

Mahmoud Massoud

Engineering Thermofluids

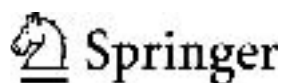
Thermodynamics, Fluid Mechanics, and Heat Transfer

Mahmoud Massoud

Engineering Thermofluids

Thermodynamics, Fluid Mechanics, and Heat Transfer

With 345 Figures and 13 Tables



Dr. Mahmoud Massoud
University of Maryland
Department Mechanical Engineering
20742 College Park, MD
USA
mmassoud@umd.edu

Library of Congress Control Number: 2005924007

ISBN 10 3-540-22292-8 **Springer Berlin Heidelberg New York**
ISBN 13 978-3-540-22292-7 **Springer Berlin Heidelberg New York**

This work is subject to copyright. All rights are reserved, whether the whole or part of the material is concerned, specifically the rights of translation, reprinting, reuse of illustrations, recitation, broadcasting, reproduction on microfilm or in other ways, and storage in data banks. Duplication of this publication or parts thereof is permitted only under the provisions of the German Copyright Law of September 9, 1965, in its current version, and permission for use must always be obtained from Springer-Verlag. Violations are liable to prosecution under German Copyright Law.

Springer is a part of Springer Science+Business Media

springeronline.com

© Springer-Verlag Berlin Heidelberg 2005

Printed in Germany

The use of general descriptive names, registered names, trademarks, etc. in this publication does not imply, even in the absence of a specific statement, that such names are exempt from the relevant protective laws and regulations and therefore free for general use.

Typesetting: PTP-Berlin Protago-TEX-Production GmbH, Germany
Final processing by PTP-Berlin Protago-TEX-Production GmbH, Germany
Cover-Design: Medionet AG, Berlin
Printed on acid-free paper 62/3141/Yu – 5 4 3 2 1 0

*In loving memory of my dear father
Ghahreman Massoud*

Preface

Thermofluids, while a relatively modern term, is applied to the well-established field of thermal sciences, which is comprised of various intertwined disciplines. Thus mass, momentum, and heat transfer constitute the fundamentals of thermofluids. This book discusses thermofluids in the context of thermodynamics, single- and two-phase flow, as well as heat transfer associated with single- and two-phase flows. Traditionally, the field of thermal sciences is taught in universities by requiring students to study engineering thermodynamics, fluid mechanics, and heat transfer, in that order. In graduate school, these topics are discussed at more advanced levels. In recent years, however, there have been attempts to integrate these topics through a unified approach. This approach makes sense as thermal design of widely varied systems ranging from hair dryers to semiconductor chips to jet engines to nuclear power plants is based on the conservation equations of mass, momentum, angular momentum, energy, and the second law of thermodynamics. While integrating these topics has recently gained popularity, it is hardly a new approach. For example, Bird, Stewart, and Lightfoot in *Transport Phenomena*, Rohsenow and Choi in *Heat, Mass, and Momentum Transfer*, El-Wakil, in *Nuclear Heat Transport*, and Todreas and Kazimi in *Nuclear Systems* have pursued a similar approach. These books, however, have been designed for advanced graduate level courses. More recently, undergraduate books using an integral approach are appearing.

In this book, a wide range of thermal science topics has been brought under one umbrella. This book is intended for graduate students in the fields of Chemical, Industrial, Mechanical, and Nuclear Engineering. However, the topics are discussed in reasonable detail, so that, with omission of certain subjects, it can also be used as a text for undergraduate students. The emphasis on the application aspects of thermofluids, supported with many practical examples, makes this book a useful reference for practicing engineers in the above fields. No course prerequisites, except basic engineering and math, are required; the text does not assume any degree of familiarity with various topics, as all derivations are obtained from basic engineering principles. The text provides examples in the design and operation of thermal systems and power production, applying various thermofluid disciplines. The goal is to give equal attention to a discussion of all power production sources. However, as George Orwell would have put it, power production from nuclear systems has been treated in this book “more equally”!

As important as the understanding of a physical phenomenon is for engineers, equally important is the formulation and solution to the mathematical model representing each phenomenon. Therefore, rather than providing the traditional mathematical tidbits, a chapter is dedicated to the fundamentals of engineering

mathematics. This allows each chapter to address the subject topic exclusively, preventing the need for mathematical proofs in the midst of the discussion of the engineering subject.

Topics are prepared in seven major chapters; Introduction, Thermodynamics, Single-Phase Flow, Single-Phase Heat Transfer, Two-Phase Flow and Heat Transfer, Applications of Thermofluids in Engineering, and the supplemental chapter on Engineering Mathematics. These chapters are further broken down into several subchapters. For example, Chapter II for Thermodynamics consists of Chapter IIa for Fundamentals of Thermodynamics, Chapter IIb for Power Cycles, and Chapter IIc for Mixtures of Non-Reactive Gases.

Each chapter opens by briefly describing the covered topic and defining the pertinent terminology. This approach will familiarize the reader with the important concepts and facilitate comprehension of topics discussed in the chapter. To aid the understanding of more subtle topics, walkthrough examples are provided, in both British and SI units. Questions at the end of each chapter remind the reader of the key concepts discussed in the chapter. Homework problems, with answers to some of the problems, are provided to assist comprehension of the related topic. Throughout this book, priority is given to obtaining analytical solutions in closed form. Numerical solutions and empirical correlations are presented as alternatives to the analytical solution, or when an analytical solution cannot be found due to the complexities involved.

Multi-authored references are cited only by the name of the first author. When an author is cited twice in the same chapter, the date of the publication follows the author's name.

A CD-ROM containing menu-driven engineering software (ToolKit) is provided for performing laborious tasks. In addition to ToolKit, the CD-ROM contains folders named after the associated chapters. These folders contain the listings of computer programs, sample input, and sample output files for various applications. The items that are included in the software are identified in the text.

The data required in various chapters are tabulated in Chapter VIII, Appendices. To distinguish the appendix tables from the tables used in various chapters, the table numbers in the appendices are preceded by the letter A.

Acknowledgement

I am grateful to my contributors listed below, who kindly answered my questions, provided useful comments and suggestions, or agreed to review several or all of the chapters of this book:

- Professor Kazys Almenas*, University of Maryland
- Professor Morton Denn, City College of New York
- Dr. Thomas L. George, Numerical Applications, Inc.
- Mr. James Gilmer, Bechtel Power Corporation
- Professor Peter Griffith, MIT
- Dr. Gerard E. Gryczkowski, Constellation Energy
- Professor Yih Yun Hsu*, University of Maryland
- Dr. Ping Shieh Kao, Computer Associates, Inc.
- Professor Mujid S. Kazimi, MIT
- Professor John H. Lienhard IV, University of Houston
- Professor Anthony F. Mills, UCLA
- Professor Mohammad Modarres, University of Maryland
- Dr. Frederick J. Moody, General Electric and San Jose State University
- Professor Amir N. Nahavandi*, Columbia University
- Mr. Farzin Nouri, Bechtel Power Corporation
- Professor Karl O. Ott, Purdue University
- Dr. Daniel A. Prelewicz, Information System Laboratories, Inc.
- Professor Marvin L. Roush, University of Maryland
- Mr. Raymond E. Schneider, Westinghouse Electric Company
- Dr. Farrokh Seifae, Framatome ANP, Inc.
- Mr. John Singleton, Constellation Energy
- Professor Neil E. Todreas, MIT
- Professor Gary Z. Watters, California State University at Chico
- Professor Frank M. White, University of Rhode Island

Technical assistance of Richard B. Mervine and Seth Spooner and editorial assistance of Ruth Martin and Edmund Tyler are gratefully acknowledged. Thanks are due my students at the University of Maryland, Martin Glaubman, Katrina Groth, Adam Taff, Keith Tetter, and Wendy Wong for providing useful feedback and suggestions. I also appreciate the efforts of my editors Gabriel Maas of Springer-Verlag and Danny Lewis and colleagues of PTP-Berlin GmbH. I commend all the contributors for assisting me in this endeavor and emphasize that any shortcoming is entirely my own.

* Retired

Table of Contents*

I.	Introduction.....	1
1.	Definition of Thermofluids	1
2.	Energy Sources and Conversion	2
3.	Energy in Perspective.....	4
4.	Power Producing Systems.....	5
5.	Power Producing Systems, Fossil Power Plants	6
6.	Power Producing Systems, Nuclear Power Plants	11
7.	Power Producing Systems, Greenpower Plants	17
8.	Comparison of Various Energy Sources	23
9.	Thermofluid Analysis of Systems.....	25
	Questions	27
	Problems	28
II.	Thermodynamics	31
Ila.	Fundamentals.....	32
1.	Definition of Terms.....	33
2.	Equation of State for Ideal Gases.....	41
3.	Equation of State for Water	46
4.	Heat, Work, and Thermodynamic Processes	55
5.	Conservation Equation of Mass for a Control Volume	64
6.	The First Law of Thermodynamics.....	66
7.	Applications of the First Law, Steady State.....	70
8.	Applications of the First Law, Transient.....	81
9.	The Second Law of Thermodynamics	96
10.	Entropy and the Second Law of Thermodynamics	105
11.	Exergy or Availability.....	116
	Questions	123
	Problems	125
Ilb.	Power Cycles	144
1.	Gas Power Systems.....	144
2.	Vapor Power Systems	161
3.	Actual Versus Ideal Cycles	174

* The related flow chart follows this section

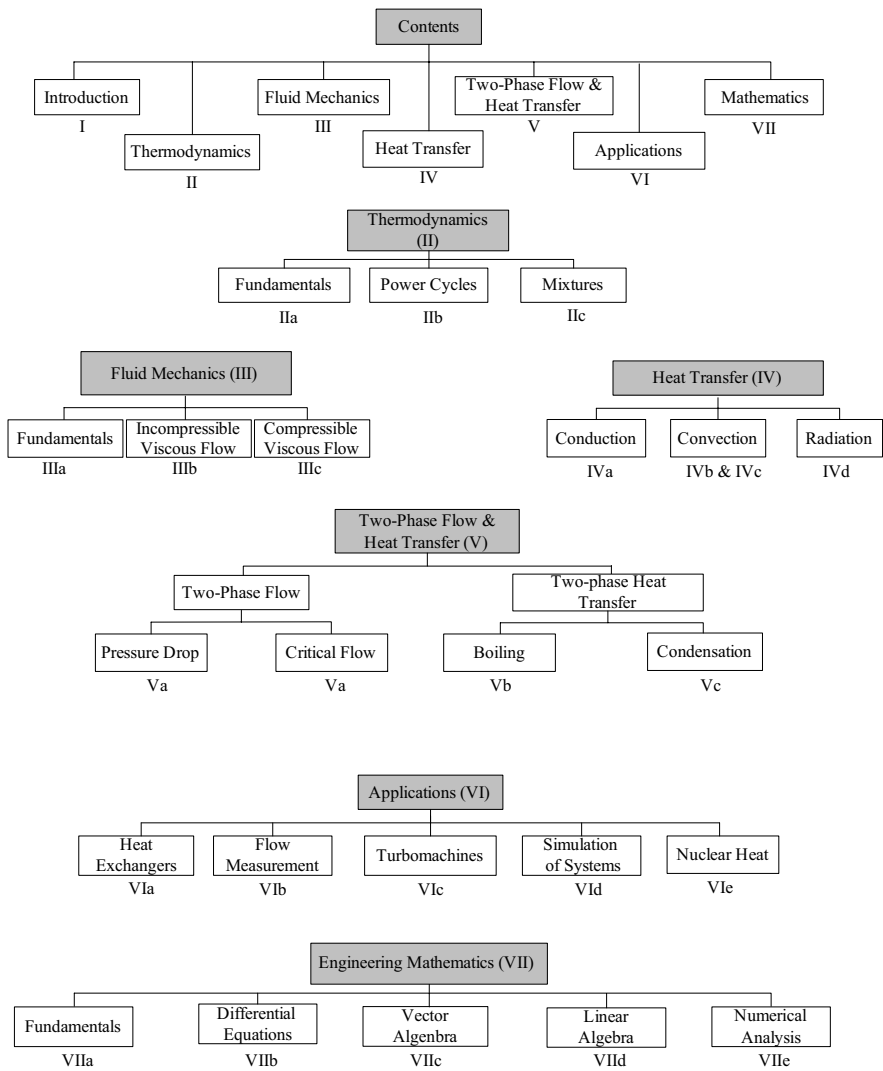
Questions	177
Problems	178
IIC. Mixtures.....	187
1. Mixture of Non-reactive Ideal Gases	187
2. Gases in Contact with Ice, Water, and Steam	193
3. Processes Involving Moist Air	196
4. Charging and Discharging Rigid Volumes	203
Questions	217
Problems	218
III. Fluid Mechanics	223
IIIa. Single-Phase Flow Fundamentals	224
1. Definition of Fluid Mechanic Terms	224
2. Fluid Kinematics	233
3. Conservation Equations	239
Questions	274
Problems	275
IIIb. Incompressible Viscous Flow	286
1. Steady Incompressible Viscous Flow	286
2. Steady Internal Incompressible Viscous Flow	289
3. Pressure Drop in Steady Internal Incompressible Viscous Flow	295
4. Steady Incompressible Viscous Flow in Piping Systems.....	310
5. Steady Incompressible Viscous Flow Distribution in Piping Networks	337
6. Unsteady Internal Incompressible Flow.....	343
7. Fundamentals of Waterhammer Transients	371
Questions	383
Problems	383
IIIc. Compressible Flow	399
1. Steady Internal Compressible Viscous Flow	399
2. The Phenomenon of Choked or Critical Flow	414
Questions	426
Problems	427
IV. Heat Transfer	431
IVa. Conduction.....	431
1. Definition of Heat Conduction Terms	432
2. The Heat Conduction Equation.....	437
3. Analytical Solution of Heat Conduction Equation.....	444

4.	Lumped-Thermal Capacity Method for Transient Heat Conduction.....	445
5.	Analytical Solution of 1-D S-S Heat Conduction Equation, Slab	448
6.	Analytical Solution of 1-D S-S Heat Conduction Equation, Cylinder	461
7.	Analytical Solution of 1-D S-S Heat Conduction Equation, Sphere	474
8.	Analytical Solution of Heat Conduction Equation, Extended Surfaces.....	477
9.	Analytical Solution of Transient Heat Conduction	485
10.	Numerical Solution of Heat Conduction Equation.....	499
	Questions	501
	Problems	502
IVb.	Forced Convection.....	518
1.	Definition of Forced Convection Terms	518
2.	Analytical Solution	521
3.	Empirical Relations.....	534
	Questions	541
	Problems	541
IVc.	Free Convection.....	549
1.	Definition of Free Convection Terms	549
2.	Analytical Solution	550
3.	Empirical Relations.....	553
	Questions	557
	Problems	558
IVd.	Thermal Radiation	561
1.	Definition of Thermal Radiation Terms.....	561
2.	Ideal Surfaces.....	568
3.	Real Surfaces	573
4.	Gray Surfaces.....	578
5.	Radiation Exchange Between Surfaces.....	579
	Questions	592
	Problems	592
V.	Two-Phase Flow and Heat Transfer.....	601
Va.	Two-Phase Flow Fundamentals	601
1.	Definition of Two-Phase Flow Terms.....	601
2.	Two-Phase Flow Relation	606
3.	Two-Phase Critical Flow	622
	Questions	632
	Problems	632

Vb.	Boiling	637
1.	Definition of Boiling Heat Transfer Terms.....	637
2.	Convective Boiling, Analytical Solutions.....	641
3.	Convective Boiling, Experimental Observation.....	648
4.	Pool Boiling Modes	650
5.	Flow Boiling Modes	658
	Questions	672
	Problems	673
Vc.	Condensation	677
1.	Definition of Condensation Heat Transfer Terms.....	677
2.	Analytical Solution	678
3.	Empirical Solution	682
4.	Condensation Degradation.....	684
	Questions	685
	Problems	686
VI.	Applications.....	687
Via.	Heat Exchangers	687
1.	Definition of Heat Exchanger Terms.....	687
2.	Analytical Solution	690
3.	Analysis of Shell and Tube Heat Exchanger.....	702
4.	Analysis of Condensers.....	710
5.	Analysis of Steam Generators.....	716
6.	Transient Analysis of Concentric Heat Exchangers.....	719
	Questions	723
	Problems	723
Vib.	Fundamentals of Flow Measurement.....	728
1.	Definition of Flow Measurement Terms.....	728
2.	Repeatability, Accuracy, and Uncertainty	729
3.	Flowmeter Types	732
4.	Flowmeter Installation	744
	Questions	745
	Problems	745
Vic.	Fundamentals of Turbomachines.....	747
1.	Definition of Turbomachine Terms	747
2.	Centrifugal Pumps	749
3.	Dimensionless Centrifugal Pumps Performance.....	755
4.	System and Pump Characteristic Curves	762
5.	Analysis of Hydraulic Turbines	769
6.	Analysis of Turbojet for Propulsion.....	777
	Questions	779
	Problems	780

VId. Simulation of Thermofluid Systems	784
1. Definition of Terms.....	784
2. Mathematical Model for a PWR Loop.....	786
3. Simplified PWR Model.....	791
4. Mathematical Model for PWR Components, Pump.....	802
5. Mathematical Model for PWR Components, Pressurizer	811
6. Mathematical Model for PWR Components, Containment	819
7. Mathematical Model for PWR Components, Steam Generator	827
Questions	829
Problems	829
 VIe. Nuclear Heat Generation.....	 841
1. Definition of Some Nuclear Engineering Terms.....	841
2. Neutron Transport Equation.....	853
3. Determination of Neutron Flux in an Infinite Cylindrical Core.....	859
4. Reactor Thermal Design	877
5. Shutdown Power Production.....	882
Questions	884
Problems	884
 VII. Engineering Mathematics	 901
VIIa. Fundamentals.....	901
1. Definition of Terms.....	901
 VIIb. Differential Equations	 911
1. Famous Differential Equations	911
2. Analytical Solutions to Differential Equations	919
3. Pertinent Functions and Polynomials.....	936
 VIIc. Vector Algebra.....	 943
1. Definition of Terms.....	943
 VIId. Linear Algebra.....	 963
1. Definition of Terms.....	963
2. The Inverse of a Matrix.....	968
3. Set of Linear Equations.....	971
 VIIe. Numerical Analysis	 976
1. Definition of Terms	976
2. Numerical Solution of Ordinary Differential Equations	979
3. Numerical Solutions of Partial Differential Equations.....	985
4. The Newton–Raphson Method	1004
5. Curve Fitting to Experimental Data	1006

VIII. Appendices	1011
I. Unit Systems, Constants and Numbers	1013
II. Thermodynamic Data	1023
III. Pipe and Tube Data.....	1049
IV. Thermophysical Data.....	1059
V. Nuclear Properties of Elements	1091
 References.....	 1097
 Index.....	 1111



Note: Roman numerals refer to the related chapters

Nomenclature

In this book, for the sake of brevity and consistency, as few symbols as possible are used. Thus, to minimize the number of symbols, yet clearly distinguish various parameters, lower case and *italic* fonts have been used whenever a symbol represents two or more parameters. For example, while V represents volume, v is used for specific volume, V for velocity, ν for kinematic viscosity, and \dot{V} for volumetric flow rate. To avoid confusion when solving problems by hand, the reader may use ∇ for volume.

Special attention must be paid whenever h representing specific enthalpy and h , standing for heat transfer coefficient, appear in the same equation. This occurs in chapters IVe and IVf, dealing with boiling and condensation. Also note that h and H stand for height. Similarly, In Chapter Va, s represents an element of length as well as entropy while S stands for slip ratio, respectively.

The units provided below in front of each symbol, are just examples of commonly used units. They do not preclude the representation of the same symbol with different sets of units. The details of the SI units are discussed in Appendix I.

English symbols	Definition	SI Unit	British Unit
a	Acceleration	m/s^2	ft/s^2
a	Radius	m	in
A	Helmholtz function	J	Btu
A	Area	m^2	ft^2
b	Width	m	ft
B	Bulk modulus	Pa	psi
B	Buckling	cm^{-2}	in^{-2}
c	Speed of sound	m/s	ft/s
c_p	Specific heat at constant pressure	$\text{W/kg}\cdot\text{C}$	$\text{Btu/lbm}\cdot\text{F}$
c_v	Specific heat at constant volume	$\text{W/kg}\cdot\text{C}$	$\text{Btu/lbm}\cdot\text{F}$
C_d	Discharge Coefficient	—	—
C_D	Drag coefficient	—	—
d, D	Diameter	m (cm)	ft (in)
e	Specific energy	W/kg	Btu/lbm
e	Uncertainty	—	—
E	Modulus of Elasticity	Pa	psi
E	Total energy	J	Btu
E	Total emissive power	W	Bu/s

symbols	Definition	SI Unit	British Unit
F	Force	N	lbf
F	View factor	-	-
F	Peaking factor	-	-
g	Gibbs function	J	Btu
g	Gravitational acceleration	m/s ²	ft/s ²
g_c	Conversion constant	kg·m/N·s ²	slug·ft/lbf·s ²
G	Mass flux	kg/s·m ²	lbm/s·ft ²
G	Irradiation	W/m ²	Btu/s·ft ²
h	Head	m	ft
h	Plank's constant	J·s	Btu·s
h	Heat transfer coefficient	W/m ² ·C	Btu/h·ft ² ·F
h	Specific enthalpy	kJ/kg	Btu/lbm
H	Height	m	ft
H	Enthalpy	J	Btu
I	Geometric inertia	m ⁻¹	ft ⁻¹
I	Irreversibility	J	Btu
I	Spectral intensity	W/m ² ·μm·sr	Btu/s·ft ² ·μm sr
j	Conversion factor	J/J	ft·lbf/Btu
J	Radiosity	W/m ² ·μm	-
J	Superficial velocity	m/s	ft/s
J	Neutron current density	s ⁻¹ ·cm ⁻²	s ⁻¹ ·ft ⁻²
J	Bessel function of first kind	-	-
k_s	Spring constant	-	-
k	Boltzmann constant	J/K	Btu/R
k	Thermal conductivity	W/m·K	Btu/h·ft·F
k_∞	Infinite medium multiplication factor	-	-
k_{eff}	Finite medium multiplication factor	-	-
K	Frictional loss coefficient	-	-
l	Mean free path	cm	in
L	Diffusion length	cm	in
m	Mass	kgm	lbm
\dot{m}	Mass flow rate	kg/s	lbm/s
M	Molecular weight	kg/kmol	lb/lbmol
N_A	Avogadro number	-	-
P	Pressure	Pa	psi
P	Perimeter	m	ft
q	Heat transfer per unit mass	J/kg	Btu/lbm
q'	Linear heat generation rate	W/m	kW/ft
q''	Heat flux	W/m ²	Btu/h·ft ²
q'''	Volumetric heat generation rate	W/m ³	Btu/h·ft ³
Q	Heat transfer	J	Btu
\dot{Q}	Rate of heat transfer	W	Btu/s
R	Gas constant	kPa·m ³ /kg·K	ft·lbf/lbm·R

English symbols	Definition	SI Unit	British Unit
r, R	Radius	m (cm)	ft (in)
R	Thermal resistance	C/W	h·F/Btu
R_u	Universal gas constant	kJ/kmol·K	ft·lbf/lbmol·R
s	Element of length	m	ft
s	Tube or rod pitch	cm	in
s	Specific entropy	J/kg·K	Btu/lbm·R
s	Volumetric neutron source strength	cm ⁻³ ·s ⁻¹	in ⁻³ ·s ⁻¹
S	Entropy	J/K	Btu/R
S	Slip ratio	—	—
S	Surface area	m ²	ft ²
S_g	Specific gravity	—	—
t	Time	s	s
T	Temperature	C (K)	F (R)
T	Torque	m·N	ft·lbf
u	Specific internal energy	J/kg	Btu/lbm
u	Unit vector	—	—
U	Internal energy	J	Btu
U	Overall heat transfer coefficient	W/m ² ·K	Btu/h·ft ² ·F
ν	Kinematics viscosity	m ² /s	ft ² /h
ν	secific volume	m ³ /kgm	ft ³ /lbm
V	Vlocity	m/s	ft/s
V	Volume	m ³	ft ³
V	Voltage	V	V
V	Volumetric flow rate	m ³ /s	ft ³ /s
W	Weight	kg	lbf
w	Work per unit mass of working fluid	J/kg	Btu/lbm
W	Work	J	Btu
\dot{W}	Power	W	Btu/s
x	Thermodynamic quality	—	—
X	Flow quality	—	—
y	mole fraction	—	—
Y	Gas expansion factor	—	—
Z	Elevation	m	ft
Greek symbols	Definition	SI Unit	British Unit
α	Void fraction, Absorptivity	—	—
β	Volumetric thermal expansion coeff.	K ⁻¹	R ⁻¹
β	Volumetric flow ratio	—	—
γ	Ratio of c_p/c_v	—	—
γ	Shearing strain	—	—

Greek symbols	Definition	SI Unit	British Unit
δ	Boundary layer thickness	mm	in
Δ	Difference in values	—	—
ε	Emissivity	—	—
ε	Strain	—	—
Σ	Macroscopic cross section	cm^{-1}	—
ζ	Effectiveness	—	—
η	Efficiency	—	—
η	Eta factor	—	—
θ	Azimuthal angle	—	—
κ	Boltzmann constant	J/K	Btu/R
κ	Isothermal compressibility	Pa^{-1}	psi^{-1}
κ	Thermal conductivity (tensor)	$\text{W/m} \cdot \text{C}$	$\text{Btu/h} \cdot \text{ft} \cdot \text{F}$
λ	System thermal length	m	ft
λ	Mean free path	cm	in
λ	Wavelength	μm	—
μ	Absorption coefficient	cm^2	—
μ	Dynamic viscosity	$\text{N} \cdot \text{s/m}^2$	$\text{bm/h} \cdot \text{ft}$
ν	Number of fast neutrons per fission	—	—
ρ	Density	kg/m^3	lbm/ft^3
ρ	Reflectivity	—	—
σ	Surface tension	N/m	lbf/ft
σ	Tensile stress	Pa	psi
σ	Stefan-Boltzmann constant	$\text{W/m}^2 \cdot \text{K}^4$	$\text{Btu/ft}^2 \cdot \text{h} \cdot \text{R}^4$
σ	Microscopic cross section	cm^{-2}	—
σ	Measure of entropy production	J/K	Btu/R
τ	Shear stress	Pa	psi
τ	Transmissivity	—	—
ϕ	Relative humidity	—	—
ϕ	Flux	$\text{s}^{-1} \cdot \text{cm}^{-2}$	$\text{s}^{-1} \cdot \text{ft}^{-2}$
ϕ	Specific availability (closed system)	kJ/kg	Btu/lbm
Φ	Availability (closed system)	kJ	Btu
Φ	Viscous Dissipation function	W	Btu/s
χ	Fission spectrum of an isotope	MeV^{-1}	Btu^{-1}
φ	Zenith angel	—	—
Ψ	Stream function	—	—
ψ	Specific availability (control volume)	kJ/kg	Btu/lbm
Ψ	Availability (control volume)	kJ	Btu
ω	Humidity ratio	—	—
ω	Impeller Speed of a turbomachine	rad/s	rad/s
Ω	Solid angle	sr	—

Subscripts

<i>B</i>	body, buoyancy
<i>CL</i>	Centerline
<i>C.V.</i>	control volume
<i>e</i>	equivalent or hydraulic diameter
<i>f</i>	saturated liquid
<i>f</i>	friction
<i>f</i>	free stream, bulk
<i>g</i>	saturated steam
<i>h</i>	equivalent or hydraulic diameter
<i>l</i>	local
<i>r</i>	reduced
<i>max</i>	maximum
<i>min</i>	minimum
<i>s</i>	surface, shaft
<i>sat</i>	saturation
<i>v</i>	vapor

Abbreviations

#	numbers of
1-D	one dimensional
Av	Avogadro number
b	Barns
C	Celsius
cm	centimeter
eV	electron volt
E	exponent (Example: $1 \times 10^3 = 1E3$)
ft	foot, feet
F	Fahrenheit
g	gram
GPM	gallon per minute
h	hour
hp	horsepower
in	inch
J	Joules
k	Kilo
K	Kelvin
ln	natural logarithm, logarithm to the base $e = 2.7182818$
log	logarithm to the base 10
m	meter
min	minute

mm	millimeter
MBtu	million Btu
MeV	Million electron volt
MWe	Mega Watt electric
MWt	Mega Watt thermal
R	Rankine
s	second
S-S	steady state
W	Watt

I. Introduction

1. Definition of Thermofluids

The study of thermofluids integrates various disciplines of the field of thermal sciences. This field consists of such topics as thermodynamics, fluid mechanics, and heat transfer, all of which are discussed in various chapters of this book. The fascinating concept of *energy* is the common denominator in all these topics. Although we are intuitively familiar with energy through our various experiences it is, nonetheless, difficult to formulate an exact definition. One might say energy is the ability to do *work*, but then we must first define work. According to Huang we may hypothesize that “energy is something that all matter has.” We leave the definitions and discussion of energy, *heat*, work, and *power* to the chapter on thermodynamics. In this chapter we introduce thermofluids and discuss the engineering applications of thermofluids in the design and operation of thermal systems, such as those used in power production.

Thermal systems deal with the storage, conversion, and transportation of energy in its many forms. These may include a jet engine that converts fuel energy to mechanical energy, an electric heater that converts electrical energy to heat energy, or even a shotgun, which converts chemical energy to kinetic energy. Having defined thermal systems, we now define fluids. In general, any substance that is not a solid can be considered as a fluid. In this book the only fluids, we consider in the design and operation of thermal systems are *liquids* and *gases* especially water and air, as they are by far the most abundant fluids on earth. Liquids and gases in thermal systems are referred to as *working fluids*. As discussed in the chapter on fluid mechanics, there are also other types of fluids such as blood, glue, lava, slurry, tar, and toothpaste, which are analyzed differently than liquids and gases.

From this brief introduction, we conclude that: *thermofluids is a subject that analyzes systems and processes involved in energy, various forms of energy, and transfer of energy in fluids*. Since fluids generally come in contact with solids, in this book we will include the study of energy transfer in both fluids and solids.

This book is prepared in seven chapters. In the present chapter, we discuss the three sources of energy for power production and describe various power producing systems. This provides sufficient background to start Chapter II and learn about thermodynamics and its associated laws governing the processes involved in thermal systems. This is followed by Chapter III on fluid mechanics and its related topics on the application of the working fluids in thermal systems. Chapter III deals exclusively with the flow of *single-phase* fluids. The topic of heat transfer in both solids and single-phase fluids is discussed in Chapter IV. Chapter V then

discusses the mechanisms associated with *two-phase flow*. Chapter V also discusses heat transfer when a fluid changes phase such as the boiling of water and condensation of steam. The knowledge gained in the first five chapters is then used in Chapter VI to discuss the applications of thermofluids in the design and operation of such thermal systems as heat exchangers (steam generators, feedwater heaters, and condensers), turbines, and pumps. Engineering mathematics covering a wide range of topics in advanced calculus is compiled in Chapter VII. This allows us in each chapter to focus exclusively on the topic at hand and prevents us from any need to discuss mathematics in these chapters.

2. Energy Source and Conversion

Energy is essential for most advances in society and the continuous improvement of the quality of life. We use a variety of means to convert energy for industrial, transportation, residential, and commercial applications.

From time to time, the world has experienced energy crises, defined as the shortage of supply of energy or the environmental consequences associated with the use of a source of energy. Such crises prove to be important reminders of how vital energy is for transportation, commerce, industry, and residential use. These crises also serve as the motivation to improve and broaden the application of energy sources and for the quests to find new sources of energy.

Figure I.2.1 shows the interaction between various forms of energy and the respective means of energy conversion. Let's examine this figure by first considering for instance, pumping water to a reservoir. The mechanical energy of the pump is used to lift water, hence increasing water's potential energy, and to fill the reservoir. The reservoir then returns the stored energy in water in the form of kinetic energy when we open the faucet in our homes. The pump itself must be powered by a prime mover such as an electric motor or an internal combustion engine, indicating conversion of electrical or chemical energies to mechanical energy.

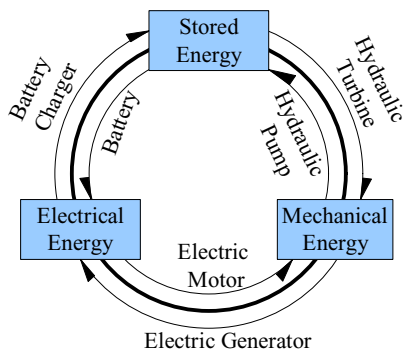


Figure I.2.1. Means of energy conversion (Marquand)

If water instead of flowing in the faucet is used to power a hydraulic turbine, the water kinetic energy would be converted back to mechanical energy. The mechanical energy in a generator is converted to electrical energy. The electrical energy may then be used to charge batteries, which then become the reservoir for stored energy. In this energy conversion process, one form of stored energy is converted to a new form of stored energy.

The converse is also possible when we use a battery to produce electrical energy, which can then be used in an electric motor to be converted to mechanical energy. The motor, in turn would serve as the prime mover of a hydraulic pump to fill a reservoir thus, converting the mechanical energy into stored energy.

Figure I.2.2 is a more comprehensive diagram of energy conversion including various types of energy and the conversion pathways between various types. For example, radiant, chemical, electrical, mechanical, and nuclear energies can be converted to thermal energy while thermal energy can be converted to mechanical and electrical energies.

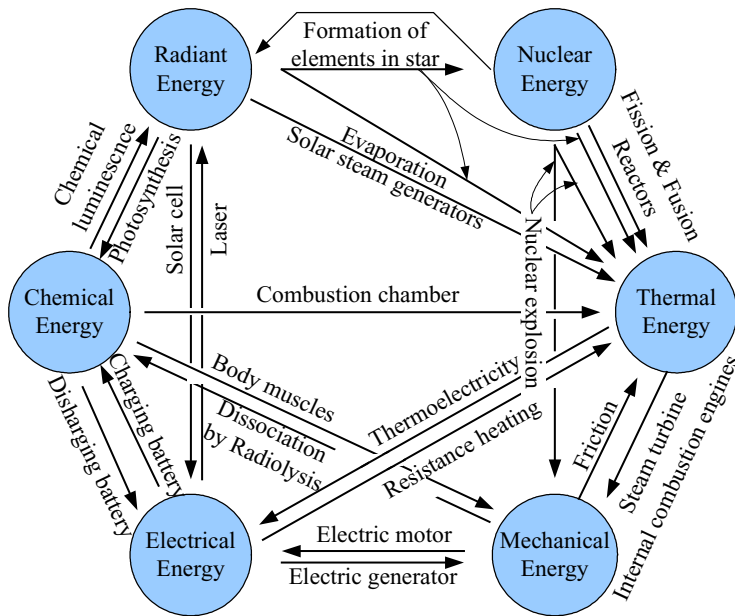


Figure I.2.2. Important forms of energy and the pathway for conversion (Marion)

The conversion of one type of energy to another takes place in what is known as a *process*. Many of such processes including the direction of a process and such concepts as efficiency are discussed in Chapter II. In the remainder of this chapter, we discuss various sources of energy and briefly describe various types of energy conversion system for power production.

3. Energy in Perspective

The world's energy resources must fulfill the needs of an increasing world population. The world energy resources are generally divided into three categories, fossil fuels, nuclear fuels, and green, renewable or alternative resources. Historically, wood was the primary source of energy before the industrial revolution. The first oil producing well was operational in 1859, which was followed by the introduction of the internal combustion engine (1876), the first steam-generated electric plant (Edison, New York city 1882), the steam turbine (1884), and the Diesel Engine (1892). We now discuss two important types of fuels; fossil and nuclear.

3.1. Fossil Fuels

This category consists of coal, oil, and natural gas. Today, over 80% of the world's energy supply is from fossil fuels, of which 60% is from oil and gas and the remaining 40% is from coal. Coal is pure carbon and natural gas is primarily methane hence, both of these fuels can be used without substantial processing. Petroleum, on the other hand, is found in the form of crude oil and must be refined for various applications. In the United States, coal is primarily used for power production and in industrial applications, while natural gas is used for industrial and residential applications as well as in power production. Petroleum in the United States is primarily used for transportation (54%) followed by industrial, residential, and power generation.

3.2. Nuclear Fuels

According to Einstein's equation $E = mc^2$, the energy obtained from 1 kg of uranium is equivalent to the burning of 3.4 thousand tons of coal¹. Similarly from the conversion of mass to energy, we find that the energy equivalent of mass in a barrel of oil is over 2 billion times more than the energy obtained by its combustion. The share of power production from nuclear energy has increased since 1950. Nuclear energy is used primarily for power production, although nuclear reactors are also used to power naval surface ships and submarines. Battery powered submarines must surface periodically to recharge their batteries using diesel engines, which require an intake of oxygen to support combustion. Since no combustion occurs in a nuclear reactor to require oxygen, nuclear powered submarines can remain submerged indefinitely. The world's first nuclear-powered submarine was commissioned in 1954 and the first commercial nuclear power plant (90 MWe) became operational in Shippingport, Pennsylvania in 1957. The physical processes occurring in nuclear reactors can be classified as either *fission* or *fusion*.

¹ The energy equivalent of 1 gram of mass is $E = (1/1,000) \text{ kg} \times (300,000,000)^2 \text{ m}^2/\text{s} = 9\text{E}13 \text{ J} = 8.53\text{E}10 \text{ Btu}$.

Fission-Based Reactors

These reactors use heavy elements like uranium and plutonium as fuel. The atoms in these elements have a high possibility of splitting (fission) when exposed to neutrons. The energy obtained from such reactions is primarily due to the kinetic energy of the fission fragments. Fission reactors may be subdivided based on energy of the neutron used for fission. Reactors using low-energy neutrons and uranium are known as *thermal* reactors and reactors using high-energy neutrons and plutonium are referred to as *fast* reactors. Most of the world's nuclear reactors are thermal. As discussed in Chapter IVe, high-energy neutrons emerge subsequent to the fission of heavy elements. Striking the atoms of a moderator slows down or thermalizes fast neutrons.

Thermal reactors in the United States use water both as coolant and as moderator thus are referred to as *Light Water Reactors* (LWRs)². Light water reactors can be divided into two major categories; *Pressurized Water Reactors* (PWRs) and *Boiling Water Reactors* (BWRs). Reactors that use gases like helium as coolant are known as *Gas Cooled Reactors* (GCR). Some fast reactors use a liquid metal, such as sodium, as coolant. These are referred to as *Liquid Metal Fast Breeder Reactors*, (LMFBR). The breeder reactors convert such *fertile* isotopes as ^{238}U and ^{232}Th to such *fissionable* isotopes as ^{239}Pu and ^{233}U , respectively. Thus, in such reactors, more fissionable nuclei are produced by conversion than are consumed by fission.

Fusion-Based Reactors

In a fusion process, two light nuclei such as deuterium and lithium fuse together in an intensely ionized electrically neutral gas known as *plasma*. The energy obtained in this reaction is in the form of the kinetic energy of the emergent nuclei. To compare the immense energy obtained from fusion in comparison with fission, we note that the energy produced by 1 kg of light nuclei in fusion is equivalent to the fission energy of about 256 kg of uranium. However, obtaining a sustained fusion reaction requires further research and development and has so far, remained elusive. To date, all fusion-based reactors are only experimental facilities.

4. Power Producing Systems

The power producing systems, used for transportation or for industrial and residential electric power consumption, can be divided into two categories. The first category includes most devices that directly convert other forms of energy into electricity, known as *direct energy conversion*. Such systems as photoelectric cells and thermoelectric generators produce electric power on smaller scale. The second category includes systems that their end result is turning the shaft of an

² As discussed in Chapter VIe, thermal reactors may also use heavy water (deuterium instead of hydrogen) both as coolant and as moderator. These types of reactors are known as HPWR or CANDU (Canadian Deuterium Uranium).

electric generator to produce electricity based on Faraday's law of induction. Faraday's law is the basic principle for current central power stations generating electricity on a large scale.

Systems in the second category can be further divided based on whether a *thermodynamic cycle* is used for their operation. A thermodynamic cycle, as shown in Figure I.4.1 and discussed in Chapter II, consists of a heat source, a heat sink, an engine, and the working fluid. In a thermodynamic cycle, the working fluid is energized in the heat source and then directed to the engine to produce power. The working fluid is then passed through the heat sink and pumped back to the heat source to continue the cycle. Systems using a thermodynamic cycle may use coal, oil, gas, or nuclear heat in the heat source. A heat sink may consist of a radiator, a condenser, or a cooling tower. Power production from renewable resources such as solar energy and geothermal plants are also included in this group. Power producing systems that do not use a thermodynamic cycle include systems using such renewable energy resources as turbomachines (hydroelectric plants and wind turbines) and tidal power as discussed in Section 7. Fundamentals of turbomachines are discussed in Chapter VIc.

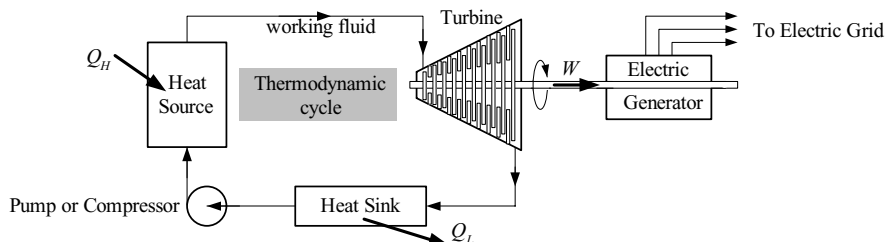


Figure I.4.1. A simplified diagram of a thermodynamic cycle for power production

5. Power Producing Systems, Fossil Power Plants

Power plants producing electricity on a large scale of hundreds to thousands of MWe, are concentrated in central power stations. Since power is extracted from the fossil fuels by combustion, systems using fossil fuels for power production are referred to as *combustion engines*. If such systems use coal or oil as fuel, they are known as *external combustion engines* in which there is no mixing of fuel with the working fluid. For example, in a coal power plant the energy obtained from the burning of coal is transferred to water flowing in the tubes through the tube wall. On the other hand, the *internal combustion engines* use refined oil, such as gasoline as well as natural gas. Thus, the working fluid in the internal combustion engines participates in the combustion process.

Internal combustion engines are used for power production in central power stations and in the automotive industry for transportation. Such engines can be divided into several categories; reciprocating piston-cylinder engines, rotary engines, and gas turbine engines as discussed next.

Reciprocating engines. The reciprocating piston-cylinder engine is a century old design that has stood the test of time and is used in an overwhelming majority of the world's automobiles. As discussed in Chapter IIb, such engines generally use the *Otto* and the *Diesel* cycles. One cycle of a four-stroke cylinder-engine consists of six phases: *intake*, *compression*, *combustion*, *expansion*, *rejection*, and *exhaust*.

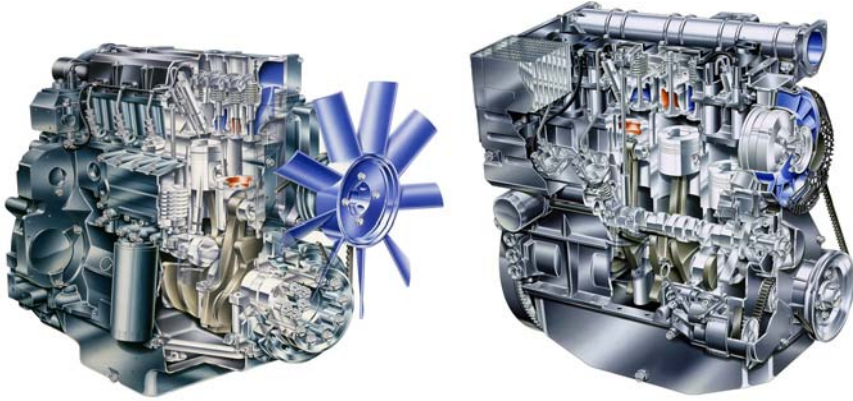


Figure I.5.1. Cutaway of an in-line six cylinder diesel engine (Courtesy Deutz AG)

The reciprocating motion of the engine piston, as transferred by the connecting rod to the crankshaft, causes the crankshaft to rotate. The crankshaft rotational motion is delivered to a gearbox to obtain the desired speed. The interface between the engine's flywheel and the gear box is provided by either a clutch or by a torque converter. These devices allow complete separation of engine and the gearbox and also provide synchronization at the time of engaging the engine with the gearbox. The output from the gearbox may be used in many ways, such as: an electric generator, a pump, the differential of a land vehicle for surface movement, the propeller of a cylinder-engine powered airplane, or the propeller of a ship for propulsion.

Reciprocating engines are equipped with camshafts to operate the intake and the exhaust valves. While the transfer of the crankshaft motion to the gearbox is through a clutch or a torque converter, the transfer of crankshaft motion to the camshaft to operate the engine's intake and exhaust valves is by gear, chain, or a belt called a timing belt. Opening of the intake and the exhaust valves is tied to the rotational motion of the crank through a rocker-arm mechanism. If the camshaft is placed below the top of the valves, the rocker-arm is operated by a push rod. If the camshaft is placed in the cylinder head then no push rod is required as the camshaft operates directly on the rocker arm. The intake and exhaust valves close by spring action.

Figure I.5.1 shows cutaways of a six-cylinder in-line diesel engine, which uses an injector and high compression ratio to reach the ignition temperature of the fuel mixture. In contrast, gasoline engines, whether using a carburetor, or a fuel injection system, use spark plugs to cause ignition for combustion. The piston is at-

tached to the connecting rod and is equipped with piston rings, which are essential components to ensure leak-tight compression. Some of the energy produced by the engine is used in an electric generator (dynamo) to charge the battery, circulate coolant around the engine jacket, or in some accessories such as car air-conditioning, and in operating the cylinder intake and exhaust valves through the camshaft.

Rotary engine. Unlike the cylinder-engine design in which pistons move in a reciprocal motion, another type of internal combustion engine uses a compartment and a rotor. The rotary combustion engine, or the Wankel engine after Felix Heinrich Wankel (1902–1988), was patented in 1936. However, problems associated with the seals at the rotor tips have prevented this type of engine from being used in a wider range of applications.

Various phases of a rotary engine cycle are shown in Figure I.5.2. As shown in Figure I.5.2-1, the rotor, rotating counterclockwise has blocked both inlet and exhaust ports, with the mixture being compressed while the combustion products are expanding. In Figure I.5.2-2, the fully expanded combustion products enter the exhaust pipe while fresh mixture enters the engine at the intake port. In Figure I.5.2-3, the fresh mixture enters the compartment, the fully compressed mixture is being ignited by the spark plug, and the combustion products leave the engine. In Figure I.5.2-4, the combustion has taken place and the mixture expands to deliver work to the rotor while the fresh mixture has filled the compartment and the inlet port is about to be blocked. The actual engine blocks of a rotary engine are shown in Figure I.5.3.

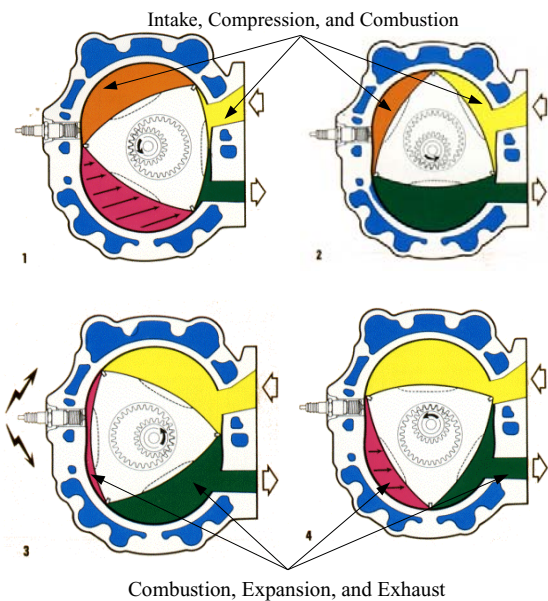


Figure I.5.2. Six phases of intake, compression, combustion, expansion, rejection, and exhaust in a rotary engine



Figure I.5.3. Rotors, shaft, compartment, and the engine block of a rotary engine

Reciprocating and rotary engines are generally water-cooled. However, some automotive engines and the pre-jet airplanes were air-cooled to reduce weight. Cylinders in the air-cooled engines of airplanes were oriented radially in a plane perpendicular to the air flow path to facilitate the flow of air through the engine. In the air-cooled engines, the rate of heat loss is enhanced by attachment of fins to the cylinder. Fins and fin efficiency are discussed in Chapter IVa.

Gas turbines are machines that convert the energy content of the working fluid to mechanical energy. Central power plants using gas turbines generally provide power at peak demand as compared with steam turbines that provide the base demand. Aviation gas turbines are referred to as jet engines. The advent of the jet engine was a turning point in aviation history as jet engines have much higher specific power, defined as power produced per engine weight, than reciprocal engines. The thrust produced by a jet engine follows Newton's third law: for every action there is an equal reaction in the opposite direction.

The principle of gas turbine operation, as discussed in Chapter IIb, is quite simple. Air entering the compressor is pressurized, to as much as 500 psia (3.4 MPa) and 1100 F (593 C) and is delivered to the combustion chamber where the mixture of air and fuel is ignited and reaches elevated temperatures (up to 3000 F, 1650 C). The energetic mixture then enters the turbine, transferring energy to the turbine rotor and leaving as exhaust gas. A portion of the turbine power is used to turn the compressor and to pump fresh air into the combustion chamber to continue the thermodynamic cycle. Figure I.5.4(a) shows the compressor and Figure I.5.4(b), a turbine rotor of a gas turbine power plant. Note that the compressor consists of combined axial (blades) and radial (disk) flow types mounted on the same shaft.

A jet engine consisting of compressor, combustion chamber, and turbine is known as a turbojet. Turbojets are well suited for crafts flying at high speeds and high altitudes. Other types of jet engines include *turbofan*, *turboprop*, and *turboshaft*. To increase the engine thrust, turbojets are equipped with a large fan, powered by the same turbine that powers the compressor and is referred to as a turbofan, as shown in Figure I.5.5. Turboprops on the other hand are turbojets that use a propeller instead of a fan. In turbofans and turboprops, about 85% of the compressed air bypasses the turbine to produce thrust, as discussed in Chapter VIc.

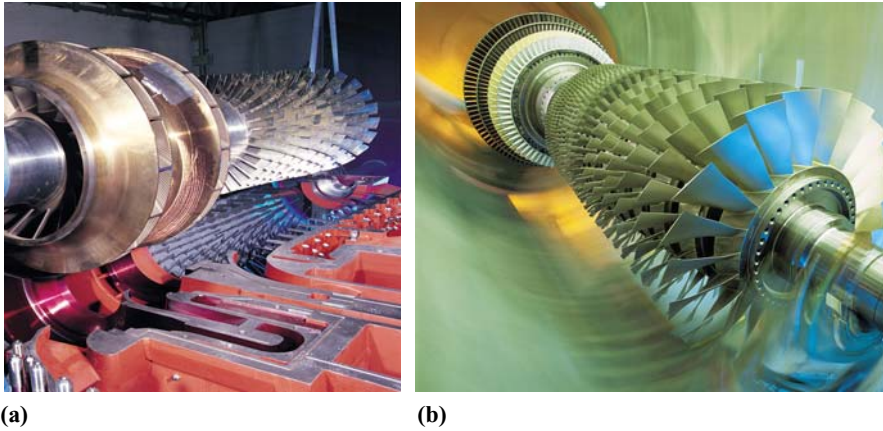


Figure I.5.4. (a) A combined axial-radial flow compressor (b) a gas turbine rotor (Courtesy Siemens AG)

In turboshaft, the turbine power is delivered to a gearbox to drive a propeller or a helicopter rotor. This arrangement allows the rotor speed to be controlled independently of the turbine. In general, however, gas turbines used in a jet engine are well suited for relatively constant loads compared with the reciprocal engines that are well suited for load varying conditions. Engine endurance generally increases if operated under a constant load.

A cutaway of a turboshaft engine is shown in Figure I.5.6. In this engine, air is compressed by two radial compressors, which are driven by an axial turbine. In general however, jet engine compressors are primarily of axial type. Axial and radial designs of turbomachines are discussed in Chapter VIc.

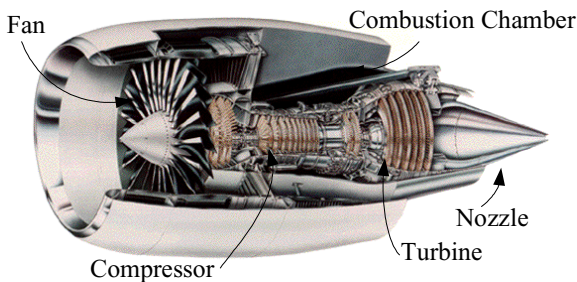


Figure I.5.5. Cutaway of a turbofan jet engine (Courtesy Pratt & Whitney)

To increase thrust, a second combustion chamber may be placed between the turbine and the nozzle. This chamber called the *afterburner*, increases the temperature of the gas before entering the nozzle hence, increasing thrust. As dis-

cussed in Chapter IIb, due to the high temperatures produced in the combustion chamber, gas turbines operate at higher thermal efficiency, defined as the ratio of power produced to the rate of energy consumed, compared with the efficiency of reciprocal engines or steam power plants.

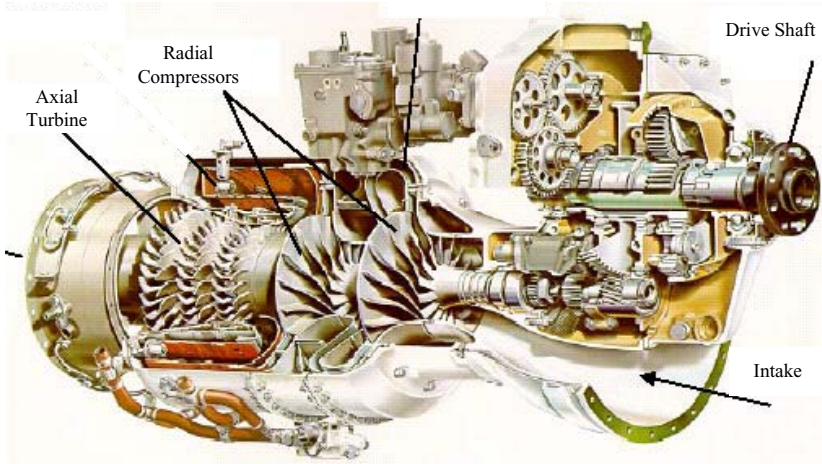


Figure I.5.6. A turboshaft engine using radial compressors and axial turbine

6. Power Producing Systems, Nuclear Power Plants

Nuclear power supplies about 17% of world's electricity. In France, about 80% of electricity is supplied by nuclear energy. In the United States, nuclear energy is the second largest source of electricity, providing power for 65 million homes. Unlike fossil fuels, nuclear energy does not produce any emissions to contribute to the greenhouse effect and global warming. Indeed if nuclear plants were to be replaced by fossil plants, the CO₂ emission worldwide would increase by 21% (Mayo). Schematics of two types of classic U.S. designed light water reactors are shown in Figure I.6.1.

Traditionally, nuclear reactors are classified based on neutron energy and the type of coolant/moderator. As mentioned in Section 3 and discussed in Chapter VIe, high-energy neutrons are referred to as fast and low energy neutrons are referred to as thermal neutrons. Reactors using high-energy neutrons for fission are referred to as fast reactors. Most commercial reactors are of the thermal type. Thermal reactors in addition to the coolant, as working fluid, also require moderator to thermalize neutrons. In most cases however, the coolant also plays the role of the moderator. There are generally three types of coolants used worldwide in power producing nuclear reactors: water, liquid metal, and gases such as helium. Water-cooled reactors are subdivided into light water (H₂O) and heavy water (D₂O) reactors, which use deuterium, an isotope of hydrogen.

All U.S. nuclear plants for power production are of the light water type being either a PWR or a BWR. In BWRs water boils inside the reactor vessel at a pressure of about 1050 psia (7.2 MPa), while in PWRs pressure is raised to about 2250 psia (15.5 MPa) to prevent water from boiling in the reactor. In PWRs, boiling takes place in the secondary side of the steam generator.

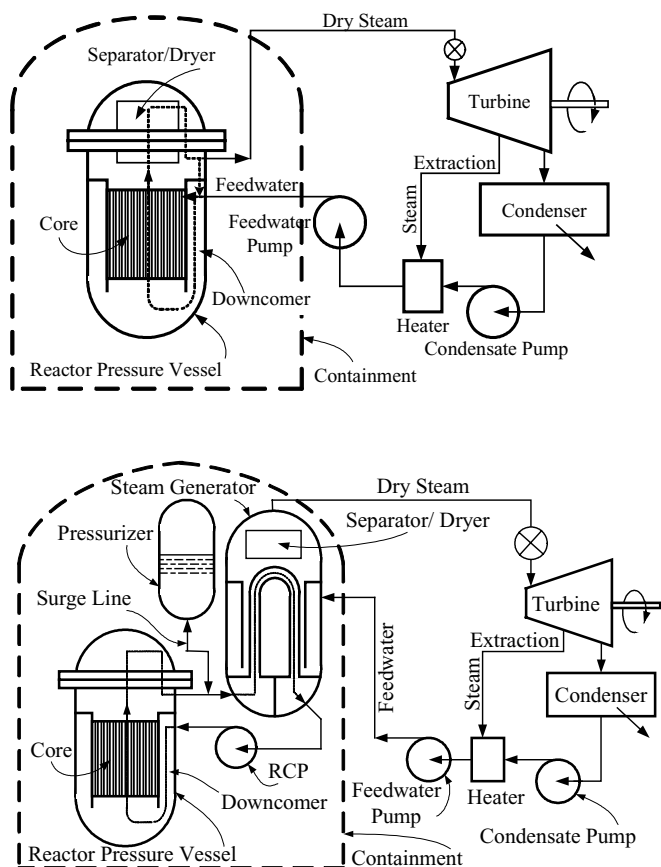


Figure I.6.1. Schematics of a BWR (*above*) and a PWR (*below*) plant

Gas cooled reactors (GCR) and advanced gas cooled reactors (AGR) use helium as the working fluid to reach high temperatures. GCRs are mostly used in England. For these types of reactors large compressors are required to circulate the coolant. Finally, a liquid metal fast breeder reactor (LMFBR) uses sodium as coolant.

6.1. Boiling Water Reactor

Since water boils in the *core* of a BWR, these types of reactors are known as direct-cycle power plants. The mixture of water and steam leaves the reactor core and enters the *separator-dryer* assembly to separate moisture from steam. As discussed in Chapter IIb, it is essential to deliver dry steam to the turbine. While dry steam enters the steam line and flows towards the turbine, the separated water at a temperature of about 550 F (288 C) flows downward towards the *downcomer* region of the reactor pressure vessel (RPV). The downcomer is an annulus between the RPV wall and the core barrel. The feedwater flow, delivered to the RPV by the main feedwater pumps also enters the downcomer but at about 375 F (190 C). These streams must mix well prior to entering the core. This task in the traditional BWR (designed by General Electric) is accomplished by two recirculation loops, each consisting of a recirculation pump, piping, and valves as shown in Figure I.6.2. The recirculation pumps withdraw water from the lower portion of the downcomer region and deliver to the inlet of up to 20 *jet pumps*. Jet pumps are made of stainless steel and consist of a suction inlet, throat (mixing section), and a diffuser. For plants operating at 1000 psia (7.2 MPa), the recirculation flow at a temperature of 545 F (285 C) then enters the *lower plenum* region of the RPV.

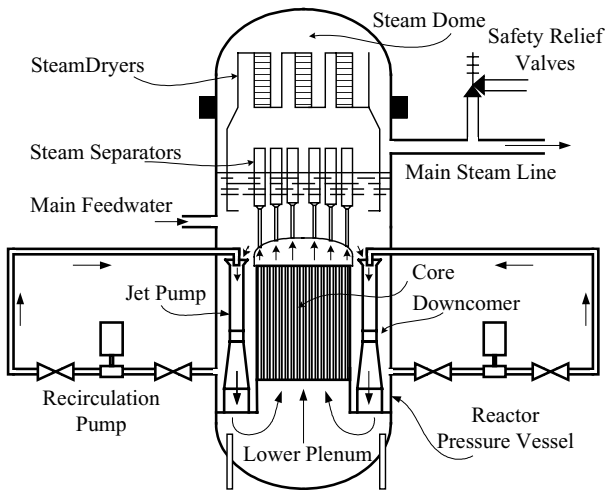


Figure I.6.2. A BWR reactor vessel

In the advanced BWR plants (ABWR, designed by Toshiba), the recirculation loops are eliminated. The recirculation in these plants takes place inside the RPV. Thus, the recirculation pumps and the jet pumps are combined and replaced by up to 10 *internal pumps* equipped with a motor (placed outside the RPV) and an impeller for forced mixing (placed in the downcomer). The recirculation pumps in BWRs and the reactor internal pumps in ABWRs play an important role in controlling the reactor power.

The well-mixed coolant entering the lower plenum flows upward into the core to remove heat from nuclear fission taking place in the fuel rods. The fuel rods are placed in square arrays of 8×8 , 9×9 , or 10×10 in a rectangular parallelepiped metal container referred to as fuel assembly or fuel bundle. The number of fuel bundles depends on the reactor power and may range from about 550 (for 800 MWe plants) to 870 (for 1350 MWe plants). Coolant, which at the core exit is a mixture of steam and water, leaves the fuel bundles and enters the upper plenum. From the upper plenum, coolant enters standpipes and is directed into the steam separator and steam dryer, as discussed earlier. The steam line leading to the turbine is equipped with safety and relief valves (SRV) as well as a main steam isolation valve (MSIV).

6.2. Pressurized Water Reactor

Unlike BWRs, no bulk boiling occurs in the core of a PWR; rather, boiling takes place in the secondary side of the steam generator (SG). Due to the presence of steam generators, PWRs are not direct-cycle power plants as they consist of a *primary side* and a *secondary side*. There is no mixing between the fluids flowing in each side, heat is transferred through the steam generator tube wall from the primary- to the secondary side. To prevent coolant from boiling in the primary side, pressure in a PWR vessel is more than twice that of a BWR (about 2250 psia, 15.5 MPa). Also, unlike BWRs, PWRs have an open core where flow can also move laterally between the fuel assemblies. There are generally over 200 fuel assemblies in the core of a PWR, each consisting of a square array of 15×15 fuel rods. The operating PWRs in the U.S. are of three designs: W (Westinghouse), CE (Combustion Engineering), and B&W (Babcock & Wilcox)³. The major differences are in the number and the type of the steam generators, as shown in Figure I.6.3.

The piping connecting the reactor vessel to the steam generator is referred to as *legs*. Pipes carrying water from the SG to the reactor vessel and from the reactor vessel to the SG are known as *Cold Leg* and *Hot Leg*, respectively. A pressure and inventory control tank, known as the *Pressurizer*, is connected to the hot leg through a *surge line*. The reactor coolant pumps (RCP) in the primary side of a PWR plant are located on the cold leg.

Shown in Figure I.6.4 is a two-loop PWR power plant. As seen in this figure, the outlet plenum of the steam generators is located on the suction of the reactor coolant pumps, delivering water through the cold leg to the downcomer region of the reactor vessel. Water then enters the lower plenum and flows to the core. Details of the reactor vessel are shown in Figure I.6.5(a). A small fraction of the coolant bypasses the core to cool the control rods. Water entering the core is at a temperature of about 550 F (288 C) and water leaving the core is about 600 F (316 C). The region on top of the core is referred to as the *core outlet plenum*. Water entering the outlet plenum from the core then flows towards the upper in-

³ CE is now owned by BNFL (Westinghouse) and B&W by Framatome ANP.

ternals of the *upper guide structure* (UGS) and leaves the vessel through the hot leg to the inlet plenum of the steam generator. In the steam generator primary side, water from the inlet plenum moves upward toward the *tubesheet* and into the U-tubes. Hot water exchanges heat with the colder water in the secondary side, through the steam generator tube wall, and enters the outlet plenum of the steam generator to be pumped back to the reactor vessel.

Details of the secondary side of a U-tube steam generator are shown in Figure I.6.5(b). In the secondary side, the main feedwater pump delivers water to the downcomer at a relatively cold temperature of about 430 F (221 C). The colder feedwater is then mixed with the warmer water, which is at a temperature on the order of 530 F (277 C) and flowing downward from the separator-dryer assembly of the steam generator. The mixed stream flows downward toward the tubesheet and then upward when entering the tube bundle. The heat of the water transferred through the tube causes this mixed stream to boil. The two-phase mixture eventually leaves the top of the U-tubes and wet steam enters the separator assembly. Swirling vanes are installed in these assemblies to separate the entrained water droplets by centrifugal force. Steam then enters the dryer assembly to further reduce the moisture content. The dry steam then leaves the dryer assembly and enters the steam line to flow to the high-pressure stage of a steam turbine.

Similar to the BWR plants, the main steam lines in the PWR plants, connecting the steam generator to the turbine, are equipped with a series of valves including SRV, a steam dump valve, and a MSIV.

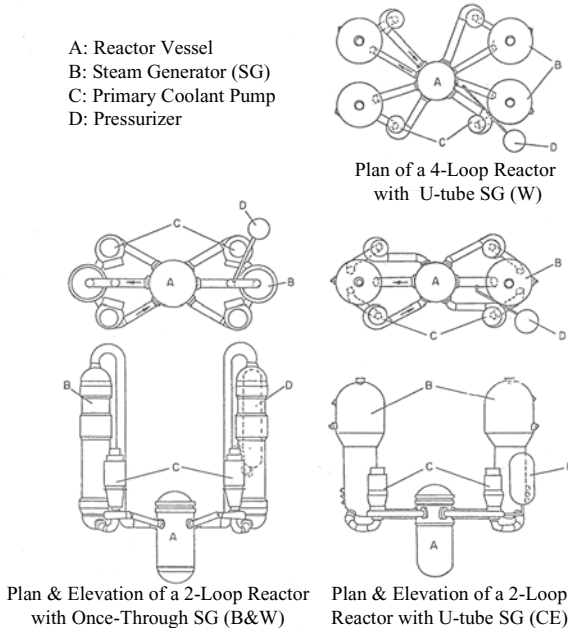


Figure I.6.3. Various classic U.S. designs of the operating PWRs (Todreas)

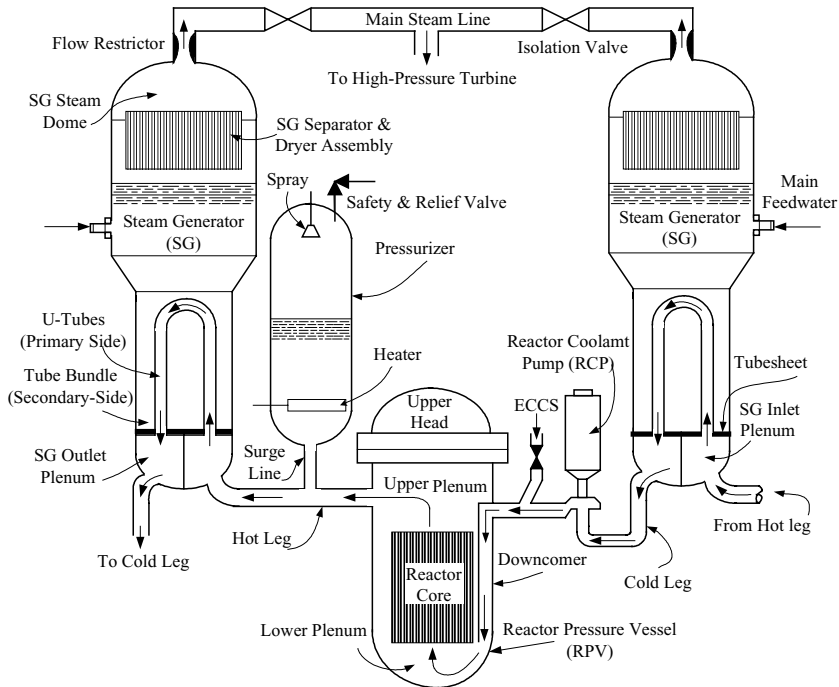


Figure I.6.4. Schematic of the RCS of a pressurized water reactor, using U-tube steam generators

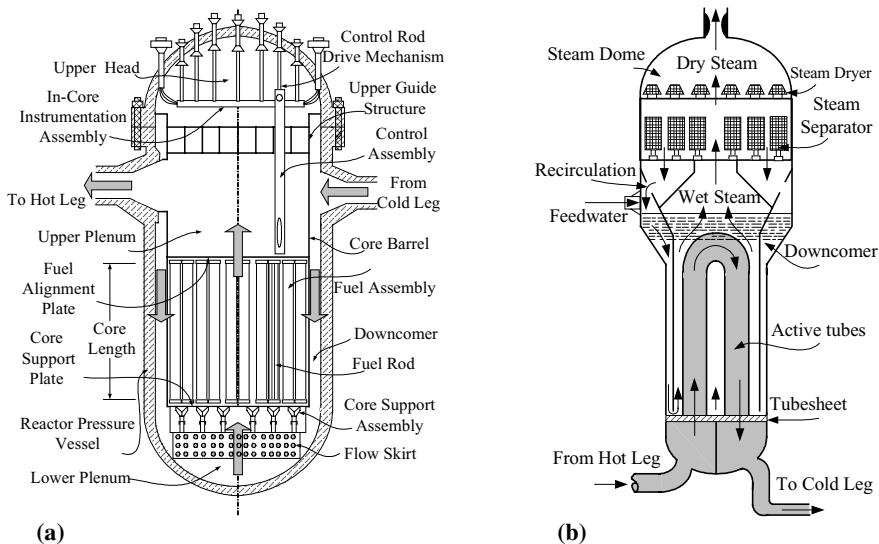


Figure I.6.5. Details of a PWR vessel (a) a PWR U-tube steam generator (b)

Fuel rods are thin hollow cylinders that are filled with uranium dioxide (UO_2) pellets. The hollow cylinder is referred to as cladding. The cladding material depends on the type of the nuclear reactor. In a LMFBFR, the cladding is made of stainless steel while in LWRs, the cladding is generally made of an alloy of zirconium, known as *zircaloy*. The small *gap* between the fuel pellets and the inside of the cladding is filled with helium. During operation the fission gases that are released from the pellet also enter the gap region.

Steam turbines are the power producing machines of systems using a thermodynamic cycle. The shaft of a steam turbine turns the rotor of the electric generator. Steam turbines are also used as *prime movers* to power pumps. The stationary blades in the casing of steam turbine act as diffuser in directing the incoming steam to the blades of the rotor. As hot, energetic steam transfers its energy to the rotor, the diameter of the rotor increases to maintain the rate of momentum transfer. Figure I.6.6 shows the combined medium and low-pressure rotor and the double-flow low pressure rotor of a steam turbine

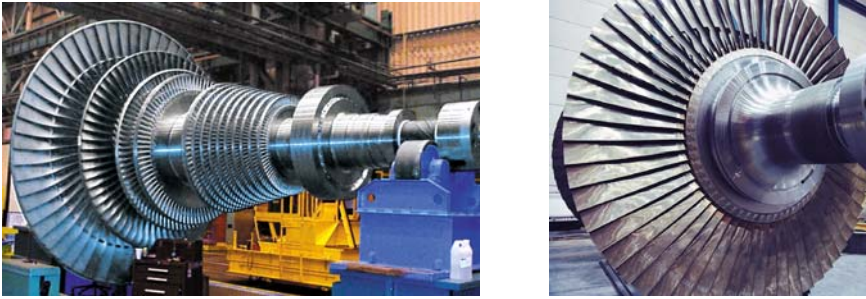


Figure I.6.6. Steam turbine rotor (courtesy Siemens AG)

7. Power Producing Systems, Greenpower Plants

The so-called greenpower or renewable energy sources consist of a wide range of sources including hydro, solar, geothermal, wind, and tidal. These sources of energy are briefly discussed next.

7.1. Hydropower Plants

After wood, falling water is the oldest source of energy. Romans used water wheels, to harness power. The first U.S. hydropower plant, built on the Fox River near Appleton, Wisconsin, generated electricity in 1882.

Figure I.7.1 shows the schematic of a hydropower plant including the turbine generator. The lake water, referred to as the head water, flows through a conduit known as the penstock towards the turbine. After turning the turbine runner, water flows in the draft tube to become the tail water to flow in the river, downstream of the turbine. As described in Chapter VIc, the turbine runner may be of *Kaplan*,

Francis, or *Pelton* type, which then turns the shaft of the electric generator. Shown in Table I.7.1 are the top 16 hydroelectric plants with respect to power production. By the late 20th century, hydroelectric produced about 25% of the global electricity and 5% of the total world energy, about 2,044 billion kilowatt-hours. The disadvantage of hydropower plants includes a large initial investment and a need for large bodies of water, with adverse effect on the river's ecological system and susceptibility to unfavorable weather conditions such as drought. Hydropower plants can be classified in terms of water flow rate and the difference between the elevations of water surface and the turbine. As discussed in Chapter III, this height is referred to as *Head*.

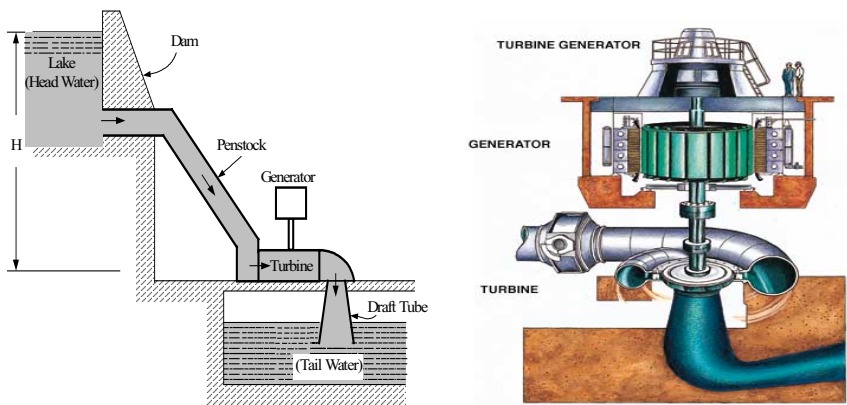


Figure I.7.1. Schematic of a hydropower plant to convert potential energy to electric power

Table I.7.1. Power output (MWe) of the world's largest hydropower plants

Name of Dam	Location	Present	Ultimate	Year operational
Itaipu	Brazil/Paraguay	12,600	14,000	1983
Guri	Venezuela	10,000	10,000	1941
Grand Coulee	U.S.A.	6,494	6,494	1967
Sayano-Shushensk	Russia	6,400	6,400	1989
Krasnoyarsk	Russia	6,000	6,096	1968
Churchill Falls	Canada	5,428	5,428	1971
La Grande 2	Canada	5,328	5,328	1979
Bratsk	Russia	4,500	4,600	1961
Moxoto	Brazil	4,328	4,328	1974
Ust-Ilim	Russia	4,320	4,320	1977
Volga	Russia	2,543	2,560	1958
Niagara	U.S.A.	2,190	2,400	1961
Volga	Russia	2,100	2,300	1955
Aswan	Egypt	1,750	2,100	1967
Chief Joseph	U.S.A.	1,024	1,950	1961
St. Lawrence	Canada – U.S.A.	1,880	1,880	1958

The Three Gorges Dam in China, 60 stories high and 2.3 kilometer long, will be the world largest dam. Upon completion in 2009, its 26 turbines will generate 18,200 MW electricity.

Low head and high flow rate are characteristics of rivers. For such condition, water is directed towards the turbine rotors known as the axial-flow turbines or *Kaplan rotor*. In this type, water flows between the vanes of the propeller and imparts its momentum to the rotor, which in turn is connected to the electric generator shaft. Figure I.7.2 shows an axial flow rotor.

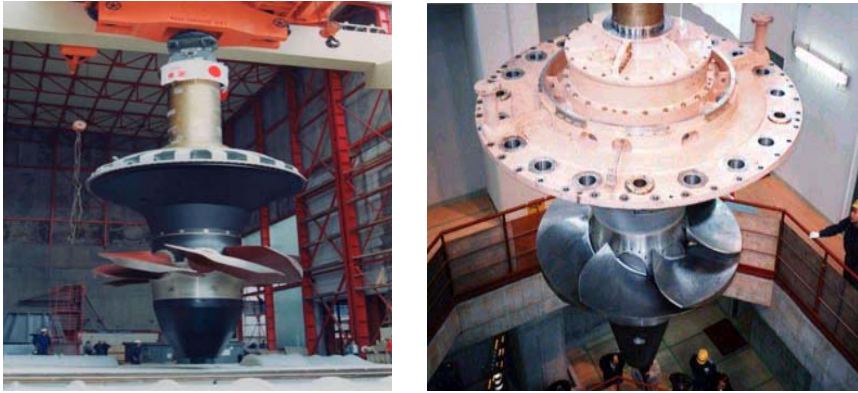


Figure I.7.2. Rotors of axial flow, Kaplan turbine (courtesy Toshiba Corporation)

High head and low flow are characteristics of water reservoirs on a mountain-top. The turbine used to harness the water power in such cases is generally of the impulse type using the *Pelton wheel* named after Lester Allen Pelton, who patented his wheel in 1889. As shown in Figure I.7.3, the Pelton wheel consists of buckets attached to the perimeter of a rotating wheel. Depending on the site, the wheel may be attached to a horizontal shaft or may be rotating horizontally connected to a vertical shaft. In this type of turbine, water is directed into injectors so that a jet of water strikes the bucket at high speed to turn the wheel. There may be one or as many as six injectors directing water towards the buckets of the wheel. The speed of the jet of water may reach values as high as 560 ft/s (171 m/s). A needle valve throttles the flow in the injectors. The wheel is placed in a casing for safety and to prevent water splashing. The principles of impulse turbines using the Pelton wheel are discussed in Chapter VIc.



Figure I.7.3. Pelton wheels of impulse turbines

Medium head, turbines are also of reaction type. Such turbines use the Francis runner, as shown in Figure I.7.4. Water enters from the side, flows between the vanes of the runner, and exits through the center.



Figure I.7.4. Runners of radial flow turbines, Francis turbine (courtesy Toshiba Corporation.)

7.2. Solar Power Plants

Solar energy, in the form of electromagnetic radiation that reaches the earth, by far surpasses all other sources of energy in magnitude. However, large scale power production by direct conversion of solar radiation to electricity by photovoltaic is still in the research and development stage. Solar collectors are now used as a residential heat source and for commercial applications such as space heating, and to a lesser extent for the generation of electricity. Large-scale power production by the use of solar collectors presently requires acres of land covered by special reflectors to divert the sun's ray to a central receiver, acting as a heat source.

Shown in Figure I.7.5 is the schematic of a thermal system for space heating using solar energy. Water is circulated in a closed flow loop. The heat source for this loop is the solar collector, heating water through the tube wall, which carries the circulating water. The heat sink is a water storage tank, which is also heated by an auxiliary heat source in cloudy weather and at night. The heat sink for the solar loop acts as a heat source for the space being heated, as the tank water is circulated in a heating coil over which the colder air flows.

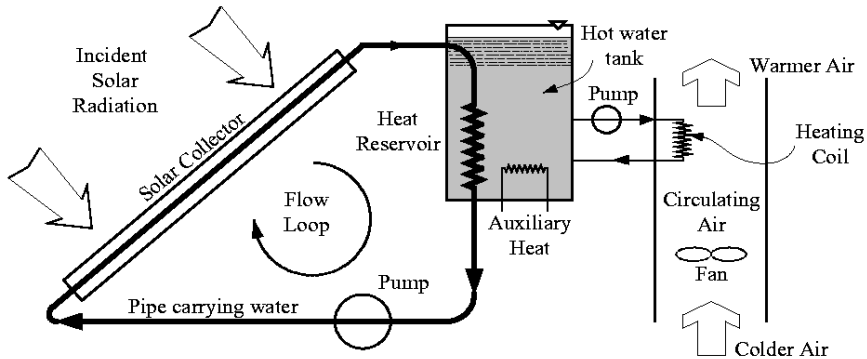


Figure I.7.5. Schematic of space heating by solar energy

7.3. Wind Turbines

Wind turbines convert wind kinetic energy into electricity. The principle of wind turbines is further discussed in Chapter VIc. Among the various types of wind turbines, the most popular is the 3-blade horizontal shaft turbine installed on a tower. The power produced by such turbines is in the range of 0.5 to 1.5 MW. Due to the low density of air, wind turbines must sweep a wide area to produce sufficient torque. One of North America's largest wind turbines produces 1.8 MW of electricity at 29 rpm. This turbine uses 39 m (128 ft) long blades installed on a 78 m (256 ft) high tower. Examples of three-blade horizontal-shaft wind turbines are shown in Figure I.7.6. Other types of such turbines include the vertical axis wind turbine. This machine resembles a giant eggbeater and was patented by George Darrieus in 1931. The advantage of the Darrieus turbine is that there is no need for a yaw mechanism to direct the blades towards the wind and the gearbox is closer to the ground hence, providing easier accessibility.



Figure I.7.6. Horizontal shaft wind turbine

7.4. Tidal Power

Power plants for harnessing tidal power are similar to hydroelectric plants, but are in the sea instead of in a river beds. The motive power comes from the fact that the moon's gravitational effect results in daily high and low tides. The daily surge of water passes through hydroturbines. The first tidal power plant, generating over 300 MWe, was built on the Rance River in France to harness the tidal power of the English channel (Marion). From low to high tide, water rises as much as 44 ft (13.4 m). The plant operates by opening the gates as tide rises to let the channel water enter the Rance River Dam. The gates are then closed at high tide. The trapped water is allowed to flow back to the English Channel at low tide through as many as 24 hydroelectric turbines each producing about 13 MWe. The total energy from tidal power worldwide is estimated at about 2 GWe

7.5. Geothermal Power

The earth's core, due to the formation of the solar system some 4.5 billion years ago, is extremely hot. Indeed at a depth of 40 km, temperature reaches as high as 1000 C. Earth's cross section is shown in Figure I.7.7(a). It is estimated that $7\text{E}11\text{ m}^3$ of superheated water (as defined in Chapter IIa) at 200 C exists beneath the earth's surface (Marion).

Geothermal energy relies on this heat source for power production. In the early part of the 20th century, the potential of geothermal energy for power was recognized. Larderello, the first geothermal power plant was developed in Italy's Tuscany in 1904. The Larderello plant now produces about 400 MWe. Several other countries such as Bolivia, Iceland, Japan, New Zealand, and the U.S. use geothermal energy for power production. In Reykjavik, Iceland, most houses are heated with pipes carrying hot volcanic water. In the United States, potential sites for geothermal energy are found mostly in the Western states such as California, Nevada, and Oregon. Figure I.7.7(b) shows that in 3 decades, power production from geothermal energy in the U.S. has increased by a factor of about 30. It is estimated that by 2010, power production from geothermal sources in the U.S. will reach 5–10 GWe. Unlike solar and wind, geothermal energy has a very high degree of availability hence; it is used as base load for power production. Indeed, the average availability for such plants exceeds 95% compared with about 70% for coal and 90% for nuclear plants. The negative aspects include a) unlike solar and wind, geothermal energy is not a 100% renewable source, as long-term use of such sites would result in steam production at lower pressures or eventual depletion of the source, b) production of such gases as hydrogen sulfide (H_2S), carbon dioxide (CO_2), and nitrogen oxide (NO_x), albeit these byproduct gases are produced in a much smaller scale compared to coal power plants, and c) the removal of underground steam and water can potentially cause the surface to subside. Despite these shortcomings, geothermal energy is indeed a very useful and clean source of energy, and with improving economical aspects it is expected to meet an increasing share of the world's energy needs.

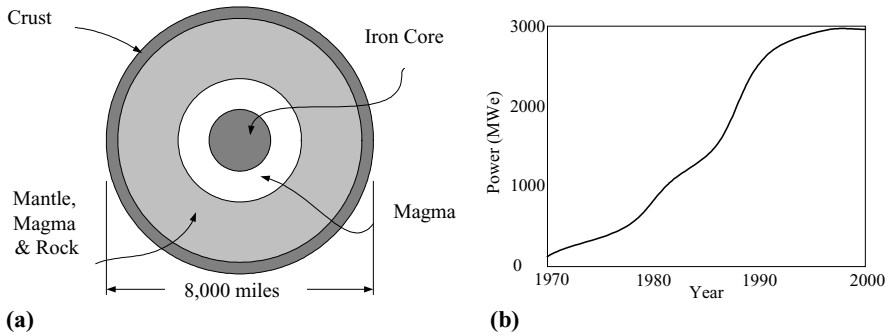


Figure 1.7.7. Depiction of: (a) Earth's cross-section; (b) growth of geothermal power in the U.S.

8. Comparison of Various Energy Sources

In Table I.8.1, we have divided the various sources of energy into three major categories as follows.

Carbon-based fuels. While this type of fuel has been the major source of energy for the past two centuries, it is coming under increasing scrutiny. This is because byproducts of carbon-based fuels include CO_2 as well as other gases, referred to as the *greenhouse gases*. Greenhouse gases in the upper atmosphere trap the sun's radiation and increase the retention of thermal energy, which otherwise would have been reflected back into space. Hence, these gases result in an increase in the earth's temperature. This phenomenon, known as the *greenhouse effect* is thought to be responsible for *global warming*.

Nuclear fuels. Nuclear-based energy is combustion free and there are therefore no emissions. However the operational safety and the safe disposal of nuclear waste remain a matter of public concern. The nuclear industry has made substantial improvement in operational safety. The new generation of reactors is designed to maximize safety and reliability by enhancing the passive safety features and reducing reliance on pumps, valves, and emergency diesel generators. Regarding nuclear waste disposal, nuclear plants store the spent fuel assemblies on-site in spent fuel pools, which in many plants have reached their maximum capacity. Nuclear plants in the U.S. have then started to store the oldest spent fuel assemblies in dry storage canisters, which are then housed on-site for passive cooling for eventual transfer to the federal repository at Yucca Mountain, Nevada.

Greenpower. The major problem associated with the renewable resources is low power density, defined as power produced per site area (MW/m^2).

Table I.8.1. Comparison of various sources of energy

Source		Advantage	Disadvantage
Carbon Based	Coal	Relatively easy to recover Established technology	Air pollution (mercury, sulfur dioxide, etc.) Contributor to acid rain and global warming Not easy to transport Acid runoff in coal mines
	Oil/ Gas	Easy to transport Established technology	Contributor to global warming Affected by geopolitical factors Expensive for energy generation Crude oil requires refinement for various use
Nuclear Based	Fission	No greenhouse or acid rain effects Compact waste Inexpensive fuel Concentrated base energy generation	Large capital cost due to regulatory requirements Long term storage of radioactive waste Potential for nuclear proliferation
	Fusion	Unlimited fuel source Low radiation level High energy output per unit mass Manageable waste	Technology for sustained fusion in development
Renew-able*	Hydro	Power source is free No greenhouse or acid rain effects	High water flow or head must be available Environmental damage if land is flooded Adverse effect on fish (salmon) population Large capital cost Susceptible to drought
	Solar	Power source is free No greenhouse or acid rain effects	Dependence on daytime clear weather Large land area for small energy generation Mirrors/panel may affect environment
	Wind	Power source is free No greenhouse or acid rain effects	Limited to suitable areas Needs expensive energy storage Noise pollution Adverse effect on birds Windstorms may damage the unit
	Tidal	Power source is free No greenhouse or acid rain effects	Low specific power Limited to suitable areas
	Geo-Therm.	Power source is free No greenhouse or acid rain effects	Associated with some CO ₂ , NO _x , and H ₂ S Economically not yet viable Not available/feasible everywhere

* Not shown in this table is the biomass energy source. Biomass includes the organic material, which convert the sunlight energy into chemical energy, which is then converted to heat when burned. Biomass fuels include such materials as wood, straw, ethanol, manure, sugar cane, and other byproducts from a variety of agricultural processes.

As Table I.8.1 shows, much research and development are needed to find an optimum solution to the issue of energy production. This is because on the one hand with an increasing world population and with energy being a major contributor in the advancement of society, one can expect that energy consumption would have only an upward trend. On the other hand, the environmental impacts associated with various sources of energy are testing the tolerance level of our planet. Regarding the greenhouse effect, while, the impact of CO₂ production on the global atmosphere is still a topic of debate and investigation, it is reasonable to conclude that the production of such gases should be limited. This would in turn limit the use of carbon-based fuels. We then face the problem of finding a suitable substitution to make up for the partial loss of power production from carbon-based energy sources. Our choice for this purpose is indeed limited, given the associated disadvantages of other sources of energy. Since fusion technology is seemingly remote, the two long term alternatives at the present time seem to be the fission reactors with enhanced safety features and geothermal power.

8.1. Saving Energy by Enhancing Efficiencies

An important factor in meeting the energy demand is the application of technology in increasing efficiency at the three stages of production, transmission, and consumption. The electricity produced in most central power plants using steam turbines, is about 1/3 of the total energy consumed. The remaining 2/3 is wasted as rejected heat to the environment. The central stations using gas turbines may have efficiencies in excess of 45% mostly due to operation at higher gas temperatures compared with steam temperature. Voltage drop in transmission lines has been a topic of investigation to find materials, which pose less resistance to the flow of electricity. Superconducting materials have such ability but they must presently operate at very low temperatures. Finally, improvement of efficiency in such home appliances as refrigerators, hot water heaters, heat pumps, washers and dryers would help reduce demand for power.

9. Thermofluid Analysis of Systems

Design and operation of any power producing system must satisfy the imposed constraints such as cost, safety, performance, size, and environmental impact. Here we focus only on the thermofluid aspects. In Section 4 we introduced such systems as pump, turbine, reactor vessel, steam generator, condenser, internal combustion engine, nuclear power plant, wind turbine, etc. There are five fundamental equations for the analysis of all such systems. These five fundamental equations in thermofluid analysis are:

- conservation equation of mass,
- conservation equation of energy,
- conservation equation of momentum (also known as linear momentum),

- conservation equation of angular momentum,
- the second law of thermodynamic

These equations are shown in the hub of Figure I.9.1. However, before these equations are applied, we first need to determine what we mean by thermofluid analysis of a system. This in turn requires us to identify the variables that we call *design parameters* of a system.

We can divide the design parameters into several categories. For example, one category includes the system dimensions such as diameter, height, flow area, and volume. Another category deals with the thermodynamic aspects such as pressure, temperature, and density. A third category might include parameters related to hydrodynamics such as power, momentum, torque, force, acceleration, and velocity.

In any system analysis, some of the design parameters are given and we need to find some other parameters of interest. This is what we refer to as thermofluid analysis of a system.

To perform thermofluid analysis of a system, we must first determine the extent of the system. This is accomplished by using techniques known as *control volume* and *control mass* as described in Chapter IIa. Once the extent of the system is defined, we consider the process applied to the system to identify the appropriate set of equations to use.

Having determined the system, the involved process, and the specified set of input data, we must then ensure that the number of applicable fundamental equations is sufficient to uniquely determine the number of the design parameters, which are unknown. Also not all the five fundamental equations listed above are applicable to the analysis of a system. For example, if there is no rotational motion involved in the analysis, the conservation equation of angular momentum is not applicable. Even when all the five fundamental equations are applicable, still we may run into the problem of having more unknowns than equations. This problem is remedied (i.e., the number of equations are increased to become equal to the number of unknowns) by introducing additional equations known as the *constitutive equations*, shown as spokes in Figure I.9.1. This figure is one way to visualize the interrelation between the fundamental and the constitutive equations.

Application of the constitutive equations depends on the type of analysis. If the analysis involves heat transfer, temperature and the rate of heat transfer are related by a constitutive equation. This constitutive equation, as discussed in Chapter IV, depends on the mode of heat transfer involved in the process. For example, in conduction heat transfer, the related constitutive equation is known as *Fourier's law* of conduction. Similarly, in convection heat transfer, the related constitutive equation is known as *Newton's law of cooling* while, in radiation heat transfer, the related constitutive equation is known as the *Stefan-Boltzmann law*.

The constitutive equations in fluid mechanics, as discussed in Chapter III, are primarily the *Newton's law of viscosity* and the *Stokes hypothesis*. The constitutive equation in mass transfer is the *Fick's law of diffusion*. The set of constitutive equations that is most often used is the *equation of state* relating the thermodynamic variables of a system. These thermodynamic variables are known as properties, as discussed in Chapter IIa.

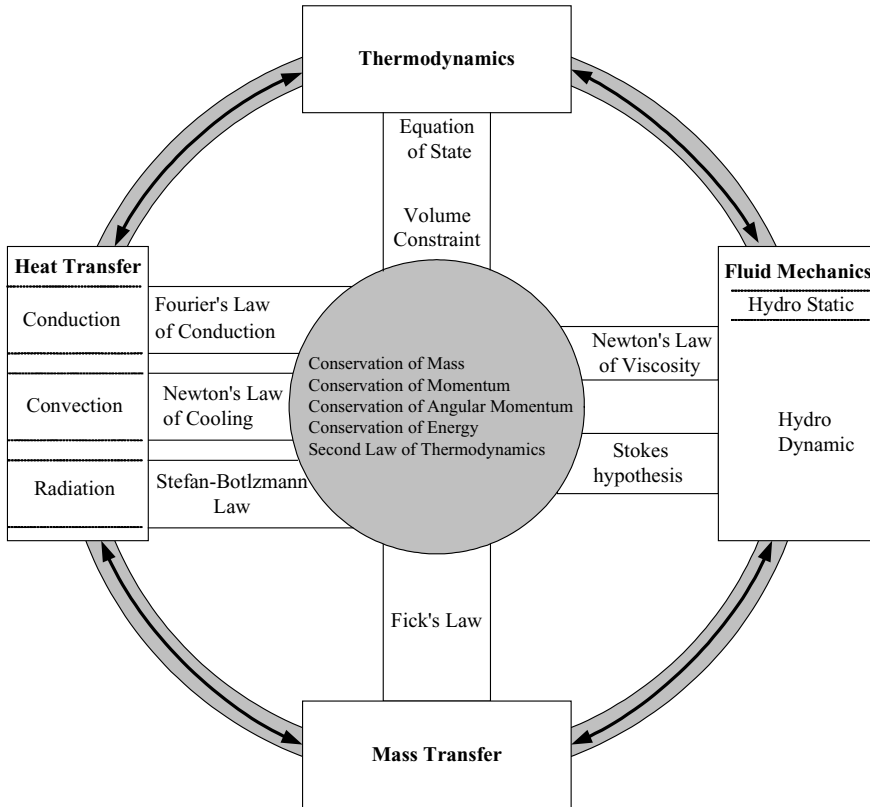


Figure I.9.1. Possible classification of the fundamental (*Hub*) and the constitutive (*Spoke*) equations in thermofluid analysis of systems

QUESTIONS

- What types of energy conversion take place in shoveling snow, rowing a canoe, and riding the elevator?
- What is the role of a transformer in the transmission of electricity through the power lines?
- How do you classify condensers, automotive radiators, and cooling towers?
- Is it true to say that the energy associated with fission is primarily due to the released radiation?
- What is the difference between fission and fusion?
- Are fossil power plants using coal for fuel, considered external or internal combustion machines?
- Why does the diameter of a steam turbine rotor increase as steam pressure decreases?
- Why is a nuclear reactor especially well suited for submarines?

- How does a gas turbine operate?
- What are the differences between turbofan, turboprop, and turboshaft?
- What is the key factor in favor of jet engines over internal combustion engines for aviation application?
- Name a disadvantage associated with hydropower plants?
- What are the disadvantages associated with wind power?
- What are the conservation equations? What do they conserve? Is the equation formulating the second law of thermodynamic a conservation equation?
- What is a constitutive equation? Why do we often need to use a constitutive equation?

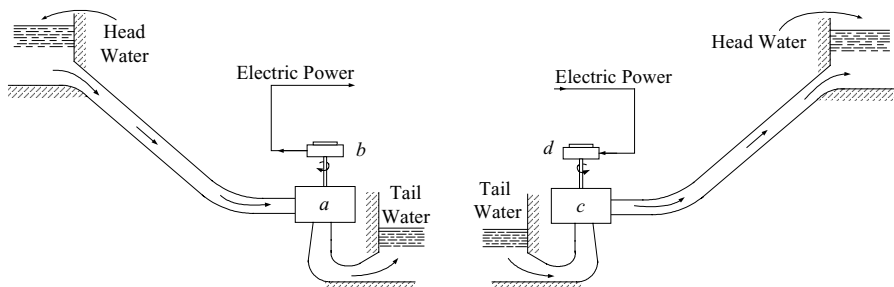
PROBLEMS

1. Match the upper case with the lower case letters that best describe the conversion of energy:

A. chemical – electrical, B. solar – electrical, C. electrical – thermal, D. nuclear – thermal, E. electrical – mechanical, F. chemical – mechanical, G. kinetic – thermal, H. potential – kinetic.

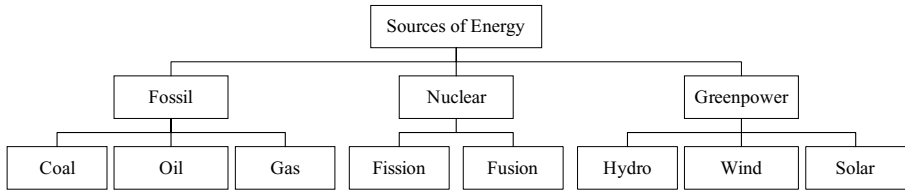
a. free fall, b. battery, c. plane crash, d. motor, e. solar calculator, f. heater, g. nuclear power plant, h. body muscles.

2. Use your knowledge of power production, power consumption, and energy conversion to find the names of the systems shown as *a* and *b* in the left hand and *c* and *d* in the right hand schematics. [Ans.: *a* is a hydraulic turbine].

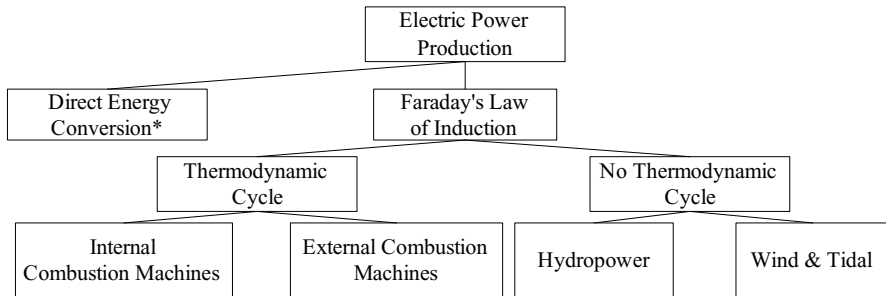


3. Explain the role of energy in water desalination and draw a diagram to represent the operation of such plant. First consider the goal and then try to find the means to accomplish your goal.

4. A simplified diagram of the three major energy sources and examples of each source of energy are shown below. Provide additional examples for sources of energy known as renewable sources or greenpower, and provide a brief description for each of the examples.

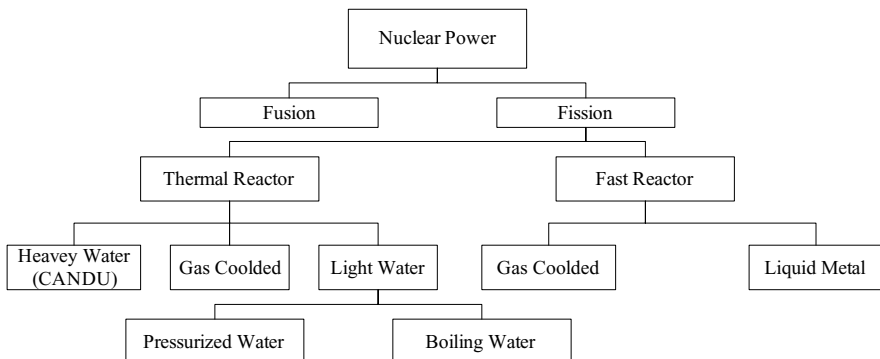


5. Principles of electrical energy production are shown in the simplified diagram. Provide a brief summary for each box comprising the thermodynamic cycle.



* Some direct energy conversion systems such as magnetohydrodynamics use the Faraday law of induction

6. A simplified diagram for nuclear power is shown below. Provide a brief description for each box comprising the light water reactor type.



7. A gas-cooled reactor uses a compressor to circulate helium as the working fluid, through the core of the reactor. The heated gas then enters a gas turbine to produce power. Helium is then cooled in the condenser and pumped back to the reactor. Another gas cooled plant uses a similar cycle but hot gases instead of entering a gas turbine enter a steam generator to boil water in the secondary side. The

cooler gas enters the compressor to be pumped back into the reactor and steam in the secondary side of the steam generator enters a steam turbine. Draw the flow path of the working fluid in each reactor type and describe the advantages and disadvantages of each design.

8. Use schematic diagrams to draw the flow path of both a BWR and a PWR. Explain the flow path in the reactor core for both types of reactors and the flow path in the steam generator of the PWR.

9. During normal operation of a PWR, feedwater enters the secondary side of the steam generator. After being heated by the hotter primary side water, feedwater boils in the tube bundle and dry steam leaves the steam generator and flows towards the turbine through the main steam line. In this condition, water level in the steam generator remains at a fixed level. Is it fair to say that the flow rate of steam out of the steam generator exactly matches the flow rate of the feedwater into the steam generator?

10. Describe the operation of a thermodynamic cycle. List and discuss the role of the various components of a thermodynamic cycle. Describe the operation of a Wankel engine in the framework of a thermodynamic cycle. In this regard, identify the heat source, the heat sink, and the working fluid in an internal combustion engine such as a Wankel rotary engine.

II. Thermodynamics

Thermodynamics, as the most fundamental subject in the field of thermal sciences, is simply defined as “the science that deals with matter, energy, and the laws governing their interactions^{*}”. Thermodynamics plays a vital role in the design and operation of power plants (fossil, nuclear, and solar), direct energy conversion (thermoelectric, thermionic, magnetohydrodynamic, and photovoltaic), heating and cooling systems (boilers, fan coolers, heat pumps, refrigerators, radiators, steam generators, and other heat exchangers), chemical plants (petrochemical refineries, water desalination, air separation, paper production, and pharmaceutical plants), bioengineering systems (lasers, life support systems, artificial heart, CAT scans), and various types of engines (automotive engines, ships, aviation gas turbines, and spacecrafts) among others. Such societal problems as energy shortages, air pollution, and waste management are better understood and remedied through the application of the laws of thermodynamics.

Historically, the development of classical thermodynamics began in late 18th century. In 1760 Joseph Black introduced the concepts of latent heat of fusion and evaporation. He also founded the *caloric theory*. In 1765 James Watt improved his steam engine through the use of an external condenser. However, it was not until the 19th century that the science of thermodynamics flourished. Below we summarize the important milestones in the development of this science in the past 200 years. The new terms and concepts mentioned in this summary are discussed later in this chapter.

- 1816, Robert Stirling patented the first engine using air as the working fluid.
- 1824, Carnot published his work on thermodynamic cycles and the second law of thermodynamics.
- Early 1840s, Julius Robert Mayer and James Prescott Joule introduced theories of the equivalency of heat and mechanical work.
- 1847, Helmholtz formulated the principle of conservation of energy and Emile Clapeyron expanded Carnot’s work
- 1848, William Thomson (Lord Kelvin) defined the absolute temperature scale based on the Carnot cycle.
- 1850, Rudolph Clausius introduced the concept of internal energy, distinguished the specific heat at constant volume from the specific heat at constant pressure, and clarified the distinction between the first and the second laws of thermodynamics.

^{*} Huang

- 1859, William Rankine who had been working towards the improvement of practical steam cycles, defined the thermodynamic efficiency of a heat engine, introduced the pressure-specific volume diagram, and published the first thermodynamics textbook.
- 1862, Nikolaus Otto introduced the Otto cycle for reciprocating internal combustion engines.
- 1865, Clausius defined the first law of thermodynamics as “the energy of the universe is constant” and the second law of thermodynamics, “the entropy of the universe tends toward a maximum”.
- 1875, Josiah Willard Gibbs developed the temperature-entropy diagram
- 1878, Gibbs published his work on thermodynamic equilibrium. Gibbs established the field of physical chemistry on the basis of thermodynamics and contributed much towards the establishment of the field of statistical thermodynamics¹.
- 1879, Gottlieb Daimler obtained a patent for a multi-cylinder engine operating on a common crankshaft.
- 1893, Rudolph Diesel introduced the diesel cycle working on the principle of compression stroke to obtain high temperatures for combustion.
- 1897, Max Planck stated the second law of thermodynamics.
- 1899, Karl Benz improved Daimler’s engine by introducing the controlled-timing electric ignition system.

In this book, the topic of thermodynamics is divided into three chapters. This chapter deals with the fundamentals of thermodynamics, the second chapter (IIb) discusses thermodynamic cycles for power production, and in the third chapter (IIc) the application of mixtures of non-reacting ideal gases is discussed.

Ila. Fundamentals

In the present chapter dealing with the fundamentals of thermodynamics, we introduce such basic concepts as a system and its surroundings, system properties, system processes, and possible direction of a process. We also explore the effect of the flow of mass and energy (in the form of heat and work) on a system. However, we first need to present the definition of these and other important terminologies as related to a thermodynamic substance and its related state. Subsequent to the definition of terms, we introduce the equations of state for two widely used working fluids: air and water. We then proceed with the definition of the three laws of thermodynamics. Examples are provided for both steady state and transient conditions using the conservation equations of mass and energy. Since these equations are dealt with in Chapter III, we use them in this chapter without further derivation.

¹ J. Willard Gibbs is also the founder of *Vector Analysis* (see Chapter VIIc).

1. Definition of Terms

1.1. Definitions Pertinent to Dimensions and Units

Dimensions are names applied to such physical quantities as length (L), mass (m), time (t), and temperature (T). These dimensions are known as the *primary dimensions**. We may also include the electric current (q) and the luminous intensity (I) as primary dimensions. All other physical quantities can be expressed in terms of these primary or fundamental dimensions. For example, velocity $V = x/t$, can be expressed as $[V] = Lt^{-1}$, density $\rho = m/V$ as $[\rho] = mL^{-3}$, force $F = ma$ as $[F] = mLt^{-2}$, pressure $P = F/A$ as $[P] = mL^{-1}t^{-2}$, etc. Symbols are placed inside brackets to signify the dimension of a physical quantity. It is of prime importance to ensure the dimensional validity of engineering formulae derived from the first principles. Hence, the dimensions of both sides of an equation must match. This is known as the *principle of dimensional homogeneity*.

Units are measures of a dimension and depend on the standard used for the unit system. There are two unit systems in use, the SI (short for its French expression, *Le Systeme Internationale d'Unites*) system of units and the English engineering system of units, referred to in this book as British Units, or BU for short. In the table below, units of the primary dimensions are expressed in both SI and BU. Other units can be derived from the basic units for such physical quantities as force, pressure, energy, power, etc. Force, for example has a derived unit that, according to Newton's second law of motion, is related to mass and acceleration so that $F \propto ma$. The derived unit for force in the SI system of units is $\text{kg}\cdot\text{m}/\text{s}^2$. In this system, force is expressed in Newton (N). Hence, one Newton, is the amount of force that would accelerate a mass of 1 kg at a rate of $1 \text{ m}/\text{s}^2$. If we now introduce a proportionality factor shown by g_c , then Newton's second law can be written as:

$$F = ma/g_c$$

Physical Quantity	Basic SI Unit	SI Symbol	Basic BU	BU Symbol
Length	Meter	m	Foot	ft
Mass	Kilogram	kg	Pound	lbm
Time	Second	s	Second	s
Temperature	Degree Kelvin	K	Degree Rankine	R

It is clear that g_c has a value of unity and units of $[g_c] = \text{kg}\cdot\text{m}/(\text{N}\cdot\text{s}^2)$. Force may also be expressed in terms of kilogram force, (kgf) which is the amount of force that would accelerate a mass of 1 kg at a rate of $9.8 \text{ m}/\text{s}^2$. To prevent confusion, the symbol for mass is also shown as kgm, which stands for Kilogram mass.

In British Units, the symbol of force is pound force (lbf), accelerating a mass of 1 slug at a rate of $1 \text{ ft}/\text{s}^2$. The most frequently used unit for mass is pound mass

* Also see Appendix I where physical quantities are expressed in both mass, length, and time (*MLT*) and force, length, and time (*FLT*) systems.

(lbm), which is accelerated at a rate of 32.1740 ft/s^2 by a force having the magnitude of one pound force. In British Units, g_c has a value of 32.174 (usually used as 32.2) and units of $[g_c] = \text{lbm} \cdot \text{ft} / \text{lbf} \cdot \text{s}^2$.

$$g_c = 1 \text{ kg} \cdot \text{m} / \text{N} \cdot \text{s}^2 \quad g_c = 32.2 \text{ lbm} \cdot \text{ft} / \text{lbf} \cdot \text{s}^2 \quad g_c = 1 \text{ slug} \cdot \text{ft} / \text{lbf} \cdot \text{s}^2$$

Derived units of some physical quantities are shown below.

Physical Quantity	Basic SI Unit	SI Symbol	Basic BU	BU Symbol
Force	Newton	N	Pound Force	lbf
Pressure	Pascal (N/m^2)	Pa	Pressure (lbf/in^2)	psi
Energy	Joule ($\text{N} \cdot \text{m}$)	J	Btu*	Btu
Power	Watt (J/s)	W	Btu/h	Btu/h

* Btu stands for British thermal unit

Example IIa.1.1. A substance has a mass equal to 2 lbm. Find the weight of this substance on the earth's surface and on a planet having $g_{\text{planet}} = \frac{1}{2} g_{\text{Earth}}$.

Solution: By definition, if a substance having mass m is exposed to the gravitational acceleration g , the resulting force is the weight of the mass given by $W = mg/g_c$. On earth, $g_{\text{Earth}} = 32.2 \text{ ft/s}^2$ hence, $W_{\text{Earth}} = 2 \times (32.2/32.2) = 2 \text{ lbf}$. On a planet with $g_{\text{planet}} = 32.2/2 = 16.1 \text{ ft/s}^2$, the weight of the substance is: $W_{\text{planet}} = 2 \times (16.1/32.2) = 1 \text{ lbf}$.

In British units, work is the result of force (lbf), multiplied by distance (ft), to obtain units of $\text{ft} \cdot \text{lbf}$. Heat, on the other hand, is generally expressed in terms of Btu. The conversion factor from $\text{ft} \cdot \text{lbf}$ to Btu is given as $1 \text{ Btu} = 778.16 \text{ ft} \cdot \text{lbf}$ (usually used as 778).

1.2. Definitions Pertinent to a Substance

Pure substance is a homogeneous substance with the same chemical composition in various phases, as defined below. Water, for example, is a pure substance as it has the same chemical composition whether in the form of steam, ice, or liquid water. Air, on the other hand, being a mixture of various gases, is not a pure substance, as in very low temperatures various components would condense at different temperatures resulting in a different chemical composition in the liquid phase.

Phase is a quantity of a pure substance that is homogeneous throughout the substance and is in the form of solid, liquid, or vapor.

Fluid is a term applied to either the liquid or the vapor phase of a pure substance. The *working fluid* is any fluid for which we are studying the thermodynamic behavior during a transformation.

System in a thermodynamic sense, refers to an entity being studied. This entity may be a pure substance such as a lump of matter, a small cylinder containing a mixture of gases, a large pipeline, or an entire power plant. The entity does not

necessarily require possessing any matter. Thus, vacuum may also constitute a thermodynamic system. The role of a system in thermodynamics is similar to the role of a free body diagram in solid mechanics, which is used to study the forces acting on a body. More specific definition for a system is given in Section 4 of this chapter.

Surroundings is anything external to a thermodynamic system. For example, if a system consists of a gas contained in a container, the rest of the universe is considered the surroundings for this system.

Boundary separates a system from its surroundings. The boundary is also known as the *control surface*.

Property such as color, pressure, temperature, density, energy, etc. is an observable characteristic of a system. As is discussed in Section 4, *heat* and *work* are not properties of a system.

Equilibrium is an important concept in thermodynamics. Systems in equilibrium do not experience any change with time. There are several types of equilibrium including thermal, mechanical, chemical, internal, and external. By thermal equilibrium we mean the temperature is the same throughout the system and is equal to the temperature of the surroundings, (which is everything external to the system). By mechanical equilibrium we mean that a system has no unbalanced force within it and the force it exerts on its boundary is balanced by an external force. By chemical equilibrium we mean that the chemical composition of a system remains unchanged. Internal equilibrium occurs in isolated systems and external equilibrium applies to systems that are in an internal equilibrium state and are also in equilibrium with their surroundings. A system is in equilibrium if pressure, temperature, and density are uniform throughout the system and do not change with time.

State. Properties of a system define the state of a system when the system is at equilibrium. For example, if certain amount of a gas at equilibrium is kept in a cylinder equipped with a piston, at pressure P_1 and temperature T_1 we refer to this condition as state 1. If, for whatever reason, the pressure and temperature of the gas are changed to P_2 and T_2 , then the state of the system is changed to state 2. Thus the state of a system changes when properties of a system change. Any change in the state is a deviation from equilibrium.

Gas, vapor, and steam. Gas is a state of matter having low density, low viscosity, high expansion, and compression ability in response to relatively small changes in pressure and temperature. Gases diffuse readily and have the ability to distribute uniformly throughout a system. Vapor is the gaseous state existing below the critical temperature (as defined in Section 1.5) of a substance that is liquid or solid in normal conditions. Steam is a special term applied only to the vapor phase of water.

1.3. Definitions Pertinent to Thermodynamic Processes

Process is applied to any transformation of a system between two equilibrium states; for the cylinder containing gas at state 1 (P_1 , T_1 , and volume V_1), compression of this gas by a piston to bring the gas to pressure P_2 , temperature T_2 , and volume V_2 is referred to as a process. A process is also known as a **Path**.

Isobaric is a process that takes place at constant pressure, such as boiling water in an open container.

Isothermal is a process that takes place at constant temperature. For example, steam condensation on the cold walls of a sauna.

Isochoric (also known as **isometric**) is a process that takes place at constant volume, such as heating a gas in a sealed rigid vessel. Other processes, such as *adiabatic*, *isentropic*, and *polytropic*, are defined in Section 4.

1.4. Definitions Pertinent to Properties of a Substance

We assume that fluid properties vary continuously (see definition of *continuum* in Chapter IIIa).

Pressure is the normal component of force per unit area exerted by a system on its boundary. The most often used pressure is referred to as absolute pressure. Zero pressure and atmospheric pressure (also known as Barometric pressure) are used as reference for absolute pressure (psia in BU). If absolute pressure is measured with respect to the atmospheric pressure, it is referred to as gage pressure (psig in BU). These are clarified in Figure IIa.1.1(a).

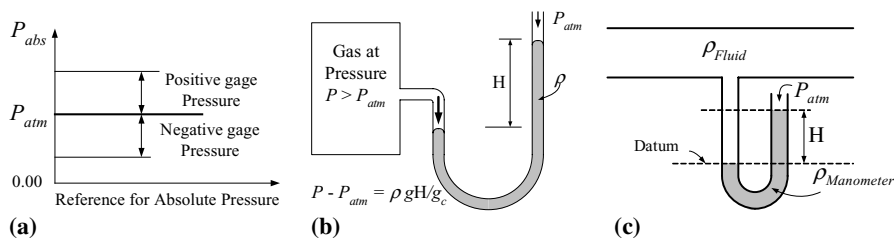


Figure IIa.1.1. (a) Absolute versus gage pressure; (b) manometer; (c) manometer with comparable densities

Manometric pressure is the pressure measured by a manometer, as shown in Figure IIa.1.1(b). In this figure ρ is the density of the manometer liquid, g is the gravitational acceleration, H is the difference in the liquid levels, and g_c is a conversion factor as described in Section 1.1. In Figure IIa.1.1(b), the density of the gas is considered negligible compared with the density of the manometer liquid.

Example IIa.1.2. Find the pressure, in N/m^2 (Pa) and in psia, at the depth of 50 m below the surface of a lake. Note that $1 \text{ atm} = 10.4 \text{ m-H}_2\text{O}$ ($\rho_{\text{Water}} = 1000 \text{ kg/m}^3$) = $14.7 \text{ psi} = 33.92 \text{ ft-H}_2\text{O} = 101.3 \text{ kPa}$.

Solution: At the depth of 50 m, the absolute pressure is $10.4 + 50 = 60.4 \text{ m H}_2\text{O}$. This is equivalent to: $P = \rho (g/g_c)h = 1000(9.8/1) \times 60.4 = 0.595\text{E}6 \text{ N/m}^2 \cong 0.595 \text{ MPa} = 0.5965\text{E}6/6,895 \cong 86 \text{ psia}$.

If the density of the fluid is comparable with the density of the manometer liquid, as shown in Figure IIa.1.1(c) then the fluid density needs to be accounted for. To find the fluid pressure, we perform a force balance with respect to the datum. Since surface areas are equal, they cancel out. The force on the left leg of the manometer is represented by $P_{\text{Fluid}} + \rho_{\text{Fluid}}gH$. This force is balanced by the force exerted in the right leg of the manometer represented as $P_{\text{atm}} + \rho_{\text{Manometer}}gH$. In equilibrium, these forces must be equal, hence:

$$P_{\text{Fluid}} = P_{\text{atm}} + (\rho_{\text{Manometer}} - \rho_{\text{Fluid}})gH$$

Shown in Figure IIa.1.2 are various units for atmospheric pressure.

Fehler! Keine gültige Verknüpfung.

Standard Temperature & Pressure (STP)		
System	Temperature	Pressure
SI	273.15 K	101.325 kPa
Scientific	0.0 C	760 mm Hg
Natural gas	60 F	14.7 psia
Engineering	32 F	14.696 psia

(a)

(b)

Figure IIa.1.2. (a) Various units for atmospheric pressure; (b) commonly used values for standard P & T

Vapor pressure. For a given temperature, every liquid has a vapor pressure at which liquid begins to boil and is at equilibrium with its own vapor. If the liquid is at a pressure greater than its own vapor pressure then there is only evaporation at the interface between the liquid and its vapor. If the liquid pressure drops below its vapor pressure, bubbles form in the liquid. Water at 102 F (39 C) has a vapor pressure of 1 psia ($\sim 7 \text{ kPa}$). Similarly, water at 212 F (100 C) has a vapor pressure of 14.696 psia (101.3 kPa). Values of the standard atmospheric pressure in various units are shown in Figure IIa.1.2(a).

Temperature is a measure of coldness or hotness of a body and is expressed in either Fahrenheit (F) or Celsius (C). Both of these temperature scales are based on

the freezing (0 C and 32 F) and boiling points of water (100 C and 212 F at atmospheric pressure). In the Celsius scale, the range between the freezing and the melting point of water is divided into 100 units. The Fahrenheit and the Celsius scales are related as

$$\frac{F - 32}{180} = \frac{C}{100}$$

Since both of these temperature scales allow for negative temperatures, an absolute temperature that has only positive values is defined. Kelvin (K) and Rankine (R) are the absolute scales for the Celsius and the Fahrenheit temperature scales, respectively. The relations are:

$$K = C + 273.15 \text{ (Generally, 273 is used in practice)}$$

$$R = F + 459.67 \text{ (Generally, 460 is used in practice)}$$

Standard condition refers to a temperature of 0 C (273 K) and atmospheric pressure (760 mm of mercury, Hg). Since volume and density of gases are sensitive to relatively small changes in temperature and pressure, it is customary to reduce all gas volumes to standard conditions for purpose of comparison. Values for standard atmosphere pressure and temperature (STP) are shown in Table IIA.1.2(b).

Specific volume of a substance is the inverse of the density of that substance. Hence, specific volume ($v = V/m$) is the volume per unit mass of a substance and is expressed in units of ft³/lbm or m³/kg. Pressure (P), temperature (T), and specific volume (v) are properties of a substance. As discussed in Section 2, the property surface of a substance is constructed based on P - T - v .

Specific gravity (S_g) of a liquid is the ratio of the density of the liquid to the density of water (62.4 lbm/ft³ or 1000 kg/m³). Specific gravity of a gas is the ratio of the molecular weight of a gas to the molecular weight of air (28.97).

Specific heat is the amount of heat required to raise the temperature of a unit mass of a homogenous phase of a substance by one degree. If the process takes place with either volume or pressure kept constant, the term is respectively referred to as constant-volume (c_v) or constant-pressure (c_p) specific heat, as defined later in this section. Specific heat has units of kJ/kg·K or Btu/lbm·F.

Energy is the ability to lift a weight to a higher elevation. The term, *energy*, is in fact a combination of two Greek words meaning *capacity* and *work*. Energy is a system quantity that describes the thermodynamic state of the system. Energy may be transferred to or from the system. Energy is generally expressed in such units as Joule (J), kilojoules (kJ), British thermal unit (Btu), or the less frequently used foot-pound force (ft·lbf).

Kinetic energy (KE) of a system is the energy associated with the motion of a system relative to a frame of reference, which is usually the earth's surface². Con-

² The relation between kinetic energy and temperature of subatomic particles is discussed in Chapter VIe

sider a body of mass m initially at rest. If an applied force F acts to accelerate mass m , then according to Newton's second law $F = ma$ where a is the resulting acceleration and g_c is implicitly accounted for. If the applied force causes the body to move by dx in the direction of the applied force, then $Fdx = madx$. Substituting for both distance and acceleration in terms of velocity, $dx = Vdt$ and $a = dV/dt$ then $Fdx = mVdV$ where V is an average velocity. Integrating the resulting equation we find³:

$$KE = \int_0^L Fdx = m \int_0^V VdV = mV^2/2$$

Potential energy (PE) of a system is the energy associated with the position or configuration of the system in a potential field such as a gravitational or electromagnetic field. Consider mass m located at height Z with respect to a reference in a gravitational field having a gravitational acceleration g . Mass m then possesses a potential energy given as $PE = mgZ$. Units for potential and kinetic energies are the same as the units for energy.

Total energy (E) of a system is the summation of all the energies possessed by the system including potential, kinetic, and internal energies.

Internal energy (U) of a system is the total energy of the system minus the potential and the kinetic energies, $U = E - (KE + PE)$. The internal energy represents the energy on the microscopic level. As described by Reynolds, it consists of such energies as nuclear and molecular binding energies, molecular rotation, translation, and vibration, intermolecular weak and strong energies, mass equivalent energy, and such other microscopic energies associated with the nuclear and electron spin.

Enthalpy (H) of a system is defined as the summation of the internal energy (U) and pressure work (PV), as in $H = U + PV$. Enthalpy and internal energy have units of J or Btu. To avoid errors associated with unit conversion, we may write $H = U + cPV$ where $c = 1$ for H and U expressed in J, P in Pa, and V in m^3 . The value of c in British Units is $c = 144/778 = 0.185$ for U and H expressed in Btu, P in psia, and V in ft^3 .

Entropy (S) is a measure of the disorder of a system. The change in the entropy of a system is always greater, or at least equal, to the heat transfer to or from the system divided by the temperature of the system. Entropy has the units of J/K or Btu/R. Specific entropy ($s = S/m$) has units of kJ/kg·K or Btu/lbm·R = 4.1868 kJ/kg·K.

Specific heat (c_v). The specific heat of a substance at constant specific volume is defined as $c_v = (\partial u / \partial T)_v$, where u , the specific internal energy, is given as $u = U/m$.

³ The rotational kinetic energy is $KE = I\omega^2/2$ where I is the moment of inertia and ω is the angular velocity given as $\omega = 2\pi N$ with N representing revolution per second.

Specific heat (c_p). The specific heat of a substance at constant pressure is defined as $c_p = (\partial h / \partial T)_P$, where h , the specific enthalpy, is given as $h = H/m$.

1.5. Definitions Pertinent to Types of Properties

Thermodynamic properties are such quantities as pressure (P), density (ρ), temperature (T), enthalpy (H), entropy (S), specific heat (c_p and c_v), coefficient of thermal expansion (β), and bulk modulus (B).

Transport properties refer to such quantities as viscosity (μ) and turbulent diffusivity (\mathcal{E}) as discussed in Chapter IIIa, and thermal conductivity (k) as discussed in Chapter IVa.

Extensive and intensive properties are defined to distinguish properties that depend on the size of the system (extensive) from those that do not depend on the size of the system (intensive). Such system properties as volume (V), mass (m), momentum (mV), enthalpy (H), and entropy (S) are examples of extensive properties. Examples of intensive properties include temperature (T), pressure (P), density ($\rho = m/V$), specific volume ($v = V/m$), specific enthalpy ($h = H/m$) and specific entropy ($s = S/m$). These are summarized in Table IIa.1.1. The state of a substance is determined by two intensive properties. These could be pressure and temperature, pressure and specific internal energy, temperature and specific enthalpy, etc.

Table IIa.1.1. Examples of extensive and intensive properties

Property	Extensive (Y)	Intensive (y)
Mass	m	ρ
Volume	V	v
Momentum	mV	V
Kinetic energy	$\frac{1}{2} mV^2$	$\frac{1}{2} V^2$
Potential energy	mgZ	gZ
Internal energy	U	u
Total energy	E	e
Enthalpy	H	h
Entropy	S	s

Critical state of a substance is a state beyond which a liquid-vapor transformation is not possible. For water, the critical pressure is $P_c = 22$ MPa (3203.6 psia), and critical temperature is $T_c = 374.15$ C (705.47 F).

Critical properties. Pressure, temperature, and specific volume (P_c , T_c , v_c) of the critical state are referred to as critical properties. Using P_c and T_c for water, the critical volume for water is given as $v_c = 0.0505$ ft³/lbm.

Reduced properties refers to the ratios of pressure and temperature normalized to corresponding critical pressure and temperature, respectively ($P_R = P/P_c$ and $T_R = T/T_c$).

2. Equation of State for Ideal Gases

The state of a substance is a function of two independent intensive properties. Mathematically, a function of two variables represents a surface in rectangular coordinates. The functional relationship between various properties of a substance in terms of the two independent intensive properties is referred to as the equation of state. For example, if we choose the two independent intensive properties as pressure (P) and temperature (T) a relation that expresses specific volume in terms of these properties, such as $v = f(P, T)$, is an equation of state with P and T being the independent variables. In this section, the equation of state for ideal gases is discussed following the definition of some pertinent terms.

2.1. Definition of Terms

Atomic mass of elements is measured with respect to the mass of Carbon 12. We define an atomic mass unit as $1/12^{\text{th}}$ of the mass of the atom of C_6^{12} . This minute amount of mass is equal to $1.660438 \text{ E-}27 \text{ kg}$. Hence, the atomic mass of an element is the mass of an atom on a scale that assigns C_{12} a mass of exactly 12.

Molecular weight of a compound is the sum of the atomic weights of the atoms that constitute a molecule of the compound.

Gram-mole. A gram-mole (mol in the SI system) of a substance is the amount of that species whose mass in gram is numerically equal to its molecular weight. For example, carbon monoxide (CO) has a molecular weight of 12 (for Carbon) + 16 (for Oxygen) = 28. In general, if the molecular weight of a substance is M , then there are $M \text{ kg/kmol}$ or $M \text{ lbm/lb-mol}$ of this substance.

Example IIa.2.1. Find the number of moles in 80 kg of CO_2 .

Solutio: Since $M_{\text{CO}_2} = 12 + 2 \times 16 = 44$, then the number of CO_2 moles are $80/44 = 1.82 \text{ kmol CO}_2$.

2.2. Equation of State

All gases at sufficiently low pressures and high temperatures (hence, at low density) obey three rules: Boyle's, Charles', and Gay-Lussac's rules. These are called the *perfect gas* rules and such gases are known as *perfect* or *ideal* gases. While the perfect gas and ideal gas are used interchangeably, an ideal gas is a perfect gas with an additional feature of having constant specific heat. *Boyle's rule* specifies that in isothermal processes, $PV = \text{constant}$. *Charles' rule* specifies that in an iso-

baric process, $V/T = \text{constant}$. Finally, *Gay-Lussac's rule* specifies that in constant volume processes, $P/T = \text{constant}$.

From any two of the above rules we conclude that for a given mass of an ideal gas, $PV/T = \text{constant}$. In order to determine the constant, we take advantage of the *Avogadro's hypothesis*, which states that, at the same pressure and temperature, equal volumes of gases contain the same number of molecules. In other words, 22.4 liters of any gas at STP, contains 1 mole or 6.023×10^{23} molecules of that gas. This is known as the *molar volume*. From the Avogadro's hypothesis we may conclude that the constant, shown by R_u , is given as $R_u = P\bar{v}/T = (1 \text{ atm} \times 22.4 \text{ liter})/(1 \text{ mole} \times 273 \text{ K}) = 0.0821 \text{ atm} \cdot \text{liter} \cdot \text{K}^{-1} \cdot \text{mole}^{-1}$. In this relation, T is the absolute temperature, \bar{v} is specific volume on a molar basis, and R_u is known as the *universal gas constant* and its value can also be found in such units as:

$$\begin{aligned} R_u &= 8.314 \text{ kJ} \cdot \text{kmol}^{-1} \cdot \text{K}^{-1} & R_u &= 0.08314 \text{ bar} \cdot \text{m}^3 \cdot \text{kmol}^{-1} \cdot \text{K}^{-1} \\ R_u &= 1545 \text{ ft} \cdot \text{lbf} \cdot \text{R}^{-1} \cdot \text{lbmol}^{-1} & R_u &= 0.73 \text{ atm} \cdot \text{ft}^3 \cdot \text{lbmol}^{-1} \cdot \text{R}^{-1} \end{aligned}$$

The equation of state for an ideal gas, $P\bar{v} = R_u T$ can be written as $Pv = RT$ where $v = \bar{v}/M$ and $R = R_u/M$. Alternatively, we can write:

$$PV = nR_u T = m(R_u/M)T = mRT \quad \text{IIa.2.1}$$

where m is mass (kgm or lbm), M is molecular weight (kg/kgmol or lb/lbmol), n is the number of moles, and R is given as $R = R_u/M$ ($\text{kPa} \cdot \text{m}^3/\text{K} \cdot \text{kg}$ or $\text{ft} \cdot \text{lbf}/\text{R} \cdot \text{lbm}$). Note that unlike R_u , which is a universal constant, the value of R depends on a specific ideal gas. Also note that in Equation IIa.2.1, we made the following substitution:

$$n = m/M$$

That is to say that one mole (mol) of any substance has a mass equal to its molecular weight.

Example IIa.2.2. A 10 ft^3 (0.283 m^3) tank contains compressed air at a pressure of 350 psia (2.41 MPa) and temperature of 80 F (27 C). We want to determine the mass of air and moles of air in this tank. $M_{\text{air}} = 28.97$.

Solution: From the equation of state for ideal gases using the air molecular weight of 28.97 lb/lbmole:

$$\begin{aligned} m &= \frac{PV}{(R_u/M)T} = \frac{\text{BU} \quad (350 \times 144) \times 10}{(1545/28.97) \times (80 + 460)} = 17.5 \text{ lbm} = \\ &\quad \text{SI} \quad \frac{(2.41 \text{E}3) \times 0.283}{(8.314/28.97) \times (27 + 273)} = 7.92 \text{ kg} \end{aligned}$$

The number of moles is found from $n = 17.5/28.97 = 0.6 \text{ lbmol}$ or alternatively, $n = 7.92/28.97 = 0.27 \text{ kmol}$.

The advantage of the equation of state for an ideal gas is its simplicity. Although in texts on thermodynamics the Boyle, Charles, and Gay-Lussac rules are generally referred to as “laws”, they were introduced here as “rules” because their application is limited only to gases that can be approximated as ideal gas. We can approximate the behavior of real gases with that of an ideal gas only if the compressibility of the gas is near unity. The compressibility of a gas is defined as $Z = Pv/RT$. When $Z \approx 1$, the gas density is low enough to allow the treatment of the gas as an ideal gas. There have been several attempts to develop an equation of state for non-ideal or real gases ($Z \neq 1$). For example, Van der Waals in the 19th century proposed the following equation of state:

$$(P + \frac{c_1}{v^2})(v - c_2) = RT \quad \text{IIa.2.2}$$

where, c_1 and c_2 are functions of P_c and T_c . Note the Van der Waals equation reduces to the ideal gas equation for large values of specific volume (occurring at low pressures or high temperatures).

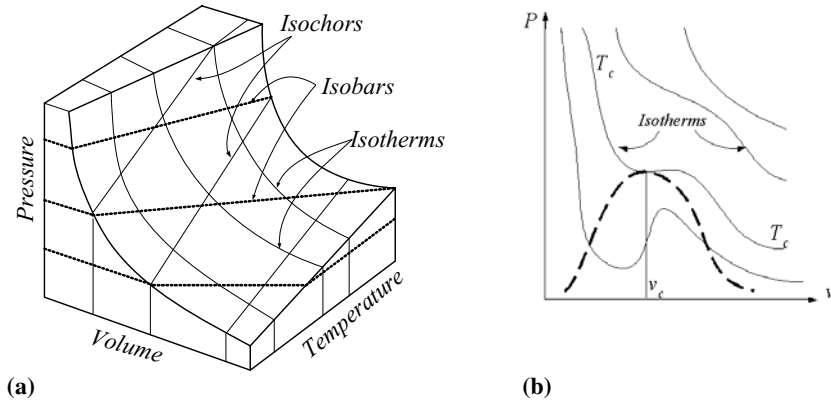


Figure IIa.2.1. Behavior of (a) an ideal gas and (b) a Van der Waals gas

To find the values of c_1 and c_2 in Equation IIa.2.2, we note that the isotherm passes through a point of inflection at the critical state hence, the first and the second derivatives of pressure with respect to specific volume at constant temperature are zero. These in addition to Equation IIa.2.2, provide three equations from which we can find $c_1 = 0.42R^2T_c^2 / P_c$, $c_2 = 0.125RT_c / P_c$ and $v_c = 0.375RT_c / P_c$. Having v_c , we can find Z from $Z = P_c v_c / (RT_c) = 0.375$.

The functional relationship between P , T , and v for the ideal gas and the Van der Waals gas are shown in Figure IIa.2.1. The Van der Waals equation, while an improvement over the ideal gas model, has limited applications. To correlate pressure, specific volume, and temperature, there have been many other equations of states since the introduction of the Van der Waals equation. Among these are Berthelot, Dieterici, and Redlich-Kwong (RK) equations. The Redlich-Kwong equation for example is an empirical correlation and is given as:

$$P = \frac{R_u T}{\bar{v} - c_2} - \frac{c_1}{\bar{v}(\bar{v} + c_2)T^{0.5}} \quad \text{IIa.2.3}$$

where $\bar{v} = Mv$ has units of ft^3/lbmol or m^3/kgmol . Constants c_1 , and c_2 in Equation IIa.2.3 are functions of the critical pressure and temperature and are given as $c_1 = 0.4275 R_u^2 T_c^{2.5} / P_c$ and $c_2 = 0.0867 R_u T_c / P_c$.

Example IIa.2.3. Use the Redlich-Kwong equation and find the pressure of superheated vapor given a specific volume of $2.7247 \text{ ft}^3/\text{lbm}$ ($0.17 \text{ m}^3/\text{kg}$) at 500 F (260 C).

Solution: For water we have $P_c = 3203.6 \text{ psia}$ and $T_c = 705 \text{ F}$. Therefore,
 $c_1 = 0.4275 [1545/(144 \times 14.7)]^2 (705 + 460)^{2.5} / (3203.6/14.7) = 48,422 \text{ atm}$
 $(\text{ft}^3/\text{lbmol})^2 \text{ R}^{0.5}$
 $c_2 = 0.0867 [1545/(144 \times 14.7)] (705 + 460) / (3203.6/14.7) = 0.338 \text{ ft}^3/\text{lbmol}$.
 $T = 500 + 460 = 960 \text{ R}$, $\bar{v} = 18 \times 2.7247 = 49.0446 \text{ ft}^3/\text{lbmol}$. Substituting in Equation IIa.2.3, we get:

$$P_{RK} = \frac{[1545/(14.7 \times 144)]960}{(49.0446 - 0.338)} - \frac{48,422}{49.0446(49.0446 + 0.338)\sqrt{960}} =$$

$$13.74 \text{ atm} = 201.9 \text{ psia} (1.39 \text{ MPa})$$

From the ideal gas model, we find $P_{IG} = [(1545/18) \times 960] / 2.7247 = 30242 \text{ lbf/ft}^2 = 210 \text{ psia}$ (1.44 MPa). The real answer is 200 psia . In this example, we do not expect to get good results from the ideal gas model, as pressure is not low enough and temperature is not high enough (try $P = 1 \text{ psia}$ and $T = 750 \text{ F}$).

It is seen from the above example that while the Redlich-Kwong model does a better job in predicting pressure, it still has an error of about 1%. To get even closer answers, more complex equations should be used. These include the Beattie-Bridgeman and the Benedict-Webb-Rubin equations.

2.3. Specific Heat of Ideal Gases

Joule showed that for ideal gases, the internal energy is only a function of temperature, $u = u(T)$. As such, for an ideal gas the partial derivative becomes a total derivative hence, we can write $du = c_v dT$. Similarly, for infinitesimal changes in enthalpy $dh = c_p dT$. By definition, enthalpy is related to internal energy as $dh = du + Pdv$. This relation can be applied to an ideal gas by substituting for the last term in the right-hand side from the equation of state, to get $dh = du + RdT$. Substituting for du and dh in terms of specific heats for an ideal gas yields:

$$c_p - c_v = R$$

Since R is constant and for an ideal gas c_v is only a function of temperature, c_p also becomes only a function of temperature. The specific heat ratio is defined as $\gamma = c_p/c_v$. Combining these two equations, we can solve for c_v and c_p in terms of R and γ :

$$c_v = \frac{R}{\gamma - 1}, \quad c_p = \frac{\gamma R}{\gamma - 1}$$

Note that c_v and c_p have the same units as R . These are kJ/kg·K, in SI or Btu/lbm·R, in British units.

Example IIa.2.4. Calculate c_v and γ of an ideal gas which has a molar mass of 16 and a $c_p = 2$ kJ/kg·K.

Solution: We first calculate R from $R = R_u/M$. Hence, $R = 8.314/16 = 0.519$ kJ/(kg·K). Having R and c_p , we can find $c_v = c_p - R$. Substituting, $c_v = 2 - 0.519 = 1.48$ kJ/kg·K. Having c_p and c_v , we find $\gamma = 2/1.48 = 1.35$.

Specific heat of ideal gases at constant pressure may be expressed in the form of a quadratic polynomial. For all practical purposes however, an average c_p and c_v may be used for most gases over the temperature range of interest.

Example IIa.2.5. We made a fit to data for c_p of air in the range of 360 R–2880 R and obtained:

$$(c_p)_{air} = 0.238534 - 6.20064 \times 10^{-6} T + 2.13043 \times 10^{-8} T^2 - 4.20247 \times 10^{-12} T^3$$

where temperature is in R and $(c_p)_{air}$ is in Btu/lbm·R. Find $(c_p)_{air}$ at $T = 80$ F according to the above fit.

Solution: At 80 F (540 R), specific heat of air at constant pressure according to the above equation becomes $(c_p)_{air} = 0.2421$ Btu/lbm·R. Compared with data in Table A.II.5(BU), the error is less than 1%.

Having c_v and c_p , we can calculate u and h by integrating $du = c_v dT$ and $dh = c_p dT$, respectively:

$$u(T_2) - u(T_1) = \int_{T_1}^{T_2} c_v(T) dT \quad \text{and} \quad h(T_2) - h(T_1) = \int_{T_1}^{T_2} c_p(T) dT$$

To simplify analysis, we may use an average value for c_v and c_p in the temperature range of interest:

$$c_v = \frac{\int_{T_1}^{T_2} c_v(T) dT}{T_2 - T_1} \approx \frac{c_v(T_1) + c_v(T_2)}{2} \quad \text{and} \quad c_p = \frac{\int_{T_1}^{T_2} c_p(T) dT}{T_2 - T_1} \approx \frac{c_p(T_1) + c_p(T_2)}{2}$$

where the arithmetic average applies to temperature ranges within which specific heat varies slightly. Having an average value for the specific heat we can calculate enthalpy, for example from:

$$h(T) - h(T_{ref.}) = c_p(T - T_{ref.})$$

Using $T_{ref.} = 0 \text{ R}$ (-460 F) and assuming $h(T_{ref.}) = 0$, then $h(T)$ can be written as $h(T) = c_p T$ where T is the absolute temperature in degrees Rankine.

3. Equation of State for Water

In this section, the equation of state for water is discussed following the definition of some pertinent terms.

3.1. Definition of Terms

Saturation temperature is the temperature at which boiling takes place at a given pressure.

Saturated liquid or vapor is a state of a substance at which change in phase takes place while the substance temperature remains constant. At saturation, the substance pressure is referred to as the *vapor pressure*. The vapor pressure is a function of temperature hence it remains constant during the phase change.

Subcooled or compressed liquid is a liquid phase of a substance, which exists at a temperature less than the saturation temperature corresponding to the substance pressure.

Superheated vapor is the vapor phase of a substance that exists at a temperature greater than the saturation temperature corresponding to the substance pressure.

Helmholtz function (a) is another thermodynamic property of a substance and is defined as $a = u - Ts$. The Helmholtz function has units of energy.

Gibbs function (g) is also a thermodynamic property of a substance and is defined as $g = h - Ts$. The Gibbs function has units of energy.

Maxwell relations are four well known thermodynamic equations written in terms of intensive properties. The Maxwell relations correlate temperature and entropy to other thermodynamic properties as follows:

$$Tds = du + Pdv \quad \text{IIa.3.1}$$

$$Tds = dh - vdP \quad \text{IIa.3.2}$$

$$sdT = -da - Pdv \quad \text{IIa.3.3}$$

$$sdT = -dg + vdP \quad \text{IIa.3.4}$$

where in these relations, a is the *Helmholtz function* (after Herman Ludwig von Helmholtz, 1821–1894) and g is the *Gibbs function* (after Josiah Willard Gibbs, 1839–1903). An example for the use of Maxwell's relations includes the calcula-

tion of entropy change of a system in terms of other thermodynamic properties. If we write Equation IIa.31 for an ideal gas as $Tds = c_v dT + RdT$ and then integrate it, we obtain the change in entropy for an ideal gas as:

$$s_2 - s_1 = R \ln \frac{v_2}{v_1} + \int_1^2 c_v \frac{dT}{T} \quad \text{IIa.3.5}$$

The specific heat of some gases, frequently used in common practice, are given in Table A.II.5. If the specific heat is taken as constant, the integral in Equation IIa.3.1 can be carried out to obtain:

$$s_2 - s_1 = R \ln \frac{v_2}{v_1} + c_v \ln \frac{T_2}{T_1} \quad \text{IIa.3.6}$$

We may apply Equation IIa.3.5 to an ideal gas and obtain a similar relation but in terms of pressure ratio.

Coefficient of volume expansivity (β) or thermal expansion coefficient is a measure of the change in specific volume with respect to temperature with pressure held constant. This coefficient is given as, $\beta = [(\partial v / \partial T)_P] / v = -[(\partial \rho / \partial T)_P] / \rho$. The coefficient of volume expansivity has the units of K^{-1} or R^{-1} .

Isothermal compressibility (κ) is a measure of change in specific volume with respect to pressure at constant temperature, $\kappa = -[(\partial v / \partial P)_T] / v$. It has the units of bar^{-1} or psi^{-1} . The minus sign is intended to maintain a positive value for κ regardless of the phase or the substance.

Isentropic compressibility (α) is a measure of change in specific volume with respect to pressure at constant entropy, $\alpha = -[(\partial v / \partial P)_S] / v$. It has the units of bar^{-1} or psi^{-1} . The minus sign is intended to maintain a positive value for κ regardless of the phase or the substance. Entropy is defined in Section 1.4.

3.2. Equation of State

Due to its availability and reasonably good physical properties, water is extensively used as a working fluid in practice. As such, water properties have been carefully measured, formulated, and tabulated. The tabulation of the thermodynamic properties of water is known as the steam tables, as presented in Tables A.II.1(SI) through A.II.4(SI) and A.II.1(BU) through A.II.4(BU) for SI and British units, respectively. Traditionally, thermodynamic properties in the steam tables are arranged with pressure and temperature as independent variables. These tables could have been arranged using any other two intensive properties such as specific volume and specific internal energy, as independent variables.

The functional relationship for water between P , T , and v is shown in Figure IIa.3.1(a). The single-phase states such as solid, liquid, and steam are identified in this figure. Also shown are two-phase regions such as liquid-vapor and solid-vapor. The projections of various regions of Figure IIa.4.1(a) on the P - T and

on the T - v surfaces are shown in Figures IIa.3.1(b) and IIIa.3.1(c), respectively. We examine these figures in more detail. Figure IIa.3.1(b) shows three distinct lines: the sublimation line, the fusion line, and the vaporization line. Pure substances at equilibrium generally exist either as solid, liquid, or gas. However, depending on the pressure and temperature two or even all of these three phases may coexist. For example, water at 32 F and 4.58 mm Hg (0.006 atm) may exists as ice, water, or steam or any combination of these phases at equilibrium. This specific point is known as the *triple point*. To further elaborate on the vaporization line, we consider a cylinder fitted with a piston. Initially, the cylinder contains superheated steam. As an example, steam can be at an absolute pressure of 18 psia and temperature of 250 F, as shown in Figure IIa.3.2 as State A.

Fehler! Keine gültige Verknüpfung.
(a)

Fehler! Keine gültige Verknüpfung.
(b)

Fehler! Keine gültige Verknüpfung.
(c)

Figure IIa.3.1. Pressure-temperature-volume plots for water (not to scale)

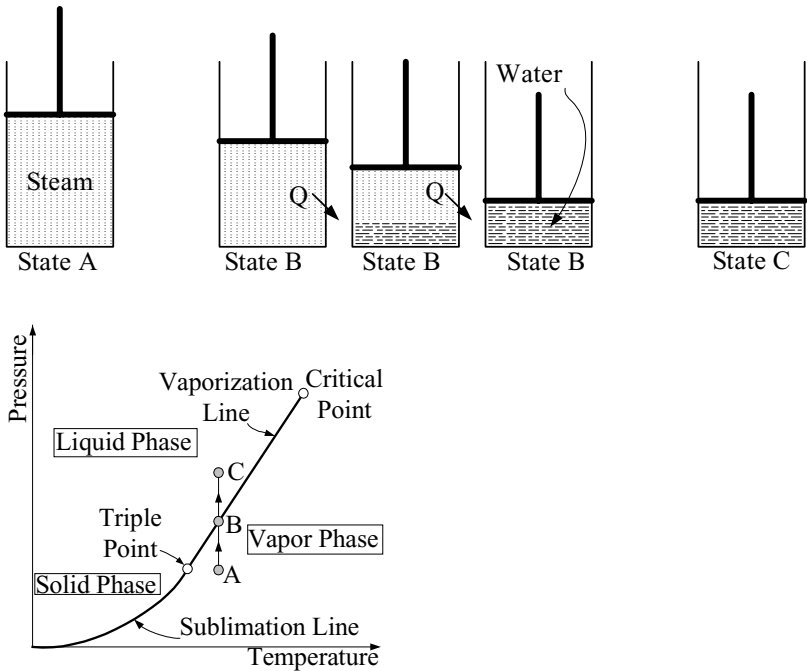


Figure IIa3.2. Steam condensation in an isothermal process

We now apply force on the piston, which increases steam pressure and temperature. To maintain temperature, the applying force on the piston must take place in an isothermal process. This is possible by allowing heat transfer from the cylinder to the surroundings, causing steam condensation. Upon condensation of all the steam in the cylinder, the pressure and temperature of state B reach 29.825 psia and 250 F, respectively. We may continue applying pressure on the piston and allowing heat transfer from the cylinder until state C is reached. For the numerical example, state C reflects a compressed or subcooled liquid at 250 F and a pressure greater than 29.825, say 34 psia.

Let's now examine an isobaric process with water in the cylinder being at state C at which $P = 34$ psia and $T = 250$ F (Figure IIa.3.3). We maintain the applied force on the piston but add heat to the water in the cylinder until water begins to boil. To maintain pressure, we let the piston move upward to accommodate the evaporation process and the expanding volume. We continue heating water until the last drop of water evaporates. This is state D where for our example, pressure is 34 psia and steam temperature has reached 257.58 F. Upon further heating with volume expansion, we reach state E at which steam is superheated. For the numerical example, state E is at 34 psia and a temperature higher than 257.58 F, say 265 F.

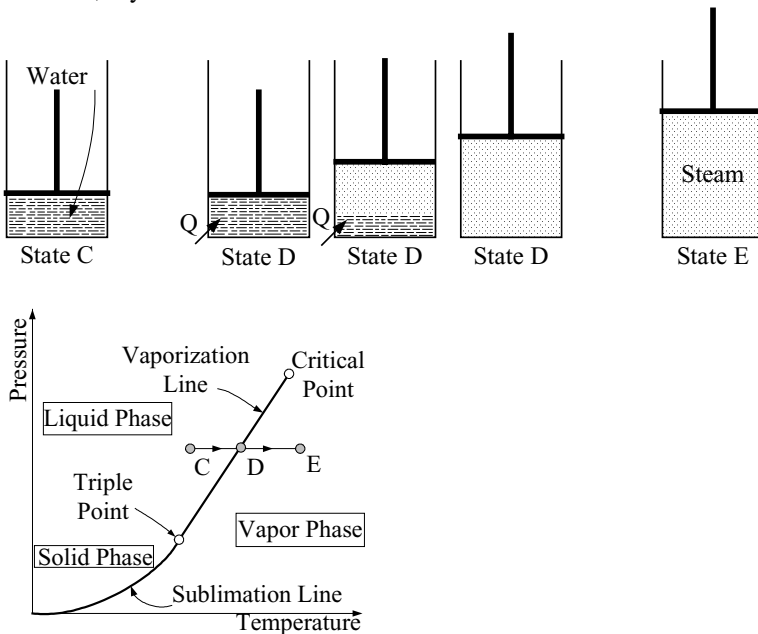


Figure IIa.3.3. Water evaporation in an isobaric process

Returning to Figure IIa.3.1, let us now examine Figure IIa.3.1(c). As shown in T - V diagram of Figure IIa.3.1(c), water goes through three major phases at a given pressure and rising temperature. On the left of the saturated-liquid line, water is subcooled otherwise known as compressed liquid. On the right of the saturation-vapor line, water is in the form of superheated vapor. A two-phase mixture exists between the two saturation lines with the mass of steam increasing from left to right. This is better determined by defining a steam static quality for a two-phase mixture:

$$x = \frac{\text{mass of steam}}{\text{mass of mixture}} = \frac{\text{mass of steam}}{\text{mass of steam} + \text{mass of liquid}}$$

When we refer to quality we generally mean static quality as defined above. Other definitions for quality are discussed in Chapter Va. Quality is zero on the saturation-liquid line and is unity on the saturation-vapor line. At any given point where A has a given steam quality of x , various thermodynamic properties are obtained as follows. We first read various saturated-liquid and saturated-vapor properties from the steam tables:

$$P_1 \rightarrow v_f \quad v_{fg} \quad v_g \quad u_f \quad u_{fg} \quad u_g \quad h_f \quad h_{fg} \quad h_g \quad s_f \quad s_{fg} \quad s_g$$

where properties of saturated liquid and saturated vapor are shown with subscripts f and g , respectively. Any property with subscript fg refers to the difference in values from saturated liquid to saturated vapor (i.e., $\pi_{fg} = \pi_g - \pi_f$ where $\pi = v, u, h, s$, etc.). In particular, h_{fg} represents the *latent heat of vaporization*. The latent heat by definition, is the energy stored in (or released from) a substance during a phase change, which occurs at constant pressure and temperature. For example, h_{fg} is that amount of heat required to vaporize saturated water to become saturated steam. Similarly, h_{fg} is that amount of heat, which is released by saturated steam to condense to saturated water. Having the saturated liquid and saturated vapor properties, we can calculate properties of a mixture of water and steam for given steam quality x as follows:

$$\begin{aligned} v &= v_f + x(v_g - v_f) = v_f + xv_{fg} \\ u &= u_f + x(u_g - u_f) = u_f + xu_{fg} \\ h &= h_f + x(h_g - h_f) = h_f + xh_{fg} \\ s &= s_f + x(s_g - s_f) = s_f + xs_{fg} \end{aligned}$$

Example IIa.3.1. Find properties of state A in Figure IIa.3.1(c) using $P_1 = 800$ psia (5.5 MPa) and $x_A = 0.7$.

Solution: From the steam tables A.II.1(BU) we find:

v_f (ft ³ /lbm)	v_{fg} (ft ³ /lbm)	u_f (Btu/lbm)	u_{fg} (Btu/lbm)
0.02087	0.54809	506.70	608.50
h_f	h_{fg}	s_f	s_{fg}

(Btu/lbm)	(Btu/lbm)	(Btu/lbm·R)	(Btu/lbm·R)
509.80	689.60	0.7111	0.7051
$v_A = 0.02087 + 0.7 \times 0.54809 = 0.4045 \text{ ft}^3/\text{lbm}$ $u_A = 506.7 + 0.7 \times 608.5 = 932.65 \text{ Btu/lbm}$ $h_A = 509.8 + 0.7 \times 689.6 = 992.52 \text{ Btu/lbm}$ $s_A = 0.7111 + 0.7 \times 0.7051 = 1.20 \text{ Btu/lbm·R}$			

Example IIa.3.2. Temperature and quality of a saturated mixture are given as 230 C and 85%, respectively. Find the thermodynamic properties for this mixture.

Solution: From the steam tables A.II.2(SI) at $T_{sat} = 230 \text{ C}$ we find:

v_f (m ³ /kg)	v_g (m ³ /kg)	u_f (kJ/kg)	u_g (kJ/kg)
1.2088E-3	0.07158	986.74	2603.90
h_f (kJ/kg)	h_g (kJ/kg)	s_f (kJ/kg·K)	s_g (kJ/kg·K)
990.12	2804.00	2.6099	6.2146

$$v = v_f + x(v_g - v_f) = 1.2088\text{E-}3 + 0.85 \times (0.07158 - 1.2088\text{E-}3) = 0.061 \text{ m}^3/\text{kg}$$

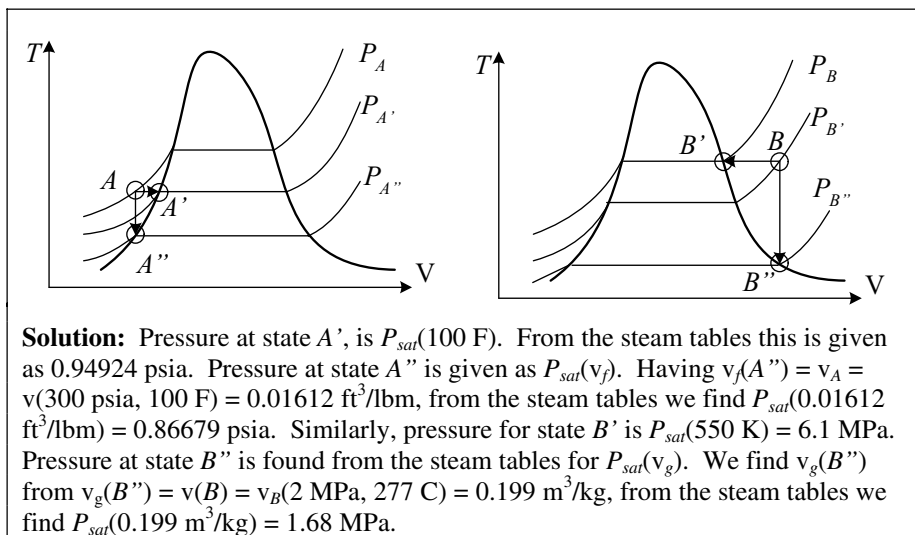
$$u = u_f + x(u_g - u_f) = 986.74 + 0.85 \times (2603.90 - 986.74) = 2,361.33 \text{ kJ/kg}$$

$$h = h_f + x(h_g - h_f) = 990.12 + 0.85 \times (2804.00 - 990.12) = 2,531.92 \text{ kJ/kg}$$

$$s = s_f + x(s_g - s_f) = 2.6099 + 0.85 \times (6.2146 - 2.6099) = 5.6739 \text{ kJ/kg·K}$$

Note that for the subcooled and superheated regions, any two intensive properties are sufficient to clearly define the state of water. These can be pressure and temperature, pressure and specific enthalpy, etc. While the same is true for the saturation region (i.e. the state of water is determined by having two independent properties), we cannot determine the state of water by having only pressure and temperature because, in the saturation region, these are functionally related and hence are not independent variables. In the saturation region, we are generally given pressure and quality, temperature and quality, pressure and enthalpy, etc.

Example IIa.3.3. State A in the left figure is subcooled water at $P = 300 \text{ psia}$ and $T = 100 \text{ F}$. Find the new pressure if the process is isothermal with final state being saturated water (A'). Also find the new pressure in a constant volume process with the final state being saturated water (A''). Repeat similar problem this time for state B in the figure on the right. State B is superheated steam at $P = 2 \text{ MPa}$ and $T = 277 \text{ C}$ with states B' and B'' being saturated steam.



Shown in Figure IIA.3.4 are the trends of saturated water and saturated steam enthalpies (h_f and h_g), water latent heat of vaporization (h_{fg}), and saturation temperature (T_{sat}) all as functions of pressure. Obtaining an equation for these or other saturation properties is much simpler than in the subcooled and superheated regions. This is due to the fact that in the saturated region we need to fit the curve to a function of a single variable as opposed to other regions which requires a curve fitting to functions of two variables. Even for the single variable function of the saturated region, a property often needs to be represented by more than one function in a piecewise fit to enhance the accuracy of the curve fit to data. Examples of curves fit to data are shown in Table A.II.6 of Appendix II. This appendix includes polynomial functions to represent P , v_f , v_{fg} , u_f , and u_{fg} in terms of temperature and are obtained by fitting curves to the steam tables data.

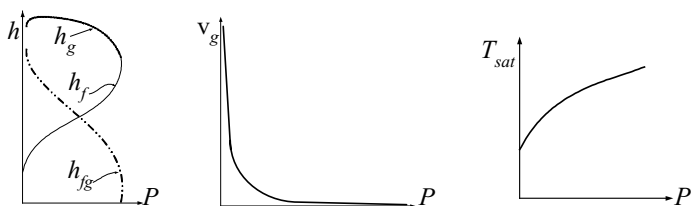


Figure IIA.3.4. Water enthalpy, steam specific volume, and saturation temperature versus pressure

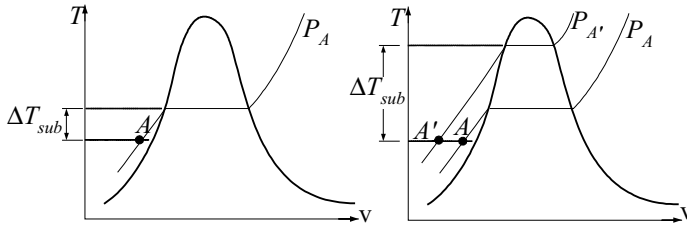
Example IIA.3.4. Consider a process where heat, mass, and work are exchanged with the surroundings. In the final state, u and v are known. Determine pressure and temperature of the final state.

Solution: The conservation equations of mass and energy are discussed later in

this chapter. For now, our purpose of presenting this example is to indicate that in thermohydraulic computer codes, mass (m) is obtained from the conservation equation of mass, total internal energy (U) from the conservation equation of energy, and volume (V) from the volume constraint. Specific internal energy (u) and specific volume (v) are obtained from $u = U/m$ and $v = V/m$, respectively. While the steam tables are traditionally arranged in terms of pressure (P) and temperature (T), it is generally the u and v that are calculated in the analysis. We should then find P and T from u and v by iteration with the steam tables. This is called the *pressure search* method. An example of such iteration is given by Program A.II.1 on the accompanying CD-ROM.

Below, we introduce the *degree of subcooling*, which is an indication of how far a system is from boiling. The degree of subcooling is an important parameter in pressurized subcooled systems, such as the primary side of a PWR, which must remain subcooled during normal operation.

Example IIa.3.5. Find the pressure required to maintain 50 C subcooling in a tank containing water at 200 C and 2 MPa.



Solution: The *degree of subcooling* is the difference between the saturation temperature and the actual temperature of a compressed liquid. At $P_A = 2$ MPa and 200 C, water is subcooled but the degree of subcooling is about $212 - 200 = 12$ C. To have a degree of subcooling increased to 50 C, we should find P_{sat} corresponding to $T = 200 + 50 = 250$ C which is about $P_{A'} = 3.97$ MPa.

Clapeyron equation is applicable to a phase change, which occurs at constant temperature and pressure. The latter is true since saturation pressure is a function of temperature. The Clapeyron equation (after Emil Clapeyron, 1799 - 1864) for a liquid-vapor phase change is:

$$\left(\frac{dP}{dT}\right)_{sat} = \frac{h_{fg}}{T v_{fg}} \quad \text{IIa.3.7}$$

From the Clapeyron equation, we can determine the latent heat of vaporization (h_{fg}), which cannot be directly measured from the PvT data. Note that T in Equation IIa.3.7 is the absolute temperature.

Clausius-Clapeyron equation is obtained by introducing simplifying approximations into the Clapeyron equation. The introduction of such approximations

limits the application of the Clapeyron equation to relatively low pressures where v_f is negligible as compared to v_g , which in turn can be approximated as $v_g = RT/P$, as explained in Section 2.2. Substituting into Equation Ila.3.7, we get:

$$\left(\frac{dP}{P}\right)_{sat} = \frac{h_{fg}}{R} \frac{dT}{T} \quad \text{Ila.3.8}$$

Upon integration, we find vapor pressure as a function of temperature:
 $\ln P_{sat} = -(h_{fg} / P_{sat})(1/T) + c$.

Example Ila.3.6. Calculate the latent heat of vaporization for water at $T = 212$ F.

Fehler! Keine gültige Verknüpfung.

Solution: To find h_{fg} , we need to determine the slope at $T = 212$ F. From the steam tables we find the following data:

T (F)	P (psia)	v_{fg} (ft ³ /lbm)
211	14.407	—
212	14.696	26.782
213	14.990	—

The slope becomes $(14.99 - 14.407)/(213 - 211) = 0.2915$ psi/F. Substituting in Equation Ila.3.7, we find:

$$h_{fg} = (dP/dT)T v_{fg} = [0.2915 \text{ lbf}/(\text{in}^2 \cdot \text{F})] \times (144 \text{ ft}^2/\text{in}^2) \times (212 + 460) \text{ R} \times 26.782 \text{ ft}^3/\text{lbm} = 755,471 \text{ ft} \cdot \text{lbf}/\text{lbm}$$

$$\text{Alternatively, } h_{fg} = (755,471 \text{ ft} \cdot \text{lbf}/\text{lbm}) / (778.17 \text{ ft} \cdot \text{lbf}/\text{Btu}) = 970.8 \text{ Btu}/\text{lbm}.$$

3.3. Determination of State

In this section, we noted that to determine the state of a substance we must have two independent intensive thermodynamic properties. In this regard, there are generally two cases that we have to deal with.

Case 1, P or T specified. In this case, either P or T and one more property (v , u , h , or s) are given. We find the state from the steam tables since one of the two known properties is either P or T . Having the saturation properties corresponding to the given P or T , we then make an assessment to see if the state is subcooled, saturated, or superheated. For example, if P & u are given to find the state, we first find $u_f(P)$ and $u_g(P)$ from the property tables. We then make the following comparison to find the thermodynamic state:

<u>Subcooled liquid</u>	<u>Saturated mixture</u>	<u>Superheated vapor</u>
$u < u_f(P)$	$u_f(P) < u < u_g(P)$	$u > u_g$

If both P and T are given and $T \neq T_{sat}(P)$ or alternatively $P \neq P_{sat}(T)$ then the state is either subcooled or superheated. This discussion is summarized in Table IIa.3.1.

Table IIa.3.1. Type of properties given for case 1

Subcooled, Saturated, Superheated			Saturated	Subcooled	Superheated
$T \ \& \ v$	or	$P \ \& \ v$	$T \ \& \ x$	$T \ \& \ P$ $T < T_{sat}(P)$	$T \ \& \ P$ $T > T_{sat}(P)$
$T \ \& \ u$	or	$P \ \& \ u$			
$T \ \& \ h$	or	$P \ \& \ h$	$P \ \& \ x$		
$T \ \& \ s$	or	$P \ \& \ s$			

Case 2, $P \& T$ not specified. If the two specified properties are not P and T , the state can not be readily determined from the steam tables. This is what was referred to in Example IIa.3.4 as the pressure search. Often in analysis we solve for $u \& v$ or $h \& v$ and would then have to find $P \& T$. In this case, we generally have to resort to iteration, an example of which is shown on the accompanying CD-ROM, Program A.II.1.

3.4. Specific Heat of Water

In many engineering applications, we may approximate values for thermodynamic properties such as v , u , and h for subcooled liquids using saturated liquid data at a specified temperature. This implies that such values are primarily a function of temperature and vary slightly with pressure at fixed temperature. We may extend this approximation to specific heat. Also note that using $du = c_v dT$, we may express the specific internal energy of water in terms of specific heat at constant volume as $\Delta u = u(T) - u_{Ref.} = c_v (T - T_{Ref.})$. Choosing the reference temperature for water as $T_{Ref.} = 32 \text{ F}$ at which $u_{Ref.} = 0$, we find $u(T) \approx c_v (T - 32)$. If we use an average value of $c_v = 1 \text{ Btu/lbm}\cdot\text{F}$ in the range of 32 F to 450 F, the internal energy of water in Btu/lbm becomes $u(T) \approx (T - 32)$ where T is in Fahrenheit. The largest error of less than 2.5% for the above temperature range occurs at 450 F.

4. Heat, Work, and Thermodynamic Processes

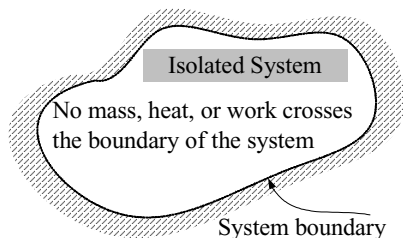
The laws of thermodynamics are known as the zeroth law, the first law, and the second law. The zeroth law is the basis for temperature measurement. This law states that if two systems are at the same temperature as a third system, the two systems would then have equal temperatures*. The first law deals with conservation of energy in a process. The second law governs the direction of the thermodynamic processes. The laws of thermodynamics are statements of fact and have no proof.

* The alternative expression for the zeroth law (also referred to as the third law of thermodynamics) is that at absolute zero, all perfect crystals have zero entropy.

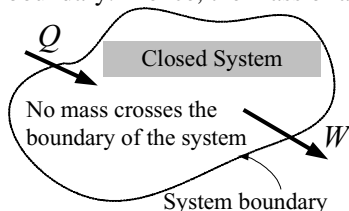
4.1. Definition of Terms

System, surrounding, and boundary are essential thermodynamics concepts, which allow us to study a substance, a region, or a process by considering it as a system and setting it apart from everything else known as the surroundings. Any interaction between the system and the surroundings takes place through the system boundary or the **control surface**. The boundary may be real or imaginary.

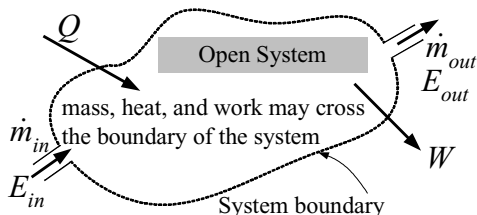
Isolated system is a system that does not have any interaction with its surroundings; hence neither mass nor energy can cross the boundaries of an isolated system.



Closed system, control mass allows transfer of energy but not mass through its boundary. Hence, the mass of a closed system is always constant.



Open system, control volume allows for transfer of mass and energy through the boundary. This is the most widely used means of analyzing thermodynamic processes. An open system may also be treated as a closed system by letting the system boundary change with the moving flow, and hence to encompass the same amount of mass at all times. Changes in the energy content of a closed system may also be due to such processes as thermal conduction, radiation, mechanical compression or expansion, and such fields as gravitational or electromagnetic.



Lumped parameter volume is a term applied to a system to emphasize the fact that there is only one temperature and pressure describing the entire system.

Distributed parameter volume, also known as subdivided volume, implies that a system is subdivided into several lumped volumes to increase the amount of detail we seek about the system while undergoing a process.

Adiabatic process refers to a thermodynamic process where there is no heat transfer to or from the system.

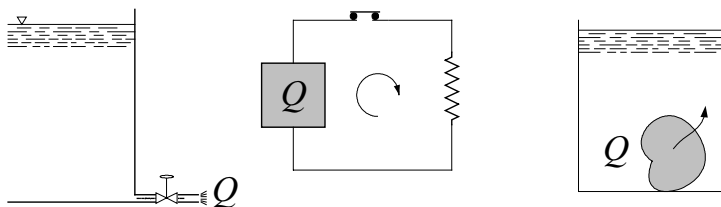
Reversible is an ideal process which, at the conclusion of the process, can be reversed to bring the system and its surroundings to the same exact condition as it was prior to the original process. Reversible processes are further discussed in Section 9 of this chapter.

Work, W is a form of energy transfer between a system and its surroundings if its net effect results in lifting a weight in a gravitational field. Various types of work are described in Section 4.3. The relation between heat (defined later in this section), work, and total energy is described in Section 6. This relation is generally referred to as the *energy equation* or *energy balance*. We assign a plus sign to the term representing work in the energy equation if work is delivered from the system to its surroundings. Otherwise we assign a minus sign. Work is not property of a system and must cross the boundary of the system. Work is expressed in J, kJ, or m·kgf in the SI system. In British units, work is given in Btu or less frequently used units of ft·lbf.

Power, \dot{W} is defined as the rate of energy transfer by work, $\dot{W} = dW/dt$. Since $W = F \times L$ where F is force and L is distance, then $\dot{W} = F \times V = (\Delta P \times A) \times V = \Delta P \times \dot{V} = (\Delta P/\rho) \times \dot{m}$. As described in Section 5, \dot{V} and \dot{m} are the volumetric flow rate and the mass flow rate, respectively.

Power is expressed in units of J/s, Watt (W, being the same as J/s), kilowatt (kW), megawatt (MW), gigawatt (GW), Btu/s, Btu/h, or horsepower (hp).

Heat, Q as a form of energy in transition is transferred due to a temperature gradient between two systems or a system and its surroundings, in the direction of decreasing temperature. The fact that heat flows solely due to temperature difference resembles the flow of water from a reservoir due to elevation difference or the flow of electricity from a capacitor (or from a battery) in an electric circuit due to potential difference. As shown in the left figure, when the valve is opened, water flows. The middle figure also shows that when the switch is turned on, electric current would be established in the circuit. Similarly, if we drop a hot block of copper into a bucket of colder water, heat flows from the copper to the water. By convention, if heat is delivered to a system we assign a plus sign to the term representing it in the energy equation. Conversely, if heat is transferred from the system to its surroundings, the sign is negative. Like work, heat is not a property of a system and it must cross the boundary of the system. Heat is expressed in J, kJ, or m·kgf in the SI system. In British units, heat is given in Btu or less frequently used units of ft·lbf.



4.2. Ideal Gas Processes

Processes involving ideal gases are referred to as polytropic when the following relation applies:

$$Pv^n = c \quad \text{IIa.4.1}$$

where c is a constant and n is the slope of the path plotted on the P - v coordinates, as shown in Figure IIa.4.1.

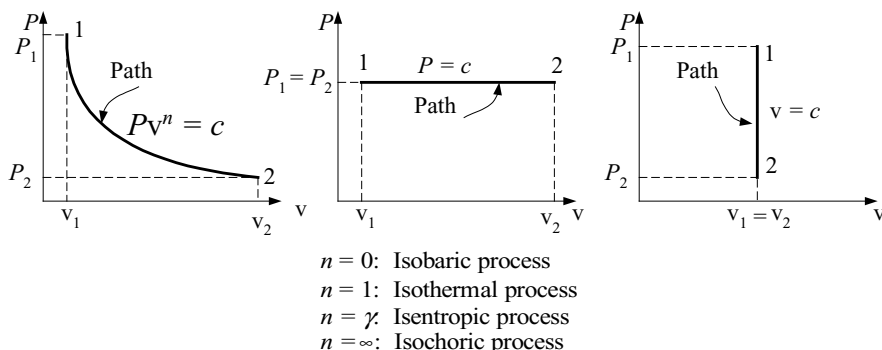


Figure IIa.4.1. Examples of Polytropic processes of an ideal gas

Special cases of the polytropic process include isobaric (constant pressure process), isochoric (constant volume process), isothermal (constant temperature process), and isentropic. Shown in Figure IIa.4.1 are also exponents of specific volume for special cases of isobaric, isochoric, isothermal, and isentropic processes. These exponents are derived by combining the equation of state ($Pv = RT$) and the polytropic process ($Pv^n = c$). To demonstrate, we take the derivative of the equation for the polytropic process and divide it by the equation for the polytropic process to obtain:

$$n = -\frac{v}{P} \frac{dP}{dv} \quad \text{IIa.4.2}$$

we now combine this equation with the equation of state for a specific case as demonstrated next.

Isothermal process. If we differentiate $Pv = RT$, we find $v dP + P dv = 0$ or $dv/dP = -v/P$. Substituting into Equation IIa.4.2, we find $n_{isotherm} = 1$.

Isobaric process. In this process, $P = c$ and $dP = 0$ hence, $n_{isobaric} = 0$.

Isochoric process is a constant volume process. For given mass, $v = c$ and $dv = 0$ hence, $n_{isochor} = \infty$

Isentropic process. An isentropic process is an adiabatic and reversible process hence constant entropy, $(dS)_{isentropic} = 0$. In an isentropic process for an ideal gas we have $n = \gamma$ where γ is given by $\gamma = c_p/c_v$. Hence, for an isentropic process we have $PV^\gamma = \text{constant}$. Combining with the equation of state, we find:

$$\frac{P_2}{P_1} = \left(\frac{V_1}{V_2}\right)^\gamma \quad \text{IIa.4.3}$$

$$\frac{T_2}{T_1} = \left(\frac{V_1}{V_2}\right)^{\gamma-1} \quad \text{IIa.4.4}$$

$$\frac{T_2}{T_1} = \left(\frac{P_2}{P_1}\right)^{\frac{\gamma-1}{\gamma}} \quad \text{IIa.4.5}$$

4.3. Types of Work

The simplest type of work is the shaft-work needed to lift a weight in a gravitational field. Examples for various types of work are as follows: *compression work* delivered to a system consisting of a piston and a gas filled cylinder, *expansion work* delivered by a system consisted of a piston and a gas filled cylinder (Figure IIa.4.2), *electric work*, representing the movement of electric charge in a field of electric potential, *magnetic work*, representing the alignment of ions with the magnetic axes, *tension work* as in a stretched wire, *surface film work* against surface tension of a liquid, *rotating shaft work* such as that delivered by a turbine, and *shear work*, due to the existence of shear forces such as that required to pull a spoon out of a jar of honey. The relation for compression or expansion work in terms of pressure and volume can be obtained from the definition of work, which is the applied force times the displacement. For both cases of compression and expansion we have:

$$\delta W = F(dl) = (P \times A)(dl) = P(A \times dl) = PdV$$

Total work is obtained from: $W_{12} = \int_1^2 PdV$. If $P_1 = P_2 = P$ then $W_{12} = P(V_2 - V_1)$.

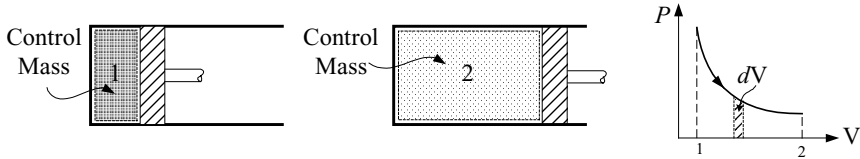


Figure IIA.4.2. Expansion work delivered by a system with moving boundary

Example IIA.4.1. The movement of the piston in the cylinder of Figure IIA.4.3 is frictionless. The spring is linear (displacement is proportional to the applied force) and is at its normal length when the piston is at the bottom of the cylinder in Figure IIA.4.3(a). We now introduce 5 kg of a mixture of water and steam to the cylinder. This causes cylinder pressure to reach 0.4 MPa at a quality of 0.2 in Figure IIA.4.3(b). At this stage, we add heat to the mixture. This causes expansion of the mixture and movement of the piston until it eventually reaches the stops in Figure IIA.4.3(c). Volume of the cylinder at this stage is $V_c = 1.0 \text{ m}^3$. We continue heating up the mixture until all water vaporizes and the mixture becomes saturated steam.

I) Show this process on a PV -diagram

II) Find pressure in stage c_2 where steam becomes saturated

III) Find pressure and steam quality at stage c_1 where piston just reaches the stops,

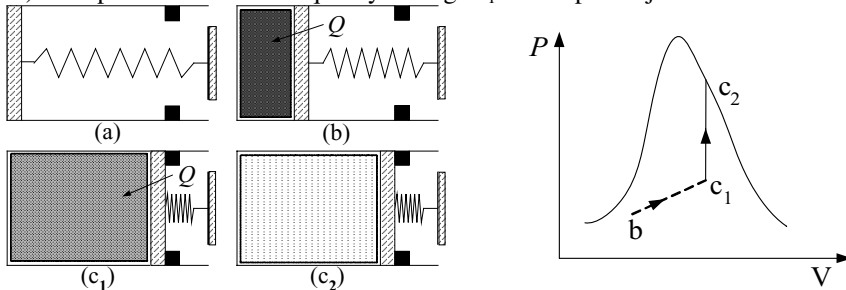


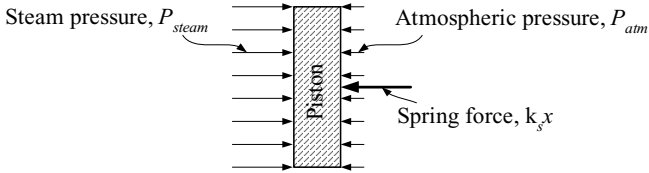
Figure IIA.4.3. Heat addition to a cylinder containing water mixture

Solution: I) This process is shown in the PV -diagram of Figure IIA.4.3. Initially, mixture has a quality of $x_b = 0.2$ at a pressure of 0.4 MPa (point b). Heat is then added to the mixture until at c_1 the piston reaches the stops. We continue heating the mixture until all water vaporizes and steam becomes saturated at c_2 . The process from state b to state c is a straight line because the spring is linear. The process from c_1 to c_2 is a vertical line, since pressure increases at a constant volume.

II) To find the pressure in state c_2 , we need to have two independent properties. We note that, in this state, steam is saturated, hence, quality is 100%. To find another independent property, we use the fact that we are dealing with a closed system hence, mass remains constant throughout states b and c. Having mass of $m = 5 \text{ kg}$, volume of $V_c = 1.0 \text{ m}^3$, and quality of $x_{c_2} = 1$, we find specific volume as $v_c = v_g = 1.0/5 = 0.2 \text{ m}^3/\text{kg}$. By interpolation in the steam tables, we find the corre-

sponding pressure of about $P_{c_2} = 1.00$ MPa.

III) To find pressure at state c_1 , we use the relation between displacement in the spring and the applied forces. This can be obtained from a free body diagram for the piston.



If we assume the spring constant is k_s and the cylinder cross sectional area is A , then from a force balance:

$$(P_{steam} - P_{atm})A = k_s x = k_s (V / A)$$

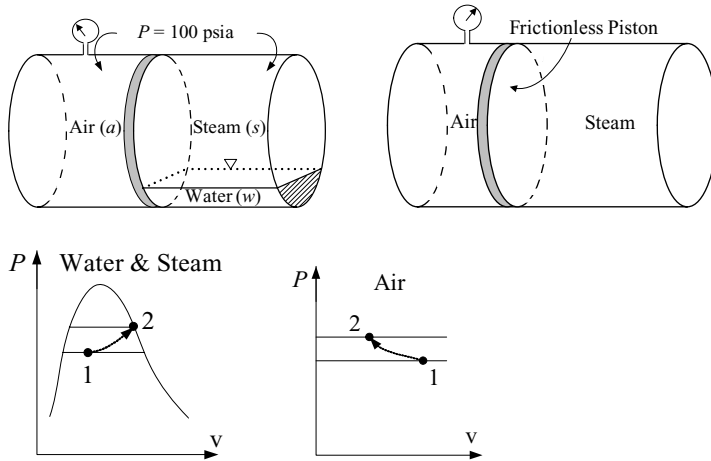
We are not given the spring constant k_s and the piston area A . We eliminate k_s and A by applying the above equation to both states b and c_1 and divide the results to obtain:

$$P_{c_1} - P_{atm} = (P_b - P_{atm})(V_{c_1} / V_b)$$

Having P_b , to find pressure at state c_1 , we need to first calculate volume at state b , which is obtained by multiplying the specific volume by the mixture mass. At $P_b = 0.4$ MPa, we find $v_b = 0.001084 + 0.2 (0.4625 - 0.001084) = 0.103$ m³/kg. Therefore, $V_b = mv_b = 5 \times 0.103 = 0.5156$ m³. Pressure at state c_1 is then found as $P_{c_1} = 0.1 + (0.4 - 0.1)(1/0.5156) = 0.682$ MPa. Note that we assumed $P_{atm} = 100$ kPa.

To find quality at c_1 , we use the fact that $v_{c_1} = v_{c_2} = 0.2$ m³/kg. Therefore, steam quality at c_1 becomes: $x_{c_1} = (v_{c_1} - v_f) / v_{fg}$. Using specific volumes at $P_{c_1} = 0.682$ MPa, $v_f = 0.001106$ m³/kg and $v_{fg} = 0.28$ m³/kg, we find $x_{c_1} = (0.2 - 0.001106) / 0.28 = 0.71$. Expectedly, the addition of heat has increased quality from 0.2 to 0.71. Further heat addition at constant volume increases quality to 100%.

Example IIa.4.2. A cylinder has a volume of 50 ft³. Half of the cylinder is filled with air and half with water and steam. The motion of the piston dividing the two chambers is frictionless while providing a perfect seal between the two chambers. The piston is a good heat conductor. Initially, the water volume is 5% of the total volume of the right chamber. We now add heat to both chambers until all of the water evaporates. Find the final pressure. Treat air as an ideal gas.



Solution: To find the final pressure we first need to determine all masses in the system. Since the motion of the piston is frictionless, both chambers are at the same pressure of 100 Psia. Since heat transfers from one chamber to the other through the piston, both chambers are also at the same temperature, $T = T_{sat}(P)$. We use subscripts a , s , and w for air, steam, and water, respectively. Subscript 1 is used for the initial equilibrium state (before heat is added to the system) and subscript 2 for final equilibrium state (after heat is added to the system). Throughout the entire process we can write the following five equations:

$$P_a = P_s = P, T_a = T_s = T_{sat}(P), \text{ and } V_a + (V_s + V_w) = 50$$

P_1 (psia)	T_1 (F)	v_{f1} (ft ³ /lbm)	v_{g1} (ft ³ /lbm)
100	327.82	0.01774	4.4310

The initial water mass is: $m_{w1} = V_{w1}/v_{f1} = (25 \times 0.05)/0.01774 = 70.462$ lbm.

The initial steam mass is: $m_{s1} = V_{s1}/v_{g1} = (25 \times 0.95)/4.4310 = 5.36$ lbm.

The initial air mass is:

$$m_{a1} = PV_{a1}/R_a T_1 = m_{a1} = (100 \times 144) \times 25 / [(1525/28.97) \times (327.82 + 460)] = 8.68 \text{ lbm.}$$

The final masses of water, steam, and air are $m_{w2} = 0$ lbm, $m_{s2} = m_{w1} + m_{s1} = 70.462 + 5.36 = 75.822$ lbm, and $m_{a2} = m_{a1} = 8.68$ lbm, respectively.

We find T_2 and P_2 by iteration:

We guess P_2 and find $T_2 = T_{sat}(P_2)$. Having P_2 and T_2 , we find $[v_{s2}(T_2)]_{Table}$. We also calculate v_{s2} from: $v_{s2}(T_2) = (50 - V_{a2})/m_{s2}$. Since $V_{a2} = (m_{a2}R_a T_2)/P_2$, therefore $[v_{s2}(T_2)]_{Calculated} = [50 - (m_{a2}R_a T_2)/P_2]/m_{s2}$.

The iteration is converged if $\left| [v_{s2}(T_2)]_{Table} - [v_{s2}(T_2)]_{Calculated} \right| \leq \varepsilon$ where ε is the convergence criterion. Following this procedure, we find $P_2 = 755$ psia and $T_2 = 511.6$ F.

4.4. Work Involving an Ideal Gas

Using special processes for an ideal gas, we can find analytical expressions for work involving moving boundaries. If the process from the initial state (1) to the final state (2) as shown in Figure IIa.4.2 is such that the volume remains the same (**isochoric**), then $dV = 0$ and we find:

$$W_{1-2} = \int_1^2 P dV = 0$$

If the process in Figure IIa.4.2 is **isobaric**, then $P_1 = P_2$ and the work done from state 1 to state 2 is:

$$W_{1-2} = \int_1^2 P dV = P_1 (V_2 - V_1)$$

If the process in Figure IIa.4.2 is **isothermal**, then from $PV = mRT$, we find $P_1 V_1 = P_2 V_2 = PV = \text{constant}$. Substituting in the integral for $P = P_1 V_1 / V$, we get:

$$W_{1-2} = \int_1^2 P dV = P_1 V_1 \int_1^2 \frac{dV}{V} = P_1 V_1 \ln \frac{V_2}{V_1}$$

In general, for a **polytropic** process from 1 to 2 in Figure IIa.4.2, we have $P_1 V_1^n = P_2 V_2^n = PV^n$. Substituting

$$W_{1-2} = \int_1^2 P dV = P_1 V_1^n \int_1^2 \frac{dV}{V^n} = P_1 V_1^n \left[\frac{V^{1-n}}{1-n} \right]_1^2 = \frac{P_2 V_2 - P_1 V_1}{1-n} \quad \text{IIa.4.4}$$

Example IIa.4.3. The cylinder in Figure IIa.4.2 is filled with air and initially is at $P_1 = 10$ kPa and $V_1 = 0.1$ m³. At the conclusion of a process the final air volume is $V_2 = 0.3$ m³. Find the work done by the piston if

a) the process is isobaric, b) the process is isothermal, c) the process is isentropic ($\gamma_{air} = 1.4$), and d) the process is polytropic with $n = 2$.

Solution:

a) In an isobaric process, $W_{1-2} = P_1 (V_2 - V_1) = 10(0.3 - 0.1) = 2$ kJ.

b) For the isothermal process, $W_{1-2} = P_1 V_1 \ln(V_2/V_1) = 10 \times 0.1 \times \ln(0.3/0.1) = 1.01$ kJ.

- c) For the isentropic process, $P_2 = P_1(V_1/V_2)^{1.4} = 10(0.1/0.3)^{1.4} = 2.148 \text{ kPa}$.
 $W_{1-2} = (P_2V_2 - P_1V_1)/(1 - n) = [2.148 \times 0.3 - 10 \times 0.1]/(1 - 1.4) = 0.89 \text{ kJ}$.
- d) For the polytropic process, $P_2 = P_1(V_1/V_2)^2 = 10(0.1/0.3)^2 = 1.111 \text{ kPa}$
 $W_{1-2} = (P_2V_2 - P_1V_1)/(1 - n) = [1.111 \times 0.3 - 10 \times 0.1]/(1 - 2) = 0.667 \text{ kJ}$.

5. Conservation Equation of Mass for a Control Volume

The conservation equation of mass, referred to as the *continuity equation*, is discussed in this section. Derivation of this equation is left to Chapter IIIa. The most intuitive way of comprehending this equation is to consider the liquid level in the tank of Figure IIa.5.1. Liquid may be added to the tank from various inlet ports and may be withdrawn from the tank through various outlet or exit ports. The liquid in this tank represents a control volume for mass or energy (note changes with time). To accumulate mass in the tank, the flow rate into the tank must exceed the flow rate out of the tank. Conversely, to deplete the tank, the flow rate out of the tank must exceed the flow rate into the tank. This intuitive statement about the rate of accumulation or depletion is also applicable to the conservation of energy, momentum, and angular momentum although its application to the conservation of mass and energy is easier to envision*. The mathematical representation of the above statement for conservation of mass is:

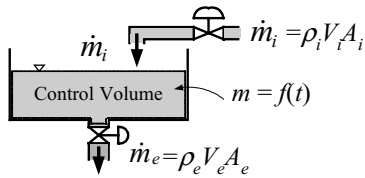


Figure IIa.5.1. Depiction of the rate equation

$$\sum_{inlet} \dot{m}_i = \sum_{exit} \dot{m}_e + \frac{dm_{C.V.}}{dt} \quad \text{IIa.5.1}$$

The subscript *C.V.* stands for control volume. The mass flow rate is related to the flow density, flow area, and flow velocity normal to the area as:

$$\dot{m} = \rho \vec{V} \cdot \vec{A} = \rho V A \quad \text{IIa.5.2}$$

It is customary to call $\dot{V} = VA$ *volumetric flow rate* and $G = \rho V$ *mass flux*. Thus, Equation IIa.5.2 can be expressed as:

* In Chapter VIe, we apply the same principle to derive the neutron transport equation.

$$\dot{m} = \rho V A = \rho \dot{V} = G A \quad \text{IIa.5.3}$$

The volumetric flow rate (\dot{V}) in SI units may be expressed as m^3/s , liter/s, etc. In British units, \dot{V} is usually given in terms of gallons per minute (gpm or GPM). Since $1 \text{ ft}^3 = 7.481$ gallons, $1 \text{ ft}^3/\text{s} = 448.86$ gpm.

Example IIa.5.1. Water at a rate of 54 GPM flows in a 3 inch-diameter pipe at 100 psia and 150 F. Find a) the volumetric flow rate, b) mass flow rate, c) mass flux, and d) flow velocity

Solution: At $P = 100$ psia and $T = 150$ F: $v = 0.01634 \text{ ft}^3/\text{lbm}$, $\rho = 1/v = 1/0.01634 = 61.2 \text{ lbm}/\text{ft}^3$.

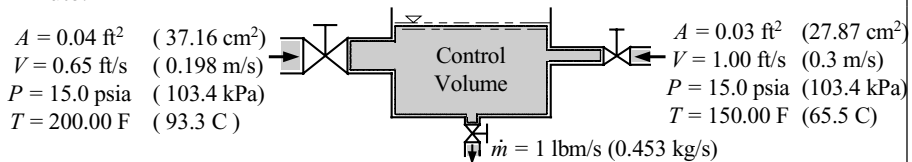
a) Volumetric flow rate of $\dot{V} = 54$ GPM is equivalent to $\dot{V} = 54/(7.481 \times 60) = 0.12 \text{ ft}^3/\text{s}$.

b) Mass flow rate becomes: $\dot{m} = \rho \dot{V} = 61.2 \times 0.12 = 7.36 \text{ lbm}/\text{s}$.

c) To find mass flux, we calculate the pipe flow area as $A = \pi d^2/4 = 3.14 \times (3/12)^2/4 = 0.049 \text{ ft}^2$. Having mass flow rate and flow area, mass flux becomes $G = \dot{m}/A = 7.36/0.049 = 150 \text{ lbm}/\text{ft}^2\cdot\text{s}$.

d) Finally, velocity is found from: $V = G/\rho = 150/61.2 = 2.45 \text{ ft}/\text{s}$. We could also find V from $V = \dot{V}/A$.

Example IIa.5.2. Water enters a mixing vessel from two inlet ports and leaves through one outlet port. Find the amount of water accumulated in the vessel in 1 minute.



Solution: We find the accumulated water by combining Equation IIa.5.1 with Equation IIa.5.2 and integrating:

$$m_2 - m_1 = [(\rho_1 V_1 A_1 + \rho_2 V_2 A_2) - \dot{m}_e] \Delta t$$

From the steam tables $v_1(15 \text{ psia} \ \& \ 200 \text{ F}) = 0.01664 \text{ ft}^3/\text{lbm}$ and $v_2(15 \text{ psia} \ \& \ 150 \text{ F}) = 0.01634 \text{ ft}^3/\text{lbm}$.

$\rho_1 = 1/v_1 = 1/0.01664 = 60.1 \text{ lbm}/\text{ft}^3$ (963 kg/m^3), $\rho_2 = 1/v_2 = 1/0.01634 = 61.2 \text{ lbm}/\text{ft}^3$ (980 kg/m^3)

$\Delta m = [(60.1 \times 0.65 \times 0.04) + (61.2 \times 1.00 \times 0.03) - 1] \times 60 = 143.92 \text{ lbm}$ (65.2 kg/s)

Steady flow steady state process: In the analysis of thermofluid systems, we often use the steady flow steady state process. Let's examine this process by con-

sidering the flow of gas through a gas turbine, representing our control volume. The steady flow condition requires that the mass flow rate of the gas entering the gas turbine to be equal to the mass flow rate of gas leaving the gas turbine. This also satisfies the steady state process during which $dm_{C.V.}/dt = 0$. However, as we will see in the next section, in a steady state process the rate of change of the energy of the control volume must also be zero, $dE_{C.V.}/dt = 0$.

Returning to the gas turbine example, it is true that the gas properties are changing as the gas flows through the blades of the turbine. That is to say the properties change spatially and there is indeed a profile for pressure, temperature, velocity, specific internal energy, and density from the entrance to the exit of the turbine. However, in the steady state condition, the spatial distribution of each property remains independent of time. On the other hand, in the unsteady state or transient situation, gas properties in the control volume not only have spatial variations but also vary with time. Hence in transient analysis, we must consider mass and energy accumulation or depletion in a control volume.

Let's now consider a case where in Figure IIA.5.1, the rate of either accumulation or depletion of mass is zero. For the conservation of mass, Equation IIA.5.1 predicts that:

$$\sum_{inlet} \dot{m}_i = \sum_{exit} \dot{m}_e \quad \text{IIA.5.4}$$

Equation IIA.5.4, also referred to as *mass balance*, is an intuitive implication of the steady flow condition.

6. The First Law of Thermodynamics

The first law of thermodynamics is a relation between heat, work, and the total energy of a closed system. The first law of thermodynamics, also known as the *conservation equation of energy* or simply the *energy equation* has the simplest mathematical form, if written for a closed system. We can intuitively obtain this equation by using logical deduction (i.e. we expect the total energy of an isolated system to remain constant). Total energy of a system, in general, is the summation of its internal, kinetic, and potential energies ($E = U + KE + PE$). Thus, for an isolated system, $dE = 0$ ¹. If the system is not isolated and heat and work are allowed to cross the moving boundary of the system (Figure IIA.4.2), we expect that addition of heat (Q) to this system and the production of some work (W) will result in a net change in the system total energy:

¹ The assertion that energy can neither be created nor destroyed is a fundamental law in classical mechanics. As discussed in Chapter VIe, on a sub-atomic basis, mass is a form of energy appearing in a nucleus as the binding energy. The binding energy, in turn, is manifested as the short term nuclear force. Thus, a more general statement is to say that mass-energy can neither be created nor destroyed.

$$\delta Q = \delta W + dE \quad \text{IIa.6.1}$$

In Equation IIa.6.1, heat is delivered from the surroundings to the system hence, a plus sign is used for the δQ term. In return, the system has delivered positive work. *Equation IIa.6.1 is the mathematical expression of the first law of thermodynamics.* It is important to remember that the sign convention described here applies only if the energy equation is written in the form of Equation IIa.6.1. In this equation, the term representing heat is in the left side and the terms representing work and the total energy are in the right side of the energy equation. Also note the distinction made in Equation IIa.6.1, between exact differential (shown by d) and non-exact differential terms (shown by δ). An exact differential, such as total energy, is independent of the process or path between the initial and the final equilibrium states. Rather, it depends only on the initial and the final state (also known as the end states) properties:

$$\int_1^2 dE = E_2 - E_1$$

On the other hand, heat and work in general cannot be integrated unless the process is known². For example, suppose we add heat to the control system in Figure IIa.4.2. By manipulating the movement of the piston, we can accomplish the path between two equilibrium states in various ways including an isobaric, an isothermal, or an isochoric process. Integrating Equation IIa.6.1, we obtain:

$$\int_1^2 \delta Q = \int_1^2 \delta W + (E_2 - E_1)$$

After integration, this equation is generally shown as:

$$Q_{12} = W_{12} + (E_2 - E_1)$$

where subscript 12 for Q and W emphasizes the change in the value of Q or W along the path from state 1 to state 2 while subscript 1 or 2 signifies condition at state 1 or at state 2. Note from this result that if system goes through a thermodynamic cycle, then $E_2 = E_1$ so that $\Delta Q = \Delta W$.

Example IIa.6.1. Find the following values for Example IIa.4.2: total heat delivered to the system, the compression work performed by the piston on the air, and the heat transfer to the air during the process.

² The only exception is when work is a result of the action of a conservative force such as the force applied by a linear spring. Mathematically, such forces are gradients of a scalar, hence:

$$W_{12} = \int_1^2 \vec{F} \cdot d\vec{r} = \int_1^2 \vec{\nabla} f \cdot d\vec{r} = \int_1^2 df = f_2 - f_1$$

Solution: To find total heat transfer, we apply the first law to the whole cylinder:

$$Q_{12} = W_{12} + U_2 - U_1$$

where $U_1 = U_{1a} + U_{1mix}$ and $U_2 = U_{2a} + U_{steam}$.

The initial mixture internal energy is: $U_{1mix} = m_{f1}u_{f1} + m_{g1}u_{g1} = 70.462(298.2) + 5.36(1105.2) = 26935.6$ Btu.

The final mixture internal energy is: $u_2 = u_g(P_2) = u_g(755 \text{ psia}) = 1116$ Btu/lbm.

$U_{2mix} = (70.462 + 5.36)(1116) = 84617$ Btu. Since for the whole cylinder $W_{12} = 0$:

$$Q_{12} = (U_{steam} - U_{1mix}) + (U_{2a} - U_{1a}) = (84617 - 26935.6) + 8.68 \times 0.171(511.6 - 327.82) = 57954 \text{ Btu.}$$

To find the amount of work done by the piston we need to have the type of process. This is because work is a path-dependent function. However, the type of the process in which heat addition takes place is not specified. We, therefore, use an approximation as follows:

$$W_{12a} = \int_1^2 P dV = \sum_1^{14} P_i V_i$$

where we have divided the interval of $755 - 100 = 655$ psia to 13 equal intervals of 50 psi and one interval of 5 psi. We then use pressures of 750 psia, 700 psia, 650 psia, etc. and find corresponding volumes from the equation of state for air. Finding the area under the PV curve by numerical summation yields:

$W_{12a} = -966$ Btu. Applying the first law to the air compartment only we find:

$$Q_{12a} = W_{12a} + (U_{2a} - U_{1a}) = -966 + 8.68 \times 0.171(511.6 - 327.82) = -693 \text{ Btu.}$$

Returning to the first law of thermodynamics, if we apply Equation Ila.6.1 to a process which brings a system from its initial equilibrium state 1 to another equilibrium state 2, substitute for the total energy term, and integrate we obtain:

$$Q_{12} = W_{12} + (U_2 - U_1) + m(V_2^2 - V_1^2)/2 + mg(Z_2 - Z_1) \quad \text{Ila.6.2}$$

As discussed earlier, enthalpy is another extensive property of a system. If we substitute for compression work in terms of PV in Equation Ila.6.2, we see that the internal energy, U and PV appear together. If we represent this summation by $H = U + PV$, the working fluid enthalpy, we simplify thermodynamic computations involving the energy equation. Since enthalpy is an extensive property, the specific enthalpy, h , as an intensive property is obtained from $h = H/m = u + Pv$. As pointed out earlier, care must be exercised in calculating enthalpy from this relation using British units. For this reason, we may write $h = u + cPv$ where in British units $c = 144/778 = 0.185$ Btu/psia-ft³ for P in psia, v in ft³/lbm, and u and h in Btu/lbm, respectively.

6.1. Conservation Equation of Energy for a Control Volume

Turning now to the conservation equation of energy for a control volume, the most frequently used form is Equation IIa.3.12 derived in Chapter IIIa and repeated below:

$$\sum_i \dot{m}_i \left(h_i + V_i^2 / 2 + gZ_i \right) + \sum \dot{Q} + \dot{q}''' V = \sum \dot{W}_s + P\dot{V}$$

$$\sum_e \dot{m}_e \left(h_e + V_e^2 / 2 + gZ_e \right) + \frac{d}{dt} \left[m \left(u + V^2 / 2 + gZ \right) \right] \quad \text{IIa.6.3}$$

where we have considered only two work terms; the shaft work and the work associated with the change in the boundary of the control volume. Also, the rate of internal heat generation is explicitly accounted for. Equation IIa.6.3 as written for a control volume is equivalent to Equation IIa.6.1, written for a control mass.

Equation IIa.6.3 expresses the fact that the rate of change of total energy of a control volume depends on the rate of net energy entering and leaving the control volume as well as the rate of heat and work exchanged with the surroundings. The last term in the right side is the rate of change of total energy of the control volume, $dE_{C.V.}/dt$.

Equation IIa.6.3 in terms of the control volume enthalpy is obtained by substituting for $u = h - Pv$ to get:

$$\sum_i \dot{m}_i \left(h_i + V_i^2 / 2 + gZ_i \right) + \sum \dot{Q} + \dot{q}''' V =$$

$$\sum \dot{W}_s + V\dot{P} + \sum_e \dot{m}_e \left(h_e + V_e^2 / 2 + gZ_e \right) + \frac{d}{dt} \left[m \left(h + V^2 / 2 + gZ \right) \right] \quad \text{IIa.6.3-1}$$

We simplify Equation IIa.6.3 or IIa.6.3-1 for cases where changes in *K.E.* and *P.E.* energies are negligible:

$$\sum_i \dot{m}_i h_i + \sum \dot{Q} = \sum \dot{W}_s + P\dot{V} + \sum_e \dot{m}_e h_e + \frac{d(mu)}{dt} \quad \text{IIa.6.4}$$

$$\sum_i \dot{m}_i h_i + \sum \dot{Q} = \sum \dot{W}_s + V\dot{P} + \sum_e \dot{m}_e h_e + \frac{d(mh)}{dt} \quad \text{IIa.6.4-1}$$

where in these equations, $\sum \dot{Q}$ now includes three major terms; the rate of heat addition to the control volume from all external sources, the rate of internal heat generation in the control volume from all internal sources, and the rate of heat removal from the control volume:

$$\sum \dot{Q} = \sum \left(\begin{array}{c} \text{Rate of heat addition} \\ \text{from all external sources} \end{array} \right) + \sum \left(\begin{array}{c} \text{Rate of Internal} \\ \text{Heat Generation} \end{array} \right) - \sum \left(\begin{array}{c} \text{Rate of heat removal} \\ \text{from the control volume} \end{array} \right)$$

Steady state analysis: We now consider a case where in Figure IIa.5.1, the rates of either accumulation or depletion of mass and energy are zero. If there is no accumulation or depletion of mass and energy and the boundary is fixed or the pressure work is negligible, Equation IIa.6.3 predicts that:

$$\sum_i \dot{m}_i \left(h_i + V_1^2 / 2 + gZ_i \right) + \sum \dot{Q} = \sum \dot{W}_s + \sum_e \dot{m}_e \left(h_e + V_2^2 / 2 + gZ_e \right) \quad \text{IIa.6.5}$$

If the *K.E.* and *P.E.* of the entering and exiting streams are negligible, Equation IIa.6.5 simplifies to:

$$\sum_i \dot{m}_i h_i + \sum \dot{Q} = \sum \dot{W}_s + \sum_e \dot{m}_e h_e \quad \text{IIa.6.6}$$

where Equation IIa.6.6 is the steady state form of Equation IIa.6.4 with no pressure work. Equation IIa.6.6 can be further simplified if there is no heat or work transfer involved in a process. This is demonstrated in the next section by applying the conservation equations of mass and energy to several important thermofluid systems.

7. Applications of the First Law, Steady State

We now proceed to examine the application of the conservation equation of energy in various thermofluid systems such as nozzles, diffusers, turbines, compressors, pumps, heat exchangers, and valves. It must be emphasized that the application of the conservation equation of energy is generally associated with the use of the conservation equation of mass and the equation of state. We begin by introducing various terms.

7.1. Definition of Terms

Nozzles are flow paths with decreasing flow area, hence, increasing velocity in the flow direction (Equation IIa.5.2 for equal densities yields $V_2 = V_1 A_1 / A_2$) as shown in the left side of Figure IIa.7.1.

Diffusers are reverse nozzles, as shown in the right-hand side of Figure IIa.7.1. A diffuser is then a flow path with increasing flow area in the flow direction. Among various applications for nozzles and diffusers is flow measurement as with a flow orifice, a nozzle plate or by using the combined nozzle-diffuser in venturi meters.

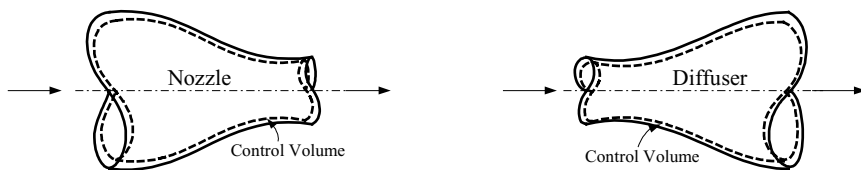


Figure IIa.7.1. Schematics of nozzle and diffuser

Turbines are mechanical devices that convert the energy of the working fluid to shaft work. Electric power is produced when the shaft work is delivered to the

rotor of a generator in a magnetic field. Turbines, if used in jet engines, deliver the shaft work to the compressor. The compressed air is then energized in the combustion chamber. A small percentage of the gas energy is used in the turbine to produce shaft work for the compressor. The rest leaves the jet engine in the form of rapid gas discharge to produce propulsion for the aircraft. A schematic of a turbine is shown in the left side of Figure IIa.7.2.

Compressors use shaft work to pressurize gases. Like turbines, the change in the potential energy from the inlet to the outlet of compressors is negligible. This is in comparison with the compression work delivered to the system. For well-insulated compressors, the rate of heat loss is also negligible. Schematic of a compressor is shown in the right side of Figure IIa.7.2.

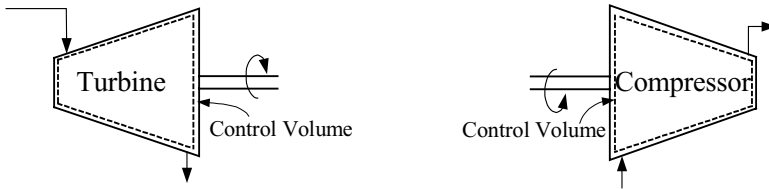


Figure IIa.7.2. Schematics of Turbine and Compressor

Pumps, like compressors, use shaft work to pressurize the working fluid, which is in the liquid phase. While the pumps and compressors perform identical functions, the difference between the density of gases and liquids results in drastic design differences for the device.

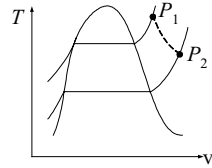
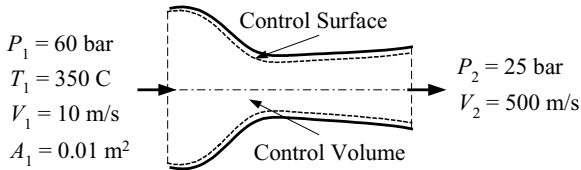
Heat exchangers are devices to transfer heat from a warmer to a colder fluid. Generally, in heat exchangers, the two streams of fluids do not mix; rather heat is transferred indirectly through tube walls or plates separating the streams. A heat exchanger in which the streams are mixed is called an open feedwater heater. Heat exchanger is a generic term which covers such diverse classes of devices as steam generators, condensers, radiators, boilers, intercoolers, and feedwater heaters.

Valves consist of a wide variety of devices to isolate or regulate flow or to control pressure. Gate valves isolate the flow, globe, ball, and butterfly valve regulate the flow, check valves prevent reverse flow, and safety and relief valves control pressure.

7.2. Conservation of Mass & Energy; Nozzles

The flow parameters that are most affected by passing through nozzles and diffusers are flow velocity and pressure. We, therefore, would have to consider change in kinetic energy. There is no work transfer and, if nozzles and diffusers are well insulated, there is also no heat transfer.

Example IIa.7.1. Steam enters a nozzle at 60 bar and 350 C and leaves through the diffuser at 25 bar at steady state condition. Use the data given below to find the outlet flow area, A_2 . The device is insulated.



Solution: We have 3 equations and 3 unknowns. The unknowns are mass flow rate, outlet temperature, and outlet flow area. The equations are the conservation equations of mass and energy as well as the equation of state. In the absence of heat and work, and in steady state steady flow conditions, Equation IIa.6.5 simplifies to:

$$h_1 + V_1^2 / 2 = h_2 + V_2^2 / 2$$

At 60 bar and 350 C for superheated steam we find $v_1 = 0.0423 \text{ m}^3/\text{kg}$ and $h_1 = 3043.67 \text{ kJ/kg}$. Substituting in the energy equation, we find, $h_2 = 3043.67 + (10^2 - 500^2)/2000 = 2918.7 \text{ kJ/kg}$. Having P_2 and h_2 , from the steam tables we obtain $v_2 = 0.0907 \text{ m}^3/\text{kg}$ and $T_2 = 264.5 \text{ C}$. From mass balance between inlet and outlet of the control volume we obtain:

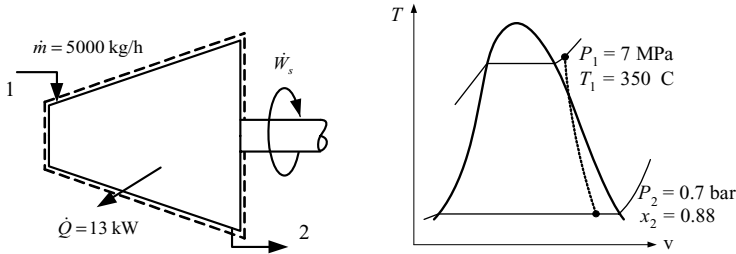
$$\dot{m} = \rho_1 V_1 A_1 = \rho_2 V_2 A_2$$

Substituting, $(10 \times 0.01) / 0.0423 = (500 \times A_2) / 0.0907$, we find $A_2 = 4.3 \text{ cm}^2$.

7.3. Conservation of Mass & Energy; Turbines

In turbines the potential and kinetic energy changes are generally negligible. Since turbines are insulated, the rate of heat transfer from turbines to the surroundings is also negligible compared to other terms in the energy equation.

Example IIa.7.2. Superheated steam enters a turbine at 7 MPa, 350 C, and a mass flow rate of 5000 kg/h. Steam leaves the turbine at 7 bar and a quality of 88%. The heat loss from the turbine is 13 kW. Calculate the rate of shaft work developed by the turbine.



Solution: To find the power output, we use Equation IIa.6.6:

$$\dot{m}_1 h_1 - \dot{Q} = \dot{W}_s + \dot{m}_2 h_2$$

We need to find the inlet and exit enthalpies. At state 1, for superheated steam we find $h_1 = 3016.6$ kJ/kg and at state 2, for a saturated mixture we find $h_{f2} = 376.47$ kJ/kg and $h_{fg2} = 2283.23$ kJ/kg. Having steam quality of $x_2 = 0.88$, $h_2 = 376.47 + 0.88 \times 2283.23 = 2359.31$ kJ/kg. From the conservation of mass we have $\dot{m}_1 = \dot{m}_2$. The rate of shaft work can then be calculated from Equation IIa.6.6 as:

$$(5000/3600) \times 3016.6 - 13 = \dot{W}_s + (5000/3600) \times 2359.3$$

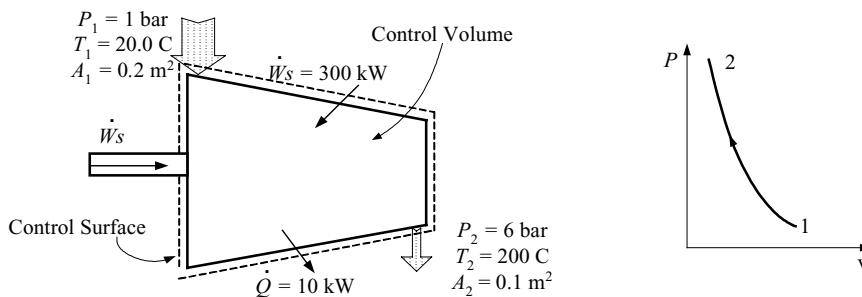
or $\dot{W} \approx 900$ kW. Note that the rate of heat loss to the surroundings is assigned a minus sign.

Ignoring heat loss, it is seen that the power produced by a turbine $\dot{W}_s = \dot{m}(h_i - h_e)$ depends on the mass flow rate and the change in enthalpy. To increase power for a fixed mass flow rate, we need to increase h_i and to lower h_e . Raising pressure, raising temperature, or raising both pressure and temperature can increase inlet enthalpy, h_i . The effects of raising P_i and T_i are discussed in Chapter IIb. The outlet enthalpy can also be reduced by lowering pressure at the outlet. This is the key feature in the design of condensers. Also note that in the design of steam turbines, it is important to ensure that dry steam flows in various stages of the turbine as moisture associated with the low-quality steam causes corrosion damage to turbine blades.

7.4. Conservation of Mass & Energy; Compressors

There are varieties of compressors to pressurize gases, including axial flow, reciprocating, rotary blower, sliding-vane, and screw-type rotary compressors.

Example IIa.7.3 . Find the mass flow rate delivered by a 300 kW air compressor with a compression ratio of 6. The maximum rate of heat loss from the compressor is estimated as 10 kW. Treat air as an ideal gas.



Solution: To find the mass flow rate, we consider a steady state condition and treat air as an ideal gas. Not having the velocities, we first assume that the change in kinetic energy is negligible. Equation Ila.6.6 simplifies to:

$$\dot{m}_1 h_1 - \dot{Q} = -\dot{W}_s + \dot{m}_2 h_2$$

From mass balance, we find that $\dot{m}_1 = \dot{m}_2 = \dot{m}$. We also note that both \dot{Q} and \dot{W} terms have minus signs as heat is lost to the surroundings and work is delivered to the system. We then solve for mass flow rate:

$$\dot{m} = \frac{\dot{W}_s - \dot{Q}}{c_p(T_2 - T_1)} = \frac{300 - 10}{1.0035(200 - 20)} = 1.6 \text{ kg/s}$$

Now we can back calculate velocities. For this, we need to find specific volumes:

$$v_1 = \frac{R_u T_1}{MP_1} = \frac{8314(20 + 273)}{28.97 \times (1 \times 10^5)} = 0.84 \text{ m}^3/\text{kg} \text{ and}$$

$$v_2 = \frac{R_u T_2}{MP_2} = \frac{8314(200 + 273)}{28.97 \times (6 \times 10^5)} = 0.226 \text{ m}^3/\text{kg}$$

We find velocities from $V = \dot{m}v / A$. At the inlet, $V_1 = 1.6 \times 0.84 / 0.2 = 6.72 \text{ m/s}$. At the outlet $V_2 = 3.62 \text{ m/s}$.

The change in kinetic energy is $[(3.62)^2 - (6.72)^2]/2 = 16 \text{ kW/kg}$. This is about 9% of the change in enthalpy. We should then correct the mass flow rate in Equation Ila.6.6 by including the inlet and exit kinetic energies:

$$\dot{m}(h_i + \frac{V_i^2}{2}) - \dot{Q} = -\dot{W}_s + \dot{m}(h_e + \frac{V_e^2}{2})$$

Solving for the mass flow rate:

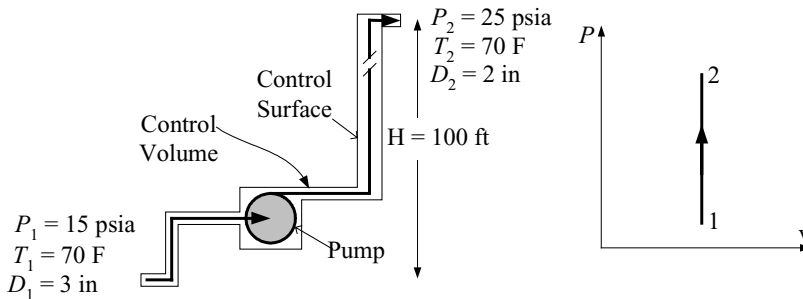
$$\dot{m} = \frac{\dot{W}_s - \dot{Q}}{c_p(T_e - T_i) + (V_e^2 - V_i^2)/2}$$

Substituting, we find the updated mass flow rate as $\dot{m} = 1.76 \text{ kg/s}$. We then update the change in kinetic energy and continue the iteration until we find the final mass flow rate as 1.81 kg/s .

7.5. Conservation of Mass & Energy; Pumps

The same fundamentals applied to compressors are applicable to pumps. However, pumps pressurize liquids with much higher density than gases. Therefore, the change in the potential energy of the liquid is substantial and must be considered in the energy equation.

Example IIa.7.4. Find the pumping power for steady flow of 360 gpm water in the pipeline below. Ignore frictional losses.



Solution: We should use Equation IIa.6.5:

$$\dot{m}(h_i + V_i^2/2 + gZ_i) - \dot{Q} = -\dot{W}_s + \dot{m}(h_e + V_e^2/2 + gZ_e)$$

For subcooled water, density and specific volume are practically functions of temperature. Hence, from the steam tables, $v_1 = v_2 = 0.01605 \text{ ft}^3/\text{lbm}$. Also, $h_1 = 38.09 \text{ Btu/lbm}$ and $h_2 = 38.12 \text{ Btu/lbm}$. Note that;

$$h_2 - h_1 \approx [h_f + v_f(P - P_{sat})]_2 - [h_f + v_f(P - P_{sat})]_1 = v_f(T)(P_2 - P_1)$$

We can verify this by substituting $h_2 - h_1 = 38.12 - 38.09 = 0.03 \text{ Btu/lbm}$.

Also $v_f(P_2 - P_1) = 0.01605(25 - 15) \times (144/778) = 0.0297 \text{ Btu/lbm}$. Hence, for pumps:

$$\Delta h_{\text{pump}} \cong v_f(T)\Delta P_{\text{pump}} \quad \text{IIa.6.7}$$

Let's now calculate the change in kinetic energy. For this, we need the inlet and outlet velocities. These can be found from $\dot{m} = \rho_1 V_1 A_1 = \rho_2 V_2 A_2$. The volumetric flow rate is $360/(60 \times 7.481) = 0.8 \text{ ft}^3/\text{s}$. Inlet flow area is $A_1 = \pi D_1^2/4 = 0.049 \text{ ft}^2$. Therefore, the inlet velocity becomes $V_1 = 0.8/0.049 = 16.3 \text{ ft/s}$. The outlet flow area is $A_2 = \pi D_2^2/4 = 0.0218 \text{ ft}^2$ and $V_2 = 36.67 \text{ ft/s}$. The change in kinetic energy is:

$$(V_2^2 - V_1^2)/2 = [36.67^2 - 16.3^2]/(2 \times 32.2 \times 778) = 0.02 \text{ Btu/lbm}$$

We now find the change in potential energy;

$$g\Delta z = 32.2 \times 100/32.2 = 100 \text{ ft} \cdot \text{lbf} = 100/778 = 0.128 \text{ Btu/lbm}$$

Substituting into Equation IIa.6.5 and setting the rate of heat loss equal to zero, yields:

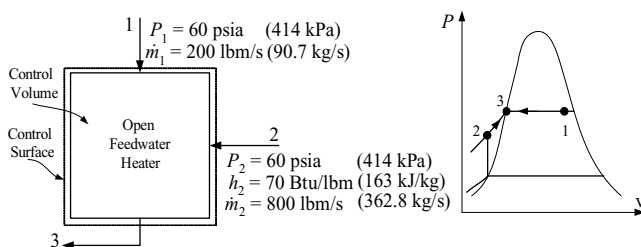
$$\dot{W}_s = (0.8/0.01605)[0.03 + 0.02 + 0.128] = 8.9 \text{ Btu/s}$$

A power of 8.9 Btu/s = 32036 Btu/h = 9.4 kW = 12.6 hp should be delivered to the pump. Actual power needed by the pump is more than 12.6 hp due to the mechanical and hydraulic losses in the pump, as discussed in Chapter VIc.

7.6. Conservation of Mass & Energy; Heat Exchangers

To demonstrate the conservation of mass and energy equations for heat exchangers, two examples are presented here. The first example deals with an open feedwater heater (also referred to as deaerator), in which the incoming streams mix.

Example IIa.7.5. Steam at quality x enters an open feedwater heater and after mixing with subcooled water, leaves as saturated water. Find the steam quality at the inlet port of the feedwater heater.



Solution: For steady state operation, we use Equation IIa.5.4 for mass balance:

$$\dot{m}_1 + \dot{m}_2 = \dot{m}_3$$

Also from Equation IIa.6.6 for energy balance, with the rate of shaft work, the rate of heat loss, and the rate of change in the kinetic and potential energies set to zero we find:

$$\dot{m}_1 h_1 + \dot{m}_2 h_2 = \dot{m}_3 h_3$$

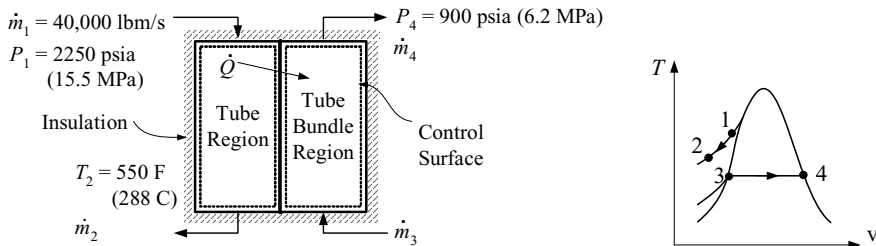
From the steam tables, $h_3 = h_f(60 \text{ psia}) = 262.2 \text{ Btu/lbm}$ and $h_{fg}(60 \text{ psia}) = 915.4 \text{ Btu/lbm}$. Hence:

$$200(262.2 + 915.4 x_1) + 800 \times 70 = (200 + 800) \times 262.2$$

Solving for the steam quality, we find $x_1 = 0.84$.

In the next example, we consider a steam generator of a PWR and will apply the conservation equations of mass and energy in conjunction with the equation of state to solve for the unknown parameters.

Example IIa.7.6. Subcooled water flows in the tubes of a steam generator in steady state condition. It leaves tubes with an enthalpy drop of 66.5 Btu/lbm. Find the rate of steam production and the rate of heat transfer from tubes for the given data.



Solution: We use Equation IIa.5.4 for mass balance and Equation IIa.6.6 for energy balance. There is no shaft work and the rate of change in the kinetic and potential energies is negligible. For the tube region:

$$\dot{m}_1 h_1 - \dot{Q} = \dot{m}_2 h_2$$

For the tube bundle region:

$$\dot{m}_3 h_3 + \dot{Q} = \dot{m}_4 h_4$$

Adding these equations and substituting from steady state continuity equation ($\dot{m}_1 = \dot{m}_2$ and $\dot{m}_3 = \dot{m}_4$), we obtain:

$$\dot{m}_1 (h_1 - h_2) = \dot{m}_3 (h_4 - h_3)$$

Since $h_1 - h_2 = 66.5$ Btu/lbm and $h_4 - h_3 = h_{fg}(900 \text{ psia}) = 669.7$ Btu/lbm.

Therefore, the rate of steam production is:

$$\dot{m}_3 = 40,000 \times 66.5 / 669.7 = 3972 \text{ lbm/s}, \approx 14.3 \times 10^6 \text{ lbm/h (1800 kg/s)}.$$

7.7. Conservation of Mass & Energy; Valves

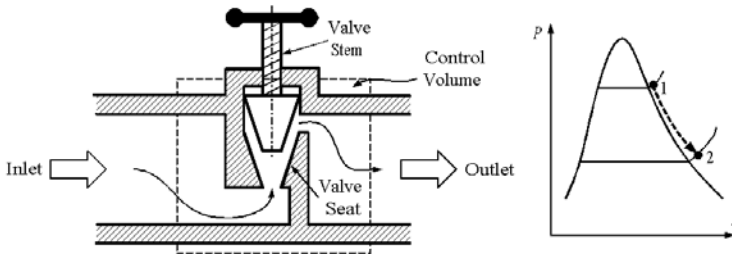
Valves that are used to control or throttle the flow rate accomplish this by introducing pressure drop to the flow. To analyze the effect of a valve on the flow, we may apply the first law of thermodynamics to a control volume taken around the valve. For this control volume, the change in potential energy is negligible. There

is also no work transfer and the rate of heat transfer is negligible, too. Combining the steady state mass and energy balance equations (Equation Ila.6.6), we obtain:

$$h_i + V_i^2 / 2 = h_e + V_e^2 / 2$$

In general, the kinetic energy terms are small compared with the enthalpies. Therefore, the process of flow going through valves and orifices can be considered isoenthalpic $h_i = h_e$

Example Ila.7.7. Steam at 900 kPa, 350 C, and a rate of 500 kg/s flows through a bypass pipe having a diameter of 1 m. The pipe is equipped with a partially open valve through which steam flows in a steady state condition. If the valve causes a 650 kPa pressure drop, find the steam temperature at the valve outlet.



Solution: First, we find h_1 (0.9 MPa & 350 C) = 3158 kJ/kg and $\rho_1 = 1/0.314 = 3.185 \text{ kg/m}^3$. We calculate velocities to show kinetic energies are small as compared with the fluid enthalpy. $A_1 = \pi 1^2 / 4 = 0.785 \text{ m}^2$ so that $V_1 = 500 / (0.785 \times 3.185) = 200 \text{ m/s}$. This amounts to $K.E. = V^2/2 = 200^2/2 = 20 \text{ kJ/kg}$. Thus; $h_2 \approx 3094 \text{ kJ/kg}$. Having $P_2 = 900 - 650 = 250 \text{ kPa}$ and $h_2 = 3094 \text{ kJ/kg}$ by iteration with the steam tables we find a steam temperature of about $T_2 \approx 308.5 \text{ C}$.

In the above example, we dealt with superheated steam entering and leaving the valve. If instead of steam, a liquid was flowing in the pipe and through the valve, we should use extra caution to ensure that the induced pressure drop to the flow would not result in flashing of the liquid. The flashing mechanism or partial vaporization of liquid would change the flow characteristics and may result in cavitation, as described in Chapter VIc.

7.8. Conservation of Mass & Energy; Heating Rigid Vessels of Constant Mass

Consider a rigid vessel containing a two-phase mixture. We want to study the heating of the mixture in this rigid vessel with no mass entering or leaving the system. As shown in Figure Ila.7.3, the vessel is initially at pressure P_1 . The control volume in this case can be viewed as a control mass. Since water and steam coex-

ist in the vessel at equilibrium, both water and steam are saturated at system pressure. Heat is now added until the vessel contains only saturated steam at pressure P_2 . The goal is to find the amount of heat added to the vessel.

The mixture mass and volume have remained the same throughout the heat up process. Therefore, $v_1 = v_2 = V/m$. This isochoric process is shown in the Pv diagram of Figure IIa.7.3.

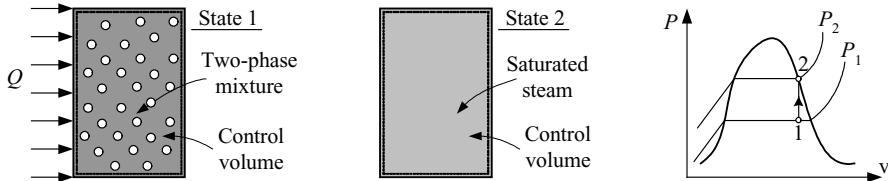


Figure IIa.7.3. Heating up a vessel containing saturated mixture

Before we embark on the solution, we must emphasize an important aspect of dealing with such problems. In Figure IIa.7.3, we have used one control volume to represent the entire mixture in the vessel. Stating that heat is transferred to the vessel implies that the separated regions of water and steam have no explicit meaning when represented with one control volume. Such *lumped* treatment of the problem does not allow specification of whether heat is added to the water or to the steam region. To obtain more details, we should at least assign one control volume to the water region and one to the steam region. To obtain even more information such as the temperature distribution in the water region, we must break down the water region into many more control volumes and apply the mass and energy equations to each control volume. Thus the allocation of only one control volume to the entire vessel implies that water and steam are homogeneously mixed at a given steam quality. This topic is discussed in more details in Section 5 of Chapter VI.

Returning to the heat up of the mixture in a rigid vessel, in order to find the amount of heat transfer to the vessel (Q), we must find at least two properties at state 2 in Figure IIa.7.3. In the case of Figure IIa.7.3 where only heat is added to the system, the vessel can be treated as a closed system. Thus, from the continuity equation we find that $m_2 = m_1 = m$. The first state property is v_2 since we know V and m hence, $v_2 = V/m$. The second property is obtained from the fact that fluid is saturated steam at P_2 (i.e., the steam quality at state 2 is $x_2 = 100\%$). If we have a function for $v_2 = f(P_2)$, we can solve for P_2 . Otherwise, we use the steam tables for $P_2 = P_g(v_g = v_2)$.

Having thermodynamic properties of both states 1 and 2, we can find heat transfer from the conservation equation of energy. The energy equation IIa.6.2 can be simplified for the following reasons. First, the work term drops as the closed system also has rigid boundary. Second, the kinetic energy terms drop as the system is at rest. Finally, the change in the potential energy (due to the change in mixture density) is negligible compared with the change in the internal energy. Therefore, Equation IIa.6.2 becomes:

$$Q_{12} = U_2 - U_1$$

It must be emphasized that, in practice, tanks must be equipped with pressure-relief valves as heating up an isolated tank would eventually lead to catastrophic failure of the tank. Rapid pressurization occurs if tanks are filled with liquids due to the lack of compressibility of the so-called “water-solid” systems.

Example Ila.7.8. A tank of 1500 ft^3 (42.5 m^3) contains steam at $P_1 = 1000 \text{ psia}$ (7 MPa) and $x_1 = 0.25$. Heat is added to the tank until steam quality becomes $x_2 = 100\%$. Find the heat transfer to the tank.

Solution: This is a closed system for which mass remains constant during the heat up process. Also the tank is rigid so volume remains constant. Hence, $v_1 = v_2$. To find mass and initial internal energy, we obtain:

P (psia)	v_f (ft ³ /lbm)	v_{fg} (ft ³ /lbm)	u_f (Btu/lbm)	u_{fg} (Btu/lbm)
1000	0.02159	0.42436	538.6	110.4

Hence, $v_1 = 0.02159 + 0.25(0.42436) = 0.12768 \text{ ft}^3/\text{lbm}$. This gives $m = V/v_1 = 1500/0.12768 = 11748 \text{ lbm}$. Also $u_1 = 538.6 + 0.25(1110.4) = 816.2 \text{ Btu/lbm}$. Since $v_2 = v_1 = 0.12768$ and the final state is saturated steam; $P_2 = P_g(v_2) = P_g(v = 0.12768 \text{ ft}^3/\text{lbm})$

A search in the steam tables for $v_g = v = 0.12768 \text{ ft}^3/\text{lbm}$ gives $P_2 = 2530 \text{ psia}$. At this pressure, $u_2 = u_g(P = 2530 \text{ psia}) = 1030 \text{ Btu/lbm}$. Hence, $Q = m(u_2 - u_1) = 11748(1030 - 816.2) = 2.5\text{E}6 \text{ Btu}$ ($2.64\text{E}6 \text{ kJ}$).

Could have we solved this problem if we were only told that state 2 was superheated steam at $P = 1000 \text{ psia}$?

7.9. Conservation of Mass & Energy; Heating Rigid Vessels at Constant Pressure

Let's now consider boiling water in a rigid vessel as shown in Figure Ila.7.4. The vessel is equipped with a control valve to discharge steam and maintain pressure at a desired value. To determine the steaming rate, we allocate two control volumes to the water and the steam regions. The makeup water, also known as *feed-water* is added to the vessel to maintain water level at a desired value. If there was no make up water to replenish the loss of inventory, the vessel would dry out. Heating up water in a vessel without providing any makeup water constitutes a transient problem. To have a heat addition process at steady flow and steady state condition, makeup water is added so that the mass flow rate of steam becomes exactly equal to the mass flow rate of the makeup water. This is shown in Figure Ila.7.4(a). The make up water may be subcooled as shown in Figure Ila.7.4(b) or saturated as shown in Figure Ila.7.4(c). If the makeup water is subcooled some of the heat is used to bring the subcooled water to saturation.

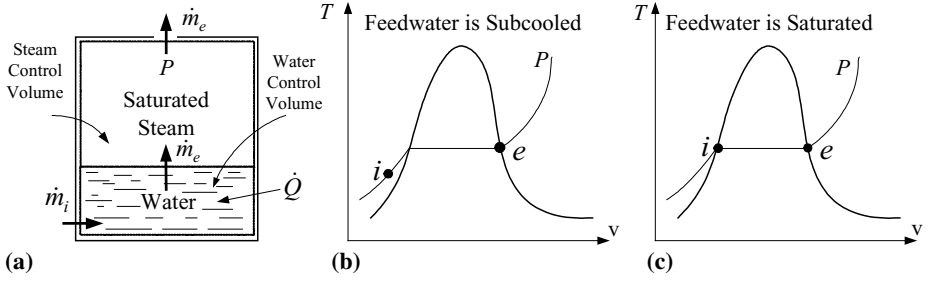


Figure IIa.7.4. Adding heat to a vessel at constant pressure

From the conservation equation of mass for steady flow and steady state conditions, $\dot{m}_i = \dot{m}_e = \dot{m}$. Also from the conservation equation of energy, $\dot{m}_i h_i + \dot{Q}_i = \dot{m}_e h_e$. Therefore, the steaming rate is found as:

$$\dot{m} = \frac{\dot{Q}}{h_g(P) - h_i} \quad \text{IIa.7.1}$$

As shown in Figure IIa.7.2-c, if the feedwater is saturated at pressure P ($h_i = h_f$), Equation IIa.7.1 reduces to:

$$\dot{m} = \frac{\dot{Q}}{h_{fg}(P)} \quad \text{IIa.7.2}$$

Note that, for a given rate of heat transfer, the steaming rate at a higher pressure is higher than the steaming rate at a lower pressure. This is due to the decrease in the latent heat of vaporization of water as pressure increases (Figure IIa.3.4).

8. Applications of the First Law, Transient

In practice, prior to establishment of steady state conditions, unsteady state or transient operation prevails. Transient operation can also be imposed on a system operating at a steady state condition. Consider for example, the steady flow of steam in a pipe when a fully open valve is throttled to a new partially open position. The flow of steam goes through a transient to reach a new steady state condition corresponding to the new position of the valve. We solve transient problems similar to problems for steady state condition by using the conservation equations of mass and energy as well as the equation of state. For a process that brings the control volume from state 1 at time t_1 to state 2 at time t_2 , we find the mass at state 2 by integrating Equation IIa.5.1:

$$\int_{t=t_1}^{t=t_2} \left(\sum_{inlet} \dot{m}_i \right) dt = \int_{t=t_1}^{t=t_2} \left(\sum_{outlet} \dot{m}_e \right) dt + [m(t_2) - m(t_1)] \quad \text{IIa.8.1}$$

Example IIa.8.1. Water is flowing in a 6 cm inside diameter pipe at a velocity of 0.75 m/s. The pipe discharges into an initially empty tank having a volume of 0.3 m³. How long will it take to fill the tank?

Solution: We first find the mass flow rate of water at atmospheric condition ($v = 0.001 \text{ m}^3/\text{kg}$) as:

$$\dot{m}_{in} = VA/v = 0.75 \times [\pi(0.06)^2/4]/0.001 = 2.12 \text{ kg/s.}$$

From Equation IIa.5.3 we have; $dm/dt = \dot{m}_{in} - \dot{m}_{out} = 2.12 - 0 = 2.12 \text{ kg/s.}$

Hence, $dm = 2.12dt$. Integrating: $m_2 - m_1 = 2.12t$. Since $m_1 = 0$, and $m_2 = V_{\text{tank}}/v = 0.3/0.001 = 300 \text{ kg}$, we find $t = 300/2.12 = 141 \text{ s.}$

Similarly, we find the internal energy of the control volume at state 2 by integrating Equation IIa.6.4:

$$\int_{t=t_1}^{t=t_2} \left(\sum_{inlet} \dot{m}_i h_i \right) dt - \int_{t=t_1}^{t=t_2} \left(\sum_{inlet} \dot{Q} \right) dt = \int_{t=t_1}^{t=t_2} \left(\sum \dot{W}_s \right) dt + \int_{t=t_1}^{t=t_2} \left(\sum_{outlet} \dot{m}_e h_e \right) dt + [m(t_2)u(t_2) - m(t_1)u(t_1)] \quad \text{IIa.8.2.}$$

ignoring changes in the *K.E.* and *P.E.* In the following examples, simple transient cases involving filling and draining containers are discussed. These include both cases of liquid and gas.

8.1. Dynamics of Mixing Tanks

Shown in Figure IIa.8.1 is a simple case of simultaneous filling and draining a heated mixing tank at atmospheric pressure. The tank is fed through several inlet ports. The shaft work is performed by the mixer and a heater may add heat to the water in the tank. Using the conservation equations of mass and energy, we can obtain two parameters in terms of other known data. For example, if the inlet mass flow rates, inlet enthalpies, mixer power, and the heater power are specified, we can solve for the mass and temperature of the tank water versus time. To perform this analysis, we make several assumptions: a) negligible *K.E.* and *P.E.* changes, b) perfect and instantaneous mixing, c) subcooled water in the tank throughout the process, d) no chemical reactions, e) no heat loss from the tank,

and f) constant tank pressure throughout the process. Applying these assumptions, Equation IIa.6.4-1 becomes:

$$\sum_1^N \dot{m}_i h_i + \dot{Q} = -\dot{W}_s + \dot{m}_e h_e + \frac{d(mh)_{C.V.}}{dt}$$

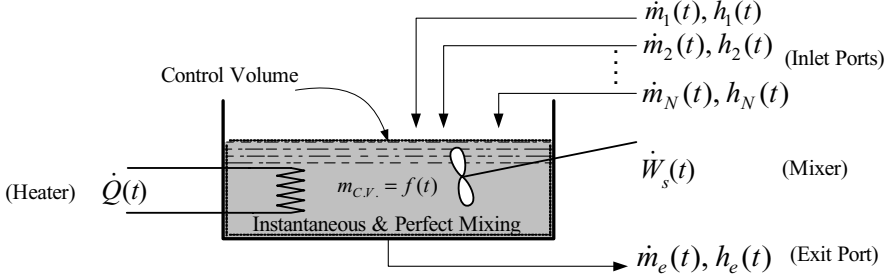


Figure IIa.8.1. Schematic of a simple mixing tank

We now take the derivative of the last term in the right side and substitute from Equation IIa.5.1 to find

$$\frac{dh_e}{dt} + \left(\frac{1}{m_{C.V.}} \sum_1^N \dot{m}_i \right) h_e = \frac{\dot{Q} + \dot{W}_s + \sum_1^N \dot{m}_i h_i}{m_{C.V.}} \quad \text{IIa.8.3}$$

where we used the perfect mixing assumption, which implies that $h_e = h_{C.V.}$. The mass of water in the tank is a function of time. For example for constant mass flow rates into and out of the tank, Equation IIa.5.1 predicts that the tank water mass varies linearly with time:

$$(m)_{C.V.} = (m_o)_{C.V.} + \left(\sum_i \dot{m}_i - \dot{m}_e \right) t$$

where $(m_o)_{C.V.}$ is the initial mass of water in the tank. Upon substitution of $(m)_{C.V.}$ into Equation IIa.8.3, we obtain a linear first-order differential equation for h_e . A general solution to such differential equations is given by Equation VIIb.2.4. Depending on the complexity of the functions representing the heater power, the shaft work, the inlet and exit mass flow rates, we may have to resort to numerical solutions, from which we obtain:

$$\text{Explicit: } h_e^{n+1} = h_e^n + \frac{\dot{Q}^n + \dot{W}_s^n + \sum_1^N \dot{m}_i^n (h_i^n - h_e^n)}{(m^n / \Delta t)};$$

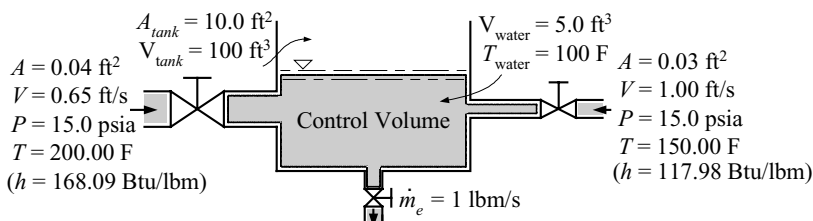
$$\text{Implicit: } h_e^{n+1} = h_e^n + \frac{\dot{Q}^n + \dot{W}_s^n + \sum_1^N \dot{m}_i^n (h_i^n - h_e^n)}{(m^n / \Delta t) + \sum_1^N \dot{m}_i^n}$$

where n is a time step index. In the above solution, a *semi-implicit* scheme is used (see Chapter VIIe and Problem 101).

Recall that for subcooled water $dh \cong c_p dT$. Assuming constant specific heat and substituting in the explicit scheme, for example, we find the water temperature at every time stop as:

$$T_e^{n+1} = T_e^n + \frac{\dot{Q}^n + \dot{W}_s^n + \sum_1^N \dot{m}_i^n (T_i^n - T_e^n)}{(m^n / \Delta t) c_p} \quad \text{IIa.8.4}$$

Example IIa.8.2. Flow enters a fully insulated tank from two inlet ports and leaves through one outlet port. Find water level in 30 minutes. Assume instantaneous and perfect mixing. Tank volume is 100 ft^3 , cross sectional area is 10 ft^2 , initial water volume is 5 ft^3 , and initial water temperature in the tank is $T_{\text{tank}} = 100 \text{ F}$.

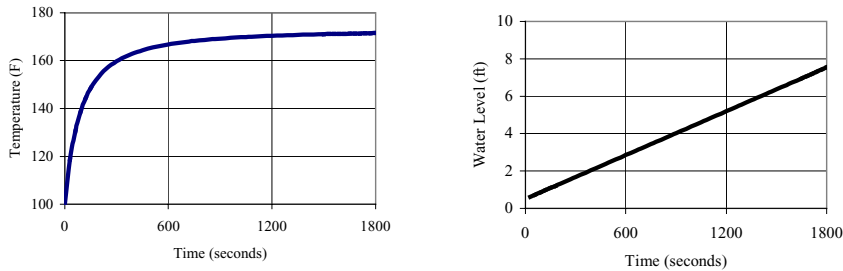


Solution: To find water level as a function of time, we first need to find water volume by dividing the mass of water by the density of water in the tank. Water level is then obtained by dividing water volume by the tank cross sectional area. Since there is no heat or work transfer to or from the control volume, temperature of water at each time step is found from the simplified form of Equation IIa.8.4:

$$T_e^{n+1} = T_e^n + \frac{\rho_1 V_1 A_1 (T_1 - T_e^n) + \rho_2 V_2 A_2 (T_2 - T_e^n)}{(m^n / \Delta t) c_p}$$

where we assumed constant specific heat. Initially (i.e., at time zero $n = 0$), the temperature, mass, and level of the tank water are $T_e^{n=0} = 100 \text{ F}$, $m^{n=0} = 5 \text{ ft}^3 \times 62 \text{ lbm/ft}^3 = 310.56 \text{ lbm}$, and $L^{n=0} = 0.5 \text{ ft}$, respectively. We now choose a time step size of $\Delta t = 0.1 \text{ s}$, for example, and find $T_e^{n=1}$ at $t = 0 + 0.1 = 0.1 \text{ s}$. Having found $T_e^{n=1}$, we proceed to find $T_e^{n=2}$ for time $t = 0.2 \text{ s}$. We continue this process until $t = 1800 \text{ s}$. The FORTRAN program representing the numerical solution is included on the accompanying CD-ROM. From the program we find that in 30

minutes, water temperature reaches to about 171.4 F at a level of 7.5 ft from the bottom of the tank, as plotted in the figure.



8.2. Charging Rigid Vessels (Fixed C.V.) with Gas

Shown in Figure IIa.8.2(a) is a tank connected to a charging line carrying pressurized gas at a known temperature. Initially, the intake valve is closed and the tank containing the same gas is at pressure P_1 and temperature T_1 . Figure IIa.8.2(b) shows the condition in the tank after the intake valve is opened. Figure IIa.8.2(c) shows the final state when the intake valve is closed. For a given initial condition of the vessel and the inlet enthalpy of the filling gas, we identify two cases to solve. In case A, having final pressure in the tank, we want to find the final gas temperature and the average gas mass flow rate entering the tank. In case B, for a given average mass flow rate of the filling gas, we want to find final pressure and temperature of the gas in the tank.

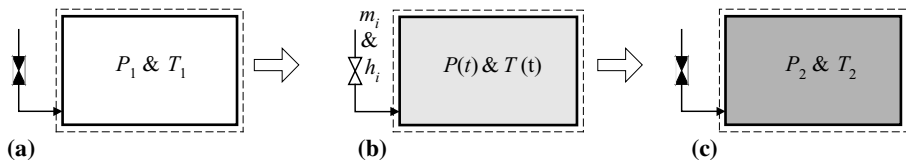


Figure IIa.8.2. Charging rigid vessels with gas and the associated control volume

Case A. For Given P_2 , Find T_2 and \bar{m}_i :

As shown in Figure IIa.8.2, the control volume representing the rigid tank contains air and is initially at pressure P_1 and temperature T_1 . The intake valve is opened to allow the flow of air into the tank from a high-pressure source. The valve is closed when the pressure in the tank reaches the specified value of P_2 . The goal is to find the average mass flow rate of air entering the tank during the charging process.

In this case, there is no heat transfer, no shaft work, and no mass leaving the control volume. Therefore, Equation IIa.6.6 simplifies to:

$$\frac{d(mu)_{C.V.}}{dt} = \dot{m}_i h_i$$

From the conservation equation of mass (Equation IIa.5.1) we have $dm_{C.V.}/dt = \dot{m}_i$. Substituting, we get:

$$\frac{d(mu)_{C.V.}}{dt} = h_i \frac{dm_{C.V.}}{dt}$$

Treating air as an ideal gas ($du = c_v dT$), h_i as a constant, and integrating from the initial state (P_1 and T_1) to the final state where P_2 is specified yields:

$$m_2 c_v T_2 - m_1 c_v T_1 = h_i \int_1^2 dm_{C.V.} = h_i (m_2 - m_1)$$

So far, we have one equation and two unknowns, m_2 and T_2 . We increase the number of equations by using the equation of state for state 2:

$$P_2 V = m_2 R_u T_2 / M_{air}$$

where $V_2 = V_1 = V$. Substituting for $m_2 T_2$ from the equation of state in the energy equation we find m_2 :

$$m_2 = \frac{P_2 V c_v (M_{air} / R_u) + m_1 (h_i - c_v T_1)}{h_i} \quad \text{IIa.8.4}$$

Total mass entering the tank is therefore $m_i = m_2 - m_1$ and the average mass flow rate is found from

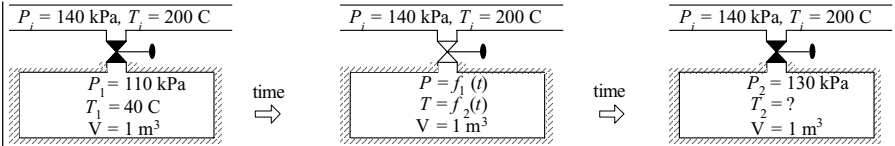
$$\bar{m}_i = m_i / \tau$$

where τ is the time it took to bring the tank pressure from P_1 to P_2 . By eliminating m_2 between the energy equation and the equation of state, we can also obtain an expression for T_2 as:

$$T_2 = \left[\left(1 - \frac{P_1}{P_2}\right) \frac{1}{\gamma T_i} + \frac{P_1}{P_2} \frac{1}{T_1} \right]^{-1} \quad \text{IIa.8.5}$$

where we have substituted for $h_i = c_p T_i$ and then $\gamma = c_p / c_v$.

Example II.8.3. A well-insulated tank contains air at 110 kPa and 40°C with the isolation valve closed. We now open the valve and let pressurized air enter the tank. We close the valve in 6 seconds when pressure in the tank reaches 130 kPa. Find the amount of air that has entered the tank. $M_{air} = 28.97 \text{ kg/kmol}$.



Solution: $P_1 = 110 \text{ kPa}$, $T_1 = 40 \text{ C}$ (313 K), $V = 1 \text{ m}^3$. Initial mass of air in the tank is:

$$m_1 = P_1 V / RT_1 = 110 \times 1 / [(8.314/28.97) \times 313] = 1.22 \text{ kg}$$

We find h_i , assuming constant c_p :

$$h_i - h_{ref} = c_p(T_i - T_{ref}) = 1.0(200 + 273 - 0) = 473 \text{ kJ/kg (note } h_{ref} = 0 \text{ at } T_{ref} = 0 \text{ K)}.$$

To find m_2 , we may use Equation IIa.8.4 (or find T_2 from Equation IIa.8.5 then m_2 from $m_2 = P_2 V / RT_2$):

$$m_2 = \frac{[130 \times 1 \times 0.72 \times (28.97 / 8.314)] + 1.22[473 - 0.72 \times (40 + 273)]}{473} = 1.33 \text{ kg}$$

The mass of air entering the tank is therefore $1.33 - 1.22 = 0.11 \text{ kg}$. To find the average flow rate, we divided $m_2 - m_1$ by the charging duration: $0.11/6 \cong 0.02 \text{ kg/s}$. To find T_2 , we use the equation of state:

$$T_2 = P_2 V / m_2 R = 340 \text{ K} = 67.6 \text{ C}.$$

In Example IIa.8.3, we were able to find an analytical solution in a closed form because the working fluid could be treated as an ideal gas, allowing the use of a simple equation of state. The reader may try the above example with steam being the working fluid. In the first try, assume that the container is initially evacuated. In the second try, assume that the container has steam at atmospheric pressure and 121 C (250 F).

Case B. For Given \dot{m}_i , Find P_2 and T_2 :

Given the initial conditions, our goal is to find the final pressure and temperature of a rigid vessel versus time while the vessel is being charged with an ideal gas at a specified mass flow rate and enthalpy. We follow the same procedure as in Case A and this time solve the equation for T_2 :

$$T_2 = (m_1 u_1 + m_i h_i) / (m_1 + m_i) c_v$$

Having T_2 , and m_2 , we can find P_2 .

Example IIa.8.4. A pressure vessel has a volume of 100 ft^3 (2.83 m^3). It contains air at 1000 psia ($\sim 7 \text{ MPa}$) and 150 F (65.5 C). A valve is now opened and highly pressurized air at a rate of 1 lbm/s (0.453 kg/s) and a temperature of 292 F (144.4 C) enters the vessel. Determine the gas pressure and temperature in the vessel after 1 minute of charging. $R_{air} = R_u / M_{air} = 1545/28.97 = 53.33 \text{ ft}\cdot\text{lbf/lbm}\cdot\text{R}$.

Solution: $m_1 = P_1 V / R_{air} T = (1000 \times 144) \times 100 / (53.33 \times 610) = 442.9 \text{ lbm (200 kg)}$

$$T_2 = [442.9 \times 0.171 \times 610 + (1 \times 60) \times 0.24 \times 752] / [(442.9 + 1 \times 60) \times 0.171] = 663 \text{ R} = 203 \text{ F (95 C)}.$$

$$m_2 = m_1 + \bar{m} \Delta t = 442.9 + 1 \times 60 = 502.9 \text{ lbm (228 kg)}$$

$$P_2 = m_2 R_{air} T / V = 502.9 \times 53.33 \times 663 / 100 = 1235 \text{ psia (8.5 MPa)}.$$

8.3. Charging Vessels with Gas (Expanding C.V.)

A cylinder equipped with a frictionless piston contains air at pressure P_1 and temperature of T_1 . Our goal is to find the mass of the air entering the cylinder when the air temperature at the final state reaches T_2 . As shown in Figure IIa.8.3(a), at the initial state (P_1, T_1) the intake valve is closed. In Figure IIa.8.3(b), the intake valve has opened, allowing air to enter the control volume. Figure IIa.8.3(c) shows the final state where the intake valve is again closed and the air temperature has reached T_2 . Since the piston is allowed to move, the pressure of the air in the cylinder remains at P_1 throughout the filling process. The moving boundary also requires accounting for the work performed by the piston moving against the atmospheric pressure.

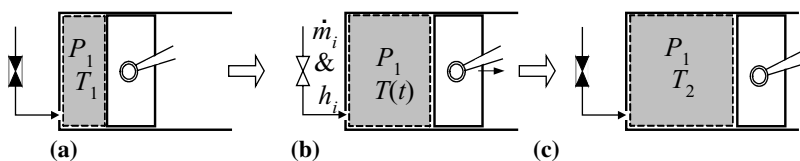


Figure IIa.8.3. Charging expanding control volumes: (a) initial state, (b) filling process, and (c) final state

We now integrate the conservation equations for mass and energy from state 1 to state 2. From the continuity equation, the mass of gas at the final stage is given as:

$$m_2 = m_1 + m_i$$

and from the conservation equation of energy we conclude that:

$$m_1 u_1 + m_i h_i + Q = P(V_2 - V_1) + m_2 u_2$$

We have two equations and three unknowns, m_i , m_2 , and u_2 for specified m_1 , u_1 , h_i , Q , P , V_1 , and V_2 . Treating air as an ideal gas, the equation of state becomes $PV_2 = m_2 RT_2$, which also satisfies the volume constraint ($v_2 = V_2/m_2$). We now solve for m_i :

$$m_i = [c_v P V_2 / R - m_1 u_1 - Q + P(V_2 - V_1)] / h_i \quad \text{IIa.8.6}$$

Example IIa.8.5. A cylinder has an initial volume of 1.0 ft^3 and contains air at 15 psia (0.1 MPa) and 120 F (49 C). Air at 150 psia (1 MPa) and 250 F (121 C) is injected into the cylinder, pushing the piston to a new position where $V_2 = 3V_1$. In the process, 0.2 Btu (211 J) heat is transferred from the cylinder to the surroundings. Find the mass of air entering the cylinder and the final air temperature in the cylinder. $R_{\text{air}} = R_u/M = 1545/28.97 = 53.33 \text{ ft}\cdot\text{lbf/lbm}\cdot\text{R}$ and $c_v = 0.171 \text{ Btu/lbm}\cdot\text{R}$.

Solution: $m_1 = PV_1/RT_1 = (15 \times 144) \times 1/[53.33(460 + 120)] = 0.07 \text{ lbm}$
 $m_i = [0.171 \times (15 \times 144) \times 3/53.33 - 0.07 \times 0.171 \times 580 - (-0.2) + 15 \times 144$
 $(3 - 1)/778]/(0.24 \times 710)$

$m_i = 0.115 \text{ lbm}$ (0.05 kg)

$T_2 = 15 \times 144 \times 3/[(0.07 + 0.115) \times 53.33] = 657 \text{ R} = 197 \text{ F}$ (92 C).

8.4. Discharging Gas-Filled Rigid Vessels (Fixed C.V.)

Determination of the rate of depressurization of vessels filled with fluids under pressure poses a challenging task, especially when the vessel is filled with liquid. Depending on fluid pressure and the rate of discharge, the liquid may change phase and flash to vapor. Vessel depressurization and flow of two-phase mixture through pipes are discussed in Chapter Va. Here we deal with an easier task of analyzing the depressurization of rigid vessels filled with an ideal gas in an isentropic process. For non-isentropic processes, see the accompanying CD-ROM.

The vessel is the control volume. In this ideal process there is no heat transfer and we assume that the depressurization process is reversible. Therefore, from Equation IIa.4.4 we have $Tv^{\gamma} = \text{constant}$. Also the volume constraint requires that $V = mv = \text{constant}$. Taking the derivative of the isentropic relation, we find:

$$\frac{dT}{T} = (1 - \gamma) \frac{dv}{v} \quad \text{IIa.8.7}$$

Similarly, the derivative of the volume constraint yields:

$$\frac{dm}{m} = - \frac{dv}{v} \quad \text{IIa.8.8}$$

Solving these equations simultaneously, we find that at any point in time we have:

$$\frac{m_2}{m_1} = \left(\frac{T_2}{T_1} \right)^{1/(\gamma-1)} \quad \text{IIa.8.9}$$

Substituting from Equation IIa.4.5 into Equation IIa.8.9 yields:

$$\frac{m_2}{m_1} = \left(\frac{P_2}{P_1} \right)^{1/\gamma} \quad \text{IIa.8.10}$$

We may also integrate Equation IIa.8.8 to obtain a relationship between mass and specific volume or between mass and density.

Example IIa.8.6. A tank is filled with air. A valve is opened to vent the tank. If pressure drops to 1/3 of its initial value find a) the mass of the gas left in the tank and b) final air temperature. The process is isentropic. Data: $V = 2 \text{ m}^3$, $P_1 = 6 \text{ bar}$, $T_1 = 230 \text{ C}$. Equilibrium within the tank during the process.

Solution: Treating air as an ideal gas, the initial mass of air is found as:

$$m_1 = \frac{P_1 V}{RT_1} = \frac{6 \times 2}{(0.08314/28.97)(230 + 273)} = 8.313 \text{ kg}$$

a) For the isentropic process $m_2 = \left(\frac{P_2}{P_1}\right)^{1/\gamma} m_1 = 8.313 \times (1/3)^{1/1.4} = 3.79 \text{ kg}$

b) The air temperature drops to: $T_2 = \left(\frac{P_2}{P_1}\right)^{\frac{\gamma-1}{\gamma}} T_1 = \left(\frac{1}{3}\right)^{0.286} \times 503 = 367 \text{ K} = 94 \text{ C}$

Rapid discharge of pressurized vessels induces thermal stresses in the vessel wall

8.5. Dynamics of Gas Filled Vessels

Earlier we derived the mass and enthalpy of mixing tanks containing a liquid at constant pressure. We want to extend the derivation to vessels containing a gas. We consider a general case of simultaneous charging of the vessel with the same gas at several inlet ports and discharging the vessel while heat and shaft work are added to the vessel as shown in Figure IIa.8.4. The derivation in this case is mathematically more involved since the gas pressure in the tank changes with time. Like before, the simplifying assumptions include a) negligible changes in the *K.E.* and *P.E.*, b) instantaneous and perfect mixing of the incoming streams with the gas in the tank, c) no chemical reaction takes place in the tank throughout the process, and d) no heat loss from the tank to the surroundings. Expanding the time derivative term in Equation IIa.6.4-1, using the perfect mixing assumption ($h_e = h_{C.V.}$) and substituting from Equation IIa.5.1, we obtain:

$$m \frac{dh}{dt} = \sum \dot{m}_i (h_i - h) + \sum \dot{Q} - \sum \dot{W}_s + V \frac{dP}{dt} \quad \text{IIa.8.11}$$

Since we already used the continuity and the energy equations and have more unknowns than equations, we now take advantage of the volume constraint; $V_{C.V.} = (mv)_{C.V.} = \text{constant}$ or alternatively $dV_{C.V.}/dt = 0$:

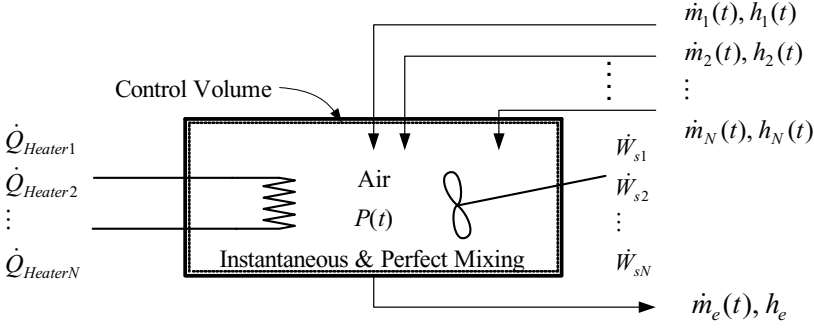


Figure IIa.8.4. A mixing tank containing an ideal gas

$$\frac{d(mv)_{C.V.}}{dt} = \frac{dm}{dt}v + m \frac{dv}{dt} = 0 \quad \text{IIa.8.12}$$

We now drop the subscript C.V., substitute for dm/dt from Equation IIa.5.1, and ponder what to do with the dv/dt term. Since P and h are the state variables, we expand dv/dt in terms of P and h , using the chain rule for composit functions:

$$\frac{dv}{dt} = \frac{\partial v}{\partial h} \frac{dh}{dt} + \frac{\partial v}{\partial P} \frac{dP}{dt} \quad \text{IIa.8.13}$$

Having all the ingredients, we proceed to substitute for dv/dt from Equation IIa.8.13 and for dh/dt from Equation IIa.8.11 into Equation IIa.8.12. We then rearrange the resulting equation and solve for dP/dt :

$$\frac{dP}{dt} = - \frac{v(\sum \dot{m}_i - \sum \dot{m}_e) + [\sum \dot{m}_i (h_i - h) + \sum \dot{Q} + \sum \dot{W}_s] (\partial v / \partial h)}{m(\partial v / \partial P) + V(\partial v / \partial P)} \quad \text{IIa.8.14}$$

At the first glance, Equation IIa.8.14 appears intimidating especially since we have introduced such unfamiliar terms as $\partial v / \partial h$ and $\partial v / \partial P$. However, this equation can be easily solved by finite difference, for example. As for the partial derivative terms, the equation of state comes to our rescue. If we are dealing with ideal gases $Pv = RT$ and therefore, $v = RT/P$. We also have $dh = c_p dT$ so that;

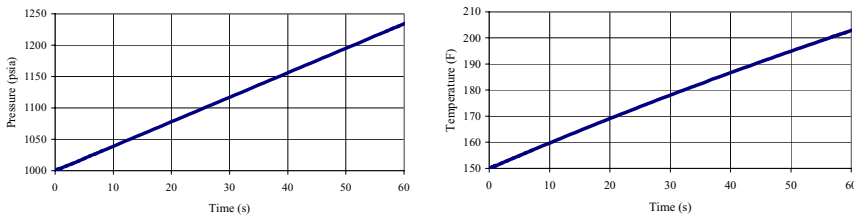
$$\frac{\partial v}{\partial P} = -\frac{v}{P} \quad \text{and} \quad \frac{\partial v}{\partial h} = \frac{\partial v}{\partial T} \frac{\partial T}{\partial h} = \frac{1}{c_p} \frac{R}{P} \quad \text{IIa.8.15}$$

We can now find dh/dt by substituting for dP/dt from Equation IIa.8.14 into Equation IIa.8.11. Pressure and enthalpy of the gas in the rigid vessel can then be calculated by subsequent integration.

In this derivation, we considered only rigid vessels thus, a control volume with fixed boundary. Control volumes with moving boundaries are analyzed in Chapter VI d.

Example IIA.8.7. Solve Example IIA.8.4 using Equations IIA.8.11 and II.8.14.

Solution: Equations IIA.8.11 and IIA.8.14 are non-linear differential equations, which we solve by the finite difference method. The solution by FORTRAN is included on the accompanying CD-ROM. The results are shown in the plots of P and T versus time. Pressure and temperature in 1 minute reach 1235 psia (8.5 MPa) and 203 F (95 C), respectively.



Special Case; Isothermal Process

Consider the rigid tank of Figure IIA.8.5. The tank is initially at T_1 and $P_1 > P_{atm}$. We open a small valve and vent the tank while simultaneously adding heat to the tank to maintain the air temperature in the tank at its initial value. We want to determine the amount of heat added to the tank when the pressure drops to P_2 .

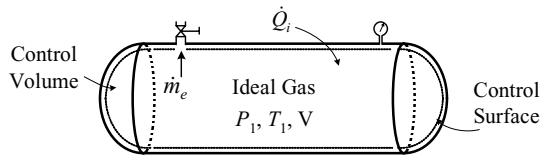


Figure IIA.8.5. Discharging gas-filled rigid vessels

While we can solve this problem by using Equations IIA.8.11 and II.8.14, we instead choose the direct solution by using Equations IIA.5.1 and IIA.6.4 in addition to the equation of state. Since there is no inlet stream, no shaft work, and only one exit port, Equation IIA.6.3 is simplified to:

$$\frac{d(mu)_{C.V.}}{dt} = m_{C.V.} \frac{du}{dt} + u_{C.V.} \frac{dm_{C.V.}}{dt} = -\dot{m}_e h_e + \dot{Q}$$

The logic for setting the term involving du/dt equal to zero is as follows: $du/dt = d(c_v T)/dt$. If we assume c_v remains constant then $du/dt = c_v(dT/dt)$. Since the proc-

process takes place at constant temperature then $dT/dt = 0$ thus, $du/dt = 0$. We now substitute from the continuity equation, $dm/dt = -\dot{m}_e$, to obtain:

$$u_{C.V.}(dm_{C.V.}/dt) = h(dm_{C.V.}/dt) + \dot{Q}$$

where due to the perfect mixing assumption, we also substituted for $h_e \equiv h$. Rearranging this equation yields:

$$\dot{Q} = (u - h)(dm/dt) = [u - (u + Pv)](dm/dt) = (Pv)(dm/dt) = RT(dm/dt)$$

where subscript C.V. is dropped. The amount of heat added to the tank is found by integrating this equation:

$$Q_{1-2} = RT \int_1^2 dm = RT(m_2 - m_1) = V(P_2 - P_1)$$

Example IIa.8.8. A 0.5 m^3 rigid tank is filled with air at 38 bar and 65 C. A valve is opened to slowly vent the tank. Find the amount of heat addition to the tank so that temperature remains at 65 C while pressure drops to 1 bar.

Solution: Treating air as an ideal gas, we find

$$Q_{1-2} = 0.5 \times (1 - 38) \times 1\text{E}5 = -1850 \text{ kJ}.$$

As an exercise, solve this problem by using Equations IIa.8.11 and II.8.14.

Calculation of P and h from Equation IIa.8.11 and II.8.14 requires specification of such input data as heater power, shaft work, inlet enthalpy and the mass flow rates at inlet and exit ports. Regarding mass flow rate at the exit port, if the control volume mass at state 2 (i.e., m_2) is specified then \dot{m}_e can be found from Equation IIa.8.1. Otherwise, \dot{m}_e is a function of tank pressure and temperature, $\dot{m}_e = f[P(t), T(t)]$ and we must calculate the mass flow rate at the exit port from an additional equation. This additional equation is the momentum equation written between the valve inlet and outlet ports. We leave further discussion of this topic to Chapter IIIc.

8.6. Discharging Rigid Vessels (Fixed C.V.) Filled with Two-Phase Mixture

In Section IIa.7.8, we examined cases where heat was added to the two-phase mixture in a control volume but no mass was allowed to enter or leave the control volume. Here we study the case of letting mass leave the control volume. Initially, the vessel contains a saturated mixture of water and steam at equilibrium (state 1 in Figure IIa.8.6). Adding heat to a rigid vessel in an isobaric process requires mass to be withdrawn. In this special case, we remove only saturated steam through a vent valve at the top of the vessel. We stop adding heat to the vessel and removing steam from the vessel when the last drop of water becomes satu-

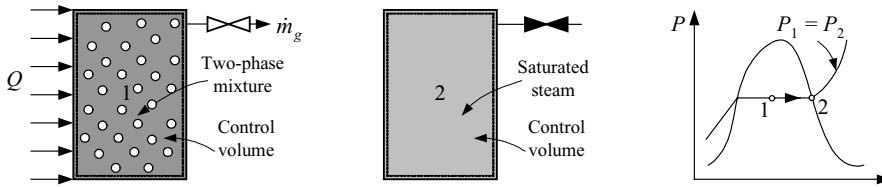


Figure Ila.8.6. Discharging steam and adding heat to a vessel at constant pressure

rated steam (state 2 in Figure Ila.8.6). We want to find the amount of heat needed for this process.

The solution to this problem is obtained from Equation Ila.8.11. However, for this isobaric process we can find an analytical solution in closed form. In this process, a carefully controlled heat addition and steam removal maintains the vessel pressure at its initial state throughout the isobaric vaporization process.

Since steam leaves the vessel at constant pressure, $\dot{m}_e = \dot{m}_g$ and $h_e = h_g$. The conservation equation for energy then becomes:

$$\dot{Q} = \dot{m}_g h_g + d(mu)_{CV} / dt$$

Multiplying both sides by dt and integrating gives;

$$\int \dot{Q} dt = h_g \int \dot{m}_g dt + (m_2 u_g - m_1 u_1).$$

We now substitute from the continuity equation to obtain:

$$Q_{12} = (m_1 - m_2) h_g + (m_2 u_g - m_1 u_1)$$

We calculate m_1 and m_2 from the equation of state and the volume constraint, $m_1 = V/v_1$ and $m_2 = V/v_g$.

Example Ila.8.9. A tank having a volume of 40 m^3 contains a mixture of water and steam at 7 MPa and a steam quality of 0.65 . Steam is withdrawn from the top of the tank while heat is added in an isobaric process until the steam quality becomes 100% . Find the amount of heat added to the tank and the mass withdrawn.

Solution:

P (MPa)	v_f (m^3/kg)	v_g (m^3/kg)	u_f (kJ/kg)	u_g (kJ/kg)	h_g (kJ/kg)
7	1.108E-3	0.2729	696.44	2572.5	2763.5

$$v_1 = 1.108\text{E-}3 + 0.65 \times 0.2718 = 0.178 \text{ m}^3/\text{kg}$$

$$m_1 = 40/0.178 = 225 \text{ kg}$$

$$m_2 = 40/0.2729 = 146.6 \text{ kg}$$

$$\begin{aligned}
 m_e &= 225 - 146.6 = 78 \text{ kg} \\
 u_1 &= 696.44 + 0.65 \times (2572.5 - 696.44) = 1915.88 \text{ kJ/kg} \\
 Q_{12} &= (m_1 - m_2)h_g + (m_2u_g - m_1u_1) = 78 \times 2763.5 + (146.6 \times 2572.5 - 225 \times 1915.88) = 162.7 \text{ MJ}
 \end{aligned}$$

8.7. Pressure Search for a Control Volume

As was discussed in Example IIa.3.4, often we calculate v and u for a control volume from which we need to find the control volume pressure and temperature. This requires a solution based on iteration with the steam tables. Let's consider a case where the final state is a saturated mixture. In this case, we may substitute for quality from $v = v_f + x v_{fg}$ into $u = u_f + x u_{fg}$ and obtain the following relation:

$$(u - u_f)v_{fg} + (v - v_f)u_{fg} = 0$$

If v_f , v_{fg} , u_f , and u_{fg} are now expressed as functions of either pressure or temperature, we can solve for pressure (or temperature) using the Newton-Raphson method, as discussed in Chapter VIIe. Having found pressure (or temperature), the corresponding saturation temperature (or pressure) can then be found. Shown in Table A.II.3 are examples of curves fits to data for v_f , v_{fg} , u_f , and u_{fg} in terms of T .

Example IIa.8.10. A tank having a volume of 500 ft³ contains a homogenous mixture of water and steam at 400 F. The initial steam quality is 15%. We now add 200 lbm of water at 450 psia and 350 F to the tank. Find pressure and temperature, assuming perfect mixing of water with the mixture in the vessel.

Solution: We follow the steps outlined below:

T (F)	P (psia)	v_f (ft ³ /lbm)	v_g (ft ³ /lbm)	u_f (Btu/lbm)	u_g (Btu/lbm)
400	247.26	0.01864	1.8630	372.45	1115.74

$$v_1 = 0.01864 + 0.15 \times (1.8630 - 0.01864) = 0.2953 \text{ ft}^3/\text{lbm}$$

$$m_1 = 500/0.2953 = 1693.23 \text{ lbm}$$

$$u_1 = 372.45 + 0.15 \times 743.29 = 483.94 \text{ Btu/lbm}$$

$$m_2 = m_1 + m_{add} = 1893.23 \text{ lbm.}$$

The enthalpy of the added water: $h_{add}(450 \text{ psia} \ \& \ 350 \text{ F}) = 322.24 \text{ Btu/lbm.}$

Applying Equation IIa.6.4 to the control volume representing the tank gives:

$\dot{m}_i h_i = d(mu) / dt$. Integrating and solving for u_2 , we obtain:

$$u_2 = \frac{m_1 u_1 + m_{add} h_{add}}{m_1 + m_{add}}$$

We also have $v_2 = V/(m_1 + m_{add})$. The numerical values for u_2 and v_2 are calculated as:

$$u_2 = [1693.23 \times 483.94 + 200 \times 322.24]/1893.23 = 466.86 \text{ Btu/lbm.}$$

$$v_2 = 500/1893.23 = 0.264 \text{ ft}^3/\text{lbm}$$

Having u_2 and v_2 , we find P_2 and T_2 by iteration with the steam tables for saturated mixture as $P_2 = 239.95 \text{ psia}$, $T_2 = 297.4 \text{ F}$, and $x_2 = 0.128$. Expectedly, adding colder water reduces the mixture enthalpy.

9. The Second Law of Thermodynamics

In the previous sections dealing with the first law of thermodynamics, we stated that both heat and work are forms of energy. We also showed the relationship between heat and work. There were several observations that were missing in those discussions. For example, we have noted from experience that work can be readily transformed to heat whereas the reverse is not readily possible. Furthermore, while 100% of work can be transformed to heat, conversion of heat to work is always less efficient. Another important fact is the effect of temperature on storage of thermal energy (i.e., the higher the temperature of the stored thermal energy, the higher the ability to be converted into work). Perhaps the most interesting observation regarding energy conversion is bringing a hot block of steel in contact with a colder block of steel. Intuitively, we know the heat flows from the warmer to the colder block. However, there is no provision in the first law to prohibit the flow of heat from the colder to the warmer block. The first law is concerned only with the conservation of energy in a process and not with the direction of the process. It is the second law that establishes the possible direction of a process. Another example includes the daily dumping of vast amounts of energy to the surroundings at power plants where work is produced in the form of electricity. Production of work equal to the same amount of energy delivered to the heat source is not prohibited by the first law. However, the loss of energy to the surroundings (i.e., the requirement for a heat sink) can be explained only if put in the framework of the second law of thermodynamics. As was stated in Chapter I, unlike the first law, the second law is a not a conservation law.

9.1. Definition of Terms

Work and heat reservoirs are two thermodynamic concepts. A work reservoir is a system for which every unit of energy crossing its boundary is in the form of work. Examples of a work reservoir include a perfectly insulated turbine and a perfectly elastic compressed spring. The heat reservoir is a constant temperature body as heat is transferred into or out of the body. A large lake acting as a heat sink for a power plant may be considered as a heat reservoir. Comparing two heat reservoirs at two different temperatures, the heat reservoir at the higher temperature is referred to as the heat source and the heat reservoir at the lower temperature, the heat sink.

Heat source is referred to any hot heat reservoir. In a gasoline engine, the heat source is the combustion chamber at the moment that the compressed gases are ignited and burn due to the action of a spark plug. In a jet engine or gas turbine power plant, the heat source is the combustion chamber where compressed air enters to mix with the injected fuel for combustion. In a fossil plant, the heat source is the boiler. In a BWR, the heat source is the reactor vessel and in a PWR, the heat source is the secondary side of the steam generator.

Heat Sink refers to any cold heat reservoir. In a gasoline engine, the heat sink is the radiator. In a power plant located next to a large body of water, the heat sink is the condenser. Power plants not having access to large bodies of water use cooling towers as heat sinks. In a heated room with no windows, the heat sink consists of the ceiling, the floor, and the walls. If an air conditioning unit is now installed to cool this room and we assume the walls quickly reach thermal equilibrium with the room, the primary heat sink for the room is the air conditioning unit. This is however, an intermediate heat sink as eventually heat is transferred to the surroundings. As a result, the environment is the *ultimate heat sink*.

Cycle is a process that, after completion, brings the system to its original state. As a result, the net change in any property of the system is zero. As an example, consider the motion of piston in cylinder of Figure IIa.9.1. We may start from a point where the piston is fully inserted and gas is at the highest pressure. The first process or path includes the expansion of the gas, which forces the piston to the bottom of the cylinder. This also turns the flywheel. The second process is when the stored energy in the flywheel pushes the piston back to its original position completing one cycle.

Clausius statement of the second law deals with the transfer of energy from a heat sink to a heat source. Simply stated, the Clausius statement specifies that “it is impossible for any device to operate in a cycle and produce no effect other than the transfer of energy by heat from the heat sink to the heat source.” In other words, the Clausius statement clarifies that the operation of heat pumps and refrigerators is possible only if work is provided to the device (compressor) to accomplish the task of removing heat from a heat sink and transferring it to the heat source.

Kelvin-Planck statement of the second law deals with the transfer of energy from a heat source to a heat sink. This statement specifies that “it is impossible for any device to operate in a cycle and produce work with only a heat source.” In other words, the Kelvin-Planck statement clarifies that no power plant can operate with a boiler, an engine, or a combustion chamber but without a radiator, a cooling tower, or a condenser.

Reversible process as defined earlier refers to a process that, if applied to a system, can be reversed exactly to the initial state with no change in the system or its surroundings. A reversible process is hard to achieve and can only be approached in a carefully planned and executed process. Examples of processes that can approach a reversible process include a smooth converging-diverging nozzle.

Among mechanical systems that are equipped with a flywheel and have the potential of approaching a reversible process we may consider the periodic motion of a pendulum in a vacuum container with negligible friction at the base. Similarly, as shown in Figure IIa.9.1, the operation of a frictionless well-insulated piston in the well-insulated cylinder while attached to a flywheel approaches a reversible process.

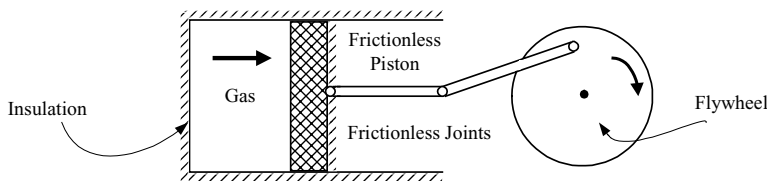


Figure IIa.9.1. A frictionless, well insulated system approaching reversible process

To illustrate how a process can be made reversible, consider the frictionless piston in Figure IIa.9.2 fixed in place by a pin. Pressure inside the cylinder is P_1 . We now release the pin and the piston reaches the stops at pressure P_2 . This process is not reversible, because during the expansion, the piston pushes against atmospheric pressure. The force needed to push the piston back to its original place is larger as the piston has to push against $P_2 > P_{atm}$. This results in work to be delivered to the piston. To approach a reversible process, consider the same piston but now it is attached to a linear spring with $k_{spring} = P_1 A/L$.

It is important to remember that there are no dissipative effects upon the conclusion of a reversible process.

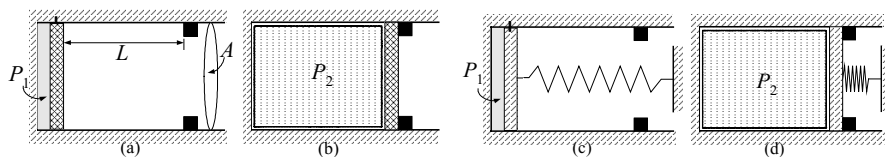


Figure IIa.9.2. Transformation of a system to approach reversible process

Irreversible process refers to any process, which is not reversible. In practice, all engineering processes are irreversible. Friction in the form of heat loss to the surroundings is one of the main reasons for this irreversibility. For example, as discussed in Chapter IIIb, the flow of fluids in pipelines and in the bends of conduits is always associated with unrecoverable pressure loss. This is due to the fluid shear stresses and roughness of the pipe wall. There are, of course, other types of irreversible processes such as shock waves resulting in sonic booms and any hysteresis effect. Inelastic deformation where a solid does not return to its original dimensions following removal of the applied force is an irreversible process. Flow of electric current through an electric resistance produces heat, causing

the process to be irreversible. Spontaneous mixing of substances of different compositions, and all actual heat transfer mechanisms are also examples of irreversible processes. The latter is an irreversible process as to reverse the process, a refrigeration cycle is needed to transfer heat from the heat sink to the heat source. This requires transfer of work from the surroundings. In practice, we can reduce certain irreversibilities by taking such actions as using smooth piping for internal flow, contoured or streamlined surfaces for external flow, and lubrication for solid to solid contact. There are always dissipative effects upon the conclusion of the irreversible process. Hence, in the design and operation of systems we must focus on reducing the irreversibilities associated with a system to minimize their dissipative effects and maximize efficiency.

Internal and external irreversibilities are two categories of irreversible processes with respect to the system boundary. Internal irreversibilities occur inside the boundary of a system and are associated with friction due to fluid shear stresses and such other processes as fluid expansion as well as fluid mixing. External irreversibilities occur across the system boundary and are associated with heat transfer to or from the system, friction due to the mechanical motion such as shaft rotation in bearing, and windage losses in electric generators.

Reversible work, W_{rev} is the work done by or on a system when it undergoes a reversible process.

Irreversible work, W_{irr} is the work done by or on a system when it undergoes an irreversible process. In a work producing system undergoing different paths, all beginning and ending in an identical change of state, the reversible work produced by the reversible path is the maximum work that can be obtained. Similarly, for a work absorbing system undergoing different paths, all beginning and ending with an identical change of state, the reversible work absorbed in the reversible path is the minimum work that can be absorbed.

Irreversibility, $I = W_{rev} - W_{irr}$ is the difference between the reversible and the irreversible work for a system when it undergoes reversible and irreversible cycles beginning and ending in an identical change of state. Since the reversible work is always larger than the irreversible work for work producing systems, and always smaller than the irreversible work for work absorbing systems, the irreversibility I is always a positive quantity. The irreversibility, also referred to as the *lost work*, is discussed further in the next section.

Heat engine is a work reservoir that goes through a cycle to produce work while heat is being transferred to and from the system across its boundary. As shown in Figure IIa.9.3, heat is transferred to the heat engine from the heat source and is transferred from the engine to the heat sink. Work is produced in this process.

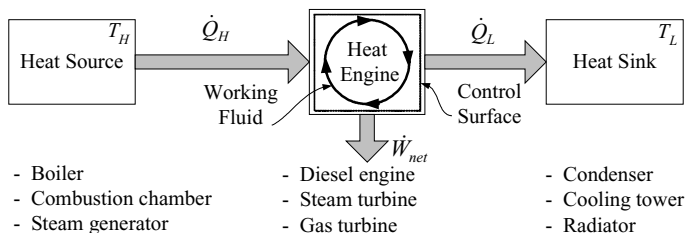


Figure IIa.9.3. Schematic of a heat engine in steady state operation

Thermal efficiency for a heat engine is defined as the net energy output in steady state operation from the engine in the form of work divided by the energy input to the heat engine from the heat source. Perhaps the most intuitive definition of efficiency is the ratio of energy obtained to energy spent. Using our sign convention (i.e., plus sign for heat transferred to the system and work delivered by the system and minus sign for heat transferred from the system and work transferred to the system) the first law for steady state operation becomes:

$$+(\dot{Q}_H) - (\dot{Q}_L) = +(\dot{W}_{net})$$

Thermal efficiency becomes:

$$\eta_{th} = \frac{\text{energy obtained}}{\text{energy spent}} = \frac{\dot{W}_{net}}{\dot{Q}_H} = \frac{\dot{Q}_H - \dot{Q}_L}{\dot{Q}_H} = 1 - \frac{\dot{Q}_L}{\dot{Q}_H} \quad \text{IIa.9.1}$$

Equation IIa.9.1, despite its simplicity, conveys important information. For example, according to the second law, $|\dot{Q}_L|$ is always greater than zero. As such, thermal efficiency of a heat engine can never be 100%. In the remainder of this chapter, we will see that thermal efficiency of a heat engine is indeed much smaller than unity. Equation IIa.9.1 also shows that to increase thermal efficiency for a given rate of heat transfer from the heat source, we must reduce the rate of heat transfer to the heat sink.

Carnot principle states that a reversible heat engine always has a higher thermal efficiency than an irreversible heat engine. The Carnot principle (Nicolas Leonard Sadi Carnot, 1796 - 1832) also states that two reversible heat engines operating between identical heat sources and heat sinks have identical thermal efficiencies.

Kelvin temperature scale provides a simple relation between the ratio of heat transfers to the heat sink and the heat source versus the temperature of these reservoirs. Referring to Figure IIa.9.3, in general the ratio of the rate of heat transfers can be expressed by several functions. Kelvin (William Thomson later became Lord Kelvin, 1824 - 1907) suggested:

$$\frac{\dot{Q}_L}{\dot{Q}_H} = f(T_L, T_H) = \frac{T_L}{T_H}$$

Carnot efficiency is derived from the Carnot principle, correlating thermal efficiency of reversible heat engines solely to the heat source and the heat sink temperatures. According to Kelvin's suggestion for a temperature scale, Equation IIa.8.3 becomes (see derivation in Chapter IIb):

$$\eta_{th, Carnot} = 1 - \frac{T_L}{T_H} \quad \text{IIa.9.2}$$

where T_L and T_H are absolute temperatures. Equation IIa.9.2 is the Carnot thermal efficiency for heat engines. This simple, yet very important equation expresses that no heat engine can have a thermal efficiency higher than that predicted by Equation IIa.9.2. Also note that the higher the temperature of the heat source, the higher the thermal efficiency. However, achievement of high temperatures in practice is limited to the metallurgical characteristics of the materials constituting the heat engine.

Example IIa.9.1. Steam pressure in the secondary side of a PWR steam generator is 900 psia (6.2 MPa). The condenser uses bay water, the lowest temperature of which is 40 F (4.4 C). Determine the maximum thermal efficiency this plant could achieve.

Solution: From Equation IIa.9.2

$$(\eta_{th})_{Max} = 1 - \frac{40 + 460}{T_{sat}(900) + 460} = 1 - \frac{40 + 460}{531.95 + 460} = 49.6\%$$

Due to irreversibilities, power plants using a steam cycle have thermal efficiency of about 30%.

Thermal pollution refers to the adverse environmental impact that power plants could have on the surroundings as the ultimate heat sink. The warm water at the exit of a once-through condenser has a temperature ranging from 12 to 25 F above the temperature of the water at the inlet. The effect of this temperature rise on the ecosystem depends on the size of the body of water ranging from a river or a lake to an estuary or an ocean.

Example IIa.9.2. An electric utility plans to operate a 1200 MWe power plant next to a lake. Agencies for protection of the environment have limited the rise in the lake water temperature to no more than 13 F (7 C). Determine the required flow of water to the condenser. Propose an alternative solution if this criterion cannot be met.

Solution: The percentage of a power plant's thermal efficiency ranges from high 20s to low 40s. Higher values of \dot{Q}_L is associated with lower thermal efficiency. Using a thermal efficient of 30% we find:

$$\dot{Q}_H = \dot{W}_{net} / \eta_{th} = 1200/0.3 = 4000 \text{ MW}$$

$$\dot{Q}_L = \dot{Q}_H - \dot{W}_{net} = 4000 - 1200 = 2800 \text{ MW}$$

This amount of energy is lost in the condenser to the environment. To find the required flow rate of cooling water to the condenser, we use an energy balance written between the inlet and outlet of the condenser, $\dot{Q}_L = \dot{m}c\Delta T$ where c is the specific heat of water. Its value between 20 C and 99.6 C is relatively constant at $c_{water} = 4.18 \text{ kJ/kg}\cdot\text{C}$. Using $\Delta T = 13 \text{ F}/1.8 = 7.2 \text{ C}$, the flow rate needed is therefore obtained from:

$$\dot{m} = 2.8\text{E}6 / [4.18 \times 7.2] = 93,000 \text{ kg/s} = 737\text{E}6 \text{ lbm/h} = 1.5\text{E}6 \text{ GPM} = 93 \text{ m}^3/\text{s}$$

This is a massive amount of water, which must be circulated through the condenser. If this flow rate cannot be sustained, the outlet temperature would exceed the limit. Cooling towers would assist in the task of removing heat as discussed in Chapter IIc.

In the above example, if we had used a thermal efficiency of 40%, which is an improvement of about 33%, the required flow rate would have dropped to 59,625 kg/s (59 m³/s). This is a reduction of about 36%, indicating that the reduction in the rate of heat loss to the surroundings, due to the increase in thermal efficiency, is greater than the increase in thermal efficiency itself. The effect of η_{th} on \dot{Q}_L and $\dot{Q}_L / \dot{W}_{net}$ for a $\dot{W}_{net} = 1000 \text{ MW}$ plant is shown in Figure IIa.9.4.

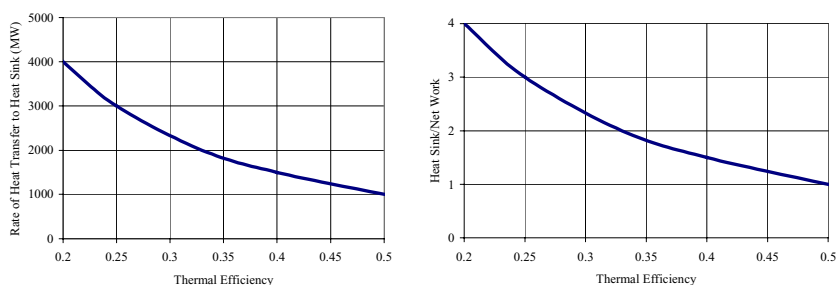


Figure IIa.9.4. Effect of Thermal efficiency on the rate of heat transfer to heat sink

Heat pump is a work reservoir that goes through a cycle and consumes work while heat is being transferred to and from the system across its boundary. As shown in Figure IIa.9.5, work is delivered to the heat pump to transfer heat from the heat sink to the heat source.

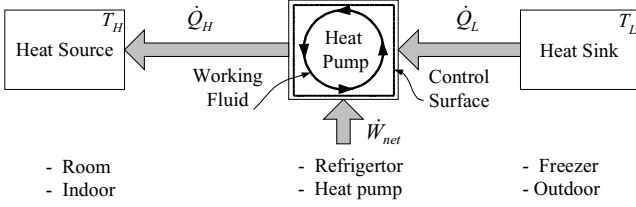


Figure IIa.9.5. Schematic of a heat pump in steady state operation

We have used the term “heat pump” as the reverse of a “heat engine”. These are both generic terms. While heat engine applies to such systems as an automobile engine, a steam turbine, and a jet engine, the heat pump applies to such systems as a refrigerator as well as a building heater/cooler. A refrigerator removes heat from the heat sink while a heat pump delivers heat to the heat source.

Coefficient of performance is a term defined for the refrigeration and heat pump cycles. In both cases, the coefficient of performance (COP) is defined similar to thermal efficiency for heat engines;

$$\text{COP} = \eta = \frac{\text{energy obtained}}{\text{energy spent}}$$

In refrigerators:

$$\eta_{\text{Refrigerator}} = \frac{\text{energy obtained}}{\text{energy spent}} = \frac{\dot{Q}_L}{\dot{W}_{\text{net}}} = \frac{\dot{Q}_L}{\dot{Q}_H - \dot{Q}_L}$$

and in heat pumps:

$$\eta_{\text{Heat pump}} = \frac{\text{energy obtained}}{\text{energy spent}} = \frac{\dot{Q}_H}{\dot{W}_{\text{net}}} = \frac{\dot{Q}_H}{\dot{Q}_H - \dot{Q}_L}$$

We now consider a reversible heat pump cycle. Such a cycle, according to the Carnot principle, consumes the least energy compared to an irreversible heat pump cycle. Using Lord Kelvin’s temperature scale for reversible cycles:

$$\left(\frac{\dot{Q}_L}{\dot{Q}_H}\right)_{\text{Reversible}} = \frac{T_L}{T_H} = r$$

The thermal efficiency and the COP for refrigerator and heat pump can be expressed as:

$$\eta_{\text{Heat engine, Carnot}} = 1 - r \quad \eta_{\text{Refrigerator, Carnot}} = \frac{r}{1 - r} \quad \eta_{\text{Heat pump, Carnot}} = \frac{1}{1 - r}$$

Example IIa.9.3. A heat pump is used for summer cooling and winter heating of a house. The heat pump COP is 5 and the rate of heat transfer to maintain the indoor temperature at 24 C when the outside temperature is 4 C is 5 kW. Find the power to operate the heat pump.

Solution: The power to operate the heat pump is obtained from $\text{COP} = 5/\dot{W}_{\text{net}}$. Therefore, $\dot{W}_{\text{net}} = 5/5 = 1 \text{ kW}$. We may also find the maximum COP. If the heat pump was operating in a reversible cycle, the COP would have been $(\text{COP})_{\text{max}} = 1/(1 - r)$ where $r = T_L/T_H = (4 + 273)/(24 + 273) = 0.93$ and $\text{COP} = 14.3$, indicating that the heat pump design could improved substantially to reduce the irreversibilities.

Carnot cycle for a heat engine results in the highest thermal efficiency of all power cycles. A cycle can be shown on pressure-volume (Pv) or temperature-entropy (Ts) coordinates. Consider the Carnot cycle, shown in the Ts diagram of Figure IIa.9.6. The first Ts diagram shows the Carnot cycle as an isentropic-isothermal cycle. Starting from Point 1, the working fluid is compressed isentropically to Point 2, which is at the temperature of the heat source. Heat is then transferred to the working fluid isothermally to Point 3 where the working fluid expands isentropically to produce work. Heat at Point 4 is then transferred isothermally until the cycle is completed at point 1. The cycle then would repeat. In the second Ts diagram, the area under the heat addition curve is shown to be equal to Q_H . In the third Ts diagram, the area under the heat rejection curve is shown to be Q_L . The net area is W_{net} . Hence:

$$W_{\text{net}} = Q_H - Q_L.$$

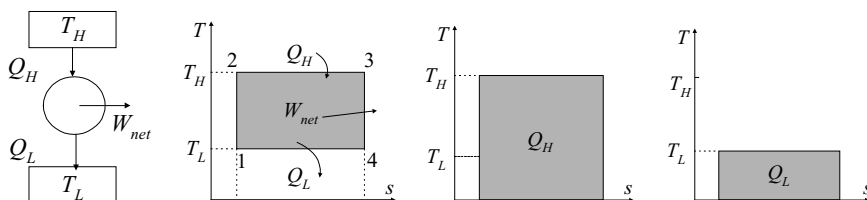


Figure IIa.9.6. Demonstration of a heat engine and Ts diagrams for the Carnot cycle

The Clausius inequality is expressed as:

$$\left[\oint \left(\frac{\delta Q}{T} \right)_{C.S.} = -\sigma \right] \leq 0$$

where the integral is taken over the control surface and the entire cycle. In this relation, σ is a measure of entropy production due to the existing irreversibilities in the system going through a cycle hence, σ is always positive for practical processes and can never be negative. The minimum value of σ is zero, occurring for only reversible processes. Later in this section we will show that σ is related to irreversibility (I) as $\sigma = I/T$.

Entropy, as a property of a system is the change in value of $\delta Q/T$ in a reversible process. We can then write:

$$S_2 - S_1 = \left(\int_1^2 \frac{\delta Q}{T} \right)_{rev} \quad \text{IIa.9.3}$$

Equation IIa.9.3 can also be written in differential form as $TdS = \delta Q$. If we now substitute for the right-hand side from Equation IIa.5.1, we get $TdS = \delta W + dE$. This can be simplified to:

$$TdS = dU + PdV \quad \text{IIa.9.4}$$

where only compression work in a reversible process is considered and the kinetic and potential energies are negligible. Entropy of a system may decrease, remain the same, or increase, depending on the process applied to the system. However, the net entropy of the system and its surroundings increases unless the process is reversible.

Exergy or availability determines the potential of a system to produce work. Any system can be at various levels of its availability. While availability is related to energy, unlike energy, availability is not conserved.

Power system refers to a heat engine that goes through a thermodynamic cycle to produce net work.

10. Entropy and the Second Law of Thermodynamics

Earlier we discussed the fact that energy is conserved and cannot be created or destroyed. We also learned about the first law of thermodynamics, which expresses the conservation of energy in various processes and noted that the first law does not provide any guideline for the direction of a process. It is the second law that clarifies the direction of a process. We also compared reversible with irreversible processes and noted that there are always dissipative effects associated with the irreversible processes. Such dissipative effects are evaluated in the context of availability versus *unavailability*. These terms are applied to the energy of a system. As such, the available energy is that amount of the energy of the system that can perform work. That portion of the energy of the system that cannot perform work is referred to as the unavailable energy. We can then write:

$$E_{\text{System}} = E_{\text{Available}} + E_{\text{Unavailable}} \quad \text{IIa.10.1}$$

Unlike energy, availability is not conserved. To elaborate consider an isolated system that includes fuel and air. Availability of this system prior to the combustion of the fuel is at its maximum as the fuel can be used to produce work. After combustion, the mixture of slightly warmer air and the combustion products has much less potential to perform work. Among various definitions for the entropy and the second law, entropy of a closed system can be defined as a property that is proportional to the unavailability of the system:

$$dS = C[dE_{\text{Unavailable}}] \quad \text{IIa.10.2}$$

where C in Equation IIa.10.2 is a proportionality constant. We can use Equation IIa.10.2 to readily show that the entropy change of a work reservoir is zero since, in a work reservoir, the unavailable energy is zero:

$$dS_{\text{Work reservoir}} = 0$$

In general however we can say that the unavailable energy is always positive or at least is equal to zero. Hence, we can write the second law for an isolated system as:

$$dS_{\text{Isolated system}} \geq 0 \quad \text{IIa.10.3}$$

Equation IIa.10.3 is the mathematical expression of the second law of thermodynamics for an isolated system and it describes the fact that the entropy of an isolated system can never decrease. Since we can consider any system and its surroundings as an isolated system, we can therefore write:

$$dS_{\text{System}} + dS_{\text{Surroundings}} \geq 0 \quad \text{IIa.10.4}$$

That is to say:

$$\text{For reversible processes:} \quad dS_{\text{System}} + dS_{\text{Surroundings}} = 0 \quad \text{IIa.10.4-1}$$

$$\text{For irreversible processes:} \quad dS_{\text{System}} + dS_{\text{Surroundings}} > 0 \quad \text{IIa.10.4-2}$$

Equation IIa.10.2 can also be used to determine the change in entropy for a heat reservoir. For this purpose, we first use the first law as given by Equation IIa.6.1 but expanded as:

$$\delta Q = \delta W + dE_{\text{Available}} + dE_{\text{Unavailable}} \quad \text{IIa.10.5}$$

Since for a heat reservoir, $dE_{\text{Available}}$ is only a fraction of δQ , Equation IIa.10.5 for a heat reservoir becomes:

$$\delta Q = C_1 dS$$

Rearranging in terms of dS , for a heat reservoir we obtain, $dS = \delta Q/C_1$. As shown by Hatsopoulos C_1 , the proportionality constant becomes $C_1 = 1/T$. Hence, for a heat reservoir:

$$dS_{\text{Heat reservoir}} = \frac{\delta Q}{T}$$

Since temperature of a heat reservoir remains constant, we can readily integrate the differential change in entropy to find that for a heat reservoir;

$$(S_2 - S_1)_{\text{Heat reservoir}} = \frac{Q_{12}}{T} \quad \text{IIa.10.6}$$

Using the sign convention, if the heat reservoir has gone through a process in which heat has been added to the reservoir, then $Q_{12} > 0$ and $S_2 - S_1 > 0$. On the other hand, if heat has been transferred from the reservoir $S_2 - S_1 < 0$.

10.1. Change in Entropy for Cycles

Shown in Figure IIa.10.1, are three cycles. Figure IIa.10.1(a) shows a cycle in which heat is transferred from a heat reservoir at high temperature to another heat reservoir at lower temperature. Figure IIa.10.1(b) shows the cycle for a heat engine. Finally, Figure IIa.10.1(c) shows a cycle for a heat pump. The goal is to find the change in entropy for each cycle. Starting with Figure IIa.10.1(a), we first note that in steady state operation, $Q_H = Q_L = Q$. The device can simply be a conducting metal, which transfers heat from the heat source to the heat sink. To find the change of entropy for this cycle, we use Equation IIa.10.4:

$$\Delta S_{\text{System}} + \Delta S_{\text{Surroundings}} = \Delta S_{\text{System}} + \Delta S_{\text{Heat source}} + \Delta S_{\text{Heat sink}} \geq 0$$

noting that the device operates in a cycle, hence, $(\Delta S)_{\text{System}} = 0$. Therefore, the change in entropy becomes:

$$\Delta S_{\text{Heat source}} + \Delta S_{\text{Heat sink}} = -\frac{Q}{T_H} + \frac{Q}{T_L} \geq 0 \quad \text{IIa.10.7}$$

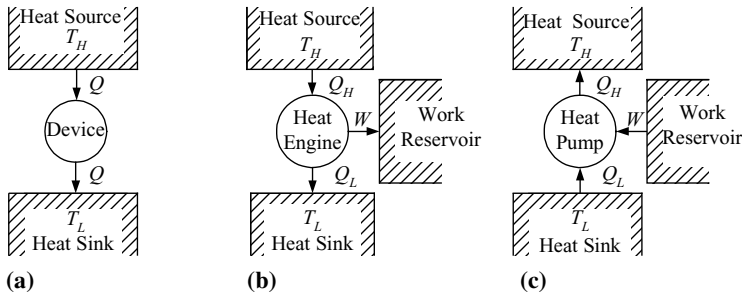


Figure IIa.10.1. Two reservoirs for (a) heat transfer, (b) heat engine, (c) heat pump

For the heat transfer to take place, the above relation must be satisfied. Since the absolute value of Q is greater than zero, it requires that $1/T_H + 1/T_L \geq 0$ or $T_H \geq T_L$. This conclusion satisfies our intuition based on experimental observations that heat flow from the hot to the cold system and if temperatures are the same then there is no heat transfer. This also supports the Clausius statement of the second law.

Example IIa.10.1. Consider two heat reservoirs, one at 550 C and another at 20 C. These reservoirs are connected by a device, resulting in a rate of heat transfer between the two reservoirs equal to 2700 MW. Find the rate of increase in the entropy of the universe as a result of this process.

Solution: To find the rate of entropy increase, we use Equation IIa.10.7:

$$\Delta S = -\frac{Q}{T_H} + \frac{Q}{T_L} = Q\left(\frac{1}{T_L} - \frac{1}{T_H}\right) = 2700\left(\frac{1}{20 + 273} - \frac{1}{550 + 273}\right) = 5.93 \text{ MW/K}$$

Let's now examine the entropy change for the heat engine. We know that for a heat engine,

$$Q_H - Q_L = W$$

Substituting for the entropy change of the heat source and heat sink and noting that for a work reservoir $\Delta S_{\text{Work reservoir}} = 0$, we obtain:

$$\Delta S_{\text{Heat source}} + \Delta S_{\text{Heat sink}} = -\frac{Q_H}{T_H} + \frac{Q_L}{T_L} + 0 \geq 0 \quad \text{IIa.10.8}$$

If the heat engine operates in a reversible process, then we can write:

$$-\frac{Q_H}{T_H} + \frac{Q_L}{T_L} = 0$$

From the above relation we conclude that $Q_L/Q_H = T_L/T_H$. If this conclusion is substituted in Equation IIa.9.1, it results in the Carnot efficiency as given by Equation IIa.9.2. It is evident that a 100% efficiency is obtained if $T_L = 0$ K. In practice T_L is about 288 K (15 C, 60 F). Therefore, it is important to increase T_H , which has its own limitations as discussed in Section 9. The conclusion that resulted in obtaining Equation IIa.9.2 also supports the Kelvin-Planck statement of the second law of thermodynamics.

The reader may try the same method used for Figures IIa.10.1(a) and IIa.10.1(b) to obtain the change of entropy for the heat pump of Figure IIa.10.1(c).

10.2. Change in Entropy for Closed Systems

We defined the closed system as a system with constant mass. Hence, in all thermodynamic processes only heat and work can cross the boundary of the system. To find the change in entropy of a closed system, we use the following inequality:

$$\Delta S_{\text{System}} + \Delta S_{\text{Surroundings}} = \Delta S_{\text{System}} + \Delta S_{\text{Heat reservoir}} + \Delta S_{\text{Work reservoir}} \geq 0 \quad \text{IIa.10.9}$$

The change in the entropy of the work reservoir is zero. The change in the entropy of the heat reservoir (*HR*) is given in Equation IIa.10.6 as $\Delta S_{\text{HR}} = Q_{\text{HR}}/T_{\text{HR}}$. Therefore, for a closed system, $\Delta S_{\text{System}} + Q_{\text{HR}}/T_{\text{HR}} \geq 0$. Whether heat is transferred from the heat reservoir to the system or from the system to the heat reservoir, we always have $Q_{\text{System}} = -Q_{\text{HR}}$, substituting we find $\Delta S_{\text{System}} - Q_{\text{System}}/T_{\text{HR}} \geq 0$. To find the differential change in entropy for a differential change in state, we replace ΔS by dS , Q_{System} by δQ_{System} , and T_{HR} by $T + dT$ of the system. If we ignore $dSdT$, then Equation IIa.10.9 simplifies to:

$$dS \geq \frac{\delta Q}{T}$$

It is apparent that the entropy increase is larger than the $\delta Q/T$ due to irreversibility. Should we add the lost work to the left-hand side, the inequality can be replaced by the equal sign. To do so, we consider two processes for the system, namely, a reversible and an irreversible process. To be able to apply the first law of thermodynamics to both processes and have the same change in the total energy of the system, we must require an identical change in the state for both processes. We start with the first law for the reversible process;

$$\delta Q_{\text{rev}} = dE + \delta W_{\text{rev}}$$

Similarly, we write the first law for the irreversible process:

$$\delta Q_{\text{irr}} = dE + \delta W_{\text{irr}}$$

Canceling dE between the two equations, we obtain:

$$\delta Q_{\text{rev}} = \delta Q_{\text{irr}} + \delta W_{\text{rev}} - \delta W_{\text{irr}} = \delta Q_{\text{irr}} + \delta I$$

where the incremental irreversibility δI is given by $\delta I = \delta W_{\text{rev}} - \delta W_{\text{irr}}$. For the reversible path we can write $dS = \delta Q_{\text{rev}}/T$. If we then substitute for $\delta Q_{\text{rev}} = TdS$, divide by T , and rearrange we obtain:

$$dS = \frac{\delta Q_{\text{irr}}}{T} + \frac{\delta I}{T} \quad \text{IIa.10.10}$$

Equation IIa.10.10 shows that the change in entropy for a closed system is solely due to the heat transfer and the irreversibility. To minimize the change in entropy, both terms should be minimized.

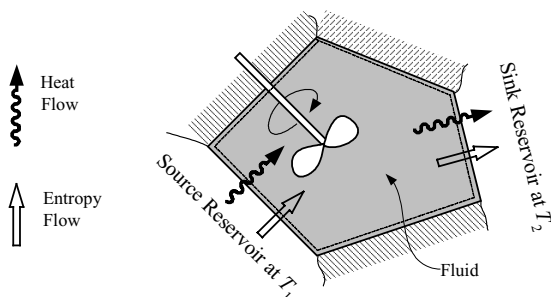


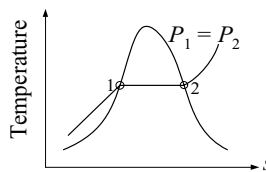
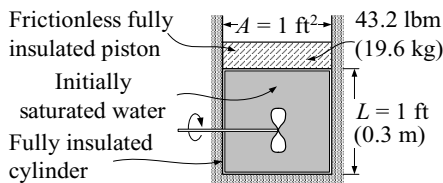
Figure IIa.10.2. Entropy transfer and production for a closed system

We are now set to examine the relation between irreversibility (I) and the measure of entropy production (σ). For this purpose, we consider the closed system of Figure IIa.10.2 in which its contents, either gas or liquid, is stirred by the action of the paddle wheel. The entropy production due to system irreversibility, such as friction, is equal to σ . Heat is introduced to the system from the hot reservoir at T_1 (transferring entropy into the system equal to Q_1/T_1) and is rejected to the cold reservoir at T_2 (transferring entropy out of the system equal to Q_2/T_2). The change in entropy can be written as:

$$S_2 - S_1 = \sum_j \frac{Q_j}{T_j} + \sigma \quad \text{IIa.10.11}$$

where j is an index to include all boundaries participating in heat transfer into or out of the system, including $j = 0$, to the surroundings. In Figure IIa.10.2, $j = 2$. The right side of Equation IIa.10.11 consists of two terms. The first term accounts for the entropy transfer into or out of the system due to exchanges with the heat reservoirs and the second term accounts for entropy production. Differentiating Equation IIa.10.11 and comparing with Equation IIa.10.10, we conclude that $\sigma = I/T$. This conclusion confirms our expectation that neither σ nor I is a property of the system as the value of both quantities depends on the type of process the system would go through.

Example IIa.10.2. A cylinder contains saturated water. The piston is frictionless and free to move. We heat the water by a mixer adiabatically to produce saturated vapor. Find the entropy produced in this process.



Solution: Boiling takes place in a closed system in a process, which is isobaric and adiabatic. Find pressure $P_{water} = P_{atm} + (Mg/A) = 14.7 + (43.2/144) = 15$ psia.

Find water mass as $m = \rho V = 59.8$ lbm (27.1 kg).

Since $Q = 0$, then Equation IIa.10.11 simply becomes $\Delta S = \sigma$. Hence, $\sigma = m(s_2 - s_1)$. Substituting, we find:

$$\sigma = m(s_g - s_f) = 59.8 \times (1.7551 - 0.3137) = 86.19 \text{ Btu (91 kJ)}.$$

10.3. Useful Work, Optimum Useful Work, and Irreversibility (Closed Systems)

If the total work obtained from a closed system is W , we define the useful work as the portion of the total work that excludes the expansion or contraction work involved with the surroundings, being at pressure P_o . In differential form, we have $\delta W_{use} = \delta W - P_o dV$. We can derive a relation for δW_{use} using the first and the second law. The first law $\delta Q = dE + \delta W$ as given by Equation IIa.6.1 can be written as:

$$\delta Q_o + \sum_j \delta Q_j = dE + \delta W_{use} + P_o dV$$

where the heat transfer term is expanded to include heat transfer to or from the surroundings and heat transfer to or from a heat source or heat sink reservoirs. Also the work transfer term is expanded to include the useful work and the expansion or contraction work with the surroundings. Writing Equation IIa.10.11 in differential form and expanding, we find:

$$dS = \frac{\delta Q_o}{T_o} + \sum_j \frac{\delta Q_j}{T_j} + \delta \sigma$$

where term $\sum_j Q_j/T_j$ is expanded to account for the surroundings separately hence, in the above equation $j \neq o$. We now find δQ_o from the second law equation (i.e., $\delta Q_o = T_o dS - \sum_j Q_j/T_j - \delta \sigma$) and substitute it into the first law equation to obtain $T_o dS - \sum_j Q_j/T_j - \delta \sigma + \sum_j \delta Q_j = dE + \delta W_{use} + P_o dV$. Solving for δW_{use} , we find:

$$\delta W_{use} = -dE - P_o dV + T_o dS + \sum_j \delta Q_j (1 - T_o/T_j) - T_o \delta \sigma$$

Useful work is optimum in the absence of any irreversibility. Thus, the *optimum useful work* is given as:

$$\delta W_{use, opt} = -dE - P_o dV + T_o dS + \sum_j \delta Q_j (1 - T_o/T_j)$$

We now integrate this equation between states 1 and 2, divide by total mass, and ignore *K.E.* and *P.E.* to get:

$$w_{use, opt} = -(u_2 - u_1) - P_o(v_2 - v_1) + T_o(s_2 - s_1) + \sum_j q_j(1 - T_o/T_j) \quad \text{IIa.10.12}$$

where $q = Q/m$. Recall that the difference between W_{use} and $W_{use, opt}$ lies in the irreversibility of the process. Therefore, the irreversibility per unit mass basis becomes:

$$w_{use, opt} - w_{use} = I/m = T_o \sigma / m \quad \text{IIa.10.13}$$

Example IIa.10.3. A rigid tank of 2 m^3 contains air at 0.4 MPa and 310 K . We now heat up the tank from a heat source at 800 K until the air temperature in the tank reaches 620 K . The surrounding atmosphere is at 1 bar and 288 K . Find a) useful work, b) optimum useful work, and c) the irreversibility of the process.

Solution: a) Since $V = \text{constant}$ and no shaft crosses the boundary, $w_{use} = 0$. Find m and P_2 for part b:

The process is isochoric; $P_2 = P_1 T_2 / T_1 = 0.8 \text{ MPa}$. Also $m = PV / RT = 0.4 \text{E}3 \times 2 / (0.287 \times 310) = 9 \text{ kg}$

b) To find $w_{use, opt}$ we need, (u_1, u_2) , (v_1, v_2) , and (s_1, s_2) . We find these properties in the following steps:

$$v_2 = v_1 = V / m = RT / P = (8.314 / 28.97) \times 310 / 0.4 \text{E}3 = 0.22 \text{ m}^3 / \text{kg}.$$

$$s_2 - s_1 = c_p \ln(T_2 / T_1) - R \ln(P_2 / P_1) = 1 \times \ln(620 / 310) - 0.287 \times \ln(0.8 / 0.4) = 0.494 \text{ kJ/kg} \cdot \text{K}$$

$$u_2 - u_1 = c_p(T_2 - T_1) = 0.72(620 - 310) = 223 \text{ kJ/kg. We find } Q \text{ from the first law: } Q / m - w_{use} = 223 \text{ kJ/kg.}$$

$$w_{use, opt} = -(223) + 288 \times 0.494 - 0.1(0) + 223(1 - 288 / 800) = 62 \text{ kJ/kg.}$$

$$\text{Thus } W_{use, opt} = 62 \times 9 = 558 \text{ kJ}$$

c) $I = W_{use, opt} - W_{use} = 558 - 0 = 558 \text{ kJ}$. This may be viewed as the work that could not be used.

Example IIa.10.4. Saturated steam condenses to saturated water in a cylinder fitted with a frictionless piston. Find a) work, b) useful work, c) optimum useful work, and d) irreversibility associated with this process.

Data: $V_1 = 2 \text{ ft}^3$ (0.057 m^3), $P_1 = 100 \text{ psia}$ (0.69 MPa), $P_o = 14.7 \text{ psia}$ (1 bar), $T_o = 525 \text{ R}$ (291 K).

Solution: We find $T_1 = 327.82 \text{ F}$, $v_g = 4.431 \text{ ft}^3 / \text{lbm}$, and $v_f = 0.0177 \text{ ft}^3 / \text{lbm}$. Thus, $m = 2 / 4.431 = 0.45 \text{ lbm}$

$$\text{a) The process is isobaric; } W = \int_1^2 P dV \quad W = Pm(v_2 - v_1) = 100 \times 144 \times 0.45(0.0177 - 4.431) / 778 = -36.7 \text{ Btu}$$

$$\text{b) } W_{use} = W - P_o m(v_{fg}) = -36.7 - 14.7 \times 144 \times 0.45(-4.4133) / 778 = -31.3 \text{ Btu}$$

$$\text{c) } w_{use, opt} = -(u_2 - u_1) - P_o(v_2 - v_1) + T_o(s_2 - s_1) + \sum_j q_j(1 - T_o / T_j).$$

In this problem, $j = o$. Substituting, we get:

$$w_{use, opt} = 807 + (14.7 \times 144 \times 4.4133 / 778) + 525(-1.1284) = 807 + 12 - 592.4 = 226.6 \text{ Btu/lbm.}$$

d) $I = mw_{use, opt} - W_{use} = 0.45 \times (226.6) - (-31.3) = 133.3 \text{ Btu}$ (140.6 kJ). This is the loss of work production.

10.4. Change in Entropy for Control Volumes

Change in the entropy of open systems can be readily obtained from Equation IIa.10.10 noting that in open systems, entropy may be brought into the system by crossing the boundary of the system through the inlet ports. Similarly, entropy may leave the system through the outlet ports, hence, for open systems:

$$dS = \sum_i \dot{m}_i s_i - \sum_e \dot{m}_e s_e + \sum_j \frac{dQ_j}{T_j} + \sum_{C.V.} \frac{I}{T} \quad \text{IIa.10.14}$$

where we have generalized the equation for the change of entropy by considering all $\delta Q/T$ terms in the control volume to account for variation of temperature within the control volume. Similarly, we considered all the lost work due to the internal irreversibility in the control volume. Equation IIa.10.14 can be readily modified for unsteady state conditions:

$$\frac{dS_{C.V.}}{dt} = \sum_i \dot{m}_i s_i - \sum_e \dot{m}_e s_e + \sum_{C.V.} \frac{\delta \dot{Q}_{C.V.}}{T} + \sum_{C.V.} \frac{\dot{I}}{T} \quad \text{IIa.10.15}$$

It is evident from Equation IIa.10.15 that, for irreversible processes in a control volume, we would have:

$$\frac{dS_{C.V.}}{dt} \geq \sum_i \dot{m}_i s_i - \sum_e \dot{m}_e s_e + \sum_{C.V.} \frac{\delta \dot{Q}_{C.V.}}{T} \quad \text{IIa.10.16}$$

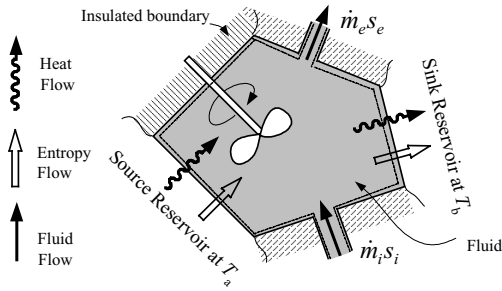
For steady flow ($\dot{m}_i = \dot{m}_e$) and steady state ($dS_{C.V.}/dt = 0$) processes we can write:

$$\dot{m}(s_e - s_i) \geq \sum_{C.V.} \frac{\delta \dot{Q}_{C.V.}}{T} \quad \text{IIa.10.17}$$

where the equals sign applies to reversible processes. For isentropic processes, $\delta \dot{Q} = 0$ hence, $s_i = s_e$.

Similar to the closed system, where we made a parallel between Equations IIa.10.10 and IIa.10.11, we are now set to find the parallel with Equation IIa.10.15 for open systems or control volumes. We do this in conjunction with Figure IIa.10.3, showing the transfer of entropy into and out of the control volume by both heat and mass transfer. We can intuitively derive the rate of change of entropy of a control volume. This is equal to the summation of the total rate of entropy transferred into the system (by heat and mass transfer), plus the rate of entropy production in the system, minus the summation of the total rate of entropy transferred out of the system. The mathematical expression of the entropy rate balance for the control volume is:

$$\frac{dS_{C.V.}}{dt} = \left(\sum_i \dot{m}_i s_i - \sum_e \dot{m}_e s_e \right) + \left(\sum_j \frac{\dot{Q}_j}{T_j} \right) + \dot{\sigma}_{C.V.} \quad \text{IIa.10.18}$$



$$\text{Rate of entropy transfer by heat flow: } \frac{\dot{Q}_a}{T_a} - \frac{\dot{Q}_b}{T_b}$$

$$\text{Rate of entropy transfer by fluid flow: } \dot{m}_i s_i - \dot{m}_e s_e$$

$$\text{Rate of entropy production by friction: } \dot{\sigma}$$

Figure IIa.10.3. Entropy transfer and production for an open system

Comparing Equation IIa.10.18 with Equation IIa.10.15 indicates that $\dot{\sigma}_{C.V.} = \dot{I}_{C.V.} / T$. At steady state, $dS_{C.V.}/dt = 0$, hence, Equation IIa.10.18 becomes:

$$\left(\sum_i \dot{m}_i s_i - \sum_e \dot{m}_e s_e \right) + \sum_j \left(\dot{Q}_j / T_j \right) + \dot{\sigma}_{C.V.} = 0 \quad \text{IIa.10.19}$$

10.5. Useful Work, Optimum Useful Work, and Irreversibility (Control Volumes)

Recall that for the closed systems, we combined the first and second law, Equations IIa.6.1 and Equation IIa.10.11 to obtain Equation IIa.10.12. Similarly, we may combine Equation IIa.6.3 and Equation IIa.10.18 to obtain the equation for useful work for a control volume. In specific, for flow entering and leaving a rigid control volume under steady state conditions (i.e. Equations IIa.6.5 and IIa.10.19) we find that the optimum useful shaft work at steady state (ss) operation is given by (see Problem 117):

$$\dot{W}_{opt,ss} = \sum_j \dot{m}_i \left(h_i + V_i^2 / 2 + gz_i - T_o s_i \right) - \sum_j \dot{m}_e \left(h_e + V_e^2 / 2 + gz_e - T_o s_e \right) + \sum_j \dot{Q} \left(1 - \frac{T_o}{T_j} \right) \quad \text{IIa.10.20}$$

If flow through the control volume at steady state condition is also steady flow, then the irreversibility per unit mass flow rate is given by Equation IIa.10.16 and Equation IIa.10.20 becomes:

$$w_{opt,ss} = \sum_j \left(h_i + V_i^2 / 2 + gz_i - T_o s_i \right) - \sum_j \left(h_e + V_e^2 / 2 + gz_e - T_o s_e \right) + \sum_j q \left(1 - \frac{T_o}{T_j} \right) \quad \text{IIa.10.21}$$

Example Ila.10.5. A globe valve is used to throttle steam in a steady state process from 10 MPa and 360 C to 4 MPa. The valve is fully insulated. Find the rate of entropy production in this process.

Solution: The throttling process in the valve is iso-enthalpic, $h_e = h_i$.

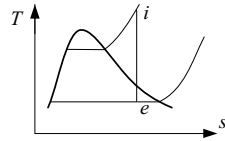
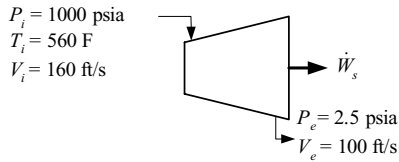
At $P_i = 10$ MPa and $T_i = 360$ C, $s_i = 6.006$ kJ/kg·K and $h_i = 2962.1$ kJ/kg.

At $P_e = 4$ MPa and $h_e = 2962.1$ kJ/kg, $s_e = 6.362$ kJ/kg·K.

From Equation Ila.10.16 with $Q = 0$ and $\dot{m}_i = \dot{m}_e$:

$$\dot{\sigma} / \dot{m} = 6.362 - 6.006 = 0.356 \text{ kJ/kg·K}$$

Example Ila.10.6. Superheated steam enters a turbine at $P_1 = 1000$ psia, $T_1 = 560$ F, and $V_1 = 160$ ft/s. Steam expands isentropically to a pressure of 2.5 psia and leaves the turbine at 100 ft/s. The inlet flow area of the turbine is $A_i = 22$ ft². Find a) work delivered by the turbine, b) entropy produced in this expansion process, c) the optimum useful work, and d) irreversibility. For the surroundings use $P_o = 14.7$ psia and $T_o = 70$ F.



Solution: a) We first find superheated properties at 1000 psia and 560 F from the steam tables:

P_i (psia)	T_i (F)	v_i (ft ³ /lbm)	h_i (Btu/lbm)	s_i (Btu/lbm·R)
1000	560	0.4668	1210.4	1.4082

We then find the exit conditions at 2.5 psia from the steam tables as follows:

P_e (psia)	$h_{f,e}$ (Btu/lbm)	$h_{g,e}$ (Btu/lbm)	$s_{f,e}$ (Btu/lbm·R)	$s_{g,e}$ (Btu/lbm·R)
2.5	101.71	1119.4	0.188	1.9029

To find the work performed by the turbine we use the first law, Equation Ila.6.5. Since there is no heat loss from the turbine, the change in elevation is negligible and the work is delivered under steady flow, steady state condition, this equation simplifies to:

$$\dot{m} \left(h_i + \frac{V_i^2}{2} \right) = \dot{W}_s + \dot{m} \left(h_e + \frac{V_e^2}{2} \right)$$

To find the rate of work delivered, we need to find h_e and \dot{m} . The exit enthalpy is given by $h_e = h_{f,e} + x_e h_{fg,e}$. Having $h_{f,e}$ and $h_{fg,e}$, we must find x_e . This is obtained from the isentropic expansion of steam in the turbine:

$$s_i = s_e = s_{f,e} + x_e s_{fg,e}$$

$$x_e = \frac{s_i - s_{f,e}}{s_{g,o} - s_{f,e}} = \frac{1.4082 - 0.188}{1.9029 - 0.188} = \frac{1.2202}{1.7149} = 0.712$$

$h_e = h_{f,e} + x_e(h_{g,e} - h_{f,e}) = 101.71 + 0.712(1119.4 - 101.71) = 826.3$ Btu/lbm. We find the mass flow rate from $\dot{m} = \rho_i V_i A_i = (1/0.4668) \times 160 \times 22 = 7540.7$ lbm/s. Thus, the power produced by the turbine is obtained as:

$$\dot{W}_s = \dot{m} \left((h_i - h_e) + \left(\frac{V_i^2}{2} - \frac{V_e^2}{2} \right) \right) =$$

$$7540.7 \times \left((1210.4 - 826.3) + \left(\frac{160^2 - 100^2}{2 \times 32.2 \times 778} \right) \right) = 2.898\text{E}6 \text{ Btu/s}$$

b) In an isentropic process, no entropy is produced. This is confirmed by Equation Ila.10.16, since $s_1 = s_2$ and $\dot{Q} = 0$, therefore, $\sigma_{C.V.} = 0$.

c) and d) In this problem, $w_{use} = w_{use, opt}$ and $I = 0$.

11. Exergy or Availability

Our goal is to determine the maximum work that can be obtained in a work-producing process from a given system. Such system may contain various forms of energy including kinetic, potential, chemical, electrical, and nuclear. The necessary and sufficient conditions for obtaining the maximum work from a system are satisfied in a reversible process that brings the system to the *dead state*. The dead state for pressure (P) and temperature (T) of the system is when P and T reach P_o and T_o of the surroundings, respectively. When this occurs, the system is in chemical, mechanical, and thermal equilibrium with the surroundings. Such equilibrium with the surroundings is required if work can be extracted by any means. For example, if system contains kinetic energy then its velocity should be brought to zero. Similar argument applies to potential energy, etc. Next we investigate the availability (exergy) of closed systems and of control volumes focusing on the systems that contain only mechanical and thermal energies.

11.1 Availability (Exergy), Closed Systems

Shown in Figure Ila.11.1 is a closed system containing a hot gas with the frictionless piston held in place by a stop. We now remove the stop and let the gas expand. The work delivered by the piston in an infinitesimal move is $\delta W_{use} = \delta W - P_o dV$. To bring temperature down to that of the surrounding (T_o), δQ heat must

be rejected to the surrounding. If used in a reversible machine, this amount of heat can produce work given by:

$$\delta W_{\text{equivalent}} = -\delta Q(1 - T_o/T)$$

where T is the system temperature during the process, ranging from $T_1 \leq T \leq T_o$. Therefore the net work in this expansion process is found by deducting the work corresponding to the heat rejection from the useful work (i.e. $\delta W_{\text{net}} = \delta W_{\text{use}} - \delta W_{\text{equivalent}}$). Substituting, we obtain $\delta W_{\text{net}} = \delta W - P_o dV - \delta Q(1 - T_o/T)$. Since we assumed a reversible expansion due to the frictionless piston, this is the maximum work that can be obtained in this process. For closed systems, we consider the system internal energy, substitute for δW from the first law ($\delta W = \delta Q - dU$), and for δQ from the second law ($\delta Q = TdS$) to find the relation for the infinitesimal work as $\delta W_{\text{use,opt}} = -dU - P_o dV + T_o dS$. Integrating, the net work in this process is found as:

$$W_{\text{use,opt}} = (U - U_o) + P_o(V - V_o) - T_o(S - S_o) \quad \text{IIa.11.1}$$

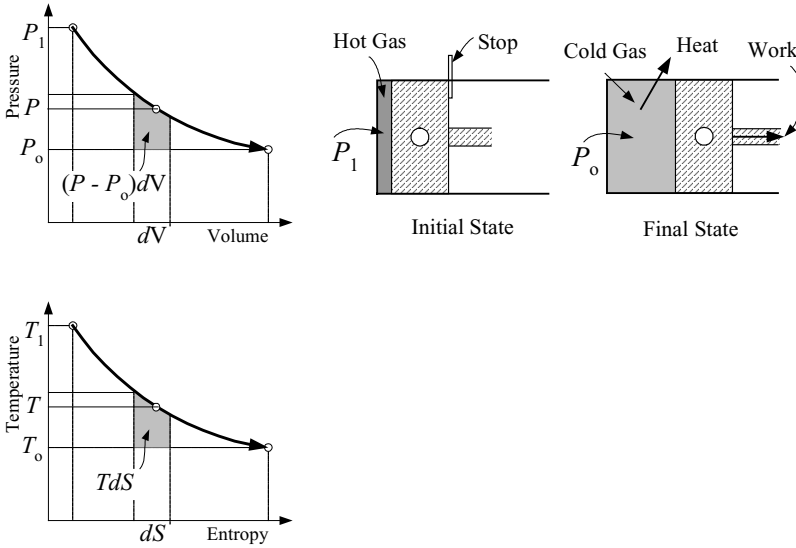


Figure IIa.11.1. A process for bringing a closed system from state 1 to the dead state

where the *opt* in the subscript is added to emphasize the reversible process. The work obtained in Equation IIa.11.1 is the closed system availability (Φ). Written on a specific basis, the specific availability becomes:

$$\phi = (u + P_o v - T_o s) - (u_o + P_o v_o - T_o s_o) \quad \text{IIa.11.2}$$

Equation IIa.11.2 can alternatively be written as:

$$\phi = (u - u_o) + P_o(v - v_o) - T_o(s - s_o) \quad \text{IIa.11.3}$$

so that $\Phi = m\phi$. Assuming the surroundings condition is at atmospheric pressure (14.7 psia = 101 kPa) and room temperature (77 F = 25 C), then the specific exergy, ϕ can be considered as yet another property.

Example IIa.11.1. A cylinder contains 5 kg of air (treated as an ideal gas) at 1 MPa and 350 C. The piston is held in place by a stop pin. Find the maximum useful work when the frictionless piston is set free to move.

Solution: Find $v = RT/P = (8.314/28.97) \times (350 + 273)/1E3 = 0.179 \text{ m}^3/\text{kg}$ and $v_o = 0.847 \text{ m}^3/\text{kg}$

$$P_o(v - v_o) = 101 \times (0.179 - 0.847) = -67.468 \text{ kJ/kg}$$

$$u - u_o = c_v(T - T_o) = 0.7165 \times (350 - 25) = 232.86 \text{ kJ/kg}$$

$$s - s_o = c_v \ln(T_1/T_o) + R \ln(v_1/v_o) = 0.7165 \times \ln(623/298) + (8.314/28.97) \times \ln(0.179/0.847) = 0.0823 \text{ kJ/kg}$$

$$\phi = (u - u_o) + P_o(v - v_o) - T_o(s - s_o) = 232.86 - 67.468 - 298 \times 0.0823 = 140.86 \text{ kJ/kg}$$

$$\Phi = 5 \times 140.86 = 704.33 \text{ kJ. } W_{use,opt} = 704.33 \text{ kJ.}$$

Change in Availability

We can readily derive the change in availability for closed systems by combining the first and the second law of thermodynamics, Equations IIa.6.1 and IIa.10.11, respectively. The first law, $E_2 - E_1 = \int_1^2 \delta Q - W$ added to the second law, while multiplied by T_o , and rearranged results in:

$$\Phi_2 - \Phi_1 = \int_1^2 \left(1 - \frac{T_o}{T_b} \right) \delta Q - [W - P_o(V_2 - V_1)] - T_o \sigma \quad \text{IIa.11.4}$$

Equation IIa.11.4 demonstrates that the change in availability is due to the availability transfer (the first three terms in the right side) and the availability destruction (the fourth term in the right-hand side). The terms representing availability transfer itself consists of availability transfer associated with heat (the first term in the right side) and the availability transfer associated with work (the second and third term in the right side).

Example IIa.11.2. A piston-cylinder assembly contains m lbm of saturated water at 212 F. We now add heat to the cylinder from a reservoir at temperature T , in a reversible process (the frictionless piston is free to move) until all water becomes saturated steam. Verify Equation IIa.10.18 for this process.

Solution: On the one hand, change in specific availability is given by:

$$\Delta\phi = (u_g - u_f) + P_o(v_g - v_f) - T_o(s_g - s_f).$$

On the other hand, $\Delta\Phi$ from Equation IIa.11.4 for $\sigma = 0$ is:

$$\Delta\Phi = (1 - T_o/T)Q - [W - P_o(V_2 - V_1)].$$

The availability transfer due to work is:

$$W - P_o(V_2 - V_1).$$

Since expansion work is given by $W = P\Delta V$, if we substitute for W , we find:

$$P\Delta V - P_o(\Delta V) = 0.$$

Therefore, $\Delta\Phi = (1 - T_o/T)Q$. Heat transfer is given by $Q/m = h_{fg}$. Thus, $\Delta\Phi = (1 - T_o/T)mh_{fg}$. This can be written as

$$\Delta\Phi/m = \Delta\phi = h_{fg} - T_o(h_{fg}/T) = (u_{fg} + P_o v_{fg}) - T_o s_{fg}.$$

Since availability can be viewed as a property of the system, which by definition, is independent of the path and depends only on the end states, we can find the change in system availability when the system goes from state 1 to state 2 as $\phi_2 - \phi_1 = (u_2 - u_1) + P_o(v_2 - v_1) - T_o(s_2 - s_1)$. Upon comparing with Equation IIa.10.12, we find the change in availability given as:

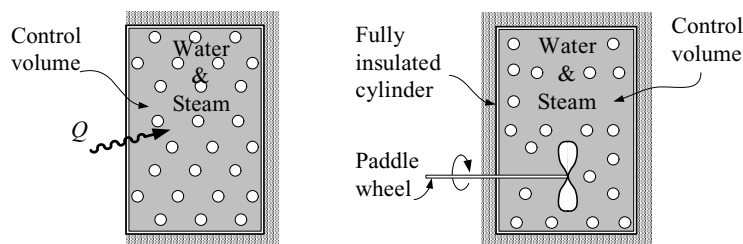
$$\phi_1 + \sum_j \dot{q}_j (1 - T_o/T) = W_{use,opt} + \phi_2$$

this equation can also be written as:

$$w_{use,opt} = -(\phi_2 - \phi_1) + \sum_j q_j (1 - T_o/T_j) \quad \text{IIa.11.5}$$

If the change in availability has been solely due to work transfer, Equation IIa.11.5 for adiabatic processes simplifies to $w_{use,opt} = -(\phi_2 - \phi_1)$.

Example IIa.11.3. A tank of 2 ft³ contains two-phase mixture of water and steam at 200 psia with $x = 10\%$. We want to increase the mixture temperature to 456.3 F by one of the following two processes. Find the irreversibility if a) heating the tank from a reservoir at 600 F and b) insulating the tank and using a paddle wheel. The surrounding pressure and temperature are 15 psia and 59 F.



Solution: We first find the mixture properties at the initial and the final states:

P (psia)	T (F)	v_f (ft ³ /lbm)	v_g (ft ³ /lbm)
200	381.8	0.01839	2.2873
450	456.3	0.01954	1.0318

u_f (Btu/lbm)	u_g (Btu/lbm)	s_f (Btu/lbm·R)	s_g (Btu/lbm·R)
354.8	1113.7	0.5438	1.5454
435.7	1118.9	0.636	1.4738

$v_2 = v_1 = 0.01839 + 0.1(2.2689) = 0.245 \text{ ft}^3/\text{lbm}$. Thus $x_2 = (0.245 - 0.0195)/1.01224 = 22.3\%$.

$m = V/v = 2/0.245 = 8.154 \text{ lbm}$. We now find change in availability for a closed system:

$$\phi_2 - \phi_1 = (u_2 - u_1) + P_o(v_2 - v_1) - T_o(s_2 - s_1) = (157.37) + 0 - 519 \times 0.1789 = 64.52 \text{ Btu/lbm or } \Delta\Phi = 526 \text{ Btu}$$

a) Since $W = 0$, we find Q from the first law, $Q = \Delta u = 8.154(157.37) = 1283.2 \text{ Btu}$. Next we find $W_{\text{use, opt}}$:

$$(W_{\text{use, opt}})_a = -\Delta\Phi + Q(1 - T_o/T) = -526 + 1283.2(1 - 519/1060) = 129 \text{ Btu}.$$

b) Since $Q = 0$, we find W from the first law, $W = -\Delta u = 8.154(157.37) = -1283.2 \text{ Btu}$. We find $W_{\text{use, opt}}$:

$$(W_{\text{use, opt}})_a = -\Delta\Phi = -526 \text{ Btu}.$$

In both process, $I = W_{\text{use, opt}} - W$. Thus $I_a = 129 - 0 = 129 \text{ Btu}$ and $I_b = -526 - (-1283.2) = 757.2 \text{ Btu}$

Since $I_b \gg I_a$, from a thermodynamic view point, heat transfer is preferred than using work to produce heat.

We may also use Equation IIa.10.19 to define a second law effectiveness (ζ) for a work producing process:

$$\zeta = \frac{w}{w_{\text{use, opt}}} = \frac{w}{-(\phi_2 - \phi_1) + \sum_j q_j (T_o / T_j)} \quad \text{IIa.11.6}$$

Example IIa.11.4. A cylinder contains steam at 3 MPa and 320 C. The frictionless piston is set free to move. After expansion, steam pressure and temperature drop to 0.7 MPa and 180 C. The work resulting from this expansion is 185 kJ/kg and the sink reservoir to exchange heat is at 100 C. Find the effectiveness.

Solution: We set up the following table for the data

P (MPa)	T (C)	v (m^3/kg)	u (kJ/kg)	s (kJ/kg·K)
3.00	350	0.0850	2788.4	6.6245
0.75	180	0.2847	2599.8	6.7880

Use the first law to find q_{1-2} gives:

$$q_{1-2} = w_{1-2} + (u_2 - u_1) = 185 + (2599.8 - 2788.4) = -3.6 \text{ kJ/kg}$$

$$w_{1-2} = \phi_1 - \phi_2 + q_{1-2}(1 - T_o/T_s) = (u_1 - u_2) + P_o(v_1 - v_2) - T_o(s_1 - s_2) + q_{1-2}(1 - T_o/T_s)$$

$$w_{1-2} = (2788.4 - 2599.8) + 101(0.085 - 0.2847) - 298(6.788 - 6.6245) - 3.6(1 - 298/373) = 256.77 \text{ kJ/kg}$$

$$\zeta = 185/256.77 = 72\%.$$

11.2. Availability (Exergy), Control Volumes

We define the flow exergy for open systems in a manner similar to that of the closed systems except for the fact that the specific flow exergy must account for the potential and kinetic energies of the fluid, knowing that at the dead state the system should reach the velocity of the surroundings (zero) and the same elevation as the surroundings. As a result, the exergy for a control volume per unit mass basis is defined as:

$$\psi = (h - h_o) - T_o(s - s_o) + (V^2/2) + g(Z - Z_o) \quad \text{IIa.11.7}$$

where Z_o is the elevation at the dead state. Therefore, the change in the inlet and exit availabilities becomes:

$$\Delta\psi = (h_e - h_i) - T_o(s_e - s_i) + (V_e^2 - V_i^2)/2 + g(Z_e - Z_i) \quad \text{IIa.11.8}$$

In most practical applications, the kinetic and potential energies are neglected compared to the fluid enthalpy. Using Equation IIa.11.8, the optimum useful work at steady state for a control volume can be obtained if we stipulate multiple input and exit ports and an exchange of heat and work with the surroundings and heat reservoirs. This work is the difference between the availabilities of the inlet and exit streams plus the work associated with the exchange of heat with heat reservoirs:

$$\dot{W}_{opt,ss} = \sum_i \dot{m}_i \psi_i - \sum_e \dot{m}_e \psi_e + \sum_j \dot{Q}_j \left(1 - \frac{T_o}{T_j} \right) \quad \text{IIa.11.9}$$

It then follows that the irreversibility associated with the steady flow of fluids through a control volume with multiple ports, while exchanging heat and work with the surroundings and heat reservoirs, is given as:

$$\dot{I}_{c.v.} = \sum_i \dot{m}_i \psi_i - \sum_o \dot{m}_o \psi_o + \sum_j \dot{Q}_j \left(1 - \frac{T_o}{T_j} \right) - \dot{W}_{c.v.} \quad \text{IIa.11.10}$$

Example IIa.11.5. Steam enters a fully insulated turbine at 800 psia and 550 F. Steam leaves the turbine at 10 psia with $x_e = 80\%$. Find the following items: a) work delivered by the turbine, b) the maximum useful work, c) the availability of the exit stream, d) the effectiveness, and e) the irreversibility. Use $T_o = 530$ R.

Solution: a) From the first law with $q = 0$, we find $w = h_i - h_e = 1230.1 - 964.94 = 283.2$ Btu/lbm.

b) $w_{opt,ss} = \psi_i - \psi_e = (h_i - h_e) - T_o(s_i - s_e)$. Thus $w_{opt,ss} = 283.2 - 530(1.447 - 1.487) = 304.42$ Btu/lbm

c) $\psi_e = (h_e - h_o) - T_o(s_e - s_o)$. For h_o and s_o of the dead state we use saturated properties for a subcooled liquid corresponding to T_o :

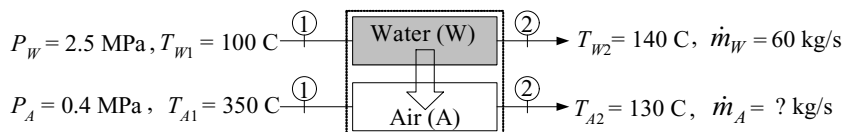
$\psi = (964.94 - 38.05) - 530(1.487 - 0.0745) = 178.3$ Btu/lbm.

d) $\zeta = w/w_{opt,ss} = 283.2/304.42 = 93\%$ and finally

e) $I_{c.v.} = w_{opt,ss} - w = 304.42 - 283.2 = 21.22$ Btu/lbm

In the thermal design of turbines it is important to minimize the availability of the exit stream to increase the effectiveness. In the above example, the irreversibility associated with the adiabatic expansion of steam is due to the increase in entropy during the expansion of the steam in various stages of the turbine.

Example Ila.11.6. Water is heated by a stream of hot air in a heat exchanger as shown. Use the data as given in the figure to find the system irreversibility. Ignore pressure drop in both streams. Use $T_o = 295$ K.



Solution: We ignore the *K.E.* and *P.E.* of both streams and treat air as an ideal gas. Stream availabilities are:

$$\Delta\psi_W = (h_{W2} - h_{W1}) - T_o(s_{W2} - s_{W1}) = (590.52 - 420.85) - 295(1.7369 - 1.3050) = 42.26 \text{ kJ/kg}$$

$$\Delta\psi_A = (h_{A2} - h_{A1}) - T_o(s_{A2} - s_{A1}) = (130 - 350) - 295(-0.3365) = -120.73 \text{ kJ/kg}$$

$\Delta\dot{\psi}_W = \dot{m}_W \Delta\psi_W = 60 \times 42.26 = 2535.6 \text{ kJ}$. We find \dot{m}_A from an energy balance for the heat exchanger:

$$\dot{m}_W(h_{W2} - h_{W1}) = \dot{m}_A c_{p,A}(T_{A1} - T_{A2}). \text{ Thus } \dot{m}_A = 60(590.52 - 420.85)/(350 - 130) = 46.27 \text{ kg/s}$$

$$\Delta\dot{\psi}_A = \dot{m}_A \Delta\psi_A = 46.27 \times (-120.73) = -5586.6 \text{ KJ}$$

$$\dot{I}_{c.v.} = \sum_i \dot{m}_i \psi_i - \sum_o \dot{m}_o \psi_o - \dot{W}_{c.v.} = \dot{m}_W \psi_W + \dot{m}_A \psi_A = 2535.6 - 5586.6 = -3051 \text{ kJ}$$

Example Ila.11.7. Cooling water at a rate of 170,000 lbm/s enters the condenser of an electric utility from a lake at 60 F and leaves at 75 F. The plant also produces exhaust gases at a rate of 450 lbm/s and 455 F. Find the more wasteful stream leaving this electric plant. Use $T_o = (60 + 460) = 520$ R.

Solution: We ignore the *K.E.* and *P.E.* and take the exhaust gases to be air, behaving as an ideal gas. Thus, for both water as compressed liquid and air as ideal gas, $\Delta h \approx c_p \Delta T$. We need to compare ψ_W with ψ_A .

Since the process for both streams is isobaric, $s - s_o = c_p \ln(T/T_o)$.

$$\psi_W = \dot{m}_W [c_{pW}(T_W - T_o) - c_{pW}T_o \ln(T_W/T_o)] = 1.7E5[1.0(75 - 60) - 1.0 \times 520 \ln(535/520)] = 36,086 \text{ Btu}$$

$$\psi_A = \dot{m}_A [c_{pA}(T_A - T_o) - c_{pA}T_o \ln(T_A/T_o)] = 450[0.24(455 - 60) - 0.24 \times 520 \ln(915/520)] = 10,924 \text{ Btu}$$

The cooling water carries more untapped energy than the stack gases by a factor of 3.

QUESTIONS

Section 1

- What are the primary dimensions?
- Mention three derived units.
- What is barometric pressure? What is the absolute pressure of total vacuum?
- Pressure of a gas container is 2 psig. What is the absolute pressure of the gas container?
- What is a pure substance? Is water a pure substance?
- What is the difference between a system and its surrounding?

Section 2

- Explain the difference between ideal, perfect, and real gases.
- Comparing the Van der Waals equation with the ideal gas law, can we conclude that the former accounts for the existence of gas molecule, hence, reduces the available volume in a gas container ($v - c_2$)?
- Comparing the Van der Waals equation with the ideal gas law, which equation of state accounts for the intermolecular attractive force ($P + c_1/v^2$)?
- By accounting for the net attraction of the molecules within a gas on an individual molecule, does the Van der Waals equation account for the reduction in the impulse the molecule would have otherwise exerted on the wall of a gas container?

Section 3

- What is degree of subcooling?
- Consider the saturation temperature of water, $T_{sat} = f(P)$. Does T_{sat} increase, remain the same, or decrease with increasing pressure?
- What is the difference between a polytropic and an isentropic process?
- A system has pressure P_1 at one instant and pressure P_2 at another instant. Is the change in pressure an exact differential?
- Is it fair to say that any change in the properties of a system in any process is always an exact differential?

Section 4

- Give an example for the “insulated system”
- What is the difference between control mass and control volume?
- Define control surface
- Since no mass crosses the boundaries of a closed system, how can its energy content change?
- Which of heat, work, and total energy of a system is an exact differential?
- Is there any work associated with the rotation of a shaft in a well lubricated journal bearing?

Section 5

- What is the difference between steady flow and steady state?

- Consider heating up a steel rod. Is this a steady state process? Give an example for a steady state process.
- Consider a compressor as a control volume. The air density changes as air flows through the inlet towards the outlet. If $dm_{C.V.}/dt = 0$ and $dE_{C.V.}/dt = 0$, is this process a steady state process?

Section 6

- What is the difference between a nozzle and a diffuser?
- What is the difference between a turbine and a compressor?
- What is the difference between a compressor and a pump?

Section 7

- Is it a good idea to insulate compressors and turbines?
- Is it fair to say that water density remains constant from the suction to the discharge of a pump?
- Does one control volume allow determination of the temperature distribution inside the control volume?

Section 8

- What is the key assumption in the dynamic analysis of mixing tanks?
- How do we find the mass flow rate through a control valve while discharging gas filled rigid vessels?
- How can we add heat to a rigid vessel in an isobaric process?

Section 9

- Can any process that does not violate the first law of thermodynamics be reversed?
- Which process takes place more readily, conversion of work to heat or conversion of heat to work?
- What is the Kelvin-Planck statement on the transfer of energy from a heat source to a heat sink?
- What is the difference between internal and external irreversibility?
- We bring a hot block of metal in contact with a cold block of metal. Is the heat transfer between these two blocks of metal reversible?
- Is any reversible process necessarily an adiabatic process?
- What is the difference between a reversible and an isentropic process?
- Is it possible to transfer heat from a heat sink to a heat source? Doesn't this violate the second law?
- A heat engine is operating between T_H and T_C . Which temperature do you change to increase efficiency?
- What is the function of a heat pump? How do you define the coefficient of performance for a heat pump?

Section 10

- Is entropy, like energy, conserved in any process?

- Describe unavailability in the context of dissipative effects of an irreversible process.
- What is the change in entropy of a work reservoir ($dS_{\text{Work reservoir}} = ?$)
- What is the proportionality constant for the change of entropy of a heat reservoir ($dS_{\text{Heat reservoir}} = ?$)
- Support the Clausius statement of the second law using entropy change for a device that works in a cycle and transfers heat from the heat source to the heat sink.
- Does entropy change in an isolated system?
- In what ways does entropy change for a closed system? Answer the same question for an open system.
- How do you define useful work, the optimum useful work, and irreversibility?

PROBLEMS

Sections IIa.1 and IIa.2

1. A system is left alone for a long time. During this time, no mass, no heat, and no work have crossed its boundary. Is this system at equilibrium?
2. A system is left alone for a long time. During this time no mass, no heat, and no work have crossed its boundary. Are properties of this system (i.e., such macroscopically measurable quantities as pressure, volume, and temperature) independent of time?
3. Find the weight in lbf of a substance having a mass equal to 4536 g. [Ans.: 10 lbf].
4. a) At certain flow conditions, the maximum mass flow rate of an ideal gas through a cross section, known as the critical flow, is given by $\dot{m} = bP/\sqrt{T}$. Find units of b if units of \dot{m} , P and T are lbm/s, psia, and degree Rankine, respectively.
b) The critical flow of saturated steam per unit area may be estimated from a relation known as Rateau correlation: $G = P[16.367 - 0.96\log_{10}P]/1000$. In this correlation, units of P and G are psia and lbm/s-in², respectively. Convert this relation so that for P in MPa, we obtain G in kg/s-cm².
5. Partial vacuum is often measured in torr where 1 torr is 133.322 Pa or 1.316E-3 atm. A vacuum pump is used to bring pressure in a tank down to 2.8 torr. Find the tank pressure in cm Hg and cm H₂O.
6. Find the *K.E.* of a substance having a mass of 2 kg and moving at a velocity of 5 m/s. [Ans. 50 J].
7. Find the *K.E.* of a substance having a mass of 2 lbm and moving at a velocity of 5 ft/s. [Ans.: 1.55 ft·lbf = 2E-3 Btu].

8. Find the kinetic and potential energies of a ball having a mass of 2 lbm and travelling at 5 ft/s at an elevation of 10 ft above the ground. [Ans.: 0.776 ft·lbf and 20 ft·lbf].
9. Find the *K.E.* of a 5000 lbm car traveling at 55 miles per hour. [Ans.: 0.5E6 ft·lbf]
10. A 100 lb rock is lifted to a height of 100 ft. Find the change in the potential energy of the rock in Btu.
11. Find the atmospheric pressure in feet of water and cm of mercury. The specific weight of mercury is 13.6. [Ans.: 33.92 ft and 76 cm-Hg].
12. Water at atmospheric pressure in a standpipe is supplied to a hydrant. Water pressure at the hydrant must be 65 psig. Find the height of the standpipe with respect to the hydrant to meet this requirement. Use $\rho_{\text{water}} = 62.4 \text{ lbm/ft}^3$. [Ans.: 150 ft]
13. A U-tube containing mercury is used as a manometer. This manometer is now connected to a container containing gas at 0.404 atm. Find the difference in the mercury height in the U-tube after being connected to the container. [Ans.: 1 ft].
14. A gas is drawn in a pipe by a vacuum pump. The manometer reads -3 in Hg. Find the gas gage pressure in inches of mercury and the absolute pressure in psia.
15. A mercury manometer reads a pressure of 5 in Hg. We now want to substitute a manometer filled with oil having a density of 45 lbm/ft³. Find the reading on the oil-filled manometer. [Ans.: 94.3 in Oil].
16. A liquid of unknown density is used in a manometer. When $P_{\text{atm}} = 14.7 \text{ psia}$, we read $H_1 = 6.72 \text{ m}$. Find the liquid density in lbm/ft³. [Ans.: 96 lbm/ft³].

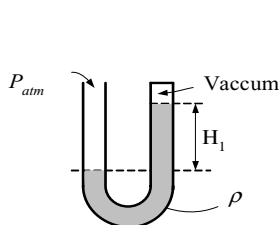


Figure for Problem 16

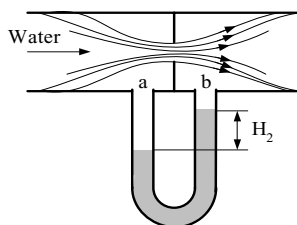


Figure for Problem 17

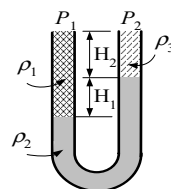
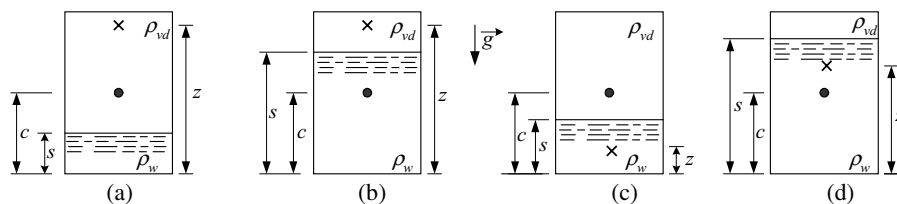


Figure for Problem 18

17. The liquid in Problem 16 is now used in measuring the pressure drop of water flowing through a thin plate orifice. For $H_2 = 60 \text{ cm}$, find pressure drop over the orifice. [Ans.: 0.46 psi].
18. For the heights and densities in the U-tube, find $P_1 - P_2$ in terms of H_1 , H_2 , ρ_1 , ρ_2 , and ρ_3 .
19. A tank contains a pool of water (density ρ_w) and a mixture of water vapor and water droplets (density ρ_{vd}). Pressure at height c (center of the tank) is given. Find

pressure at height z of each tank in terms of P_c and given heights and densities.

[Ans.: a) $P_z = P_c + (c - z) \rho_{vd}g$].



20. Find the Kmols of ammonia (NH_3) that is equivalent to 34 kg of NH_3 . [Ans.: 2 kmol]

21. Find the lb-moles of CO_2 contained in 120 g of CO_2 . [Ans.: 6.02E-3 lb-mole].

22. Find the mass of air in a 1 m^3 tank. Pressure in the tank is 1 MPa and air temperature in the tank is 40 C. [Ans. 11.11 kg].

23. A pressure vessel having a volume of 171 ft^3 contains 1.523 lbmoles of helium at a pressure of 7 atm. Find the temperature of helium in this tank. [Ans.: 620 F].

24. In this problem we want to compare the prediction of three equation of states for gases. These are the ideal gas, $Pv = RT$, the Van Der Waals $(P + c_1/v_2)(v - c_2) = RT$, and the Beattie-Bridgeman equation:

$$P = \frac{RT}{\bar{v}^2} \left(1 - \frac{c}{\bar{v}T^3} \right) (\bar{v} + B) - \frac{A}{\bar{v}^2}$$

For this comparison, use CO_2 at $T = 300 \text{ K}$ and $v = 0.0040 \text{ m}^3/\text{kg}$. Compare the results with the value of 6.6 MPa obtained experimentally. Note that in the Beattie-Bridgeman equation v is in m^3/kmol , T is in K, and P is in kPa. Also $A = A_0(1 - a/v)$ and $B = B_0(1 - b/v)$. For CO_2 , $A_0 = 507.2836$, $a = 0.07132$, $B_0 = 0.10476$, $b = 0.07235$, and $c = 660,000$. [Ans. $P_{IG} = 14.17 \text{ MPa}$, $P_{VDW} = 6.95 \text{ MPa}$, and $P_{BB} = 6.741 \text{ MPa}$].

25. Use a Maxwell relation and show that the change in entropy of an ideal gas is given as:

$$s_2 - s_1 = c_p \ln \frac{T_2}{T_1} - R \ln \frac{P_2}{P_1}$$

Section IIa.3

26. Plot water density as a function of temperature in the range of 32 F to 100 F. Find the peak water density.

27. Find the enthalpy of a water mixture at 2000 psia and a quality of 50%. [Ans.: 905 Btu/lbm].

28. Use the steam tables and find the specific volume of water at a) $P = 550$ psia and $T = 580$ F, b) $P = 600$ psia and $T = 180$ F, c) $P = 500$ psia and $u = 800$ Btu/lbm, d) $P = 500$ psia and $h = 1000$ Btu/lbm.

29. Use the steam tables and find steam quality for a) $T = 120$ C and $v = 0.6$ m³/kg, b) $P = 2250$ psia, $h = 1000$ Btu/lbm, and c) $P = 10$ MPa, $v = 0.015$ m³/kg.

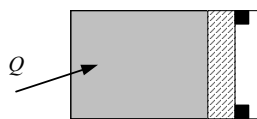
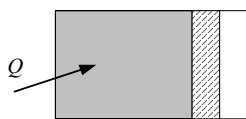
30. Use the steam tables and find the specific entropy of water at a) $P = 10$ MPa and $T = 180$ C, b) $P = 2$ MPa and $T = 370$ C, c) $P = 5$ MPa and $u = 1200$ kJ/kg, d) $P = 5$ psia and $h = 1200$ F.

31. Use the steam tables and find the temperature and the thermodynamic state of water at $P = 7.5$ MPa and $h = 1200$ kJ/kg.

32. For water, we are given $P = 350$ psia and $T = 134.604$ F. Can we find other thermodynamic properties such as v , u , h , and s ? Explain your answer.

Sections Ila.4 through Ila.8

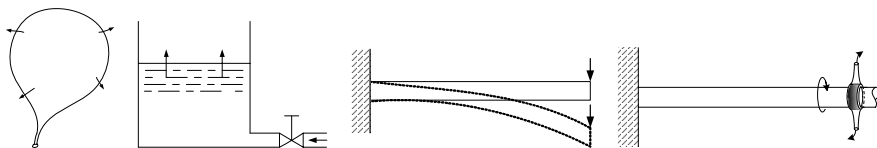
33. Heat is added to a cylinder as shown in the figure. Find the type of process in both cases.



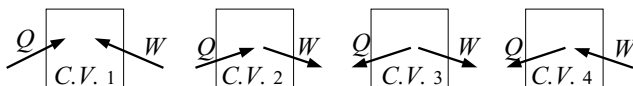
34. Write the conservation of mass and the first law of thermodynamic for a closed system undergoing a cycle.

35. Determine if any work is associated with the following actions and the type of the work if applicable:

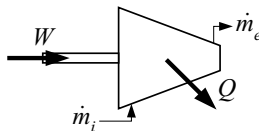
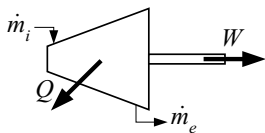
a) inflating a balloon, b) filling a tank from the bottom, c) depressing the free end of a cantilever and d) twisting a free end of a cantilever.



36. Select the sign of the heat and work terms in the equation for the first law of thermodynamics written for a closed system (i.e., $E_1 + Q = W + E_2$) given the following cases:



37. Select the sign of the heat and work terms in the equation for the first law of thermodynamics written for a control volume given the following cases:



38. Specify the type of work in the following examples, a) crushing an empty soda can, b) pulling a spoon out of a honey jar, c) cranking an engine, d) pumping water, e) turning a shaft inside a lubricated bearing.

39. The solar collector shown in Figure I.7.5 is used to provide domestic hot water. Assuming a person needs about 20 gallon/day (76 liter) of hot water at 140 F (60 C), find the collector surface area to meet this demand. Use a tap water temperature of 60 F (15.5 C). For solar radiation, use a heat flux (radiant energy divided by the collector surface area) of 236 W/m². Due to the collector thermal properties, only 80% of the sun's energy is available to warm the flowing water in the solar collector. [Ans.: 1.57 m²].

40. We want to evaluate the operation of the relief valve in the radiator cap of a car on a hot summer day while the car is driven up a hill. Before the engine is started, water is at atmospheric pressure and room temperature (P_1 and T_1 , respectively). At this condition, the volume of water in the engine block, radiator, water pump, and the connecting hoses is V_1 . The volume between the water surface and the top of the radiator is ΔV . We now start the engine and begin driving the car on the long road leading to the hill. The relief valve opens when the pressure reaches P_H . 1) Plot the expansion and the pressurization processes on the T - v diagram of Figure IIa.3.1(c) and 2) Explain how you find the amount of heat transferred to the water when pressure reaches P_H . For this evaluation you may assume: a) water is incompressible (i.e., changes in water density are negligible), and b) air is removed so that water expansion is an isobaric process.

41. A tank contains air treated as an ideal gas initially at 100 psia and 200 F. We now heat up this tank until its pressure reaches 110 psia. Find the air temperature at this pressure.

42. A cylinder equipped with a piston contains saturated steam at 2 MPa. We now compress the steam in an isentropic process until its volume becomes equal to 2/3 of its original volume. Find the steam pressure, temperature, and its thermodynamic state.

43. A cylinder contains air at 150 psia and 250 F. The air is kept in the cylinder with a tightly fit piston. At this state, the cylinder volume is 5 ft³. We now compress the air, treated as an ideal gas, while heat is removed so that compression takes place in constant pressure until the air volume becomes 2 ft³. Find the amount of heat removed from the cylinder.

44. In this problem we want to find the work associated with the compression of an ideal gas. A cylinder-piston assembly contains 2 kg of air, treated as an ideal gas. The air in the cylinder is initially at 10 bar pressure and 25 C. We now push the piston and compress the air but keep the pressure at 10 bar by letting heat

transfer out of the cylinder. Find the work delivered to the system when volume reaches 1/3 of the initial volume.

45. In this problem we want to find the work associated with the torsion of a solid bar. If τ is the applied torsion resulting in an elemental twist of $d\theta$, the work delivered to the bar is $\delta\dot{W} = \tau d\dot{\theta}$. Consider the shaft of an electric motor receiving a torque equal to 35 N m at a constant angular velocity of 1200 rpm. Find the rate of work delivered by the electric motor to the shaft. [Ans.: $\dot{W} \cong 4.4$ kW].

46. In this problem we want to find electric work. A current of I amp at a voltage of V volt, is associated with a power of VI . Find the work associated with charging a battery for 5 hours at a voltage of 12 V and a current of 2.5 A. [Ans.: 540 kJ].

47. In this problem, we want to find the work associated with a change in the surface area of fluids. As described in Chapter III, surface tension as force per unit length, is a liquid property tending to maintain liquid surface. The work associated with a differential change in the liquid surface area is found as $\delta W = 2\sigma dA$, where σ is surface tension. Find the work required to blow a bubble 5 cm in diameter from soapy water. At 25 C temperature, soapy water has a surface tension of about $\sigma = 0.073$ N/m. [Ans.: 1.15E-3 J].

48. In this problem, we want to find the heat produced in a gearbox. The work brought into the system at steady state condition by the high-speed drive shaft is 1 MW. The work carried away on the low-speed shaft is 0.95 MW. Find the amount of heat produced. [Ans. 50 kW].

49. To compress air in a cylinder, 1000 Btu of energy is required. This compression process results in the internal energy of the air to increase by 100 Btu. Find the amount of heat transfer involved in the process. Is this amount of heat transferred to the cylinder or transferred from the cylinder? [Ans.: -900].

50. The steam in a cylinder undergoes a process in which 1000 kJ of heat is transferred to a cylinder. The addition of heat to the cylinder results in the internal energy of the steam to be increased to 800 kJ. Find the amount of work delivered to the piston. [Ans.: 200 kJ].

51. Find the thermal power of the PWR of the nuclear ship *Savannah*. The reactor operated at 1,750 psia. The coolant entered the reactor vessel at rate of 9.4E6 lbm/h and a temperature of 497 F and exited at 519 F. [Ans. 71.33 MWth].

52. Pressurized air at a rate of 4.5 kg/s flows in a rectangular duct. The air pressure and temperature at a point in the duct is measured as 33 C and 250 kPa. The duct cross section is a rectangle of 50 cm by 20 cm. Find a) the volumetric flow rate, b) the mass flux, c) the average velocity at this location. [Ans.: c) 15.8 m/s].

53. Liquid sodium enters the core of a liquid metal fast breeder reactor (LMFBR) at 400 C and leaves at 560 C. The reactor operates at 750 MW. Find the sodium flow rate. $c_p = 0.3$ Btu/lbm·F. [Ans.: 12,471 lbm/s].

54. Use the Maxwell relations to show that, for an isentropic process of an ideal gas, $Pv^\gamma = \text{constant}$ where γ is given as $\gamma = c_p/c_v$. [Hint: Use $ds = (c_v dT/T) + R (dv/v) = 0$ and $ds = (c_p dT/T) - R (dP/P) = 0$. Cancel dT/T and integrate.]

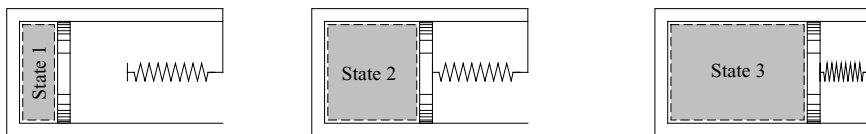
55. Use the equation of state for ideal gases in conjunction with the Maxwell relations to derive an alternative equation to Equation IIa.3.6 (calculation of the change in the entropy of a system in a reversible process. [Ans.:

$$s_2 - s_1 = \int_{T_1}^{T_2} c_p (dT/T) - R \ln(P_2/P_1)] .$$

56. A tank at atmospheric pressure contains two inlets and one outlet port. The first inlet port has a flow area of 0.05 ft^2 and the flow area of the second inlet port is 0.025 ft^2 . Water enters the first inlet port at 5 ft/s and 100 F . Water enters the second inlet port at 8 ft/s and 175 F . Water leaves the tank at a rate of 2 lbm/s . Find the rate of change of the tank water level.

57. We compress air at 1 MPa and 150 C to a pressure of 5 MPa in an isentropic process. Treat air as an ideal gas and find its temperature at this pressure. [Ans.: $T_2 \approx 240 \text{ C}$].

58. A mixture of water and steam is contained in a cylinder equipped with a well-fitted leak-tight piston of cross sectional area A . At state 1, the mixture is at pressure P_1 having a steam quality of x_1 and a volume of V_1 . Heat is added to the cylinder until the piston just touches the spring. At this stage, the volume of the cylinder content is $V_2 = V_1 + \Delta V$. We keep adding heat to the cylinder. The piston would travel further to the right and start compressing the spring. We terminate the heating process when the pressure of the cylinder content reaches P_3 . Write a procedure from which P_2 , T_2 , and T_3 can be determined. Assume a linear spring ($F = k_s x$) with known k_s .

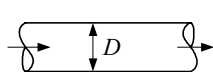


59. Show that for steady-flow, steady state isentropic process of an ideal gas the work from going from state 1 to state 2 is found from:

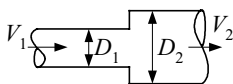
$$W_{12} = \frac{\gamma R T}{\gamma - 1} \left[1 - \left(\frac{P_2}{P_1} \right)^{\frac{\gamma - 1}{\gamma}} \right]$$

60. Flow enters a heat exchanger at a rate of $25\text{E}6 \text{ lbm/h}$ and a density of 1.5 slugs/ft^3 . There are 9000 tubes in this heat exchanger. If flow is distributed evenly among the tubes, find the flow velocity in each tube. Use a diameter of 0.63 in for all the tubes. [Ans.: 7.38 ft/s].

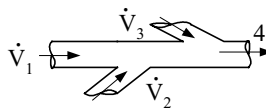
61. Water at 20 C enters the pipe of Figure (a) at a velocity of 2.5 m/s . The pipe has an inside diameter of 5 cm . Find the mass flow rate, mass flux, and volumetric flow rate. [Ans. 4.9 kg/s , $2497.5 \text{ kg/m}^2\cdot\text{s}$, $4.9\text{E}-3 \text{ m}^3/\text{s}$].



(a)



(b)



(c)

62. Show that for the pipe of Figure (b) flow velocity at the exit is given by $V_2 = V_1 (D_2/D_1)^2$.

63. For the pipe in Figure (c), find mass flow rate (\dot{m}_4) and velocity (V_4) at the exit of the pipe.

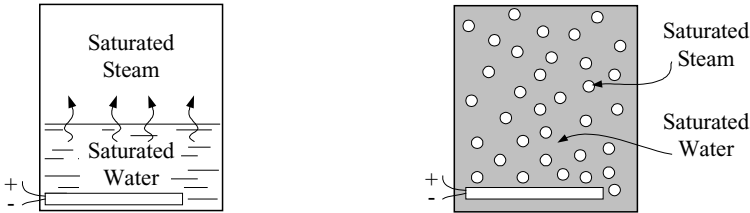
64. The mass flow rate through the core of a 2×4 PWR (i.e., 2 hot legs and four cold legs) is $62.82\text{E}6$ kg/h. The inside diameter (I.D.) of the hot leg is 1 m. Estimate the I.D. of the cold leg. Data: $T_{HL} = 320$ C, $T_{CL} = 288$ C, and $P = 15.5$ MPa. [Hint: $V_{HL} = V_{CL}$].

65. The core of a nuclear reactor produces 2772 MWth at 2155 psia. The volumetric flow rate through the core is given as $122.71\text{E}6$ GPM. The core outlet temperature is 604 F. Find the core inlet temperature. [Hint. Guess T_{in} , find T_{avg} , find $\rho_{avg}(P, T_{avg})$, find \dot{m} , update T_{avg} and continue iteration]. [Ans.: 549 F].

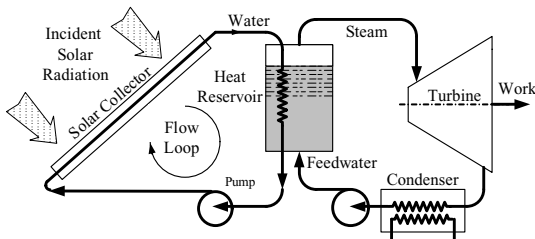
66. Consider the pressurizer of a PWR, having an internal volume of 1500 ft³. The pressurizer contains 750 ft³ of water and steam at 2000 psia at equilibrium. Due to a turbine trip, an in-surge of 100 GPM and 600 F enters the pressurizer for 5 minutes. Find the temperature of the water region after termination of the in-surge. Assume perfect mixing between the in-surge and water in the water region. Ignore work due to boundary change and heat transfer with the steam region. [Ans. $T_2 = 662.5$ F].

67. The pressurizer of a PWR is at 2250 psia. Water through the letdown line leaves the pressurizer at a rate of 44 GPM and enters the volume control tank (VCT) for 30 minutes. If no other process has taken place in either tank, use the data below and find the change in water level in the two tanks. Assume instantaneous and perfect mixing in VCT. Data: $V_{\text{Pressurizer}} = 1500$ ft³, $(V_{\text{water}})_{\text{Pressurizer}} = 750$ ft³, $A_{\text{Pressurizer}} = 50$ ft², $V_{\text{VCT}} = 1000$ ft³, $(V_{\text{water}})_{\text{VCT}} = 385$ ft³, $A_{\text{VCT}} = 44.3$ ft², $T_{\text{VCT}} = 150$ F.

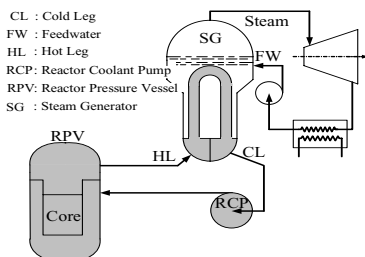
68. A rigid vessel is filled with saturated water and steam. In the left figure, water and steam constitute two separate regions while in the right figure the water and steam make a homogenous mixture. Under what condition can the right figure represent the left figure?



69. We plan to design a 1 MWth solar power station, as shown in the figure. Solar radiation heats up the circulating water in the solar collectors, which is then transferred to a heat reservoir to produce steam. The reservoir is maintained at 1 MPa. Dry, saturated steam, after expansion in the turbine, is cooled down in the condenser and is pumped back to the reservoir. Find the steady state mass flow rate of feedwater and of steam. The steam enthalpy at the exit of the turbine is 2300 kJ/kg. List the advantages and drawbacks of this design. Changes in the kinetic and potential energies are negligible. [Ans.: 2 kg/s].



70. Total heat in the primary side of a PWR, as shown in the figure, is 2700 MWth. This amount of heat consists of the fission heat produced in the core and the reactor coolant pump (RCP) heat. The steam generator is maintained at a pressure of 900 psia. The enthalpy of feedwater entering the steam generator is 430 Btu/lbm. Find the steady state mass flow of the dry saturated steam leaving the steam generator towards the turbine. [Ans.: 11.7E6 lbm/s].



71. Shown in Figure (a) is the flow path of a BWR vessel. Find the steam mass flow rate (\dot{m}_g) in terms of total reactor core power (\dot{Q}), feedwater enthalpy (h_d), and thermodynamic properties at vessel pressure.

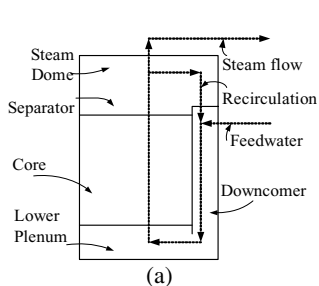
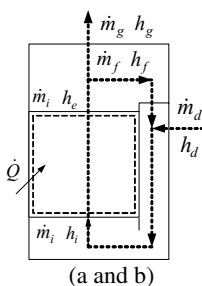


Figure for Problem 71



(a and b)

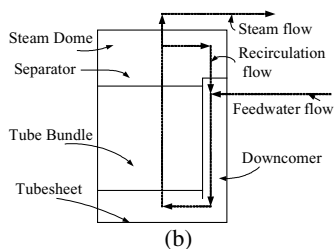


Figure for Problem 73

[Ans: $\dot{m}_g = \dot{Q} / (h_g - h_d)$].

72. In Problem 71, defining the recirculation flow rate as $r = \dot{m}_f / \dot{m}_g$, show that $r = (1 - x_e) / x_e$ where x_e is the steam quality at the core exit.

73. Shown in Figure (b), is the flow path in the secondary side of a PWR steam generator. For the steady state operation, find the steam mass flow rate in terms of the following parameters:

h_{in} : water enthalpy at the inlet to the tube bundle region

h_f : saturated water enthalpy at the steam generator pressure

h_{fg} : latent heat of vaporization at the steam generator pressure

\dot{Q}_{Core} : total rate of heat transfer in the core,

\dot{m}_i : mass flow rate in the tube bundle region,

N_{SG} : number of steam generators (N_{SG})

[Ans.: $\dot{m}_s = \{(\dot{Q}_{Core} / N_{SG}) - \dot{m}_i(h_f - h_{in})\} / h_{fg}$].

74. A PWR steam generator at steady state operation produces dry, saturated steam. Pressure in the tube bundle region is 6 MPa (875 psia). The PWR power plant is equipped with two steam generators and is producing a total electric power of 810 MWe at a thermal efficiency of 30%. Use a feedwater enthalpy of 1007 kJ/kg (433 Btu/lbm), a recirculation ratio of 3.3 to find:

a) the feedwater flow rate entering the steam generator downcomer, b) the steam flow rate c) the flow rate entering the tube bundle region, d) the recirculation flow rate entering the downcomer region, e) water enthalpy entering the tube bundle region, f) mixture enthalpy at the exit of the tube bundle region, g) the degree of subcooling at the inlet to the tube bundle region.

75. Start with Equation IIa.6.3 and show that, for rigid control volumes with no internal heat generation, the first law for control volumes simplifies to:

$$\sum_i \dot{m}_i \left(h_i + \frac{V_i^2}{2g_c} + \frac{g}{g_c} Z_i \right) + \sum \dot{Q} = \sum \dot{W}_s + \sum_e \dot{m}_e \left(h_e + \frac{V_e^2}{2g_c} + \frac{g}{g_c} Z_e \right) + \frac{d}{dt} \left[m \left(u + \frac{V^2}{2g_c} + \frac{g}{g_c} Z \right) \right]$$

76. Saturated steam enters a turbine at 7 MPa and a rate of 6E3 kg/h. Steam leaves turbine at 7 bar and $x_e = 85\%$. There is a total of 20 kW heat loss from the turbine. Find the power developed by this turbine. [Ans.: 0.93 MW].

77. Hot water enters the steam generator tubes of a PWR at a rate of 138.5E6 lbm/h, pressure of 2250 psia and temperature of 600 F. Water leaves the tubes at 550 F. Steam is produced in the secondary side at 1000 psia. Find the steam mass flow rate. [Ans.: 7E6 lbm/h].

78. Find the rate of steam produced in a BWR operating at 1,600 MWth. Water enters the core from the lower plenum at a rate of 50E6 lbm/h and a temperature of 526 F. Reactor pressure is 1050 psia. [Ans.: 6E6 lb/h].

79. A high temperature gas-cooled reactor (HTGR) is designed to operate at 330 MWe with a $\eta_{th} = 39.23\%$. Helium enters the reactor at a pressure of 710 psia and temperature 760 F and leaves at 1,430 F. Find the He flow rate through the core. $c_p = 1.24$ Btu/lbm·F. [Ans.: 3.455E6 lbm/h]

80. For a PWR steam generator, we define the recirculation ratio as $R = \dot{m}_r / \dot{m}_s$, where \dot{m}_s is the steam mass flow rate and \dot{m}_r is the recirculation mass flow rate. Express R in terms of core exit average quality ($X_e = \dot{m}_s / \dot{m}$). [Ans.: $R = X_e / (1 - X_e)$].

81. Obtain an analytical solution in closed form for the set of mass and energy equations in Example IIa.8.2. [Hint, since the inlet mass flow rates and enthalpies as well as the outlet mass flow rate are all uniform with time, the rate of change of mass in the tank is constant, hence, water level is a linear function of time].

[Ans.: Mass of water in the tank as a function of time is found from

$$m(t) = \left(\sum_{i=1}^2 \dot{m}_i - \dot{m}_e \right) t + m(t=0) \quad \text{and water temperature in the tank from}$$

$$\theta = e^{-\int p(t) dt} \left\{ \left[\int q(t) e^{\int p(t) dt} dt \right] + C \right\} \quad \text{where } p(t) \text{ and } q(t) \text{ are obtained from}$$

$$p(t) = \left[\left(\sum_{i=1}^2 \dot{m}_i - \dot{m}_e \right) c_v + \left(\sum_{i=1}^2 \dot{m}_i \right) c_p \right] / m(t), \quad q(t) = \left(\sum_{i=1}^2 \dot{m}_i h_i \right) / m(t), \text{ and } C \text{ is}$$

found from the initial condition for water temperature.]

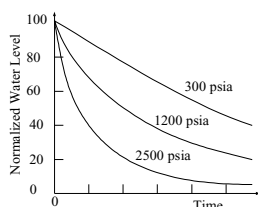
82. Find an analytical solution for Example IIa.8.2 if heat is also added to the tank at a constant rate of \dot{Q} Btu/s. [Ans.: The only modification is in $q(t)$ which be-

$$\text{comes } q(t) = \left(\dot{Q} + \sum_{i=1}^2 \dot{m}_i h_i \right) / m(t).]$$

83. If in Example IIa.8.2 heat is added to the water at a rate of 2000 Btu/s, find the time it takes for water to reach saturation at atmospheric pressure.

84. A tank contains 5 ft³ of water at 100 F and 1 atm. Heat, at a constant rate of 1,000 Btu/s, is added to the tank in an isobaric process. Find the time it takes for the last drop of water to evaporate. Properties of subcooled water at 1 atm and 100 F are $v = 0.01613$ ft³/lbm and $h = 68.04$ Btu/lbm. [Ans.: 4.6 min.]

85. A tank contains 5 ft³ of water at 100 F. Heat, at a constant rate of 1,000 Btu/s is added to the tank in an isobaric process. Find the time it takes for the last drop of water to evaporate. Solve this problem for three cases. In case 1, the tank pressure is 300 psia. In case 2, the tank pressure is 1200 psia. In case 3, the tank pressure is 2500 psia. a) What conclusion do you reach from this study? b) Assume a tank cross sectional area of 1 ft² and plot water level as a function of time for all three cases. [Ans.: a) As shown in Figures Ila.3.1(c) and Ila.3.4, latent heat of vaporization decreases as pressure increases. Hence, the tank loses water faster at higher pressures. b) the plot should have the trend shown below:



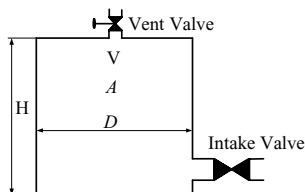
].

86. A tank of 8000 ft³ (225 m³) contains a two-phase mixture of water and steam at $P_i = 1000$ psia (7 MPa) and $x_i = 28.233\%$. Heat is now added to the tank, treated as a single control volume at a rate of:

$$\dot{Q}(t) = \dot{Q}_o e^{\alpha t}$$

where $\dot{Q}_o = 34.4$ MW and $\alpha = 18$ h⁻¹. Find the time it takes for pressure to reach 3000 psia (21 MPa). [Hint: At state 2, we have P_2 and $v_2 = v_1$]. [Ans.: 5 min].

87. A cylindrical tank has a base diameter of $D = 3$ ft and a height of $H = 7$ ft. The tank contains air at 100 psia and 100 F. The intake valve is now opened to allow 100 F water at a constant rate of 10 lbm/s to enter the tank. Assume that no air is dissolved in the water and no heat transfer takes place at the air - water and air - wall interfaces. Find air pressure in the tank 62 seconds after the intake valve is opened. Treat air as an ideal gas and the compression of air as an isentropic process. The vent valve remains closed. [Ans.: 137.2 psia].



88. A rigid vessel having a volume of V contains air, initially at a pressure of P_1 and a temperature of T_1 . An intake valve is now opened to allow pressurized air at a temperature of T_i to enter the vessel. The intake valve is closed when pressure in the vessel reaches P_2 . Use the conservation equations of mass and energy as well as the equation of state to derive a relation for the final temperature. Consider the process adiabatic and neglect any storage of heat in the tank wall. [Ans.: $T_2 = P_2 c_p T_i / \{c_v (P_2 - P_1) + (P_1 c_p T_i / T_1)\}$].

89. A rigid tank has a volume of $V = 1.0 \text{ ft}^3$ and contains air at $P_1 = 14.7 \text{ psia}$ and $T_1 = 70 \text{ F}$. An admission valve is now opened to allow pressurized air at $P_i = 100 \text{ psia}$ and $T_i = 70 \text{ F}$ enter the tank. The valve is closed when $P_2 = 30 \text{ psia}$. Find T_2 . [Ans.: $T_2 = 161 \text{ F}$].

90. The volume of the water in the secondary side of a PWR steam generator is 130 m^3 . The power deposited to the water ten minutes after the reactor is shut-down is 58 MW . If there is no feedwater delivered to the steam generator, find the time to boil the steam generator dry. The secondary side pressure is 9 MPa .

91. A tank with a volume of $V = 2 \text{ m}^3$ contains air at 3 MPa and 200 C . The vent valve is now opened. Find the tank pressure and temperature when $1/3$ of the air escapes through the vent valve. The intake valve remains closed.

92. A tank with a volume of 10 m^3 contains air at 0.1 MPa and 15 C . The intake valve is opened to allow pressurized air enter the tank at an average mass flow rate of 0.5 kg/s and temperature of 100 C . If the tank is fully insulated, find the tank pressure after 60 seconds. The vent valve remains closed. [Ans.: $P = 0.55 \text{ MPa}$, $T = 182 \text{ C}$].

93. A tank with a volume of $V = 10 \text{ m}^3$ contains air at 0.1 MPa and 15 C . The intake valve is opened to allow pressurized air enter the tank at an average mass flow rate of 0.5 kg/s and temperature of 100 C . During the charging process, heat is transferred to the atmosphere at a rate of $0.01(T - T_s) \text{ Btu/s}$ where T is the air temperature in the tank and $T_s = 10 \text{ C}$ is temperature of the surroundings. Find the tank pressure after 60 seconds. The vent valve remains closed. [Ans.: $P = 0.53 \text{ MPa}$, $T = 168 \text{ C}$].

94. A pressurized rigid vessel having a volume of 10 ft^3 is filled with air to 600 psia and 185 F . We want to vent this tank so that the final pressure drops to atmospheric pressure (14.7 psia). However, we would like to maintain the air temperature in the tank at 185 F throughout the venting process. Find the amount of heat necessary to accomplish this task. Treat air as an ideal gas with constant specific heat and ignore changes in the air kinetic and potential energies compared to its internal energy. [Ans.: 898 Btu].

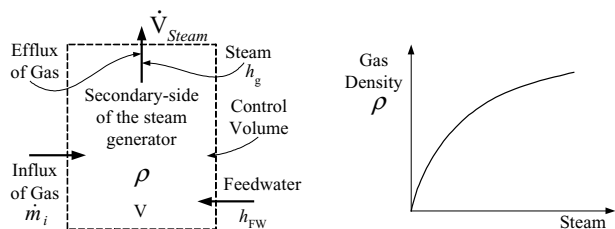
95. A rigid vessel is depressurized from 3 MPa to 101 kPa through a small vent. Heat is added in this process to maintain temperature at its initial value. The tank has a volume of 5 m^3 and its inventory is an ideal gas. Find the amount of heat required for accomplishing this task. [Ans.: $14,495 \text{ kJ}$].

96. A cylindrical pressurized vessel is filled with air to 500 psia at an initial temperature of 250 F. The vessel has a diameter of $D = 4$ ft and total volume of $V = 200$ ft³. A small, 1 inch vent valve is now opened. Find pressure (P) and temperature (T) of the gas in the vessel 20 seconds into the venting event. Treat air as an ideal gas. The tank is fully insulated. The valve discharge coefficient is 0.65. The intake valve remains closed [Hint: Flow rate through the valve should be multiplied by the specified discharge coefficient]. [Ans.: $P = 133$ psia, $T = 10$ F].

97. A cylindrical pressurized vessel is filled with air to 500 psia at an initial temperature of 250 F. The vessel has a diameter of $D = 4$ ft and total volume of $V = 200$ ft³. A small, 1 inch vent valve is now opened. Find pressure (P) and temperature (T) of the gas in the vessel 20 seconds into the venting event. Treat air as an ideal gas. The rate of heat transfer from the tank to the surroundings is estimated at $0.008(T - T_s)$ Btu/s where the surrounding is at a temperature of $T_s = 35$ F. The valve discharge coefficient is 0.65. The intake valve remains closed. [Ans.: $P = 132$ psia, $T = 6$ F].

98. The pressurizer of a PWR is a cylindrical tank having a volume of 1500 ft³. Initially, the tank is full of a mixture of water and steam. Consider this saturated mixture to be distributed uniformly in the tank at $P_1 = 2250$ psia. The initial steam quality is 70%. We now start heating the tank but would like to keep pressure at its initial value of 2250 psia. To achieve this goal, we must simultaneously remove mass from this tank. If only steam is removed by a valve at the top of the tank and the kinetic and potential energies are negligible, find the amount of the mass removed and heat added when the last drop of water boils and becomes steam.

99. A small amount of leakage exists in the steam generator of a PWR operating at the rated power of \dot{W}_{100} . A noble gas escapes the primary side and enters the secondary side at a fixed rate of \dot{m}_i . Find the density of the gas in the secondary side of the steam generator versus time. The volume of the secondary side is V .



[Hint: Since the leak is small, we treat gas as a component. Find $\rho_{100}(t)$, density of the gas at 100% power from $V(d\rho_{100}/dt) = \dot{m}_i - \rho_{100} \dot{V}_{\text{Steam}}$ where \dot{V}_{Steam} is the steam volumetric flow rate at 100% with $\rho_{100}(0) = 0$].

[Ans.: $\rho_{100}(t) = (1 - e^{-\beta t})\alpha$ where $\alpha = \dot{m}_i / \dot{V}_{\text{Steam}}$ and $\beta = \dot{V}_{\text{Steam}} / V$].

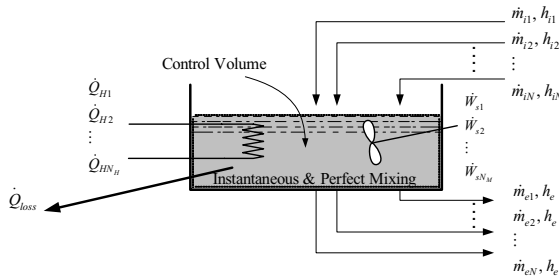
100. A small amount of leak exists in the steam generator of a PWR operating at the rated power of \dot{W}_{100} . A noble gas escapes the primary side and enters the sec-

secondary side at a fixed rate of \dot{m}_i . At θ seconds into the operation at nominal power, we reduce power to 20% of nominal. a) If the primary side and the secondary side pressure remain about the same value as at nominal power, find the steam flow rate (\dot{m}_{20}) in terms of \dot{W}_{100} , \dot{W}_{20} , and steam mass flow rate at full power (\dot{m}_{100}). b) Find the partial density of the noble gas in the secondary side (ρ_{20}), at the reduced power of 20%, versus time.

[Ans.: $\rho_{20}(t') = \alpha' + (\rho_{100}(t = \theta) - e^{-\beta' t'}) \alpha'$ where $t' = t - \theta$, $\alpha' = \dot{m}_i / \dot{V}'_{\text{Steam}}$, and $\beta' = \dot{V}'_{\text{Steam}} / V$].

[Note, the above answers assume that the noble gas is stable. If radioactive gases such as Xe-135 are involved, the Xe buildup in the primary side and decay in the secondary side must be factored in.]

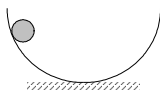
101. Consider a mixing tank that contains m_o kg of water initially at T_o C. This tank is fed by N feed lines carrying water at various temperatures. The mass flow rate and enthalpy of water in the feed lines are known functions of time. There are N_M mixers and N_Q heaters. The tank is poorly insulated. The rate of heat loss is given as $\beta(T_{C.V.} - T_f)$ where β has units of W/C and T_f is temperature of the surroundings. Both β and T_f are known functions of time. There are N inlet ports and M outlet ports. Assume instantaneous and perfect mixing so that water in the tank can be represented by one control volume.



a) Use other simplifying assumptions, as used in Section 8, and obtain the governing differential equations for the control volume mass and enthalpy. b) Assume a constant specific heat and obtain an analytical solution for the water temperature leaving the tank in terms of the specified forcing functions. c) Use the definitions in Chapter VIIe and obtain the solution in explicit, semi-implicit, and fully-implicit numerical schemes.

Section IIa.9 through IIa.11

102. Is the motion of the sphere a reversible process in the absence of any air resistance and friction?



103. A smooth pipe equipped with an isolation valve connects two tanks containing air. When the valve is closed $P_A > P_B$. We now open the valve until both tanks reach equilibrium. Is this a reversible process?



104. A pendulum, placed in an enclosure, is operating in a vacuum. The connecting rod is attached to a frictionless joint. Is the motion of this pendulum a reversible process?

105. An adiabatic and reversible process is an isentropic process. Can an irreversible process in which heat is allowed to transfer have no change in entropy? Clarify your answer. [Ans.: Yes].

106. Consider two heat engines operating between the same heat source and heat sink in the Carnot cycle. One heat engine uses gas and the other uses water as working fluid. Which heat engine would have higher thermal efficiency?

107. We want to heat up the contents of a closed system. We may use a paddle wheel or a heat reservoir. Thermodynamically, which method is preferred?

108. A cylinder, fitted with a frictionless piston, contains saturated steam at a specified pressure. We now let heat transfer take place from the cylinder to the surroundings until saturated steam becomes saturated water. Does this constitute a reversible process? Does this constitute an isentropic process?

109. Heat is added to a cylinder containing air. The cylinder has a volume of 0.12 m^3 and initially is at $P_1 = 1 \text{ MPa}$ and $T_1 = 50 \text{ C}$. Find a) the air pressure when the air temperature reaches 150 C , b) the amount of heat added to the cylinder, and c) the change in the air entropy. [Ans.: 1.31 MPa , 94 kJ , 0.252 kJ/C].

110. A cylinder contains 3 kg of air at $P_1 = 1 \text{ bar}$ and $T_1 = 27 \text{ C}$. In a polytropic compression, the pressure and temperature of the air are raised to $P_2 = 15 \text{ bar}$ and $T_2 = 227 \text{ C}$. Find the polytropic exponent, the final volume, the amount of compression work delivered to the system, and the amount of heat rejected to the surroundings. [Ans.: 1.23 , 0.287 m^3 , -763 kJ , and -316 kJ].

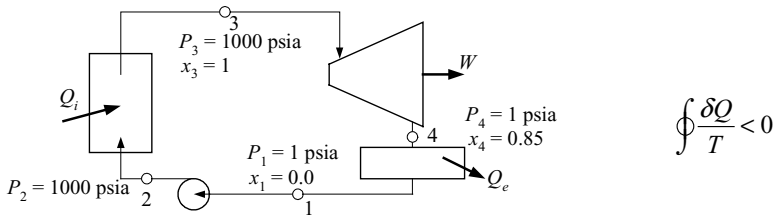
111. Thermal efficiency of a power plant is calculated as 30% . The electrical output of the plant is 1000 MWe . How much heat is transferred in the heat source to the working fluid (i.e., MWth)?

112. In a 1000 MW power plant, steam at 1000 F enters the turbine. Pressure in the primary side of the condenser is 4 psia . Find the least possible amount of heat rejected to the surroundings.

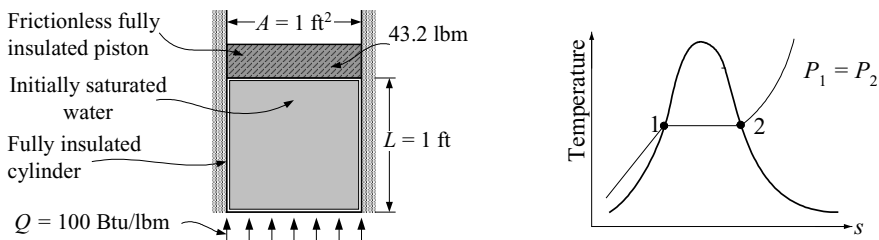
113. A power plant operates at a thermal efficiency of 32% . The rate of heat transfer in the heat source is 2700 MW . Find the power produced by the turbine.

114. A refrigerator operates at 1 kW power to maintain the temperature of the freezer compartment at -7°C while the room temperature is 25°C . The power transferred to the room from the refrigerator is 4 kW. Find the COP ($\eta_{\text{Refrigerator}}$) and compare it with the maximum COP ($\eta_{\text{Refrigerator, Carnot}}$).

115. We want to verify the validity of the data reported for the following power plant. Water leaving the condenser is saturated at $P_1 = 1$ psia. Water entering the boiler is subcooled at $P_2 = 1000$ psia and $T_2 = 79.26^\circ\text{F}$ ($h_2 = 50$ Btu/lbm). Steam leaving the boiler and entering the turbine is saturated at $P_3 = 1000$ psia. Finally, the mixture leaving the turbine and entering the condenser is at $P_4 = 1$ psia and $x_4 = 0.85$. [Hint: You must verify the Clausius inequality noting that heat is added in the boiler and rejected at the condenser].



116. Heat is added from the bottom to an otherwise well-insulated cylinder until all the initially saturated water becomes saturated steam then the heat addition is terminated and the bottom is rapidly insulated. Use the data shown in the figure to find a) the amount of work produced, b) the entropy transfer to the cylinder, and c) the entropy produced in the cylinder.



117. Derive Equation IIa.10.20 by expanding the rate of heat transfer term in Equation IIa.10.19 as:

$$\sum_j (\dot{Q}_j / T_j) = \dot{Q}_o / T_o + \sum_k (\dot{Q}_k / T_k)$$

where j is the summation over all thermal boundaries except for o (i.e., $k \neq o$). Substitute this relation into Equation IIa.10.19, solve for \dot{Q}_o and substitute into Equation IIa.6.5, where in Equation IIa.6.5 you should also make a similar expansion for the heat transfer term, $\sum_j \dot{Q}_j = \dot{Q}_o + \sum_k \dot{Q}_k$. Equation IIa.10.20 gives

the optimum useful work. Find the equation from which the useful work w_{use} can be calculated.

118. Superheated steam is throttled at steady state conditions from 10 MPa and 480 C to 6 MPa. Find the entropy production in this process.

[Ans.: 0.158 kJ/kg·K].

119. Saturated steam enters a condenser at 1 psia and saturated water leaves the condenser. The cooling water enters the condenser tubes at 65 F and leaves at 77 F. Ignore the changes in the kinetic and potential energies and find the steady state entropy production for this fully insulated condenser.

120. A steam turbine operates at a steady state condition with superheated steam entering the turbine at 3 MPa and 450 C. Steam velocity at the inlet is 150 m/s and the inlet steam pipe has a diameter of 0.75 m. After expansion in the turbine, saturated steam leaves the turbine at 100 C and 90 m/s. The power produced by this turbine is 0.32 MW. The turbine is not insulated and heat transfer takes place at an average temperature at the turbine control surface of 225 C. Ignore changes in the potential energy of the steam and find the entropy production rate in the turbine. [Ans.: $\dot{m} = 613.6$ kg/s, $\dot{Q} = -0.0118$ MW, and $\dot{\sigma} \cong 1.91$ MW/K].

121. A cylinder contains 10 kg of air (treated as an ideal gas) at 2 MPa and 365 C. The frictionless piston is held in place by a stop pin. The pin is now removed and the piston is set free to move. Find the special optimum useful work this process. For the surroundings use $P_o = 101$ kPa and 25 C. [Ans.: 3476.2 kJ].

122. A cylinder contains 16 lbm of air at 220 psia. We wish the optimum useful work corresponding with the expansion of a frictionless piston to be 1000 Btu. Find the volume of the tank and air initial temperature to satisfy this requirement. Treat air as an ideal gas and use $P_o = 15$ psia and $T_o = 77$ F.

123. A cylinder contains steam at 460 psia and 600 F. The frictionless piston is held in place by a stop pin. The pin is now removed and the piston is set free to move. After expansion, steam pressure and temperature drop to 100 psia and 360 F while producing 74 Btu/lbm of work and exchanging heat with a sink reservoir at 305 F. Determine the effectiveness of the steam expansion. Use $P_o = 15$ psia and $T_o = 77$ F. [Ans.: 78%].

124. The stored energy of a system containing compressed air can be used in various work processes. Consider a tank containing 5 kg of compressed air at 1.5 MPa and 350 C. Find the maximum useful work. Treat air as an ideal gas and use $P_o = 0.101$ MPa and $T_o = 298$ K. [Ans.: 1635 kJ].

125. We want to compare two methods of heating the same tank. For this purpose, consider increasing the quality of a two-phase mixture in a rigid tank. The tank has a volume of 1 m³. Initially the mixture pressure is 2 MPa and the mixture quality is 8%. The tank temperature is raised to 300 C. The pressure and temperature of the surroundings are 0.101 MPa and 25 C, respectively. In the first method, we fully insulate the tank and use a paddle wheel. In the second method,

we remove the insulation and add heat from a reservoir at 450 C. Find the irreversibility of each method and comment on the result. [Ans.: $I_a = 120,000$ kJ & $I_b = 12,355$ kJ].

126. To maximize the productivity of an electric power plant, we need to determine wasteful processes. Two obvious candidates are the heat carry out of the plant in the heat sink and in the exhaust of stack gases. Use the data and find which stream is more wasteful. The power plant produces 12,000 MWe having an overall efficiency of 31%. The power plant exhausts the stack gases at a rate of 500 lbm/s and a temperature of 445 F. The condenser uses 190,000 lbm/s of cooling water, which enters condenser at 65 F. Treat the stack gases as air and air as an ideal gas. [Ans.: $T_{w2} = 78$ F, $\psi_w = 45,285$ Btu, $\psi_A = 11,294$ Btu].

127. In a heavy duty truck, the circulating water to cool the 600 hp engine enters radiator at 0.2 MPa, 98 C and 3.6 kg/s. Air flows over the radiator tubes at a rate of 8 kg/s. Find the irreversibility of the radiator. Use $T_o = 25$ C and ignore pressure drop in both streams. [Ans.: $T_{w2} = 71.4$ C, $T_{A2} = 78$ C].

128. Find the steady flow special availability of a geothermal energy source. Water from this source is at 0.6 MPa and 152 C.

129. When the combustion products in a diesel engine ignite, temperature reaches 4850 F and 1950 psia. If the combustion products are treated as air, find the associated special availability of the products.

IIb. Power Cycles

Power cycles are an important application of the thermodynamic principles. In this chapter we discuss power cycles that use a heat source to develop a net power output. The heat source may be the energy from fossil fuel, nuclear fuel, solar heating, or geothermal energy.

1. Gas Power Systems

Power production systems using gases as the working fluid have a wide range of applications in automotive, aircraft, and large-scale land-based power plants. The working fluid in such systems always remains in the gas phase throughout a cycle.

1.1. Definition of Terms

Internal combustion engines are power systems in which the working fluid changes composition. Such systems generally use air in addition to the fuel (resulting in combustion products). Examples of such systems include gasoline engines using a spark-ignition system, diesel engines, and gas turbines.

External combustion engines are power systems in which the working fluid does not change composition; rather heat is transferred to the working fluid from the combustion products. An example includes a fossil power plant where heat is transferred to steam, which is the working fluid in a boiler. In nuclear power plants no combustion takes place. Rather, heat is produced by fission and transferred to the coolant. Hence, a nuclear power plant can be simply considered as an external engine or machine. Although external engines generally use steam as working fluid, gas cooled reactors, by definition, are external machines that use a gaseous working fluid to produce work in conjunction with a gas turbine.

Open cycle is a term applied to internal combustion engines because the working fluid changes from cycle to cycle. This occurs, for example, in the intake process of a spark-ignition engine where, air is admitted and mixed with the combustible products. The mixture is then ignited, expanded, and at the end of the cycle the combustion products leave the engine in the exhaust process. The cycle is then repeated.

Reciprocating engines are of the cylinder-piston type. In contrast, a Wankel engine is equipped with a rotor. As discussed in Chapter I, the piston slides inside the cylinder by the connector rod, which is attached to the crankshaft. In a reciprocating engine, depending on the manner the air-fuel mixture enters, the exhaust leaves the cylinder (chamber), and the power stroke per revolution of the crankshaft, the engine may be of a *two-* or a *four-stroke* type.

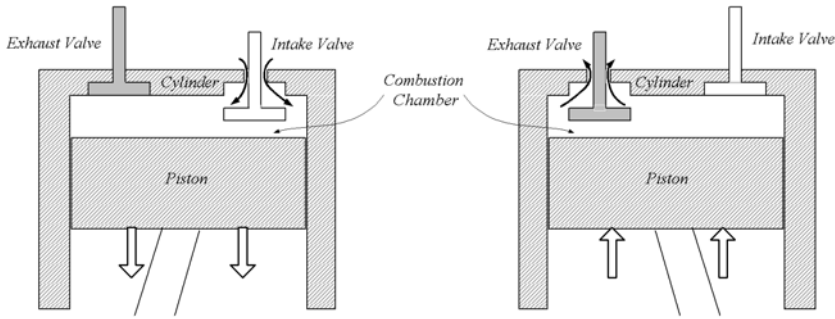


Figure IIb.1.1. Intake and exhaust in a reciprocal open cycle four-stroke internal combustion engine

Shown in Figure IIb.1.1 is a four-stroke open cycle internal combustion engine. The *head-end dead center* and *crank-end dead center* are the positions at which the volume of the combustion chamber is a minimum or a maximum, respectively. At the head-end dead center for example, the piston is fully inserted into the cylinder. In the intake process, the intake valve opens to deliver air from the engine manifold (not shown in Figure IIb.1.1) while the exhaust valve is closed. This condition is reversed when the piston pushes the exhaust gases out of the cylinder.

Figure IIb.1.2 shows the start and the end states of all the processes that constitute one cycle of the operation of an open cycle internal combustion engine. The cycle begins at the *intake* stage when the piston is at the head-end dead center and just begins to move downward to admit the mixture of air and fuel in to the cylinder by suction. At this stage, the exhaust valve is fully closed and the intake valve is fully open. When the piston reaches the crank-end dead center, the intake valve closes. The *compression* process starts at the conclusion of the intake process when the piston begins to move toward the head-end dead center. At the end of the compression process, *ignition* takes place resulting in the *combustion* of the mixture*. This pushes the piston towards the crank-end dead center. Work is delivered in this *expansion* process. Finally, the cycle is completed when the piston moves towards the head-end dead center to discharge the combustion products. In this stage, known as the *exhaust* process, the exhaust valve opens while the intake valve is fully closed. A cylinder-piston engine and the corresponding P - v diagram are shown in Figure IIb.1.3.

* While four-stroke engines have ignition in every other revolution of the crankshaft, two-stroke engines have ignition in every revolution. In two-stroke engines, the lubrication system is eliminated as oil is directly added to the fuel. Thus a two-stroke engine has a higher specific power than a similar four-stroke engine and is used in such appliances as chain saw and leaf blower and in small airplanes. Having ignition per every revolution requires simultaneous compression of the air-fuel-oil mixture while the combustion products are expanding. Similarly, by combining the intake and exhaust processes, the incoming compressed mixture expels the combustion products through the exhaust port. In this process some of the fresh mixture may also escape through the exhaust.

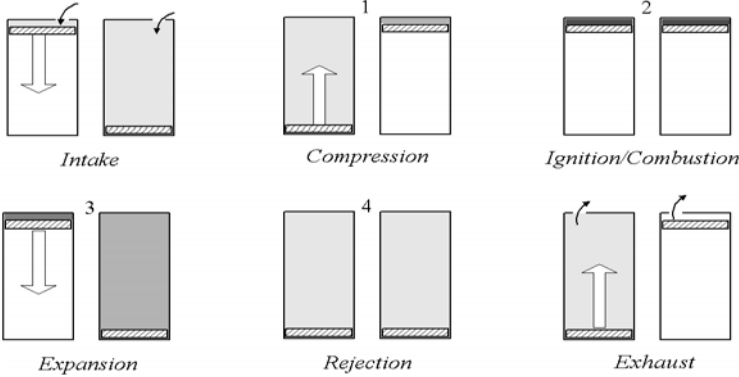


Figure IIb.1.2. Start and end states of processes in an open-cycle internal combustion engine. (Numbers refer to the air standard cycle)

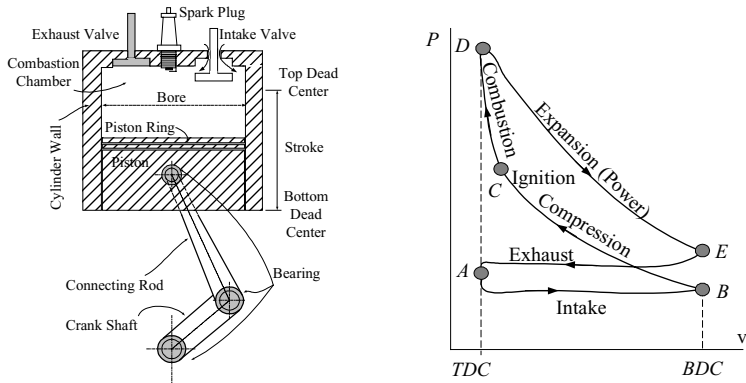


Figure IIb.1.3. A piston-cylinder engine and corresponding pressure-displacement plot

Gas turbine is an internal combustion engine where shaft work is produced by a rotor rather than the moving boundary of a deformable control volume. Air enters at the suction end of a compressor that is driven by the turbine shaft (Figure IIb.1.4). Compressed air leaves the compressor and enters the combustion chamber. This leads to high-energy gases entering the gas turbine. Inside the turbine, the gas flows between the static blades, which act as a diffuser by directing the flow of gas over the rotating blades. The rotating blades are attached to the rotor to transfer momentum and energy. A portion of the work produced by the high-energy gas is delivered to the compressor. The gas finally leaves the turbine by transferring the remaining of energy to the heat sink.

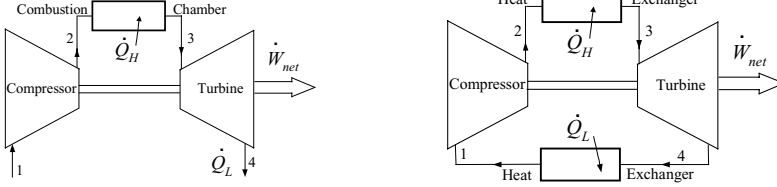


Figure IIb.1.4. Schematics of an open and a closed cycle gas turbine

Closed cycle, also referred to as *air standard cycle*, is a theoretical cycle resembling an actual open cycle for analysis purposes. In an air standard cycle, we make several simplifying assumptions. First, we assume that the working fluid - air - is behaving as an ideal gas. This assumption allows us to use the equation of state for ideal gases and to describe internal energy in terms of the product of temperature and specific heat. Next we assume that the mass of air used as working fluid is fixed in the entire cycle. Hence, there is no intake and no exhaust processes. Heat of ignition is transferred to this fixed mass of air at the heat source and is rejected to the heat sink. Hence, the same mass of air is analyzed throughout a cycle and the composition of air remains intact. We also assume all processes are internally reversible and the effects of kinetic and potential energies are assumed to be negligible.

Compression ratio (r_v) for a process is defined as the ratio of the gas volume before compression to the gas volume after compression, $r_v = V_1/V_2$. Therefore, the compression ratio is always greater than one.

Pressure ratio (r_p) for a process is defined as the ratio of gas pressure after compression to gas pressure before compression, $r_p = P_2/P_1$. Therefore, the pressure ratio is always greater than one. This term is also referred to as the *compressor pressure ratio*. For an isentropic compression, $r_p = r_v^\gamma$.

Temperature ratio (r_T) is defined as the ratio of the maximum to the minimum temperature in a cycle, $r_T = T_3/T_1$.

1.2. Air Standard Carnot Cycle

The air standard Carnot cycle (Figure IIb.1.5) is a theoretical cycle in which heat transfer to air at the heat source and heat rejection at the heat sink take place as isothermal processes while the compression and expansion processes are isentropic. Thus, in the Carnot cycle $s_1 = s_4$, $s_2 = s_3$, $T_1 = T_2 = T_L$, and $T_3 = T_4 = T_H$.

The efficiency for the Carnot cycle is obtained by using Equation IIa.9.1 and substituting for Q_L and Q_H from the T - s diagram of Figure IIb.1.5:

$$\eta_{th} = 1 - \frac{Q_L}{Q_H} = 1 - \frac{T_L(s_1 - s_2)}{T_H(s_4 - s_3)} = 1 - \frac{T_L}{T_H} = \frac{T_1}{T_4} = 1 - \frac{T_2}{T_3} \quad \text{IIb.1.1}$$

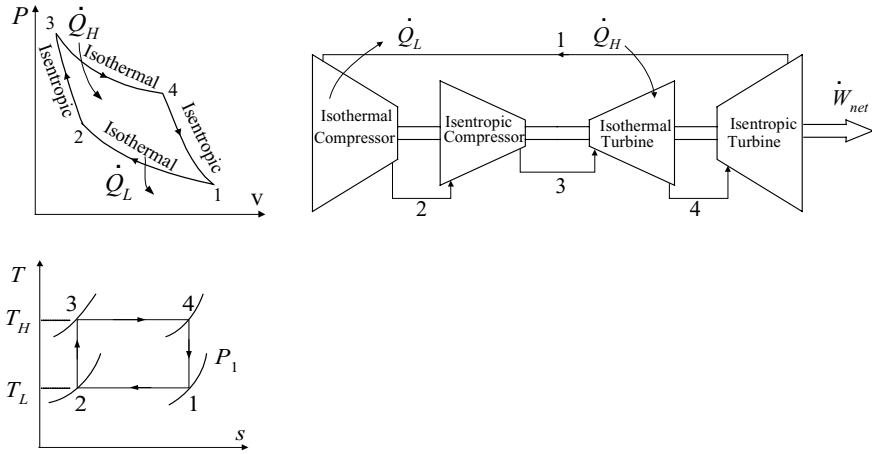


Figure IIb.1.5. The air standard Carnot cycle

For the isentropic process of gas compression we define the compression ratio, r_v as:

$$r_v = \frac{V_1}{V_4} = \frac{V_2}{V_3}$$

Using the relation between pressure and volume for an isentropic process, $PV^\gamma = \text{constant}$ where $\gamma = c_p/c_v$ and the equation of state for an ideal gas, $PV = mRT$, we can relate r_v to temperature ratio as follows:

$$r_v = \frac{V_2}{V_3} = \left(\frac{T_2}{T_3}\right)^{\frac{1}{1-\gamma}} = \left(\frac{P_3}{P_2}\right)^{\frac{1}{\gamma}} \quad \text{IIb.1.2}$$

Since heat transfer to air at the heat source takes place in an isothermal process, we calculate heat from the definition of entropy:

$$Q_{3-4} = \int_3^4 \delta Q = \int_3^4 T ds = T_3(s_4 - s_3)$$

We now use Equation IIa.3.6 with the last term set to zero:

$$s_4 - s_3 = R \ln \frac{V_4}{V_3} + \int_1^2 c_v \frac{dT}{T} = R \ln \frac{V_4}{V_3}$$

Therefore, the amount of heat transferred at the heat source is given as:

$$Q_{34} = T_3 R \ln \frac{V_4}{V_3} = T_3 R \ln \left(\frac{P_3}{P_4} \right)^{\frac{1}{\gamma}} \quad \text{I Ib.1.3}$$

The amount of heat transferred to the heat sink can be found from similar procedure.

Example I Ib.1.1. Find the thermal efficiency of a Carnot cycle for $T_L = 25^\circ\text{C}$ and $T_{H1} = 250^\circ\text{C}$, $T_{H2} = 500^\circ\text{C}$, and $T_{H3} = 750^\circ\text{C}$.

Solution: From Equation I Ib.1.1 $\eta_{th1} = 1 - \frac{T_L}{T_H} = 1 - \frac{25 + 273}{250 + 273} = 1 - 0.57 = 43\%$.

Similarly, for T_{H2} , and T_{H3} we find $\eta_{th1} = 1 - (298/773) = 61\%$ and $\eta_{th3} = 1 - (298/1023) = 70\%$. Thus, for fixed T_L , η_{th} increases with T_H .

In the next problem, we find the important cycle parameters such as pressure, temperature, and the rate of heat transfer.

Example I Ib.1.2. An air standard Carnot cycle operates at an efficiency of 75%. The amount of heat transferred to air at the heat source is 50 Btu/lbm. The highest and the lowest cycle pressures are 2710 psia and 14.7 psia, respectively. Find cycle pressures and temperatures. ($\gamma_{air} = 1.4$).

Solution: We have to find 2 temperatures ($T_1 = T_2$ and $T_3 = T_4$) and 2 Pressures (P_2 and P_4) given Q_{34} , η_{th} , P_1 , and P_3 . To find these unknowns, we use Equations I Ib.8.1, I Ib.8.2, I Ib.8.3, and the isentropic relation. From Equation I Ib.8.1, we have:

$$\eta_{th} = 1 - (T_1 / T_4) = 1 - (P_1 / P_4)^{\frac{1-\gamma}{\gamma}}$$

We find P_4 from here, substitute it into Equation I Ib.8.3, and solve the result for T_3 to get:

$$T_3 = \frac{Q_{34}}{R \ln \left[\frac{P_3}{P_1} (1 - \eta_{th})^{\frac{\gamma}{1-\gamma}} \right]} = \frac{50 \times 778}{53.34 \ln \left[\frac{2710(1 - 0.75)^{3.5}}{14.7} \right]} \approx 2000 \text{ R}$$

Having T_3 , we also have $T_4 = T_3 = 2000 \text{ R}$. We can use Equation I Ib.8.1 again to find other temperatures:

$$\eta_{th} = 1 - \frac{T_2}{T_3} = 0.75$$

Hence, $T_2 = T_1 = 500 \text{ R}$. Having found all temperatures, we can obtain the two remaining pressures. For this purpose we apply the isentropic relation between

states 4 and 1:

$$P_4/P_1 = (T_4/T_1)^{\gamma/(\gamma-1)} = (2000/500)^{3.5} = 128$$

Substituting, we find $P_4 = 14.7 (128) = 1882$ psia. Finally, P_2 is obtained from an isentropic relation between states 2 and 3: $P_2 = (T_2/T_3)^{\gamma/(\gamma-1)} P_3 = 21.2$ psia.

The Carnot cycle is not practical. This is due to the fact that isentropic processes cannot be achieved in practice. Furthermore, heat addition and rejection take place at isothermal processes, which are also difficult to obtain in practice. In theoretical form, the Carnot cycle still serves to predict the maximum efficiency for cycles operating between the same reservoir temperatures. Means of approaching the performance of the Carnot cycle are discussed later in this chapter.

1.3. Air Standard Cycles for Reciprocating Engines

The air standard Otto cycle is the theoretical version of the actual Otto cycle (after Nikolaus August Otto, 1832 – 1891) in spark-ignition reciprocating engines, used extensively in the automotive industry. As shown in Figure I Ib.1.6 (a), the air standard Otto cycle is an isentropic-isochoric cycle where heat addition and rejection take place at constant volume, and compression and expansion processes are at constant entropy.

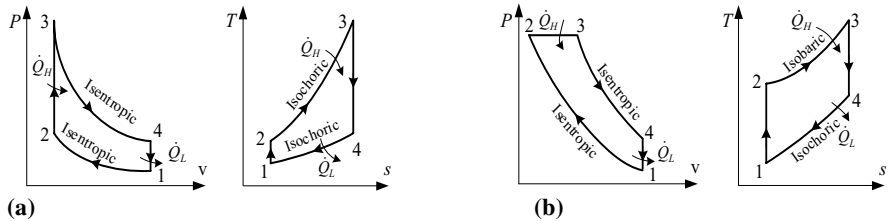


Figure I Ib.1.6. The air standard Pv and Ts diagrams for (a)- Otto and (b)- Diesel Cycles

The efficiency of the Otto cycle is obtained from:

$$\eta_{th} = \frac{\dot{W}_{net}}{\dot{Q}_H} = \frac{\dot{Q}_H - \dot{Q}_L}{\dot{Q}_H} = 1 - \frac{\dot{Q}_L}{\dot{Q}_H} = 1 - \frac{\dot{m}c_v(T_4 - T_1)}{\dot{m}c_v(T_3 - T_2)} = 1 - \frac{(T_4/T_1 - 1)}{(T_3/T_2 - 1)} \frac{T_1}{T_2} \quad \text{I Ib.1.4}$$

We can manipulate Equation I Ib.1.4 to obtain thermal efficiency only as a function of the pressure ratio. To do this, we take advantage of the isentropic process relating temperature ratio to volume ratio, $T_2/T_1 = (V_1/V_2)^{\gamma-1}$. Finally, we note that the cylinder volume for compression is the same as the volume for expansion ($V_1 = V_4$ and $V_2 = V_3$), hence, $T_2/T_1 = (V_1/V_2)^{\gamma-1} = (V_4/V_3)^{\gamma-1} = T_3/T_4$. Therefore, $T_4/T_1 = T_3/T_2$:

$$\eta_{th} = 1 - \frac{T_1}{T_2} = 1 - \left(\frac{V_2}{V_1}\right)^{\gamma-1} = 1 - \frac{1}{r_V^{\gamma-1}} = 1 - \frac{1}{r_P^{(\gamma-1)/\gamma}} \quad \text{Iib.1.5}$$

This relation shows that theoretically, the larger the compression ratio, the higher the thermal efficiency of the Otto cycle. In practice, however, the larger the compression ratio, the more likely the occurrence of engine knock due to the phenomena known as *detonation*. Combustion is associated with a *flame front* where burning proceeds in combustible gases. Detonation on the other hand is when combustible gases explode rather than burn. The resulting shock waves damage the cylinder, piston, and other engine components. Fuel chemical composition affects the occurrence of detonation in engines with higher compression ratios. For example, leaded fuels reduce the likelihood of detonation hence, allow higher compression ratio. However, the environmental concern regarding lead has resulted in most spark-ignition engines operating at a compression ratio generally in the range of 8 to 9.

Example Iib.1.3. An air standard Otto cycle operates at an efficiency of 55%. The amount of heat transferred to air at the heat source is 1700 kJ/kg. The lowest cycle pressure and temperature are 0.1 MPa and 20 °C, respectively. Find cycle pressures and temperatures at the end of each process.

Solution: We first find the compression ratio from thermal efficiency, Equation Iib.1.5:

$$r_V = \left(\frac{1}{1 - \eta_{th}}\right)^{\frac{1}{\gamma-1}} = \frac{1}{(1 - 0.55)^{2.5}} = 7.36$$

The compression process from 1 to 2 is isentropic for which from Equation Iia.4.4 we have;

$$\frac{T_2}{T_1} = \left(\frac{V_1}{V_2}\right)^{\gamma-1} = r_V^{\gamma-1} = \frac{1}{1 - \eta_{th}} = 2.22$$

Solving for T_2 we find $T_2 = 2.22 T_1 = 2.22(20 + 273) = 651$ K. We can also find P_2 from:

$$\frac{P_2}{P_1} = \frac{T_2}{T_1} \frac{V_1}{V_2} = r_V^{\gamma} r_V = r_V^{\gamma} = (7.36)^{1.4} = 16.36$$

Resulting in $P_2 = 1.636$ MPa. We find T_3 from the following heat balance at the heat source:

$$Q = 1700 = c_v(T_3 - T_2) = 0.7165(T_3 - 651)$$

Hence, we find $T_3 = 3024$ K. Since the process from state 2 to state 3 is isochoric, we find P_3 from

$$P_3 = \frac{T_3}{T_2} P_2 = 3024 \times 1.636 / 651 = 7.6 \text{ MPa}$$

The expansion process from 3 to 4 is isentropic, hence:

$$P_4 = \left(\frac{V_3}{V_4}\right)^\gamma P_3 = \frac{P_3}{r_V^\gamma} = \frac{7.6}{7.36^{1.4}} = 0.465 \text{ MPa}.$$

In the above example, we calculated a gas temperature as high as 3024 K. This is the temperature of the bulk of the gas. The cylinder wall has a temperature much lower than the gas maximum temperature due to the film thermal resistance adjacent to the wall, as discussed in Chapter IVa.

The air standard Diesel cycle is the theoretical version of the actual diesel cycle in reciprocating engines, used extensively in trucking, heavy industry, and irrigation. The diesel cycle (after Dr. Rudolph Christian Karl Diesel, 1858 – 1913) does not have a spark ignition rather it is a compression-ignition cycle. Air is compressed to the ignition temperature of the fuel. As such, diesel engines have a high compression ratio since only air is being compressed. As shown in Figure IIb.1.6, the air standard diesel cycle is an isentropic-isobaric-isochoric cycle where heat is added in an isobaric process and is rejected in an isochoric process. To find thermal efficiency in an air standard diesel cycle, we write:

$$\eta_{th} = \frac{\dot{W}_{net}}{\dot{Q}_H} = \frac{\dot{Q}_H - \dot{Q}_L}{\dot{Q}_H} = 1 - \frac{\dot{Q}_L}{\dot{Q}_H} = 1 - \frac{\dot{m}c_v(T_4 - T_1)}{\dot{m}c_p(T_3 - T_2)} = 1 - \frac{(T_4/T_1 - 1) T_1}{\gamma(T_3/T_2 - 1) T_2}$$

IIb.1.6

To simplify Equation IIb.1.6, similar to Equation IIb.1.5, we introduce a new variable called *cutoff ratio* (also referred to as *the degree of isobaric expansion*), $r_c = V_3/V_2$. We now try to find temperature ratios in terms of r_V and r_c . Using the isentropic relations between states 1 and 2, we find

$$P_2 = P_1 r_V^\gamma$$

Using the ideal gas relation between states 2 and 3, noting that $P_2 = P_3$, and taking advantage of the cutoff ratio, we find:

$$\frac{T_3}{T_2} = \frac{P_3}{P_2} \frac{V_3}{V_2} = r_c$$

From the ideal gas relation between states 4 and 1 we find $T_4 = (P_4/P_1)T_1$. To cancel P_4 , we use:

$$\frac{P_4}{P_3} = \left(\frac{V_3}{V_4}\right)^\gamma = \left(\frac{V_3}{V_1}\right)^\gamma = \left(\frac{V_3}{V_2}\right)^\gamma \left(\frac{V_2}{V_1}\right)^\gamma = \left(\frac{r_c}{r_V}\right)^\gamma$$

From the isochoric process between states 1 and 4 we find $T_4/T_1 = P_4/P_1$. Substituting for P_4 in terms of P_3 from the above relation, we obtain:

$$\frac{T_4}{T_1} = \frac{P_3}{P_1} \left(\frac{r_c}{r_V}\right)^\gamma = \frac{P_2}{P_1} \left(\frac{r_c}{r_V}\right)^\gamma = \frac{P_1 r_V^\gamma}{P_1} \left(\frac{r_c}{r_V}\right)^\gamma = r_c^\gamma$$

We need to find similar relations for the remaining temperature ratio. Using the ideal gas relation, we find:

$$\frac{T_1}{T_2} = \frac{P_1}{P_2} \frac{V_1}{V_2} = \frac{1}{r_V^\gamma} r_V = \frac{1}{r_V^{\gamma-1}}$$

Substituting in Equation IIb.1.6, we obtain η_{th} for the diesel cycle:

$$\eta_{th} = 1 - \frac{(T_4/T_1 - 1)}{\gamma(T_3/T_2 - 1)} \frac{T_1}{T_2} = 1 - \frac{r_c^\gamma - 1}{\gamma(r_c - 1)} \frac{1}{r_V^{\gamma-1}} = 1 - \beta \frac{1}{r_V^{\gamma-1}} \quad \text{IIb.1.7}$$

where β is only a function of r_c .

Example IIb.1.4. An air standard Diesel cycle operates at an efficiency of 65% and a compression ratio of 20. The lowest cycle pressure and temperature are 14.5 psia and 70 F, respectively. Find pressures and temperatures of the cycle at the conclusion of each process.

Solution: We first find pressure and temperature of state 2 from state 1 by using the isentropic relations, Equation IIa.4.1:

$$P_2 = P_3 = \left(\frac{V_1}{V_2}\right)^\gamma P_1 = 20^{1.4} \times 14.50 = 961.2 \text{ psia}$$

Similarly,

$$T_2 = \left(\frac{P_2}{P_1}\right)^{\frac{\gamma-1}{\gamma}} T_1 = r_V^{\gamma-1} T_1 = 20^{0.4} (70 + 460) = 1756.6 \text{ R}$$

Having P_1 , P_2 , P_3 , T_1 , and T_2 , we need to find P_4 , T_3 , and T_4 . These can be found from these 3 equations:

$$\begin{cases} \frac{P_4}{P_1} = \frac{T_4}{T_1} \\ \frac{T_3}{T_4} = \left(\frac{P_3}{P_4}\right)^{\frac{\gamma-1}{\gamma}} \\ \eta_{th} = 1 - \frac{T_4 - T_1}{\gamma(T_3 - T_2)} \end{cases}$$

To solve this set, we first eliminate P_4 , by substituting it from the first to the second equation. We would then have two equations and two unknowns, T_3 and T_4 . From the first equation we find, $P_4 = (P_1/T_1)T_4$. Substituting into the second equation, we get:

$$T_3 = \left(\frac{P_2}{P_1}\right)^{\frac{\gamma-1}{\gamma}} \frac{T_1}{T_4} \quad T_4 = \left(\frac{P_2 T_1}{P_1}\right)^{\frac{\gamma-1}{\gamma}} \frac{1}{T_4^\gamma}$$

We now substitute T_3 into the third equation for thermal efficiency and solve for T_4 :

$$T_4 - (1 - \eta_{th}) \gamma \left(\frac{P_2 T_1}{P_1}\right)^{\frac{\gamma-1}{\gamma}} \frac{1}{T_4^\gamma} + [(1 - \eta_{th}) \gamma T_2 - T_1] = 0$$

This is a nonlinear algebraic equation for the unknown T_4 . Substituting for $T_1 = 530$ R, $T_2 = 1756.6$ R, $P_1 = 14.5$ psia, $P_2 = 961.2$ psia, $\gamma = 1.4$, and $\eta_{th} = 0.65$, we get:

$$T_4 - 9.749 T_4^{1/\gamma} + 330.73 = 0$$

The answer can be found by iteration as $T_4 = 1329.5$ R. Back substitution results in $P_4 = (14.5/530)T_4 = 36.4$ psia. Finally, we find $T_3 = (961.2 \times 530/14.5)^{2/7} 1329.5^{1/1.4} = 3388.4$ R. We can find the amount of heat added to the cycle as:

$$q_H = c_p(T_3 - T_2) = 0.24(3388.4 - 1756.6) = 391.6 \text{ Btu/lbm}$$

Similarly,

$$q_L = c_v(T_4 - T_1) = 0.171(1329.5 - 530) = 136.7 \text{ Btu/lbm}$$

$$w_{net} = 392.6 - 136.7 = 254.88 \text{ Btu/lbm}$$

We may check on thermal efficiency as

$$\eta_{th} = 254.88/391.6 = 0.65$$

Note, $(\eta_{th})_{\text{Carnot}} = 1 - (530/3388.4) = 0.84$

1.4. Air Standard Cycle for Gas Turbines

The air standard Brayton cycle* (after George Bailey Brayton, 1830–1892) is an ideal cycle for gas turbine plants as shown in Figure IIb.1.7. Gas compression and expansion takes place in isentropic processes and heat addition and rejection in isobaric processes. By increasing the pressure ratio, the efficiency of the Brayton cycle can be increased. To demonstrate, let's increase the pressure ratio from P_2/P_1 to P_2'/P_1 . This cycle is associated with higher heat addition at the heat source but the same heat transfer to the heat sink as the original cycle hence, higher thermal efficiency. To derive thermal efficiency in terms of the pressure ratio, we start with the definition of thermal efficiency:

* Also known as the Joule cycle.

$$\eta_{th} = 1 - \frac{\dot{Q}_L}{\dot{Q}_H} = 1 - \frac{\dot{m} c_p (T_4 - T_1)}{\dot{m} c_p (T_3 - T_2)} = 1 - \frac{(T_4 / T_1 - 1) T_1}{(T_3 / T_2 - 1) T_2}$$

For the isentropic process 3-4 we can write $P_4/P_3 = (V_3/V_4)^k$. Since $P_1 = P_4$ and $P_2 = P_3$, then $V_1/V_2 = V_3/V_4$. From the ideal gas equation of state we have $T_4/T_1 = V_4/V_1$ and $T_3/T_2 = V_3/V_2$. Therefore, $T_4/T_1 = T_3/T_2$. Upon substitution and the application of Equation IIa.4.5, thermal efficiency simplifies to:

$$\eta_{th} = 1 - \frac{T_1}{T_2} = 1 - \left(\frac{P_1}{P_2}\right)^{(\gamma-1)/\gamma} = 1 - \frac{1}{r_p^{(\gamma-1)/\gamma}} \quad \text{IIb.1.8}$$

where in Equation IIb.1.8, we also made use of the definition of r_p , the pressure ratio.

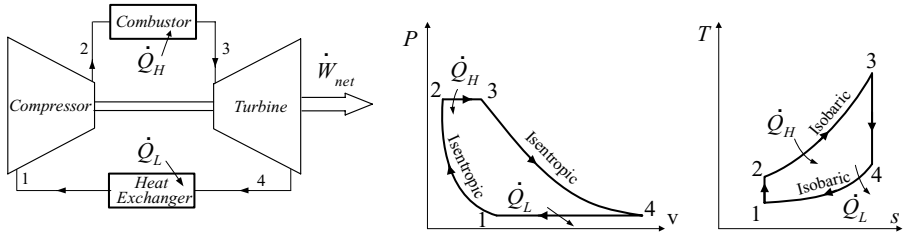


Figure IIb.1.7. The air standard P - v and T - s diagrams for Brayton cycle

Maximum work in the air standard Brayton cycle is a function of the pressure and temperature ratio. To derive this function we start with the following relations for a Brayton cycle as obtained from Equation IIa.4.5:

$$\frac{T_2}{T_1} = r_p^\alpha, \quad \frac{T_4}{T_3} = \frac{1}{r_p^\alpha}$$

where in these relations $\alpha = (\gamma - 1)/\gamma$. The net work per unit mass of the Brayton cycle is found as:

$$\begin{aligned} w_{net} &= w_t - w_c = c_p (T_3 - T_4) - c_p (T_2 - T_1) = c_p T_1 \left[\left(1 - \frac{T_4}{T_3}\right) \frac{T_3}{T_1} - \left(\frac{T_2}{T_1} - 1\right) \right] \\ &= c_p T_1 \left[\left(1 - \frac{1}{r_p^\alpha}\right) r_T - \left(r_p^\alpha - 1\right) \right] \end{aligned}$$

Where w_t and w_c are work per unit mass delivered by the turbine and work per unit mass delivered to the compressor, respectively. We also substituted for the temperature ratios in terms of r_p .

For a given temperature ratio, we optimize the net work by taking its derivative with respect to r_p and setting the result equal to zero:

$$\frac{\partial w_{net}}{\partial r_p} = c_p T_1 \left[r_T \frac{\partial}{\partial r_p} \left(1 - \frac{1}{r_p^\alpha} \right) - \frac{\partial}{\partial r_p} (1 - r_p^\alpha) \right] = 0$$

After simplification, we find;

$$r_p = (r_T)^{\frac{\gamma}{2(\gamma-1)}} \quad \text{I Ib.1.9}$$

where in Equation I Ib.1.9, $r_T = T_3/T_1$. The maximum net work occurs when r_p is given by Equation I Ib.1.9 since the second derivative of w_{net} is positive.

Example I Ib.1.5. Air enters the compressor of an air standard Brayton cycle at 15°C and 0.1 MPa. The cycle pressure and temperature ratios are given as $r_p = 11$ and $r_T = 5$, respectively. Find:

- pressure and temperature at the end of each process,
- thermal efficiency,
- work per unit mass,
- cycle pressure ratio for optimum work,
- the required mass flow rate to produce 10 MW power.

Solution: a) The inlet temperature to the compressor is $T_1 = 15 + 273 = 288$ K. Air pressure at the exit of the compressor is $P_2 = 0.1 r_p = 0.1 \times 11 = 1.1$ MPa. Hence, $T_2 = T_1 (r_p)^{(\gamma-1)/\gamma} = (15 + 273)(11)^{(1.4-1)/1.4} = 571$ K. Air pressure at the inlet to the turbine is $P_3 = P_2 = 1.1$ MPa and $T_3 = T_1 (r_T) = 288 \times 5 = 1440$ K. Finally, $P_4 = P_1 = 0.1$ MPa and $T_4 = T_3 (1/r_p)^{(\gamma-1)/\gamma} = 1440/(11)^{1.4-1/1.4} = 726$ K.

b) Thermal efficiency is:

$$\eta_{th} = 1 - \frac{1}{r_p^{(\gamma-1)/\gamma}} = 1 - 1/(11)^{0.4/1.4} = 49.6\%$$

c) Work per unit mass is found from:

$$w_{net} = c_p (T_3 - T_4) - c_p (T_2 - T_1) = 1.0035(1449 - 726 - 571 + 288) = 432.5 \text{ kJ/kg}$$

d) The optimum r_p is found from Equation I Ib.8.9 as $r_p = (5)^{1.4/[2(1.4-1)]} = 16.72$. This is a high compression ratio due to a high temperature ratio. For a temperature ratio of 4, the pressure ratio is found to be 11.3. Therefore, in the above example with pressure ratio of 11, if the temperature ratio is maintained at 4, the cycle would produce near maximum work. This is important for transportation applications of the gas turbine to maximize net work per unit mass of the working fluid. This, in turn, is related to *specific power* (power produced by the engine divided by the weight of the engine).

e) The relationship between power and net work per unit mass is:

$$\dot{W}_{net} = \dot{m}w_{net}$$

where \dot{m} is the mass flow rate of the working fluid in the cycle. For the air standard cycle, the mass flow rate of air needed to produce 10 MW of power is found as $\dot{m} = 10,000 \text{ kW}/432.5 \text{ kJ/kg} = 23 \text{ kg/s}$.

Gas turbine with regenerator is designed to recover some energy from the hot exhaust gases. A counter flow heat exchanger (regenerator), uses the turbine exhaust gases to heat up the compressed gases before they enter the turbine. Heating the gas from state 2 to state “a” before entering the combustor saves fuel.

According to the second law of thermodynamics, $T_a \leq T_4$ (Figure IIb.1.8). This is expressed in terms of the regenerator efficiency:

$$\eta_{reg} = \frac{T_a - T_2}{T_4 - T_2}$$

Generally, regenerator efficiency ranges from 60 to 80%. While addition of the regenerator helps to save fuel, it also introduces an additional initial investment.

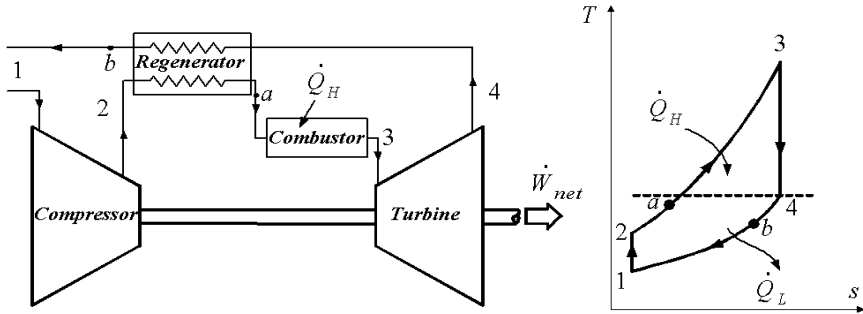


Figure IIb.1.8. A Regenerative modified Brayton Cycle

Example IIb.1.6. Consider the addition of a regenerative heat exchanger with an efficiency of 75% to the cycle of Example IIb.1.5. Find the improvement in thermal efficiency.

Solution: The same $w_{net} = 432.5 \text{ kJ/kg}$ as in Example IIb.1.5 also applies here. However, the amount of heat addition at the heat source is reduced due to the addition of the regenerator. To calculate the amount of heat addition, we first find T_a from:

$$T_a = T_2 + (T_4 - T_2)\eta_{reg} = 571 + 0.75(726 - 571) = 687 \text{ K}$$

Total heat addition is:

$$Q_H = c_p(T_3 - T_a) = 1.0035(1440 - 687) = 755 \text{ kJ/kg}$$

Thermal efficiency becomes:

$$\eta_{th} = \frac{w_{net}}{Q_H} = \frac{432.5}{755} = 57\%$$

The improvement in thermal efficiency is in excess of 15%, justifying the addition of the regenerator.

Air standard Stirling and Ericsson cycles are examples of how to approach the Carnot efficiency in common practice. One impractical aspect of the Carnot cycle is the fact that the heat addition and rejection are isothermal processes. The Stirling cycle (after Rev. Robert Stirling, 1790–1878) and Ericsson cycle (after Captain John Ericsson, 1803–1889) can be approximated if the heat addition and rejection processes take place in multiple stages. Heating and cooling of gas in the Stirling cycle take place in isochoric processes and in the Ericsson cycle in isobaric processes. As shown in Figure I Ib.1.9, these cycles can achieve the thermal efficiency of the Carnot cycle operating within the same T_H and T_L temperature limits.

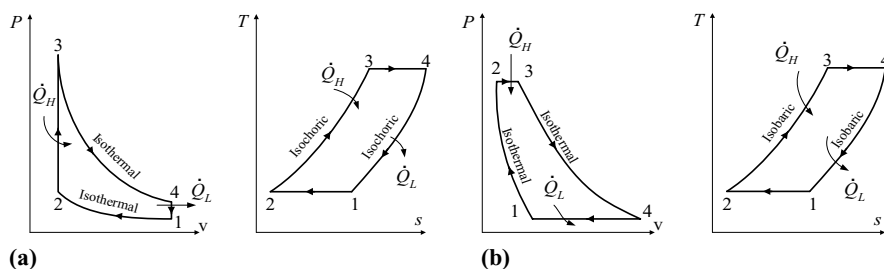


Figure I Ib.1.9. The air standard Pv and Ts diagrams for (a) Stirling and (b) Ericsson cycles

Approaching Ericsson and Stirling cycles is possible by devising systems for heating and cooling in multiple stages so that the average temperature at each process represent the intended temperature of the theoretical Stirling and Ericsson cycles (Figure I Ib.1.10). Systems allowing multiple stage heat addition and heat rejection are called reheat and intercooler, respectively.

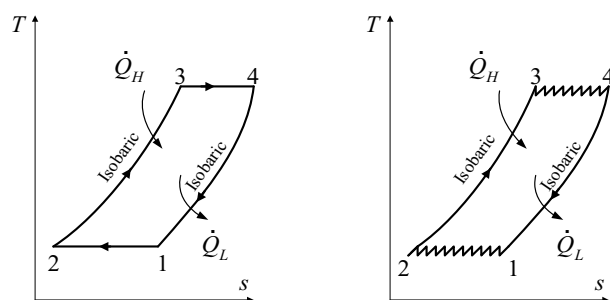


Figure I Ib.1.10. Ericsson and the approximate Ericsson cycle

Gas turbine with intercooler is shown in Figure IIb.1.11. Addition of the intercooler increases the net work of the gas turbine cycle. A cycle equipped with an intercooler compresses the working fluid at two stages. The compressed gas at the exit of the first stage is cooled in a heat exchanger and compressed to the intended pressure in the second stage. The use of an intercooler increases net work hence, the cycle thermal efficiency, but there is a limit to the number of stages that can be added to the cycle due the associated cost and diminishing gain.

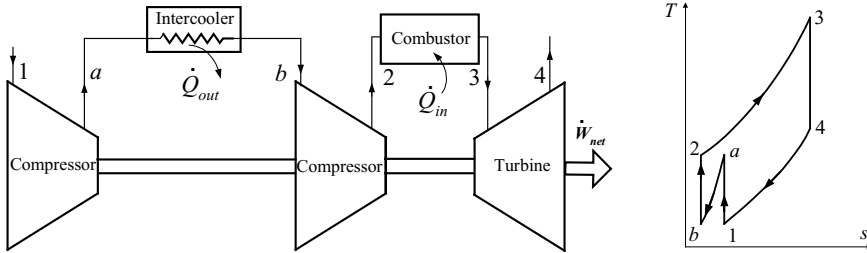


Figure IIb.1.11. Gas turbine equipped with intercooler

Gas turbine with reheat allows for gas expansion in multiple stages. Hot gases enter the first stage of the turbine and are heated up to the same temperature before entering the second stage of the turbine (Figure IIb.1.12). The reheat increases net work of the cycle, hence, the cycle efficiency.

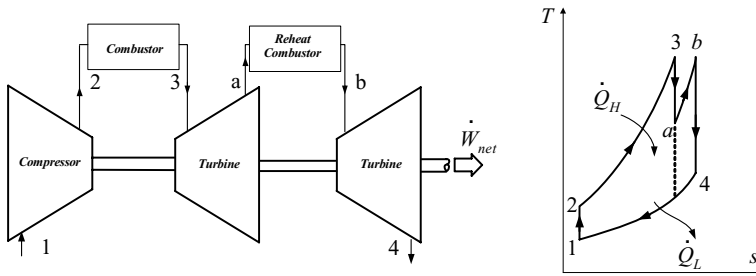


Figure IIb.1.12. The reheat modified Brayton Cycle

1.5. Air Standard Cycle for Reaction Engines

Reaction engines are gas turbines where the bulk of the work developed by the turbine is converted into the kinetic energy and used as thrust for propulsion. Towards the end of World War II, aircraft equipped with reciprocating engines could reach a maximum speed of up to 500 miles/hour. The advent of aircraft with reaction engines increased the maximum speed to over 1000 miles/hour. This was possible because reaction engines have a much higher specific power compared with reciprocating engines.

Gas turbine for jet propulsion¹ is shown in Figure I Ib.1.13. Air pressure is increased in a diffuser before entering the compressor. The work produced by the turbine is primarily delivered to the compressor and the remaining power is used as auxiliary power for lighting, air conditioning, and other electrical needs of the aircraft. The exhaust gases from the turbine are expanded to the atmospheric pressure in a nozzle. The change in the momentum due to this expansion produces the force required to thrust the aircraft.

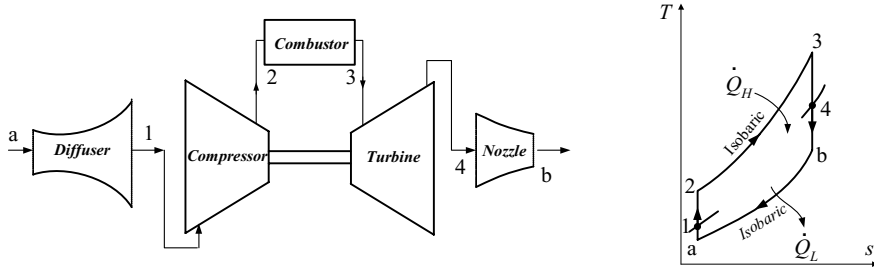


Figure I Ib.1.13. Schematic of a gas turbine for jet propulsion²

Example I Ib.1.7. Air enters a jet engine diffuser at 650 miles/h (1046 km/h), 5 F (-15 C) and 12 psia (83 kPa). The compression ratio of the compressor is 10. The gas temperature at the exit of the combustor is 1700 F (927 C). If all processes are ideal and turbine work is delivered entirely to the compressor, find the velocity of gases at the nozzle exit. The diffuser inlet diameter is 6 ft (1.83 m).

Solution: We first determine properties at the end of various processes. For this, we ignore all potential and kinetic energies except for the nozzle. Having $P_a = 12$ psia, $T_a = 5 + 460 = 465$ R (258 K), and $V_a = 650$ miles/hr = 953.3 ft/s (290.5 m/s) we find properties at state 1 from the first law of thermodynamics:

$$h_1 = h_a + \frac{V_a^2}{2} = 0.24 \times 465 + \frac{953.3^2}{2 \times 32.2 \times 778} = 129.7 \text{ Btu/lbm} \quad (301.7 \text{ kJ/kg})$$

Therefore $T_1 = h_1/c_p = 540.5$ R. To find P_1 , we use the isentropic process for the diffuser:

$$P_1 = P_a \left(\frac{T_1}{T_a} \right)^{\gamma/(\gamma-1)} = 12 (540.5/465)^{0.4/1.4} = 12.5 \text{ psia} \quad (86.2 \text{ kPa})$$

¹ This topic is discussed in more details in Chapter VIc.

² Sir Frank Whittle (1907–1996) and Hans J. P. von Ohain independently developed jet airplane engine. Whittle obtained his jet-propulsion patent in 1930. The first British experimental jet flew in 1941.

Having P_1 , we find P_2 from the compression ratio; $P_2 = 10 \times 12.5 = 125$ psia. To find T_2 , we use the isentropic relation for the compression process;

$$T_2 = T_1 r^{\gamma-1/\gamma} = 540.5(10)^{0.4/1.4} = 1043.5 \text{ R } (579.4 \text{ K})$$

Since process 2–3 is an isobaric process, $P_3 = P_2 = 125$ psia and T_3 is given as $T_3 = 1700 + 460 = 2160$ R. To find the state of air at the turbine exit, we note that $w_T = w_C$. If written in terms of enthalpies we find:

$$h_2 - h_1 = h_3 - h_4$$

Treating air as an ideal gas, which allows us to use a constant specific heat, we find that:

$$T_4 = T_3 + T_1 - T_2 = 2160 + 540.5 - 1043.5 = 1657 \text{ R } (920.2 \text{ K})$$

Air pressure at state 4 can be found from the isentropic relation written for the expansion process in turbine:

$$P_4 = P_3 \left(\frac{T_4}{T_3} \right)^{\gamma/(\gamma-1)} = 125(1657/2160)^{0.4/1.4} = 115.9 \text{ psia } (0.8 \text{ MPa})$$

We can also find temperature at state 5 from the isentropic expansion in the nozzle where air reaches the atmospheric pressure, $P_b = P_a$:

$$T_b = T_4 \left(\frac{P_b}{P_4} \right)^{(\gamma-1)/\gamma} = 1657(12/115.9)^{0.4/1.4} = 866.8 \text{ R } (499 \text{ K})$$

We can find velocity at the nozzle exit by writing the energy equation for a control volume encompassing the nozzle:

$$V_b = \sqrt{2c_p(T_4 - T_b)} = \sqrt{2 \times 0.24 \times 32.2 \times 778(1657 - 866.8)} = 3082.5 \text{ ft/s } (939.65 \text{ m/s})$$

The thrust developed by various types of gas turbines for aircraft propulsion is discussed in Chapter VIc.

2. Vapor Power Systems

Unlike the gas power systems in which the working fluid is constantly changing, the vapor power cycles use a closed system in which the working fluid remains the same but its phase changes during a cycle. The vapor power systems are primarily based on the Rankine cycle. To improve thermal efficiency, the Rankine cycle is modified with reheat and regenerative cycles. In the calculations, we use the first and the second law of thermodynamics in conjunction with the steam tables thermodynamics properties.

2.1. Definition of Terms

Rankine and modified Rankine cycle are extensively used in electric power plants using steam as working fluid.

Balance of plant is a term generally applied to include all the components in a power plant except the heat source. This includes turbine, condenser, pump, feedwater heater, and the associated piping.

Feedwater is the water flowing from the condenser to the heat source.

Extraction steam is a term applied to that portion of steam that bypasses the turbine to heat up feedwater.

Feedwater heater is a heat exchanger used to heat up feedwater from the extraction steam to increase η_{th} .

High-, intermediate-, and low-pressure turbines are stages of a steam turbine that admit steam at progressively decreasing pressures.

Reheater is a heat exchanger to heat up the steam exiting the high-pressure turbine prior to entering the intermediate-pressure turbine. The warmer stream is extraction steam from the heat source that bypasses the high-pressure turbine.

Moisture separator transfers the condensate of the reheater to a tank to be pumped to the feedwater line. The tank is known as the drain tank and the pump as the drain pump.

Trap is a valve that reduces steam pressure by introducing a large, non-recoverable pressure drop to the flow and allows the condensate to pass to a lower pressure region. Pressure drop is discussed in Chapter IIb.

2.2. The Rankine Cycle

A schematic of a Rankine cycle (after William John Maquorn Rankine, 1820 – 1872) used for a steam power plant is shown in Figure IIb.2.1. Water is pumped isentropically into the heat source at state 1. The heat source can be a boiler, the vessel of a BWR, the steam generator of a PWR, etc. Water is boiled at constant pressure and the saturated or superheated steam enters the high-pressure stage of the steam turbine. The stationary blades direct high-energy steam toward the rotating blades on the turbine shaft, which then turns the rotor of the electric generator. In the Rankine cycle, the steam expansion process in the turbine is isentropic ($s_3 = s_4$). The low-energy steam leaves the turbine at stage 4 and enters the condenser. After rejecting heat in the heat sink at constant pressure, it is again pumped into the heat source for the next cycle.

Thermal efficiency of a Rankine cycle is calculated from:

$$\eta_{th} = \frac{\dot{W}_{net}}{\dot{Q}_H} = \frac{\dot{W}_t - \dot{W}_p}{\dot{Q}_H} = \frac{\dot{m}(h_3 - h_4) - \dot{m}(h_2 - h_1)}{\dot{m}(h_3 - h_2)} \quad \text{IIb.2.1}$$

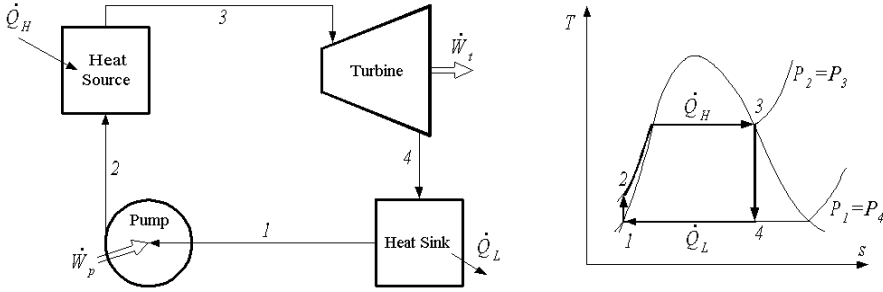


Figure Iib.2.1. Rankine cycle for a steam power plant

where subscripts p and t stand for pump and turbine, respectively. Recall that, per Equation Iia.6.7, the enthalpy rise through the pump is found as $\Delta h_{pump} \cong v_f(T)\Delta P_{pump}$. Substituting into Equation Iib.2.1, thermal efficiency becomes:

$$\eta_{th} = \frac{(h_3 - h_4) - (h_2 - h_1)}{(h_3 - h_2)} = \frac{(h_3 - h_4) - v_f(T)\Delta P_{pump}}{(h_3 - h_1) - v_f(T)\Delta P_{pump}} \quad \text{Iib.2.2}$$

Example Iib.2.1. Saturated steam in a Rankine cycle enters a turbine at 5.86 MPa (850 psia) and leaves the condenser at 6.895 kPa (1 psia). Find the cycle thermal efficiency.

Solution: We first find the relevant thermodynamic properties at the heat sink and heat source pressures:

P (MPa)	v_f (m ³ /kg)	h_f (kJ/kg)	h_g (kJ/kg)	s_f (kJ/kg·K)	s_g (kJ/kg·K)
0.00689	0.10074E-2	162.178	2571.07	0.5552	8.2791
5.86	—	1205.44	2785.44	3.0125	5.8998

The energy used in pumping the condensate is found from:

$$w_p = v_f(T)\Delta P_{pump} = 0.10074 \text{E-}2 \times (5.86 \text{E}3 - 0.00689 \text{E}3) = 5.89 \text{ kJ/kg}$$

Therefore, $h_2 = h_1 + w_p = 162.178 + 5.89 = 168 \text{ kJ/kg}$. To find η_{th} , we need h_1 through h_4 (Equation Iib.2.2).

We have $h_1 = 162.178 \text{ kJ/kg}$, $h_2 = 168 \text{ kJ/kg}$, and $h_3 = 2785.44 \text{ kJ/kg}$. To find h_4 , we first find x_4 from the second law of thermodynamics. Process 3-4 is isentropic

From Equation IIa.10.14 we conclude that, $s_3 = s_4$:

$$x_4 = \frac{s_3 - s_{f4}}{s_{g4} - s_{f4}} = \frac{5.8998 - 0.5552}{8.2791 - 0.5552} = 0.692$$

We can now find $h_4 = 162.178 + 0.692(2571.07 - 162.178) = 1829.13$ kJ/kg. Thus thermal efficiency is:

$$\eta_{th} = \frac{w_{net}}{\dot{q}} = \frac{(2785.44 - 1829.13) - 5.89}{(2785.44 - 162.178) - 5.89} = \frac{950.42}{2617.37} = 36.3\%$$

As discussed in Example IIb.1.5, the total power produced by a power plant is the product of flow rate and the net work per unit mass of the working fluid.

Example IIb.2.2. In Example IIb.2.1, find the steam mass flow rate for a 1000 MW power plant.

Solution: The net power per unit mass flow rate is found from $w_{net} = w_t - w_p = (h_3 - h_4) - w_p$. Substituting, the net work becomes $w_{net} = 950.42$ kJ/kg. Hence, the required steam mass flow rate to produce 1000 MW power is $\dot{m}_s = \dot{W} / w_{net} = 1\text{E}6 / 950.42 = 1052$ kg/s (8.35×10^6 lbm/h).

Effects of pressure and temperature on cycle performance. We now investigate the effects of lowering heat sink pressure, superheating steam, and increasing steam pressure on the cycle thermal efficiency. Given heat source pressure and temperature, lowering heat sink pressure increases cycle efficiency. To verify, we use the Rankine cycle in Figure IIb.2.2. Lowering heat sink pressure for the same amount of heat addition, causes the amount of heat rejection to be reduced by area 1-4-4'-1'-2'-2-1 in Figure IIb.2.2(a). On the other hand, lowering the heat sink pressure results in $x_{4'} < x_4$. This decrease in steam quality is disadvantageous for the turbine blades as excessive moisture would lead to pitting and erosion. For a given heat sink pressure, cycle efficiency increases by superheating steam. This is shown in Figure IIb.2.2(b) where work is increased by the enclosed area in 3-3'-4'-4-3. This amount of extra work is obtained at the expense of more heat input in the heat source shown by the enclosed area in 3-3'-a'-a. Further advantage of superheating steam is the increase in steam quality leaving the last stage of the turbine. Finally, given heat sink pressure and steam temperature, increasing heat source pressure increases cycle efficiency but reduces steam quality leaving the last stage of the turbine, Figure IIb.2.2(c). To remedy this problem, we use a modified Rankine cycle by reheating steam, as discussed later in this chapter. In the following example we investigate the effect of steam superheat on cycle efficiency.

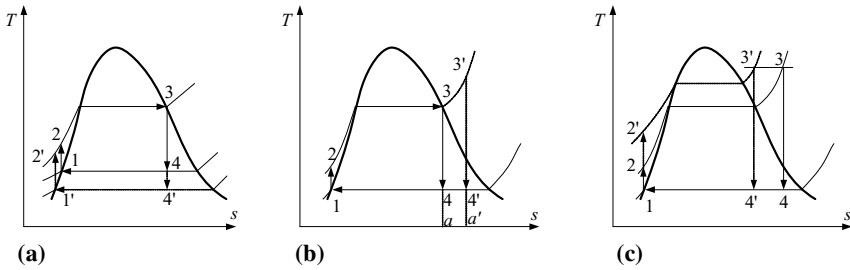


Figure IIB.2.2. Pressure and temperature effects on Rankine cycle

Example IIB.2.3. In Example IIB.2.1, instead of saturated steam, suppose we use superheated steam at a temperature of 650 F (616 K). The rest of the cycle remains unchanged. Find the effect on cycle efficiency.

Solution: We find the relevant thermodynamic properties at the given heat source pressure and temperature as well as the given heat sink pressure. Saturation properties at the heat sink pressure remain the same:

P (psia)	v_f (ft ³ /lbm)	h_f (Btu/lbm)	h_g (Btu/lbm)	s_f (Btu/lbm·F)	s_g (Btu/lbm·F)
1.000	0.016136	69.730	1105.8	0.1326	1.9781

Superheated properties at heat source pressure and temperature are:

P (psia)	T (F)	v (ft ³ /lbm)	h (Btu/lbm)	s (Btu/lbm·F)
850.0	680	0.71250	1323	1.5283

We note that the pump work remains unchanged. Thermal efficiency is found from Equation IIB.2.2. We have $h_1 = 69.73$, $h_2 = 72.27$, and $h_3 = 1198$ Btu/lbm. To find h_4 , we first find x_4 :

$$x_4 = \frac{s_3 - s_f}{s_g - s_f} = \frac{1.5283 - 0.1326}{1.9781 - 0.1326} = 0.76$$

Therefore, $h_4 = 69.73 + 0.76 (1105.8 - 69.73) = 857$ Btu/lbm. Thus, thermal efficiency becomes:

$$\eta_{th} = \frac{(h_3 - h_4) - v_f(T) \Delta P_{pump}}{(h_3 - h_1) - v_f(T) \Delta P_{pump}} = \frac{(1323 - 857.0) - 2.54}{(1323 - 69.73) - 2.54} = 37\%$$

In the above example, we were only interested in finding the improvement in the thermal efficiency. For the sake of completion, it is important to also calculate

such key design parameters as turbine work, the energy deposited in the heat source, and the energy rejected to the environment in the heat sink.

Example I Ib.2.4. In Example I Ib.2.3, find the heat added in the heat source and rejected in the heat sink.

Solution: To find the heat added to the working fluid, we write an energy balance for the heat source:

$$q_H = h_3 - h_2 = 1323 - 72.27 = 1250.73 \text{ Btu/lbm (2909 kJ/kg)}$$

The amount of energy rejected to the surroundings is also found from an energy balance written for the heat sink:

$$q_L = h_4 - h_1 = 857 - 69.73 = 787.27 \text{ Btu/lbm (1831 kJ/kg)}$$

The net work is $w_{net} = q_H - q_L = 1250.73 - 787.27 = 463.5 \text{ Btu/lbm}$. Thermal efficiency can be found from $\eta_{th} = w_{net} / q_H = 463.5 / 1250.73 = 37\%$. Turbine work is $w_t = h_3 - h_4 = 1323 - 857 = 466 \text{ Btu/lbm (1804 kJ/kg)}$. Finally, $w_{net} = w_t - w_p = 466 - 2.54 = 461.75 \text{ Btu/lbm (1074 kJ/kg)}$.

To numerically verify the effect of the heat source and heat sink pressures on thermal efficiency, we may perform a parametric study the results of which are shown in Figure I Ib.2.3.

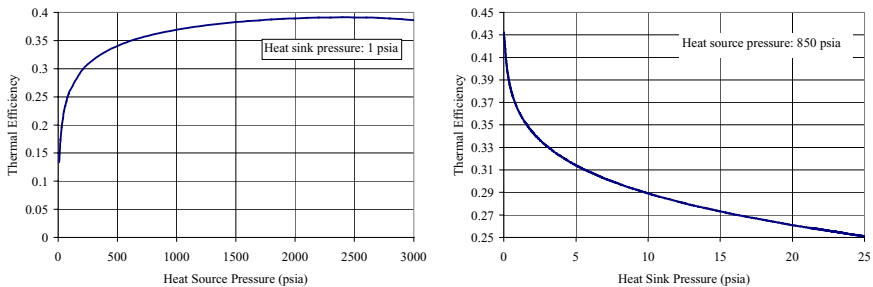


Figure I Ib.2.3. Effect of pressure on thermal efficiency of an ideal Rankine cycle

Figure I Ib.2.3 indicates that, for a given heat sink pressure, thermal efficiency increases with increasing heat source pressure. Conversely, for a given heat source pressure, thermal efficiency decreases substantially with increasing heat sink pressure.

2.3. Reheat-Modified Rankine Cycle

As discussed above, increasing heat source pressure or decreasing heat sink pressure increases thermal efficiency. However, such changes in pressure also increase the moisture content in the last stage of the turbine, Figures I Ib.2.2(a) and I Ib.2.2(c). The reheat cycle helps alleviate the high moisture content, as

shown in Figure IIb.2.4. After expansion to some intermediate pressure, steam is heated up in an isobaric process before entering the next stage of the turbine. By doing so, we increase steam quality from $x_{6'}$ to x_6 .

To accomplish the same goal and also increase thermal efficiency, we could have increased the degree of superheat to state $3'$ (Figure IIb.2.4).

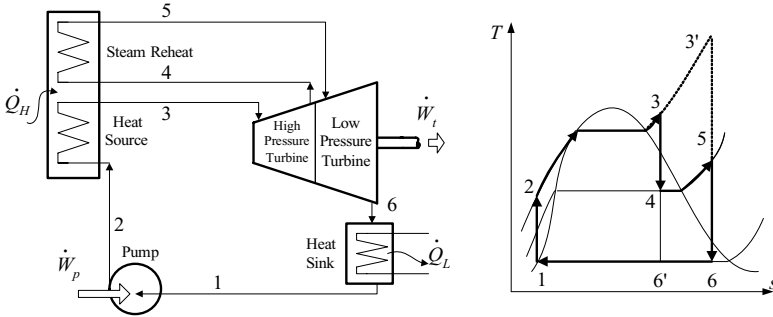


Figure IIb.2.4. The reheat-modified Rankine cycle

2.4. Regenerative-Modified Rankine Cycle

In this modification, feedwater is heated by steam extraction from the turbine prior to entering the heat source. This increases the average temperature in the heat source, thereby increasing thermal efficiency. Heating up of water takes place in a heat exchanger referred to as the *feedwater heater* (FWH). In such systems, steam condenses on the tubes carrying the feedwater. Hence, the two streams do not mix and are generally at different pressures. Since the two streams do not mix, these are known as *closed feedwater heaters*. Occasionally, streams may be allowed to mix, which takes place when the two streams are at the same pressure. This is referred to as *open feedwater heaters*, as shown in Figure IIb.2.6(a) and discussed in Example IIa.7.5. In closed feedwater heaters, the condensate is either pumped to a higher-pressure FWH, Figure IIb.2.6(b), or allowed to flow to a lower pressure region, such as either a FWH or the condenser, Figure IIb.2.6(c). In the latter case, the condensate is passed through a special valve referred to as steam trap. Ideally, the mixture pressure in the steam trap drops in an isentropic process to the pressure of the up-stream system. Such a system is either a low pressure FWH or the condenser.

To determine the fraction of steam extraction from the turbine to be used in an open feedwater heater so that state 3 is saturated liquid, we use an energy balance written for the feedwater heater. From Figure IIb.2.5, for perfect mixing, we have:

$$\dot{m}_{es}h_6 + (\dot{m}_s - \dot{m}_{es})h_2 = \dot{m}_sh_3$$

where \dot{m}_s and \dot{m}_{es} are mass flow rates of steam and the extraction steam, respectively. Dividing terms by the steam mass flow rate and showing the fraction of steam used as extraction steam by y , we get:

$$yh_6 + (1 - y)h_2 = h_3$$

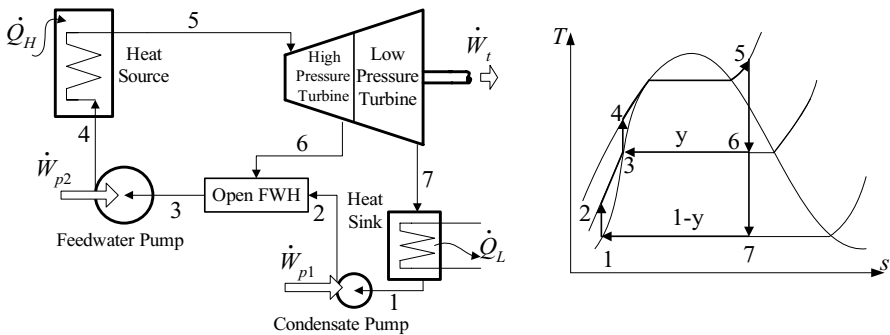


Figure I Ib.2.5. Regenerative-modified Rankine cycle. Open feedwater heater.

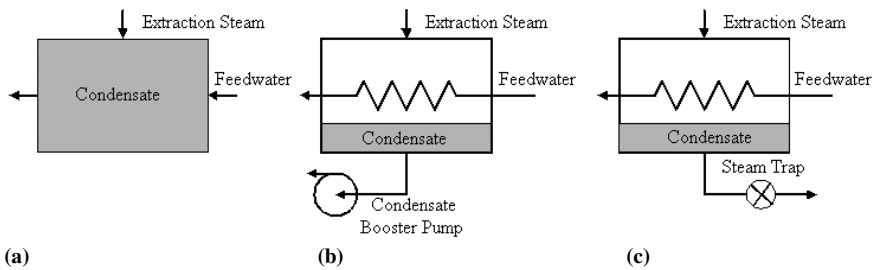


Figure I Ib.2.6. Schematics of open and closed feedwater heaters

Example I Ib.2.5. In Example I Ib.2.1, we now introduce an open feedwater heater with steam extraction to heat up the feedwater. For the FWH operating at 100 psia (0.7 MPa), find the revised thermal efficiency.

Solution: We first find the relevant thermodynamic properties at the given pressures.

P (psia)	v_f (ft ³ /lbm)	h_f (Btu/lbm)	h_g (Btu/lbm)	s_f (Btu/lbm·F)	s_g (Btu/lbm·F)
1.000	0.016136	69.730	1105.8	0.1326	1.9781
100.0	0.017740	298.50	1187.2	0.4743	1.6027
850.0	0.021500	518.40	1198.0	—	1.4096

To find steam quality at state 6, we use $s_6 = s_5$ (unlike Figure I Ib.2.5, here state 5 is saturated), hence:

$$1.4096 = 0.4743 + x_6 (1.6027 - 0.4743)$$

From here, $x_6 = 0.83$ and $h_6 = 298.5 + 0.83(1187.2 - 298.5) = 1036.1$ Btu/lbm (2410 kJ/kg). The energy used in the condensate pump, which delivers the con-

densate to the FWH is found from:

$$w_{cp} = v_f(T)\Delta P_{pump} = 0.016695 \times (100 - 1) \times (144 / 778) = 0.31 \text{ Btu/lbm} \quad (0.72 \text{ kJ/kg})$$

where subscript cp stands for condensate pump. Therefore, $h_2 = h_1 + 0.31 = 70 \text{ Btu/lbm}$ (163 kJ/kg). We can find y , the fraction of steam used as steam extraction, from an energy balance for the FWH:

$$\begin{aligned} y h_6 + (1 - y) h_2 &= h_3 \\ 1036.1 y + 70(1 - y) &= 298.5 \end{aligned}$$

Therefore, $y = 0.236$. Having the fraction of steam used for steam extraction, we can calculate w_t and w_p . To do this, we first find the enthalpy of state 4. The energy used in the feedwater pump is found from:

$$\begin{aligned} w_{fwp} &= v_f(T)\Delta P_{pump} = 0.01774 \times (850 - 100) \times (144 / 778) = 2.46 \text{ Btu/lbm} \\ & \quad (5.72 \text{ kJ/kg}) \end{aligned}$$

where subscript fwp stands for feedwater pump. Therefore, $h_4 = h_3 + w_p$. Finding $h_4 = 298.50 + 2.46 = 301 \text{ Btu/lbm}$. Total pumping power is:

$$w_p = (1 - y)w_{cp} + w_{fwp} = (1 - 0.236) \times 0.31 + 2.46 = 2.69 \text{ Btu/lbm} \quad (6.26 \text{ kJ/kg})$$

Total power produced by the turbine is:

$$\begin{aligned} w_t &= h_5 - [y h_6 + (1 - y) h_7] = 1198 - [0.236 \times 1036.1 + (1 - 0.236) \times 786.7] = 352.4 \text{ Btu/lbm} \\ & \quad (819.7 \text{ kJ/kg}) \end{aligned}$$

Total energy input is:

$$q_H = h_5 - h_4 = 1198 - 301 = 897 \text{ Btu/lbm} \quad (2086 \text{ kJ/kg})$$

The cycle thermal efficiency is, therefore,

$$\eta_{th} = (w_t - w_p) / q_H = (352.4 - 2.69) / 897 = 0.389.$$

This is an improvement of over 6%. To maximize thermal efficiency, we can find an optimum pressure for the FWH by trial as discussed later in this chapter. There is an initial investment for the reheat and regenerative modifications that will be recovered due to higher efficiency. Also note that w_n has dropped 14% from 408.7 to 349.7 Btu/lbm.

Regenerative Cycle with Closed Feedwater Heater

In general, steam power plants use closed feedwater heaters, as shown in Figure II.2.7. To determine the fraction of steam extraction from turbine to be used in the feedwater heater, we use an energy balance written for the feedwater heater to obtain:

$$y = \frac{(h_3 - h_2)}{(h_5 - h_7)}$$

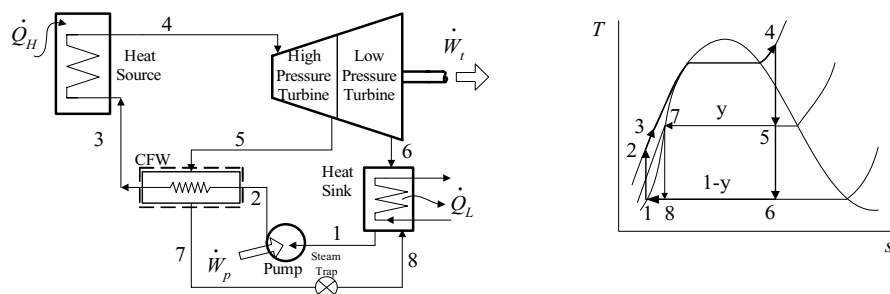


Figure I Ib.2.7. Regenerative-modified Rankine cycle. Closed feedwater heater

The calculation procedure is similar to that of the open feedwater heater as shown in the next example.

Example I Ib.2.6. In Example I Ib.2.5, we use a closed feedwater heater and steam extraction to heat up the feedwater. The extraction steam enters the FWH at 80 psia (0.55 MPa), find thermal efficiency.

Solution: We first find the relevant thermodynamics properties at the given pressures.

P (psia)	T (F)	v_f (ft ³ /lbm)	h_f (Btu/lbm)	h_g (Btu/lbm)	s_f (Btu/lbm·F)	s_g (Btu/lbm·F)
1.000	101.74	0.016136	69.730	1105.8	0.1326	1.9781
80.0	312.04	0.017573	282.10	1183.0	0.4534	1.6208
850.0	525.24	0.021500	518.40	1198.0	—	1.4096

To find steam quality at state 5, we use $s_5 = s_4$ (unlike Figure II.9.7, here steam entering the turbine is saturated), hence:

$$1.4096 = 0.4534 + x_5 (1.6208 - 0.4534)$$

From here, $x_5 = 0.82$ and $h_5 = 282.1 + 0.82(1183.0 - 282.1) = 1020$ Btu/lbm. The energy used in the condensate pump, which delivers the condensate to the FWH is $w_p = 2.54$ Btu/lbm. Hence, $h_2 = 72.27$ Btu/lbm. To find the fraction of steam used as steam extraction we ignore the temperature difference and assume that $T_3 \approx T_5 = 312.04$ F. Having $P = 850$ psia and $T = 312.04$, $h_3 \approx 283.5$ Btu/lbm. Hence

$$y = (283.5 - 72.27)/(1020 - 282.1) = 0.286$$

Turbine work is found from $w_t = (h_4 - h_5) + (1 - y)(h_5 - h_6) = (1198 - 1020) + 0.714(1020 - 786.7) = 344.5$ Btu/lbm. Also $q_H = h_4 - h_3 = 1198 - 283.5 = 914.5$ Btu/lbm. Hence, $\eta_{th} = (344.4 - 2.54)/914.5 = 0.374$

Regenerative Cycle with Moisture Separation

Steam cycles generally employ a moisture separator for steam extraction from the high-pressure turbine, as shown in Figure IIb.2.8. This would introduce dry, saturated steam to the next stage of the turbine. This also reduces the moisture content of steam at the last stage of the low-pressure turbine. For given P_H , P_M , P_L , and h_5 , we can design the cycle if either state 3 is specified or y is given. Note that h_6 is obtained from the isentropic expansion in the high pressure turbine ($s_6 = s_5$) and the first law of thermodynamics written for the moisture separator. Next, we find h_3 or y from an energy balance written for the open feedwater heater:

$$\dot{m}_f h_A + y \dot{m}_g h_7 + (1 - y) \dot{m}_g h_2 = \dot{m}_s h_3 \quad \text{IIb.2.3}$$

where we assumed perfect mixing in the open feedwater heater. Subscripts f and g stand for saturated water and steam flowing out of the moisture separator, respectively. Subscript s stands for the total steam flowing out of the heat source so that $\dot{m}_f + \dot{m}_g = \dot{m}_s$, $\dot{m}_f = (1 - x_6) \dot{m}_s$ and $\dot{m}_g = x_6 \dot{m}_s$.

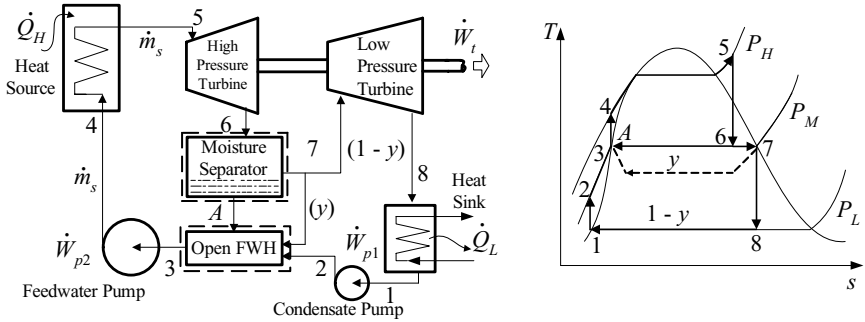
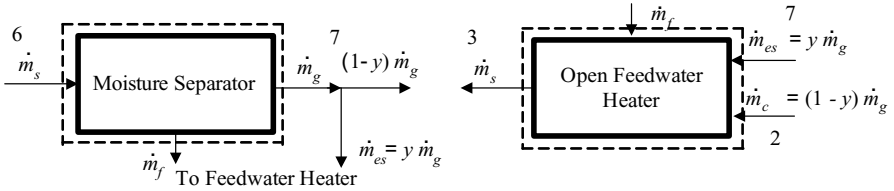


Figure IIb.2.8. A regenerative-modified ideal Rankine cycle with moisture separator



We find h_3 from Equation IIb.2.3 for given y or solve for y if state 3 is specified. If y is given, h_3 is found from Equation IIb.2.3 as $h_3 = x_6 h_A + x_6 y h_7 + x_6 (1 - y) h_2$. If h_3 is given, for example, state 3 is saturated water at pressure P_M (i.e., $h_3 = h_A$ on Figure IIb.2.8) then y is found from Equation IIb.2.3 as:

$$y = (h_3 - h_2) / (h_7 - h_2) \quad \text{IIb.2.4}$$

Example I Ib.2.7. Saturated steam enters a turbine at 1125 psia (7.75 MPa). Heat is rejected in the condenser at 1 psia (6.895 kPa). Find η_{th} for a regenerative cycle using a moisture separator and an open feedwater heater at 50 psia (0.34 MPa). In this case, water leaving the feedwater heater is saturated ($h_3 = h_A$).

Solution: We first find the relevant thermodynamic properties at the given pressures.

P (psia)	v_f (ft ³ /lbm)	h_f (Btu/lbm)	h_g (Btu/lbm)	s_f (Btu/lbm·F)	s_g (Btu/lbm·F)
1.000	0.016136	69.730	1105.8	0.1326	1.9781
50.00	0.017274	250.20	1174.1	0.4112	1.6586
1125.	—	—	1188.0	—	1.37655

We now find the unknown enthalpies in successive steps as follows:

$$w_{p1} = v_f(T) \Delta P_{pump} = 0.016136 \times (50 - 1) \times (144 / 778) = 0.146 \text{ Btu/lbm} \quad (0.34 \text{ kJ/kg})$$

$$h_2 = 69.73 + 0.146 = 69.88 \text{ Btu/lbm} \quad (162.5 \text{ kJ/kg})$$

$$w_{p2} = v_f(T) \Delta P_{pump} = 0.017274 \times (1125 - 50) \times (144 / 778) = 3.44 \text{ Btu/lbm} \quad (8 \text{ kJ/kg})$$

$$h_4 = 250.2 + 3.437 = 253.64 \text{ Btu/lbm} \quad (590 \text{ kJ/kg})$$

$$x_6 = (1.37655 - 0.4112) / (1.6586 - .4112) = 0.774$$

$$h_6 = 250.2 + 0.774(1174.1 - 250.2) = 965.2 \text{ Btu/lbm} \quad (2245 \text{ kJ/kg})$$

$$x_8 = (1.6586 - 0.1326) / (1.9781 - .1326) = 0.827$$

$$h_8 = 69.73 + 0.827(1105.8 - 69.73) = 926.43 \text{ Btu/lbm} \quad (2155 \text{ kJ/kg})$$

Having h_3 , we now find the fraction of the total steam used as extraction steam from Equation I Ib.2.4: $y = (250.2 - 69.88) / (1174.1 - 69.88) = 0.163$

Having all enthalpies and the steam extraction fraction, we can calculate the pump work, the turbine work, the net work, the heat addition, and thermal efficiency in successive steps as follows:

$$w_p = (\dot{W}_{p1} + \dot{W}_{p2}) / \dot{m}_s = x_6(1 - y)w_{p1} + w_{p2} = 0.774 \times (1 - 0.163) \times 0.146 + 3.44 = 3.53 \text{ Btu/lbm} \quad (8.2 \text{ kJ/kg})$$

$$w_t = (h_5 - h_6) + x(1 - y)(h_7 - h_8) = (1188 - 965.2) + 0.774(1 - 0.163)(1174.1 - 926.43) = 383.25 \quad (891 \text{ kJ/kg})$$

$$w_n = w_t - w_p = 383.25 - 3.53 = 379.72 \text{ Btu/lbm} \quad (883 \text{ kJ/kg})$$

$$q_H = h_5 - h_4 = 1188 - 253.64 = 934.36 \text{ Btu/lbm} \quad (2173 \text{ kJ/kg})$$

$$\eta_{th} = 379.72 / 934.36 = 0.406$$

Selection of pressure at which a feedwater heater is operating is not arbitrary. As shown in Figure I Ib.2.10, a regenerative-modified Rankine cycle using an open FWH and a moisture separator while operating between $P_H = 1000$ psia, and $P_L = 1$ psia, has a maximum thermal efficiency at a FWH pressure of about 100 psia.

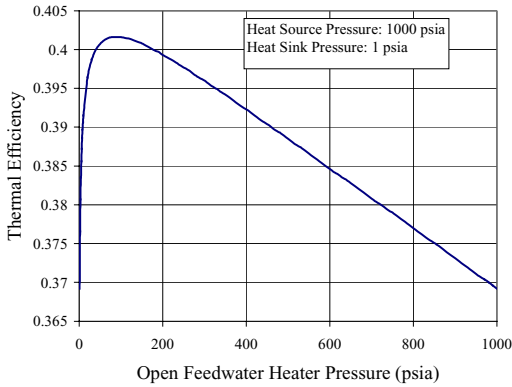


Figure Iib.2.9. Effect of the FWH pressure (P_M) on thermal efficiency

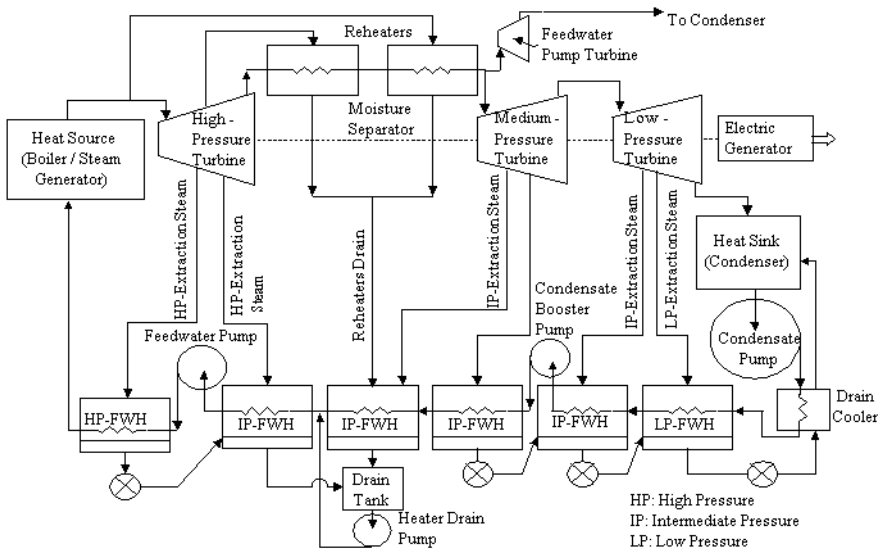


Figure Iib.2.10. A steam power plant utilizing multiple feedwater heaters

In steam power plants, several stages of feedwater heaters operating at various pressures (Figure Iib.2.10) are used. This requires at least four sets of pumps including the condensate pump, the condensate booster pump, the heater drain pump, and the feedwater pump. The condensate pump takes suction from the condenser and delivers water to the first stage of the low pressure FWHs via an external drain cooler. The cooler has two functions. First, it subcools the FWH drain water to prevent flashing in the drain line. Second, it preheats the incoming condensate water before being exposed to the higher energy extraction steam. The feedwater enters the first set of the low-pressure feedwater heaters (LP-FWH) after flowing through the drain cooler. The condensate booster pump takes suction

from the LP-FWH to discharge the feedwater to the intermediate-pressure feedwater heaters. Finally, the feedwater pump delivers water through the high-pressure feedwater heater (HP-FWH) to the heat source. The condensed steam in the secondary side of the IP-FWH and HP-FWH is collected in the *heater drain tank* to be pumped into the feedwater line by the *heater drain pump* also known as the *drip pump*.

In steam power plants, thermal hydraulic loads are generally divided between sets of pumps, coolers, and feedwater heaters to facilitate maintenance and increase system reliability. As shown in Figure I Ib.2.11, three condensate pumps, three feedwater booster pumps, and two feedwater pumps are used to deliver water through 3 coolers and 14 feedwater heaters.

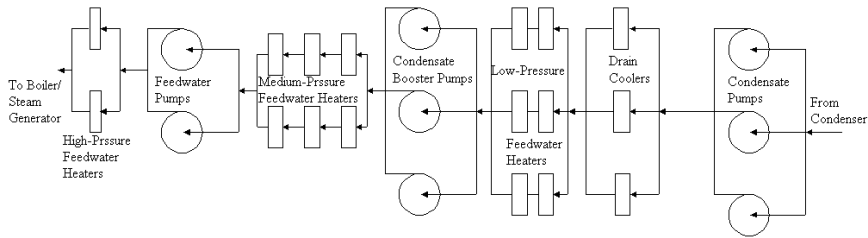


Figure I Ib.2.11. Schematics of a typical steam plant feedwater

3. Actual Versus Ideal Cycles

In the discussion about the vapor and the gas power cycles, we assumed ideal conditions for the involved processes. For example, in the steam power cycles we used the same pressure and temperature for the steam entering the turbine as that leaving the heat source. In reality however, there are pipelines carrying steam from the heat source to the turbine. This is associated with some heat loss even though the pipe is well insulated. Additionally, the flow of steam in the pipe causes a frictional pressure drop. Such non-isentropic effects would adversely affect thermal efficiency.

3.1. Losses in Mechanical Components

In the discussion below, we consider non-isentropic conditions, which result in losses in pipes, turbines, pumps/compressors, and nozzles. In this discussion we consider a steam power plant that utilizes the Rankine cycle as shown in Figure I Ib.3.1. We first consider the pump and turbine losses, then losses in the piping and the condenser.

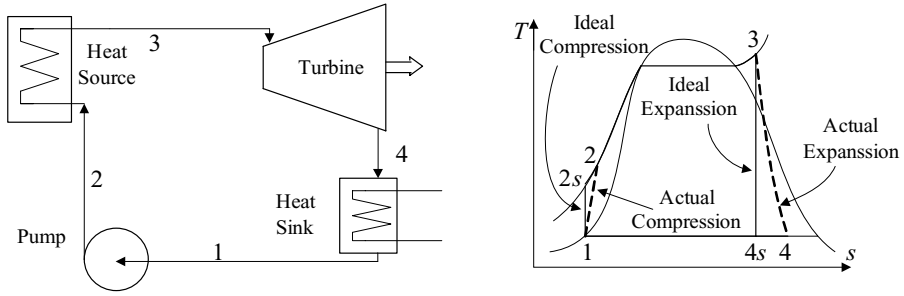


Figure IIb.3.1. Losses associated with pump and turbine

Pump losses are primarily associated with the irreversibilities due to friction between the flow of water and the interior pump surfaces. As shown in Figure IIb.3.1, if the compression process was isentropic, the state at the pump exit would have been $2s$. However, irreversibilities cause entropy to increase and the actual state is 2. To facilitate analysis, we calculate work delivered to the pump by multiplying the isentropic work by the pump efficiency, a value smaller than unity:

$$w_p = w_{ps}\eta_p = h_2 - h_1 = (h_{2s} - h_1)\eta_p$$

Turbine losses are similar to the pump losses and are primarily associated with irreversibilities due to the friction between the flow of steam and the interior turbine surfaces such as the stationary and moving turbine blades. Since there are some heat losses to the environment, the expansion process is non-adiabatic. As shown in Figure IIb.3.1, if the expansion process was isentropic, the state at the turbine exit would have been $4s$. However, irreversibilities cause entropy to increase and the actual state is 4. Interestingly, this decreases the moisture content, which is the only helpful aspect of turbine irreversibilities. To facilitate analysis, we then calculate work obtained from the turbine by multiplying the isentropic work by turbine efficiency, being a value smaller than unity:

$$w_t = w_{ts}\eta_t = h_3 - h_4 = (h_3 - h_{4s})\eta_t$$

Losses in pipes include the losses due to friction as well the heat transfer to the surroundings. These losses are further discussed in Chapter IIIb where they are divided into two categories of *major* and *form* losses. The major loss (skin friction) accounts for friction between the working fluid and the pipe wall. Form loss accounts for the existence of such pipe fitting as elbows, tees, reducers, and valves.

Effects of pipe, pump, and turbine losses on the ideal Rankine cycle are shown in Figure IIb.3.2. Water is first pumped from the condenser to the heat source. If the compression process was isentropic, the state of fluid at the entrance to the heat source would have been at $2s$. However, due to pump irreversibilities, the state of water at the pump discharge is 2. From point 2 to point 3, which is the heat source inlet, pressure and temperature drop due to losses in the pipe ($P_3 < P_2$).

Then water is boiled and superheated steam leaves the heat source at $P_4 = P_3$. Due to pipe losses, superheated steam enters the turbine at $T_5 < T_4$ and $P_5 < P_4$. In this discussion, we ignored losses in the heat source and the heat sink.

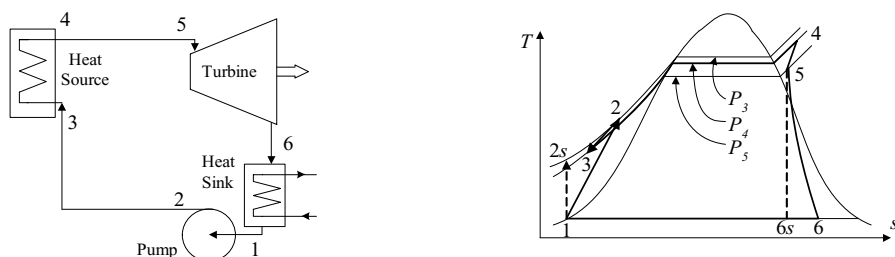
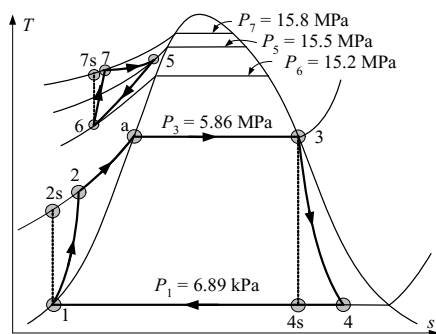
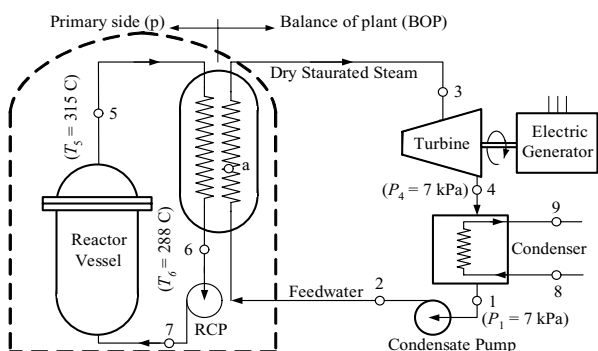


Figure I Ib.3.2. Effect of pipe, pump, and turbine losses on the ideal Rankine cycle

Example I Ib.3.1. The top figure shows the schematics of the primary side of a PWR and the Rankine cycle of the secondary side. The bottom figure shows the associated T - s diagram for both primary and secondary sides. Find a) thermal efficiency, and b) the power produced by the plant. Additional data: mass flow rate in vessel: 60E6 kg/h, $\eta_t = 0.90$, and $\eta_p = 0.85$.



Solution: The ideal cycle is solved in Example Iib.2.1 and the following enthalpies are obtained:

$$h_1 = 162.178 \text{ kJ/kg}, h_{2s} = 168 \text{ kJ/kg}, h_3 = 2785.44 \text{ kJ/kg}, \text{ and } h_{4s} = 1829.13 \text{ kJ/kg}.$$

Due to irreversibilities, the pumping power is increased and turbine work is decreased. To find the revised w_p and w_t , we use the specified isentropic efficiencies:

$$w_p = (h_{2s} - h_1)/\eta_p = (168 - 162.178)/0.85 = 6.85 \text{ kJ/kg}.$$

$$\text{We also find } h_2 = 162.178 + 6.85 = 169.03 \text{ kJ/kg}$$

$$w_t = (h_3 - h_{4s})\eta_t = (2785.44 - 1829.13) \times 0.90 = 860.68 \text{ kJ/kg}$$

$$q_H = h_3 - h_2 = 2785.44 - 169.03 = 2616.4 \text{ kJ/kg}$$

a) We find $\eta_{th} = (w_t - w_p)/q_H = (860.68 - 6.85)/2616.4 = 32.6\%$ (versus 36.3 in Example Iib.2.1)

b) To find the power produced, we use an energy balance in the steam generator:

$$\dot{m}_p(h_5 - h_6) = \dot{m}_s(h_3 - h_2).$$

We need h_5 and h_6 . These are found as $h_5(15.5 \text{ MPa} \ \& \ 315 \text{ C}) = 1421.94 \text{ kJ/kg}$ and $h_6(15.2 \text{ MPa} \ \& \ 288 \text{ C}) = 1273.24 \text{ kJ/kg}$. Therefore,

$$\dot{m}_s = 60\text{E}6 \times (1421.94 - 1273.24)/2616.4 = 3.41\text{E}6 \text{ kg/h}.$$

$$\dot{W} = 3.41\text{E}6 \times (860.68 - 6.85) = 808.7 \text{ MW}$$

QUESTIONS

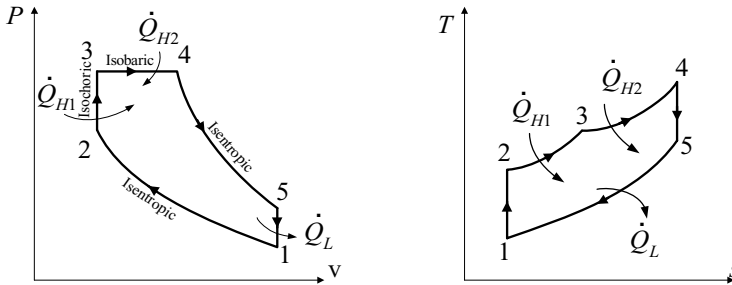
- Would a machine gun be considered an internal combustion or an external combustion engine?
- In an automotive engine, what are the BDC and TDC?
- Is the Wankel engine a reciprocating engine?
- In an internal combustion engine, where is the position of the piston during the rejection process?
- What is the key advantage of a gas turbine over traditional piston-cylinder engine for aviation?
- What is compression ratio?
- During which process in an Otto cycle does heat rejection take place?
- During which process in a Diesel cycle does heat addition take process?
- What is the ultimate heat sink for an automotive engine?
- Why does an increase in heat source pressure of an ideal Rankine cycle increase the cycle thermal efficiency? Assume heat sink pressure and steam temperature are held constant.
- What is the major difference between the Ericsson and the Stirling cycles?
- What is the advantage of an intercooler in a gas turbine?
- By the use of what processes can we approach the Stirling and Ericsson cycles?
- During which process does heat addition take place in a Rankine cycle?
- Why should dry steam enter a turbine?

- What is a reheat-modified Rankine cycle?
- What is a regenerative-modified Rankine cycle?
- What is a moisture separator?
- Explain the effect of feedwater heater pressure on cycle thermal efficiency in a regenerative modified ideal Rankine engine which also uses a moisture separator.

PROBLEMS

1. Consider two cycles. One cycle for a gas turbine and the other cycle for a vapor power plant. Assume that the two cycles have the same power output from the turbine per unit mass flow rate (\dot{W}_t / \dot{m}). Compare the compression work per unit mass flow rate of the gas turbine cycle (\dot{W}_c / \dot{m}) with that of the vapor power cycle (\dot{W}_p / \dot{m}). What conclusion do you reach? Explain the result.
2. An air standard Otto cycle operates at a compression ratio of 4 and a pressure ratio (P_3/P_2) of 4. Find the cycle thermal efficiency for $P_1 = 1$ bar and $T_1 = 320$ K.
3. The compression and the pressure ratios of an Otto cycle are both equal to 4. Air enters the engine at 1 bar and 320 K. Find all pressures and temperatures of this cycle. [Ans.: $P_2 = 7.4$ bar, $P_3 = 29.6$ bar, $P_4 = 4.2$ bar, $T_2 = 592$ K, $T_3 = 368$ K, $T_4 = 1340$ K].
4. An air standard diesel cycle has an efficiency of 0.58 and a compression ratio of 17. Determine pressures and temperatures of the cycle at the conclusion of each process. Pressure and temperature at the start of the compression process are 0.1 MPa and 16 C, respectively. [Ans.: $P_2 = 765.6$ Psia, $P_4 = 67.23$ psia, $T_2 = 1615$ R, $T_3 = 4830$ F, $T_4 = 2411$ R.]
5. An air standard Diesel cycle operates at a compression ratio of 20 and a cutoff ratio of 2. Find the cycle thermal efficiency for $P_1 = 1$ bar and $T_1 = 320$ K.
6. An air standard diesel cycle has a compression ratio of 20 and an isobaric expansion ratio (V_3/V_2) of 2. Pressure and temperature at the start of the compression process are $P_1 = 1$ bar and $T_1 = 350$ K. Find the cycle thermal efficiency. Compare the result with the Carnot efficiency. [Ans.: $\eta = 64.8\%$]
7. Given the same compression ratio for both air standard Otto and air standard Diesel cycle, which cycle has higher thermal efficiency? Answer the same question this time for the Otto cycle versus the Brayton cycle.
8. In this problem we are asked to perform a parametric study for thermal efficiency of an air standard Diesel cycle as a function of the cutoff ratio, r_c , and the compression ratio, r . Use Equation Iib.1.7 and plot thermal efficiency for $r_c = 0.5, 1, 2, 4, 6$, and 8 while the compression ratio is held constant at $r = 10$. Repeat this for $r = 12, 15, 17$, and 20. What conclusion can be reached from this plot? [Ans.: Thermal efficiency increases as r increases and decreases as r_c increases.]

9. Consider the dual cycle shown in the figure. Find thermal efficiency in terms of γ , r , r_P , and r_c . Where $\gamma = c_p/c_v$, $r_V = V_1/V_2$, $r_P = P_3/P_2$, and $r_c = V_4/V_3$.



$$[\text{Ans.: } \eta_{th} = 1 - \frac{r_P r_c^\gamma - 1}{[(r_P - 1) + \gamma r_P (r_c - 1)]} \frac{1}{r_V^{\gamma-1}}].$$

10. Use the following information for a dual cycle internal combustion engine and find a) the state parameters (P & T) at stages 1 through 5 shown in the Problem 9 figure, b) the expansion work, c) the compression work, d) the net cycle work, and the cycle efficiency. Data: $P_1 = 1$ bar, $T_1 = 300$ K, $r_V = 12.7$, $r_P = P_3/P_2 = 1.4$, and $r_c = 1.6$, the working fluid is air ($c_v = 0.72$ kJ/kg·C, $c_p = 1.01$ kJ/kg·C, $R = 287$ J/kg·C, $\gamma = 1.4$). [Ans.: $P_2 = 35$ bar, $P_3 = 49$ bar, $P_4 = 49$ bar, $P_5 = 2.7$ bar, $T_2 = 555$ C, $T_3 = 887$ C, $T_4 = 1585$ C, $T_5 = 535$ C)].

11. Find thermal efficiency of an air standard Brayton cycle with the ratio $T_4/T_3 = 0.45$. [Ans.: 55%]

12. Air enters an ideal gas turbine cycle at 1 bar and 27 C. The maximum temperature in the cycle is 727 C. Find the cycle efficiency for a compression ratio of 10. [Ans.: 0.482].

13. Air enters the compressor of an air standard Brayton cycle at 27 C and 0.1 MPa. The cycle pressure and temperature ratios are given as $r_P = 11$ and $r_T = 4$, respectively. Find a) pressure and temperature at the end of each process, b) thermal efficiency, c) work per unit mass, d) cycle pressure ratio for optimum work, and e) the required mass flow rate to produce 1 MW power.

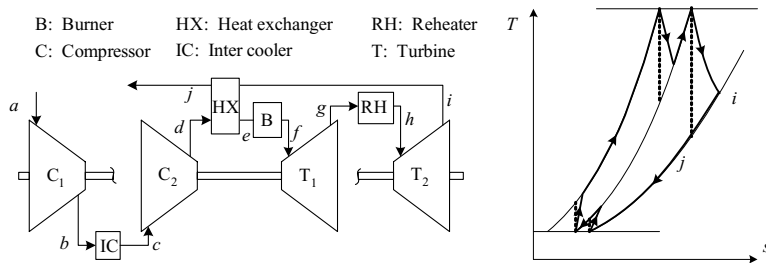
14. Air enters the compressor of an air standard Brayton cycle at 70 F and 14.7 psia. The cycle pressure ratio is $r_P = 11$ and the temperature ratio is such that the net work produced by the cycle corresponds to the maximum net work. Find a) pressure and temperature at the end of each process, b) thermal efficiency, and c) the required mass flow rate to produce 300 horsepower.

15. To improve thermal efficiency, a gas turbine uses a two-stage compression and one intercooler. Assume ideal processes and isentropic compression to show that the compressor work is at a minimum when the two compressors have identical compression ratios. Gas enters both compressors at the same temperature.

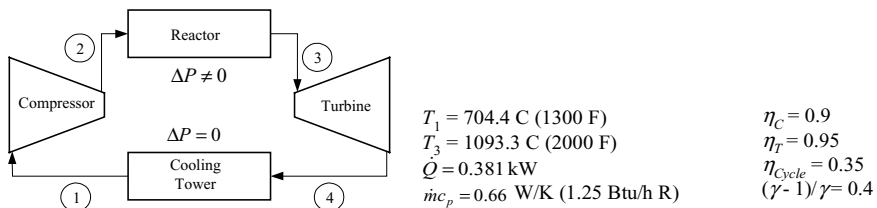
16. In a steam power plant, saturated steam at a pressure of 400 psia enters the turbine. The condenser pressure is atmospheric. Find the ideal Rankine cycle and the maximum thermal efficiency. [Ans.: 23% and 26%].

17. Derive a relation for the optimum r_p of a gas turbine operating on a Brayton cycle having the turbine and the compressor efficiencies of η_t and η_c , respectively.
[Ans.: $r_p = (\eta_c \eta_t r_T)^\beta$ where $\beta = \gamma/2(\gamma - 1)$].

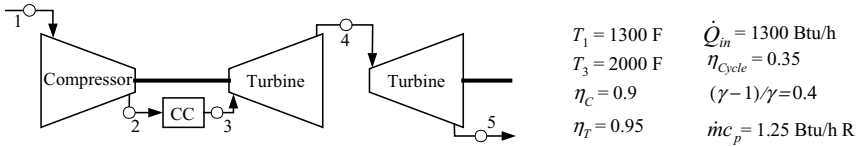
18. A gas turbine power plant consisting of high pressure (HP) and low pressure (LP) compressors and turbines is shown in the figure. The HP and LP turbines drive the HP and LP compressors, respectively. a) Place letters “a” through “j” on the accompanying T - s diagram and b) use the given data to find the net work and the cycle thermal efficiency. Data: $T_a = 20^\circ\text{C}$, $T_f = 850^\circ\text{C}$, $(r_p)_{\text{C1}} = (r_p)_{\text{C2}} = 4$, $\eta_c = 80\%$, $\eta_t = 85\%$, and the heat exchanger effectiveness is 75%.



19. In the Brayton cycle shown in the figure, pressure drop at the heat sink is negligible hence, $r_C \neq r_T$. a) Draw the T - s diagram and explicitly show the differences between the pressure levels of states 1 and 3. b) Use the given data to find r_C and r_T , assuming the working fluid is an ideal gas.

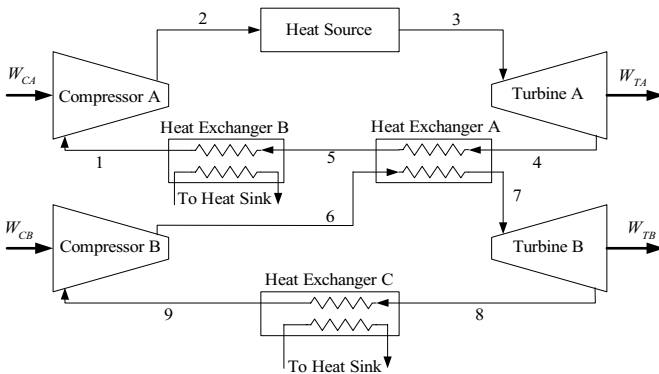


20. Air enters the compressor of a helicopter engine. The pressurized air is then delivered to the combustion chamber (CC). High energy mixtures then enter the first turbine, referred to as the *gas generator* and then the second turbine, referred to as the *power turbine*. Use the data given and find the power produced by the system in the following two cases: a) assume all the processes are ideal and b) assume the compressor and the turbine efficiencies are 90% and 85%, respectively.



21. Two ideal Brayton cycles are shown in the Figure. The working fluid is cooled in Heat Exchanger A prior to entering the heat sink (Heat Exchanger B). Heat Exchanger A is the heat source for a simple Brayton cycle. a) Draw the T - s diagram for this combined cycle, b) find the pressure ratio of turbine B, which maximizes the cycle thermal efficiency, and c) find the cycle thermal efficiency.

Data: $T_1 = T_9 = 5 \text{ C}$, $T_3 = 700 \text{ C}$, $T_4 - T_7 = 15 \text{ C}$, $P_2 = 4P_1$, $c_p = 5.23 \text{ kJ/kg}$, $\gamma = 1.658$. $\dot{m}_2 = 2\dot{m}_6$. The working fluid in both cycles is the same.



22. In a steam power plant, saturated steam at a pressure of 400 psia enters the turbine. The condenser pressure is 1 psia. Find the ideal Rankine cycle and the maximum thermal efficiency. [Ans: 33% and 38%]

23. Saturated steam in a Rankine cycle enters the turbine at 850 psia and leaves the condenser at 3.5 inches of Mercury (in Hg). Find: a) thermal efficiency of the cycle, b) power obtained from the turbine for steam mass flow rate of 11E6 lbm/hr. [Ans.: a) 34.8%, b) 1246 MW]

24. Superheated steam at a pressure of 4 MPa and a temperature of 350 C leaves the heat source and enters the turbine. The heat sink is at a pressure of 10 kPa. Calculate net work produced by the cycle and the cycle efficiency.

25. In Example IIb.2.1, we use an open FWH in conjunction with some extraction steam to heat up the feedwater. For the FWH operating at 250 psia, find the revised thermal efficiency and compare your calculated value with the results obtained in Example IIb.2.5. [Ans.: 0.385]

26. Saturated steam enters a turbine at 1000 psia. Heat is rejected in the condenser at 1 psia. Find thermal efficiency for a regenerative cycle, using a moisture separator and an open feedwater heater at 200 psia. Also find the steam extraction fraction, total pump work, and total turbine work. [Ans.: $\eta = 0.399$, $y = 0.2528$, $w_p = -3.098$ Btu/lbm, $w_t = 336.39$ Btu/lbm,]

27. In a Rankine cycle, dry saturated steam ($x = 100\%$), enters the turbine at 8 MPa and saturated liquid ($x = 0\%$) leaves the condenser at 0.008 MPa. Net power produced by this cycle is 100 MW. Find the turbine work, the cycle mass flow rate, the rate of heat transfer to the cycle, the rate of heat removal from the cycle, and thermal efficiency. [Ans.: $\eta_{th} = 37.1\%$ and mass flow rate = $3.77E5$ kg/h].

28. Perform a parametric study for a steam power plant operating between pressures of 7 MPa and 7 kPa on an ideal Rankine cycle. Use feedwater heater pressure as the variable. Produce plots similar to Figure I Ib.2.3 for such parameters as fraction of the steam extraction, pump work, and turbine work.

29. Consider the secondary side of a simplified PWR plant consisting only of the steam generator, turbine, condenser, and the feedwater pump. This plant is operating in an ideal Rankine cycle and producing dry saturated steam at a rate of $5.674E6$ kg/h and at a pressure of 7 MPa. A two-phase mixture leaves turbine and enters the condenser at 0.0075 MPa. The feedwater pump demands 9.4 kJ/kg at steady state to pump water from the condenser to the steam generator. A river flowing adjacent to the plant provides the cooling water to the condenser. According to regulations, the rise in the temperature of the river water exiting the plant must not exceed 8 C. Find a) plant thermal efficiency, b) maximum efficiency, and c) the flow rate of the circulating water through the condenser tubes. [Ans.: 36.7%, 43.9%, and $9.3E8$ kg/h].

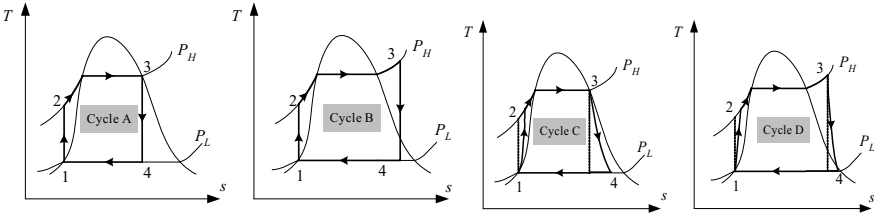
30. Superheated steam leaves the boiler of an ideal regenerative cycle at 600 psia and 800 F. Pressure in the feedwater heater and in the condenser is 60 psia and 1 psia, respectively. Find η_{th} . [Ans.: 39.1%].

31. Consider an air standard Otto cycle. The compression ratio is 8. At the beginning of the compression stroke, pressure is at 14.7 psia and 60 F. The heat transfer to the air per cycle is 800 Btu/lbm. Find the cycle thermal efficiency. [Ans.: $\eta_{th} = 56\%$].

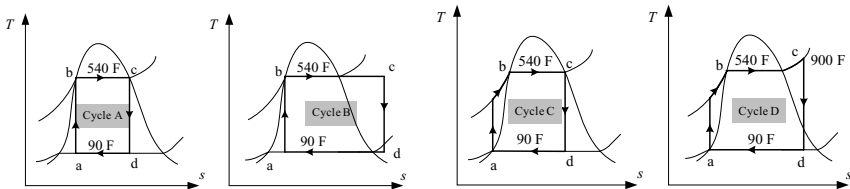
32. In a hypothetical 350 MWe nuclear power plant, cold water enters the reactor, steam leaves the reactor to enter the turbine, and the hot water from the turbine is returned to a nearby lake. Use the given data to find a) the temperature of the water at the inlet and outlet of the core, b) the maximum available work, c) the governing equation for the lake water temperature while ignoring any heat transfer by evaporation, and d) the plant lifetime based on the lake water temperature not exceeding 60 F.

Data: reactor power = 350 MWe, thermal efficiency = 0.333, temperature of water leaving the plant = 150 F, water mass flow rate = $1E4$ lbm/s, lake water volume = $1E12$ ft³, lowest water temperature = 50 F.

33. For the ideal Rankine cycles shown in the figure, find the minimum number of properties that we need to know in order to solve for the rest of unknowns such as pressures, temperatures, net work, and thermal efficiency. [Ans.: For cycle A we need, P_H and P_L . For Cycle D, we need P_H , P_L , T_3 , η_{turbine} , and η_{pump}].



34. Four designs for a steam power plant are shown in the figure. a) Find the heat supplied, the heat rejected, the net work, and the cycle thermodynamic efficiency for each design. b) Compare the results and comment on the advantage of each design.



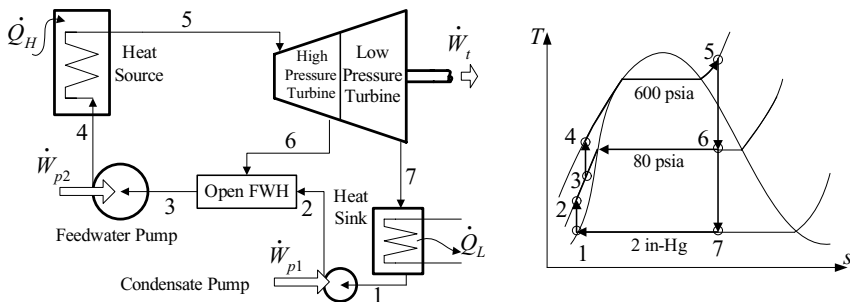
35. Find the efficiency of an ideal Rankine cycle using a steam temperature of 500 C and a condenser pressure of 0.1 bar. Try three steam pressures of 20 bar, 50 bar, and 100 bar. [Ans.: 34%, 38%, and 40%].

36. Find the efficiency of an ideal Rankine cycle in which superheated steam enters the turbine at 773 K and 40 bar. Try three condenser pressures of 2 bar, 0.5 bar, and 0.05 bar. [Ans.: 0.25, 0.31, and 0.38].

37. In a Rankine cycle, steam enters the turbine at 160 bar and 823 K. Pressure in the condenser is 0.05 bar. Find the cycle efficiency for the following isentropic efficiencies; $\eta_{\text{turbine}} = 0.88$, $\eta_{\text{pump}} = 0.9$.

38. In a regenerative modified Rankine cycle (Figure Iib.2.5), steam leaves the boiler and enters the turbine at 8 MPa and 753 K. Pressure in the open feedwater heater and the condenser are 0.7 MPa and 0.008 MPa, respectively. Water entering the feedwater pump is saturated. Each turbine has an isentropic efficiency of 0.85. a) Find the plant thermal efficiency, b) given a steam mass flow rate of 1E5 kg/h, find the net power.

39. A regenerative-modified Rankine cycle with moisture separator is shown in the figure. Use the given data in the figure to find the net cycle efficiency. Ignore the pump work.



40. Saturated steam at 1000 psia enters the high pressure turbine of an ideal regenerative Rankine cycle. The cycle is equipped with a moisture separator, delivering saturated water to an open feedwater heater at 100 psia. Saturated steam from the feedwater heater enters the low pressure turbine. Pressure in the condenser is 1 psia. The condensate leaving the open feedwater heater is saturated water. Draw the cycle schematic and the corresponding T - s diagram. Find a) the cycle thermal efficiency, b) the work per unit mass flow rate of water consumed by the condensate pump, c) the work per unit mass flow rate of water consumed by the feedwater pump, d) the work per unit mass flow rate of water produced by the high pressure turbine, e) the work per unit mass flow rate of water produced by the low pressure turbine, f) the heat per unit mass flow rate of water delivered to the heat source, and g) the fraction of steam used as the extracted steam in the open feedwater heater. [Ans.: 40.2%, 0.2 Btu/lbm, 3 Btu/lbm, 172.6 Btu/lbm, 188.6 Btu/lbm, 891.4 Btu/lbm, 20.5%].

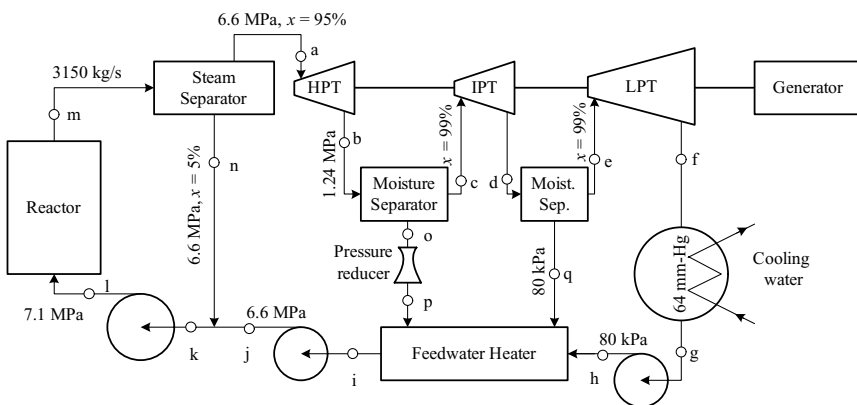
41. Superheated steam at 7.585 MPa (1100 psia) and 616.3 K (650 F) enters the high pressure turbine of an ideal regenerative Rankine cycle. The cycle is equipped with a moisture separator, delivering saturated water to an open feedwater heater at 0.689 MPa (100 psia). Saturated steam from the feedwater heater enters the low pressure turbine. Pressure in the condenser is 7 kPa (1 psia). The condensate leaving the open feedwater heater is saturated water. Find a) the cycle thermal efficiency, b) the work per unit mass flow rate of water consumed by the condensate pump, c) the work per unit mass flow rate of water consumed by the feedwater pump, d) the work per unit mass flow rate of water produced by the high pressure turbine, e) the work per unit mass flow rate of water produced by the low pressure turbine, f) the heat per unit mass flow rate of water delivered to the heat source, and g) the fraction of steam used as the extracted steam in the open feedwater heater. [Ans.: 41.1%, 0.465 kJ/kg, 7 kJ/kg, 469 kJ/kg, 474.7 kJ/kg, 2278.7 kJ/kg, 20.5%].

42. Saturated steam at 7.585 MPa (1100 psia) and 616.3 K (650 F) enters the high pressure turbine of an ideal regenerative Rankine cycle. The cycle is equipped

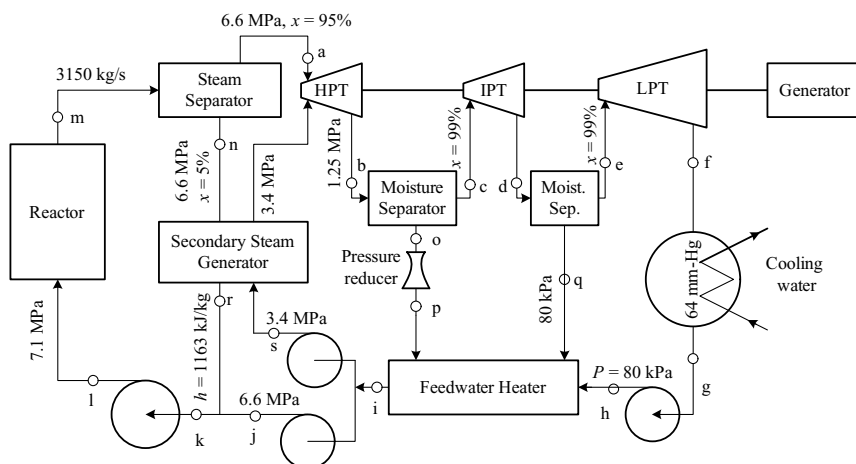
with a moisture separator, delivering saturated water to an open feedwater heater at 0.689 MPa (100 psia). Only 18% of the steam leaving the moisture separator is used in an open feedwater heater. Pressure in the condenser is 7 kPa (1 psia). Find a) the cycle thermal efficiency, b) the work per unit mass flow rate of water consumed by the condensate pump, c) the work per unit mass flow rate of water consumed by the feedwater pump, d) the work per unit mass flow rate of water produced by the high pressure turbine, e) the work per unit mass flow rate of water produced by the low pressure turbine, f) the heat per unit mass flow rate of water delivered to the heat source, and g) the enthalpy of water leaving the open feedwater heater. [Ans.: 39.3%, 0.465 kJ/kg, 62.8 kJ/kg, 469 kJ/kg, 489.4 kJ/kg, 2278.7 kJ/kg, 638.2 kJ/kg].

43. Solve problem 41 assuming an isentropic efficiency of 85% for each pump and 90% for each turbine. [Ans.: 35%, 0.697 kJ/kg, 63.96 kJ/kg, 422.15 kJ/kg, 440.3 kJ/kg, 2277.52 kJ/kg, 640.8 kJ/kg].

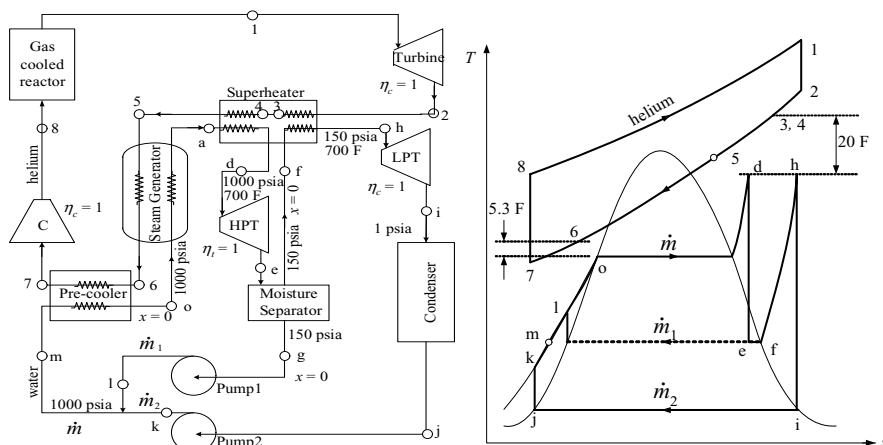
44. The schematic diagrams of two suggested designs for a boiling water reactor are shown in the figures. One uses a direct cycle and the other a dual cycle. The outlet conditions for both designs are the same. In both designs, steam leaves the steam separator assembly with a quality of 95% to enter the high pressure turbine (HPT) while the saturated liquid with 95 weight percent being recirculated to the reactor. The vapor is expanded successively in the HPT, the intermediate pressure turbine (IPT), and the low pressure turbine (LPT) before entering the condenser being at a 64 mm-Hg. Moisture separators between the HPT and IPT and between the IPT and LPT reduce the steam moisture to 1%; the separated liquid is used to heat the feedwater in an open feedwater heater. The heated condensate and the recirculated water from the steam separator are pumped through the reactor. Assume 100% efficiency in all pumps, and neglect pressure losses in the moisture separators. Take all turbine efficiencies as 75%.



In the dual cycle design, an additional steam generator is used. The 6.6 MPa saturated liquid from the steam separator produces saturated steam at 3.4 MPa in the secondary steam generator, its enthalpy being reduced to 1163 kJ/kg. The 3.4 MPa steam is introduced to the HPT at the appropriate stage with perfect mixing. Sketch the T - s diagram for the direct and dual cycles.



45. A combined Brayton – Rankine cycle is shown in the figure. Calculate a) all the flow rates shown in the diagram, b) all terms that are required to find the cycle thermal efficiency. Note the relative temperature relations; $T_6 = T_o + 5.3$ F, $T_4 = T_d + 20$ F.



IIC. Mixtures

Thermodynamic systems often include more than one component. For example, the combustion of fossil fuels results in a mixture product of several gases. Also the analyses of a PWR pressurizer and nuclear plant containment require consideration of such non-condensable gases as air in contact with water vapor. In this chapter we first study the fundamental relations related to mixtures and then apply these relations to the analysis of such interesting topics as conditioning a mixture of moist air, response of pressure suppression systems to pressurization, and the operation of cooling towers. We also study the pressure and temperature of a PWR containment following such events as the rupture of pipes carrying high energy fluids inside the containment.

Gas mixtures can be divided into two major categories: non-reactive and reactive gases. Moist air on a humid day is an example of non-reactive gases and a combustible mixture in the cylinder of an internal combustion engine is an example of the reactive gases. The non-reactive gases can be further divided into two categories: mixture of real gases and mixture of ideal gases. Air, for example, may be considered as a mixture of ideal gases. In this chapter we deal only with the mixture of non-reactive ideal gases.

1. Mixture of Non-reactive Ideal Gases

Dry air is a good example of a mixture of non-reactive ideal gases. The mole fraction of each component of dry air is shown in Table IIC.1.1.

Table IIC.1.1. Composition of dry air

Component	Mole Fraction (%)
Nitrogen	78.08
Oxygen	20.95
Argon	0.93
Carbon Dioxide	0.03
Neon, Helium, Methane, etc.	0.01

Due to the importance of air in industrial applications, air properties are identified and tabulated at various pressures and temperatures. However, in general, where various gases at various mole fractions may mix, we must find an easier way to represent the property of the mixture of gases. That is to say that we must use the properties of the pure substances that constitute the mixture and find equivalent properties as if the mixture itself is a pure substance. For example, consider a system containing N non-reactive ideal gases. There are two models to find the representative properties for this system: the *Dalton* and the *Amagat* models. Regardless of the model we use, the total number of moles in the system n is given as

$$n = \sum_{i=1}^N n_i \quad \text{IIC.1.1}$$

where n_i is the number of moles of component i and N is the number of components comprising the mixture.

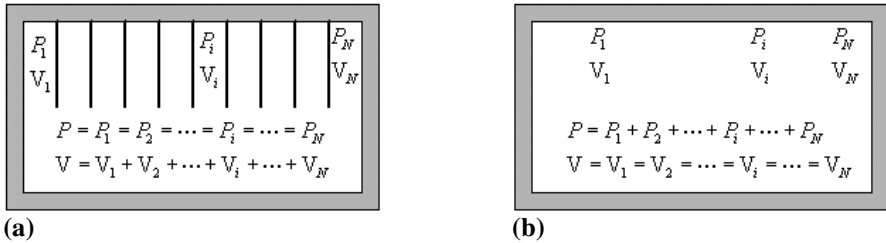


Figure IIC.1.1. (a) Amagat and (b) Dalton models for non-reactive mixture of ideal gases

Amagat Model, Equal Pressure and Temperature

Consider the system of gases shown in Figure IIC.1.1(a). In the Amagat model, all the non-reactive ideal gases are at the same pressure and temperature but at different volume so that the summation of all the volumes becomes equal to the volume of the system. This can be verified by applying the ideal gas law to each volume of gas:

$$n_i = \frac{PV_i}{R_u T}$$

and then substitute in Equation IIC.1.1, to get:

$$V = \sum_{i=1}^N V_i \quad \text{IIC.1.2}$$

See Problem 3 at the end of this section for the applicability of the Amagat model to non-ideal gases.

Dalton Model, Equal Volume and Temperature

Consider the system of gases shown in Figure IIC.1.1(b). In the Dalton model, all non-reactive ideal gases have the same volume and temperature but are at different pressure so that the summation of all pressures becomes equal to the pressure of the system. This can be verified by applying the ideal gas law to each gas:

$$n_i = \frac{P_i V}{R_u T}$$

and substitute in Equation IIc.1.1, to get:

$$P = \sum_{i=1}^N P_i \quad \text{IIc.1.3}$$

where V_i in Equations IIc.1.2, and P_i in Equation IIc.1.3 are referred to as partial volume and partial pressure, respectively. Similarly, V in Equations IIc.1.2, and P in Equation IIc.1.3 are referred to as total volume and total pressure, respectively. The Dalton model is more commonly applied to the mixture of ideal gases than the Amagat model. It is important to note that for both Amagat and Dalton models

$$T = T_1 = T_2 = \dots = T_i = \dots = T_N.$$

Example IIc.1.1. A tank having a volume of 10 m^3 is filled with nitrogen and 5 kg of carbon dioxide at a pressure and temperature of 140 kPa and 70 C, respectively. Find the partial volumes according to the Amagat model and the partial pressures according to the Dalton model.

Solution: Total volume and pressure are given. In both models, gases are at thermal equilibrium at 70 C.

a) *Amagat Model:* To find the partial volumes, we apply the ideal gas law to carbon dioxide:

$$V_{\text{CO}_2} = m \left(\frac{R_u}{M_{\text{CO}_2}} \right) \frac{T}{P} = 5 \left(\frac{8.31434}{44.01} \right) \frac{70 + 273}{140} = 2.31 \text{ m}^3$$

According to the Amagat model $V_{\text{N}_2} = V - V_{\text{CO}_2} = 10 - 2.31 = 7.69 \text{ m}^3$.

b) *Dalton Model:* We can use similar procedure to find the partial pressures from the Dalton model by applying the ideal gas law to carbon dioxide:

$$P_{\text{CO}_2} = m \left(\frac{R_u}{M_{\text{CO}_2}} \right) \frac{T}{P} = 5 \left(\frac{8.31434}{44.01} \right) \frac{70 + 273}{10} = 32.4 \text{ kPa}$$

Therefore, $P_{\text{N}_2} = P - P_{\text{CO}_2} = 140 - 32.4 = 107.6 \text{ kPa}$

Application of Dalton Model to Moist Air

The term moist air refers to a mixture of dry air, treated as a pure substance, and water vapor. Consider a volume containing moist air with n_a moles of dry air and n_v moles of water vapor at pressure P and temperature T . The total number of moles in this volume is found as

$$n = n_a + n_v$$

The mole fraction of air is given as:

$$y_a = n_a/n$$

and the mole fraction of water vapor as:

$$y_v = n_v/n$$

where subscripts a and v stand for air and water vapor, respectively. Total pressure of the moist air, partial pressure of the dry air, and partial pressure of water vapor are found as:

$$P = \frac{nR_u T}{V}, \quad P_a = \frac{n_a R_u T}{V}, \quad P_v = \frac{n_v R_u T}{V} \quad \text{IIC.1.4}$$

respectively. From these relations we conclude that $P_v = y_v P$ and $P_a = y_a P$.

Example IIC.1.2. A tank of volume 10 m^3 contains a mixture of air and superheated steam at a total pressure of 355 kPa and temperature of 100 C . The tank contains 0.05 lbmole of steam and 0.8 lbmole of air. Find the air and steam partial pressures.

Solution: Total number of moles of the mixture is $n = n_v + n_a = 0.05 + 0.8 = 0.85$. Therefore, the mole fractions of vapor and air are $y_v = 0.05/0.85 = 0.059$ and $y_a = 0.8/0.85 = 0.94$, respectively. This results in the vapor and air partial pressures of $P_v = y_v P = 21 \text{ kPa}$ and $P_a = y_a P = 334 \text{ kPa}$, respectively.

In the next example, we calculate the component masses of a mixture from partial pressures.

Example IIC.1.3. A large dry containment of a PWR has a volume of $2\text{E}6 \text{ ft}^3$. At normal operation, the mixture of air and superheated steam is at a total pressure of 14.7 psia and temperature of 120 F . If the partial pressure of superheated steam is 0.2 psia , find the masses of air and steam in the containment.

Solution: To find the masses, let's assume that both steam and air can be treated as ideal gases. Hence, for steam:

$$m_v = \frac{P_v V}{(R_u / M_v) T} = \frac{(0.2 \times 144.00) \times (2 \times 10^6)}{(1545/18)(120 + 460)} = 1157 \text{ lbm}$$

Since steam partial pressure is given, it implies that the calculation should be based on the Dalton model. Hence, $P_a = P - P_v = 14.7 - 0.2 = 14.5 \text{ psia}$. Therefore, for air:

$$m_a = \frac{P_a V}{(R_u / M_a) T} = \frac{(14.5 \times 144.00) \times (2 \times 10^6)}{(1545/28.97)(120 + 460)} = 135,000 \text{ lbm}$$

Calculation of Mixture Properties

To simplify dealing with mixtures, we calculate average mixture properties from the properties of the components comprising the mixture. The component properties are either based on mole fraction or mass fraction:

$$C_v = n\bar{c}_v = n \sum_i y_i \bar{c}_{v,i}(T, P_i) = mc_v = m \sum_i x_i c_{v,i}(T, P_i) \quad \text{IIc.1.5}$$

$$C_p = n\bar{c}_p = n \sum_i y_i \bar{c}_{p,i}(T, P_i) = mc_p = m \sum_i x_i c_{p,i}(T, P_i) \quad \text{IIc.1.6}$$

$$U = n\bar{u} = n \sum_i y_i \bar{u}_i(T, P_i) = mu = m \sum_i x_i u_i(T, P_i) \quad \text{IIc.1.7}$$

$$H = n\bar{h} = n \sum_i y_i \bar{h}_i(T, P_i) = mh = m \sum_i x_i h_i(T, P_i) \quad \text{IIc.1.8}$$

Here, the mass fraction of each component is defined as the ratio of the mass of that component to the total mass of the mixture. We examine the application of these relations in the following example.

Example IIc.1.4. Assuming air consists of only N₂, O₂, and Argon, find u , h , and c_p of air at 1 atm and $T = 80^\circ\text{F}$ (540°R) for the percentage specified below:

Component i	Molecular weight M	Volume fraction V_i/V	Mole fraction y_i	Mass fraction x_i
N ₂	28.013	0.7803	0.7803	0.7546
O ₂	31.999	0.2099	0.2099	0.2319
A	39.946	0.0098	0.0098	0.0135

Solution: We first calculate the mixture molecular weight:

$$M = \sum_i y_i M_i = 0.7803(28.013) + 0.2099(31.999) + 0.0098(39.948) = 28.967 \text{ lb/lbmole}$$

Using M , we calculate x_i according to:

$$x_i = y_i M_i / M$$

The results are listed in the above table. Obtaining c_v and c_p from Table A.II.5 (BU), for the mixture specific internal energy, we find:

$$u = \sum_i x_i u_i = 0.7546(540 \times 0.1774) + 0.2319(540 \times 0.157) + 0.0135(540 \times 0.0746) =$$

$$92.5 \text{ Btu/lbm}$$

for specific enthalpy we find:

$$h = \sum_i x_i h_i = 0.7546(540 \times 0.2483) + 0.2319(540 \times 0.2191) + 0.0135(540 \times 0.1244) =$$

$$129.5 \text{ Btu/lbm}$$

and for specific heat we find:

$$c_p = \sum_i x_i c_{pi} = 0.7546(0.2483) + 0.2319(0.2191) + 0.0135(0.1244) = 0.24 \text{ Btu/(lbm R)}$$

Example Ilc.1.5. A cylinder contains 1 lbm of CO₂ and 2 lbm of N₂ at 20 psia and 100 F. In a polytropic process ($n_{poly} = 1.3$), the content is compressed to 60 psia. Find the value of work and heat transfer.

Solution. The work done on the system can be found from Equation IIa.4.4;

$$W = \frac{P_2 V_2 - P_1 V_1}{1 - n_{poly}} = \frac{m(R_u / M)(T_2 - T_1)}{1 - n_{poly}}$$

Where m and M are the mixture mass and molecular weight. We need to find m , M , and T_2 . The mixture mass is found from:

$$m = m_{\text{CO}_2} + m_{\text{N}_2} = 1 + 2 = 3 \text{ lbm}$$

To find the molecular weight, we must first find total number of molecules:

$$n_{\text{CO}_2} = \frac{m_{\text{CO}_2}}{M_{\text{CO}_2}} = \frac{1}{44} = 0.023 \text{ lbmol}$$

$$n_{\text{N}_2} = \frac{m_{\text{N}_2}}{M_{\text{N}_2}} = \frac{2}{28} = 0.071 \text{ lbmol}$$

Therefore, $N = 0.023 + 0.071 = 0.094 \text{ lbmol}$ and $M = m/N = 3/0.094 = 31.91$. Mixture temperature following compression is found from:

$$T_2 = T_1 \left(\frac{P_2}{P_1} \right)^{(n_{poly}-1)/n_{poly}} = 560(3)^{(1.3-1)/1.3} = 722 \text{ R}$$

Substituting, we find the amount of work delivered to the system as:

$$W = \frac{m(R_u / M)(T_2 - T_1)}{1 - n_{poly}} = \frac{3(1545 / 31.91)(722 - 560)}{1 - 1.3} = -78436 \text{ ft lbf} = -100.8 \text{ Btu}$$

where the minus sign confirms that work is delivered to the system. The heat transfer is found from the first law of thermodynamics:

$$Q = W + \Delta U$$

We calculate ΔU from:

$$\Delta U = \left(\sum_{i=1}^N m_i c_{vi} \right) (T_2 - T_1) = (1 \times 0.158 + 2 \times 0.177)(722 - 660) = 31.74 \text{ Btu}$$

Therefore, the amount of heat transferred to the surroundings is found as:

$$Q = -100.8 + 31.74 = -69 \text{ Btu.}$$

Example IIc.1.6. A gas tank contains a mixture of 1.35 kmol CO_2 and 4.8 kmol of air at 1.2 bar and 37 C. Assuming air by volume consists of 21% O_2 and 79% N_2 , find:

- the masses of N_2 , O_2 , and CO_2 as well as the total mass
- the percentage of carbon in the mixture by mass
- the molecular weight of the mixture
- specific volume of the mixture

Solution. a) We first find the number of moles:

For $n_{\text{CO}_2} = 1.35$ kmol, $n_{\text{O}_2} = 4.8 \times 0.21 = 0.97$ kmol, and $n_{\text{N}_2} = 4.8 \times 0.79 = 3.79$ kmol. Having number of moles, we then find the masses from $m = nM$. Hence, for nitrogen $m_{\text{N}_2} = 3.79 \times 28 = 106.2$ kg, for oxygen

Mass of mixture: $m = m_{\text{N}_2} + m_{\text{O}_2} + m_{\text{CO}_2} = 106.2 + 31 + 59.4 = 196.6$ kg.

b) $m_C = [(12/44) \times 59.4]/196.6 = 8\%$

c) To find M , we need to find total number of moles and the mole fraction of each component.

$$n = n_{\text{CO}_2} + n_{\text{O}_2} + n_{\text{N}_2} = 3.97 + 0.97 + 1.35 = 6.29 \text{ kmol}$$

$$y_{\text{N}_2} = 3.97/6.29 = 0.63$$

$$y_{\text{O}_2} = 0.97/6.29 = 0.16$$

$$y_{\text{CO}_2} = 1.35/6.29 = 0.21$$

$$M = 0.63(28) + 0.16(32) + 0.21(44) = 34.82 \text{ kg/kmol}$$

$$\text{d) } v = RT/P = (R_u/M)T/P = (8314.5/34.82) \times (273 + 37)/(1.2 \times 10^5) = 0.62 \text{ m}^3/\text{kg}.$$

2. Gases in Contact with Ice, Water, and Steam

Moist air is one of the most important mixtures for industrial applications. Let's consider a general case of a system consisting of non-condensable gases in contact with ice, water, and water vapor, as shown in Figure IIc.2.1. The system therefore consists of three regions. The water region is generally referred to as the *pool*. The gas region consists of gases, vapor, and water droplets. Gases may include any combination of air and such other gases as carbon monoxide, ammonia, ethanol, etc. Depending on the process, which such system may undergo, various phases in this system would interact. For example, the superheated steam may condense on the droplets and droplets may vaporize in contact with hot gases. Also water may evaporate at the interface, steam would condense on the ice surface, and ice would melt in contact with warmer water and gases. Having defined this general case, in the following sections, we deal with specific cases of a mixture of air and water vapor as well as the mixture of moist air being in contact with

a pool of water. Therefore, we exclude the presence of the ice region. Additionally, if there is a pool region, we assume no gas is dissolved in the pool.

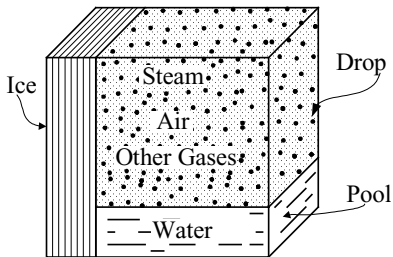


Figure IIC.2.1. Generalization of a thermodynamic system containing water and gas

Relative Humidity, a Measure of Moisture Content

Let's limit the discussion to the control volume representing the gas region of Figure IIC.2.1. We further limit the discussion to a case when the gas region consists only of a mixture of air and water vapor. This moist air mixture has n_a moles of dry air and n_v moles of water vapor at pressure P and temperature T .

<div style="display: flex; justify-content: space-between;"> Water vapor Air </div> <div style="text-align: center; padding: 5px;"> Moist Air </div> <div style="display: flex; justify-content: space-between; padding: 5px;"> $n = n_a + n_v$ $P = P_a + P_v$ </div>

Let's now bring the water vapor to saturation while maintaining the temperature and total pressure of the mixture at the above values. For the mixture of moist air, the relative humidity is defined as:

$$\phi = \left(\frac{y_v}{y_g} \right)_{P, T}$$

where the saturation state is shown by subscript g and the mole fraction of saturated steam in the mixture by $y_g = n_g/n$. Since $P_v = y_v P$ and $P_g = y_g P$, relative humidity can be written as:

$$\phi = \frac{P_v}{P_g(T)} \tag{IIC.2.1}$$

Equation IIC.2.1 is shown in Figure IIC.2.2(a). In Figure IIC.2.2(b), a relative humidity of unity is obtained by adding steam and replacing some air to maintain the same total pressure as in Figure IIC.2.2(a).

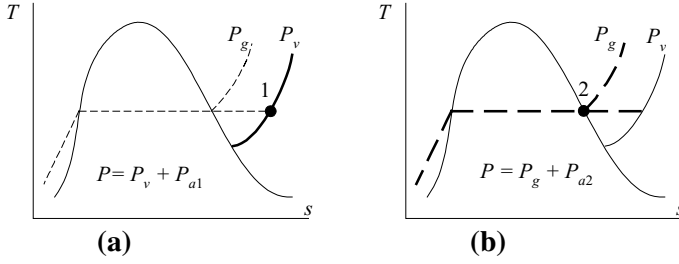


Figure IIc.2.2. (a) State of vapor in moist air and in (b) saturated mixture

Example IIc.2.1. A large dry containment of a PWR has a volume of $2\text{E}6 \text{ ft}^3$. At normal operation, the mixture of air and superheated steam is at a total pressure of 14.7 psia, temperature of 120 F, and relative humidity of 65%. Find the masses of air and steam in the containment.

Solution: To find the masses of air and steam, we need the partial pressure of each component. To find the partial pressure of steam, we use the relative humidity. $P_v = \phi P_g$. From the steam tables we find:

P_g (120 F) = 1.6927 psia. Therefore, $P_v = 0.65 (1.6927) = 1.1$ psia and $P_a = 14.7 - 1.1 = 13.6$ psia. Finally:

$$m_v = \frac{P_v V}{(R_u / M_v) T} = \frac{(1.1 \times 144.00) \times (2 \times 10^6)}{(1545 / 18)(120 + 460)} = 6364 \text{ lbm}$$

$$m_a = \frac{P_a V}{(R_u / M_a) T} = \frac{(13.6 \times 144.00) \times (2 \times 10^6)}{(1545 / 28.97)(120 + 460)} = 126,626 \text{ lbm}$$

Humidity Ratio or Specific Humidity

Another means of measuring the moisture content in moist air is calculating the humidity ratio, defined as the mass of the water vapor to the mass of dry air:

$$\omega = \frac{m_v}{m_a} = \frac{P_v V / (R_u / M_v) T}{P_a V / (R_u / M_a) T} = \frac{M_v P_v}{M_a P_a} = 0.622 \frac{P_v}{P - P_v} \quad \text{IIc.2.2}$$

Example IIc.2.2. Find the relative humidity for a sample of moist air at 14.7 psia and 80 F if the humidity ratio is 0.02.

Solution: From humidity ratio, we find $P_v = P / [1 + (0.622 / \omega)]$. Substituting for total pressure and for the humidity ratio, $P_v = 14.7 / (1 + 0.622 / 0.02) = 14.7 / 32.1 = 0.458$ psia. Also P_g (80 F) = 0.507 psia. Therefore, $\phi = 0.458 / 0.507 = 90\%$.

3. Processes Involving Moist Air

In this section we discuss isochoric, isobaric, and adiabatic processes involving moist air. We start with the isobaric process. Cooling down of moist air in many air-conditioning systems can be considered cooldown at constant pressure. The following example deals with calculating the rate of condensate produced in such systems.

Mixture Cooldown at Constant Pressure, Dew Point Temperature

To describe the dew point temperature, we consider unsaturated moist air at temperature T_1 . Steam in this mixture is superheated at state 1 (partial pressure P_1 and temperature T_1 in Figure IIC.3.1). Hence, the relative humidity is less than unity. State 2 shows saturated steam corresponding to temperature T_1 . If the moist air was at state 2, the mixture would have been saturated. The dew point of the mixture at state 1 is the temperature to which the mixture should be cooled down at constant pressure to become saturated. As shown in Figure IIC.3.1, temperature T_3 is the dew point temperature for the mixture at state 1, $T_3 = T_g(P_1)$. If any of the steam condenses, then saturated water appears at state 4. Further cooldown of the mixture occurs on the saturation line (State 5). Such cooldown results in lower steam partial pressure (P_{gs}) due to the appearance of condensate dropping out of the mixture (State 6).

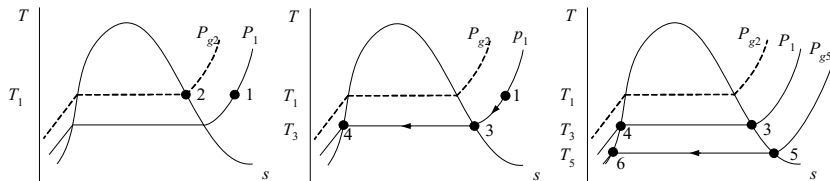


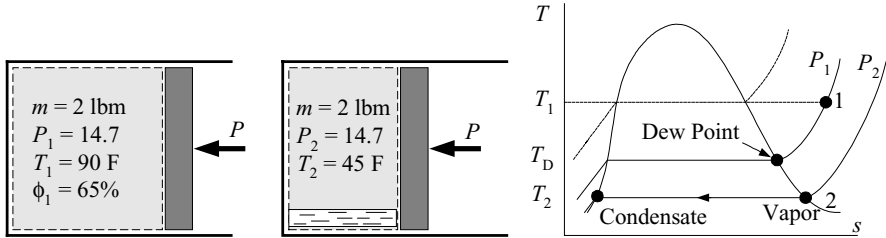
Figure IIC.3.1. Cooldown of unsaturated mixture to saturation

Example IIC.3.1. A large dry containment of a PWR has a free volume of 57000 m³. Following an event, the moist air in this containment reaches 1.5 atm, 130 C, and a relative humidity of 15%. Find the dew point temperature corresponding to this state.

Solution: To find the dew point temperature, we need to find the saturation temperature corresponding to the mixture partial pressure of steam (i.e., $T_{\text{Dew Point}} = T_g(P_v)$). To find P_v , we find $P_g(T_v) = P_g(130 \text{ C}) = 2.701 \text{ bar}$. So that:
 $P_v = 0.15(2.701) = 0.4 \text{ bar}$. The corresponding saturation temperature is:
 $T_g(0.4 \text{ bar}) = 75.8 \text{ C}$.

Example IIc.3.2. A 2-lbm sample of moist air is initially (state 1) at $P_1 = 14.7$ psia, $T_1 = 90$ F, and $\phi_1 = 65\%$. This mixture is cooled at constant pressure to $T_2 = 45$ F (state 2). Find a) the humidity ratio at state 1, b) the dew point temperature at states 1 and 2, c) the amount of condensate at state 2.

Solution: a) To find the initial humidity ratio we need to have P_v . This is found from the initial relative humidity. We first find $P_g(90 \text{ F}) = 0.698$ psia. Hence, $P_v = 0.65(0.698) = 0.4537$ psia, and $\omega_1 = 0.622 \times 0.4537 / (14.7 - 0.4537) = 0.02$.



b) The dew point temperature corresponding to state 1 is $T_{D1} = T_g(P_{v1}) \approx 76$ F and for state 2 is 45 F.

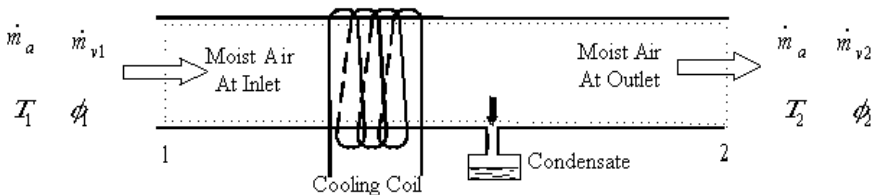
c) The mixture becomes saturated at $T_{D1} = 76$ F. Further decrease in temperature results in steam condensation. At state 2, $P_v = P_2 = P_g(T_2) = P_g(45 \text{ F}) = 0.14744$ psia. Since total pressure is kept constant,

$\omega_2 = 0.622 \times 0.14744 / (14.7 - 0.14744) = 0.0063$ hence, $m_{v2} = 0.0063 m_a$. We must find m_a . On one hand
 $m_a + m_{v1} = 2 \text{ lbm}$

On the other hand $m_{v1}/m_a = 0.02$. Solving this set we find, $m_a = 1.9608$ lbm and $m_{v1} = 0.0392$ lbm. Therefore, $m_{v2} = 0.0063 \times 1.9608 = 0.01235$ lbm. Hence, the mass of steam condensed in this process is:

$m_c = m_{v1} - m_{v2} = 0.0392 - 0.01235 = 0.02685$ lbm.

Example IIc.3.3. Moist air at 1 atm, 20 C, and a relative humidity of 70% enters a cooling duct at a rate of $1.3 \text{ m}^3/\text{s}$. Temperature of the saturated mixture at the exit of the cooling coil is 5 C. Assuming negligible pressure drop, find the mass flow rate of the condensate produced in the cooling duct.



Solution: The condensate mass flow rate is calculated as $\dot{m}_c = \dot{m}_{v1} - \dot{m}_{v2}$. To find the vapor mass flow rates, we need to calculate the air mass flow rate and

then use Equation IIc.2.2. To calculate the air mass flow rate, we need air pressure,

$$P_{a1} = P - P_{v1} = P - \phi_1 P_g(T_1) = 1.01325 - 0.7(0.02339) = 0.997 \text{ bar.}$$

Hence, air mass flow rate is obtained from:

$$\dot{m}_a = \rho_a \dot{V}_a = \frac{P_a}{(R_u / M_a)T} \dot{V}_a$$

Substituting:

$$\dot{m}_a = \frac{0.997}{(0.08314/28.97)(273+20)}(1.3) = 1.54 \text{ kg/s}$$

To find the humidity ratios, we find vapor partial pressures at the inlet and outlet.

At the inlet:

$$P_{v1} = 0.7(0.02339) = 0.0164 \text{ bar}$$

and at the outlet the mixture is saturated

$$P_{v2} = 1.0(0.00872) = 0.00872 \text{ bar.}$$

$$\text{Therefore, } \omega_1 = 0.622(0.0164)/(1.01325 - 0.0164) = 0.01$$

$$\omega_2 = 0.622(0.0087)/(1.01325 - 0.0087) = 0.005399$$

Thus $\dot{m}_C = \dot{m}_{v1} - \dot{m}_{v2} = \dot{m}_a(\omega_1 - \omega_2)$ substituting for \dot{m}_a , the mass flow rate of condensate is found as:

$$\dot{m}_C = \dot{m}_a(\omega_1 - \omega_2) = 1.54(0.01 - 0.0087) = 0.00785 \text{ kg/s} = 25.5 \text{ kg/h.}$$

Mixture Cooldown at Constant Volume

We often encounter mixture cooldown at isochoric instead of isobaric process. This occurs when a non-deformable (rigid) volume contains a fixed amount of a mixture (state 1 on Figure IIc.3.2) and the volume is then subjected to cooldown. In this case, the temperature at which condensate appears (state 2 on Figure IIc.3.2) differs from the dew point temperature (State D on Figure IIc.3.2). To find the temperature corresponding to state 2, we note that at the moment that vapor becomes saturated at constant volume we have $v_{g2} = v_{v1}$. We wrote this relation based on the fact that both volume and all masses remain constant throughout the cooldown process. Since we know P_1 and T_1 we can find v_{v1} . Then from the steam tables, we can find the temperature corresponding to the saturated steam specific volume v_{g2} .

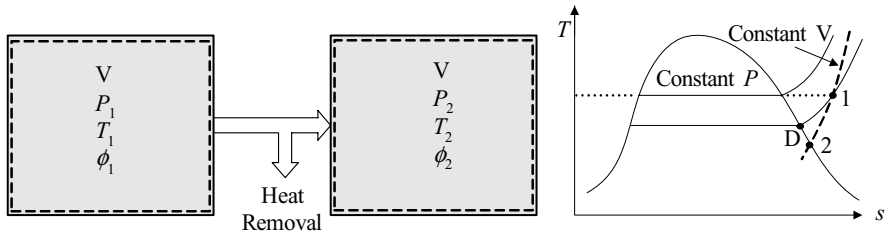
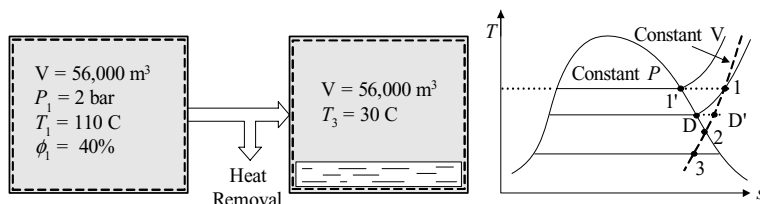


Figure IIc.3.2. Cooldown of moist air at constant volume

Example IIc.3.4. Moist air is contained in a volume of $56,000 \text{ m}^3$ at 2 bar, 110°C , and a relative humidity of 40%. This mixture is now cooled to 30°C . Find a) the dew point temperature, b) temperature at which vapor begins to condense, c) the amount of water condensed, and d) final pressure. States are shown in the figure.



Solution: a) We find the dew point temperature from $T_D = T_g(P_{v1})$. To find P_{v1} , we use the relative humidity. $P_{v1} = P_g(T_1) = P_g(110^\circ\text{C}) = 0.14327 \text{ MPa} = 1.4327 \text{ bar}$.

Hence, $P_{v1} = 0.40(1.4327) = 0.573 \text{ bar}$. We find $T_D = T_{\text{sat}}(P_{v1} = 0.573 \text{ bar}) = 84.38^\circ\text{C}$. Also note that $P_{a1} = 2 - 0.573 = 1.427 \text{ bar}$.

b) Since the cooldown is at constant volume, we know that the condensate first appears at T_2 because on the constant volume line, the pressure corresponding to T_D is smaller than the saturation pressure corresponding to the dew point temperature (i.e., $P_{D'} < P_D = P_g(T_D)$). Hence, vapor is superheated at $T_{D'} = T_D$ and $P_{D'}$. Temperature at which vapor begins to condense is found from $v_{g2} = v_1$, where v_1 is given by $P_1 v_1 = (R_u/M_a)T_1$. Subsequently, we find $v_1 = (0.08314/18)(110 + 273)/0.573 = 3.8 \text{ m}^3/\text{kg}$. This corresponds to a saturation pressure of $T_2 = 82.2^\circ\text{C}$, which is 2°C less than the dew point temperature.

c) To find the mass of the condensate, we again use the fact that cooldown is at a constant volume: $v_3 = v_2 = v_1$. From the steam tables, we find $v_f(30^\circ\text{C}) = 0.001004 \text{ m}^3/\text{kg}$ and $v_g(30^\circ\text{C}) = 32.89 \text{ m}^3/\text{kg}$. Steam quality at point 3 is found as $x_3 = (v - v_f)/v_{fg} = (3.8 - 0.001004)/(32.89 - 0.001004)$

d) The moist air volume at state 3 is $V_3 = 56,000 - 1702(0.001004) = 55998.3 \text{ m}^3$. $P_{\text{final}} = P_3 + P_{a3}$. Where $P_{a3} = m_a(R_u/M_a)T_3/V_3$. However, the dry air mass is found from $m_a = P_{a1}V_1/(R_u/M_a)T_1 = (2 - 0.573)(56,000) / (0.08314/28.97)(30 + 273) = 91898.4 \text{ kg}$. Therefore, $P_{a3} = 91898.4 (0.08314/28.97)(30 + 273)/55998.3 = 1.427 \text{ bar}$. Hence, $P_{\text{final}} = 1.427 + P_g(30^\circ\text{C}) = 1.427 + 0.0425 = 1.47 \text{ bar}$.

Humidification

In the analysis of moist air in closed systems undergoing constant pressure or constant volume processes we were able to determine conditions of the final state of the mixture from the equation of state. To find more information about the process, for example the amount of heat transfer in a constant volume process we would have to use the conservation equation of energy in addition to the equation of state. In general, we need to use the conservation equation of mass, conservation equation of energy, and the equation of state as applied to a control volume to study the thermal-hydraulic characteristics of air conditioning systems. The applicable equations for conservation of mass and energy are IIa.5.1 and IIa.6.5, respectively. For example, let's analyze heating and humidification of moist air as shown in Figure IIc.3.3.

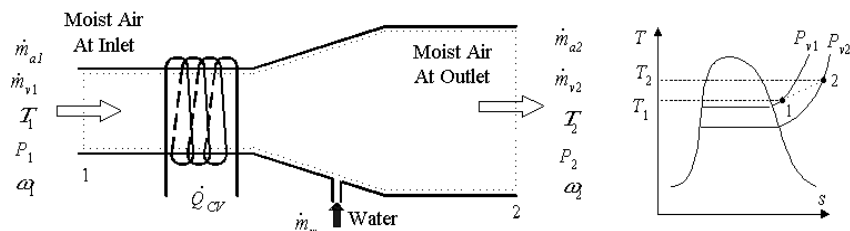


Figure IIC.3.3. Control volume for conditioning a mixture of moist air

Considering steady state operation, the conservation equation of mass for dry air becomes:

$$\dot{m}_{a1} = \dot{m}_{a2} = \dot{m}_a \quad \text{IIC.3.1}$$

and for water:

$$\dot{m}_{v1} + \dot{m}_w = \dot{m}_{v2} \quad \text{IIC.3.2}$$

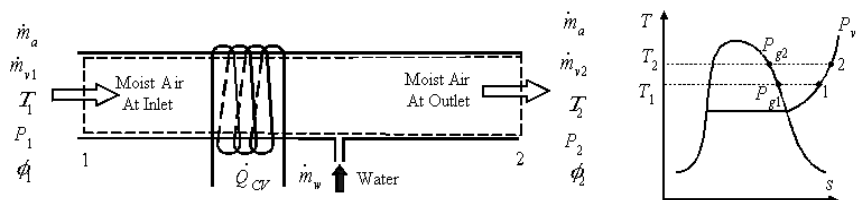
We apply the conservation equation of energy at steady state to the mixture to obtain:

$$(\dot{m}_{a1}h_{a1} + \dot{m}_{v1}h_{v1}) + \dot{m}_w h_w + \dot{Q}_{CV} = (\dot{m}_{a2}h_{a2} + \dot{m}_{v2}h_{v2}) \quad \text{IIC.3.3}$$

where we assumed no net work and ignored the kinetic and potential energies. To simplify, we substitute for the vapor mass flow rate from $\dot{m}_v = \omega \dot{m}_a$ to obtain $\dot{m}_w = (\omega_2 - \omega_1)\dot{m}_a$. Substituting in Equation IIC.3.3, we get:

$$\dot{Q}_{CV} / \dot{m}_a = c_{pa}(T_2 - T_1) + (\omega_2 h_{v2} - \omega_1 h_{v1}) - (\omega_2 - \omega_1)h_w \quad \text{IIC.3.4}$$

Example IIC.3.5. Moist air enters a heated duct at 15 psia, 50 F, 60% relative humidity and a volumetric flow rate of 5000 CFM. Water is sprayed into the moist air stream at a temperature of 80 F and a flow rate of 0.3 GPM. Assuming negligible pressure drop in the short duct, find the relative humidity at the outlet of the duct and the rate of heat transfer for steady state operation at $T_2 = 70$ F.



Solution: First, we find air density at the inlet to calculate the air mass flow rate, $\rho_{a1} = P_1 / (R_u / M_a) T_1 = 15(144) / [(1545/28.97)(50 + 460)] = 0.08 \text{ lbm/ft}^3$.

Hence, $\dot{m}_a = 0.08(5000)/60 = 6.62 \text{ lbm/s}$. We now calculate the inlet humidity

ratio $P_{v1} = 0.6P_g(50\text{ F}) = 0.6(0.178) = 0.11$ psia so that:

$$\omega_1 = 0.622(0.11)/(15 - 0.11) = 0.0045.$$

Mass flow rate of the injected water is;

$$\dot{m}_w = \rho_w \dot{V}_w = 62.2[0.3/(60 \times 7.481)] = 0.042 \text{ lbm/s} \quad (0.02 \text{ kg/s})$$

where the water density at 80 F is 62.2 lbm/ft³ and 7.481 is the conversion factor for ft³ to gallon. We find the humidity ratio at the outlet from:

$$\omega_2 = \omega_1 + (\dot{m}_w / \dot{m}_a) = 0.0045 + (0.042/6.62) = 0.$$

and $P_g(70\text{ F}) = 0.363$ psia (2.5 kPa) so that:

$$\phi_2 = 0.26/0.363 = 70\%.$$

Other parameters needed for Equation IIc.3.4 are water and vapor enthalpies. These can be found from the Steam Tables as $h_w = 48$ Btu/lbm, $h_{v1} = (P = 0.11, T = 50) = 1085$ Btu/lbm, and $h_{v2} = (0.11, 70) = 1092$ Btu/lbm (2540 kJ/kg). Substituting in Equation IIc.3.4, we get:

$$\dot{Q}_{CV} = 6.62[0.24(70 - 50) + (0.01 \times 1092 - 0.0045 \times 1085) - (0.01 - 0.0045)48] = 70 \text{ Btu/s} \quad (74 \text{ kW})$$

The Adiabatic Saturation Process

Another example of gases in contact with phases of water is the adiabatic saturation process. As shown in Figure IIc.3.4, moist air with an unknown relative humidity is passed over a pool of water contained in a well insulated duct. The mixture pressure and temperature at the inlet are specified. If the entering air is not saturated, some of the water in the pool would evaporate and enter into the mixture stream. For sufficiently long duct, the mixture at the outlet would be saturated. Temperature of the mixture at the outlet is less than the inlet temperature ($T_2 < T_1$) due to the fact that some energy of the mixture is used to evaporate water in the pool. This temperature is referred to as the *adiabatic saturation temperature* since the saturation of the mixture occurred without any need for heat transfer from the surroundings. Saturated make up water is added to the pool to maintain the process at steady state condition.

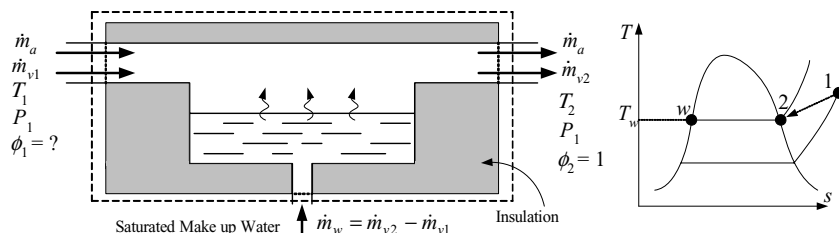


Figure IIc.3.4. Steady flow of moist air over a pool of water to produce saturated mixture

Measurement of Relative Humidity

We can use the above adiabatic saturation process to determine the unknown humidity ratio as well as the relative humidity. If the pressure drop in the duct is negligible, we can apply the same procedure that led to the derivation of Equation IIC.3.4 except for the heat transfer term which should be dropped:

$$c_{pa}(T_2 - T_1) + (\omega_2 h_{v2} - \omega_1 h_{v1}) - (\omega_2 - \omega_1)h_w = 0$$

We solve this equation for the unknown humidity ratio to obtain:

$$\omega_1 = \frac{c_{pa}(T_2 - T_1) + \omega_2(h_{v2} - h_f)}{(h_{v1} - h_f)} \quad \text{IIC.3.5}$$

Where ω_2 is given by Equation IIC.2.2. Note that $h_{v2} = h_g(T_2)$. Having ω_1 , we can find the unknown relative humidity from:

$$\phi = \frac{\omega}{(0.622 + \omega)} \frac{P}{P_g(T_v)} \quad \text{IIC.3.6}$$

Wet- and Dry-Bulb Temperatures

We measure the dry-bulb temperature of a mixture by a thermometer. To measure the wet-bulb temperature, we cover the bulb of the thermometer by a wet wick. We can then measure the wet-bulb temperature by either drawing the flow of the mixture over the wet bulb by a fan or moving the thermometer in the mixture. If the mixture is not saturated, some heat transfer takes place, transferring energy from the mixture to the wick for liquid evaporation. This results in the temperature shown by the thermometer to be lower than the dry-bulb temperature. We can then measure the humidity ratio by using Equations IIC.3.5, from which we can find the relative humidity.

Example IIC.3.6. Temperature of a room is measured as 72 F. The wet-bulb temperature is measured as 65 F. Find the relative humidity.

Solution: We can find the relative humidity from Equation IIC.1.20. This, in turn, requires the humidity ratio, which we can find from Equation IIC.1.19. Note that there is no make-up water hence Equation IIC.3.5 becomes

$$\omega_1 = [c_{pa}(T_2 - T_1) + \omega_2 h_g(T_2)] / h_{v1}(T_1)$$

To find ω_2 , we use Equation IIC.2.2: $\omega_2 = 0.622P_{v2} / (P - P_{v2})$ where $P = 14.7$ psia and $P_{v2} = P_g(T_2)$. For $T_2 = 65^\circ\text{F}$, $P_g(65) = 0.30545$ psia. Therefore, $\omega_2 = 0.622(0.30545) / (14.77 - 0.30545) = 0.0132$. Then $\omega_1 = [0.24(65 - 72) + 0.0132(1089.9)] / 1093 = 0.0116$. Using in Equation IIC.3.6, we get:

$$\phi_1 = \frac{\omega_1}{(0.622 + \omega_1)} \frac{P}{P_g(T_{v1})} = \frac{0.0116}{(0.622 + 0.0116)} \frac{14.7}{0.38844} = 69\%$$

Note that we assumed $h_{v1} \cong h_g(T_1)$ to avoid iteration.

4. Charging and Discharging Rigid Volumes

This is a more general case of the topic discussed in Section 8 of Chapter IIa. The rigid container (i.e. constant volume process) initially contains moist air at specified pressure, temperature, and relative humidity. Fluid at a specified rate is now injected into the container. The intention is to find the equilibrium pressure and temperature. Similarly, we can consider a case where a valve is opened to allow a specified amount of the mixture to leave the container. Such a process, where the final equilibrium-state is not known, frequently occurs in common practice. Determination of the final equilibrium-state generally requires iteration with the steam tables. A special case is shown in Example IIc.4.2 where a mixture of water and steam enters a control volume and final pressure is sought.

Rigid Volumes Initially at Non-equilibrium Condition

First we consider a simple case where moist air is in contact with water. Note that both air and water are at the same temperature. Figure IIc.4.1(a) shows a system containing moist air with relative humidity less than 1. In such a system, water evaporates until the mixture of air and water vapor becomes saturated in steam and the system reaches equilibrium, Figure IIc.4.1(b). In such an equilibrium condition, all components are again at the same temperature albeit $T_2 < T_1$. In the thermodynamic analysis of such systems, we may assume that no gas is dissolved in water.

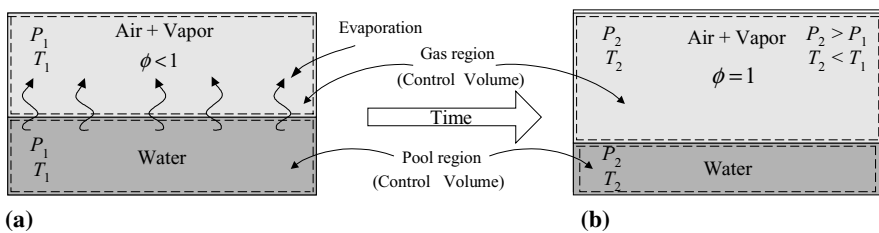
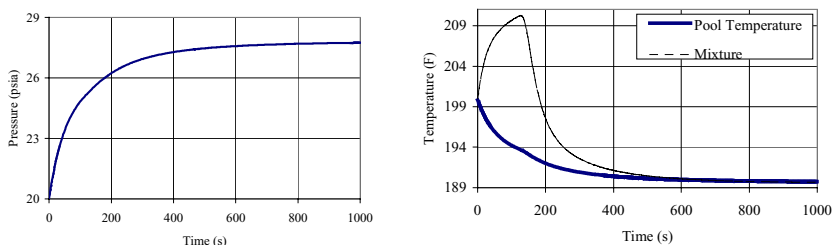


Figure IIc.4.1. (a) Water evaporation to reach and (b) Equilibrium state

Example IIc.4.1. The system in Figure IIc.4.1(a) has two distinct regions, the pool and the gas region. Subcooled water in the pool region is initially at pressure P_1 and temperature T_1 where $T_1 < T_{g1}(P_1)$. The mixture in the gas region is initially at total pressure P_1 , temperature T_1 , and relative humidity $\phi_1 < 1$. A thermally conducting plate separates these two regions. At time zero, the plate is removed

and the regions begin to exchange mass and energy. Assuming no heat transfer between the system and the surroundings, discuss the response of the system to the removal of the plate, Figure IIc.4.1(b).

Solution: What drives this transient is the gas region not being saturated. The transient begins at time zero, when the plate is removed and the regions are allowed to exchange mass and energy. To bring the gas region to saturation, water vaporizes, carrying saturated water enthalpy, $h_g(P)$ into the gas region. This increases pressure and temperature. Since, the energy for vaporization is provided by the pool water, this also causes water temperature and water level to drop. Water in the pool is subcooled at total pressure and will remain subcooled throughout the transient due to increasing pressure. However, at equilibrium water and steam reach saturation at the steam partial pressure. Vapor temperature would eventually stop rising as relative humidity approaches unity. With the gas region saturated, the warmer mixture exchanges heat with the colder water. Hence, the mixture temperature reverses direction and merges with the pool water temperature until it eventually reaches equilibrium. This discussion is depicted in the plots of pressure and temperatures for a system having a volume of 100 ft^3 and being at initial conditions of $P = 20 \text{ psia}$, $T = 200 \text{ F}$, and $\phi = 10 \%$. The initial water volume fraction (water volume divided by total volume) in this example is 3%.



Filling Rigid Volumes, Equilibrium Saturation Condition

In this case, we analyze a control volume initially at equilibrium state with specified initial pressure, temperature, relative humidity, and water volume fraction. Such a control volume may represent the suppression pool of a BWR, or the quench tank of a PWR. The role of such systems is to condense the injected mixture of water and steam. Although the injection, condensation, and subsequent pressurization of the control volume constitute a transient process, we only consider the initial and the final equilibrium states. The goal is to find the final pressure given the total mass and enthalpy of the injected mixture of water and steam (Figure IIc.4.2). Since the moist air is initially saturated and a saturated mixture is also injected into the control volume, then the moist air remains saturated throughout the event and the water in the pool also remains saturated at the steam partial pressure. To find the final pressure, we use the conservation equations of mass,

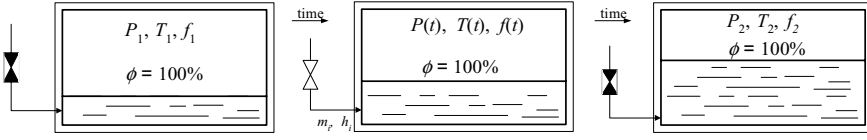


Figure IIc.4.2. A control volume representing a steam suppression system

energy, the equation of state, and the volume constraint. Mass balance for water and steam gives:

$$(m_{f1} + m_{g1}) + m_i = m_{f2} + m_{g2}$$

For energy balance, we use Equation IIa.8.2 as applied to the control volume, assuming a constant h_i :

$$(m_{f1}u_{f1} + m_{g1}u_{g1}) + (m_a u_a) + m_i h_i = (m_{f2}u_{f2} + m_{g2}u_{g2}) + (m_a u_a)$$

Finally, the volume constraint gives:

$$m_{f2}v_{f2} + m_{g2}v_{g2} = V$$

There are four unknowns: T_2 , v_2 (u_2), m_{f2} , and m_{g2} . There are also four equations, three of which are listed above and the fourth is the equation of state. We begin solving the above set by eliminating m_{g2} from mass and volume constraint to find $m_{f2} = [(m_{f1} + m_{g1} + m_i)v_{g2} - V] / v_{fg2}$. Hence,

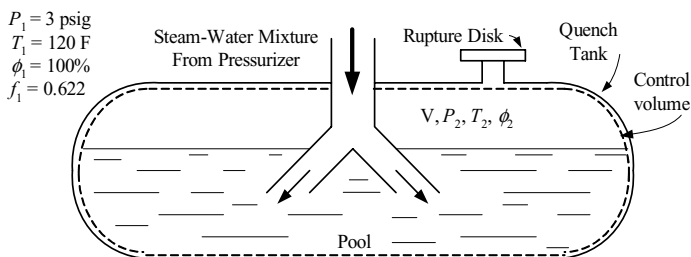
$$m_{g2} = [V - (m_{f1} + m_{g1} + m_i)v_{f2}] / v_{fg2}.$$

Substituting into the energy equation, we get:

$$C_1[(v_{g2} / v_{fg2})u_{f2} - (v_{f2} / v_{fg2})u_{g2}] + V(u_{fg2} / v_{fg2}) + C_2(T_2 - T_1) = C_3 \quad \text{IIc.4.1}$$

where C_1 , C_2 , and C_3 are constants given as $C_1 = m_{f1} + m_{g1} + m_i$, $C_2 = m_a c_{va}$, and $C_3 = (m_{f1}u_{f1} + m_{g1}u_{g1}) + m_i h_i$, respectively. We may substitute for $v_{f2} = v_f(T_2)$, $v_g = v_g(T_2)$, and other thermodynamic properties in Equation IIc.4.1. This would result in a non-linear algebraic equation, that is only a function of T_2 and can be solved by the Newton-Raphson method. Alternatively, we may assume a value for T_2 and iterate with the steam tables.

Example IIc.4.2. The quench tank of a PWR, as shown in the figure, has a volume of 217 ft³ (6 m³). Initial pressure, temperature, relative humidity, and water volume fraction (f_1) are specified in the figure. During an event, a total of 536 lbm (243 kg) of steam at an average enthalpy of 1133 Btu/lbm (2635.3 kJ/kg) enters the pool. The rupture disk will fail at a pressure of 145 psia (≈ 1 MPa). Find whether the disk remains intact or if it fails.



Solution: We first find the initial masses and internal energies as follows:

$$m_{f1} = f_1 V / v_{f1} = 0.622(217/0.01620) = 8331.3 \text{ lbm} \text{ (3779 kg)}$$

Since $P_{v1} = \phi_1 P_g(T_1) = 1.6927 \text{ psia}$ hence, $P_{a1} = P_1 - P_{v1} = 17.70 - 1.6927 = 16 \text{ psia}$. We can now find the mass of air in the tank from:

$$m_a = P_a V_a / (R_u / M_a) T_1 = (16 \times 144) \times 82 / [(1545/28.97) \times (460 + 120)] = 6.11 \text{ lbm} \text{ (2.77 kg)}$$

To find the mass of vapor we may either use $m_{v1} = V_a / v_{g1} = 82 / 203.26 = 0.403 \text{ lbm}$ or use the definition of the humidity ratio $m_{v1} = \omega_1 m_a$ with $\omega_1 = 0.622 P_{v1} / (P - P_{v1}) = 0.622 \times 1.6927 / (17.7 - 1.6927) = 0.0657$ to get $m_{v1} = \omega_1 m_a = 0.0657 \times 6.11 = 0.402 \text{ lbm}$. Finally, $u_{f1} = 87.97 \text{ Btu/lbm}$ and $u_{g1} = 1113.6 \text{ Btu/lbm}$. Thus $C_1 = 8331.3 + 0.403 + 536 = 8868 \text{ lbm} \text{ (4022.5 kg)}$

$$C_2 = 6.11(0.171) = 1.045 \text{ Btu/F} \text{ (1.984 J/C)}$$

$$C_3 = (8331.3 \times 87.97 + 0.403 \times 1113.6 + 536 \times 1133) = 1.341\text{E6 Btu} \text{ (1414.8 MJ)}$$

Upon substitution into Equation Ilc.4.1, we get:

$$\{8868[(v_{g2}/v_{fg2})u_{f2} - (v_{f2}/v_{fg2})u_{g2}] + 217(u_{fg2}/v_{fg2}) + 1.045(T_2 - 120)\} - \{1.3406\text{E6}\} = 0$$

To solve this equation iteratively with steam tables, we guess a T_2 , say $T_2 = 250 \text{ F}$. From the steam tables, we find $v_{f2} = 0.01787 \text{ ft}^3/\text{lbm}$, $v_{g2} = 3.7875 \text{ ft}^3/\text{lbm}$, $v_{fg2} = 3.7697 \text{ ft}^3/\text{lbm}$, $u_{f2} = 311.3 \text{ Btu/lbm}$, and $u_{g2} = 1190.1 \text{ Btu/lbm}$

The answer converges to $T_2 = 182.5 \text{ F}$ after 6 trials as shown below.

T_2 (F)	v_{f2} (ft ³ /lbm)	v_{fg2} (ft ³ /lbm)	v_{g2} (ft ³ /lbm)	u_{f2} (Btu/lbm)	u_{fg2} (Btu/lbm)	u_{g2} (Btu/lbm)	Residue
340	0.01787	3.76970	3.78750	311.3	878.8	1190.1	112
250	0.01701	13.8020	13.8190	218.7	868.7	1087.4	67.6
200	0.01664	33.6220	33.639	168.1	905.5	1073.4	11.3
160	0.01639	77.2700	77.290	127.8	934.2	1062.1	-22.5
182	0.01652	48.1720	48.189	149.8	918.5	1068.3	-1.13

The moist air volume becomes

$$V_{a2} = 217 - (135 + 536 \times 0.01652) = 73.15 \text{ ft}^3 \text{ (2.07 m}^3\text{)}$$

At $T_2 = 182.5 \text{ F}$, tank pressure is $P_2 = P_{g2}(T_2) + P_{a2}(T_2) = 7.94 + [6.11 (1454/28.97) (182.5 + 460) / 73.15] = 7.94 + 11.57 = 19.5 \text{ psia} \text{ (0.134 MPa)}$.

This pressure is too low to cause the failure of the rupture disk. However, we assumed that all the steam is condensed in the pool. Pressure rises substantially even if a small fraction of steam is not condensed and escapes to the moist region above the pool. This is shown in Example IIc.4.3.

Filling Rigid Volumes, Equilibrium Saturation Condition, Alternate Solution

To avoid iteration, we may choose an approximate solution for problems similar to Example IIc.4.2. In this method, we ignore the presence of air (and other non-condensable gases) in the vapor region. This is a valid assumption only if a small amount of air exists in the volume. We then use a “lumped parameter” approach in which the mixture of the pool water and the moist air is assumed to be mixed homogeneously. We also assume that the incoming mixture of water and steam mixes instantaneously and perfectly with the content of the control volume. The mass balance for water gives:

$$m_1 + m_i = m_2$$

The volume constraint gives:

$$v_{f2} + x_2 v_{fg2} = V/m_2$$

and the energy equation for the mixture becomes:

$$m_2(u_{f2} + x_2 u_{fg2}) = (m_1 u_1 + m_i h_i)$$

Substituting for m_2 from the mass balance and eliminating x_2 between the energy equation and the volume constraint, we find an equation equivalent to Equation IIc.4.1:

$$u_{f2} + (V/m_2 - v_{f2})u_{fg2}/v_{fg2} = (m_1 u_1 + m_i h_i)/(m_1 + m_i) \quad \text{IIc.4.2}$$

Solving Equation IIc.4.2 for $P_{sat}(T_2)$, we then find $P_2 = P_{sat}(T_2) + m_{air}RT/V$.

Filling Rigid Volumes, Equilibrium Superheated Condition

In the previous section we considered control volumes in which water vapor remains saturated throughout the charging process. We now consider cases in which water vapor is superheated steam at the final state. The solution procedure is similar to the derivation for the saturation condition however, unlike the saturation condition in this case, pressure is not a function of temperature and has to be calculated separately. An example for such cases includes a main steam line break inside the containment building of a PWR and subsequent pressurization of the containment. From the volume constraint we have:

$$v_2 = V/(m_1 + m_i) = A_1 \quad \text{IIc.4.3}$$

The energy balance for the control volume, assuming no heat transfer to or from the control volume, yields:

$$(m_1 + m_i) u_2 + m_a c_{va}(T_2 - T_1) = m_1 u_1 + m_i h_i$$

This equation may be written as:

$$u_2 + A_2(T_2 - T_1) = A_3 \quad \text{IIC.4.4}$$

where $A_2 = m_a c_{va}/(m_1 + m_i)$ and $A_3 = (m_1 u_1 + m_i h_i)/(m_1 + m_i)$. Equations IIC.4.3, IIC.4.4, and the equation of state provide three equations for three unknowns P_2 , T_2 , and v_{v2} (u_{v2}). Since iteration on both P_2 and T_2 is very laborious, we treat the vapor as an ideal gas and find the vapor pressure from $P_{v2} = m_{v2} R_v T_2 / V$. In this approach, we have implicitly accounted for and hence, superseded the volume constraint for vapor. Having P_{v2} and T_2 , we read u_2 from the steam tables and compare it with u_2 calculated from Equation IIC.4.4. We continue this iterative process until the convergence criterion is met. We then find the final pressure from:

$$P_2 = \frac{m_a R_a T_2}{V} + \frac{m_2 R_v T_2}{V} \quad \text{IIC.4.5}$$

Example IIC.4.3. An initially drained quench tank contains moist air at 120 F (48.9 C) at a relative humidity of 50%. A total of 54 lbm (24.5 kg) of steam at an average enthalpy of 1133 Btu/lb (2635.27 kJ/kg) enters the tank. Find the tank final temperature and pressure. Tank has a volume of 217 ft³ ($\approx 6 \text{ m}^3$).

Solution: In this case, moist air occupies the entire volume of the tank. Initial mass of vapor in the tank is found from $P_v = 0.5(1.6927) = 0.85 \text{ psia}$. Therefore, $v_1 = (0.85 \times 120) = 405.5 \text{ ft}^3/\text{lbm}$ and $m_1 = 217/405.5 = 0.535 \text{ lbm}$. Thus, $m_2 = 0.535 + 54 = 54.535 \text{ lbm}$. Again, from the steam tables, $u_1 = 1049.14 \text{ Btu/lbm}$ and:

$$A_3 = (0.535 \times 1049.14 + 54 \times 1133)/54.535 = 1132.17 \text{ Btu (1194.5 kJ/kg)}$$

To find air mass, we calculate $P_{a1} = P_1 - P_{v1} = 17.70 - 0.85 = 16.85 \text{ psia}$. Therefore, the mass of air in the tank is:

$$m_a = P_a V_a / (R_a / M_a) T_1 = (16.85 \times 144) \times 217 / [(1545/28.97) \times (460 + 120)] = 17 \text{ lbm (7.71 kg)}.$$

Hence, $A_2 = 17(0.171)/m_2 = 0.053$ and Equation IIC.4.4 becomes $u_2 + 0.053(T_2 - 120) = 1132.17$.

We start the iteration process by guessing $T_2 = 400 \text{ F}$.

$$P_{v2} = 54.535(1545/18)(460 + 400)/217 = 128.83 \text{ psia giving } u_2 = 1132.33 \text{ Btu/lbm}.$$

From Equation IIC.4.4 for $u_2 + 0.053(T_2 - 120) = 1132.17$ we find $u_2 = 1132.17 - 0.053(400 - 120) = 1117.24 \text{ Btu/lbm}$. The trials are tabulated as follows:

T_2 (F)	P_{v2} (psia)	$(u_2)_{\text{Table}}$ (Btu/lbm)	$(u_2)_{\text{Energy Eq.}}$ (Btu/lbm)
400	128.8	1132.3	1117.24
350	121.3	1111.1	1119.98
355	122.1	1113.3	1119.97
370	124.3	1119.7	1118.92
368	124.0	1118.9	1119.02

Having the final equilibrium temperature at about $T_2 = 368.5 \text{ F}$, final pressure becomes $P_2 = 124 + [17 \times (1545/28.97) \times (460 + 368.5) / (217 \times 144)] = 124 + 24 = 148 \text{ psia (1.02 MPa)}$. This indicates that the quench tank rupture disk of Example IIC.4.3 fails during this event.

Thermal Design of Cooling Towers

Cooling towers are ultimate heat sinks. They are used in power production and other applications such as production of chilled water. Cooling towers are used when naturally occurring heat sinks such as lakes and other large bodies of water are not available or are available but the flow of water is not sufficient to comply with regulations for prevention of thermal pollution. Cooling towers for power production are either of induced draft or of natural draft type. Cooling towers may also be of wet or of dry type. In the dry cooling tower, atmospheric air passes through tubes carrying turbine exhaust. Hence, in dry cooling towers, the only means of transferring heat to the atmospheric air is through sensible heat. In the wet cooling towers as shown in Figure IIc.4.3, the circulating water cooling the turbine exhaust is sprayed inside the tower and is cooled by both sensible and latent heat removal due to the counter current flow of atmospheric air drawn into the cooling tower. The packing facilitates contact between the warmer sprayed water and the colder atmospheric air hence, increasing the rate of heat transfer. It also causes breakup of water droplets to enhance evaporation. The energy for evaporation is supplied by the warmer, sprayed water at 1. As a result, water exiting at 2 is cooler than the water sprayed at 1. The evaporation also causes the moist air exiting the tower at 4 to be near or at saturation. The makeup water that flows into the tower at 5 is meant to compensate for the loss of water through evaporation.

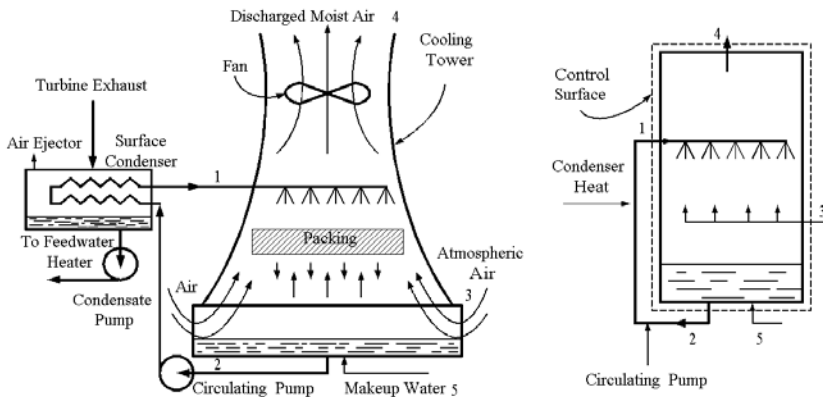


Figure IIc.4.3. A wet, induced-draft cooling tower

Conservation Equations for Wet Cooling Towers

Let's consider the control volume representing the ideal wet cooling tower. The streams entering the control volume include atmospheric air, warm circulating water, and makeup water. The streams leaving the control volume include the nearly saturated moist air and colder water. Thermal analysis of the cooling tower is based on two conservation equations of mass, one for air and one for water, and one energy equation for the mixture of air and water. For steady state operation, mass balance for air gives:

$$\dot{m}_{a3} = \dot{m}_{a4} = \dot{m}_a$$

Mass balance for water gives:

$$\dot{m}_1 + \dot{m}_{w3} + \dot{m}_5 = \dot{m}_2 + \dot{m}_{w4}$$

Since $\dot{m}_1 = \dot{m}_2$, then:

$$\dot{m}_{w3} + \dot{m}_5 = \dot{m}_{w4}$$

We now solve for the mass flow rate of the make up water in terms of the differential rate of moisture content at the outlet and inlet to the control volume:

$$\dot{m}_5 = \dot{m}_{w4} - \dot{m}_{w3} = (\omega_4 - \omega_3)\dot{m}_a \quad \text{IIC.4.6}$$

The energy balance gives:

$$\dot{m}_1 h_1 + (\dot{m}_{w3} h_{w3} + \dot{m}_a c_{pa} T_3) + \dot{m}_5 h_5 = \dot{m}_2 h_2 + (\dot{m}_{w4} h_{w4} + \dot{m}_a c_{pa} T_4) \quad \text{IIC.4.7}$$

We may now approximate the enthalpies of the moisture content of the incoming and exiting streams of moist air as saturated enthalpies at the specified temperatures. After simplifications, substitutions, and rearrangement of Equation IIC.4.7, we find the required mass flow rate of air as:

$$\dot{m}_a = \frac{\dot{m}_1 (h_1 - h_2)}{(\omega_4 h_{g4} - \omega_3 h_{g3}) - (\omega_4 - \omega_3) h_5 + c_{pa} (T_4 - T_3)} \quad \text{IIC.4.8}$$

Having the mass flow rate of air from Equation IIC.4.8, we can choose the fan for induced-draft tower or size the tower for natural-draft cooling towers. The mass flow rate of makeup water is also found (Equation IIC.4.6) based on the mass flow rate of air.

Example IIC.4.4. The condenser of a power plant is cooled by a circulating water flow rate of 100×10^6 lbm/h. The circulating water enters the cooling tower at 110 F and leaves the tower for the condenser at 95 F. Atmospheric air enters the tower at 75 F and 35% relative humidity. Moist air leaves the tower at 90 F and 95% relative humidity. The make up water enters the tower at 70 F. Find the mass flow rate of air and the make up water.

Solution: We first find the pertinent thermodynamic properties:

T (F)	P (psia)	h_f (Btu/lbm)	h_g (Btu/lbm)
70	-	38.05	1092.1
75	0.43	43.05	1094.3
90	0.69	58.02	1100.8
95	-	63.01	1102.9
110	-	77.98	1109.3

Having vapor pressure and relative humidity, we can find the humidity ratios. For air entering the tower $P_{v3} = 0.35(0.43) = 0.15$ psia. For air leaving the tower, $P_{v5} = 0.95(0.69) = 0.65$ psia. Therefore,

$$\omega_3 = 0.622(0.15)/(14.7 - 0.15) = 0.00641. \text{ Similarly,}$$

$$\omega_4 = 0.622(0.65)/(14.7 - 0.65) = 0.0287.$$

Substituting in Equation Ilc.4.8, we get:

$$\dot{m}_a = \frac{1E8(77.98 - 63.01)}{(0.0287 \times 1100.8 - 0.0064 \times 1094.3) - (0.0287 - 0.0064)38 + 0.171(90 - 75)} \approx 57E6 \text{ lbm/hr}$$

Substituting in Equation Ilc.4.6, we find

$$\dot{m}_5 = (0.0287 - 0.0064)57E6 \approx 1.3E6 \text{ lbm/hr.}$$

Thermal Design of Containment

The containment building is the last barrier against release of radioactive materials to the environment in the case of a hypothetical accident. There are several types of containments, the design of which depends on the type of the nuclear reactor and the architect engineer. For example, to deal with thermalhydraulic loads, BWR containments are equipped with a suppression pool while some types of PWR containment utilize large blocks of ice. Figure Ilc.4.4 shows the schematic of a PWR *large, dry containment*. With respect to thermalhydraulic loads, PWR containments should withstand the consequences of two types of postulated accidents; a loss of coolant accident (LOCA) and a main steam line break (MSLB). A LOCA refers to a primary side pipe break of the hot or the cold leg, such as a double-ended guillotine break at location a-a in Figure Ilc.4.4, for example. A MSLB refers to rupture of the main steam line inside the containment such as a double-ended guillotine break at break location b-b. The LOCA and MSLB are referred to as design basis accidents.

The PWR containment analysis for both LOCA and MSLB requires two key inputs, mass flow rate and enthalpy of the fluid flowing through the break into the containment. We analyze containment in both the design phase and during operation. In the design phase, our intention is to find the free volume, that can accommodate the mass and energy transfer so that the peak pressure and temperature are kept below the specified design limits. During operation, containment analysis is required subsequent to any modification that may impact the containment response to above postulated accidents. During plant operation, we therefore seek containment peak pressure and temperature for given free volume.

A containment building, or simply containment, is generally equipped with active safety systems such as spray and air coolers to provide a heat sink in the case of an accident. The containment structure and internals also absorb a substantial amount of energy during an accident, thus they are referred to as *passive heat sinks*. In the case of the containment structure, some heat is also transferred to the surroundings through the primer, paint, steel liner plate, and the one meter thick concrete wall. The heat source for the containment depends on the postulated accident and the reactor type. For a LOCA, the heat source includes the latent heat

of the primary-system inventory, the sensible heat stored in the reactor system metals, and the decay heat of the fission fragments. For a MSLB in a PWR, the heat source includes the latent heat of water inventory of the secondary side, the sensible heat from the stored energy in the steam generator metals, and the heat transfer from the primary side through the tubes. Additionally, some exothermic chemical reactions, such as zirconium reacting with water at high temperatures, add to the containment thermal load. Handling the hydrogen produced in such chemical reactions is another constraint for the design of the containment. This discussion is summarized in Table IIc.4.1.

Below we perform a containment response analysis for both LOCA and MSLB to find peak pressure and temperature for a PWR large dry containment. Similar analysis exists for a BWR containment.

Table IIc.4.1. Factors affecting PWR containment response to accidents

Event	Heat Source	Heat Sink	Source of Emergency Cooling
LOCA	Decay heat*	Containment spray	High-pressure safety injection
	Coolant internal energy	Containment air coolers	Low pressure safety injection
	Metal Stored energy	Passive heat sinks	Safety water tanks
	Reactor pump heat		
	Exothermic reactions		
MSLB	Latent heat of coolant	Containment spray	Auxiliary feedwater
	Stored energy	Containment air coolers	
	Exothermic reactions	Passive heat sinks	

* See description in Chapter VIe.

Case A: Containment Response Analysis to LOCA in PWRs

In this case, we seek peak pressure for given containment volume. To obtain pressure and temperature versus time, we need to have the mass flow rate and enthalpy of the flow at the break as a function of time. We leave this rigorous treatment of containment analysis to Chapter VI d. For now, we include the primary side of the reactor in the containment control volume (Figure IIc.4.5). For this control volume, there is no flow entering or exiting and no shaft or expansion work. We then find containment peak pressure by integrating the simplified form of Equation IIa.8.1 from the initial to the final state. The initial state refers to the primary system being intact. The final state refers to a condition at which the primary side has discharged most of its inventory to the containment and has reached thermal equilibrium with the containment.

In the analysis that follows, m_{v1} is the initial mass of water vapor in the containment atmosphere, m_{w1} is the initial mass of water in the primary-system. Similarly, V_{v1} is the free volume of the containment (according to the Dalton’s model, $V_{v1} = V_a$) and V_{w1} is the volume of the primary-system. Finally, m_{w2} is the total mass of water and steam in $V_{v1} + V_{w1}$. Similar subscripts are used for the internal energy terms.

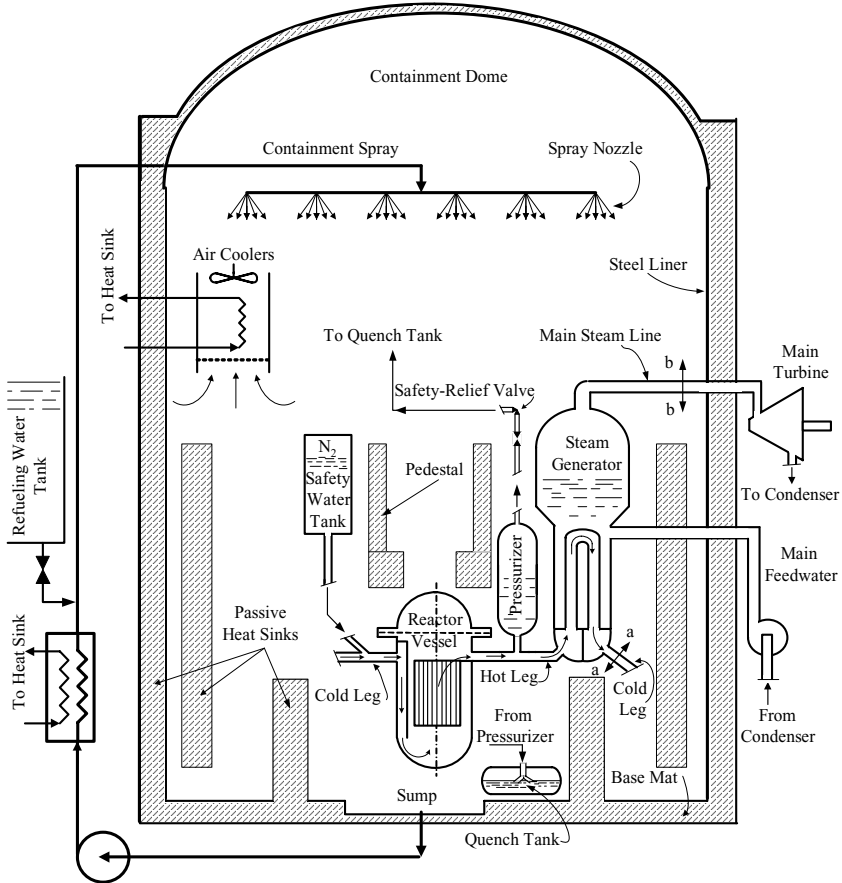


Figure IIc.4.4. Schematic of a PWR Large Dry Containment

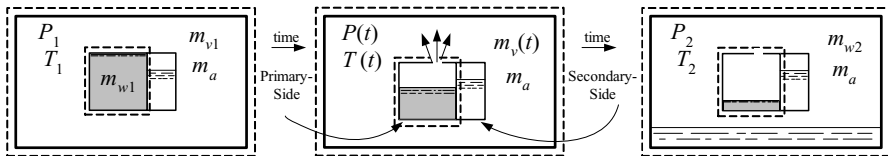


Figure IIc.4.5. Depiction of a LOCA in a PWR containment

From Equation IIa.8.1 for water and steam we find:

$$m_{v1} + m_{w1} = m_{w2} \quad \text{IIc.4.9}$$

From Equation IIa.8.2 for air, water, and steam we find (see Table IIc.4.1 for sources and sinks of energy):

$$m_a u_{a1} + m_{v1} u_{v1} + m_{w1} u_{w1} + Q_{Decay} + Q_{Metal} + Q_{Pump} - Q_{Spray} - Q_{Cooler} - Q_{Structure} \\ = m_a u_{a2} + m_{w2} u_{w2}$$

To maximize the energy transfer to the containment atmosphere, we drop all energy removal terms due to the action of spray and air cooler, as well as the heat absorption in the containment structure:

$$m_a u_{a1} + m_{v1} u_{v1} + m_{w1} u_{w1} + Q_{Decay} + Q_{Metal} + Q_{Pump} = m_a u_{a2} + m_{w2} u_{w2} \quad \text{IIc.4.10}$$

We have three unknowns, m_{w2} , u_{w2} , and T_2 . To complete the set, we use the volume constraint:

$$v_{w2} = (V_{w1} + V_{v1})/m_{w2} \quad \text{IIc.4.11}$$

Since the mass transfer in a LOCA from the primary side to the containment is primarily in the form of a two-phase mixture, we expect that the containment atmosphere becomes saturated in steam, yielding $\phi_2 = 1$. To solve the above set of three equations, we substitute for m_{w2} from the continuity equation into the energy equation and the volume constraint. We then assume a steam quality x_2 , and iterate on T_2 between the two equations and the steam tables.

Example IIc.4.5. The primary side of a PWR has a volume of 11,000 ft³ (311.5 m³). The reactor is operating at an average pressure of 2200 psia (15 MPa) and average temperature of 575 F (302 C). Containment initial conditions are given as 16.5 psia (114 kPa), 125 F (52 C), and 20% relative humidity. Containment volume is 2E6 ft³ (56,636 m³). Find final equilibrium pressure following a LOCA.

Solution: For containment, we first find the initial steam partial pressure:

$$P_{v1} = \phi P_g(125) = 0.2 \times 1.9424 = 0.388 \text{ psia (2.67 kPa)}$$

We now find initial masses and energies for which we first find the thermodynamic properties as follows:

P (psia)	T (F)	$P_g(T)$ (psia)	v (ft ³ /lbm)	u (Btu/lbm)
0.388	125	1.9424	898	1052.4
2250	575	—	0.0221	569.84

$m_{v1} = V_{v1}/v_1 = 2,000,000/898 = 2227 \text{ lbm}$. The air mass is found from $m_a = P_{a1}V_d/(R_aT_1)$. Since air pressure is $P_{a1} = P_1 - P_{v1} = 16.5 - 0.388 = 16.11 \text{ psia}$:

$$m_a = \frac{P_{a1}V_{a1}}{R_aT_1} = \frac{(16.11 \times 144) \times (2 \times 10^6)}{(1545/28.97)(460 + 125)} = 150015 \text{ lbm (68,047 kg)}$$

We now find the mass of water in the primary system as $m_{w1} = V_{w1}/v_{w1} = 11,000/0.0221 = 497737$ lbm. Hence,

$$m_{w2} = m_{v1} + m_{w1} = 2227 + 497737 = 499,964 \text{ lbm.}$$

From Equation Ilc.4.11 we find $v_2 = (2,000,00 + 11,000)/499,964 = 4 \text{ ft}^3/\text{lbm}$. Having v_2 , we guess a value for T_2 and read v_{f2} and v_{g2} from the steam tables to find x_2 as $x_2 = (v_2 - v_f)/v_{fg}$.

$$T_2 = T_1 + \frac{(m_{v1}u_{v1} + m_{w1}u_{w1}) - m_{w2}u_{w2}}{m_a c_{va}}$$

where we have only considered the coolant internal energy (see the comment below). We summarize the data we have found so far:

m_a lbm	m_{v1} lbm	m_{w1} lbm	u_{v1} Btu/lbm	u_{w1} Btu/lbm	m_{w2} lbm	v_{w2} ft ³ /lbm
150015	2227	497737	1052.4	569.84	499,964	4

$$m_{v1}u_{v1} + m_{w1}u_{w1} = 2227(1052.4) + 497737(569.84) = 2.859\text{E}8 \text{ Btu (3E8 kJ)}$$

We begin the iteration process by assuming a value for T_2 and find an updated value for T_2 as follows:

T_2 (F)	v_f (ft ³ /lbm)	v_{fg} (ft ³ /lbm)	u_f (Btu/lbm)	u_{fg} (Btu/lbm)	x_2 (-)	u_{w2} (Btu/lbm)	T_2 (F)
268.10	0.0172	10.3941	236.90	854.62	0.383	564.4	270

Since $\varepsilon = (270 - 268.10)/268.10 = 0.7\%$, we use 270 F as a reasonably accurate final temperature. Having final equilibrium temperature, we find:

$$P_{w2} = P_g(268.1 \text{ F}) = 40.73 \text{ psia (281 kPa)}$$

$$P_{a2} = m_a R_a T_2 / (V_{w1} + V_{v1}) = 150015 \times 53.33(268.1 + 460) / 2,011,000 = 8.68 \text{ psia (59.8 kPa)}$$

Therefore, final equilibrium pressure is $P_2 = P_{w2} + P_{a2} = 40.73 + 8.68 = 49.4 \text{ psia (341 kPa)}$.

Comment: In this solution, we only accounted for the internal energy of the primary side coolant and did not consider the heat addition from all other sources. If the pumps are tripped, their contribution to the energy equation is eliminated. However, inclusion of the decay heat and the sensible heat of the reactor structure and its internals (metal stored energy) requires detailed knowledge of the system. If we assume that the contribution from the decay heat and stored energy in the above example is $Q_{Total} = 25\text{E}6 \text{ Btu}$, we may follow the same steps outlined above to find $T_2 = 276 \text{ F}$ and $P_2 = 64.7 \text{ psia}$. The method of obtaining the pressure and temperature trends for containment response is discussed in Chapter VI d.

Case B: Containment Response Analysis to MSLB in PWRs

In this case, we also seek the final equilibrium pressure for given containment volume, where the initial state refers to the steam generator being intact. The final state refers to thermal equilibrium between the broken steam generator and the containment. The control volume we choose consists of the containment and the

broken steam generator (Figure Ilc.4.6). As explained in Case A, the selection of such a control volume eliminates the need for having the break mass flow rate and enthalpy versus time. On the other hand, such treatment precludes us from predicting the trend of the containment pressure and temperature during the event. The same sets of equations we developed for LOCA are also applicable here. However, in a MSLB, mass transfer from the broken steam generator to the containment is primarily in the form of dry steam. Therefore, we expect that the containment atmosphere becomes superheated in steam, yielding $\phi_2 < 1$.

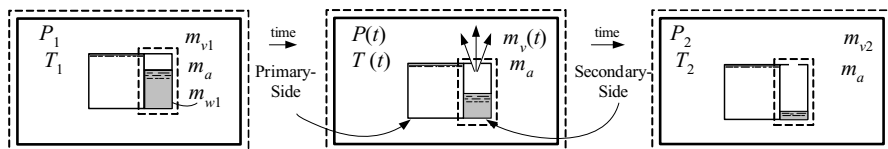


Figure Ilc.4.6. Depiction of a MSLB in a PWR containment

In this case, like Case A, we use the Dalton law of partial pressures for volume constraint. However, we calculate the partial pressure of the superheated steam from the ideal gas law, per Equation Ilc.4.5. This is a reasonable approximation in the range of interest for pressure and temperature:

$$P_2 = m_a R_a T_2 / (V_{v1} + V_{w1}) + m_{v2} R_v T_2 / (V_{v1} + V_{w1}) \quad \text{Ilc.4.12}$$

Example Ilc.4.6. The secondary side of a PWR steam generator has a volume of 227 m³ of which 75 m³ is water. Steam generator pressure is 6.21 MPa. Initial containment pressure, temperature, and relative humidity are 0.101 MPa, 50 C, and 50%, respectively. Containment volume is 56,636 m³. Find the final equilibrium pressure and temperature following a MSLB. The amount of heat transferred from the primary side to the secondary side is 897.6E8 J.

Solution: The initial vapor mass in the containment is found from

$$P_{v1} = \phi P_g(50 \text{ C}) = 0.5 \times 0.0123 = 0.00615 \text{ MPa}$$

We can find vapor mass from either the steam tables or the ideal gas law. From the steam tables

$$v(0.00615 \text{ MPa} \text{ \& } 50 \text{ C}) = 24.7 \text{ m}^3/\text{kg}.$$

Hence, the vapor mass is found as:

$$m_{v1} = 56,636 / 24.7 = 2293 \text{ kg}$$

From the ideal gas law, $m_{v1} = 6150 \times 56,636 / [(8314/18) \times (273 + 50)] = 2335 \text{ kg}$. The error in the calculation of vapor mass by using the ideal gas law is less than 2%. Similarly, for air mass

$$m_a = (101000 - 6150) \times 56,636 / [(8314/28.97) \times (273 + 50)] = 58,000 \text{ kg}$$

The initial mass of water and steam in the secondary side of the steam generator can be calculated from the specific volumes, found from the steam tables. For water, $m_{f1} = 75/0.0013 = 57,692$ kg. For steam, $m_{g1} = (227 - 75)/1.69 = 4,841$ kg. Therefore, $m_{w1} = 4841 + 57,692 = 62,533$ kg. We also find $x_1 = m_{\text{steam}}/m_{\text{water}} = 4841/62,533 = 0.077$. Therefore,

$$u_{w1} = 1216.75 + 0.077 \times 1370.79 = 1322.86 \text{ kJ/kg.}$$

To summarize;

m_a (kg)	m_{v1} (kg)	m_{w1} (kg)	u_{v1} (kJ/kg)	u_{w1} (kJ/kg)	m_{v2} (kg)
58,000	2293	62,533	2441.36	1323	64,826

We now guess T_2 , and find P_{v2} , from Equation IIc.4.12. Assuming $T_2 = 210$ C we find P_{v2} :

$$P_{v2} = [67826 \times 462 \times 483/56863] = 0.254 \text{ MPa}$$

We use the calculated P_{v2} and the assumed T_2 to find u_{v2} from the steam tables as $u_{w2} = 2,667$ kJ/kg. Having the final internal energies, the final temperature can be found from Equation IIc.4.10:

$$T_2 = T_1 + \frac{(m_{v1}u_{v1} + m_{w1}u_{w1} + Q_{\text{Primary-Secondary}}) - m_{w2}u_{w2}}{m_a c_{va}}$$

Substituting values for masses, internal energies, and heat transfer between primary and the secondary:

$$T_2 = 50 + \frac{(2293 \times 2441.36 + 62,533 \times 1323 + 0.898\text{E}8) - 64,826 \times 2.667}{58000 \times 0.713} = 176 \text{ C}$$

We continue the iteration until the convergence criterion is met. The final answer is $T_2 = 200$ C and $P_2 = 0.393$ MPa.

Comment: This is a useful method to find the final state inside the containment following a MSLB (or a LOCA). In practice, the conservation equations of mass and energy are integrated over a small time step to obtain u and v . The corresponding P and T are found in a pressure search process. This process is repeated until the end of the specified duration is reached.

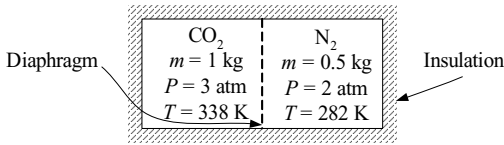
QUESTIONS

- What is the difference between the Dalton and the Amagat model?
- Apply the Amagat model to Example IIc.1.2. What conclusion do you reach?
- In a containment of a nuclear plant, the relative humidity is measured as 35% and in the containment of another plant, it is measured as 70%. If both containments are at the same temperature and total pressure, which containment has higher steam pressure? If both containments have also equal volumes, which containment has higher air mass?
- Consider an unsaturated moist air at total pressure P , temperature T , and relative humidity ϕ . What is the significance of $P_g(T)$ and of $T_g(P_v)$?

- Is the dew point temperature reached in an isochoric or an isobaric process?
- Describe the humidification process.
- Consider a fully insulated system consisting of two regions. The first region contains water at P_1 and T_1 . This region is separated from the second region by a thermally conducting membrane. The second region contains moist air also at P_1 and T_1 with $\phi = \phi_1 < 1$. The membrane is now removed and $\phi_2 = 1$. Is $P_2 > P_1$?
- Why is there a need for makeup water in the operation of cooling towers?
- Consider the large dry containment of a PWR. There are many internals in the containment such as pedestals, pipe supports, polar crane, stairways, etc. The obvious disadvantage of the containment internals is to reduce the free volume of the containment. From a thermodynamic point of view, what is the advantage of having the internals in the containment during a design basis accident?
- With respect to containment response, what are the two major differences between a LOCA and a MSLB?

PROBLEMS

1. A tank, having a volume of 5 m^3 , is filled with N_2 and 2 kg of CO_2 at a pressure and temperature of 150 kPa and 50 C, respectively. Find the partial volumes according to the Amagat and the partial pressures according to the Dalton model.
2. A rigid tank contains 1 kg of nitrogen at 38 C and 2 MPa. We now add oxygen to the tank in an isothermal process until the pressure in the tank reaches 2.76 MPa. Find the mass of oxygen that entered the tank in this process. [Ans.: 0.35 kg].
3. Consider a room having a volume of 75 m^3 maintained at $P = 1 \text{ atm}$, $T = 25 \text{ F}$ and $\phi = 70\%$. a) Use the Dalton model to find the partial pressures of air and water vapor. b) Use the Amagat model to find the partial volumes of air and water vapor. What conclusion do you reach about the applicability of the Amagat model to water vapor? [Hint: In case b, find the state of the water vapor from the steam tables by having its pressure and temperature].
4. A large dry containment of a PWR has a volume of $2\text{E}6 \text{ ft}^3$. At normal operation, the mixture of air and superheated steam is at a total pressure of 1.8 psig (16.5 psia) and temperature of 125 F. The relative humidity in the containment is measured as 30%. Find the masses of air and steam in the containment.
5. A cylinder contains 0.8 lbm of CO_2 and 0.5 lbm of N_2 at 18 psia and 80 F. In a polytropic process ($n = 1.25$), the content is compressed to 65 psia. Find final temperature, the work, the heat transfer, and the change in the mixture entropy.
6. Consider two well insulated-tanks as shown in the figure. The tanks contain carbon dioxide and nitrogen at the given pressures and temperatures. The thermally non-conductive diaphragm is now removed. Find the final temperature and pressure of the mixture at equilibrium.



[Hint: Since the tanks are well insulated, there is no heat transfer with the surroundings. Since the boundaries are fixed, there is no work. Hence, from the first law, $U_2 = U_1$].

7. Two steady flow streams of gases at different pressure and temperature are merged into one stream in a adiabatic process. Use the given data to find the temperature of the merged streams. Data: One stream consists of 2.3 kg of nitrogen at 103.5 kPa and 150 C. The other stream consists of 1 kg of CO_2 at 138 kPa and 38 C. [Ans.: 120 C].

8. A cylinder contains gases with the following volumetric analysis: 13% CO_2 , 12% O_2 , and 75% N_2 . Find c_p , c_v , and R for this mixture of gases. Specific heat at constant pressure of CO_2 , O_2 , and N_2 are given as 1.271 kJ/kg K, 1.11 kJ/kg K, and 1.196 kJ/kg K, respectively.

9. Find the dew point temperature for an unsaturated moist air at $P = 15 \text{ psia}$, $T = 120 \text{ F}$, and $\phi = 30\%$. [Ans: $T_{\text{Dew Point}} = T_g(P_v) \approx 80 \text{ F}$].

10. Find an expression for relative humidity in terms of ω

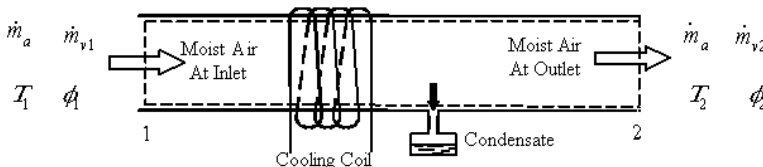
[Ans: $\phi = (\omega/0.622)\{P_a/P_g(T_v)\}$ or alternatively $\phi = \{\omega/(0.622 + \omega)\}\{P/P_g(T_v)\}$].

11. Find the mass fraction of water vapor in moist air at 30 psia, 200 F, and 65%.

12. Consider 5-lbm sample of moist air initially at 20 psia, 150 F, and 50% relative humidity. This mixture is cooled at constant pressure to 70 F. Find a) the humidity ratio at state 1, b) the dew point temperature at states 1 and 2, and c) the amount of condensate at state 2.

13. A rigid tank contains 0.5 kg of moist air at 1.034 MPa, 160 C, and $\phi = 100\%$. We now cool the tank until its temperature drops to 82 C. Find a) the amount of heat removed and b) the amount of condensate produced in this process. [Ans.: - 914 kJ and 0.4 kg].

14. Moist air at 15 psia, 90 F, and a relative humidity of 60% enters a cooling duct at a rate of 1200 ft^3/m . Temperature of the saturated mixture at the exit of the cooling coil is 65 F. Assuming negligible pressure drop, find the mass flow rate of the condensate produced in the cooling duct.



15. Determine the amount of condensate, the final pressure, and heat transfer in the cooldown process of a sample of moist air. The process takes place in a rigid container having a volume of 35 m^3 . Moist air is initially at 1.5 bar, 120 C, and 10%. The final temperature is 22 C. [Ans.: 3.15 kg].

16. Consider constant-volume cooldown of a mixture of water vapor and nitrogen in a 17.66 ft^3 container. The mixture is originally at 122 F, 290 psia, and 40% relative humidity. The mixture is cooled to 50 F. Find the heat transfer in this process. [$Q_{CV} = -321 \text{ Btu}$]

17. Find the relative humidity in a room at a temperature of 20 C. The wet bulb temperature is 15.5 C.

[Ans.: 63%].

18. In Example IIC.4.2, we assumed that all of the incoming steam is condensed in the quench tank. Find the final pressure assuming that 5% of the steam escapes from the pool region to the vapor region.

19. A power plant uses a cooling tower as the heat sink. The net power produced by the plant is 270 MWe. The plant thermal efficiency is 35%. Use these and other pertinent data given below to find a) the mass flow rate of air and b) the mass flow rate of make up water.

circulating water: inlet temperature $T_{wi} = 104 \text{ F}$ (40 C) and exit temperature $T_{we} = 86 \text{ F}$ (30 C)

air: inlet temperature $T_{ai} = 77 \text{ F}$ (25 C), relative humidity $\phi_i = 35\%$, air exit temperature $T_{ae} = 95 \text{ F}$ (35 C) and relative humidity $\phi_e = 90\%$

make-up water: inlet temperature $T_{mw} = 68 \text{ F}$ (20 C).

[Ans.: for air: $57.83\text{E}6 \text{ lbm/h}$, for makeup water: $1.366\text{E}6 \text{ lbm/h}$].

20. A BWR containment design is suggested as shown in the Figure. The reactor is isolated within a drywell compartment. A rupture disk caps the end of a duct leading into a vapor suppression pool of water. The pool is inside a secondary compartment. The rupture disk fails at a differential pressure of 60 psi (0.414 MPa). Now consider the case of a main steam line break. Use the following data to find the time that the rupture disk fails.

Drywell: initial temperature $T_i = 100 \text{ F}$ (38 C), initial pressure $P_i = 14.7 \text{ psia}$ (0.1013 MPa), initial relative humidity $\phi_i = 0\%$, and free volume $V_{drywell} = 5\text{E}5 \text{ ft}^3$ ($14.16\text{E}3 \text{ m}^3$).

Secondary-containment: initial pressure = 14.7 psia (0.1013 MPa), and free volume = $5\text{E}6 \text{ ft}^3$ ($14.16\text{E}4 \text{ m}^3$)

Suppression pool: water volume = $2.3\text{E}5 \text{ ft}^3$ ($6.5\text{E}3 \text{ m}^3$) and initial temperature = 100 F (38 C).

Steam blowdown: steam mass flow rate from the steam line to the drywell $\dot{m} = 500 \text{ lbm/s}$ (227 kg/s) for the duration of $t < 360 \text{ s}$ and $\dot{m} = 500e^{-t/\theta} \text{ lbm/s}$ ($227e^{-t/\theta} \text{ kg/s}$) for $t \geq 360 \text{ s}$ and $\theta = 100 \text{ s}$. In order to avoid the necessity of an iterative solution, use the following simplifying assumptions:

- a) the atmosphere components are uniformly mixed and in thermodynamic equilibrium,
 b) air can be treated as an ideal gas,
 c) no heat loss from the reactor to the drywell atmosphere,
 d) no steam condensation on the drywell walls,
 e) blowdown takes place at a constant reactor pressure of 500 psia (3.45 MPa) for the duration of interest
 f) no heat loss from drywell through the walls
 g) steam may be treated as an ideal gas so that $u_{\text{Steam}} = u_g + c_{v,\text{Steam}}(T - T_{\text{sat}})$ and $h_{\text{Steam}} = h_g + c_{p,\text{Steam}}(T - T_{\text{sat}})$, where $u_g = 1098$ Btu/lbm (2554 kJ/kg), $h_g = 1180$ Btu/lbm (2744 kJ/kg), and $T_{\text{sat}} = 776$ R (431 K).
 [Ans.: $t = 89$ s, $P_2 = 70$ psia, $T_2 = 475$ F (246 C), $\phi_2 = 12\%$, $m_a = 35,439$ lbm (16,286 kg)].

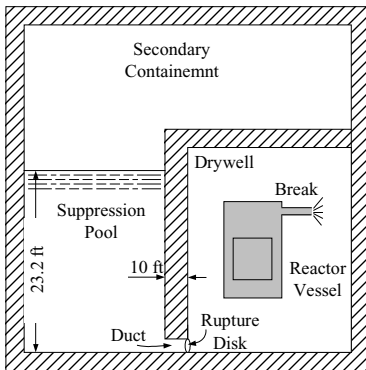


Figure for Problem 20

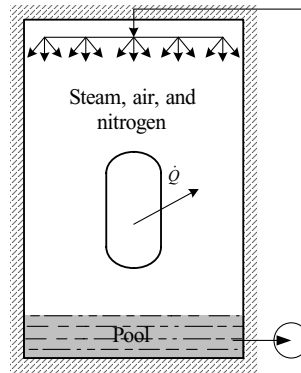


Figure for Problem 21

21. A large containment is filled with steam, air, and nitrogen. The containment also has a pool of water, which is sprayed in the containment atmosphere. Heat is added to the containment at a specified rate. Use the given data to find a) the initial containment pressure and b) the time it takes for the containment pressure to reach the pressure limit of 145 psia (1 MPa).

Total mass of water (water in the pool and steam) $m_w = 3.42\text{E}6$ lbm (1.55E6 kg)

Water-steam quality $x = 0.03$

Air mass $m_a = 0.132\text{E}6$ lbm (6E4 kg)

Nitrogen mass $m_n = 2200$ lbm (998 kg)

Containment initial temperature $T_i = 688$ R (109 C)

Initial relative humidity $\phi_i = 100\%$

Rate of heat addition to containment atmosphere $\dot{Q} = 1.02\text{E}8$ Btu/h (30 MW)

[Ans.: 7.66 h].

III. Fluid Mechanics

Topics in single-phase flow range from such simple phenomena as the flow of water in a pipe to such exotic phenomena as supersonic flow and shock waves. The study of fluid mechanics is based on thermodynamic principles and Newton's* second law of motion. Fluid mechanics is the basis for such diverse fields as acoustics, aerodynamics, biofluids, combustion, fire protection, magnetohydrodynamics, meteorology, and oceanography. Since the field of fluid mechanics is vast, it is traditionally divided into several categories to facilitate the study of its related topics. Here we briefly discuss the various categories involved in the study of fluid mechanics. The unfamiliar terms used in this discussion are defined and dealt with as we pace through the chapter.

One way to categorize the field of fluid mechanics is to consider the number of phases involved in the flow. Single-phase flow considers only the flow of one fluid such as water, air, steam, etc. On the other hand if water and steam for example coexist in the flow, we then need to use the two-phase flow principles to study such a condition. Single-phase flow is discussed in Chapter IIIa through IIIc and two-phase flow in Chapter Va.

Another way to categorize the study of fluid mechanics is to consider whether the flow of fluid is confined to a conduit or whether the fluid is flowing over an object placed in the flow field. If the flow is confined to a conduit we are dealing with internal flow. In such cases, we may be interested in determining the pumping power required to establish certain flow rate. If the conduit is a piping network, flow distribution in the network is of interest. On the other hand, if fluid flows over an object, the condition is known as external flow such as the flow of air over an airplane or the motion of a boat in water. External flow covers such topics as lift and drag as well as flow of fluids in open channels. Chapter III is mostly concerned with the internal flow of fluids. Some aspects of external flow are discussed in Chapter IV.

Further categorization may be based on such physical properties of the fluid as density and viscosity. As discussed later in this chapter with regard to density, fluid may be considered incompressible like flow of liquids in a pipe or a fluid may be compressible like flow of a gas in compressor. With regard to viscosity, we consider two cases of real and ideal fluids also referred to as viscous and inviscid, respectively. Viscous effects are associated with friction. The advantages inherent in the ideal flow assumption enable us to obtain analytical solutions in closed form to describe the flow behavior in certain conditions. Unlike ideal flu-

* Sir Issac Newton (1643–1727) also contributed to calculus, optics, astronomy, fluid mechanics, and heat transfer

ids, which are incompressible and inviscid, dealing with real fluids involves pipe roughness and such topics as unrecoverable frictional pressure drop. Chapter III deals primarily with the flow of real fluids.

All of the above categories may be analyzed under steady state or transient conditions. At steady state, there is no change in flow properties such as pressure, velocity, and density with time. Transient analysis on the other hand is required when there is a change in flow conditions. Examples of flow transients include throttling a valve on a pipe carrying flow, turning off a running pump, or draining a vessel. Chapter IIIb deals with both steady state and transient analysis of viscous incompressible internal flows.

There are still other categorizations such as *hydrostatics* versus *hydrodynamics* and the type of flow regime, (i.e. laminar versus turbulent). In this book, fluid mechanics is divided into four chapters. In Chapter IIIa, we first discuss the fundamentals that are applicable throughout fluid mechanics. This includes derivation of the conservation equations for single-phase flow. The conservation equations for linear momentum and energy are used in conjunction with multiple simplifying assumptions to derive the Bernoulli equation. This is followed by the discussion on the concept of “*head loss*”. Chapter IIIb deals with incompressible viscous flow through pipes, fittings, and in piping networks. Chapter IIIb is then concluded with the study of unsteady flow of incompressible fluids. This includes the discussion of such topics as tracking liquid level in surge tanks, time to drain vessels, time to fill drained pipelines, and learning the fundamentals of such fast transients as “*waterhammer*”. Flow of compressible viscous fluids including critical flow through pipe breaks is discussed in Chapter IIIc and the fundamentals of two-phase flow in Chapter Va.

IIIa. Single-Phase Flow Fundamentals

1. Definition of Fluid Mechanics Terms

Stress is the result of applied force per unit area. The applied force acting on a surface consists of two components one normal to the surface and the other parallel or tangent to the surface. The component normal to the surface if divided by the surface area is referred to as normal stress (σ). A shear stress (τ) is developed due to the action of the tangential component on a surface.

Fluid is a substance that, under an applied shear stress deforms continuously. A deformation always exists regardless of how small the applied stress might be. There is no shear stress only when fluid is at rest. Depending on the magnitude of the acting shear force, solids would initially deform. However, unlike fluids, such deformation is not continuous. Any substance that is not fluid may be considered solid. Fluids we are familiar with include liquids and gases. There are a few substances, such as toothpaste categorized as fluid even though they are neither a fluid nor a solid. These are known as Bingham Plastic.

Continuum hypothesis is the fundamental principle in thermofluids. In most cases, it is impractical to study fluid behavior on a molecular basis. Therefore, we use a macroscopic approach, defining a differential volume to represent a point in the fluid. By using the average values for each point, fluid properties then vary continuously throughout the fluid. Thus by ignoring the behavior of individual molecules of the fluid and assuming that the fluid consists of continuous matter*, we can define unique values for the flow variables; P , T , V , τ , ρ , etc. For example, we define density at a point for fluid as a continuum according to:

$$\rho = \lim_{\delta V \rightarrow \delta V'} (\delta m / \delta V) \quad \text{IIIa.1.1}$$

where $\delta V'$ is a differential volume yet contains sufficient number of molecules to make statistical averages meaningful. For all liquids and for gases at atmospheric pressure, the limiting volume is about 10^{-9} mm^3 . Having defined flow field variables at a point, we use partial derivatives to determine the change in such variables between two points separated by elements of length. For example, if pressure at point x, y, z is P , pressure at a point located dx, dy , and dz apart is $P + dP$ where $dP = (\partial P / \partial x)dx + (\partial P / \partial y)dy + (\partial P / \partial z)dz$.

Field refers to the flow variables (or parameters), such as pressure, velocity, temperature, or density, as a function of position in a given region, which may also be a function of time. For density for example, this is shown as $\rho = \rho(t, x, y, z)$.

Coordinate systems are used to represent the properties of a flow field in space at any point in time. A fluid element in the flow field is determined by its position vector. The position vector in Cartesian coordinates for example is expressed as $\vec{r} = r_x \vec{i} + r_y \vec{j} + r_z \vec{k}$ where \vec{i} , \vec{j} , and \vec{k} are the unit vectors. Similarly, the velocity vector in Cartesian coordinates is comprised of three components; V_x , V_y , and V_z . In the literature, these are often represented with u , v , and w . The components of flow velocity in cylindrical and spherical coordinates are represented by V_r, V_θ, V_z and V_r, V_θ, V_ϕ respectively.

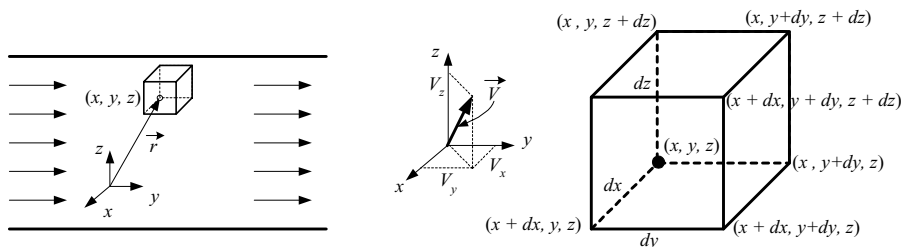


Figure IIIa.1.1. Position vector, velocity vector, and a differential volume in Cartesian coordinates

* A statistical approach is used for special cases to which the continuum assumption does not apply. An example of such cases includes the passage of a rocket through the outer layer of the atmosphere.

Body and surface forces are encountered in fluid statics and fluid dynamics. Body forces consist of all forces that are developed in the fluid without physical contact. Body forces are distributed over the volume of the fluid. Electromagnetic and gravitational forces are examples of body forces arising in a fluid. Surface forces such as shear and normal stresses on the other hand act on the boundaries of a fluid through direct contact. A body force therefore is proportional to the volume or mass, whereas surface forces, such as pressure and shear stress, are proportional to the area. An element of a fluid in the Cartesian coordinate system consists of six boundaries. Each boundary experiences two shear stresses tangent to the boundary and a normal stress perpendicular to the boundary. These are shown with two-letter subscript. The first index in the subscript refers to the axis to which the boundary is perpendicular and the second index in the subscript refers to the axis to which the stress component is in parallel. Hence, τ_{yz} refers to the shear stress in the boundary the plane of which is perpendicular to the y -axis and the direction of the stress, which is parallel to the z -axis. The nine component stress tensor, also referred to as the stress matrix, is also shown in Figure IIIa.1.2. Note, that $\sigma_x = -P + \tau_{xx}$, $\sigma_y = -P + \tau_{yy}$, and $\sigma_z = -P + \tau_{zz}$ where σ implies normal to the plane of its associated index.

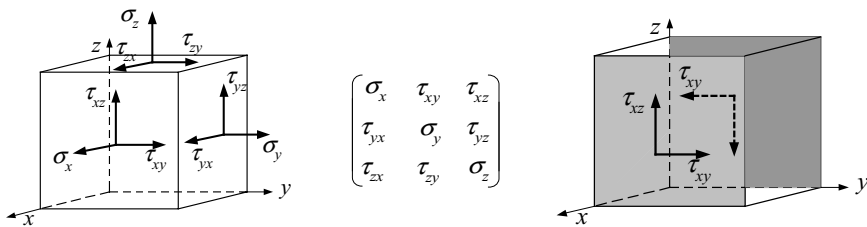


Figure IIIa.1.2. Normal and shear stress components of an elemental control volume

Fluid kinematics and fluid dynamics both describe a flow field. The motion of a fluid in a flow field is the basis of fluid kinematics. The effects of forces on fluid motion are studied in fluid dynamics.

Kinematic properties refer to such quantities as linear velocity, angular velocity, vorticity, strain rate, and acceleration. Note that these are properties of the flow field rather than the fluid. Thermodynamics and transport properties as well as extensive and intensive properties were discussed in Chapter II.

Shearing strain is described below by comparing the response of a piece of solid to an applied shearing force with the response of a liquid to the same applied force. Shown in the left side of Figure IIIa.1.3 is a solid such as steel, firmly attached to two plates. The lower plate is fixed while the upper plate is allowed to move. If we now apply force F to the upper plate, in the case of steel we cause point B to move a small distance to point B'. The application of force F also causes shear stresses to be created at the interface between the steel and the upper

plate to resist the applied force. The free-body diagram of the moving plate shows (the center figure) that at equilibrium, $F = \tau A$. The angle $\delta\alpha$ is referred to as the shearing strain ($\gamma = \lim(\delta\alpha/\delta t)$ as δt approaches zero). If we now apply the same force to the plate in the right side of the Figure IIIa.1.3, it moves continuously.

In solids, the shear stress (τ) is related to the shearing strain, $\tau = f(\gamma)$. For viscous fluids, $\delta\alpha$ is a function of time as the upper plate is moving continuously due to the applied force. In fluids, we therefore relate the shear stress to the *rate of change of the shearing strain* ($\dot{\gamma}$) also known as shear rate, $\tau = f(\dot{\gamma})$. From the linear velocity profile we can easily show that the rate of strain is equal to the slope of velocity $\dot{\gamma} = dV_x/dy$.

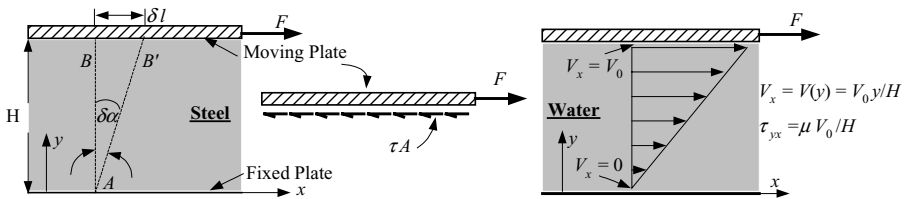


Figure IIIa.1.3. Shear stress as a function of velocity gradient

On the other hand, we also know that the rate of shearing strain is proportional to the shear stress ($\tau \propto \dot{\gamma}$), which in turn is proportional to the applied force F , ($\tau A = F$). Thus $\dot{\gamma}$ increases as τ increases. Therefore, the shear stress is proportional to the slope of the velocity profile $\tau \propto dV_x/dy$. For this relation to be equal, we need a proportionality factor as discussed next.

Dynamic viscosity is the proportionality factor for shear stress and the velocity profile. The dynamic viscosity, also referred to as molecular viscosity or simply viscosity, is the most important property of a fluid. It is a measure of the response of a fluid to an applied shear force. Mathematically we can write:

$$\tau = \mu(T) dV_x/dy \quad \text{IIIa.1.2}$$

where μ is viscosity and V_x is the component of velocity along the x -axis. In this case, shear stress acts on a plane normal to the y -axis. This mathematical relation is a statement of *Newton's law of viscosity*, showing that the velocity gradient is the driving force for momentum transfer. Viscosity, similar to density, is a function of temperature. Change of viscosity versus temperature depends on the type of fluid. For gases, viscosity increases with temperature. For liquids, viscosity decreases as temperature increases.

Units of viscosity can be obtained from the definition of viscosity. Using shear stress as force per area and velocity gradient as the inverse of time, units of viscosity can be found as FT/L^2 . In British units, viscosity is expressed as $\text{lbf}\cdot\text{s}/\text{ft}^2$.

However, in most cases, viscosity is multiplied by g_c to obtain units of $\text{lbm/ft}\cdot\text{s}$. In SI units, viscosity is generally given in centi-poise where $1 \text{ poise} = 1 \text{ g/s}\cdot\text{cm}$ or in units of $\text{Pa}\cdot\text{s}$. Note: $1 \text{ centi-poise} = 2.419 \text{ lbm/ft}\cdot\text{hr}$.

Kinematic viscosity is defined as the ratio of dynamic viscosity to density, $\nu = \mu / \rho$. Kinematic viscosity has units of ft^2/h or m^2/s . Note: in SI units, $1 \text{ Stoke} = 1 \text{ cm}^2/\text{s}$. Hence, $1 \text{ ft}^2/\text{s} = 92,903 \text{ cs}$ (centistokes).

Viscous and inviscid fluids are identified in the context of friction. A viscous fluid causes friction when it flows. If the friction is negligible, then the fluid is inviscid and the flow is considered to be ideal.

Ideal gas versus ideal fluid. To avoid any confusion, recall that we used the term “ideal gas” in Chapter IIa for any gas that conforms to the ideal gas rules. In this chapter, we use the “ideal fluid” term for any fluid which is incompressible and inviscid. Therefore while ideal gases at certain conditions may also behave as an ideal fluid, ideal gases are generally not ideal fluids. Conversely, many liquids under certain conditions may behave as an ideal fluid but they are clearly not ideal gases.

Newtonian fluid is a type of fluid where the rate of deformation due to the act of a shear stress is linearly proportional to the magnitude of the acting shear stress. Therefore, all fluids that obey the above relation for shear stress are Newtonian fluids. For example, water, benzene, alcohol and air are Newtonian fluids. Strictly speaking, for a fluid to be Newtonian, four criteria should be met. These criteria are discussed following the definition of the non-Newtonian fluids.

Non-Newtonian fluid is a fluid that does not conform to Newton’s law of viscosity, in that viscosity for these fluids is a function of shear rate, $\tau_{yx} = \mu(\dot{\gamma})dV_x/dy$. Non-Newtonian fluids include pseudo plastic, Bingham plastic, and Dilatants. Pseudo plastic materials include polymer solutions, most slurries, mud, and motor oil. Bingham plastic may indeed be considered Newtonian as they tolerate shear stress until the magnitude of the shear stress is equal to the yield stress of the fluid. Then the fluid flows. Examples of Bingham plastic include toothpaste, jellies, some slurries, bread dough, blood, and mayonnaise. Dilatant fluids are rare. The viscosity of such fluids increases with the increasing rate of deformation. The suspensions of starch and sand serve as an example of dilatant fluids, also referred to as shear thickening fluids. Finally, some non-Newtonian fluids demonstrate a transient period before reaching the intended velocity. These are known as viscoelastic materials, such as molten low-density polyethylene. Viscoelastics return only partially to their original configuration after being subjected to shear stress.

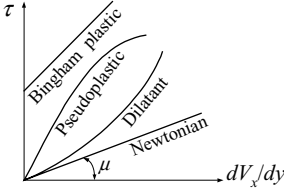


Figure IIIa.1.4. Shear stress versus the deformation rate for Newtonian and non-Newtonian fluids

Newtonian fluid criteria. Newtonian fluids meet four criteria. a) As discussed earlier, the stress is linearly dependent on the velocity gradient. b) Stresses due to an applied force are symmetric. Before discussing the other criteria let's elaborate. We derived a relation between flow velocity in the x -direction and the shear stress in a plane normal to the y -axis and parallel to the x -axis. The first criterion requires that $\tau_{yx} = \mu dV_x/dy = \tau_{xy}$. We also note that if the fluid flows in the direction of the y -axis, we can similarly write $\tau_{xy} = \mu dV_y/dx = \tau_{yx}$. In general, a fluid can flow in any arbitrary direction in the xy -plane. Hence, in general we should write:

$$\tau_{xy} = \tau_{yx} = \mu(dV_x/dy + dV_y/dx)$$

We can also write similar relations for flow in the xz - and yz - planes. In tensor notation;

$$\tau_{ij} = \tau_{ji} = \mu(dV_i/dx_j + dV_j/dx_i) \quad \text{IIIa.1.3}$$

c) Shear stress is related to the instantaneous value of the derivative of velocity. This criterion rules out the effect of some non-Newtonian fluids such as viscoelastic materials. d) For stationary fluids stress is isotropic. This is to exclude such other non-Newtonian fluids as Bingham plastic. Figure IIIa.1.4 shows the behavior of shear stress for various materials.

No-slip condition for Newtonian and non-Newtonian viscous fluids is an important concept in that a fluid does not have any motion relative to the solid boundary in contact with the fluid. Hence if the solid boundary is at rest, fluid velocity is zero. Likewise, if the solid boundary is a plate in motion, the fluid particle at the surface also moves at the same speed as the plate. Thus, as a boundary condition ($V_{\text{fluid}}|_{\text{surface}} = V_{\text{surface}}$).

Surface tension is a liquid property. There are inter-molecular forces in the interior of a liquid, which result in no net force applied to a molecule as the molecules are equally attracted to each other. However, for the molecules on the liquid surface, while the inter-molecular forces act towards the interior of the liquid, there are no forces to counter act. Hence, there is a net unbalanced cohesive force towards the interior of the liquid. Considering a semi-hemispheric drop of a liquid of radius R , we can represent the net unbalanced force as ΔP acting on the cross sectional area, πR^2 . Where $\Delta P = P_{\text{interior}} - P_{\text{exterior}}$. This force gives rise to surface

tension (σ) acting on the perimeter, $2\pi R$. Thus, the surface tension becomes $\sigma = \Delta P(\pi R^2)/2\pi R = \Delta PR/2$.

Bulk modulus is an indication of the fluid compressibility (i.e., density variation within a flow) and is defined as $E_v = dP/(d\rho/\rho)$. High values of bulk modulus indicate the fluid is nearly incompressible. Liquids have generally high bulk modulus hence, liquids, for most practical purposes, can be considered incompressible. Per above definition, the bulk modulus has the same dimensions as pressure. In British Units it can generally be written as psi and in SI units as Pa.

Speed of sound is a measure of propagation of disturbances in a fluid. The speed of sound is related to the fluid properties in which the disturbance is propagating. This relationship is expressed as $c = \sqrt{dP/d\rho}$. It can be shown that for ideal gases undergoing an isentropic process, the speed of sound is given as $c = \sqrt{\gamma RT}$ where T is the absolute temperature of the fluid and $\gamma = c_p/c_v$. The ratio of the speed of an object to the speed of sound in the same medium as that of the object is called the *Mach number* (Ma). If Ma is less than, equal, or greater than 1.0, the object is moving at a *subsonic*, *sonic*, or *supersonic* speed, respectively.

Streamlines are useful in relating the fluid flow velocity components to the geometry of the flow field. A streamline is defined as the line drawn tangent to the velocity vector at each point in a flow field. By definition, there is no flow across a streamline.

Steady and unsteady flows depend on the frame of reference. In the Eulerian approach, as described in Section 2, if flow at every point in the fluid is independent of time, then the flow is steady, otherwise it is unsteady (Figure IIIa.1.5).

Laminar and turbulent flows are applicable only to viscous fluid flow and are identified based on the streamlines. The laminar or purely viscous flow moves along laminas or layers. In laminar flow, there is no microscopic mixing of adjacent fluid layers. Turbulent flow has velocity components with random turbulent fluctuations superimposed on their mean values. The *Reynolds number*, after Osborne Reynolds (1842-1912), is a dimensionless variable whose value determines whether flow is laminar or turbulent. The Reynolds number is defined as $Re = \rho V \Delta / \mu$ where in this relation Δ is an element of length. For flow over a flat plate for example, $\Delta = L$ and for flow inside pipes, $\Delta = D$ where D is the pipe diameter. For external flow over flat plates, flow remains laminar as long as $Re < 5E5$ and for internal flow inside conduits flow remains laminar as long as $Re \leq 2000$.

Turbulent flow viscosity is of two types; molecular, μ as defined earlier, and eddy as defined in Chapter IIIb. The molecular viscosity of Newtonian fluids is independent of location, boundaries, and the flow regime (i.e., laminar or turbulent). The eddy viscosity on the other hand depends on all of these factors.

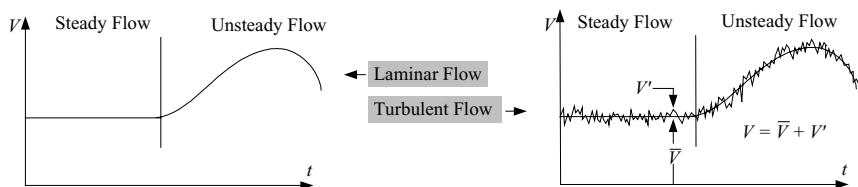


Figure IIIa.1.5. Variation of axial velocity with time for laminar and turbulent flows

Compressibility and incompressibility are flow properties in addition to being fluid properties and are based on the variation in fluid density. In an incompressible flow, the variation of density within the flow field is negligible. Generally, liquids may be considered incompressible, whereby density is a function of temperature and a weak function of pressure (hence, according to Equation IIa.6.7, $\Delta h \approx v \Delta P$). For water, the bulk modulus is about 3E5 psi (2 GPa) and as predicted by $dP = E_v d\rho/\rho$, it requires very high change in pressure to obtain a slight change in density. Therefore, in most cases flow of water may be considered *incompressible*. However, there are special cases (such as waterhammer, discussed in Chapter IIIc) that the compressibility of the liquid must be accounted for and the flow must be analyzed as *compressible*.

Compressibility in gases is more subtle. While gases are easily compressed (such as gas pressurization in compressors), in many applications gases may be treated as incompressible flow. Generally speaking, the compressibility effects for gases may be neglected as long as the flow velocity remains below 30% of the sonic velocity in the fluid. If a fluid is compressible, an abrupt change in pressure is not felt instantaneously throughout the flow field. In contrast, for incompressible fluids, such pressure disturbances are propagated at very high sonic wave velocity.

Boundary layer is a thin layer of fluid, developed whenever a flowing viscous fluid comes in contact with a solid. Velocity within this layer drops from the bulk fluid velocity, $(V_x)_f$ to zero at the surface of the solid. Laminar and turbulent boundary layers are compared in Figure IIIa.1.6. This figure also shows the comparison between the flow over a flat plate and inside a pipe. In both cases, flow velocity at the surface of the solid is zero and at the edge of the boundary reaches practically the velocity of the bulk stream. Hence, inside the boundary layer, viscous effects are present as the shear stress retards the flow. In the free stream, the viscous flow behaves as if it is inviscid. In the case of the flow inside a pipe, the region from the entrance to the pipe where the boundary layer is developing is known as the *entrance length* or *entrance region*. Subsequently, the boundary layer is established where flow is fully developed and a unique velocity profile exists. For flow over flat plates, transition from laminar to turbulent flow most likely occurs at $Re \cong 5E5$. For flow inside tubes, transition begins at $Re = 2000$ and flow becomes fully turbulent at $Re \geq 4000$.

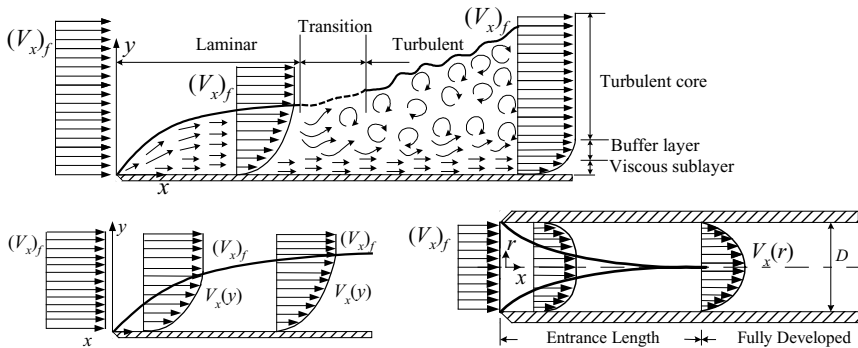


Figure IIIa.1.6. Comparison of boundary layers over a flat plate and in a pipe

Thickness of the boundary layer over a flat plate is a function of the distance from the leading edge and the Reynolds number. For example, for flow of air over a flat plate at 2 m/s and 27 C, the boundary layer thickness at 0.5 m from the leading edge is about 1 cm or 0.4 in.

Flow dimensions refer to the number of velocity components in a given coordinate system. Fluid flow, in general, is three-dimensional such as the plume from a cooling tower. However, in some applications, flow may be considered two or even one-dimensional, which greatly simplifies analysis. An example for the one-dimensional flow includes the fully developed region of viscous flows in a pipe as shown in Figure IIIa.1.7(a). Figure IIIa.1.7(b) shows the two-dimensional flow of a viscous fluid in a nozzle (variable flow area). Another example for a two-dimensional flow includes the developing flow of viscous flows in the entrance region of a pipe.

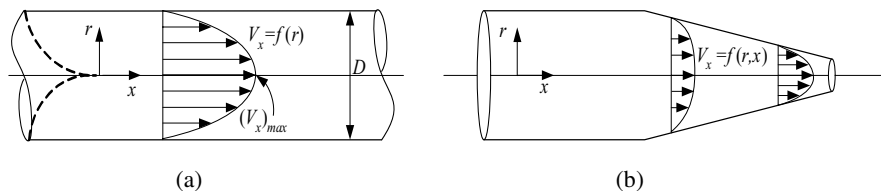


Figure IIIa.1.7. Examples of (a) one-dimensional and (b) two-dimensional flow

External and internal flows refer to conditions where a solid boundary is immersed in the flow or contains the flow, respectively. Analysis of external flow is essential for such engineering applications as tube banks, airfoils, ship hull, or blunt bodies. Lift and drag are phenomena pertinent to external flow. Analysis of internal flow is essential for such engineering applications as flow of fluids in pipelines, pumps, turbines, and compressors.

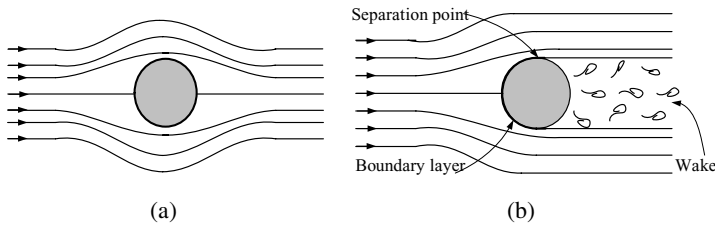


Figure IIIa.1.8. External flow over cylinder (a) ideal flow and (b) real flow

Shown in Figure IIIa.1.8 is a cylinder exposed first to an ideal flow and then to a real flow. In either case, the flow far from the body can be considered ideal, even in the case of the real flow. This is because far away from the cylinder, friction in the real flow is negligible especially for low velocity flow. As the flow approaches the cylinder (in the case of an ideal flow) the streamlines are squeezed to accommodate the cylinder and there is no friction. In the case of real flow, the boundary layer is developed in which flow velocity at the wall is zero. The velocity profile inside the boundary layer depends on the flow Reynolds number (i.e., laminar or turbulent). For ideal flow, the streamlines recover downstream of the cylinder to produce a symmetric pattern. Hence, pressures upstream and downstream of the cylinder are equal (i.e. there is no drag acting on the cylinder). This did not conform to the results obtained in experiments. Therefore, in the early days of fluid dynamics, this phenomenon was known as the d'Alembert's Paradox. With the introduction of the boundary layer by Prandtl in 1904, the existence of drag in real fluids was confirmed and the paradox resolved. Division of the flow by Prandtl into two regions of free stream with negligible friction and boundary layer where frictional effects are important is one of the most important contributions to the field of fluid mechanics.

Boundary layer separation. In real fluids, as flow passes the cylinder, there is a region in which a fluid particle moving in the boundary layer lacks sufficient kinetic energy to convert to enthalpy. The particle cannot then move into the higher-pressure region and the external pressure causes the particle to move in the opposite direction of the velocity profile. When this happens, separation of the boundary layer ensues. A vortex created as the result of this reverse flow is eventually detached from the surface to drift downstream of the cylinder to produce a turbulent wake behind the cylinder. This leads to the appearance of a wake behind the cylinder. The subsequent pressure drop gives rise to a drag acting on the cylinder. To reduce drag, the object must be streamlined. That is to say that if the cylinder is replaced with an airfoil, the gradual tapering of the trailing edge prevents separation of the boundary layer to a large extent, which then substantially reduces drag.

2. Fluid Kinematics

Earlier we defined the continuum hypothesis, allowing us to treat a fluid as a continuous matter and using such terms as *fluid element* and *fluid particle*. We shall

use this hypothesis to derive the conservation equations of mass, momentum, and energy. However, before we embark on the derivation, we need to define the frame of reference. In fluid mechanics, there are two frameworks. A flow field can either be described based on the motion of a specific fluid element or the motion of the fluid through a specific region in space. These frameworks are referred to as *Lagrangian* and *Eulerian* descriptions, respectively. In the Lagrangian approach, the trajectory of an individual particle is followed. In the Eulerian approach, the flow at every fixed point as a function of time is described. These frameworks are further described in the context of acceleration for a fluid element.

2.1. Fluid Acceleration

Prior to studying the dynamics of the fluid flow, we begin by deriving the acceleration of a fluid element in a flow field. Other aspects of fluid kinematics, such as fluid rotation, are discussed later in this chapter. The velocity of an infinitesimal fluid element in the Cartesian coordinate system based on the Eulerian description is expressed as:

$$\mathbf{V}(\vec{r}, t) = V_x[x(t), y(t), z(t), t]\vec{i} + V_y[x(t), y(t), z(t), t]\vec{j} + V_z[x(t), y(t), z(t), t]\vec{k}$$

IIIa.2.1

In Equation IIIa.2.1 \vec{i} , \vec{j} , and \vec{k} are the unit vectors of Cartesian coordinates. Also x , y , z , and t are four variables representing space and time. Finally, V_x , V_y , and V_z are the components of the velocity vector in the x , y , and z directions, respectively. In Figure IIIa.2.1, vector $\mathbf{V}(\vec{r}, t)$ represents the velocity of a fluid element at location \vec{r} at time t , while vector $\mathbf{V}(\vec{r} + d\vec{r}, t + dt)$ represents the velocity of the same fluid element, which has moved in time dt by $d\vec{r}$. According to the Lagrangian approach, the acceleration of the fluid element is given by $\vec{a} = d\vec{V}/dt$. Using the chain rule for differentiation (Chapter VIIa):

$$\vec{a} = \frac{d\vec{V}}{dt} = \frac{\partial \vec{V}}{\partial t} + \frac{\partial \vec{V}}{\partial x} \frac{dx}{dt} + \frac{\partial \vec{V}}{\partial y} \frac{dy}{dt} + \frac{\partial \vec{V}}{\partial z} \frac{dz}{dt}$$

IIIa.2.2

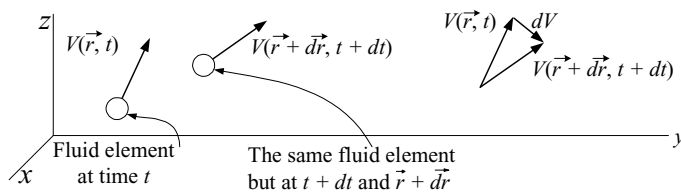


Figure IIIa.2.1. Velocity of a fluid element in Cartesian coordinates

By substituting for $dx/dt = V_x$, $dy/dt = V_y$, and $dz/dt = V_z$, Equation IIIa.2.2 can be rearranged to obtain:

$$\vec{a} = \frac{d\vec{V}}{dt} = \left(\frac{\partial \vec{V}}{\partial t} \right) + \left(V_x \frac{\partial \vec{V}}{\partial x} + V_y \frac{\partial \vec{V}}{\partial y} + V_z \frac{\partial \vec{V}}{\partial z} \right) \quad \text{IIIa.2.3}$$

Equation IIIa.2.3 is a vector equation. Therefore, it has three components for $\vec{a} = a_x \vec{i} + a_y \vec{j} + a_z \vec{k}$. Also the term in the first parenthesis represents the *local acceleration*, due to the change of flow velocity with time. This is because the *local derivative* ($\partial/\partial t$), is the rate of change of a fluid flow property as seen by an observer at a fixed position in space. Term d/dt is the total derivative.

Terms in the second parenthesis represent the *convective acceleration* due to the change of flow velocity in space*. The above relation can be simplified by noticing that the last three terms in the second parenthesis are dot products of the velocity vector and the gradient operator (see Chapter VIIc for the definition of the gradient operator in the three coordinate systems). Thus, in Cartesian coordinates we write:

$$\vec{a} = \frac{D\vec{V}}{Dt} = \left[\frac{\partial}{\partial t} + (\vec{V} \cdot \vec{\nabla}) \right] \vec{V} \quad \text{IIIa.2.4}$$

Note the change of notation in the left side of Equation IIIa.2.4 from d/dt to D/Dt , which is referred to as the *substantial derivative* (since one moves with the substance). Thus the substantial derivative (D/Dt) refers to the time rate of change of a fluid flow property as viewed by an observer at the origin of the coordinate system, which is moving at the flow velocity \vec{V} . Also note that in the right-hand side of Equation IIIa.2.4 the derivative terms are placed in a bracket. This allows us to express the substantial derivative as a mathematical operator:

$$\frac{D}{Dt} = \frac{\partial}{\partial t} + (\vec{V} \cdot \vec{\nabla})$$

Calling the substantial derivative an operator implies that it can operate on all the flow field properties such as pressure, temperature, velocity, density, etc. This is described later in this section.

Example IIIa.2.1. Find the acceleration of a fluid particle in the Cartesian coordinate system.

Solution: We substitute Equation IIIa.2.1 into Equation IIIa.2.3 and evaluate each term as follows:

$$\frac{\partial \vec{V}}{\partial t} = \frac{\partial V_x}{\partial t} \vec{i} + \frac{\partial V_y}{\partial t} \vec{j} + \frac{\partial V_z}{\partial t} \vec{k}$$

* If the observer's reference is accelerating then the acceleration of a particle with respect to a fixed reference is given in Chapter VIb by Equation VIb.3.9.

$$V_x \frac{\partial \vec{V}}{\partial x} = V_x \left(\frac{\partial V_x}{\partial x} \vec{i} + \frac{\partial V_y}{\partial x} \vec{j} + \frac{\partial V_z}{\partial x} \vec{k} \right)$$

$$V_y \frac{\partial \vec{V}}{\partial y} = V_y \left(\frac{\partial V_x}{\partial y} \vec{i} + \frac{\partial V_y}{\partial y} \vec{j} + \frac{\partial V_z}{\partial y} \vec{k} \right)$$

$$V_z \frac{\partial \vec{V}}{\partial z} = V_z \left(\frac{\partial V_x}{\partial z} \vec{i} + \frac{\partial V_y}{\partial z} \vec{j} + \frac{\partial V_z}{\partial z} \vec{k} \right)$$

Summing up terms, fluid acceleration in the Cartesian coordinates may be written as:

$$\begin{aligned} \vec{a} = & \left(\frac{\partial V_x}{\partial t} + V_x \frac{\partial V_x}{\partial x} + V_y \frac{\partial V_x}{\partial y} + V_z \frac{\partial V_x}{\partial z} \right) \vec{i} + \left(\frac{\partial V_y}{\partial t} + V_x \frac{\partial V_y}{\partial x} + V_y \frac{\partial V_y}{\partial y} + V_z \frac{\partial V_y}{\partial z} \right) \vec{j} + \\ & \left(\frac{\partial V_z}{\partial t} + V_x \frac{\partial V_z}{\partial x} + V_y \frac{\partial V_z}{\partial y} + V_z \frac{\partial V_z}{\partial z} \right) \vec{k} \end{aligned}$$

IIIa.2.3-1

Example IIIa.2.2. Find the acceleration of a fluid particle at $x = 1$ cm, $y = 2$ cm, and $z = -1$ cm at $t = 3$ s in a flow field with Eulerian velocity in the Cartesian coordinates given as $\vec{V} = xt\vec{i} - y\vec{j} + (1-t)z\vec{k}$ cm/s.

Solution: We first note that $V_x = xt$, $V_y = -y$, $V_z = (1-t)z$. We then carry out derivatives as follows:

For V_x : $\partial V_x / \partial t = x$, $\partial V_x / \partial x = t$, $\partial V_x / \partial y = 0$, and $\partial V_x / \partial z = 0$.

For V_y : $\partial V_y / \partial t = 0$, $\partial V_y / \partial x = 0$, $\partial V_y / \partial y = -1$, and $\partial V_y / \partial z = 0$

For V_z : $\partial V_z / \partial t = -z$, $\partial V_z / \partial x = 0$, $\partial V_z / \partial y = 0$, and $\partial V_z / \partial z = (1-t)$

Substituting into Equation IIIa.2.3-1, we obtain: $\vec{a} = x(1+t^2)\vec{i} + y\vec{j} + (t-2)tz\vec{k}$ cm/s². For the specified point at the specified time, the acceleration becomes:

$$\vec{a} = 10\vec{i} + 2\vec{j} - 3\vec{k} \quad \text{with} \quad |\vec{a}| = \sqrt{10^2 + 2^2 + (-3)^2} = 10.63 \text{ cm/s}^2.$$

Example IIIa.2.3. The flow velocity in a flow field is given as $V_x(x) = V_0[1 - (2x/3L)]$. Find the flow acceleration of a point located at $x = 0.75$ m. Use $L = 1$ m and $V_0 = 3$ m/s.

Solution: This is a one-dimensional, steady flow hence the local acceleration is zero. We can find the convective acceleration from

$$a_x = V_x(dV_x/dx) = V_0[1 - (2x/3L)][-2V_0/3L] = -2V_0^2[1 - (2x/3L)]/3L$$

For the specified location, we find $a_x = -3$ m/s². The minus sign indicates that flow decelerates.

We now further elaborate on the two types of accelerations defined earlier. Let's generalize the discussion by using a flow property c , being a function of both space and time $c = f(\vec{r}, t)$ where c may represent P , T , V , ρ , etc. Equation IIIa.2.4 for the flow property c is then written as:

$$\frac{Dc}{Dt} = \frac{\partial c}{\partial t} + (\vec{v} \cdot \vec{\nabla} c) \quad \text{IIIa.2.5}$$

If the property c of the flow field is being observed from a fixed point with respect to the flow field, we show the time rate of change of property c by the partial derivative $\partial c / \partial t$, which we referred to as the local acceleration when $c = V$. An example for the case where c represents velocity, $c = V$ includes acceleration of stagnant water in a constant diameter pipe when a pump is turned on. Similarly, an example for the case that c represents temperature, $c = T$ is when we place a container of cold water in a warm room.

Regarding the convective acceleration, an example for $c = V$ is when fluid steadily flows through a converging or diverging channel as shown in Figures IIIa.2.2(a) and IIIa.2.2(b), respectively. From the point of view of a stationary observer, for this steady state fluid flow, velocity at any point along the channel is independent of time. Hence, according to the Eulerian approach we have $\partial V / \partial t = 0$. However, from the point of view of an observer moving with the flow, velocity at any point along the channel is changing with time because the flow area is changing. If the observer moves at the same velocity as the flow velocity, according to the Lagrangian approach, DV/Dt is not zero*. Using the substantial derivative, Equation IIIa.2.5 for this case predicts that $DV/Dt = (\vec{v} \cdot \vec{\nabla})\vec{v}$. As a result, in Equation IIIa.2.5, the left side describes the rate of change of flow property in the Lagrangian and the right hand sides describe the rate of change of flow property c in the Eulerian framework.

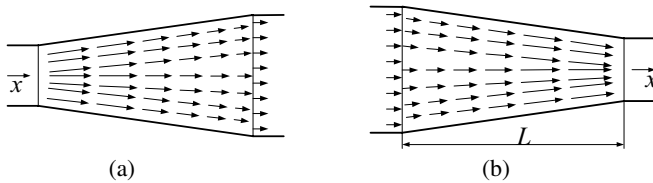


Figure IIIa.2.2. 1-D velocity vectors in a steady ideal flow field. a) decelerating flow and b) accelerating flow

So far we discussed the case that the observer is either fixed or moves in the flow with the same velocity as the flow velocity. But what if the observer is moving in the flow field at a velocity \vec{v}_o , which is different than the flow velocity

* Try an example in which $c = \rho$. For solution, search for “acceleration pressure drop” in Chapters IIIb and Va.

($\vec{V}_o \neq \vec{V}$)? In this case, we use the same chain rule as given by Equation IIIa.2.2 but the derivatives of the location become the components of the observer velocity vector:

$$\frac{dc}{dt} = \frac{\partial c}{\partial t} + \frac{\partial c}{\partial x} \frac{dx}{dt} + \frac{\partial c}{\partial y} \frac{dy}{dt} + \frac{\partial c}{\partial z} \frac{dz}{dt} = \frac{\partial c}{\partial t} + \frac{\partial c}{\partial x} V_{ox} + \frac{\partial c}{\partial y} V_{oy} + \frac{\partial c}{\partial z} V_{oz}$$

where we used d/dt in the left side to distinguish this case from the case that the observer is moving at the flow velocity. This derivative is referred to as the *total time derivative*. Similar to the substantial derivative, we can write the right side in a more familiar manner:

$$\frac{dc}{dt} = \left[\frac{\partial}{\partial t} + (\vec{V}_o \cdot \vec{\nabla}) \right] c \quad \text{IIIa.2.6}$$

By canceling the partial derivative $\partial c / \partial t$ between Equations IIIa.2.5 and IIIa.2.6, we find the relation between the total and the substantial derivatives as:

$$\frac{Dc}{Dt} = \frac{dc}{dt} + (\vec{V} - \vec{V}_o) \cdot \vec{\nabla} c \quad \text{IIIa.2.7}$$

The substantial derivative is equal to the total derivative when the observer velocity is equal to the flow velocity.

The Lagrangian approach is well suited for solid mechanics where the focus is on the motion of individual particles. The continuum hypothesis also makes the Lagrangian approach useful for the derivation of the conservation equation in fluid mechanics. For example, the conservation equation of mass, using the Lagrangian framework simply becomes $m = \text{constant}$ ($Dm/Dt = 0$). Similarly, the momentum equation for fluids as given by Newton's second law of motion has its simplest form when written in the Lagrangian framework; $\vec{F} = D(m\vec{V})/Dt$. Finally, the simplest form of the conservation equation of energy is the one written for a closed system, using the Lagrangian description, as given by Equation IIa.6.1. As described in the next section, we can either use the Lagrangian approach to derive the set of conservation equations and then substitute from the Eulerian equivalent (Equation IIIa.2.5) or directly derive the Eulerian formulation by observing flow entering and leaving a stationary control volume (the Lagrangian free-body diagram).

Example IIIa.2.4. Find the framework that, from the fluid mechanics point of view, best describes the following situations: a) a lion chasing a deer in a herd, b) a traffic engineer surveying the traffic pattern at an intersection, c) a bird carrying a tag to study the migration pattern of a flock of birds, d) a cameraman filming a school of fish entering and leaving a coral reef, and e) a chemist sampling river water for pollution.

Solution: The answers are a) Lagrangian, b) Eulerian, c) Lagrangian, d) Eulerian, and e) Eulerian.

Next, we solve an example for convective acceleration in a fluid flowing at steady state condition.

Example IIIa.2.5. Consider the conduit shown in Figure IIIa.2.2(b). The conduit has a width of 1 ft (3.28 m). The flow area at $x = 0$ is 2.5 ft^2 (0.23 m^2) and at $x = L = 6 \text{ ft}$ (1.83 m) is 1 ft^2 (0.1 m^2). Fluid flows steadily at a volumetric flow rate of $\dot{V} = 12 \text{ ft}^3/\text{s}$ ($0.34 \text{ m}^3/\text{s}$). Find the acceleration of a point located at $x = 3 \text{ ft}$.

Solution: To find acceleration, we first need to find velocity. Since we are given the volumetric flow rate, we find velocity from $V_x = \dot{V}/A(x)$. The flow area between $x = 0$ and $x = L$ is a function of x and can be found as $A = A_1 + (A_2 - A_1)x/L$. Substituting values, we find $A = 2.5 - 1.5x/L$. Hence, $V(x) = \dot{V}/A = 12/(2.5 - 1.5x/L)$. For the one-dimensional flow, $V_y = V_z = 0$ and acceleration from Equation IIIa.2.2 is found as:

$$a_x = \frac{d\vec{V}}{dt} = \left(\frac{\partial V_x}{\partial t} \right) + \left(V_x \frac{\partial V_x}{\partial x} \right)$$

Since fluid flows steadily $\partial V_x / \partial t = 0$. We find $dV_x/dx = (18/L)/(2.5 - 1.5x/L)^2$. Therefore,

$$a_x = [12/(2.5 - 1.5x/L)](18/L)/(2.5 - 1.5x/L) = (18/L)/(2.5 - 1.5x/L)^3 = (216/6)/(2.5 - 1.5/2)^3 = 6.72 \text{ ft/s}^2.$$

In the next example, we find the total acceleration due to the presence of local and convective accelerations.

Example IIIa.2.6. Find the acceleration in Example IIIa.2.5 if the flow is increasing at a rate of $2.5 \text{ ft}^3/\text{s}^2$.

Solution: The convective acceleration remains the same. The local acceleration must now be calculated from $\partial V_x / \partial t$. We found $V_x = \dot{V}/A(x)$. Thus, $\partial V_x / \partial t = \partial [\dot{V}/A(x)] / \partial t = 2.5/A(x)$. At $x = 3$, $\partial V_x / \partial t = 2.5/1.75 = 1.43 \text{ ft/s}^2$. Total acceleration is then found as $a_x = 1.43 + 6.72 = 8.15 \text{ ft/s}^2$.

3. Conservation Equations

Information about a flow field can be obtained from the solution to the conservation equations, which can be derived either in an *integral form for a finite control volume* or in *differential form for an infinitesimal control volume*. The latter approach is necessary if the goal is to obtain detailed information in the flow field such as determination of pressure, temperature, or velocity distributions. Additionally, there is dimensional analysis. Therefore, we may say that in general, there are three types of analyses for solving the single-phase fluid flow problems namely, differential, integral, and dimensional. Each type of analysis has its own benefits and drawbacks. For example, in the differential analysis, the three con-

ervation equations of mass, momentum, and energy are applied to an infinitesimal element of the flow field. These three differential equations are then integrated over the specific region of interest with specified boundary conditions peculiar to that region. The integrated equations in conjunction with the thermodynamic equation of state provide sufficient number of equations to find such key flow parameters as pressure, temperature, velocity, and density. The advantage of the differential analysis is the detailed information it provides about the region being analyzed. This includes distribution of pressure and velocity in the flow field. The disadvantage of this method is the intensive computational efforts required for solving the problem. This is due to the fact that, except in special cases, analytical solutions in closed form cannot be obtained hence, seeking numerical solutions is inevitable. Depending on the extent of details desired, such numerical solutions, even with today's computational abilities, remain labor intensive and are used only if no other method provides the required information.

In integral analysis, a control volume of finite size is assigned to the region of interest and the three conservation equations are applied. These equations already include the boundary conditions. The advantage of this method is the ease in setting up and solving the integral equations. The obvious disadvantage is the loss of details within the control volume. However, depending on the case being analyzed, the analyst may not require such details, average values representing the region may be quite sufficient.

Finally, in dimensional analysis we try to find relevant dimensionless parameters without knowing the related differential equations. In this chapter we discuss only the integral and the differential analyses.

3.1. Integral Analysis of Conservation Equations

This method is applied to control volumes with finite size. We take advantage of the Lagrangian approach to set up the conservation equations and by using the Eulerian approach, we then convert these equations to suit fluid flow applications. Since the Lagrangian approach is applied to a closed system (an entity having a constant mass), the *Reynolds transport theorem* is used to relate the rate of change of properties of the system to that of a control volume. As was discussed in Chapter IIa, if Y represents an extensive property of a system, then y represents the intensive property so that $y = dY/dm$. According to the Reynolds transport theorem*, we can write:

$$\frac{d}{dt}(Y_{System}) = \frac{\partial}{\partial t} \left(\iiint_{C.V.} y \rho dV \right) + \iint_{C.S.} y \rho (\vec{V} \cdot d\vec{S}) \quad \text{IIIa.3.1}$$

where dV is the differential volume and dS is the differential surface area encompassing the control volume. As was discussed in Section 2, the left side in Equa-

* This theorem is derived in Chapter VIIc from the general transport theorem and the Leibnitz rule for the differentiation of integrals. See Equation VIIc.1.31 for the Reynolds transport theorem as applied to a fixed control volume.

tion IIIa.3.1 represents the Lagrangian definition and the right side represents the Eulerian equivalent. We use Equation IIIa.3.1 to derive the integral form of the conservation equations of mass, momentum, and energy as discussed next.

Conservation Equation of Mass, Integral Approach

In the case of conservation equation of mass, $Y = m$ and $y = dY/dm = 1$. These can be substituted in Equation IIIa.3.1 noting that the left side becomes zero, as the system mass is constant:

$$\frac{D}{Dt}(m)_{System} = 0$$

Therefore, Equation IIIa.3.1 simplifies to:

$$\frac{\partial}{\partial t} \left(\iiint_{C.V.} \rho dV \right) + \iint_{C.S.} \rho(\vec{V} \cdot d\vec{S}) = 0 \quad \text{IIIa.3.2}$$

Equation IIIa.3.2 is the Eulerian description of the conservation equation of mass. It expresses the fact that the rate of change of mass in a control volume is due to the algebraic summation of mass flow rates entering and leaving the control volume. For steady state and incompressible flow, Equation IIIa.3.2 becomes:

$$\iint_{C.S.} \rho(\vec{V} \cdot d\vec{S}) = \sum_{Exit Ports} (\rho VA)_e - \sum_{Inlet Ports} (\rho VA)_{in} = \sum_{Exit Ports} \dot{m}_e - \sum_{Inlet Ports} \dot{m}_{in} = 0 \quad \text{IIIa.3.3}$$

Note that for incompressible fluids at constant temperature, density remains the same in the flow field hence, it cancels out in the above equation.

Conservation Equation of Momentum, Integral Approach

In the case of conservation equation of momentum, $Y = mV$ and $y = V$. These can be substituted in Equation IIIa.3.1 to obtain:

$$\frac{D}{Dt}(m\vec{V})_{System} = \frac{\partial}{\partial t} \left(\iiint_{C.V.} \vec{V} \rho dV \right) + \iint_{C.S.} \vec{V} \rho(\vec{V} \cdot d\vec{S}) \quad \text{IIIa.3.4}$$

The left-hand side is the Lagrangian description of momentum of the system. According to Newton's second law, the system momentum is related to the algebraic summation of all forces acting on the system:

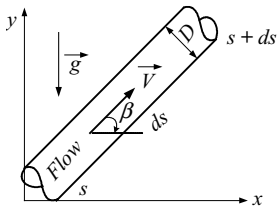
$$\frac{D}{Dt}(m\vec{V})_{System} = \sum \vec{F} = \sum \vec{F}_{Body Force} + \sum \vec{F}_{Surface Force} \quad \text{IIIa.3.5}$$

The conservation equation for momentum can then be written as:

$$\sum \vec{F}_{Body\ Force} + \sum \vec{F}_{Surface\ Force} = \frac{\partial}{\partial t} \left(\iiint_{C.V.} \vec{V} \rho dV \right) + \iint_{C.S.} \vec{V} \rho (\vec{V} \cdot d\vec{S}) \quad \text{IIIa.3.6}$$

where in Equation IIIa.3.6, the first term in the right side is the rate of change of momentum within the control volume and the second term is the net *momentum flux* through the control volume. Equation IIIa.3.6 is a vector equation having components in three dimensions. Application of the one-dimensional momentum equation is explored in various Chapters of this book.

Example IIIa.3.1. Write the integral momentum equation for a one-dimensional (1-D) flow.



Solution: We use the control volume in the figure ($dV = A ds$) and follow Equation IIIa.3.6. The first term in the right side of this equation is the rate of change of momentum in the control volume which becomes $(d\dot{m}/dt)ds$. The second term in the right side is the momentum flux $[(\dot{m}^2/\rho A)_{s+ds} - (\dot{m}^2/\rho A)_s]$. The body force is the fluid weight and the surface forces are the friction force (F_F) and the pressure force.

$$\sum dF = A(P_s - P_{s+ds}) - \rho(A ds)g \sin \beta - dF_F$$

where β is measured from the horizontal plane. Substituting:

$$\frac{d\dot{m}}{dt} ds + \left[\left(\frac{\dot{m}^2}{\rho A} \right)_{s+ds} - \left(\frac{\dot{m}^2}{\rho A} \right)_s \right] = A(P_s - P_{s+ds}) - A \rho g ds (\sin \beta) - dF_F$$

We rearrange this equation by dividing both sides by $A ds$ and letting ds approach zero:

$$\frac{1}{A} \frac{\partial \dot{m}}{\partial t} = \frac{\partial P}{\partial s} - \rho g (\sin \beta) - \frac{1}{A} \frac{\partial (\dot{m}^2 / \rho A)}{\partial s} - \left(\frac{\partial P}{\partial s} \right)_F \quad \text{IIIa.3.6-1}$$

where the differential friction force is now written in terms of the friction pressure drop.

Conservation Equation of Energy, Integral Approach

In the case of conservation equation of energy, $Y = E$ and $y = dE/dm = e$ where E and e are total and specific energy of the system, respectively. Substituting these in Equation IIIa.3.1 yields:

$$\frac{D}{Dt}(E)_{System} = \frac{\partial}{\partial t} \left(\iiint_{C.V.} e \rho dV \right) + \iint_{C.S.} e \rho (\vec{V} \cdot d\vec{S}) \quad \text{IIIa.3.7}$$

The left side in the above equation is the Lagrangian expression of the rate of change of total system energy. This according to the first law of thermodynamics is related to the rate of work and heat transfer to or from the system as follows:

$$\frac{D}{Dt}(E)_{System} = \sum \dot{Q} - \sum \dot{W} \quad \text{IIIa.3.8}$$

Substituting yields:

$$\sum \dot{Q} - \sum \dot{W} = \frac{\partial}{\partial t} \left(\iiint_{C.V.} e \rho dV \right) + \iint_{C.S.} e \rho (\vec{V} \cdot d\vec{S}) \quad \text{IIIa.3.9}$$

As was discussed in Chapter II, The rate of work transfer to or from the control volume may consist of several types including the shaft work, the pressure work, the viscous work (due to the surface shear stresses), and work due to electric and magnetic fields, etc. Therefore, the rate of work transfer becomes:

$$\sum \dot{W} = \dot{W}_s + \iint_{C.S.} P(\vec{V} \cdot d\vec{S}) - \iint_{C.S.} \vec{\tau} \cdot d\vec{S} + \dot{W}_{Electric} + \dot{W}_{Magnetic} + \dots \quad \text{IIIa.3.10}$$

We may partition the pressure work by taking the surface integral on all the ports (both inlet and exit) and the remaining of the control surface:

$$\iint_{C.S.} P(\vec{V} \cdot d\vec{S}) = \iint_{C.S., ports} P(\vec{V} \cdot d\vec{S}) + \iint_{C.S., remaining} P(\vec{V} \cdot d\vec{S}) = \iint_{C.S., ports} P(\vec{V} \cdot d\vec{S}) + P\dot{V}$$

By partitioning the integral, we explicitly consider the work due to changes in the boundary of a deformable control volume. If the control surface is not deformable, then the last term on the right side is zero. As for the viscous work, except in the case of very slow or so called creep flow, where viscosity effects are dominant, the rate of work transfer due to viscous forces is negligible compared to the shaft work. Substituting for the total rate of work transfer in the integral energy equation and using the constituents of the total specific energy (i.e., specific internal u , kinetic $\rho V^2/2$, and potential ρgZ energies):

$$e = u + \rho V^2 / 2 + \rho gZ$$

the first law of thermodynamics can be written as:

$$\sum \dot{Q} = \sum \dot{W}_s + P\dot{V} + \frac{\partial}{\partial t} \iiint_{C.V.} \left(u + \frac{V^2}{2} + gZ \right) \rho dV + \iint_{C.S., ports} \left(u + \frac{P}{\rho} + \frac{V^2}{2} + gZ \right) \rho (\vec{V} \cdot d\vec{S}) \quad \text{IIIa.3.11}$$

In Equation IIIa.3.11, we have considered only shaft work and pressure work due to changes in the control surface. Also note that the triple integral over the control volume represents total energy of the C.V.:

$$E_{C.V.} = \iiint_{C.V.} \left(u + \frac{V^2}{2} + gZ \right) \rho dV$$

Using the definition of enthalpy ($h = u + Pv$), Equation IIIa.3.11 can be written in terms of flow enthalpy entering and leaving the control volume:

$$\sum_i \dot{m}_i \left(h_i + \frac{V_i^2}{2} + gZ_i \right) + \sum \dot{Q} + \dot{q}''V = \sum \dot{W}_s + P\dot{V} + \sum_e \dot{m}_e \left(h_e + \frac{V_e^2}{2} + gZ_e \right) + \frac{d}{dt} \left[m \left(u + \frac{V^2}{2} + gZ \right) \right] \quad \text{IIIa.3.12}$$

where in Equation IIIa.3.12, \dot{q}'' is the volumetric heat generation rate (kJ/m³ or Btu/ft³, for example) in the control volume due to such effects as electric resistance, exothermic chemical reactions, nuclear heat generation, etc. The volumetric heat generation rate from nuclear reactions is discussed in Chapter VIe.

It is important to recall our sign convention as discussed in Chapter II, for \dot{Q} and \dot{W} , the rate of heat transfer and power, respectively. The rate of heat transfer has a plus sign if heat is added to the system and has a minus sign if heat is removed from the system. Power, has a plus sign if work is performed by the system and has a minus sign if work is delivered to the system. Therefore, power delivered by a turbine is positive and power delivered to a pump or a compressor is negative. Similarly, the heat transfer delivered to a boiler or to the core of a nuclear reactor is positive and the heat loss from a pump or a turbine is negative.

Equation IIIa.3.12 represents the integral form of the energy equation for a deformable control volume. For steady state processes and control volumes with fixed boundaries and no internal heat generation, Equation IIIa.3.12 simplifies to:

$$\sum_i \dot{m}_i \left(h_i + \frac{V_i^2}{2} + gZ_i \right) + \sum \dot{Q} = \sum \dot{W}_s + \sum_e \dot{m}_e \left(h_e + \frac{V_e^2}{2} + gZ_e \right) \quad \text{IIIa.3.12-1}$$

For steady state and steady flow processes Equation IIIa.3.12-1 is further simplified to:

$$\left(h_i + \frac{V_i^2}{2} + gZ_i \right) + \sum q = \sum w_s + \left(h_e + \frac{V_e^2}{2} + gZ_e \right) \quad \text{IIIa.3.12-2}$$

where q and w_s are heat and shaft work transfer per unit mass of the working fluid, respectively. Although the equations for conservation of momentum and conservation of energy are independent, as is shown later in this section, under certain circumstance they would lead to a similar conclusion. The case in point is the well-known Bernoulli equation.

3.2. Differential Analysis of Conservation Equations

There are generally three methods to derive the conservation equations in their differential forms. In the first method, the differential forms for the conservation equations are derived from the integral form by using the vector calculus, specifically the Gauss divergence theorem (Chapter VIIc). In the second method, the integral approach is applied to a control volume and the differential formulation is derived by taking the limit as the volume becomes infinitesimal. In the third method, the conservation equations are directly derived for an infinitesimal control volume using the Eulerian approach.

Conservation Equation of Mass, Differential Analysis

To derive the differential form of the continuity equation, we consider flow of fluid through an elemental control volume, $dx dy dz$, as shown in Figure IIIa.3.1. For simplicity, we have only shown flow through the yz -plane in the x -direction. The rate of mass entering the control volume at $x = 0$ is $(\rho V_x) dA = (\rho V_x)(dy dz)$. Similarly, we can find the mass flow rate entering the control volume through the xy - and xz -planes. Since mass is a scalar quantity, we can add all these mass flow rates to find the total rate of mass entering the control volume from all directions as:

$$(\rho V_x) dy dz + (\rho V_y) dx dz + (\rho V_z) dx dy$$

We now find the mass flow rate leaving the control volume in the x -direction through the yz -plane located at $x = dx$. This is found from the Taylor expansion of the function $(\rho V_x) dy dz$, by using only the first two terms. This amounts to $[\rho V_x + \partial(\rho V_x)/\partial x](dy dz)$. Similarly, we find the mass flow rate into the control volume in the y - and z -directions. Hence, total mass of fluid flowing out of the control volume becomes:

$$\left\{ (\rho V_x) dy dz + \left[\frac{\partial(\rho V_x)}{\partial x} dx \right] dy dz \right\} + \left\{ (\rho V_y) dx dz + \left[\frac{\partial(\rho V_y)}{\partial y} dy \right] dx dz \right\} + \left\{ (\rho V_z) dx dy + \left[\frac{\partial(\rho V_z)}{\partial z} dz \right] dx dy \right\}$$

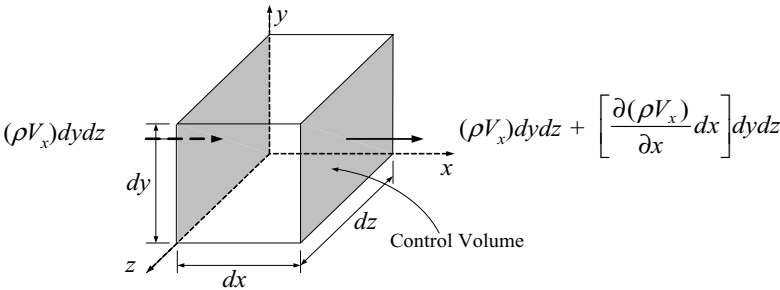


Figure IIIa.3.1. Flow of fluid through an elemental control volume in Cartesian coordinates

The rate of change of mass of the control volume is due to the difference in the incoming and outgoing flows:

$$\frac{\partial}{\partial t}(\rho dx dy dz) = - \left[\frac{\partial(\rho V_x)}{\partial x} dx \right] dy dz + \left[\frac{\partial(\rho V_y)}{\partial y} dy \right] dx dz + \left[\frac{\partial(\rho V_z)}{\partial z} dz \right] dx dy$$

This equation simplifies to:

$$\frac{\partial \rho}{\partial t} + \left[\frac{\partial(\rho V_x)}{\partial x} + \frac{\partial(\rho V_y)}{\partial y} + \frac{\partial(\rho V_z)}{\partial z} \right] = 0$$

The general form of the continuity equation that is independent of any coordinate system can be written as:

$$\frac{\partial \rho}{\partial t} + \bar{\nabla} \cdot \rho \bar{V} = 0 \quad \text{IIIa.3.13}$$

where in Equation IIIa.3.13, density is a function of space and time $\rho = f(x, y, z, t)$. Equation IIIa.3.13 is valid for any flow field condition whether it is steady or unsteady, viscous or frictionless, compressible or incompressible. However, this equation is not valid when there is any source or sink singularities in the control volume such as occurrence of condensation or boiling. Also, nuclear reactions in which conversion of mass and energy may exist are excluded.

Under a steady state condition, the second term is identically zero as, despite the possible existence of a spatial distribution for density, such a distribution would not change with time. The continuity equation is in its simplest form if a fluid is incompressible, since density at constant temperature in an incompressible flow field is constant. Gases can be treated as incompressible fluid as long as the gas velocity remains less than about 30% of the speed of sound in the gas (≈ 300 ft/s or 91.5 m/s). Next we solve several examples using various forms of the continuity equation.

Example IIIa.3.2. Use Equation IIIa.3.13 and derive the continuity equation in terms of the substantial derivative of density.

Solution: We first carryout the differentiation in Equation IIIa.3.13:

$$\frac{\partial \rho}{\partial t} + \bar{\nabla} \cdot \rho \bar{V} = \frac{\partial \rho}{\partial t} + \rho \bar{\nabla} \cdot \bar{V} + \bar{V} \cdot \bar{\nabla} \rho = 0$$

in Cartesian coordinates:

$$\frac{\partial \rho}{\partial t} + \rho \left(\frac{\partial V_x}{\partial x} + \frac{\partial V_y}{\partial y} + \frac{\partial V_z}{\partial z} \right) + (V_x \frac{\partial \rho}{\partial x} + V_y \frac{\partial \rho}{\partial y} + V_z \frac{\partial \rho}{\partial z}) = 0$$

We now collect the first term and the terms in the second parenthesis and use Equation IIIa.2.2:

$$\frac{D\rho}{Dt} + \rho \bar{\nabla} \cdot \bar{V} = 0$$

Example IIIa.3.3. Write the continuity equation in Cartesian coordinates for a) steady flow and b) incompressible flow.

Solution: a) For steady flow, we use Equation IIIa.3.13 and drop the first term. We also note that for steady flow $\rho = f(x, y, z)$:

$$\bar{\nabla} \cdot \rho \bar{V} = \frac{\partial(\rho V_x)}{\partial x} + \frac{\partial(\rho V_y)}{\partial y} + \frac{\partial(\rho V_z)}{\partial z} = 0$$

b) For incompressible flow $\rho = \text{constant}$ (i.e., $\partial\rho/\partial t = 0$). Hence, Equation IIIa.3.13 becomes $\bar{\nabla} \cdot \rho \bar{V} = 0$ or alternatively $\bar{\nabla} \cdot \rho \bar{V} = \rho \bar{\nabla} \cdot \bar{V} = 0$. That is to say

$$\frac{\partial V_x}{\partial x} + \frac{\partial V_y}{\partial y} + \frac{\partial V_z}{\partial z} = 0. \text{ In two dimensions, we have:}$$

$$\frac{\partial V_x}{\partial x} + \frac{\partial V_y}{\partial y} = 0 \quad \text{IIIa.3.13-1}$$

Example IIIa.3.4. Consider a planar flow with the component of velocity along the x -axis given as $V_x = xy$ and the component of velocity along the y -axis given as $V_y = -2y$. Do these components represent an incompressible flow?

Solution: To have a planar incompressible flow, we must be able to show that $\partial V_x/\partial x + \partial V_y/\partial y = 0$ is met. Taking the derivative and substituting, we get $y - 2 \neq 0$ which does not satisfy the continuity equation. Therefore, the above components do not represent an incompressible flow. The reader may verify that the following components do represent an incompressible flow; $V_x = 2xy$ and $V_y = -y^2$.

Example IIIa.3.5. Does vector $\bar{v} = (axy + bz)\bar{i} - ayz^2\bar{j} + (ayz + bxz)\bar{k}$ represent the velocity vector of an incompressible flow field?

Solution: For incompressible flow, we must have $\partial v_x/\partial x + \partial v_y/\partial y + \partial v_z/\partial z = 0$. Finding components:

$\partial v_x/\partial x = ayt$, $\partial v_y/\partial y = -az^2$, and $\partial v_z/\partial z = ay + bx$. The summation is not zero thus v is not a velocity vector in an incompressible flow.

Example IIIa.3.6. Consider a planar incompressible flow with the component of velocity along the x -axis given as $V_x = c_1x^2y + c_2x$. Find V_y .

Solution: Since for a two-dimensional flow, the continuity equation simplifies to $\partial V_x/\partial x + \partial V_y/\partial y = 0$. Having V_x , we find $dV_x/dx = 2c_1xy + c_2$. Hence, $\partial V_y(x, y)/\partial y = -(2c_1xy + c_2)$. Integrating, $V_y = -(c_1xy + c_2)y + c_3$, where c_3 is the constant of integration and is found from the boundary condition.

Example IIIa.3.7. Start with integral analysis and obtain the differential equation of the conservation of mass for the control volume of Example IIIa.3.1 for $\beta = 0$.

Solution: For a horizontal control volume, we replace s with x . According to Equation IIIa.3.2, the rate of change of mass in the control volume is equal to the mass flux through the control volume, hence

$$\frac{\partial(\rho V)}{\partial t} = \rho V A - \left[\rho V A + \frac{\partial(\rho V A)}{\partial x} dx \right]$$

This equation simplifies to $\partial(\rho)/\partial t + \partial(\rho V)/\partial x = 0$. Carrying out the differentiation and rearranging

$$\frac{1}{\rho V} \frac{\partial \rho}{\partial t} + \frac{1}{V} \frac{\partial V}{\partial x} + \frac{1}{\rho} \frac{\partial \rho}{\partial x} = 0$$

Conservation Equation of Momentum, Differential Analysis

Shown in Figure IIIa.3.2 is an elemental control volume of a fluid being traced in a flow field. The applied forces on this control volume, due to the acting stresses, consist of body and surface forces:

$$\sum d\vec{F} = \sum (d\vec{F})_{\text{Body Force}} + \sum (d\vec{F})_{\text{Surface Force}}$$

The body forces include weight and forces induced by an electromagnetic field, for example:

$$\sum (d\vec{F})_{\text{Body Force}} = \rho \vec{g} + \vec{B}$$

The surface forces are due to pressure and shear stresses. To find the expression for these forces, let's look only at the surface forces in the x -direction:

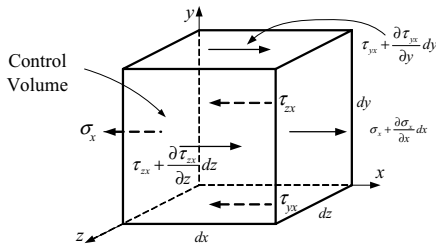


Figure IIIa.3.2. Components of normal and shear stresses in the x -direction for an infinitesimal fluid element

The net surface force in the x -direction due to the normal and tangential (shear) stresses becomes:

$$dF_{s,x} = \left(\frac{\partial \sigma_x}{\partial x} + \frac{\partial \tau_{yx}}{\partial y} + \frac{\partial \tau_{zx}}{\partial z} \right) dx dy dz$$

Similarly, the body forces with components in the x -direction become:

$$dF_{B,x} = (\rho g_x + B_x) dx dy dz$$

We can write similar expressions for differential force components in the y - and z -directions as act on the differential element $dx dy dz$. According to Newton's second law of motion, the applied forces result in the fluid particle acceleration. Thus, in this Lagrangian approach we can then write:

$$dm \left(\frac{\partial \vec{V}}{\partial t} + V_x \frac{\partial \vec{V}}{\partial x} + V_y \frac{\partial \vec{V}}{\partial y} + V_z \frac{\partial \vec{V}}{\partial z} \right) = d\vec{F}$$

Substituting for $dm = \rho dx dy dz$, where ρ is expressed in kg/m^3 in SI units or slug/ft^3 in BU, yields:

$$\begin{aligned} \rho \left(\frac{\partial V_x}{\partial t} + V_x \frac{\partial V_x}{\partial x} + V_y \frac{\partial V_x}{\partial y} + V_z \frac{\partial V_x}{\partial z} \right) &= \rho g_x + B_x + \frac{\partial \sigma_x}{\partial x} + \frac{\partial \tau_{yx}}{\partial y} + \frac{\partial \tau_{zx}}{\partial z} \\ \rho \left(\frac{\partial V_y}{\partial t} + V_x \frac{\partial V_y}{\partial x} + V_y \frac{\partial V_y}{\partial y} + V_z \frac{\partial V_y}{\partial z} \right) &= \rho g_y + B_y + \frac{\partial \tau_{xy}}{\partial x} + \frac{\partial \sigma_y}{\partial y} + \frac{\partial \tau_{zy}}{\partial z} \\ \rho \left(\frac{\partial V_z}{\partial t} + V_x \frac{\partial V_z}{\partial x} + V_y \frac{\partial V_z}{\partial y} + V_z \frac{\partial V_z}{\partial z} \right) &= \rho g_z + B_z + \frac{\partial \tau_{xz}}{\partial x} + \frac{\partial \tau_{yz}}{\partial y} + \frac{\partial \sigma_z}{\partial z} \end{aligned}$$

These are the three components of the momentum equation (known as the Cauchy momentum equation), written in terms of normal and shear stresses. These equations are applicable to both Newtonian and non-Newtonian fluids as long as the continuum hypothesis is satisfied. It is the substitution for the normal and shear stresses that makes the equations peculiar to either Newtonian or non-Newtonian fluids.

Momentum Equation for Newtonian Fluids (The Navier-Stokes Equations)

In Section 1 we discussed that one of the criteria for a Newtonian fluid is to be able to relate the shear stress to velocity in the form of:

$$\begin{aligned} \tau_{xy} = \tau_{yx} &= \mu \left(\frac{\partial V_y}{\partial x} + \frac{\partial V_x}{\partial y} \right), \quad \tau_{yz} = \tau_{zy} = \mu \left(\frac{\partial V_z}{\partial y} + \frac{\partial V_y}{\partial z} \right), \text{ and} \\ \tau_{zx} = \tau_{xz} &= \mu \left(\frac{\partial V_x}{\partial z} + \frac{\partial V_z}{\partial x} \right) \end{aligned}$$

According to the Stokes hypothesis, we can show (Aris, Daily, and Schlichting) that for Newtonian fluids:

$$\sigma_x = -P - \frac{2}{3}\mu(\bar{\nabla} \cdot \bar{V}) + 2\mu \frac{\partial V_x}{\partial x}, \quad \sigma_y = -P - \frac{2}{3}\mu(\bar{\nabla} \cdot \bar{V}) + 2\mu \frac{\partial V_y}{\partial y}, \text{ and}$$

$$\sigma_z = -P - \frac{2}{3}\mu(\bar{\nabla} \cdot \bar{V}) + 2\mu \frac{\partial V_z}{\partial z}$$

Substituting the above expressions, for stress in terms of velocity, in the momentum equation we obtain:

$$\begin{aligned} \rho \left(\frac{\partial V_x}{\partial t} + V_x \frac{\partial V_x}{\partial x} + V_y \frac{\partial V_x}{\partial y} + V_z \frac{\partial V_x}{\partial z} \right) &= -\frac{\partial P}{\partial x} + \rho g_x + B_x + \frac{\partial}{\partial x} \left(-\frac{2}{3}\mu(\bar{\nabla} \cdot \bar{V}) + 2\mu \frac{\partial V_x}{\partial x} \right) \\ &\quad + \frac{\partial}{\partial y} \left[\mu \left(\frac{\partial V_y}{\partial x} + \frac{\partial V_x}{\partial y} \right) \right] + \frac{\partial}{\partial z} \left[\mu \left(\frac{\partial V_z}{\partial x} + \frac{\partial V_x}{\partial z} \right) \right] \\ \rho \left(\frac{\partial V_y}{\partial t} + V_x \frac{\partial V_y}{\partial x} + V_y \frac{\partial V_y}{\partial y} + V_z \frac{\partial V_y}{\partial z} \right) &= -\frac{\partial P}{\partial y} + \rho g_y + B_y + \frac{\partial}{\partial x} \left[\mu \left(\frac{\partial V_y}{\partial x} + \frac{\partial V_x}{\partial y} \right) \right] \\ &\quad + \frac{\partial}{\partial y} \left(-\frac{2}{3}\mu(\bar{\nabla} \cdot \bar{V}) + 2\mu \frac{\partial V_y}{\partial y} \right) + \frac{\partial}{\partial z} \left[\mu \left(\frac{\partial V_z}{\partial y} + \frac{\partial V_y}{\partial z} \right) \right] \\ \rho \left(\frac{\partial V_z}{\partial t} + V_x \frac{\partial V_z}{\partial x} + V_y \frac{\partial V_z}{\partial y} + V_z \frac{\partial V_z}{\partial z} \right) &= -\frac{\partial P}{\partial z} + \rho g_z + B_z + \frac{\partial}{\partial x} \left[\mu \left(\frac{\partial V_z}{\partial x} + \frac{\partial V_x}{\partial z} \right) \right] \\ &\quad + \frac{\partial}{\partial y} \left[\mu \left(\frac{\partial V_y}{\partial z} + \frac{\partial V_z}{\partial y} \right) \right] + \frac{\partial}{\partial z} \left(-\frac{2}{3}\mu(\bar{\nabla} \cdot \bar{V}) + 2\mu \frac{\partial V_z}{\partial z} \right) \end{aligned}$$

These equations can be generalized in the vector form of:

$$\rho \frac{D\bar{V}}{Dt} = \sum d\bar{F} \quad \text{IIIa.3.14}$$

Substitution of forces in Equation IIIa.3.14 yields the momentum equation in the Cartesian coordinates:

$$\rho \frac{D\bar{V}}{Dt} = -\bar{\nabla}P + \rho\bar{g} + \bar{B} + \bar{\nabla} \left[\frac{4\mu}{3} \bar{\nabla} \cdot \bar{V} \right] + \bar{\nabla} \times [\mu(\nabla \times \bar{V})] \quad \text{IIIa.3.15}$$

This equation allows for variation of fluid viscosity as a function of position. In many applications viscosity is independent of location. In this case, Equation IIIa.3.15 simplifies to:

$$\rho \left(\frac{\partial}{\partial t} + \bar{V} \cdot \bar{\nabla} \right) \bar{V} = \rho\bar{g} + \bar{B} - \bar{\nabla}P + \frac{\mu}{3} \bar{\nabla}(\bar{\nabla} \cdot \bar{V}) + \mu \nabla^2 \bar{V} \quad \text{IIIa.3.16}$$

where the left side of Equation IIIa.3.16 is expanded according to Equation IIIa.2.3. The assumption of constant viscosity (i.e., independent of spatial position) allowed us to take the viscosity term outside the differentiation. This simplified set of vector equations (IIIa.3.16) is known as the *Navier-Stokes equations* as Louis Marie Henri Navier (1785 – 1836) first derived these equations for incompressible fluids in 1822. George Gabriel Stokes (1819–1903) generalized the derivation in 1845⁺.

Definition of terms in the Navier-Stokes equations is as follows.

$(\partial \vec{V} / \partial t):$	local acceleration
$(\vec{V} \cdot \nabla) \vec{V}$	convective acceleration
$\rho \vec{g}:$	gravity force
$\vec{B}:$	remaining body force (electrical force in a magnetic field)
$\nabla P:$	pressure force
$\frac{\mu}{3} \nabla(\nabla \cdot \vec{V}) + \mu \nabla^2 \vec{V}:$	viscous shear forces

To this date no analytical solution in closed form exists for the Navier-Stokes equation. We therefore investigate special cases by neglecting certain terms in these equations as the flow condition permits.

The Navier-Stokes equations in the cylindrical and spherical coordinate systems are given in Tables A.III.4 and A.III.5, respectively.

Steady flow: In steady flow, local acceleration from the Eulerian point of view is zero ($\partial \vec{V} / \partial t = 0$). Hence, the Navier-Stokes equation:

$$\rho \left(\cancel{\frac{\partial}{\partial t} + \vec{V} \cdot \nabla} \right) \vec{V} = \rho \vec{g} + \vec{B} - \nabla P + \frac{\mu}{3} \nabla(\nabla \cdot \vec{V}) + \mu \nabla^2 \vec{V}$$

for steady flow simplifies to:

$$\rho (\vec{V} \cdot \nabla) \vec{V} = \rho \vec{g} + \vec{B} - \nabla P + \frac{\mu}{3} \nabla(\nabla \cdot \vec{V}) + \mu \nabla^2 \vec{V}$$

Incompressible flow: Variation in fluid density in incompressible flow is negligible. Hence, as shown in Example IIIa.3.2, $\nabla \cdot \vec{V} = 0$ so that the Navier-Stokes equation:

$$\rho \left(\frac{\partial}{\partial t} + \vec{V} \cdot \nabla \right) \vec{V} = \rho \vec{g} + \vec{B} - \nabla P + \cancel{\frac{\mu}{3} \nabla(\nabla \cdot \vec{V})} + \mu \nabla^2 \vec{V}$$

for incompressible flow simplifies to:

⁺ According to Eckert, “these equations were first derived by N. Navier and S. P. Poisson from a consideration of intermolecular forces and by B. de Saint Venant and Stokes based on the assumption that the normal and shear stresses in a fluid are proportional to the deformation velocities.”

$$\rho \left(\frac{\partial}{\partial t} + \vec{V} \cdot \vec{\nabla} \right) \vec{V} = \rho \vec{g} + \vec{B} - \vec{\nabla} P + \mu \nabla^2 \vec{V} \quad \text{IIIa.3.17}$$

A one-dimensional form of the incompressible flow may be written as:

$$\rho \left(\frac{\partial V_z}{\partial t} + V_z \frac{\partial V_z}{\partial z} \right) = \rho g_z + B_z - \frac{\partial P}{\partial z} - dF_z \quad \text{IIIa.3.18}$$

where the fourth term on the right side of Equation IIIa.3.17 is written as a viscous force in Equation IIIa.3.18. Velocity and viscous force terms always have different signs. Determination of the viscous force is discussed in Section 4.

Ideal Flow (Euler Equation): For inviscid (frictionless, $\mu = 0$), incompressible, and constant property flow, in the absence of body forces other than gravity, the Navier-Stokes equation

$$\rho \left(\frac{\partial}{\partial t} + \vec{V} \cdot \vec{\nabla} \right) \vec{V} = \rho \vec{g} + \vec{B} - \vec{\nabla} P + \frac{\mu}{3} \vec{\nabla} (\vec{\nabla} \cdot \vec{V}) + \mu \nabla^2 \vec{V}$$

simplifies to:

$$\rho \left(\frac{\partial}{\partial t} + \vec{V} \cdot \vec{\nabla} \right) \vec{V} = \rho \vec{g} - \vec{\nabla} P \quad \text{IIIa.3.19}$$

This is the Euler equation. As discussed in Section 1, although all fluids possess viscosity, some fluids behave as if they are inviscid. Hence, the Euler equation has practical applications. Indeed, for high Reynolds numbers, the viscous effects for most fluids are confined to a thin layer near the solid surface (i.e., the boundary layer).

Very slow flow: in very slow or creeping flows, the Reynolds number is small, indicating that the inertia effects can be neglected as the viscosity effects become dominant. Hence, the convective acceleration term can be dropped. The Navier-Stokes equation:

$$\rho \left(\frac{\partial}{\partial t} + \vec{V} \cdot \vec{\nabla} \right) \vec{V} = \rho \vec{g} + \vec{B} - \vec{\nabla} P + \frac{\mu}{3} \vec{\nabla} (\vec{\nabla} \cdot \vec{V}) + \mu \nabla^2 \vec{V}$$

for very slow flow, in the absence of other body forces simplifies to:

$$\rho \frac{\partial \vec{V}}{\partial t} = -\vec{\nabla} P + \mu \nabla^2 \vec{V} \quad \text{IIIa.3.20}$$

Static fluid: in a static fluid, velocity is zero. Hence, the Navier-Stokes equation:

$$\rho \left(\frac{\partial}{\partial t} + \vec{V} \cdot \vec{\nabla} \right) \vec{V} = \rho \vec{g} + \vec{B} - \vec{\nabla} P + \frac{\mu}{3} \vec{\nabla} (\vec{\nabla} \cdot \vec{V}) + \mu \nabla^2 \vec{V}$$

for static fluid, in the absence of other body forces except for gravity simplifies to

$$\rho \bar{g} - \bar{\nabla} P = 0 \quad \text{IIIa.3.21}$$

Integrating, the component in the z -direction can be written in the familiar form of:

$$\Delta P = \rho g \Delta Z \quad \text{IIIa.3.22}$$

Next, we solve several problems regarding the application of the momentum equation.

Example IIIa.3.8. Write the momentum equation for an ideal flow in Cartesian coordinates.

Solution: The momentum equation for an ideal fluid is the Euler's equation as given by Equation IIIa.3.19 in the general form. To obtain the components in Cartesian coordinates, we develop each term separately:

– Local acceleration:

$$\rho \frac{\partial \bar{V}}{\partial t} = \rho \left(\frac{\partial V_x}{\partial t} \bar{i} + \frac{\partial V_y}{\partial t} \bar{j} + \frac{\partial V_z}{\partial t} \bar{k} \right)$$

– Convective acceleration:

$$\rho (\bar{V} \cdot \bar{\nabla}) \bar{V} = \rho [(V_x \bar{i} + V_y \bar{j} + V_z \bar{k}) \cdot \left(\frac{\partial}{\partial x} \bar{i} + \frac{\partial}{\partial y} \bar{j} + \frac{\partial}{\partial z} \bar{k} \right)] \bar{V}$$

$$\rho (\bar{V} \cdot \bar{\nabla}) \bar{V} = \rho \left[(V_x \frac{\partial}{\partial x} + V_y \frac{\partial}{\partial y} + V_z \frac{\partial}{\partial z}) (V_x \bar{i} + V_y \bar{j} + V_z \bar{k}) \right]$$

$$\rho (\bar{V} \cdot \bar{\nabla}) \bar{V} = \rho \left[(V_x \frac{\partial V_x}{\partial x} + V_y \frac{\partial V_x}{\partial y} + V_z \frac{\partial V_x}{\partial z}) \bar{i} + (V_y \frac{\partial V_y}{\partial x} + V_y \frac{\partial V_y}{\partial y} + V_y \frac{\partial V_y}{\partial z}) \bar{j} + \right. \\ \left. (V_z \frac{\partial V_z}{\partial x} + V_z \frac{\partial V_z}{\partial y} + V_z \frac{\partial V_z}{\partial z}) \bar{k} \right]$$

– Gravity force:

$$\rho \bar{g} = \rho (g_x \bar{i} + g_y \bar{j} + g_z \bar{k})$$

– Pressure force:

$$-\bar{\nabla} P = -\left(\frac{\partial P}{\partial x} \bar{i} + \frac{\partial P}{\partial y} \bar{j} + \frac{\partial P}{\partial z} \bar{k} \right).$$

Therefore, the momentum equation for ideal flow in the Cartesian coordinate system becomes:

$$\rho \left(\frac{\partial V_x}{\partial t} + V_x \frac{\partial V_x}{\partial x} + V_y \frac{\partial V_x}{\partial y} + V_z \frac{\partial V_x}{\partial z} \right) = \rho g_x - \frac{\partial P}{\partial x}$$

$$\rho \left(\frac{\partial V_y}{\partial t} + V_x \frac{\partial V_y}{\partial x} + V_y \frac{\partial V_y}{\partial y} + V_z \frac{\partial V_y}{\partial z} \right) = \rho g_y - \frac{\partial P}{\partial y}$$

$$\rho \left(\frac{\partial V_z}{\partial t} + V_x \frac{\partial V_z}{\partial x} + V_y \frac{\partial V_z}{\partial y} + V_z \frac{\partial V_z}{\partial z} \right) = \rho g_z - \frac{\partial P}{\partial z}$$

Example IIIa.3.9. Find the governing equation for steady state incompressible flow over a flat plate.

Solution: Starting with Equation IIIa.3.16, the first term in the left side and the fourth term in the right side are canceled due to the steady and incompressible fluid assumptions, respectively. If all body forces are also negligible then:

$$\rho(\vec{V} \cdot \nabla) \vec{V} = -\nabla P + \mu \nabla^2 \vec{V}$$

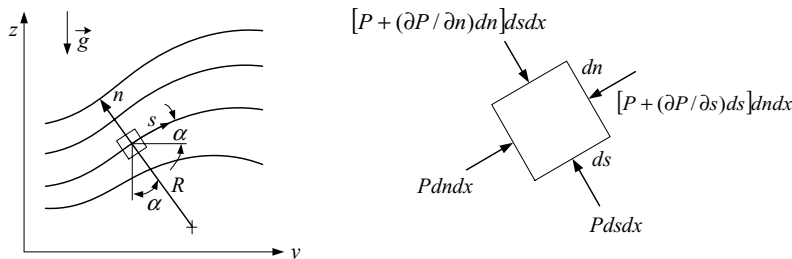
If fluid flows in the x -direction over the surface then the x -component of the momentum equation is:

$$V_x \frac{\partial V_x}{\partial x} + V_y \frac{\partial V_x}{\partial y} = -\frac{1}{\rho} \frac{\partial P}{\partial x} + \nu \left(\frac{\partial^2 V_x}{\partial x^2} + \frac{\partial^2 V_x}{\partial y^2} \right)$$

In the boundary layer over the plate, variation in V_x in the x -direction is much less than variation in V_x in the y -direction and the first term in the parenthesis can be neglected:

$$V_x \frac{\partial V_x}{\partial x} + V_y \frac{\partial V_x}{\partial y} = -\frac{1}{\rho} \frac{\partial P}{\partial x} + \nu \frac{\partial^2 V_x}{\partial y^2} \quad \text{IIIa.3.20-1}$$

Example IIIa.3.10. Find the two-dimensional Euler's equation along a streamline (sn coordinate).



Solution: The Euler's equation along the streamlines can be derived directly by applying Newton's second law of motion to a differential control volume ($dsdn$) along the streamlines. For an ideal flow, only pressure and gravity forces need to be considered. Along the streamline, the net pressure force becomes $-(\partial P / \partial s) ds dn$.

The component of the gravity force along the streamline becomes:

$$-\rho g \cos(\alpha) = -\rho g \partial z / \partial s.$$

The summation of forces must be equal to mass times acceleration:

$$-(\partial P / \partial s) ds dn - (\rho g \partial z / \partial s) ds dn = \rho (ds dn) a_s$$

Canceling out $dsdn$ from both sides of the equation and substituting for the acceleration in terms of the total derivatives yields:

$$\frac{\partial V}{\partial t} + V \frac{\partial V}{\partial s} + \frac{1}{\rho} \frac{\partial P}{\partial s} + g \frac{\partial z}{\partial s} = 0$$

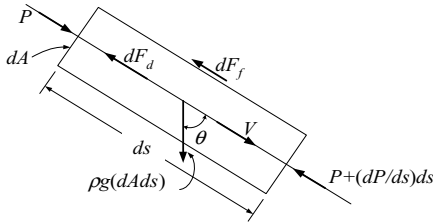
A similar procedure yields Euler's equation in the direction of the n -axis.

Example IIIa.3.11. Find the one-dimensional momentum equation for the flow of a viscous fluid.

Solution: We consider the differential control volume where all dimensions are lumped except for the dimension along the s -axis. In applying Equation IIIa.3.14 to this control volume, we note the pressure force, gravitational force, friction force, and another body or surface force (dF_d) other than friction and weight. Finally;

$$\frac{\partial P}{\partial s} + \rho g \cos \theta - \left(\frac{dF_f}{ds} + \frac{dF_d}{ds} \right) = \rho \left(\frac{\partial V}{\partial t} + V \frac{\partial V}{\partial s} \right)$$

where F_f and F_d are expressed as force per unit area.



Applicability of the Navier-Stokes Equations

These equations are applicable only to Newtonian fluids in laminar flow having constant viscosity, (i.e., independent of spatial position). Adjustments must be made to apply these equations to turbulent flow. It is interesting to note that the non-linearity of these second order partial differential equations is not due to viscous effects of the fluid, rather it is due to the inertial effects manifested in the convective acceleration term. Except for the very slow flow, we were not able to eliminate the source of non-linearity, even for the special flow cases discussed above.

Conservation Equation of Energy, Differential Analysis

Compared with the momentum equation, derivation of the energy equation is simpler since energy, like mass, is a scalar quantity. Hence, we find the rates of energy into and out of an elemental control volume from the three directions of x , y , and z and simply add them up. Since similar processes exist in these three directions, we consider only the processes in the x -direction and apply the results to the y - and z -directions. The rate of change of total energy of the elemental control volume is due to the net exchange of energy into and out of the control volume. This Eulerian approach for the energy equation is described next.

The flow of energy into and out of the control volume can be divided into two groups. The first group includes the rate of energy exchange due to convection, conduction, radiation, and internal heat generation. Convection is associated with the flow of fluid carrying internal, kinetic, and potential energies, $e_i = u + K.E. + P.E.$ Since the potential energy is very small, we only consider the internal and the kinetic energies. To simplify the notations, we use the *stagnation specific energy*, defined as¹ $u^o = u + K.E.$ Total energy brought into the control volume from face $dydz$ is $(\rho V_x u^o) dydz$. Total energy leaving the control volume, is found by Taylor expansion, using only the first two terms; $(\rho V_x u^o) dydz + [\partial(\rho V_x u^o)/\partial x] dx dydz$. Hence, the net exchange of energy due to convection is found as $-[\partial(\rho V_x u^o)/\partial x] dx dydz$. Similarly, for the y - and z -directions, we find the net energy exchange as $-[\partial(\rho V_y u^o)/\partial y] dx dydz$ and $-[\partial(\rho V_z u^o)/\partial z] dx dydz$, respectively.

$$-\left[\frac{\partial(\rho V_x u^o)}{\partial x} + \frac{\partial(\rho V_y u^o)}{\partial y} + \frac{\partial(\rho V_z u^o)}{\partial z} \right] = -\bar{\nabla} \cdot (\rho u^o \bar{V})$$

The internal heat generation is $(\dot{q}''' dx dy dz)$, where \dot{q}''' is the volumetric heat generation rate. This term accounts for electric heating or fission heat generation in a nuclear reaction. Conduction heat transfer needs to be expressed in terms of temperature. As discussed in Chapter IVa, Fourier's law relating heat flux to temperature gradient $(-k \partial T / \partial x)$ provides such a relation, where k is thermal conductivity. Hence, the net exchange due to conduction heat transfer in the x -direction is $[\partial(k \partial T / \partial x) / \partial x] dx dy dz$. Considering the y - and z -directions, the net energy exchange due to conduction becomes:

$$\frac{\partial(k \partial T / \partial x)}{\partial x} + \frac{\partial(k \partial T / \partial y)}{\partial y} + \frac{\partial(k \partial T / \partial z)}{\partial z} = \bar{\nabla} \cdot (k \bar{\nabla} T)$$

For now, we represent the radiation heat transfer simply by \dot{q}_r'' . In Chapter IVd we shall see that the Stefan-Boltzmann law relates \dot{q}_r'' to temperature. The net exchange due to radiation is, therefore, $(\partial \dot{q}_r'' / \partial x) + (\partial \dot{q}_r'' / \partial y) + (\partial \dot{q}_r'' / \partial z)$ per unit volume. This can be expressed as $\bar{\nabla} \cdot \dot{\bar{q}}_r''$ per unit volume.

The second group of energy for the control volume includes the rate of work. This in turn consists of three types of work. First, shaft work, which is clearly zero for this elemental control volume. Second, work performed by the surface forces. Third the work performed by the body forces. Work performed by the surface forces consists of work performed by the normal and shear stresses. Since work is defined as force multiplied by distance and the rate of work is defined as force times velocity, work performed by the surface forces is non-zero only for the velocity components, which are in the same direction as the surface force. For example, as shown in Figure IIIa.3.3, the rate of work at $x=0$ due to normal stress in the x -direction is given by $-(\sigma_x dy dz) V_x$ and the rate of work due to shear stresses

¹ The stagnation state is attained when a flowing fluid is brought to rest in an isentropic process. Thus, $h^o = h + V^2/2$.

in the x -direction is given by $-(\tau_{xy}dxdy)V_y$ and by $-(\tau_{xz}dxdz)V_x$ (see also Figure IIIa.3.2). Hence, the total rate of work in the x -direction at $x = 0$ is found as:

$$-(\sigma_x dydz)V_x - (\tau_{yx}dxdy)V_x - (\tau_{zx}dxdy)V_x$$

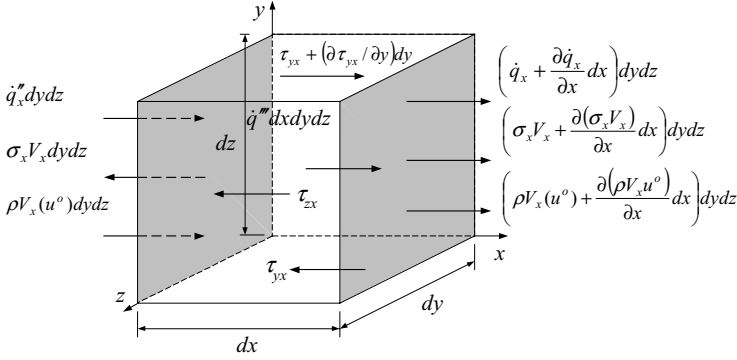


Figure IIIa.3.3. Influx and efflux of energy in the x -direction for an elemental control volume

The rate of work at $x = dx$ is given by $(\sigma_x dydz)V_x + [\partial(\sigma_x dydz)V_x / \partial x]dxdydz$ for the normal stress and by $(\tau_{yx} dydz)V_y + [\partial(\tau_{yx} dydz)V_y / \partial x]dxdydz$ and $(\tau_{zx} dydz)V_z + [\partial(\tau_{zx} dydz)V_z / \partial x]dxdydz$, for the shear stress. Hence, the net rate of work exchange in the x -direction is:

$$\left[\frac{\partial(\sigma_x V_x)}{\partial x} + \frac{\partial(\tau_{xy} V_y)}{\partial x} + \frac{\partial(\tau_{xz} V_z)}{\partial x} \right] dxdydz$$

Thus the net rate of work exchange from all directions is found as:

$$\frac{\partial}{\partial x}(\sigma_x V_x + \tau_{xy} V_y + \tau_{xz} V_z) + \frac{\partial}{\partial y}(\sigma_y V_y + \tau_{yx} V_x + \tau_{yz} V_z) + \frac{\partial}{\partial z}(\sigma_z V_z + \tau_{zx} V_x + \tau_{zy} V_y) = P(\bar{\nabla} \cdot \bar{V}) + \Phi$$

where Φ , referred to as *viscous dissipation function*, now stands for

$$\Phi = \frac{\partial}{\partial x}(\tau_{xy} V_y + \tau_{xz} V_z) + \frac{\partial}{\partial y}(\tau_{yx} V_x + \tau_{yz} V_z) + \frac{\partial}{\partial z}(\tau_{zx} V_x + \tau_{zy} V_y) = \bar{\nabla} \cdot (\bar{\tau} \cdot \bar{V})$$

where the right-hand side term is the short hand representation of Φ using tensor notations for τ .

Example IIIa.3.12. Express the viscous dissipation function only in terms of velocity components.

Solution: We can elegantly accomplish this task only for laminar flow. To do this, we expand the terms comprising the net rate of work exchange and then substitute for the shear and normal stresses from the Newtonian fluid criteria and the Stokes hypothesis, respectively. Expanding the net rate of work exchange:

$$\left(\frac{\partial \sigma_x}{\partial x} + \frac{\partial \tau_{yx}}{\partial y} + \frac{\partial \tau_{zx}}{\partial z} \right) V_x + \left(\frac{\partial \sigma_y}{\partial y} + \frac{\partial \tau_{zy}}{\partial z} + \frac{\partial \tau_{xy}}{\partial x} \right) V_y + \left(\frac{\partial \sigma_z}{\partial z} + \frac{\partial \tau_{xz}}{\partial x} + \frac{\partial \tau_{yz}}{\partial y} \right) V_z +$$

$$\left(\sigma_x \frac{\partial V_x}{\partial x} + \sigma_y \frac{\partial V_y}{\partial y} + \sigma_z \frac{\partial V_z}{\partial z} \right) + \tau_{xy} \left(\frac{\partial V_y}{\partial x} + \frac{\partial V_x}{\partial y} \right) + \tau_{yz} \left(\frac{\partial V_z}{\partial y} + \frac{\partial V_y}{\partial z} \right) + \tau_{zx} \left(\frac{\partial V_x}{\partial z} + \frac{\partial V_z}{\partial x} \right)$$

We now substitute for the normal and shear stresses in terms of velocity from the constitutive relations:

$$-P \left(\frac{\partial V_x}{\partial x} + \frac{\partial V_y}{\partial y} + \frac{\partial V_z}{\partial z} \right) + 2\mu \left[\left(\frac{\partial V_x}{\partial x} \right)^2 + \left(\frac{\partial V_y}{\partial y} \right)^2 + \left(\frac{\partial V_z}{\partial z} \right)^2 \right] - \frac{2\mu}{3} \left(\frac{\partial V_x}{\partial x} + \frac{\partial V_y}{\partial y} + \frac{\partial V_z}{\partial z} \right)^2 +$$

$$\mu \left[\left(\frac{\partial V_y}{\partial x} + \frac{\partial V_x}{\partial y} \right)^2 + \left(\frac{\partial V_z}{\partial y} + \frac{\partial V_y}{\partial z} \right)^2 + \left(\frac{\partial V_x}{\partial z} + \frac{\partial V_z}{\partial x} \right)^2 \right] = -P(\bar{\nabla} \cdot \bar{V}) + \Phi$$

The first term represents the rate at which fluid is being compressed and the remaining terms comprise the *viscous-dissipation function*. The viscous-dissipation function in Cartesian coordinates becomes:

$$\Phi = 2\mu \left[\left(\frac{\partial V_x}{\partial x} \right)^2 + \left(\frac{\partial V_y}{\partial y} \right)^2 + \left(\frac{\partial V_z}{\partial z} \right)^2 \right] + \mu \left[\left(\frac{\partial V_y}{\partial x} + \frac{\partial V_x}{\partial y} \right)^2 + \left(\frac{\partial V_z}{\partial y} + \frac{\partial V_y}{\partial z} \right)^2 + \left(\frac{\partial V_x}{\partial z} + \frac{\partial V_z}{\partial x} \right)^2 \right]$$

By using an order-of-magnitude analysis Φ may be approximated as

$$\Phi = \mu(\delta V_x / \delta y)^2.$$

Finally, the rate of work performed by body forces is simply found as $\bar{V} \cdot \bar{B}$. The summation of all these rates of exchanges must be equal to the rate of change of total energy of the elemental control volume (i.e., $\partial(\rho u_o) dx dy dz / \partial t$). Before we write the final energy equation, we use the continuity equation as given by Equation IIIa.3.13, to simplify the rate of change of the control volume total energy, $\partial(\rho u_o) / \partial t$ and the net energy exchange due to convection, as follows:

$$\frac{\partial(\rho u_o)}{\partial t} + \bar{\nabla} \cdot (\rho u_o \bar{V}) = \rho \left(\frac{\partial u_o}{\partial t} + \bar{V} \cdot \bar{\nabla} u_o \right) + u_o \left(\frac{\partial \rho}{\partial t} + \bar{\nabla} \cdot \rho \bar{V} \right)$$

Thus we find:

$$\rho \left(\frac{\partial(u_o)}{\partial t} + \bar{V} \cdot \bar{\nabla} u_o \right) = \rho \frac{Du_o}{Dt} = \bar{\nabla} \cdot (k \bar{\nabla} T) - \bar{\nabla} \cdot \bar{q}_r'' + \dot{q}''' - P(\bar{\nabla} \cdot \bar{V}) + \Phi + \bar{V} \cdot \bar{B}$$

Definition of terms from the left side is as follows:

$\rho \frac{\partial(u^o)}{\partial t}$: local rate of change of the stagnation energy of the infinitesimal control volume
$\rho \vec{V} \cdot \vec{\nabla} u^o$: rate of change in stagnation energy due to convection
$\vec{\nabla} \cdot (k \vec{\nabla} T)$: net rate of heat transfer due to conduction
$\vec{\nabla} \cdot \vec{q}_r''$: net rate of heat transfer due to radiation
\dot{q}'''	: rate of volumetric heat generation (electrical, chemical, or nuclear reactions)
$P(\vec{\nabla} \cdot \vec{V})$: rate of work performed by pressure forces
Φ	: rate of work performed by viscous forces (viscous-dissipation function)
$\vec{V} \cdot \vec{B}$: rate of work performed by body forces, such as weight

The first and the second terms on the left side of Equation IIIa.3.23 are the Eulerian representation of the Lagrangian term for the net rate of change of the stagnation energy. Next, we discuss the simplification of the energy equation for special cases.

Inviscid fluid: For frictionless fluid flow, the rate of work performed by viscous forces is zero. Hence,

$$\rho \frac{\partial(u^o)}{\partial t} + \rho \vec{V} \cdot \vec{\nabla} u^o = \vec{\nabla} \cdot (k \vec{\nabla} T) - \vec{\nabla} \cdot \vec{q}_r'' + \dot{q}''' - P(\vec{\nabla} \cdot \vec{V}) + \vec{V} \cdot \vec{B}$$

Incompressible flow: For an incompressible flow, the rate of work performed by pressure forces becomes zero. Hence;

$$\rho \frac{\partial(u^o)}{\partial t} + \rho \vec{V} \cdot \vec{\nabla} u^o = \vec{\nabla} \cdot (k \vec{\nabla} T) - \vec{\nabla} \cdot \vec{q}_r'' + \dot{q}''' + \Phi + \vec{V} \cdot \vec{B}$$

Ideal flow: For incompressible and inviscid flow, the energy equation further simplifies to:

$$\rho \frac{\partial(u^o)}{\partial t} + \rho \vec{V} \cdot \vec{\nabla} u^o = \vec{\nabla} \cdot (k \vec{\nabla} T) - \vec{\nabla} \cdot \vec{q}_r'' + \dot{q}'''$$

where in this equation the rate of work performed by body forces is also dropped as compared with more dominant terms. If the net rate of heat transfer due to thermal radiation can be ignored (as discussed in Chapter IVd, thermal radiation becomes noticeable at elevated temperatures), we obtain

$$\rho \frac{\partial(u^o)}{\partial t} + \rho \vec{V} \cdot \vec{\nabla} u^o = \vec{\nabla} \cdot (k \vec{\nabla} T) + \dot{q}'''$$

Solid materials: Further simplification can be made in the energy equation if applied to solids, in which case, the net rate of heat transfer due to convection does not exist:

$$\rho \frac{\partial(u)}{\partial t} = \bar{\nabla} \cdot (k \bar{\nabla} T) + \dot{q}''' \quad \text{IIIa.3.24}$$

Equation IIIa.3.24 is the basis of the conduction heat transfer, which is discussed in Chapter IVa.

Example IIIa.3.13. Find the governing equation for steady state incompressible flow over a flat plate.

Solution: Starting with Equation IIIa.3.23, the first term in the left-hand side and the fourth term in the right-hand side are canceled due to the steady and incompressible fluid assumptions, respectively. The equation then reduces to:

$$\rho \bar{V} \cdot \bar{\nabla} u^o = \bar{\nabla} \cdot (k \bar{\nabla} T) - \bar{\nabla} \cdot \bar{\dot{q}}_r'' + \dot{q}''' + \Phi + \bar{V} \cdot \bar{B}$$

If the effect of all body forces is also negligible, there is no internal heat generation, and we ignore contribution by thermal radiation then we get:

$$\rho \bar{V} \cdot \bar{\nabla} u = \bar{\nabla} \cdot (k \bar{\nabla} T) + \Phi$$

Substituting for u in terms of temperature, developing terms, substituting for viscous-dissipation function, and considering only two-dimensional flow, the equation becomes:

$$V_x \frac{\partial T}{\partial x} + V_y \frac{\partial T}{\partial y} = \alpha \left(\frac{\partial^2 T}{\partial x^2} + \frac{\partial^2 T}{\partial y^2} \right) + 2 \frac{v}{c} \left(\frac{\partial V_x}{\partial x} \right)^2 + 2 \frac{v}{c} \left(\frac{\partial V_y}{\partial y} \right)^2 + \frac{v}{c} \left(\frac{\partial V_x}{\partial x} + \frac{\partial V_x}{\partial y} \right)^2$$

In the boundary layer, variation in V_x in the x -direction is much less than variation in V_x in the y -direction and the first term in the second parenthesis can be neglected. Also neglecting $\partial V_y / \partial y$ and temperature variations in the x -direction, the above equation simplifies to:

$$V_x \frac{\partial T}{\partial x} + V_y \frac{\partial T}{\partial y} = \alpha \frac{\partial^2 T}{\partial y^2} + \frac{v}{c} \left(\frac{\partial V_x}{\partial y} \right)^2$$

Ignoring viscous dissipation, the above equation further simplifies to:

$$V_x \frac{\partial T}{\partial x} + V_y \frac{\partial T}{\partial y} = \alpha \frac{\partial^2 T}{\partial y^2} \quad \text{IIIa.3.23-1}$$

Note the striking resemblance between Equations IIIa.3.20-1 (in the absence of the pressure gradient term) and IIIa.3.23-1.

As we shall see in Chapter IIIb, the viscous dissipation function results in a pressure drop, which is traditionally expressed as head loss. Due to analytical

complexities associated with flow fluctuations, pressure drop in turbulent flow due to viscous effects are generally obtained in experiments.

3.3. Derivation of the Bernoulli Equation

The Bernoulli equation is a simplified form of the one-dimensional momentum equation. The goal here is to show that under certain circumstance, the Bernoulli equation can also be derived from the conservation equation of energy. The Bernoulli equation written as:

$$P + \frac{\rho V^2}{2} + \rho gZ = \text{constant}$$

states that the total mechanical energy of an incompressible, inviscid flow along a streamline always remains a constant as shown in Figure IIIa.3.4(a). This is discussed in more detail in the next two sections.

Derivation of Bernoulli Equation from Energy Equation

Although the Bernoulli equation and the equation for conservation of energy are, in general, independent equations, the purpose here is to show that in certain circumstances, the Bernoulli equation can be derived from the equation for conservation of energy. These include the assumptions of steady flow, no heat, and no work transfer. To demonstrate, consider Equation IIIa.3.11 for steady and uniform flow at the inlet and outlet ports of a fixed control volume:

$$\sum \dot{Q} = \sum \dot{W}_s + \dot{W}_v + \dot{m} \int_{inlet}^{exit} \left(du + \frac{dP}{\rho} + \frac{dV^2}{2} + gdZ \right) \quad \text{IIIa.3.25}$$

where in Equation IIIa.3.25 we have retained the work done by the viscous forces. Dividing Equation IIIa.3.25 by mass flow rate, and integrating the specific internal energy, yields:

$$q = w_s + w_v + (u_e - u_i) + \int_{inlet}^{exit} \left(\frac{dP}{\rho} + \frac{dV^2}{2} + gdZ \right) \quad \text{IIIa.3.26}$$

This equation can be slightly rearranged to get:

$$[w_s + w_v + (u_e - u_i - q)] + \int_{inlet}^{exit} \left(\frac{dP}{\rho} + \frac{dV^2}{2} + gdZ \right) = 0 \quad \text{IIIa.3.27}$$

Let's now evaluate the left side term. This term consists of shaft work, viscous work, heat transfer, and dissipation. In the absence of any of these effects, Equation IIIa.3.27 becomes the Bernoulli equation provided that the flow is incompressible. Therefore, we were able to derive the Bernoulli equation from the conservation equation for energy for an incompressible flow and for the condition that

the terms in the brackets sum up to zero. Since in the next section we will also derive the Bernoulli equation from the conservation equation for momentum, we leave the discussion about the Bernoulli equation to the next section and here we only concern ourselves with the terms in the bracket:

$$[w_s + w_v + (u_e - u_i - q)]$$

In order for this bracket to sum up to zero, we should have no viscous work, no shaft work and show that $(u_e - u_i - q) = 0$. Let's see under what circumstance this parenthesis becomes zero. Obviously one case is when $u_e = u_i$ and $q = 0$ (i.e., for adiabatic flow). Another case is when $u_e - u_i = q$. The latter condition indicates that even if heat transfer is involved for the flow going from point i to point e , as long as the heat transfer is equal to the increase in the flow specific internal energy, still the terms in the parenthesis sum up to zero. This condition exists for inviscid and incompressible flow.

If the term $(u_e - u_i - q) \neq 0$ we cannot then use the Bernoulli equation. To take into account the effects of the parenthesis when not summing up to zero, we retain this term in Equation IIIa.3.27. However, for simplicity, we represent the unrecoverable energy loss as $(u_e - u_i - q) = gh_f$. Term h_f is referred to as the unrecoverable *head loss*. Substituting this definition, Equation IIIa.3.27 becomes:

$$g \int_{inlet}^{exit} (dh_s + dh_f) + \int_{inlet}^{exit} \left(\frac{dP}{\rho} + \frac{dV^2}{2} + gdZ \right) = 0 \quad \text{IIIa.3.28}$$

where in Equation IIIa.3.28, we ignored the shear work in comparison with the shaft work and we wrote the shaft work as *head*. Carrying out the integral, Equation IIIa.3.28 is further simplified to:

For Steady Compressible Flow:

$$(h_s + h_f) + \frac{V_e^2 - V_i^2}{2g} + (Z_e - Z_i) + \frac{1}{g} \int (dP / \rho) = 0 \quad \text{IIIa.3.29}$$

Or alternatively,

For Steady Incompressible Flow:

$$(h_s + h_f) + \frac{V_e^2 - V_i^2}{2g} + (Z_e - Z_i) + \frac{1}{g} \left(\frac{P_e}{\rho_e} - \frac{P_i}{\rho_i} \right) = 0 \quad \text{IIIa.3.29}$$

For incompressible flow, density can be treated as a constant ($\rho_e = \rho_i$) and Equation IIIa.3.29 becomes:

For Steady Incompressible Flow:

$$\frac{1}{g} \frac{P_i}{\rho} + \frac{V_i^2}{2g} + Z_i = \frac{1}{g} \frac{P_e}{\rho} + \frac{V_e^2}{2g} + Z_e + h_s + h_f \quad \text{IIIa.3.30}$$

Equation IIIa.3.30 is the basis for the field of hydraulics. In this equation, each term has the dimension of length and all terms are written in terms of head. Rearranging Equation IIIa.3.30, we find

$$\frac{1}{\rho g}(P_i - P_e) + \frac{1}{g}\left(\frac{V_i^2}{2} - \frac{V_e^2}{2}\right) + (Z_i - Z_e) = h_s + h_f \quad \text{IIIa.3.31}$$

In Equation IIIa.3.31, the first term in the left side is the *pressure head*, the second term is the *velocity head*, and the third term is the *elevation head*. In the right side, the first term is the shaft head (*pump head* with $-h_p$ or *turbine head* with $+h_t$) and the second term is the *head loss*. The velocity head is a recoverable head whereas the head loss, as the name implies, is *unrecoverable*. If the fluid is frictionless, then $h_f = 0$. These terms, especially the head loss for internal flow, are discussed in detail in Chapter IIIb.

It is important to emphasize that in this derivation we have been consistent with the sign convention we defined in Chapter IIa (see Problem 60). Hence $+h_s$ should be chosen if the control volume to which Equation IIIa.3.31 is applied includes a turbine. Similarly, $-h_p$ should be chosen if the control volume to which Equation IIIa.3.31 is applied includes a pump or compressor. Regarding h_f , it always represents a negative value since friction produces heat, which is transferred to the surroundings. Hence, $+h_f$ should always be used in Equation IIIa.3.30 or IIIa.3.31. Equation IIIa.3.31 may also be written as:

$$(P_i + \frac{\rho V_i^2}{2} + \rho g Z_i) - \rho g h_f = \rho g h_s + (P_e + \frac{\rho V_e^2}{2} + \rho g Z_e) \quad \text{IIIa.3.32}$$

Means of calculating h_f are discussed in Chapter IIIb. If friction is negligible and there is no shaft work, Equation IIIa.3.31 simplifies to:

Steady ideal Flow, and no Work:

$$\frac{P_i}{\rho} + \frac{V_i^2}{2} + g Z_i = \frac{P_e}{\rho} + \frac{V_e^2}{2} + g Z_e \quad \text{IIIa.3.33}$$

This is the famous Bernoulli equation, first introduced in Bernoulli's *Hydrodynamics*, published in 1738. The Bernoulli equation is also applicable to a compressible fluid as long as flow velocity remains about 30% of the speed of sound in the fluid. Cautions on the use of this equation are discussed later in this section. Equation IIIa.3.33 shows that the summation of pressure work, kinetic energy, and potential energy for steady ideal flow with no shaft work remains a constant along the streamlines.

Terms in Equation IIIa.3.31 are divided by g to obtain *head* and the equation is then applied to a flow path as graphically shown in Figure IIIa.3.4(a). Note that the energy grade line (EGL) represents the summation of all the terms and the hydraulic grade line (HGL) represents the summation of pressure and elevation terms. We assume that the flow path and the bends in Figure IIIa.3.4(a) are smooth and frictionless.

Example IIIa.3.14. Flow of water enters the conduit shown in Figure IIIa.3.4(b) at a rate of $10 \text{ ft}^3/\text{s}$ (283 lit/s). For the given data, find the pressure head at point 2. Assume frictionless flow path. Data: $D_1 = 1 \text{ ft}$ (0.3 m), $D_2 = 2 \text{ ft}$ (0.6 m), $Z_1 = 10 \text{ ft}$ (3 m), $Z_2 = 20 \text{ ft}$ (6 m) and $(\text{Pressure head})_1 = 25 \text{ ft}$ (7.6 m).

Solution: We first find water velocity at points 1 and 2 using $V = \dot{V}/A = 4\dot{V}/\pi d^2$. Hence, $V_1 = 4 \times 10/\pi \times 1^2 = 12.73 \text{ ft/s}$ (3.88 m/s) and $V_2 = 4 \times 10/\pi \times 2^2 = 3.18 \text{ ft/s}$ (0.97 m/s). Equation IIIa.3.33 in terms of head is:

$$\frac{P_1}{\rho g} + \frac{V_1^2}{2g} + Z_1 = \frac{P_2}{\rho g} + \frac{V_2^2}{2g} + Z_2$$

Substituting values, we find,

$$25 + (12.73)^2/(2 \times 32.2) + 10 = (P_2/\rho g) + (3.18)^2/(2 \times 32.2) + 20.$$

Thus, $(P_2/\rho g) = 17.36 \text{ ft}$ (5.3 m).

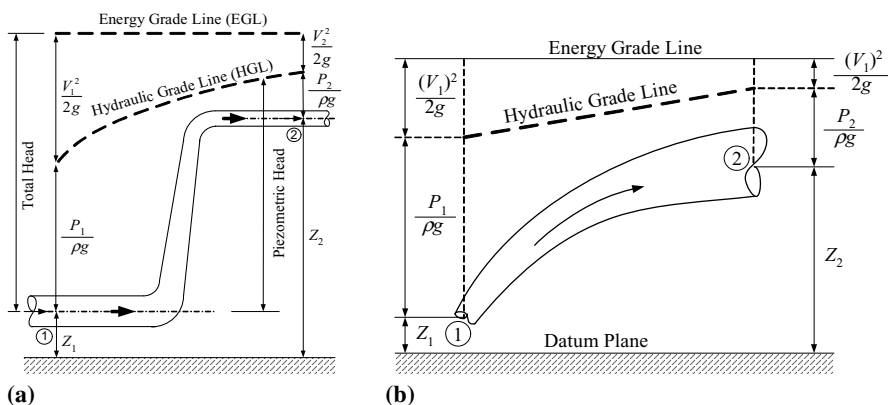


Figure IIIa.3.4. (a) An arbitrary flow path representing HGL. (b) Figure for Example IIIa.3.14

Having derived the Bernoulli equation from the energy equation with the imposed restrictions, we set out to derive the Bernoulli equation from the momentum equation. However, we first need to learn about the fluid rotation.

Fluid Rotation

Earlier, as part of fluid kinematics we studied the acceleration of a fluid element in a flow field. Another aspect of fluid motion is fluid deformation, consisting of linear and angular deformations (see Figure IIIa.3.5). In linear deformation, the fluid particle moves about without any distortion. In contrast, there is a change in the orientation of the fluid element when undergoing an angular deformation. Fluid rotation is, therefore, a linear deformation. It can be shown (see Problem 55) that the angular velocity in fluid rotation is given as:

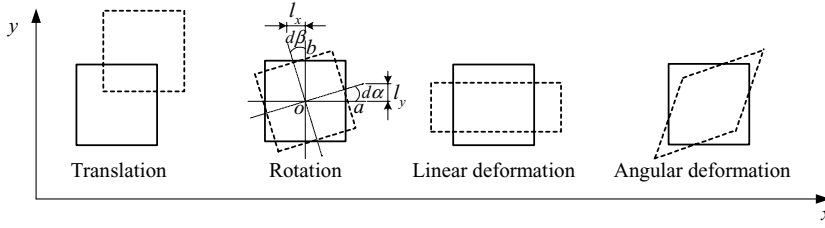


Figure IIIa.3.5. Types of fluid motion (Fox)

$$\vec{\omega} = (\vec{\nabla} \times \vec{V})/2$$

For definition of curl and positive sign of the product of two vectors see Chapter VIIc. Another related variable is defined as *Vorticity*, being twice the rotation vector (i.e. $\vec{\zeta} = 2\vec{\omega} = \vec{\nabla} \times \vec{V}$).

Example IIIa.3.15. Find the vorticity of a fluid particle at $x = 1$ cm, $y = 2$ cm, and $z = -1$ cm in a flow field given as $\vec{V} = 2xy\vec{i} - (y^2 + yz)\vec{j} + 0.5z^2\vec{k}$ cm/s.

Solution: Using the definition of the curl operator from Chapter VIIc, we find $\vec{\zeta} = y\vec{i} - 2x\vec{k}$ s⁻¹. At the specified point, the velocity and the vorticity vector are; $\vec{V} = 4\vec{i} - 2\vec{j} + 0.5\vec{k}$ cm/s and $\vec{\zeta} = 2\vec{i} - 2\vec{k}$ s⁻¹, respectively.

Derivation of Bernoulli Equation from Differential Momentum Equation

The Bernoulli equation can be derived from the Euler form of the Navier-Stokes equations. Recall that the Euler equation is for an inviscid, incompressible, and constant property fluid with gravity as the only body force:

$$\frac{\partial \vec{V}}{\partial t} + \vec{V} \cdot \vec{\nabla} \vec{V} = \vec{g} - \frac{1}{\rho} \vec{\nabla} P$$

Also recall that the convective acceleration term is the source of non-linearity in the conservation equation of momentum. To be able to deal with this troublesome term, we notice that it can be substituted from the following vectorial identity:

$$(\vec{V} \cdot \vec{\nabla}) \vec{V} = \frac{1}{2} \vec{\nabla} (\vec{V} \cdot \vec{V}) - \vec{V} \times (\vec{\nabla} \times \vec{V})$$

to get:

$$\frac{\partial \vec{V}}{\partial t} + \frac{1}{2} \vec{\nabla} (\vec{V} \cdot \vec{V}) - \vec{V} \times (\vec{\nabla} \times \vec{V}) = \vec{g} - \frac{1}{\rho} \vec{\nabla} P$$

The third term represents the cross product of the velocity vector and the vorticity vector, which is now the only troublesome term. This term can be eliminated for two conditions. The first condition is when we are dealing with irrotational flow. Because for irrotational flow vorticity is zero hence, $\vec{\nabla} \times \vec{V} = 0$. With the third term eliminated, the above equation can be integrated between point i and point e . The second condition is when point i and point e are located on a streamline. In this case, the third term in integration goes to zero. To demonstrate, we multiply both sides of the equation by an element of length, $d\vec{r}$, which lies on the streamline. It can be easily shown that the non-linear term is eliminated, as $[\vec{V} \times (\vec{\nabla} \times \vec{V})] \cdot d\vec{r} = 0$, and the rest of the equation after integration becomes:

$$\int_i^e \frac{\partial \vec{V}}{\partial t} \cdot d\vec{s} + \int_i^e \left(\frac{dV^2}{2} + g dz + \frac{dP}{\rho} \right) = 0 \quad \text{IIIa.3.34}$$

where points i and e are located on a streamline. Equation IIIa.3.34 is the time dependent form of the Bernoulli equation. For steady and incompressible flow, this equation reduces to the Bernoulli equation (Equation IIIa.3.33).

Derivation of Bernoulli Equation from the Integral Momentum Equation

We begin by analyzing the one-dimensional steady flow of a fluid in an arbitrary conduit as shown in Figure IIIa.3.6. The steady state continuity equation results in $d(\rho VA) = 0$ hence, $\dot{m} = \rho VA = \text{constant}$. The steady state momentum balance relates the body (weight of the fluid) and surface forces (pressure and viscous forces) to the momentum flux:

$$(dP/ds)Ads + \tau_w(\pi D_h)ds + \rho g Ads \sin \theta + (\rho VA)(dV/ds)ds = 0$$

Dividing through by Ads , we obtain:

$$-dP = \rho V dV + 4\tau_w(ds/D_h) + \rho g dZ \quad \text{IIIa.3.35}$$

We may now integrate this equation between points 1 and 2 along the length of the channel. There are several problems that we must resolve to be able to perform the integration. The first problem is flow velocity, which may not be uniform at a given location along the conduit. To resolve this problem, we consider

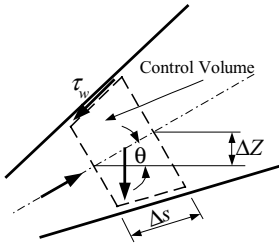


Figure IIIa.3.6. One-dimensional flow of fluid in an arbitrary conduit

the case of highly turbulent flow so that velocity is approximately uniform over the flow cross section. The second problem is the fact that the flow cross section may vary along the conduit. To be able to integrate, let's only consider the case of fluid flow in a conduit with a uniform cross section, such as a circular pipe or tube. The third problem to resolve is the fact that, for compressible fluids, density changes from point 1 to point 2 along the length of the conduit. This change in density may be as a result of heating or cooling the flow. To deal with this problem, we use densities at point 1 (ρ_1) and at point 2 (ρ_2) to obtain an average density $\bar{\rho}$. Since the average specific volume is given as $\bar{v} = v_1 + v_2$, we substitute for $v = 1/\rho$ to obtain the average density as:

$$\frac{1}{\bar{\rho}} = \frac{1}{\rho_1} + \frac{1}{\rho_2}$$

With these modifications in mind, we now integrate Equation IIIa.3.35 to obtain:

$$P_1 - P_2 = \left(\frac{1}{\rho_2} - \frac{1}{\rho_1} \right) \frac{\dot{m}^2}{A^2} + \Delta P_{fric} + \bar{\rho}g(Z_2 - Z_1) \quad \text{IIIa.3.36}$$

where the first term in the right side of Equation IIIa.3.36 was obtained by the following substitution:

$$\int_1^2 \rho V dV = \int_1^2 \frac{\dot{m}^2}{A^2} d\left(\frac{1}{\rho}\right) = \left(\frac{1}{\rho_1} - \frac{1}{\rho_2} \right) \frac{\dot{m}^2}{A^2}$$

For incompressible flow, $\rho_1 \equiv \rho_2 \equiv \bar{\rho}$ hence, the first term in the right side of Equation IIIa.3.36 is practically zero. The second term in the right side of Equation IIIa.3.36, is the frictional pressure drop, which is discussed in Chapter IIIb. Application of Equation IIIa.3.36 is discussed in Chapter IIIb (Example IIIb.4.7). For inviscid flow ($\Delta P_{fric} = 0$), Equation IIIa.3.36 reduces to Equation IIIa.3.33, the Bernoulli equation.

Derivation of the Bernoulli Equation from Euler's Equation for Streamlines

In Example IIIa.3.10, we derived the Euler's equation in streamline coordinates (sn) as:

$$\frac{\partial V}{\partial t} + V \frac{\partial V}{\partial s} + \frac{1}{\rho} \frac{\partial P}{\partial s} + g \frac{\partial z}{\partial s} = 0 \quad \text{IIIa.3.37}$$

To integrate this equation along the streamlines between points 1 and 2, we multiply the above equation by ds and integrate:

$$\int \frac{\partial V}{\partial t} ds + \int_1^2 \left(V dV + \frac{1}{\rho} dP + g dz \right) = 0 \quad \text{IIIa.3.38}$$

or alternatively;

$$\int_1^2 \frac{\partial V}{\partial t} ds + \frac{V_2^2 - V_1^2}{2} + \frac{1}{\rho}(P_2 - P_1) + g(Z_2 - Z_1) = 0 \quad \text{IIIa.3.39}$$

Equation IIIa.3.39 for steady flow reduces to Equation IIIa.3.33 (i.e., the Bernoulli equation).

One-Dimensional Momentum Equation for Viscous Flow

If we are dealing with viscous flow, the applicable equation should account for frictional losses. Hence, we can use the modified form of Equation IIIa.3.37 written as

$$\int_1^2 \frac{\partial V}{\partial t} ds + \int_1^2 \left(V dV + \frac{1}{\rho} dP + g dZ + g dh_f + g dh_s \right) = 0 \quad \text{IIIa.3.40}$$

Integrating;

$$\int_1^2 \frac{\partial V}{\partial t} ds + \frac{V_2^2 - V_1^2}{2} + \int_1^2 \left[\frac{1}{\rho} dP + g(Z_2 - Z_1) + gh_f + gh_s \right] = 0 \quad \text{IIIa.3.41}$$

If the flow is incompressible, then Equation IIIa.3.41 can be integrated to obtain:

$$\int_1^2 \frac{\partial V}{\partial t} ds + \frac{V_2^2 - V_1^2}{2} + \frac{1}{\rho}(P_2 - P_1) + g(Z_2 - Z_1) + gh_f + gh_s = 0 \quad \text{IIIa.3.42}$$

The integral term can be written as:

$$\int_1^2 \frac{\partial V}{\partial t} ds = \int_1^2 \frac{d(\dot{m} / \rho A)}{dt} ds = \frac{d\dot{m}}{dt} \int_1^2 \frac{ds}{\rho A} = \frac{I}{\rho} \frac{d\dot{m}}{dt}$$

Substituting for the integral term and dividing through by g , Equation IIIa.3.42 becomes:

$$\frac{1}{\rho g} I \frac{d\dot{m}}{dt} + \frac{V_2^2 - V_1^2}{2g} + \frac{1}{\rho g}(P_2 - P_1) + (Z_2 - Z_1) + h_f + h_s = 0 \quad \text{IIIa.3.43}$$

where $I = \Sigma(L/A)$ is called the *geometrical inertia*. Note that Equation IIIa.3.43 is written in terms of heads;

$(I/\rho g) d\dot{m}/dt$:	Inertia head
$(V_2^2 - V_1^2)/(2g)$:	Velocity head
$(P_2 - P_1)/(\rho g)$:	Static pressure head
$(Z_2 - Z_1)$:	Elevation head

h_f :	Friction head
h_s :	Shaft head

For steady incompressible flow with $h_s = h_f = 0$, Equation IIIa.3.43 reduces to the Bernoulli equation. If we multiply the terms of Equation IIIa.3.43 by ρg , each term can be expressed as a differential pressure term:

$$\Delta P_{Inertia} + \Delta P_{vel-acc} + \Delta P_{static} + \Delta P_{gravity} + \Delta P_{friction} + \Delta P_{shaft} = 0 \quad \text{IIIa.3.44}$$

If the shaft work is due only to the pump in the flow path, Equation IIIa.3.44 can be written as

$$\Delta P_{pump} - (\Delta P_{Inertia} + \Delta P_{vel-acc} + \Delta P_{static} + \Delta P_{gravity} + \Delta P_{friction}) = 0 \quad \text{IIIa.3.45}$$

or alternatively as

$$\sum \left(\frac{L}{A} \right) \frac{dm}{dt} = \Delta P_{pump} - (\Delta P_{stat} + \Delta P_{grav} + \Delta P_{accl} + \Delta P_{fric}) \quad \text{IIIa.3.45}$$

Note that the differential pressure shown by ΔP is generally defined as $\Delta P = P_2 - P_1$. In the case of the differential pressure due to friction, ΔP is always a negative number. To avoid the use of a minus sign, we define $\Delta P_{friction}$ as $\Delta P_{friction} = P_1 - P_2$ throughout this book.

Applicability of the Bernoulli Equation

The Bernoulli equation is the most widely known equation in the field of hydraulics due to its simplicity, which came at a high price including the following restrictions:

- flow must be at steady state conditions
- there should not be any shaft work, viscous work, or any other work
- flow must be inviscid, incompressible, with uniform properties
- flow must be either irrotational or the end points i and e must lie on a streamline.

These are stringent conditions to meet. The lack of frictional effects implies that the Bernoulli equation cannot be applied where flow encounters obstacles that cause unrecoverable pressure loss to the flow. The no shaft work requirement precludes using the Bernoulli equation across a pump, compressor, or a turbine, for example. The uniform properties requirement precludes applying the Bernoulli equation to situations where density at the exit is substantially different than density at the inlet. Hence, the Bernoulli equation cannot be applied across a cooling or heating coil over which a gas is flowing.

These restrictions require careful assessment of a problem before a solution based on the Bernoulli equation is embarked upon. For example, a *hydraulic jump* (Figure IIIa.3.7) is an irreversible process (associated with head loss) which occurs at certain conditions for a liquid flowing at high speed in a wide, horizontal open channel. While it is tempting to apply the Bernoulli equation at end points before and after the jump, the associated irreversibility and the fact that we cannot

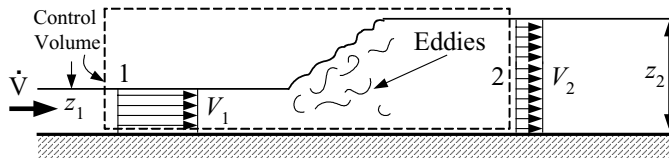
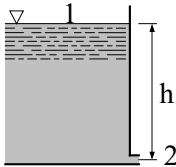


Figure IIIa.3.7. Hydraulic jump in a rectangular channel

trace a streamline between the end points, precludes doing so. Regarding the incompressibility requirement of the flow, we can apply the Bernoulli equation to a compressible flow as long as flow velocity remains about 30% of the speed of sound in the fluid.

Next, we shall solve several examples to which the Bernoulli equation can be applied. It is important to note that for cases that the Bernoulli equation does not apply, we should use the applicable momentum equation such as Equation IIIa.3.31 or Equation IIIa.3.43.

Example IIIa.3.16. Water flows through a small opening located at depth h in a large reservoir. Find water velocity.

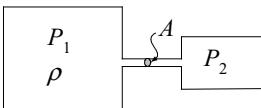


Solution: Applying the Bernoulli equation between points 1 and 2, noting equal pressures ($P_1 = P_2$), and the fact that $V_1 \approx 0$ compared with V_2 , we can solve for V_2 to obtain:

$$V_2 = \sqrt{2gh} \quad \text{IIIa.3.46}$$

The mass flow rate is, therefore, found as $\dot{m} = \rho A_2 V_2$. In Chapter IIIb we shall see that flow rate is reduced due to a *discharge coefficient*. The actual mass flow rate is then $\dot{m} = \rho C_d A_2 \sqrt{2gh}$.

Example IIIa.3.17. A horizontal and frictionless flow path connects two reservoirs. The cross sectional area of reservoir 1 is much larger than that of the flow path. If pressure is maintained in both reservoirs, find the mass flux in the flow path.



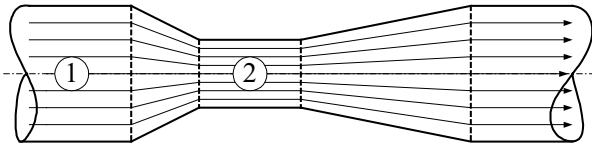
Solution: Applying the Bernoulli equation between points 1 and 2, we obtain:

$$P_1 = P_2 + \frac{\rho V_2^2}{2}$$

Solving for V_2 , we find, $V_2 = \sqrt{2(P_1 - P_2)/\rho}$. Multiplying both sides by density, yields:

$$G = \rho V_2 = \sqrt{2\rho(P_1 - P_2)} \quad \text{IIIa.3.47}$$

Example IIIa.3.18. The device shown in the figure is known as a *venturi*. In this specific venturi, the differential pressure between locations 1 and 2 is 5 psi and the diameter ratio is $D_2/D_1 = 0.35$. If $D_2 = 8$ inches, find the air flow rate through the frictionless venturi.



Solution: Applying the Bernoulli equation between points 1 and 2, noting equal elevations ($Z_1 = Z_2$), and solving for V_2 , we get:

$$V_2^2 - V_1^2 = \left[\frac{2(P_1 - P_2)}{\rho} \right]$$

To get rid of velocity at point 1, we use the continuity equation; $V_1 A_1 = V_2 A_2$ so that $V_1 = V_2 A_2/A_1$. If we now substitute for V_1 in terms of V_2 and use $A_2/A_1 = (D_2/D_1)^2 = \beta^2$ we obtain:

$$V_2^2 = \frac{2(P_1 - P_2)}{\rho(1 - \beta^4)}$$

Substituting for $\dot{V} = V_2 A_2$, we find volumetric flow rate in terms of pressure drop, throat flow area and β :

$$\dot{V} = A_2 \sqrt{\frac{2(P_1 - P_2)}{\rho(1 - \beta^4)}} \quad \text{IIIa.3.48}$$

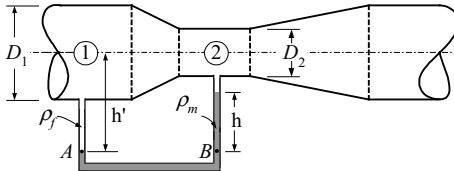
To calculate the volumetric flow rate from Equation IIIa.3.48, we have $A_2 = 3.14(8/12)^2/4 = 0.349 \text{ ft}^2$. Using density of air at standard condition, we find:

$$\dot{V} = 0.349 \sqrt{\frac{2(5 \times 144)}{0.076(1 - 0.35^4)}} \approx 2900 \text{ ft}^3/\text{min}$$

In this problem we demonstrated the usefulness of the Bernoulli equation in de-

termining the flow rate of fluids. However, we assumed ideal conditions such as frictionless venturi as well as steady, inviscid, and incompressible fluid flow. To account for non-ideal conditions, the above flow rate is reduced by a discharge coefficient as discussed in Section IIIb.4.2.

Example IIIa.3.19. For the venturi shown in the figure, derive a relation for flow velocity, V_1 in terms of h , $\beta = D_1/D_2$, and $\rho^* = \rho_m/\rho_f$ where ρ_m is the density of the manometer liquid.



Solution: Applying Equation IIIa.3.33 between points 1 and 2, noting equal elevations ($Z_1 = Z_2$) gives

$$P_1 + (\rho_f V_1^2 / 2) = P_2 + (\rho_f V_2^2 / 2)$$

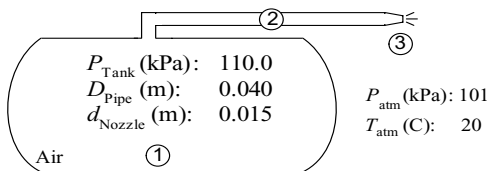
From Equation IIa.5.3, velocity V_2 can be expressed in terms of V_1 as $V_2 = V_1 (D_1/D_2)^4$. Substituting, we get:

$$(\rho_f / 2g) (\beta^4 - 1) V_1^2 = P_1 - P_2$$

We now express P_1 and P_2 in terms of h . To do this, we know that $P_A = P_B$. But $P_A = P_1 + \rho_f h' g$ and $P_B = P_2 + \rho_f (h' - h) g + \rho_m h g$. Therefore, $P_1 - P_2 = gh(\rho_m - \rho_f)$. Substituting, we obtain:

$$V_1 = \sqrt{\frac{2gh(\rho^* - 1)}{\beta^4 - 1}} \quad \text{IIIa.3.49}$$

Example IIIa.3.20. A large pressurized tank filled with air discharges into the atmosphere. The flow path is a short and frictionless smooth pipe connected to a discharge nozzle. Find a) the flow rate of air and b) pressure in the pipe for the given data. Ignore all frictional losses, including head losses at the entrance to the pipe, at the bend, and at the nozzle.



Solution: a) To find the flow of air we need to find $\dot{V} = V_3 A_3$ where point 3 is taken at the nozzle exit. Having $A^3 = \pi t^2/4 = 3.14(0.015)^2/4 = 1.77\text{E-}4 \text{ m}^2$, we find V_3 by using the Bernoulli equation between points 1 and 3:

$$P_1 + \frac{\rho V_1^2}{2} + \rho g Z_1 = P_3 + \frac{\rho V_3^2}{2} + \rho g Z_3$$

We note that $P_3 = P_{\text{atm}}$, $Z_1 \approx Z_3$, and $V_1 \approx 0$. We ignored the elevation head here primarily because the working fluid (air) has low density. We assume that air velocity at point 1 is negligible because the tank is large. Hence;

$$\frac{\rho V_3^2}{2} = P_1 - P_3$$

We now need air density, $\rho = P_1 / RT_1 = 110\text{E}3 / [286.9(20 + 273)] = 1.3 \text{ kg/m}^3$. Substituting;

$$V_3 = \sqrt{2(P_1 - P_3) / \rho} = \sqrt{2(110,000 - 101,000) / 1.3} = 118 \text{ m/s}$$

Therefore, $\dot{V} = V_3 A_3 = 118 \times 1.77\text{E-}4 = 0.021 \text{ m}^3/\text{s}$. We now should calculate the speed of sound in air to ensure that $V_3 < 0.3c$. Assuming air is an ideal gas:

$$c = \sqrt{\gamma RT} = \sqrt{1.4 \times 286.9 \times (20 + 273)} = 1085 \text{ m/s}$$

Therefore application of the Bernoulli equation is valid here.

b) To find pressure in the pipe, we write the Bernoulli equation between points 1 and 2:

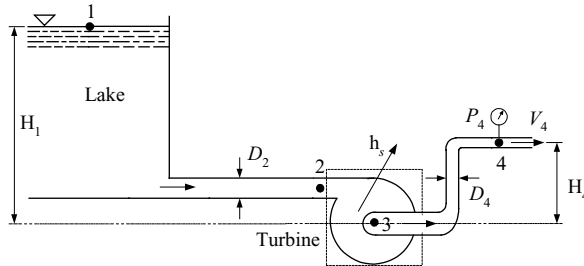
$$P_2 = P_1 - \frac{\rho V_2^2}{2}$$

But we do not have V_2 . We can calculate it from the continuity equation:

$$\dot{V} = V_2 A_2 = V_3 A_3$$

Since $A_2 = 3.14(0.04)^2/4 = 1.257\text{E-}3 \text{ m}^2$ therefore, $V_2 = 0.021/1.257\text{E-}3 = 16.7 \text{ m/s}$. So that $P_2 = 110,000 - [1.3 \times (16.7)^2/2] = 109.82 \text{ kPa}$.

Example IIIa.3.21. Find the maximum power developed by the turbine. Data: $H_1 = 37 \text{ m}$, $H_4 = 2 \text{ m}$, $D_2 = 56 \text{ cm}$, $D_4 = 35 \text{ cm}$, $V_4 = 8.5 \text{ m/s}$, $P_4 = 200 \text{ kPa}$, $P_{\text{atm}} \cong 100 \text{ kPa}$, $\rho = 1000 \text{ kg/m}^3$.



Solution: Since the Bernoulli equation does not apply here, we use Equation IIIa.3.31. The maximum power is obtained when we ignore all frictional losses. Equation IIIa.3.31 is applied between locations 1 and 4 noticing that $V_1 \approx 0$ and there is a turbine on the path:

$$(P_1 + \cancel{\frac{\rho V_1^2}{2}} + \rho g Z_1) - \cancel{\rho g h_f} = \rho g h_s + (P_4 + \frac{\rho V_4^2}{2} + \rho g Z_4)$$

where we ignored velocity at point 1. Solving for h_s , we find the head developed by the turbine as:

$$\begin{aligned} \rho g h_s &= \rho g (Z_1 - Z_4) + (P_1 - P_4) - \frac{\rho V_4^2}{2} = 1000 \times 9.81(37 - 2) - (200 - 100) \times \\ &1000 - \frac{1000 \times 8.5^2}{2} \\ \rho g h_s &= 343.35\text{E}3 - 100\text{E}3 - 36.125\text{E}3 = 207.23 \text{ kPa} \end{aligned}$$

The volumetric flow rate is $\dot{V} = VA = [\pi(35/100)^2 / 4] \times 8.5 \cong 0.82 \text{ m}^3/\text{s}$. Turbine power is then found as:

$$\dot{W} = (\rho g h_s) \dot{V} = 207.23 \text{ kPa} \times 0.82 \text{ m}^3/\text{s} \cong 170 \text{ kW} \cong 228 \text{ hp}$$

QUESTIONS

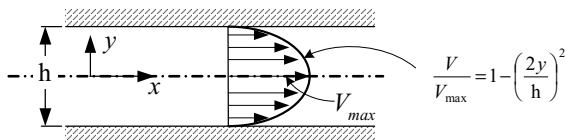
- What is continuum and why do we use such a concept in thermodynamics and fluid mechanics?
- Is pressure a body force or a surface force?
- What is the difference between fluid static, fluid kinematics, and fluid dynamics?
- Consider an ideal gas going through an isentropic process. Does the speed of sound in this gas increase as the gas temperature increases?
- Is blood a Newtonian fluid?
- Why does the rate of shearing strain in viscous fluids increase with the increase in shear stress?
- For what type of fluid is a yield stress defined?
- What approach best describes watching a school of fish while paddling in a canoe?
- Is Equation IIIa.3.14 the Eulerian or the Lagrangian description of the conservation of momentum?
- What is the significance of the Reynolds number?
- What is the d'Alembert's paradox?
- What is the contribution of Prandtl to the field of fluid mechanics?
- Is flow external or internal in a wind tunnel where objects of study are placed in a controlled flow of air?

- What is an unrecoverable pressure drop? Is there also a recoverable pressure drop?
- The Navier-Stokes equations are highly non-linear partial differential equations. Can we get rid of the non-linear terms if we use an inviscid fluid?
- What is mechanical energy? Is it correct to say that there is no conversion of mechanical energy to internal energy for the incompressible inviscid flow?
- What is vorticity and for what condition is the vorticity of a fluid flow zero?

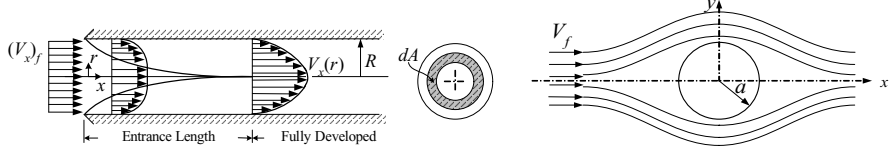
PROBLEMS

Section 1

1. A fluid element in a flow field at time t is identified with the three components of its location vectorgiven as: $r_x = 1$ cm, $r_y = -4$ cm, and $r_z = 2$ cm. Find a) the magnitude and b) sketch the direction this fluid element is heading. [Ans.: a) 4.58 cm].
2. Use Table A.IV.4(SI) to find the dynamic viscosity of air at the temperatures of 100, 300, 400, 600, 800, and 1000 K. Air is the atmospheric pressure. Plot the viscosities versus temperature and describe the trend.
3. Use Table A.IV.5(SI) to find the dynamic and kinematic viscosities of satuaertd water at 300, 400, 500, and 600 K. Plot the viscosities versus time and describe the trend. Compare the results for water with the results for air in Problem 2 and explain the difference.
4. The velocity vectors of three flow fileds are given as $\vec{V}_1 = ax\vec{i} + bx(1+t)\vec{j} + t\vec{k}$, $\vec{V}_2 = ax\vec{i} + bx(1+t)\vec{j}$, and $\vec{V}_3 = ax\vec{i} - bzy(1+t)\vec{k}$ where coefficients a and b have constant values. Is it correct to say that flow field 1 is one-, flow filed 2 is two-, and flow filed 3 is three-dimensional? Are these flow fields steady or unsteady?
5. Two large flat plates are sparated by a narrow gap filled with water. The lowr plate is stationary and the top plate moves at velocity V_f . The velocity profile in water is linear $\vec{V} = V_f(y/h)\vec{i}$ where y is the vertical distance. Find the shear stress at the wall. $T_{\text{Water}} = 20$ C, $h = 5$ mm, and $V_f = 0.5$ cm/s.
6. Water is flowing between two stationary parallel plates. For laminar flow, the velicity is a parabolic function of the vertical distance y as shown in the figure. Find a) the force applied on the lower plate and b) the average flow velocity in the fully developed region of the flow field. Data: $V_{\text{max}} = 0.1$ m/s, $h = 0.8$ cm, plate length is 1 m and the plate width is 10 cm.



7. The velocity profile for the laminar flow of water in a pipe is $V_x(r) = (V_x)_{\max}[1 - (r/R)^2]$. Find velocity at $r = R/8$, $r = R/4$, and $r = R/2$. [Ans.: $V_x(r = R/8) = 0.015625(V_x)_{\max}$].



Problems 7 and 8

Problems 9 and 22

8. In the above problem find the average flow velocity and the volumetric flow rate if the maximum velocity at the pipe centerline is 2 m/s and pipe diameter is 8 cm. [Ans.: $V_{av} = (V_x)_{\max}/2 = 1$ m/s, $5E-3$ m³/s].

9. The components of the velocity vector for the flow of an ideal fluid over a circular cylinder are:

$V_r = V_f(1 - a^2/r^2)\cos\theta$ and $V_\theta = -V_f(1 + a^2/r^2)\sin\theta$ where a and V_f are the radius of the cylinder and the velocity of the approaching flow, respectively. Find a) the magnitude of velocity at $\theta = \pi/4$ for fluid particles at $r_1 = 1.1a$, $r_2 = 1.2a$, $r_3 = 1.3a$ and b) the maximum velocity and its location. [Ans.: $V_2 = 1.22V_f$].

10. Fluid is flowing between two large plates. Flow enters the gap between the two plates at $x = 0$ and leaves the gap at $x = L$, where $L = 5$ m. The two plates are not parallel so that the flow area at $x = 0$ is twice the flow area at $x = L$. The flow enters the gap at $x = 0$ at a velocity of $V_1 = 1$ m/s. Find a) the flow velocity at $x = L$ and b) the velocity vector.

11. In Cartesian coordinates, the Eulerian description of an unsteady, two-dimensional velocity field is given as $\vec{V}(x, y, t) = e^{xt}\vec{i} + e^{yt}\vec{j}$. Find the velocity of a particle located at $x = 2$ and $y = 3$ at time $t = 1$.

12. In the polar coordinate system, as defined in Chapter VIIc, r and θ are related to x and y as $r^2 = x^2 + y^2$ and $\tan\theta = y/x$. a) Use the chain rule for differentiation to show that

$$\frac{\partial}{\partial x} = \cos\theta \frac{\partial}{\partial r} - \frac{\sin\theta}{r} \frac{\partial}{\partial \theta} \quad \text{and} \quad \frac{\partial}{\partial y} = \sin\theta \frac{\partial}{\partial r} + \frac{\cos\theta}{r} \frac{\partial}{\partial \theta}$$

b) Take the derivative of $f(r, \theta) = r\sin(2\theta)$ in the Cartesian coordinate system.

13. Use the chain rule for taking the derivative of composite functions and find dG/ds where $G = F[f_i(s), s]$. Next, find the acceleration of a fluid particle for a case in which $G = V$, $s = t$, and $f_1(s) = x(t)$, $f_2(s) = y(t)$, and $f_3(s) = z(t)$. [Ans.: $dG/ds = \sum_i (\partial G/\partial f_i) df_i/ds + \partial G/\partial s$].

Sections 2

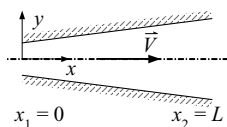
14. Find the fluid acceleration if the velocity profile is given as a) $\vec{V} = V_f(y/h)\vec{i}$ and b) $\vec{V} = V_f(yt/h)\vec{i}$.

15. The three components of a velocity vector of a fluid particle in the Cartesian coordinate system are $V_x = x^2yt^2$, $V_y = -xy^2(1+t)t$, and $V_z = 2xyt$. Find the acceleration of a fluid particle located at $x = y = z = 1$ at $t = 1$ s.

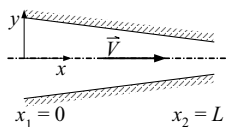
16. Consider a high-rise building. Balloons are being released steadily from each floor of the building such that the balloon population at any elevation z is given by $N = N_o[1 + (z/H)]$ where N_o is the number of balloons released at the ground and H is the elevation of the last floor. Find the observed rate of change of the balloon population as seen by a) an observer on the first floor looking up and b) an observer traveling upward in a hot-air balloon at velocity V_o . [Ans.: 0 and $V_o N_o(2z/H^2)$].

17. Specify the framework that best describes the following situations; a) a helicopter pilot following a Police chase, b) a hunter targeting a bird in a flock of birds, c) a lion chasing a wildebeast in a herd, d) a geologist watching lava flowing from a volcano, e) studying blood flow in the arteries by using suitable dyes.

18. Air flows in a duct with a rectangular flow area. At the entrance, the rectangle is 1 m by 0.5 m and at the exit, the rectangle is 1.5 m by 0.8 m. The duct is 10 m long and the volumetric flow rate of air in the duct is $1 \text{ m}^3/\text{s}$. Find the acceleration of air halfway through the duct. Is flow accelerating or decelerating? [Ans.: 0.114 m/s^2].



Problem 18



Problem 19

19. The velocity vector for a one-dimensional, steady, incompressible flow in the channel shown below is given as $\vec{V} = V_1[1 + (x/L)]\vec{i}$. Find a) the x -component of the acceleration vector and b) the position vector of a fluid particle located at $x = 0$ and time $t = 0$. [Ans.: a) $a_x = (1 + x/L)V_1^2/L$ and b) $x = L(e^{V_1 t/L} - 1)$].

20. A velocity vector is given as $\vec{V} = xyt\vec{i} - x^2yt^2\vec{j}$. Find a) the local acceleration vector. b) the convective acceleration vector. [Ans. for part a: $\vec{a}_{local} = xy\vec{i} - 2x^2yt\vec{j}$].

21. A position vector is given as $\vec{R} = R_x\vec{i} + R_y\vec{j} + R_z\vec{k}$ where $R_x = 0.334xy^2t^3 + 1.5zt^2$, $R_y = 0.5xyt^2 - x^2t$, and $R_z = -(0.334y^2zt^3 - 0.25z^2t^2)$. Find the velocity and the acceleration vectors. Calculate the acceleration of a point located at $x = 1 \text{ m}$, $y = -1 \text{ m}$, and $z = 1 \text{ m}$ at time $t = 2 \text{ s}$. [Ans.: $\vec{a} = 7\vec{i} - \vec{j} - 4.5\vec{k}$ and $|\vec{a}| = 8.38 \text{ m/s}^2$].

22. Use the components of steady flow velocity around a cylinder as given in Problem 9 and find the acceleration of a fluid element located at $r = 2a$ and $\theta = \pi/2$. [Ans.: $-(V_0)^2/(4a)$].

Section 3 (Continuity Equation)

23. Do the following vectors represent the velocity vector of an incompressible flow?

$$\vec{V}_1 = (xyzt)\vec{i} - (xyzt^2)\vec{j} + 0.5z^2(xt^2 - yt)\vec{k} \quad \text{and}$$

$$\vec{V}_2 = (xyzt)\vec{i} - (xyzt^2)\vec{j} + 0.5z^2(xt^2 - yt)\vec{k}$$

24. In a two-dimensional incompressible flow, the component V_x of the velocity vector is given as $V_x = -x^2y$. Find V_y . [Ans.: $V_y = xy^2 + C$].

25. In a three dimensional incompressible flow, V_x and V_y are given as $V_x = 3x^2 + xy^2$, $V_y = xzy$. Find V_z . [Ans.: $V_z = -(6x + y^2)z - 0.5xz^2$].

26. Two components of a two-dimensional flow in polar coordinates are given as $V_r = V_0 \cos \theta [1 - (a/r)^2]$ and $V_\theta = -V_0 \sin \theta [1 + (a/r)^2]$. Is this a steady incompressible flow?

27. The velocity vector in a flow field is represented by $\vec{V} = 2\vec{u}_r + 3\vec{u}_\theta + 4\vec{u}_\phi$ where \vec{u}_r , \vec{u}_θ , and \vec{u}_ϕ are the unit vectors of the spherical coordinate system. Does this represent an incompressible flow field?

28. The velocity vector of a steady, two-dimensional, incompressible flow in polar coordinates is shown as $\vec{V} = V_r \vec{i}_r + V_\theta \vec{i}_\theta$. If the r -component is given as $V_r = (\theta/2\pi) + V_0 \cos \theta$, find the θ -component. [Ans.: $V_0 \sin \theta$].

29. Density of a two-dimensional steady compressible flow field in the Cartesian coordinate system is given as $\rho = xy$. If the component V_x of the velocity vector is $V_x = x^2y^2$, find the differential equation from which V_y can be determined. [Ans.: $dV_y/dy + V_y/y + 3xy^2 = 0$].

30. A velocity vector is given as $\vec{V} = (xyzt)\vec{i} - (xyzt^2)\vec{j} + 0.5z^2(xt^2 - yt)\vec{k}$. Find the vector representing the applied differential force on a unit mass of the fluid (i.e., $d\vec{F}/dm$).

[Hint, $d\vec{F}/dm = (\partial \vec{V}/\partial t) + (V_x \partial \vec{V}/\partial x + V_y \partial \vec{V}/\partial y + V_z \partial \vec{V}/\partial z)$].

31. Show that the velocity of an incompressible flow has zero divergence.

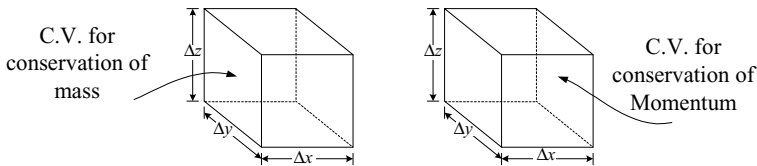
32. Velocity profile for turbulent flow in smooth circular pipes may be empirically expressed as $V(r) = V_{\max}(1 - \eta)^m$. The value of the exponent m depends on the flow condition and varies from 1/6 to 1/10, with 1/7 being used for wide ranges of turbulent flow. Find the ratio of the average to the maximum velocity in the flow field $\bar{V}/V_{\max} = f(m)$. [Ans.: $\bar{V}/V_{\max} = 2/[(m+1)(m+2)]$].

33. Derive the relation between ρ , V , and A for one-dimensional flow under steady state condition.

[Ans.: $\frac{d\rho}{\rho} + \frac{dV}{V} + \frac{dA}{A} = 0$].

34. Use the Gauss divergence theorem to obtain Equation IIIa.3.13 from IIIa.3.2.

35. Two infinitesimal elements of the same fluid in the Cartesian coordinates taken in a flow field are shown in the figure. One is used as a control volume through which fluid flows to derive the conservation equation of mass. The other is used as a differential fluid element in a free body diagram to relate the net applied forces to the acceleration of the fluid element. Specify which of these derivations uses the Eulerian and which uses the Lagrangian approach. b) Specify the conservation equation of mass in the Lagrangian approach.



36. The general form of the continuity equation that is independent of the coordinate system and applies to steady or unsteady, compressible or incompressible, viscous or inviscid flow is given by Equation IIIa.3.13. Which term of this equation represents the mass flux? Show the units of the mass flux term. Apply this equation to a compressor, which is steadily delivering compressed air to a reservoir.

37. Apply Equation IIIa.3.13 to a flow field identified with the velocity vector given as $\vec{V} = ax\vec{i}$ and density of $\rho = b + ce^{-sx} \cos ax$ where coefficients a , b , c , and s are constants.

38. Equation IIIa.3.13 for steady flow simplifies to $\vec{\nabla} \cdot \rho \vec{V} = 0$. What other condition should exist to be able to further simplify this equation and obtain $\vec{\nabla} \cdot \vec{V} = 0$?

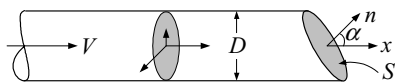
39. Regarding the differential formulation of the continuity equation, match numbers with letters:

1: $\frac{\partial \rho}{\partial t} + \vec{\nabla} \cdot (\rho \vec{V}) = 0$, 2: $\vec{\nabla} \cdot (\vec{V}) = 0$, 3: $\frac{D\rho}{Dt} + \rho(\vec{\nabla} \cdot \vec{V}) = 0$, 4: $\vec{\nabla} \cdot (\rho \vec{V}) = 0$

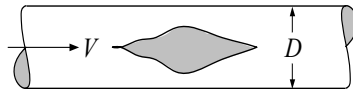
a: Lagrangian form, b: Steady flow, Eulerian form, c: Incompressible flow, d: Eulerian form

40. Water flows steadily in a pipe of inside diameter D . Flow area at exit, S is at an inclined angle α with the horizontal plane. Find α in terms of the pipe diameter and exit flow area. [Ans: $\alpha = \cos^{-1}(\pi D^2/4S)$].

- 41.** Find water flow rate at steady state condition in the above pipe for $V = 3 \text{ m/s}$, $S = 100 \text{ cm}^2$, and $\alpha = 30^\circ$.



Problems 40, 41, and 42



Problem 43

- 42.** Water is flowing steadily in a 4 in diameter pipe at a velocity of 5 ft/s. Flow area at the exit (surface S) is at an inclination angle of 30 degrees with the horizontal plane. a) Find the velocity vector as well as the vector representing surface S . b) Use the two vectors you obtained in part a to find the volumetric flow rate as:

$$\dot{V} = \int_S \vec{V} \cdot d\vec{s} = \vec{V} \cdot \vec{S}$$

- 43.** Water at 7 ft/s and 65 F flows in a 10 in schedule 40 pipe (inside diameter from Table A.III.1(SI) is 254.5 mm or 10.02 in from Table A.III.1(BU)). The pipe now bursts with an effective rupture area of twice the flow area of the pipe ($A_{\text{Rupture}} = \pi D^2/2$). Find the mass flow rate of water through the ruptured area. Assume that the flow velocity remains at 7 ft/s after the pipe ruptures. [Ans.: 239 lbm/s].

- 44.** Consider a cylinder, equipped with a piston. The cylinder contains a gas, having a density of 20 kg/m^3 when the piston is $L_o = 20 \text{ cm}$ from the closed end of the cylinder. We now pull the piston away from the closed end at a velocity of $V_{\text{piston}} = 15 \text{ m/s}$. Find the gas density at $t = 0.5 \text{ s}$ after the piston is pulled. Assume that $V_{\text{gas}} = V_{\text{piston}}(x/L)$. Note that at time zero, $L = L_o$. [Ans.: 14.5 kg/m^3].

Section 3 (Momentum Equation)

- 45.** For the flow of fluids, Newton's second law of motion can be expressed as:

$$\rho \frac{D}{Dt} \begin{bmatrix} V_x \\ V_y \\ V_z \end{bmatrix} = \begin{bmatrix} \sigma_x & \tau_{xy} & \tau_{xz} \\ \tau_{yx} & \sigma_y & \tau_{yz} \\ \tau_{zx} & \tau_{zy} & \sigma_z \end{bmatrix} \begin{bmatrix} \partial/\partial x \\ \partial/\partial y \\ \partial/\partial z \end{bmatrix} + \rho \begin{bmatrix} g_x \\ g_y \\ g_z \end{bmatrix}$$

- a) Is this equation applicable to non-Newtonian fluids?
 b) Draw the free body diagram and show all the forces applied on the infinitesimal fluid element.
 c) By taking moments about axes passing through the center of the infinitesimal element, show that the shear stresses become $\tau_{xy} = \tau_{yx}$, $\tau_{yz} = \tau_{zy}$, and $\tau_{xz} = \tau_{zx}$ (this is an implication of the Stokes hypothesis).
 d) The constitutive equations for the normal stresses are $\sigma_x = -P + \tau_{xx}$, $\sigma_y = -P + \tau_{yy}$, $\sigma_z = -P + \tau_{zz}$ where
 $\tau_{xx} = 2\mu(\partial V_x/\partial x) + \lambda \vec{\nabla} \cdot \vec{V}$, $\tau_{yy} = 2\mu(\partial V_y/\partial y) + \lambda \vec{\nabla} \cdot \vec{V}$,
 and $\tau_{zz} = 2\mu(\partial V_z/\partial z) + \lambda \vec{\nabla} \cdot \vec{V}$ where $\lambda = -2\mu/3$. Use the Stokes hypothesis to show that:

$$P = -(\sigma_x + \sigma_y + \sigma_z)/3$$

Thus, pressure at a point in a fluid is a compressive stress, having an absolute value equal to the average value of the three normal stresses applied at that point.

46. Consider the case of an ideal fluid flow in the conduit of Problem 19. Find pressure at the exit of the conduit in terms of the flow density and velocities at the inlet and the outlet. [Ans.: $P_2 = P_1 - (V_{x2}^2 - V_{x1}^2)$].

47. Show that the Navier-Stokes equations for a three dimensional, incompressible, and Newtonian fluid are:

$$\rho \frac{DV_x}{Dt} = \rho g_x - \frac{\partial P}{\partial x} + \mu \left(\frac{\partial^2 V_x}{\partial x^2} + \frac{\partial^2 V_x}{\partial y^2} + \frac{\partial^2 V_x}{\partial z^2} \right)$$

$$\rho \frac{DV_y}{Dt} = \rho g_y - \frac{\partial P}{\partial y} + \mu \left(\frac{\partial^2 V_y}{\partial x^2} + \frac{\partial^2 V_y}{\partial y^2} + \frac{\partial^2 V_y}{\partial z^2} \right)$$

$$\rho \frac{DV_z}{Dt} = \rho g_z - \frac{\partial P}{\partial z} + \mu \left(\frac{\partial^2 V_z}{\partial x^2} + \frac{\partial^2 V_z}{\partial y^2} + \frac{\partial^2 V_z}{\partial z^2} \right)$$

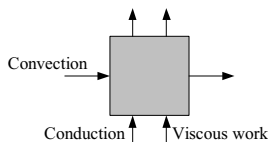
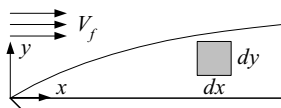
48. Two components of a two-dimensional flow are given as $V_x = x^2 - y^2$ and $V_y = -2xy$. Use the result of Problem 47 to find the condition for this velocity vector to be the solution to the Navier-Stokes equations.

49. The velocity components of a two dimensional steady ideal fluid flow (frictionless and incompressible) are given as $V_x = axy$ and $V_y = -by^2$ where coefficients a and b are constants. Find the pressure gradient in terms of a , b , x , and y . Find the value of the pressure gradient for $a = b = 1$ at point $x = y = 1$.

50. Assuming air behaves as an ideal gas use the equation of state and Equation IIIa.3.22 to find the air pressure in the upper atmosphere as a function of elevation. Use the result to find air pressure at an elevation of 1 km (3280.8 ft) from the sea level. In a winter night temperature at this elevation is measured as -16°C . [Ans.: $P = P_s e^{-Mzg/(R_u T)}$, 88.7 kPa].

Section 3 (Energy Equation)

51. Solve Example IIIa.3.13 by direct derivation. For this purpose, consider the elemental control volume inside the boundary layer as shown in the figure. Write a steady state energy balance for this control volume by considering the net convection in the flow direction, net conduction perpendicular to the flow direction, and viscous work.



52. Express the first law as is given by Equation IIIa.3.12 in terms of the enthalpy of the control volume.

53. Use Equation IIIa.3.23 to derive the rate of change of entropy for a Newtonian fluid as:

$$\frac{ds}{dt} = \frac{k}{\rho} \frac{\nabla^2 T}{T} + \frac{\Phi}{T}$$

54. Use the velocity profile of Problem 6 for laminar flow between two parallel plates to find the temperature distribution in the flow in terms of T_s , the plates temperature.

Section 3 (Fluid Rotation)

55. Derive the relation for angular velocity in terms of the velocity components for fluid rotation in a two-dimensional flow field. [Hint: Use the schematic for rotation in Figure IIIa.3.5 and find the angular velocity for line oa as $\omega_{oa} = d\alpha/dt$. Substitute for $d\alpha = dl_y/dx$ and for dl_y from $dl_y = (\partial V_y/\partial x)dxdt$. Do the same for line ob to find ω_{ob} . The z -component of rotation vector is the average of ω_{oa} and ω_{ob} . Do the same for x - and y - components].

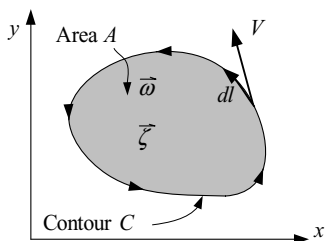
56. Show that the convective acceleration for an irrotational flow is given by $\bar{\nabla}(\bar{V} \cdot \bar{V})/2$. [Hint: Expand the relation for convective acceleration $\bar{a}_x = (\bar{V} \cdot \bar{\nabla})\bar{V}$ and set the curl of the velocity vector equal to zero].

57. Use the definition of vorticity (ζ) to find the value of $(\bar{V} \times \bar{\zeta}) \cdot d\bar{r}$ where V is the velocity vector and $d\bar{r}$ is an element of length of a streamline. [Ans.: 0].

58. The two components of the velocity vector are given as $V_x = -ay/(x^2 + y^2)^{1/2}$ and $V_y = ax/(x^2 + y^2)^{1/2}$ where a is a constant in cm/s. Find the vorticity of a fluid element located at $x = y = 1$ cm. [Ans.: $1.41a\bar{k}$].

59. An area closed by the contour C in a flow field is shown in the figure. Circulation is defined as the summation of the tangential velocity component around the contour C :

$$\Gamma = \oint_C \bar{V} \cdot d\bar{l} = \int_A \bar{\omega} \cdot d\bar{A}$$



a) Find the units of circulation Γ and b) show that $\Gamma = \oint \nabla \times \bar{V} \cdot d\bar{A}$.

Section 3 (Bernoulli Equation)

60. Flow is pumped from point A to point B in a steady state steady flow process. Start with Equation IIIa.3.12 and obtain the governing equation as given in Equation IIIa.3.31. [Hint: Equation IIIa.3.12 for steady state steady flow with one inlet port and one outlet port becomes;

$$\left(h_i + \frac{V_i^2}{2} + gZ_i \right) + q = w_s + \left(h_e + \frac{V_e^2}{2} + gZ_e \right) \quad 1$$

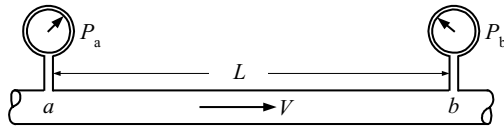
Substituting for $h = u + Pv$, noting that $u_i = u_e$, and rearranging we obtain:

$$\frac{1}{\rho g} (P_i - P_e) + \frac{1}{g} \left(\frac{V_i^2}{2} - \frac{V_e^2}{2} \right) + (Z_i - Z_e) - h_f = -h_p \quad 2$$

where q in Equation 1 is the heat produced by frictional losses and delivered from the control volume to the surroundings. Also w_s in Equation 1 is the shaft work delivered to the control volume as pump head hence, carrying a minus sign in Equation 2].

61. An inviscid fluid flows steadily at low speed in a horizontal and well-insulated pipe.

a) Consider locations a and b along the length of the pipe and chose the correct answers for velocity (V), pressure (P), and temperature (T):

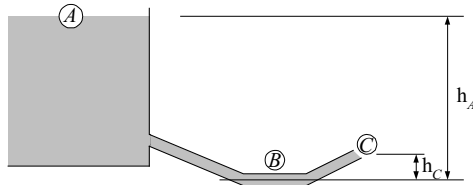


$$\begin{array}{lll} V_b < V_a, & V_b = V_a, & V_b > V_a \\ P_b < P_a, & P_b = P_a, & P_b > P_a \\ T_b < T_a, & T_b = T_a, & T_b > T_a \end{array}$$

b) Answer the same questions but for the pipe oriented so that $Z_b > Z_a$.

c) Answer the same questions but for the pipe oriented so that $Z_b < Z_a$.

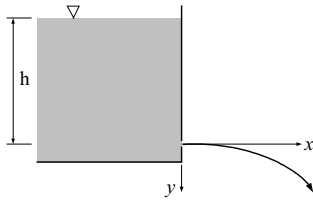
62. A large reservoir is connected to a frictionless flow path, having a small flow area, as shown in the figure.



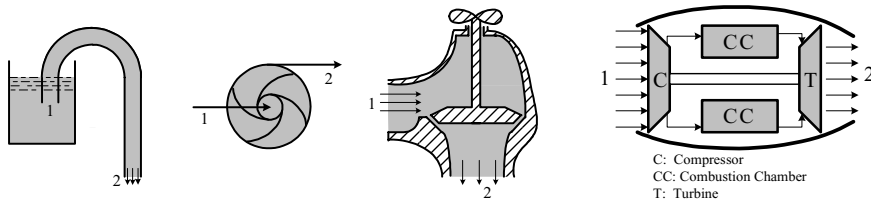
	K.E.	P.E.	K.E. + P.E.
A			
B			
C			

Specify the kinetic energy, potential energy, and total energy for points A, B, and C located on the flow path.

63. Water is flowing out of a small hole located at a depth of h below the free surface of a large reservoir. Find the equation of the stream leaving the hole in the coordinate shown in the figure. [Ans.: $y = x^2/4h$].



64. Four cases are shown in the figure: water flowing through a smooth siphon, water flowing through a pump, water flowing through an angle valve, and air flowing through an operating turbo jet. Identify the case to which the Bernoulli equation is applicable between locations 1 and 2.



For cases that the Bernoulli equation is not applicable, specify the alternative equation that should be used.

65. A turbine (see the figure of Example IIIa.3.21) is located at an elevation H_1 from the surface of a lake with the discharge pipe located at an elevation H_2 from the turbine centerline. Find flow velocity, V_4 in terms of H_1 , H_2 , P_1 , P_4 , h_s , and ρ where subscript 4 refers to the discharge piping.

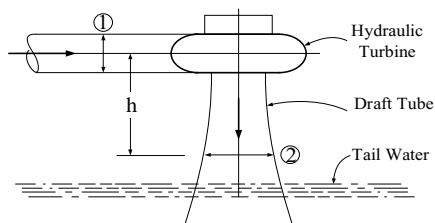
[Ans.: $V_4 = \sqrt{(2/\rho)[(P_1 - P_4) + \rho g(Z_1 - Z_4 - h_s)]}$].

66. A turbine is operating at 150 ft below the surface of a lake. Flow rate of water through the turbine is 100 ft³/s. The discharge pipe is located 10 ft above the turbine. In the discharge pipe, where velocity is 25 ft/s, pressure is measured as 12 psig. Find the maximum power developed by this turbine. [Ans.: 1164 hp].

67. A turbine is located 100 m below the surface of a lake. The discharge pipe has an elevation of 5 m from the turbine centerline. The head developed by the turbine is 81.5 m. Pressure at the discharge pipe is 15 psig. Find flow velocity and the power developed by the turbine. Ignore frictional losses and use $D_i = 4$ m. [Ans.: $V_4 = 7.62$ m/s, 76.5 MW].

68. Water at a rate of 1 m³/s enters a small hydraulic turbine from the horizontal supply line, having a diameter of 50 cm. The pressure at the inlet (stage 1 in the figure) is 200 kPa. Pressure in the turbine discharge conduit (the draft tube) at

location 2, which is 2 m below the turbine centerline, is measured as 55 kPa. Find the shaft head and the horsepower developed by this turbine. Use $D_2 = 65$ cm.



69. Consider the hydraulic jump as shown in Figure IIIa.3.7. Use the continuity and the momentum equations to derive a relation for z_2 in terms of V_1 and z_1 . [Hint: Cancel V_2 between the two equations, then cancel out $(z_1 - z_2)$ to obtain $z_2^2 + z_1 z_2 - a z_1 = 0$]. [Ans.: $z_2 = -(z_1 / 2) + \sqrt{(z_1 / 2)^2 + a z_1}$; where $a = V_1^2 / 2g$].

70. A siphon (an inverted U-tube) is used to steadily withdraw water from a large reservoir. The top of the siphon is 1.5 m higher than the surface of the water in the reservoir and the discharge side of the siphon is 8 m below the water surface. Ignore all frictional losses in the siphon. Find a) the mass flow rate of water discharged to the atmosphere and b) the pressure at the top of the siphon. Water is at $T = 27^\circ\text{C}$ and 1 atm. The diameter of the siphon tube is 5 cm. [Ans.: a) 24.6 kg/s and b) 7.86 kPa].

71. In Problem 70, find the height of the top of the siphon at which pressure reaches the vapor pressure of the water in the reservoir and the flow becomes disrupted.

72. A pipe is connected vertically to the discharge side of a pump. The top of the pipe is a short horizontal segment connected to a nozzle. The vertical length of the pipe (i.e., from the pump discharge to the horizontal segment) is 12 ft long and the pipe diameter is 4 in. The nozzle discharges water to the atmosphere at a velocity of 65 ft/s. Ignore all frictional losses and find the required pressure at the pump discharge.

IIIb. Incompressible Viscous Flow

In the previous chapter, we used Newton's second law of motion to obtain both the integral and differential forms of the momentum equation. In this chapter, we focus on the one-dimensional internal incompressible viscous flow. We use Newton's second law to find the frictional losses associated with the flow of fluids in pipes, fittings, and valves in steady state conditions. We then conclude this chapter with the study of unsteady state incompressible fluid flow.

1. Steady Incompressible Viscous Flow

Incompressible inviscid flow is a special case for which even analytical solutions in closed form can be obtained if the flow is also irrotational (known as potential flow). For incompressible viscous fluids, the task of analyzing the flow is still well developed provided the flow remains laminar. If the flow is turbulent, the traditional techniques need to be enhanced by experimental data. Hence, due to the complexity of turbulent flow, the existing theories are semi-empirical. As shown in Figure IIIa.1.5, turbulent flow is subject to large lateral fluctuations. The term turbulent stands for the chaotic nature of the fluid motion, which involves lateral mixing superimposed on the motion of the main stream. The cross-wise mixing causes additional shear stresses and friction, which results in additional energy loss for turbulent flow compared with laminar flow. The momentum transfer by crosswise mixing is shown in Figure IIIb.1.1.

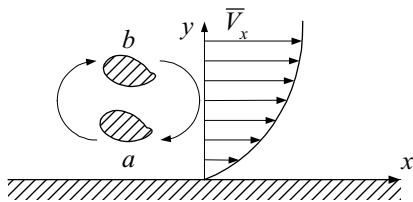


Figure IIIb.1.1. Momentum transfer in turbulent flow

Two particles of fluid having masses m_a and m_b are exchanged due to the turbulent fluctuations in a flow. In this process, due to the continuity equation, no net mass is exchanged but the momentum transfer is equal to $m[\bar{V}_x(b) - \bar{V}_x(a)]$ where $m = m_a = m_b$ and \bar{V}_x represents the average velocity. Next, we investigate the modification of the conservation equations to account for such momentum transfer due to the turbulent fluctuations.

Modification of Conservation Equations to Accommodate Turbulent Flow

Viscous Newtonian fluids follow Newton's law of viscosity for laminar flow. In turbulent flow as explained above, the shear stress is enhanced due to the existence of the local momentum transfer between the layers of the fluid. The best description for turbulent phenomena is offered by Hines, "*turbulence may be defined as an irregular condition of flow in which various quantities show a random variation with time and space, so that statistically distinct average values can be discerned.*"

The Navier-Stokes equations are valid for laminar flow. The difficulty in applying these equations to turbulent flow lies in the fact that the variables in these equations refer to the instantaneous values at the point under consideration. Reynolds modified the Navier-Stokes equations so that the variables would be time averaged. Additional terms were introduced to account for fluctuations in flow. Scores of experiments have shown that turbulent fluctuations are randomly distributed. Hence, the frequency spectrum of the fluctuations shows continuous variations with no peak, as discrete peaks imply periodicity. Mathematically, this means that the time average of the fluctuating velocity is zero.

$$\frac{1}{\theta} \int_0^\theta V'_x dt = 0$$

To modify the conservation equations, each laminar term in the equation is replaced by the turbulent equivalent such as $V_x = \bar{V}_x + V'_x$, $V_y = \bar{V}_y + V'_y$, $V_z = \bar{V}_z + V'_z$, $P = \bar{P} + P'$, etc. These are then integrated over the domain of interest (θ) noting that for V'_x , for example:

$$\frac{1}{\theta} \int_0^\theta V_x dt = \frac{1}{\theta} \int_0^\theta (\bar{V}_x + V'_x) dt = \bar{V}_x$$

This is known as the *Reynolds rule of averages*. To apply this to the conservation equation for mass, we note that the equation for steady incompressible flow is given as:

$$\frac{\partial V_x}{\partial x} + \frac{\partial V_y}{\partial y} + \frac{\partial V_z}{\partial z} = 0$$

Substituting terms and integrating yields:

$$\int_0^\theta \left(\frac{\partial V_x}{\partial x} + \frac{\partial V_y}{\partial y} + \frac{\partial V_z}{\partial z} \right) dt = \frac{\partial \bar{V}_x}{\partial x} + \frac{\partial \bar{V}_y}{\partial y} + \frac{\partial \bar{V}_z}{\partial z} = 0$$

Therefore, the conservation equation of mass is directly applicable to both laminar and turbulent flows. Let's try the same procedure for the conservation equation of momentum (Equation IIIa.3.17):

$$\rho \frac{d\bar{V}}{dt} = -\bar{\nabla}P + \rho\bar{g} + \mu\nabla^2\bar{V}$$

We may use the component of this equation along the x -axis. After substitution and integration:

$$\rho \frac{d\bar{V}_x}{dt} = -\frac{\partial \bar{p}}{\partial x} + \rho g_x + \frac{\partial}{\partial x} \left(\mu \frac{\partial \bar{V}_x}{\partial x} - \rho \overline{V'_x V'_x} \right) + \frac{\partial}{\partial y} \left(\mu \frac{\partial \bar{V}_x}{\partial y} - \rho \overline{V'_x V'_y} \right) + \frac{\partial}{\partial z} \left(\mu \frac{\partial \bar{V}_x}{\partial z} - \rho \overline{V'_x V'_z} \right)$$

Note that now some unfamiliar terms, such as $\overline{\rho V'_x V'_x}$, appear. We could not get rid of them the same way we got rid of the fluctuations by time averaging. These terms are referred to as *turbulent, eddy, or Reynolds shear stress* even though they are not shear stress. Rather, they appear as a result of fluid inertia manifested as convective acceleration. These terms are called shear stress because they appear next to the laminar shear stress term. As a result, shear stress in general is given as:

$$\tau = \mu \frac{\partial \bar{V}_x}{\partial x} - \rho \overline{V'_x V'_y} = \tau_{\text{Laminar}} + \tau_{\text{Turbulent}}$$

A similar procedure can be applied to the two other components of the momentum equation.

Let's now consider a boundary layer developed when a fluid flows over a flat plate. As shown in Figure IIIb.1.2, near the free stream, shear stress is all due to turbulent shear. This contribution diminishes rapidly as we approach the wall, dominated by viscous shear. Turbulent shear for incompressible fluid is a two-dimensional tensor. The structure of this tensor in the Cartesian coordinate system is given as:

$$\tau_{\text{Turbulent}} = \begin{pmatrix} \tau_{xx} & \tau_{xy} & \tau_{xz} \\ \tau_{yx} & \tau_{yy} & \tau_{yz} \\ \tau_{zx} & \tau_{zy} & \tau_{zz} \end{pmatrix} = -\rho \begin{pmatrix} \overline{V'_x V'_x} & \overline{V'_x V'_y} & \overline{V'_x V'_z} \\ \overline{V'_y V'_x} & \overline{V'_y V'_y} & \overline{V'_y V'_z} \\ \overline{V'_z V'_x} & \overline{V'_z V'_y} & \overline{V'_z V'_z} \end{pmatrix}$$

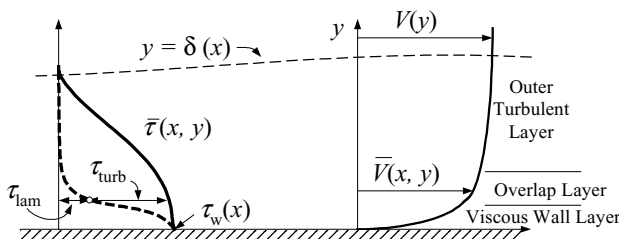


Figure IIIb.1.2. Profiles of shear stress and velocity in boundary layer

Reynolds shear can be expressed in terms of velocity gradient, similar to the Newton law of viscosity. Boussinesq made this analogy by introducing the concept of eddy viscosity to obtain:

$$\overline{V'_x V'_y} = -\varepsilon \frac{d\overline{V}_x}{dy}$$

where ε is known as eddy diffusivity for momentum. The quantity $\rho\varepsilon$ is usually interpreted as an eddy viscosity analogous to μ , the molecular viscosity, but whereas the μ is a fluid property, $\rho\varepsilon$ is a parameter of fluid motion. We study the shear stresses in internal flow in the next section.

2. Steady Internal Incompressible Viscous Flow

The topic of internal flow covers the vast field of fluid flow in pipelines, fittings, valves, pumps, and turbines.

Velocity Distribution

In Section 1 we noted that unlike laminar flow, in turbulent flow no simple relation exists between the shear stress and the mean velocity field. Hence, there is no fundamental theory to determine the velocity distribution on a purely theoretical basis. As a result, semi-empirical relations are used to determine the velocity field in turbulent flow. In this section, both laminar and turbulent flows inside pipes are studied and relevant correlations are presented.

Shown in Figure IIIb.2.1 are the boundary layers for flow inside a pipe. For the fully developed flow, flow can either be laminar or turbulent.

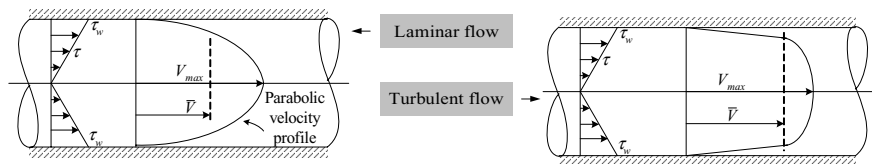


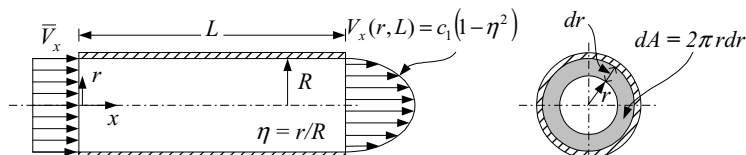
Figure IIIb.2.1. Shear stress and laminar and turbulent boundary layers in pipes

Our goal is to derive the profile for shear stress as well as the velocity profile for both laminar and turbulent flow regimes. In these derivations, we will see that the shear stress has a linear profile regardless of the flow regime. We will also see that the laminar flow has a parabolic velocity profile where the maximum velocity is much larger than the average velocity. In turbulent flow, the velocity profile is much flatter than the laminar velocity profile. Thus, the maximum velocity is just slightly larger than the average velocity. In the fully developed region, $V_r = 0$ and so is $\partial V_x / \partial x = 0$. In both flow regimes, the average velocity is obtained from:

$$\bar{V}_x = \frac{1}{A} \int_{Area} V_x(r, x) dA = \frac{1}{A} \int_{Area} V_x(r) dA$$

In this chapter, we use the average flow velocity at each cross section.

Example IIIb.2.1. The velocity distribution at the exit of a pipe is given. Find the uniform inlet velocity in terms of the maximum velocity.



Solution: To find the uniform inlet velocity, we make use of the definition of average flow velocity:

$$\bar{V}_x = \frac{1}{A} \int_{Area} V_x(r, x) dA = \frac{1}{\pi R^2} \int_0^R c_1 \left[1 - \left(\frac{r}{R} \right)^2 \right] (2\pi r dr) = \frac{2c_1}{R^2} \left[\frac{r^2}{2} - \frac{r^4}{4R^2} \right]_0^R = \frac{2c_1}{R^2} \frac{R^2}{4} = \frac{c_1}{2}$$

Shear Stress Distribution in Incompressible Viscous Flow in Pipes

Before deriving the shear stress profile, it is interesting to note that for an ideal flow, pressure changes between two points if there is a change in flow area or elevation. For viscous fluids, due to the existence of shear stresses, pressure changes even though there is no change in flow area or elevation. To derive the shear stress profile for steady incompressible viscous flow in pipes, a force balance for a control volume as shown in Figure IIIb.2.2 is used. For fluid flowing in the x -direction, pressure acting at the left area of the control volume is balanced by the pressure acting on the right surface area and by the shear stress acting on the surface area of the control volume. Note that we have used the first two terms of the Taylor expansion for pressure. From a steady state force balance, we then find that:

$$P\pi r^2 - \left(P + \frac{dP}{dx} dx \right) \pi r^2 - 2\pi r dx \tau_{rx} = 0$$

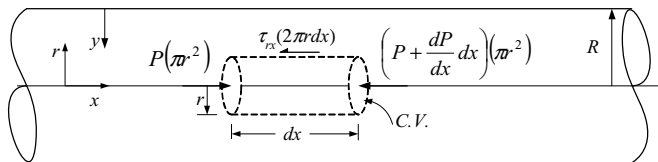


Figure IIIb.2.2. Control volume for shear stress profile in laminar and turbulent flow in pipes

which then simplifies to:

$$\tau_{rx} = -\frac{r}{2} \frac{\partial P}{\partial x}$$

The maximum shear stress occurs at the surface or wall of the pipe ($r = R$). Therefore, at the wall of the pipe:

$$\tau_w = -\frac{R}{2} \frac{\partial P}{\partial x}$$

We could obtain the same result by using the conservation equation for momentum directly, as described in the next section.

Fully Developed Laminar Flow Inside Pipes

Once past the entrance region, the steady flow of an incompressible viscous flow inside pipes would become fully developed. If the flow is laminar, the velocity profile can be derived analytically by using the conservation equations of momentum in a cylindrical coordinate system. As fluid flows along the x -axis, by using symmetry, we note that velocity at any cross section changes only in the r -direction (i.e., $V_x = V_x(r)$). Note that the same conclusion can be reached by using the conservation equation of mass. The conservation equation of momentum in a cylindrical coordinate system in the direction of flow (x -axis) gives:

$$\rho V_x \frac{\partial V_x}{\partial x} = -\frac{dP}{dx} - \frac{1}{r} \frac{\partial}{\partial r} (r\tau) = 0$$

where the only body force is gravity, which for horizontal flow has no component in the x -direction. If flow is not horizontal, the term representing gravity should be considered in the above equation. Integrating this equation, with boundary condition of $\tau = 0$ at $r = 0$, yields the same results obtained in the previous section for shear stress. To derive the velocity profile, the Newton law of viscosity can be substituted in the profile for shear stress:

$$\tau_{rx} = -\frac{r}{2} \frac{\partial P}{\partial x} = \mu \frac{\partial V_x}{\partial y}$$

This equation can now be integrated with the boundary condition of $V_x = 0$ at $r = R$. Radially, r and y are in opposite direction. Thus, for the purpose of integration, we make a change of variable from dy to $-dr$ to obtain:

$$V_x(r) = -\frac{R^2}{4\mu} \left(\frac{\partial P}{\partial x} \right) \left[1 - \left(\frac{r}{R} \right)^2 \right] \quad \text{IIIb.2.1}$$

indicating that velocity in laminar flow is a parabolic function in the r -direction. This is known as *Hagen-Poiseuille flow*. The maximum velocity occurs at $r = 0$. Hence, maximum velocity for laminar flow inside a pipe is given as:

$$(V_x)_{\max} = -\frac{R^2}{4\mu} \left(\frac{\partial P}{\partial x} \right)$$

Therefore, the velocity profile in terms of maximum velocity at any axial location can be written as:

$$\frac{V_x(r)}{(V_x)_{\max}} = 1 - \left(\frac{r}{R} \right)^2 \quad \text{IIIb.2.2}$$

The volumetric flow rate can be obtained by using its definition:

$$\dot{V} = \int \vec{V} \cdot d\vec{A} = \int_0^R (2\pi r) V_x dr = -\frac{\pi D^4}{128\mu} \frac{\partial P}{\partial x} = \frac{\pi D^4}{128\mu} \frac{\Delta P}{L} \quad \text{IIIb.2.3}$$

where the differential pressure ΔP over length L due to friction is defined as $\Delta P = P_1 - P_2$.

Wall Shear Stress In Terms of Average Velocity

To obtain a relationship between shear stress at the wall and flow average velocity, we first note that:

$$\tau_w = \tau_{rx}(r=R) = -\frac{R}{2} \frac{\partial P}{\partial x}$$

All we need to do is to relate the pressure gradient to the average flow velocity. This can be accomplished by using the results obtained in Example IIIb.2.1 by substituting for c_1 from Equation IIIb.2.1 to obtain:

$$\bar{V} = -\frac{R^2}{8\mu} \frac{\partial P}{\partial x}$$

Later in various chapters, the average flow velocity is also shown by V . Solving for pressure gradient, we find:

$$\frac{\partial P}{\partial x} = -\frac{8\mu\bar{V}}{R^2} = -32 \frac{\mu\bar{V}}{D^2}$$

To write P/x in terms of $K.E.$, we divide and multiply by $\bar{V}/2$:

$$\frac{\partial P}{\partial x} = -32 \frac{\mu\bar{V}}{D^2} = -\left(\frac{64\mu}{\rho D \bar{V}} \right) \frac{1}{D} \left(\frac{\rho \bar{V}^2}{2} \right) \quad \text{IIIb.2.4}$$

The first bracket can be written as $(64/Re)$ and shown as $f = 64/Re$, where f is known as *friction factor* or the *Darcy-Weisbach resistance coefficient*. We discuss

the friction factor in more details later in this chapter. Substituting the result obtained for $\partial P/\partial x$ in the relation for τ_w , the wall shear becomes:

$$\tau_w = -\frac{R}{2} \frac{\partial P}{\partial x} = \frac{f}{4} \left(\frac{\rho \bar{V}^2}{2} \right) \quad \text{IIIb.2.5}$$

Fully Developed Turbulent Flow Inside Pipes

Similar to the laminar flow, once past the entrance region, the steady turbulent viscous flow inside pipes becomes fully developed. In most engineering applications, flow is generally turbulent and the profile for shear stress distribution remains the same as derived in the previous section. However, unlike laminar flow, we can not use the Newton law of viscosity to derive the velocity distribution from shear stress.

As discussed in Section 1, in turbulent flow, shear stress is enhanced by addition of the Reynolds shear stress to the Newton law of viscosity:

$$\frac{\tau}{\rho} = \nu \frac{d\bar{V}_x}{dy} - \overline{V'_x V'_y}$$

where y is the distance from the pipe wall. To determine a velocity profile for turbulent flow, we would have to use the experimental data obtained for a smooth pipe, as shown in Figure IIIb.2.3.

To simplify the task of model making using the experimental data, Hinze identifies two major regions in the velocity profile. The first region is located close to the wall. In this region, viscous forces are dominant and the flow is laminar. This region is referred to as the viscous wall layer or *viscous sub-layer*. The second region includes the bulk of the flow and is referred to as the *turbulent core*. In this region, turbulent shear is dominant. The overlap or the *buffer layer* is located between the above regions. In the buffer layer both turbulent shear and viscous shear exist. Prandtl, von Karman, and Millikan used the experimental data to formulate the velocity profile in the viscous sub-layer, the turbulent core, and the buffer layer, respectively. These profiles are expressed in terms of dimensionless velocity versus dimensionless distance from the wall. To obtain non-dimensional values, a factor called the *friction velocity*, V_x^* , is used:

$$V_x^* = \sqrt{\tau_w / \rho}$$

Note that V_x^* is not actually a flow velocity, rather it is a term that has dimensions of length per unit time. Defining $V_x^+ = \bar{V}_x / V_x^*$ and $y^+ = y V_x^* / \nu$ where $\nu = \mu / \rho$ is the kinematic viscosity, we get a plot of V_x^+ versus y^+ as shown in the semi-log scale of Figure IIIb.2.3. The velocity profiles that best fit data for each region are given as:

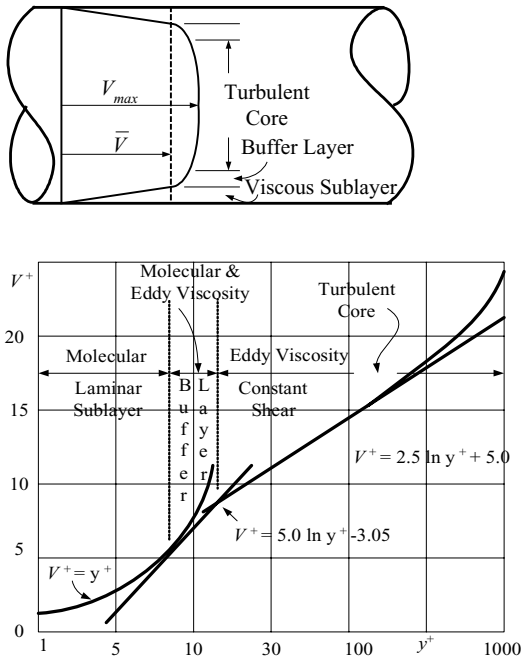


Figure IIIb.2.3. Universal turbulent velocity distribution

$$V_x = y^+ \quad y^+ < 5$$

$$V_x^+ = 5 \ln(y^+) - 3 \quad 5 \leq y^+ \leq 30$$

$$V_x^+ = 2.5 \ln(y^+) + 5 \quad y^+ > 30$$

While these profiles are representative of flow inside pipes they have two disadvantages for practical applications. First, a three-region model would need to be used to represent the flow. Second, there is a discontinuity between the formula for one region and the formula for another region. This results in a system of equations with discontinuities in the derivatives. Therefore, it is preferable to find a single velocity profile that reasonably describes turbulent flow in pipes. Pai recommended a profile in the form of a power series:

$$\frac{\bar{V}_x}{(V_x)_{\max}} = 1 + C_1 \left(\frac{r}{R}\right)^2 + C_2 \left(\frac{r}{R}\right)^m$$

for both laminar and turbulent flows. Brodkey extended this solution to non-Newtonian fluids. An even simpler profile originally suggested by Nikuradze for the turbulent core region is:

$$\frac{\overline{V_x}}{(V_x)_{\max}} = \left(\frac{y}{R}\right)^{1/n} = \left(1 - \frac{r}{R}\right)^{1/n} \quad \text{IIIb.2.6}$$

where R is pipe radius. Hinze showed that the exponent n is a function of the Reynolds number, ranging from 6 to 10. In most applications, a value of 7 is used for the exponent n . Hence, the profile for fully developed turbulent flow is referred to as a *one-seventh power profile*. Although the one-seventh power profile is very easy to use, it has its own drawbacks. For example, a simple profile is not applicable close to the wall nor does it give zero slope at the pipe centerline.

Now that velocity profiles of laminar and turbulent flows were discussed, we return to Equation IIIb.2.3 to derive a very important relation in fluid mechanics applications namely, the calculation of pressure drop in pipes for the flow of viscous fluids.

3. Pressure Drop in Steady Internal Incompressible Viscous Flow

Here we are primarily concerned with one-dimensional flow. As discussed in Section IIIa.3.3, the unrecoverable pressure drop is intrinsically associated with the flow of viscous fluids. For comparison, recall from the Bernoulli equation that any change in pressure in the flow of an ideal fluid occurs only due to a change in flow area or elevation. This is referred to as recoverable pressure drop. Conversely, the flow of viscous fluids is associated with pressure drop even if both the flow area and the flow path elevation remain the same. This is referred to as unrecoverable pressure drop. Therefore, the goal here is to calculate the unrecoverable pressure drop for both fully developed laminar and turbulent flows in pipes. Expectedly, we should be able to derive an analytic relation for pressure drop in laminar flow whereas the turbulent flow pressure drop would have to be obtained from experimental data.

Pressure drop is either due to the surface condition of the conduit wall carrying the fluid or due to the presence of fittings and valves. We begin with the study of pressure drop in straight pipes.

Pressure Drop in Fully Developed Laminar Flow

Pressure drop in steady, incompressible, fully developed laminar flow inside pipes was obtained from the solution to the conservation equation for momentum in Section 1. The pertinent relation to this discussion is Equation IIIb.2.3, which may be rearranged to obtain a relation for pressure drop:

$$\Delta P = P_1 - P_2 = \frac{128\mu L \overline{V} (\pi D^2 / 4)}{\pi D^4} = 32 \frac{L}{D} \frac{\mu \overline{V}}{D}$$

which states that pressure drop in a pipe depends on three factors, type of fluid (appears as viscosity), pipe dimensions (appears as the ratio of pipe length over pipe diameter), and average flow velocity. As discussed in Chapter IIIa, to com-

ply with tradition in hydraulics, the pressure drop may be expressed in terms of height of fluid or head. This loss in fluid head between two points is due to fluid viscosity. Hence, the pressure drop associated with friction head, h_f , is given as:

$$P_1 - P_2 = \rho g h_f \quad \text{IIIb.3.1}$$

Substituting for pressure drop, the frictional head loss becomes:

$$h_f = \frac{1}{g} \frac{1}{\rho} \left[64 \frac{L}{D} \left(\frac{\mu}{\bar{V}D} \right) \frac{\bar{V}^2}{2} \right]$$

where two times the average flow velocity is multiplied in both numerator and denominator. The terms are then grouped in separate ratios. There are two advantages for the multiplication by twice the average flow velocity. First, if density is positioned in the denominator of dynamic viscosity, this ratio constitutes the dimensionless Reynolds number, accounting for the inertial to viscous effects. The second advantage is that the square of velocity divided by 2 provides the specific kinetic energy associated with the flow of fluid. The net results can be summarized as:

$$(h_f)_{\text{Laminar}} = 64 \left(\frac{\mu}{\rho \bar{V}D} \right) \frac{L}{D} \frac{\bar{V}^2}{2g} = \left(\frac{64}{\text{Re}} \right) \frac{L}{D} \frac{\bar{V}^2}{2g} \quad \text{IIIb.3.2}$$

This relation applies to laminar flow i.e. as long as the Reynolds number stays below 2200. Recall that the ratio of $(64/\text{Re})$ is referred to as the friction factor (i.e. $f_{\text{Laminar}} = 64/\text{Re}$) and the Reynolds number is the ratio of inertial to viscous forces:

$$\text{Re} = \frac{\rho \bar{V}D}{\mu} = \frac{\dot{m}D}{\mu A} = \frac{4\dot{m}}{\pi \mu D} = \frac{\dot{V}D}{\nu A} \quad \text{IIIb.3.3}$$

Pressure Drop in Fully Developed Turbulent Flow

An analogy with laminar flow head loss can be used to derive a formula for turbulent flow to get:

$$(h_f)_{\text{Turbulent}} = f_{\text{Turbulent}} \frac{L}{D} \frac{\bar{V}^2}{2g} \quad \text{IIIb.3.4}$$

Expectedly, the friction factor in turbulent flow depends not only on fluid viscosity but also on the pipe wall roughness. Colebrook used the experimental data obtained by Prandtl's student Nikuradze to develop a correlation for friction factor as an implicit function of pipe roughness and Reynolds number. Subsequently, Moody plotted the correlation in a semi-log chart, which has become the well-known Moody diagram, as shown in Figure IIIb.3.1 (Moody 44). The Colebrook correlation is given as:

$$\frac{1}{\sqrt{f_{\text{Colebrook}}}} = -2.0 \log \left(\frac{\epsilon/D}{3.7} + \frac{2.51}{\text{Re} \sqrt{f_{\text{Colebrook}}}} \right) \quad \text{IIIb.3.5}$$

In this correlation, D is the pipe inside diameter and ε is the roughness of the pipe wall. Typical values for pipe roughness for some commercial pipes are shown in Table IIIb.3.1. Equation IIIb.3.5 is implicit in f . Hence, it requires iteration to solve for the friction factor. An example for such iteration is provided in Chapter VII. Haaland suggested an explicit formulation for friction factor as a function of pipe roughness and Reynolds number:

$$\frac{1}{f_{\text{Haaland}}^{1/2}} \approx -1.8 \log \left[\frac{6.9}{\text{Re}} + \left(\frac{\varepsilon/D}{3.7} \right)^{1.11} \right] \quad \text{IIIb.3.5-1}$$

As shown in Table IIIb.3.1, the pipe roughness (ε) is on the order of 0.00085 ft for cast iron pipes, 0.0005 ft for galvanized iron, and 0.00015 ft for commercial steel. Churchill suggests the following explicit formula:

$$f_{\text{Churchill}} = \frac{1.325}{[\ln(\varepsilon/3.7D + 5.74/\text{Re}^{0.9})]^2} \quad \text{IIIb.3.5-2}$$

The friction factor calculated from Churchill's formula is within 1% of that calculated from the Colebrook correlation and at the same time prevents iteration. Moody has recommended a similar friction factor:

$$f_{\text{Moody}} = 0.0055 \left[1 + \left(2 \times 10^4 \frac{\varepsilon}{D} + \frac{10^6}{\text{Re}} \right)^{0.333} \right] \quad \text{IIIb.3.5-3}$$

Table IIIb.3.1. Typical values of average roughness of commercial pipes

Material	ε (ft)	ε (mm)	C Hazen-Williams	n Manning
Asbestos cement	—	—	140	0.011
Asphalt cast iron	0.0004	0.120	—	0.013
Cast iron	0.00085	0.260	130	0.013
Commercial steel	0.00015	0.046	—	—
Concrete	0.001 – 0.01	0.3 – 3.0	120 – 140	0.011 – 0.014
Copper tube	smooth	smooth	150	0.010
Drawn tubing	0.000005	0.0015	—	—
Galvanized iron	0.0005	0.15	—	0.016
Glass	smooth	smooth	150	0.010
PVC, plastic	smooth	smooth	150	0.009
Riveted steel	0.003 – 0.3	0.9 – 9.0	110	0.013 – 0.017
Welded Steel	0.00015	0.046	120	0.012
Wood stave	0.0006 – 0.003	0.18 – 0.9	—	—
Wrought iron	0.00015	0.046	120	0.012

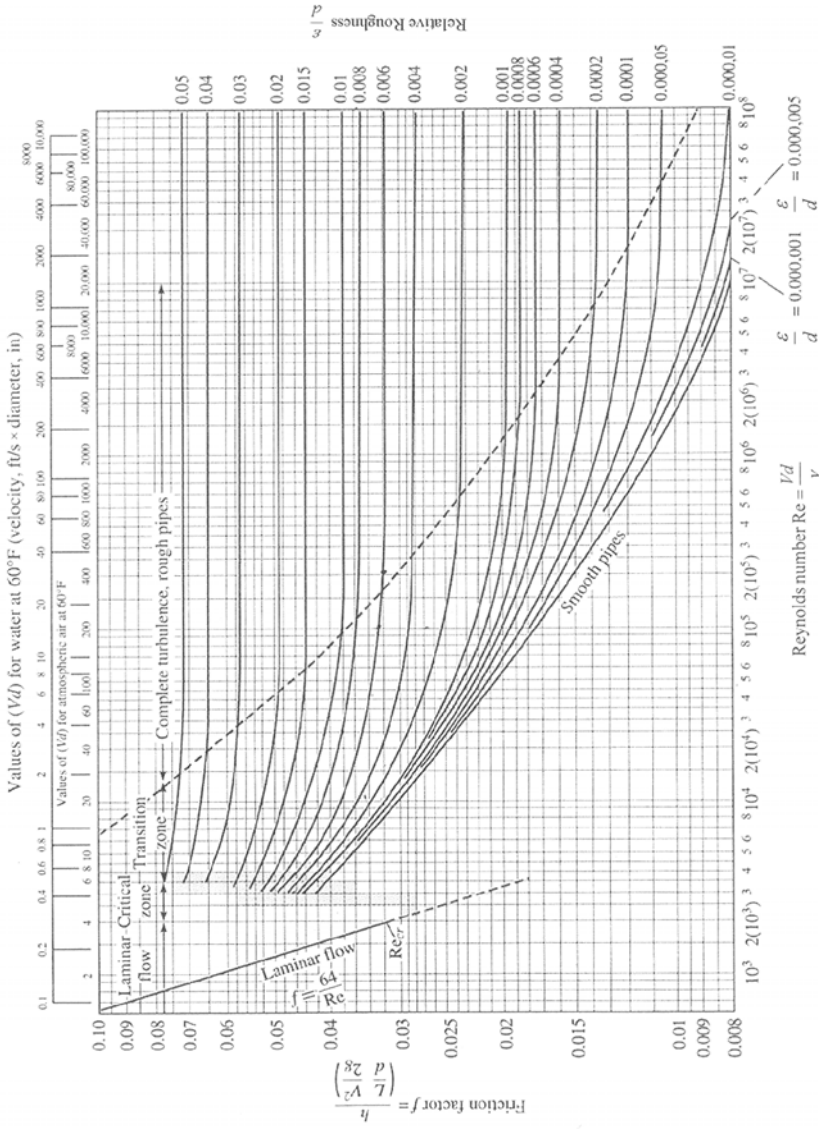


Figure IIIb.3.1. Friction factor for fully developed flow in pipes and tubes

In most engineering applications, especially in nuclear engineering, smooth pipes are used. McAdams recommends the following friction factor for fully developed turbulent flow in smooth pipes:

$$f_{\text{McAdams}} = \frac{0.184}{(\text{Re})^{0.2}} = \frac{0.184}{(\rho \bar{V} D / \mu)^{0.2}} \quad \text{IIIb.3.6}$$

For fully rough (wholly turbulent flow) and high Reynolds number, the frictional effects are produced by roughness alone without the viscous action. For this region, Vennard derives the friction factor as:

$$f_{\text{Vennard}} = [1.14 + 2 \log_{10}(D/\epsilon)]^{-2}$$

Having f , we can find pressure drop. To do this we note that the Reynolds number is dimensionless, density in British Units is in lbm/ft^3 , velocity in ft/hr , diameter in ft , and dynamic viscosity in $\text{lbm/ft}\cdot\text{hr}$. Having the head loss associated with internal flow of fluids, pressure drop can be readily found by back substitution of Equations IIIb.3.4 into Equation IIIb.3.1. Therefore, pressure drop corresponding to the frictional head loss for a viscous fluid flowing between two points can be calculated as:

$$\Delta P = P_1 - P_2 = \left(f \frac{L}{D}\right) \frac{\rho V^2}{2} = \left(f \frac{L}{D}\right) \frac{\rho \dot{V}^2}{2A^2} = \left(f \frac{L}{D}\right) \frac{\dot{m}^2}{2\rho A^2} \quad \text{IIIb.3.7}$$

To have pressure drop in British units expressed as lbf/ft^2 , the pipe length and diameter should be in ft , density in slug/ft^3 , and velocity in ft/s . Equation IIIb.3.7 is known as the *Darcy formula*. This equation is used in pipe sizing, in a pump selection analysis, and other engineering applications. It must be emphasized that Equation IIIb.3.7 should be used to calculate pressure drop due to flow friction between two points located on a straight piece of pipe. Should there be an exception to this limitation, additional pressure drops may need to be considered, as discussed later in this chapter.

Example IIIb.3.1. Fluid flows into a 3 in pipe with $\text{Re} = 200,000$. Compare the friction factor if the pipe is smooth with the friction factor if the pipe is made of cast iron.

Solution: First, for the smooth pipe, we can get reasonably accurate values by using correlation IIIb.3.7:

$$f = 0.184 \text{Re}^{-0.2} = 0.184(200,000)^{-0.2} = 0.016$$

For the cast iron pipe, we get a reasonably accurate value from the Churchill correlation without any need for iteration:

$$f = \frac{1.325}{[\ln(\epsilon/3.7D + 5.74/\text{Re}^{0.9})]^2} = \frac{1.325}{\{\ln[0.00085/(3.7 \times 3/12) + 5.74/200,000^{0.9}]\}^2} \approx 0.028$$

The corresponding pressure drop for the cast iron pipe is almost twice that of the smooth pipe.

Example IIIb.3.2. A pipeline, made of commercial steel, carries oil at a rate of $0.5 \text{ m}^3/\text{s}$. The pipe length and diameter are 1 km and 300 mm, respectively. Find pressure drop in this pipeline. Oil properties: $\rho_{oil} = 850 \text{ kg/m}^3$ and $\nu_{oil} = 1.5\text{E}-5 \text{ m}^2/\text{s}$.

Solution: We use the Churchill correlation to find f to be used in Equation IIIb.3.7. This in turn requires us to calculate the Reynolds number:

$$\text{Re} = VD/\nu = VDA/(\nu A) = \dot{V} D/\nu A$$

$$\text{Pipe flow area is } A = \pi D^2/4 = 3.14(300/1000)^2/4 = 0.0707 \text{ m}^2$$

$$\text{Hence, } \text{Re} = 0.5(300/1000)/(1.5\text{E}-5 \times 0.0707) = 141,443$$

$$f = \frac{1.325}{[\ln(\varepsilon/3.7D + 5.74/\text{Re}^{0.9})]^2} = \frac{1.325}{\{\ln[0.046/(3.7 \times 300) + 5.74/141,444^{0.9}]\}^2} \approx 0.0177$$

$$\Delta P = \left(f \frac{L}{D}\right) \frac{\dot{m}^2}{2\rho A^2} = (0.0177 \frac{1000}{0.3}) \frac{(850 \times 0.5)^2}{2 \times 850 \times (0.0707)^2} = 1.25 \text{ MPa}$$

Example IIIb.3.3. The riser of a containment spray system carries water at a rate of 1250 GPM (78.86 lit/s) to the spray header located 190 ft from the pump center line. The riser is an 8 in (20 cm) smooth pipe. Find the pump pressure rise to offset the pressure drop in the riser due to friction and elevation. Water is at 60 F.

Solution: We find the pressure drop due to friction and elevation by following the steps outlined below:

$$D = 8/12 = 0.667 \text{ ft (20.32 cm)}$$

$$A = \pi (0.667)^2/4 = 0.349 \text{ ft}^2 (0.0324 \text{ m}^2)$$

$$\dot{V} = 1250 (60/7.481) = 10,025 \text{ ft}^3/\text{h} = 2.785 \text{ ft}^3/\text{s} (78.86 \text{ lit/s})$$

$$\mu(60 \text{ F}) = 2.76 \text{ lbm/ft-h}, \rho(60 \text{ F}) = 62.35 \text{ lbm/ft}^3, \nu(60 \text{ F}) = 0.0443 \text{ ft}^2/\text{h} (1.143\text{E}-6 \text{ m}^2/\text{s})$$

$$\text{Re} = \dot{V} D/\nu A = [10,025 \times 0.667] / [0.0443 \times 0.349] = 432,608$$

$$f = 0.184/\text{Re}^{0.2} = 0.0137$$

$$h_f = f(L/D) (\dot{V}^2/2gA^2) = 0.0137(190/0.667) \times (2.785^2/2 \times 32.2 \times 0.349^2) = 4 \text{ ft}$$

Equation IIIa.3.31 is applicable:

$$\frac{1}{\rho g} (P_i - P_e) + \frac{1}{g} \left(\frac{V_i^2}{2} - \frac{V_e^2}{2} \right) + (Z_i - Z_e) = -h_s + h_f$$

We simplify this equation for the following reasons. First, the kinetic energy terms cancel out since $V_i = V_e$. Next, we note that there is no pump between point i and e hence, $h_s = 0$. This is because the control volume includes the pipe run from the discharge of the pump to the spray header. Also noting that $Z_e - Z_i = H$, thus:

$$P_i - P_e = \rho(H + h_f)g$$

Substituting

$$P_i - P_e = 62.35(190 + 4) 32.2/32.2 = 84 \text{ psi (0.58 MPa)}$$

In this problem, we did not consider frictional losses due to valves and fittings. These are included in the so-called *minor losses*, which are discussed later in this chapter.

Other Pipe Friction Models

The Darcy formula, also known as *Darcy-Weisbach*, is the most widely used model for the calculation of pipe friction. An empirical equation known as *Hazen-Williams* is often used in the calculation of frictional losses in piping networks for water. Another empirical equation, known as *Manning* is an adaptation of open-channel equation applied to the flow of water in rough pipes. The Darcy-Weisbach formula is given in Equation IIIb.3.7. The Hazen-Williams formula is given as:

$$V = 0.55CD^{0.63} \left(\frac{h_f}{L} \right)^{0.54} \quad \text{IIIb.3.8}$$

and the Manning formula as:

$$V = 0.59D^{2/3} \frac{1}{n} \left(\frac{h_f}{L} \right)^{1/2} \quad \text{IIIb.3.9}$$

where constants C and n are given in Table IIIb.3.1. Note that in the Hazen-Williams and Manning formulae D is in ft and V in ft/s. Vennard shows that both the Hazen-Williams and Manning models can be cast into the Darcy formula if f is expressed as $f_{H-W} = 1090/(C^{1.85} \text{Re}^{0.15})$ and as $f_M = 185n^2/D^{1/3}$, respectively. The advantage of the Hazen-Williams and Manning formulae is that to find the pipe diameter for a given head loss, no iteration is needed. This is demonstrated in the following example.

Example IIIb.3.4. Two water reservoirs are located 5 miles apart and have an $h_f = 250$ ft. Find the pipe diameter to carry a steady flow of $25 \text{ ft}^3/\text{s}$. The pipe is welded steel.

Solution: We first use the Hazen-Williams formula. From Table IIIb.3.1, $C = 120$ hence,

$$[25 / (\pi D^2/4)] = 0.55 \times 120 D^{0.63} [250/(5 \times 5280)]^{0.54}$$

Solving for D , we find, $D_{H-W} = 1.973$ ft or 23.7 inches. We next use the Manning formula:

$$[25 / (\pi D^2/4)] = 0.59 D^{2/3} (250/5 \times 5280)^{0.5}/0.012$$

Solving for D , we find $D_M = 2$ ft or 24 inches. The reader should now try the Darcy-Weisbach formula.

Finding the pipe diameter, D , from the Darcy equation requires iteration as we should solve Equations IIIb.3.4 and IIIb.3.5 simultaneously. Another way to avoid iteration is to use the Swamee and Jain's correlation:

$$D = 0.66 \left[\varepsilon^{1.25} \left(\frac{L \dot{V}^2}{gh_f} \right)^{4.75} + \nu \dot{V}^{9.4} \left(\frac{L}{gh_f} \right)^{5.2} \right]^{0.04} \quad \text{IIIb.3.10}$$

where ε is in ft, \dot{V} is in ft³/s, L is in ft, $g = 32.2$ ft/s², h_f in ft, ν in ft²/s, and D is in ft. Note that Equation IIIb.3.10 is applicable for $10^{-6} \leq \varepsilon \leq 0.02$ and $3 \times 10^3 \leq \text{Re} \leq 3 \times 10^6$.

Example IIIb.3.5. Solve Example IIIb.3.4 using the Swamee and Jain's correlation. Use water at $T = 65$ F.

Solution: From Table IIIb.3.1 we find $\varepsilon = 0.00015$ ft. Also for water, $\nu = 0.041$ ft²/hr = $1.13\text{E-}5$ ft²/s. We now substitute in Equation IIIb.3.10:

$$D = 0.66 [0.00015^{1.25} \left(\frac{26,399.7(25)^2}{32.2 \times 250} \right)^{4.75} + 1.13\text{E-}5 \times (25)^{9.4} \left(\frac{26,399.7}{32.2 \times 250} \right)^{5.2}]^{0.04} = 1.854 \text{ ft} \\ = 22.3 \text{ in}$$

Pressure Drop Associated with Fittings and Valves

Earlier we studied pressure drop in straight pipes due to the viscosity of the fluid and the surface condition of the pipe wall. This is known as *skin friction*. We now consider other conditions that also result in pressure drop by disturbing the flow such as twist, turn, or partial obstruction of the flow. These may result in flow separation and consequently irreversible energy loss to the fluid flow. Similar to the Darcy pressure drop, this also results in unrecoverable pressure drop.

Losses due to twist, turn, and flow obstruction are generally due to the presence of valves and fittings such as reducers, enlargers, bends, T for flow division, and invasive flowmeters. The losses due to the fittings and valves are referred to as the *minor losses*. The term *minor* should not be taken literally as depending on the flow condition the pressure drop due to the presence of pipe fittings, flowmeters, and valve may by far surpass the pressure drop caused by the skin friction.

Using an electrical engineering analogy, fluid flow is similar to electric current, pressure loss is equivalent to voltage difference and disturbance to the flow is equivalent to electrical resistance. The term "*hydraulic resistance*" for such disturbances to the flow is therefore well suited. To be consistent with Darcy pres-

sure drop (Equation IIIb.3.7), ΔP due to fittings and valves is also expressed in terms of specific kinetic energy:

$$\Delta P = K \frac{\rho V^2}{2} = K \frac{\rho \dot{V}^2}{2A^2} = K \frac{\dot{m}^2}{2\rho A^2} \quad \text{IIIb.3.11}$$

where K is referred to as *loss coefficient*. Since combined molecular and turbulent viscosity is the mechanism that converts mechanical work into heat, it is difficult to find analytical solutions to the hydraulic resistance-induced pressure drops. For this reason, each specific hydraulic resistance must be evaluated separately. Experimental data are obtained for various hydraulic resistance configurations. These data are generally correlated in terms of dimensionless numbers to account for the type of fluid (density and viscosity), flow properties (flow velocity), and the hydraulic resistance geometry (diameter, thickness, etc.) These correlations can be found in such handbooks as Idelchik, Lyons, and Crane.

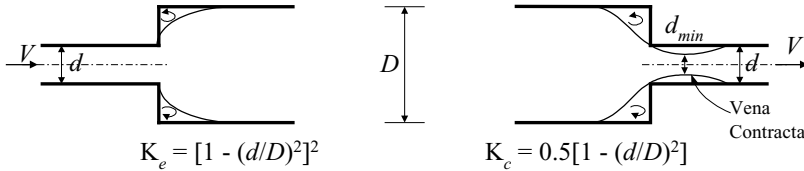


Figure IIIb.3.2. Loss coefficient associated with sudden change in flow area

As shown in Figure IIIb.3.2, a sudden expansion occurs in a flow when a pipe is connected to a larger diameter pipe without gradual increase in diameter. This results in flow separation downstream of the connection edge. In this case, the loss coefficient is derived as (Example IIIb.3.6):

$$K_e = [1 - (d/D)^2]^2$$

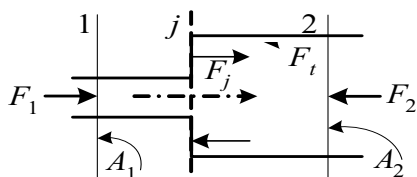
This figure also shows a sudden contraction at a junction between two pipe sizes. In a sudden contraction, flow separation in the downstream pipe causes the main stream to contract through a minimum diameter, referred to as *vena contracta*. The loss coefficient for sudden contraction is:

$$K_c = 0.5[1 - (d/D)^2]$$

For both cases of sudden expansion and contraction, the corresponding head loss is found in terms of the velocity in the smaller pipe (i.e., $h = K V_d^2 / 2g$).

Example IIIb.3.6. Derive the loss coefficient for a sudden expansion.

Solution: To find K for a sudden expansion, we write the steady-state form of the momentum equation. To do this, we consider a control volume the extent of which is from cross section 1 to cross section 2. The surface forces acting on this control volume are pressure and shear forces. Hence, we can write:



$$F_1 - F_2 - F_t + F_j = \dot{m}(V_2 - V_1) = \rho(A_2 V_2^2 - A_1 V_1^2)$$

where $F_1 = P_1 A_1$, $F_2 = P_2 A_2$, F_j is a force due to the interaction between the fluid and the channel wall at the expansion plane j , acting on area $A_2 - A_1$ and F_t is the shear force. To reduce the number of unknowns, let's assume that the friction force in the short distance between planes 1 and 2 is negligible (i.e., $F_t \approx 0$). Hence, the momentum equation simplifies to:

$$P_1 A_1 - P_2 A_2 + P_j (A_2 - A_1) = \rho(A_2 V_2^2 - A_1 V_1^2)$$

Still, we have more unknowns than equations. To get rid of P_j , we note that pressure at 1 is practically the same as pressure at cross section j due to the short distance between cross sections 1 and j , the constant flow area, and the zero shear force assumption. Substituting for $P_j = P_1$ we get:

$$A_2 (P_1 - P_2) = \rho(A_2 V_2^2 - A_1 V_1^2)$$

Relating velocities by the continuity equation, $V_2 = V_1 A_1 / A_2$ and substituting, we get:

$$P_1 - P_2 = \rho(A_2 V_2^2 - A_1 V_1^2) / A_2 = \rho V_1^2 \left[(A_1 / A_2)^2 - A_1 / A_2 \right] \quad (1)$$

We also note that Equation IIIa.3.30 gives the relation between $P_1 - P_2$ and head loss with $Z_1 = Z_2$ and $h_s = 0$:

$$P_1 - P_2 = \rho(V_2^2 - V_1^2) / 2 + \rho g h_f \quad (2)$$

We substitute for $P_1 - P_2$ from Equations (2) into Equation (1) and solve for h_f :

$$h_f = \left[1 - 2(A_1 / A_2) + (A_1 / A_2)^2 \right] (V_1^2 / 2g) \quad (3)$$

By comparing with $h_f = K V_1^2 / 2g$ we find $K \equiv (1 - A_1 / A_2)^2$. Equation (3) is known as the Borda-Carnot equation.

In a sudden contraction, if the upstream diameter approaches infinity, the loss coefficient is associated with “pipe entrance”. As shown in Figure IIIb.3.3, the smoother the entrance to a pipe, the lower the loss coefficient. For example, in the reentrant type, the pipe penetrates the flow field, causing perturbation of streamlines, some flow separation, and large head loss.

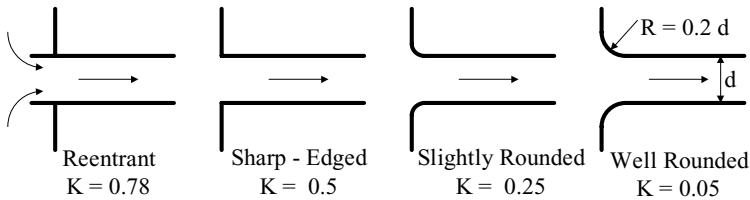


Figure IIIb.3.3. Loss coefficient associated with various pipe entrances

Table IIIb.3.2 (Crane) gives the friction factor for clean commercial steel pipe for fully turbulent flow in terms of nominal pipe size. To find loss coefficient in various valves and fittings (Table IIIb.3.3), we can either calculate the friction factor or use approximate value from Table IIIb.3.2 based on the pipe diameter.

Table IIIb.3.2. Turbulent flow friction factor for clean commercial steel pipe

Nominal Size (inch)	1/2"	3/4"	1"	1 1/4"	1 1/2"	2"	2 1/2", 3"
Nominal Size (mm)	15	20	25	32	40	50	65 - 80
f	0.027	0.025	0.023	0.022	0.021	0.019	0.018
Nominal Size (inch)	4"	5"	6"	8" - 10"	12" - 16"	18" - 24"	
Nominal Size (mm)	100	125	150	200 - 250	300 - 400	450 - 600	
f	0.017	0.016	0.015	0.014	0.013	0.012	

The loss coefficient (K) for a variety of valves and fittings is presented in Table IIIb.3.3. In this table, the loss coefficient is given in terms of an equivalent length, $K = fL_e/D$. Dependence of K on D , for flow through valves and fittings, is similar to the dependence of f on D , for flow in straight pipes. Hence, the L_e/D term tends towards a constant value for various pipe sizes of a given type of fitting. For example, consider flow through a fully opened gate valve installed on a 2 inch diameter pipe ($K = 8$ from Table IIIb.3.3). The L_e associated with this valve is found from $L_e/D = K/f = 8/0.019 = 421$. Thus $L_e = 421D = 70$ ft where f is estimated from Table IIIb.3.2 as $f = 0.019$.

Pipe and tube data are provided in Tables A.III.1 through A.III.3. In summary, total pressure drop is the summation of that given by Equations IIIb.3.7 and IIIb.3.11:

$$\Delta P = \left(f \frac{L}{D} + \sum K \right) \frac{\rho V^2}{2} = \left(f \frac{L}{D} + \sum K \right) \frac{\dot{m}^2}{2\rho A^2} \quad \text{IIIb.3.12}$$

Equation IIIb.3.12 can alternatively be written as:

$$\Delta P = f \left(\frac{L}{D} + \frac{L_e}{D} \right) \frac{\rho V^2}{2} = f \left(\frac{L + L_e}{D} \right) \frac{\rho \dot{V}^2}{2A^2} = f \frac{L'}{D} \frac{\rho \dot{V}^2}{2A^2} = f \frac{L'}{D} \frac{\dot{m}^2}{2\rho A^2} \quad \text{IIIb.3.13}$$

The frictional losses in fittings and valves are often referred to as *form losses*. Note that we may write Equation IIIb.3.13 as:

$$\dot{m} = A \sqrt{\frac{2\rho\Delta P}{K}} \quad \text{IIIb.3.14}$$

where $K = fL/D + \sum K_i$ where index i refers to various fittings and valves on the piping system. As discussed in Chapter IIIc, Equation IIIb.3.14 may also be applied to compressible flow with some modifications.

Application and Various Types of Valves

Schematics of various control and check valves are shown in Figure IIIb.3.4. Design details of a chemical, food processing, or power plant including the interrelationship of various systems and components are generally documented in so called *Piping & Instrumentation Diagrams* (P&IDs). To simplify drafting and the application of the P&IDs, symbols representing various components are devised. For example, Figure IIIb.3.5 shows symbols used to represent various types of valves. We can divide valves into two categories, flow control valves and pressure control valves. We first discuss flow control valves.

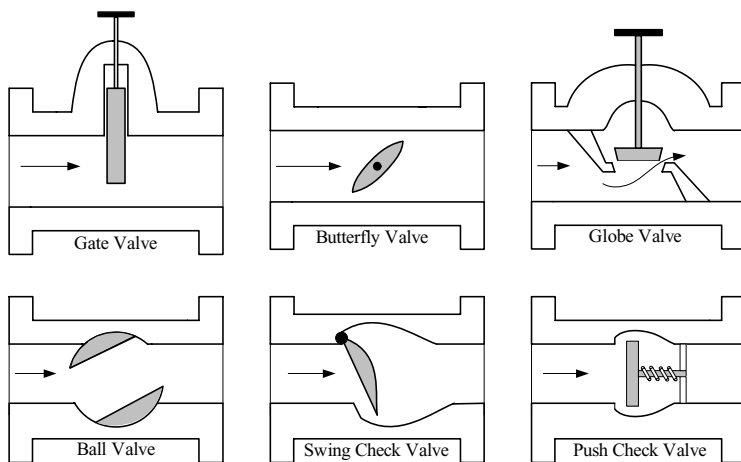


Figure IIIb.3.4. Schematics of various valves

A *gate valve* is generally used to isolate components. As such, a gate valve is either fully open or fully closed. On the other hand, to throttle the flow, *globe valves* are utilized. Expectedly, globe valves are associated with much higher-pressure drop for the flow than open gate valves. Other flow control valves include *butterfly valves*, *ball valves*, and *needle valves*. Directional valves include various types of *check valves*. For example, in a tilting disc and a swing check valve, the disc is readily lifted in the flow direction due to the flow momentum acting on the disc. However, if flow reverses, the pressure exerted on the disc would keep the valve tightly shut.

Safety valves (SVs), to control pressure, are generally spring loaded. If the pressure exceeds the high-pressure set point, the valve will lift and is then reset when pressure drops below the low-pressure set point. *Pilot Operated Relief Valves (PORVs)* can be manually or remotely operated (lifted) to relieve pressure. PORVs operate on a minimum and maximum pressure differential. In remotely operated valves, the action of obstructing or allowing the flow of fluids can be accomplished by a driver to change the position of the gate, disc, plunger, etc. Valves equipped with such drivers are generally known as *motor operated valves (MOV)*s. Depending on the type and size of a valve, the driver is an electric motor, an air operated (*pneumatic*) system, or electromagnetic (*solenoids*). For example, PORVs are generally solenoid valves.

Table IIIb.3.3. Loss coefficient (K) in L/D for valves and fittings

Category	Item	Loss Coefficient (K/f)
Elbow	90 Threaded	30
	45 Threaded	16
	90 Welded	14
	45 Welded	10
Tee	Line Flow	20
	Branch Flow	60
Valve	Gate (fully open)	8
	Gate (75% open)	35
	Gate (50% open)	160
	Gate (25% open)	900
	Swing check (fully open)	50
	Lift check (fully open)	600
	Globe (fully open)	340
	Angle (fully open)	150
	Ball (fully open)	3
	Butterfly (fully open)	50

Valve flow rate is also defined in terms of the flow coefficient C_v (also known as *valve sizing coefficient*) being the ratio of the theoretical and the actual flow rates. In applications however, C_v for the flow of incompressible fluid is defined as the flow rate of water in GPM at 60 F and at a pressure drop of 1 psi across a valve (Crane). The metric equivalent of flow coefficient is flow factor K_v , defined as the flow rate of water in m^3/h at 20 C, which results in a pressure drop of 1 bar.

Having the C_v of a valve, flow rate through the valve at temperatures other than 60 F (or liquid other than water) and pressure drops other than 1 psi may be calculated from:

$$\dot{V} = C_v \sqrt{\Delta P / S_g} \quad \text{IIIb.3.15}$$

where S_g is the liquid specific gravity, ΔP is in psi, and the volumetric flow rate is in GPM.

Example IIIb.3.7. A valve with a flow coefficient of 1000 results in a pressure drop of 2 psi (13.8 kPa) across the valve for water flowing at 110 F (43 C). Find the corresponding flow rate.

Solution: At 15 psia, we find $\rho(60 \text{ F}) = 62.4 \text{ lbm/ft}^3$ and $\rho(110 \text{ F}) = 61.88 \text{ lbm/ft}^3$. The flow rate is found from Equation IIIb.3.15 as $\dot{V} = 1000 \times [2/(61.88/62.4)]^{1/2} = 1420 \text{ GPM (89.6 lit/s)}$.

The valve loss, or resistance coefficient, can be expressed as a function of the valve C_v and the pipe inside diameter by substituting for the definition of C_v into Equation IIIb.3.11, which results in $K = 891d^4 / C_v^2$ where pipe inside diameter d is in inches. We may also find C_v for a given K and d from $C_v = 29.84d^2/K^{0.5}$.

Example IIIb.3.8. A valve of $C_v = 500$ is installed on a 5-inch pipe. Find the valve loss coefficient.

Solution: The corresponding loss coefficient for this valve is found as $K = 891d^4 / C_v^2 = 891(5)^4 / 500^2 = 2.23$

Example IIIb.3.9. Find the pressure drop over a half-open gate valve located on a horizontal 6-inch pipe carrying SAE 10W oil at 92 F and 1000 GPM. ($\varepsilon = 0.025$ in, $\nu = 0.00018 \text{ ft}^2/\text{s}$, and $S_g = 0.88$).

Solution: In the absence of a pump and for steady flow in a horizontal pipe, Equation IIIa.3.31 simplifies to Equation IIIb.3.12. For a half-open gate valve, $K = 160f$. We find f from:

$$f = [1.14 + 2 \log_{10}(D/\varepsilon)]^{-2} = [1.14 + 2 \log(6/0.025)]^{-2} = 0.029$$

Therefore, $K = 0.029 \times 160 = 4.64$. Flow area is: $A = \pi(6/12)^2/4 = 0.196 \text{ ft}^2$

Flow rate is: $\dot{V} = 1000/(60 \times 7.481) = 2.228 \text{ ft}^3/\text{s}$. Flow density is: $\rho = 62.4 \times 0.88 = 54.9 \text{ lbm/ft}^3$

Pressure drop becomes $\Delta P = 4.64 \times 54.9 (2.228)^2 / [2 \times 32.2 \times 0.196^2] = 511 \text{ lbf/ft}^2 = 3.5 \text{ psi}$.

Checking on Re to ensure flow is turbulent; $Re = [2.228 \times (6/12)] / [0.00018 \times 0.196] = 3.2E4 > 4000$

Note that from Figure IIIb.3.1, for $\epsilon/D = 0.004$ and $Re = 3.2E4$, we find $f \approx 0.03$.

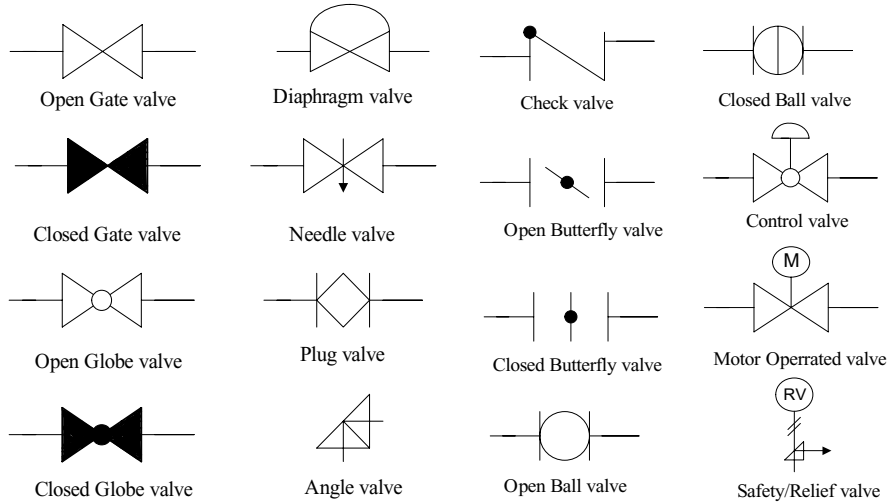
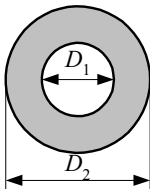


Figure IIIb.3.5. Symbols for various valves

Hydraulic diameter (D_h) is defined for channels having a flow area, different than pipes and tubes. Since flow area and perimeter for a circle are given as $A_{flow} = \pi D^2/4$ and $P = \pi D$, respectively we conclude that $A_{flow} = PD/4$. We use the same concept of dividing four times flow area by the *wetted* perimeter for other conduits to obtain an equivalent diameter $D_h = 4 A_{flow}/P_{wetted}$.

Example IIIb.3.10. Consider an annular conduit between two concentric cylinders of diameters D_1 and D_2 . Find an equivalent diameter for this conduit.

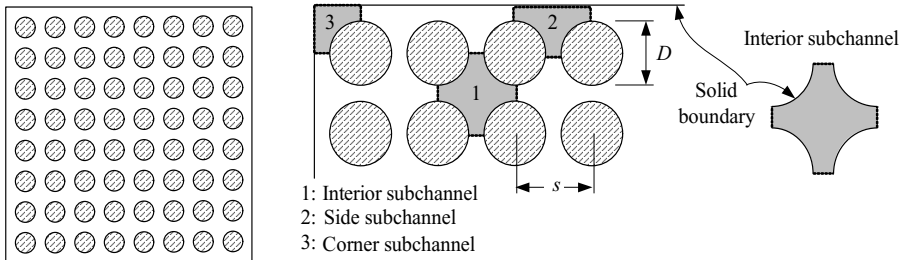


Solution: As shown in the figure, the flow area and the wetted perimeter are found as:

$A_{flow} = \pi(D_2^2 - D_1^2)/4$ and $P_{wetted} = \pi(D_2 + D_1)$. Therefore,

$$D_h = 4 \frac{\pi(D_2^2 - D_1^2)/4}{\pi(D_2 + D_1)} = D_2 - D_1$$

Example IIIb.3.11. In a BWR, fuel rods are arranged in a square array within a fuel assembly. Find the hydraulic diameter for an interior, side, and corner subchannel as shown in the figure.



Solution: With respect to the interior subchannel, we note that the control surface is bounded by the surface of the four surrounding fuel rods and the gap between the rods. The wetted perimeter consists only of the solid surfaces (i.e., the four quadrants of the four surrounding rods, as the gap is only an imaginary boundary). These are summarized in the table where D is the fuel rod outside diameter and s is the rod pitch.

No.	Type	Perimeter	Flow Area	Hydraulic diameter
1	Interior	πD	$s^2 - \pi D^2/4$	$4[s^2 - \pi D^2/4]/\pi D$
2	Side	$(\pi D/2) + s$	$[s^2 - \pi D^2/4]/2$	$2[s^2 - \pi D^2/4]/[(\pi D/2) + s]$
3	Corner	$(\pi D/4) + s$	$[s^2 - \pi D^2/4]/4$	$[s^2 - \pi D^2/4]/[(\pi D/4) + s]$

where we have assumed the rod to wall distance to be half of the rod to rod pitch.

4. Steady Incompressible Viscous Flow in Piping Systems

In this section we study the internal flow of incompressible viscous fluids in pipelines under steady-state conditions. We first begin with the flow analysis in a single-path system, the most familiar example of which is pumping liquids from a suction reservoir to a discharge reservoir, as shown in Figure IIIb.4.1. Gas and oil pipelines are examples of single-path systems. The flow path may consist of any number of valves, fittings, and instruments such as pressure gages, flowmeters, temperature probes, etc.

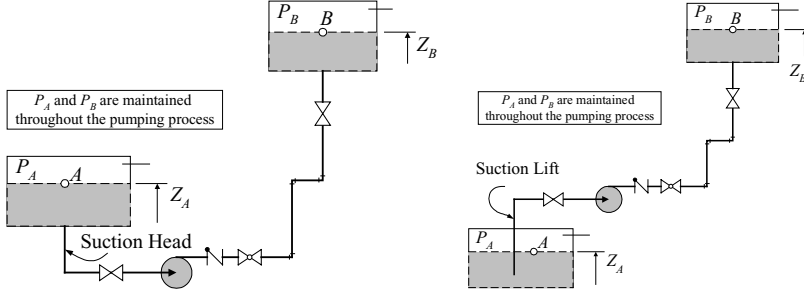


Figure IIIb.4.1. Pumping liquid in a single path system

To analyze such systems, we may apply Equation IIIb.3.31 between points A and B , located on the liquid surface of the suction and discharge reservoirs, respectively. Alternatively, we may use Equation IIIa.3.44 in steady-state resulting in:

$$\Delta P_{\text{pump}} = \Delta P_{\text{stat}} + \Delta P_{\text{grav}} + \Delta P_{\text{fric}} + \Delta P_{\text{vel-acc}} \quad \text{IIIb.4.1}$$

The definition of various differential pressure terms in Equation IIIb.4.1 is as follows:

$$\begin{aligned} \Delta P_{\text{stat}} &= P_B - P_A \\ \Delta P_{\text{grav}} &= \rho g (Z_B - Z_A) \\ \Delta P_{\text{fric}} &= \left(f \frac{L}{D} + \sum K \right) \frac{\dot{m}^2}{2 \rho A^2} \\ \begin{cases} \Delta P_{\text{vel}} = \left[\frac{1}{A_B^2} - \frac{1}{A_A^2} \right] \frac{\dot{m}^2}{2 \rho} \\ \Delta P_{\text{acc}} = \left[\frac{1}{\rho_2} - \frac{1}{\rho_1} \right] \frac{\dot{m}^2}{A^2} \end{cases} \end{aligned}$$

Writing the momentum equation in terms of differential pressures makes comprehension of the momentum equation intuitively simple. The left side of Equation IIIb.4.1 represents pressure increase in the flow while moving from pump suction to pump discharge due to momentum transfer from the pump impeller to the flow. In steady-state operation, this increase in pressure must overcome frictional losses and provide for pumping the liquid to a higher elevation. The first term on the right side, $\Delta P_{\text{stat}} = P_B - P_A$, is the difference in static pressure of point A and point B . If pressure at the suction reservoir is higher than pressure in the discharge reservoir, this term would assist the pump head and if there is no pump, this term would provide the driving force.

The second term in the right side is pressure difference due to gravity (ΔP_{grav}). A significant portion of ΔP_{pump} is used to lift liquid from point A and deliver it to

point B . This is calculated based on the elevation of the liquid level in each reservoir (measured from the same datum). If the suction reservoir has a higher elevation than the pump centerline, this term assists the pump head. If there is no pump and there is no difference in the static pressures between point A and point B , then there would be a reverse flow if point B is at a higher elevation than point A . Otherwise this term would provide the driving force. The third term in the right side is the friction pressure drop (ΔP_{fric}) which always impedes the flow.

Finally, the fourth term in the right side is the differential pressure term due to a change in flow velocity. This is either due to change in the flow area (ΔP_{vel}) or in the fluid density (ΔP_{acc}). If there is a sudden change in flow area, the associated frictional loss is accounted for by ΔP_{fric} . Hence, ΔP_{vel} accounts only for the recoverable pressure difference. In this case, as shown in Figure IIIb.4.2, the fluid densities at locations 1 and 2, i.e. before and after the area change, are practically equal. On the other hand, the flow velocity may change from location 1 to location 2 even if the flow area remains the same. This occurs when the fluid flow is heated up or cooled down. In the case of heat addition, $\rho_2 < \rho_1$ and flow is accelerated. If the flow is cooled down, $\rho_2 > \rho_1$ and flow is decelerated. In either case, the related pressure differential term is referred to as the acceleration pressure difference. In this chapter, we assume that flow remains single-phase whether heated up or cooled down. In Chapter Va, we discuss the acceleration pressure difference for two-phase flow.

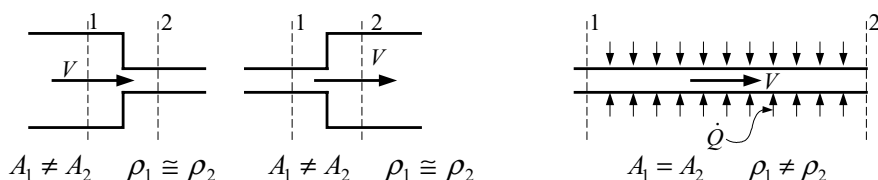


Figure IIIb.4.2. ΔP_{vel} due to sudden area change and ΔP_{acc} due to density change

4.1. Types of Problems for Flow in Single-Path Systems

For the single-path system of Figure IIIb.4.1, we can consider a total of 10 variables: pipe length (L), pipe diameter (D), pipe relative roughness ($e = \varepsilon/D$), suction reservoir pressure (P_1), discharge reservoir pressure (P_2), suction reservoir elevation (Z_1), discharge reservoir elevation (Z_2), flow temperature (T , to find μ and ρ), flow rate ($\dot{m} = \rho \dot{V}$), and pump head (h_s) or alternatively pump pressure rise (ΔP_{pump}). Let's consider a case where 5 of these variables such as L , e , Z_1 , Z_2 , and T are given. In this case, we can calculate any of the 5 remaining variables if the other four are also given. This discussion is summarized in Table IIIb.4.1 where 5 arbitrarily selected parameters of L , ε , Z_1 , Z_2 , and T are assumed to be known. Then four types of problems are identified.

Table IIb.4.1. Matrix of parameters for given L , ε , Z_1 , Z_2 , and T

Type	Known	Find
I	P_1, P_2, D, \dot{m}	ΔP_{pump}
II	$P_1, P_2, D, \Delta P_{\text{pump}}$	\dot{m}
III	$P_1, P_2, \dot{m}, \Delta P_{\text{pump}}$	D
IV	$D, \dot{m}, \Delta P_{\text{pump}}$	P_1 (or P_2)

The following four examples are solved for each of the above four types.

Type I. For Given Data Find Pump Head

Problems in which flow rate and diameter are specified have a straightforward solution as shown below.

Example IIb.4.1. The following data are given for Figure IIb.4.1. Find pump head.

Data: $L = 1000$ ft (304.8 m), smooth pipe, $Z_1 = 5$ ft (1.5 m), $Z_2 = 100$ ft (30.5 m), water at $T = 60$ F (15.5 F), $P_1 = 15$ psia (103.4 kPa), $P_2 = 30$ psia (206.8 kPa), $D = 4''$ (10.16 cm), $\dot{V} = 200$ GPM (12.6 lit/s).

Solution: To find the pump head, we need to find the various pressure differential terms of Equation IIb.4.1:

$$D = 4/12 = 0.334 \text{ ft}$$

$$A = \pi D^2/4 = \pi(0.334)^2/4 = 0.087 \text{ ft}^2 \text{ (8.08E-3 m}^2\text{)}$$

$$\text{At } T = 60 \text{ F, } \rho = 62.4 \text{ lbm/ft}^3 \text{ (998 kgm}^3\text{)}, \mu = 2.71 \text{ lbm/ft}\cdot\text{h, and } \nu = \mu / \rho = 0.044 \text{ ft}^2/\text{h (1.135E-6 m}^2\text{/s)}$$

$$\dot{V} = 200 \text{ GPM}/7.481 = 26.73 \text{ ft}^3/\text{min} = 0.445 \text{ ft}^3/\text{s (12.6 lit/s)}. \text{ Assuming turbulent flow and using Equation IIb.3.3, we find:}$$

$$\text{Re} = \dot{V} D / \nu A = 1603.8(0.334) / [0.044(0.087)] = 139,940$$

$$f = 0.184/\text{Re}^{0.2} = 0.184/(139940)^{0.2} = 0.017$$

We now calculate the pressure drop terms:

$$\Delta P_{\text{grav}} = 62.4 (32.2/32.2) (100 - 5) = 5928 \text{ lbf/ft}^2 = 41.2 \text{ psi (284 kPa)}$$

$$\Delta P_{\text{stat}} = 30 - 15 = 15 \text{ psia (103.4 kPa)}$$

To calculate Δp_{fric} , we need to find K :

$$K = K_{\text{sharp-edged}} + 4K_{90} + 2K_{\text{gate}} + K_{\text{check}} + K_{\text{globe}} + K_{\text{expansion}}$$

$$K = 0.5 + 4(14f) + 2(8f) + 50f + 340f + 1 = 8.5$$

$$\Delta P_{\text{fric}} = \left[0.017 \times \frac{1000}{0.334} + 8.5 \right] \frac{(62.4 \times 0.445)^2}{2 \times 32.2 \times 62.4 \times 0.087^2} = 10.5 \text{ psi (72.4 kPa)}$$

Therefore, $\Delta P_{\text{pump}} = 41.2 + 15 + 10.5 = 66.7 \text{ psi} = 154 \text{ ft (47 m) of water}$. We may also find the pumping power from the pump head:

$$\dot{W} = \dot{V} \Delta P = 0.445 \times (66.7 \times 144) = 15.4\text{E}6 \text{ ft}\cdot\text{lbf/h} = 5.8 \text{ kW} = 7.8 \text{ hp}$$

Assuming a pump efficiency of 70%, the required pumping power is 11 hp.

Type II. For Given Data Find Flow Rate

These types of problems generally require iteration. However, this can be avoided by using a friction factor from Table IIIb.3.2 for a clean commercial steel pipe.

Example IIIb.4.2. The following data are given for Figure IIIb.4.1. Find the flow rate of water from tank A to tank B. Data: $L = 150 \text{ m}$, smooth pipe, $Z_1 = -3 \text{ m}$, $Z_2 = 15 \text{ m}$, water at $T = 15 \text{ C}$, $P_1 = 103 \text{ kPa}$, $P_2 = 117 \text{ kPa}$, $D = 6 \text{ cm}$, pump head = 37 m, total loss coefficient = 8.5.

Solution: To find the pump flow rate, we find the various pressure differential terms:

$$D = 6/100 = 0.06 \text{ m}$$

$$A = \pi(0.06)^2/4 = 2.83\text{E}-3 \text{ m}^2$$

$$\text{At } T = 15 \text{ C}, \rho = 1000 \text{ kg/m}^3, \mu = 0.114\text{E}-2 \text{ N}\cdot\text{s/m}^2, \nu = \mu/\rho = 0.114\text{E}-5 \text{ m}^2/\text{s}$$

$$\Delta P_{\text{pump}} = \rho g h_{\text{pump}} = 1000 \times 9.81 \times 37 = 363 \text{ kPa}$$

Unlike case A, we do not have the flow rate to calculate the Reynolds number and hence f . However, to avoid iteration, we may use Table IIIb.3.2 to find $f = 0.018$. Next, we calculate all the pressure drop terms:

$$\Delta P_{\text{grav}} = \rho g (\Delta Z) = 1000 \times 9.81 [15 - (-3)] = 176.6 \text{ kPa}$$

$$\Delta P_{\text{stat}} = 117 - 103 = 14 \text{ kPa}$$

$$\Delta P_{\text{fric}} = (fL/D)\rho \dot{V}^2/2A^2 = [(0.018 \times 150/0.06) + 8.5] \times 1000 \times \dot{V}^2/[2 \times (2.83\text{E}-3)^2] = (3.34\text{E}6) \dot{V}^2 \text{ kPa}$$

According to Equation IIIb.4.1:

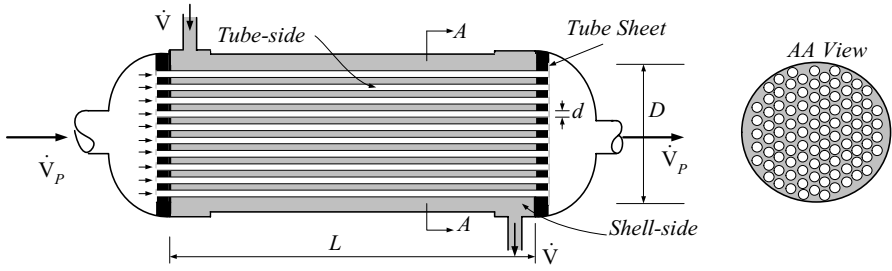
$$363 = 176.6 + 14 + (3.34\text{E}6) \dot{V}^2$$

Solving for the volumetric flow rate we find $\dot{V} = 7.2\text{E}-3 \text{ m}^3/\text{s} = 7.2 \text{ lit/s (114 GPM)}$.

Comment: Using the calculated rate, we find $\text{Re} = 133,904$ and the friction factor from Equation IIIb.3.6 as $f = 0.0174$, which is in good agreement (within 5%) with the value we used from Table IIIb.3.2.

Example IIIb.4.3. Find water flow rate at an average temperature of 60 F (15.5 C) in the shell-side of the heat exchanger. Use tube length $L = 20 \text{ ft (6 m)}$, shell inside diameter $D = 2 \text{ ft (0.6 m)}$, tube outside diameter $d = 1 \text{ in (2.54 cm)}$, number

of tubes $N_{\text{tube}} = 150$, $\Delta P = 10$ psi (69 kPa), and total loss coefficient $K = 20$.



Solution: We first find the physical properties at the average temperature:
 At $T = 60$ F, $\rho = 62.4$ lbm/ft³ (998 kg/m³), $\mu = 2.71$ lbm/ft·h ($\approx 1089\text{E}-6$ N·s/m²)
 Since we want the flow rate in the shell-side, we must calculate the hydraulic diameter;

$$A_f = \pi(D^2 - Nd^2)/4 = \pi(2^2 - 150 \times 0.0833^2)/4 = 2.32 \text{ ft}^2 \text{ (0.216 m}^2\text{)}$$

$$P_w = \pi(D + Nd) = \pi(2 + 150 \times 0.0833) = 45.553 \text{ ft (13.88 m)}$$

$$D_h = 4A_f/P_w = 0.204 \text{ ft} = 2.448 \text{ in} = 0.204 \text{ ft (6.2 cm)}$$

We now calculate the pressure differential terms:

$$\Delta P_{\text{pump}} = \Delta P_{\text{grav}} = 0$$

$$\Delta P_{\text{stat}} = P_2 - P_1 = -10 \text{ psi (69 kPa)}$$

$$\Delta P_{\text{fric}} = [(fL/D) + K] \rho \dot{V}^2 / (2 A_f^2) = L' \rho \dot{V}^2 / (2 A_f^2)$$

$$\text{where } L' = L + L_e = L + (D_h \times \Sigma K)/f = 20 + [(0.204 \times 20)/f]$$

$$\text{Substituting in Equation IIIb.4.1, we get } \Delta P_{\text{stat}} = P_2 - P_1 = -f \frac{L'}{D} \frac{\dot{m}^2}{2\rho A_f^2}$$

The solution to this equation depends on the roughness of the surfaces, which in turn determines the degree of complexity. If the surface is sufficiently rough for which an ε can be defined, then the above equation should be solved by iteration with either the Moody chart (Figure IIIb.3.1) or the Colebrook correlation (Equation IIIb.3.5). Here, we solve the above equation for smooth surface and leave the solution for a case where for example $e = 0.006$ to the reader.

Solution 1: We assume that f is a function of D_h , from Table IIIb.3.2, $f = 0.018$

$$L_e = KD/f = 20 \times 0.204/0.018 = 227 \text{ ft. Hence, } L' = L + L_e = 247 \text{ ft (72.3 m)}$$

The mass flow rate is found from Equation IIIb.3.14:

$$\dot{m} = A_f \sqrt{\frac{2\rho g_c D_h \Delta P_{\text{stat}}}{fL'}} = 2.32 \sqrt{\frac{2 \times 62.4 \times 32.2 \times 0.204 \times (10 \times 144)}{0.018 \times 247}} = 1197 \text{ lbm/s}$$

(543 kg/s)

Solution 2: If we treat friction factor as $f = f(D_h, \text{Re})$ then to solve for flow rate, we should write the friction factor as $f = 0.184/\text{Re}^{0.2}$ for smooth pipes. Since $\text{Re} = \dot{m}D_h / \mu A$ then $f = 0.184(\mu A / D_h)^{0.2} \dot{m}^{-0.2}$. We should substitute f into Equation IIIb.3.12. Note that we cannot use Equation IIIb.3.13 because we cannot find L_e from the given total K . Upon substitution into Equation IIIb.3.12 and rearrangement, we obtain:

$$\frac{K}{2\rho A_f^2} \dot{m}^2 + \frac{0.184\mu^{0.2}}{2\rho D_h A_f^{1.8}} \dot{m}^{1.8} - \Delta P_{stat} = 0 \quad \text{IIIb.4.2}$$

Substituting numerical values into Equation IIIb.4.2 we find:

$$\frac{20}{2 \times 62.4 \times 32.2 \times 2.3235^2} \dot{m}^2 + \frac{0.184 \times (2.71 \times 3600)^{0.2}}{2 \times 62.4 \times 32.2 \times 0.204 \times 2.3235^{1.8}} \dot{m}^{1.8} - (10 \times 144) = 0$$

This equation simplifies to $\dot{m}^2 + 0.335\dot{m}^{1.8} - 1.562\text{E}6 = 0$. We find by iteration $\dot{m} = 1200 \text{ lbm/s}$ (544 kg/s). This is equivalent to $\dot{V} = 8,646 \text{ GPM}$ (545 lit/s). Thus the Reynolds number is found as $\text{Re} = 140193$ and $f = 0.0172$. This shows that solution 1 provided a reasonably accurate answer while being simpler to carry out.

Comment: As discussed in Chapter VIa, heat exchangers use baffle plates to hold tubes in place and prevent flow-induced vibration. An exact value for K is peculiar to the specific design of a given heat exchanger. It is shown in Chapter VIa, that design of a heat exchanger is a compromise between both thermal and hydraulic aspects in addition to other design parameters such as cost, size, material, structure, and performance. In this problem we dealt with a few parameters such as L , ε , ΔP , D , d , N , K , and \dot{V} . The reader may perform a parametric study to see the effect of each parameter on pressure drop or the flow rate.

Type III. For Given Data Find Pipe Diameter

In problems where the pipe diameter is an unknown, we resort to iteration as shown in the next example.

Example IIIb.4.4. The following data are given for Figure IIIb.4.1. Find the pipe diameter.

Data: $L = 100 \text{ m}$, $Z_1 = 0 \text{ m}$, $Z_2 = 25 \text{ m}$, water at $T = 16 \text{ C}$, $P_1 = 105 \text{ kPa}$, $P_2 = 140 \text{ kPa}$, $\dot{V} = 0.01 \text{ m}^3/\text{s}$, pump head, $h_p = 85 \text{ m}$. The pipe is smooth and $K = 8.5$.

Solution: To find the pump flow rate, we calculate the ΔP terms for Equation IIIb.4.1:

At $T = 16 \text{ C}$, $\rho = 1000 \text{ kgm/m}^3$, $\mu = 0.111\text{E-}2 \text{ N}\cdot\text{s/m}^2$, $\nu = \mu/\rho = 0.111\text{E-}5 \text{ m}^2/\text{s}$

Since we do not have the pipe diameter, we cannot calculate the Re number and

hence f (or find f) in Table IIIb.3.2. Thus, f remains an unknown, being a function of pipe diameter, D .

To find D , we proceed as follows:

$$\Delta P_{pump} = 1000 \times 9.81 \times 85 = 833.85 \text{ kPa}$$

$$\Delta P_{grav} = 1000 \times 9.81 \times 25 = 245.3 \text{ kPa}$$

$$\Delta P_{stat} = 140 - 105 = 35 \text{ kPa}$$

$$\Delta P_{fric} = [(fL/D) + K] \dot{m}^2 / [2\rho(\pi D^2/4)^2] = \Delta P_{pump} - (\Delta P_{grav} + \Delta P_{stat}) = c_1$$

Assuming flow is turbulent, solution to this equation depends on the correlation we use for f . Let's use the simple explicit relation given by Equation IIIb.3.6 for smooth pipes, $f = 0.184/\text{Re}^{0.2}$. Substituting for $\text{Re} = VD/\nu = \dot{V}D/\nu A = 4\dot{V}/\pi \nu D$, $f = [0.184(\pi/4\dot{V})^{0.2}]D^{0.2}$. The above equation then simplifies to:

$$c_2 D^4 - c_3 D^{-0.8} - K = 0$$

where $c_2 = (\pi)^2 c_1 / (8\rho \dot{V}^2)$, $c_3 = 0.184(\pi \nu / 4\dot{V})^{0.2} L$, and $c_1 = \Delta P_{pump} - (\Delta P_{grav} + \Delta P_{stat})$

Substituting numerical values, we get:

$$c_1 = 833.85 - (245.3 + 35) = 553.55 \text{ kPa.}$$

$$c_2 = (3.14)^2 \times 553.55 / (8 \times 1000 \times 0.01^2) = 6829.15$$

$$c_3 = 0.184[3.14 \times 0.111\text{E-}5 / (4 \times 0.01)]^{0.2} \times 100 = 2.837$$

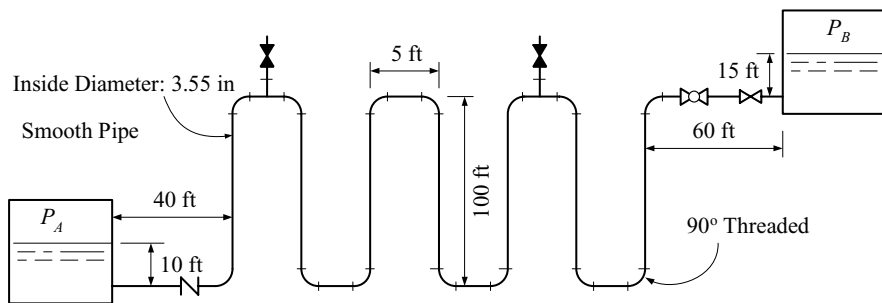
Therefore, we should solve $(6829.15 \times 1000)D^4 - 2.837D^{-0.8} - 8.5 = 0$. By iteration we find $D \approx 4.92 \text{ cm}$.

Type IV. For Given Data Find Reservoir Pressure

Solution to these types of problems is straightforward and does not require any iteration, as shown next.

Example IIIb.4.5. The steady flow rate of water in the coil from tank A to tank B is given as 200 GPM (12.6 lit/s). Find the pressure in tank A. The pressure in tank B is 250 psia (1.72 MPa) and water temperature is $T = 100 \text{ F}$ (37.8 C).

Solution: To find the pressure in tank A, we use Equation IIIb.4.1 between points A and B located on the water surface of tanks A and B, respectively.



At $T = 100\text{ F}$, $\rho = 62\text{ lbm/ft}^3$ (993 kg/m^3), $\mu = 1.647\text{ lbm/ft}\cdot\text{h}$ hence, $\nu = 0.0266\text{ ft}^2/\text{h}$ ($6.86\text{E-}7\text{ m}^2/\text{s}$).

$$L = 7 \times 100 + 6 \times 5 + 40 + 60 = 830\text{ ft (253 m)}$$

$$D = 3.55/12 = 0.296\text{ ft (0.09 m)}$$

$$A = \pi D^2/4 = \pi(0.296)^2/4 = 0.0687\text{ ft}^2\text{ (6.38E-3 m}^2\text{)}$$

$$\text{Re} = \frac{\dot{V}D}{\nu A} = \frac{(200 \times 60 / 7.481)\text{ ft}^3/\text{h} \times 0.296\text{ ft}}{0.0266\text{ ft}^2/\text{h} \times 0.0687\text{ ft}^2} = 260,000$$

$$f = 0.184/\text{Re}^{0.2} = 0.184/12.656 = 0.0152$$

The total loss coefficient is found as:

$$K = K_{\text{entrance}} + K_{\text{Check Valve}} + 14K_{90^\circ \text{ elbow}} + 2K_{\text{tee}} + K_{\text{Globe Valve}} + K_{\text{Gate Valve}} + K_{\text{exit}}$$

$$K = 0.5 + (50 + 14 \times 30 + 2 \times 20 + 340 + 8)f + 1 \cong 15$$

We now calculate the differential pressure terms including ΔP_{fric} :

$$\Delta P_{\text{stat}} = 250 - P_A$$

$$\Delta P_{\text{grav}} = 62 \times (100 + 15 - 10) = 6510\text{ lbf/ft}^2 = 45.2\text{ psi (311.6 kPa)}$$

$$\Delta P_{\text{fric}} = \left(f \frac{L}{D} + K \right) \frac{\dot{m}^2}{2\rho A^2} = \left(0.0152 \frac{830}{0.296} + 15 \right) \frac{[62 \times 200 / (7.481 \times 60)]^2}{2 \times 32.2 \times 62 \times 0.0687^2} = 2333\text{ lbf/ft}^2 = 16.2\text{ psi}$$

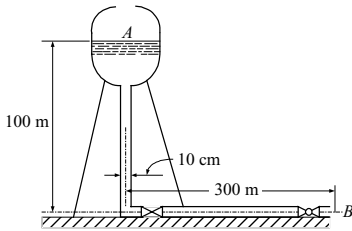
Substituting into Equation IIIb.4.1 and noting that $\Delta P_{\text{pump}} = \Delta P_{\text{vel-acc}} = 0$:

$$(250 - P_A) + 45.2 + 16.2 = 0$$

Solving for P_A , we find: $P_A = 311\text{ psia (2.14 MPa)}$.

The above example provided a situation where the piping does not conform to Figure IIIb.4.1 yet has a similar solution. The driving force in the above example was the difference in the static pressures between the supply and the receiving reservoirs. An example in which the driving force is the gravity head follows.

Example IIIb.4.6. A reservoir for water distribution is connected to a 10-cm pipe. Water surface in the reservoir is 100 m above the pipe. The pipe delivers water to a point 300 m away from the reservoir. Find the maximum flow rate.



Solution: The maximum flow rate occurs when water level is at its highest elevation and the gate and the globe valves are fully open. We now calculate the pressure terms one by one:

$$A = \pi D^2/4 = 3.140 \times 0.1^2/4 = 7.85\text{E-}3 \text{ m}^2$$

$$\Delta P_{stat} = P_B - P_A = P_{atm} - P_{atm} = 0$$

$$\Delta P_{grav} = \rho g (Z_B - Z_A) = 999 \times 9.81 (0.0 - 100) = -980,000 \text{ Pa}$$

$$\Delta P_{vel} = \left[\frac{1}{A_B^2} - \frac{1}{A_A^2} \right] \frac{\dot{m}^2}{2\rho} = \left(\frac{1}{7.85\text{E-}3} \right)^2 \frac{\dot{m}^2}{2 \times 999} = 8.12 \dot{m}^2 \text{ Pa}$$

$$fL/D = 0.017 \times (100 + 300)/0.1 = 68 \text{ (} f \text{ from Table IIIb.3.2)}$$

$$K = K_c + K_{90} + K_{gate} + K_{globe} + K_e = 0.5 + (14 + 8 + 340) \times 0.017 + 1 = 7.65$$

$$\Delta P_{fric} = \left(f \frac{L}{D} + K \right) \frac{\dot{m}^2}{2\rho A^2} = (68 + 7.65) \frac{\dot{m}^2}{2 \times 999 \times (7.85\text{E-}3)^2} = 614.5 \dot{m}^2 \text{ Pa}$$

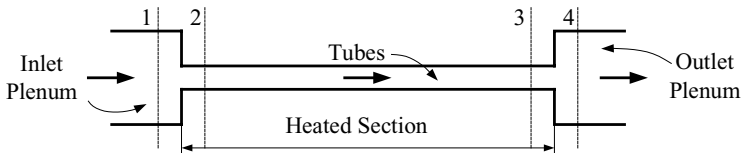
Substituting into Equation IIIb.4.1 and noting that $\Delta P_{pump} = 0$:

$$-980,000 + (8.12 + 614.5) \dot{m}^2 = 0$$

$$\dot{m}^2 = 1574 \text{ (kg/s)}^2. \text{ Thus, } \dot{m} = 39.7 \text{ kg/s and } \dot{V} \approx 40 \text{ lit/s.}$$

In the above example, we avoided iteration by using f from Table IIIb.3.2. The next example deals with the acceleration pressure drop.

Example IIIb.4.7. Air, at a rate of 12000 lbm/h enters the inlet plenum of a shell-and tube heat exchanger at 14.7 psia and 200 F. Air is heated to 800 F upon leaving the heated section and entering the outlet plenum. Find $P_1 - P_4$. Data: $N_{tube} = 50$, tube inside diameter (I.D.) = 1 in, tube length, $L = 12$ ft. Also $D_1 = D_4 = 1$ ft.



Solution: We note that $P_1 - P_4 = (P_1 - P_2) + (P_2 - P_3) + (P_3 - P_4)$.

We also note that $\Delta P_{pump} = \Delta P_{grav} = 0$.

$$A_1 = A_4 = \pi(1)^2/4 = 0.785 \text{ ft}^2, \text{ and } A_2 = A_3 = 50[\pi(1/12)^2/4] = 0.273 \text{ ft}^2$$

$$K_c = 0.5(1 - A_2/A_1) = 0.5 \times (1 - 0.273/0.785) = 0.33$$

$$K_e = (1 - A_3/A_4)^2 = (1 - 0.273/0.785)^2 = 0.43$$

$$\bar{T} = (200 + 800)/2 = 500 \text{ F}, \mu_{\text{air}} = 0.068 \text{ lbm/h}\cdot\text{ft}$$

$$\rho_2 = (14.7 \times 144)/[(1545/28.97) \times (200 + 460)] = 0.06 \text{ lbm/ft}^3$$

$$\rho_3 = (14.7 \times 144)/[(1545/28.97) \times (800 + 460)] = 0.03 \text{ lbm/ft}^3$$

$$V_1 = \frac{\dot{m}}{\rho_1 A_1} = \frac{12000/3600}{0.06 \times 0.785} = 70.7 \text{ ft/s}, V_2 = 203.5 \text{ ft/s}, V_3 = 407, V_4 = 142 \text{ ft/s}$$

$$\Delta P_{12} = \Delta P_{vel} + \Delta P_{fric} = \rho_2(V_2^2 - V_1^2)/2 + K_c \dot{m}^2 / 2\rho_2 A_2^2$$

$$\Delta P_{vel} = \rho_2(V_2^2 - V_1^2)/2 = 0.06 \times (203.5^2 - 70.7^2)/(2 \times 32.2) = 34 \text{ lbf/ft}^2 = 0.24 \text{ psi}$$

$$\Delta P_{fric} = K_c \frac{\dot{m}^2}{2\rho_2 A_2^2} = 0.33 \times \frac{(12000/3600)^2}{2 \times 0.06 \times 32.2 \times 0.273^2} = 12.7 \text{ lbf/ft}^2 = 0.09 \text{ psi}$$

$$\Delta P_{12} = 0.24 + 0.09 = 0.33 \text{ psi (2.3 kPa)}$$

$$\text{For } \Delta P_{23}, \text{Re} = \frac{\dot{m}D}{\mu A_2} = \frac{12000 \times (1/12)}{0.068 \times 0.273} = 53870$$

$$f = 0.184/\text{Re}^{0.2} = 0.184/(53820)^{0.2} = 0.02$$

$$\Delta P_{fric} = f \frac{L}{D} \frac{\dot{m}^2}{2\rho A_2^2} = 0.02 \times \frac{12}{(1/12)} \times \frac{(12000/3600)^2}{2 \times 32.2 \times 0.045 \times 0.273^2} = 1 \text{ psi}$$

Due to the considerable density change from 2 to 3, we calculate ΔP_{acc} :

$$\Delta P_{acc} = \left(\frac{1}{\rho_3} - \frac{1}{\rho_2} \right) \frac{\dot{m}^2}{A_2^2} = \left(\frac{1}{0.03} - \frac{1}{0.06} \right) \frac{(12000/3600)^2}{32.2 \times 0.273^2} = 0.53 \text{ psi}$$

$$\Delta P_{23} = \Delta P_{fric} + \Delta P_{acc} = 1 + 0.53 = 1.53 \text{ psi (10.5 kPa)}$$

$$\Delta P_{34} = \Delta P_{vel} + \Delta P_{fric} = \rho_3(V_4^2 - V_3^2)/2 + K_e \dot{m}^2 / 2\rho_3 A_3^2$$

$$\Delta P_{vel} = \rho(V_4^2 - V_3^2)/2 = 0.03 \times (142^2 - 407^2)/(2 \times 32.2) = -67.7 \text{ lbf/ft}^2 = -0.47 \text{ psi}$$

$$\Delta P_{fric} = K_e \frac{\dot{m}^2}{2\rho_3 A_3^2} = 0.43 \times \frac{(12000/3600)^2}{2 \times 0.03 \times 32.2 \times 0.273^2} = 33.2 \text{ lbf/ft}^2 = 0.23 \text{ psi}$$

$$\Delta P_{34} = -0.47 + 0.23 = -0.24 \text{ psi}$$

$$P_1 - P_4 = \Delta P_{12} + \Delta P_{23} + \Delta P_{34} = 0.33 + 1.53 - 0.24 = 1.62 \text{ psi (11 kPa)}.$$

Problems involving flow in single-path systems can be easily solved by using the software on the accompanying CD-ROM.

4.2. Application of Bernoulli Equation in Flow Measurement

Flowmeters are discussed in Chapter VIb. Our purpose here is to demonstrate one of the practical applications of the Bernoulli equation. In Example IIIa.3.18, we showed that a reduction in flow area results in the conversion of some pressure head to velocity head. By measuring the induced pressure difference we then calculated the volumetric flow rate (Equation IIIa.3.48). Depending on the manner in which the reduction in flow area is introduced, the device is called either *venturi*, *nozzle*, or *thin-plate orifice*. The schematic of these devices is shown in Figure IIIb.4.3. As seen in this figure, the smoothest reduction in flow area, hence the least unrecoverable pressure drop takes place in a venturi. This is in contrast to a thin plate orifice, with the most abrupt change in flow area, introducing the largest pressure drop. By comparison, the flow nozzle causes a medium pressure drop. Since these devices are based on the Bernoulli equation and used invasively to measure the flow rate, we refer to them as the *Bernoulli-obstruction meters*.

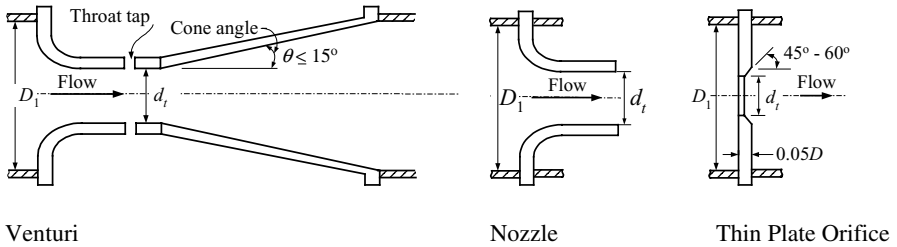


Figure IIIb.4.3. Standard shapes of various Bernoulli meters

Returning to Example IIIa.3.18, we concluded that for a frictionless venturi and an ideal fluid, flow rate can be measured from the recoverable pressure drop. In common practice however, we deal with real fluids. Hence, we must account for the non-recoverable pressure drop due to the frictional losses. This is generally accounted for by multiplication of the flow rate by a parameter known as the *discharge coefficient*, $C_d < 1$. Therefore, in common practice, the volumetric flow rate through such devices is calculated from a relation similar to Equation IIIa.3.48 but with some modifications as follows:

$$\dot{V} = \frac{C_d}{\sqrt{1-\beta^4}} A_2 \left(\frac{2(P_1 - P_2)}{\rho} \right)^{1/2} \quad \text{IIIb.4.3}$$

where β is the ratio of the diameter of the reduced area (throat) to the pipe diameter ($\beta = d_2/D$) and A_2 is the flow area at the throat as shown in Figure IIIb.4.4. For venturi meters, depending on the Reynolds number, C_d is in the range of $0.8 \leq C_d < 1.0$ and for orifice meters in the range of $0.6 \leq C_d < 0.95$. Note that in the case of the thin-plate orifice, the flow area is further reduced due to the formation of *vena contracta* (also see Figure IIIb.3.2 for sudden contraction).

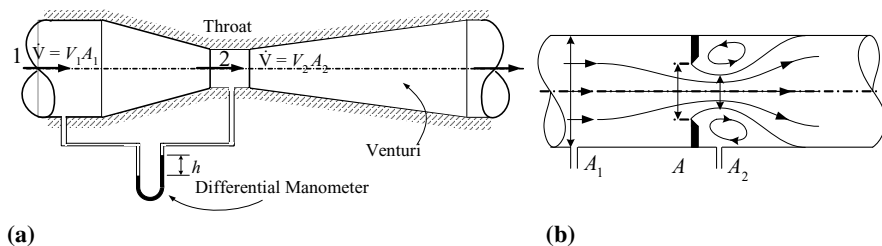


Figure IIIb.4.4. (a) A venturi equipped with a manometer and (b) an orifice meter

The multiplier in Equation IIIb.4.3 is referred to as the *Velocity of Approach Factor* given as $1/\sqrt{1-\beta^4}$. To simplify, we may represent $\alpha = C_d / \sqrt{1-\beta^4}$ to get:

$$\dot{m} = \rho \dot{V} = \alpha A_2 \sqrt{2\rho(P_1 - P_2)} \quad \text{IIIb.4.4}$$

where α is known as the *flow coefficient*. The discharge coefficient (C_d) corrects the theoretical equation for the influence of several parameters including velocity profile, the energy loss between taps, type of meter, and pressure tap locations. In general, the discharge coefficient is the product of two coefficients, the *velocity coefficient* (C_v) and the *coefficient of contraction* (C_c). The latter accounts for losses in the device and the former accounts for the flow area reduction due to the vena contracta, therefore, $C_v = \dot{V}_{\text{actual}} / \dot{V}_{\text{theoretical}}$.

The velocity coefficient, C_v , must be determined experimentally, as there is no theoretical means of calculating it. The coefficient of contraction is obtained from the ratio of the flow area at the vena contracta to the flow area at the throat; $C_c = A_{\text{vena}}/A_t$. Finally, we find the discharge coefficient from $C_d = C_v C_c$. Note that Equation IIIb.4.4 is applicable only if changes in the fluid density are negligible. The applicable equation for cases where the change in density is noticeable is discussed in Chapter IIIc.

Determination of the Discharge Coefficient

The C_d for Bernoulli-type devices are obtained as curve fits to data by ISO and recommended by ASME, as follows:

Thin Plate Orifice

$$C_d = 0.5959 + 0.0312\beta^{2.1} - 0.184\beta^8 + F_1 \frac{0.09\beta^4}{1-\beta^4} - 0.0337F_2\beta^3 + 91.71\beta^{2.5} \text{Re}_D^{-0.75}$$

In this correlation, F_1 and F_2 depend on the location of the pressure taps. For the upstream tap located at a distance equal to the pipe diameter (D) from the inlet face and the downstream tap located at a distance of ($D/2$), these factors are

0.4333 and 0.47, respectively. This is referred to as $D: D/2$ tap. For the corner taps where the meter plate meets the pipe wall, $F_1 = F_2 = 0$, hence C_d becomes:

$$C_d = 0.5959 + 0.0312\beta^{2.1} - 0.184\beta^8 + 91.71\beta^{2.5} \text{Re}_D^{-0.75} \quad \text{IIIb.4.5}$$

Long Radius Nozzle

$$C_d = 0.9965 - 0.00653 \left(\frac{10^6}{\text{Re}_D} \right) \quad \text{IIIb.4.6}$$

Venturi Nozzle

$$C_d = 0.9858 - 0.196\beta^{4.5} \quad \text{IIIb.4.7}$$

The above discharge coefficients for orifice ($D: D/2$ tap), nozzle and venturi are plotted in Figure IIIb.4.5.

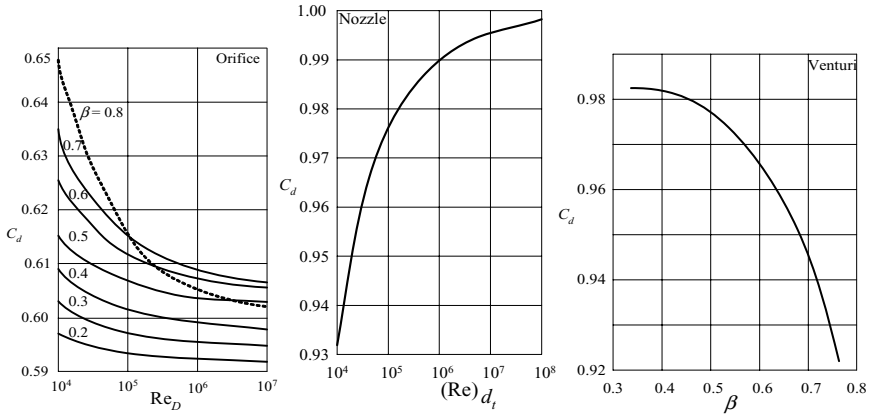


Figure IIIb.4.5. Discharge coefficient for Bernoulli obstruction meters (ISO-ASME)

4.3. Unrecoverable Head Loss for Bernoulli Obstruction Meters

Let's consider three pressure taps for the venturi and the orifice meter, as shown in Figures IIIb.4.4, and IIIb.4.6(a). The first tap is located at least one pipe diameter upstream of the meter, the second tap located at the throat of the meter and the third tap located downstream where the flow is fully recovered.

Pressure at these locations may be shown as P_1 , P_t (or P_2) and P_3 , respectively. Total pressure drop for the meter is given by the differential pressure term $P_1 - P_t$. A portion of the total pressure drop is recoverable when flow reaches location 3 where, for incompressible fluid flow velocity, V_3 becomes equal to V_1 . The remaining portion of the total pressure drop is the unrecoverable pressure drop given by $P_1 - P_3$. The ratio of the unrecoverable head loss and the total pressure differential, for the square edged orifice, flow nozzle, and venturi with 15-degree cone angle, is given in Figure IIIb.4.6(b).

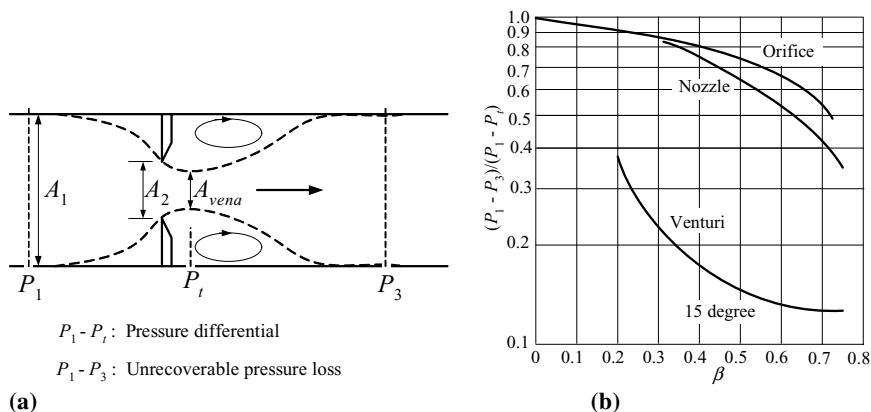


Figure IIIb.4.6. (a) Schematic of pressure taps for a thin plate orifice and (b) Pressure loss rate (Miller)

The unrecoverable head loss may also be found from the loss coefficient and the flow velocity. The loss coefficient for the three Bernoulli obstruction meters is shown in Figure IIIb.4.7. Expectedly, the flow meter that causes less disturbance to the flow is associated with smaller loss coefficient. As such, a venturi with a cone angle of 7 degrees results in the lowest and a thin-plate orifice results in the highest loss coefficient.

Having the pipe and the throat diameters, we find β and then K for a specific meter from Figure IIIb.4.7. The unrecoverable head loss is then calculated from K and the throat velocity $h_f = KV_t^2 / 2g$.

The head obtained from this equation using the loss coefficient from Figure IIIb.4.7 must agree with the head loss obtained from Figure IIIb.4.6(b).

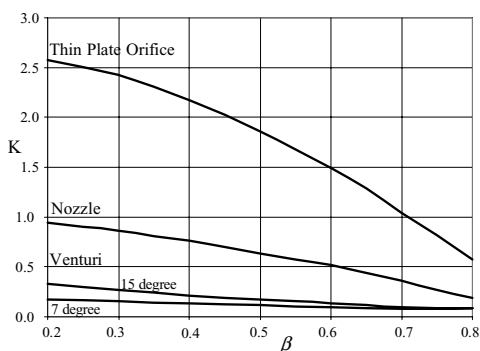


Figure IIIb.4.7. Frictional loss coefficient for Bernoulli obstruction meters (Bean)

4.4. Types of Problems for Bernoulli Obstruction Meters

Similar to the single-path piping systems, the type of problems for Bernoulli meters can be divided into three groups as shown in Table IIIb.4.2. For a given pipe diameter (D) and fluid (ρ), there are 3 parameters in Equation IIIb.4.3. Since we have only one equation, we can solve for only one unknown. Hence, the other two parameters must be given. For types I and III, the unknown must be determined by iteration. The examples that follow examine all of the types listed in Table IIIb.4.2. As we shall see in Chapter IIIc, when Equation IIIb.4.34 is applied to compressible fluids, an additional parameter (Y) will have to be dealt with.

Table IIIb.4.2. Matrix of parameters for Bernoulli-obstruction meters

Type	Known	Find
I	\dot{V}, β	ΔP
II	$\beta, \Delta P$	\dot{V}
III	$\dot{V}, \Delta P$	β

Type I. Find Pressure Drop, Given Throat Diameter and Flow Rate

Type I problems are generally used in the design process. For example, to size the pump in a flow loop to provide for the induced pressure drop due to the installation of the Bernoulli obstruction meter. Problems of this type are straightforward as no iteration is necessary. This is because, C_d can be easily calculated since the flow rate (hence, the Re number) and β are known. Having C_d , we find ΔP from Equation IIIb.4.4.

Example IIIb.4.8. A long radius nozzle is used to measure the flow rate of water in a pipeline. The pipe inside diameter is 10 in (25.4 cm) and the nozzle throat diameter is 2.5 in (6.35 cm). The nominal volumetric flow rate measured by this meter is 500 GPM (31.54 lit/s). Find the recoverable and unrecoverable pressure drops. Water flows at 100 F (38 C).

Solution: To find ΔP over the nozzle we use Equations IIIb.4.4 and IIIb.4.7:

At 100 F: $\rho = 62 \text{ lbm/ft}^3$ (993 kg/m³) and $\nu = 7.39\text{E-}6 \text{ ft}^2/\text{s}$ (6.86E-7 m²/s)

$$\dot{V} = 500 \text{ GPM} = (500/7.481)/60 = 1.11 \text{ ft}^3/\text{s} \text{ (31.54 lit/s)}$$

$$D = 10/12 = 0.833 \text{ ft}, d_t = 2.5/12 = 0.208 \text{ ft}, \text{ and } \beta = 2.5/10 = 0.25$$

$$A_1 = \pi(0.833)^2/4 = 0.545 \text{ ft}^2, \text{ hence, } V_1 = \dot{V}/A_1 = 1.11/0.545 = 2.04 \text{ ft/s}$$

$$A_t = \pi(0.208)^2/4 = 0.034 \text{ ft}^2, \text{ hence, } V_t = \dot{V}/A_t = 1.11/0.034 = 32.65 \text{ ft/s}$$

$$\text{Re}_D = V_1 D / \nu = 2.04 \times 0.833 / 7.39\text{E-}6 = 230,000$$

Finding C_d from Figure IIIb.4.4 or Equation IIIb.4.6 as:

$$C_d = 0.9965 - 0.00653 \left(\frac{10^6}{\text{Re}_D} \right) = 0.9965 - 0.00653 \left(\frac{10^6}{230,000} \right) = 0.97$$

$$\alpha = \frac{C_d}{\sqrt{1 - \beta^4}} = \frac{0.97}{\sqrt{1 - 0.25^4}} = 0.972$$

Since $\dot{V} = \alpha A_t \sqrt{2\Delta P / \rho}$, solving for ΔP :

$$\Delta P = \frac{\rho \dot{V}^2}{2\alpha^2 A_t^2} = \frac{62 \times 1.11^2}{2 \times 32.2 \times 0.972^2 \times 0.034^2} = 1086 \text{ lbf/ft}^2 = 7.54 \text{ psi}$$

For $\beta = 0.25$ from Figure IIIb.4.7 for a nozzle we find $K = h_m / [V_t^2 / 2g] \cong 0.8$

$$h_m = K \frac{V_t^2}{2g} = 0.8 \times \frac{32.65^2}{2 \times 32.2} = 13.24 \text{ ft}$$

This amounts to a pressure drop of:

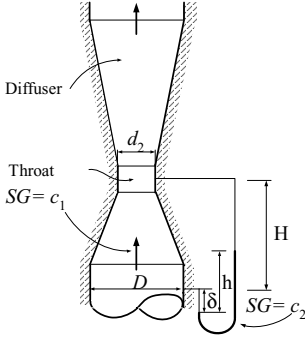
$$\Delta P_m = \rho g h_m = 62 \times 32.2 \times 13.24 / 32.2 = 821 \text{ lbf/ft}^2 = 5.7 \text{ psi}$$

Thus, of 7.54 psi total pressure drop, 5.7 psi is unrecoverable and 1.84 psi is recoverable.

Type II. Find Flow Rate, Given Throat Diameter and Pressure Drop

Type II problems are generally used for analysis of already designed and installed flowmeters. Problems of this type are rather straightforward. Iteration is generally necessary (except for the venturi nozzle) to find C_d . Then flow rate is obtained from Equation IIIb.4.4.

Example IIIb.4.9. A venturi is used to measure the flow of oil. Use the following data to find the oil flow rate. $D = 55 \text{ cm}$, $H = 75 \text{ cm}$, $h = 175 \text{ cm}$, $d_t = 22 \text{ cm}$. Specific gravity (SG) of oil is $c_1 = 0.8$ and of the manometer liquid is $c_2 = 1.3$.



Solution: Writing the Bernoulli equation between the venturi inlet and venturi throat, we get:

$$P_1 + \rho V_1^2 / 2 + \rho g Z_1 = P_2 + \rho V_2^2 / 2 + \rho g Z_2$$

Expressing velocities in terms of volumetric flow rate and rearranging terms, we get:

$$(P_1 - P_2) + \rho / 2 [1 / A_1^2 - 1 / A_2^2] \dot{V}^2 + \rho g (Z_1 - Z_2)$$

Writing in terms of $\beta = d_t/D$ and solving for \dot{V} yields:

$$\dot{V} = A_t \sqrt{2[\Delta P - \rho g H] / [\rho(1 - \beta^4)]}$$

Finally factoring in the discharge coefficient C_d and substituting in terms of the flow coefficient yields:

$$\dot{V} = \alpha A_t \sqrt{2[\Delta P - \rho g H] / \rho}$$

We find ΔP by writing the Bernoulli equation between the two ends of the manometer to get:

$$P_1 + \rho g \delta = P_t + \rho g (H + \delta - h) + \rho_m g h$$

where ρ and ρ_m are densities of fluids in the venturi and the manometer, respectively. Solving for ΔP , we get:

$$\Delta P = g[\rho(H - h) + \rho_m h]$$

Substituting numerical values, we find

$$\Delta P = 9.81[(0.8 \times 999)(0.75 - 1.75) + (1.3 \times 999)(1.75)] = 14.455 \text{ kPa}$$

Since $\beta = 0.22/0.55 = 0.4$, $C_d = 0.9858 - 0.196(0.4)^{4.5} = 0.983$. We also find

$$\alpha = 0.983 / \sqrt{1 - 0.4^4} = 0.996$$

$$A_t = \pi(0.22)^2/4 = 0.038 \text{ m}^2,$$

$$\dot{V} = 0.996 \times 0.038 \sqrt{2[14455 - (999 \times 0.8) \times 0.75] / (999 \times 0.8)} = 0.223 \text{ m}^3/\text{s}$$

Type III. Find Throat Diameter, Given Flow Rate and Pressure Drop

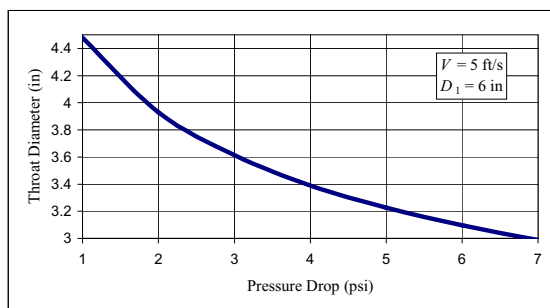
Type III problems are used in the design process to calculate the throat diameter for the intended flow rate and pressure drop. Problems of this type are generally solved by iteration.

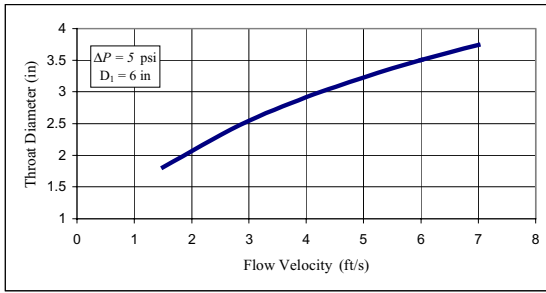
Example IIIb.4.10. We need to simulate a pressure drop of 5.0 psi caused by a pump with a seized rotor in a test section. To induce this pressure drop to the flow, we use a thin-plate orifice with corner taps. The test section is a 6 inch pipe with water flowing at 352 GPM and 60 F. Find the throat diameter of the orifice.

Solution: To find the throat diameter, we should first find $C_d(\beta)$ from $\dot{V} = [A_1 C_d / \sqrt{1 - \beta^4}] \sqrt{2\Delta P / \rho}$ and set it equal to C_d from the ISO curve fit for thin-plate orifice. Since both of these equations are highly non-linear functions of β , we have to resort to iteration.

$D = 6/12 = 0.5$ ft hence, $A_1 = 3.14(0.5)^2/4 = 0.196$ ft². Since $\dot{V} = 352/(7.481 \times 60) = 0.784$ ft³/s, therefore $V_1 = 0.784/0.196 = 4$ ft/s and $Re_D = V_1 D / \nu = 4 \times 0.5 / 1.23E-5 = 0.163E6$. Final results of the iteration are:

$\beta = d_2/D_1$ (-):	0.485	Throat diameter (in):	2.913
Throat velocity (ft/s):	16.96	Reynolds number (-):	0.16E6
Discharge Coefficient (-):	0.602	Loss coefficient (-):	1.910
Head loss (ft):	8.536	Pressure loss (psi):	3.696
Velocity of approach factor (-):	1.029	Flow coefficient (-):	0.620





Having solved the problem, we now want to find how the throat diameter changes with flow or with pressure drop. Intuitively, we know that for given D_1 and ΔP , the larger the flow rate, the larger the throat diameter. This is because pressure drop increases with flow velocity. That lessens demand on the thin-plate orifice for pressure drop. Conversely, for given flow velocity and pipe inside diameter, the higher the pressure drop (ΔP), the smaller the throat diameter. These are shown in the above plots.

Problems involving flow in single-path systems and the Bernoulli obstruction meters can be easily solved by using the software on the accompanying CD-ROM.

4.4. Flow in Compound Conduits

In common practice, pipes of different lengths and diameters are connected via reducers and enlargers. This constitutes a serial-path system as shown in Figure IIIb.4.8(a). For example, the riser of a containment spray system consists of a serial flow path. On the other hand, pipes may be connected at both ends to a common plenum, or header, such that flow entering the inlet plenum is divided between the pipes. This constitutes a system with parallel flow paths. There are two types of parallel flow path systems. In the first type, flow is mixed only at the inlet and exit plenum, as shown in Figure IIIb.4.8(b). We refer to this type as closed parallel flow path. This is the type that we study in this chapter. In the second type, flow is also intermixing between various flow paths. For example, the fuel assemblies of a BWR core constitute a closed parallel path system where flow is mixed in the lower plenum prior to entering the core and in the upper plenum after leaving the core. On the other hand, the core of a PWR consists of many open parallel flow paths where flows are mixed due to the existing cross flow between the subchannels, having lateral communication.

We now compare the hydraulic characteristics of the serial and closed parallel path systems with respect to flow rate and pressure drop. For simplicity, we refer to the closed parallel flow path as parallel flow path.

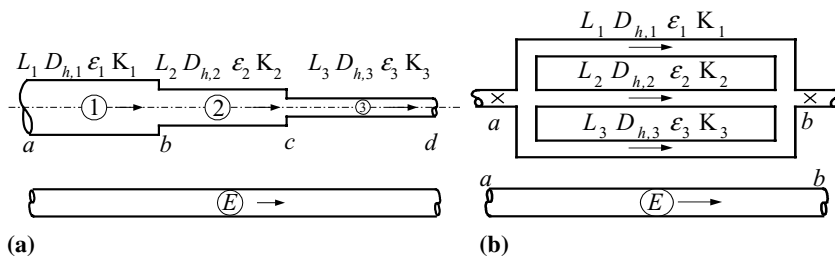


Figure IIIb.4.8. Flow paths connected in series and in parallel and their equivalent flow path

Comparison of Serial-Path Systems with Parallel-Path Systems

For the steady flow of incompressible viscous fluids, we first consider pipes connected in series as shown in Figure IIIb.4.8(a). Pipes in series have generally different length, diameter, and loss coefficient. Therefore, while flow rate is the same for all the pipe segments, pressure drops are generally different:

Pipes in Series

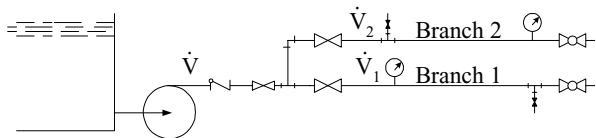
$$\dot{V}_1 = \dot{V}_2 = \dot{V}_3 \quad \Delta P_1 \neq \Delta P_2 \neq \Delta P_3 \quad \Delta P = \Delta P_1 + \Delta P_2 + \Delta P_3$$

Similarly, as shown in the right side of Figure IIIb.4.8(b), parallel pipes may also have different diameter, length, and loss coefficient. In this case however;

Pipes in Parallel

$$\dot{V}_1 \neq \dot{V}_2 \neq \dot{V}_3 \quad \dot{V} = \dot{V}_1 + \dot{V}_2 + \dot{V}_3 \quad \Delta P_1 = \Delta P_2 = \Delta P_3$$

Example IIIb.4.11. A pump delivers water at a steady rate of $\dot{V} \text{ m}^3/\text{s}$ to a branch containing two parallel lines. Find flow rate in branch 1 in terms of \dot{V} and the known diameters, lengths, flow areas, and loss coefficients.



Solution: We use $\Delta P_1 = \Delta P_2$ and then substitute from the continuity equation to obtain:

$$\sum \left[\left(f \frac{L}{D} \right) + K \right]_1 \left(\frac{\rho \dot{V}_1^2}{2A_1^2} \right) = \sum \left[\left(f \frac{L}{D} \right) + K \right]_2 \rho \left(\frac{\dot{V} - \dot{V}_1}{2A_2^2} \right)^2$$

If we represent $\sum [(fL/D) + K]/A^2 = R$ then the above equation reduces to:

$$(R_1 - R_2)\dot{V}_1^2 + 2(R_2\dot{V})\dot{V}_1 - R_2\dot{V}^2 = 0$$

From this equation we find branch 1 flow rate as:

$$\dot{V}_1 = \frac{\left[-R_2\dot{V} \pm \sqrt{R_2^2\dot{V}^2 + (R_1 - R_2)R_2\dot{V}^2} \right]}{R_1 - R_2}$$

or

$$\dot{V}_1 / \dot{V} = \left(-R_2 \pm \sqrt{R_1 R_2} \right) / (R_1 - R_2)$$

The plus sign is chosen if $R_1 > R_2$. Otherwise, we choose the minus sign.

System Curve for Serial-Path Systems

We consider a serial-path system, consisting of pipes of various lengths (L), diameters (D), and loss coefficients (K). This piping system has, in general, an elevation change ($Z_e - Z_i$). Equation IIIa.3.31 for this system can be written as:

$$H_{System} = \frac{P_i - P_e}{\rho g} = (Z_e - Z_i) + \left(\sum f \frac{L}{DA^2} + \sum \frac{K}{A^2} \right) \frac{\dot{V}^2}{2g}$$

where due to the lack of any pump in the system, h_s is dropped and h_f is replaced by Equation IIIb.3.12. Depending on the flow regime, H_{system} is either a linear function of velocity or a parabolic function. If flow is laminar then $f = 64/\text{Re} = 64\mu A/\rho \dot{V} D$. Substituting, for the friction factor, we find:

$$H_{System} = c_1 + c_2 \dot{V} \quad \text{IIIb.4.8-1}$$

where $c_1 = Z_e - Z_i$ and $c_2 = \Sigma 64\mu L'/(2g\rho DA)$. For turbulent flow in smooth pipes, if we use an approximate value for the friction factor as given in Table IIIb.3.2, we find

$$H_{System} = c_1 + c_3 \dot{V}^2 \quad \text{IIIb.4.8-2}$$

where $c_3 = \Sigma fL'/(2gDA^2)$. The plot of H_{system} versus \dot{V} is known as the *system curve*.

In the analysis we often choose to simplify a piping network by substituting one pipe to represent a series of pipes connected together. Thus, it is important to determine the characteristics of the equivalent pipe.

Equivalent Pipe for Serial-Path and Parallel-Path Systems

To simplify the thermal-hydraulic analysis of a multi piping system connected in series or in parallel, having different L , D_h , ε and K , we substitute such a system with an equivalent flow path (E). This substitution should be performed such that the equivalent flow path retains the characteristics of the original system. Hence the conservation equations of mass, momentum, and energy as well as the volume constraint for the original system must also satisfy the equivalent flow path. The volume constraint can be expressed in terms of equal transit time. As for the conservation equation of momentum, Equation IIIa.3.42 yields:

$$\frac{1}{g} \frac{L}{A} \frac{d\dot{V}}{dt} + \frac{1}{\rho g} (P_2 - P_1) + h_f - h_p + (Z_2 - Z_1) = 0 \quad \text{IIIa.3.42}$$

We now apply the concept of equivalent flow path first to the serial and then to the parallel systems.

Flow Paths Connected in Series

The continuity equation requires that $\dot{V}_E \equiv \dot{V}_1 = \dots = \dot{V}_i \dots = \dot{V}_N$. The energy equation requires thermal properties to remain the same. The volume constraint requires that $\tau_E = \sum \tau_i$ where τ is the liquid transit time. Substituting for τ yields, $V_E / \dot{V}_E \equiv V_1 / \dot{V}_1 \dots + V_i / \dot{V}_i \dots + V_N / \dot{V}_N$, which simplifies to:

$$V_E = \sum V_i = \sum L_i A_i \quad \text{IIIb.4.9}$$

Applying Equation IIIa.3.42, the momentum equation to each pipe segment in Figure IIIb.4.5(a), we obtain:

$$\begin{aligned} \frac{1}{g} \frac{L_1}{A_1} \frac{d\dot{V}}{dt} + \frac{1}{\rho g} (P_b - P_a) + h_{f1} - h_{p1} + (Z_b - Z_a) &= 0 \\ &\vdots \\ \frac{1}{g} \frac{L_N}{A_N} \frac{d\dot{V}}{dt} + \frac{1}{\rho g} (P_{N+1} - P_N) + h_{fN} - h_{pN} + (Z_{N+1} - Z_N) &= 0 \end{aligned} \quad \text{IIIb.4.10}$$

adding up terms, we get:

$$\left(\frac{1}{g} \sum \frac{L_i}{A_i} \right) \frac{d\dot{V}}{dt} + \frac{1}{\rho g} (P_{N+1} - P_a) + \sum h_{fi} - \sum h_{pi} + (Z_{N+1} - Z_a) = 0 \quad \text{IIIb.4.11}$$

We now apply Equation IIIa.3.42, the momentum equation to the equivalent flow path:

$$\frac{1}{g} \frac{L_E}{A_E} \frac{d\dot{V}}{dt} + \frac{1}{\rho g} (P_{N+1} - P_a) + h_{fE} - h_{pE} + \Delta Z_E = 0 \quad \text{IIIb.4.12}$$

To have similar dynamic response, similar terms must be equal. Hence, $\Delta Z_E \equiv Z_{N+1} - Z_1$, $h_{p,E} = \sum h_{p,i}$ and

$$\frac{L_E}{A_E} = \sum \frac{L_i}{A_i} \quad \text{IIIb.4.13}$$

Additionally, $h_{fE} = \sum h_{fi}$, hence:

$$\left(\frac{K_E^*}{A_E^2} \right) \frac{\rho \dot{V}^2}{2} = \sum \left(\frac{K_i^*}{A_i^2} \right) \frac{\rho \dot{V}^2}{2} \quad \text{IIIb.4.14}$$

where in Equation IIIb.4.14, $K^* = fL/D + K$. So far we have three equations; Equations IIIb.4.9, IIIb.4.13, and IIIb.4.14. To find the five unknowns, V_E , A_E , L_E , D_E , and K_E we need two more equations. The fourth equation is obtained from $V_E = L_E A_E$, as noted in Equation IIIb.4.9 and the fifth equation from the definition of the hydraulic diameter:

$$D_h = 4 \frac{A_{Flow}}{P_{wetted}} = 4 \frac{V}{S_{wetted}} \quad \text{IIIb.4.15}$$

Requiring equal wetted surfaces (S_{wetted}) between the equivalent and the serial flow paths and using Equations IIIb.4.9 and IIIb.4.14, we obtain the hydraulic diameter of the equivalent pipe as:

$$D_{h,E} = \frac{\sum L_i A_i}{\sum (L_i A_i / D_{h,i})} \quad \text{IIIb.4.16}$$

We now use the remaining three equations to find A_E , L_E , and K_E . If we substitute for A_E in Equation IIIb.4.13 from $A_E = V_E/L$, to find $L_E^2/V_E = \sum (L_i/A_i)$ and then substitute for V_E from Equation IIIb.4.9, we obtain:

$$L_E = \left[\sum (L_i A_i) \sum \left(\frac{L_i}{A_i} \right) \right]^{0.5} \quad \text{IIIb.4.17}$$

having V_E and L_E , we can also express the flow area of the equivalent flow path, A_E as:

$$A_E = \left[\frac{\sum (L_i A_i)}{\sum (L_i / A_i)} \right]^{0.5} \quad \text{IIIb.4.18}$$

Finally, we find K_E from Equation IIIb.4.14 as:

$$K_E = A_E^2 \left[\sum \frac{K_i^*}{A_i^2} \right] - (f_E \frac{L_E}{D_E}) \quad \text{IIIb.4.19}$$

The results are summarized in Table IIIb.4.3.

Flow Paths Connected in Parallel

The volume constraint requires Equation IIIb.4.9 to be applicable here as well. The momentum equation for each pipe segment in Figure III.8.1(b), is given by the sets of Equation IIIb.4.10.

$$\begin{aligned} \frac{1}{g} \frac{L_1}{A_1} \frac{d\dot{V}_1}{dt} + \frac{1}{\rho g} (P_b - P_a) + h_{f1} + \Delta Z_1 &= 0 \\ &\vdots \\ \frac{1}{g} \frac{L_N}{A_N} \frac{d\dot{V}_N}{dt} + \frac{1}{\rho g} (P_b - P_a) + h_{fN} + \Delta Z_N &= 0 \end{aligned} \quad \text{IIIb.4.20}$$

and for the equivalent flow path:

$$\frac{1}{g} \frac{L_E}{A_E} \frac{d\dot{V}_E}{dt} + \frac{1}{\rho g} (P_b - P_a) + h_{fE} + \Delta Z_E = 0$$

Pump terms are not shown as they develop equal heads. Since pressure terms are equal, it requires that

$$\frac{L_E}{A_E} \frac{d\dot{V}_E}{dt} = \frac{L_1}{A_1} \frac{d\dot{V}_1}{dt} = \frac{L_2}{A_2} \frac{d\dot{V}_2}{dt} = \dots = \frac{L_N}{A_N} \frac{d\dot{V}_N}{dt} \quad \text{IIIb.4.21}$$

This results in finding each flow rate in terms of the equivalent pipe flow rate as:

$$d\dot{V}_i = \frac{L_E}{A_E} \left(\frac{A_i}{L_i} \right) d\dot{V}_E \quad \text{IIIb.4.22}$$

We now use, the mass balance requirement that:

$$d\dot{V}_E = d\dot{V}_1 + d\dot{V}_2 + \cdots d\dot{V}_N \quad \text{IIIb.4.23}$$

Substituting for each flow rate in terms of the equivalent pipe flow rate from Equation IIIb.4.22 in Equation IIIb.4.23, we obtain:

$$A_E / L_E = \sum (A_i / L_i) \quad \text{IIIb.4.24}$$

Canceling A_E between $V_E = L_E A_E$ and Equation IIIb.4.24, we find an expression for L_E in terms of A_i and L_i :

$$L_E = \left[\frac{\sum (L_i A_i)}{\sum (A_i / L_i)} \right]^{0.5} \quad \text{IIIb.4.25}$$

Back substitution gives A_E :

$$A_E = \left[\sum (L_i A_i) \sum (A_i / L_i) \right]^{0.5} \quad \text{IIIb.4.26}$$

To find the equivalent loss coefficient, from equal pressure drop requirement we get:

$$\left(f_E \frac{L_E}{D_E} + K_E \right) \frac{\dot{V}_E^2}{2gA_E^2} = \left(f_1 \frac{L_1}{D_1} + K_1 \right) \frac{\dot{V}_1^2}{2gA_1^2} = \cdots = \left(f_i \frac{L_N}{D_N} + K_N \right) \frac{\dot{V}_N^2}{2gA_N^2} \quad \text{IIIb.4.27}$$

We find each flow rate in terms of the flow rate in the equivalent path and substitute it in the mass balance:

$$\dot{V}_E = \dot{V}_1 + \dot{V}_2 + \cdots + \dot{V}_N \quad \text{IIIb.4.28}$$

we find:

$$\dot{V}_E \equiv \left(K_E^* / K_1^* \right)^{1/2} (A_1 / A_E) \dot{V}_E + \cdots + \left(K_E^* / K_N^* \right)^{1/2} (A_N / A_E) \dot{V}_E$$

where $K^* = K + (fL/D)$. Solving for K_E , we get:

$$K_E = \left[A_E / \sum \left(A_i / \sqrt{K_i^*} \right) \right]^2 - (f_E L_E / D_E)$$

Finally, the hydraulic diameter for the equivalent pipe is obtained from Equation IIIb.4.16. The results are summarized in Table IIIb.4.3.

Table IIb.4.3. Equivalent pipe characteristics

	Pipes Connected in Series	Pipes Connected in Parallel
Volume	$V_E = \sum V_i = \sum L_i A_i$	$V_E = \sum V_i = \sum L_i A_i$
Area	$A_E = \sqrt{\sum (L_i A_i) / \sum (L_i / A_i)}$	$A_E = \sqrt{\sum (L_i A_i) \sum (A_i / L_i)}$
Length	$L_E = \sqrt{\sum (L_i A_i) \sum (L_i / A_i)}$	$L_E = \sqrt{\sum (L_i A_i) / \sum (A_i / L_i)}$
Loss coefficient	$K_E = A_E^2 \left[\sum (K_i^* / A_i^2) \right] - (f_E L_E / D_E)$	$K_E = A_E^2 \left[\sum \left(A_i / \sqrt{K_i^*} \right) \right]^{-2} - (f_E L_E / D_E)$

$$K^* = K + fL/D$$

Example IIb.4.12. Find the characteristics of an equivalent pipe to represent a piping system connected in series. Individual pipe length, diameter, and loss coefficients are given below. A flow rate of 100 GPM enters the piping system. Use $\rho = 62.4 \text{ lbm/ft}^3$ and $\mu = 0.7\text{E-}3 \text{ lbm/ft}\cdot\text{s}$. Pipe is smooth commercial steel.

Pipe No.	L (ft)	D (in)	K (-)
1	100.00	3.50	5.00
2	180.00	3.00	4.00
3	50.00	2.50	6.00
4	90.00	2.00	1.00

Solution: We use Table IIb.4.3 for pipes connected in series. Results are summarized below:

Pipe No.	L (ft)	D (in)	A (ft ²)	V (ft/s)	K (-)	\dot{V} GPM	$\text{Re} \times 10^{-6}$	f (-)	ΔP (psi)
1	100	3.5	0.067	3.32	5.00	100	0.087	0.0189	0.86
2	180	3.0	0.049	4.55	4.00	100	0.101	0.0184	2.39
3	50	2.5	0.034	6.55	6.00	100	0.121	0.0177	2.95
4	90	2.0	0.022	10.1	1.0	100	0.152	0.0169	7.12
Equivalent:									
	454.26	2.78	0.042	5.30	35.65	100	0.109	0.0181	13.3

Example IIb.4.13. Find the characteristics of an equivalent pipe to represent a piping system connected in parallel. Individual pipe length, diameter, and loss coefficients are given below. A flow rate of 19 lit/s enters the piping system. Use $\rho = 998 \text{ kg/m}^3$ and $\mu = 1.1\text{E-}6 \text{ N}\cdot\text{s/m}^2$. Pipe is smooth commercial steel.

Pipe No.	L (m)	D (cm)	K (-)
1	30.48	8.89	5.00
2	54.86	7.62	4.00
3	15.24	6.35	6.00
4	27.43	5.08	1.00

Solution: We use Table IIb.4.3 for pipes connected in parallel. Results are summarized below:

Pipe No.	L (m)	D (cm)	A (m ²)	V (m/s)	K (-)	\dot{V} lit/s	Re $\times 10^{-6}$	f (-)	ΔP (kPa)
1	30.48	8.89	6.207E-3	1.25	5.00	7.735	0.260	0.018	8.7
2	54.86	7.62	4.560E-3	1.00	4.00	4.613	0.303	0.018	8.7
3	15.24	6.35	3.167E-3	1.28	6.00	4.059	0.364	0.019	8.7
4	27.43	5.08	2.027E-3	1.22	1.00	2.516	0.455	0.019	8.7
Equivalent:									
	30.91	14.96	0.0175	1.08	11.5	18.92	0.292	0.016	8.7

5. Steady Incompressible Viscous Flow Distribution in Piping Networks

In most engineering applications, fluid flows in multi-paths piping. Examples include water and gas distribution in municipalities, a nuclear plant emergency core cooling system (ECCS), division of a PWR hot leg flow to steam generator tubes, division of a BWR core flow rate between fuel bundles, and variety of piping systems in the balance of plant. In Section 4.4 we considered special cases of serial and parallel piping systems. In this section, we consider more general case of piping networks, which may consists of a combination of serial and parallel piping configurations.

Figure IIb.5.1(a) shows an example of a piping network consisted of loops and nodes (X_1 through X_{15}). A node is any point in the system at which either three or more flows meet or network geometric dimensions change. A branch, link, or flow path is referred to the conduits connecting two nodes. In general, a flow path may also include pump, valves and fittings, as shown in Figure IIb.5.1(b). Flow paths that do not have circular flow area are modeled with the use of a hydraulic diameter. Flow between various paths in a piping network is divided based on the path resistance i.e. the least resistance path carries the most flow rate and vice

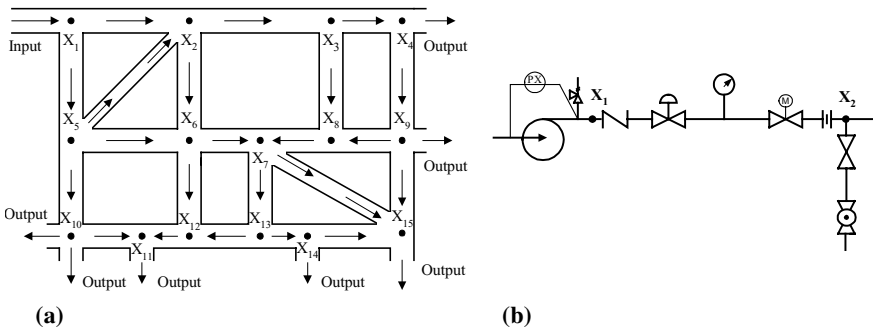


Figure IIb.5.1. (a) A piping network and (b) Example of a flow path details

versa. A node may be connected to a boundary. There are two types of boundaries namely, pressure boundary and flow boundary. Mathematically, these serve as boundary conditions for the related differential equations. Flow boundaries are of two types. A source-flow boundary, which supplies fluid to the network, and a sink-flow boundary to which the nodal fluid flows. The sink fluid boundary is also referred to as an output.

The goal is to find the steady-state nodal pressures and inter-nodal flow rates. The boundary condition, generally include the output flow rates and either input flow rate to or nodal pressure at the inlet of the network. In this example there are 15 unknown nodal pressures and 22 unknown branch flow rates. We have also 15 continuity equations and 22 inter-nodal momentum equations. There are 8 flow boundary conditions (at nodes 1, 4, 9, 10, 11, 14, and 15). Of these, the flow to node 1 is the supply flow and the rest are output flows.

To solve piping network problems, we seek simultaneous solution to a set of continuity and momentum equations. The continuity equation is written for each node and the momentum equation for each branch. Therefore, we obtain a set of coupled non-linear differential equations, which are solved iteratively. In this chapter we discuss three methods. The first two methods, known as Hardy Cross and Carnahan method, are applicable to steady incompressible flow. The third method, developed by Nahavandi, applies to both steady-state and transient incompressible flow. We discuss the first two methods here and leave the discussion about the Nahavandi method to the transient flow analysis discussion in Section 6.

The Hardy Cross Method

This method applies only to incompressible fluids, flowing under steady state and isothermal conditions. In this method, the algebraic summation of all flow rates associated with a node is set equal to zero. This results in as many equations as the number of nodes. The reason for setting the summation of all flow rates associated with a node equal to zero is that at steady-state, the conservation equation for mass written for each node resembles the Kirchhoff's law as applied to electric circuits. According to the Kirchhoff's law, the algebraic summation of nodal electric currents (flow rates) must be equal to zero:

$$\sum_{j=1}^N \dot{m}_{ji} = \sum_{j=1}^N \dot{V}_{ji} = 0 \quad \text{IIIb.5.1}$$

where N is the number of branches stemming from a node, j is an index representing a branch to node i . In Figure IIIb.5.1, for example, N is equal to 15.

To find the flow distribution in the piping networks by the Hardy Cross method, an initial best estimate is used to allocate flow rates to each loop comprising the piping network. We then set the algebraic summation of the flow rates in each loop equal to zero. Then a correction to the flow rate in each loop is applied to bring the net flow rate into closer balance. Consider the piping network of Fig-

ure IIIb.5.1. Suppose the initial guess in a branch is \dot{V}_0 . The correction to this initial guess is $\Delta\dot{V}$ such that the correct flow rate is now:

$$\dot{V} = \dot{V}_0 + \Delta\dot{V} \quad \text{IIIb.5.2}$$

We use the estimated flow rate of each loop in the momentum equation for that loop. We know that in a closed loop, we can write:

$$\sum_j (\Delta P)_j = 0 \quad \text{IIIb.5.3}$$

Using Equation IIIb.3.6 for turbulent flow in a smooth pipe, pressure drop becomes a function of $\dot{V}^{1.8}$. In general, pressure drop can be expressed as $\Delta P = c\dot{V}^n$ where n is some power depending on friction factor relation and c is the proportionality constant as given in Equation IIIb.3.7. For example, if we treat f as a constant then $n = 2$ and $c = (fL/D)\rho/(2A^2)$. Substituting for \dot{V} from Equation IIIb.5.2 and expanding terms according to the Taylor series, we obtain:

$$\Delta P = c\dot{V}^n = c(\dot{V}_0 + \Delta V)^n = c(\dot{V}_0^n + n\dot{V}_0^{n-1}\Delta V + \dots) \quad \text{IIIb.5.4}$$

If $\Delta\dot{V}$ is small compared with \dot{V}_0 , we may ignore higher order terms not shown in the right side of Equation IIIb.5.4 and apply this equation to a chosen loop in the piping network, Equation IIIb.5.3, to get:

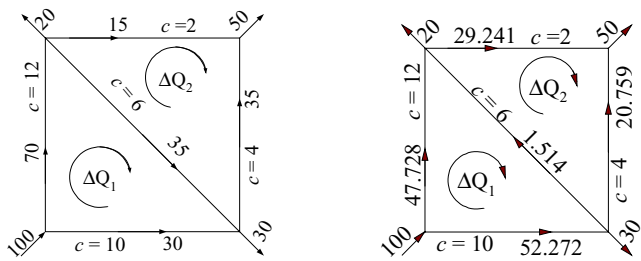
$$\sum \Delta P = \sum c\dot{V}|\dot{V}|^{n-1} = \sum c\dot{V}_0|\dot{V}_0|^{n-1} + \Delta V \sum cn|\dot{V}_0|^{n-1} = 0 \quad \text{IIIb.5.5}$$

where first, $\Delta\dot{V}$ is taken outside the summation since it is the same for the entire loop and second, an absolute value sign is used to account for the flow direction. We may choose an arbitrary direction for the flow but once chosen, use it consistently. For example, we may choose all the clockwise flows as positive and all counterclockwise flows as negative. From Equation IIIb.5.5 we find:

$$\Delta V = - \frac{\sum c\dot{V}_0|\dot{V}_0|^{n-1}}{\sum cn|\dot{V}_0|^{n-1}} \quad \text{IIIb.5.6}$$

The solution procedure is as follows. We first use best engineering judgment to allocate initial flow distribution to each loop. Next, we choose the flow directions in each branch so that Equation IIIb.5.1 is satisfied at each node. We then assign positive value to each branch flow rate in a loop that flows counterclockwise, for example. Finally, we find the numerator and the denominator of Equation IIIb.5.6 to calculate the correction factor. Subsequently, we update flow rates using the correction factor to calculate a new correction factor. We continue this process until the calculated correction factor becomes exceedingly small.

Example IIIb.5.1. Find flow distribution in the left side network, for $n = 2$. Units of the c factors are such that the flow rates are in GPM (for example, for pipe with $c = 2$, $\dot{V}_{c=2} = 15$ GPM, etc.).



Solution: We assume the clockwise direction as positive and use an initial guess for the flow in each loop to be corrected in the following steps. We first correct the assumed flow distribution in the lower loop:

<u>1</u>				
c	6	10	12	
\dot{V}_0	35	-30	70	
$c\dot{V}_0 \dot{V}_0 ^{n-1}$	7350	-9000	58800	Summation: 57150
$cn \dot{V}_0 ^{n-1}$	420	600	1680	Summation: 2700 $\Delta\dot{V}_1 = -21.17$
Updated \dot{V}_0	13.83	-51.17	48.83	

We now update the upper loop as follows:

c	2	4	6	
\dot{V}_0	15	-35	-13.83	
$c\dot{V}_0 \dot{V}_0 ^{n-1}$	450	-4900	-1147.6	Summation: -5597.6
$cn \dot{V}_0 ^{n-1}$	60	280	165.96	Summation: $\Delta\dot{V}_2 = 11.06$
Updated \dot{V}_0	26.06	-23.94	-2.77	

In the second trial, we revise values in the lower loop, using the updated flow rate for the common flow path:

2

c	6	10	12	
\dot{V}_0	2.77	-51.17	48.83	
$c\dot{V}_0 \dot{V}_0 ^{n-1}$	46.04	-26183.69	28612.43	Summation: 2474.77
$cn \dot{V}_0 ^{n-1}$	33.24	1023.4	1171.92	Summation: 2228.56 $\Delta\dot{V}_1 = -1.11$
Updated \dot{V}_0	1.66	-52.28	47.72	

We now revise values in the upper loop flows, using the updated flow rate for the common flow path:

c	2	4	6	
\dot{V}_0	26.06	-23.94	-1.66	
$c\dot{V}_0 \dot{V}_0 ^{n-1}$	1358.25	-2292.49	-16.53	Summation: -950.77
$cn \dot{V}_0 ^{n-1}$	104.24	191.52	19.92	Summation: 315.68 $\Delta\dot{V}_2 = 3.01$
Updated \dot{V}_0	29.07	-20.93	1.353	

We follow the same procedure in the third trial:

3

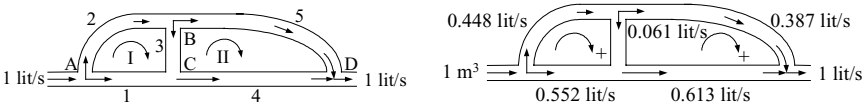
c	6	10	12	
\dot{V}_0	-1.353	-52.28	47.72	
$c\dot{V}_0 \dot{V}_0 ^{n-1}$	-10.98	-27,332	27,326	Summation: -16.6
$cn \dot{V}_0 ^{n-1}$	16.23	1045.6	1145.28	Summation: 2228.56 $\Delta\dot{V}_1 = -0.007$
Updated \dot{V}_0	-1.345	-52.27	47.727	

Revising the upper loop flows, using the updated flow rate for the common flow path, in the third trial:

c	2	4	6	
\dot{V}_0	29.07	-20.93	1.345	
$c\dot{V}_0 \dot{V}_0 ^{n-1}$	1690.13	-1752.26	10.85	Summation: -51.27
$cn \dot{V}_0 ^{n-1}$	116.28	167.44	-33.24	Summation: 250.48
$\Delta\dot{V}_2$	= 0.168			

Final results are shown in the right side figure. Although, we could have made better initial guesses such as $(c = 6, 5)$, $(c = 10, 60)$, $(c = 12, 40)$, $(c = 2, 15)$, and $(c = 4, 35)$, the number of trials would still be 3.

Example IIIb.5.2. Find flow distribution in the left side network for the given data. Use $n = 2$.



Pipe	L (m)	D (m)	A (m ²)	f	c (from Equation IIIb.3.7)
1	507.6	0.55	0.237	0.012	10
2	143.7	0.40	0.126	0.013	15
3	47.9	0.40	0.126	0.013	5
4	628	0.50	0.196	0.012	20
5	114	0.30	0.071	0.013	50

Solution: We assume the clockwise direction as positive for each loop and use an initial guess for the flow in each loop to be corrected in the following steps. Using the procedure of Example IIIb.5.1, we obtain:

Trial	\dot{V}_1	\dot{V}_2	\dot{V}_3	\dot{V}_4	\dot{V}_5	Δ_1	Δ_2
0	-0.60	0.40	-0.100	-0.500	0.500	0.0	0.0
1	-0.55	0.45	0.565	-0.60556	0.3934	0.05	0.10656
2	-0.5511	0.4488	0.06113	-0.6123	0.3877	-0.00114	-0.00571
3	-0.5513	0.44873	0.06101	-0.61228	0.38772	-0.00013	-0.00001
4	-0.55127	0.44873	0.06101	-0.61228	0.38772	0.00000	0.00000

The results are shown in the right side figure.

The Carnahan Method

In this method, we express flow rates in terms of pressure difference between the adjacent nodes. The summation of all the flow rates at each node, according to Equation IIIb.5.1 must be zero. Hence, we obtain as many equations as the number of nodes. To elaborate, let's consider two adjacent nodes, i and j , the momentum equation for the flow path connecting these nodes is given by Equation IIIb.4.1:

$$(P_j - P_i) + \left(f \frac{L}{D} + \sum K\right)_{ij} \frac{\dot{m}_{ij}^2}{2\rho A^2} + \rho g(Z_j - Z_i) = 0$$

where we assumed that there is no pump in flow path ij . Treating friction factor as a constant and considering the special case of flow distribution in the horizontal plane, this equation becomes:

$$\dot{m}_{ij} = (P_i - P_j) \sqrt{\frac{1}{|P_i - P_j| c_{ij}}} \quad \text{IIIb.5.7}$$

where in Equation IIIb.5.7, $c_{ij} = (fL/D + \sum K)_{ij} / (2\rho A^2)$. Per Carnahan, the advantage of factoring out the nodal pressure difference in Equation IIIb.5.7 is that the square root would always have a real value. Additionally, if pressure of node i is higher than that of node j , then flow would leave node i with a plus sign. Otherwise, flow would enter node i , with a minus sign as it should. Similar equations can be written for other flow paths connected to j . The summation of all the flow rates for node j must be equal to zero:

$$\sum_{i=1}^n \dot{m}_{ij} = \sum_i \left[(P_i - P_j) \sqrt{\frac{1}{|P_i - P_j| c_{ij}}} \right] = 0$$

Where n represents total number of flow paths connected to node j . Similar equations can be written for the rest of the nodes, resulting in a set of non-linear algebraic equations. Such set can be solved by the Newton-Raphson iteration method as discussed in Chapter VII or by the *successive-substitution* method. In the latter method, P_j is calculated from:

$$P_j = \left(\sum_{i=1}^n P_i \sqrt{\frac{1}{|P_i - P_j| c_{ij}}} \right) / \left(\sum_{i=1}^n \sqrt{\frac{1}{|P_i - P_j| c_{ij}}} \right)$$

Similar relations can be obtained for all other nodes. An initial guess is made for all the nodes. These initial guesses are then used in the right side of the above equations to update the guesses. The process continues until the difference in successive guesses becomes exceedingly small. The process is converged when the absolute value of the pressure difference divided by the updated pressure becomes smaller than a specified convergence criterion. Having calculated nodal pressures, inter-nodal flow rates can then be determined. Care must be exercised when flow encounters valves and fittings that induce large pressure drops. In such cases, the local pressure may drop below the vapor pressure corresponding to the liquid temperature, which may lead to cavitation as discussed in Chapter VI.

6. Unsteady Internal Incompressible Flow

In this section we analyze the unsteady, internal, one-dimensional flow of a single-phase incompressible fluid in single-path systems and flow distribution in multi-

path systems. Transient or unsteady fluid flow is due to the departure from steady state and stagnation conditions. Changing the flow area, such as throttling of a regulating valve or the speed of an operating pump would induce flow transients. Other examples of flow transients include pipe ruptures, loss of power to pumps, and actuation of safety and relief valves. Flow transients can be divided into two categories. The first category includes slow transients also referred to as *rigid column theory*. In these types of transients, the assumption is that the entire body of fluid moves as a rigid body. Also the liquid is assumed to be incompressible and the conduit carrying the liquid fully rigid. Hence, any disturbance in the medium is propagated instantly throughout the system.

The second category includes fast transients when there is a rapid change in flow velocity or fluid density. Analysis of fast transients is more complicated than the analysis of slow transients. This is because the compressibility of the fluid and the elasticity of the conduit containing the fluid must be accounted for. Although in many applications liquids may be treated as incompressible, in reality even liquids possess some degree of compressibility. Mathematically, problems involving slow transients can be solved with ordinary differential equations while the analysis of fast transients includes solution to partial differential equations as pressure, $P(\vec{r}, t)$ and velocity, $V(\vec{r}, t)$ are in general functions of both space and time. This type of transient is known as *waterhammer* or *elastic analysis*.

In discussing slow transients, we study such topics as transients in flow loops, time to fill drained pipelines, and time to empty vessels. We start with simpler examples of unsteady flow involving the application of the momentum equation. We then analyze waterhammer in the fast transient category. Employing Equation IIIa.3.38, we study two types of slow transients. The first type includes problems for which we may ignore the viscous effects of the incompressible fluid. The second type includes the unsteady flow of incompressible viscous flow. We start with the unsteady flow of incompressible inviscid fluids.

6.1. Unsteady Flow of Internal Incompressible Inviscid Flow

We apply Equation IIIa.3.39 for incompressible inviscid flow along the streamlines to a few examples, assuming the working fluid can be treated as an ideal fluid.

Time To Reach Steady-State Flow Rate

Consider a large reservoir discharging water through a small hole, as shown in Figure IIIb.6.1(a). In this case, the first term of Equation IIIa.3.39 is negligible hence we may use the Bernoulli equation at steady-state condition between points 1 and 2. Noticing that in a large reservoir, water velocity is zero everywhere except at the hole, we get (See Example IIIa.3.16)

$$(V_2)_{\text{steady-state}} = \sqrt{2gh_0}$$

Therefore the mass flow rate is calculated as:

$$\dot{m}_{\text{steady-state}} = \rho \sqrt{2gh_0} (\pi d^2 / 4)$$

We now consider another case where the same tank is connected to a pipe of length L and the same diameter d as shown in Figure IIIb.6.1(b). Initially, a fast acting gate valve with zero resistance is fully closed. At time zero the valve is fully opened. We want to find the time it takes for the water velocity to reach from zero to its steady-state value.

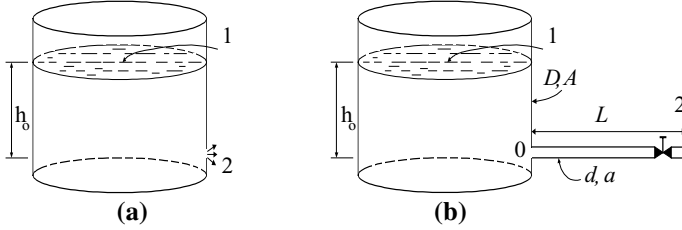


Figure IIIb.6.1. Flow of liquid from a large reservoir with fixed height

Since $P_1 = P_2$ and $V_1 = 0$, Equation IIIa.3.39 for this case is simplified to:

$$\int_1^2 \frac{\partial \bar{V}}{\partial t} \cdot \vec{ds} + \frac{V_2^2}{2} + g(Z_2 - Z_1) = 0$$

To integrate the first term along the streamline from point 1 to 2, we note that:

$$\int_1^2 \frac{\partial \bar{V}}{\partial t} \cdot \vec{ds} = \int_1^0 \frac{dV_1}{dt} dl + \int_0^2 \frac{dV_2}{dt} \approx \int_0^2 \frac{dV_2}{dt} dl = L \frac{dV_2}{dt}$$

Substituting we obtain,

$$L \frac{dV_2}{dt} + \frac{V_2^2}{2} - gh_0 = 0 \quad \text{IIIb.6.1}$$

Although this is a non-linear differential equation, we can find an analytical solution by the method of separation of variables, which results in $dt/2L = dV_2/(2gh - V_2^2)$. We now integrate this equation between time $t = 0$ when velocity is $V_2 = 0$ to an arbitrary time t to find $V_2(t)$:

$$\int_0^t \frac{dt}{2L} = \int_0^{V_2} \frac{dV_2}{2gh_0 - V_2^2} = \left[\frac{1}{\sqrt{2gh}} \tanh^{-1} \left(\frac{V}{\sqrt{2gh}} \right) \right]_0^{V_2}$$

resulting in:

$$V_2 / V_o = \tanh(V_o t / 2L) \quad \text{IIIb.6.2}$$

where $V_o = \sqrt{2gh_o}$. Time for velocity to reach its steady-state value is found from $\tanh(V_o t / 2L) = 1$.

Example IIIb.6.1. The initially closed valve in Figure IIIb.6.1(b) suddenly opens. Find the time it takes for the velocity to reach 50% of its steady-state value. Data: $L = 6$ m, $h_o = 3$ m, $d = 15$ cm.

Solution: We find t from $\tanh(t\sqrt{2gh_o}/2L) = 0.5$. The argument becomes $(t\sqrt{2gh_o}/2L) = (t\sqrt{2 \times 9.81 \times 3}/12) = 0.64t$. Hence, for $\tanh(0.64t) = 0.5$ by iteration we find $t \cong 0.87$ s.

Static Head as a Function of Time

Liquid is flowing through a small hole in the bottom of a reservoir having a diameter of D , as shown in Figure IIIb.6.1(a). In obtaining $V = \sqrt{2gh_o}$, we considered the reservoir to be large enough so that the available head for flow through the pipe remains constant. However, if the available head is decreasing as more flow leaves the tank, then the variation of $h = f(t)$ should be considered. To see how h is changing versus time, we write the continuity equation for the tank; $d/dt(m_{\text{tank}}) = -\dot{m}_o$. Substituting yields:

$$A \frac{d}{dt} h(t) = -V_2 a = -a \sqrt{2gh(t)}$$

where d is the diameter of the pipe. From this relation we obtain,

$$\frac{dh}{dt} + \sqrt{2g} \left(\frac{d}{D}\right)^2 h^{1/2} = 0 \quad \text{IIIb.6.3}$$

This is a non-linear differential equation that can be solved by separation of variables to obtain:

$$\sqrt{h(t)} = \sqrt{h_o} - [\sqrt{g/2}(a/A)]t$$

In the case of the reservoir connected to a pipe with static head decreasing as a function of time, we must solve Equations IIIb.6.1 and IIIb.6.3 simultaneously, as discussed in Section IIIb.6.2.

Flow Oscillation in a U-Tube

Another example of unsteady flow is the oscillation of inviscid liquid in a U-tube. At time zero, we push point 1 causing point 2 to reach the height H (Fig-

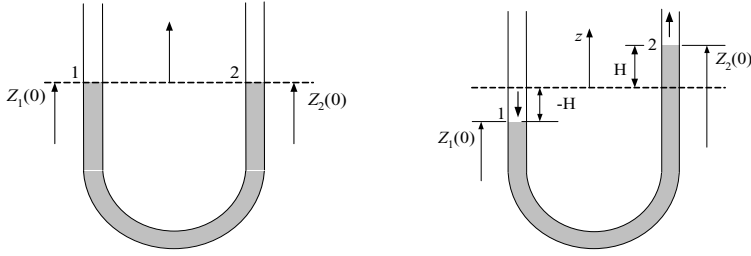


Figure IIIb.6.2. Flow oscillation of an inviscid fluid in a U-tube

ure IIIb.6.2). We then let go so that the oscillation can begin. Since streamlines are well defined in this problem and fluid is inviscid, we can apply Equation IIIa.3.38:

$$\int_1^2 \frac{\partial V}{\partial t} ds + \frac{V_2^2 - V_1^2}{2} + \frac{1}{\rho}(P_2 - P_1) + g(Z_2 - Z_1) = 0$$

where Z_1 and Z_2 are measured from an arbitrary datum. Since during the oscillation $P_1 = P_2$ and $V_1 = V_2$, Equation IIIa.3.39 reduces to:

$$L \frac{dV}{dt} + g(Z_2 - Z_1) = 0$$

where in this equation, L is the length of the liquid column. Substituting for $V = dz/dt$, we get:

$$\frac{d^2 z}{dt^2} + \frac{2g}{L} z = 0$$

where z is measured from the line connecting points 1 and 2 at time zero. The solution to this second order, linear differential equation is given as:

$z = c_1 \cos \sqrt{(2g/L)} t + c_2 \sin \sqrt{(2g/L)} t$. Using initial conditions, at $t = 0$, $dz/dt = 0$ gives $c_2 = 0$. Also at $t = 0$, $z = H$ hence, $c_1 = H$. Therefore, the liquid level at any given time can be found from:

$$z = H \cos \sqrt{(2g/L)} t$$

Velocity of the column of liquid versus time can be obtained by differentiating with respect to t , $V = dz/dt$ so that; $V = H \sqrt{(2g/L)} \sin \sqrt{(2g/L)} t$. This derivation shows that for inviscid liquids, the column has a simple harmonic motion with a period of $T = 2\pi \sqrt{(L/2g)}$.

Draining Tanks in a Quasi-steady Process

This is a useful method for cases in which the fluid acceleration in Equation IIIa.3.39 is so small, in comparison with the other terms, that we can approximately ignore the time derivative term. Hence, the process is referred to as *quasi-steady*. To elaborate let's try the tank in Figure IIIb.6.1(a), which is now shown in Figure IIIb.6.3. In this tank, water is covered by a blanket of pressurized air, initially at P_i having a volume of V_i . The tank cross sectional area is A_t and the initial water level from the drain centerline is h_i . In Figure IIIb.6.3, H is the fixed elevation of the tank from the drain centerline. The drain flow area is $A_e \ll A_t$. At time zero, we remove the plug and let water drain from the tank. Since the ratio of A_e/A_t is very small, we ignore the initial acceleration and assume that the tank is being drained in a quasi-steady manner. The quasi-steady assumption also lets us assume reversible expansion of the air region. We may treat the gas expansion as an isentropic process if the tank is fully insulated. This is to prevent any heat transfer to the expanding air from the surroundings.

In Figure IIIb.6.3, we have identified two control volumes, one for the expanding air region and another for the shrinking water region. We apply Equation IIIa.3.33, the Bernoulli equation to the water region:

$$\frac{P}{\rho} + \frac{V_t^2}{2} + gZ = \frac{P_{atm}}{\rho} + \frac{V_e^2}{2} + gZ_e$$

where $V_t A_t = V_e a_e$, $V_t = -dh/dt$, and $Z - Z_e = h(t)$ and . For the gas region, we use Equation IIa.4.3:

$$\frac{P}{P_i} = \left(\frac{V_i}{V} \right)^\gamma = \left(\frac{H - h_i}{H - h} \right)^\gamma$$

We substitute for V_t , V_o , and P in terms of the known values of H , h_i , A_t , a and the only unknown, dh/dt in the Bernoulli equation to obtain:

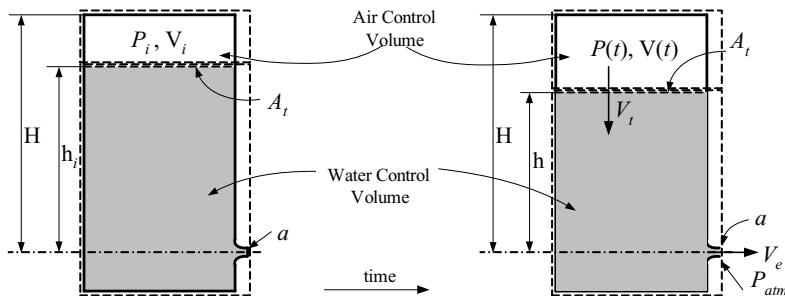


Figure IIIb.6.3. Draining of a fully insulated tank in a quasi-steady process

$$\frac{dh}{dt} = -\sqrt{2} \sqrt{\frac{P_i}{\rho} \left(\frac{H-h_i}{H-h} \right)^{\gamma} - \frac{P_{atm}}{\rho} + (gh)} / \sqrt{\left(\frac{A_t}{a} \right)^2 - 1}$$

To plot $h = f(t)$, we should solve the above first order non-linear differential equation numerically.

Example IIIb.6.2. Find the time to drain the water tank of Example IIIa.3.16. Data: $h_i = 10$ ft, $a/A_t = 0.01$.

Solution: We note that $V_o a = V_t A_t = -A_t dh/dt$. Substituting into $V_o = (2gh)^{1/2}$, we find:

$$\frac{dh}{h^{1/2}} = -\left(\frac{a}{A_t} \right) \sqrt{2g} dt$$

Although a non-linear, differential equation, due to its simplicity we can find the following analytical solution:

$$h = \left(\sqrt{h_i} - \frac{1}{2} \frac{a}{A_t} \sqrt{2g} t \right)^2$$

Substituting, we find time for $h = 0$ as

$$t_{h=0} = \sqrt{2h_i / g} / (a / A_t) = \sqrt{2 \times 10 / 32.2} / 0.01 = 79 \text{ s.}$$

6.2. Unsteady Flow of Internal Incompressible Viscous Flow

In Section 6.1 we ignored the viscous effect of the flow. In this section we solve the same transient problems while accounting for the viscosity of the fluid.

Flow Oscillation in a U-Tube

Previously, we considered flow oscillations in U-tubes for inviscid fluids. We now consider a U-tube containing a viscous fluid, initially at rest. The column of viscous fluid is set in motion by imposition of a pressure difference $P_1 - P_2$. The exact solution of viscous flow oscillations in U-tubes is described by Bird. Here we find an approximate solution by considering an average flow velocity at each cross section and a friction factor corresponding to the laminar flow. We start with Equation IIIa.3.42 noting that there is no shaft head. Using the continuity equation ($V_1 = V_2$), $h_f = f(L/D)(V^2/2g)$, and $f = 64/\text{Re}$, we find:

$$L \frac{dV}{dt} + 2gz + \frac{1}{\rho} (P_2 - P_1) + \frac{8\mu L}{\rho R^2} V = 0$$

Substituting for $V = dz/dt$:

$$\frac{d^2 z}{dt^2} + \frac{8\mu}{\rho R^2} \frac{dz}{dt} + \frac{2g}{L} z + \frac{1}{\rho L} (P_2 - P_1) = 0$$

subject to two initial conditions, at $t = 0$, $z = 0$ and $V = dz/dt = 0$. To solve the above second order non-homogenous differential equation, we substitute for $2z = s - (P_2 - P_1)/\rho g$ to get:

$$\frac{d^2 s}{dt^2} + \left(\frac{8\mu}{\rho R^2}\right) \frac{ds}{dt} + \left(\frac{2g}{L}\right) s = 0$$

Expectedly, this is the general form of the second order differencial equation describing the oscillation of a damped system such as a linear spring-dash pot system or an electrical circuit consisting of resistance, capacitance, and inductance (RLC circuit). The solution to this homogenous equation can be found by substituting $s = e^{\lambda t}$.

Time To Reach Steady-State Flow Rate

Consider the pipe connected to the reservoir of Figure IIIb.6.1(b). The valve is suddenly opened. We want to find the time it takes for water to reach its steady state or nominal value for flow rate, considering the friction in the pipe that results in a head loss. Here, point 1 is taken at the pipe entrance. Hence, $V_1 = V_2$ and $Z_1 = Z_2$ so Equation IIIb.3.42 simplifies to:

$$\frac{dV}{dt} \int_1^2 ds + \frac{1}{\rho} (P_2 - P_1) + gh_f = 0$$

Since $P_2 = P_{\text{atm}}$ and $P_1 = \rho gh_o + P_{\text{atm}}$, the governing equation simplifies to:

$$\frac{L}{g} \frac{dV}{dt} = h_o - f \frac{L}{d} \frac{V^2}{2g}$$

Since friction factor is a function of velocity, which in turn is changing with time, the above first order non-linear differential equation does not in general have an analytical solution. However, if we treat the friction factor as a constant equal to its steady-state value, throughout the transient, we find that:

$$t = \frac{LV_o}{2gh_o} \ln \left(\frac{V_o + V}{V_o - V} \right) \quad \text{IIIb.6.4}$$

where V_o is the flow velocity at steady-state condition. Note that velocity approaches the steady-state value, asymptotically. If we assume that the steady-state flow rate is reached when $V = 0.99 V_o$ then we find the approximate time as $t = 2.65LV_o/gh_o$.

Example IIIb.6.3. The initially closed valve in Figure IIIb.6.1 suddenly opens. Find the time it takes for the velocity to reach 99% of its final value. Data: $L = 3660$ m, $h_o = 24.5$ m, $d = 63.5$ cm, $f = 0.02$.

Solution: Time is given by $t_{99} = 2.65LV_o/gh_o$. But we must first find the steady-state velocity from:

$h_o = f(L/d)V_o^2/2g$. Substituting data;

$$V_o = \{[24.5 \times 2 \times 9.81]/[0.02 \times 3660/0.635]\}^{0.5} = 2 \text{ m/s.}$$

Hence, $t_{99} = 2.65 \times 3660 \times 2/(9.81 \times 24.5) \cong 81$ s.

Example IIIb.6.4. Compare time to reach steady-state flow rate for the two cases of inviscid and viscous flow. Data: $L = 100$ ft, $h_o = 20$ ft, $d = 6$ in, $f = 0.02$.

Solution: First we consider the case of inviscid flow. Equation IIIb.6.2 gives velocity as a function of time

Since $V_o = (2 \times 32.2 \times 20)^{0.5} = 35.9$ ft/s, the velocity ratio becomes:

$$(V/V_o)_{\text{inviscid}} = \tanh(35.9t/200) = \tanh(0.18t)$$

For the case of viscous flow, Equation IIIb.6.4 gives velocity as a function of time. Rearranging this equation, we obtain $V/V_o = (e^{t/\lambda} - 1)/(e^{t/\lambda} + 1)$ where $\lambda = LV_o/2gh_o$

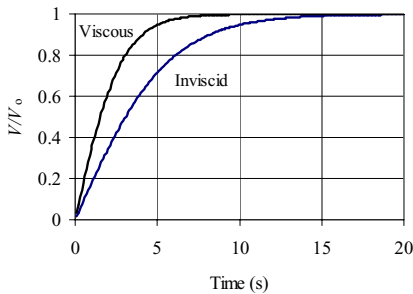
$$V_o = [2g h_o d/(fL)]^{1/2} = \{20 \times 2 \times 32.2/[0.02 \times 100/(6/12)]\}^{0.5} = 18 \text{ ft/s}$$

$$\lambda = 100 \times 18/(2 \times 32.2 \times 20) = 1.4 \text{ s}$$

Hence, the velocity ratio is found as:

$$(V/V_o)_{\text{viscous}} = (e^{t/1.4} - 1)/(e^{t/1.4} + 1)$$

Velocities versus time are plotted in the figure.



As shown in the figure, it takes a longer time for the inviscid flow to establish (i.e., flow velocity reaching the steady state value).

Flow Between Reservoirs in a Quasi-steady Process (Gravity Fill)

In this problem we are interested in finding the time it takes for the height between two large water reservoirs to drop to a specified value. The reservoirs are connected by a pipe, which also includes valves and fittings (Figure IIIb.6.4). Initially, both valves are closed and the height difference in water levels is h_1 . At time zero, both valves are fully opened. We use continuity and momentum equations. If s and s' show change in water level at time t , then $sA_1 = s'A_2$. At time t , we also have $h(t) = h_1 - (s + s')$, thus $dh = -(1 + A_1/A_2)ds$. From a mass balance:

$$V\left(\frac{\pi d^2}{4}\right) = A_1 ds / dt = A_1 \frac{-dh}{1 + A_1 / A_2} = -\frac{dh}{1/A_1 + 1/A_2}$$

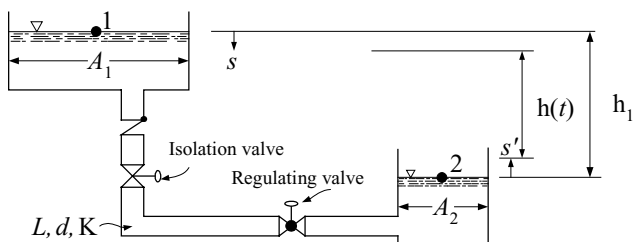


Figure IIIb.6.4. Unsteady flow of viscous fluid between reservoirs

Having found velocity in terms of h , we use the momentum equation to find another relation for V and h . This is given by Equation IIIa.3.41 (with $h_s = 0$):

$$\int_1^2 \frac{\partial V}{\partial t} ds + \frac{V_2^2 - V_1^2}{2} + \frac{1}{\rho}(P_2 - P_1) + g(Z_2 - Z_1) + gh_f = 0$$

substituting for $Z_2 - Z_1 = -h(t)$, for $h_f = (fL/d + K)V^2/2g$, and for V in terms of h , we find

$$dt = -\frac{4(fL/d + K)^{1/2}}{\pi d^2 \sqrt{2g} (1/A_1 + 1/A_2)} \frac{dh}{\sqrt{h}}$$

Integrating this relation between time zero ($h = h_1$) to any time at which $h = h_2$, we find that the time t is given by:

$$t = \frac{8(fL/d + K)^{1/2}}{\pi d^2 \sqrt{2g} (1/A_1 + 1/A_2)} (\sqrt{h_1} - \sqrt{h_2}) \quad \text{IIIb.6.5}$$

Time to Fill Drained Pipelines

The time it takes to fill a drained pipeline is of special interest in many engineering applications. Examples include buildings spray system for fire protection or a nuclear reactor containment building spray train for protection against excessive pressurization in the case of a high-energy line break. Let's consider a simple case of filling a straight vertical pipe of diameter d and flow area a with water as shown in Figure IIIb.6.5. Initially, water height in the reservoir is h_0 and at an elevation $Z_1 = Z_T + h_0$, with respect to the pump centerline. Also the control valve is closed, the pump is circulating water, and the discharge pipe is full of water up to the control valve elevation, Z_V . At time zero, the bypass line is shut and the control valve starts to open. It takes θ_0 seconds for the control valve to reach the full open position. The control valve loss coefficient K_V versus area is known. We want to find the time it takes to fill the drained piping downstream of the control valve.

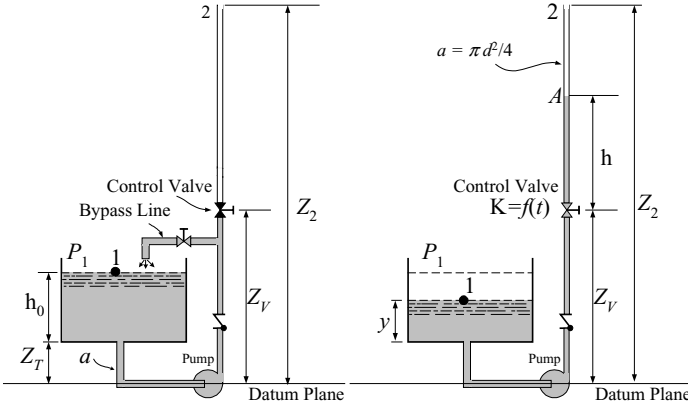


Figure IIIb.6.5. Filling of a partially drained pipeline

The bypass line is considered in this problem to avoid dealing with pump start up and the associated inertia, as discussed in Chapter VIc. To find the fill up time, we note that at time t , water has reached point A at an elevation Z_A . We write the momentum equation between points 1 and A. Equation IIIa.3.45 for water:

$$\sum \left(\frac{L_V + h}{a} \right) \frac{d\dot{m}_W}{dt} = \Delta P_{\text{pump}} - (\Delta P_{\text{stat}} + \Delta P_{\text{grav}} + \Delta P_{\text{vel}} + \Delta P_{\text{fric}})_W \quad \text{IIIb.6.6}$$

where L_V is the length of the suction and discharge piping up to the control valve. We also have:

$$\Delta P_{\text{stat}} = P_A - P_1$$

$$\Delta P_{\text{grav}} = \rho_W g (h + Z_V - Z_1) = \rho_W g (h + Z_V - Z_T - y)$$

$$\Delta P_{\text{vel}} = [1 - (a/A_1)^2] \dot{m}_W^2 / (2\rho_W a^2)$$

$$\Delta P_{fric} = [f(L_V + h)/d + \Sigma K(t)] \dot{m}_W^2 / (2\rho_{air}a^2)$$

$$\Delta P_{pump} = c_1 \dot{m}^2 + c_2 \dot{m} + c_3$$

where we have expressed pressure increase over the pump in terms of mass flow rate, with coefficients c_1 , c_2 , and c_3 are constants to match pump data. For the sake of generality, we also apply Equation IIIa.3.45 to the air region:

$$\sum \left(\frac{Z_2 - Z_V - h}{a} \right) \frac{d\dot{m}_{air}}{dt} = -(\Delta P_{stat} + \Delta P_{grav} + \Delta P_{vel} + \Delta P_{fric})_{air} \quad \text{IIIb.6.7}$$

Assuming Ma number remains below 0.3, we may ignore the compressibility effect of air hence, $\dot{m}_{air} = \dot{m}_W$

$$\Delta P_{stat} = P_2 - P_A$$

$$\Delta P_{grav} = \rho_{air}g(Z_2 - Z_V - h)$$

$$\Delta P_{vel} = 0.0$$

$$\Delta P_{fric} = [f(Z_2 - Z_V - h)/d + \Sigma K_{air}] \dot{m}_W^2 / (2\rho_{air}a^2)$$

If we substitute for the pressure differential terms and add up the two momentum equations, we get:

$$\begin{aligned} \sum \left(\frac{L}{a} \right) \frac{d\dot{m}}{dt} = & (c_1 \dot{m}^2 + c_2 \dot{m} + c_3) - (P_2 - P_1) - [\rho_W g(h + Z_V - Z_T - y) + \rho_{air} g(Z_2 - Z_V - h)] \\ & - [1 - (a/A_1)^2] \dot{m}^2 / (2a^2) - \{ [f(L/d) + \Sigma K]_W / \rho_W + [f(L/d) + \Sigma K]_{air} / \rho_{air} \} \dot{m}^2 / (2a^2) \end{aligned} \quad \text{IIIb.6.8}$$

where L and ΣK are the total length and total loss coefficient of the suction and discharge pipe, respectively. The loss coefficient is a given function of time since the control valve is not a quick open valve. Also note that we dropped the subscript for the mass flow rate. The governing equation is a non-linear differential equation. Since h and y appear in this equation, we must relate these to the mass flow rate. Using the continuity equation will accomplish this. On the one hand we know $A_1(h_0 - y) = ah$. On the other hand

$$-A_1 dy/dt = \dot{m} / \rho_W \quad \text{IIIb.6.9}$$

Eliminating h in Equation IIIb.6.8, we obtain two simultaneous differential equations for y and \dot{m} . The initial conditions are $y(t=0) = h_0$ and $\dot{m}(t=0) = \dot{m}_o$ where \dot{m}_o is the mass flow rate in the bypass loop prior to opening the control valve. Since this set of equations must be solved numerically, P_1 and P_2 can be specified as known functions of time. Indeed, in the case of a PWR or BWR containment during an accident, P_2 is a rapidly changing parameter. As discussed in Chapter IIIc.2, we must also make sure that the flow of air out of the pipe remains subsonic. Equation IIIb.6.8 can be simplified by ignoring the less significant terms.

Time to Drain Vessels in Quasi-steady Process

An example of unsteady incompressible flow is given here in the context of time it takes to fill or drain vessels with liquid. The time dependent flow rate is obtained from the solution to the conservation of mass and momentum equations. Figure IIIb.6.6 shows vessels, having a flow cross sectional area as a function of height. In special cases such as a right circular cylinder, the flow area is a constant, as was studied in Section 6.1. A general solution can be sought for simultaneous filling and draining. But we assume that liquid is drained only by gravity. The rate of change of liquid mass in an elemental control volume is:

$$\frac{dm}{dt} = \frac{d[\rho A(y)y]}{dt} = -\dot{m}_o$$

where in the above equation, the vessel cross sectional area is assumed to be a function of elevation. Time to empty a vessel can then be calculated if the function for $A = f(y)$ is specified. If the cross sectional area is constant, $A = A_v$, the time to empty the tank from a height of y_1 to a height of y_2 can be readily found as:

$$\theta = \frac{2A_v}{C_d a \sqrt{2g}} \left[\sqrt{y_1} - \sqrt{y_2} \right] \quad \text{IIIb.6.10}$$

where a and C_d are the drain flow area and discharge coefficient (generally between 0.65 and 1.0), respectively. Next we analyze a more comprehensive case of a spherical reservoir.

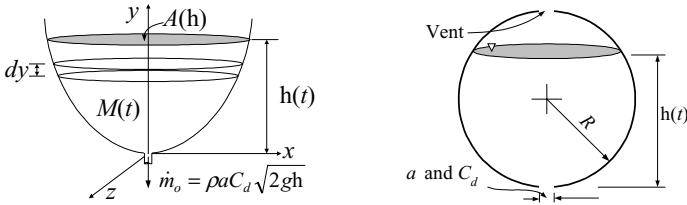


Figure IIIb.6.6. Draining of an arbitrary and a spherical vessel containing incompressible fluid

Time to Drain Spherical Reservoirs in Quasi-steady Process

To determine the time to empty a spherical reservoir with gravity draining, as shown in Figure IIIb.6.7, we again use the continuity and the momentum equations, noting that the gravity head acts against the velocity head and the friction. In this case however, the flow cross section in the tank also varies with elevation, and thus with time. Ignoring initial liquid acceleration, noticing that $P_1 = P_2$ and $V_1 = 0$, Equation IIIa.3.42

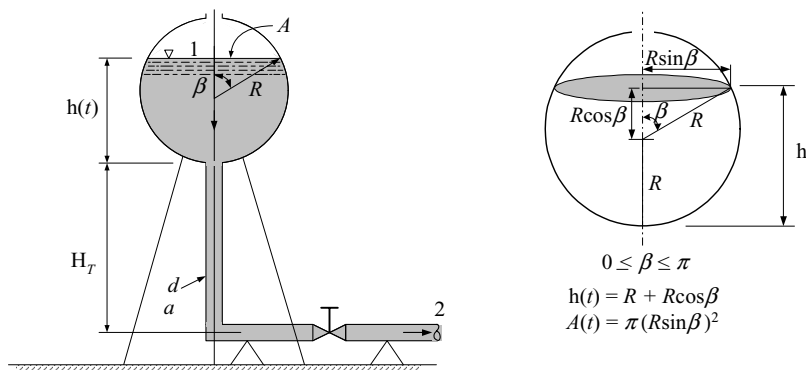


Figure IIIb.6.7. Spherical water reservoir connected to the discharge piping

$$\cancel{\frac{1}{\rho}(P_1)} + \cancel{\frac{V_1^2}{2}} + gZ_1 = \cancel{\frac{1}{\rho}(P_2)} + \cancel{\frac{V_2^2}{2}} + gZ_2 + gh_f + \cancel{\int_1^2 \frac{\partial V}{\partial t} ds}$$

simplifies to:

$$H_T + h = KV^2/2g \quad \text{IIIb.6.11}$$

where $K = fL/d + \sum K_i$ and we dropped the subscript of the velocity term. We obtain the second relation between $V(t)$ and $h(t)$ from the continuity equation, as flow rate in the pipe is due to the rate of drop in water level in the reservoir, thus $-Adh/dt = VaC_d$ where the exit flow area is aC_d . Eliminating V between the mass and the momentum equations yields:

$$aC_d \sqrt{\frac{2g}{K}} dt = -A \frac{dh}{\sqrt{H_T + h}}$$

We should now solve the above differential equation, for which we make a change of variable from h to β . While the range of h is $0 \leq h \leq 2R$, the range of β is $0 \leq \beta \leq \pi$. Using the new variable, we find water level as a function of time from:

$$\pi R^3 \int_0^\pi \frac{\sin^3 \beta d\beta}{\sqrt{H_T + R + R \cos \beta}} = \int_0^\theta aC_d \sqrt{\frac{2g}{K}} dt$$

We may switch to yet another variable, $\zeta = \cos \beta$ and $d\zeta = -\sin \beta d\beta$, with $-1 \leq \zeta \leq 1$. The resulting integral can be carried out twice by the method of separation of variables. The result, expressed again in terms of β is

$$\left[\int_1^{-1} \frac{(1-\zeta^2)\zeta}{\sqrt{H_T + R(1+\zeta)}} d\zeta \right] = - \int_0^\theta \frac{aC_d}{\pi R^3} \sqrt{\frac{2g}{K}} dt$$

Developing the left side integral by using three times, the method of integration by part, yields:

$$\left[\frac{2}{R} \zeta(1-\zeta^2)B^{1/2} - \frac{4}{3R^2}(1-3\zeta^2)B^{3/2} - \frac{16}{5R^3}\zeta B^{5/2} + \frac{32}{3R^4}B^{7/2} \right]_1^{-1} = - \frac{aC_d}{\pi R^3} \sqrt{\frac{2g}{K}} t$$

where $B = \sqrt{H_T + R(1+\zeta)}$. Moody has evaluated various containers for gravity *draining*. These include spherical and conical vessels as well as vertical and horizontal cylinders.

Time Dependent Water Level In Surge Tanks

In hydroelectric power plants, a tunnel delivers water from the reservoir via the penstock to the turbine. As shown in Figure IIIb.6.8, the control valve aborts the flow of water to protect the turbine in a sudden loss of electric load. As is discussed in the next section, sudden acceleration or deceleration of fluid flow results in the imposition of hydraulic forces, which may damage piping. A surge tank located upstream of the control valve prevents such damage by diverting the flow and damping oscillations. The surge tank also provides water in the case of a sudden load increase. The goal is to determine the surge tank water level as a function of time. The maximum water level occurs in the case of a loss of load followed by sudden closure of the control valve. Water initially flows in the tunnel at a speed of V_0 . Diameters of the tunnel and the surge tank are d and D , respectively. The tunnel length from the dam inlet to the surge tank is L . At steady-state operation, water in the surge tank is below the water level in the reservoir due to the frictional head loss, $H_L = Z_A - Z_B$ where elevations Z_A and Z_B are measured from an arbitrary datum.

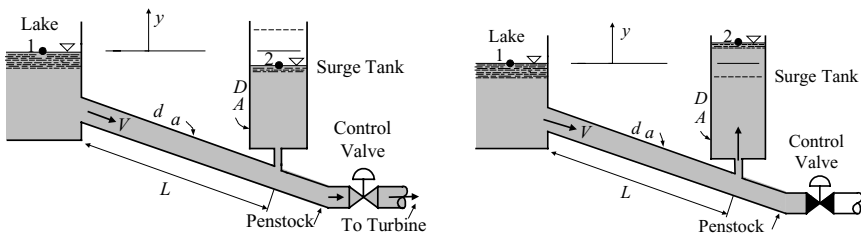


Figure IIIb.6.8. Surge tank to regulate the operation of a hydraulic turbine

Upon a sudden closure of the control valve, water rushes into the surge tank. This problem is similar to flow between reservoirs. However, we cannot use the “quasi-steady” assumption. To determine the surge tank water level as a function of time, we again use the conservation equations of mass and momentum. From the conservation equation of mass for the surge tank we conclude:

$$\rho \frac{dy}{dt} A = \rho V a \quad \text{IIIb.6.13}$$

where V is flow velocity after the control valve is shut and y is measured from the water surface in the reservoir. We now apply the one-dimensional momentum equation, IIIa.3.44 between points 1 and 2. Since flow velocities inside the two reservoirs are very small, we ignore both velocity heads and frictional losses in the reservoirs. Integrating between points 1 and 2 along the streamlines, we get:

$$\frac{dV}{dt} + g \frac{y}{L} + K \frac{V^2}{2L} = 0 \quad \text{IIIb.6.14}$$

where $K = fL/d + \Sigma K_i$, V is flow velocity in the penstock, and L is the friction length in the penstock. Note that the slope of the penstock does not appear in the final equation. Hence, this analysis is applicable to any inclination including a horizontal tunnel. We can now summarize Equations IIIb.6.13 and IIIb.6.14 as:

$$\frac{dy}{dt} = c_1 V$$

$$\frac{dV}{dt} = c_2 V^2 + c_3 y$$

Coefficients c_1 , c_2 , and c_3 in these coupled first order and non-linear differential equations are given as $c_1 = d^2/D^2$, $c_2 = -(fL/D + \Sigma K)/(2L)$, and $c_3 = -g/L$. The boundary condition for the first differential equations is that at time zero, $y = -H_L$ and for the second equation that at time zero, $V = V_0$. One way to solve this set is to take derivative of the first equation. Then substituting for dV/dt and for V from the second and the first equation, respectively to obtain:

$$\frac{d^2 y}{dt^2} + a \left(\frac{dy}{dt} \right)^2 + by = 0$$

Where $a = -c_2/c_1$ and $b = -c_1 c_3$. This is a second-order non-linear differential equation, which could be solved numerically. It is interesting to explore the response of the system in the absence of friction for which we can find an analytical solution in closed form. In the absence of friction, the governing equation is:

$$\frac{d^2 y}{dt^2} + by = 0$$

Since b is positive, the solution to this second order linear homogenous differential equation is given as:

$$y(t) = C_1 \sin \sqrt{b} t + C_2 \cos \sqrt{b} t$$

Coefficients C_1 and C_2 can be found from two boundary conditions. First, at $t = 0$, $y = 0$. Recall that earlier we said that at $t = 0$, $y = -H_L$. However, we are not considering friction in this case, and hence, the surge tank water level is about the same as the reservoir. For the second condition, we note that the flow rate going to turbine at time zero would enter the surge tank right after the closure of the valve at the same velocity. Hence, at $t = 0$, $dy/dt = V_o$. Using the first boundary condition, $C_2 = 0$. Using the second boundary condition, we can find C_1 which upon substitution, we get:

$$y = \left(\frac{D}{d} \sqrt{\frac{L}{g}} V_o \right) \sin \left(\frac{d}{D} \sqrt{\frac{g}{L}} t \right)$$

Expectedly, the oscillation of the water level in the surge tank is sinusoidal with no damping effect due to lack of friction. The amplitude of the oscillation is given by $\lambda = (D \sqrt{L/g} V_o) / d$ with a period of $T = (2\pi D \sqrt{g/L}) / d$. There are various designs for the surge tank. Examples include an orifice tank, a differential tank, and a closed tank. In an orifice tank the inlet is equipped with an orifice to enhance friction. In a differential tank, the overflow is contained in a secondary tank encompassing the primary surge tank. In a closed tank, the damping effect is provided by the work required to compress the air trapped on top of the tank water inventory. Chaudhry, Parmakian, and Streeter discuss design and operation of surge tanks.

Liquid Level Fluctuation in Open Tanks

We now consider a case similar to the surge tank. Water enters an open tank at a constant rate of \dot{V}_i and leaves through a long pipe (Figure IIIb.6.9). Unlike the surge tank problem, in this problem we let pressure downstream of the tank change in a prescribed manner. The goal is to determine the response of the tank water level to such pressure changes. For this purpose, we again combine the conservation equations of mass and momentum. We write the continuity equation for the control volume representing the tank:

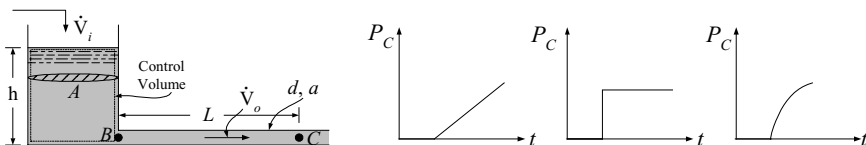


Figure IIIb.6.9. Dynamic response of a tank to influx and efflux of an incompressible fluid

$$A dh/dt = \dot{V}_i - \dot{V}_o$$

where A is the tank flow area and \dot{V}_o is the rate of flow leaving the tank. We now write the momentum equation for the long pipe extending between points B and C as given by Equation IIIb.3.7:

$$P_B - P_C = (fL/d)\rho\dot{V}_o^2/(2a^2)$$

At this point, all we need to do is to substitute for P_B and P_C in terms of h and combine the continuity and the momentum equations. To find an analytical solution we consider the case of laminar flow in the pipe. For this case, $f = 64\mu/(\rho Vd)$. For P_B , we write $P_B = P_{atm} + \rho gh$, where we ignored the velocity heads. Similarly, for P_C , we write $P_C = P_{atm} + \rho gh_C$. Substituting, we obtain:

$$\frac{dh}{dt} + c_1 h = c_2 \quad \text{IIIb.6.15}$$

where $c_1 = 1/(BA)$, $c_2 = (\dot{V}_i + h_C/B)/A$, and $B = 128\nu L/(\pi g d^4)$. Vennard considers three cases of linear, step, and sinusoidal fluctuations for h_C . The solution to Equation IIIb.6.15 is given by Equation VIIb.2.4. For example, for a step increase in the downstream pressure, we find:

$$h = Ce^{-t/BA} + B\dot{V}_i + h_C \quad \text{IIIb.6.16}$$

where C is the constant of integration to be found from the initial condition. That is to say, at steady state, $h_C = h_{C0}$ and $h = h_0$. We can find the relation between h_{C0} and h_0 by setting $dh/dt = 0$ in Equation IIIb.6.15:

$$h_0 = B\dot{V}_i + h_{C0} \quad \text{IIIb.6.17}$$

After a step increase from $h_C = h_{C0}$ to say $h_C = h_{C1}$, Equation IIIb.6.16 gives the response in water level as:

$$h = Ce^{-t/BA} + B\dot{V}_i + h_{C1}$$

Since at $t = 0$, $h = h_0$, therefore $h_0 = C + B\dot{V}_i + h_{C1}$. Substituting from IIIb.6.17, C is found as $C = h_{C0} - h_{C1}$ and Equation IIIb.6.16 becomes:

$$h = (h_{C0} - h_{C1})e^{-t/BA} + B\dot{V}_i + h_{C1}$$

This equation gives the tank water level as a function of time. The new steady state value for water level, h_1 , is found by letting t approach ∞ . Thus $h_1 = B\dot{V}_i + h_{C1}$ and water level can be expressed as:

$$h = (h_{C0} - h_{C1})e^{-t/BA} + h_1 \quad \text{IIIb.6.18}$$

Finally, by substituting the derivative of h from Equation IIIb.6.18 into the tank mass balance we find:

$$\dot{V}_o = \dot{V}_i + \frac{h_{C0} - h_{C1}}{B} e^{-t/BA}$$

Example IIIb.6.5. Oil ($\nu = 1\text{E-}4 \text{ m}^2/\text{s}$), enters an open tank at a steady rate of $1.2 \text{ m}^3/\text{min}$ and leaves through a 30 m long pipe. The tank has a constant cross sectional area of 2.5 m^2 and the pipe has an inside diameter of 12 cm . At steady state conditions, the exit pressure is 1.65 m of oil. While the inlet flow remains constant, we increase the exit pressure instantaneously to 2.2 m of oil. Find the effect on oil level and exit flow rate.

Solution: We first check the Reynolds number to ensure Equations IIIb.6.15 through IIIb.6.18 are applicable:

$$\text{Re} = d \dot{V}_i / (\nu A) = (0.12 \times 1.2/60) / (1\text{E-}4 \times \pi 0.12^2/4) = 2122$$

Flow is laminar, thus:

$$B = 128\nu L / (\pi g d^4) = 128 \times 1\text{E-}4 \times 1 \times 30 / (\pi \times 9.81 \times 0.12^4) = 60 \text{ s/m}^2$$

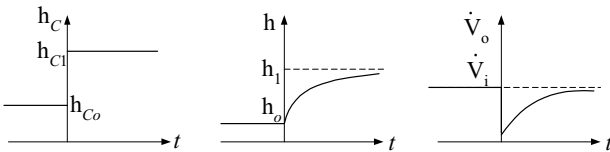
$$A = \pi 0.12^2/4 = 0.0113 \text{ m}^2$$

$$h_o = B \dot{V}_i + h_{C0} = 60 \times (1.2/60) + 1.65 = 2.85 \text{ m}$$

$$h_1 = h_o + (h_{C1} - h_{C0}) = 2.85 + (2.2 - 1.65) = 3.4 \text{ m}$$

$$h(t) = (h_{C0} - h_{C1})e^{-t/BA} + h_1 = (1.65 - 2.2)e^{-t/(60 \times 0.0113)} + 3.4 = -0.55e^{-t/0.678} + 3.4$$

$$\dot{V}_o = \dot{V}_i + (h_{C0} - h_{C1})e^{-t/BA} / B = 1.2 + (1.65 - 2.2)e^{-t/0.678} = 1.2 - 0.55 e^{-t/0.678} \text{ m}^3/\text{s}$$



Pressure Fluctuation in Gas Tanks

We now consider the situation where the pressure at the exit of a gas filled tank is changed. Our goal is to find the tank pressure response to the change in the downstream pressure. Figure IIIb.6.10(a) shows the gas tank of volume V . Under steady state conditions, the tank pressure is P_o , temperature T , and pressure at point C is P_{C0} . Flow rate into and out of the tank is \dot{m}_i . We now increase pressure at point C to P_{C1} . To see the effect on the tank pressure, we again use the mass and momentum equations. From the mass balance;

$$\dot{m}_i - \dot{m}_e = \frac{dm}{dt} = \frac{d}{dt} \left(\frac{PV}{RT} \right) = \frac{V}{RT} \left[\frac{dP}{dt} + \frac{P}{T} \frac{dT}{dt} \right] \quad \text{IIIb.6.19}$$

where in Equation IIIb.6.19, the temperature derivative is set equal to zero since the process is assumed to be isothermal. This is a reasonable assumption if the tank is not insulated. Equation IIIb.3.7 for momentum balance becomes $P - P_C = (fL/d) \dot{m}_e^2 / (2\rho A^2)$. Since we have assumed that tank pressure is uniform at all times, $P_B = P$. Furthermore, for this slow gas flow rate we ignored compressibility effects. Substituting for \dot{m}_e from the momentum balance into Equation IIIb.6.19, we obtain:

$$\frac{dP}{dt} + \left(\frac{RT}{V} \right) \sqrt{(P - P_C) / \beta} - \left(\frac{RT}{V} \right) \dot{m}_i \quad \text{IIIb.6.20}$$

where $\beta = (fL/d) / (2\rho A^2)$ and f is treated as a constant. Equation IIIb.6.20 is a non-linear first order differential equation, predicting the tank pressure as a function of time, for a specified forcing function for $P_C(t)$. We can find analytical solution in closed form for special cases of laminar flow in the pipe or for charging vessels with no gas withdrawal. For the latter case (i.e. $\dot{m}_e = 0$, as shown in Figure IIIb.6.10(b)) the momentum equation for the pipe becomes $P_B - P_C = \beta \dot{m}_i^2$. If we again assume that pressure is uniform in the tank at all times, then $P_C = P$. Substituting in Equation IIIb.6.19 yields:

$$\frac{dP}{dt} = \frac{RT}{V} \sqrt{(P_B - P) / \beta}$$

an analytical solution exists for charging vessels if the line pressure, P_B is kept constant:

$$P = P_B - \left(\sqrt{P_B - P_o} - \frac{RT}{2V\sqrt{\beta}} t \right)^2 \quad \text{IIIb.6.21}$$

The mass flow rate into the tank that results in a tank pressure of $P(t)$ is found from Equation IIIb.6.19 as:

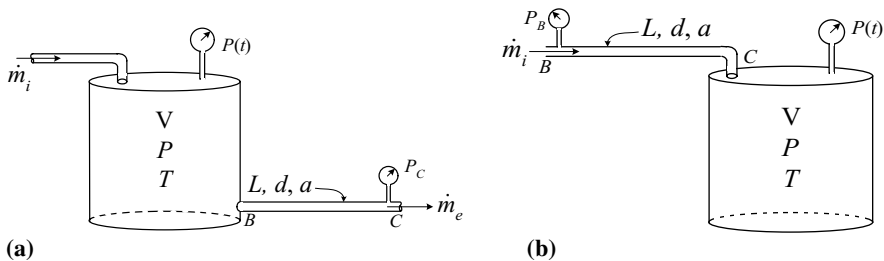


Figure IIIb.6.10. Pressure of a gas tank to downstream pressure change

$$\dot{m}_i = \sqrt{\frac{P_B - P_o}{\beta}} - \frac{RT}{2\beta V} t \quad \text{IIIb.6.22}$$

The study of the level response in an open tank holding liquid or the pressure response of a tank containing gas to changes in upstream or downstream pressure showed an interesting phenomenon. It indicated that we may maintain the liquid level or the gas pressure at specified values by manipulating the upstream or downstream pressures. Design of the devices which manipulate the upstream and downstream pressure to maintain level or pressure at specified values are generally discussed in books on feedback control systems.

Example IIIb.6.6. A tank having a volume of 50 m^3 contains air at 600 kPa. We intend to charge this tank through a feed line having a diameter of 6 cm and a length of 35 m. Pressurized air at 1200 kPa and 20 C enters the feed line. Find the time it takes for the tank pressure to reach 1200 kPa.

Solution: We find time for $P(t) = P_B$ from Equation IIIb.6.21:

$$t = \frac{\sqrt{P_B - P_o}}{RT / (2V\sqrt{\beta})}$$

$P_B = 1200 \text{ kPa}$, $P_o = 600 \text{ kPa}$, $R = 8314/28.97 = 287 \text{ m N/kg K}$, $V = 50 \text{ m}^3$, $T = 273 + 20 = 293 \text{ K}$,

$\rho = \bar{P} / (RT) = 900 / (0.287 \times 293) = 10.7 \text{ kg/m}^3$

$\beta = (fL/d) / (2\rho A^2) = 0.012 \times 35 / [2 \times 0.06 \times 10.7 \times (\pi \times 0.06^2/4)^2] = 0.41\text{E}5 \text{ (m kg)}^{-1}$

Substituting, we find:

$$t = \sqrt{(1200 - 600) \times 1000} / [287 \times 293 / (2 \times 50 \times \sqrt{0.41\text{E}5})] = 186.5 \text{ s.}$$

Vent Clearing, Liquid Expulsion

Our goal is to determine the time for liquid expulsion from a submerged pipe, which is also referred to as vent clearing. As shown in Figure IIIb.6.11(a), a pipe of constant cross sectional area A , is submerged in a liquid pool while connected to a reservoir of pressurized gas or vapor, having pressure P_g . As an example, this situation may represent the discharge of steam into the subcooled water of a BWR suppression pool. Our control volume extends from point 1 to point 2. As before, we use the same conservation equations for mass and momentum to determine the time for liquid expulsion from the pipe. The implicit assumption in this derivation is that the propagation time ($t_p = L/c$ where c is the speed of sound) is much shorter than the expulsion time. We apply Equation IIIa.3.44 to the control volume, with terms expanded below:

$$\Delta P_{inertia} = \rho(H - s)dV/dt$$

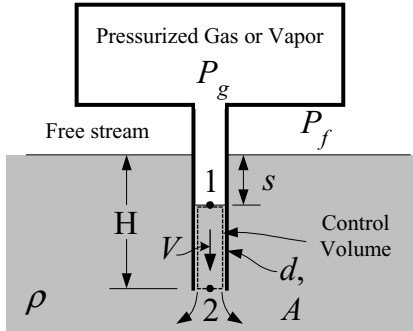
$$\Delta P_{pump} = 0$$

$$\Delta P_{stat} = P_2 - P_1$$

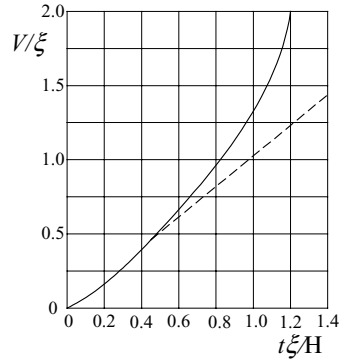
$$\Delta P_{vel} = 0$$

$$\Delta P_{grav} = \rho g(Z_2 - Z_1)$$

$$\Delta P_{fric} = f[(H - s)/d]\rho V^2/2$$



(a)



(b)

Figure IIIb.6.11. Expulsion of liquid from a submerged pipe

Since the gas density is generally negligible, $P_1 = P_g$. Also, from a simple force balance we find that:

$$P_2 = P_f + \rho gH$$

We also note that $Z_2 - Z_1 = (s - H)$. The conservation equation of mass takes the form of $V = ds/dt$. If we substitute for P_1 , P_2 , $Z_2 - Z_1$, and V in Equation IIIa.3.44, we obtain:

$$(H - s) \frac{d^2 s}{dt^2} + gs + f \frac{H - s}{d} \left(\frac{ds}{dt} \right)^2 = \frac{1}{\rho} (P_g - P_f) \quad \text{IIIb.6.23}$$

where in Equation IIIb.6.23, P_f is the free stream pressure. For the initial condition, we assume s is known. For example, if the pipe is full of water up to height H then $s(t = 0) = 0$. Also at time zero, liquid is at rest hence, $ds(t = 0)/dt = 0$. The solution to Equation IIIb.6.23 depends on the manner in which P_g is increased to expel liquid. Moody obtained solution for the cases of step increase ($P_g = P_o$) as well as a ramp increase ($P_g = P_f + Ct$, where C is a positive constant). The solution for the step increase in pressure is given as:

$$t = \left(\frac{L}{\xi} \sqrt{\frac{\pi}{2}} \right) \operatorname{erf} \sqrt{\frac{1}{2} \ln \left(\frac{H}{H-s} \right)^2} \quad \text{IIIb.6.24}$$

where $\xi = \sqrt{(P_o - P_f)/\rho}$ and the error function, $\operatorname{erf}(x)$, is defined in Chapter VIIb.3. Values of $\operatorname{erf}(x)$ are given in Figure IVa.9.3. Equation IIIb.6.24 is plotted with the solid line in Figure IIIb.6.11(b). The time to expel all the liquid from the pipe is found by letting s approach H :

$$\theta = 1.253H/\xi \quad \text{IIIb.6.25}$$

The dotted line in Figure IIIb.6.11(b) is for a case where the step increase in pressure is just enough to push the liquid to the exit of the pipe. The step increase in this case is for P_g to be increased to $P' = P_f + \rho gH$.

An interesting observation is that for cases where $P_g > P'$, velocity increases rapidly as s approaches H . Indeed Equation IIIb.6.24 shows that the denominator becomes zero. This is expected, as the mass of liquid approaches zero. In reality, the mass expelled from the pipe would accelerate the surrounding liquid, which was not considered in the above analysis. Thus, real velocity remains at a finite value.

Dynamics of Gas Bubbles

Analysis of rising bubbles in liquids is an involved task and the phenomenon is still a topic of investigation. The reason is due to the associated complexities such as; bubble shape, friction force (referred to as drag), geometry of the liquid container (bubble rise in an infinite liquid versus in a bank of tubes), liquid motion (stagnant versus flowing liquid), type of process (adiabatic versus thermal), and gas diffusion into liquid.

Gas bubbles are introduced into a liquid whereas vapor bubbles are primarily induced into the liquid such as in boiling. Here we discuss only gas bubbles. Steam bubbles are discussed in Chapter Vb.

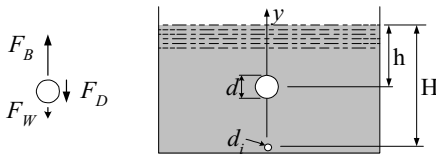


Figure IIIb.6.12. Gas bubble rising in a pool of liquid

Let's consider a simple case of a single non-condensable spherical* gas bubble in infinite stagnant water. Our goal is to find the bubble velocity and diameter as a function of time while the bubble is rising to the liquid surface. To obtain an analytical solution in closed form, we make several simplifying assumptions, which limit the results to cases for which the assumptions are valid. Suppose a small nitrogen bubble ($3 \text{ mm} \leq d_i \leq 9 \text{ mm}$) is just released in a pool of water at elevation H below the water surface. Due to buoyancy, the bubble rises to the surface while friction in the form of the drag force resists the bubble motion. The net force acting on the bubble results in the acceleration of the bubble according to Newton's second law. If the bubble trajectory does not significantly deviate from the vertical, then the bubble acceleration is along the y -axis:

$$F_B - F_W + F_D = m_b a_y \quad \text{IIIb.6.26}$$

where subscripts B , W , D , and b stand for buoyancy, weight, drag, and bubble, respectively. We now assume that after the initial acceleration period, the bubble reaches a terminal velocity at which point $a_y = 0$. All then we need to do is to express F_B , F_W , and F_D in terms of the system parameters. The bubble weight is found from $F_W = \rho_b V g$ where V is the bubble volume. The buoyancy force arises as a result of the displaced water by the presence of the bubble. Therefore, $F_B = \rho_w V g$ where subscript w stands for water. The drag force is due to frictional pressure drop; $F_D = (\Delta P) A_b$ where A_b in this relation is the projected area of the spherical bubble, $A_b = \pi d^2 / 4$ where d is the bubble diameter. Pressure drop, due to drag on the bubble, is similar to Equation IIIb.3.11. Therefore, the drag force on the bubble, F_D becomes:

$$F_D = \Delta P A_b = \left(C_D \frac{\rho_w V^2}{2} \right) \left(\pi d^2 / 4 \right) \quad \text{IIIb.6.27}$$

where in Equation IIIb.6.27, C_D is the *drag coefficient*. Solution of Equation IIIb.6.26 depends on the expression used for the drag coefficient, which in turn depends on a variety of factors such as bubble velocity and liquid properties (viscosity, density, and liquid surface tension). For laminar flow, $C_D = 16/\text{Re}$ where $\text{Re} = \rho_w V d / \mu_w$. Substituting C_D into Equation IIIb.6.27, we find $F_D = 2\pi\mu V d$. Stokes derived the drag force for very low Re numbers with negligible inertial forces as $F_D = 3\pi\mu V d$ (Fox). Substituting the Stokes drag force in Equation IIIb.6.26, noting that $\rho_b \ll \rho_w$, and substituting the results in Equation IIIb.6.26 (with $a_y = 0$), we find $\rho_w V g = 3\pi\mu V d$. Solving for the terminal velocity, we get:

$$V = \frac{\rho_w g d^2}{18\mu} \quad \text{IIIb.6.28}$$

As the bubble rises, pressure keeps dropping thus d changes with time and so does the bubble velocity. To express d as a function of time, we use the equation of

* An aspect ratio is defined for ellipsoidal bubbles, given as the ratio of the bubble minor over its major axis. For spherical bubbles the aspect ratio is unity.

state for the isothermal bubble. At any depth along the bubble flow path; $PV = P_i V_i$ where i refers to the bubble initially released at depth H . Substituting for $V = \pi d^3/6$ and for $P = P_{atm} + \rho_w g h$ in the equation of state, the bubble diameter is found as:

$$d = \left(\frac{P_i}{P_{atm} + \rho_w g h} \right)^{1/3} d_i \quad \text{IIIb.6.29}$$

where d_i is the initial bubble diameter at depth H . Substituting Equation IIIb.6.29 into Equation IIIb.6.28, we find the bubble velocity as a function of time. However, these are implicit relations in time as $h = f(t)$, is yet to be determined. To find h , we use the fact that $dh/dt = V$ with the initial condition of $h(t = 0) = H$. Substituting from Equations IIIb.6.28 and IIIb.6.29 and integrating, we find h as a function of time given by:

$$h = \frac{1}{\rho_w g} \left[\left(P_i^{5/3} - \frac{5(\rho_w g d_i)^2}{54\mu} \right)^{3/5} t - P_{atm} \right] \quad \text{IIIb.6.30}$$

where $P = P_{atm} + \rho_w g H$. We then find $V = f(t)$ and $d = f(t)$ by back substitution of Equation IIIb.6.30 into Equations IIIb.6.29 and the result in III.6.28, respectively.

Flow Distribution in Piping Networks, the Nahavandi Method

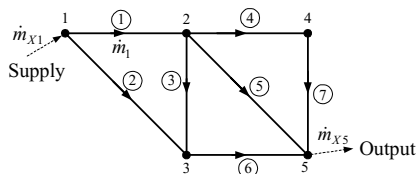
Two methods for determination of flow distribution in piping networks were discussed in Section 3. Here, we discuss the Nahavandi method, which is based on solving the transient form of the conservation equations of mass and momentum. To determine flow under steady-state condition, a null transient is analyzed. The null transient, also known as dynamic relaxation, finds solutions for time dependent problems without any imposed forcing function in the boundary conditions. In this method, the same concept of node and inter-nodal flow path, branch, or link, as discussed in Section 3 applies. The continuity equation is applied to each node and the momentum equation to each flow path. However, no mass storage at a node or in a flow path is allowed. This assumption, while greatly simplifying the analysis, introduce only slight inaccuracy if applied to incompressible flow. Additionally, the liquid must remain single-phase as no heat transfer is considered in the network. Since the method is applicable only to slow transients, the wave propagation effect, as discussed in Section 7 is also neglected. The Nahavandi method is well suited for computer programming since the formulation is based on matrix algebra.

The Continuity Equation: To write the continuity equation in matrix form, we first define a *connection matrix* $[C]$ with elements being either +1, -1, or 0. This matrix is obtained from the fact that pressure drop between two nodes is related to the nodal pressures as:

$$\{\Delta P_{stat}\} = -[C] \{P\} \quad \text{IIIb.6.31}$$

where the number of rows of matrix $[C]$ is equal to the number of branches and the number of columns in matrix A is equal to the number of nodes of the piping network. In Equation IIIb.6.31, a matrix is represented by $[]$ and an array by $\{ \}$. Matrix algebra is discussed in Chapter VIId.

Example IIIb.6.7. Find the connection matrix for the piping network shown in the figure.



Solution: There are 5 nodes and 7 flow paths. To distinguish the number representing a node from the number representing a flow path, the latter is placed inside a circle next to the related flow path. The flow to node 1 is from a source for which the source pressure is given. The output flow rate to a sink is from node 5. Subscript X indicates that the flow is an external flow (i.e., enters or leaves the piping network). The supply pressure and the external flow are given and we must find the unknown inter-nodal flow rates. Recall that according to our sign convention, any flow leaving a node would be assigned a plus and any flow entering a node would be assigned a minus sign. Pressure drop is related to nodal pressure through $\Delta P = P_B - P_A$:

$$\Delta P_1 = \Delta P_{1-2} = -(P_1 - P_2)$$

$$\Delta P_2 = \Delta P_{1-3} = -(P_1 - P_3)$$

$$\Delta P_3 = \Delta P_{2-3} = -(P_2 - P_3)$$

$$\Delta P_4 = \Delta P_{2-4} = -(P_2 - P_4)$$

$$\Delta P_5 = \Delta P_{2-5} = -(P_2 - P_5)$$

$$\Delta P_6 = \Delta P_{3-5} = -(P_3 - P_5)$$

$$\Delta P_7 = \Delta P_{4-5} = -(P_4 - P_5)$$

Hence, Equation IIIb.6.31 becomes:

$$\begin{Bmatrix} \Delta P_1 \\ \Delta P_2 \\ \Delta P_3 \\ \Delta P_4 \\ \Delta P_5 \\ \Delta P_6 \\ \Delta P_7 \end{Bmatrix} = - \begin{bmatrix} 1 & -1 & 0 & 0 & 0 \\ 1 & 0 & -1 & 0 & 0 \\ 0 & 1 & -1 & 0 & 0 \\ 0 & 1 & 0 & -1 & 0 \\ 0 & 1 & 0 & 0 & -1 \\ 0 & 0 & 1 & 0 & -1 \\ 0 & 0 & 0 & 1 & -1 \end{bmatrix} \begin{Bmatrix} P_1 \\ P_2 \\ P_3 \\ P_4 \\ P_5 \end{Bmatrix}$$

The connection matrix is thus a 7×5 matrix with elements of only -1 , 1 , and 0

Having determined the connection matrix $[C]$, the continuity equation for the piping network becomes:

$$[C]^T \{\dot{m}\} + \{\dot{m}_X\} = \{0\} \quad \text{IIIb.6.32}$$

Example IIIb.6.8. For the piping network of Example IIIb.6.7, verify the Kirchhoff's law for nodes 2 and 5.

Solution: To verify Equation IIIb.6.32, we need to find the transpose of matrix C and multiply it by the mass flow rates while considering the output flows:

$$\begin{bmatrix} 1 & 1 & 0 & 0 & 0 & 0 & 0 \\ -1 & 0 & 1 & 1 & 1 & 0 & 0 \\ 0 & -1 & -1 & 0 & 0 & 1 & 0 \\ 0 & 0 & 0 & -1 & 0 & 0 & 1 \\ 0 & 0 & 0 & 0 & -1 & -1 & -1 \end{bmatrix} \begin{Bmatrix} \dot{m}_1 \\ \dot{m}_2 \\ \dot{m}_3 \\ \dot{m}_4 \\ \dot{m}_5 \\ \dot{m}_6 \\ \dot{m}_7 \end{Bmatrix} + \begin{Bmatrix} -\dot{m}_{X1} \\ 0 \\ 0 \\ 0 \\ 0 \\ \dot{m}_{X5} \end{Bmatrix} = \begin{Bmatrix} 0 \\ 0 \\ 0 \\ 0 \\ 0 \end{Bmatrix}$$

From this matrix equation, we get confirmation that for node 2, for example:

$$-\dot{m}_1 + \dot{m}_3 + \dot{m}_4 + \dot{m}_5 = 0$$

Similarly for node 5 we have:

$$-\dot{m}_5 - \dot{m}_6 - \dot{m}_7 + \dot{m}_{X5} = 0$$

A piping network having N nodes and M flow paths has a total of $M + N$ unknowns. These are N nodal pressures and M flow rates. There are N continuity equations given by Equation IIIb.6.32 and M momentum equations written for the M flow paths as discussed next.

The Momentum Equation: We may use Equation IIIa.3.44 for each flow path:

$$\sum \left(\frac{L}{A} \right) \frac{d\dot{m}}{dt} = \Delta P_{pump} - (\Delta P_{stat} + \Delta P_{grav} + \Delta P_{accl} + \Delta P_{fric})$$

Approximating the time dependent term by finite difference and multiplying both sides by A/L we obtain:

$$\left\{ \frac{\dot{m}^{n+1} - \dot{m}^n}{\Delta t} \right\} = \left\{ \frac{A}{L} \right\} \left\{ \Delta P_{pump} - (\Delta P_{stat} + \Delta P_{vel} + \Delta P_{grav} + \Delta P_{fric}) \right\} \quad \text{IIIb.6.33}$$

where various pressure terms in Equation IIIb.6.33 are defined in Equation IIIb.4.1. Note that in Equation IIIb.6.33, the mass flow rates with superscript

$n+1$ are the unknown mass flow rates to be calculated at time $n+1$ having mass flow rates at time n . Mass flow rates at time zero are obtained from our initial guesses based on engineering judgment. These estimated flow rates must satisfy the Kirchhof's law at each node. We now rearrange Equation IIIb.6.33 for the unknown mass flow rates:

$$\{\dot{m}^{n+1}\} = \{\dot{m}^n\} + \{B(\Delta P_{pump} - \Delta P_{stat}) - B(\Delta P_{grav} + \Delta P_{fric})\} \quad \text{IIIb.6.34}$$

where in Equation IIIb.6.34, $\{B\} = \{A_i \Delta t / L_i\}$ with A representing the flow area and L the flow length.

Matrix Solution: To find nodal pressures, we substitute for $\{\Delta P_{stat}\}$ from Equation IIIb.6.31 into Equation IIIb.6.34 and then substitute the resulting equation into Equation IIIb.6.32 to obtain:

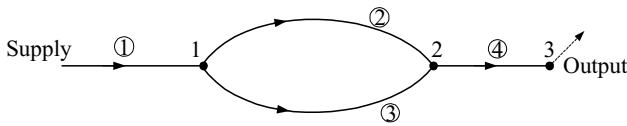
$$[C]^T \{\dot{m}^n\} + [C]^T [B][C]\{P\} + [C]^T \{B\Delta P_{pump} - B(\Delta P_{grav} + \Delta P_{fric})\} + \{\dot{m}_X\} = \{0\} \quad \text{IIIb.6.35}$$

We can now solve Equation IIIb.6.35 for the unknown nodal pressures. The solution is as follows:

$$\{P\} = [E]^{-1} [C]^T \{B\Delta P_{pump} - B(\Delta P_{grav} + \Delta P_{fric}) - \dot{m}^n\} - [E]^{-1} \{\dot{m}_X\} \quad \text{IIIb.6.36}$$

where in Equation IIIb.6.36, $[E] = [C]^T [B][C]$ is a square matrix and $[B]$ a diagonal matrix with diagonal elements of $[B_i] = \{A_i \Delta t / L_i\}$. Having found nodal pressures, we can find inter-nodal flow rates from Equation IIIb.6.34.

Example IIIb.6.9. Determine matrix $[E]$ for the network shown in the figure.



Solution: Using the supply pressure as the reference pressure, we find $\Delta P_1 = -(0 - P_1)$. Thus we find:

$$\begin{Bmatrix} \Delta P_1 \\ \Delta P_2 \\ \Delta P_3 \\ \Delta P_4 \end{Bmatrix} = - \begin{bmatrix} -1 & 0 & 0 \\ 1 & -1 & 0 \\ 1 & -1 & 0 \\ 0 & 1 & -1 \end{bmatrix} \begin{Bmatrix} P_1 \\ P_2 \\ P_3 \end{Bmatrix}$$

Using the connection matrix, the continuity equation becomes:

$$\begin{bmatrix} -1 & 1 & 1 & 0 \\ 0 & -1 & -1 & 1 \\ 0 & 0 & 0 & -1 \end{bmatrix} \begin{Bmatrix} \dot{m}_1 \\ \dot{m}_2 \\ \dot{m}_3 \\ \dot{m}_4 \end{Bmatrix} + \begin{Bmatrix} 0 \\ 0 \\ \dot{m}_{x3} \end{Bmatrix} = \begin{Bmatrix} 0 \\ 0 \\ 0 \end{Bmatrix}$$

The momentum equation becomes:

$$\begin{Bmatrix} \frac{\dot{m}_1^{n+1} - \dot{m}_1^n}{\Delta t} \\ \frac{\dot{m}_2^{n+1} - \dot{m}_2^n}{\Delta t} \\ \frac{\dot{m}_3^{n+1} - \dot{m}_3^n}{\Delta t} \\ \frac{\dot{m}_4^{n+1} - \dot{m}_4^n}{\Delta t} \end{Bmatrix} = \begin{Bmatrix} \frac{A_1}{L_1} (\Delta P_{pump} - \Delta P_1 - \Delta P_{grav1} - \Delta P_{fric1}) \\ \frac{A_2}{L_2} (\Delta P_{pump} - \Delta P_2 - \Delta P_{grav2} - \Delta P_{fric2}) \\ \frac{A_3}{L_3} (\Delta P_{pump} - \Delta P_3 - \Delta P_{grav3} - \Delta P_{fric3}) \\ \frac{A_4}{L_4} (\Delta P_{pump} - \Delta P_4 - \Delta P_{grav4} - \Delta P_{fric4}) \end{Bmatrix}$$

The $[E]$ matrix is obtained from:

$$[E] = (g\Delta t) \begin{bmatrix} -1 & 1 & 1 & 0 \\ 0 & -1 & -1 & 1 \\ 0 & 0 & 0 & -1 \end{bmatrix} \begin{bmatrix} A_1/L_1 & 0 & 0 & 0 \\ 0 & A_2/L_2 & 0 & 0 \\ 0 & 0 & A_3/L_3 & 0 \\ 0 & 0 & 0 & A_4/L_4 \end{bmatrix} \begin{bmatrix} -1 & 0 & 0 \\ 1 & -1 & 0 \\ 1 & -1 & 0 \\ 0 & 1 & -1 \end{bmatrix}$$

Thus the elements of the $[E]$ matrix are:

$$[E] = (g\Delta t) \begin{bmatrix} (A_1/L_1) + (A_2/L_2) + (A_3/L_3) & -(A_2/L_2) - (A_3/L_3) & 0 \\ -(A_2/L_2) - (A_3/L_3) & (A_2/L_2) + (A_3/L_3) + (A_4/L_4) & -(A_4/L_4) \\ 0 & -(A_4/L_4) & (A_4/L_4) \end{bmatrix}$$

We can then find the nodal pressures by inverting matrix $[E]$, substituting the results into Equation IIIb.6.36, and performing the matrix operations.

7. Fundamentals of Waterhammer Transients

Analysis of waterhammer or rapid flow transients, where acoustic waves travel through the flow path, is much more involved than the rigid column theory. In this section we just introduce the concept of waterhammer analysis for liquids only and discuss some preliminary derivations of governing equations. For more information on this topic, the interested reader may review works of Parmakian,

Watters, and Wiley & Streeter. An added complication in waterhammer analysis, in addition to the effects of fluid compressibility, is the fact that the elasticity of the conduit containing the fluid must also be taken into account. For this reason, waterhammer analysis is also called *elastic* analysis.

To introduce the concept of rapid transient analysis, let's consider a simple case of steady fluid flow in a frictionless horizontal pipe at a speed of V_1 , as shown in Figure IIIb.7.1(a). Since the pipe is frictionless, pressure head at point B, where a control valve is located, is the same as that of point A hence, the hydraulic grade line (HGL) is horizontal. Our goal is to find the pressure head caused by throttling of the valve. In Figure IIIb.7.1(b), the valve is instantaneously throttled so that flow velocity has dropped to $V_2 < V_1$. The reduction in flow velocity, according to the Bernoulli equation is associated with an increase in pressure head just upstream of the valve. The increased pressure head is now a driving force, which causes the disturbance to travel upstream of the valve at the acoustic velocity in the medium, c . The increased pressure head (ΔH) also affects the liquid via compression and the pipe wall via expansion.

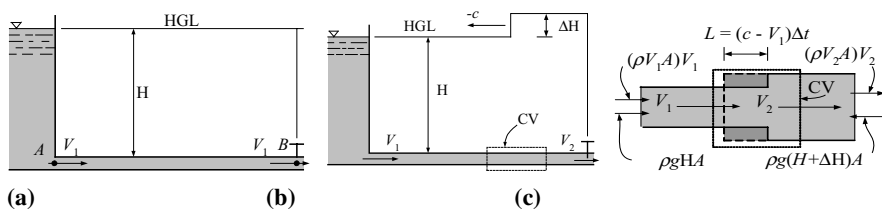


Figure IIIb.7.1. Flow from a reservoir through a frictionless pipe.

We now write the momentum equation for a control volume through which the disturbance would pass as shown in Figure IIIb.7.1(c). The summation of all the forces is equal to the rate of change of momentum in the control volume, plus the net momentum flux per Equation IIIa.3.6. Net force is found as:

$$-\rho g H A - \rho g (H + \Delta H) A = -\rho g A \Delta H$$

Note that we ignored the slight increase in the pipe flow area due to expansion. Net momentum flux is obtained as $[\rho V_2^2 A - \rho V_1^2 A]$. Throttling of the valve has resulted in a ΔV reduction in the flow velocity therefore, $\Delta V = V_1 - V_2$. Substituting for V_2 and ignoring ΔV^2 , momentum flux reduces to:

$$[\rho V_2^2 A - \rho V_1^2 A] = [\rho (V_1 - \Delta V)^2 A - \rho V_1^2 A] \cong -(2\rho A V_1 \Delta V)$$

Finally, we find the rate of change of momentum as follows. We note that flow is moving at a velocity of V_1 towards the right and the disturbance is moving at the speed of sound in the liquid towards the left. Hence, at the time increment Δt , the control volume has a length of $(c - V_1)\Delta t$ and a mass of $\rho(c - V_1)\Delta t A$. In the inter-

val Δt , velocity has changed from V_1 to V_2 . Hence, the rate of change of momentum is given by $[\rho g(c - V_1)\Delta t A][(V_2 - V_1)/\Delta t]$. The momentum equation for the control volume becomes:

$$-\rho g A \Delta H = [\rho g(c - V_1)\Delta t A](\Delta V/\Delta t) - (2\rho A V_1 \Delta V_1)$$

This simplifies to:

$$\Delta H = c\Delta V(1 + V_1/c)/g \quad \text{IIIb.7.1}$$

We can further simplify this relation by comparing typical flow velocities with the speed of sound in various mediums as shown in Table IIIb.7.1. Hence, ignoring V_1/c as compared with unity, we find $\Delta H \cong c\Delta V/g$.

Example IIIb.7.1. Flow velocity of a liquid, for which $c = 4900$ ft/s, is reduced from 2 ft/s to 1 ft/s. Find the resulting head rise.

Solution: From Equation IIIb.7.1, since $V \ll c$, we find $\Delta H = 4900 \times (2 - 1)/32.2 = 152$ ft. This is a substantial rise in head for such a small change in flow rate indicating that waterhammer subjects piping to a large magnitude force with potential of damaging the piping system. If the liquid is water, then $\Delta P \cong 66$ psi.

The magnitude of waterhammer forces depends on the elasticity of the piping material and liquid compressibility. The more rigid the piping material, the higher the magnitude of the waterhammer force. As for liquid compressibility, the lower the compressibility, the higher the waterhammer force. Equation IIIb.7.1 can be extended to multiple incremental changes of velocity. In particular,

$$H \cong \Sigma c\Delta V/g \quad \text{IIIb.7.2}$$

Here we ignored pipe friction as well as any reflecting wave traveling towards the regulating valve. In a more rigorous analysis, we shall consider both pipe friction and forward and reflecting waves due to pressure wave propagation. However, we first discuss effects of various parameters on the wave speed.

7.1. Factors Affecting The Speed of Acoustic Waves

Speed of sound in several mediums is shown in Table IIIb.7.1. In liquid flow inside pipes, the wave speed depends not only on the elasticity of the piping material but also on such parameters as diameter and thickness of the pipe as well as density and bulk modulus of the liquid. To mathematically demonstrate the dependency of the sound wave on these parameters we consider flow of a liquid in the pipe of Figure IIIb.7.1 with valve instantly shut. In this case, $V_2 = 0$ and $\Delta V = V_1$. Instant closure of the valve results in development of a pressure head, which compresses the liquid and causes the pipe to expand both axially and in the radial direction. However, axial direction is generally much smaller as compared with radial expansion of the pipe. Expansion of the pipe combined with compression of the liquid result in a certain amount of the liquid mass from the reservoir entering

Table IIIb.7.1. Speed of sound in various mediums

Gas	c (m/s)	c (ft/s)	Liquid	c (m/s)	c (ft/s)	Solid	c (m/s)	c (ft/s)
H ₂	1,294	4,246	Glycerin	1,859	6,100	Aluminum	5,151	16,900
He	1,000	3,281	Water	1,490	4,890	Steel	5,060	16,600
Air	340	1,117	Mercury	1,451	4,760	Brick	3,652	11,980
Ar	317	1,040	Ethyl Alcohol	1,201	3,940	Copper	3,557	11,670
CO ₂	266	873				Brass	3,500	11,480
CH ₄	185	607				Ice	3,200	10,500
UF ₆	91	297				Cork	500	1,640

At 1 atm and 60 F

the pipe. This amount of mass can be found from the following mass balance. If L is the length of the pipe, it takes $t = L/c$ seconds for the pressure wave to reach the reservoir after the instant closure of the valve. During this time, a total of $(\rho V_1 A)L/c$ mass of liquid has entered the pipe. The mass of liquid entering the pipe due to pipe expansion is $\rho L \Delta A$ and the mass entering due to liquid compression is $L A \Delta \rho$. Therefore,

$$(\rho V_1 A) L/c = \rho L \Delta A + L A \Delta \rho$$

This equation simplifies to $V_1/c = \Delta A/A + \Delta \rho/\rho$. Noting that $V_1 = \Delta V$, we substitute for ΔV from Equation IIIb.7.1 for $V_1 \ll c$ and solve for c^2 to obtain:

$$c^2 = g \Delta H / [\Delta A/A + \Delta \rho/\rho] \quad \text{IIIb.7.3}$$

To relate the wave speed to the liquid and the pipe wall properties, we first replace $\Delta H = \Delta P / \rho(g/g_c)$ and take advantage of the definition of liquid bulk modulus, as defined in Chapter IIIa, $E_v = \Delta P / (\Delta \rho/\rho)$. Equation IIIb.7.3 becomes:

$$c^2 = (E_v/\rho) / [1 + E_v \Delta A/A \Delta P] \quad \text{IIIb.7.4}$$

Now, we can relate ΔP and $\Delta A/A$ to pipe properties. To do this, we consider the free body diagram of the pipe as shown in Figure IIIb.7.2 and perform a simple force balance.

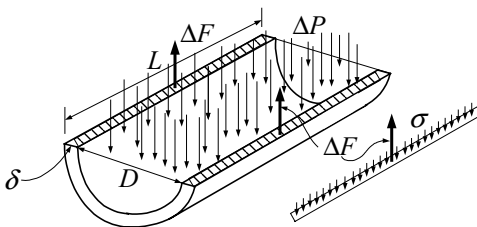


Figure IIIb.7.2. The free body diagram of a pipe carrying fluid

The incremental internal pressure in the pipe is balanced by the circumferential tensile force per unit length; $2\Delta FL = \Delta P(LD)$. Since the incremental tensile force in turn is balanced by the tensile stress $\Delta F/L = \sigma(L\delta)$, then we can relate stress to incremental pressure $2\sigma\delta = \Delta PD$ or $\sigma = \Delta PD/2\delta$. Having related ΔP to pipe stress, we seek to relate ΔA to pipe strain. We then would relate strain to stress through E , the modulus of elasticity as $\varepsilon = \sigma/E$. The incremental increase in flow area is given by $\Delta A = \pi D (\Delta D/2)$. But by definition, $\varepsilon = \Delta D/D$. Hence, $\Delta A = \pi D^2 \varepsilon/2$. We now substitute for ε in terms of σ and for σ in terms of ΔP to get; $\Delta A/A = \Delta PD/E\delta$. Substituting in Equation IIIb.7.4, we obtain:

$$c = \sqrt{(E_v/\rho) / [1 + (E_v/E)(D/\delta)]} = [C_{Liquid} / (1 + C_{Pipe})]^{1/2} \quad \text{IIIb.7.5}$$

where we have called $g_c E_v/\rho = C_{Liquid}$ and $(E_v/E)(D/\delta) = C_{Pipe}$. Elasticity of some piping materials is given in Table IIIb.7.2.

Table IIIb.7.2. Elasticity for some piping materials

	Steel	Ductile Cast Iron	Copper	Brass	Aluminum	PVC	Fiber- Glass	Plastic	Asbestos Cement
E (psi)	30E6	24E6	16E6	15E6	10.5E6	4.0E6	4.0E6	1.3E6	3.4E6
E (GPa)	206.8	165.5	110.3	103.4	72.397	27.58	27.58	8.964	23.44

Example IIIb.7.2. Water at 60 F is flowing in a 22-inch Schedule 60 steel pipe. Find the wave speed for the system. $\rho_{\text{water}} = 62.37 \text{ lbm/ft}^3$, $(E_v)_{\text{water}} = 3.11 \times 10^5 \text{ psi}$ and $E_{\text{steel}} = 30 \times 10^6 \text{ psi}$.

Solution: For 22-inch Schedule 60 pipe, $D = 20.25 \text{ in}$ and $\delta = 0.875 \text{ in}$. From Equation IIIb.7.5 we have:

$$c = \sqrt{\frac{32.2 \times (144 \times 3.11 \text{E}5) / 62.37}{1 + (3.11 \text{E}5 / 3 \text{E}7)(20.25 / 0.875)}} = 4318 \text{ ft/s}$$

If the pipe was fully rigid (i.e., $E \rightarrow \infty$), then the wave speed would have been found from:

$$c = \sqrt{E_v/\rho} = \sqrt{32.2 \times 144 \times 3.11 \text{E}5 / 62.37} = 4808 \text{ ft/s}$$

Speed of sound in water from Table IIIb.7.1 is 4890 ft/s.

To determine the effect of wall thickness, we may perform similar analysis as in Example IIIb.7.1 with wall thickness as a variable. The results of such analysis for two types of piping materials are shown in Table IIIb.7.3.

Table IIIb.7.3. Wave speed in piping systems

D/δ	Steel		Cast Iron*	
	m/s	ft/s	m/s	ft/s
5	1,430	4,680	1,400	4,590
10	1,365	4,478	1,341	4,400
20	1,310	4,300	1,250	4,100
40	1,219	4,000	1,097	3,600
60	1,158	3,800	1,021	3,350
80	1,097	3,600	945	3,100
100	1,036	3,400	884	2,900

* $E = 16\text{E}6$ psi (110.32 GPa)

Having the wave speed enables us to compare the head rise subsequent to sudden closure of a valve in various piping systems. In the example below, we compare the head rise in two piping systems.

Example IIIb.7.3. Water flows at 80 F in a 20-inch Schedule 40 pipe. Find the head rise due to instantaneous closure of a valve (a) for steel pipe and (b) for a PVC pipe having the same dimensions as the steel pipe. $\rho_{\text{water}} = 62.22 \text{ lbm/ft}^3$, $(E_v)_{\text{water}} = 3.22\text{E}5$ psi. Water flow rate is 5198 GPM.

Solution: For a 20 in (51 cm) nominal pipe size Schedule 40, $D = 18.812$ in (48 cm), $\delta = 0.594$ in (1.5 cm), $E_{\text{steel}} = 30\text{E}6$ psi (206.85 GPa) and $E_{\text{PVC}} = 4\text{E}5$ psi (2.758 GPa). For the steel pipe, we calculate:

$$(C_{\text{Pipe}})_{\text{Steel}} = (E_v/E)(D/\delta) = 1 + (3.22/300)(18.812/0.594) = 0.34$$

and for the PVC pipe, we have:

$$(C_{\text{Pipe}})_{\text{PVC}} = (E_v/E)(D/\delta) = 1 + (3.22/4)(18.812/0.594) = 25.49$$

For both cases:

$$C_{\text{Liquid}} = E_v/\rho = 32.2 \times (144 \times 3.22\text{E}5/62.22) = 24\text{E}6$$

The wave speed for the steel pipe is found as:

$$c = [C_{\text{Liquid}} / (1 + C_{\text{Pipe}})]^{1/2} = [24\text{E}6 / (1 + 0.34)]^{0.5} = 4232 \text{ ft/s (1290 m/s)}$$

and for the PVC pipe as:

$$c = [C_{\text{Liquid}} / (1 + C_{\text{Pipe}})]^{1/2} = [24\text{E}6 / (1 + 25.49)]^{0.5} = 970 \text{ ft/s (296 m/s)}$$

Water velocity is found as:

$$V = \dot{V} / A_{Pipe} = [5198 / (60 \times 7.481)] / [\pi(18.812/12)^2/4] = 6 \text{ ft/s (1.83 m/s)}$$

Hence, the head rise from Equation IIIb.7.1 for $V \ll c$, i.e., $\Delta H \equiv c\Delta V/g$ for flow in the steel pipe is:

$$\Delta H \equiv c\Delta V/g = 4232 \times 6/32.2 = 788.6 \text{ ft (240.3 m)}$$

In the case of the PVC pipe we find the head rise as:

$$\Delta H \equiv c\Delta V/g = 970 \times 6/32.2 = 180 \text{ ft (55 m)}$$

So far we noticed how analysis of a fast transient differs from the rigid column theory. We performed some hand calculations to determine the head rise following instantaneous closure of a valve. We were also able to express the speed by which disturbances in a fluid are propagated in terms of the factors affecting it. Next, we perform a more rigorous analysis to obtain the conservation equations in the form of partial differential equations. To be able to solve the set of governing equations, we use the method of characteristics. This method allows us to solve the converted equations by finite difference.

7.2. Analysis of Fast Transients in Piping Systems

Our goal is to analyze the response of a piping system containing the flow of a fluid to a fast transient. For this purpose, we consider the internal, one-dimensional flow of a fluid in a pipe. The free body diagram of an element of this piping system is shown in Figure IIIb.7.3. In general, the pipe may have an angle θ with the horizontal plane. Initially, fluid is flowing steadily in the pipe. At time zero, a valve is instantly closed causing in pressure waves to propagate at the speed of sound in the system. As a result of the perturbation, the fluid is compressed and the pipe expands. We now set up the conservation equations of mass and momentum for the elemental control volume assuming that the elongation in the axial direction is negligible compared with the elongation in the radial direction.

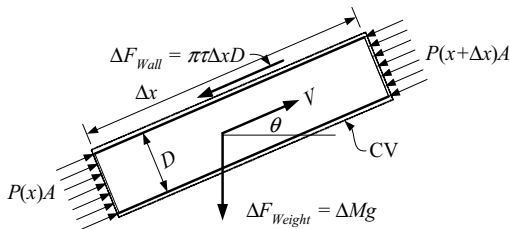


Figure IIIb.7.3. Free-body diagram of an elemental control volume

Continuity Equation is derived in Example IIIa.3.7 as $(1/A)dA/dt + (1/\rho)d\rho/dt + (dV/dx) = 0$. We may now substitute for:

$$dA/A = dP/D/E\delta = \rho g dH/D/E\delta$$

that was derived earlier to couple the continuity equation with the pipe structural properties. Similarly, $d\rho/\rho$ can be replaced by taking advantage of the definition of the liquid bulk modulus:

$$d\rho/\rho = dP/E_v = \rho g dH/E_v$$

Substituting and rearranging we obtain the relation between the velocity and the head rise:

$$\frac{dH(x,t)}{dt} + \frac{c^2}{g} \frac{\partial V(x,t)}{\partial x} = 0 \quad \text{IIIb.7.6}$$

where we have also substituted from Equation IIIb.7.5. This is a partial differential equation in two unknowns. We need one more equation to be able to solve the set, which is obtained as follows.

Momentum Equation for a one-dimensional flow is derived as (see Example IIIa.3.10)

$$\rho \left(\frac{\partial V}{\partial t} + V \frac{\partial V}{\partial x} \right) + \frac{\partial P}{\partial x} + \pi D \tau + \rho g \sin \theta = 0 \quad \text{IIIb.7.7}$$

We may now substitute for pressure, friction, and gravity terms as follows. For the friction term, we substitute for wall shear stress from Equation IIIb.2.5 or alternatively from the Darcy equation as given by Equation IIIb.3.7 so that:

$$\pi D \tau = \pi D \frac{f}{4} \frac{\rho V |V|}{2} = f \frac{A}{D} \frac{\rho V |V|}{2}$$

where A is the flow area. For the gravity force term we notice that $\sin \theta = \partial z / \partial x$ (see Figure IIIb.7.3). Finally, we replace the pressure term with the piezometric head so that:

$$\frac{\partial P}{\partial x} = \rho g \frac{\partial (H - z)}{\partial x}$$

where $H = P/(\rho g/g_c) + z$. Substituting in Equation IIIb.7.7 we obtain;

$$\rho \left(\frac{\partial V}{\partial t} + V \frac{\partial V}{\partial x} \right) + \rho g \left(\frac{\partial H}{\partial x} - \frac{\partial z}{\partial x} \right) + f \frac{\rho V |V|}{2D} + \rho g \frac{\partial z}{\partial x} = 0$$

Note that by replacing the pressure term with piezometric head, the resulting equation applies only to liquids. Dividing through by ρ and canceling the $\partial z / \partial x$ terms, the momentum equation reduces to

$$\left(\frac{\partial V}{\partial t} + V \frac{\partial V}{\partial x}\right) + g \frac{\partial H}{\partial x} + f \frac{V|V|}{2D} = 0 \quad \text{IIIb.7.8}$$

Now that we have derived the governing equations, we embark on finding mathematical means of solving Equation IIIb.7.6 and IIIb.7.8.

Solving the Governing Equations. The reason problems involving fast transients are more complicated, is the fact that we have to solve a set of coupled, non-linear, partial differential equations,

$$\begin{aligned} \left(\frac{\partial H}{\partial t} + V \frac{\partial H}{\partial x}\right) + \frac{c^2}{g} \frac{\partial V(x,t)}{\partial x} &= 0 \\ \left(\frac{\partial V}{\partial t} + V \frac{\partial V}{\partial x}\right) + g \frac{\partial H}{\partial x} + f \frac{V|V|}{2D} &= 0 \end{aligned}$$

where the first term of Equation IIIb.7.6 is now expanded. To be able to tackle this set of equations, we first try to eliminate as many nonlinear terms as possible. Such elimination undoubtedly leads to the introduction of some uncertainties in the results. However, if the eliminated terms are negligible as compared with other terms, then the degree of uncertainty will be much less. As was discussed in Section IIIa.3.2, the non-linearity is due to the convective acceleration term. Fortunately, $V\Delta H/\Delta x$ in the continuity equation and $V\Delta V/\Delta x$ in the momentum equation are small terms compared with the other terms. That is, the temporal changes in velocity and the head rise ($\Delta V/\Delta t$ and $\Delta H/\Delta t$) are much longer than the spatial changes. Also note that such terms as $\Delta H/\Delta x$ and $\Delta V/\Delta x$ are multiplied by large values such as g and c^2/g , respectively. Dropping the less significant terms, the set simplifies to:

$$\frac{\partial H}{\partial t} + \frac{c^2}{g} \frac{\partial V}{\partial x} = 0 \quad \text{IIIb.7.9}$$

$$\frac{\partial V}{\partial t} + g \frac{\partial H}{\partial x} + f \frac{V|V|}{2D} = 0 \quad \text{IIIb.7.10}$$

Despite the above simplification, no general solution to this set of equations exists. An interesting way to make this set more amenable to a solution is the method of characteristics, which converts the set of coupled non-linear partial differential equation into a set of coupled ordinary differential equations. As demonstrated by Equation IIIa.2.2, total derivative of velocity for example, in one dimension is found as:

$$\frac{dV}{dt} = \frac{\partial V}{\partial t} + \frac{\partial V}{\partial x} \frac{dx}{dt} \quad \text{IIIb.7.11}$$

We then note that for V , the space derivative exists in Equation IIIb.7.9 and the time derivative exists in Equation IIIb.7.10. For H , the time derivative exists in Equation IIIb.7.9 and the space derivative exists in Equation IIIb.7.10. It then ap-

pears that if these equations are added together, the resulting equation will contain all the terms that we need for setting up the total derivatives. However, we add these by multiplying the first equation by an unknown factor λ and then add it to the second equation:

$$\left(\frac{\partial V}{\partial t} + \frac{\lambda c^2}{g} \frac{\partial V}{\partial x} \right) + \lambda \left(\frac{\partial H}{\partial t} + \frac{g}{\lambda} \frac{\partial H}{\partial x} \right) + f \frac{V|V|}{2D} = 0 \quad \text{IIIb.7.12}$$

By comparing Equation IIIb.7.12 with Equation IIIb.7.11, we note that if $dx/dt = \lambda c^2/g$, then the first bracket, for velocity, would have the form of the total derivative. Similarly, for the second bracket, we need to have $dx/dt = g/\lambda$. We then conclude that $\lambda c^2/g = g/\lambda$. From here, we find $\lambda = \pm g/c$. We also find that $dx/dt = \pm c$. Hence, the governing equations known as the *compatibility equations* become:

$$(C^-) \quad \frac{dV}{dt} - \frac{g}{c} \frac{dH}{dt} + f \frac{V|V|}{2D} = 0 \quad \text{For } \frac{dx}{dt} = -c \quad \text{IIIb.7.14}$$

$$(C^+) \quad \frac{dV}{dt} + \frac{g}{c} \frac{dH}{dt} + f \frac{V|V|}{2D} = 0 \quad \text{For } \frac{dx}{dt} = +c \quad \text{IIIb.7.13}$$

Let's consider the case of the reservoir and the instant closure of a valve, as shown in Figure IIIb.7.4. We first divide the pipe length into N equally spaced segments $\Delta x = L/N$. In this case $N = 4$ hence, there are five nodes. Initially liquid is steadily flowing in the pipe. At time t the valve is instantly closed. Closure of the valve results in the appearance of a pressure wave, having a magnitude of $\Delta H \equiv c\Delta V/g$, as predicted by Equation IIIb.7.1 for $V_1 \ll c$, traveling upstream. Our goal is to find V and H for all the nodes along the pipe. The time it takes the disturbance to reach node 4 is given by $\Delta t = \Delta x/c$. The information about velocity and head at node 4 is related to $dx/dt = -c$ hence, it is predicted by the C^- equation. The C^+ equation transmits information in the $+c$ direction. We therefore can find H_4 and V_4 from similar information at nodes 3 and 5, which are known at time t .

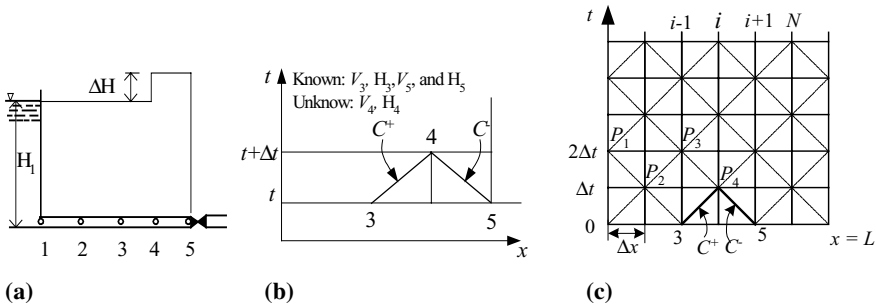
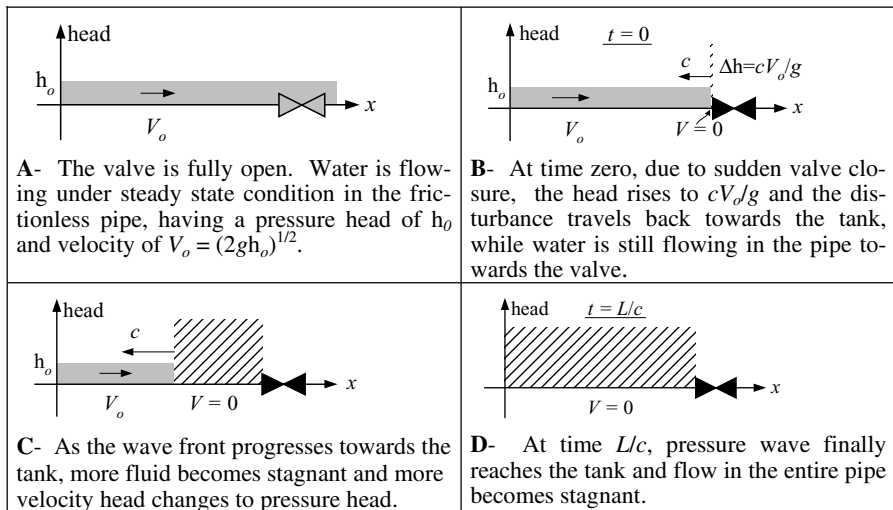
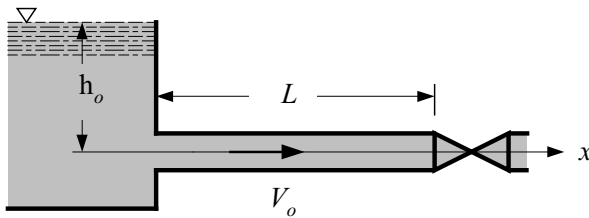


Figure IIIb.7.4. Graphical representation of C^- and C^+ solutions for an instant valve closure

Period of Pressure Pulse. Let's now find the time it takes for the wave to travel back and forth from the valve to the tank and returning to the valve. Consider the tank of Figure IIIb.7.5. Water is steadily flowing from the tank in the pipe. We then suddenly close the valve and examine the system response to the valve closure. To simplify the discussion, we make the following three assumptions:

- the connecting pipe is frictionless. This assumption eliminates the consideration of damping.
- water level in the tank is constant (pressure head is h_o from the pipe centerline) prior to the closure of the valve. This assumption implies steady flow of water in the pipe.
- the magnitude of the negative pressure pulse is such that the absolute pressure remains higher than water vapor pressure. This assumption eliminates the consideration of liquid flashing to vapor.

As shown in Figure IIIb.7.5, the period for the pressure pulse to complete a cycle, in a frictionless pipe of length L , is $4L/c$.



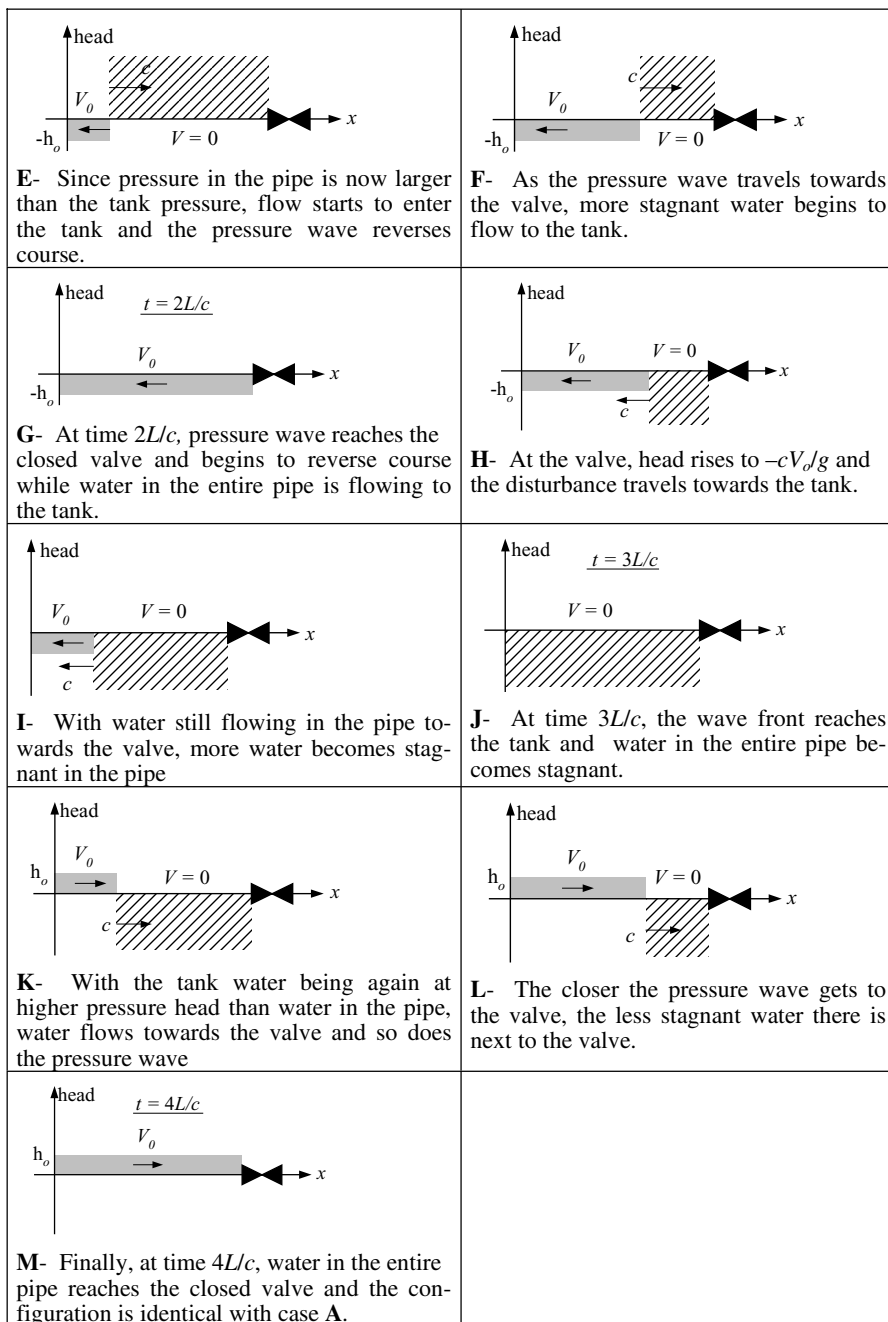


Figure IIIb.7.5. Head versus pipe length for flow in a frictionless pipe with sudden valve closure

QUESTIONS

- Does a boundary layer develop for the flow of inviscid fluids?
- Are the Navier-Stokes equations directly applicable to turbulent flow? What is an eddy?
- What is the molecular viscosity?
- What are the two types of stresses in the boundary layer over a flat plate?
- Is it fair to say that the shear stress profile in pipe flow remains linear regardless of the flow regime?
- What is the Hagen-Poiseuille flow?
- For the flow of a viscous fluids in a pipe, specify the location of the viscous sub-layer.
- What is the friction velocity? Does it exist in an ideal flow?
- What is the Darcy formula? Define the difference between Darcy-Weisbach and Hazen-Williams formulae.
- What is a valve flow coefficient?
- What is vena contracta? Define the discharge coefficient.
- What is the difference between a globe and a gate valve? For what applications is each valve used?
- Specify the difference between waterhammer, rigid column, and quasi-steady problems.
- What is an elastic analysis?
- Instant throttling of a valve disturbs the steady flow of a liquid in a pipe. At what velocity does this disturbance propagate upstream?
- What factors affect the speed that a disturbance would propagate in a pipe flow?
- Consider the flow of water in two identical piping systems except for one pipe being copper and the other plastic. In which system is the head rise higher following an instantaneous closure of a valve?

PROBLEMS

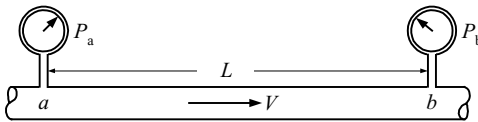
Sections 1 and 2

1. a) A viscous fluid at a specified flow rate enters a pipe of diameter d . The Reynolds number indicates that the flow is laminar. The same fluid at the same mass flow rate enters another pipe of diameter $d/2$ and flow becomes turbulent. What flow property is the reason for the change in the Reynolds number?
 b) Water at room temperature enters a pipe having I.D. = 4 in at a rate of 30 lbm/s. Determine the flow regime (i.e., whether the flow is laminar or turbulent).
2. The x -component of a flow velocity is given as $V(x, y, z, t)$. Use the definition of the time-averaged mean velocity $\bar{V}_x = \left(\oint_0^\theta V_x dt \right) / \theta$ to show that the time-averaged fluctuating velocity (V'_x) in the time domain of interest (θ) is zero.

3. Find the minimum diameter of a smooth tube to ensure the flow of water at an average velocity of 100 cm/s remains turbulent. Use $\nu_{\text{water}} = 1\text{E-}6 \text{ m}^2/\text{s}$. [Ans.: 4 mm].
4. Show that the Re number for the flow of fluids in pipes and tubes ($A = \pi D^2/4$) is given as $\text{Re} = 4 \dot{m} / (\pi \mu D)$. Find the maximum tube diameter to ensure the flow of water at a rate of 100 kg/h remains turbulent. Use $\mu_{\text{water}} = 1\text{E-}3 \text{ N}\cdot\text{s}/\text{m}^2$. [Ans.: 8.8 mm].
5. Air at 1 atm and 20 C flows through a smooth pipe. The centerline velocity and the pipe diameter are 6 m/s and 15 cm, respectively. Find a) the wall shear stress and b) the average velocity in the pipe.
6. Air flows over a sphere at 77 C. The diameter of the sphere is 10 cm. Find the air velocity that results in the Reynolds number to reach the transition from the laminar to turbulent flow if such transition takes place at a Reynolds number of about 250,000. [Ans.: 52.3 m/s].

Section 3

7. Water flows steadily in a horizontal and well-insulated pipe. Consider locations a and b along the length of the pipe and chose the correct answers for velocity (V), pressure (P), and temperature (T):



$$V_b < V_a, V_b = V_a, V_b > V_a, P_b < P_a, P_b = P_a, P_b > P_a, T_b < T_a, T_b = T_a, T_b > T_a$$

8. Plot and compare the friction factors obtained from the Colebrook, Haaland, Churchill, and McAdams correlations (Equations IIIb.3.5, IIIb.3.5-1, IIIb.3.5-2, and IIIb.3.6) as a function of Reynolds number for a smooth pipe.
9. Compare the frictional pressure drop, due to skin friction, of air and water for a smooth circular pipe of inside diameter D and length L . For this comparison, consider the mass flow rate of air to be equal to the mass flow rate of water. [Ans.: Using the McAdams' correlation for f we find, $\Delta P_a / \Delta P_w = (\rho_w / \rho_a)^{1.2}$].
10. A large water tank is connected to a small nozzle located 5 ft below the water surface in the tank (Figure a). The nozzle diameter at the exit is 1 in. Find the flow rate through the nozzle. We now attach a diffuser to the nozzle (Figure b). Will the flow rate a) increase, b) remain the same, or c) decrease?



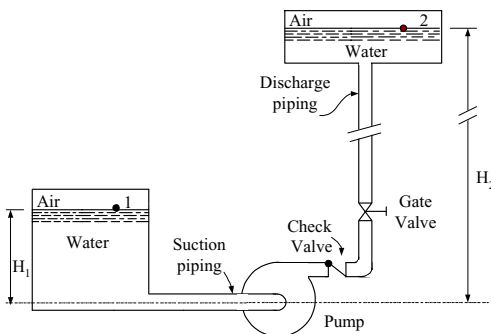
11. An incompressible fluid flows steadily in a pipe of diameter d . This pipe is connected to a pipe of larger diameter D by a sudden expansion. Use the continuity and the momentum equations to derive a relation for the sudden expansion loss coefficient, K_e in terms of the dimensionless diameter $\beta = d/D$.

12. A pump, having a pump head of h_{pump} delivers a liquid at a volumetric flow rate of \dot{V} . Show that the power consumed by the pump is $\dot{W} = (\rho g) \dot{V} h_{\text{pump}}$ where ρ is the liquid density. Find the pump head of a 10 hp pump, delivering water at a rate of 400 GPM. [Ans.: ≈ 100 ft].

13. Find the water flow rate at an average temperature of 15 C in the shell-side of a heat exchanger. Use $L = 7.62$ m, shell inside diameter $D = 0.914$ m, tube outside diameter $d = 3.81$ cm, number of tubes $N_{\text{tube}} = 200$, $\Delta P = 110.32$ kPa, and total loss coefficient $K = 35$. [Ans.: $0.492 \text{ m}^3/\text{min}$].

14. Consider the flow of water at 70 F and a rate of 2.5 GPM in a wrought iron pipe of $\frac{3}{4}$ in diameter pipe (I.D. = 0.824 in.) There are two 90-degree medium sweep elbows, a swing check valve, and a fully open angle valve. Find the pressure drop over 100 ft of this piping system. [Ans.: 0.83 psi].

15. A pump operating at 660 hp delivers water, from a large pressurized supply tank to a large pressurized reservoir, at a rate of $150 \text{ ft}^3/\text{s}$. Total length of the suction and the discharge piping is 1000 ft. Pressures in the supply and the reservoir tanks are 30 psig and 15 psig, respectively. These pressures are maintained throughout the pumping process. Water level heights with respect to the pump centerline are 15 ft and 50 ft, respectively. Find the pipe diameter. Ignore variations in water level in both tanks. [Ans.: $D_i \approx 3.5$ ft].



16. Consider the pumping system of Problem 15 but with both reservoirs at atmospheric pressure. Total length of the suction and the discharge piping, from the supply to the discharge reservoir is L , having an inside diameter of D . Our goal is to deliver the same flow rate to the same elevation but without using a pump. Find the elevation of the bottom of the supply reservoir to provide sufficient gravity head for this purpose. [Ans.: $H = c_1/c_2$ where $c_1 = (fL/D + \Sigma K)(\dot{V}^2/2gA^2)$ and $c_2 = 1 - (f\dot{V}^2/2gDA^2)$].

17. In problem 16 we investigated the effect of gravity head to provide the desired flow rate without using a pump. In this problem we want to investigate the effect of static pressure to provide the same flow rate without using a pump. For this purpose, we maintain the same configuration of the piping system of Problem 15. However, we maintain the discharge reservoir at atmospheric pressure. Find the required pressure in the supply reservoir to deliver the desired flow rate. [Ans. $P_1 - P_{\text{atm}} = (fL/D + \Sigma K)(\dot{V}^2/2gA^2)$].

18. A pump delivers water to a differential elevation of $H_B - H_A = 40$ ft. Diameter of the suction and discharge piping is 5 in and total length of the piping is 450 ft. Pressure in the supply tank is 10 psig and in the receiving reservoir 5 psig. Find the water flow rate. The head developed by the pump is 65 ft and $\Sigma K = 5$. [Ans.: 630 GPM].

19. A piping system is to be designed to deliver $0.5 \text{ m}^3/\text{s}$ water from a lake to a reservoir located at an elevation of 78 m from the pump centerline. The reservoir is at atmospheric pressure. The pump centerline is 1 m above the surface of the lake. The total pipe run from the lake to the reservoir is 420 m. Both intake and discharge pipings should have the same nominal pipe size of 12 in schedule 40. The list of the fittings and valves of the piping system includes one globe valve, two gate valves, two swing check valves, twelve elbows (90°), and two standard Ts. Find the required pump head and pumping power. Assume a pump efficiency of 70%. [Ans.: $\approx 1.2 \text{ MW}$].

20. Find the pressure drop between locations a and b for flow in a pipe using the following data:

Working fluid:	Water
Pipe:	Stainless steel, Schedule No. 120
Nominal pipe size (cm):	10
Flow rate (m^3/min):	2.271
Temperature (C):	38
Length (m):	45.72

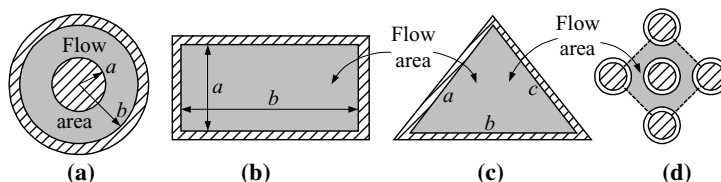
Solve for the following 3 cases: a) $Z_a = Z_b = 33.5$ m, b) $Z_a = Z_b + 15$ m, and c) $Z_a = Z_b + 46$ m.

21. Find the head loss over 15 ft of 1 in pipe carrying oil (S.G. = 0.86 and $\mu = 3 \text{ lbm/ft}\cdot\text{h}$) at 0.5 GPM. Is the flow laminar or turbulent? [Ans.: $h_f = 1.74 \text{ ft}$].

22. Head loss in 1000 ft of a 12 in cast-iron pipe, for water at 60 F, is 15 ft. Find the flow rate, $\varepsilon/D = 85\text{E-}4$. [Ans.: $V = 7.4$ ft/s and volumetric flow rate = 5.8 ft³/s].

23. Find the water flow rate at 15 C in a welded steel pipe of diameter 250 mm. Head loss is 5m/500m.

24. Find the hydraulic diameter for the conduits shown in Figures (a), (b), (c) and (d). For Figure (d), the rod pitch (the distance between the centerline of the neighboring rods) is 2 inch and the sides of the square do not constitute solid boundaries.



Section 4

25. Find pressure drop for the sudden contraction and sudden expansion as shown in the figure, $d_2 = d_3 = 1$ in and $D_1 = D_4 = 5$ in. a) Find pressure drop for the flow of water at 65 F, 14.7 psia and a rate of 5000 lbm/h. b) Find pressure drop for air at the same conditions as water.



26. In this problem our goal is to compare pressure drop for the flow of an incompressible fluid in a straight pipe to the pressure drop of a compressible fluid in the same pipe and under the same conditions. For the incompressible case, consider the flow of water at a rate of 5000 lbm/s in the pipe. Then compare the results with the flow of air. The pipe is smooth and has a diameter of 1 in and length of 20 ft. For both cases, fluid enters the pipe at 14.7 psia and 100 F and leaves the pipe at the same temperature.

27. Water enters a heated pipe at a rate of 5000 lbm/s, pressure of 14.7 psia and temperature of 100 F. The pipe is smooth and has a diameter and length of 1 in and 20 ft, respectively. Water temperature at the exit of the pipe is 200 F. Find the total pressure drop from A to B.



Figure for Problems 27, 28, 29, and 50

28. Water enters a pipe at a rate of 5000 lbm/s, pressure of 14.7 psia and temperature of 200 F. The pipe is smooth and has diameter and length of 1 in and 20 ft, respectively. A cold fluid flows over the pipe so that water temperature at exit is 100 F. Find total pressure drop from A to B.

29. Air enters a heated pipe at a rate of 2265 kg/s, pressure of 1 atm and temperature of 38 C. The pipe is smooth and has a diameter and length of 2.54 cm and 6 m, respectively. Air temperature at the exit of the pipe is 371 C. Find the total pressure drop from A to B.

30. Air enters a pipe at a rate of 5000 lbm/s, pressure of 14.7 psia and temperature of 700 F. The pipe is smooth and has a diameter and length of 1 in and 20 ft, respectively. A cold fluid flows over the pipe so that air temperature at the exit is 100 F. Find the total pressure drop from A to B.

31. Water at 60 F flows in a tube with $d = 1/2$ in and $L = 5$ ft. Find the friction pressure drop associated with the flow of water in the tube if water flows at a velocity of a) 0.5 ft/s and b) 5 ft/s.

32. Water at 100 F is pumped at a rate of 125 gpm to a reservoir 50 ft higher. The pipe length is 200 ft and the pipe inside diameter, I.D. = 2.067 in. The fittings include 3 standard 90-degree elbows, two 45-degree elbows, and an open gate valve. Pump efficiency is 70%. Find pump horsepower for a) $\epsilon = 0$ ft, b) $\epsilon = 0.0008$ ft.

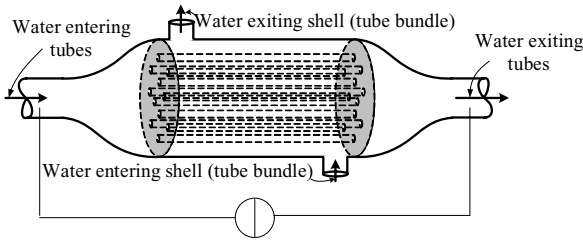
33. A shell-and-tube heat exchanger has 40 tubes of I.D. = 1 in and $L = 10$ ft. Hot stream enters the shell side and air at 14.7 psia and 200 F at a rate of 1000 lbm/h enters the tubes. Find the total tube-side pressure drop. The diameter of both inlet and outlet plenums is 0.75 ft. [Ans.: 2 lbf/ft²].

34. Fully developed air flows inside the $1/4$ in tubes of an air-cooled heat exchanger at a rate of 1.5 lbm/h. The conditions at the inlet of the tube are atmospheric pressure and 60 F. After being heated in the 2 ft long tube, air leaves at 780 F. Find the pressure drop in the heat exchanger.

35. Oil flows in a pipe at a rate of 4000 GPM. The head loss over a length of 10,000 ft of the pipe having a surface roughness of 0.0018 in, is 75 ft. Find the pipe diameter. Assume oil $\nu = 0.36$ ft²/h. [Ans. 16.85 in].

36. The number of tubes of a shell and tube heat exchanger N is given but we do not know the tube diameter, d . To determine the tube diameter, a pump is used to circulate flow inside the tubes. The flow rate and the pressure drop are then carefully measured. Use the specified data and find the tube inside diameter.

Data: $N = 40$, $L_{\text{tube}} = 3$ m, $\Delta P = 34.5$ kPa, $\dot{V} = 31.55$ lit/s, $T = 20$ C.
[Ans.: ≈ 1.6 cm].

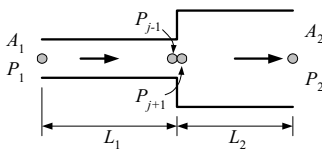


37. Use the definition of the flow coefficient C_v and substitute the appropriate equivalent units in the Darcy equation to show that the valve resistance or loss coefficient in terms of C_v is given as $K = 891d^4/C_v^2$ where the pipe diameter, d is in inches.

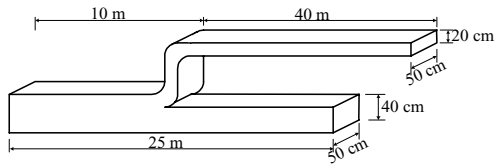
38. Find a) the loss coefficient of a valve installed on a 8 in schedule 40 steel pipe and b) the equivalent pipe length. The flow is fully turbulent and the valve has a discharge coefficient of 2000. [Ans.: 0.9 and 43 ft].

39. Find K , C_v , and L_e for a 3 in Schedule 40 fully open lift check valve. [Ans.: $L_e = 153$ ft].

40. An incompressible viscous fluid flows in a pipe of length L_1 and flow area A_1 , which is connected to a pipe of flow area A_2 and length L_2 as shown in the figure. Write the momentum equation for both sections of the pipe and add them together to obtain an equation for the combined piping system. Find the key assumption that you have to make to obtain the results listed in Table IIb.4.3-1. [Ans.: $P_{j-1} = P_{j+1}$ where P_{j-1} and P_{j+1} are pressures right before and right after the sudden enlargement, respectively].



Problem 40

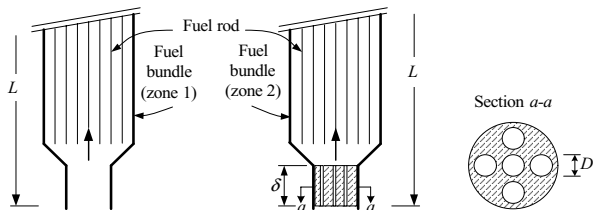


Problem 41

41. Air flows at 60 C in a duct as shown in the figure at a rate of $100 \text{ m}^3/\text{min}$. The duct divides into two branches, A and B, having lengths of 15 m and 40 m, respectively. The depth of the duct remains constant at 50 cm. Branch A has a width of 40 cm and branch B has a constant width of 20 cm. The discharge of both branches is into the same outlet. The 90 elbows are well rounded with each having a loss coefficient of 0.25. For the smooth surface of the ducts use a friction factor of 0.022 and find flow of air in each branch.

42. In a conceptual nuclear reactor design, we want to divide the core into two zones. Zone one contains N_1 bundles surrounded by zone two with N_2 bundles. The design criteria requires the total power generated in zone one to be equal to the total power produced in zone two. Additionally, the temperature rise in zone

one must also be equal to the temperature rise in zone two. To meet these design criteria, it is necessary to reduce the flow rate in zone two by adding orifice blocks to the inlet of the fuel bundles located in zone two. Each orifice block has five orifices. Use the given data to find the diameter of the orificing (D). Assume smooth surfaces and negligible pressure losses in all parts of the fuel assemblies other than the fuel bundle and the orifice block. Data: $\Delta P_{Core} = 0.745$ MPa, $\dot{m}_{Core} = 17.5$ E6 kg/h, $N_1 = 65$, $N_2 = 85$, $L = 4$ m, $\delta = 40$ cm, $\rho_{water} = 800$ kg/m³, $\mu_{water} = 2$ E-4 N·s/m², $K_c = 0.5$, $K_e = 1.0$, and all five channels in the orifice block have equal diameters. [Ans.: 2 cm].



43. A thin-plate orifice is used to measure water flow rate. The water temperature is 27 C and a mass flow rate of 50 lit/s is measured by the orifice. The pipe diameter is 26 cm and the orifice diameter is 7 cm. Find the non-recoverable pressure drop. [Ans.: 21 m, $C_d = 0.6$, $K = 2.5$].

44. We want to measure the flow rate of water at 20 C by a thin plate orifice. The pipe diameter carrying the water is 20 cm and the thin-plate orifice diameter is 5 cm. A pressure drop of 70 kPa is measured between the taps. Find the flow rate and the throat velocity. [Ans.: 23 lit/s, 11.6 m/s].

45. Obtaining the characteristics of an equivalent pipe (L_E , A_E , V_E , D_E , and K_E) to represent a compound piping (i.e. pipes connected in series or in parallel) depends on the imposed constraint. In this problem, you are asked to develop a table similar to Table IIIb.4.3.

a) First, for several pipes connected in series, find the characteristics of an equivalent pipe using the following constraints $L_E = \sum L_i$, $(\Delta P_{skin})_E = (\sum \Delta P_{skin})_i$, and $(\Delta P_{fittings-valves})_E = (\sum \Delta P_{fitting-valves})_i$.

b) Next, consider several pipes connected in parallel. Find the characteristics of an equivalent pipe using the following constraints $A_E = \sum A_i$, $(\Delta P_{skin})_E = (\Delta P_{skin})_i$, and $(\Delta P_{fittings-valves})_E = (\sum \Delta P_{fitting-valves})_i$.

[Ans.:

Pipes in series
V: $V_E = \sum V_i$

L: $L_E = \sum L_i$

A_{flow} : V_E/L_E

Pipes in parallel

$V_E = \sum V_i$

$L_E = \sum \dot{m}_i L_i / \sum \dot{m}_i$

$A = \sum A_i$

$$\begin{array}{lll}
 I: & I_E = L_E A_E & I_E = \sum_i \dot{m}_i L_i / \sum_i \dot{m}_i L_i \\
 K: & K_E = A_E^2 \sum_i (K_i / A_i^2) & K_E = A_E^2 \left(\sum_i \left(A_i / \sqrt{K_i} \right) \right)^{-2}
 \end{array}$$

46. For part b of Problem 35, find the flow rate in a parallel flow branch. Assume all branches consist of smooth pipes and use the friction factor as given by Equation IIIb.3.6.

$$[\text{Ans. } \dot{V}_i = \left[\left(\frac{D_i}{D_1} \right)^{4.8/1.8} \left(\frac{L_1}{L_i} \right)^{1/1.8} \right] \left[\sum_N \left[\left(\frac{D_i}{D_1} \right)^{4.8/1.8} \left(\frac{L_1}{L_i} \right)^{1/1.8} \right] \right]^{-1} \dot{V}].$$

47. Water enters a system of parallel piping at a rate of 500 GPM. The pipes length and inside diameter are $L_1 = 10$ ft, $D_1 = 2.5$ in, $L_2 = 20$ ft, $D_2 = 3.0$ in, $L_3 = 5$ ft, $D_3 = 2$ in, and $L_4 = 25$ ft, $D_4 = 3.5$ in. All pipes are smooth and loss coefficients are negligible. Find the diameter of the equivalent pipe. [Ans.: 6.06 in].

48. The riser of a spray system consists of 3 pipe segments connected in series. The data for these three pipes are shown below. If we want to represent this system with only one pipe, what diameter should we choose? The flow rate, density, and viscosity are 1250 GPM, 62.4 lbm/ft³, and 0.7E-3, respectively.

Pipe No.	L (ft)	D (in)	K (-)
1	110.00	8.00	15.0
2	120.00	7.50	1.50
3	100.00	7.00	3.00

[Ans.:

Flow In Serial Pipes

Pipe No.	L (ft)	D (in)	A (ft ²)	V (ft/s)	K (-)	\dot{V} GPM	$Re \times 1E-6$	f (-)	ΔP (psi)
1	110	8.00	0.349	7.98	15.0	1250	0.474	0.01348	7.38
2	120	7.50	0.307	9.07	1.50	1250	0.506	0.01331	2.25
3	100	7.00	0.267	10.43	3.00	1250	0.542	0.01312	3.84

Data For The Equivalent Pipe Representing The Compound Piping System

L (ft)	D (in)	A (ft ²)	V (ft/s)	K (-)	\dot{V} (GPM)	I (ft ^{0.1})	ΔP (psi)
331.87	7.34	0.307	9.07	17.08	1250.00	1080.4	13.50].

49. Water flows at a rate of 200 GPM into a piping system connected in series. Length, diameter, and loss coefficient of each pipe are given below. For $\rho = 62.4$ lbm/ft³ and $\mu = 0.7E-3$ lbm ft/s find total pressure drop and the diameter of an equivalent pipe representing this system.

Pipe No.	L (ft)	D (in)	K (-)
1	100.00	5.00	50.00
2	80.00	4.50	45.00
3	70.00	4.00	65.00
4	120.00	3.50	55.00
5	90.00	3.00	15.00

[Ans.:
Flow In Serial Pipes

Pipe No.	L (ft)	D (in)	A (ft ²)	V (ft/s)	K (-)	\dot{V} GPM	$Re \times 1E-6$	f (-)	ΔP (psi)
1	100	5.00	0.136	3.27	50.00	200	0.121	0.01770	3.90
2	80	4.50	0.110	4.05	45.00	200	0.135	0.01732	5.33
3	70	4.00	0.087	5.12	65.00	200	0.152	0.01692	12.03
4	120	3.50	0.067	6.65	55.00	200	0.173	0.01648	18.49
5	90	3.00	0.049	9.09	15.00	200	0.202	0.01598	11.51

Data For The Equivalent Pipe Representing The Compound Piping System

L (ft)	D (in)	A (ft ²)	V (ft/s)	K (-)	\dot{V} (GPM)	I (ft ^{0.1})
ΔP (psi)						
491.48	3.06	0.083	5.37	233.02	200.00	5159.06 51.3].

50. Water flows at a rate of 5000 GPM into a piping system connected in parallel. Length, diameter, and loss coefficient of each branch are given below. For $\rho = 62.4 \text{ lbm/ft}^3$ and $\nu = 9.305E-6 \text{ ft}^2/\text{s}$ find total pressure drop and the length and diameter of an equivalent pipe representing this system.

Pipe No.	L (ft)	D (in)	K (-)
1	1000.0	10.00	150.00
2	1500.0	11.00	100.00
3	500.00	8.00	10.00
4	2000.0	9.00	50.00
5	900.00	7.00	5.00

[Ans.:
Flow In Parallel Pipes

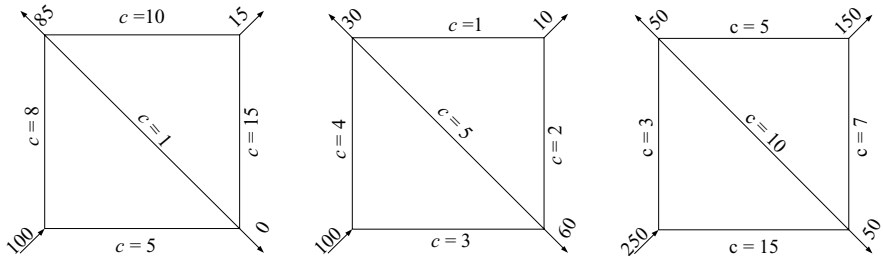
Pipe No.	L (ft)	D (in)	A (ft ²)	V (ft/s)	K (-)	\dot{V} GPM	$Re \times 1E-6$	f (-)	ΔP (psi)
1	1000	10.00	0.545	5.20	150.00	1272.69	0.47	0.01353	3.39
2	1500	11.00	0.660	4.61	100.00	1365.92	0.45	0.01359	3.39
3	500	8.00	0.349	7.04	10.00	1102.76	0.50	0.01331	3.39
4	2000	9.50	0.442	3.51	50.00	696.99	0.28	0.01494	3.39
5	900	7.00	0.267	4.68	5.00	561.64	0.29	0.01484	3.39

Date of the Equivalent Pipe Representing the Compound Piping System

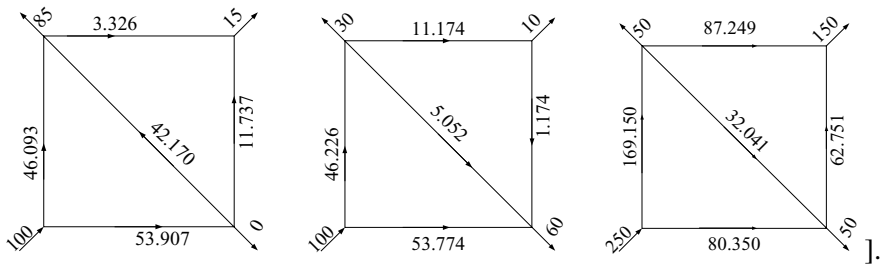
L (ft)	D (in)	A (ft ²)	V (ft/s)	K (-)	\dot{V} (GPM)	I (ft ⁰⁻¹)	ΔP (psi)
1154.48	10.51	2.263	4.922	31.56	5000	510.05	3.39].

Section 5

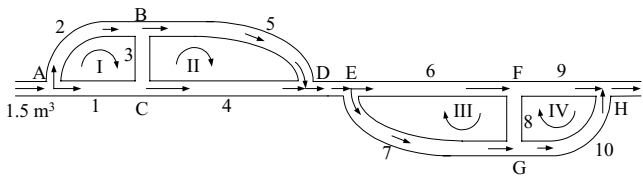
51. Find flow distribution in each network by the Hardy Cross method. Assume $n = 2$. Try the same cases for $n = 1.8$.



[Ans.:



52. Find the absolute value of the flow rate and the direction of the flow in branches BC and FG.



Pipe	1	2	3	4	5	6	7	8	9	10
L (m)	585	253.8	223.2	9.77	18.1	1269	565.3	201.3	19.6	6.8
D (m)	0.65	0.55	0.45	0.35	0.30	0.55	0.50	0.40	0.35	0.30

[Ans.: 0.0 and 0.007 m³/s from G to F].

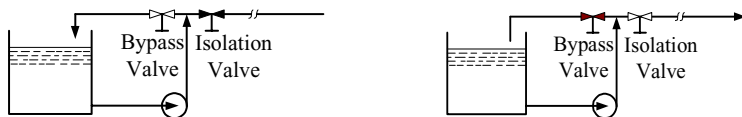
53. Write a computer program based on the Hardy Cross method for determination of flow distribution in piping networks. First, start with simple cases and use the methods outlined in Chapter IIIb.5 before extending to more general cases.

Section 6

54. Derive the time to drain the tank of Example IIIb.6.2 from the observation that $t = V_t/V_o A_o$. [Hint: Use an average value for $V_o = \sqrt{2gh_1}/2$ and the fact that $V_t = h_t A_t$.]

55. An emergency water tank is pressurized with nitrogen to 1.0 MPa. The tank has a diameter of 2 m. Height of water in the tank is 15 m. The tank is located above a reactor and is connected to the reactor by a pipe having a diameter of 0.2 m. At time zero the reactor pressure drops to 0.2 MPa. Find the maximum flow rate delivered by the tank to the reactor. Treat water as an ideal fluid (incompressible and inviscid). [Ans.: 1367 kg/s].

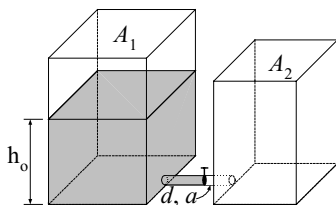
56. A pump is operating in recirculation mode. At time zero, we close the bypass valve and simultaneously open the isolation valve to fill the initially drained supply line. Use the data to find the time it takes to fill the supply line. Data: $\dot{V}_{\text{pump}} = 200 \text{ GPM}$, $L_{\text{Supply Line}} = 1200 \text{ ft}$, $D_{\text{Supply Line}} = 3 \text{ in.}$ [Ans.: $\sim 132 \text{ s}$].



57. A water tank, in the shape of a right circular cylinder, has an inside diameter D . The tank, being open to the atmosphere is initially filled with water up to a height of h_o , measured from the drain centerline. The drain has an inside diameter d and a discharge coefficient of C_d . We now open the drain to drain the tank by gravity. Show that the time to drain the tank is obtained from $t = \sqrt{h_o} / [C_d (d/D)^2 \sqrt{g/2}]$.

58. A water tank is at atmospheric pressure. Initially, the tank water level is at 20 ft from the drain centerline. We now open the drain and assume there are no frictional losses. If $A_e/A_t = 0.015$, find the time to drain the tank.

59. Consider two rectangular tanks having constant flow areas of A_1 and A_2 . The tanks are connected at the bottom by a frictionless pipe of diameter d . The first tank is filled with water up to an elevation h_o from the connecting pipe. We now open the isolation valve. a) Show that the time for levels to equalize is given by:



$$\theta = \frac{2A_1 A_2 \sqrt{h_o}}{a \sqrt{2g} (A_1 + A_2) C_d}$$

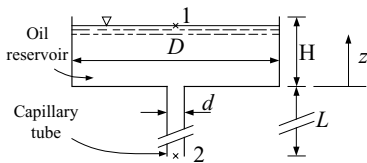
b) Find the time in second if $h_0 = 3$ m, $d = 5$ cm, $A_1 = 3$ m², $A_2 = 2$ m², and $C_d = 0.61$. [Ans. 7 m, 21 s].

60. The initially closed valve in Figure IIIb.6.1(b) suddenly opens. Find the time it takes velocity to reach 99% of its steady-state value. Assume that fluid is inviscid and $L = 30$ ft, $h_0 = 7$ ft, $D = 1$ in. [Ans.: 7.5 s].

61. The initially closed valve in Figure IIIb.6.1(b) suddenly opens. Find the flow velocity 5 seconds after the valve is opened. Data: $L = 1000$ ft, $h_0 = 50$ ft, $V_0 = 10$ ft/s. [Ans.: $\lambda = 3.1$ s. and $V = 6.7$ ft/s].

62. A tank in the shape of a right circular cylinder (Figure IIIb.6.3.) contains water and is pressurized to 50 psia. Water level from the drain centerline is 15 ft. The tank height is 20 ft, tank diameter is 10 ft and the drain diameter is 1 in. Find the time to completely drain the tank. The water tank is fully insulated. Do you expect some water flashing to steam when level becomes near zero? What happens if we use an exceedingly small hole for the drain? [Ans.: 200 min]

63. A capillary tube viscometer, as shown in the figure, is a reservoir containing oil, connected to a capillary tube (d on the order of 1 mm). Find the time to drain oil from the reservoir.



$$[\text{Ans.: } \theta = \frac{32\mu L}{\rho g d^2} \left(\frac{D}{d}\right)^2 \ln\left(1 + \frac{H}{L}\right)].$$

64. Oil ($\nu = 1\text{E-}4$ m²/s), enters an open tank at a steady rate of 2 m³/min and leaves through a 25 m long pipe. The Tank has a constant cross sectional area of 3 m² and the pipe has an inside diameter of 15 cm. At steady state conditions, the exit pressure is 2 m of oil. While the inlet flow remains constant, we increase the exit pressure instantaneously to 3 m of oil. Find the effect on oil level and exit flow rate.

65. Oil ($\nu = 1\text{E-}4$ m²/s), enters an open tank at a steady rate of 2 m³/min and leaves through a 25 m long pipe. The Tank has a constant cross sectional area of 3 m² and the pipe has an inside diameter of 15 cm. At steady state conditions, the exit pressure is 2 m of oil. While the inlet flow remains constant, we increase the exit pressure linearly to 4 m of oil in 5 minutes. Find the tank oil level at 5 minutes, i.e., when $h_{Co} = 4$ meters.

66. A gas tank of volume V contains pressurized gas at pressure P_o and temperature T . Flow rate of gas into and out of the tank under steady-state conditions is \dot{m}_i . Pressure at point C, Figure IIIb.6.10(a), jumps to: $P_{C1} = P_{Co} + \Delta P$. Find the

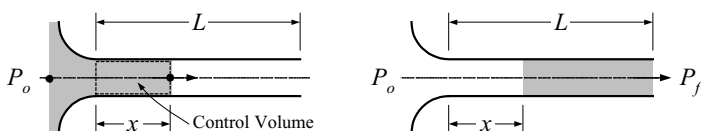
tank pressure versus time. Tank is not insulated hence process is isothermal. Assume laminar flow in the discharge pipe.

[Ans.: $P(t) = (P_{Co} - P_{C1})e^{-t/(KV/RT)} + P_o - (P_{Co} - P_{C1})$].

67. A tank having a volume of 30 m^3 contains air at 400 kPa. We intend to charge this tank through a feed line having a diameter of 4 cm and a length of 30 m. Pressurized air at 900 kPa and 15 C enters the feed line. Find the time it takes for the tank pressure to reach 900 kPa.

68. A tank having a volume of 40 m^3 contains air at 500 kPa. We intend to charge this tank through a feed line having a diameter of 4 cm and a length of 30 m. Pressurized air at 900 kPa and 15 C enters the feed line. Find the tank pressure after 2 minutes. Plot the tank pressure and the inlet mass flow rate versus time.

69. Consider two identical pipes. One pipe is to be filled with water by suddenly raising the liquid pressure upstream of the pipe to P_o . The other pipe is already filled with water. We would like to expel the water from the pipe by suddenly increasing the upstream pressure of the gas to P_o . Find the time to fill and to drain each pipe and compare the results. The atmospheric pressure for both cases is shown by P_f . Pipe area is A .



[Hint: For the filling the pipe example, write the momentum equation for the control volume shown in the figure as $\Sigma F = d(mV)/dt + \Delta(\text{momentum flux})$. Since no mass is leaving, momentum flux at the exit is zero and momentum flux at the inlet is the flow rate into the control volume. The momentum equation then becomes:

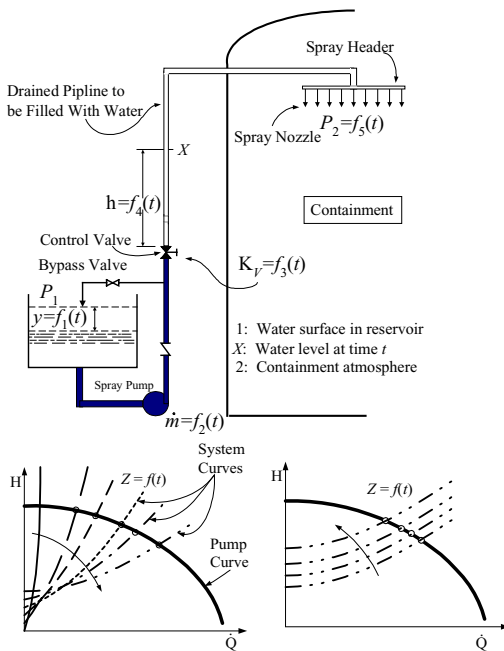
$$(P_o - P_f)A - F_{\text{friction}} = d(mV)/dt + (0 - \dot{m}_i V)$$

Relate \dot{m}_i to m from the continuity equation and substitute for m from ρAx and for V from $V = dx/dt$].

70. Shown in the figure is a normally closed control valve known as the containment spray isolation valve, being generally a motor operated globe valve. In case of a hypothetical accident that leads to containment pressurization, a spray signal is sent to turn on the pump and open the control valve. The piping upstream of the spray valve is filled with water whereas the piping downstream of the control valve is drained. When the signal is sent to activate the spray system, the control valve begins to open, water starts to flow in the empty piping until it eventually reaches the spray header located at an elevation of about 200 ft. Water is then sprayed into the containment atmosphere at a desired droplet diameter by 100 spray nozzles attached to the header ring. You are to determine the time it takes to

fill the pipeline and to calculate the flow rate out of the nozzles once the header is filled.

[Hint: This can be calculated by dividing the volume of the drained pipe by the volumetric flow rate. Since, flow rate is changing with time this should be done in a discretized manner. To simplify the analysis, you may assume that the pump is operating at rated conditions and flow is bypassed to the reservoir. Then a signal is sent to the control valve to open. This signal simultaneously closes the bypass valve. The first plot shows the system curve when the control valve is opening and the second plot shows the system curve when the control valve is fully opened].

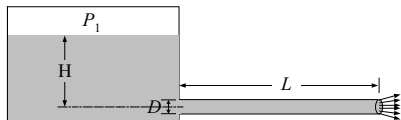


71. A spherical bubble of nitrogen, having an initial diameter of 5 mm is released at a depth of 10 m in a pool of water. Assume the bubble instantly reaches its terminal velocity. Find the time it takes for the bubble to reach the water surface. Plot d , V , and h as a function of time and comment on the validity of the results.

72. A pipe equipped with a nozzle is used to deliver water to the wheel of a hydraulic turbine. The pipe has a diameter of 35 cm and a length of 1 km. The nozzle has a diameter of 10 cm and provides a velocity head of 35 m when turbine operates at steady state condition. Now, consider a case where the fully closed turbine stop valve is suddenly opened. Find the time it takes the wheel of the turbine to reach 97% of its full speed.

Section 7

73. A large tank is connected to a pipe of diameter D and length L . Water is flowing steadily in the pipe, which is discharged to the atmosphere. A blanket of gas is used to maintain pressure in the tank at $P_1 = P_0$. At time zero, we increase the gas pressure so that $P_1(t) = f(t)$. Use the assumptions consistent with the rigid column theory and find the governing differential equation for the flow rate in the pipe. Plot flow rate versus time for the following data. By adding water, the tank water level is constantly maintained at H . Data: $P_0 = 20$ psia, $H = 10$ ft, $L = 1$ ft, $D = 1$ in, $f(t) = (2P_0/5)t + P_0$ for $t \leq 5$ s and $f(t) = 3P_0$ for $t > 5$ s. Assume smooth pipe.



74. Water flows at 60 F in a 12-inch Schedule 40 pipe ($D = 11.938$ in. and $\delta = 0.406$ in.). Find the head rise due to the instantaneous closure of a valve a) for steel pipe and b) for a PVC pipe having the same dimensions as the steel pipe. $\rho_{\text{water}} = 62.37$ lbm/ft³, $(E_v)_{\text{water}} = 3.11\text{E}5$ psi. $\dot{V} = 2442$ GPM.

75. Consider flow of water in a frictionless pipe at 7 ft/s. An isolation valve is instantaneously closed. Find the resulting pressure head just upstream of the valve. [Ans.: $4890 \times 7/32.2 = 1,063$ ft]

76. Water at 60 F is flowing in an 18-inch Schedule 80 steel pipe. Find the wave speed for the system. $\rho_{\text{water}} = 62.37$ lbm/ft³, $(E_v)_{\text{water}} = 3.11 \times 10^5$ psi.

IIIc. Compressible Flow

1. Steady Internal Compressible Viscous Flow

In compressible fluids, changes in the fluid density due to the variation in pressure and temperature may become significant and the treatment of the flow discussed in the previous sections should be applied here with added vigilance. Due to the complexity of the subject, flow of compressible fluids is generally divided into three categories. These include, flow of gas, flow of two-phase mixture (such as steam and water), and two-phase flow mixed with non-condensable gases. The flow path may include a pipe, a Bernoulli obstruction meter (nozzle, thin-plate orifice, and venturi), valves, fittings, and pipe breaks. Compressible fluids may encounter a phenomenon known as choked or critical flow. This phenomenon imposes an added constraint on the internal flow of compressible fluids and must be considered in all of the above categories. Failure to do so results in gross errors in the related analysis.

In this section, we study only the flow of gases in pipes, Bernoulli obstruction meters, and pipe breaks. In all these cases, the compressible fluid is considered to behave as an ideal gas undergoing such processes as isothermal, adiabatic, or isentropic. In general, flow of gases in pipelines is associated with heat transfer and friction. We therefore begin the analysis of steady, one-dimensional, internal flow of compressible fluids in a variable area conduit with friction and heat transfer. We then reduce the general formula to obtain the formulation for some specific processes such as isothermal and adiabatic.

1.1. Compressible Viscous Flow in Conduits

To derive the general formula for one-dimensional flow of ideal gases with friction and heat transfer, we consider the one-dimensional flow of a compressible fluid in the variable area conduit of Figure IIIc.1.1. At any location x from the entrance to the conduit, the flow field is defined by four parameters $P(x)$, $T(x)$, $V(x)$, and $\rho(x)$. To determine these parameters, we use continuity, energy, and momentum equations as well as the equation of state written for differential control volume $A(x)dx$. Using the mass, momentum, and energy at steady state conditions entering the control volume at x , we find the mass, momentum and energy at $x + dx$ by Taylor's series expansion. The continuity equation becomes $d(\rho VA) = 0$. The energy equation for steady state, no shaft work, negligible changes in potential energy, and no internal heat generation becomes:

$$dq = c_p dT + VdV \quad \text{IIIc.1.1}$$

where the first term on the right side represents the change in enthalpy from x to $x + dx$. The net momentum flux at steady state is equal to the summation of forces acting on the control volume:

$$-dP - 4(dx/D)\tau_w = \rho VdV \quad \text{IIIc.1.2}$$

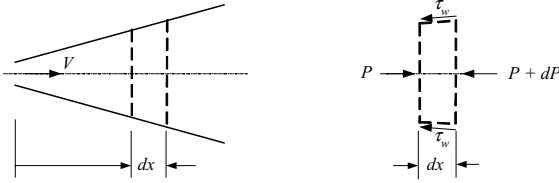


Figure IIIc.1.1. Flow of ideal gas in a variable area conduit with heat transfer and friction

To simplify the momentum equation, we define:

$$dF = (4/\rho)(dx/D)\tau_w \quad \text{IIIc.1.3}$$

where dF is the frictional head loss per unit mass. Substituting for τ_w from Equation IIIc.1.3 into Equation IIIc.1.2, we obtain;

$$-dP - \rho dF = \rho V dV \quad \text{IIIc.1.4}$$

The last equation to use is the equation of state for an ideal gas:

$$d(P/R\rho T) = 0 \quad \text{IIIc.1.5}$$

The formulation of the problem ends here. To find the four parameters P , T , V and ρ , we solve these four equations simultaneously. First, we carry out the differentials in the continuity equation and in the equation of state. We then divide the result by the argument. For example, for the continuity equation we have:

$$d(\rho VA) = VAd\rho + \rho AdV + V\rho dA = 0 \quad \text{IIIc.1.6}$$

Dividing by ρVA , we obtain:

$$\frac{d\rho}{\rho} + \frac{dV}{V} + \frac{dA}{A} = 0 \quad \text{IIIc.1.7}$$

Similarly, differentiating the equation of state and dividing through by $P = R\rho T$ yields:

$$-\frac{dP}{P} + \frac{d\rho}{\rho} + \frac{dT}{T} = 0 \quad \text{IIIc.1.8}$$

For the energy equation, we divide Equation IIIc.1.1 by $c_p T$:

$$\frac{dq}{c_p T} = \frac{dT}{T} + \frac{V^2 dV(\gamma-1)}{V\gamma RT} \quad \text{IIIc.1.9}$$

and for the momentum equation, we divide Equation IIIc.1.4 by P :

$$-\frac{dP}{P} - \frac{\rho dF}{P} = \frac{\mathcal{W}^2}{\gamma \mathcal{R}T} \frac{dV}{V} \quad \text{IIIc.1.10}$$

Note that in the energy and momentum equations we also made use of $c_p = \gamma \mathcal{R}/(\gamma-1)$ where $\gamma = c_p/c_v$. We now manipulate the definition of the Mach number $\text{Ma} = V/c$ by substituting for the speed of sound in the medium $c^2 = \gamma \mathcal{R}T$ to obtain $\text{Ma}^2 = V^2/(\gamma \mathcal{R}T)$. Taking the derivative and dividing by the argument yields:

$$\frac{d\text{Ma}^2}{\text{Ma}^2} = \frac{TdV^2 - (V^2 dT/T^2)}{V^2/T} = \frac{dV^2}{V^2} - \frac{dT}{T} = \frac{2dV}{V} - \frac{dT}{T} \quad \text{IIIc.1.11}$$

which simplifies to:

$$\frac{dV}{V} = \frac{1}{2} \left(\frac{d\text{Ma}^2}{\text{Ma}^2} + \frac{dT}{T} \right)$$

Substituting for dV/V in the energy and momentum equations, we obtain a system of four algebraic equations for four unknowns dP , dT , dV , and $d\rho$. Solving by the method of elimination and substitution, yields:

$$\frac{dP}{P} = \frac{-\gamma \text{Ma}^2}{1 - \text{Ma}^2} \left(\frac{dq}{c_p T} \right) + \frac{\gamma \text{Ma}^2}{1 - \text{Ma}^2} \left(\frac{dA}{A} \right) - \frac{(\gamma-1)\text{Ma}^2 + 1}{1 - \text{Ma}^2} \left(\frac{dF}{\mathcal{R}T} \right) \quad \text{IIIc.1.12}$$

$$\frac{dT}{T} = \frac{1 - \gamma \text{Ma}^2}{1 - \text{Ma}^2} \left(\frac{dq}{c_p T} \right) + \frac{(\gamma-1)\text{Ma}^2}{1 - \text{Ma}^2} \left(\frac{dA}{A} \right) - \frac{(\gamma-1)\text{Ma}^2}{1 - \text{Ma}^2} \left(\frac{dF}{\mathcal{R}T} \right) \quad \text{IIIc.1.13}$$

$$\frac{dV}{V} = \frac{1}{1 - \text{Ma}^2} \left(\frac{dq}{c_p T} \right) + \frac{1}{1 - \text{Ma}^2} \left(\frac{dA}{A} \right) + \frac{1}{1 - \text{Ma}^2} \left(\frac{dF}{\mathcal{R}T} \right) \quad \text{IIIc.1.14}$$

$$\frac{d\rho}{\rho} = \frac{1}{1 - \text{Ma}^2} \left(\frac{dq}{c_p T} \right) + \frac{\text{Ma}^2}{1 - \text{Ma}^2} \left(\frac{dA}{A} \right) - \frac{1}{1 - \text{Ma}^2} \left(\frac{dF}{\mathcal{R}T} \right) \quad \text{IIIc.1.15}$$

where in these equations, q , A , and F are known functions. Upon the integration of Equations IIIc.1.12 through IIIc.1.15, we find pressure P , temperature T , velocity V , and fluid density ρ , respectively. Next, we derive analytical solutions for the three important processes: isothermal, adiabatic, and isentropic.

1.2. Isothermal Process For Compressible Flow

To analyze the flow of compressible fluids in an isothermal process, we may use the general formula obtained above and apply the isotherm constraint or derive the formulation directly. Both methods are described here.

A. Pressure Drop for Flow of Compressible Fluids in Pipelines, Reduction from General Formula

Consider the flow of an ideal gas in a pipe with diameter D . If flow properties are known at the inlet (i), we want to find flow properties at the outlet (e) for $T_i = T_e$. We try this method only for pressure. Here, $dA = 0$ (pipe with constant flow area) and $dT = 0$ (isothermal process). Equation IIIc.1.12 reduces to:

$$\frac{dP}{P} = \frac{\gamma \text{Ma}^2}{1 - \text{Ma}^2} \left(\frac{dq}{c_p T} \right) - \frac{(\gamma - 1) \text{Ma}^2 + 1}{1 - \text{Ma}^2} \left(\frac{dF}{RT} \right)$$

and Equation IIIc.1.13 yields:

$$\frac{1 - \gamma \text{Ma}^2}{1 - \text{Ma}^2} \left(\frac{dq}{c_p T} \right) - \frac{(\gamma - 1) \text{Ma}^2}{1 - \text{Ma}^2} \left(\frac{dF}{RT} \right) = 0$$

We find $(dq/c_p T)$ from the second equation and substitute in the first. After simplification we find:

$$\frac{dP}{P} = \frac{1}{\gamma \text{Ma}^2 - 1} \left(\frac{dF}{RT} \right)$$

If we substitute for $\text{Ma}^2 = V^2/\gamma RT$, for $dF = (4/\rho)(dx/D)\tau_w$, and for $\tau_w = (f/4)(\rho V^2/2)$, we get

$$\frac{dP}{dx} = \frac{Pf}{2D} \left(1 - \frac{P}{\rho V^2} \right)^{-1} \quad \text{IIIc.1.16}$$

Equation IIIc.1.16 can be integrated to obtain ΔP . We will further study Equation IIIc.1.16 in Section 2.

B. Pressure Drop for Flow of Compressible Fluids in Pipelines, Direct Derivation

Here we derive the equation for pressure drop between two points i and e directly from the conservation equations. These points are located at a distance L from each other on a horizontal pipe having diameter D . For this section of pipe, assuming steady flow, Equation IIIa.3.28 simplifies to:

$$\frac{1}{g} \frac{dP}{\rho} + \frac{VdV}{g} + dh_f = 0$$

where dh_s is also dropped since there is no shaft work between the points. Substituting for the frictional head loss from Equation IIIb.3.4 for a differential length dx given as:

$$dh_f = f \frac{dx}{D} \frac{V^2}{2g}$$

we obtain:

$$\frac{dP}{\rho} + VdV + f \frac{dx}{D} \frac{V^2}{2} = 0 \quad \text{IIIc.1.17}$$

To be able to differentiate Equation IIIc.1.17, we eliminate both density and velocity. To accomplish this, we first divide through by V^2 , knowing that $V \neq 0$:

$$\frac{dP}{\rho V^2} + \frac{dV}{V} + f \frac{dx}{2D} = 0 \quad \text{IIIc.1.18}$$

To eliminate ρ and V , we need two additional equations. First we use the continuity equation. The density and velocity at any point along the flow path can be related to the given density and velocity at the production source for steady flow:

$$\rho VA = \rho_i V_i A = \dot{m} = GA$$

The second equation is the ideal gas equation of state, $P/\rho = RT$ from which, $1/\rho = RT/P$. The first term in Equation IIIc.1.18 can be manipulated, noting that for $T_i = T$ we have $P_i/\rho_i = P/\rho$, to get:

$$\frac{dP}{\rho V^2} = \frac{dP}{\rho_i V_i} \frac{1}{V} = \left(\frac{RT_i dP}{P_i V_i} \right) \left(\frac{\rho}{\rho_i} \frac{1}{V_i} \right) = \left(\frac{RT_i dP}{P_i V_i} \right) \frac{P}{P_i V_i}$$

Similarly, we manipulate the second term of Equation IIIc.1.18, using $V = G/\rho = GRT/P$, to get:

$$\left(\frac{1}{V} \right) dV = \left(\frac{P}{GRT} \right) \left(- \frac{GRT dP}{P^2} \right) = - \frac{dP}{P}$$

Equation IIIc.1.18 then simplifies to:

$$- \frac{dP}{P} + RT_i \frac{PdP}{(P_i V_i)^2} + f \frac{dx}{2D} = 0$$

This equation can now be integrated for flow from one point to another:

$$- \int_{P_i}^{P_e} \frac{dP}{P} + \frac{RT_i}{(P_i V_i)^2} \int_{P_i}^{P_e} P dP + \int_{x_i}^{x_e} f \frac{dx}{2D} = 0$$

where x_i and x_e are points where pressure is P_i and P_e , respectively and $x_e - x_i = L$. Integrating yields:

$$-\ln\left(\frac{P_e}{P_i}\right)^2 - \frac{RT}{V_i^2} \left[1 - \left(\frac{P_e}{P_i}\right)^2 \right] + f \frac{L}{D} = 0 \quad \text{IIIc.1.19}$$

where the subscript for temperature is dropped, as $T_e = T_i$. Equation IIIc.1.19 may alternatively be written as:

$$c_1 \xi - \ln \xi - (c_1 - c_2) = 0 \quad \text{IIIc.1.19}$$

where the dummy variable ξ and coefficients c_1 and c_2 are given as:

$$\begin{aligned} \xi &= (P_e/P_i)^2 \\ c_1 &= RT / V_i^2 \\ c_2 &= fL/D \end{aligned}$$

In this integration, we assumed the friction factor remains constant between the two points. This is a valid assumption as the friction factor for smooth pipes is a function of the Reynolds number (Equation IIIb.3.3), which is in turn a function of viscosity ($\text{Re} = \rho V D / \mu$). For ideal gases, viscosity is only a function of temperature, which was assumed to remain constant (isothermal flow).

Equation IIIc.1.19 is a non-linear algebraic equation, which should be solved by iteration. As the first guess, we may ignore $\ln \xi$, compared with the absolute value of the other two terms, and find ξ from:

$$\xi = \left(\frac{P_e}{P_i} \right)^2 = 1 - f \frac{L}{D} \frac{V_i^2}{RT} = 1 - f \frac{L}{D} \gamma \text{Ma}_i^2 \quad \text{IIIc.1.20}$$

Example IIIc.1.1. Air flows isothermally in a smooth, 1 ft (0.3 m) diameter, 1500 ft (457 m) long horizontal pipe at a rate of 7500 CFM (212.4 m³/min). Air enters the pipe at 600 psia (4.1 MPa) and 300 F (149 C). Find the pressure drop in the pipe.

Solution: At given P_i and T_i , air viscosity is $\nu_i = 1.27\text{E-}5 \text{ ft}^2/\text{s}$. We now perform the following steps:

$$A = 3.14 D^2 / 4 = 3.14 / 4 = 0.785 \text{ ft}^2 \text{ (0.073 m}^2\text{)}$$

$$V_1 = \dot{V} / A = 7500 / (0.785 \times 60) = 159.15 \text{ ft/s (48.5 m/s)}$$

$$\text{Re}_i = V_i D / \nu_i = 159.15 \times 1 / 1.27\text{E-}5 = 1.25\text{E}7;$$

$$f_i = 0.184 / \text{Re}_i^{0.2} = 0.184 / (5.88\text{E}6)^{0.2} = 0.007. \text{ Since } f_i = f_e, \text{ we drop the subscript.}$$

$$c_1 = RT / V_i^2 = (1545 / 28.97)(300 + 460) / (159.15^2 / 32.2) = 51.53,$$

$$c_2 = fL / D = 0.007 \times 1500 / 1 = 10.5. \text{ Therefore, Equation IIIc.1.19 becomes:}$$

$$51.53 \xi - \ln(\xi) - 41.03 = 0$$

By iteration, we find; $\xi \approx 0.792$. Thus, $(P_e/P_i) = (0.792)^{1/2} = 0.8899$
 $P_e = 0.8899 \times (600) = 534$ psia and pressure drop is $\Delta P = P_i - P_e = 600 - 534 = 66$ psi (0.455 MPa)
 If estimated from Equation IIIc.1.20, ξ is found as:
 $\xi = 1 - [0.007 \times (1500/1.0) \times (159.15^2/32.2)] / [(1545/28.97) \times (300 + 460)] = 0.796$.

Caveat: Pressure drop associated with the isothermal flow of compressible viscous fluids results in a decrease in the fluid density, which in turn results in an increase in the flow velocity to preserve the specified steady state mass flow rate. Equation IIIc.1.19 is valid only if flow remains subsonic. As is discussed in Section 2, flow becomes sonic when $dP/dL \rightarrow \infty$. We then take the derivative of Equation IIIc.1.19:

$$\frac{dP_e}{dL} = \frac{f/D}{2(RT/V_i^2)(P_e/P_i^2) - (2/P_i)} \quad \text{IIIc.1.21}$$

Setting the denominator of Equation IIIc.1.21 equal to zero, we find the condition for sonic velocity as:

$$\xi = \left(\frac{P_e}{P_i} \right)^2 = \frac{V_i^2}{RT} \quad \text{IIIc.1.22}$$

Alternatively, we may express Equation IIIc.1.22 in terms of the Ma number by noting that:

$$\frac{P_e}{P_i} = \frac{\rho_e/(RT)}{\rho_i/(RT)} = \frac{\dot{m}/(V_e A)}{\dot{m}/(V_i A)} = \frac{V_i}{V_e} = \frac{\text{Ma}_i}{\text{Ma}_e} \quad \text{IIIc.1.23}$$

where we also took advantage of $c^2 = \gamma RT$ and $\text{Ma} = V/c$. Substituting for the pressure ratio in terms of the Mach number ratio in Equation IIIc.1.22, we find the limiting Mach number:

$$\text{Ma}^* = \sqrt{1/\gamma} \quad \text{IIIc.1.24}$$

Thus Equation IIIc.1.19 is valid as long as the Ma number at the pipe exit remains less than $(1/\gamma)^{1/2}$.

Equation IIIc.1.19 may also be expressed in terms of the Ma number by using the relation between the pressure ratio and the Mach number ratio, as given by Equation IIIc.1.23:

$$\left(\frac{\text{Ma}_i}{\text{Ma}_e} \right)^2 = 1 + \gamma \text{Ma}_i^2 \left[\ln \left(\frac{\text{Ma}_i}{\text{Ma}_e} \right)^2 - f \frac{L}{D} \right] \quad \text{IIIc.1.25}$$

Example IIIc.1.2. Methane enters a pipeline at a rate of 50 kg/s. The pipe is 1200 m long, having an inside diameter of 0.5 m. Find the pipe length over which Equation IIIc.1.19 is applicable.

Data: $P_i = 0.5$ MPa, $T_i = 27$ C, $f = 0.015$, $M_{\text{CH}_4} = 16$, and $\gamma_{\text{CH}_4} = 1.3$.

Solution: We first calculate the Mach number at the pipe inlet:

$$A = \pi D^2/4 = \pi(0.5)^2/4 = 0.196 \text{ m}^2$$

$$\rho_i = P_i/RT = 500/[(8.314/16) \times (27 + 273)] = 3.207 \text{ kg/m}^3$$

$$V_i = \dot{m}/(\rho_i \times A) = 50/[3.207 \times 0.196] \approx 79.55 \text{ m/s}$$

$$c = \sqrt{\gamma RT} = \sqrt{1.3 \times (8314/16) \times (27 + 273)} = 450 \text{ m/s}$$

$$\text{Ma}_i = 79.55/450 = 0.177$$

The limiting Mach number is then found as $\text{Ma}^* = (1/1.3)^{0.5} = 0.877$. Thus, $\xi = (\text{Ma}_i/\text{Ma}^*)^2 = 0.078$

From Equation IIIc.1.25 we find:

$$L = \frac{D}{f} \left[\ln \xi - \left(\frac{\xi - 1}{\gamma \text{Ma}_i^2} \right) \right] = \frac{1.5}{0.015} \left[\ln(0.078) - \left(\frac{0.078 - 1}{1.3 \times 0.177^2} \right) \right] = 2008 \text{ m}$$

Example IIIc.1.3. Express the relation for pressure drop for incompressible flow in terms of the Ma number.

Solution: We substitute for $\rho = P/(RT)$ and $V^2 = c^2 \text{Ma}^2 = (\gamma RT) \text{Ma}^2$ in Equation IIIb.3.7, $P_i - P_e = (fL/D)\rho V^2/2$:

$$\frac{P_e}{P_i} = 1 - f \frac{L}{2D} \gamma \text{Ma}^2 \quad \text{IIIc.1.26}$$

$$\Delta P = f \frac{L}{2D} \gamma \text{Ma}^2$$

1.3. Adiabatic Process for Compressible Fluids

Consider the same condition as discussed before. However, this time $T_e \neq T_i$ but the pipe is insulated so that $dq = 0$. Note that if there is also not any friction, the problem can be easily solved using isentropic relations. However, we are considering adiabatic flow of gases with friction. To derive the formulation, we note that for adiabatic ($dq = 0$) and constant area channel ($dA = 0$), Equations IIIc.1.13 and IIIc.1.14 reduce to:

$$\frac{dT}{T} = - \frac{(\gamma - 1) \text{Ma}^2}{1 - \text{Ma}^2} \left(\frac{dF}{RT} \right) \quad \text{IIIc.1.27}$$

$$\frac{dV}{V} = \frac{1}{1 - \text{Ma}^2} \left(\frac{dF}{RT} \right) \quad \text{IIIc.1.28}$$

Dividing Equation IIIc.1.27 by Equation IIIc.1.28 and substituting from Equation IIIc.1.28 yields:

$$\frac{dT}{T} = -(\gamma - 1)\text{Ma}^2 \left(\frac{dV}{V} \right) = -(\gamma - 1)\text{Ma}^2 \left(\frac{dV}{V} \right) = \frac{-(\gamma - 1)\text{Ma}^2}{1 - \text{Ma}^2} \left(\frac{dF}{RT} \right) \quad \text{IIIc.1.29}$$

Next, we substitute for dT/T from Equation IIIc.1.29 and for dV/V from Equation IIIc.1.28 into Equation IIIc.1.11. To deal with the dF/RT term, we find dF from Equation IIIc.1.3 and V^2 from the definition of the Ma number $dF/RT = f(dx/2D)V^2/RT = f(dx/2D)\text{Ma}^2 \gamma RT/RT = f(dx/2D)\text{Ma}^2 \gamma$ to obtain:

$$\frac{d\text{Ma}^2}{\text{Ma}^2} = \frac{\gamma \text{Ma}^2}{1 - \text{Ma}^2} \left[1 + \frac{(\gamma - 1)}{2} \text{Ma}^2 \right] f \frac{dx}{D} \quad \text{IIIc.1.30}$$

To make interesting conclusions from Equation IIIc.1.30, we also simplify Equation IIIc.1.12 and like before substitute for $dF = (4/\rho)(dx/D)\tau_w$, $\tau_w = (f/4)(\rho V^2/2)$, and $\rho = P/RT$ to obtain:

$$\frac{dP}{dx} = -\frac{1 + (\gamma - 1)\text{Ma}^2}{1 - \text{Ma}^2} f \frac{1}{D} \frac{\rho V^2}{2} \quad \text{IIIc.1.31}$$

Subsonic flow, $\text{Ma} < 1$ ($d\text{Ma} > 0$). The pressure drop resulted from subsonic flow of compressible viscous fluids in constant area conduits results in an increase in the flow temperature, which combined with decrease in pressure ($dP/dx < 0$) causes density to decrease ($\rho = P/RT$) and velocity ($V = \dot{m}/\rho A$) and Ma number to increase. Thus, friction causes the subsonic flow to accelerate.

Supersonic flow, $\text{Ma} > 1$ ($d\text{Ma} < 0$). The supersonic flow of compressible viscous fluids in constant area conduits results in a decrease in Ma number and velocity, requiring flow density and consequently pressure ($dP/dx > 0$) to increase. Thus, supersonic flow decelerates due to friction. We further deal with this topic in Section 2. But for now, let's integrate Equation IIIc.1.30 from the pipe entrance to the pipe exit:

$$\int_{\text{Ma}_i}^{\text{Ma}_e} \frac{[2 + (\gamma - 1)\text{Ma}^2]}{2\gamma \text{Ma}^4 (1 - \text{Ma}^2)} d\text{Ma}^2 = \frac{1 - \text{Ma}_i^2}{\gamma \text{Ma}_i^2} + \frac{\gamma + 1}{2\gamma} \ln \frac{(\gamma + 1)\text{Ma}_i^2}{2 \left[1 + \frac{\gamma - 1}{2} \text{Ma}_i^2 \right]} = \int_0^L f \frac{dx}{D} = \frac{\bar{f}}{D} L \quad \text{IIIc.1.32}$$

where in Equation IIIc.1.32, we have used an average value for the friction factor and specified $\text{Ma}_e = 1$. This results in the maximum pipe length beyond which flow becomes sonic and supersonic. Since a supersonic flow decelerates, the tran-

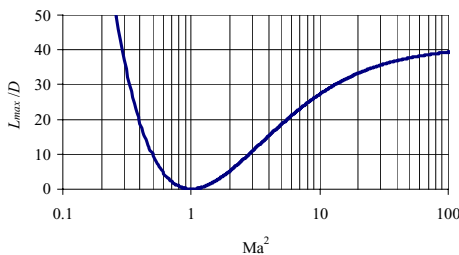
sition to subsonic is followed by a *shock wave*. The phenomenon is similar to a *hydraulic jump* for the flow of incompressible fluids in open channels where a fast and shallow flow becomes a slow and deep flow. As a result, Equation IIIc.1.32 gives the maximum pipe length for a continuous flow.

Example IIIc.1.4. Find the L_{\max}/D versus Ma^2 for air. Use an average friction factor of 0.02.

Solution: We use Equation IIIc.1.32, which for air ($\gamma = 1.4$) becomes:

$$\frac{L_{\max}}{D} = \frac{1}{1.4f} \left(\frac{1 - \text{Ma}_i^2}{\text{Ma}_i^2} + 1.2 \ln \frac{1.2 \text{Ma}_i^2}{1 + 0.2 \text{Ma}_i^2} \right)$$

The plot shows that as Ma^2 approaches ∞ , L_{\max}/D asymptotically approaches about 40.



1.4. Isentropic Process of Compressible Fluids

Under the isentropic process, we discuss two topics. First, we discuss the calculation of pumping power in compressors. Second, we consider compressible flow through Bernoulli obstruction meters. The latter topic is especially important in the measurement of compressible flow.

A. Calculation of Compressor Pumping Power

Pumping compressible fluids is an example of noticeable change in fluid density during a process. Let's consider a pipeline in which an ideal gas enters at pressure P_1 (Figure IIIc.1.2). Due to the frictional losses, pressure drops downstream to P_2 . Our goal is to find the pumping power required for increasing the pressure of a compressible fluid from pressure P_2 to pressure P_3 . In a special case, $P_3 = P_1$. For the compressor as the control volume, we use Equation IIIa.3.28 while ignoring frictional pressure drop and the change in elevation from the inlet to the outlet of the compressor:

$$\frac{1}{g} \frac{dP}{\rho} + \frac{VdV}{g} + dh_s = 0$$

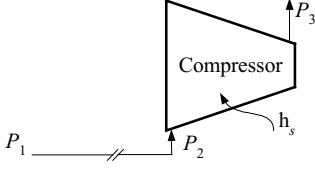


Figure IIIc.1.2. Isentropic compression of an ideal gas

Using subscript 2 for the inlet to the compressor and subscript 3 at the exit of the compressor, the rate of work delivered to the compressor shaft, in terms of shaft head is found by integrating the above equation:

$$h_s = - \left[\frac{V_3^2 - V_2^2}{2g} + \frac{1}{g} \int_2^3 \frac{dP}{\rho} \right] \quad \text{IIIc.1.33}$$

If heat transfer in the compressor is neglected, the compression process between points 2 and 3 becomes adiabatic. Since we also assumed no frictional losses in the compressor, we can write:

$$\frac{P_2}{\rho_2^\gamma} = \frac{P}{\rho^\gamma}$$

Therefore, $1/\rho = (1/\rho_2)(P_2/P)^{1/\gamma}$ and upon substitution, the second term on the right side of Equation IIIc.1.33 becomes:

$$\frac{1}{\rho_2 g} P_2^{\frac{1}{\gamma}} \int_2^3 P^{1/\gamma} dP = \frac{\gamma}{\gamma-1} \frac{1}{g} \frac{P_2}{\rho_2} \left[\left(\frac{P_3}{P_2} \right)^{\frac{\gamma-1}{\gamma}} - 1 \right] = \frac{\gamma}{\gamma-1} \frac{1}{g} R T_2 \left[\left(\frac{P_3}{P_2} \right)^{\frac{\gamma-1}{\gamma}} - 1 \right]$$

The first term in the right side of Equation IIIc.1.33 can also be rearranged to obtain:

$$\frac{V_3^2 - V_2^2}{2g} = \frac{V_3^2}{2g} \left(1 - \frac{V_2^2}{V_3^2} \right) = \frac{V_3^2}{2g} \left(1 - \frac{\rho_3^2}{\rho_2^2} \right) = \frac{V_1^2}{2g} \left(1 - \frac{P_3^2}{P_2^2} \right)$$

Note that conditions at point 3 must be identical to conditions at point 1. Substituting for the first and the second terms in the right side of Equation IIIc.1.33, the required shaft head is calculated as:

$$h_s = - \left[\frac{V_1^2}{2g} (1 - r^2) + \frac{\gamma}{\gamma-1} \frac{1}{g} R T_2 (r^{\frac{\gamma-1}{\gamma}} - 1) \right] \quad \text{IIIc.1.34}$$

where the compression ratio $r = P_3/P_2$. Finally, the pumping power is determined from:

$$\dot{W}_s = \dot{m}gh_s \quad \text{IIIc.1.35}$$

where \dot{m} is the mass flow rate of the compressible fluid through the compressor.

Example IIIc.1.5. Transferring natural gas by pipelines from the production source to a distant destination is accomplished by providing multiple pumping stations connected in series and located at equal distances along the path between the production source and the receiving reservoir, as shown in Figure IIIc.1.3.

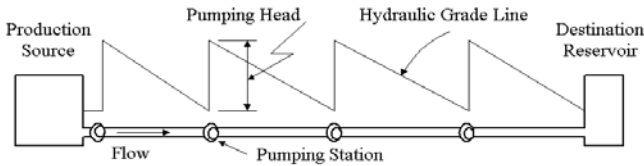


Figure IIIc.1.3. Cross-country pipeline for delivery of natural gas

In each pumping station, gas is compressed and pressurized to compensate for the frictional losses in the pipeline until the next pumping station. The pressurization and the cooling of inter-coolers bring pressure and temperature to the values where gas first enters the pipeline from the production source.

- Find the pressure drop in the pipeline between the successive pumping stations and
- find the pumping power for each pumping station for given pipe diameter, flow rate (\dot{m}), pressure (P_1), and temperature (T_1) at the production source.

Data: Natural gas is compressed to $P_1 = 120$ psia (0.827 MPa), then cooled to the ambient temperature of $T_1 = 80$ F (26.67 C), as shown in Figure IIIc.1.4. Gas then enters the pipeline at a velocity of 45 ft/s (13.72 m/s). The pipe has an inside diameter of 2.25 ft (68.6 cm). The pumping stations are located every 15 miles (24.14 km). Natural gas (considered as methane) molecular weight is 16, its kinematic viscosity at 80 F (26.67 C) is about $2.62\text{E-}5$ ft²/s ($2.434\text{E-}6$ m²/s), and $\gamma = c_p/c_v = 1.3$.

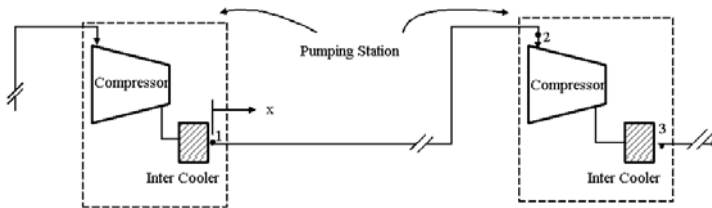


Figure IIIc.1.4. Pumping stations for pressure recovery

Solution: a) We assume ideal gas behavior for natural gas, uniform properties at each cross section, and negligible changes in elevation. We find frictional pressure drop at 15 mile intervals from Equation IIIc.1.19, assuming isothermal flow in the pipe:

$Re = VD/\nu = 45 \times 2.25/2.62E-5 = 3.864E6$. Hence, $f = 0.184/Re^{0.2} = 0.00886$ (for smooth pipe)

$$c_1 = RT_1/V_1^2 = (1545/16) \times (460 + 80)/(45 \times 45/32.2) = 829.15$$

$$c_2 = fL/D = 0.00886 \times (15 \times 5280)/2.25 = 311.87$$

$$829.15\xi - \ln \xi - 517.28 = 0$$

By iteration (or simply ignoring $\ln \xi$) we find $\xi \approx 0.6233$. Hence, $P_2/P_1 = \xi^{1/2} = (0.6233)^{1/2} = 0.7895$. Therefore, $P_2 = 0.7895(120) = 94.74$ psia and $\Delta P = 120 - 94.74 = 25.26$ psi (0.174 MPa).

b) The pumping power is needed to compensate for the unrecoverable pressure loss over the 15 miles of piping between successive pumping stations. Pumping power is given by Equation IIIc.1.34 and IIIc.1.35:

$$\dot{W}_s = -\dot{m} \left[\frac{V_1^2}{2} (1 - r^2) + \frac{\gamma}{\gamma - 1} RT_2 (r^{\frac{\gamma-1}{\gamma}} - 1) \right]$$

where

$$A = \pi D^2/4 = 3.14 \times (2.25)^2/4 = 3.976 \text{ ft}^2 \text{ (0.369)}$$

$$R = R_u/M = 1545/16 = 96.56 \text{ ft}\cdot\text{lbf/lbmole}\cdot\text{R} \text{ (0.519 kJ/kmol}\cdot\text{K)}$$

$$\rho_1 = P_1/RT_1 = 144 \times 120/[96.56(460 + 80)] = 0.331 \text{ lbm/ft}^3 \text{ (5.3 kg/m}^3\text{)}$$

$$\dot{m} = \rho_1 V_1 A = 0.331 \times 45 \times 3.976 = 59.22 \text{ lbm/s (26.86 kg/s)}$$

$$r = P_3/P_2 = P_1/P_2 = 120/94.74 = 1.267$$

$$\dot{W} = -59.22 \left[\frac{45^2}{2 \times 32.2} (1 - 1.267^2) + \frac{1.3}{0.3} 96.56(460 + 80)(1.267^{0.3/1.3} - 1) \right] = -7.5E5 \text{ ft}\cdot\text{lbf/s (-1 MW)}$$

B. Flow Rate Measurement of Compressible Fluids

In measuring flow rate of compressible fluids with Bernoulli obstruction meters, we must take into account the compressibility effect, due to the noticeable change in the density of the compressible fluid through such devices. The pressure drop associated with the flow of compressible fluids, especially through a thin-plate orifice, causes the flow to expand adiabatically and density to decrease downstream of the throat. Our goal is to find an expression similar to Equation IIb.4.4, that was derived for the mass flow rate of incompressible fluids. Recall that in the derivation of Equation IIb.4.4, which was based on Equation IIIa.3.33, we used the Bernoulli equation. Here, however, due to the change in the fluid density, we cannot use the Bernoulli equation. We then start with the energy equation. To begin the derivation, consider flow through the venturi of Figure IIb.4.3 where

the extent of the control volume is from inlet (1) through the throat (2). We make the following simplifying assumptions: the fluid behaves as an ideal gas, the flow velocity is less than the speed of sound in the fluid, and the process is steady as well as isentropic. The energy equation between stages 1 and 2, $h_1 + V_1^2/2 = h_2 + V_2^2/2$, can be written as:

$$\left(\frac{1}{\rho_1^2 A_1^2} - \frac{1}{\rho_2^2 A_2^2} \right) \dot{m}^2 = 2c_p(T_2 - T_1)$$

where we substituted for velocities from the continuity equation, $\dot{m} = \rho_1 V_1 A_1 = \rho_2 V_2 A_2$. Also substituting for temperature in terms of pressure from the isentropic relation IIa.4.3 (i.e., $\rho_1/\rho_2 = (P_1/P_2)^{1/\gamma}$), for c_p from $c_p = R\gamma/(\gamma-1)$, and for density from $\rho = P/RT$ and after some algebraic manipulation, we find:

$$\dot{m} = A_2 \sqrt{\left(\frac{2\gamma}{\gamma-1} \right) P_1 \rho_1 \left[\frac{r^{2/\gamma} (1 - r^{(\gamma-1)/\gamma})}{1 - \beta^4 r^{2/\gamma}} \right]}$$

where A_2 is the flow area at the throat, $\beta = D_2/D_1$, and $r = P_2/P_1$. Using the same argument as in Section IIIb.4.2 for incompressible flow measurement by Bernoulli obstruction meters, the above relation becomes:

$$\dot{m} = C_d A_2 \sqrt{\left(\frac{2\gamma}{\gamma-1} \right) P_1 \rho_1 \left[\frac{r^{2/\gamma} (1 - r^{(\gamma-1)/\gamma})}{1 - \beta^4 r^{2/\gamma}} \right]} \quad \text{IIIc.1.36}$$

Comparing Equation IIIc.1.36 with relation IIIb.4.4, we seek a means to express the flow rate of both compressible and incompressible fluids with an identical relation. To do so, we define a factor Y (referred to as the *adiabatic expansion factor* or *net expansion factor*):

$$Y = \frac{\text{mass flow rate of a compressible flow}}{\text{mass flow rate of an incompressible flow}}$$

Substituting for the numerator from Equation IIIc.1.36 and for the denominator from Equation IIIb.4.4 yields:

$$\dot{m} = \alpha Y A_2 \sqrt{2\rho_1 \Delta P} \quad \text{IIIc.1.37}$$

where A_2 is the venturi throat diameter, $\alpha = C_d / \sqrt{1 - \beta^4}$, $\beta = D_2/D_1$, $\Delta P = P_1 - P_2$, and Y is given as:

$$Y_{\text{Venturi}} = \sqrt{\frac{\gamma}{\gamma-1} \frac{(r^{2/\gamma} - r^{(\gamma+1)/\gamma})}{1 - \beta^4 r^{2/\gamma}} \frac{1 - \beta^4}{1 - r}} \quad \text{IIIc.1.38}$$

Knowing the type of gas (γ) and the inlet pressure and temperature, we know the gas density (ρ). If we also know the throat pressure (P_2 and alternatively $r = P_2/P_1$) and the venturi size (β), we can calculate Y from Equation IIIc.1.38 and then find mass flow rate from Equation IIIc.1.37. Since the calculation of Y is laborious, values of Y have been provided in tables and figures for various gases (γ) and venturi sizes β . The expansion coefficient as calculated above applies to nozzles and venturies. ASME has provided the following correlation for a thin-plate orifice:

$$Y_{\text{Orifice}} = 1 - (0.41 + 0.35\beta^4)[(1-r)/\gamma] \quad \text{IIIc.1.39}$$

Values for the adiabatic expansion factor as given by Equations IIIc.1.38 and IIIc.1.39 are plotted in Figure IIIc.1.5. Note that the differential pressure taps are located one-pipe diameter upstream and a half-pipe diameter downstream of the inlet face of the nozzle and the orifice plate ($D:D/2$).

Example IIIc.1.6. A venturi meter is used to measure the flow of carbon dioxide. The inlet and the throat diameters are 5 (12.7 cm) and 2 (5.08 cm) inches, respectively. Inlet pressure and temperature are 150 psia (1.034 MPa) and 200 F (93.33 C). Pressure at the throat of the venturi is 145 psia (1 MPa). Carbon dioxide kinematic viscosity is $1.32\text{E-}5 \text{ ft}^2/\text{s}$ ($1.23\text{E-}6 \text{ m}^2/\text{s}$) and for carbon dioxide, $\gamma = 1.3$. Find the mass flow rate.

Solution: To use Equation IIIc.1.37, we need to find A , ρ , r , and Y :

$$A_2 = \pi D_2^2 / 4 = \pi (2/12)^2 / 4 = 0.0218 \text{ ft}^2 \text{ (2 cm}^2\text{)}$$

$$\rho_1 = P_1 / RT_1 = 150 \times 144 / [(1545 / 44) \times (460 + 200)] = 0.932 \text{ lbm/ft}^3 \text{ (14.93 kg/m}^3\text{)}$$

Having $\gamma = 1.3$, $\beta = 2/5 = 0.4$ and $r = P_2/P_1 = 145/150 = 0.967$, we find Y :

$$Y_{\text{Venturi}} = \sqrt{\frac{1.3 \left(0.967^{2/1.3} - 0.967^{2.3/1.3} \right) 1 - 0.4^4}{0.3 \frac{1 - 0.4^4}{1 - 0.967} \times 0.967^{2/1.3}}} = 0.98$$

The discharge coefficient is found from Equation IIb.4.7 as:

$$C_d = 0.9858 - 0.196\beta^{4.5} = 0.983$$

The flow coefficient becomes $\alpha = C_d / \sqrt{1 - \beta^4} = 0.983 / (1 - 0.4^4)^{0.5} = 0.995$. Finally, mass flow rate from Equation IIIc.1.37 is found as:

$$\dot{m} = \alpha Y A_2 \sqrt{2 \rho_1 \Delta P} = 0.995 \times 0.98 \times 0.0218 \sqrt{2 \times 32.2 \times 0.932 \times (5 \times 144)} = 4.419 \text{ lbm/s} \text{ (2 kg/s)}$$

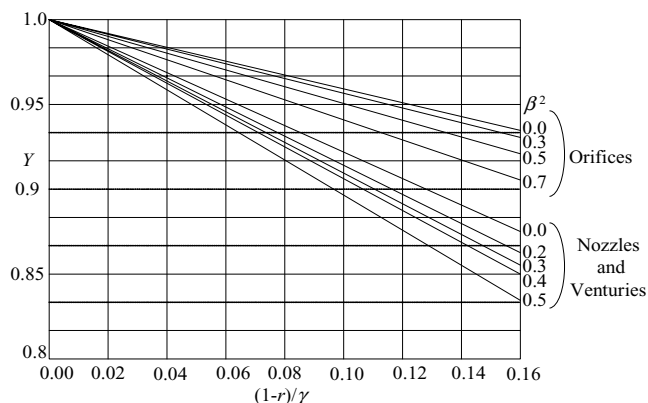


Figure IIIc.1.5. Values of the net expansion factor Y for Bernoulli obstruction meters

2. The Phenomenon of Choked or Critical Flow

In the flow of fluids, any downstream perturbation travels upstream at the speed of sound in that fluid. We now consider two tanks connected by a pipe as shown in Figure IIIc.2.1. The tanks are filled with a compressible fluid and are initially at the same thermodynamic condition. Hence, there is no flow of fluid from the left tank to the right tank and vice versa. If we maintain pressure in the left tank and begin to reduce pressure in the right tank, a flow rate will be established. The more we reduce pressure in the right tank the higher the rate of flow will be between the two tanks. As was discussed in Section IIIb.7, this is due to the fact that reduction in the downstream pressure, being a disturbance, is carried upstream faster than the flow velocity. Once this reduction in pressure is “felt” upstream, the rate of flow increases.

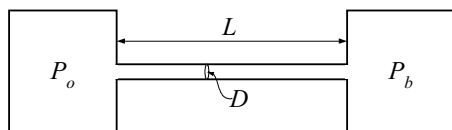


Figure IIIc.2.1. Tanks filled with compressible fluid and connected by a pipe.

There is of course a limit to the increase in the flow rate. This limit is reached when the flow velocity itself reaches the speed of sound. In this case, the speed of the disturbance to travel upstream is the same as the flow velocity. Hence, the perturbation cannot be “communicated” upstream. As a result, the flow rate remains the same regardless of further reduction in the downstream pressure. Flow rate under such circumstance is *choked*. The choked or *critical* flow rate is, therefore, only a function of the upstream pressure in the flow field. For ideal gases,

we can derive an analytical relation for the choked flow rate. For non-ideal fluids, we have to resort to hybrid solutions, being a blend of theory and experimental data in the form of a correlation. In this chapter, we are concerned only with the choked flow of single-phase compressible fluids such as ideal gases, saturated, and superheated steam. Choked flow for two-phase (water and steam) conditions is discussed in Chapter Va.

Assuming the process is isothermal, we examine Equation IIIc.1.16. As shown in Figure IIIc.2.2(a), the ratio of $P/\rho V^2$ determines the slope, dP/dx . For $P/\rho V^2 > 1$, the slope is negative. This is the region on the curve between points A and B. For $P/\rho V^2 < 1$, the slope is positive. This is the region between points B and C. For $P/\rho V^2 = 1$, which occurs at point B, the tangent to the curve is vertical. The condition corresponding to point B is called the critical condition and the pressure at point B, the critical pressure. Let's now examine Equation IIIc.1.19. Figure IIIc.2.1(b) shows the plot of P_b/P_o versus fL/D for various Mach numbers. The straight line represents the incompressible flow behavior from Equation IIIc.1.20.

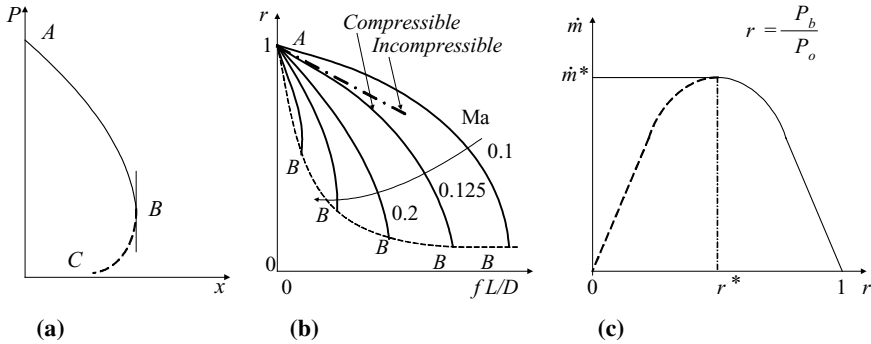


Figure IIIc.2.2. (a) and (b) Depiction of Equation IIIc.1.16 and (c) Equation IIIc.1.19

Note in Figure IIIc.2.2(b) similar to Figure IIIc.2.2(a), as flow velocity approaches the speed of sound in the fluid, the denominator approaches zero. At sonic velocity, the tangent to the curve becomes vertical. Finally, in examining Equation IIIc.1.19, we obtain a parabolic plot of mass flow rate versus $r = P_b/P_o$ as shown in Figure IIIc-2-2(c). At $r = 1$ ($P_b = P_o$) there is no flow. As P_2 is lowered, flow rate increases. As discussed above, there is a critical pressure (shown by P_e^* and the corresponding ratio by r^*) beyond which the flow becomes independent of the downstream pressure. Equation IIIc.1.31 shows that the mass flow rate peaks when the downstream pressure causes flow to become sonic. El-Wakil has summarized the above discussion in the plots of Figure IIIc.2.3. As shown in this Figure IIIc.2.3, when the source pressure is equal to the downstream, back, or the receiving tank pressure, there is no flow and velocity is zero (line number 0). Line numbers 1 and 2 show subsonic flow, which increases with further reduction in

back pressure. Line 3 shows the back pressure at which flow has become sonic. Lines 4 and 5 show that further reduction in back pressure beyond that of line 3 does not result in further flow increase.

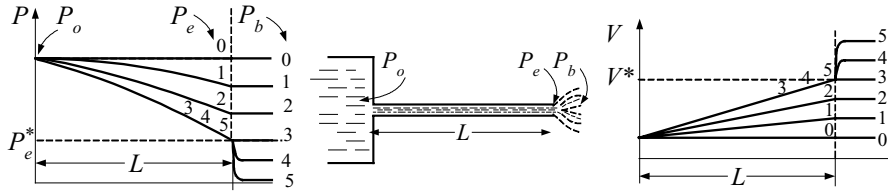


Figure IIIc.2.3. Pressure and Flow Velocity of Compressible Fluids (El-Wakil)

Example IIIc.2.1. Show that for an isentropic condition the critical flow of a compressible fluid in a horizontal constant area pipe is identical to the mass flow rate at sonic speed.

Solution: For choked flow $d\dot{m}/dP = 0$. We find from the continuity equation under steady state condition:

$$\frac{d\dot{m}}{dP} = \frac{d(\rho VA)}{dP} = VA \frac{d\rho}{dP} + \rho A \frac{dV}{dP} = 0$$

from which we find $dP/dV = (-\rho/V)dP/d\rho$. From Equation IIIc.1.4 for frictionless flow:

$$\frac{dP}{\rho V^2} + \frac{dV}{V} + \frac{f dx}{2D} = 0$$

from which we find $dP/dV = -\rho V$. Therefore, $(-\rho/V)dP/d\rho = -\rho V$. Since $G = \rho V$, then:

$$G^2 = \rho^2 \left(\frac{dP}{d\rho} \right)_s = \rho^2 (c^2)$$

where we substituted for the speed of sound as given by $c = \sqrt{(dP/d\rho)_s}$. Note that subscript s , for entropy, is added to emphasize that the process is adiabatic and frictionless (isentropic).

2.1. Calculation of Choked Flow for Ideal Gases

We can readily derive the flow rate of ideal gases under choked condition from the energy equation written between the flow upstream and the receiving tank downstream as:

$$h_o = h_b + V_b^2 / 2 \quad \text{IIIc.2.1}$$

where the stagnation enthalpy (i.e., the enthalpy plus the associated kinetic energy) is used for the upstream flow. Substituting for enthalpies, we find:

$$V_b^2 = 2c_p T_b (T_o / T_b - 1) \quad \text{IIIc.2.2}$$

Relating velocity to Mach number via $\text{Ma}^2 = V^2 / c^2$ and substituting for $c^2 = \gamma R T$, we obtain:

$$\text{Ma}^2 = \frac{2c_p T (T_o / T_b - 1)}{\gamma R T_b} = \frac{2c_p (T_o / T_b - 1)}{\gamma R} = \frac{2[\gamma R / (\gamma - 1)](T_o / T_b - 1)}{\gamma R} = \frac{2}{\gamma - 1} (T_o / T_b - 1)$$

so that

$$T_o / T_b = 1 + \zeta \text{Ma}^2 \quad \text{IIIc.2.3}$$

where $\zeta = (\gamma - 1)/2$. Using the isentropic relations given by Equations IIa.4.4 and IIa.4.5, we further find that:

$$P_o / P_b = \left(1 + \zeta \text{Ma}^2\right)^{\gamma/(\gamma-1)} \quad \text{IIIc.2.4}$$

$$\rho_o / \rho_b = \left(1 + \zeta \text{Ma}^2\right)^{1/(\gamma-1)} \quad \text{IIIc.2.5}$$

It is important to note that when flow is choked, $\text{Ma} = 1$, hence

$$T^*/T_o = \lambda \quad \text{IIIc.2.6}$$

$$\rho^*/\rho_o = \lambda^{1/(\gamma-1)} \quad \text{IIIc.2.7}$$

$$P^*/P_o = \lambda^{\gamma/(\gamma-1)} \quad \text{IIIc.2.8}$$

where $\lambda = 2/(\gamma + 1)$ and * represents properties at the choked condition. From the last relation we can identify two cases. First, back pressure less than critical pressure, $P_b > P^*$ and second, back pressure greater than critical pressure, $P_b < P^*$. These cases are discussed next.

Case A. $P_b > P^*$

We can find mass flux from Equation IIIc.2.2 by substituting from $T_b/T_o = (P_b/P_o)^{(\gamma-1)/\gamma}$ and $\rho_b = P_b/RT_b = (P_o/RT_o)(P_b/P_o)^{1/\gamma}$ to obtain:

$$G = \dot{m} / A = P_o \sqrt{\frac{2}{RT_o} \frac{\gamma}{\gamma-1} \left[\left(\frac{P_b}{P_o} \right)^{2/\gamma} - \left(\frac{P_b}{P_o} \right)^{(\gamma+1)/\gamma} \right]} \quad \text{IIIc.2.9}$$

Case B. $P_b \leq P^*$

We can find mass flux from $G = \dot{m} / A = \rho V$ with V and ρ substituted from Equations IIIc.2.2, IIIc.2.6, and IIIc.2.7, respectively to obtain:

$$G = \dot{m} / A = \sqrt{\frac{\gamma}{R}} \lambda^{\left(\frac{\gamma+1}{\gamma-1}\right)} \frac{P_o}{\sqrt{T_o}} \quad \text{IIIc.2.10}$$

Expectedly, when flow is choked, P_b does not appear in the equation for mass flux.

Example IIIc.2.2. A tank contains air at stagnation properties of 100 psia (0.69 MPa) and 75 F (23.89 C). A 1 inch (2.54 cm) diameter vent valve is opened. Find a) air flow rate if $P_b = 60$ psia (0.36 MPa) and b) air flow rate if $P_b = 14.7$ psia (1 atm).

Solution: For Air, $\gamma = c_p/c_v = 0.24/0.17 = 1.4$ hence $\lambda = 2/(1 + 1.4) = 0.8334$. Also $R = R_u/M_{air} = 1545/28.97 = 53.33$ ft lbf/lbm R (0.287 kJ/kmol·K), $T_o = 75 + 460 = 535$ R (297 K), and $A = 5.454\text{E-}3$ ft² (5.07E-4 m²). We first find P^* , the pressure at which flow is choked. This is found from Equation IIIc.2.8 as:

$$P^* = P_o \lambda^{\gamma(\gamma-1)} = 100(0.8334)^{1.4/0.4} = 52.83 \text{ psia (0.36 MPa)}$$

a) Since $P_b > P^*$, we use Equation IIIc.2.9:

$$G = \sqrt{\frac{2 \times 32.2}{53.33} \times \frac{1.4}{0.4} \left(\left(\frac{65}{100} \right)^{2/1.4} - \left(\frac{65}{100} \right)^{2.4/1.4} \right)} \frac{(100 \times 144)}{\sqrt{535}} = 320.2 \text{ lbm/s} \cdot \text{ft}^2$$

(1612.2 kg/s·m²)

Therefore, $\dot{m} = 320.2 \times 5.454\text{E-}3 = 1.745$ lbm/s (0.79 kg/s)

b) We can find the choked flow rate from either Equation IIIc.2.9:

$$G = \sqrt{\frac{2 \times 32.2}{53.33} \times \frac{1.4}{0.4} \left(\left(\frac{52.83}{100} \right)^{2/1.4} - \left(\frac{52.83}{100} \right)^{2.4/1.4} \right)} \frac{(100 \times 144)}{\sqrt{535}} = 331.24 \text{ lbm/s} \cdot \text{ft}^2$$

(1617.24 kg/s·m²)

or from Equation IIIc.2.10:

$$G = \sqrt{\frac{1.4 \times 32.2}{53.33}} (0.8334)^{2.4/4} \frac{(100 \times 144)}{\sqrt{535}} = 331.24 \text{ lbm/s} \cdot \text{ft}^2 \text{ (1617.24 kg/s} \cdot \text{m}^2\text{)}$$

The choked mass flow rate is $\dot{m} = 331.24 \times 5.454\text{E-}3 = 1.81$ lbm/s (0.821 kg/s).

To expedite arithmetic, we may calculate the constants in Equation IIIc.2.10 for a specified ideal gas. If for example air is the working fluid, then the choked mass flux of air in British Units becomes:

$$G_{BU} = 76.63 P_o / \sqrt{T_o} \quad \text{IIIc.2.11-1}$$

where P_o is the source pressure in psia, T_o is the source temperature in degree Rankine, and G is mass flux in $\text{lbm/s}\cdot\text{ft}^2$. Similarly, for P_o in kPa and T_o in degree Kelvin, mass flux of air in $\text{kg/s}\cdot\text{m}^2$ is given by:

$$G_{SI} = 40.42 P_o / \sqrt{T_o} \quad \text{IIIc.2.11-2}$$

Example IIIc.2.3. Air in an isentropic process and at a rate of 5 kg/s is expanded through the throat to an exit Mach number of 2. The air pressure and temperature at the inlet are $P_o = 350$ kPa and $T_o = 250$ C (523 K). Find a) the throat area, b) the air pressure and temperature at the exit, c) exit velocity and exit area.

Solution: For Air, $\gamma = c_p/c_v = 0.24/0.17 = 1.4$, $\zeta = (\gamma - 1)/2 = 0.2$, and $\lambda = 2/(1 + \gamma) = 2/(1 + 1.4) = 0.8334$.

a) Since $V_{exit} > 1$ then $V_{throat} = 1$:

$$G = 40.42 P_o / \sqrt{T_o} = 40.42 \times 350 / (523)^{0.5} = 618.6 \text{ kg/s}\cdot\text{m}^2$$

$$A_{throat} = \dot{m} / G = 5 / 618.6 = 8.08\text{E-}3 \text{ m}^2. \text{ Therefore,}$$

$$D_{throat} = (4A/\pi)^{0.5} = (4 \times 8.08\text{E-}3/\pi)^{0.5} = 10 \text{ mm}$$

b) We use Equations IIIc.2.3 and IIIc.2.4:

$$T_{exit} = T_o / [1 + \zeta \text{Ma}^2] = 523 / [1 + 0.2 \times 2^2] = 290.5 \text{ K}$$

$$P_{exit} = P_o / [1 + \zeta \text{Ma}^2]^{\gamma/(\gamma-1)} = 350 / [1 + 0.2 \times 2^2]^{3.5} = 44.73 \text{ kPa}$$

$$c) V_{exit} = c \text{Ma and } c = \sqrt{\gamma R T} = [1.4 \times (8,314/28.97) \times 290.5]^{0.5} = 339.58 \text{ m/s}$$

To find A_{exit} , we find ρ_{exit} having P_{exit} and T_{exit} :

$$\rho_{exit} = P_{exit} / (R T_{exit}) = 44.73 / [(8.314/28.97) \times 290.5] = 0.536 \text{ kg/m}^3$$

$$A_{exit} = \dot{m} / (\rho V) = 0.0274 \text{ m}^2.$$

$$\text{Therefore, } D_{throat} = (4A/\pi)^{0.5} = (4 \times 0.0274/\pi)^{0.5} = 18.7 \text{ mm}$$

2.2. Steady Flow of Ideal Gases Through Pipe Breaks

The rate of discharging compressible fluids to the atmosphere depends generally on the source and the sink pressures as well as the flow path length and diameter. As shown in Figure IIIc.2.4, the flow path may be equipped with fittings and valves and hence, the frictional losses due to skin friction and form losses in valves and fittings must be accounted for in the analysis. As a result, the flow may be either subsonic or choked.

It is therefore important to determine the flow condition prior to the calculation of the flow rate, as discussed next.

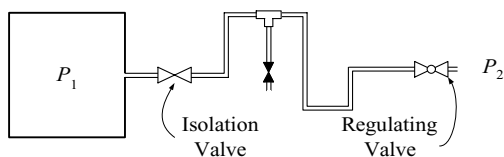


Figure IIIc.2.4. Discharging compressible fluids to the atmosphere through valves and fittings

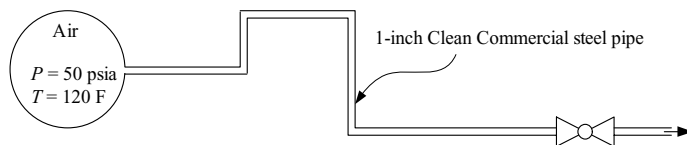
A. Steady Flow of Ideal Gases Through Pipe Breaks, Subsonic Flow

To obtain the mass flow rate, we use Equation IIIb.3.14 as was derived for incompressible fluids. To account for the changes in density due to the associated pressure drop through the flow path, we find fluid density at the source pressure and temperature (ρ_1) while introducing Y , the adiabatic expansion factor. Additionally, as was discussed in the derivation of Equations IIIb.4.4 and IIIc.1.37, to account for the deviation from ideal conditions, we apply α , the flow coefficient. Therefore, mass flow for compressible fluids (Equation IIIb.3.14) becomes:

$$\dot{m} = YA \sqrt{2 \frac{\rho_1 (P_1 - P_2)}{K}} \quad \text{IIIc.2.12}$$

where $K = fL/D + \sum K_i$. Equation IIIc.2.12 applies if flow remains subsonic. The Y factor is given in Figure IIIc.2.5 for gases with $\gamma = 1.3$ and $\gamma = 1.4$. Flow remains subsonic as long as we can find K from the plots of Figure IIIc.2.5. An application of Equation IIIc.2.12 is discussed in the following example.

Example IIIc.2.4. Pressure in a large tank containing air is maintained at 50 psia (0.34 MPa) and 120 F (49 C) while air is discharged to the atmosphere through a 1 in (2.54 cm) clean commercial steel pipe. The 50 ft (164 m) long pipe includes four 90-degree elbows and a fully open globe valve. Find a) If flow is choked and b) the mass flow rate of air.



Solution: a) To see if flow is choked, we need K and $\Delta P/P_1$:

$$K = [L/D + K_{\text{Entrance}} + 4 \times K_{90\text{-Elbow}} + K_{\text{Globe-Valve}} + K_{\text{Exit}}]f$$

We find $f = 0.023$ from Table IIIb.3.2 and loss coefficients from Table IIIb.3.3:

$$K = [(50 \times 12/1) + 0.5 + 4 \times 30 + 340 + 1] \times 0.023 = 24.4$$

$$\Delta P/P_1 = (50 - 14.7)/50 = 0.706$$

To find Y , we use Figure IIIc.2.5 to get; $Y = 0.77$

Since we found Y from the figure, flow is not choked.

b) To find the mass flow rate from Equation IIIc.2.12, we need A and ρ :

$$A = \pi D^2/4 = \pi (1/12)^2/4 = 0.00545 \text{ ft}^2 \text{ (5.063E-4 m}^2\text{)}$$

$$\rho_1 = P_1/RT_1 = 50 \times 144/[(1545/28.97) \times (460 + 120)] = 0.233 \text{ lbm/ft}^3$$

$$\dot{m} = 0.77 \times 0.00545 [2 \times 32.2 \times 0.233 \times (50 \times 144 - 14.7 \times 144) / 24.4]^{0.5} = 0.23 \text{ lbm/s.}$$

B. Steady Flow of Ideal Gases Through Pipe Breaks, Choked Flow

The minimum value of Y corresponding to the maximum value of $\Delta P/P_1$ is circled on each plot in Figure IIIc.2.5 and tabulated next to the figure for a specified loss coefficient K . If for a given gas (γ), given loss coefficient (K), and given $\Delta P/P_1$, we cannot find the corresponding Y factor from Figure IIIc.2.5, we should then use the associated table next to these plots, as specified in CRANE. This would imply that the flow is choked. In this case, the choked flow rate is found from:

$$\dot{m} = YA \sqrt{2 \frac{\rho_1 \Delta P_{\max}}{K}} \quad \text{IIIc.2.13}$$

where ΔP_{\max} must be obtained from the tables associated with Figure IIIc.2.5.

Example IIIc.2.5. Use the same data as in Example IIIc.2.3 but for a tank pressure of 450 psia (3.1 MPa). Find a) if flow is choked and b) the maximum mass flow rate of air.

Solution: a) Having K , to see if flow is choked we need $\Delta P/P_1$:

$$\Delta P/P_1 = (450 - 14.7)/450 = 0.967$$

We cannot find Y from Figure IIIc.2.4. Thus, Y must be found from the related table adjacent to Figure IIIc.2.4. Using $K = 24.5$, we find $Y = 0.71$ by interpolation. This implies that flow is choked. From the same table, maximum $\Delta P/P_1$ by interpolation is found as 0.8487.

$$\Delta P = 0.8487 \times 450 = 381.9 \text{ psia (2.633 MPa)}$$

b) Having A , to find the mass flow rate from Equation IIIc.2.13, we need ρ :

$$\rho_1 = P_1/RT_1 = 450 \times 144/[(1545/28.97) \times (460 + 120)] = 2.1 \text{ lbm/ft}^3 \text{ (33.64 kg/m}^3\text{)}$$

$$\dot{m} = 0.71 \times 0.00545 \sqrt{2[(32.2 \times 2.1) \times (381.9 \times 144)] / 24.4} = 2.1 \text{ lbm/s.}$$

Standard Condition: Due to the change of density in compressible fluids, flow rate is either expressed as mass per unit time or the volumetric flow rate per hour at standard condition ($P_s = 14.7$ psi and $T_s = 60^\circ \text{F} = 520^\circ \text{R}$). To express flow rate in terms of standard condition, since the mass flow rates must remain the same, we write

$$\dot{V}_S = \dot{V} \frac{\rho}{\rho_S}$$

where subscript S stands for standard condition. Substituting from Equation IIIc.2.13, we obtain:

$$\dot{V}_S = \frac{YA}{\rho_S} \sqrt{2\rho_1 \frac{\Delta P}{K}} = YA \frac{RT_s}{P_S} \sqrt{2\rho_1 \frac{\Delta P}{K}} = YA \frac{T_s}{P_S} \sqrt{2 \frac{P_1}{T_1} R \frac{\Delta P}{K}} \quad \text{IIIc.2.14}$$

where ρ_1 is substituted from the ideal gas law. We may further express Equation IIIc.2.14 in terms of S_g , the gas specific gravity defined as:

$$S_g = \frac{M}{M_{air}} = \frac{R_{air}}{R}$$

Equation IIIc.12.14 therefore becomes:

$$\dot{V}_S = YA \frac{T_S}{P_S} \sqrt{2 \frac{P_1}{T_1} \frac{R_{air}}{S_g} \frac{\Delta P}{K}} \quad \text{IIIc.2.15}$$

Example IIIc.2.6. A tank contains carbon dioxide at 113 F (45 C) and 145.1 psia (1 MPa). The tank is equipped with a 15.28 ft (4.66 m) long, 0.5 in schedule 40 pipe (I.D. = 0.622 in = 15.8 mm). Find the flow rate in standard cubic feet per minute corresponding to the specified pressure and temperature. ($\gamma_{\text{CO}_2} = 1.28$ and $M_{\text{CO}_2} = 44$).

Solution: We first find the flow rate at the given conditions:

$$A = \pi D^2/4 = \pi (0.622/12)^2/4 = 2.11\text{E-}3 \text{ ft}^2 \text{ (1.96E-4 m}^2\text{)}$$

$$\rho_1 = P_1/RT_1 = 145.1 \times 144/[(1545/44) \times (460 + 113)] = 1 \text{ lbm/ft}^3 \text{ (16.6 kg/m}^3\text{)}$$

$$f = 0.027 \text{ (Table IIIb.3.2).}$$

Finding the loss coefficients from Table IIIb.3.3:

$$K = [L/D + K_{\text{Entrance}} + K_{\text{Exit}}]f = [(15.28 \times 12/0.622) + 0.5 + 1] \times 0.027 = 8$$

$$\Delta P/P_1 = (145.1 - 14.7)/145.1 = 0.9.$$

From the table adjacent to Figure IIIc.2.5 for air, the maximum ΔP corresponding to $K = 8$ is 0.75. Since the calculated $\Delta P/P_1 = 0.9 > 0.75$, the flow is choked. We find the net expansions coefficient corresponding to $K = 8$ as $Y = 0.698$ and $\Delta P_{\text{max}} = 0.762 \times 145.1 = 145.86 \text{ psi}$

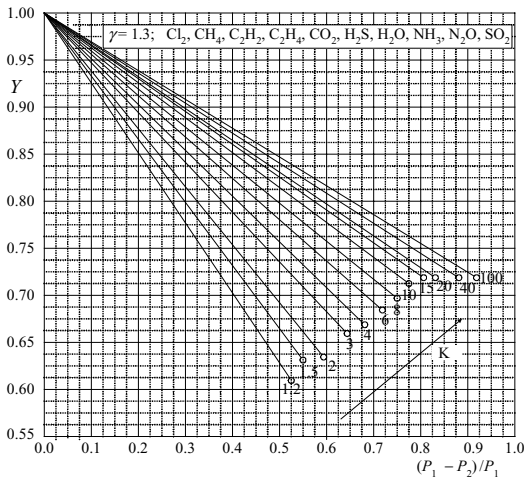
The volumetric flow rate is found from Equation IIIc.2.15 given $S_g = 44/28.97 = 1.52$

$$\begin{aligned} \dot{V}_S &= 0.698 \times 2.11\text{E-}3 \times \frac{520}{14.7 \times 144} \sqrt{2 \times 32.2 \frac{145.1 \times 144}{(113 + 460)} \times \frac{1545/28.97}{44/28.97} \times \frac{0.75}{8}} \\ &= 0.032 \text{ ft}^3/\text{s} \end{aligned}$$

To expedite arithmetic, we may calculate the constants in Equation IIIc.2.10. Substituting for $A = \pi d^2/4$, R_{air} , T_S , and P_S , Equation IIIc.2.15 in British Units simplifies to:

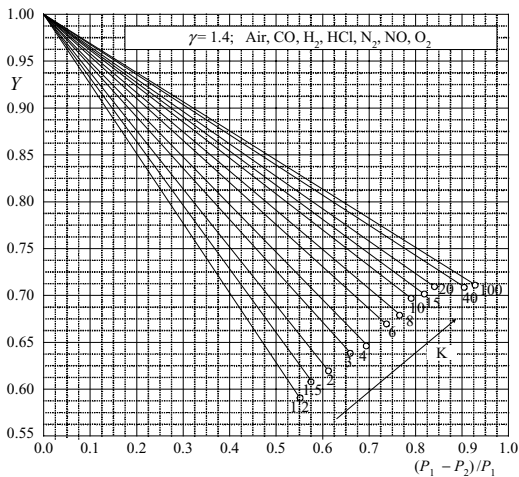
$$(\dot{V}_S)_{BU} = 678.4 Y d^2 \sqrt{\frac{P_1}{T_1 S_g} \frac{\Delta P}{K}}$$

where d is in inch, P_1 and ΔP in psi, T in degree Rankine, and the volumetric flow rate is in ft^3/min .



Limiting Parameters for sonic velocity
($\gamma = 1.3$)

K	$(P_1 - P_2)/P_1$	Y
1.2	0.525	0.612
1.5	0.550	0.631
2.0	0.593	0.635
3.0	0.642	0.658
4.0	0.673	0.670
6.0	0.722	0.685
8.0	0.750	0.698
10.	0.773	0.705
15.	0.807	0.718
20.	0.831	0.718
40.	0.877	0.718
100.	0.920	0.718



Limiting Parameters for sonic velocity
($\gamma = 1.4$)

K	$(P_1 - P_2)/P_1$	Y
1.2	0.552	0.588
1.5	0.576	0.606
2.0	0.612	0.622
3.0	0.662	0.639
4.0	0.697	0.649
6.0	0.737	0.671
8.0	0.762	0.685
10.	0.784	0.695
15.	0.818	0.702
20.	0.839	0.710
40.	0.883	0.710
100.	0.926	0.710

Figure IIIc.2.5. Adiabatic expansion factor for flow of ideal gases for $\gamma = 1.3$ and 1.4 (Crane)

2.3. Critical Flow Correlations for Steam

We conclude the single-phase choked flow analysis with presentation of the critical flow correlations for steam. In this regard, we consider two cases of saturated and superheated steam.

A. Critical Flow Correlation for Superheated Steam

If steam is superheated, the critical flow can be reasonably found from Equation IIIc.2.10 so that mass flux is calculated as:

$$G_{BU} = 59.35 C_d P_o / \sqrt{T_o} \quad \text{IIIc.2.16-1}$$

$$G_{SI} = 31.31 C_d P_o / \sqrt{T_o} \quad \text{IIIc.2.16-2}$$

where P_o is in psia (kPa) and T_o is in degree Rankine (Kelvin) for G to be in $\text{lbm/s}\cdot\text{ft}^2$ ($\text{kg/s}\cdot\text{m}^2$).

However a more accurate relation is:

$$G_{BU} = 45.25 C_d \sqrt{\frac{P}{v(P, h)}} \quad \text{IIIc.2.17}$$

where P is in psia, specific volume (v) is in ft^3/lbm , and mass flux (G) is in $\text{lbm/s}\cdot\text{ft}^2$.

B. Critical Flow Correlations for Saturated Steam

There are several empirical correlations for critical flow of saturated steam. A correlation that results in reasonable agreement with models such as Moody and isoenthalpic (as discussed in Chapter Va for two-phase critical flow) is Critco (Nahavandi 62):

$$(G_{\text{Critco}})_{BU} = \frac{13.734P}{h_g(P) - 185} \quad \text{IIIc.2.18-1}$$

$$(G_{\text{Critco}})_{SI} = \frac{325.726P}{h_g(P) - 430.28} \quad \text{IIIc.2.18-2}$$

where P is in psia (MPa), h_g in Btu/lbm (kJ/kg), and G in $\text{lbm/s}\cdot\text{in}^2$ ($\text{kg/s}\cdot\text{cm}^2$). Other critical flow correlations for steam include the Napier correlation (Moody 75):

$$(G_{\text{Napier}})_{BU} = \frac{P}{70} \quad \text{IIIc.2.19-1}$$

$$(G_{\text{Napier}})_{SI} = \frac{P}{7} \quad \text{IIIc.2.19-2}$$

the Grashof correlation (Baumeister):

$$(G_{Grashof})_{BU} = 0.0165P^{0.97} \quad \text{IIIc.2.20-1}$$

$$(G_{Grashof})_{SI} = 0.0149P^{0.97} \quad \text{IIIc.2.20-2}$$

and the Rateau correlation (Baumeister):

$$(G_{Rateau})_{BU} = P[16.367 - 0.96 \log_{10} P]/1000 \quad \text{IIIc.2.21-1}$$

$$(G_{Rateau})_{SI} = P[14.292 - 0.96 \log_{10} P]/100 \quad \text{IIIc.2.21-2}$$

In Equations IIIc.2.19 through IIIc.2.21, P is in psia (MPa) and G is in lbm/s·in² (kg/s·cm²). As a rough estimate, the critical flow of saturated steam can be guessed from Napier's correlation as $G \approx 2P$ where P is in psia and G is in lbm/s·ft². Thompson compared the results from Napier's correlation with data and observed that the Napier's correlation overpredicts data between pressures from 100 to 1500 psia and underpredicts data for pressures greater than 1500 psia. Hence, a pressure correction factor is used for this correlation for the source pressure in the range of $1500 < P < 3200$ psia as follows:

$$C_{Napier} = \frac{0.1906P - 1000}{0.2292P - 1061} \quad \text{IIIc.2.22}$$

where P is in psia. The ASME Boiler and Pressure Vessel Code uses the Napier's correlation with the above correction factor. The choked flow rate is then calculated from:

$$\dot{m}_{\max} = 0.9C_d C_{Napier} (A_c P / 70) \quad \text{IIIc.2.23}$$

where mass flow rate is in lbm/s, A_c is the choking area in square inch, P is in psia, and C_d is the discharge coefficient.

Example IIIc.2.7. Saturated steam at 1000 psia (6.89476 MPa) is discharged to the atmosphere through a 1/8 in (3.175 mm) diameter valve. Find mass flow rate of steam.

Solution: Since flow of steam discharged from 1000 psia to 14.7 psia is choked, we may use Critco or other correlations IIIc.2.19 through IIIc.2.21. For Critco, $h = h_g = 1192.9$ Btu/lbm (2774.5 kJ/kg):

$$G_{Critco} = 13.734 \times 1000 / (1192.9 - 185) = 13.63 \text{ lbm/s} \cdot \text{in}^2 \text{ (0.958 kg/s} \cdot \text{cm}^2\text{)}$$

$$G_{Napier} = 1000/70 = 14.28 \text{ lbm/s} \cdot \text{in}^2 \text{ (1 kg/s} \cdot \text{cm}^2\text{)}$$

$$G_{Grashof} = 0.0165(1000)^{0.97} = 13.41 \text{ lbm/s} \cdot \text{in}^2 \text{ (0.943 kg/s} \cdot \text{cm}^2\text{)}$$

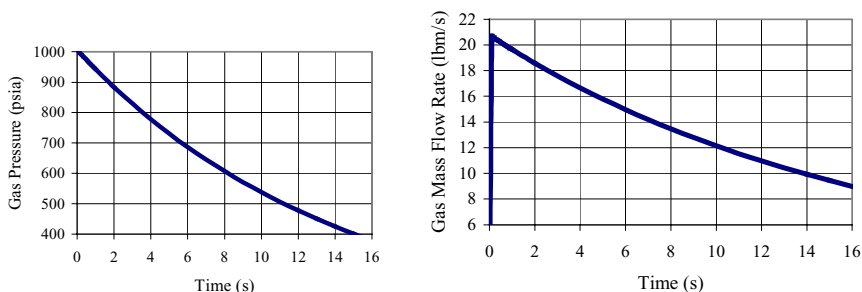
$$G_{Rateau} = [16.267 - 0.92(2.158 + \log_{10} 1000)] = 13.48 \text{ lbm/s} \cdot \text{in}^2 \text{ (0.948 kg/s} \cdot \text{cm}^2\text{)}$$

$$G_{rough\ estimate} = 2 \times 1000 = 2000 \text{ lbm/s} \cdot \text{ft}^2 = 13.88 \text{ lbm/s} \cdot \text{in}^2 \text{ (0.976 kg/s} \cdot \text{cm}^2\text{)}$$

Note that Napier's correlation has predicted the largest choked flow rate.

Example IIIc.2.8. A pressure vessel is filled with air. A small valve is opened to vent the vessel. Find the vessel pressure after 15 s. The mass flow rate through the valve is given as $\dot{m}_e = bP/\sqrt{T}$. In BU; \dot{m}_e in lbm/s, P in psia, and T in R, the value of b is given as $b = 0.5148 \text{ lbm}\cdot\text{ft}^2\cdot\text{R}^{1/2}/(\text{s}\cdot\text{lbf})$. Other data are as follows; $P_1 = 1000 \text{ psia}$, $T_1 = 150 \text{ F}$, $V = 100 \text{ ft}^3$, $d_{\text{valve}} = 1 \text{ inch}$, $A_{\text{valve}} = 5.454 \times 10^{-3} \text{ ft}^2$, $(C_d)_{\text{valve}} = 0.65$.

Solution: We must solve the conservation equations for mass and energy as well as the volume constraint simultaneously. The involved equations constitute a set of first-order non-linear differential equations, thus we use a finite difference approach. The FORTRAN program used to solve this problem is included on the accompanying CD-ROM and is the same that was used to solve Example IIa.8.7. The results for pressure and mass flow rate are plotted versus time.



From the pressure plot versus time, we find $P(t = 15 \text{ s}) = 400 \text{ psia}$. Discharging pressurized vessels results in a rapid drop of the gas temperature. Thus, pressure vessels undergoing rapid discharge should be designed to withstand high thermal stresses. Also, note that in this problem we ignored any heat transfer to or from the tank structure. If the tank is poorly insulated, the rate of heat transfer should be included in the formulation.

QUESTIONS

- How does pressure drop calculation of compressible fluids differ from incompressible fluids?
- What manipulation do you use to express Equation IIIb.3.7 in terms of the Ma number?
- Why is it a reasonable assumption for friction factor to remain constant in the isothermal flow in pipes?
- Is Equation IIIc.1.19 applicable to the flow of compressible fluids in any pipe length?
- Why does the subsonic flow accelerate?
- Is it correct to say that in supersonic flow, pressure actually increases in the flow direction?
- Why is a maximum pipe length calculated for the flow of compressible fluids in pipes?

- Why do we have to define the adiabatic expansion factor for the flow of compressible fluids?
- What is the value of the adiabatic expansion factor for incompressible fluids?
- What is the value of Y for CO_2 flowing through an orifice with $D_{\text{throat}} = D_{\text{pipe}}/2$?
- What is the critical or choked flow?
- When does flow become choked?
- Is choked flow associated only with the flow of the compressible fluids?
- What is the critical pressure? What happens when the back pressure is less than, equal to or greater than the critical pressure?
- What is the critical pressure of air at a stagnation pressure of 2 MPa?
- Why is flow choked if we cannot find Y from the plots of Figure IIIc.2.5?

PROBLEMS

1. Consider the flow of a compressible fluid in a conduit under steady state and isothermal conditions. The flow density changes from point a to point b that is located downstream of point a . Compare the flow Reynolds number at these points and specify whether $\text{Re}_a > \text{Re}_b$, $\text{Re}_a = \text{Re}_b$, or $\text{Re}_a < \text{Re}_b$.

2. Air at pressure P_1 , temperature T_1 , and mass flow rate of \dot{m} enters a compressor. Air pressure rise over the compressor is ΔP_1 . Water at the same conditions enters a pump and its pressure is raised by the same amount. Compare the required pumping powers for air, \dot{W}_a and for water, \dot{W}_w .
[Hint. $\dot{W} = \Delta P \dot{V} = \Delta P \dot{m} / \rho$].

3. Use Equation IIIc.1.14 to show that:

$$\frac{d\text{Ma}^2}{\text{Ma}^2} = \frac{1 + \gamma \text{Ma}^2}{1 - \text{Ma}^2} \left(\frac{dq}{c_p T} \right) - \frac{2 + (\gamma - 1)\text{Ma}^2}{1 - \text{Ma}^2} \left(\frac{dA}{A} \right) + \frac{2 + (\gamma - 1)\text{Ma}^2}{1 - \text{Ma}^2} \left(\frac{dF}{RT} \right)$$

Use this result and substitute for dF/RT term to directly derive Equation IIIc.1.30 for the adiabatic flow of compressible fluids in constant flow area channels.

4. Methane at a rate of 1 kg/s is flowing inside a pipeline. The pipe inside diameter is 1 m. Find the Ma number at a location where pressure and temperature are measured as 1 MPa and 27 C, respectively. $M_{\text{CH}_4} = 16.043$, $\gamma_{\text{CH}_4} = 1.304$. [Ans.: 0.44].

5. Carbon dioxide is flowing in a conduit at 50 psia, 100 F, and a velocity of 50 ft/s. Find the flow Ma number at this location. $M_{\text{CO}_2} = 44.01$, $\gamma_{\text{CO}_2} = 1.28$. [Ans.: 0.056].

6. Air enters a duct at 700 kPa and $\text{Ma} = 0.05$. The duct has a wetted perimeter of 1 m and a flow area of 0.1 m^2 . Find the air pressure at a length of 150 m from the pipe entrance. The air temperature remains constant in the pipe.

7. Air flows in a pipeline at a rate of 25 kg/s. The pipe is 1000 m long and has an inside diameter of 0.35 m. Assuming isothermal process, find the pipe length over which the flow remains subsonic. Data: $P_i = 0.5 \text{ MPa}$, $T_i = 27 \text{ C}$, $f = 0.015$.

8. Compressed air in a facility. For this purpose, a compressor delivers 1 lbm/s of air in a 2 in schedule 40 pipe at 50 psia and 80 F. Assuming the flow is isothermal, find the length of the pipe at the end of which flow becomes sonic.

9. Natural gas is flowing in a pipeline of 2.5 m diameter at a rate of 100 kg/s. The pipeline is well insulated. The gas at the exit of the pumping station's compressor has a pressure of 700 kPa and a temperature of 40 C. Find the maximum pipe length for continuous flow.

10. Air enters a pipe at a Mach number of 0.1. The pipe is 1000 m long, having an inside diameter of 0.25 m. The flow is isothermal and the friction factor remains constant over the entire length of the pipe at 0.013. Find the Mach number at the exit of the pipe.

11. Natural gas, compressed to $P_1 = 100$ psia then cooled to $T_1 = 70$ F, flows in a cross-country pipeline at a velocity of 40 ft/s. The pipe is smooth and has an inside diameter of 2 ft. To maintain pressure, pumping stations are established every 10 miles along the route. In each pumping station, natural gas is compressed to its original pressure and cooled to its original temperature. Find the pressure drop between each pumping station and the required pumping power. Assume natural gas as pure methane with $k = 1.3$, molecular weight of 16 and kinematic viscosity of $2.61\text{E-}5$ ft²/s.

[Ans.: $\text{Re} = 0.31\text{E}7$, $f = 0.00928$, $P_2 = 87.29$, $c_2 = 264$, $\Delta P = 12.71$ psi,

$\dot{m} = 35.36$ lbm/s, $\text{Ma} = 0.03$, and $\dot{W} = 454$ hp].

12. Show that in an isentropic process involving flow in a horizontal flow path, $v dP + V dV = 0$.

13. Show that $G_{critical} = \sqrt{-(dP/dv)_s}$.

14. A tank contains air at stagnation properties of 200 kPa and 30 C. A vent of 3 cm diameter is opened. a) Find air flow rate if $P_b = 150$ kPa and b) if $P_b = 101.35$ kPa. [Ans.: For $C_d = 1$, a) 0.29 and b) 0.33 kg/s].

15. Air in an isentropic process and at a rate of 6 kg/s is expanded through the throat to an exit Mach number of 3. The air pressure and temperature at the inlet are $P_o = 300$ kPa and $T_o = 300$ C, respectively. Find a) the throat area, b) the air pressure and temperature at the exit, c) exit velocity and area.

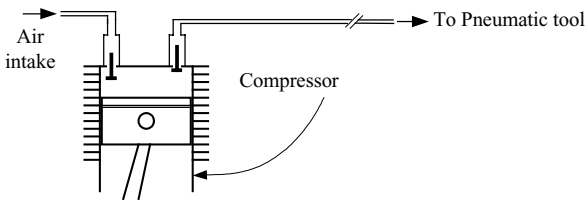
16. Air in an isentropic process and at $P_o = 250$ kPa and $T_o = 600$ K is expanded through the throat to an exit Mach number of 2.5. The throat diameter is 11 cm. Find a) the mass flow rate of air, b) the air pressure and temperature at the exit, c) exit velocity and area.

17. A fully inflated tire has a volume of 15 ft³. The pressure and temperature of the air in the tire are 65 psia and 75 F, respectively. At this condition, the air intake needle is depressed for 3 s and then released. Treating air as an ideal gas and assuming small changes in the tire temperature and volume, Find the amount of air that left the tire. Assume a discharge coefficient of 0.61 and a flow area of 0.01 in².

18. Air flows steadily from a high pressure container (A) to a low pressure container (B) through an ideal convergent-divergent nozzle. Find the flow area at the throat and at the exit of the nozzle. Data: mass flow rate: 2 kg, air pressure in container A: 700 kPa, inlet temperature: 116 C, air pressure in container B: 70 kPa.

19. A tank contains carbon dioxide maintained at 50 C and 0.5 MPa. The tank is equipped with a 4.5 m long pipe. The pipe has in inside diameter of 1 cm. Find the flow rate in standard cubic feet per minute corresponding to the specified pressure and temperature. ($\gamma_{\text{CO}_2} = 1.28$ and $M_{\text{CO}_2} = 44$).

20. In a repair shop compressed air is used to operate pneumatic tools. The total length of the airline including all the loss coefficients in terms of equivalent length is about 152.5 m (500 ft). The airline consists of smooth pipe of I.D. = 1.27 cm. Air is compressed to 0.345 MPa (50 psia) and then cooled to 24 C (75 F) when entering the line at a velocity of 2.4 m/s (8 ft/s). Find pressure when air is used to operate the pneumatic tool.



21. In a repair shop compressed air is used to operate pneumatic tools. The total length of the airline including all the loss coefficients in terms of equivalent air is about 500 ft. The airline consists of smooth pipe of I.D. = 0.5 inch. The compressed air is cooled to 75 F when entering the line. A pneumatic tool requires 35 psia of compressed air to operate. To what pressure should the air be pressurized by a compressor to provide the desired pressure for the tool? What power is required to obtain such pressure if the compression process can be assumed isentropic? Air velocity at the inlet is 10 ft/s.

22. A fully inflated tire has a volume of 15 ft³. The pressure and temperature of the air in the tire are 65 psia and 75 F, respectively. At this condition, the air intake needle is depressed for 5 seconds. Treating air as an ideal gas and assuming small changes in the tire temperature and volume, plot the mass flow rate of air versus time. Assume a discharge coefficient of 0.61 and a flow area of 0.01 in².

23. Find the value of the adiabatic expansion factor, Y for CO₂ flowing through an orifice with $\beta = 0.5$ and $r = P_2/P_1 = 0.85$. [Ans.: 0.95]

24. A PWR plant is equipped with atmospheric dump valves (ADV) and turbine bypass valves (TBV). The role of an ADV, installed on the steam line, is to dump steam to the atmosphere in case of a plant trip, while the role of the TBV is to diert steam to the condenser in the case of a turbine trip. The specification sheet as provided by the manufacturer specifies flow rates of 292,500 lbm/h and 1,173,000

lbm/h at the saturation temperature of 556 F for the ADV and the TBV, respectively. Assuming a C_d of 0.61 for both valves find the ADV and the TBV effective flow areas. [Ans.: 8.87 in^2 and 35.58 in^2].

25. Air flows through a nozzle with differential pressure taps located at D : $D/2$ upstream and downstream, respectively. For this nozzle, $D_{throat} = 0.75D_{pipe}$. What is the value of Y if $r = 0.85$?

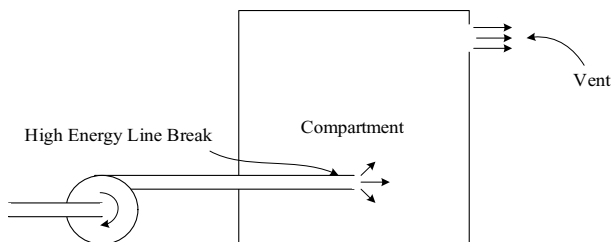
26. A tank containing air is pressurized to 1.7 MPa and 30 C. A valve is now opened to discharge air to the atmosphere through a flow area of 6.45 cm^2 . Find the maximum flow rate. [Ans.: 372 kg/s].

27. Compare Critco, Napier, Grashof, and Rateau critical flow correlations for the range of 50 – 2500 psia.

28. The steam generator of a PWR is operating at 6.55 MPa (950 psia). Due to a sudden plant trip, the *atmospheric dump valve* opens (ADV) to discharge steam. Find the steam flow rate through the ADV. The valve flow area is 40.88 cm^2 (0.044 ft^2). The valve discharge coefficient is 0.61.

29. A pressure vessel is filled with pressurized saturated steam. A small valve is opened to vent the vessel. Find the vessel pressure after 30 s. Data: $P_1 = 1000 \text{ psia}$, $V = 100 \text{ ft}^3$, $D_{Valve} = 1 \text{ inch}$, $(C_d)_{Valve} = 0.65$.

30. A pipe carrying a high pressure air ruptures inside a compartment. The compartment has a vent to discharge air to the atmosphere. Assuming steady state condition, derive an algorithm for the calculation of peak pressure in the compartment.



[Hint: Assuming an isothermal process, the compartment pressure keeps rising as long as the flow rate from the broken pipe exceeds the flow through the vent. The compartment pressure peaks when these flow rates become equal. Apply a discharge coefficient to Equation IIIc.2.9 and set the result equal to Equation IIIc.2.10].

31. A high energy pipe, carrying nitrogen ruptures inside a compartment. Use the given data to find the peak pressure reached in the compartment following the event. Treat nitrogen as air. Data: Nitrogen pressure is 1600 psia (11 MPa), room and nitrogen are at the same initial temperature of 75 F (24 C), diameter of the pipe is 10 in (25.4 cm) and the vent flow area of the compartment is 120 ft^2 (11 m^2).

IV. Heat Transfer

The processes that a given control volume may go through were discussed in chapters on thermodynamics and fluid flow. We showed that to find the conditions at the end of a process, given specified conditions at the beginning of the process, we should use the conservation equations of mass, momentum, and energy in conjunction with the equation of state. In most cases, the rate of heat transfer to or from a control volume is not known, thus it must be determined from a constitutive relation. The topic of heat transfer helps us identify the applicable mode of heat transfer and provides us with the constitutive relation, which correlates temperature to the rate of heat transfer.

There are three modes of heat transfer; conduction, convection, and radiation. Conduction is more pronounced in solids and stems from molecular diffusion due to an existing temperature gradient. The radiation mechanism is less understood. In certain conditions, radiation can be explained according to wave mechanics and in other situations according to quantum mechanics. Radiation heat transfer applies to solids, liquids, and gases. On the other hand, convection is solely due to the bulk motion of a fluid, transferring heat in the process. As such, convection heat transfer is pertinent only to fluids. Convection heat transfer is the dominant mode not only in single-phase but also in two-phase flow such as heat transfer associated with phase change in boiling and condensation. As discussed in Chapter I, the constitutive relation in heat conduction, heat convection, and thermal radiation is known as Fourier's law, Newton's law of cooling, and the Stefan-Blotzmann law, respectively.

IVa. Conduction

The goal of studying conduction heat transfer is to determine the temperature distribution within a substance and the rate of heat transfer to or from the substance. The entire topic of conduction heat transfer is based on the energy equation as derived in Chapter III. Fortunately, in conduction heat transfer, the energy equation can be significantly simplified due to the absence of such terms as the rate of work performed by pressure forces and the rate of work performed by viscous forces. In most cases, change in stagnation energy due to convection is also absent. As shown later in this chapter, the elimination of these terms allows the use of analytical solutions in closed form for certain classes of problems.

In this chapter, following the introduction of pertinent terms, we first derive the heat conduction equation in its general form. We then discuss the concept of lumped parameter versus one-, two-, or three-dimensional analysis. The primary

goal is to find analytical solutions to both steady state and transient heat conduction problems. In this regard, we start with one-dimensional geometry in the Cartesian, cylindrical, and spherical coordinate systems. We consider such cases as heat conduction with internal heat generation, which may in turn be a function of space (i.e., location) or temperature. We then consider transient response of multi-dimensional objects to heat conduction. This is followed by the introduction of numerical methods.

1. Definition of Heat Conduction Terms

Homogenous versus heterogeneous: In conduction heat transfer*, a substance is considered homogenous if its thermal conductivity, as defined later in this section, does not vary from point to point within the substance. Otherwise, the substance is heterogeneous. Water and iron, are examples of homogenous substances and such porous materials as wood and cork are examples of heterogeneous material.

Isotropic versus anisotropic: A substance is considered isotropic with respect to heat conduction when its thermal conductivity is the same in all directions. Otherwise, the substance is anisotropic. Water and iron are examples of isotropic and wood and asbestos are examples of anisotropic materials. In this chapter we deal only with homogenous and isotropic materials.

Volumetric heat generation rate ($\dot{q}''' = \dot{Q}/V$) is the rate of energy produced in the unit volume of the substance by chemical, electrical, or nuclear reactions. In British units, this term can be expressed as Btu/hr-ft³ and in SI units it is generally expressed as W/m³. Nuclear reactions are discussed in Chapter V.

Heat flux ($\dot{q}'' = \dot{Q}/A$) is the rate of heat transfer per unit area. In British units, it is generally expressed as Btu/hr-ft² and in SI units as W/m².

Linear heat generation rate ($\dot{q}' = \dot{Q}/L$) is the rate of heat transfer per unit length. In British units, it can be expressed as Btu/ft and in SI units as W/m. In nuclear engineering, this term is often expressed in the hybrid unit of kW/ft.

Transport by diffusion is the mechanism responsible for thermal conduction. For example, in gases at atmospheric pressure and temperature, a molecule travels a short distance before colliding with another molecule. This collision results in the transfer of energy in the gas in a tortuous path. The mean free path of a molecule (l) is much smaller than the characteristic length of the system (L).

Fourier's law of heat conduction, published in *Theorie Analytique de la Chaleur* by Baron Jean Baptist Joseph Fourier (1768–1830) in 1822, provides the most essential relation between the rate of heat transfer and the temperature gradient in heat conduction. In a substance, heat flows from a higher to a lower tem-

* Although *conductive* and *convective* heat transfer are more proper, we retain the more traditional *coduction* and *convection* heat transfer.

perature region. The higher the temperature difference ($\Delta T = T_2 - T_1$) between these regions (i.e. the temperature gradient) the higher the rate of heat transfer. The rate of heat transfer is also proportional to the area normal to the direction of heat (A), but the rate of heat transfer decreases as the distance between the two region (Δx) increases. We then conclude that:

$$\dot{Q} \propto A \Delta T / \Delta x \quad \text{IVa.1.1}$$

Equation IVa.1.1, in which $l \ll L$, is Fourier's law for homogenous isotropic continua.

Thermal conductivity as a transport property of a substance, is the proportionality factor between the rate of heat flux and the temperature gradient with respect to distance;

$$\frac{\dot{Q}}{A} = -k \frac{\partial T}{\partial x} \quad \text{IVa.1.2}$$

Since the temperature gradient is negative, the minus sign is inserted to get positive value for the rate of heat transfer in the direction of decreasing temperature. Fourier's law for heterogeneous isotropic continua can be generalized by using the gradient operator:

$$\dot{q}'' = -k \bar{\nabla} T \quad \text{IVa.1.3}$$

which is applicable in all three coordinate systems. In Cartesian coordinates, Equation IVa.1.3 becomes:

$$\bar{q}'' = -k \left(\frac{\partial T}{\partial x} \bar{i} + \frac{\partial T}{\partial y} \bar{j} + \frac{\partial T}{\partial z} \bar{k} \right)$$

Thermal conductivity for some materials, such as wood for example, is directionally dependent and must be treated as a tensor. The vectorial form of Fourier's law for heterogeneous anisotropic continua is:

$$\bar{q}'' = \bar{K} \cdot \bar{\nabla} T$$

where \bar{K} is thermal conductivity tensor. This equation in Cartesian coordinate is written as:

$$\begin{pmatrix} \dot{q}_x'' \\ \dot{q}_y'' \\ \dot{q}_z'' \end{pmatrix} = - \begin{pmatrix} k_{xx} & k_{xy} & k_{xz} \\ k_{yx} & k_{yy} & k_{yz} \\ k_{zx} & k_{zy} & k_{zz} \end{pmatrix} \begin{pmatrix} \partial T / \partial x \\ \partial T / \partial y \\ \partial T / \partial z \end{pmatrix}$$

Thermal conductivity in British units is expressed as Btu/h·ft·F and in SI units as W/m·C. The value of k for a continuum depends on several factors including thermodynamic state (phase, pressure, and temperature) as well as chemical composition and structure. Values for some materials are shown in Figure IVa.1.1 and

in Appendix Tables A.IV.1 through A.IV.6. In metals where properties are primarily a function of temperature, thermal conductivity can be correlated to temperature as:

$$k = k_0[1 + \beta_0(T - T_0)] \quad \text{IVa.1.4}$$

where k_0 is thermal conductivity at a given reference temperature T_0 .

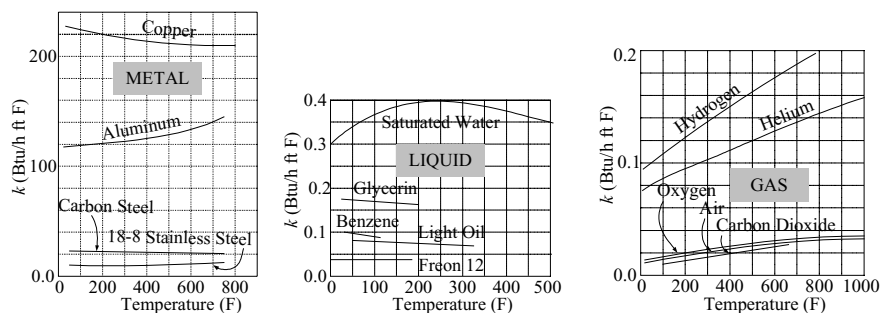


Figure IVa.1.1. Thermal conductivity of some metals, liquids, and gases*

Due to its dependence on space and temperature, thermal conductivity can complicate heat conduction analysis. Fortunately, in most cases thermal conductivity over the temperature range of interest can be treated as a constant, which greatly simplifies analysis. Even in cases, such as calculation of heat transfer in nuclear fuels, where thermal conductivity may not be treated as a constant, an average value for k may be determined over the temperature range of interest as:

$$\bar{k} = \frac{\int_{T_1}^{T_2} k dT}{T_2 - T_1} \quad \text{IVa.1.5}$$

Using a constant value, a linear function, or an average value over the temperature range of interest for k are all simplifying techniques in seeking analytical solutions for heat conduction problems. In numerical solutions, there is no such limitation for the specification of thermal conductivity.

Thermal capacitance, a thermodynamic property of a substance is defined as the product of density and specific heat (ρc). Thermal capacitance is an indication of energy storage of a substance. As shown in Equation IVa.1.1, in conduction heat transfer, density and specific heat always appear as an entity and only in tran-

* Thermal conductivity of gases shown in this figure is for the viscous state. At the molecular state where gas pressure becomes exceedingly small (partial vacuum), k also becomes a function of pressure. Roth gives the threshold pressure for the molecular state as $P = [C_1 L(1 + C_2 T)]$ where L is the mean free path and constants C_1 and C_2 for air are 118.76 m/N and 0.00885 K⁻¹, respectively. In this relation, P is in bar and T in degrees Kelvin.

sient conduction. Thermal capacitance has units of $\text{Btu/ft}^3\cdot\text{F}$ in British units and $\text{J/m}^3\cdot\text{C}$ in SI units.

Thermal diffusivity is defined as the ratio of thermal conductivity to thermal capacitance $\alpha = k/\rho c$. Although, this property is obtained by dividing a transport property by a thermodynamic property, thermal diffusivity itself is the key transport property for transient conduction. A small value for α indicates that the substance has a higher potential to store energy than to transfer energy. A large value for α indicates that the substance is more effective in transferring than in storing energy. In British units, thermal diffusivity is expressed as ft^2/s and in SI units as m^2/s .

Convection heat transfer (\dot{q}_c''), is a mechanism by which heat is transferred due to the bulk motion of a fluid. Of specific interest is the heat transfer between a fluid in motion at one temperature and a solid at a different temperature. If the fluid bulk motion is solely due to the existing temperature gradient between the fluid and the solid, the convection is known as *natural* or *free convection* as opposed to *forced convection*. Mixed convection is a mode of heat transfer in which the rate of heat transfer from free convection is comparable to that of forced convection. Convection heat transfer is discussed in Chapter IVb.

Heat transfer coefficient. Similar to conduction, the rate of heat flux in convection heat transfer is proportional to the temperature gradient, $\dot{q}'' \propto \Delta T$. The proportionality constant is known as the *heat transfer coefficient*, $h = \dot{q}''/\Delta T$. In British units, h is expressed as $\text{Btu/h}\cdot\text{ft}^2\cdot\text{F}$ and in SI units as $\text{W/m}^2\cdot\text{K}$. The relationship expressed as $\dot{q}'' = h\Delta T$ is known as *Newton's law of cooling*. Orders of magnitude of h for various heat transfer regimes are shown in Table IVa.1.1.

Table IVa.1.1. Approximate range of convection heat transfer coefficient

Regime	h ($\text{Btu/ft}^2\cdot\text{h}\cdot\text{F}$)	h ($\text{W/m}^2\cdot\text{K}$)
Free convection (air):	1 – 5	5 – 25
Free convection (Water)	10 – 250	50 – 1200
Forced convection (air):	5 – 50	25 – 250
Forced convection (water)	10 – 5000	50 – 20,000
Condensation of steam on walls	500 – 5,000	2,000 – 20,000
Condensation of steam on pipes	500 – 10,000	2,000 – 50,000
Pool boiling of water	500 – 10,000	2,000 – 50,000
Flow boiling of water	500 – 20,000	2,000 – 100,000

Thermal resistance, (R_{th}) depends on thermal conductivity of a substance, however, it is not a property of the substance, as its value depends on the geometry in a specific problem. According to Fourier's law, $\dot{Q} = kA(\Delta T/\Delta x)$. Using an electrical engineering analogy, the temperature gradient resembles applied voltage and the rate of heat transfer resembles electric current. Thus, $R_{th} = \Delta x/(kA)$ can be viewed as thermal resistance. Obviously, substances with higher thermal conduc-

tivity and larger surface area pose smaller resistance to the flow of heat. Conversely, the larger the distance between two regions of higher and lower temperatures, the lower the rate of heat transfer. Thermal resistance in convection heat transfer can also be obtained as $R_{th} = 1/(hA)$ where h is the heat transfer coefficient.

Contact resistance occurs in thermal conduction between two attached solids. In such cases, there is always a gap between the two solids due to surface roughness. The only exception is when surfaces in contact are *mirror finished*. In most applications, the gap between the two surfaces of solids in contact is filled with stagnant air, which is a poor conductor of heat. As a result, there is a thermal resistance in addition to the heat conduction resistance for surfaces in contact. Expectedly, the contact resistance depends on both the pressure applied to the composite solids and the fluid filling the gap. As a rough estimate, the contact resistance may be taken into account by increasing the thickness of the solid with lower thermal conductivity by about 0.2 in (5 mm).

Radiation heat transfer (\dot{q}_r'') refers to the exchange of thermal radiation between surfaces. Thermal radiation is the energy emitted due to the internal energy of the surface, manifested as temperature. Unlike the conduction and convection modes, radiation does not require a medium as the emitted energy is transported by photons capable of traveling through perfect vacuum. The mean free path in radiation heat transfer is very long compared with the diffusion mechanism since photons travel in straight lines without colliding. The Stefan-Boltzmann law gives the maximum rate of heat transfer radiated from a surface as $\dot{q}_r'' = \sigma T^4$ where T is the absolute temperature of the surface and the Stefan-Boltzmann constant is given as $\sigma = 0.1714\text{E-}8 \text{ Btu/h}\cdot\text{ft}^2\cdot\text{R}^4 = 5.67\text{E-}8 \text{ W/m}^2\cdot\text{K}^4$. A surface exhibiting the maximum rate of heat transfer is known as a *black body*. Real surfaces are those that emit less energy by a factor of ε , known as *emissivity*. The net radiation heat flux between two surfaces, located in a radiationally non-participating medium, is found from $\dot{q}_r'' = \varepsilon\sigma(T_1^4 - T_2^4)$. In this equation, ε is the surface emissivity and T_2 is the temperature of surface 2, which encompasses surface 1. It is shown in Chapter IVd that the net heat flux should be reduced by a *view factor* if only some of the radiation leaving surface 1 reaches surface 2. While radiation heat transfer is always present, at low temperatures it may become insignificant when compared with the rate of heat transfer by forced convection mechanism. An example of neutron and gamma radiations, which must be treated differently than thermal radiation, is given in Section 5.5 of this chapter.

Steady state (S-S) conduction refers to a condition where temperature distribution in a substance does not change with time. As such, any heat added to the substance or internally produced in the substance is transferred away from the substance. Selection of insulation to minimize heat loss from a piping system carrying superheated steam is based on a steady state analysis. Similarly, design of fins or extended surfaces to maximize the rate of heat dissipation from electronic devices or air-cooled engines involves steady state application of the conduction heat transfer. Steady state operation of a nuclear core implies that the rate

of heat production by fission in the fuel rods is exactly equal to the rate of heat removal by the coolant. Mathematically speaking, the solution to steady state problems is obtained if the algebraic summation of all energy addition, generation, and removal from a control volume is set equal to zero. This reflects the fact that while temperature changes from point to point inside the object, the distribution of temperature remains the same and is independent of time.

Unsteady, time-dependent, or transient conduction heat transfer deals with the temperature response of an object to changes in the rate of internal heat generation (if any) or changes in the boundary conditions. Problems dealing with cooling down or heating up of a substance are transient in nature. Mathematically speaking, changes in the rate of internal heat generation (if any) or changes in the boundary conditions are *forcing functions* for temperature distribution.

Heat transfer area. Distinction must be made between the surface and the cross sectional areas. For the solid cylinder shown in Figure IVa.1.2, area at $x = 0$ is $A = \pi r_o^2 = \pi D^2/4$ while area at $y = r_o$ is $S = \pi DL$.

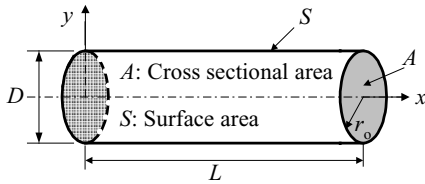


Figure IVa.1.2. Identification of cross sectional area and surface area

Fourier number ($Fo = \alpha / x^2$) is a dimensionless number pertinent to transient analysis in conduction.

2. The Heat Conduction Equation

We may directly derive the heat conduction equation by using the differential analysis for heat diffusion in an infinitesimal control volume. The analysis is performed in the Cartesian coordinate system as shown in Figure IVa.2.1. The derivation is based on the first law of thermodynamic We simplify Equation IIa.6.3 by noting that for the infinitesimal control volume $\sum \dot{m}_i = \sum \dot{m}_e = \sum \dot{W} = 0$ so that:

$$\sum \left(\text{Rate of heat addition by} \right) + \sum \left(\text{Rate of internal} \right) = \sum \left(\text{Rate of heat removal by} \right) + \left(\text{Rate of change} \right)$$

$$\sum \left(\text{conduction \& radiation} \right) + \sum \left(\text{heat generation} \right) = \sum \left(\text{conduction \& radiation} \right) + \left(\text{of internal energy} \right)$$

The total rate of energy entering the C.V. from all sides by conduction is:

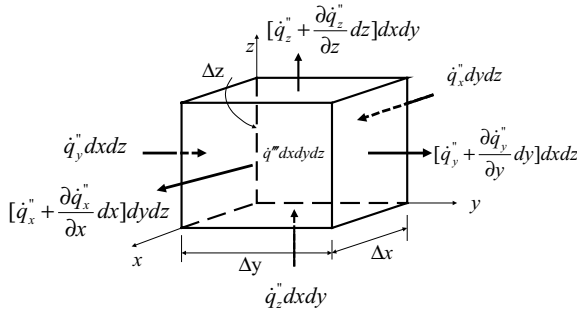


Figure IVa.2.1. Diffusion of heat in an elemental control volume in Cartesian coordinates

$$(\dot{q}_x'' + \dot{q}_y'' + \dot{q}_z'')dx dy dz$$

The total rate of energy leaving the C.V. from all sides by conduction is:

$$[\dot{q}_x'' + (\partial \dot{q}_x'' / \partial x) \Delta x] \Delta y \Delta z + [\dot{q}_y'' + (\partial \dot{q}_y'' / \partial y) \Delta y] \Delta x \Delta z + [\dot{q}_z'' + (\partial \dot{q}_z'' / \partial z) \Delta z] \Delta x \Delta y$$

If there is any internal heat generation (due to nuclear reaction, electrical resistance, or exothermic chemical reaction, for example), then the total rate of energy produced in the C.V. is:

$$\dot{q}''' \Delta x \Delta y \Delta z$$

Using our sign conventions of Chapters II and III, we find the rate of change of total energy of the C.V. as:

$$[\partial \dot{q}_x'' / \partial x + (\partial \dot{q}_y'' / \partial y) + (\partial \dot{q}_z'' / \partial z)] + \dot{q}''' = \partial(\rho u) / \partial t$$

Taking advantage of Fourier's law, the result in the absence of noticeable thermal radiation can be cast in the general form of:

$$\nabla \cdot [k(\vec{r}, T) \nabla T(\vec{r}, t)] + \dot{q}'''(\vec{r}, t) = \rho(\vec{r}, T) c(\vec{r}, T) \frac{\partial T(\vec{r}, t)}{\partial t} \quad \text{IVa.2.1}$$

The definition of each term in Equation IVa.2.1 is as follows:

$\nabla \cdot [k(\vec{r}, T) \nabla T(\vec{r}, t)]$: rate of heat transfer by conduction mechanism

$\dot{q}'''(\vec{r}, t)$: rate of internal heat generation per unit volume

$\rho(\vec{r}, T) c(\vec{r}, T) \frac{\partial T(\vec{r}, t)}{\partial t}$: rate of change of internal energy of the control volume

It is emphasized in Equation IVa.2.1 that in general the material thermal properties are functions of space and temperature. This is especially true for thermal conductivity as discussed earlier. In special cases where thermal properties can be con-

sidered constant over the temperature range of interest, the above equation can be simplified to obtain the *general heat conduction equation*:

$$\nabla^2 T + \frac{\dot{q}'''}{k} = \frac{1}{\alpha} \frac{\partial T}{\partial t} \quad \text{IVa.2.2}$$

In the absence of any internal heat generation, the equation takes the form of the *Fourier equation*:

$$\nabla^2 T = \frac{1}{\alpha} \frac{\partial T}{\partial t} \quad \text{IVa.2.3}$$

In steady state with internal heat generation, the equation becomes the *Poisson equation*:

$$\nabla^2 T + \frac{\dot{q}'''}{k} = 0 \quad \text{IVa.2.4}$$

In one-dimension, Equation IVa.2.4 in the Cartesian coordinate simplifies to:

$$\frac{d^2 T}{dx^2} + \frac{\dot{q}'''}{k} = 0 \quad \text{IVa.2.4-1}$$

If the internal heat generation is not uniform, rather is a linear function of temperature, the Poisson equation becomes the *Helmholtz equation*:

$$\nabla^2 T + C^2 T = 0 \quad \text{IVa.2.5}$$

where C is a constant. The Laplacian term (∇^2) can be expanded depending on the application of the Poisson equation in the Cartesian, cylindrical, or spherical coordinate systems. Under steady state conditions and with $\dot{q}''' = 0$, the Poisson equation reduces to:

$$\nabla^2 T = 0 \quad \text{IVa.2.6}$$

And in the one-dimensional Cartesian coordinate, Equation IVa.2.6 can be simply written as $d^2 T/dx^2 = 0$. The following example deals with conduction equation in the cylindrical coordinates.

Example IVa.2.1. Write the general heat conduction equation in the cylindrical coordinate system. ($k = \text{constant}$)

Solution: Substituting for the Laplacian operator from Equation VIIc.1.10, we find;

$$\frac{1}{r} \frac{\partial}{\partial r} \left(r \frac{\partial T}{\partial r} \right) + \frac{1}{r^2} \frac{\partial^2 T}{\partial \theta^2} + \frac{\partial^2 T}{\partial z^2} + \frac{\dot{q}'''}{k} = \frac{1}{\alpha} \frac{\partial T}{\partial t} \quad \text{IVa.2.7}$$

For long cylinders having symmetry in the θ -direction, temperature becomes only a function of r . Hence, Equation IVa.2.7 reduces to the one-dimensional heat conduction equation in polar coordinate:

$$\frac{1}{r} \frac{\partial}{\partial r} \left(r \frac{\partial T}{\partial r} \right) + \frac{\dot{q}'''}{k} = \frac{1}{\alpha} \frac{\partial T}{\partial t} \quad \text{IVa.2.8}$$

Example IVa.2.2. Write the general heat conduction equation in the spherical coordinate system. ($k = \text{constant}$)

Solution: Substituting for the Laplacian operator from Equation VIIc.1.11, we find;

$$\frac{1}{r^2} \frac{\partial}{\partial r} \left(r^2 \frac{\partial T}{\partial r} \right) + \frac{1}{r^2 \sin^2 \phi} \frac{\partial^2 T}{\partial \theta^2} + \frac{1}{r^2 \sin \phi} \frac{\partial}{\partial \phi} \left(\sin \phi \frac{\partial T}{\partial \phi} \right) + \frac{\dot{q}'''}{k} = \frac{1}{\alpha} \frac{\partial T}{\partial t} \quad \text{IVa.2.9}$$

For symmetrical conditions along θ and ϕ , temperature becomes only a function of distance r . Hence, Equation IVa.2.9 reduces to one-dimensional heat conduction in the spherical coordinate system:

$$\frac{1}{r^2} \frac{\partial}{\partial r} \left(r^2 \frac{\partial T}{\partial r} \right) + \frac{\dot{q}'''}{k} = \frac{1}{\alpha} \frac{\partial T}{\partial t} \quad \text{IVa.2.10}$$

2.1. Initial and Boundary Conditions

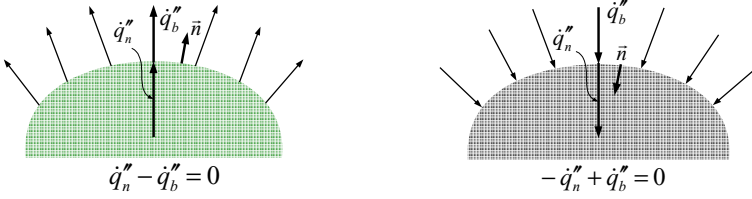
Once the differential equation for heat conduction is obtained, we need to have the boundary and the initial conditions to obtain the solution for a specific problem.

Boundary conditions (BC) are required whether we seek analytical or numerical solutions to steady state or transient problems. As Equation IVa.2.1 shows, the heat conduction equation is a second order differential equation in space and a first order differential equation in time. Hence, it requires two boundary conditions and one initial condition. Basically, there are four types of boundary conditions* that may be prescribed; temperature at the boundary, constant heat flux, thermal radiation, and a convection boundary. An insulated boundary is a special case of the constant heat flux boundary condition where $\dot{q}'' = 0$. Let's now discuss each of these four types.

Temperature BC: The prescribed surface temperature is referred to as the *Dirichlet* boundary condition. If the specified boundary temperature is T_s , then $T(\bar{r})_b = T_s$ where subscript b stands for boundary. The specified temperature at the boundary may not necessarily be a constant. Rather the prescribed temperature in general may vary as a function of time.

* Other more complicated boundary conditions include such cases as phase change and thermal resistance.

Heat flux BC is also known as the *Neumann* boundary condition. The prescribed heat flux may be into or away from the boundary. We assign a positive sign to the heat flux if it is towards the boundary and a negative sign if it leaves the boundary. Hence, for a heat flux BC we write $\pm \dot{q}_n'' \pm \dot{q}_b'' = 0$, where \dot{q}_n'' is the heat transfer by conduction in the solid at the boundary and \dot{q}_b'' is the prescribed heat flux at the boundary. Alternatively, we can write $\pm [-k(\partial T / \partial n)_b] \pm \dot{q}_b'' = 0$, where n is the direction normal to the boundary. Note that if the heat flux at the boundary is prescribed as zero ($\dot{q}_b'' = 0$), it implies that the boundary is insulated. A zero heat flux is also an indication of temperature symmetry in a substance.



Radiation BC may be due to thermal radiation of the solid at the boundary or a prescribed radiation heat flux at the boundary. The effect of incoming thermal radiation is to raise the boundary temperature. This is different than a bombardment of solids with high-energy radiation, such as gamma heating, which results in internal heat generation in the solid, as discussed in Section 5.5.

Convection BC: Specification of a heat transfer coefficient at the boundary implies the exchange of heat by the conduction and convection mechanisms so that $\pm [-k(\partial T / \partial n)_b] \pm h(T_b - T_f) = 0$ where T_f is the fluid temperature at the boundary. A convection boundary condition is usually shown by h, T_f . Figure IVa.2.2 shows three examples for convection boundary conditions.

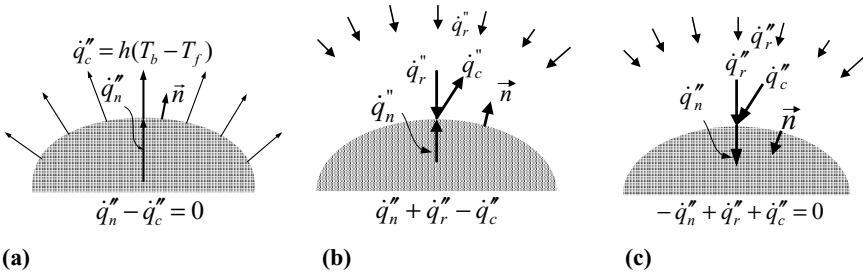


Figure IVa.2.2. Examples of convection and radiation boundary conditions

In case (a), heat brought to the boundary by conduction is carried away from the boundary by convection. In case (b), heat brought to the boundary by conduc-

tion and heat added to the boundary by radiation are carried away from the boundary by convection. In case (c), heat brought to the boundary by convection and heat added to the boundary by radiation are carried away from the boundary by conduction. For case (b), for example, an energy balance gives:

$$-k(\partial T / \partial n)_b + \dot{q}_r'' - h(T_b - T_f) = 0$$

As seen from this example, Kirchhoff's law also applies for steady state conditions, similar to the flow of electricity or flow of fluids in piping networks.

It is important to take advantage of any existing symmetrical condition for the temperature profile. This generally happens for substances having familiar geometry such as plate, parallelepiped, cylinder, or sphere as shown in Figure IVa.2.3. For uniform internal heat generation and external heat removal, we note that in the case of a plate, $dT/dx = 0$ at $x = 0$ and in the case of a cylinder and sphere, $dT/dr = 0$ at $r = 0$. This also implies that for a plate, for example, the mid-plane is at an adiabatic condition.

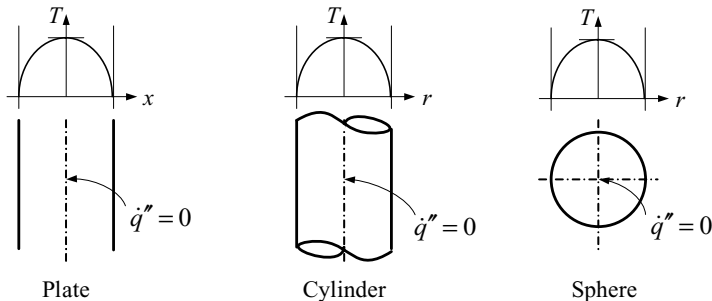


Figure IVa.2.3. Symmetrical temperature profiles in plates, cylinders, and spheres

Conduction BC is applied between two bodies. Equal temperature and equal heat flux apply at the point of contact so that for bodies A and B in perfect contact, $T_A = T_B$ and $-k_A dT_A/dn = -k_B dT_B/dn$.

Initial condition (IC) is required to find a solution for problems involving transient conduction because to find temperature at other points in time, temperature distribution in the substance must be known at time zero. If the time zero distribution is given as $T_o(\bar{r})$, the solution must satisfy $T(\bar{r}, t = 0) = T_o(\bar{r})$.

2.2. Determination of Heat Conduction in Various Dimensions

While heat conduction in solids is generally three dimensional, we often encounter cases in practice that conduction may be considered predominantly two or even one dimensional. The dimensionless number most helpful in this regard is the Biot number.

Biot number ($Bi = R_{cond}/R_{conv} = hL_c/k$), after J. B. Biot, is the ratio of two thermal resistances. Considering a solid with a convection boundary condition at its surface, the numerator is thermal resistance to conduction within the solid and the denominator is thermal resistance to convection across the fluid boundary layer. Also h , k , and L_c are heat transfer coefficient, thermal conductivity of a solid, and a characteristic length, respectively.

Lumped formulation of heat conduction is often used in evaluating the temperature response of objects to changes in the environmental temperature. This is the simplest type of analysis, providing useful information. On the other hand, since the entire object is represented by only one temperature, no knowledge about temperature distribution in the object can be obtained. Conditions for the applicability of the lumped-thermal capacity formulation are discussed in Section 3.

One-dimensional (1-D) heat conduction generally provides sufficient information about temperature distribution, and is the most commonly used technique in engineering applications. Due to the symmetry and large dimensions in two of the three directions in most cases, application of a 1-D analysis not only is a simplifying but also a reasonable assumption. Examples of such cases are shown in Figure IVa.2.4. A plate also referred to as a slab, is a solid, which is limited only in the x -direction. A long, slender cylinder is another example for which a 1-D conduction for obtaining temperature distribution is a reasonable assumption. In these solids, it is reasonable to assume that $T = f(x)$ and $T = f(r)$, respectively.

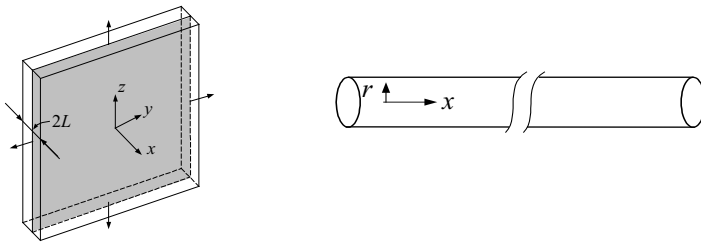


Figure IVa.2.4. Solids suitable for 1D heat conduction, a plate (slab) and a long slender rod

Regarding the latter example, let's consider the thin, solid cylinder of Figure IVa.2.5(a). If heat in this long solid cylinder is being generated uniformly while exposed to a convection boundary, the diffusion of heat is in the radial direction and for a given r , temperature is the same at any axial location (any x). Now let's assume that the solid cylinder is of finite length and rather than heat is being generated in the cylinder, it is added at one end as shown in Figure IVa.2.5(b). If this thin cylinder is fully insulated, the heat diffusion is basically in the axial direction. In this cylinder, for a given x , temperature is practically the same across any cross section.

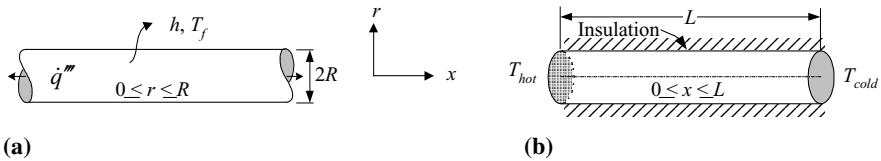


Figure IVa.2.5. One-dimensional heat conduction; (a) $T = f(r)$ and (b) $T = f(x)$

Example IVa.2.3. Find the rate of heat transfer if the cylinder in Figure IVa.2.5(b) is a stainless steel rod.

$k = 15 \text{ W/m}\cdot\text{K}$ ($8.7 \text{ Btu/h}\cdot\text{ft}\cdot\text{F}$), $L = 1 \text{ m}$ (3.3 ft), $T_h = 200 \text{ C}$ (392 F), $T_c = 100 \text{ C}$ (212 F), $A = 5 \text{ cm}^2$ (0.8 in^2).

Solution:

$$\dot{Q} = kA \frac{\Delta T}{L} = 15 \times (5 \times 10^{-4}) \frac{200 - 100}{1} = 0.75 \text{ W} = 8.7 \times (0.8 / 144) \frac{392 - 212}{3.3} = 2.6 \text{ Btu/h}$$

Two- and three-dimensional heat conduction must be used when an object cannot be accurately analyzed with the one-dimensional heat conduction method. For example, temperature distribution in a short, fat cylinder and in a parallelepiped, as shown in Figure IVa.2.6 requires a two- and a three-dimensional analysis, respectively. In these solids, temperature distribution is given as $T = f(x, r)$ and $T = f(x, y, z)$, respectively. In multi-dimensional problems, it is essential to choose a coordinate system that best fits the object geometry.

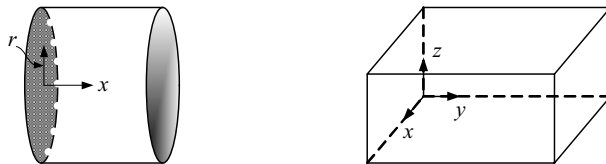


Figure IVa.2.6. Solids requiring multi-dimensional heat conduction, a short cylinder and a parallelepiped

3. Analytical Solution of Heat Conduction Equation

Due to the importance of analytical solutions, this topic is discussed first, followed by the discussion of numerical solutions. One of the important aspects of seeking analytical solutions is the fact that it enhances our intuition about the nature of the problem. The understanding of how to formulate a problem, what to expect, and how to interpret the results becomes an asset when using numerical methods for problems that are not amenable to analytical solutions. The term *analytical solution* refers to a solution found by mathematical modeling of the problem, which

provides an exact answer. Despite our preference to seek analytical solutions in closed form, and the availability of many mathematical techniques for solving problems in conduction heat transfer, analytical solutions are not always possible. This is due to the involved complexities such as multi-dimensional conduction in complex geometries with temperature dependent properties. In such cases, numerical methods are employed. The disadvantage of numerical methods is that every problem has to be modeled and solved separately. Analytical solutions not only provide exact answers in most cases, but may also provide applicable solutions to groups of similar problems. Another advantage of analytical solutions is in verifying the correctness and accuracy of numerical solutions of problems for which analytical solutions can be found.

Even if analytical solutions exist, for the sake of simplicity, there are occasions where we settle for solutions with some degree of approximation. For example, we can find an infinite series solution for temperature distribution as a function of time in a slab. If $Fo > 0.2$, we can show that the transient temperature distribution in the slab can be approximated by only the first term of the infinite series.

In the foregoing discussions, both steady state and transient problems are discussed. This allows us to learn about the inherent differences. We begin the discussion with the lumped formulations and proceed to one, two, and three-dimensional problems in various coordinates.

4. Lumped-Thermal Capacity Method for Transient Heat Conduction

The lumped-thermal capacity method is a convenient means of solving transient conduction problems. The term lumped implies that temperature distribution in the object is not a concern since the entire object is represented by only one temperature. This method of analysis is useful when we need to estimate the temperature response of an object suddenly exposed to a different temperature. By temperature response, we mean the change in temperature of the object as a function of time. To derive the relation for temperature versus time, consider the object shown in Figure IVa.4.1. This object is initially at a temperature of T_i when is suddenly exposed to a temperature of T_f . In this derivation, we make two important assumptions: a) the medium temperature T_f remains constant and is not affected by the energy transfer with the object and b) heat transfer between the object and the medium is due only to heat convection from the object to the medium. To find the governing equation, we may derive the equation directly from the conservation equation for energy, using the control volume as shown in Figure IVa.4.1. If the body is hotter than the environment ($T_i > T_f$), then the rate of internal energy depletion of the object is due to the heat loss to the environment.

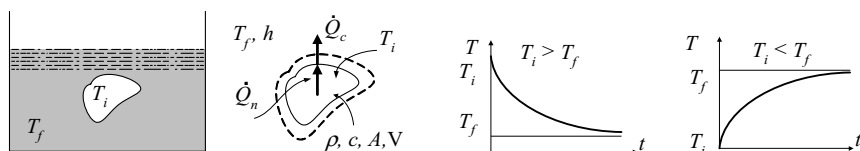


Figure IVa.4.1. Sudden exposure of an object to a lower or higher temperature medium

Using Equation IIa.6.4 where $\sum \dot{m}_i h_i = \sum \dot{m}_e h_e = \sum \dot{W} = \dot{q}'' = 0$ and $\sum \dot{Q} = -\dot{Q}_c$ we obtain:

$$-\dot{Q}_c = \frac{d(\rho c V T)}{dt}$$

where ρ , c , V , and T are density, specific heat, volume and temperature of the object, respectively. If we substitute for the convection heat transfer, $\dot{Q}_c = hA(T - T_f)$, we obtain:

$$\frac{dT}{dt} = -\frac{1}{\rho c V} [hA(T - T_f)] \quad \text{IVa.4.1}$$

where h and A are the heat transfer coefficient at the boundary and the heat transfer area of the object, respectively. To find the solution to this first order linear differential equation, we may introduce a change in function as $\theta = T - T_f$. Since T_f remains constant $dT/dt = d(T - T_f)/dt = d\theta/dt$. Substituting for T in terms of θ in Equation IVa.4.1 and integrating yield:

$$\int_{\theta_0}^{\theta} \frac{d\theta}{\theta} = - \int_{t=0}^t \left(\frac{hA}{\rho c V} \right) dt$$

where θ_0 is obtained by applying the initial condition $T(t=0) = T_0$. Thus, $\theta_0 = T_0 - T_f$ is a known value. We find the object temperature as a function of time by carrying out the integral and substituting for θ and θ_0 in terms of T , T_0 , and T_f :

$$T(t) = T_f + (T_0 - T_f)e^{-t/\tau} \quad \text{IVa.4.2}$$

where the constant in this solution represents:

$$\tau = \frac{\rho c V}{hA} \quad \text{IVa.4.3}$$

Note that τ , known as the *time constant* of the object, depends on both properties of the object (density, specific heat, and geometry) and heat transfer coefficient at the boundary. The time constant indicates how quickly an object responds to a change in temperature. The numerator has units of energy per temperature and $1/hA$ represents thermal resistance. We can also derive a similar equation when the object is colder than the surroundings ($T_i < T_f$), as shown in last graph of Figure IVa.4.1. Whether the object is colder or warmer than the surroundings to which it is suddenly exposed, the object temperature reaches the temperature of the surroundings asymptotically.

The absolute value of the exponent in Equation IVa.4.2 increases with time resulting in the exponential term to diminish and temperature of the object to eventually reach T_f . The major assumption that allowed us to use this simple transient analysis is the uniform temperature distribution within the object. This in turn implies that the Biot number is much smaller than unity (i.e., the resistance to conduction is much smaller than the resistance to convection). Generally, for the lumped capacitance analysis to be valid, we should have $Bi = h(V/A)/k < 0.1$. The characteristic length appearing in the numerator of the Biot number for a slab is half of the slab thickness, for a long cylinder is half its radius, and for a sphere is one third of its radius.

Shown in Figure IVa.4.2 are three geometrically identical slabs ($k_1 \gg k_2 \gg k_3$) initially at temperature T_i and suddenly exposed to a convection boundary condition of h and T_f . Temperature gradients for these slabs are presented as functions of both space and time. In the first slab, thermal conductivity is so high that temperature anywhere within the slab can reasonably be considered the same. In the second slab, thermal conductivity is smaller by a factor of 10. We see that temperature varies noticeably within the slab. In the third slab, thermal conductivity is smaller by a factor of 100. In this case, temperature varies markedly within the slab.

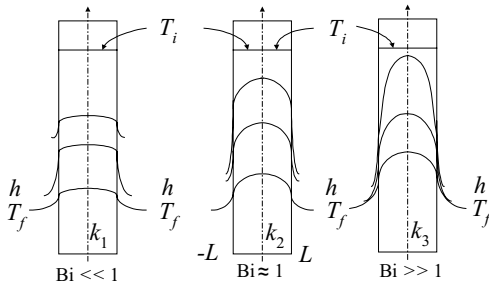


Figure IVa.4.2. Comparison of temperature profile in slabs with different Biot numbers

To determine the temperature response of objects with large Biot numbers, we need to use the conduction equation in one or more dimension as discussed later in this chapter.

Example IVa.4.1. A piece of copper wire is initially at 150 C when suddenly immersed in an environment at 38 C. Find the wire temperature after 1 minute, a) if the environment is water and b) if the environment is air. Assume highly polished copper ($\varepsilon = 0.02$) so that heat transfer is primarily due to convection.

Data: For copper at 150 C; $k = 374 \text{ W/m}\cdot\text{K}$, $c = 381 \text{ J/kg}\cdot\text{K}$, and $\rho = 8938 \text{ kg/m}^3$. Wire diameter is 1 mm, and the heat transfer coefficient for water and air is $h = 50 \text{ W/m}^2\cdot\text{K}$ and $h = 5 \text{ W/m}^2\cdot\text{K}$, respectively.

Solution: We first calculate the Biot number:

$$Bi = h(V/A)/k = h[(\pi d^2 L/4)/(\pi d L)]/k = hd/4k = 50 \times (1/1000)/(4 \times 374) = 3.3\text{E-}5$$

Since $Bi \ll 1$ we can use the lumped capacitance method. For immersion in water:

$$\tau_w = \rho c V / (hA) = 8938 \times 381 \times (\pi l^2/4)L / [50 \times (\pi l)L] = 17 \text{ s.}$$

$$T = 38 + 112 \times \exp(-1 \times 60/17) = 41 \text{ C}$$

For exposure to air:

$$\tau_a = \tau_w (h_w/h_a) = 170 \text{ s and } T = 38 + 112 \times \exp(-60/170) = 117 \text{ C.}$$

5. Analytical Solution of 1-D S-S Heat Conduction Equation, Slab

Our goal in this section is to solve the conduction equation in one-dimension (1-D) in Cartesian coordinates under steady state (S-S) condition with and without internal heat generation. In the subsequent sections, we solve 1-D, S-S problems in cylindrical and spherical coordinates. We then extend the solution method to multi-dimensional transient problems.

By 1-D we mean that the geometry of the object and the specified boundary conditions are such that the rate of heat transfer is predominantly one-dimensional and is negligible in the other two dimensions.

5.1. 1-D S-S Heat Conduction in Slabs ($\dot{q}''' = 0$)

The goal is to find the steady state ($\partial T / \partial t = 0$) temperature distribution in a slab with constant thermal conductivity ($\partial k / \partial T = 0$) and with no internal heat generation ($\dot{q}''' = 0$). Recall that we defined a slab as a plate with a finite dimension along the x -axis and infinite dimensions along the y - and z -axis. Applying the Cartesian coordinate system to the slab and for the one-dimensional heat transfer, the Laplacian simplifies to:

$$\nabla^2 T = \frac{d}{dx} \left(\frac{dT}{dx} \right) = \frac{d^2 T}{dx^2} \quad \text{IVa.5.1}$$

Substituting in Equation IVa.2.4 and simplifying terms that drop due to steady state and no internal heat generation, we get $d^2 T / dx^2 = 0$. The solution to this problem is readily found to be $T = c_1 x + c_2$ where coefficient c_1 and c_2 can be found by applying the boundary conditions. If surface temperatures are specified (Figure IVa.5.2(a)), the equation for temperature distribution inside the slab is determined as:

$$T = -(T_{s1} - T_{s2}) \frac{x}{2L} + \frac{1}{2} (T_{s1} + T_{s2}) \quad \text{IVa.5.2}$$

In this case, we can find the rate of heat transfer from the slab as $\dot{q} = kA(\Delta T / \Delta x)$
 $= kA(T_{s1} - T_{s2}) / 2L$.

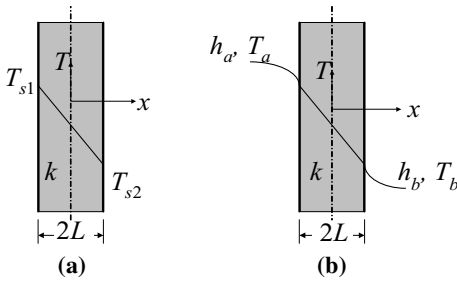


Figure IVa.5.2. (a) Slab with specified surface temperature and (b) Slab with a specified convection BC

For the case that convection heat transfer is specified at the boundaries, Figure IVa.2.1(b), determination of the constants is more involved. At $x = -L$, convection heat enters the node while conduction heat leaves the node, hence a heat balance at the left boundary according to our sign convention, yields:

$$h_a(T_a - T_{-L}) - \left[-k \frac{\partial T}{\partial x} \right]_{x=-L} = 0$$

At the right boundary, heat by conduction enters the node while heat by convection leaves the node:

$$\left[-k \frac{\partial T}{\partial x} \right]_{x=L} - h_b(T_L - T_b) = 0$$

Substituting for temperature and its derivative, constants c_1 and c_2 are determined as $c_1 = -h_a h_b (T_a - T_b) / c_3$ and $c_2 = T_a - [h_b(k + Lh_a)(T_a - T_b) / c_3]$ where $c_3 = h_a(k + Lh_b) + h_b(k + Lh_a)$. Regardless of the type of the boundary condition, the temperature profile in a one-dimensional slab with constant k at steady state and no internal heat generation is always a straight line. The rate of heat transfer for Figure IVa.5.2(b) where a convection boundary is specified is still given by $\dot{Q} = kA(T_{s1} - T_{s2}) / (\Delta x)$ where, in this case $\Delta x = 2L$.

Example IVa.5.1. Heat loss through an insulation ($k = 0.05 \text{ W/m}\cdot\text{C}$) is 125 W/m^2 . The temperature gradient across the insulation is 100 C . Find the thickness of the insulation.

Solution: From Fourier's law of conduction we have:

$\dot{Q} / A = 125 = k(T_{s1} - T_{s2}) / \Delta x$. Substituting for k and ΔT , the thickness is found from $125 = 0.05 \times 100 / \Delta x$. Therefore, $\Delta x = 0.04 \text{ m} = 4 \text{ cm}$.

In the next example, we examine temperature distribution in a plate, given the plate surface temperatures.

Example IVa.5.2. Surface temperature at the mid-plane of a carbon steel plate ($k = 30 \text{ Btu/h}\cdot\text{ft}\cdot\text{F}$) is maintained at 250 F. The plate thickness is 1 in and surface heat flux is $3250 \text{ Btu/h}\cdot\text{ft}^2$. Find the temperature of each face of this plate.

Solution: The temperature profile is linear, $T = c_1x + c_2$. If the plate thickness is $2L$ and x is on the left surface, at $x = L$, $T = T_{mp}$ and at $x = 0$, $\dot{q}'' + k(dT/dx)_{x=0} = 0$. Solving for c_1 and c_2 to get $T = T_{mp} + (\dot{q}''/k)(L - x)$, where mp stands for mid-plane. We then find $T_1(x = 0) = T_{mp} + (\dot{q}''L/k)$ and $T_2(x = 2L) = T_{mp} - (\dot{q}''L/k)$.

An alternative solution is to use $T_1 + T_2 = 2T_{mp}$ and $\dot{q}'' = k\Delta T / \Delta x$, where $\Delta x = 2L$. Substituting values, we find $T_1 + T_2 = 500$ and $T_1 - T_2 = 3250 \times (1/12)/30$. Solving this set, we obtain $T_1 = 254.5 \text{ F}$ and $T_2 = 245.5 \text{ F}$.

Thermal conduction in slabs subject to the convection boundary condition is solved in the next example.

Example IVa.5.3. A 1 in thick plate ($k = 30 \text{ Btu/h}\cdot\text{ft}\cdot\text{F}$) separates two rooms. The ambient temperature and associated heat transfer coefficient in one room are 150 F and $25 \text{ Btu/h}\cdot\text{ft}^2\cdot\text{F}$, respectively. The other room is at 50 F with a heat transfer coefficient of $15 \text{ Btu/h}\cdot\text{ft}\cdot\text{F}$. Find surface temperatures of the plate, temperature at the mid-plane, and heat flux through the plate between the rooms.

Solution: Temperature distribution in the plate is given as $T = c_1x + c_2$

$$c_3 = h_a(k + Lh_b) + h_b(k + Lh_a) = 25(30 + 15 \times 0.5/12) + 15(30 + 25 \times 0.5/12) = 1231.25$$

$$c_1 = -h_a h_b (T_a - T_b) / c_3 = -25 \times 15(150 - 50) / 1231.25 = -30.46 \text{ F/ft}$$

$$c_2 = T_a - [h_b(k + Lh_a)(T_a - T_b) / c_3] = 150 - [15(30 + 25 \times 0.5/12)(150 - 50) / 1231.25] = 112.18 \text{ F}$$

$$T = -30.46x + 112.18$$

Having the temperature profile, we find the surface temperatures; at $x = -0.5/12 = -0.042 \text{ ft}$, $T_{-L} = 113.45 \text{ F}$ and at $x = 0.5/12 = 0.042 \text{ ft}$ $T_{+L} = 110.91 \text{ F}$. At the mid-plane $T_{x=0} = 112.18 \text{ F}$.

Heat flux is found from $\dot{q}'' = k\Delta T / \Delta x$ where, $T_1 - T_2 = 2.54 \text{ F}$, thus

$$\dot{q}'' = 30 \times 2.54 / (1/12) = 914.4 \text{ Btu/h}\cdot\text{ft}^2.$$

The rate of heat transfer for Figure IVa.5.2(b) where the convection boundary condition is specified can be found from an electrical engineering analogy

$$\dot{Q} = \frac{T_a - T_b}{\sum R} \quad \text{IVa.5.3}$$

where

$$\sum R = R_a + R_{slab} + R_b$$

In this relation, the thermal resistance of the slab is $R_{slab} = \Delta x / kA$. For the convection boundary, thermal resistances for the left and the right boundaries are $R_a = 1/h_a A$ and $R_b = 1/h_b A$, respectively. Substituting, we can find the rate of heat transfer as:

$$\dot{Q} = \frac{T_a - T_b}{\frac{1}{h_a A} + \frac{\Delta x}{kA} + \frac{1}{h_b A}} \quad \text{IVa.5.4}$$

The concept of thermal resistance becomes even more helpful in problems involving a multi-layer wall.

For example, consider a composite wall in series (Figure IVa.5.3). In general, layers may consist of stacked conductors, as shown in Figure IVa.5.4. In such cases, we should use parallel thermal resistance as the flow of heat is divided between the stacks so that the stack with least thermal resistance conducts more heat.

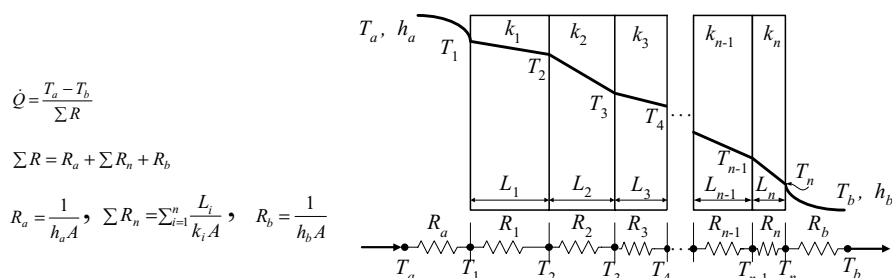


Figure IVa.5.3. Composite wall, all layers arranged in series

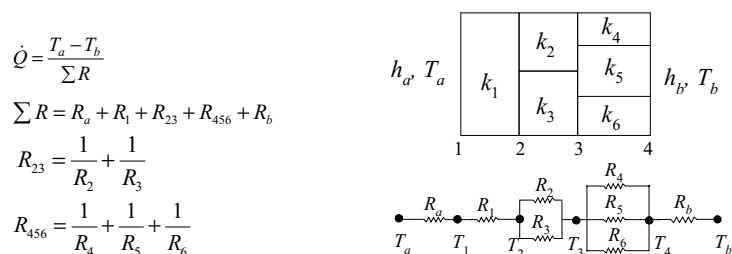


Figure IVa.5.4. A composite wall, which consists of stacked conductors arranged in series

Example IVa.5.4. The wall of a containment building consists of 6 mm steel liner and 50 cm concrete. The steel liner facing the interior is coated with 2 mm of primer and 3 mm of paint. The outside of the concrete is coated with 3 mm paint. Find the heat loss through the wall, treated as a slab. Ignore contact resistance.

Data: $T_a = 127^\circ\text{C}$, $T_b = 27^\circ\text{C}$, $k_{\text{concrete}} = 3.5 \text{ W/m}\cdot\text{C}$, $k_{\text{steel}} = 60 \text{ W/m}\cdot\text{C}$, $k_{\text{paint}} = 0.5 \text{ W/m}\cdot\text{C}$, $k_{\text{primer}} = 1.7 \text{ W/m}\cdot\text{C}$, $h_a = 120 \text{ W/m}^2\cdot\text{C}$, and $h_b = 25 \text{ W/m}^2\cdot\text{C}$.

Solution: We first calculate thermal resistances per unit surface area (1 m^2) of the wall from inside to outside:

$$R_a = 1/(h_a A) = 1/(120 \times 1) = 8.3\text{E-}3 \text{ C/W}$$

$$R_{\text{paint}} = \Delta x_{\text{paint}}/(k_{\text{paint}} A) = 3\text{E-}3/(0.5 \times 1) = 6\text{E-}3 \text{ C/W}$$

$$R_{\text{primer}} = \Delta x_{\text{primer}}/(k_{\text{primer}} A) = 2\text{E-}3/(1.7 \times 1) = 1.2\text{E-}3 \text{ C/W}$$

$$R_{\text{steel}} = \Delta x_{\text{steel}}/(k_{\text{steel}} A) = 6\text{E-}3/(60 \times 1) = 1\text{E-}4 \text{ C/W}$$

$$R_{\text{concrete}} = \Delta x_{\text{concrete}}/(k_{\text{concrete}} A) = 0.50/(3.5 \times 1) = 0.14 \text{ C/W},$$

$$R_{\text{paint}} = \Delta x_{\text{paint}}/(k_{\text{paint}} A) = 3\text{E-}3/(0.5 \times 1) = 6\text{E-}3 \text{ C/W}$$

$$R_b = 1/(h_b A) = 1/(25 \times 1) = 0.04 \text{ C/W}$$

Thus, $\Sigma R = 8.3\text{E-}3 + 6\text{E-}3 + 1.2\text{E-}3 + 1\text{E-}4 + 0.14 + 6\text{E-}3 + 0.04 = 0.2016 \text{ C/W}$

Therefore, we find $\dot{q}'' = (127 - 27)/0.2016 = 496 \text{ W/m}^2$. The rate of heat loss without any paint and primer increases by 7%.

5.2. 1-D S-S Heat Conduction in Slabs ($\dot{q}''' \neq 0$)

A slab with internal heat generation is shown in Figure IVa.5.5. The goal is to find the steady state ($\partial T / \partial t = 0$) temperature distribution in the slab, assuming constant thermal conductivity ($\partial k / \partial T = 0$). Equation IVa.2.4 simplifies to:

$$\frac{\partial^2 T(x)}{\partial x^2} + \frac{\dot{q}'''}{k} = \frac{1}{\alpha} \frac{\partial T(x)}{\partial t} = 0 \quad \text{IVa.5.5}$$

For a uniform volumetric heat generation rate, Equation IVa.5.5 can be integrated to obtain:

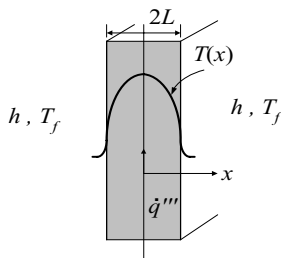


Figure IVa.5.5. Slab with internal heat generation

$$T(x) = -\frac{\dot{q}'''}{2k}x^2 + c_1x + c_2 \quad \text{IVa.5.6}$$

where constants c_1 and c_2 can be determined from a set of boundary conditions. Since a convection boundary condition of h , T_f is specified for both sides of the slab, we can find the constants by taking advantage of the fact that the center plane is adiabatic due to symmetry $-kdT/dx(0) = 0$:

$$-k \left[-\frac{\dot{q}'''}{2k}(2x) + c_1 \right]_{x=0} = 0$$

resulting $c_1 = 0$. This also implies that the center plane has the maximum temperature. We now use the second boundary condition, which specifies that the heat transfer by conduction at $x = L$ is removed by convection:

$$-k \frac{dT}{dx} \Big|_{x=L} - h(T|_{x=L} - T_f) = 0$$

Substituting for $T(L)$, from Equation IVa.5.6, we find coefficient c_2 as $c_2 = (\dot{q}'''L/h) + (\dot{q}'''L^2/2k) + T_f$. Thus, the profile is:

$$T(x) = T_f + \frac{\dot{q}'''}{2k}(L^2 - x^2) + \frac{\dot{q}'''L}{h} \quad \text{IVa.5.7}$$

Having the temperature profile for the slab with internal heat generation, we can find temperature of the center plane (i.e., at $x = 0$):

$$T(x=0) = T_{\max} = T_f + \dot{q}'''(L^2/2k + L/h)$$

If we substitute for T_f in Equation IVa.5.7 we find the temperature profile in terms of T_{\max} :

$$T(x) = T_{\max} - \frac{\dot{q}'''}{2k}x^2 \quad \text{IVa.5.8}$$

The surface temperature can be found by setting $x = L$:

$$T(L) = T_{\max} - \frac{\dot{q}'''}{2k}L^2 \quad \text{IVa.5.9}$$

The rate of heat transfer from each surface is equal to the rate of volumetric heat generation rate in half of the slab volume (i.e., $\dot{Q} = \dot{q}''' \times AL$) where A is the heat transfer area of the slab. If we substitute for \dot{q}''' from the Equation IVa.5.9 we get $\dot{Q} = 2(k\Delta T/L)$. This is twice the rate of heat transfer from an identical slab but with no internal heat generation.

5.3. 1-D S-S Heat Conduction in Composite Slabs ($\dot{q}''' \neq 0$)

If the slab with internal heat generation is made of fissile materials (referred to as fuel), sheath or cladding is used to contain the by-products of nuclear fission. Suppose the thickness of the slab representing the fuel material is $2L$ and the thickness of slab representing each cladding is δ . The goal is to find the steady state ($\partial T/\partial t = 0$) temperature distribution in the slab assuming constant thermal conductivity ($\partial k/\partial T = 0$) for both fuel and cladding but with internal heat generation ($\dot{q}''' \neq 0$) produced uniformly only in the inner slab (fuel) as shown in Figure IVa.5.6.

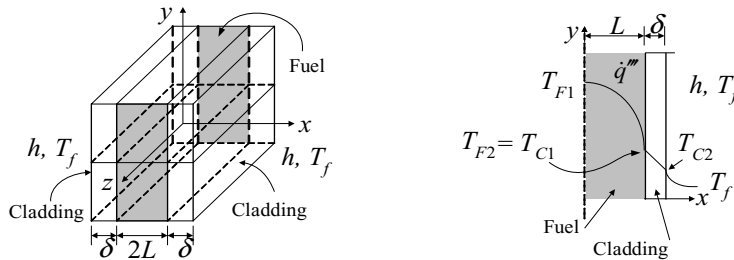


Figure IVa.5.6. Slab with internal heat generation and cladding

This is a two-region problem. For a specified convection boundary condition, we can determine the temperature profile and the rate of heat transfer by solving the heat conduction equation in the fuel region (shown by subscript F) and in the clad region (shown by subscript C). Due to symmetry, we only consider half of the composite slab. For the fuel region Equation IVa.5.6 is applicable:

$$T_F(x) = -\frac{\dot{q}'''}{2k_F}x^2 + c_1x + c_2, \quad 0 \leq x \leq L$$

For the clad region, where $L \leq x \leq L + \delta$ with δ being the clad thickness, Equation IVa.5.1 is applicable so that $d^2T_C/dx^2 = 0$ resulting in $T_C(x) = c_3(x - L) + c_4$ where we assumed that no heat is generated in the cladding. Since there are four unknowns (c_1 , c_2 , c_3 , and c_4) we need four boundary conditions. One boundary condition takes advantage of symmetry and sets heat transfer at the adiabatic yz -plane to zero. The second boundary condition takes into account heat transfer by convection at $x = L + \delta$. The third and the fourth boundary conditions deal with equal temperature and equal heat flux at the boundary between the two regions of fuel and cladding, assuming no contact resistance.

From the first boundary condition we find that $c_1 = 0$. Using the second boundary condition we write:

$$-k_C \frac{\partial T_C(x=L+c)}{\partial x} - h[T_C(x=L+c) - T_f] = 0$$

From the third boundary condition (i.e., equal temperatures at the common surface) we get:

$$T_F(x=L) = -\frac{\dot{q}'''}{2k_F}L^2 + c_1L + c_2 = T_C(x=L) + c_4$$

Finally from the fourth boundary condition (i.e., equal heat flux at the common surface) we obtain:

$$-k_F \frac{\partial T_F(L)}{\partial x} - [-k_C \frac{\partial T_C(L)}{\partial x}] = 0$$

Solving for c_1 through c_4 , the temperature profile for the fuel region, in dimensionless terms, becomes:

$$\frac{T_F(x) - T_f}{\dot{q}'''L^2 / 2k_F} = 1 - \left(\frac{x}{L}\right)^2 + 2\frac{k_F}{k_C} \left[\frac{\delta}{L} + \frac{k_C}{Lh} \right] \quad 0 \leq x \leq L$$

and for the cladding region:

$$\frac{T_C(x) - T_f}{\dot{q}'''L^2 / k_C} = 1 - \left(\frac{x}{L}\right) + \left[\frac{\delta}{L} + \frac{k_C}{Lh} \right] \quad L \leq x \leq L+c$$

Note that we neglected contact resistance and assumed that thermal conductivity of the fuel region is independent of temperature. For nuclear fuels, such as uranium, these are not accurate assumptions.

5.4. 1-D S-S Heat Conduction in Slabs ($\dot{q}''' = f(T)$)

So far we dealt with a uniform internal heat generation rate that remained constant regardless of the fuel temperature. However, due to a phenomenon known as the *Doppler effect*, as fuel temperature increases, there is a mechanism known as the *negative reactivity coefficient*, which tends to reduce the rate of fission and thereby the rate of heat generation. A simple way to account for the dependency of the internal heat generation rate on temperature is to assume a linear function so that $\dot{q}''' = c_1 + c_2T$ where c_1 and c_2 are known constants. By substituting this relation in Equation IVa.2.4, we obtain the Poisson equation:

$$\nabla^2 T + \frac{c_1 + c_2T}{k_F} = 0 \quad \text{IVa.5.10}$$

We can transform Equation IVa.5.10 to a Helmholtz equation by introducing a linear transformation as:

$$T' = T + (c_1 / c_2) \quad \text{IVa.5.11}$$

Upon substitution of Equation IVa.5.11 in Equation IVa.5.10, we get:

$$\nabla^2 T' + \frac{c_2}{k_F} T' = 0 \quad \text{IVa.5.12}$$

For the slab in Figure IVa.5.5, the equation becomes $d^2 T' / dx^2 + B^2 T' = 0$ where $B^2 = c_2 / k_F$. This is a second order linear differential equation. Since B^2 is positive, the answer is a trigonometric function (Chapter VIIa):

$$T'(x) = A_1 \sin(Bx) + A_2 \cos(Bx)$$

where coefficients A_1 and A_2 can be found from specified boundary conditions. For example, for the conditions of Figure IVa.5.5, A_1 must be zero due to symmetry hence, $T'(x) = A_2 \cos(Bx)$. Finding A_2 from the convection boundary, the temperature profile for a slab fuel with a temperature-dependent heat generation rate becomes:

$$T'(x) = \frac{hT_f}{h \cos(BL) - Bk_F \sin(BL)} \cos(Bx)$$

Example IVa.5.5. Find temperature at $x = L/2$ for a plate-type fuel.

Data: $c_1 = -0.01 \text{ kW/m}^3$, $c_2 = 125 \text{ kW/m}^3 \cdot \text{C}$, $k_F = 2 \text{ W/m} \cdot \text{C}$, $T_f = 288 \text{ C}$, $h = 8 \text{ kW/m}^2 \cdot \text{C}$, $2L = 0.6 \text{ cm}$.

Solution: Using the data, we first find the argument BL :

$$B = (c_2 / k_F)^{1/2} = (125/2)^{1/2} = 7.9 \text{ m}^{-1}. \text{ Thus } BL = 7.9 \times 0.003 = 0.237$$

$$T'(x) = \frac{8 \times 288}{8 \cos(0.237) - 7.9 \times 0.002 \sin(0.237)} \cos(7.9x) = 296 \cos(7.9x)$$

$$T_{L/2} \cong 296 \cos(0.237) \approx 294 \text{ C. We find } T_{L/2} = T'_{L/2} - (c_1 / c_2) \approx 294 \text{ C.}$$

5.5. Bombardment of Slabs with Energetic Radiation ($\dot{q}''' = f(x)$)

We now discuss an interesting conduction problem where the volumetric heat generation rate is a function of location. This occurs when materials are exposed to high-energy radiation. Consider exposure of a cold iron plate to solar radiation. Temperature penetration in the plate is a function of the radiation intensity at the plate surface exposed to radiation. Mathematically, this affects the solution via boundary condition at the exposed surface. By contrast, if the same plate is exposed to neutron or gamma radiation, the energetic beam penetrates deep into the plate, interacting with the iron atoms, and depositing energy in each interaction.

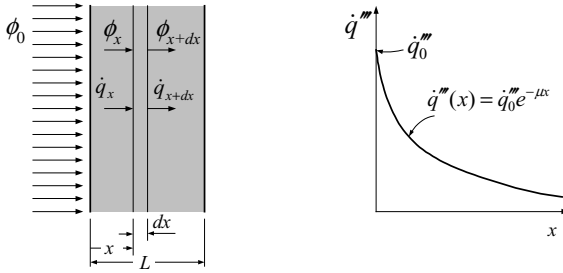


Figure IVa.5.7. Bombardment of a slab by high-energy radiation

The interaction of the high-energy radiation with the atoms of the medium attenuates the radiation intensity. Since the rate of interaction at any location in the medium is directly proportional to the number of particles in that location, it can be easily shown that the rate of interaction decreases exponentially. To demonstrate, let's say that ϕ represents the number of particles of the high energy radiation that have penetrated the medium to depth x per unit time and per unit surface area of the medium. We call this quantity, flux. If the particles are photons, ϕ represents the flux of gamma radiation and if the particles are neutrons, ϕ is neutron flux. We now consider the elemental control volume located at x and extended to dx . Particles that enter this control volume interact with the atoms of the material comprising the control volume. Since in each interaction a particle is removed, the number of particles leaving this control volume (at $x + dx$) has decreased by ϕ_{lost} . A particle balance yields $\phi_x = \phi_{x+dx} + \phi_{\text{lost}}$. To find the rate of particles which have had interaction (i.e., dropped out ϕ_{lost}) we introduce the absorption coefficient, μ . This coefficient represents the likelihood that a particle would have an interaction with an atom of the medium per unit distance of travel in the medium. Hence, in traveling dx , there is a chance equal to $\phi(\mu dx)$ that a particle would have an interaction in the medium. Substituting for $\phi_{\text{lost}} = \phi(\mu dx)$ and for $\phi_{x+dx} \equiv \phi_x + (d\phi/dx)dx$ in the particle balance, we find:

$$\phi_x = [\phi_x + (d\phi/dx)dx] + \phi_x(\mu dx) \quad \text{IVa.5.13}$$

Equation IVa.5.13 simplifies to $d\phi/dx = -\mu\phi$. Upon integration from $x = 0$ where particle flux is ϕ_0 to any x , the radiation flux in the medium is obtained as:

$$\phi(x) = \phi_0 e^{-\mu x} \quad \text{IVa.5.14}$$

The absorption coefficient (μ) introduced above is the probability of interaction per unit distance of travel. This is usually expressed in cm^{-1} . Values of μ for various shielding materials are given in Table A.V.1(SI)*.

* The type of interaction of the incident radiation with the atoms of the medium depends on the nature and the energy of the incident radiation as well as the material of the medium. If the radiation consists of neutrons, then the type of interaction may be absorption or scat-

If ΔE is the energy transferred to the atoms of the medium in each collision, then the rate of energy transfer is given as $I = \phi \Delta E$ where I has the units of energy per unit time and unit surface area. Hence, the amount of heat generated in the medium per unit volume is $\dot{q}''' = \mu I$, having the units of energy per unit time and unit volume. Substituting for I in terms of flux from Equation IVa.5.14, for gamma bombardment we obtain:

$$\dot{q}'''(x) = \dot{q}_0''' e^{-\mu x} \quad \text{IVa.5.15}$$

The governing equation for heat conduction can either be derived from an energy balance using the control volume of Figure IVa.5.7 or obtained from the simplified form of Equation IVa.2.4:

$$\frac{d^2 T}{dx^2} + \frac{\dot{q}_0'''}{k} e^{-\mu x} = 0 \quad \text{IVa.5.16}$$

Equation IVa.5.16 has an analytical solution. Integrating this equation twice, yields:

$$T(x) = -\frac{\dot{q}_0'''}{\mu^2 k} e^{-\mu x} + c_1 x + c_2 \quad \text{IVa.5.17}$$

where constants c_1 and c_2 in Equation IVa.5.17 are found from a specified set of boundary conditions. We shall consider two types of boundary conditions; specified surface temperature and specified heat convection.

Case 1. Specified Surface Temperature: If the surface temperatures are specified at $T(x=0) = T_0$ and $T(x=L) = T_L$ as boundary conditions, we can then find the solution as:

$$T(x) = T_0 + (T_L - T_0) \frac{x}{L} + \frac{\dot{q}_0'''}{\mu^2 k} \left[\left(e^{-\mu L} - 1 \right) \frac{x}{L} - \left(e^{-\mu x} - 1 \right) \right] \quad \text{IVa.5.18}$$

Since the slab temperature is maintained at both sides, there is a maximum temperature within the slab obtained by setting the derivative of temperature in Equation IVa.5.18 equal to zero $dT(x)/dx = 0$:

$$x_{\max} = -\frac{1}{\mu} \ln \left[\frac{\mu k}{\dot{q}_0''' L} (T_0 - T_L) + \frac{1}{\mu L} (1 - e^{-\mu L}) \right] \quad \text{IVa.5.19}$$

We then find the maximum temperature by substituting x_{\max} from Equation IVa.5.19 into Equation IVa.5.18. Since the flux decreases exponentially, about 90% of the total energy is usually absorbed in the 15% of the thickness of

tering. In this case, the probability is shown as Σ and is known as the macroscopic cross section. If the gamma rays are striking the surface of the medium, the type of interaction may be pair production, Compton scattering, or photo electric. For more information see El-Wakil and Lamarsh.

the medium, which is closer to the radiation source. Especially for thick mediums, term $e^{-\mu L}$ becomes exceedingly small and can be ignored.

Case 2. Specified Convection BC. In problems involving radiation heating, the medium is generally cooled from both sides by convection heat transfer. At $x = 0$, the convection boundary condition h_1, T_{f1} and at $x = L$, the convection boundary condition h_2, T_{f2} is specified. In this case, coefficients c_1 and c_2 are found from:

$$\text{At } x = 0, \quad -(-kdT/dx) - h_1(T - T_{f1}) = 0$$

$$\text{At } x = L, \quad -kdT/dx - h_2(T - T_{f2}) = 0$$

Solving for c_1 and c_2 , while ignoring $e^{-\mu L}$, we find the temperature profile in the medium as:

$$T - T_{f2} = -\frac{\dot{q}_0'''}{\mu^2 k} e^{-\mu x} - \frac{T_{f1} - T_{f2} + (1 + h_1 / \mu k)(\dot{q}_0''' / \mu h_1)}{L + (1/h_1 + 1/h_2)k} x +$$

$$(L + k/h_2) \frac{T_{f1} - T_{f2} + (1 + h_1 / \mu k)(\dot{q}_0''' / \mu h_1)}{L + (1/h_1 + 1/h_2)k}$$

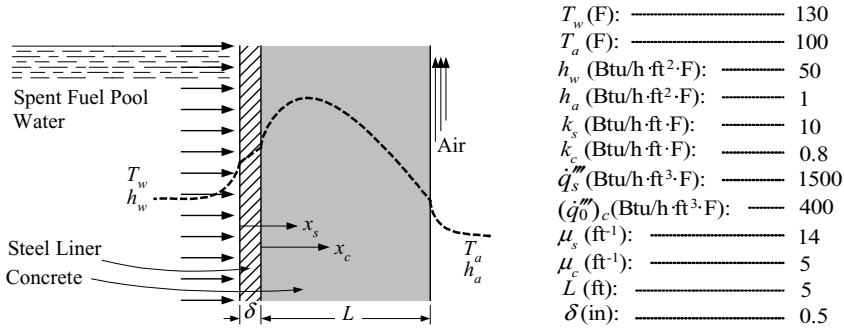
Similar to Case 1, the location of the maximum temperature is found from:

$$x_{\max} = -\frac{1}{\mu} \ln \left[\frac{\mu k}{\dot{q}_0'''} \frac{T_{f1} - T_{f2} + (1 + h_1 / \mu k)(\dot{q}_0''' / \mu h_1)}{L + (1/h_1 + 1/h_2)k} \right]$$

It is important to note that in both Cases 1 and 2, the total heat removed from the medium being bombarded with radiation must exactly match the heat generated in the medium by radiation (what if the heat removed is less than the heat generated?). Mathematically, the following balance at steady state operation must exist:

$$h_1(T - T_1) + h_2(T - T_2) = \int_0^L \dot{q}_0''' dx$$

Example IVa.5.6. In nuclear plants, the spent fuel assemblies are placed in a spent fuel pool (SFP) filled with borated water. The pool wall consists of a steel liner attached to thick concrete. It is important to maintain the humidity content of the concrete. Thus, we want to determine the maximum temperature in the concrete due to the pool wall being irradiated by gamma rays emitted from the spent fuel rods. In the solution we must account for heat generation in both steel and concrete. Use the given data and the following subscripts; a : air, c : concrete, s : steel liner, w : water. Ignore contact resistance.



Solution: Since the steel liner is thin, a constant \dot{q}_s''' is specified. Steel temperature is given by:

$$T_s = -(\dot{q}_s''' / 2k_s)x_s^2 + c_1x_s + c_2 \text{ and concrete temperature by}$$

$$T_c = -\frac{\dot{q}_0'''}{\mu_c^2 k_c} e^{-\mu_c x_c} + c_3 x_c + c_4. \text{ There are four unknown coefficients } c_1, c_2, c_3, \text{ and } c_4 \text{ and four boundary conditions at } x_s = 0, \text{ at } x_s = \delta, \text{ and at } x_c = L:$$

$$\text{At } x_s = 0, \text{ we have: } -[k_s dT_s/dx_s] - h_w(T_s - T_w) = 0$$

$$\text{At } x_s = \delta, \text{ we have: } T_s = T_c$$

$$\text{At } x_s = \delta, \text{ we have: } -[k_c dT_c/dx_c] - [-k_s dT_s/dx_s] = 0$$

$$\text{At } x_c = L, \text{ we have: } [-k_c dT_c/dx_c] - h_a(T_c - T_a) = 0$$

Representing $\alpha = \dot{q}_s''' / (2k_s)$ and $\beta = \dot{q}_0''' / (\mu_c^2 k_c)$, the four equations are found as:

$$k_s c_1 + h_w c_2 = h_w T_w$$

$$-\alpha \delta^2 + c_1 \delta + c_2 = -\beta + c_4$$

$$k_c(c_3 + \mu \beta) + k_s(-2\alpha \delta + c_1) = 0$$

$$(k_c + Lh_a)c_3 + h_a c_4 = h_a T_a$$

we find c_1, c_2, c_3 , and c_4 from:

$$\begin{pmatrix} k_s & h_w & 0 & 0 \\ \delta & 1 & 0 & -1 \\ k_s & 0 & k_c & 0 \\ 0 & 0 & k_c + h_a L & h_a \end{pmatrix} \begin{pmatrix} c_1 \\ c_2 \\ c_3 \\ c_4 \end{pmatrix} = \begin{pmatrix} h_w T_w \\ \alpha \delta^2 - \beta \\ 2\alpha \delta k_s - \mu \beta k_c \\ h_a T_a \end{pmatrix}$$

For the given set of data, we find $c_1 = -5.74$, $c_2 = 126$, $c_3 = -7.96$, and $c_4 = 146$. Hence, T_s and T_c become:

$$T_s = -83.33x_s^2 - 5.74x_s + 126 \text{ and } T_c = -20e^{-5x_c} - 7.96x_c + 146, \text{ respectively.}$$

The maximum temperature of $T_c = 140$ F occurs in the concrete at $x_c = 6$ in.

6. Analytical Solution of 1-D S-S Heat Conduction Equation, Cylinder

Determination of the heat transfer rate and temperature distribution in cylinders is essential in many practical applications. This includes heat transfer from hollow cylinders such as pipes and tubes as well as heat transfer from solid cylinders such as nuclear fuel rods. In the discussion that follows, we have divided the topic of heat transfer in cylinders into two sections based on whether internal heat generation exists in the cylinder or not. Each section is further divided into two subsections based on whether the cylinder is solid or hollow. The major distinction is the type of boundary conditions applied to each case.

6.1. 1-D S-S Heat Conduction in Hollow Cylinders ($\dot{q}''' = 0$)

Shown in Figure IVa.6.1 is a pipe with inside radius of r_1 and an outside radius of r_2 , carrying a fluid at the bulk temperature of T_{fa} . The pipe is exposed to the convection boundary of T_{fb} and h_b . If temperatures of both inside and outside fluids remain constant along the length of the pipe, the heat diffusion will be in the radial direction. While similar solution applies whether $T_{fa} > T_{fb}$ or $T_{fa} < T_{fb}$, in the derivation below we have assumed $T_{fa} > T_{fb}$.

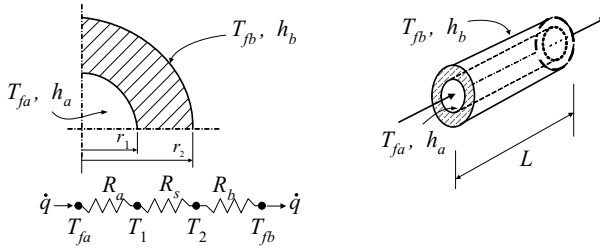


Figure IVa.6.1. Hollow cylinder without internal heat generation

Our goal is to determine the steady state ($\partial T / \partial t = 0$) temperature distribution in this hollow cylinder, assuming constant thermal conductivity ($\partial k / \partial T = 0$) and no internal heat generation ($\dot{q}''' = 0$). Since the thermal conductivity remains constant, the applicable equation in this case is Equation IVa.2.7. Since we are only concerned with heat diffusion in the r -direction, we use the Laplacian in polar coordinates as given by Equation IVa.2.8. For steady state, the Poisson equation reduces to:

$$\nabla^2 T = \frac{1}{r} \frac{d}{dr} \left(r \frac{dT}{dr} \right) = 0 \quad \text{IVa.6.1}$$

Integrating this equation, we find $dT/dr = c_1/r$. Hence, temperature in the cylinder, as a function of radius, is given as $T(r) = c_1 \ln r + c_2$. We find coefficient c_1 and c_2 from the boundary conditions for three cases.

Case 1. Temperature Boundary Condition. In this case, the inside and outside temperatures are specified (i.e., $T(r_1) = T_1$ and $T(r_2) = T_2$). Substituting these in the cylinder temperature profile yields:

$$c_1 \ln r_1 + c_2 = T_1$$

$$c_1 \ln r_2 + c_2 = T_2$$

We find c_1 and c_2 from this set of equations. By back substitution in the temperature profile, we get:

$$T(r) = T_1 - \frac{T_1 - T_2}{\ln(r_2 / r_1)} \ln(r / r_1)$$

To find the rate of heat transfer, we use Fourier's law for a region of the wall between r and $r + dr$:

$$\dot{Q} = -kA \frac{dT}{dr} = -k(2\pi r L) \frac{dT}{dr}$$

While temperature is a function of radius, the rate of heat transfer at steady state remains constant at any radius. Hence, we rearrange Fourier's law, and integrate from inside $r = r_1$ to outside $r = r_2$:

$$\int_{T_1}^{T_2} dT = -\frac{\dot{Q}}{2\pi k L} \int_{r_1}^{r_2} \frac{dr}{r}$$

Carrying out the integration, we find:

$$\dot{Q} = \frac{T_1 - T_2}{\frac{\ln(r_2 / r_1)}{2\pi k L}} \quad \text{IVa.6.2}$$

Using the electrical resistance analogy, we find that for cylinders, the thermal resistance is given as:

$$R_s = R_{\text{cylinder}} = \frac{\ln(r_2 / r_1)}{2\pi k L} \quad \text{IVa.6.3}$$

Case 2. Convection Boundary Condition. Having derived the rate of heat transfer between two radial locations in the cylinder and the corresponding thermal resistance, we now consider the case where convection boundary conditions are specified for the inside and outside of the cylinder. To find the equation for temperature profile in the cylinder, we first find coefficients c_1 and c_2 by using the convection boundary condition inside the cylinder:

$$h_a [T_{fa} - T(r = r_1)] - \left[-k \frac{\partial T(r = r_1)}{\partial r} \right] = 0$$

Substituting for temperature profile and its derivative we obtain;
 $h_a[T_{fa} - (c_1 \ln r_1 + c_2)] + kc_1 / r_1 = 0$. Similarly, from the convection boundary condition outside the cylinder we find that:

$$-k \frac{\partial T(r)}{\partial r} \Big|_{r=r_2} - h_b [T(r)_{r=r_2} - T_{fb}] = 0$$

Substituting for temperature profile and its derivative, we obtain:

$$kc_1 / r_2 + h_b [(c_1 \ln r_2 + c_2) - T_{fb}] = 0$$

Solving these two equations for c_1 and c_2 and substituting, we find the temperature profile in the cylinder as:

$$\frac{T(r) - T_{fa}}{T_{fa} - T_{fb}} = - \frac{\ln(r / r_1) + (k / r_1 h_a)}{(k / r_1 h_a) + \ln(r_2 / r_1) + (k / r_2 h_b)} \quad \text{IVa.6.4}$$

The inside surface temperature is:

$$\frac{T(r_1) - T_{fa}}{T_{fa} - T_{fb}} = - \frac{(k / r_1 h_a)}{(k / r_1 h_a) + \ln(r_2 / r_1) + (k / r_2 h_b)}$$

Similarly, the outside surface temperature of the cylinder can be found as:

$$\frac{T(r_2) - T_{fa}}{T_{fa} - T_{fb}} = - \frac{\ln(r_2 / r_1) + (k / r_1 h_a)}{(k / r_1 h_a) + \ln(r_2 / r_1) + (k / r_2 h_b)}$$

We can find the rate of heat transfer from an electrical analogy:

$$T_{fa} - T_1 = \frac{\dot{Q}}{h_a (2\pi r_1 L)}$$

$$T_1 - T_2 = \frac{\dot{Q}}{\frac{\ln(r_2 / r_1)}{2\pi k L}}$$

$$T_2 - T_{fb} = \frac{\dot{Q}}{h_b (2\pi r_2 L)}$$

Summing up, the intermediate temperatures cancel out. We then rearrange terms to find \dot{Q} as:

$$\dot{Q} = \frac{T_{fa} - T_{fb}}{\frac{1}{2\pi r_1 L h_a} + \frac{\ln(r_2 / r_1)}{2\pi k L} + \frac{1}{2\pi r_2 L h_b}} \quad \text{IVa.6.5}$$

Case 3. Steady State Heat Loss from Insulated Cylinders: This is similar to Case 2. Insulation of piping systems is necessary in power production for example, to reduce the rate of heat loss from the hotter fluid and in cryogenics to reduce the rate of heat transfer to the fluid. To accomplish this, as shown in Figure IVa.6.2, pipes are encapsulated in layers of insulation made of materials with low thermal conductivity. To determine the rate of heat transfer, we extend the method of Case 2 by writing the boundary temperatures in terms of total rate of heat transfer and the related thermal resistance and add them up to obtain:

$$\dot{Q} = \frac{T_{fa} - T_{fb}}{\frac{1}{2\pi_1 L h_a} + \frac{\ln(r_2/r_1)}{2\pi k_1 L} + \frac{\ln(r_3/r_2)}{2\pi k_2 L} + \frac{1}{2\pi_3 L h_b}} \quad \text{IVa.6.6}$$

$$\dot{Q} = \frac{T_a - T_b}{\sum R}$$

$$\sum R = R_a + \sum R_n + R_b$$

$$R_a = \frac{1}{h_a A_a}, \quad \sum R_n = \sum_{i=1}^{n-1} \frac{\ln(r_{i+1}/r_i)}{2\pi k_i L}, \quad R_b = \frac{1}{h_b A_b}$$

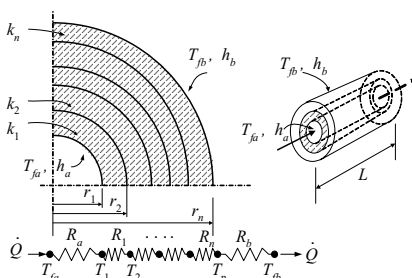


Figure IVa.6.2. Reduction of heat loss through pipe wall with multiple layers of insulation

Example IVa.6.1. A layer of paint and 3 layers of insulators cover a pipe carrying steam. Find the rate of heat loss to ambient.

No.	Region	d_i (in)	d_o (in)	k (Btu/ft·h·F)
1	Pipe	24.0	28.0	10.0
2	Paint	28.0	28.05	0.50
3	Insulator	28.05	40.0	0.03
4	Insulator	40.0	50.0	0.02
5	Insulator	50.0	55.0	0.01

Other data are specified as: $T_{fa} = 650$ F, $h_a = 500$ Btu/ft²·h·F, $h_b = 5$ Btu/ft²·h·F, $T_{fb} = 75$ F, and $L = 400$ ft.

Solution: Thermal resistances from inside to outside are as follows:

Pipe bulk to wall: $R_{f,a} = 1/(\pi d_i L h_a) = 1/[\pi \times (24/12) \times 400 \times 500] = 7.95\text{E-}7$ h·F/Btu

Region 1: $R_{pipe} = \ln(r_1/r_i)/(2\pi k_{pipe} L) = \ln(28/24)/[2 \times \pi \times 10 \times 400] = 6.13\text{E-}6$ h·F/Btu

Region 2: $R_{paint} = \ln(r_2/r_1)/(2\pi k_{paint} L) = \ln(28.05/28)/[2 \times \pi \times 0.5 \times 400] = 1.42\text{E-}6$ h·F/Btu

Region 3: $R_1 = \ln(r_3/r_2)/(2\pi k_{ins. a} L) = \ln(40/28.05)/[2 \times \pi \times 0.03 \times 400] = 4.71\text{E-}3$ h·F/Btu

Region 4: $R_2 = \ln(r_4/r_3)/(2\pi k_{ins. b} L) = \ln(50/40)/[2 \times \pi \times 0.02 \times 400] = 4.44\text{E-}3$ h·F/Btu

Region 5: $R_3 = \ln(r_5/r_4)/(2\pi k_{ins. c} L) = \ln(55/50)/[2 \times \pi \times 0.01 \times 400] = 3.79\text{E-}3$ h·F/Btu

Loss to ambient: $R_{f,b} = 1./(\pi d_s L) h_b = 1./[\pi \times (55/12) \times 400 \times 5] = 3.47\text{E-}5 \text{ h-F/Btu}$

$\Sigma R = 7.95\text{E-}7 + 6.13\text{E-}6 + 1.42\text{E-}6 + 4.71\text{E-}3 + 4.44\text{E-}3 + 3.79\text{E-}3 + 3.47\text{E-}5 = 0.013 \text{ h-F/Btu}$

The thermal resistance is practically due to the three layers of insulation.

$\dot{Q}_{loss} = (T_{f,a} - T_{f,b})/\Sigma R = (650 - 75)/0.013 = 44,288 \text{ Btu/hr} = 13 \text{ kW.}$

Note that if there was no insulation,

$\dot{Q}_{loss} = (650 - 75)/(7.95\text{E-}7 + 6.13\text{E-}6 + 3.47\text{E-}5) = 4 \text{ MW!}$

Let's now consider the rate of heat transfer in a concentric or simple shell & tube heat exchanger as shown in Figure IVa.6.3.

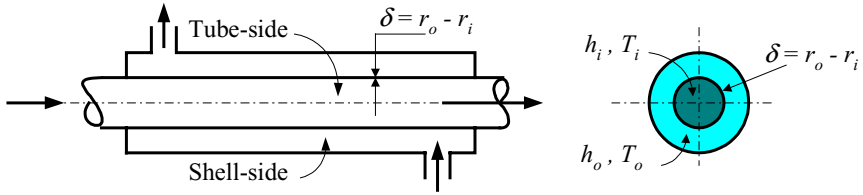


Figure IVa.6.3. Schematics of a concentric or simple shell & tube heat exchange

Applying the thermal resistance concept to this heat exchanger results in:

$$\dot{Q} = UA\Delta T \quad \text{IVa.6.7}$$

where

$$UA = \left[\frac{1}{2\pi r_i L h_i} + \frac{\ln(r_o / r_i)}{2\pi k_s L} + \frac{1}{2\pi r_o L h_o} \right]^{-1} \quad \text{IVa.6.8}$$

In Equation IVa.6.8, U is called the “overall heat transfer coefficient.” The value of U is based on the area it is associated with so that

$$UA = U_i (2\pi r_i L) = U_o (2\pi r_o L)$$

where U_i and U_o are referred to as the overall heat transfer coefficients based on the inside and outside tube diameter, respectively. Hence, U_o becomes:

$$U_o = [R_i + R_s + R_o]^{-1} \quad \text{IVa.6.8-1}$$

where $R_i = (1/h_i)(d_o/d_i)$, $R_s = \ln(d_o/d_i)/[d_o/(2k_s)]$, and $R_o = 1/h_o$ where k_s is thermal conductivity of the tube metal. Substituting we find;

$$U_o = \left[\frac{d_o}{d_i h_i} + \frac{d_o \ln(d_o / d_i)}{2k_s} + \frac{1}{h_o} \right]^{-1} \quad \text{IVa.6.8-2}$$

The overall heat transfer coefficient is an essential factor in the design and operation of heat exchangers.

6.2. 1-D S-S Heat Conduction in Solid Cylinders ($\dot{q}''' \neq 0$)

Solution for steady state temperature distribution in the axial direction in solid cylinders without internal heat generation is given by Equation IVa.5.2. This equation is applicable to an axially-insulated solid cylinder of length $2L$ where heat is added to one end and removed from the other end. The solution to steady state heat conduction in the radial direction for solid cylinders without internal heat generation is trivial as the solid cylinder has to be at uniform and constant temperature at any cross section. Considering cylinders with internal heat generation, our goal is to find the steady state temperature profile for two cases of solid and hollow cylinders. For the case of solid cylinders we analyze fuel rods in nuclear reactors. For hollow cylinders, we find temperature distribution in an annular fuel rod where coolant flows both inside and outside of the rod. The governing equation for both cases is Equation IVa.2.10 with $\partial T / \partial t = 0$.

For solid cylinders with internal heat generation we study temperature distribution in a nuclear fuel pellet. For light water reactors, such pellets are made of uranium dioxide (UO_2). A nuclear fuel rod (see Chapter I) consists of stacks of such pellets contained within cladding. Nuclear heat is produced when fuel rods in the core are exposed to neutron flux. In the discussion below, we analyze two cases. In Case 1 we consider a bare fuel rod to determine thermal resistance of a pellet. In Case 2 we analyze a fuel rod with cladding.

Case 1. Nuclear Fuel Pellet. Typical fuel pellet for PWRs is a right circular cylinder with both diameter and height being about 1 cm. The active length of a fuel rod is about 3.6 m or 144 in so that a fuel rod has as over 300 fuel pellets. To derive the thermal resistance of a fuel rod, let's assume that a bare rod is placed in the core. To find thermal resistance, we find the temperature gradient of the fuel (i.e., $T_{F1} - T_{F2}$):

$$\frac{1}{r} \frac{d}{dr} \left(k_F r \frac{dT_F}{dr} \right) + \dot{q}''' = 0 \quad \text{IVa.6.9}$$

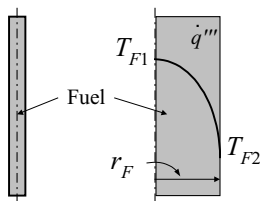


Figure IVa.6.4. A solid cylinder with internal volumetric heat generation

Thermal conductivity of UO_2 is temperature dependent however, replacing it with an average value allows us to integrate Equation IVa.6.9:

$$\int d\left(r \frac{dT_F}{dr}\right) = -\frac{\dot{q}'''}{k_F} \int r dr$$

This results in:

$$\frac{dT_F}{dr} = -\frac{\dot{q}'''}{2k_F} r + \frac{c_1}{r}$$

Upon further integration we obtain:

$$T_F(r) = -\frac{\dot{q}'''}{4k_F} r^2 + c_1 \ln(r) + c_2 \quad \text{IVa.6.10}$$

Coefficients c_1 and c_2 are found from boundary conditions. Coefficient c_1 must be zero for two reasons. First, at $r = 0$, temperature must be finite. Second, due to symmetry, temperature is a maximum at the centerline. Coefficient c_2 is found from temperature $T_F(r = 0) = T_{F1}$, resulting in a temperature profile of:

$$T_F(r) = T_{F1} - \frac{\dot{q}'''}{4k_F} r^2$$

Temperature gradient across the bare fuel rod is obtained by finding temperature at $r = r_F$:

$$T_{F1} - T_{F2} = \frac{\dot{q}'''}{4k_F} r_F^2 \quad \text{IVa.6.11}$$

Relating \dot{q}''' to the rate of heat transfer according to $(\pi r_F^2 L) \dot{q}''' = \dot{Q}$ and substituting in Equation IVa.6.11 yields:

$$\dot{Q} = 2k_F A \frac{T_{F1} - T_{F2}}{r_F} \quad \text{IVa.6.12}$$

Where, in Equation IVa.6.12, $A = \pi r_F L$ is the surface area. Thermal resistance of a pellet is found as:

$$R_F = \frac{r_F}{2k_F A} = \frac{1}{4\pi L k_F} \quad \text{IVa.6.13}$$

Note that by substituting for the volumetric heat generation rate in Equation IVa.6.11, we find:

$$T_{F1} - T_{F2} = \frac{\dot{Q}}{4\pi L k_F} = \frac{\dot{q}'}{4\pi k_F} \quad \text{IVa.6.14}$$

Equation IVa.6.14 is now in terms of the linear heat generation rate and shows that temperature difference across the fuel is only a function of \dot{q}' (the linear heat generation rate) and is independent of fuel diameter. The linear heat generation rate is a key factor in the design and operation of nuclear plants.

Case 2. Nuclear Fuel Rod. A fuel rod of a light water reactor consists of a hollow cylinder made of Zircaloy, filled with UO_2 pellets. The cylinder is about 12 ft long (Figure IVa.6.4). The space between the fuel and the clad is referred to as *gap*, being originally filled with helium and pressurized to several hundred psi. Fission gases released during the nuclear reaction also diffuse into the gap region further pressurizing the rod.

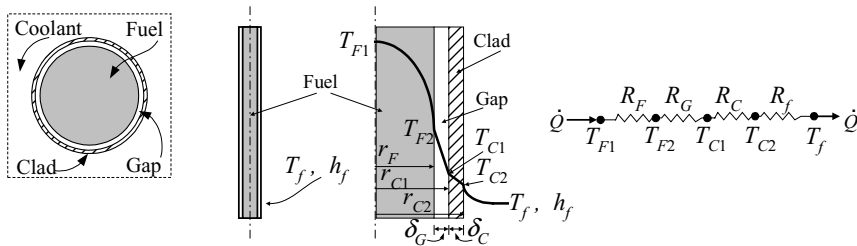


Figure IVa.6.5. Temperature profile in a cylindrical fuel rod

Our goal is to find the rate of steady state heat transfer. Due to symmetry, we consider temperature distribution only in one half of the fuel rod. At steady state operation, the rate of heat transfer is the same in all the fuel rod regions, the fuel pellet region, the gap region, and the cladding region. We use subscript *F* for fuel, *C* for cladding, *G* for Gap, and *f* for the coolant. To find the rate of heat transfer in each region, we use Fourier's law but rearrange the equation in terms of temperature difference. Starting from the fuel centerline and moving toward the coolant, the rate of heat transfer in each region of fuel, gap, cladding and coolant becomes:

$$\text{Temperature gradient in fuel:} \quad T_{F1} - T_{F2} = \frac{\dot{Q}}{4\pi L k_F}$$

$$\text{Temperature gradient in gap:} \quad T_{F2} - T_{C1} = \frac{\dot{Q}}{2\pi r_{C1} L h_G}$$

$$\text{Temperature gradient in clad:} \quad T_{C1} - T_{C2} = \frac{\dot{Q}}{[2\pi k_C L / \ln(r_{C2} / r_{C1})]}$$

$$\text{Temperature gradient in coolant:} \quad T_{C2} - T_f = \frac{\dot{Q}}{2\pi r_{C2} L h_f}$$

Summing up these relations, the intermediate temperatures cancel out and after rearrangement we get:

$$\dot{Q} = \frac{T_{F1} - T_f}{R_F + \frac{1}{2\pi r_G L h_G} + \frac{\ln(r_{C2}/r_{C1})}{2\pi k_C L} + \frac{1}{2\pi r_{C2} L h_f}} \quad \text{IVa.6.15}$$

where in Equation IVa.6.15, R_F is given by Equation IVa.6.13 and r_G and h_G are effective gap radius and heat transfer coefficient, respectively.

Example IVa.6.2. Find the centerline temperature of an average fuel rod in a PWR core.

Parameter	Value	Parameter	Value
Core power (MW):	2700	Clad inside diameter (in):	0.388
Number of fuel rods:	38,000	Gap thickness (in):	0.0075
Fuel rod length (ft):	12.2	Water temperature (F):	575
Clad outside diameter (in):	0.44	h_f (Btu/ft ² ·h·F):	6000
k_F & k_C (Btu/ft·h·F):	1 & 3	h_G (Btu/ft ² ·h·F):	1000

Solution: We find $d_{C2} = 0.44$ in, $d_{C1} = 0.388$ in and $d_{F2} = d_{C1} - 2\delta_{Gap} = 0.194 - 2 \times 0.0075 = 0.373$ in

We now find the individual thermal resistances in Equation IVa.6.15:

$$R_F = 1/(4\pi L k_F) = 1/(4 \times \pi \times 12.2 \times 1) = 6.53\text{E-}3 \text{ h·F/Btu}$$

$$R_G = 1/(2\pi r_{F1} L h_G) = 1/[(0.373/12) \times \pi \times 12.2 \times 1000] = 8.39\text{E-}4 \text{ h·F/Btu}$$

$$R_C = \ln(r_{C2}/r_{C1})/(2\pi L k_C) = \ln(0.44/0.388)/[2 \times \pi \times 12.2 \times 3] = 5.47\text{E-}4 \text{ h·F/Btu}$$

$$R_f = 1/(2\pi r_{C2} L h_f) = 1/[(0.44/12) \times \pi \times 12.2 \times 6000] = 1.18\text{E-}4 \text{ h·F/Btu}$$

$$\Sigma R = 6.53\text{E-}3 + 8.53\text{E-}4 + 5.56\text{E-}4 + 6.03\text{E-}5 = 8\text{E-}3 \text{ h·F/Btu}$$

The fuel centerline temperature is found from:

$$\dot{Q} = (T_{F1} - T_f)/\Sigma R$$

where total core power is: $\dot{Q} = (2700 \times 1000 \times 3412)/38000 = 0.2424\text{E}6 \text{ Btu/h}$

$0.2424\text{E}6 = (T_{F1} - 575)/8\text{E-}3$. Solving for T_{F1} , we find $T_{F1} = 2514 \text{ F}$

6.3. 1-D S-S Heat Conduction in Hollow Cylinders ($\dot{q}''' \neq 0$)

An annular nuclear fuel pellet is a good example for a hollow cylinder with internal heat generation. In this section, we analyze three cases of such fuel pellets.

Case 1. Two-Stream Coolant. Shown in Figure IVa.6.6 is the conceptual design of an annular fuel rod. Fluid flows both around the fuel (similar to a solid fuel rod) and through the central channel for further cooling. Our goal is to determine the temperature distribution in the fuel pellet. We use Equation IVa.6.10 while assuming an average thermal conductivity for the fuel. To find the coefficients c_1 and c_2 , we must use either of the following boundary conditions:

Surface Temperatures Specified. For specified fuel surface temperatures at r_i and r_o (i.e., T_{Fi} and T_{Fo}) we find the coefficients and upon substitution in Equation IVa.6.10, temperature profile in the bare annular fuel becomes:

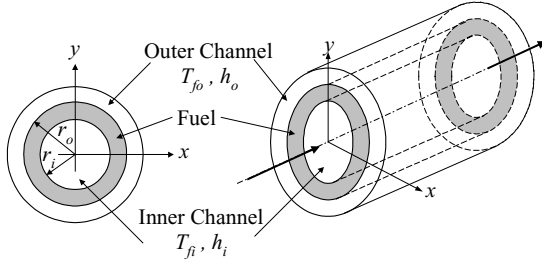


Figure IVa.6.6. A conceptual annular fuel rod with neither inner nor outer cladding

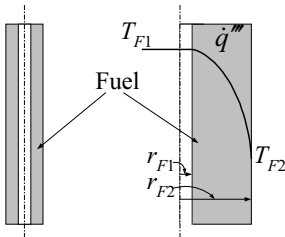
$$T_F(r) = T_{Fi} - \frac{\dot{q}'''}{4k_F}(r^2 - r_i^2) + \frac{T_{Fo} - T_{Fi} + (\dot{q}'''/4k_F)(r_o^2 - r_i^2)}{\ln(r_o/r_i)} \ln(r/r_i) \quad \text{IVa.6.16}$$

Convection Boundary Specified. For specified convection boundary, temperature distribution in the fuel is:

$$T_F(r) = T_{Fi} - \frac{\dot{q}'''}{4k_F}(r^2 - r_i^2) + \frac{T_{Fo} - T_{Fi} - (\dot{q}'''/4k_F)(r_o^2 - r_i^2) - (\dot{q}'''/2k_F)(r_i/h_i + r_o/h_o)}{k_F(1/r_i h_i + 1/r_o h_o) + \ln(r_o/r_i)} \ln(r/r_i)$$

Case 2. One-Stream Coolant. In this case, the annular fuel pellets are encased inside the clad and the fuel rod is cooled only by coolant flowing around the clad. To calculate the annular fuel thermal resistance, we consider the case of power production in a bare annular fuel rod. The answer to this case is also given by Equation IVa.6.10. To find coefficients c_1 and c_2 we use the following boundary conditions. At $r = r_{F1}$, there is no heat flux, hence $dT_F(r_{F1})/dr = 0$ and at $r = r_{F1}$, we have $T(r) = T_{F1}$. Using these boundary conditions, temperature distribution in the fuel becomes:

$$T_F(r) - T_{F1} = -\frac{\dot{q}'''}{4k_F}[(r^2 - r_{F1}^2) - r_{F1}^2 \ln(r/r_{F1})^2]$$



We can now calculate temperature gradient across the fuel pellet by taking $r = r_{F2}$ to obtain:

$$\Delta T = T_{F1} - T_{F2} = \frac{\dot{q}''' r_{F2}^2}{4k_F} [(1 - \zeta^2) + \zeta^2 \ln \zeta^2]$$

where $\zeta = r_{F1} / r_{F2}$. The volumetric heat generation rate is related to the rate of heat transfer from a bare annular fuel as:

$$\dot{Q} = \dot{q}''' \pi (r_{F2}^2 - r_{F1}^2) L = \dot{q}''' \pi r_{F2}^2 L (1 - \zeta^2)$$

Substituting for the volumetric heat generation rate in terms of the rate of heat transfer and rearranging:

$$\dot{Q} = \frac{\Delta T}{\left(1 - \frac{\zeta^2 \ln \zeta^2}{1 - \zeta^2}\right) / (4\pi L k_F)} \quad \text{IVa.6.17}$$

Thus, thermal resistance of an annular fuel cooled only from outside is therefore given by:

$$R = \left(1 - \frac{\zeta^2 \ln \zeta^2}{1 - \zeta^2}\right) / (4\pi L k_F) \quad \text{IVa.6.18}$$

If we compare Equation IVa.6.18 with Equation IVa.6.14 derived for a solid fuel, we conclude that for the same thermal conductivity and linear heat generation rate, the annular fuel operates at a lower temperature gradient. Similarly, for the same temperature gradient and thermal conductivity, the annular fuel can be operated at higher linear heat generation rate:

$$R = \frac{\dot{q}'_{\text{AnnularFuel}}}{\dot{q}'_{\text{SolidFuel}}} = \frac{1 - \zeta^2 (1 + \ln \zeta^2)}{1 - \zeta^2}$$

Case 3. *Annular Fuel Rod* consists of annular fuel pellets inside a clad as shown in Figure IVa.6.7. The rate of heat transfer is obtained from Equation IVa.6.15 but with R_F given by Equation IVa.6.18.

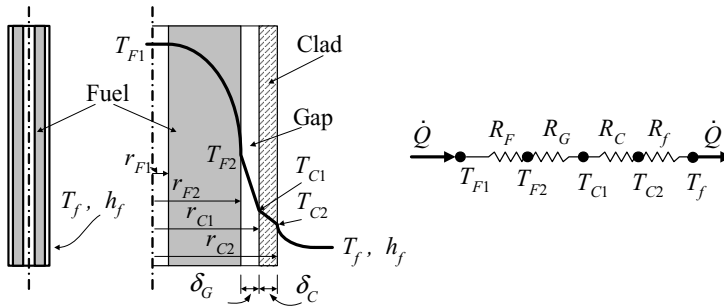
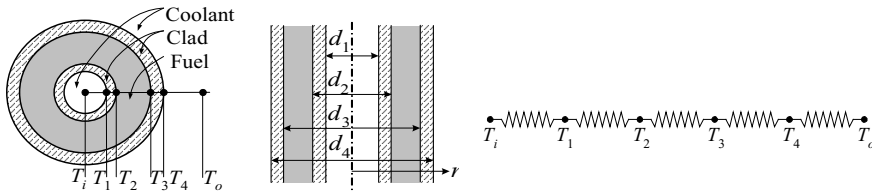


Figure IVa.6.7. Annular fuel rod with cladding

The next example deals with temperature distribution in an annular fuel rod with two-stream coolant and inner as well as outer cladding. In this example, we have assumed no contact resistance hence, no gap exists between the fuel and both inner and outer cladding.

Example IVa.6.3. Find the maximum temperature and its location in a two-stream annular fuel rod with inner and outer cladding. Data: $T_i = 325^\circ\text{C}$, $T_o = 300^\circ\text{C}$, $h_i = 6000 \text{ W/m}^2\cdot\text{C}$, $h_o = 4500 \text{ W/m}^2\cdot\text{C}$, $k_F = 3.5 \text{ W/m}\cdot\text{C}$, $k_C = 11 \text{ W/m}\cdot\text{C}$, $\dot{q}' = 10 \text{ kW/ft}$, $d_1 = 0.6 \text{ cm}$, $d_2 = 0.8 \text{ cm}$, $d_3 = 1.4 \text{ cm}$, and $d_4 = 1.6 \text{ cm}$.



Solution: This is a one-dimensional, steady state problem with heat generation in a two-stream annular fuel rod, having constant thermal conductivity and negligible contact resistance. Solution for temperature distribution in the inner cladding (i.e., for the region between r_1 to r_2) is found from Equation IVa.6.10:

$$T_C = c_1 \ln r + c_2 \quad r_1 \leq r \leq r_2$$

Similarly, Equation IVa.6.10 is the solution to temperature distribution in the fuel region:

$$T_F = -(\dot{q}''/4k_F)r^2 + c_3 \ln(r) + c_4 \quad r_2 \leq r \leq r_3$$

Finally, temperature distribution in the outer clad region (i.e., for the region between r_3 and r_4) is given by:

$$T_C = c_5 \ln r + c_6 \quad r_3 \leq r \leq r_4$$

There are 6 coefficients, which can be found from the following 6 boundary conditions:

Location	Boundary Condition	Location	Boundary Condition
$r = r_1$	$k_C dT_C/dr = h_i(T_C - T_i)$	$r = r_3$	$T_F = T_C$
$r = r_2$	$T_C = T_F$	$r = r_3$	$-k_F dT_F/dr = -k_C dT_C/dr$
$r = r_2$	$-k_C dT_C/dr = -k_F dT_F/dr$	$r = r_4$	$-k_C dT_C/dr = h_o(T_C - T_o)$

Upon substitution we find;

$$\begin{pmatrix} h_i \ln r_1 - k_C / r_1 & h_i & 0 & 0 & 0 & 0 \\ \ln r_2 & 1 & -\ln r_2 & -1 & 0 & 0 \\ k_C / r_2 & 0 & -k_F / r_2 & 0 & 0 & 0 \\ 0 & 0 & \ln r_3 & 1 & -\ln r_3 & -1 \\ 0 & 0 & k_F / r_3 & 1 & -k_C / r_3 & 0 \\ 0 & 0 & 0 & 0 & h_o \ln r_4 + k_C / r_4 & h_o \end{pmatrix} \begin{pmatrix} c_1 \\ c_2 \\ c_3 \\ c_4 \\ c_5 \\ c_6 \end{pmatrix} = \begin{pmatrix} h_i T_i \\ -\dot{q}''' r_2^2 / 4k_F \\ -\dot{q}''' r_2 / 2 \\ \dot{q}''' r_3^2 / 4k_F \\ \dot{q}''' r_3 / 2 \\ h_o T_o \end{pmatrix}$$

Since $r_1 = 0.3$ cm, $r_2 = 0.4$ cm, $r_3 = 0.7$ cm, $r_4 = 0.8$ cm, and $\pi(r_3^2 - r_2^2)\dot{q}''' = \dot{q}'$ then

$$\dot{q}''' = \frac{\dot{q}'}{\pi(r_3^2 - r_2^2)} = \frac{(10 \text{ kW/ft} \times 1000 \text{ W/kW}) \times 3.2802 \text{ ft/m}}{\pi(0.7^2 - 0.4^2) \text{ cm}^2 \times 1\text{E-4 m}^2/\text{cm}^2} = 3.165\text{E8 W/m}^3 = 316.5 \text{ MW/m}^3$$

Substituting numerical values, the above matrix equation becomes:

$$\begin{pmatrix} -38521.5 & 6000 & 0 & 0 & 0 & 0 \\ -5.521 & 1 & 5.521 & -1 & 0 & 0 \\ 2750 & 0 & -875 & 0 & 0 & 0 \\ 0 & 0 & -4.9618 & 1 & 4.9618 & -1 \\ 0 & 0 & 500 & 1 & -1571.43 & 0 \\ 0 & 0 & 0 & 0 & -20352.4 & 4500 \end{pmatrix} \begin{pmatrix} c_1 \\ c_2 \\ c_3 \\ c_4 \\ c_5 \\ c_6 \end{pmatrix} = \begin{pmatrix} 0.1950\text{E7} \\ -0.36167\text{E3} \\ -0.63294\text{E6} \\ 0.110760\text{E4} \\ 0.110760\text{E7} \\ 0.1350\text{E7} \end{pmatrix}$$

Thus, $c_1 = 213.84$, $c_2 = 1697.94$, $c_3 = 1395.44$, $c_4 = 8443.67$, $c_5 = -255.46$, and $c_6 = -855.37$

Location of the maximum temperature is found from:

$$r(T_{\max}) = \sqrt{2c_3 k_F / \dot{q}'''}$$

and the maximum temperature itself is obtained from:

$$T_{\max} = -22.6r^2 + c_3 \ln[r(T_{\max})] + c_4$$

Substituting values, we find $r(T_{\max}) = 0.556$ cm and $T_{\max} = 1894.6$ C.

6.4. 1-D S-S Heat Conduction in Solid Cylinders ($\dot{q}''' = f(T)$)

If we can express $\dot{q}''' = c_1 + c_2 T$ then Equation IVa.2.8 for steady state conditions can be written as:

$$\frac{d^2 T'}{dr^2} + \frac{1}{r} \frac{dT'}{dr} + B^2 T' = 0 \quad \text{IVa.6.19}$$

Where $B^2 = c_2/k_f$. Equation IVa.6.19 is a Bessel differential equation having the solution of:

$$T'(r) = A_1 J_0(Br) + A_2 Y_0(Br)$$

Where J_0 and Y_0 are zero order Bessel functions of first and second kind, respectively. From symmetry we conclude that $A_2 = 0$ as Y_0 approaches infinity and r approaches zero. A_1 can be found from the boundary condition at the surface. Bessel functions are discussed in Section 3 of Chapter VIIb.

7. Analytical Solution of 1-D S-S Heat Conduction Equation, Sphere

We seek temperature distribution only in the radial direction due to the symmetry in the ϕ and θ directions. If such symmetry does not exit, we must find a multi-dimensional solution.

We consider several cases for steady state heat transfer in a sphere. These include temperature profile in hollow spheres with no heat generation, heat loss from insulated spheres, and temperature profile in solid and hollow spheres without and with volumetric heat generation.

7.1. 1-D S-S Heat Conduction in Hollow Spheres ($\dot{q}''' = 0$)

A spherical container holds a liquid at constant temperature (Figure IVa.7.1). We assume that the liquid is warmer than ambient and the heat loss is steadily supplemented by an electric heater, heating the liquid.

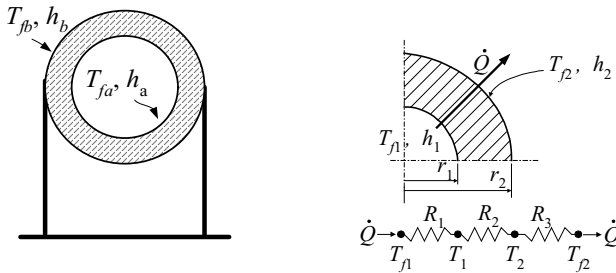


Figure IVa.7.1. Heat conduction in a hollow sphere

The resistances represent the internal convection, conduction through the sphere wall, and the external convection, respectively. To obtain thermal resistance of the sphere wall, we note that the same amount of heat passes through all the wall layers. Since the surface area of a layer at radius r is $4\pi r^2$:

$$\dot{Q} = -kAdT/dr = -k(4\pi r^2)dT/dr$$

We may now rearrange this equation to obtain:

$$dT = \dot{Q} dr / (4\pi k r^2)$$

Integrating between $T(r = r_1) = T_1$ and $T(r = r_2) = T_2$ results in:

$$\Delta T = \dot{Q} (1/r_1 - 1/r_2) / 4\pi k = \dot{q} R$$

where the sphere thermal resistance is given as $R_{\text{sphere}} = (1/r_1 - 1/r_2) / 4\pi k$.

Steady State Heat Loss from Insulated Spheres

We may extend the above result to find thermal resistance of a spherical wall and layers of insulation. These thermal resistances are summarized in Figure IVa.7.2.

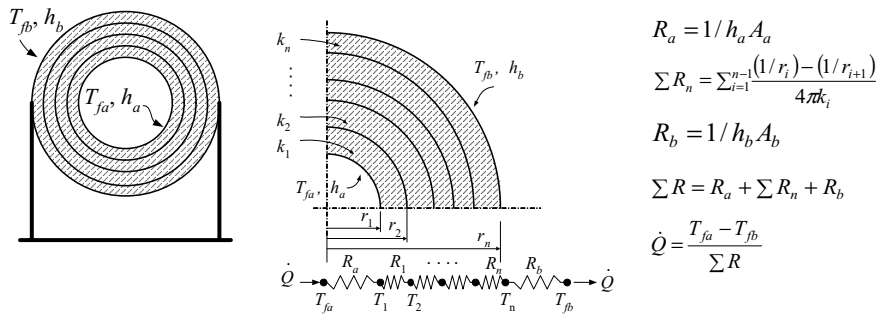


Figure IVa.7.2. Electric resistance analogy for heat conduction in spheres with multiple layers of insulation

Example IVa.7.1. Liquid at 180 C is stored in a steel spherical container, which is covered with three layers of insulation. Find the rate of heat loss. Data: $r_1 = 5$ m, $r_2 = 5.1$ m, $r_3 = 5.3$ m, $r_4 = 5.4$ m, $r_5 = 5.6$ m, $h_a = 500$ W/m²·C, $h_b = 100$ W/m²·C, $T_{fb} = 35$ C, $k_{\text{Carbon Steel}} = 55$ W/m·C, $k_1 = 0.05$ W/m·C, $k_2 = 0.03$ W/m·C, $k_3 = 0.08$ W/m·C.

Solution: We find thermal resistances as follows:

Inside sphere: $R_a = 1/[(\pi r_1^2) h_a] = 1/[(\pi \times 5^2) \times 500] = 2.55\text{E-}5$ C/W

$$\sum R_n = \sum_{i=1}^{n-1} \frac{(1/r_i) - (1/r_{i+1})}{4\pi k_i}$$

$$= \frac{(1/5) - (1/5.1)}{4\pi \times 55} + \frac{(1/5.1) - (1/5.3)}{4\pi \times 0.05} + \frac{(1/5.3) - (1/5.4)}{4\pi \times 0.03} + \frac{(1/5.4) - (1/5.6)}{4\pi \times 0.08}$$

$$\sum R_n = 5.67\text{E-}6 + 0.118 + 9.27\text{E-}3 + 6.58\text{E-}3 = 0.134 \text{ C/W}$$

Outside sphere: $R_b = 1/[(\pi r_s^2)h_b] = 1/[(\pi \times 5.6^2) \times 100] = 1\text{E-}4 \text{ C/W}$
 $\Sigma R = 2.55\text{E-}5 + 0.134 + 1\text{E-}4 \cong 0.134 \text{ C/W}$

Rate of heat transfer: $\dot{Q} = (T_{fa} - T_{fb})/\Sigma R = (180 - 35)/0.134 = 1.08 \text{ kW}$.

To find the temperature distribution in the wall of a bare hollow sphere without internal heat generation, we use Equation IVa.2.10 and retain only the first term in the left side of the equation:

$$\frac{1}{r^2} \frac{d}{dr} \left(r^2 \frac{dT}{dr} \right) = 0$$

When integrated we get $r^2 dT/dr = c_1$ or alternatively, $dT/dr = c_1/r^2$. Integration of this equation gives:

$$T = -c_1/r + c_2r \quad \text{IVa.7.1}$$

Coefficients c_1 and c_2 are found from a specified set of boundary condition. For a convection boundary of T_{fa} and h_a for the inside ($r = r_a$) and T_{fb} and h_b for the outside ($r = r_b$) of the sphere we write:

$$h_a [T_{fa} - (T)_{r=r_a}] = -k \left(\frac{dT}{dr} \right)_{r=r_a} \quad \text{and} \quad -k \left(\frac{dT}{dr} \right)_{r=r_b} = h_b [(T)_{r=r_b} - T_{fb}]$$

where we assumed that $T_{fa} > T_{fb}$. Upon substitution of Equation IVa.7.1 in the above boundary conditions, coefficients c_1 and c_2 are calculated and temperature profile in the sphere wall is obtained.

7.2. 1-D S-S Heat Conduction in Solid Spheres ($\dot{q}''' \neq 0$)

An example of one-dimensional heat conduction in spheres with internal heat generation is the fuel balls in a gas cooled nuclear reactor. Fission heat is generated inside the fuel ball and removed at the surface by the coolant. Temperature distribution in spherical fuels is the solution to Equation IVa.2.10 at steady state;

$$\frac{1}{r^2} \frac{\partial}{\partial r} \left(r^2 \frac{\partial T}{\partial r} \right) + \frac{\dot{q}'''}{k} = 0$$

This equation can be easily integrated to obtain $T = -(\dot{q}'''/6k)r^2 + c_1/r + c_2$ and, recognizing that at $r = 0$ temperature is finite, $c_1 = 0$. We obtain c_2 from an appropriate boundary condition.

Example IVa.7.2. Temperature at the center of a spherical fuel element is 2000 C. Find the surface temperature. Data: $d = 1 \text{ cm}$, $k_F = 3.5 \text{ W/m}^2\cdot\text{C}$, and $\dot{q}''' = 630 \text{ MW/m}^3$.

Solution: At $r = 0$ m, $T = 2000$ C hence, $c_2 = 2000$ C. The profile becomes:

$$T = -(\dot{q}'''/6k)r^2 + 2000$$

We now find temperature at $r = 0.5/100$ m, $T = -[630\text{E}6/(6 \times 3.5) \times (5\text{E}-3)^2 + 2000 = 1250$ C.

7.3. 1-D S-S Heat Conduction in Spheres ($\dot{q}''' \neq 0$)

For spherical fuel pellets where $\dot{q}''' = c_1 + c_2T$, the Helmholtz equation becomes:

$$\frac{d^2T'}{dr^2} + \frac{2}{r} \frac{dT'}{dr} + B^2T' = 0 \quad \text{IVa.7.2}$$

where $B_2 = c_2/k_f$. The solution to this linear second-order differential equation is:

$$T' = A_1 \frac{\cos(Br)}{Br} + A_2 \frac{\sin(Br)}{Br}$$

where coefficients A_1 and A_2 can be found from the boundary conditions. From symmetry we conclude that $A_2 = 0$. Having A_2 , we can find A_1 from the boundary conditions specified at the surface.

8. Analytical Solution of Heat Conduction Equation, Extended Surfaces

In Section IVa.3 we studied surfaces covered with multiple layers of insulation used to reduce the rate of heat transfer. In this section, we will study means of enhancing the rate of heat transfer, which is accomplished by the use of extended heat transfer surfaces or *fins*. There is a variety of designs for fins that can be categorized in three classes: longitudinal, circular, and spine. Each class has its own variety of designs depending on the fin profile. Figure IVa.8.1 shows four profiles of longitudinal fins.

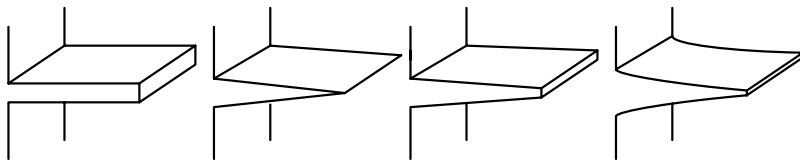


Figure IVa.8.1. Longitudinal fins of rectangular, triangular, trapezoidal, and parabolic profiles

The purpose of fin thermal analysis is to determine temperature gradient in the fin and the rate of heat transfer from the fin. We begin with the analysis of a longitudinal fin with variable area as shown in Figure IVa.8.2. In the derivation that follows, we assume that the fin is made of homogeneous material with constant thermal conductivity. We will also assume that the conduction-convection arrangement guarantees a low Biot number so that heat transfer can be treated primarily as one-dimensional. Additionally, the heat transfer coefficient and temperature of the convection boundary are assumed constant.

8.1. 1-D S-S Heat Conduction in Fins ($\dot{q}''' = 0$)

To be able to analyze fins using the one-dimensional heat conduction equation, we assume that both sides of the fin (parallel to the xy -plane) are insulated, or $L \gg l$. Since the direction of heat transfer is perpendicular to the shaded and the cross-hatched areas and these areas change as a function of x , we need to write the conservation equation of energy for the elemental control volume shown in the right side of Figure IVa.8.2. At steady state, the rate of energy leaving the top area by convection, the front area by conduction, and the bottom area by convection is equal to the rate of energy entering from the rear (shaded) area by conduction:

$$\dot{Q}_x = (\dot{Q}_x + \frac{d\dot{Q}_x}{dx} dx) + h dS (T - T_f)$$

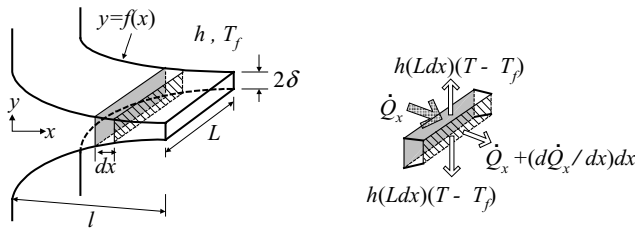


Figure IVa.8.2. Longitudinal fin with variable cross-sectional area

Two observations must be made at this point. First, we represented the whole control volume by only one temperature. Second, the surface area for convection heat transfer of the control volume (dA) is equal to the perimeter times the width of the control volume (i.e., $dS = 2(L + y)dx = Pdx$ where $P = 2(L + y)$ is the control volume perimeter). We now introduce an approximation by ignoring y compared with L . The control volume perimeter is, therefore, approximated as $P \approx 2L$. In other words, we have ignored heat transfer from the sides of the fin to be consistent with 1-D assumption. After substitution and simplification we find:

$$\frac{d\dot{Q}_x}{dx} + Ph(T - T_f) = 0$$

Where I_0 and K_0 are order-zero modified Bessel functions of the first and second kind, respectively. To find coefficients c_1 and c_2 , we use two boundary conditions. The first boundary condition deals with temperature at $x = 0$ which must be finite. However, as Figure VIIb.3.1 shows, K_0 approaches infinity as x approaches zero. Since temperature is finite, this implies that c_2 must be set equal to zero $c_2 = 0$. The second boundary condition is at $x = l$ (i.e. $T(l) = T_b$ where subscript b stands for base). Since $\theta = T - T_f$, then $\theta_0 = T_0 - T_f$. Substituting, we find $c_1 = \theta_0 / I_0(2ml^{1/2})$. Temperature profile in the fin then becomes:

$$\frac{T - T_f}{T_0 - T_f} = \frac{I_0(2mx^{1/2})}{I_0(2ml^{1/2})}$$

The rate of heat transfer from the entire fin is equal to the rate of heat diffusion at the base given by $\dot{Q}_{fin} = -kA_b dT/dx$. Upon substitution, we obtain:

$$\frac{\dot{Q}_{fin}}{k(bL)(T_0 - T_f)/l} = ml^{1/2} \frac{I_1(2ml^{1/2})}{I_0(2ml^{1/2})}$$

Case 2: Annular Fins with Rectangular Profile. Annular fins, as shown in Figure IVa.8.4, are another example of fins with a variable heat conduction area. We may derive the governing equation similar to Case 1 or use the result obtained for Case 1 in Equation IVa.8.1. The reader may perform the derivation by taking advantage of the energy balance in the elemental control volume of Figure IVa.8.4 and note that the rate of thermal energy steadily provided by the base, at radius r_b and temperature of T_b , is dissipated by convection to the environment by the fin. To use Equation IVa.8.1, the perimeter is found as $P = 2(2\pi r)$ and the heat conduction area as $A(r) = (2\pi r)(2\delta)$. Thus the governing equation becomes:

$$\frac{d^2\theta}{dr^2} + \frac{1}{r} \frac{d\theta}{dr} - m^2\theta = 0 \quad \text{IVa.8.3}$$

where $m^2 = h/k\delta$. Equation IVa.8.3 is a Bessel differential equation with the following solution:

$$T(r) - T_f = c_1 I_0(mr) + c_2 K_0(mr)$$

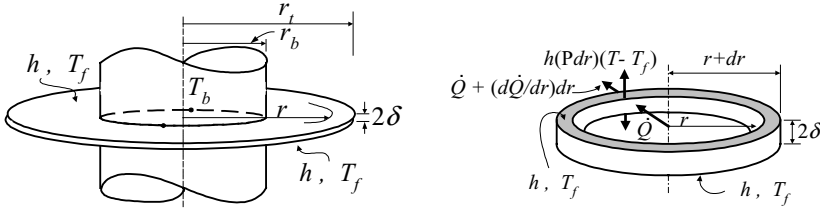


Figure IVa.8.4. Schematic of an annular fin with rectangular profile

To find the coefficients we use the boundary conditions at the base and at the tip of the fin. Temperature of the base, T_b is generally specified so that $T(r_b) = T_b$. For the second boundary condition, we should use the convection boundary condition at $r = r_t$ over the surface area of $S = 2\pi r_t(2\delta)$. However, a mathematically simpler means to accomplish this is to have an insulated boundary at the tip and add the surface area to the top and the bottom of the fin. This is acceptable if the heat transfer coefficient for the vertical surface is the same as for the horizontal surfaces. By adding the vertical surface area to the horizontal area, the new fin diameter becomes $r_t + \delta$ and the second boundary condition at $r' = r_t + \delta$ can be written as $dT/dr = 0$.

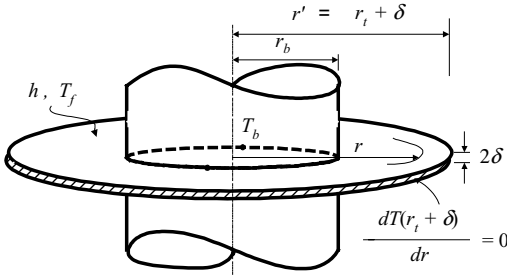


Figure IVa.8.5. Annular fin with insulated tip

We use these boundary conditions to find coefficients c_1 and c_2 . Upon substitution, the temperature profile in the fin is found as :

$$\frac{T - T_f}{T_b - T_f} = \frac{I_1(mr')K_0(mr) + K_1(mr')I_0(mr)}{I_0(mr_b)K_1(mr') + I_1(mr')K_0(mr_b)} \quad \text{IVa.8.4}$$

where I and K are the modified Bessel functions of the first and second kind. Some Bessel functions for $0 < x < 4$ are given in Table VIIb.3.1. The rate of heat transfer can then be calculated from:

$$\frac{\dot{Q}}{r_b \sqrt{hk\delta}(T_b - T_f)} = \left(\frac{4}{\pi}\right) \frac{I_1(mr')K_1(mr_b) + K_1(mr')I_1(mr_b)}{I_0(mr_b)K_1(mr') + I_1(mr')K_0(mr_b)} \quad \text{IVa.8.5}$$

Example IVa.8.1. Find temperature in an annular fin at $r = 6$ in. Data: $k = 10$ Btu/h·ft·F, $T_b = 400$ F, $T_f = 65$ F, $h = 50$ Btu/h·ft²·F, $r_b = 5$ in, $r_t = 9$ in and $\delta = 0.25$ in. Also find the total rate of heat transfer.

Solution: We use Equations IVa.8.4 to find T and Equation IVa.8.5 to find the rate of heat transfer. We first find $m = [50/(10 \times 0.25/12)]^{0.5} = 15.5 \text{ ft}^{-1}$ and then $r' = r_t + \delta = 9 + 0.25 = 9.25$ in so that $mr' = 11.95$ and $mr_b = 6.46$. We find the following Bessel functions:

Argument	I_0	I_1	K_0	K_1
$mr_b = 6.46$	0.254	-0.165	0.758E-3	0.814E-3
$mr = 7.75$	0.225	—	0.192E-3	—
$mr' = 11.95$	—	0.226	—	0.241E-5

$$T = 65 + (400 - 65) \frac{0.225 \times 0.192\text{E}-3 + 0.241\text{E}-5 \times 0.225}{0.254 \times 0.241\text{E}-5 + 0.226 \times 0.758\text{E}-3} = 150.6 \text{ F}$$

Similarly, for total rate of heat transfer we have:

$$\dot{Q} = (5/12) \sqrt{50 \times 10 \times 0.25/12} (400 - 65) (4/\pi) \frac{0.226 \times 0.814\text{E}-3 - 0.165 \times 0.241\text{E}-5}{0.254 \times 0.241\text{E}-5 + 0.226 \times 0.758\text{E}-3} = 612.5 \text{ Btu/h}$$

Without the fin, $\dot{Q} = 2\pi r_b \times 2\delta (T_b - T_f) = 2\pi(5/12)(2 \times 0.25/12)(400 - 65) = 36.54 \text{ Btu/h}$.

Case 3: Fins with Constant Heat Diffusion Area. Examples of such fins include longitudinal fins of rectangular profile and cylindrical spines as shown in Figure IVa.8.6. Since the conduction area is constant alongside the fin, the second term in Equation IVa.8.1 is zero and this equation simplifies to:

$$\frac{d^2\theta(x)}{dx^2} - \frac{P}{A} \frac{h}{k} \theta(x) = 0$$

In the case of a fin with a rectangular profile, the perimeter is $P = 2(b + 2\delta)$ and the heat diffusion area is $A = 2b\delta$. In the case of cylindrical spines $P = 2\pi\delta$ and heat diffusion area is $A = \pi\delta^2$. Therefore, m^2 for the fin with rectangular profile is given as:

$$m_{\text{rectangular}}^2 = \frac{(b + 2\delta)h}{b\delta k} \equiv \frac{h}{\delta k}$$

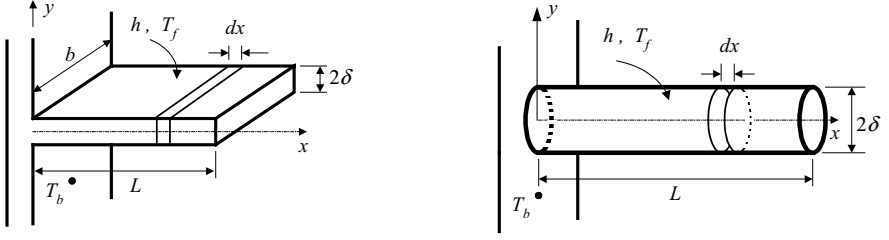


Figure IVa.8.6. Longitudinal fin of rectangular profile and cylindrical spine

and for cylindrical spines as $m_{\text{cylinder}}^2 = \frac{2h}{\delta k}$. Hence, the governing equation for such fins becomes:

$$\frac{d^2\theta(x)}{dx^2} - m^2\theta(x) = 0 \quad \text{IVa.8.6}$$

The general solution for Equation IVa.8.6 is given in Chapter VIIb as $\theta = c_1 e^{-mx} + c_2 e^{mx}$. Coefficients c_1 and c_2 can be found from the boundary conditions at the base, $x = 0$ and at the tip, $x = L$. At the base, the temperature must be equal to the specified base temperature of $T = T_b$. At the tip, three types of boundary conditions can be specified as follows.

BC, Type 1: the tip of the fin is insulated, hence $-k dT(L)/dx = 0$.

BC, Type 2: fin is so long that heat transfer through convection has caused tip temperature to reach T_f .

BC, Type 3: the tip of the fin is also losing heat to the environment by convection, $-kdT(L)/dx - hA(T - T_f) = 0$.

The solution for types 1 and 2 is left to the reader. As was discussed in Case 2, we can reduce type 3 to type 1. However, this case is much simpler than the annular fin and we can treat it with a convection boundary at the tip. The solution for temperature distribution in the fin for type 3 boundary condition is:

$$\frac{T - T_f}{T_b - T_f} = \frac{\cosh m(L - x) + (h/mk) \sinh m(L - x)}{\cosh mL + (h/mk) \sinh mL} \quad \text{IVa.8.7}$$

Having the temperature profile, we can find total rate of the fin heat loss from $\dot{Q} = -k(dT/dx)_{x=0}$:

$$\dot{Q} = \sqrt{hPkA}(T_b - T_f) \frac{\sinh mL + (h/mk) \cosh mL}{\cosh mL + (h/mk) \sinh mL} \quad \text{IVa.8.8}$$

8.2. 1-D S-S Heat Conduction in Fins ($\dot{q}''' \neq 0$)

If nuclear fuel rods are equipped with fins, an internal heat generation can take place in the fin due to the bombardment by γ radiation as discussed in Section IVa.5.5. Assuming such internal heat generation is uniform, Equation IVa.8.1 should then include an additional term to have:

$$\frac{d^2\theta(x)}{dx^2} + \left[\frac{1}{A(x)} \frac{dA(x)}{dx} \right] \frac{d\theta(x)}{dx} - \frac{P}{A(x)} \frac{h}{k} \theta(x) = -\frac{\dot{q}'''}{k} \quad \text{IVa.8.9}$$

Therefore, the general solution we obtained for various fin profiles is also applicable to the case that such fins have internal heat generation. However, the specific solution must also be found due to the addition of the constant term in the right side of Equation IVa.8.9 as explained next.

Case 1. Annular fin with internal heat generation. The governing equation is:

$$\frac{d^2\theta}{dr^2} + \frac{1}{r} \frac{d\theta}{dr} - m^2\theta = -\frac{\dot{q}'''}{k} \quad \text{IVa.8.10}$$

and the solution is given by El-Wakil is:

$$\frac{T - T_f}{T_b - T_f} = R_g + (1 - R_g) \frac{I_1(mr')K_0(mr) + K_1(mr')I_0(mr)}{I_0(mr_b)K_1(mr') + I_1(mr')K_0(mr_b)} \quad \text{IVa.8.11}$$

where I and K are the modified Bessel functions of the first and second kind. The rate of heat transfer from the fin from the base material is found from:

$$\frac{\dot{Q}}{r_b \sqrt{hk\delta}(T_b - T_f)} = (1 - R_g) \left(\frac{4}{\pi} \right) \frac{I_1(mr')K_1(mr_b) + K_1(mr')I_1(mr_b)}{I_0(mr_b)K_1(mr') + I_1(mr')K_0(mr_b)} \quad \text{IVa.8.12}$$

where R_g in these equations is a dimensionless number known as the *generation ratio* and is given by:

$$R_g = \frac{\dot{q}'''}{m^2 k (T_b - T_f)}$$

Case 2: Fins with Constant Heat Diffusion Area and Internal Heat Generation. Here, the governing equation simplifies to:

$$\frac{d^2\theta(x)}{dx^2} - m^2\theta(x) = -\frac{\dot{q}'''}{k} \quad \text{IVa.8.13}$$

To find the solution, we use the insulated tip boundary condition by extending the length in Figure IVa.8.6 by $L' = L + \delta$, resulting in:

$$\frac{T - T_f}{T_b - T_f} = R_g + (1 - R_g) \frac{\cosh m(L' - x)}{\cosh mL'} \quad \text{IVa.8.14}$$

The rate of heat transfer dissipated from the fin (from the base material) obtained by using Fourier's law $\dot{Q} = -kA dT/dx$. Taking the derivative of temperature profile and substituting, we find:

$$\dot{Q} = (1 - R_g) mkA(T_b - T_f) \tanh mL' \quad \text{IVa.8.15}$$

where $A_{\text{rectangular}} = b\delta$ and $A_{\text{cylinder}} = 2\pi\delta$. If there is no internal heat generation, $R_g = 0$.

The analytical solution to the two-dimensional heat conduction equation at steady state condition is discussed in Section IVa.9.2. It is demonstrated that a product solution in the form of $T(x, y) = X(x)Y(y)$ can be found for the Laplace equation $\partial^2 T / \partial x^2 + \partial^2 T / \partial y^2 = 0$.

9. Analytical Solution of Transient Heat Conduction

We can find analytical solutions to transient heat conduction for two types of one-dimensional problems. The first type includes the so-called *semi-infinite* solids. The second type includes solids having familiar geometries such as slab, cylinder, and sphere. Both types of problems are discussed in this section.

9.1. 1-D Transient Heat Conduction, Semi-infinite Solid

An interesting application of one-dimensional transient heat conduction is in finding the response of semi-infinite objects to sudden imposition of various boundary conditions at the surface. Although the semi-infinite solid is a mathematical concept, it can be used in many practical applications. Considering buried pipelines carrying water for example, we are interested in knowing the penetration depth of sudden freeze on the ground. This would determine how deep a water main should be buried for protection from freeze rupture. The ground can then be treated as a semi-infinite solid. The reason we are able to find an analytical solution is that we treat ground, where the pipe is buried, to be infinite in the y and z directions ($-\infty < y < \infty$ and $-\infty < z < \infty$) and semi-infinite only in the x -direction ($0 \leq x < \infty$) as shown in Figure IVa.9.1. The semi-infinite model implies that temperature deep inside the solid remains unaffected by the changes in temperature at the surface. This is used as a boundary condition. The governing equation for a semi-infinite solid is the 1-D form of Equation IVa.2.3 in the x -direction:

$$\alpha \frac{\partial^2 T}{\partial x^2} = \frac{\partial T}{\partial t} \quad \text{IVa.2.3}$$

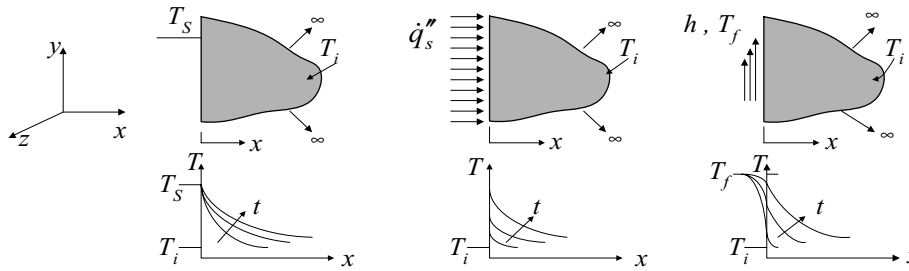


Figure IVa.9.1. Imposition of various boundary conditions at the surface of a semi-infinite solid

The solution requires two boundary conditions and one initial condition. The initial condition is the uniform temperature of the solid before the imposition of any instantaneous change at its surface, $T(x,0) = T_i$. One boundary condition deals with the heat transfer mechanism at the surface and the other deals with the fact that, far away from the surface, the temperature remains at its initial value, $T(\infty,t) = T_i$. The heat transfer mechanism at the surface is either in the form of imposition of an instantaneous temperature, or instantaneous exposure to either a heat flux or a convection boundary. We will use these three types of boundary conditions in three Cases A, B, and C as discussed below. For now, we try to find a solution to the 1-D form of Equation IVa.2.3. Among the several methods to solve this equation, one deals with the integral technique where a profile for temperature distribution is assumed. The coefficients are then found by setting the total rate of heat transfer equal to the rate of heat transfer at the surface. Another method is to use the Laplace transform. The approach discussed here uses the transformation of variables method.

Our goal is to find a single variable such as $s = f(x, t)$ so that we can express temperature only in terms of s rather than both x and t . We choose the function $f(x, t)$ as $s = x/g(t)$. At $x = 0$ and any t , variable s also becomes zero and at $t = 0$ and any x , variable s also becomes infinity. The latter constraint would represent the entire solid and will be used as an initial condition. Therefore, the goal is now to find the unknown function $g(t)$. Keeping this goal in mind, we will try to express temperature in Equation IVa.2.3 in terms of s . To do this, we need to find out the partial derivative of temperature with respect to x and t . The first derivative is found as:

$$\frac{\partial T}{\partial x} = \frac{\partial T}{\partial s} \frac{\partial s}{\partial x} = \frac{1}{g(t)} \frac{\partial T}{\partial s}$$

and the second derivative as:

$$\frac{\partial^2 T}{\partial x^2} = \frac{\partial}{\partial x} \left[\frac{1}{g(t)} \frac{\partial T}{\partial s} \right] = \frac{1}{g(t)} \left[\frac{\partial^2 T}{\partial s^2} \frac{\partial s}{\partial x} \right] = \frac{1}{g^2(t)} \frac{\partial^2 T}{\partial s^2} \quad \text{IVa.9.1}$$

Having defined the left side of Equation IVa.2.3 in terms of $g(t)$, we now seek to express the temperature derivative with respect to time (i.e., the right side of Equation IVa.2.3) in terms of the temperature derivative with respect to s :

$$\frac{\partial T}{\partial t} = \frac{\partial T}{\partial s} \frac{\partial s}{\partial t} = \left[\frac{\partial T}{\partial s} \right] \left[-\frac{x}{g^2(t)} \frac{dg(t)}{dt} \right] = \left[\frac{\partial T}{\partial s} \right] \left[-s \frac{1}{g(t)} \frac{dg(t)}{dt} \right] \quad \text{IVa.9.2}$$

We can now substitute Equations IVa.9.1 and Equation IVa.9.2 into Equation IVa.2.3 to obtain:

$$\frac{d^2 T}{ds^2} + 2s \frac{dT}{ds} \left[\frac{2}{4\alpha} g(t) \frac{dg(t)}{dt} \right] = 0 \quad \text{IVa.9.3}$$

Our goal of finding $g(t)$ to express temperature in terms of $s = x/g(t)$, is now reduced to finding $g(t)$ so that the bracket in Equation IVa.9.3 becomes equal to unity;

$$\frac{2}{4\alpha} g(t) \frac{dg(t)}{dt} = 1$$

This is a first order linear differential equation from which, $g(t)$ can be found as $g(t) = 2\sqrt{\alpha t}$. Having found $g(t)$ and consequently the variable s as $s = x/2\sqrt{\alpha t}$, we now return to Equation IVa.9.3 to find a solution for the second-order linear differential equation:

$$\frac{d^2 T / ds^2}{dT / ds} = -2s$$

This equation can be integrated to obtain:

$$\ln(dT / ds) = -s^2 + \ln c_1 \quad \text{IVa.9.4}$$

where c_1 is the constant of integration and is conveniently chosen as a logarithmic term. Equation IVa.9.4 can be written as:

$$dT/ds = c_1 \exp(-s^2) \quad \text{IVa.9.5}$$

which, upon integration, gives temperature distribution in the semi-infinite solid. To find the constants of integration, we need to use the boundary and initial conditions. There are generally three types of boundary conditions specified at the surface. These are discussed below as Cases 1, 2, and 3.

Case 1. *Imposition of an instantaneous temperature at the surface.* In this case, we investigate the response of a semi-infinite solid to a sudden change of temperature at its surface. To determine temperature, we integrate Equation IVa.9.5 from zero to any s :

$$\int_0^s \frac{dT}{ds} ds = T(s) - T(0) = c_1 \int_0^s e^{-s^2} ds$$

where $T(s = 0) = T(0, t) = T_S$ where T_S is the temperature of the semi-infinite solid at its surface. To find constant c_1 , we use the initial condition at $t = 0$ and any x . This implies that as $s \rightarrow \infty$, $T(s) = T_i$. Therefore;

$$T_i - T(0) = c_1 \int_0^\infty e^{-s^2} ds \quad \text{IVa.9.6}$$

as is shown in Section 3 of Chapter VIIb, $\int_0^\infty e^{-s^2} ds = \sqrt{\pi}/2$. By substituting into Equation IVa.9.6, we conclude that $c_1 = 2[T_i - T(0)]/\sqrt{\pi}$. Thus, the temperature distribution in the semi-infinite body becomes:

$$\frac{T(x, t) - T_S}{T_i - T_S} = \frac{2}{\sqrt{\pi}} \int_0^s e^{-s^2} ds \quad \text{IVa.9.7}$$

Therefore, we successfully managed to find the temperature distribution in a semi-infinite solid subject to an instantaneous change of temperature from T_i to T_S at its surface. The following integral is known as the *Gaussian error function* and is plotted in Figure IVa.9.3.

$$\text{Error function: } \frac{2}{\sqrt{\pi}} \int_0^s e^{-s^2} ds \quad \text{IVa.9.8}$$

The penetration of the surface disturbance at any distance x from the surface at any time t is given by:

$$S(x, t) = \frac{T(x, t) - T_S}{T_i - T_S} = \text{erf}\left(\frac{x}{2\sqrt{\alpha t}}\right) \quad \text{IVa.9.9}$$

To find the heat flux at the surface, we use Leibnitz's rule (Equation VIIc.1.26) to carryout differentiation of an integral. Note that in this case, the first and the last terms in the right side of Equation VIIc.1.26 are zero. Hence, the surface heat flux is found as:

$$\dot{q}_S'' = -k \frac{\partial T}{\partial x} = -k(T_i - T_S) \frac{2}{\sqrt{\pi}} e^{-\frac{x^2}{4\alpha t}} \frac{\partial}{\partial x} \left(\frac{x}{2\sqrt{\alpha t}} \right) = \frac{k(T_S - T_i)}{\sqrt{\pi \alpha t}} \quad \text{IVa.9.10}$$

Example IVa.9.1. The surface temperature of a large aluminum slab is suddenly raised and maintained at 135 C. The slab is originally at a uniform temperature of 30 C. Find the temperature at a depth of 20 cm and the surface heat flux 10 min after the event. Aluminum properties: $k = 204 \text{ W/m}\cdot\text{C}$ and $\alpha = 8.42\text{E-}5 \text{ m}^2/\text{s}$.

Solution: We first find the argument (arg) then the related function as follows:

$arg = x/2(\alpha)^{0.5} = 0.2/2(8.42\text{E-}5 \times 600)^{0.5} = 0.44$ and the corresponding value is $erf(0.44) = 0.466$

$$T = T_s + (T_i - T_s)erf(0.44) = 135 + (30 - 135) \times 0.466 = 86 \text{ C}$$

$$\dot{q}'' = k(T_s - T_i)/\sqrt{\pi\alpha t} = 204(135 - 30)/(\pi \times 8.42\text{E-}5 \times 600)^{1/2} = 53.77 \text{ kW}$$

Case 2. *Imposition of an instantaneous heat flux at the surface.* At any time, the temperature of any point within a semi-infinite solid, the surface of which is exposed to an instantaneous and uniform heat flux, is obtained from:

$$S(x, t) = T - T_i = \frac{2\dot{q}_s''\sqrt{\alpha t/\pi}}{k} \exp\left(\frac{-x^2}{4\alpha t}\right) - \frac{\dot{q}_s''}{k} \operatorname{erfc}\left(\frac{x}{2\sqrt{\alpha t}}\right) \quad \text{IVa.9.11}$$

where the complementary error function is defined as $\operatorname{erfc}(x) = 1 - \operatorname{erf}(x)$.

Case 3. *Imposition of an instantaneous convection at the surface.* In this case, the transient is a result of exposing the surface of a semi-infinite solid to convection heat transfer. The objective is to determine the penetration of convection temperature into the solid at a given time. The solution to this problem is given as:

$$S(x, t) = \frac{T - T_f}{T_i - T_f} = \operatorname{erf}\left(\frac{x}{2\sqrt{\alpha t}}\right) - \exp\left(\frac{hx}{k} + \frac{h^2\alpha t}{k^2}\right) \times \operatorname{erfc}\left(\frac{x}{2\sqrt{\alpha t}} + \frac{h\sqrt{\alpha t}}{k}\right) \quad \text{IVa.9.12}$$

Example IVa.9.2. The surface of a large steel slab is suddenly cooled with flowing air. Find temperature at a depth of 15 in, 1 hour after exposure to the cold air at the surface. Steel properties: $k = 25 \text{ Btu/ft}\cdot\text{h}\cdot\text{F}$ and $\alpha = 1.3\text{E-}4 \text{ ft}^2/\text{s}$. Air flows at $T_f = 65 \text{ F}$ and $h = 10 \text{ Btu/ft}\cdot\text{h}\cdot\text{F}$. Initial steel temperature is 850 F .

Solution: We first find the arguments then the values of the corresponding error functions:

$$arg_1 = x/2(\alpha)^{0.5} = (15/12)/2(1.3\text{E-}4 \times 3600)^{0.5} = 0.914,$$

$$\operatorname{erf}(arg_1) = 0.804$$

$$arg_2 = hx/k + h^2\alpha t/k^2 = 10 \times (15/12)/25 + 100 \times 1.3\text{E-}4 \times 3600/625 = 0.575,$$

$$\exp(arg_2) = 1.78$$

$$arg_3 = arg_1 + h(\alpha t)^{0.5}/k = 0.914 + 10 \times (1.3\text{E-}4 \times 3600)^{0.5}/25 = 1.187,$$

$$\operatorname{erfc}(arg_3) = 0.093$$

$$S(x, t) = \frac{T - 65}{850 - 65} = [0.804 - 1.78 \times 0.093] = 0.6385$$

Therefore, temperature at $x = 15$ in is found as:

$$T - T_f = (T_i - T_f) \times S(x, t). \text{ Substituting, } T = 65 + (850 - 65) \times 0.6385 = 566 \text{ F.}$$

Now that we have dealt with three types of boundary conditions for a semi-infinite solid, we will discuss two interesting aspects. First, we consider two semi-infinite solids brought in contact. Second, we analyze the response of a semi-infinite solid to a harmonically oscillating temperature boundary condition.

9.2. Semi-infinite Bodies in Contact

Experience shows that we can sense the relative temperature of various objects in a room by touching. While counterintuitive, we can explain this phenomena by treating our hand and the object we touch as semi-infinite solids in contact. Each semi-infinite solid is originally at uniform temperature, for example $T_{1,i}$ and $T_{2,i}$, respectively. When these solids are brought in perfect contact (Figure IVa.9.2), the interface must satisfy two boundary conditions for each solid. First, both solids must have the same temperature at the interface. Second, the heat flux leaving the warmer solid must be equal to the heat flux entering the colder solid. The assumption of perfect contact allows us to use a zero thermal resistance at the interface.

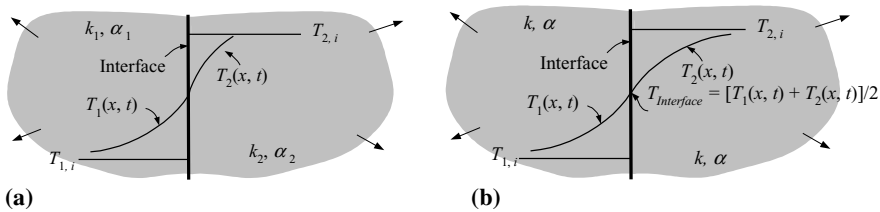
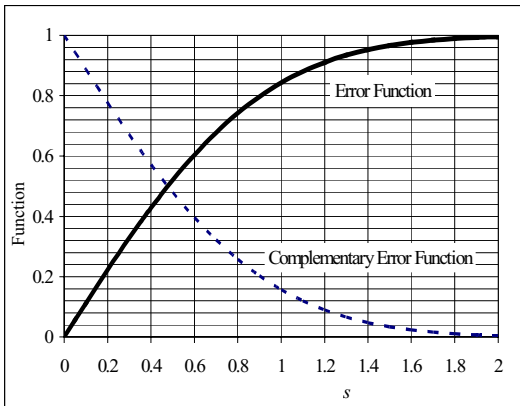


Figure IVa.9.2. Semi-infinite solids in perfect contact (a) $(\rho ck)_1 \neq (\rho ck)_2$ and (b) $(\rho ck)_1 = (\rho ck)_2$

Applying Equation IVa.9.10 and solving for the interface temperature, $T_{1,s} = T_{2,s} = T_s$, we find:

$$T_s = \frac{\sqrt{(\rho ck)_1} T_{1,i} + \sqrt{(\rho ck)_2} T_{2,i}}{\sqrt{(\rho ck)_1} + \sqrt{(\rho ck)_2}} \quad \text{IVa.9.13}$$

Equation IVa.9.13 indicates that the surface temperature approaches the temperature of solid, which has higher ρck . If both solids are made of the same material, then the interface temperature is $T_s = [T_{1,i} + T_{2,i}]/2$. This case is shown in Figure IVa.9.2(b).



s	erf	$erfc$
0	0	1
0.05	0.05637	0.94363
0.1	0.11246	0.88754
0.15	0.168	0.832
0.2	0.2227	0.7773
0.25	0.27633	0.72367
0.3	0.32863	0.67137
0.35	0.37938	0.62062
0.4	0.42839	0.57161
0.5	0.5205	0.4795
0.6	0.60385	0.39615
0.7	0.6778	0.3222
0.8	0.7421	0.2579
0.9	0.79691	0.20309
1	0.8427	0.1573
1.1	0.8802	0.1198
1.2	0.91031	0.08969
1.3	0.93401	0.06599
1.4	0.95228	0.04772
1.5	0.9661	0.0339
1.6	0.97635	0.02365
1.7	0.98379	0.01621
1.8	0.98909	0.01091
1.9	0.99279	0.00721
2	0.99532	0.00468

Figure IVa.9.3. Gaussian error function and complementary error function

Example IVa.9.3. Two blocks, treated as semi-infinite solids, are brought into perfect contact. The blocks are made of aluminum ($\alpha = 9.7\text{E-}5 \text{ m}^2/\text{s}$) and are initially at 0 C and 150 C. Find temperature at a depth of 11 cm in each block 2 minutes into the perfect contact.

Solution: Since both blocks are made of the same material ($k_A = k_B$), the slopes of the temperature profile are the same in the two blocks. Hence, $T_s = (0 + 150)/2 = 75 \text{ C}$.

$$\arg = x/2(\alpha)^{0.5} = 0.11/[2(9.7\text{E-}5 \times 2 \times 60)^{0.5}] = 0.5, \quad erf(\arg_1) = 0.52$$

$$S_1(x, t) = \frac{T_1 - 75}{0 - 75} = 0.52 \quad \text{and} \quad S_2(x, t) = \frac{T_2 - 75}{150 - 75} = 0.52$$

We find $T_1 = 36 \text{ C}$ and $T_2 = 114 \text{ C}$.

9.3. Semi-infinite Bodies and Harmonically Oscillating Temperature at the Boundary

An example of rapidly oscillating temperature is exposure of the cylinder wall of an internal combustion engine to the combustible gas and the combustion products. Another example, but for low frequency oscillation, includes exposure of the earth's surface to the seasonal changes in the weather temperature. Let's treat earth as a semi-infinite solid and examine the latter case in more detail. Note that for oscillating temperature at the boundary, we do not need an initial condition, as the temperature penetration is also oscillatory, satisfying the steady state solution. Equation IVa.2.3 still applies, however, we introduce dimensionless ratios to simplify the equation. For a sinusoidal oscillation, we show the average surface temperature with \bar{T} , the amplitude of the oscillation with ΔT , and the angular frequency with ω . The three dimensionless ratios are for temperature, time, and location:

$$\theta = \frac{T - \bar{T}}{\Delta T}, \quad \Omega = \omega t, \quad \text{and} \quad \zeta = x / \sqrt{\omega / 2\alpha}$$

We first find T in terms of θ as $T = \bar{T} + \Delta T \theta$. We then carry out the derivatives for Equation IVa.2.3 using the chain rule for differentiation to obtain $\partial T / \partial x = (dT/d\zeta)(d\zeta/dx)$ and $\partial T / \partial t = (\partial \theta / \partial \Omega)(d\Omega/dt)$ resulting in:

$$\frac{\partial^2 T}{\partial x^2} = \Delta T \frac{\omega}{2\alpha} \frac{\partial^2 \theta}{\partial \zeta^2} \quad \text{and} \quad \frac{\partial T}{\partial t} = \omega \Delta T \frac{\partial \theta}{\partial \Omega}$$

Substituting in Equation IVa.2.3, the governing equation for harmonically oscillating boundary temperature becomes:

$$\frac{1}{2} \frac{\partial^2 \theta}{\partial \zeta^2} = \frac{\partial \theta}{\partial \Omega}$$

subject to $\theta_{\zeta=0} = \cos \Omega$ and $\theta_{\zeta \rightarrow \infty} = 0$. As derived by Carslaw and described by Lienhard, we try a solution in the form of $\theta = e^{-\zeta} \cos(\Omega - \zeta)$, resulting in the following answer:

$$\frac{T - \bar{T}}{\Delta T} = e^{-x\sqrt{\omega/2\alpha}} \cos\left[\Omega - \sqrt{\frac{\omega}{2\alpha}} x\right]$$

Example IVa.9.4. How deep should we dig the ground in high summer to find the coldest part of the earth? $\alpha_{\text{Earth}} = 0.139\text{E-6 m}^2/\text{s}$.

Solution: The coldest part is due to the temperature penetration during the preceding winter. In this case, the angular frequency is $\omega = 2\pi \text{ rad/year}$. To find the location of T_{\min} , we try a solution in the following form: $\theta = e^{-\zeta} \cos(\Omega - \zeta) =$

$e^{-\zeta} \cos \zeta$. Initially, $\Omega = \alpha = 0$. To find ζ , we take the derivative of θ and set it equal to zero:

$$\frac{d\theta}{dt} = -[(\cos \zeta) + \sin \zeta]e^{\zeta} = 0$$

This results in $\tan \zeta = -1$, corresponding to $\zeta = 3\pi/4, 7\pi/4, 11\pi/4$, etc. For the first answer, we find: $x\sqrt{\omega/(2\alpha)} = 3\pi/4$. Substituting for $\omega = 2\pi\nu = 2 \times \pi(365 \times 24 \times 3600) = 0.199\text{E-}6$ s, we find $x = (3\pi/4)/[0.199\text{E-}6/(2 \times 0.139\text{E-}6)]^{1/2} = 2.783$ m.

9.4. 1-D Transient Heat Conduction, Plate, Cylinder, and Sphere

Our goal here is to find analytical solutions to one-dimensional transient heat conduction in an infinite plate, infinite cylinder, and sphere. In all three cases, the object is initially at the uniform temperature of T_i and suddenly exposed to a convection boundary specified as T_f and h . Similar to the steady state solution for a rectangular plate, the technique of separation of variables can be used to find analytical solutions in series form for such objects. Heisler has shown that the center temperature (T_o) in these objects is obtained within 1% approximation by using only the first term of the series solution:

$$\frac{T_o - T_f}{T_i - T_f} = C_B \exp\left(-A_B^2 \frac{\alpha t}{s^2}\right) \quad \text{IVa.9.13}$$

where coefficients C_B and A_B are only functions of the Biot number, $\text{Bi} = hs/k$ and are given in Table IVa.9.1. In Equation IVa.9.13, $s = L$ for a slab, and $s = R$ for a thin solid cylinder and solid sphere. Equation IVa.9.13 applies only if the Fourier number $\text{Fo} = \alpha t/s^2 > 0.2$.

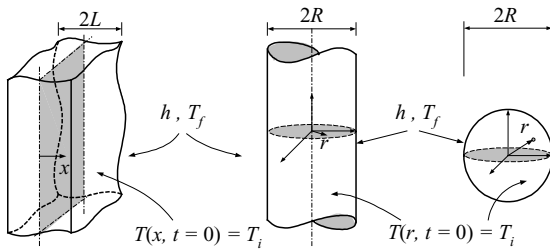


Figure IVa.9.3. Plate (slab), infinite cylinder and sphere

Next, we examine plates, cylinders, and spheres. The approach is to first find the center temperature of the object from Equation IVa.9.13 in conjunction with Table IVa.1.9. Then use the center temperature to find the off center temperatures.

Case 1. *Temperature Distribution in a Thin Plate.* Having the center-plane temperature from Equation IVa.9.13, temperature of any other point is found from:

$$P(x, t) = \frac{T - T_f}{T_i - T_f} = C_B \exp(-A_B^2 Fo) \cos(A_B x / L) \quad \text{IVa.9.14}$$

and the total heat transfer from:

$$\frac{Q}{Q_0} = 1 - P(x, t) \frac{\sin(A_B)}{A_B} \quad \text{IVa.9.15}$$

where $Q_0 = mc(T_i - T_f)$ where A_B and C_B are obtained from Table IVa.9.1.

Case 2. *Temperature Distribution in an Infinite Solid Thin Cylinder.* In the case of a cylinder with diameter of $2R$ ($s = R$), having the centerline temperature as a function of time, temperature of any point within the infinite cylinder can be obtained from:

$$C(r, t) = \frac{T - T_f}{T_i - T_f} = C_B \exp(-A_B^2 Fo) J_0(A_B r / R) \quad \text{IVa.9.16}$$

and the total heat transfer from:

$$\frac{Q}{Q_0} = 1 - 2 \times C(r, t) \frac{J_1(A_B)}{A_B} \quad \text{IVa.9.17}$$

where A_B and C_B are obtained from Table IVa.9.1.

Case 3. *Temperature Distribution in a Sphere.* In a solid sphere of diameter $2R$ ($s = R$), temperature at any point is obtained from the center temperature as:

$$K(r, t) = \frac{T - T_f}{T_i - T_f} = \frac{R}{r A_B} \sin(A_B r / R)$$

and total heat transfer by:

$$\frac{Q}{Q_0} = 1 - 3K(r, t) \frac{\sin A_B - A_B \cos A_B}{A_B^3}$$

where A_B and C_B are obtained from Table IVa.9.1. Note that the arguments of the trigonometric functions are in radians. Methods of the analysis of transient heat conduction in plates, cylinders and spheres are shown in the following examples.

Example IVa.9.5. A brick wall, 30 cm thick and 80 C is suddenly exposed to an environment of 10 C and 120 W/m² C. Find temperature at 5 cm from the center plane 10 h after exposure.

Brick properties; $k = 0.69$ W/m·C, $c = 840$ kJ/kg·C, and $\rho = 1602$ kg/m³ ($\alpha = 5.127\text{E-}7$ m²/s).

Solution: We first find the Biot and the Fourier numbers:

$$\text{Bi} = hL/k = 120 \times (0.30/2)/0.69 = 26 \text{ and } \text{Fo} = 5.127\text{E-}4 \times 36000/(0.15)^2 = 0.82$$

From Table IVa.9.1 we find $A_B = 1.5106$ and $C_B = 1.2709$. From Equation IVa.9.14:

$$P(x, t) = C_B \exp(-A_B^2 \text{Fo}) \cos(A_B x/L) = [1.2709 \exp(-1.5106^2 \times 0.82)] \cos(1.5106 \times 5/15) = 0.171$$

$$T = T_f + (T_i - T_f) \times P(x, t) = 10 + (80 - 10) \times 0.171 = 22 \text{ C.}$$

In the next example, we examine transient analysis in infinite solid cylinders.

Example IVa.9.6. A long steel cylinder with a diameter of 8 cm and an initial temperature of 250 C is suddenly exposed to a convection boundary of 25 C and 500 W/m²·C. Find the temperature at $r = 0$ cm and at $r = 2$ cm at 2 minutes after the exposure. ($k = 35$ W/m·C, $\rho = 7800$ kg/m³, and $c = 0.48$ kJ/kg·C).

Solution: We need the Biot and the Fourier numbers:

$$\text{Bi} = hR/k = 500 \times (4/100)/35 = 0.571 \text{ and } \alpha = k/\rho c = 35/(7800 \times 480) = 9.35\text{E-}6 \text{ m/s}^2$$

$$\text{Fo} = 9.35\text{E-}6 \times 120/0.04^2 = 0.7$$

To find the centerline temperature from Equation IVa.9.13, we find coefficients A_B and C_B from Table IVa.9.1 as $A_B = 0.996$ and $C_B = 1.1286$. Hence,

$$C_o(r, t) = C_B \exp(-A_B^2 \text{Fo}) = 1.1286 \exp(-0.996^2 \times 0.7) = 0.563$$

Therefore, the center temperature is:

$$T_o = T_f + (T_i - T_f) C_o(r, t) = 25 + 0.563(250 - 25) = 152 \text{ C}$$

From Equation IVa.9.16 we find:

$$C(r, t) = C_o(r, t) J_0(A_B r/R) = 0.563 \times J_0(0.996 \times 2/4) = 0.528$$

Therefore, temperature at $r = 2$ is found as:

$$T(r = 2) = T_f + (T_i - T_f) C(r, t) = 25 + (250 - 25) \times 0.528 = 143.9 \text{ C}$$

Total heat transfer per meter of this cylinder in this period is $\dot{q}' = 2135$ kJ/m.

The next example deals with transient heat conduction in spheres.

Example IVa.9.7. A sphere with $D = 12$ cm and $T_i = 300$ C is suddenly exposed to a convection boundary of 25 C and $100 \text{ W/m}^2\cdot\text{C}$. Find temperature at a radius of $r = 0$ and $r = 2$ cm, 85 s after the exposure.

($k = 52 \text{ W/m}\cdot\text{C}$, $\rho = 7270 \text{ kg/m}^3$, $c = 420 \text{ J/kg}\cdot\text{K}$).

Solution: We find α as: $\alpha = 52/(7270 \times 420) = 1.7\text{E-}5 \text{ m}^2/\text{s}$.

For $\text{Bi} = 100 \times 0.06/52 = 0.115$, from Table IVa.9.1 we also find $A_B = 0.576$ and $C_B = 1.034$

$$\arg = -A_B^2 \text{Fo} = -A_B^2 \alpha t / s^2 = -(0.576)^2 (1.7\text{E-}5)(85)/(0.06)^2 = -0.133$$

$$T_o = T_f + (T_i - T_f) \exp(\arg) = 25 + 1.034(300 - 25) \exp(-0.133) = 273.97 \text{ C}$$

$$T(r = 2) = T_f + (T_o - T_f)(R/A_B r) \sin(A_B r/R) = 25 + (273.97 - 25)(6/2 \times 0.576) \sin(2 \times 0.576/6)$$

$$T(r = 2) = 25 + (273.97 - 25)(5.208) \sin(0.192) = 272.4 \text{ C}$$

Is the lumped capacitance method appropriate here? Find the sphere temperature by using Equation IVa.4.2 (note, $\text{Bi} \ll 1$).

9.5. Multi-dimensional Transient Heat Conduction

Analytical solution to the steady state heat conduction in a rectangular plate and to the transient heat conduction in infinite plates, infinite cylinders, and spheres is obtained by the method of the separation of variables. In this method, temperature distribution is in the form of the product of various functions. An example of such analytical solution is discussed in Chapter VIIb where temperature distribution is sought in a rectangular plate subject to one non-homogenous and three homogeneous boundary conditions. Equation VIIb.2.27 gives the series solution obtained for this case.

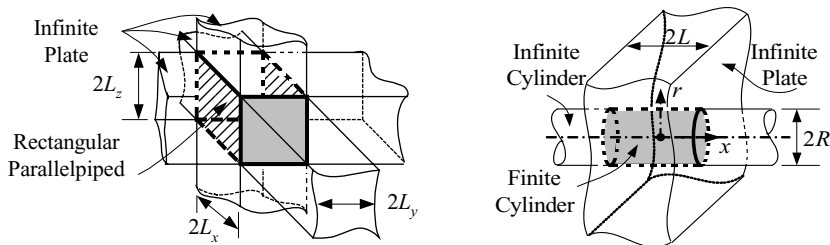


Figure IVa.9.4. Obtaining multidimensional objects from one-dimensional solids

Similar approach can be used to find transient temperature distribution in other objects if they can be reduced to such basic configurations for which analytical solutions already exist. For example, we can use two infinite plates to construct an

infinite parallelepiped. To find temperature distribution in an infinite parallelepiped, we can then multiply the solutions of the two infinite plates. Similarly, we can obtain a finite cylinder from the intersection of an infinite cylinder and an infinite plate. Temperature distribution in the finite cylinder is the product of the solutions of the infinite plate and the infinite cylinder. These are shown in Figure IVa.9.4 and Table IVa.9.2.

Table IVa.9.1. Heisler coefficients for center temperature

Biot Number	Thin Plate		Infinite Cylinder		Sphere	
	A_B	C_B	A_B	C_B	A_B	C_B
0.01	0.0998	1.0017	0.1412	1.0025	0.1730	1.0030
0.02	0.1410	1.0033	0.1995	1.005	0.2445	1.0060
0.04	0.1987	1.0066	0.2814	1.0099	0.3450	1.0120
0.06	0.2425	1.0098	0.3438	1.0148	0.4217	1.0179
0.08	0.2791	1.0130	0.3960	1.0197	0.4860	1.0239
0.1	0.3111	1.0161	0.4417	1.0246	0.5423	1.0298
0.2	0.4328	1.0311	0.6170	1.0483	0.7593	1.0592
0.3	0.5218	1.0451	0.7465	1.0712	0.9208	1.0880
0.4	0.5932	1.058	0.8516	1.0931	1.0528	1.1164
0.5	0.6533	1.0701	0.9408	1.1143	1.1656	1.1441
0.6	0.7051	1.0814	1.0185	1.1345	1.2644	1.1713
0.7	0.7506	1.0919	1.0873	1.1539	1.3525	1.1978
0.8	0.7910	1.1016	1.1490	1.1724	1.4320	1.2236
0.9	0.8274	1.1107	1.2048	1.1902	1.5044	1.2488
1	0.8603	1.1191	1.2558	1.2071	1.5708	1.2732
2	1.0769	1.1785	1.5995	1.3384	2.0288	1.4793
3	1.1925	1.2102	1.7887	1.4191	2.2889	1.6227
4	1.2646	1.2287	1.9081	1.4698	2.4556	1.7202
5	1.3138	1.2403	1.9898	1.5029	2.5704	1.787
6	1.3496	1.2479	2.0490	1.5253	2.6537	1.8338
7	1.3766	1.2532	2.0937	1.5411	2.7165	1.8674
8	1.3978	1.257	2.1286	1.5526	2.7654	1.8920
9	1.4149	1.2598	2.1566	1.5611	2.8044	1.9106
10	1.4289	1.262	2.1795	1.5677	2.8363	1.9249
20	1.4961	1.2699	2.2881	1.5919	2.9857	1.9781
30	1.5202	1.2717	2.3261	1.5973	3.0372	1.9898
40	1.5325	1.2723	2.3455	1.5993	3.0632	1.9942
50	1.5400	1.2727	2.3572	1.6002	3.0788	1.9962
100	1.5552	1.2731	2.3809	1.6015	3.1102	1.9990

Table IVa.9.2. Solution for multidimensional solids

Solid Geometry	Semi-infinite Solid	Infinite Plate	Infinite Cylinder
Semi-infinite Plate	$S(x, t)$	$P(x, t)$	—
Infinite Rectangular Bar	—	$P_1(x, t) \times P_2(x, t)$	—
Semi-infinite Rectangular Bar	$S(x, t)$	$P_1(x, t) \times P_2(x, t)$	—
Rectangular Parallelepiped	—	$P_1(x, t) \times P_2(x, t) \times P_3(x, t)$	—
Semi-infinite Cylinder	$S(x, t)$	—	$C(r, t)$
Short Cylinder	—	$P(x, t)$	$C(r, t)$

Example IVa.9.8. A stainless steel cylinder with a diameter of 2 in, length of 3 in, and initial temperature of 650 F is suddenly exposed to a convection boundary of 65 F and 50 Btu/ft²·h·F. Find the temperature at a radius of $r = 0.5$ in and height of 1 in from the mid-plane, 2 minutes after the exposure.

Solution: From Table IVa.9.2, we note that temperature distribution in a short cylinder is given by: $T(r, x, t) = P(x, t)C(r, t)$. We then find Bi number for the plate and for the cylinder:

	Bi	Fo	A_B	C_B	$P(x, t)$	$C(r, t)$
Plate	0.716	0.323	0.757	1.093	0.796	—
Cylinder	0.478	0.724	0.921	1.110	—	0.569

Hence, for the short cylinder:

$$\Theta(r, t) = [T(r, t) - T_f]/[T_i - T_f] = P(x, t) \times C(r, t) = 0.796 \times 0.569 = 0.453$$

$$T(r, t) = 65 + (650 - 65) \times 0.453 = 330 \text{ F. Also, } Q = 340.22 \times (3/12) = 85 \text{ Btu.}$$

Example IVa.9.9. An aluminum cylinder is exposed to a convection boundary. Find temperature at the specified location and time.

Data: $k = 124 \text{ Btu/ft} \cdot \text{h} \cdot \text{F}$, $c = 0.2 \text{ Btu/lbm} \cdot \text{F}$, $\rho = 170 \text{ lbm/ft}^3$, $T_i = 400 \text{ F}$, $T_f = 50 \text{ F}$, $h = 100 \text{ Btu/ft}^2 \cdot \text{h} \cdot \text{F}$, $2R = 2 \text{ in}$, $2L = 5 \text{ in}$, $r = 0.5 \text{ in}$, $x = 1.5 \text{ in}$, $t = 30 \text{ s}$.

Solution: $\text{Bi(plate)} = hL/k = 100(5/12)/124 = 0.168$ and $\text{Bi(cylinder)} = hR/k = 100(1/12)/124 = 0.067$. We then use Table IVa.5.1 and Equations IVa.5.14 and IVa.5.16.

	Bi	Fo	A_B	C_B	$P(x, t)$	$C(r, t)$
Plate	0.168	0.700	0.394	1.026	0.903	—
Cylinder	0.067	4.376	0.363	1.017	—	0.567

Hence, for the short cylinder:

$$\Theta(r, t) = [T(r, t) - T_f]/[T_i - T_f] = P(x, t) \times C(r, t) = 0.903 \times 0.567 = 0.512$$

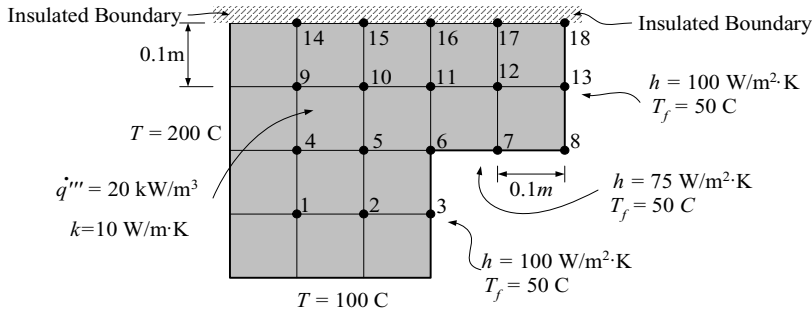
$$T(r, t) = 50 + (400 - 50) \times 0.512 = 229 \text{ F.}$$

Problems involving temperature distribution in solids can be easily solved by using the software on the accompanying CD-ROM.

10. Numerical Solution of Heat Conduction Equation

As much as we try to find analytical solutions for engineering problems, there are many cases for which analytical solutions cannot be found. In heat conduction, this occurs when we are dealing with complex geometries, when properties are strongly dependent on temperature, when internal heat generation rate is a function of space and time, when boundary conditions are non-linear, or in some cases due to all these factors combined. Therefore, it becomes indispensable to resort to modeling the problem numerically and solving the set of equations by computer. Since numerical techniques are described in Chapter VIIe, we only apply the results in this chapter. In the following example, a plate with a specified internal heat generation and unit depth is subjected to three types of boundary conditions, temperature, convection, and insulated boundaries.

Example IVa.10.1. Use the information given in the figure to find temperature distribution in the plate.



Solution: Nodes 1, 2, 4, 5, 9, 10, 11, and 12 are interior nodes to which Equation VIIe.3.5 applies. Nodes 3, 7, and 13 are plane surface nodes subject to convection boundary. Nodes 6 and 8 are corner nodes. Nodes 14 through 17 are plane surface nodes subject to insulated boundary condition. Node 18 is on an insulated boundary and also faces a convection boundary. For internal nodes we have:

$$\begin{aligned} \text{Node 1:} & \quad T_2 + T_4 - 4T_1 + 20 = -300 \\ \text{Node 2:} & \quad T_1 + T_3 + T_5 - 4T_2 + 20 = -100 \\ \text{Node 4:} & \quad T_1 + T_5 + T_9 - 4T_4 + 20 = -200 \\ \text{Node 5:} & \quad T_2 + T_4 + T_6 + T_{10} - 4T_5 + 20 = 0 \\ \text{Node 9:} & \quad T_4 + T_{10} + T_{14} - 4T_9 + 20 = -200 \\ \text{Node 10:} & \quad T_5 + T_9 + T_{11} + T_{15} - 4T_{10} + 20 = 0 \end{aligned}$$

$$\text{Node 11:} \quad T_6 + T_{10} + T_{12} + T_{16} - 4T_{11} + 20 = 0$$

$$\text{Node 12:} \quad T_7 + T_{11} + T_{13} + T_{17} - 4T_{12} + 20 = 0$$

For plane surface nodes with convection boundary we have different heat transfer coefficient for vertical and for horizontal planes. For nodes on a vertical plane, the Biot number is $Bi = h\Delta x/k = 1$ whereas for nodes on a horizontal plane the Biot number is $Bi = h\Delta x/k = 0.75$:

$$\text{Node 3:} \quad 2T_2 + T_6 + 100 - 2(2+1)T_3 + 20 = -100$$

$$\text{Node 7:} \quad T_6 + T_8 + 2T_{12} - 2(2+0.75)T_7 + 20 = -1.5T_f$$

$$\text{Node 13:} \quad 2T_{12} + T_8 + T_{18} - 2(2+1)T_{13} + 20 = -100$$

For the internal corner node subject to convection boundaries we have:

$$\text{Node 6:} \quad 2(T_5 + T_{11}) + (T_3 + T_7) - (6 + 1.75)T_6 + 30 = -1.75T_f$$

For the corner node subject to convection boundaries we have:

$$\text{Node 8:} \quad (T_7 + T_{13}) - (2 + 1.75)T_8 + 10 = -1.75T_f$$

For plane surface nodes subject to the insulated boundary we have:

$$\text{Node 14:} \quad 200 + T_{15} + 2T_9 - 4T_{14} + 20 = 0$$

$$\text{Node 15:} \quad T_{14} + T_{16} + 2T_{10} - 4T_{15} + 20 = 0$$

$$\text{Node 16:} \quad T_{15} + T_{17} + 2T_{11} - 4T_{16} + 20 = 0$$

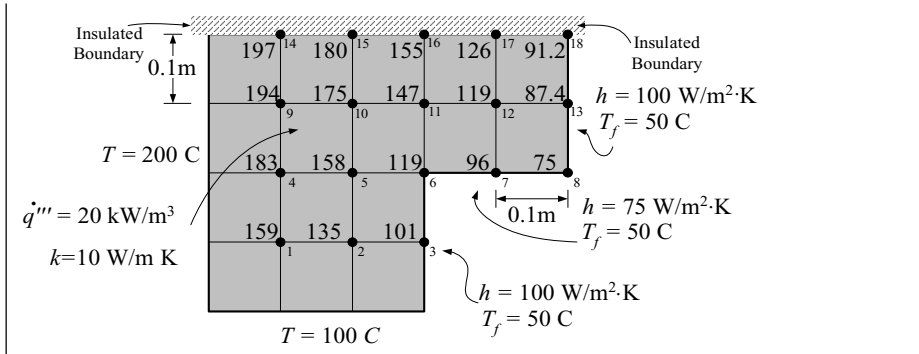
$$\text{Node 17:} \quad T_{16} + T_{18} + 2T_{12} - 4T_{17} + 20 = 0$$

Finally, for the corner node subject to insulation and convection boundaries we have:

$$\text{Node 18:} \quad (T_{13} + T_{17}) - (2 + 1)T_{18} + 10 = -T_f$$

$$\begin{pmatrix} -4 & 1 & 0 & 1 & 0 & 0 & 0 & 0 & 0 & 0 & 0 & 0 & 0 & 0 & 0 & 0 & 0 & 0 \\ 1 & -4 & 1 & 0 & 1 & 0 & 0 & 0 & 0 & 0 & 0 & 0 & 0 & 0 & 0 & 0 & 0 & 0 \\ 0 & 2 & -6 & 0 & 0 & 1 & 0 & 0 & 0 & 0 & 0 & 0 & 0 & 0 & 0 & 0 & 0 & 0 \\ 1 & 0 & 0 & -4 & 1 & 0 & 0 & 0 & 1 & 0 & 0 & 0 & 0 & 0 & 0 & 0 & 0 & 0 \\ 0 & 1 & 0 & 1 & -4 & 1 & 0 & 0 & 0 & 1 & 0 & 0 & 0 & 0 & 0 & 0 & 0 & 0 \\ 0 & 0 & 1 & 0 & 2 & -7.75 & 1 & 0 & 0 & 0 & 20 & 0 & 0 & 0 & 0 & 0 & 0 & 0 \\ 0 & 0 & 0 & 0 & 0 & 1 & -5.5 & 1 & 0 & 0 & 0 & 2 & 0 & 0 & 0 & 0 & 0 & 0 \\ 0 & 0 & 0 & 0 & 0 & 0 & 1 & -3.75 & 0 & 0 & 0 & 0 & 1 & 0 & 0 & 0 & 0 & 0 \\ 0 & 0 & 0 & 1 & 0 & 0 & 0 & 0 & -4 & 1 & 0 & 0 & 0 & 1 & 0 & 0 & 0 & 0 \\ 0 & 0 & 0 & 0 & 1 & 0 & 0 & 0 & 1 & -4 & 1 & 0 & 0 & 0 & 1 & 0 & 0 & 0 \\ 0 & 0 & 0 & 0 & 0 & 1 & 0 & 0 & 0 & 1 & -4 & 1 & 0 & 0 & 0 & 1 & 0 & 0 \\ 0 & 0 & 0 & 0 & 0 & 0 & 1 & 0 & 0 & 0 & 1 & -4 & 1 & 0 & 0 & 0 & 1 & 0 \\ 0 & 0 & 0 & 0 & 0 & 0 & 0 & 2 & 0 & 0 & 0 & 1 & -6 & 1 & 0 & 0 & 0 & 1 \\ 0 & 0 & 0 & 0 & 0 & 0 & 0 & 0 & 2 & 0 & 0 & 0 & 1 & -4 & 1 & 0 & 0 & 0 \\ 0 & 0 & 0 & 0 & 0 & 0 & 0 & 0 & 0 & 2 & 0 & 0 & 0 & 1 & -4 & 1 & 0 & 0 \\ 0 & 0 & 0 & 0 & 0 & 0 & 0 & 0 & 0 & 0 & 2 & 0 & 0 & 0 & 1 & -4 & 1 & 0 \\ 0 & 0 & 0 & 0 & 0 & 0 & 0 & 0 & 0 & 0 & 0 & 2 & 0 & 0 & 0 & 1 & -4 & 1 \\ 0 & 0 & 0 & 0 & 0 & 0 & 0 & 0 & 0 & 0 & 0 & 0 & 1 & 0 & 0 & 0 & 1 & -3 \end{pmatrix} \begin{pmatrix} T_1 \\ T_2 \\ T_3 \\ T_4 \\ T_5 \\ T_6 \\ T_7 \\ T_8 \\ T_9 \\ T_{10} \\ T_{11} \\ T_{12} \\ T_{13} \\ T_{14} \\ T_{15} \\ T_{16} \\ T_{17} \\ T_{18} \end{pmatrix} = \begin{pmatrix} -320 \\ -120 \\ -220 \\ -220 \\ -20 \\ -117.5 \\ -95 \\ -97.5 \\ -220 \\ -20 \\ -20 \\ -20 \\ -120 \\ -220 \\ -20 \\ -20 \\ -20 \\ -20 \\ -60 \end{pmatrix}$$

The results are shown in the figure.



In this example, we assumed a uniform heat generation rate. However, if the rate of heat generation is a function of location, we could easily account for spatial dependence of the internal heat generation. To obtain more accurate values for temperatures, we should use smaller mesh sizes. The above example dealt with rectangular coordinates. We can use the same procedure and solve problems in orthogonal but not rectangular, such as cylindrical and spherical coordinates.

QUESTIONS

- Are homogeneous substances necessarily isotropic?
- Does conduction heat transfer apply only to solids?
- Does convection heat transfer apply only to fluids?
- What is the difference between heat flux and the linear heat generation rate?
- Consider a solid sphere of diameter D in which heat is produced in the center of the sphere and is steadily removed at the surface. Is heat flux at $r = D/6$ equal to the heat flux at $r = D/3$?
- Consider a solid sphere of diameter D in which heat is produced in the center of the sphere and is steadily removed at the surface. Is the rate of heat transfer at $r = D/6$ equal to the rate of heat transfer at $r = D/3$?
- What is the difference between a gas thermal conductivity at the viscous state versus the molecular state?
- Regarding thermal conduction, what type of a substance is wood?
- What is the thermal capacitance of silver at 300 F?
- Define thermal diffusivity. Consider solids A and B being at the same temperature. However, solid A has a higher thermal diffusivity than solid B. Which is more effective in transferring than in storing energy?
- Is aluminum more effective in storing energy than zinc at the same temperature?
- Define thermal resistance. One side of a plate is warmer than the other side. Is thermal resistance in this plate inversely related to the thickness of the plate?
- What is radiation heating? If a plate is bombarded by γ -radiation why is there a maximum temperature in the plate? How do you find the location and the magnitude of the maximum temperature?

- How do you define the heat transfer coefficient? What is the range of h in free convection for gases?
- A thin disk is being welded at a point located at r and θ with $0 < r < D/2$ and $0 < \theta < 2\pi$ and D is the disk radius. Is temperature distribution in this disk 1-D? What coordinate system do you use to find temperature distribution in the disk?
- What is the difference between heat transfer coefficient and the overall heat transfer coefficient?
- Temperature difference across a fuel pellet, operating at $\dot{q}' = 10 \text{ kW/ft}$ is 700 F. Maintaining the same \dot{q}' , what is the change in temperature gradient across the pellet if the pellet diameter was 10% smaller?
- What is the advantage of an annular fuel as compared with a solid fuel pellet?
- A cylinder has $Fo = 0.05$. Is the Heisler solution applicable to this cylinder?
- What is the advantage of analytical solution compared with numerical solutions or experimental correlations?

PROBLEMS

Sections 1 and 2

1. Find an average thermal conductivity for copper in the temperature range of 200 F to 600 F.
2. Two plates are placed in a container. The gap between the plates is 0.01 inches. A vacuum pump is used to remove air from the container. However, a small amount of air has remained in the container so that air pressure is measured as 0.1 mbar. Can the air thermal conductivity be obtained from Figure IVa.1.1?
3. Thermal conductivity of a substance is measured as $k = k_0 \sqrt{T/T_0}$. Find an average value for thermal conductivity in the temperature range of T_1 and T_2 .
[Ans. $\bar{k} = (k_0 / 2T_0^{1/2})(T_2^{3/2} - T_1^{3/2}) / (T_2 - T_1)$].
4. Heat is being generated in a fuel element at a volumetric heat generation rate of $\dot{q}''' = 1300 \text{ kW/m}^3$. The fuel element is a rectangular parallelepiped of thickness 2 cm with a height of 2 m and width of 1 m. The fuel thermal conductivity is $k = 3.5 \text{ W/m}\cdot\text{C}$. Find the rate of heat transfer from the fuel element at steady state condition. [Ans.: 52 kW].
5. Heat at a rate of 5 kW is being uniformly produced in a solid cylinder. The cylinder has a diameter and a length of 2 cm and 4 m, respectively. Find a) the volumetric and the linear heat generation rates for this cylinder and b) heat flux at $r = D/2$. [Ans.: $\dot{q}' = 0.25 \text{ kW/m}$, $\dot{q}'' = 19.9 \text{ kW/m}^2$, and $\dot{q}''' = 3979 \text{ kW/m}^3$].
6. Consider a solid spherical fuel in which heat at a rate of 1 kW is uniformly produced in the solid sphere and is removed steadily at the surface. The sphere

has a radius of 1 cm. Find the volumetric and the linear heat generation rates for this sphere.

7. Derive Equation IVa.2.1 from the general form of the conservation equation for energy as given by Equation IIIa.3.23.

8. A large block of concrete with a thickness of 50 cm is exposed to thermal radiation resulting in the surface temperature to be maintained at 100 C. If the opposing surface is kept at 50 C, find a) the rate of heat transfer at steady state condition per unit surface area and b) temperature at a distance 30 cm from the hot surface. Assume the concrete thermal conductivity remains constant throughout the block at 1.4 W/m·K. [Ans.: a) 140 W/m² and b) 70 C].

9. A large sheet of steel is exposed to a temperature of 250 C. The sheet has a thickness of 5 cm and loses heat to an area maintained at 85 C. Find the rate of heat transfer at steady state condition. The heat transfer coefficients from the hot side to the sheet is 45 W/m·K and from the sheet to the room is 8 W/m·K.

10. A garment is rated at 150 F for ironing. An iron is set at 200 W. Is this setting appropriate? Assume heat flows primarily from the surface for ironing, having an area of $A_{\text{iron}} = 0.4 \text{ ft}^2$. Other data include $h = 10 \text{ Btu/ft}^2 \cdot \text{h} \cdot \text{F}$ and $T_{\text{ambient}} = 70 \text{ F}$. [Ans.: $T_{\text{iron}} = 240 \text{ F}$].

11. As shown in the figure, two plates made of the same material and having constant k are exposed on one side to hot water at T_w and h_w and on the other to cold air at T_a and h_a . Using the direction of the x -axis as shown, write the boundary condition at a) $x = 0$ and b) $x = L$ for each case.

[Ans. a- at $x = 0$, B.C.: $h_w(T_w - T_{1,0}) - [-k dT_1/dx]_0 = 0$ and $[k dT_2/dx]_0 - h_a(T_{2,0} - T_a) = 0$].

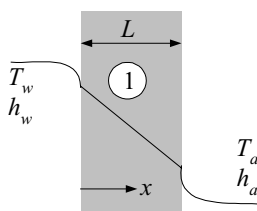


Figure for Problem 11

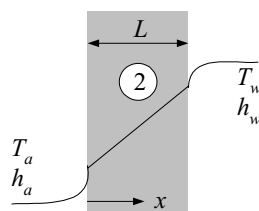


Figure for Problem 20

Section 4

12. A piece of copper wire is initially at 150 C. We now expose this wire to air at 38 C. Find a) the rate of heat transfer at the moment of exposure and b) compare this rate of heat transfer to the rate of heat transfer from thermal radiation at the moment of exposure.

Data: For copper at 150 C; $k = 374 \text{ W/m} \cdot \text{K}$, $c = 381 \text{ J/kg} \cdot \text{K}$, $\rho = 8938 \text{ kg/m}^3$, $\epsilon = 0.8$. The heat transfer coefficient is $h = 5 \text{ W/m}^2 \cdot \text{K}$. [Ans.: Initial heat loss is 64% due to radiation and 36% due to convection].

13. A small copper ball is placed in a room to cool down. Assuming the room temperature and the heat transfer coefficient remain constant throughout the transient, find the time at which the sphere temperature reaches half of its initial value. Data: $d = 1$ cm, $T_i = 200$ C, $T_f = 27$ C, $h = 8$ W/m²·C. [Ans.: 10 min].

14. An fuel ball, originally at 100 F is suddenly exposed to a convection boundary. Find the time it takes the fuel to reach 99% of the free stream temperature. Data: $d = 1$ in, $T_f = 550$ F, $h = 180$ Btu/h·ft²·F. Fuel density = 750 lbm/ft³ and fuel specific heat = 0.05 Btu/lbm·F.

15. Consider a fuel pellet of volume V , surface area A , density ρ , and specific heat c . The pellet is initially at temperature T_i . At time zero, heat is produced in the pellet at a constant rate of \dot{Q} . At the same time, the pellet is exposed to the surroundings being at the constant free stream temperature of T_f . The heat transfer coefficient between the pellet and the free stream is h . Assuming a lumped heat capacity method applies a) set up the governing differential equation, b) show that the pellet temperature versus time (t) is given as:

$$T(t) = T_f + \left[(T_i - T_f) + \frac{\dot{Q}}{\rho c V} \tau \right] e^{-t/\tau} + \frac{\dot{Q}}{\rho c V} \tau$$

where $\tau = \rho c V / h A$ and c) find the pellet equilibrium temperature (i.e., when $t \gg \tau$). [Hint: Use Equation IIa.6.4 to obtain the governing differential equation. Then use Equation VIIb.2.5 to solve the equation].

16. Use the result of the above problem to plot temperature versus time for a cylindrical pellet subject to the simultaneous internal heat generation and exposure to a convection boundary at time zero. Data: $d = 1.00$ cm, $h = 1.00$ cm, $\rho = 10.4$ g/cm³, $c = 0.35$ kJ/kg·K, $T_i = T_f = 65$ C, $h = 1200$ W/m²·C, $\dot{Q} = 0.05$ kW. Use $t_1 = 0.001$ s, $t_2 = 0.7$ s, $t_3 = 1$ s, $t_4 = 3$ s, $t_5 = 6$ s, $t_6 = 9$ s, $t_7 = 20$ s, $t_8 = 30$ s, $t_9 = 50$ s, and $t_{10} = 100$ s.

Section 5

17. Shown in the figure is a storage facility built in the shape of a parallelepiped. Details of the walls and the roof are also shown. The thickness of the paint, is 5 mm. The thickness of the sheet rock, insulation, and brick is 4 cm, 15 cm, and 5 cm, respectively. Estimate the heat loss in a Winter day where $T_f = 0$ C and the indoor temperature is maintained at 25 C. Use $h_i = 4$ W/m K and $h_o = 10$ W/m K.

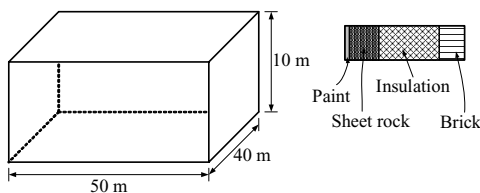


Figure for Problem 17

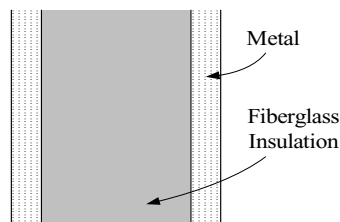


Figure for Problem 18

18. Consider the fiberglass insulation in a kitchen oven, which is sandwiched between two sheets of metal. The maximum temperature on the inside surface of the oven may reach 260 C. Find the minimum thickness of the fiberglass insulation to ensure that the temperature on the outside surface of the oven does not exceed 40 C. The kitchen temperature varies between 18 C to 37 C. The heat transfer coefficient between the oven surface and the kitchen is 15 W/m²·K. The thermal conductivity of fiberglass is $k_{\text{fiberglass}} = 0.04$ W/m·K.

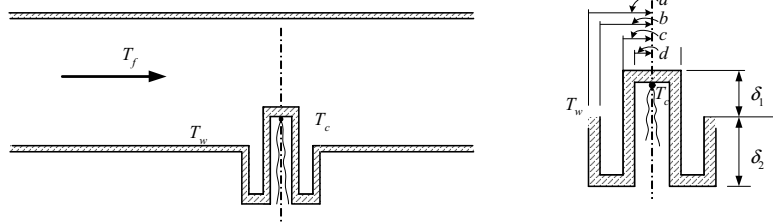
19. Compare the heat losses from a single-pane with a double-pane window. In a cold Winter day, the room temperature is maintained at 23 C while the outside temperature is -10 C. The glass thickness is 5 mm and the 2 cm gap in the double-pane window is filled with stagnant air. The inside and outside heat transfer coefficients are 5 W/m²·K and 20 W/m²·K, respectively. Use $k_{\text{glass}} = 1.4$ W/m·K and $k_{\text{air}} = 0.025$ W/m·K.

20. The two plates of Problem 11 made of the same material and having constant k are exposed on one side to hot water at T_w and h_w and on the other to cold air at T_a and h_a . Find a) the equation for temperature profile in these plates and b) temperatures at $x = 0$ and at $x = L$ if $h_w = h_a = h$.

[Ans.: a) $T_1(x) = c_1x + c_2$ where, $c_1 = h_w(T_a - T_w)/c_3$ and $c_2 - T_a = -h_w(h_aL + k)(T_a - T_w)/(h_ac_3)$ where $c_3 = (k + h_wL + h_wk/h_a)$.]

21. The 1 ft thick walls of a building are made of concrete ($k = 2$ Btu/h·ft·F). The outside temperature and heat transfer coefficient are 50 F and 2 Btu/h·ft²·F, respectively. Find the rate of heat transfer through 1000 ft² of the wall if the inside temperature and heat transfer coefficient are 120 F and 1 Btu/h·ft²·F, respectively. Both the inside and the outside of the wall are coated with 20 mils of paint ($k = 0.1$ Btu/h·ft·F) where 1 mil = 1E-3 in. Compare the results with a bare wall.

22. Shown in the figure is a thermocouple well to measure the temperature of a high pressure fluid flowing at a distance δ_1 from the wall. The piping and the thermocouple well are made of steel. Use the given data to estimate the error in the thermocouple measurement of the fluid temperature.



Data: $T_f = 120$ F (49 C), $T_w = 60$ F (15.5 C), $k_f = 0.1$ Btu/h·ft·F (0.173 W/m·C), $k_w = 10$ Btu/h·ft·F (17.2 W/m·C), $h = 20$ Btu/h·ft²·F (113.6 W/m²·C), $a = 0.625$ in (1.587 cm), $b = 0.5$ in (1.27 cm), $c = 0.25$ in (0.635 cm), $d = 0.125$ in (0.3175 cm), $\delta_1 = 0.5$ in (1.27 cm), $\delta_2 = 2$ in (5.08 cm). Ignore thermal radiation.

23. Surface temperature of a bare slab fuel ($2L = 2$ cm, $k = 3.5$ W/m C) is 300 C. The volumetric heat generation rate in the slab is $\dot{q}''' = 1300$ kW/m³. Find the temperature of points located on a vertical plane 0.5 cm from the center plane. [Ans.: 314 C].

24. Fuel slabs are used in an experimental reactor. Find the maximum fuel temperature for the following data $T_f = 1090$ F, $L = 0.25$ in, $\delta = 0.025$ in, $k_F = 1$ Btu/ft-h-F, $k_C = 3$ Btu/ft-h-F, $h = 350$ Btu/ft²-h-F, and $\dot{q}''' = 1.0E7$ Btu/ft³-h. [Ans.: 4000 F].

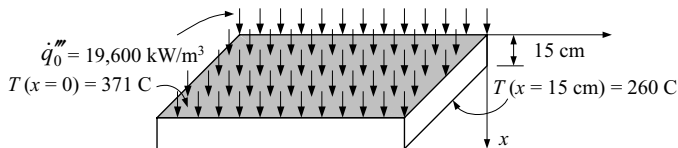
25. Surface temperatures of a plate are maintained at $T_0(x = 0)$ and $T_L(x = L)$. Thermal conductivity of the plate in the temperature range of interest remains constant. Find temperature distribution in the plate for a constant volumetric heat generation rate. [Ans.: $T(x) - T_0 = (\dot{q}'''L^2 / 2k)(1 - \xi)\xi + (T_L - T_0)\xi$ where $\xi = x/L$].

26. Surface temperatures of a plate are maintained at $T_0(x = 0)$ and $T_L(x = L)$. Thermal conductivity of the plate in the temperature range of interest remains constant. Find a) the maximum temperature in the plate and b) the location of the maximum temperature for a constant volumetric heat generation rate.

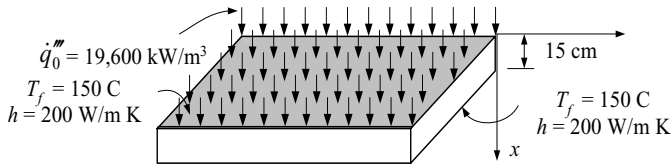
[Ans.: $x = (1 + \lambda)(L/2)$ where $\lambda = (T_L - T_0)/(\dot{q}'''L^2 / 2k)$].

27. Derive Equation IVa.5.16 directly from an energy balance using the elemental control volume of Figure IVa.5.7.

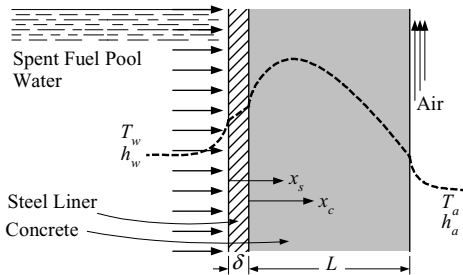
28. Gamma radiation is bombarding an iron plate as shown in the Figure. Temperatures of the surface at $x = 0$ and at $x = 15$ cm are maintained at 371 C and 260 C, respectively. Find the maximum temperature and its location in the plate. Also find temperature at 1 cm from the side facing the irradiation and the rate of heat removal from the side not being irradiated. $k = 48.5$ kW/m-K, $\mu = 24.6$ m⁻¹. [Ans.: $T_{max} = 594$ C, $x_{max} = 4.8$ cm].



29. Gamma radiation is bombarding an iron plate as shown in the figure. A convection boundary condition of $T_f = 150$ C and $h = 200$ W/m-K removes heat from the plate. Find the maximum temperature and its location in the plate. Also find temperature at 1 cm from the side facing irradiation and the rate of heat removal from the side not being irradiated. $k = 48.5$ kW/m K, $\mu = 24.6$ m⁻¹.



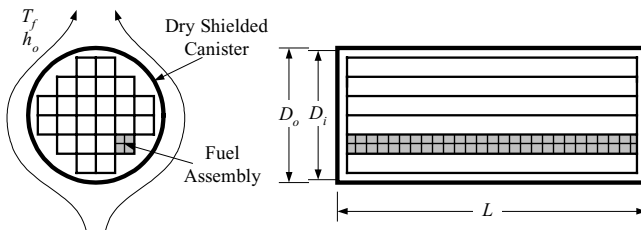
30. Regarding the radiation heating of a spent fuel pool wall, we want to determine the maximum temperature in the concrete. In the solution, you must account for heat generation in both steel and concrete. The rate of heat generation in these mediums follows an exponential profile, $\dot{q}'''(x) = \dot{q}_0'''e^{-\mu x}$. Find the maximum temperatures and their locations in both steel liner and concrete. Subscripts *a*, *c*, *s*, and *w* are used for air, concrete, steel liner, and water, respectively.



T_w (F):	130
T_a (F):	100
h_w (Btu/h·ft ² ·F):	50
h_a (Btu/h·ft ² ·F):	1
k_s (Btu/h·ft·F):	10
k_c (Btu/h·ft·F):	0.8
\dot{q}_s''' (Btu/h·ft ³ ·F):	1500
$(\dot{q}_0''')_c$ (Btu/h·ft ³ ·F):	400
μ_s (ft ⁻¹):	14
μ_c (ft ⁻¹):	5
L (ft):	5
δ (in):	0.5

Section 6

31. A dry shielded canister (DSC) is a hermetically sealed circular cylinder, containing spent nuclear fuel assemblies for long time storage. Consider a design in which the DSC is filled with helium and placed horizontally for passive cooling in the ambient.



If there are 26 fuel assemblies in a DSC and each fuel assembly produces a design decay power of 0.5 kW, estimate the amount of helium mass the DSC should be filled with so that at the thermodynamic equilibrium, the helium pressure does not exceed 5 psig. Assume $T_f = 105$ F, $D_o = 68$ in, $D_i = 65$ in, $L = 10$ ft, $h_o = 10$ Btu/h·ft²·F. The DSC shell is made of stainless steel. The end plates have the same thickness as the shell and are made of the same material. An internal heat transfer coefficient of $h_i = 20$ Btu/h·ft²·F is found to represent the combined ther-

mal radiation, heat conduction, and heat convection inside the canister. Ignore thermal radiation from the canister to the ambient.

32. A bare fuel rod has a diameter of 0.373 in and length of 12 ft. The volumetric heat generation rate for this rod is $\dot{q}''' = 10,000 \text{ kW/ft}^3$. The heat produced by the rod is removed by water used as the coolant, at 2250 psia and 575 F. Find the heat transfer coefficient between the bare fuel rod and the coolant. The fuel rod surface temperature is 675 F. [Ans.: $h = 2651 \text{ Btu/h}\cdot\text{ft}^2\cdot\text{F}$].

33. Working fluid at 35 F flows in a 2 in pipe. Ambient temperature is 125 F. The pipe is covered with 2 layers of insulation each having a thickness of 5 in with $k_1 = 0.015 \text{ Btu/ft}\cdot\text{h}\cdot\text{F}$ and $k_2 = 0.04 \text{ Btu/ft}\cdot\text{h}\cdot\text{F}$. The pipe is 0.2 in thick with $k = 8 \text{ Btu/ft}\cdot\text{h}\cdot\text{F}$. Find the rate of heat transfer to the working fluid in 100 ft of pipe. Assume $h_a = 200 \text{ Btu/ft}^2\cdot\text{h}\cdot\text{F}$ and $h_b = 15 \text{ Btu/ft}^2\cdot\text{h}\cdot\text{F}$. [Ans.: $UA = 5 \text{ Btu/h}\cdot\text{F}$ and $\dot{Q} = 454.5 \text{ Btu/h}$].

34. A steam pipe, made of copper, has an inside diameter of 5 cm and an outside diameter of 6.2 cm. To reduce thermal loss to the surroundings, the pipe is insulated with 2.55 cm thick fiberglass. An aluminum foil of thickness of 0.2 mm covers the insulation. Find the rate of heat loss from the pipe using the following data: $h_i = 142 \text{ W/m}^2\cdot\text{K}$, $T_i = 150 \text{ C}$, $h_o = 68 \text{ W/m}^2\cdot\text{K}$, $T_o = 27 \text{ C}$, $L_{\text{pipe}} = 98.5 \text{ m}$. [Ans.: 0.43 kW].

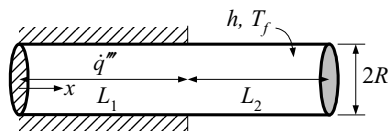
35. Superheated steam flows in an insulated pipe. Find the rate of heat loss for the following data.

Region	d_i (cm)	d_o (cm)	k (W/m \cdot K)
Pipe	89.0	92.0	50.
Paint	92.0	92.2	3.0
Insulator 1	92.2	100.0	0.2
Insulator 2	100	120.0	0.1

Additional data: $T_a = 350 \text{ C}$, $h_a = 1000 \text{ W/m}^2\cdot\text{K}$, $h_b = 20 \text{ W/m}^2\cdot\text{K}$, $T_b = 20 \text{ C}$, $L = 100 \text{ m}$. [Ans.: $UA = 271.3 \text{ W/C}$ and $\dot{Q} = 0.3 \text{ MW}$].

36. Find the surface temperature, surface heat flux, and linear heat generation rate of an electric resistor. The resistor is in the form of a solid cylinder of diameter 0.2 in and $k = 50 \text{ Btu/h}\cdot\text{ft}\cdot\text{F}$. Heat is produced uniformly in the cylinder so that $\dot{q}''' = 5\text{E}7 \text{ Btu/h}\cdot\text{ft}^3$. Assume the center temperature is maintained at 300 F. [Ans.: 282.6 F, $\dot{q}'' = 2.08 \text{ Btu/h}\cdot\text{ft}^2$, and $\dot{q}' = 3.2 \text{ kW/ft}$].

37. A long and slender shaft of diameter $2R$ and length $L_1 + L_2$ is insulated over length L_1 and produces heat only in this section while over length L_2 , it is exposed to a convection boundary (h , T_f). Write the governing differential equations and the associated boundary conditions from which temperatures in sections L_1 and L_2 can be obtained. Both ends may be treated as adiabatic surfaces.



38. An electric resistor, $R = 0.1$ in, is steadily generating heat at a rate of $\dot{q}''' = 5E7$ Btu/h·ft³. The centerline temperature is maintained at 300 F, find surface temperature, surface heat flux, and \dot{q}' . $k = 50$ Btu/ft·h·F. [Ans.: $T_s = 282.6$ F, $\dot{q}'' = 2.1E5$ Btu/h·ft², and $\dot{q}' = 3.2$ kW/ft].

39. A fuel rod of a PWR consists of about 320 solid fuel pellets inside a zircaloy cladding. Use the specified data to plot the distribution of temperature in the fuel rod. The temperature distribution should include the fuel region, the gap region, the cladding region, and end at the bulk coolant for two cases of low and high linear heat generation rates. Data: $D_{\text{Fuel}} = 0.96$ cm, $D_{\text{Inside Clad}} = 0.985$ cm, $D_{\text{Outside Clad}} = 1.12$ cm, $k_{\text{Fuel}} = 1.73$ W/m·C, $k_{\text{Clad}} = 5.2$ W/m·C, $T_{\text{Water}} = 300$ C, $\dot{q}'_{\text{Low}} = 5$ kW/ft (164 W/cm), and $\dot{q}'_{\text{High}} = 15$ kW/ft (492 W/cm). The heat transfer coefficient from the fuel rod to bulk coolant is 34 kW/m²·C. The heat transfer coefficient in the gap region is 5.7 kW/m²·C for the low and is 11.4 kW/m²·C for the high linear heat generation rate.

40. Use the following data to plot the temperature distribution in a cylindrical fuel rod for a) a linear heat generation rate of 5 kW/ft and b) a linear heat generation rate of 15 kW/ft. Data: Fuel diameter = 0.377 in, Clad inside diameter = 0.388 in, Clad outside diameter = 0.44 in, fuel thermal conductivity = 1 Btu/h·ft·F, cladding thermal conductivity = 13 Btu/h·ft·F, gap heat transfer coefficient = 1000 Btu/h·ft²·F. Heat transfer coefficient to coolant is 6000 Btu/h·ft²·F and coolant temperature is 575 F. The fuel has a central hole but no coolant flows in the central hole. The hole has a diameter of 0.04 in.

41. Find the maximum temperature and its location in a two-stream annular fuel rod with inner and outer cladding. $T_i = 350$ C, $T_o = 340$ C, $h_i = 10,000$ W/m²·C, $h_o = 8,000$ W/m²·C, $k_F = 3.5$ W/m·C, $k_C = 11$ W/m·C, $\dot{q}' = 9$ kW/ft, $d_1 = 5$ mm, $d_2 = 9$ mm, $d_3 = 17$ mm, $d_4 = 21$ mm. [Ans.: $c_1 = 141$, $c_2 = 1250$, $c_3 = 965$, $c_4 = 5970$, $c_5 = -282$, $c_6 = -908$, $r_{\text{max}} = 6.11$ mm, $T_{\text{max}} = 568.6$ C].

42. A fuel rod is producing heat at a rate of 8 kW/ft. The rod has a central hole. Helium flows over the rod as well as inside the central hole. Find the maximum temperature and its location for this fuel rod.

Fuel geometry data: diameter of the central hole: 0.25 in, thickness of the inner clad: 1/8 in, outside diameter of fuel: 1 in, thickness of outer clad: 1/8 in. Thermal conductivity data: clad: 30 Btu/h·ft·F, fuel: 1 Btu/h·ft·F. Temperature and heat transfer coefficient data: bulk fluid temperature in the central hole: 595 F, heat transfer coefficient in the central hole: 3000 Btu/h·ft²·F, bulk fluid temperature outside the fuel rod: 590 F, heat transfer coefficient outside fuel rod: 2500 Btu/h·ft²·F.

43. A two-stream annular fuel rod includes inner and outer cladding. Use the following data and determine equation for temperature as a function of radius for the inner clad, fuel, and the outer clad regions. Also find the maximum temperature and its location.

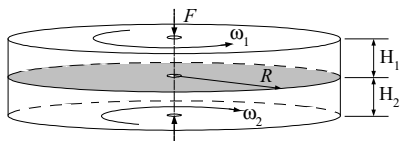
Data: $R_1 = 0.25$ in, $R_2 = 0.27$ in, $R_3 = 0.55$ in, $R_4 = 0.58$ in, $\dot{q}' = 11$ kW/ft, $k_F = 3.5$ W/m·C, $k_C = 11$ W/m·C, $T_i = 350$ C, $T_o = 300$ C, $h_i = 6,000$ W/m²·C, $h_o = 4500$ W/m²·C.

[Ans.: $r(T_{max}) = 0.39$ in, $T_{max} = 546$ C, $T_{ci} = 182\ln r + 1330$, $T_F = -5.543E6r^2 + 1090\ln r + 6120$, $T_{co} = -332\ln r - 1040$ where r is in meter and T in degrees Centigrade].

44. Plot the steady state temperature distribution for the fuel rod of Problem 43.

[Ans.: The key temperatures are $T_{fi} = 350$ C, $T(R_1) = 409$ C, $T(R_2) = 423$ C, $T_{max} = 546$ C, $T(R_3) = 0.378$ C, $T(R_4) = 360$ C, $T_{fo} = 300$ C. Find the temperature of several other points, especially in the fuel region].

45. Two rigid circular cylinders, in perfect contact are pressed together by the action of force F . Initially, the cylinders are in thermal equilibrium with the ambient at temperature T_f . At time zero cylinders begin to rotate at nominal speeds of ω_1 and ω_2 as shown in the figure. The bottom cylinder rotates clockwise and the upper cylinder rotates counterclockwise. The coefficient of dry friction between the cylinders is μ . The heat resulting from the friction of the rotating cylinders, raises their temperature. Heat transfer coefficient for the upper cylinder surface area is h_{s1} and for the horizontal area is h_{a1} . Similarly, heat transfer coefficient for the bottom cylinder surface area is h_{s2} and for the horizontal area is h_{a2} . Use these data and those given in the figure to a) write the differential equations from which temperature distribution in each cylinder can be obtained and b) identify the initial and the boundary conditions.



[Hint: Temperatures are obtained from Equation IVa.2.7 with $\partial T / \partial \theta = 0$ due to symmetry in the θ direction. There are 2 initial and 8 boundary conditions].

46. Find the governing differential equation for temperature distribution in spheres with symmetry in θ and ϕ directions.

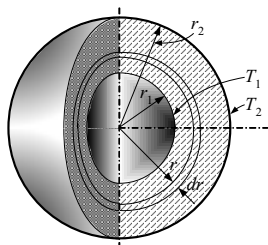
[Ans. $1/r^2 d/dr(r^2 dT/dr) + \dot{q}'''/k = 0$].

Section 7

47. Derive the temperature profile in a thick-wall sphere for a temperature boundary condition (i.e., $T(r_1) = T_1$ and $T(r_2) = T_2$). {Ans.: $T(r) = [(A/r) - B]/C$ where $A = (r_1 r_2 T_1 - r_1 r_2 T_2)$, $B = r_1 T_1 - r_2 T_2$, and $C = r_2 - r_1$ }.

48. Derive a temperature profile in a thick-wall sphere for a convection boundary, $h_1[T_{f1} - T(r_1)] = -kdT(r_1)/dr$ and $h_2[T(r_2) - T_{f2}] = -kdT(r_2)/dr$. {Ans.: $T = T_{f1} - [(T_{f1} - T_{f2})/B][A - 1/r]$ where $A = 1/r_1 + k/h_1 r_1^2$ and $B = C + D$ where $C = 1/r_1 - 1/r_2$ and $D = k/h_1 r_1^2 + k/h_2 r_1^2$ }

49. To find the thermal conductivity of a substance, two hemispheres of this substance are made to form a sphere. A heat source is placed in the center of this sphere. Assuming perfect contact of the two halves and isotropic heating of the inner surface, use the given data to find thermal conductivity. [Ans.: 2 W/m·K].



$$R_1 = 10 \text{ cm}$$

$$R_2 = 15 \text{ cm}$$

$$T_1 = 340 \text{ C}$$

$$T_2 = 300 \text{ C}$$

$$\dot{Q} = 300 \text{ W}$$

50. A thick-wall spherical container is filled with a hot liquid. A pump circulates the liquid to maintain the bulk temperature at 150 C. Ignore temperature gradient in the liquid. Find temperature in the middle of the wall and the energy required to keep liquid temperature at 150 F for an hour. $D_i = 3 \text{ m}$, $\delta_{\text{wall}} = 20 \text{ cm}$, $k = 20 \text{ W/m} \cdot \text{C}$, $T_{f1} = 150 \text{ C}$, $T_{f2} = 25 \text{ C}$, $h_i = 500 \text{ W/m}^2 \cdot \text{C}$, and $h_o = 10 \text{ W/m}^2 \cdot \text{C}$.

51. A spherical fuel element has a center temperature of 3600 F. The fuel element is covered by two layers of coating. The fuel ball is cooled by helium. Find the rate of heat transfer. Data: $r_{\text{fuel}} = 0.5 \text{ in}$, $r_1 = 0.7 \text{ in}$, $r_2 = 0.9 \text{ in}$. $k_{\text{fuel}} = 2 \text{ Btu/ft} \cdot \text{h} \cdot \text{F}$, $k_{\text{coating}} = 7 \text{ Btu/ft} \cdot \text{h} \cdot \text{F}$, $T_f = 700 \text{ F}$ and $h = 5000 \text{ Btu/ft}^2 \cdot \text{h} \cdot \text{F}$. [Ans.: 4100 Btu/h].

52. Derive the temperature profile in a hollow and bare spherical fuel ball. [Ans.: $T = -(\dot{q}'''/6k_F)r^2 - c_1/r + c_2$ where $c_1 = \dot{q}''' r_1^3/3k_F$ and $c_2 = T_f + c_1[\alpha - (\beta k_F/h)]$ where $\alpha = 1/r_2 + r_2^2/2 r_1^3$ and $\beta = r_2/r_1^3 + 1/r_2^2$]

Section 8

53. A stainless steel spoon is used to stir hot tea maintained at 49 C. The spoon can be approximated as a rectangular parallelepiped having a length of 15 cm, a width of 6 mm and a thickness of 2 mm. The exposed length of the spoon to the ambient at 18 C is 5 cm. Find a) the rate of heat loss from the spoon assuming an average heat transfer coefficient of 6 W/m²·K with the ambient and b) fin efficiency. [Ans.: $\approx 0.1 \text{ W}$, 25%].

54. As shown in the figure, to dissipate heat from an electrical appliance, thin plates of metal with a thermal conductivity of 10 Btu/h·ft·F are used. Find the

number of the plates to dissipate 10.55 W at steady state operation. Data: $T_{base} = 85^\circ\text{F}$, $T_f = 65^\circ\text{F}$, $h = 1 \text{ Btu/h}\cdot\text{ft}^2\cdot\text{F}$, $L = 10 \text{ in}$, $b = 1 \text{ in}$, $\delta = 0.03 \text{ in}$. [Ans.: 15].

55. A longitudinal fin of triangular profile is made of aluminum. The base temperature is 350°C . The top and the bottom of the fin are exposed to a convection boundary given as $T_f = 30^\circ\text{C}$ and $h = 50 \text{ W/m}^2\cdot\text{K}$. Find a) the fin temperature at $x = l/2$ and b) the heat removed by the fin. Additional data: $b = 1 \text{ cm}$ and $l = 1.5 \text{ cm}$.

56. An annular fin is used to cool an internal combustion engine. Find a) the total rate of heat transfer from the fin b) fin temperature at $r = r_i/2$, c) fin effectiveness, defined as the rate of heat loss from the fin to the rate of heat loss without the fin, and d) fin efficiency, defined as the rate of heat loss from the fin to the rate of heat loss from the fin if the entire fin were at the base temperature. The fin is made of commercial bronze. Data: $r_i = 20 \text{ cm}$, $r_b = 10 \text{ cm}$, fin thickness = 5 mm , base temperature = 250°C , $T_f = 15^\circ\text{C}$, and $h = 100 \text{ W/m}^2\cdot\text{K}$.

[Ans.: $T(15 \text{ cm}) =$ a) 136°C , b) 611 W , c) about 8.3, and d) about 52%].

57. A longitudinal fin of rectangular profile is used to enhance heat removal from a wall maintained at 450°F . The fin is made of carbon steel. The fin is exposed to a convection boundary. Find a) temperatures at the tip of the fin and b) the rate of heat loss from the fin, c) fin effectiveness, defined as the rate of heat loss from the fin to the rate of heat loss without the fin, and d) fin efficiency, defined as the rate of heat loss from the fin to the rate of heat loss from the fin if the entire fin were at the base temperature. Fin length = 1 in , fin thickness = $1/8 \text{ in}$, fin width = 6 in , $T_f = 72^\circ\text{F}$, $h = 5 \text{ Btu/h}\cdot\text{ft}^2\cdot\text{F}$. [Ans.: b) 159 Btu/h].

58. We plan to design an engine with an outside diameter of 10 cm and height of 12 cm . The outside surface is at 200°C . Several means of cooling the engine are to be evaluated including the use of cylindrical spines. The spines to be evaluated have a diameter of 1 in and a length of 3 cm . Find a) the amount of heat removed by a total of 240 equally spaced spines and b) find the fin efficiency. Assume the surface temperature is uniform over the entire surface of the engine. Data: $k = 50 \text{ W/m}\cdot\text{K}$, $T_b = 200^\circ\text{C}$, $T_f = 12^\circ\text{C}$, and $h = 13 \text{ W/m}^2\cdot\text{K}$. [Ans.: a) 0.6 kW].

59. A pressure vessel containing a mixture of water and steam is shown in the figure. The flange attached to the vessel head is secured tightly to the lower flange attached to the rest of the vessel by 24 bolts. If the base temperature in the bolt at the connection to the upper nut is 350°F , find the amount of heat lost by the last 3 in of the stainless steel bolts. Use $T_f = 70^\circ\text{F}$, $h_f = 1 \text{ Btu/h}\cdot\text{ft}^2\cdot\text{F}$, and $k_{Bolt} = 10 \text{ Btu/h}\cdot\text{ft}\cdot\text{F}$. [Ans. 0.125 kW].

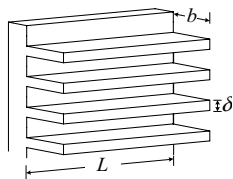


Figure for Problem 54

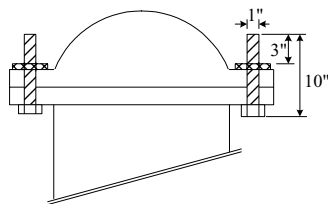


Figure for Problem 59

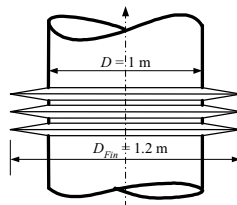
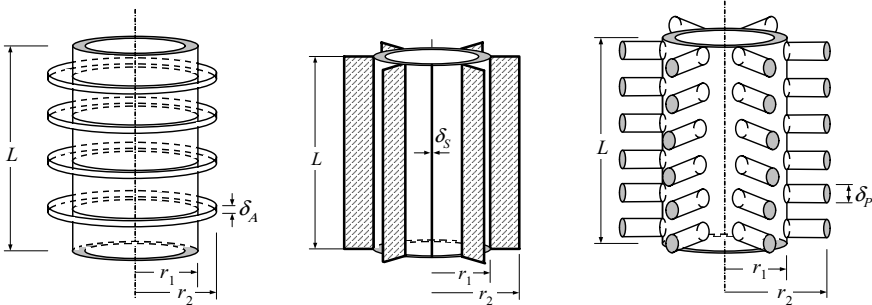


Figure for Problem 60

60. A pipe carrying superheated steam is equipped with an expansion joint to prevent structural damage in the case of temperature driven transients. The expansion joints are thin stainless steel plates welded at the tip to other plates and at the base to the steel pipe. Find the amount of heat loss to the surroundings in the case where the plates are not insulated. There are 3 sets of expansion joints as shown in the figure. In the pipe, steam is flowing at 150 C while the surrounding is at 20 C. Additional data: $h_a = 250 \text{ W/m}^2\cdot\text{K}$, $h_b = 15 \text{ W/m}^2\cdot\text{K}$.

61. Due to the manufacturing preferences, only three types of fins are to be considered for the cooling of an air-cooled internal combustion engine.. These are annular fins with rectangular profile, straight fins of uniform cross section, and pin fins (cylindrical spines). The cylinder height is 20 cm and has a base diameter ($2r_1$) of 8 cm. All fins have insulated tips. The cylinder base temperature is 200 C, the cooling air temperature is 30 C, and the heat transfer coefficient is estimated at about $50 \text{ W/m}^2\cdot\text{K}$. Fins are spaced equally and uniformly. Subscripts A, S, and P are used to represent annular fin, straight fin, and pin fin, respectively. Use the following data to find: a) the rate of heat removal from each type of fin and b) temperature at the tip ($r = r_2$) of each fin.



Data: $L = 20 \text{ cm}$, $r_1 = 4 \text{ cm}$, $r_2 = 9.55 \text{ cm}$, $\delta_A = 8 \text{ mm}$, $\delta_S = 3 \text{ mm}$, $d_p = 2 \text{ cm}$, $N_A = 4$, $N_S = 6$, $N_P = 36$.

62. Two cylindrical aluminum spines, having equal length and equal outside diameter are attached to a hot wall. One of the spines is made of a solid rod and the other is a pipe. Compare the rate of heat loss from these otherwise identical fins. The outside diameter is 5 cm and the pipe inside diameter is 4 cm. The wall is at 300 C and the ambient temperature and heat transfer coefficient are 35 C and $15 \text{ W/m}^2\cdot\text{K}$, respectively. Assume the same heat transfer coefficient for the inside of the pipe.

Section 9

63. Consider two blocks of nickel, treated as semi-infinite solids. Initially, one block is at 0 C and the other at 100 C. We now bring these blocks in contact. Ignore the contact thermal resistance and find the temperature of a point located 5 cm from the common boundary in either block, 5 minutes after the contact. Use $\alpha_{\text{Nickel}} = 2.3\text{E-}5 \text{ m}^2/\text{s}$. [Ans.: 34 C and 66 C].

64. Consider two blocks treated as semi-infinite solids. One block is made of copper and the other of stainless steel. Initially, the block made of copper is at 0 C and the block made of stainless steel at 100 C. We now bring these blocks in contact. Ignore the contact thermal resistance and find the temperature of a point located 5 cm from the common boundary in either block, 5 minutes after the contact.

65. A PWR pressurizer is at 2200 psia. A sudden outsurge results in all the water leaving the pressurizer. Find the temperature at a depth of 1 in, 10 minutes into the event. Steel properties; $k = 25 \text{ Btu/ft}\cdot\text{h}\cdot\text{F}$ and $\alpha = 1.3\text{E-}4 \text{ ft}^2/\text{s}$. $h = 75 \text{ Btu/ft}\cdot\text{h}\cdot\text{F}$. Initial water volume 850 ft^3 . Pressurizer volume 1700 ft^3 . [Hint: $T_i = T_{\text{sat}}(2200 \text{ psia}) = 649.5 \text{ F}$ and $T_f = T_{\text{sat}}(P_2)$ where $P_2 = P_1 (V_1/V_2)^k$]. (Ans. $P_2 = 875 \text{ psia}$, $T_f = 528.6 \text{ F}$, $\arg_1 = 0.15$, $\arg_2 = 0.952$, $\arg_3 = 0.988$, and $T = 545 \text{ F}$)

66. A long steel rod is suddenly exposed to a convection boundary. Find the temperature at $r = 0.35 \text{ in}$ after a duration of 75 s . Data: rod diameter = 2 in , $k = 20 \text{ Btu/ft}\cdot\text{h}\cdot\text{F}$, $c = 0.1 \text{ Btu/lbm}\cdot\text{F}$, $\rho = 488 \text{ lbm/ft}^3$, $T_i = 550 \text{ F}$, $T_f = 75 \text{ F}$, $h = 100 \text{ Btu/ft}^2\cdot\text{h}\cdot\text{F}$. [Ans.: $T_o = 282 \text{ F}$, $T(r = 0.35 \text{ in}) = 277 \text{ F}$, $Q = 305 \text{ Btu/ft}$].

67. A long slender steel bar initially at 400 C is exposed to a convection boundary of $T_f = 35 \text{ C}$ and $h = 375 \text{ W/m}^2\cdot\text{C}$. The bar diameter is 5 cm . Find the temperature at $r = 0.75 \text{ cm}$ after 85 seconds of exposure. [Ans.: $T_o = 241.5 \text{ C}$, $T_r = 239 \text{ C}$].

68. Aluminum balls are heated up to 580 K and then exposed to air at 283 K to cool down with an average heat transfer coefficient of $25 \text{ W/m}^2\cdot\text{K}$. The balls are 3 cm in diameter. Find the temperature at $r = 0.5 \text{ cm}$ after 75 seconds of exposure. Is the lumped capacitance an acceptable solution here? [Ans.: 329 K].

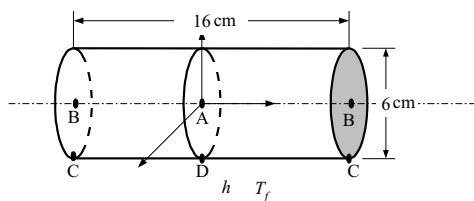
69. A sphere made of fire-clay brick is heated to 500 C and cooled in ambient air at $T_f = 35 \text{ C}$ and $h = 250 \text{ W/m}\cdot\text{C}$. The sphere has a diameter of 10 cm . Find the temperature at a radius of 2.5 cm after 30 minutes. Data: $k = 1 \text{ W/m}\cdot\text{C}$, $c = 1 \text{ kJ/kg}$, $\rho = 2000 \text{ kg/m}^3$. [Ans.: $K(r, t) = 0.663$. $T = 343 \text{ C}$].

70. A short stainless steel cylinder ($D = 8 \text{ cm}$ and $2L = 6 \text{ cm}$) is initially at 327 C . Find the temperature at a location identified as $r = D/2$ and $x = 0$ after being suddenly exposed for 3 minutes to air at $T_f = 27 \text{ C}$ and a heat transfer coefficient of $h = 500 \text{ W/m}\cdot\text{C}$. [Ans.: $P(x, t) = 0.635$ and $C(r, t) = 0.337$. $T = 91 \text{ C}$].

71. A long stainless steel rod ($\rho = 7900 \text{ kg/m}^3$, $c = 0.526 \text{ kJ/kg}\cdot\text{K}$, and $k = 17.4 \text{ W/m}\cdot\text{K}$) having a diameter of 5 cm , is initially at 200 C when its surface is exposed to an ambient at 300 K with a heat transfer coefficient of $600 \text{ W/m}^2\cdot\text{K}$. After 2 min exposure, find: a) the centerline temperature and b) the temperature at a distance of 1 cm from the rod centerline. c) Find the temperature of 10 equally-spaced points inside the rod after 2 min of exposure and plot the results. d) Track the centerline temperature every 5 seconds and plot the results for the 2 minutes of exposure. [Ans.: a) 93 C and b) 90 C].

72. A solid rectangular parallelepiped is made of aluminum and is initially at 20 C. The base is a 2 cm by 3 cm rectangle and the height of the parallelepiped is 5 cm. The parallelepiped is now dropped into hot oil at 150 C. Find: a) the temperature of point P and b) the temperature of the center of the parallelepiped after 2 min of exposure to hot oil. Point P is located 1 cm above the center plane and 1 cm from each side.

73. A short cylinder having an initial temperature of 40 C is suddenly exposed to a convection boundary of $300 \text{ W/m}^2\cdot\text{K}$. Use the data given below to find the temperatures of points A, B, C, and D. Data: $k = 26 \text{ W/m}\cdot\text{K}$, $c_p = 0.349 \text{ kJ/kg}\cdot\text{K}$, $\rho = 8,666 \text{ lbm/m}^3$. [Ans.: $T_A = 176 \text{ C}$, $T_B = 184 \text{ C}$, $T_C = 186.5 \text{ C}$, $T_D = 180 \text{ C}$].



Section 10

74. A cylindrical spine is used is shown in the figure. a) Use the given data to find the temperature distribution in the solid rod. The tip of the fin loses heat by convection. b) Find the temperature of a node by numerical methods as described in Section 3 of Chapter VII. First divide the fin into 5 equally spaced nodes. Repeat the solution for the number of nodes increased to 10 and finally to 20. c) Compare the results obtained in part b with the analytical solution of part a. Data: $L = 20 \text{ cm}$, $D = 2 \text{ cm}$, $k = 50 \text{ W/m}\cdot\text{C}$, $T_B = 250 \text{ C}$, $T_f = 35 \text{ C}$, $h = 10 \text{ W/m}^2\cdot\text{C}$.

75. Two surfaces of a long L-shape object are maintained at temperatures T_{s1} (along the x -axis) and T_{s2} (along the y -axis) as shown in the figure. All other surfaces are exposed to a convection boundary (T_f and h). Use the method described in Section 3 of Chapter VII to find temperatures at location 1, 5, and 7. Data: $a = 2 \text{ cm}$, $T_{s1} = 50 \text{ C}$, $T_{s2} = 100 \text{ C}$, $T_f = 15 \text{ C}$, $h = 10 \text{ W/m}^2\cdot\text{C}$.

76. All surfaces of an infinitely long heating element, having a cross section in the shape of a cross, are maintained at 300 C. Due to symmetry, only a quarter of the cross section is shown in the figure. Heat is uniformly produced in the element at a rate of 100 kW/m^3 . Find the temperature distribution in the element at the locations shown in the figure. The element thermal conductivity is $35 \text{ W/m}\cdot\text{K}$. All surfaces are exposed to a convection boundary condition of $T_f = 40 \text{ C}$ and $h = 1200 \text{ W/m}^2\cdot\text{C}$.

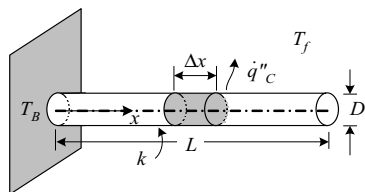


Figure for Problem 74

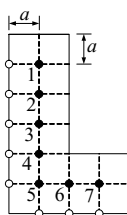


Figure for Problem 75

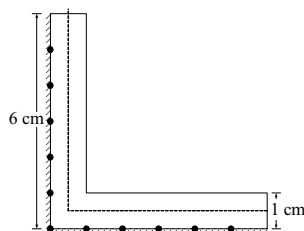


Figure for Problem 76

77. The surfaces of a long solid square bar are maintained at the temperatures shown in the figure. The solid thermal conductivity is 25 W/m-C. Find the temperatures of the nodes shown in the figure.

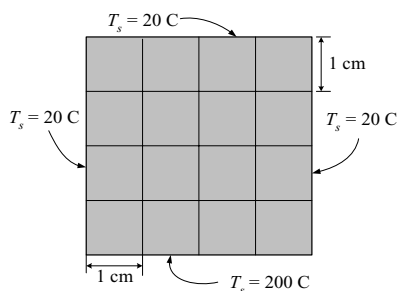


Figure for Problem 77

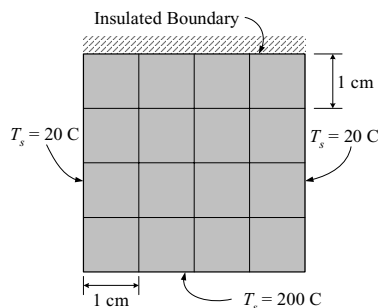


Figure for Problem 78

78. One side of the bar of Problem 76 is now insulated. Find the temperature distribution in the bar.

79. Use the given data to find the temperature distribution in the plate with one side insulated, three sides are isothermal and the indentation is exposed to a convection boundary.

80. A plate-type fuel element, having a thermal conductivity of 2 W/m-K, produces heat. The heat source is uniformly distributed, having a source strength of 2.4×10^8 W/m³. One side of the fuel is insulated (due to symmetry), one side is maintained at 200 F, and remaining sides are exposed a convection boundary of 300 C and $34 \text{ kW/m}^2 \cdot \text{K}$. Find the two-dimensional temperature distribution in the fuel at steady state condition.

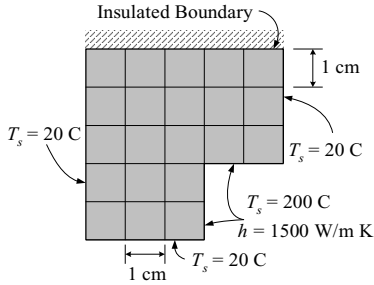


Figure for Problem 79

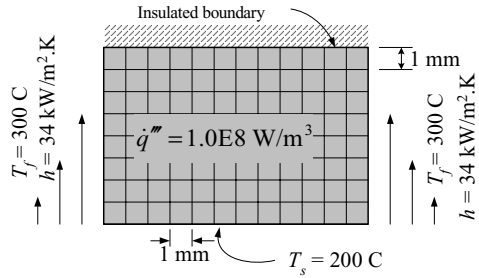
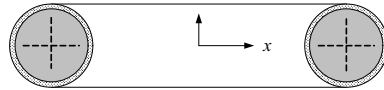
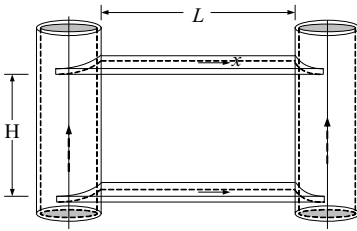


Figure for Problem 80

81. Shown in the figures are the elevation and the plan views of two pipes carrying hot air. The air flow rate is 200 kg/s in each of the two 12 inch, schedule 40 steel pipes. The pipes are connected to each other by 2 steel support plates. The plates have a thickness of 2 cm and are placed 50 cm apart from each other. The distance between the pipes is 55 cm. Find a) temperature at $x = 0$ for steady state operation in the bottom plate and b) find the temperature of the top plate at the same location. Data: Assume a constant heat transfer coefficient of $2500 \text{ W/m}^2 \cdot \text{K}$ inside the pipe. The air pressure and bulk temperature at the entrance to the pipe (where the bottom plate is located) are 3 MPa and 300 C, respectively. The ambient temperature is 37 C and the heat transfer coefficient with the ambient is $12 \text{ W/m}^2 \cdot \text{K}$. Assume that the pipes are smooth.



IVb. Forced Convection

In Chapter IVa we often used the convection boundary condition to determine temperature distribution in such cases as fuel rods, fins, and multi-dimensional solids. However in all such cases, the heat transfer coefficient, h was specified. Our primary goal in this chapter is to find the heat transfer coefficient for a given set of conditions. As we shall see, the magnitude of the heat transfer coefficient depends on such factors as the type of fluid, the flow velocity, and the type of application. The type of fluid in turn defines such fluid properties as viscosity, density, thermal conductivity, and specific heat. Flow velocity is a key parameter, which is used in conjunction with temperature to determine the flow regime, being laminar or turbulent. Finally, the type of application determines whether flow is external such as flow over flat plates, cylinders, and spheres or internal such as flow inside conduits. The immediate application of the heat transfer coefficient is in finding the temperature distribution and the rate of heat transfer to or from a substance. In this chapter we exclusively deal with forced convection heat transfer. The characteristic of this heat transfer mode is the fact that the flow of fluid is due to the operation of a pump, a compressor, or the rapid movement of an object in the flow field.

1. Definition of Forced Convection Terms

Newton's law of cooling is the result of applying the Isaac Newton's suggestion in 1701 that if a body is placed in a medium at a lower temperature, then the rate of change of temperature of the body is proportional to $T_{body} - T_f$ where T_f in this relation is the temperature of the colder medium. Since the rate of change of temperature of the body is also proportional to the rate of heat transfer from the body, we may then conclude:

$$\dot{q}'' = h(T_{body} - T_f)$$

where h , the proportionality factor is known as *heat transfer coefficient*. To be consistent, we replace T_{body} with T_s where subscript s represents a surface such as a flat plate or the wall of a conduit.

Thermal boundary layer over a flat plate develops whenever there is a temperature difference between a surface and the fluid flowing over the surface. The hydrodynamic boundary layer and the associated velocity profile for flow of a viscous fluid over a flat plate are shown in the left side of Figure IVb.1.1. Development of a similar boundary layer, for a case where the flat plate is hotter than the fluid, is shown in the right side of Figure IVb.1.1. The viscous forces are dominant in the hydrodynamic boundary layer resulting in a velocity profile as shown in the figure. Similarly, a temperature gradient exists in the thermal boundary layer. At the edge of the boundary, both velocity and temperature inside the boundary layer reach 99% of the free stream velocity (V_f) and temperature (T_f), respectively. Also at the edge of the boundary layer where $y = \delta$, we find that

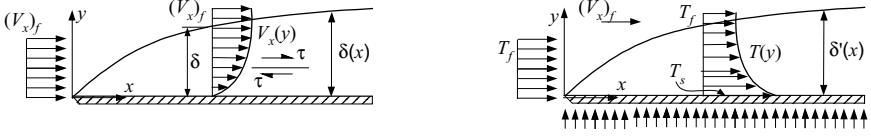


Figure IVb.1.1. Hydrodynamic and thermal boundary layers for flow over a heated flat plate

$\partial V_x(\delta)/\partial y = 0$. The amount of heat transferred from the flat plate to the boundary layer at any given x is obtained from the local heat flux by applying Fourier's law to the flowing fluid;

$$\dot{q}_s'' = -k_f \frac{dT(0)}{dy}$$

Also from Newton's law of cooling, we have $\dot{q}_s'' = h(T_s - T_f)$. Hence, the heat transfer coefficient h is found by setting the left sides of these two equations equal to each other:

$$h = \frac{-k_f \partial T(0)/\partial y}{T_s - T_f} \quad \text{IVb.1.1}$$

Since temperatures are changing with x , then $h = f(x)$. An average value for h is found from:

$$\bar{h} = \frac{\int_0^L h(x) dx}{\int_0^L dx} \quad \text{IVb.1.2}$$

Leading edge of a plate is defined as the location on the plate where $x = 0$.

Trailing edge of a plate is defines as the location on the plate where $x = L$ with L being the plate length.

Bulk temperature or the *mixing cup* temperature for a fluid flowing in a conduit is given as:

$$\bar{T}_f(x) = \frac{\int_A \{\rho V_x(r) dA\} \{c_p T(r, x)\}}{\int_A \{\rho V_x(r) dA\} \{c_p\}} \quad \text{IVb.1.3}$$

where A is the flow area. If the conduit is a circular cylinder, then the bulk temperature becomes;

$$\bar{T}_f(x) = \frac{\int_0^R \rho V_x(2\pi r dr) \{c_p T(r, x)\}}{\int_0^R \rho V_x(2\pi r dr) (c_p) dx} \quad \text{IVb.1.4}$$

Equation IVb.1.4 indicates that the bulk fluid temperature, being averaged at a given cross section, varies from cross-section to cross-section along the axis of the conduit. The inlet temperature of fluid, refers to the bulk fluid temperature entering a conduit.

Film temperature is an arithmetic average between fluid bulk temperature (T_f) and the surface temperature (T_s) (i.e., $T_{Film} = (\bar{T}_f + T_s)/2$).

Prandtl number, after Ludwig Prandtl (1875–1953), is a measure of diffusion of momentum, as compared to the diffusion of heat in a fluid. The momentum diffusion appears as kinematic viscosity and diffusion of heat as thermal diffusivity. Hence, $Pr = \nu/\alpha = (\mu/\rho)/(k/\rho c_p) = \mu c_p/k$. Since the diffusion of momentum and heat are also associated with the thickness of the boundary layer, the Prandtl number is then a parameter which relates δ , the thickness of the hydrodynamic boundary layer to δ' , the thickness of the thermal boundary layer. See Table A.I.6 for the list and the significance of various dimensionless numbers.

The range of Pr number for some fluids is shown in Table VIb.1.1. For water temperature in the range of 330 F (165 C) $\leq T \leq$ 430 F (221 C), the Prandtl number for water is about unity, $Pr_{Water}(T) \approx 1$.

Table IVb.1.1. Range of Pr number for various fluids

Fluid	Liquid metals	Gases	Water	Light Organic Liquids	Oils	Glycerin
Range of Pr	0.003–0.05	0.7–1	1–13	5–50	50–10000	2E3–8.5E3

The Pr number for various fluids is given in the tables of Appendix IV.

Nusselt number, after Ernest Kraft Wilhelm Nusselt (1882–1957), is a measure of the temperature gradient at the surface. Dividing heat flux due to convection by the heat flux due to conduction, both expressed at the surface, we find:

$$Nu = \frac{(\dot{q}_s'')_{Convection}}{(\dot{q}_s'')_{Conduction}} = \frac{h\Delta T}{-kdT/dx} \approx \frac{h\Delta T}{k(\Delta T/\Delta x)} = \frac{h\Delta x}{k}$$

This dimensionless ratio shows that for a flat plate, Nu number is a function of the distance from the leading edge, $Nu = f(x)$. Additionally, at any given x , temperature ranges from T_s to T_f . Hence at any x , thermal properties may be evaluated at the film temperature.

Stanton number is the division of the Nu number by the product of the Re and the Pr numbers. Therefore, $St = Nu/(RePr)$. Substituting for Nu, Re, and Pr numbers in terms of the fluid and the flow properties, we find the Stanton number given as $St = h/(\rho V c_p)$.

Eckert number after E. R. G. Eckert, is the ratio of the temperature rise due to energy conversion to the overall temperature gradient. The Eckert number is then given by $Ec = V_f^2 / c_p \Delta T$.

Reynolds-Colburn analogy is a convenient means of allowing the measurement of heat transfer coefficient from the frictional drag on a flat plate in an adiabatic process. By using the Reynolds-Colburn analogy, it can be shown that the friction factor is given as $f = 2\text{StPr}^{2/3}$.

2. Analytical Solution

To find the heat transfer coefficient in forced convection analytically, we have to limit our analysis to the simplest cases of laminar flow over a flat plate or in conduits. Even these seemingly simple cases require the introduction of several simplifying assumptions to enable us to reach a solution. Before embarking on such analysis, it should be added that the application of such simple cases in practice is rather limited. However, the advantage of such analytical solutions is that they allow us to seek solutions having the same functional relationship for more complicated cases such as those involved in turbulent flow. That is to say that the functional relationship assists us in finding experimentally-based empirical correlation for cases, which are not amenable to analytical solution.

2.1. External Laminar Flow

Consider the steady laminar flow of an incompressible viscous fluid over a flat surface ($\text{Re} < 5\text{E}5$). If fluid temperature differs from that of the plate then both hydrodynamic and thermal boundary layers would develop over the plate. Let us further assume that the plate is isothermal, such fluid properties as k , μ , and c_p are independent of temperature, and conduction heat transfer in the fluid in the x -direction is negligible.

Determination of Velocity and Temperature Profiles for Laminar Flow over Flat Plate

The governing equation for the hydrodynamic boundary layer is Equation IIIa.3.20-1, repeated below:

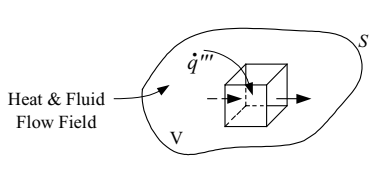
$$V_x \frac{\partial V_x}{\partial x} + V_y \frac{\partial V_x}{\partial y} = -\frac{1}{\rho} \frac{\partial P}{\partial x} + \nu \frac{\partial^2 V_x}{\partial y^2} \quad \text{IIIa.3.20-1}$$

If the pressure is also constant throughout the flow, then in the above equation $\partial P / \partial x = 0$. For the temperature boundary layer, the governing equation is Equation IIIa.3.23-1, also repeated below:

$$V_x \frac{\partial T}{\partial x} + V_y \frac{\partial T}{\partial y} = \alpha \frac{\partial^2 T}{\partial y^2} \quad \text{IIIa.3.23-1}$$

Example IVb.2.1. Derive Equation IIIa.3.23-1 directly from an energy balance written for a control volume.

Solution: The derivation is similar to heat conduction in a solid. However, while solid is stationary, we know that there is fluid motion inside the boundary layer. Hence, our derivation must take this into account. We begin by considering flow into and out of an elemental control volume taken inside the boundary layer, as shown in the figure. An energy balance for the elemental control volume takes the form of:



$$\begin{aligned}
 & \text{Net Flux of Energy By Conduction} \\
 & \text{Net Flux of Energy By Convection} \\
 & + \text{Rate of Energy Production}
 \end{aligned}
 = \text{Rate of Change of Internal Energy}$$

We integrate the energy balance over the entire heat and fluid flow fields to obtain:

$$-\int_S (-k \bar{\nabla} T) \cdot \bar{n} dS - \int_S (\rho \bar{V} h) \cdot \bar{n} dS + \int_V \dot{q}''' dV = \int_V \rho c \frac{\partial T}{\partial t} dV$$

We can convert the surface integrals to volume integrals by using Gauss's theorem, Equation VIIc.1.25:

$$\int_V \left(\bar{\nabla} \cdot k \bar{\nabla} T - \rho c_p \bar{\nabla} \cdot \bar{V} T - \rho c_p \frac{\partial T}{\partial t} + \dot{q}''' \right) dV = 0$$

where we have assumed incompressible flow for which, $dh = c_p dT$. For constant k , we obtain:

$$k \nabla^2 T - \rho c_p (\bar{V} \cdot \bar{\nabla} T + T \bar{\nabla} \cdot \bar{V}) + \dot{q}''' - \rho c_p \frac{\partial T}{\partial t} = 0$$

For incompressible flow, the second term in the parentheses is zero (see Example IIIa.3.3). Dividing by k and introducing thermal diffusivity ($\alpha = k / \rho c_p$), the above equation reduces to:

$$\nabla^2 T + \dot{q}''' = \frac{1}{\alpha} \left(\frac{\partial T}{\partial t} + \bar{V} \cdot \bar{\nabla} T \right) \quad \text{IIIa.3.23-2}$$

Equation IIIa.3.23-2 reduces to Equation IVa.2.2 for stagnant fluid. Using the substantial derivative D/Dt , Equation IIIa.3.23-2 may also be written as:

$$\nabla^2 T + \dot{q}''' = \frac{1}{\alpha} \frac{DT}{Dt} \quad \text{IIIa.3.23-3}$$

Equations IIIa.3.20-1 and IIIa.3.23-1 are second-order, coupled partial differential equations. Finding an analytical solution by integration is not an easy task. However, in this case we know how the profiles of both variables look like. Therefore, we try to solve these equations by guessing the functional relationship for $V_x = f_1(y)$ and $T = f_2(y)$. Since for each equation we have four boundary conditions, two at the surface and two at the edge of boundary layer, we use a third order polynomials. Thus, we express velocity as a function of y as:

$$V_x = c_1 + c_2 y + c_3 y^2 + c_4 y^3$$

All we have to do now is to find the four unknown coefficients, c_1 through c_4 , so that the above polynomial fits both Equation IIIa.3.20-1 and the specified sets of boundary conditions. The sets of boundary conditions are:

$$\text{at } y = 0: V_x = 0 \text{ and } \partial^2 V_x / \partial y^2 = 0$$

$$\text{at } y = \delta: V_x = V_f \text{ and } \partial V_x / \partial y = 0$$

Using conditions at $y = 0$, we find $c_1 = c_3 = 0$. We now use conditions at $y = \delta$ to find c_2 and c_4 . From $y = \delta$, $V_x = V_f$, we find $c_2 \delta + c_4 \delta^3 = V_f$. From $y = \delta$, $\partial V_x / \partial y = 0$, we find $c_2 + 3c_4 \delta^2 = 0$. Solving this set, we find c_2 and c_4 in terms of δ , V_x , and V_f as $c_2 = 3V_f/2\delta$ and $c_4 = -V_x/2\delta^3$. Therefore, the velocity profile becomes:

$$\frac{V_x}{V_f} = \frac{3}{2} \frac{y}{\delta} - \frac{1}{2} \left(\frac{y}{\delta} \right)^3 \quad \text{IVb.2.1}$$

Due to the similarity of the governing Equations IIIa.3.20-1 and IIIa.3.23-1, we expect that temperature can be described by a similar function:

$$\frac{T - T_s}{T_f - T_s} = \frac{3}{2} \frac{y}{\delta'} - \frac{1}{2} \left(\frac{y}{\delta'} \right)^3 \quad \text{IVb.2.2}$$

Although we were able to find an analytical solution for these profiles, we are far from declaring victory. This is because in Equation IVb.2.1, V_x is expressed in terms of the unknown δ , yet to be determined. We did expect this additional twist, as we used our engineering intuition and picked a profile. We then found the coefficients of the function representing the profile from the boundary conditions. But we still have no guarantee that the chosen profile would satisfy the governing equation itself. The thickness of the boundary layer, δ , is indeed the final requirement to ensure the chosen profile does satisfy the governing equation. We should then embark on finding δ . Similar to the profile for V_x , we first guess a profile for δ and then try to find the related coefficient. However, the solution for δ is not as straightforward as the solution we managed to find for the velocity profile.

Determination of the Hydrodynamic Boundary Layer Thickness for Laminar Flow over Flat Plate

To find the thickness of the hydrodynamic boundary layer, δ , we first note that δ is only a function of x . To find this function, we resort to the conservation equation of mass, Equation IIIa.3.13-1:

$$\frac{\partial V_x}{\partial x} + \frac{\partial V_y}{\partial y} = 0$$

this equation can be approximated as $V_f/x + V_y/\delta = 0$. Therefore V_y is proportional to $V_y \propto V_f \delta/x$. We now apply the same approximation to the governing momentum equation, Equation IIIa.3.20-1 while substituting for V_y . This results in:

$$V_f \frac{V_f}{x} + V_f \frac{\delta}{x} \frac{V_f}{\delta} \approx \nu \frac{V_f}{\delta^2}$$

from which δ is found to have a functional relationship as $\delta \propto \sqrt{\nu x / V_f}$.

Having obtained the shape of the function for δ , we substitute it into Equation IIa.3.20-1, being a partial differential equation. Fortunately, we can convert this equation to an ordinary differential equation by noticing that both V_x and V_y can be expressed in terms of a stream function ψ . That is to say that if $V_x = \partial\psi/\partial y$ and $V_y = -\partial\psi/\partial x$ then the continuity equation (Equation IIIa.3.13-1) is automatically satisfied. To find the stream function, we integrate either of these relations while noting from Equation IVb.2.1 that $V_x/V_f = f(\beta)$ where $\beta = y/\delta$. Hence

$$\psi = \int V_x dy = \int V_f f(\beta) dy = \int V_f \sqrt{\frac{\nu x}{V_f}} f(\beta) d\beta = V_f \sqrt{\frac{\nu x}{V_f}} \int f(\beta) d\beta = V_f \sqrt{\frac{\nu x}{V_f}} F(\beta)$$

Thus $F(\beta) = \psi(x, y)/(\nu x V_f)^{1/2}$. Having ψ and $F(\beta)$, we find V_x and V_y :

$$V_x = \partial\psi/\partial y = (dF/d\beta) V_f / 2$$

$$V_y = -\partial\psi/\partial x = [\beta F'(\beta) - F(\beta)] (\nu V_f / x)^{1/2} / 2$$

Having V_x and V_y , we can find other derivatives and substitute the results in Equation IIIa.3.20-1 to obtain:

$$2 \frac{d^3 F}{d\beta^3} + F \frac{d^2 F}{d\beta^2} = 0 \quad \text{IVb.2.3}$$

This equation is subject to three boundary conditions, two of which deal with $y = 0$ (i.e., $V_x(x, 0) = V_y(x, 0) = 0$). This is equivalent with $F(\beta = 0) = dF(\beta = 0)/d\beta = 0$. The third boundary condition is at $y = \infty$, i.e., $V_x(x, \infty) = V_f$. This is equivalent with $dF(\infty)/d\beta = 1$.

Blasius recommended the above method for solving Equation IVb.2.3. A strict analytical solution has not been found for Equation IVb.2.3. Schlichting found a

solution by series expansion and Howarth solved the equation numerically. The numerical results are tabulated for $F(\beta)$ as a function of β , which indicate that $V_x = 0.99V_f$ if $\beta = 5$. Recall that $\beta = y/\delta = y/\sqrt{\nu x/V_f}$. Hence at $y = \delta$, $\beta = 5$. Rearranging, we find δ as:

$$\delta_{\text{Laminar}} = \delta = \frac{5}{\sqrt{V_f/x}} = \frac{5x}{\text{Re}_x^{1/2}} \quad \text{IVb.2.4}$$

Example IVb.2.2. Water flows over a flat plate at a speed of 4 m/min and a temperature of 50 C. The length of the plate is 25 cm. Find the thickness of the boundary layer at the trailing edge.

Solution: We first find water kinematic viscosity at $T = 50$ C to be $\nu = 0.554\text{E-}6$ m²/s. We now find Re_L :

$$\text{Re}_L = V_f/\nu L = (4/60)/(0.554\text{E-}6 \times 0.25) = 481,348$$

This indicates that flow at the trailing edge is laminar:

$$\delta_L = 5L/\text{Re}_L^{1/2} = 5 \times 0.25/(481,348)^{0.5} = 1.8 \text{ mm}$$

Determination of the Thermal Boundary Layer Thickness for Laminar Flow over Flat Plate

Now that we found a relation for the thickness of the hydrodynamic boundary layer in terms of the Reynolds number, we set out to find a relation for the thickness of the thermal boundary layer. As we shall see in the next section, the relation for the thickness of the thermal boundary layer will be especially useful in the calculation of the heat transfer coefficient for laminar flow over a flat plate. To derive a relation for δ' , we consider flow over a heated flat plate as shown in Figure IVb.2.1. This figure shows a case where heating of the plate starts at $x = x_o$, Figure IVb.2.1(a). For the derivation of a relation for δ' , we may either reduce the set of conservation equations of Chapter IIIa, for the control volume shown in

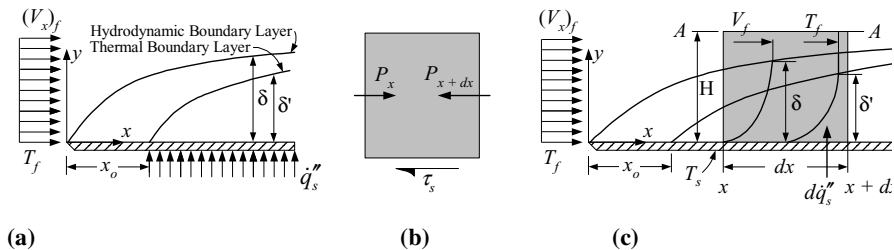


Figure IVb.2.1. Hydrodynamic and thermal boundary layers for flow over a flat plate heated at $x = x_o$

Figure IVb.2.1(c) or directly derive the conservation equations for this control volume. Choosing the direct derivation by an integral approach*, we consider the mass, momentum, and energy of the fluid entering and leaving this differential control volume. These transfer processes enter from the vertical side located at x and from the horizontal side (A-A) located in the free stream. Mass, momentum and energy then leave the control volume through the vertical side located at $x + dx$. These processes are summarized in Table IVb.2.1.

Table IVb.2.1. The transfer processes for the elemental control volume of Figure IVb.2.1

	Entering from side x	Leaving from side $x + dx$	Entering from side A – A
Mass	$\int_0^H \rho V_x dy$	$\int_0^H \rho V_x dy + \frac{d}{dx} \left(\int_0^H \rho V_x dy \right) dx$	$\frac{d}{dx} \left(\int_0^H \rho V_x dy \right) dx$
Momentum	$\int_0^H \rho V_x^2 dy$	$\int_0^H \rho V_x^2 dy + \frac{d}{dx} \left(\int_0^H \rho V_x^2 dy \right) dx$	$(V_x)_f \frac{d}{dx} \left(\int_0^H \rho V_x dy \right) dx$
Energy	$\int_0^H \rho V_x (c_p T) dy$	$\int_0^H \rho V_x (c_p T) dy + \frac{d}{dx} \left[\int_0^H \rho V_x (c_p T) dy \right] dx$	$(c_p T_f) \frac{d}{dx} \left[\int_0^H \rho V_x dy \right] dx$

We first deal with the momentum equation for which at steady state, the resultant of all forces is equal to the net momentum flux (i.e., the net momentum entering minus the net momentum leaving the control volume, Equation IIIa.3.6). As shown in Figure IVb.2.1(b), the forces applied on the control volume are the shear at the solid surface and the pressure forces. The shear force at the free stream (side A-A) is zero, thus:

$$-\tau_s - \left(\frac{dP}{dx} \right) H = \frac{d}{dx} \left(\int_0^H \rho V_x^2 dy \right) dx - (V_x)_f \frac{d}{dx} \left(\int_0^H \rho V_x dy \right) dx \quad \text{IVb.2.5}$$

We may simplify Equation IVb.2.5 by considering a case of constant pressure, $dP/dx = 0$. The right side of Equation IVb.2.5 can also be simplified (see Problem 11) to obtain:

$$\rho \frac{d}{dx} \left[\int_0^H ((V_x)_f - V_x) V_x dy \right] = \tau_s = \mu \frac{\partial V_x (y=0)}{\partial y} \quad \text{IVb.2.6}$$

If we substitute the velocity profile of Equation IVb.2.1 into Equation IVb.2.6 and integrate, we conclude:

$$\delta \frac{d\delta}{dx} = \frac{140}{13} \frac{\nu}{(V_x)_f} \quad \text{IVb.2.7}$$

Equation IVb.2.7 can be integrated to obtain an approximate value for δ . This value differs by only 7.2% as compared with the exact value given by Equation IVb.2.4.

* This method is originally developed by T. von Karman.

We now consider the energy equation for the differential control volume of Figure IVb.2.1(c). The steady state form of Equation IIIa.3.9 relates the net energy addition to the control volume (by convection, conduction, and internal heat generation as well as the viscous work) to net energy removal from the control volume. Noting that the net viscous work is $\mu(\partial V_x/\partial y)^2 dx dy$ (Example IIIa.3.12) and considering only heat convection into and out of the control volume and heat transfer from the solid surface, we find:

$$\frac{d}{dx} \left[\int_0^H (T_f - T) V_x dy \right] + \frac{\mu}{\rho c_p} \left[\int_0^H \left(\frac{dV_x}{dy} \right)^2 dy \right] = \alpha \left[\frac{\partial T}{\partial y} \right]_s \quad \text{IVb.2.8}$$

Note that in the derivation of Equation IVb.2.8, we made several assumptions including steady state flow, fluid with constant properties, and the free stream with constant velocity and temperature.

The rate of heat transfer from the surface, the right side of Equation Vb.2.8, can be determined by substituting for the profiles of velocity and temperature from Equations IVb.2.1 and IVb.2.2. However, the viscous dissipation term introduces non-linearity, which precludes the development of an exact solution in closed form. Fortunately, the net viscous work in laminar flow is generally negligible compared with the rate of heat transfer by the convection or the conduction mechanism. The viscous work becomes significant for high kinetic energy flows or very viscous fluids.

Ignoring the net viscous work term, Equation IVb.2.8 simplifies to (see Problem 12):

$$(V_x)_f \left[2\delta^2 \zeta^2 \frac{d\zeta}{dx} + \zeta^3 \delta \frac{d\delta}{dx} \right] = 10\alpha$$

where $\zeta = \delta'/\delta$. Introducing Equation IVb.2.7 and rearranging, we find the following differential equation:

$$\frac{4}{3} x \frac{d\zeta}{dx} + \zeta - \frac{13}{14} \frac{\alpha}{v} = 0$$

where $\zeta = \zeta^3$. The boundary conditions for this differential equation is $\zeta = 0$ (since $\delta' = 0$) at $x = x_o$. Thus

$$\zeta = \frac{\delta}{\delta'} = \frac{1}{1.026} \text{Pr}^{-1/3} \left[1 - \left(\frac{x_o}{x} \right)^{3/4} \right]^{1/3} \quad \text{IVb.2.9}$$

If the plate is heated at the leading edge then $\zeta = \delta'/\delta = (\text{Pr}^{-1/3}/1.026)$.

Determination of Heat Transfer Coefficient for Laminar Flow over Flat Plate

Since h is defined as heat flux at the surface divided by ΔT , Equation IVb.1.1 gives:

$$h = \frac{-k(\partial T / \partial y)_s}{T_s - T_f}$$

We now need to find $(\partial T / \partial y)_s$, which is obtained from Equation IVb.2.2. Substituting, we find:

$$h = \frac{-k(\partial T / \partial y)_s}{T_s - T_f} = \frac{3}{2} \frac{k}{\delta'} = \frac{3}{2} \frac{k}{\delta} (1.026 \text{Pr}^{1/3})$$

where we substituted for the thermal boundary layer thickness, δ' in terms of the hydrodynamic boundary layer thickness, δ . We can further simplify this equation by substituting for δ from Equation IVb.2.4:

$$h = \frac{-k(\partial T / \partial y)_s}{T_s - T_f} = \frac{3}{2} \frac{k}{\delta} (1.026 \text{Pr}^{1/3}) = \frac{3}{2} \frac{k}{5x} \text{Re}^{1/2} (1.026 \text{Pr}^{1/3}) = 0.3 \frac{k}{x} \text{Re}^{1/2} (\text{Pr}^{1/3})$$

Using the definition of the Nusselt number, $\text{Nu} = hx/k$, we find;

$$\text{Nu}_x = 0.3 \text{Re}_x^{1/2} \text{Pr}^{1/3} \quad 0.6 < \text{Pr} < 50 \quad \text{IVb.2.10}$$

Equation IVb.2.10 was derived analytically for the range of Pr number shown above. However, we would have to resort to empirical correlations to be able to include all fluids ranging from liquid metal (Pr in the order of 0.01) to motor oil (Pr in the order of 50,000). One such correlation is that suggested by Churchill and Ozoe:

$$\text{Nu}_x = C \text{Re}_x^{1/2} \text{Pr}^{1/3} \quad \text{Re}_x \text{Pr} > 100 \quad \text{IVb.2.11}$$

In Equation IVb.2.11, C is used to represent $C = a / \left[1 + (b / \text{Pr})^{2/3} \right]^{1/4}$ where coefficients a and b for constant temperature are given as 0.3387 and 0.0468 and for constant heat flux as 0.4637 and 0.0207. Thus, the Churchill and Ozoe correlation for constant temperature is:

$$\text{Nu}_x = \frac{0.3387}{\left[1 + \left(\frac{0.0468}{\text{Pr}} \right)^{2/3} \right]^{1/4}} \text{Re}_x^{1/2} \text{Pr}^{1/3} \quad (T_s = \text{constant}) \quad \text{IVb.2.11-1}$$

and for constant heat flux is:

$$\text{Nu}_x = \frac{0.4637}{\left[1 + \left(\frac{0.0207}{\text{Pr}}\right)^{2/3}\right]^{1/4}} \text{Re}_x^{1/2} \text{Pr}^{1/3} \quad (\dot{q}_s'' = \text{constant}) \quad \text{IVb.2.11-2}$$

The fluid properties in these correlations are developed at the film temperature.

Equations IVb.2.10 and IVb.2.11 demonstrate the dependency of the Nu number on Re and Pr numbers for laminar flow over a flat plate. These equations also show that we should expect similar functional relationship for the Nu number even if flow is not laminar. Thus for all practical purposes, we should expect:

$$\text{Nu} = c_1 \text{Re}^{c_2} \text{Pr}^{c_3} \quad \text{IVb.2.11}$$

where constants c_1 , c_2 , and c_3 depend on a specific case. Such functional relationship between Nu, Re, and Pr numbers is indeed confirmed in many experiments for forced convection heat transfer as discussed later in this chapter.

Determination of Average Heat Transfer Coefficient for Laminar Flow over Flat Plate

To find the average heat transfer coefficient for laminar flow over a flat plate, we note that in Equations IVb.2.11, the Nu number is a function of $\text{Re}^{1/2}$. We may then express the Nusselt number as $\text{Nu} = C_1 \text{Re}^{1/2}$ where C_1 represents all other terms. Substituting for $\text{Re} = V_f x / \nu$ and for $\text{Nu} = h x / k$, we may write the heat transfer coefficient as:

$$h_x = (k/x) C_1 (V_f x / \nu)^{1/2} = B_1 x^{-1/2} \quad \text{IVb.2.12}$$

where $B_1 = C_1 k (V_f / \nu)^{1/2}$. If we now substitute for h_x from Equation IVb.2.12 into Equation IVb.1.2 and integrate over the entire length of the flat plate, we find the average heat transfer coefficient as:

$$\bar{h} = \int_0^L h_x dx / \int_0^L dx = \int_0^L B_1 x^{-1/2} dx / L = 2B_1 L^{1/2} / L = 2B_1 L^{-1/2} = 2h_L$$

Substituting for the heat transfer coefficient from $h = \text{Nu}(k/x)$, we find $\bar{\text{Nu}} = 2\text{Nu}_L$.

Example IVb.2.3. Water at high pressure and temperature flows over a heated plat at 0.25 m/s. Temperature of water is 250 C and the plate temperature is maintained at 260 C. The length of the heated plate is 5 cm. Find the average heat flux over the plate.

Solution: We find water properties at the film temperature $T_{film} = (250 + 260)/2 = 255 \text{ C}$

At $T_{film} = 255 \text{ C}$, $\nu = 0.132\text{E-}6 \text{ m}^2/\text{s}$, $k = 0.6106 \text{ W/m}\cdot\text{K}$, and $\text{Pr} = 0.8458$

$\text{Re}_L = VL/\nu = 0.25 \times 0.05/0.132\text{E-}6 = 94,697$. Flow is laminar so we use Equation IVb.2.11-1:

$$\begin{aligned}
 C &= 0.3387/[1 + (0.0468/0.8458)^{0.666}]^{0.25} = 0.327 \\
 Nu_L &= 0.312(94,697)^{0.5}(0.8458)^{0.333} = 95.28 \\
 h_L &= Nu_L k/L = 95.28 \times 0.6106/0.05 = 1163.6 \text{ W/m}^2\cdot\text{K} \\
 \bar{h} &= 2h_L = 2 \times 1163.6 = 2327 \text{ W/m}^2\cdot\text{K} \\
 \bar{q}'' &= 2327(260 - 250) = 23.27 \text{ kW/m}^2.
 \end{aligned}$$

We now solve a similar example but for the flow of air over a heated flat plate. In this example, we also find the thickness of the hydrodynamic boundary layer as well as the thermal boundary layer.

Example IVb.2.4. A heated plate has a length of 0.5 m and width of 0.65 m. The plate temperature is held constant at 119 C. Air at 15 m/s and 35 C flows over the plate. Find a) the average heat transfer coefficient over the plate, b) total heat transferred from the plate to the colder air and c) δ , and δ' at the trailing edge.

Solution: We find air properties at the film temperature

$$T_{film} = (35 + 115)/2 = 77 \text{ C}$$

At $T_{film} = 75 \text{ C}$, $\nu = 2.06\text{E-}5 \text{ m}^2/\text{s}$, $k = 0.0297 \text{ W/m}\cdot\text{K}$, and $Pr = 0.706$

$$Re_L = VL/\nu = 15 \times 0.5/2.06\text{E-}5 = 364,077.$$

Flow is laminar so we use Equation IVb.2.11-1:

$$C = 0.3387/[1 + (0.0468/0.8458)^{0.666}]^{0.25} = 0.327$$

$$Nu_L = 0.327(364,077)^{0.5}(0.8458)^{0.333} = 186$$

$$\text{a) } h_L = Nu_L k/L = 186 \times 0.0297/0.5 = 11.08 \text{ W/m}^2\cdot\text{K}$$

$$\bar{h} = 2h_L = 2 \times 11.08 = 22.16 \text{ W/m}^2\cdot\text{K}$$

$$\text{b) } \bar{Q} = 22.16(0.5 \times 0.65)(119 - 35) = 0.605 \text{ kW}$$

$$\text{c) } \delta_L = 5 \times L / Re_L^{1/2} = 5 \times 0.5 / 364,077^{0.5} = 4.14 \text{ mm}$$

$$\delta' = \delta / (1.026 Pr^{1/3}) = 4.14 / (1.026 \times 0.706^{0.333}) = 4.53 \text{ mm}.$$

So far we mostly dealt with the isothermal flow of fluids in the laminar flow regime over a flat plate. For constant heat flux boundary condition see Problems 28 and 29. Next, we examine the internal laminar flow of fluids.

2.2. Internal Laminar Flow of Viscous Fluids

Velocity profile for fully developed, laminar flow in a pipe is a parabolic function given by Equation IVb.2.1. Temperature profile for the same conditions can be obtained from the two-dimensional steady state form of the conservation equation of energy in the cylindrical coordinate system. Equation IIIa.3.23 assuming steady state, no radiation heat transfer, no internal heat generation, no body force, no viscous dissipation, and incompressible flow can be written as:

$$\rho \vec{V} \cdot \vec{\nabla} u^o = \vec{\nabla} \cdot (k \vec{\nabla} T)$$

Expanding this equation in two-dimensional cylindrical coordinates, while assuming constant thermal conductivity, yields:

$$\rho(V_r \vec{u}_r + V_x \vec{u}_x) \cdot \left[\frac{\partial(c_p T)}{\partial r} \vec{u}_r + \frac{\partial(c_p T)}{\partial x} \vec{u}_x \right] = k \left[\frac{1}{r} \frac{\partial}{\partial r} \left(r \frac{\partial T}{\partial r} \right) + \frac{\partial}{\partial x} \left(\frac{\partial T}{\partial x} \right) \right] \quad \text{IVb.2.13}$$

where \vec{u}_x and \vec{u}_r are the unit vectors. Since \vec{u}_x is perpendicular to the conduit flow area and hence to \vec{u}_r , we find that $\vec{u}_r \cdot \vec{u}_x = \vec{u}_x \cdot \vec{u}_r = 0$. If we also assume that the fluid properties are weak functions of temperature, Equation IVb.2.13 reduces to:

$$\frac{1}{\alpha} \left(V_r \frac{\partial T}{\partial r} + V_x \frac{\partial T}{\partial x} \right) = \frac{1}{r} \frac{\partial}{\partial r} \left(r \frac{\partial T}{\partial r} \right) \quad \text{IVb.2.14}$$

Equation IVb.2.14 is the same as Equation IIIa.3.23-1 but written in polar coordinates. In Equation IVb.2.14 we have used the constant heat flux assumption, $d\dot{q}_s''/dx = 0$. This implies that the last term in the right side of Equation IVb.2.13 is equal to zero (i.e., $\partial(\partial T/\partial x)/\partial x = 0$). Since in the fully developed region, $V_r = 0$ (and so is $\partial V_x/\partial x = 0$), Equation IVb.2.14 further simplifies to:

$$\frac{1}{r V_x} \frac{\partial}{\partial r} \left(r \frac{\partial T}{\partial r} \right) = \frac{1}{\alpha} \frac{\partial T}{\partial x} \quad \text{IVb.2.15}$$

To solve Equation IVb.2.15, we substitute the velocity profile for V_x from Equation IVb.2.1 to obtain:

$$\frac{\partial}{\partial r} \left(r \frac{\partial T}{\partial r} \right) = \frac{1}{\alpha} \frac{\partial T}{\partial x} (V_x)_{\max} \left(1 - \frac{r^2}{R^2} \right) r$$

where R is the pipe radius. This equation can be easily integrated to find:

$$r \frac{\partial T}{\partial r} = \frac{1}{\alpha} \frac{\partial T}{\partial x} (V_x)_{\max} \left(\frac{r^2}{2} - \frac{r^4}{4R^2} \right) + c_1$$

and the temperature distribution is finally obtained by another integration so that;

$$T = \frac{1}{\alpha} \frac{\partial T}{\partial x} (V_x)_{\max} \left(\frac{r^2}{4} - \frac{r^4}{16R^2} \right) + c_1 \ln r + c_2$$

The constants of integration c_1 and c_2 can be found from the following boundary conditions. At $r = 0$, due to symmetry, $\partial T / \partial r = 0$. This results in $c_1 = 0$. If temperature at $r = 0$ is known (i.e., $T_{CL} = T(r = 0)$), then $c_2 = T_{CL}$. Substituting for c_1 and c_2 , temperature profile in the flow is found as:

$$T = T_{CL} + \frac{1}{\alpha} \frac{\partial T}{\partial x} (V_x)_{\max} \frac{R^2}{4} \left[\left(\frac{r}{R} \right)^2 - \frac{1}{4} \left(\frac{r}{R} \right)^4 \right] \quad \text{IVb.2.16}$$

Given the fluid velocity and temperature at the pipe centerline, we can find fluid temperature at any cross section for a given axial and radial location by using Equation IVb.2.16. For example, the wall temperature T_s at any axial location is obtained by setting $r = R$ to find:

$$T_s = T_{CL} + \frac{3}{4} \frac{1}{\alpha} \frac{\partial T}{\partial x} (V_x)_{\max} \frac{R^2}{4}$$

However, the most important application of Equation IVb.2.16 is in finding the fluid bulk temperature. This is obtained by substituting for temperature profile in Equation IVb.1.4 and carrying out the integrals to find:

$$\bar{T}_f = T_{CL} + \frac{7}{24} \frac{1}{\alpha} \frac{\partial T}{\partial x} (V_x)_{\max} \frac{R^2}{4} \quad \text{IVb.2.17}$$

We now find heat transfer coefficient from the fact that:

$$\dot{q}'' = h(T_s - T_f) = -k(\partial T / \partial y)_{y=0} = k(\partial T / \partial r)_{r=R}$$

The derivative of temperature in the radial direction is found as $(\partial T / \partial r)_{r=R} = [(V_x)_{\max} R / 4\alpha] \partial T / \partial x$ then

$$h = \frac{-k(\partial T / \partial r)_{r=R}}{T_s - \bar{T}} = \frac{k[(V_x)_{\max} R / 4\alpha] \partial T / \partial x}{(11/24)[(1/\alpha)(\partial T / \partial x)(V_x)_{\max} (R^2/4)]} = \frac{24}{11} \frac{k}{R} = \frac{48}{11} \frac{k}{D} \quad \text{IVb.2.18}$$

From $h = 48k/11D$ we find $Nu = hD/k = 48/11$. Thus, for laminar flow inside pipes $Nu = \text{constant}$.

The topic of internal flow of fluids in heated conduits is discussed in more details in Section 2 of Chapters VIa and VIe. Figure IVb.2.2 shows the temperature profiles for two interesting cases of constant heat flux specified at the channel wall (Figure IVb.2.2(a)) and an isothermal channel wall (Figure IVb.2.2(b)).

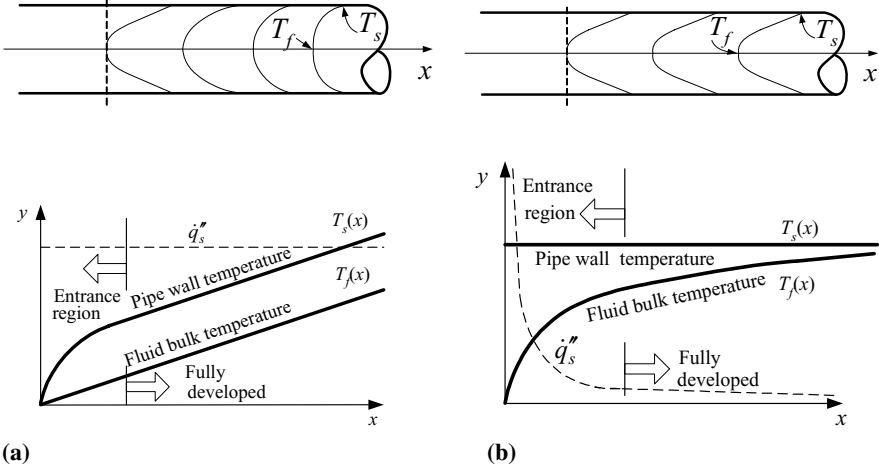
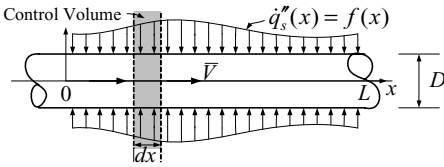


Figure IVb.2.2. Axial temperature profiles (a) constant wall heat flux and (b) constant wall temperature

Example IVb.2.5. Consider the fully developed flow of an incompressible viscous flow at velocity \bar{V} in a heated pipe of diameter D and length L . Heat flux of $\dot{q}_s'' = f(x)$ is applied to the channel wall. Derive the axial temperature distribution in terms of \dot{q}_s'' , \bar{V} , D , L , and ρ .



Solution: We write the mass and energy balance for the shaded control volume at steady state condition:

$$\left[\rho \bar{V} (\pi D^2 / 4) \right] dh = \dot{q}_s''(x) [\pi D dx]$$

Since flow is subcooled, $dh = c_p dT$. Substituting and integrating from $x = 0$ to any x yields:

$$T_f(x) = T_f(0) + (4D / \rho \bar{V}) \int_0^x \dot{q}_s''(x) dx$$

where $T_f(x)$ is the fluid bulk temperature. If the function representing the wall heat flux is specified, we can find $T_f(x)$. For a special case of constant wall heat flux, $\dot{q}_s'' = \text{constant} = \dot{q}_s''$, we find:

$$T_f(x) = T_f(0) + (4D\dot{q}''x / \rho\bar{V}) \quad \text{IVb.2.19}$$

Equation IVb.2.19 (Figure IVb.2.2(a)) is applicable to any flow regime whether laminar or turbulent as long as flow remains subcooled so that $T_f(x = L) < T_{sat}(P_{system})$. In Equation IVb.2.19, for $x = L$, we have $T_f = T_f(L)$ confirming that the results are consistent with an overall energy balance over the tube length:

$$\dot{Q} = \dot{m}c_p(T_{x=L} - T_{x=0}) \quad \text{IVb.2.20}$$

3. Empirical Relations

In Section 2 we were able to find analytical solutions only for such limited cases as forced convection heat transfer for flow over flat plate and inside conduits. In these cases, we considered steady and laminar flow. Additionally, we used such simplifying assumptions as incompressible laminar flow, thermal properties independent of temperature, no internal heat generation, and negligible heat transfer from thermal radiation. Still we had to resort to empirical correlations to increase the range of applicability of Nu number.

In common practice an ideal situation to satisfy all the required conditions generally does not exist. While in many cases a steady incompressible flow can be assumed with approximately constant thermal properties in a specified range of temperature, flow cannot be guaranteed to remain laminar. Indeed, except in some special cases, flow is generally turbulent. Fortunately, in the majority of cases the Nusselt number for forced convection heat transfer in turbulent flow has the same functional relationship with the Pr and the Re numbers as shown in Equation IVb.2.11. Thus, all we need to do is to find constants c_1 , c_2 , and c_3 . These are generally found in experiments, hence the relations are known as *empirical correlations*. To demonstrate the relation between theory and experiment, let's rearrange Equation IVb.2.11 and take the logarithm of each side of the rearranged formula:

$$\log(\text{Nu} / \text{Pr}^{c_3}) = \log c_1 + c_2 \log \text{Re}$$

This equation shows that the logarithm of $(\text{Nu} / \text{Pr}^{c_2})$ is a linear function of the logarithm of the Reynolds number. This functional relation is verified by variety of tests using different fluids and pipe diameters.

3.1. External Turbulent Flow over Flat Plates

Assuming a turbulent velocity profile $V_x/(V_x)_f = (y/\delta)^{1/7}$, substituting in Equation IVb.2.5 and integrating, we find the boundary layer thickness for turbulent flow over a flat plate, heated at the leading edge as:

$$\delta_{\text{Turbulent}} = 0.37x / \text{Re}_x^{1/5} \quad 5\text{E}5 < \text{Re}_x < 1\text{E}7 \quad \text{IVb.3.1}$$

Comparing the thickness of turbulent versus laminar boundary layer, given by Equation IVb.2.4, we find that $\delta_{\text{Turbulent}} = 0.074\delta_{\text{Laminar}} \text{Re}_x^{0.3}$. Since $\text{Re}_x > 5\text{E}5$, then $\delta_{\text{Turbulent}}$ is at least 4 times thicker than δ_{Laminar} . Since turbulence is associated with the eddy diffusivity, being random fluctuations as opposed to the molecular diffusion in the laminar flow, the fluid Pr number does not influence the boundary layer thickness in turbulent flow. This implies that in turbulent flow, $\delta = \delta'$. The local Nu number is given by:

$$\text{Nu}_x = 0.0296 \text{Re}_x^{4/5} \text{Pr}^{1/3} \quad 0.6 < \text{Pr} < 60 \quad \text{IVb.3.2}$$

and the average Nu number by (Whitaker):

$$\overline{\text{Nu}} = 0.036(\text{Re}_L^{4/5} - 9200) \text{Pr}^{0.43} (\mu_f / \mu_s)^{1/4} \quad \text{IVb.3.3}$$

where properties are found at T_f except for μ_s , which is found at T_s . This correlation is valid for $2\text{E}5 < \text{Re}_L < 5.5\text{E}6$, $0.7 < \text{Pr} < 380$, and $0.26 < \mu_f / \mu_s < 3.5$.

3.2. External Flow over Conduits

We already analyzed external flow over flat plates. There are two more cases to be considered in external turbulent flow. These are flow over single cylinders and spheres as well as flow over a cluster of cylinders and spheres. For example, flow across tube banks is of much interest in heat exchanger technology.

Cross Flow over Cylinders

This includes flow over cylinders with circular or non-circular cross section. When a fluid flows over curved surfaces, depending on the Reynolds number of the flow, the boundary layer may become separated from the surface. This phenomenon is too complicated to have analytical solutions. Ironically, the boundary layer separation occurs mostly at very low to moderate Reynolds numbers (10 – 1000). When Re becomes greater than 3E5, the boundary layer separation is delayed. Therefore, for flow over curved surfaces, even for laminar flow we have to resort to empirical correlations such as that recommended by Whitaker:

$$\overline{\text{Nu}} = (0.4 \text{Re}^{1/2} + 0.06 \text{Re}^{2/3}) \text{Pr}^{2/5} (\mu_f / \mu_s)^{0.25} \quad \text{IVb.3.4}$$

Equation IVb.3.4 is valid for $40 < \text{Re} < 1\text{E}5$, $0.65 < \text{Pr} < 300$, and $0.25 < \mu_f / \mu_s < 5.2$. All properties are found at the free stream temperature except for the μ_s , which is developed at the surface temperature.

Example IVb.3.1. The surface of a cylinder ($D = 10$ cm and $L = 20$ cm) is maintained at 127 C. The cylinder is exposed to the cross flow of air. The air velocity, temperature, and pressure are 40 m/s, 27 C, and 1 atm, respectively. Assuming a very low surface emissivity, find the rate of heat transfer by convection.

Solution: We find air properties at $T_f = 300$ K: $\nu = 15.89\text{E-}6$ kg/m³, $\mu_f = 18.46\text{E-}6$ N·s/m², $\mu_s = 2.3\text{E-}6$ N·s/m², $\text{Pr} = 0.707$, and $k = 0.0263$ W/m·C.

We now find the Reynolds number:

$$\text{Re} = VD/\nu = 40 \times 0.1/15.89\text{E-}6 = 251,730$$

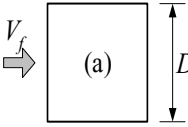
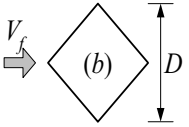
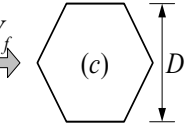
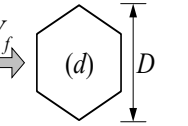
$$\text{Nu} = [0.4 \times (251,730)^{1/2} + 0.06 \times (251,730)^{2/3}] \times (5.83)^{2/5} \times (18.46\text{E-}6/2.3\text{E-}6)^{0.25} \approx 1500$$

$$h = \text{Nu}(k/D) = 1500 \times (0.0263/0.1) = 394 \text{ W/m}^2\cdot\text{C}.$$

$$\dot{Q} = h(\pi DL)(T_s - T_f) = 394 \times (\pi \times 0.1 \times 0.2) \times (127 - 27) \approx 2.5 \text{ kW}.$$

For non-circular cylinders, we use Table IVb.3.1 as recommended by Jakob. All properties are found at the film temperature

Table IVb.3.1. Coefficients c_1 and c_2 for non-circular cylinders $\text{Nu} = c_1 \text{Re}^{c_2} \text{Pr}^{1/3}$

				
c_1	0.102	0.246	0.153	0.160
c_2	0.675	0.588	0.638	0.638

The range for Re number in Table IVb.3.1 is $5\text{E}3 < \text{Re} < 1\text{E}5$ except for case (d) which the range is $5\text{E}3 < \text{Re} < 1.95\text{E}4$.

Flow over Spheres

The Nusselt number over a sphere having diameter D can be found from Whitaker's correlation:

$$\text{Nu} = 2 + \left(0.4 \text{Re}^{1/2} + 0.06 \text{Re}^{2/3}\right) \text{Pr}^{2/5} \left(\mu_f / \mu_s\right)^{1/4} \quad \text{IVb.3.5}$$

applicable for $3.5 < \text{Re} < 8\text{E}4$ and $0.7 < \text{Pr} < 380$. The Reynolds number is developed based on D . All properties are found at the free stream temperature except for μ_s , which is found at T_s .

Cross Flow over Bank of Tubes

Shown in Figure IVb.3.1 is cross flow over a tube bank arranged in either in-line or staggered configuration.

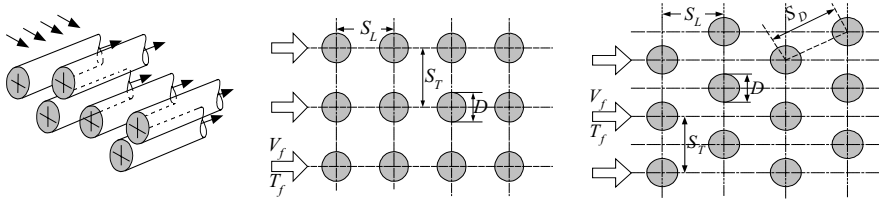


Figure IVb.3.1. Cross Flow over tube banks arranged in in-line and staggered configurations

Note that in both configurations the velocity vector of the fluid flowing over the tubes is perpendicular to the velocity vector of the fluid flowing inside the tubes. Our goal is to obtain the heat transfer coefficient for the fluid which is flowing over the tubes. For the fluid flowing inside the tubes, the heat transfer coefficient is discussed in Sections 2.2 and 3.3 for laminar and for turbulent flows, respectively. Tubes are spaced by longitudinal pitch (S_L) and transverse pitch (S_T). Lateral pitch S_D is pertinent to the staggered arrangement. Maximum flow velocity occurs in the gap between the adjacent rods having a height of $S_T - D$. Form a mass balance we find $V_{\max} = V_f S_T / (S_T - D)$. The average Nu number is recommended by Zhukauskas as:

$$\overline{\text{Nu}} = c_1 \text{Re}_{\max}^{c_2} \text{Pr}^{0.36} (\text{Pr} / \text{Pr}_s)^{0.25} \quad \text{IVb.3.6}$$

where c_1 and c_2 are given in Table IVb.3.2. This correlation is valid for $0.7 < \text{Pr} < 500$, $1000 < \text{Re}_{\max} < 2\text{E}6$, and tubes bundles with 20 or more rows of tubes. If the number of rows is less than 20, then a correction factor must be used. To apply the correction factor, the Nusselt number is calculated for a tube bundle with 20 rows of tubes. Then the correction factor C is obtained from Table IVb.3.3 so that

$$\text{Nu}_{<20} = C \text{Nu}_{20}$$

All fluid properties in Equation IVb.3.6 are found at the arithmetic mean of the fluid inlet and outlet temperatures except for Pr_s , which is found at the surface temperature T_s .

Table IVb.3.2. Coefficients in Equation IVb.3.6

Geometry	Re_{\max}	c_1	c_2
In-line	10 – 100	0.80	0.40
	100 – 1E3	(Treat as a single cylinder)	
	1E3 – 2E5	0.27	0.63
	> 2E5	0.21	0.84
Staggered	10 – 100	0.90	0.40
	100 – 1E3	(Treat as a single cylinder)	
	1E3 – 2E5 ⁱ	$0.35(S_T/S_L)^{0.2}$	0.60
	1E3 – 2E5 ^j	0.40	0.60
	> 2E5	0.02	0.84

ⁱ For $S_T/S_L < 2$

^j For $S_T/S_L > 2$

Table IVb.3.3. Correction factor C for bundles with less than 20 tubes

No. of Rows	1	2	3	4	5	7	10	13	16
In-line	0.70	0.80	0.86	0.90	0.92	0.95	0.97	0.98	0.99
Staggered	0.64	0.76	0.84	0.89	0.92	0.95	0.97	0.98	0.99

3.3. Internal Turbulent Flow

A frequently used correlation in internal turbulent flow for single-phase heat transfer is the Dittus-Boelter correlation, originally developed in the 1930s for automotive engineering:

$$\text{Nu}_D = 0.023 \text{Re}_D^{0.8} \text{Pr}^n \quad \text{IVb.3.4}$$

where $n = 0.4$ if $T_s > T_f$ and 0.3 if $T_s < T_f$. Therefore;

$$\text{Nu}_D = 0.023 \text{Re}_D^{0.8} \text{Pr}^{0.3} \quad (\text{Fluid is cooled}) \quad \text{IVb.3.4-1}$$

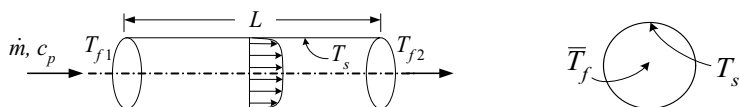
$$\text{Nu}_D = 0.023 \text{Re}_D^{0.8} \text{Pr}^{0.4} \quad (\text{Fluid is heated}) \quad \text{IVb.3.4-2}$$

The range of applicability includes $0.7 < \text{Pr} < 160$, $\text{Re}_D > 10,000$, and $L/D > 10$. Seider-Tate later modified this correlation for cases with large differences between the surface and the fluid bulk temperature by accounting for fluid viscosity evaluated at the bulk (μ_f) and at the surface temperature (μ_s):

$$\text{Nu}_D = 0.027 \text{Re}_D^{0.8} \text{Pr}^{0.3} (\mu_f / \mu_s)^{0.14} \quad \text{IVb.3.5}$$

All properties in Equations IVb.3.4 and IVb.3.5 should be found at the fluid bulk temperature except for μ_s .

Example IVb.3.2. Water at a rate of 4 kg/s enters a heated pipe at 10 C and leaves at 30 C. The pipe has a diameter of 5 cm and its wall is maintained at 95 C. Find the required pipe length.



Solution: To find L , we use Equation IVb.2.20 in conjunction with Newton's law of cooling:

$$\dot{m} c_p (T_{f2} - T_{f1}) = h A (T_s - \bar{T}_f)$$

where T_{f1} and T_{f2} are the water bulk temperature at the inlet and at the exit of the pipe. The bulk average temperature is shown by \bar{T}_f :

$\bar{T}_f = (T_{f1} + T_{f2})/2 = (10 + 30)/2 = 20$ C. To find A , having \dot{m} , T_s , T_{f1} , T_{f2} , and \bar{T}_f we need to find h :

At 20 C, $\rho = 998.37 \text{ kg/m}^3$, $c_p = 4.18 \text{ kJ/kg}\cdot\text{C}$, $\mu_f = 0.001 \text{ N}\cdot\text{s/m}^2$, $k = 0.6 \text{ W/m}\cdot\text{C}$, and $\text{Pr} = 6.9$

$$\text{Re} = \frac{\rho V D}{\mu} = \frac{\dot{m} D}{\mu A} = \frac{4 \times 0.05}{0.001 \times (\pi \times 0.05^2 / 4)} = 101,859$$

$$\text{Nu} = 0.023 \text{Re}^{0.8} \text{Pr}^{0.4} = 0.023 \times 101,859^{0.8} \times 6.9^{0.4} = 505.4 \text{ (580 if Equation IVb.3.5 is used)}$$

$$h = \text{Nu} \times k/D = 505.4 \times 0.6/0.05 = 6065 \text{ W/m}^2\cdot\text{C}$$

$$A = \dot{m} c_p (T_{f2} - T_{f1}) / h (T_s - \bar{T}_f)$$

Substituting values:

$$A = \pi D L = \pi \times 0.05 \times L = 4 \times 4180 \times (30 - 10) / [6065 \times (95 - 20)]$$

Solving for the pipe length, we find $L = 4.68 \text{ m}$.

Equations IVb.3.4 is applicable to fluids flowing inside conduits. However, the heat transfer coefficient of water flowing in rod or tube bundles parallel to the axis of the rods or tubes should be calculated from:

$$\text{Nu}_D = C \text{Re}_D^{0.8} \text{Pr}^n \quad \text{IVb.3.6}$$

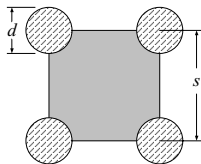
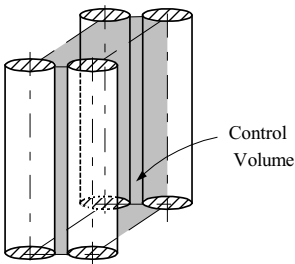
where coefficient C is found from:

$$C = 0.042 \frac{s}{D} - 0.024 \quad \text{Square array } (1.1 \leq s/D \leq 1.3) \quad \text{IVb.3.7(a)}$$

$$C = 0.026 \frac{s}{D} - 0.024 \quad \text{Triangular array } (1.1 \leq s/D \leq 1.5) \quad \text{IVb.3.7(b)}$$

as recommended by Weisman. In these relations s and D are the pitch and the diameter of a tube or a rod, respectively.

Example IVb.3.3. Consider the fully developed flow of water in a rod bundle at a rate of 2845 lbm/h. System pressure is 1020 psia and water bulk temperature is 525 F. Find the heat transfer coefficient. Use rod pitch = 0.738 in and rod diameter = 0.563 in.



Solution: We first find the channel flow area and the equivalent diameter:

$$A_{Flow} = s^2 - 4(\pi l^2/16) = 0.738 \times 0.738 - \pi(0.563)^2/4 = 0.2956 \text{ in}^2 = 2\text{E-}3 \text{ ft}^2.$$

$$P_{Wetted} = 4(\pi l/4) = \pi d = 1.768 \text{ in}$$

$$D_e = 4[0.2956 / 1.768] = 0.668 \text{ in}$$

Water properties at $P = 1020$ psia and $T = 525$ F are $v = 0.02166 \text{ ft}^3/\text{lbm}$ or $\rho = 46.17 \text{ lbm/ft}^3$

$$V = \dot{m}/(\rho A) = (2845/3600)/(47.62 \times 2\text{E-}3) = 8.08 \text{ ft/s}$$

$$\text{Re} = \rho V D_e / \mu = [47.62 \times 8.08 \times (0.668/12)] / (0.23766/3600) = 323,568$$

Since water is heated up, we use:

$$\text{Nu} = \frac{h D_{channel}}{k_{Water}} = C \text{Re}^{0.8} \text{Pr}^{0.4}$$

At $T = 525$ F, we also find $\text{Pr} = 0.8726$ and $k = 0.3377 \text{ Btu/h}\cdot\text{ft}\cdot\text{F}$. Since $s/D \approx 1.3$, C is calculated as:

$$C = 0.042 \times (0.738/0.563) - 0.024 = 0.031055$$

$$\text{Nu} = \frac{h D_{channel}}{k_{Water}} = C \text{Re}^{0.8} \text{Pr}^{0.4} = 0.031055 \times 323,568^{0.8} (0.8726)^{1/3} = 759$$

$$h = \text{Nu} \times k_{Water} / D_e = 759 \times 0.3377 / (0.668/12) = 4606 \text{ Btu/h}\cdot\text{ft}^2\cdot\text{F}$$

3.4. Internal Flow of Liquid Metals

An interesting feature of liquid metals, such as bismuth, mercury, and sodium, is that due to their high thermal conductivity, heat transfer by conduction plays a much more important role than in ordinary liquids and gases. For liquid metal properties see Table A.IV.6(SI). Thus, the Nu number for liquid metals includes a constant, to account for heat transfer by conduction superimposed on the term accounting for flow velocity and hence heat transfer by convection.

For flow in circular tubes, Lyon-Martinelli correlation is recommended for isothermal wall:

$$\text{Nu} = 5.0 + 0.025 \text{Pe}^{0.8} \quad \text{IVb.3.8}$$

where Pe is the Peclet number given by $\text{Pe} = \text{Re} \text{Pr}$. For uniform wall heat flux, The Seban-Shimazaki correlation, valid only for $s/D > 1.35$ is used:

$$\text{Nu} = 7.0 + 0.025 \text{Pe}^{0.8} \quad \text{IVb.3.9}$$

For flow of liquid metals parallel to heated rods, arranged in a hexagonal array, Dwyer recommends:

$$\text{Nu} = 6.66 + 3.126(s/D) + 1.184(s/D)^2 + 0.0155(\psi \text{Pe})^{0.86}$$

where s/D is the ratio of the pitch to diameter for the array and ψ is given by (Lamarsh and Baratta):

$$\psi = 1 - \frac{0.942(s/D)^{1.4}}{\text{Pr}(\text{Re}/1000)^{1.281}}$$

QUESTIONS

- What does k in Biot number and in Nusselt number stand for? State the interpretation of each number.
- What is the difference between V_x and $(V_x)_f$? Similarly, identify the difference between T and T_f .
- Which scientist first identified the boundary layer? What is the significance of the Prandtl number?
- In the analytical derivation of external and internal temperature profiles, we assumed thermal properties to be independent of temperature. Is it then correct to say that in such circumstance the temperature and the velocity fields are independent?
- What is the von Karman method for the development of the energy equation in the boundary layer?
- How accurate is the thickness of boundary layer obtained from a force balance in the boundary layer?
- What are the key assumptions, which were made to obtain an analytical solution for the thickness of the thermal boundary layer?
- Consider heat convection for laminar flow of water in a pipe. What is the effect of doubling the flow rate on the Nusselt number? What is the effect of using motor oil instead of water on h ?
- What is the difference between the Dittus-Boelter and the Seider-Tate correlations? What is the range of applicability for the Pr number? Are these correlations applicable to liquid metals?

PROBLEMS

1. Start with Equation IVb.2.7 and obtain an approximate relation for the thickness of the hydrodynamic boundary layer. Compare your result with the exact solution.
2. Start with Equation IVb.2.6 and derive a relation for the thickness of the hydrodynamic boundary layer by assuming a linear relation for velocity versus distance, i.e., $V_x/(V_x)_f = y/\delta$.
3. Assume a two-dimensional flow over a flat plate. Use the result of Problem 1 for the thickness of the boundary layer and the velocity profile for V_x , as given by

Equation IVb.2.1 and obtain a relation for V_y . [Hint: Use the equation for continuity given by Equation IIIa.3.13-1].

4. Find the Pr number of a fluid having $\nu = 0.001 \text{ ft}^2/\text{s}$, $k = 0.08 \text{ Btu/ft h F}$, $c_p = 0.45 \text{ Btu/lbm}\cdot\text{F}$, and $\rho = 58 \text{ lbm/ft}^3$. [Ans.: 1175].

5. Consider a flat plate 15.3 cm long. Find the free stream velocity, V_f so that the flow regime remains laminar for such fluids as water, air, and helium at 1 atm and 20 C. [Ans.: 3.3, 51, and 387 m/s].

6. Air at atmospheric pressure and room temperature (27 C) flows over a flat plate at a speed of 2 m/s. The length of the plate is 0.5 m. Find the thickness of the boundary layer at the middle of the plate ($x = 25 \text{ cm}$) and at the trailing edge ($x = L$). [Ans. 7 mm and 1 cm].

7. A flat plate has a length of 40 cm and width of 1 m. Air, at pressure of 2 atm, temperature of 57 C, and velocity of 3 m/s flows over the plate. Find the thickness of the boundary layer at $x = L$.

8. Use the result of Problem 3 and find the y -component of velocity over the plate of Problem 6 at the outer edge of the boundary layer for two locations; a) the middle of the plate and b) the trailing edge of the plate.

9. Solve Problem 3 using the velocity profile of Problem 2. Use the result and find the y -component of velocity over the plate of Problem 6. Calculate numerical values for V_y at the outer edge of the boundary layer for two locations; a) the middle of the plate and b) the trailing edge of the plate.

10. Plot the thickness of the boundary condition as a function of the length of a flat plate ($\delta = C x^{0.5}$), starting from the leading and ending at the trailing edge. For this purpose consider the flow of air at a pressure of 2 atm and temperature of 27 C over the flat plate. Find δ at $x = 0.45 \text{ m}$.

11. Start with Equation IVb.2.5 and obtain Equation IVb.2.6. [Hint: By assuming constant pressure throughout the flow, the left hand side is simplified as $dP/dx = 0$. To simplify the right hand side, first substitute for the last term from the integration-by-part technique. Now write the Bernoulli equation and conclude that $d(V_x)/dx$ is also zero.]

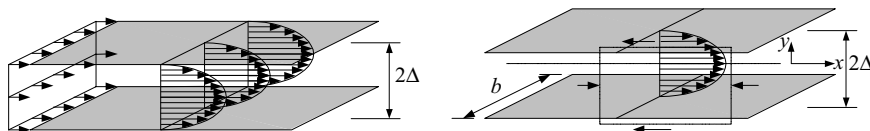
12. Start with Equation IVb.2.8 and obtain Equation IVb.2.9. For this purpose, first ignore the non-linear term compared with the two dominant terms. Then substitute for the velocity and temperature profiles. To develop the integral, consider a case where the hydrodynamic boundary layer is thicker than the thermal boundary layer (thus the integral is zero for $y > \delta'$). Arrange the result in terms of $\zeta = \delta'/\delta$ and ignore ζ^4 .

13. Air at a pressure of 1 atm and temperature of 30 C flows over a flat plate. The plate has a length of 120 cm, a width of 200 cm and a temperature of 10 C.

14. To derive an analytical solution for the thickness of the thermal boundary layer, Equation IVb.2.9, it was qualitatively argued that the net viscous work term is generally negligible compared with the more dominant terms. The goal of this problem is to quantify the above argument for fluids having low, medium, and high Prandtl numbers. Assume constant fluid properties and equal hydrodynamic and thermal boundary layer thicknesses to determine cases that the above approximation is valid. [Hint: Define a figure of merit being the ratio of the viscous dissipation to the surface conduction. Use an order of magnitude analysis to relate this ratio to the Prandtl number multiplied by the Eckert number].

15. Equation IVb.2.9 was derived by using the cubic-parabola profiles for velocity and temperature as given in Equations IVb.2.1 and IVb.2.2. Use the same cubic-parabola profile for temperature but a linear velocity profile, as for Problem 2, and obtain the Nu number in terms of the Re and Pr numbers.

16. Consider the flow of a fluid between two large parallel flat plates located at a distance of 2Δ apart.



Find the governing momentum equation for the flow between the plates for the condition that the velocity profile is fully developed. [Hint: In this case, the net momentum flux is zero].

17. Use the momentum equation of Problem 16 and obtain the velocity profile in terms of y , Δ , and the maximum velocity at $y = 0$. [Ans.: $V_x = (1 - y^2/\Delta^2)/(V_x)_0$].

18. Find $\xi = \delta' / \delta$ for the fluids of Table IVb.1.1 at $P = 1$ at and $T = 20^\circ\text{C}$. [Ans.: $\xi_{\text{Water}} = 0.5$].

19. Consider a heat exchanger made of sheets of parallel flat plates. Water at 25°C , 1 atm, and 4 m/s flows over a plate. Find the water flow rate in the boundary layer of one plate at 10 cm from the leading edge.

20. Air is flowing at 1 atm, 130°C , and 20 m/s over a flat plate. Find the thickness of the boundary layer at 5 cm from the leading edge and the air flow rate in the boundary layer at this location.

21. A heated flat plate is exposed to the colder air flowing over the plate at a velocity of 35 ft/s. The plate is at a temperature of 200°F while air is at atmospheric pressure and 70°F . Find the rate of heat transfer if the plate is a) heated at the leading edge and b) at a distance of 3 in from the leading edge.

22. Two parallel flat plates are placed 2 cm apart. Water, at 20 C, flows between these plates at a velocity of 1.6 m/s. Find: a) if the flow becomes fully developed and b) the distance from the leading edge if it does.

23. A flat plate having a length of 75 cm and width of 50 cm is maintained at 85 C. Cold air at 10 kPa and 30 C flows over the plate at 10 m/s. Find the total rate of heat loss from the plate.

24. Water at 80 F is flowing over a flat plate with a velocity of 8 ft/s. The plate is 5 ft long. Find and plot the heat transfer coefficient as a function of the plate length.

25. Air at a temperature of 95 F and a velocity of 20 ft/s flows over a hot flat plate, maintained at 482 F. Find the rate of heat transfer from this 1 ft by 1 ft square plate. [Ans. ~ 423 Btu/hr].

26. In Problem 25, find the distance from the surface of the plate where flow velocity becomes 75% of the free stream velocity at $x = L/2$.

27. A plate is heated over its entire length and maintained at 140 F. Air at atmospheric pressure and 80 F is flowing over the plate at velocity of 6.6 ft/s. Find the heat transfer coefficient and the rate of heat transfer from at a distance of 1.6 ft from the leading edge. The depth of plate is 1 ft. [Ans. ~ 392 Btu/hr].

28. For flow over a flat plate, the average temperature difference (i.e., $\overline{T_s - T_f}$) when the plate temperature is kept constant is readily calculated. This is not the case if a constant heat flux to or from the surface is imposed. Use the averaging scheme over the plate length as given by:

$$\overline{T_s - T_f} = \frac{\int_0^L (T_s - T_f) dx}{\int_0^L dx}$$

to find the average temperature difference. [Hint: Substitute for ΔT in the numerator from the Nu number and for Nu number from Equation IVb.2.11 and integrate].

29. Obtain the average temperature difference for the laminar flow of fluids over a heated plate ($L \times b$), for constant heat flux boundary condition, in terms of the Re and the Pr numbers. For this purpose, use the result of Problem 28 and the local Nu_x number for constant heat flux boundary condition given as:

$$Nu_x = 0.453 Re_x^{1/2} Pr^{1/3} \quad (\dot{q}_s'' = \text{constant})$$

where in this relation properties are developed at the film temperature.

[Ans.: $\overline{T_s - T_f} = 1.47 Re_L^{-1/2} Pr^{-1/3} \dot{q}_s'' (L/k)$].

30. A heated flat plate is exposed to the flow of cold air. Find h_x at $x = L/2$ and the total rate of heat transfer for two types of boundary conditions: a) isothermal plate and b) constant heat flux. Data: plate dimensions are 50 cm \times 50 cm, $T_{air} = 10^\circ\text{C}$, $P_{air} = 0.5$ atm, $V_{air} = 4$ m/s, $\bar{T}_{plate} = 100^\circ\text{C}$. [Ans.: 157 W, 70 W].

31. A uniformly heated square plate of 2 ft \times 2 ft is exposed to cold air at 80 F. The heater output remains at a constant value of 1 kW. Air, at atmospheric pressure, flows over the plate at a velocity of 16.5 ft/s. Find the average temperature of this plate. [Ans.: $\sim 513^\circ\text{F}$].

32. A flat square plate is uniformly heated over its entire surface. One side of the plate is insulated and the other is exposed to cold air flowing over the plate. Find the plate average temperature. Data: $L = 35$ cm, $T_{air} = 20^\circ\text{C}$, $V_{air} = 5$ m/s, $P_{air} = 1$ atm, $\dot{q}'' = 900$ W/m². [Ans.: 80°F].

33. Water at 25°C flows in a smooth tube, having a diameter of 5 cm, at a rate of 1 kg/s. The tube is unheated and the temperature difference between the tube wall and the water is negligible. Determine the flow regime.

34. Show that the mass flow rate of water in a pipe or tube of diameter D is given by $\dot{m} = \pi D \mu \text{Re}/4$.

35. Water enters a heated tube of 2 mm diameter at 30°C and leaves the tube at 60°C . Find the water mass flow for the average Reynolds number of 1000. [Ans.: 0.00564 kg/s].

36. Air at 10 atm and 77°C flows in a duct of rectangular cross section, 20 cm by 10 cm, at a rate of 0.001 kg/s. Find a) the flow regime and b) the heat transfer coefficient. The duct is also at 77°C .

37. We want to establish fully turbulent flow in a smooth circular tube carrying water at a velocity of 5.75 ft/s. Find the maximum tube diameter that still ensures the flow is fully turbulent. What size tube should be used if air instead of water is flowing in the tube? Both fluids are at 1 atm and 68°F . What conclusion you draw from your solution?

38. Water is flowing at a rate of \dot{m} in a smooth pipe of diameter D . A section of this pipe having a length of L is heated. Water at the inlet to the heated section has a temperature of T_{f1} . Water temperature at the exit of the heated section is T_{f2} . The heated section of the pipe wall is maintained at T_s . Show that for turbulent flow in the pipe and a specified pipe diameter, the required heated length is given by:

$$L = 11.407 \left(\frac{\text{Pr}^{0.6}}{\mu^{0.2}} \right) \left(D^{0.8} \dot{m}^{0.2} \right) \left(\frac{\Delta T_f}{\Delta T_s} \right)$$

where $\Delta T_f = T_{f2} - T_{f1}$, $\Delta T_s = T_s - \bar{T}_f$, and $\bar{T}_f = (T_{f1} + T_{f2})/2$. [Hint: Use Newton's law of cooling in conjunction with Equations IVb.2.20 and IVb.3.4].

39. Water at a rate of 5 kg/s is flowing inside a heated tube. The tube has a diameter of 6 cm and its wall is maintained at 85 C. Find the required tube length so that the water can be heated from 10 to 20 C.

40. Water is flowing at a rate of \dot{m} in a smooth pipe of diameter D . A section of this pipe having a length of L is heated. Water at the inlet to the heated section has a temperature of T_{f1} . Water temperature at the exit of the the heated section is T_{f2} . The heated section of the pipe wall is maintained at T_s . Show that for turbulent flow in the pipe and a specified heated length, the pipe diameter is given by:

$$D = 0.0477 \left[\frac{L}{\dot{m}^{0.2} c_p^{0.6}} \left(\frac{k}{\mu} \right)^{0.4} \left(\frac{\Delta T_s}{\Delta T_f} \right) \right]^{1.25}$$

41. Water flows in a heated round tube at a rate of 3 kg/s. The heated section of the tube is 4 m long. The tube wall is maintained at 90 C. Water enters the tube at 35 C and leaves the heated section at 45 C. Find the tube diameter. [Ans.: 10.3 cm].

42. Water is flowing in a smooth pipe of diameter D . A section of this pipe having a length of L is heated. Water at the inlet to the heated section has a temperature of T_{f1} . Water temperature at the exit of the heated section is T_{f2} . The heated section of the pipe wall is maintained at T_s . Show that for turbulent flow in the pipe and a specified heated length and pipe diameter, pressure drop in the heated section is given by:

$$\Delta P = 0.0159 \left(\frac{L^{1.9}}{D^{5.52}} \right) \left(\frac{\mu^{0.38} \text{Pr}^{0.54}}{\rho} \right) \left(\frac{\Delta T_s}{\Delta T_f} \right)^{0.9}$$

[Hint: Use Newton's law of cooling in conjunction with Equations IIIb.3.6, IIIb.3.7, and IVb.2.20].

43. As described in Chapter VIb, one way to measure the mass flow rate is to use a heated duct. Consider the flow of air in a duct. To measure the air flow rate, we first raise the temperature of a segment of this duct and maintain the wall temperature at a desired value. We then measure the air pressure and temperature at the inlet and exit of the heated segment. Use this technique and the given data to find the air flow rate in the duct. Data: Air pressure: 17 psia, air temperature at the inlet: 65 F, air temperature at the exit: 125 F, duct wall temperature 230 F, duct cross section is 1.5 ft by 1 ft, and the length of the heated segment is: 8 ft.

44. Consider a small double pipe heat exchanger. Hot air flows in the inner and cold water in the outer pipe. The heat exchanger is well insulated. The inner pipe

is thin and made of copper tubing. Use the given data to find the required heat exchanger length. Data: Inner pipe diameter: 3 cm, wall thickness: 2 mm, outer pipe diameter: 6 cm, $P_{air} = 1$ atm, $\dot{m}_{air} = 1$ kg/s, $\dot{m}_{water} = 2$ kg/s, total rate of heat transfer: 20 kW, average air temperature: $T_{air} = 450$ C, average water temperature: $T_{water} = 160$ C, water pressure 5 atm.

45. Water flows in a heated tube. The constant heat flux of 2 MW/m^2 is applied to the tube wall. Water enters the tube at a rate of 1 kg/s and an inlet temperature of 35 C. Find the water exit temperature. The tube inside diameter is 2 cm and the tube length is 1 m. [Ans.: 65 C].

46. Consider the flow of water in a heat flux controlled channel. The channel length and diameter are D and L , respectively. The heat flux at the wall varies linearly along the channel. Show that the water temperature at the exit of the channel is given by:

$$T_{exit} = T_{inlet} + \frac{\pi D}{\dot{m} c_p} (\dot{q}_{inlet}'' + \dot{q}_{exit}'') \frac{L}{2}$$

47. Consider the flow of water in a heat flux controlled channel. The wall heat flux varies linearly. Find the water temperature at the exit of the channel. Data: $D = 3$ cm, $L = 1.5$ m, $\dot{m}_{water} = 1$ kg/s, $\dot{q}_{inlet}'' = 1 \text{ MW/m}^2$, $\dot{q}_{outlet}'' = 2 \text{ MW/m}^2$, $T_{in} = 30$ C. [Ans.: 81 C].

48. Water is flowing in a smooth pipe of diameter D . A section of this pipe having a length of L is heated. Water at the inlet to the heated section has a temperature of T_{f1} . Water temperature at the exit of the heated section is T_{f2} . The heated section of the pipe wall is maintained at a constant heat flux so that a constant temperature difference of $\Delta T_s = T_s - \bar{T}_f$ exists between the wall and the bulk water temperature. Show that for turbulent flow in the pipe and a specified heated length and pipe diameter, water temperature at the exit of the heated section is given by:

$$T_{f2} = T_{f1} + 0.0876 \left(\frac{L}{D^{0.8}} \right) \left(\frac{\mu^{0.2}}{\text{Pr}^{0.6}} \right) \left(\frac{\Delta T_s}{\dot{m}^{0.2}} \right)$$

49. Water flows in a heated tube at a velocity of 2 m/s. The tube length and diameter are 20 cm and 6 mm, respectively. A constant heat flux is imposed on the tube wall to maintain a constant temperature difference of 8 C between the tube wall temperature and the bulk water temperature. For a water temperature of 40 C at the inlet, find the water temperature at the outlet of the tube. [Ans.: ≈ 44 C].

50. The surface of a cylinder, having a diameter of 25 cm, is maintained at 140 C. Air flows over the cylinder at a steady state velocity of 50 m/s, a temperature of 35 C, and a pressure of 1 atm. Assuming the surface emissivity is very low, find

the rate of heat transfer to the cylinder to make up the loss by convection to the cross flow of air and maintain its temperature at the specified value.

51. The surface of a cylinder, having a diameter of 6 in and a length of 2 ft, is maintained at 300 F. The cylinder is exposed to the cross flow of carbon dioxide flowing at a steady state velocity of 150 ft/s, a temperature of 70 F, and a pressure of 1 atm. Assuming the surface emissivity is very low, find the rate of heat transfer to the cylinder to make up the heat loss by convection to the cross flow of air and to maintain its temperature at the specified value.

52. A sphere made of copper, having a diameter of 2 cm, is heated to 50 C. We now place this sphere in air flowing over the sphere at a velocity of 15 m/s, a temperature of 17 C, and a pressure of 1 atm. Find the time the sphere temperature drops to 25 C.

53. A steel pellet is heated up to 400 F and placed in air, flowing at a velocity of 155 ft/s over the pellet. The pellet has a diameter of 0.5 in. We want to estimate the cooldown rate of the pellet by using a lumped capacitance method. Plot the pellet temperature versus time for 30 minutes. Data: $\varepsilon = 0.8$, $T_{air} = 100$ F and $P_{air} = 1$ atm, $\rho = 488$ lbm/ft³, $c = 0.1$ Btu/lbm·F.

54. A cross flow heat exchanger consists of a cluster of 25 tubes, arranged in a staggered square array. Thus, there are 5 rows, each consists of 5 tubes. The tube diameter, the longitudinal pitch, and the transverse pitch are 15 mm, 35 mm, and 32 mm, respectively. Air flows over the tube bank at a velocity of 8 m/s and an inlet temperature of 27 C. The tube surface temperature is maintained at 77 C. Find the rate of heat transfer and the air exit temperature.

IVc. Free Convection

Free or natural convection is that mode of heat transfer where fluid flows only due to the presence of buoyancy forces. This in turn is the result of the action of body forces, most notably gravity, in the presence of density gradient, generally due to a temperature gradient. Although the rate of heat transfer by free convection is generally smaller than that of forced convection, the most notable advantage associated with free convection is in its passive nature, which in turn increases system reliability. Since the lower rate of heat transfer results in higher thermal resistance, making the application of this mode of heat transfer essential in enhancing insulation. Free convection in flow loops results in the circulation of the working fluid, referred to as natural circulation, which plays a major role in nuclear plants during shutdown. Free convection does not always lead to natural circulation as the latter requires the heat source to be located at a lower elevation than the heat sink. Even in such case, the buoyancy force must be sufficient to overcome the friction force caused by the fluid shear stresses. As shown in Section 2 of this chapter, the interesting feature of free convection heat transfer is the fact that the thermal and the hydrodynamic aspects are intertwined.

1. Definition of Free Convection Terms

Volumetric expansion coefficient (β) for a fluid, as defined in Chapter II, is the change of fluid volume with temperature at constant pressure. The volumetric expansion coefficient is given by $\beta = (\partial V / \partial T)_P / V$ and has units of inverse temperature. We may approximately express the volumetric expansion coefficient as: $\beta \cong [(V_1 - V_2) / (T_1 - T_2)] / V_1 = [(\rho_1 - \rho_2) / (T_1 - T_2)] / \rho_1$. For ideal gases, $\beta = 1/T$ where T is the gas absolute temperature in degrees K or R.

Characteristic length is the length over which free convection is established. For vertical flat plates and cylinders, this is the height of the plate. For horizontal cylinders and sphere, this is the diameter. Finally, for horizontal plates, $L = A_s / P$ where A_s and P are the plate surface area and perimeter, respectively.

Grashof number, after Franz Grashof, is a measure of buoyancy as compared with the viscous forces in the hydrodynamic boundary layer. Due to the appearance of the buoyancy forces, the Grashof number plays an important role in heat transfer by free convection. For flow of fluid over a plate, the Grashof number is:

$$Gr = g\beta(T_s - T_f)x^3/\nu^2$$

The Gr number is used to determine relative importance of the modes of heat transfer by convection. If $Gr \ll Re^2$, then the forced convection mode is dominant. For $Gr \gg Re^2$, the free convection mode is dominant.

Mixed Convection is that mode of convection heat transfer for which $Gr \approx Re^2$.

Modified Grashof Number (Gr^*) is the product of Gr and Nu numbers, $Gr^* = GrNu = g\beta\dot{Q}_s x^4 / (kv^2)$

Rayleigh number (Ra) is the product of the Grashof and the Prandtl numbers, $Ra = GrPr$.

2. Analytical Solution

Figure IVc.1 shows the free convection boundary layers for a hot vertical plate, a hot horizontal wire and a cold vertical plate. Note that outside the boundary layer, fluid is quiescent and $V_f = 0$ since fluid away from the surface is stagnant. To show the significance of the Grashof number, we obtain the kinetic energy of the fluid in the boundary layer from an energy balance. Ignoring the frictional losses on the wall we find that:

$$(\rho_f - \rho_s) gx/2 = \rho_f V^2/2$$

where we have approximated the average density difference in the boundary layer as $(\rho_f - \rho_s)/2$. For the flow in the boundary layer, we can find $Re^2 = (Vx/\nu)^2$. Substituting for V^2 from the energy balance, we find $Re^2 = [(\rho_f - \rho_s)gx/\rho_f](x/\nu)^2$, which is an alternative way to represent the Gr number. If we substitute from the definition of the volumetric expansion coefficient, we find $Gr = g\beta(T_s - T_f)x^3/\nu^2$.

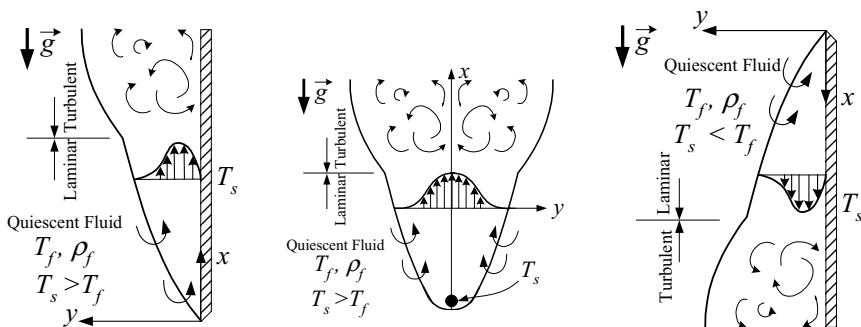


Figure IVc.1.1. Free convection boundary layers

2.1. External Laminar Flow

Consider the steady laminar flow of an incompressible fluid over a vertical flat plate. Similar assumptions used in the forced convection analysis are applicable here.

Determination of Velocity and Temperature Profiles

The governing equation for the hydrodynamic boundary layer is Equation III.3.20-1 repeated here as:

$$V_x \frac{\partial V_x}{\partial x} + V_y \frac{\partial V_x}{\partial y} = -\frac{1}{\rho} \frac{\partial P}{\partial x} + \nu \frac{\partial^2 V_x}{\partial y^2} + \frac{1}{\rho} X \quad \text{IIIa.3.20-1}$$

where body force is now accounted for. Since $\partial P/\partial x = -\rho g$ and $X = -\rho g$, the momentum equation becomes:

$$V_x \frac{\partial V_x}{\partial x} + V_y \frac{\partial V_x}{\partial y} = g \left(\frac{\rho - \rho_f}{\rho} \right) + \nu \frac{\partial^2 V_x}{\partial y^2} = g\beta(T - T_f) + \nu \frac{\partial^2 V_x}{\partial y^2} \quad \text{IVc.2.1}$$

The temperature boundary layer is given by Equation III.3.23-1. Similar to the forced convection case, we may find the velocity and the temperature profile in the boundary layer from the boundary conditions:

Profile	$y = 0$	δ	δ
Temperature	$T = T_s$	$T = T_f$	$\partial T/\partial y = 0$
Velocity	$V_x = 0$	$V_x = 0$	$\partial V_x/\partial y = 0$

For temperature profile we then find:

$$\frac{T - T_f}{T_s - T_f} = \left(1 - \frac{y}{\delta} \right)^2$$

For the velocity profile at $y = 0$ from Equation IVc.2.1 we find an additional condition:

$$\frac{\partial^2 V_x}{\partial y^2} = -g\beta(T - T_f)/\nu$$

Hence, the velocity profile becomes:

$$\frac{V_x}{V_{xo}} = \left(1 - \frac{y}{\delta} \right)^2$$

where V_{xo} is an assumed velocity since in free convection, $V_f = 0$. Note that the velocity profile also satisfies the continuity Equation IIIa.3.13-1 as it should. To be able to solve the governing equations analytically, similar to forced convection, we seek to convert the partial differential equations to ordinary differential equations. Ostrach used a change of variables from x and y to ξ so that $\xi = (\text{Gr}_x/4)^{1/4} y/x$ and a stream function ψ given by $\psi(x, y) = 4\nu(x/y)\xi f(\xi) = 4\nu(\text{Gr}_x/4)^{1/4} f(\xi)$ where $f(\xi)$ is a function to be determined. Having the stream function, V_x and V_y are found in terms of ξ . For V_x , we take the derivative of ψ with respect to y :

$$V_x = \frac{\partial \psi}{\partial y} = \frac{\partial \psi}{\partial \xi} \frac{\partial \xi}{\partial y} = \left[4\nu(\text{Gr}_x/4)^{1/4} f'(\xi) \right] \left[(\text{Gr}_x/4)^{1/4} / x \right] = \frac{2\nu}{x} \text{Gr}_x^{1/2} f'(\xi)$$

To obtain V_y , we may either use $V_y = -\partial\psi/\partial x$ or use the continuity Equation IIIa.3.13-1 to find V_y in terms of ξ and $f(\xi)$ as $V_y = \nu c_1 x^{-1/4} [\xi f'(\xi) - 3f(\xi)]$. Having found V_x and V_y in terms of ξ and $f(\xi)$, Ostrach introduced a dimensionless temperature $\theta = (T - T_f)/(T_s - T_f)$. Substituting for V_x , V_y , T_s , and their related derivatives in terms of ξ , $f(\xi)$, and θ , the set of partial differential equations given by Equations IIIa.3.13-1, IIIa.3.20-1, and IVc.2.1 are reduced to the following set of two ordinary differential equations:

$$\frac{d^3 f(\xi)}{d\xi^3} + 3f \frac{d^2 f(\xi)}{d\xi^2} - 2 \left(\frac{df(\xi)}{d\xi} \right)^2 + \theta = 0$$

$$\frac{d^2 \theta}{d\xi^2} + 3\text{Pr}_f \frac{d\theta}{d\xi} = 0$$

This set is subject to the following boundary condition. For $\xi = 0$, $f = df/d\xi = 0$ and $\theta = 1$. The other boundary condition is for $\xi \rightarrow \infty$, $df/d\xi = 0$ and $\theta = 0$. We do not expect to find an analytical solution to the above set of coupled non-linear second and third order differential equations. But we know that $\theta'(0) = -f(\text{Pr})$ is a part of the solution since it is the dimensionless temperature gradient at the wall. We now tie this condition to the heat transfer coefficient through the heat transfer gradient at the wall:

$$h = \frac{-k(\partial T/\partial y)_0}{T_s - T_f} = \frac{-k}{T_s - T_f} \frac{\partial T}{\partial \theta} \frac{\partial \theta(0)}{\partial \xi} \frac{d\xi}{dy} = -k\theta'(0) \frac{1}{\sqrt{2}} \text{Gr}_x^{1/4} \frac{1}{x} = \frac{1}{\sqrt{2}} \frac{k}{x} \text{Gr}_x^{1/4} f(\text{Pr})$$

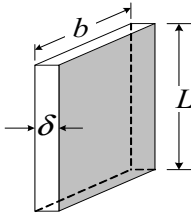
The above relation can be written in terms of $\text{Nu} = f(\text{GrPr}) = f(\text{Ra})$. Seemingly, we obtained an analytical solution for this problem. However, $f(\text{Pr})$ is yet to be determined. One way to find this function is to solve the above set of differential equations numerically, plot $\theta = f(\xi)$ and find the slope of the curves in such plots. Ostrach obtained numerical solutions for $f(\xi)$ and θ in terms of Pr number. An empirical fit to the results of Ostrach solution is $f(\text{Pr}) = 0.676\text{Pr}^{1/2}(0.861 + \text{Pr})^{-1/4}$. Hence, Nu and $\overline{\text{Nu}}$ becomes:

$$\text{Nu}_x = 0.478\text{Ra}_x^{1/4} [1 + (0.861/\text{Pr})]^{-1/4} \quad \text{IVc.2.2}$$

$$\text{Nu}_L = 0.637\text{Ra}_L^{1/4} [1 + (0.861/\text{Pr})]^{-1/4} \quad \text{IVc.2.3}$$

All properties are evaluated at the film temperature except for β which for gases is found at T_f .

Example IVc.2.1. A vertical plate is maintained at 40 C. This plate is placed in a quiescent hot air at 114 C, find the rate of heat transfer to the plate. Use $L_{plate} = 0.3$ m, $b_{plate} = 0.42$ m, $\delta = 1$ mm, and $P_{air} = 1$ bar.



Solution: We first find the air properties from Table A.IV.4 at $T_{av} = (40 + 114)/2 = 350$ K:

$$\nu = 20.92\text{E-}6 \text{ m}^2/\text{s}, k = 0.03 \text{ W/m}\cdot\text{C}, \text{Pr} = 0.7, \beta = 1/T_f = 1/(114 + 273) = 1/387 = 2.584\text{E-}3 \text{ K}^{-1}.$$

$$\text{Ra}_L = \text{Gr}_L \text{Pr} = [g\beta(T_s - T_f)L^3/\nu^2]\text{Pr} \\ = [9.81 \times (2.584\text{E-}3) \times (114 - 40) \times 0.3^3/(20.92\text{E-}6)^2] \times 0.7 = 1.157\text{E}8$$

$$\text{Nu}_L = 0.637\text{Ra}_L^{1/4} [1 + (0.861/\text{Pr})]^{-1/4} \\ = 0.637 \times (1.157\text{E}8)^{0.25} \times [1 + (0.861/0.7)]^{-0.25} = 54$$

$$h = \text{Nu}_L \times k/L = 54 \times 0.03/0.3 = 5.4 \text{ W/m}^2\cdot\text{C} (\approx 1 \text{ Btu/h}\cdot\text{ft}^2\cdot\text{F})$$

$$\dot{Q} = hA(T_f - T_{plate}) = 5.4 \times (0.3 \times 0.42) \times (114 - 40) = 50 \text{ W}.$$

Heat transfer to both sides is $2 \times 50 = 100$ W.

3. Empirical Relations

While the foregoing derivation was for a simple case of laminar flow over flat plate, we expect the same functional relationship $\text{Nu} = f(\text{Ra})$ for more complicated cases involving turbulent flow over inclined flat plates, cylinders, and spheres. In free convection, the transition between laminar to turbulent flow takes place at a critical $\text{Ra} = 1\text{E}9$ for vertical plates. Due to the inherent complexities of turbulent flow coupled with the fact that the surface may be oriented at angles or being curved, the only solution we find is in the form of empirical correlations. Such correlations are generally devised for the entire range of the Ra number.

3.1. Flow over Vertical Plates and Cylinders

Isothermal vertical plate: For flow over an isothermal vertical plate, Churchill and Chu recommend:

$$\overline{\text{Nu}}_L = \left\{ 0.825 + 0.387 \left[1 + (0.492 / \text{Pr})^{0.5625} \right]^{-0.296} \text{Ra}_L^{1/6} \right\}^2 \quad \underline{1.0\text{E}-1 < \text{Ra} < 1.0\text{E}12} \quad \text{IVc.3.1}$$

Isothermal vertical cylinders: Equation IVc.3.1 is also applicable to isothermal vertical cylinders provided that $(D/L)_{\text{cylinder}} \geq 35/\text{Gr}_L^{1/4}$. Fluid properties should be evaluated at $T_{\text{Film}} = (T_s + T_f)/2$ but β is found at T_f .

Example IVc.3.1. A radiator consists of 36 vertical plates, each maintained by an electrical element at a temperature of 62 C, to heat a room at 12 C. The plates have a height of 45 cm, a width of 10 cm, and a thickness of 10 mm. Find the rate of heat transfer from this radiator. Pressure in the room is atmospheric.

Solution: We first find the air properties from Table A.IV.4 at $T_{\text{av}} = (12 + 62)/2 = 37 \text{ C} = 310 \text{ K}$:

$$\nu = 16.89\text{E-}6 \text{ m}^2/\text{s}, k = 0.0274 \text{ W/m}\cdot\text{C}, \text{Pr} = 0.706, \beta = 1/T_f = 1/(12 + 273) = 3.508\text{E-}3 \text{ K}^{-1}.$$

$$\text{Gr}_L = g\beta(T_s - T_f)L^3/\nu^2 = 9.81 \times (3.508\text{E-}3) \times (62 - 12) \times 0.45^3/(16.89\text{E-}6)^2 = 5.484\text{E}8$$

$$\text{Ra}_L = \text{Gr}_L \text{Pr} = 5.484\text{E}8 \times 0.706 = 3.87\text{E}8$$

For isothermal vertical plates, we use Equation IVc.3.1:

$$\text{Nu}_L = \{0.825 + 0.387[1 + (0.492/0.706)^{0.5625}]^{-0.296}(3.87\text{E}8)^{0.16667}\}^2 = 91.78$$

$$h = \text{Nu} \times k/L = 91.78 \times 0.0274/0.45 = 5.59 \text{ W/m}\cdot\text{C} (\approx 1 \text{ Btu/h}\cdot\text{ft}^2\cdot\text{F})$$

$$\dot{Q} = N_{\text{plates}} \times hA(T_{\text{plate}} - T_f)$$

$$A_{\text{plate}} = 2(L \times b + b \times \delta + L \times \delta)$$

$$A_{\text{plate}} = 2(0.45 \times 0.10 + 0.45 \times 0.01 + 0.1 \times 0.01) = 0.101 \text{ m}^2$$

$$\dot{Q} = 36 \times 5.59 \times 0.101 \times (62 - 12) = 1 \text{ kW}.$$

Vertical plates and cylinders with constant heat flux: For flow over vertical plates and cylinders in constant heat flux, Churchill & Chu correlation is:

$$\overline{\text{Nu}}_L^{-1.25} - 0.68\overline{\text{Nu}}_L^{-0.25} - 0.67 \left[1 + (0.492 / \text{Pr})^{0.5625} \right]^{-0.445} \text{Pr}^{0.25} (\text{Gr}_L^*)^{0.25} = 0$$

$$\underline{1.0\text{E}-1 < \text{Ra} < 1.0\text{E}12} \quad \text{IVc.3.2}$$

where in Equation IVc.3.2, $\overline{\text{Nu}}_L = \dot{Q}_s L / (k \Delta T)$ with ΔT calculated from $\overline{\Delta T} = [T_s(L/2) - T_f]$. Fluid properties should be evaluated at $T_{\text{Film}} = (T_s + T_f)/2$ but β is found at T_f .

3.2. Flow over Horizontal Plates and Cylinders

Heat transfer coefficient in free convection over horizontal plates strongly depends on the orientation of the plate with respect to temperature as the flow pattern depends on the side of plate under consideration (Figure IVc.3.1).

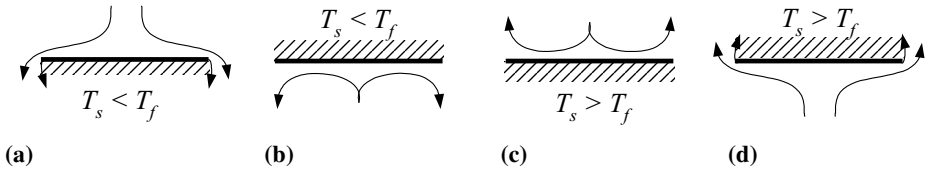


Figure IVc.3.1. Horizontal plates in free convection

Consider for example a cold horizontal flat plate in a hotter fluid (a). Fluid on the top would move over the plate, get cooler, and would flow downward from the side of the plate. On the other hand, in case (b), fluid moves underneath the plate, gets cooler and freely rushes downward leading to a more effective heat transfer in case (b) than in case (a). A similar situation exists for cases of (c) and (d) where cooler fluid moves over the plate, gets warmer and freely moves upward where in case (d), fluid moves underneath the plate, gets warmer, and can move upward only when it reaches the edges of the plate.

Isothermal horizontal plates: For the more effective cases of (b) and (c), the average Nu number originally suggested by McAdams, for the indicated ranges of the Rayleigh numbers, should be calculated from:

$$\overline{Nu}_L = 0.54 Ra_L^{0.25} \quad 1.0E4 \leq Ra_L \leq 1.0E7 \quad \text{IVc.3.3}$$

$$\overline{Nu}_L = 0.15 Ra_L^{0.33} \quad 1.0E7 \leq Ra_L \leq 1.0E11 \quad \text{IVc.3.4}$$

For the less effective cases of (a) and (d), the average Nu number may be calculated from

$$\overline{Nu}_L = 0.27 Ra_L^{0.25} \quad 1.0E5 \leq Ra_L \leq 1.0E10 \quad \text{IVc.3.5}$$

In these correlations, the characteristic length L used in the calculation of the Grashof number is found from $L = A/P$ where A is the surface area and P the perimeter. Fluid properties in Equations IVc.3.3 through IVc.3.5 should be evaluated at the $T_{Film} = (T_s + T_f)/2$.

Example IVc.3.2. An air-cooled compressor uses 15 thin, annular fins. When the engine is operating at steady state, each fin is at an average temperature of 200 F. The ambient is at 1 atm and 60 F. The inside and the outside diameters are 6 in and 1.6 ft, respectively. Find the steady state rate of heat transfer.

Solution: We first find the air properties from Table A.IV.4 at $T_{av} = (200 + 60)/2 = 130\text{ F} = 590\text{ R}$:

$$\nu = 1.72\text{E-}4\text{ ft}^2/\text{s}, k = 0.016\text{ Btu/h}\cdot\text{ft}^2\cdot\text{F}, \text{Pr} = 0.705, \beta = 1/T_f = 1/590 = 0.00169\text{ R}^{-1}.$$

$$A_{plate} = \pi(D^2 - d^2)/4 = \pi[1.6^2 - (6/12)^2]/4 = 1.81\text{ ft}^2$$

$$P_{plate} = \pi D = \pi \times 1.6 = 5\text{ ft}$$

$$L_{characteristic} = A/P = 1.81/5 = 0.362\text{ ft}$$

$$\text{Gr}_L = g\beta(T_s - T_f)L^3/\nu^2 = 32.2 \times 0.00169 \times (200 - 60) \times 0.362^3/(1.72\text{E-}4)^2 = 12.22\text{E}6$$

$$\text{Ra}_L = \text{Gr}_L\text{Pr} = 12.22\text{E}6 \times 0.705 = 8.61\text{E}6$$

For isothermal horizontal plates with $\text{Ra}_L = 8.61\text{E}6$, we use Equation IVc.3.3:

$$\text{Nu}_L = 0.54 \times (8.61\text{E}6)^{0.25} = 29.25$$

$$h = \text{Nu} \times k/L = 29.25 \times 0.016/0.362 = 0.77\text{ Btu/h}\cdot\text{ft}^2\cdot\text{F}$$

$$\dot{Q} = N_{plates} \times hA(T_{plate} - T_f) = 15 \times 0.77 \times 1.81 \times (200 - 60) = 2927\text{ Btu/h}$$

$= 0.86\text{ kW}$. Total rate of heat transfer is 1.56 kW.

Isothermal horizontal cylinders: For horizontal cylinders, Churchill and Chu recommend the following correlation:

$$\text{Nu}_D = \left\{ 0.6 + 0.387\text{Ra}_D^{0.1667} \left[1 + (0.559/\text{Pr})^{0.5625} \right]^{-0.296} \right\}^2$$

$1.0\text{E-}5 < \text{Ra} < 1.0\text{E}12$ IVc.3.6

The characteristic length for the calculation of the Grashof number is the cylinder diameter. Fluid properties should be evaluated at $T_{av} = (T_s + T_f)/2$ but β is found at T_f .

Example IVc.3.3. Cold water is flowing in a thin-wall tube, maintaining the tube wall temperature at 14 C. The ambient air is at 40 C. Find the rate of heat transfer to the tube wall. $D_{tube} = 6\text{ cm}$, $L_{tube} = 4\text{ m}$.

Solution: Finding the air properties from Table A.IV.4 at $T_{av} = (14 + 40)/2 = 27\text{ C} = 300\text{ K}$:

$$\nu = 15.89\text{E-}6\text{ m}^2/\text{s}, k = 0.0263\text{ W/m}\cdot\text{C}, \text{Pr} = 0.707, \beta = 1/T_f = 1/(40 + 273) = 3.195\text{E-}3\text{ K}^{-1}.$$

$$\text{Gr}_L = g\beta(T_s - T_f)L^3/\nu^2 = 9.81 \times (3.195\text{E-}3) \times (40 - 14) \times 0.06^3/(15.89\text{E-}6)^2 = 0.697\text{E}6$$

$$\text{Ra}_L = \text{Gr}_L\text{Pr} = 0.697\text{E}6 \times 0.707 = 493,000$$

For isothermal horizontal cylinders, we use Equation IVc.3.6:

$$\text{Nu}_L = \{ 0.6 + 0.387 \times 493,000^{0.1667} [1 + (0.559/0.707)^{0.5625}]^{-0.296} \}^2 = 11.94$$

$$h = \text{Nu} \times k/L = 11.94 \times 0.0263/0.06 = 5.23\text{ W/m}\cdot\text{C}$$

$$\dot{Q} = hA(T_{plate} - T_f) = 5.23 \times (\pi \times 0.06 \times 4) \times (40 - 14) = 102.6\text{ W}.$$

Spheres: For spheres immersed in fluids, having $Pr \geq 0.7$, Churchill (1983) recommends the following correlation:

$$Nu_D = 2 + 0.589Ra_D^{0.25} \left[1 + (0.469/Pr)^{0.5625} \right]^{-0.4445} \quad Ra_D \leq 1.0E11 \quad \text{IVc.3.7}$$

The characteristic length for the calculation of the Grashof number is the cylinder diameter. Fluid properties should be evaluated at $T_{Film} = (T_s + T_f)/2$ but β is found at T_f .

Example IVc.3.4. Compare the heating of a spherical metal, 6 cm in diameter, in water and in air. Water is saturated at 100 C. Air is also at 100 C and 1 atm. The metal is at 20 C.

Solution: The rate of heat transfer in the two mediums is proportional to:

$$\frac{\dot{Q}_{Water}}{\dot{Q}_{Air}} = \frac{h_{Water} A \Delta T}{h_{Air} A \Delta T} = \frac{Nu_{Water} k_{Water}}{Nu_{Air} k_{Air}}$$

The average temperature in both medium is $T_{Film} = (20 + 100)/2 = 60$ C. The air and water properties are:

Medium	ν (m/s ²)	Pr	k (W/m·C)	β (1/K)
Air	18.900E-6	0.708	0.0285	0.003003
Water	0.4748E-6	3	0.6507	0.000529

$$Ra_{Air} = [g\beta(T_s - T_f)L^3/\nu^2]Pr = [9.81 \times 0.003003 \times (100 - 20) \times 0.06^3/(18.90E-6)^2] \times 0.708 = 1.00E6$$

$$Ra_{Water} = [g\beta(T_s - T_f)L^3/\nu^2]Pr = [9.81 \times 0.000529 \times (100 - 20) \times 0.06^3/(0.4748E-6)^2] \times 3 = 1.197E10$$

$$Nu_{Air} = 2 + 0.589 \times (1E6)^{0.25} \times [1 + (0.469/0.708)^{0.5625}]^{-0.4445} = 35.4$$

$$Nu_{water} = 2 + 0.589 \times (1.197E10)^{0.25} \times [1 + (0.469/3)^{0.5625}]^{-0.4445} = 311.8$$

The rate of heat transfer in water is $(311.8/35.4) \times (0.6507/0.0285) = 201$ times faster.

QUESTIONS

- What mode of heat transfer governs the oceanic and the atmospheric motions?
- The heating system of a tall building consists only of a boiler, located in the basement, the radiators (located on each floor), and the pipe runs. What mode of heat transfer is used in this design?
- What is the difference between Nu and \overline{Nu} , between Gr and Gr^* , and between Re and Ra ?
- What is the value of the Ra number for the transition for the free convection boundary layer from laminar to turbulent?
- What is the characteristic length? How is it calculated in a horizontal cylinder?

- Consider free convection over a horizontal plate with $T_s > T_f$. Compare the heat transfer from the top of the plate with that from the bottom of the plate. Which heat transfer is more efficient?

PROBLEMS

1. A flat plate, maintained at 250 C is placed vertically in air at a pressure of 1 bar and temperature of 20 C. The plate height and width are 20 cm and 10 cm. Find the rate of heat transfer to this plate. [Ans.: 64 W].
2. Consider two identical flat plates both maintained at 400 K. These plates are placed vertically into tow large containers. One plate is placed in a container full of air at 300 K and 1 atm and the other plate in a container full of carbon dioxide at 300 K and 1 atm. Find the ratio of the Grashof numbers Gr_{air}/Gr_{CO_2} .
3. Consider two identical flat plates both maintained at 400 K. These plates are placed vertically into tow large containers. One plate is placed in a container full of air at 300 K and 1 atm and the other plate in a container full of carbon dioxide at 300 K and 1 atm. Find the ratio of the heat transfer coefficients h_{air}/h_{CO_2} and the rate of heat transfer $\dot{Q}_{air}/\dot{Q}_{CO_2}$.
4. For a flat plate, the transition from the free convection boundary layer to the free convection turbulent boundary layer takes place at a Rayleigh number of about $Ra = 1E9$. A flat plate at 70 C is placed in a colder medium at 27 C. Find the location on the plate where this transition takes if the plate is placed in: a) air, b) Ammonia, c) water. All fluids are at 1 atm.
5. A flat plate of glass, having a height of 1 ft is heated to 200 F in an annealing furnace. The plate is then removed and placed vertically in a room at 60 F and 14.7 psia to be air cooled. Find the initial rate of heat transfer from the glass plate.
6. A radiator consists of 15 vertical plates, each maintained by an electrical element at a temperature of 65 C. to heat a room at 15 C. The plates have a height of 50 cm, a width of 12 cm, and a thickness of 16 mm. Find the rate of heat transfer from this radiator. Pressure in the room is atmospheric.
7. Two identical plates (A and B), heated to 40 C, are placed in quiescent air at 15 C and 1 atm to be air-cooled. Plate A is hanged vertically and the plate B is placed horizontally. Both plates are cooled from both sides. Assuming no thermal radiation and only free convection heat transfer, which plate cools faster?
8. An air-cooled engine uses 20 thin, horizontal fins. When the engine is operating at steady state, each fin is at an average temperature of 240 F. The ambient is at 1 atm and 60 F. The inside and the outside diameters of each annular fin are 8 in and 2 ft, respectively. Find the steady state rate of heat transfer.
9. A small transformer is placed in a metal box. The box has a height of 10 cm, depth of 0.75 m, and width of 1 m. There is no heat transfer from the bottom of the box and from the four insulated sides, as heat is dissipated only from the top of

the box. The ambient air is at 20 C at 1 atm. The rate of heat transfer to be dissipated is 0.4 kW. Find the temperature of the top of the metal box.

10. The air conditioning duct in a house is 60 m long. The duct cross section is a rectangle with a height of 35 cm and width of 75 cm. The duct is bare and exposed to air at 18 C. Find the total rate of heat loss if the average surface temperature of the duct metal is 35 C.

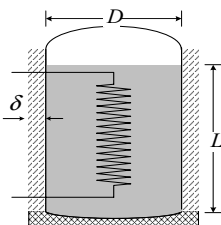
11. A block of steel is uniformly heated from inside to maintain its temperature at 100 C. The block is a rectangular parallelepiped. The base of the block is a 3 cm by 3 cm square and the height of the block is 6 cm. We place this block in air at 25 C. Find the rate of heat loss from this block by natural convection.

12. A horizontal steam line carries saturated steam at a rate of 6.0E6 lbm/h. The steam line has a diameter of 2.67 ft, a wall thickness of 2 in, and a length of 150 ft. Accounting for the steam pressure drop in the pipe, steam may be considered saturated at an average pressure of 800 psia. The pipe is insulated with a thickness of 7 inches. Find the rate of heat loss to the ambient at 23 C. The emissivity of the insulation is 0.7. Other data include $P_{ambient} = 1$ atm, $k_s = 10$ Btu/h·ft·F, $k_i = 0.7$ Btu/h·ft·F. The ambient air is quiescent.

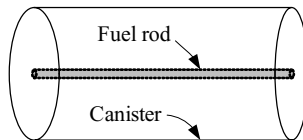
13. Slurry at a rate of 110 lbm/h and 110 F is pumped through 2 in inside diameter pipe. After traveling in a unheated length of the pipe, the slurry enters a 3 ft long heated section where the wall of the pipe is maintained at 190 F. Find the average temperature of the slurry leaving the heated section. Thermal properties of slurry are as follows $\rho = 70$ lbm/ft³, $\mu = 150$ lbm/h·ft, $c = 0.4$ Btu/lbm·F, and $k = 0.5$ Btu/h·ft·F.

14. A large tank of diameter D contains water to height L , as shown in the figure. The tank is insulated with a layer of insulation, having a thickness of δ_i . The tank wall thickness is δ_s . The water bulk temperature is maintained at T_{fi} while the ambient temperature is T_{fo} . Use the given data to find the rate of heat that is transferred to water at steady state conditions.

Data: $D = 8.04$ ft (2.45 m), $L = 32.8$ ft (10 m), $\delta_s = 4$ in, (10.16 cm), $\delta_i = 5$ in (12.7 cm), $P_{fi} = 2250$ psia (15.51 MPa), $T_{fi} = 500$ F (260 C), $P_{fo} = 1$ atm, $T_{fo} = 85$ F (29.5 C), $k_s = 10$ Btu/h·ft·F, $k_i = 0.8$ Btu/h·ft·F.



Problem 14



Problem 15

15. A spent fuel rod is placed in a canister. A vacuum pump is used to remove all air and establish vacuum in the canister. The surface temperature of the rod must

not exceed 392 F (200 C) while the temperature of the canister wall must remain at 151 F (66 C). For a heat transfer coefficient of 2 Btu/h·ft²·F (11.4 W/m²·C) find the ambient temperature. Ignore conduction heat transfer between the rod and the canister. $\varepsilon_{\text{canister}} = 0.6$.

16. A solid sphere made of polished copper has a diameter of 2 cm and is at 100 C. We now expose the solid sphere to air at 50 C and 1 atm. Use the lumped capacitance method to plot the temperature of the solid sphere versus time after five minutes of exposure. The air is quiescent.

17. A spent fuel rod is placed in a canister. A vacuum pump is used to remove all air and establish vacuum in the canister. The surface temperature of the rod must not exceed 392 F (200 C) when the temperature of the ambient is at 40 C (104 F). For a heat transfer coefficient of 1.5 Btu/h·ft²·F (8.5 W/m²·C) find the canister wall temperature. Ignore conduction heat transfer between the rod and the canister. $\varepsilon = 0.6$.

18. A spent fuel rod is placed in a canister. A vacuum pump is used to remove all air and establish vacuum in the canister. The surface temperature of the rod must not exceed 302 F (150 C) when the temperature of the ambient is at 40 C (104 F). Find the canister wall temperature. Ignore conduction heat transfer between the rod and the canister. $\varepsilon = 0.6$.

19. A longitudinal fin of rectangular profile (Figure IVa.8.6) made of aluminum is used to dissipate heat from a hot surface. Find the rate of heat transfer from this fin. Data: $T_b = 125$ C, $T_f = 27$ C, $L = 20$ cm, $b = 14$ cm, $\delta = 1$ cm. [Hint: Assume a reasonable value for h to find $T(x = L/2)$ from Equation IVa.8.7 and iterate until the convergence criterion is met].

20. A well insulated water tank contains 100 lit of water at 27 C. We want to heat the water to 90 C. For this purpose we place a coil made of copper with an outside diameter of 1.2 cm in the water. The coil carries steam at 115 kPa. Ignore the thermal resistance of the condensing steam. Find a) the required heating time and b) the amount of steam condensed in the coil.

21. A horizontal pipe delivers steam at 1 MPa and a rate of 100 kg/s to a steam turbine. The pipe (O.D. = 11.5 cm and I.D. = 9.65 cm) is made of carbon steel. You may assume that the air and the walls of the turbine building are both at 20 C. Use an emissivity of 0.81 for the pipe surface to estimate the rate of heat loss, per unit length of the pipe, due to the free convection and thermal radiation mechanisms.

IVd. Thermal Radiation

Thermal radiation is perhaps the most interesting mode of heat transfer, as it does not require a material medium. The recognition of this interesting feature, which today is commonplace, has a long history. In Chapter VII, we have discussed scientists' efforts to unify physical concepts. Up to about 100 years ago, these efforts had been focused on explaining every phenomenon in terms of two independent branches of science. First, classical mechanics for explaining the behavior of particles based on the Newton laws and electromagnetism for explaining the behavior of waves based on Maxwell's equations. The most challenging task was explaining the nature of light, which was thought to behave only as a wave. However, if light behaved only as an electromagnetic wave, how could then it travel through empty space? While filling the vacuum with fictitious ether provided a temporary solution, it was the development of modern physics, based on quantum mechanics, which allowed description of particles and waves as two distinct modes of behavior. In quantum mechanics, a wavelength is defined for particles. Max Planck ingeniously expressed energy of particle-like electromagnetic radiation in terms of wave frequency. Since wavelength is related to the speed of the particle through frequency, we conclude that the shorter the wavelength, the more energetic the particle. The term radiation encompasses a wide range of wavelengths in the electromagnetic spectrum. In this chapter we limit our discussion to thermal radiation, which covers only radiation emitted as a result of the temperature of a substance. We consider surfaces emitting or receiving radiant energy. We will see that radiation heat transfer is treated differently because the radiant energy is both directional and wavelength dependent.

1. Definition of Thermal Radiation Terms

1.1. Definitions Pertinent to Wavelength

Electromagnetic spectrum refers to such energetic radiation as cosmic rays on the one-side and such low energy radiation as radio waves and TV signals, on the other. Some types of radiation can be seen, such as light, some can be felt, such as heat, and some can only be detected by sensitive instruments.

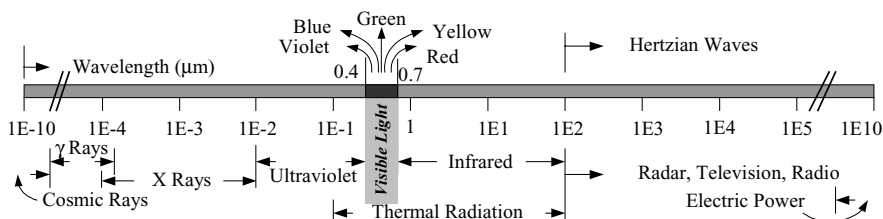


Figure IVd.1.1. Depiction of the electromagnetic spectrum on a log scale

Shown in Figure IVd.1.1 is the electromagnetic wave spectrum in terms of wavelength ($\mu\text{m} = 1\text{E-}6\text{ m}$) ranging from about $1\text{E-}10\ \mu\text{m}$ for high energy cosmic rays to $1\text{E}9\ \mu\text{m}$ for low energy electric power. On this spectrum, γ rays follow the cosmic rays. The γ rays are emitted directly from the atomic nucleus and their energy is measured in MeV. For example bombardment of oxygen, O_{16} with neutrons results in the appearance of unstable nitrogen N_{16} , which then decays by emitting energetic γ rays on the order of 6.13 MeV and 7.12 MeVs. X-rays are generally less energetic than γ rays and are emitted by atoms while in the excited state. This is subsequent to an electron dropping to a lower orbit. The ultraviolet light is much less energetic than X-rays and is harmful only to sensitive tissue. Generally γ rays, X-rays, and ultraviolet light are of interest to nuclear physicists and engineers. The visible light covers the small region between 0.4 to 0.7 μm . The monochromatic distribution of visible light is highlighted in figure IVd.1.1. The region pertinent to heat transfer falls in the 0.1 to 100 μm range. This region includes the low energy portion of ultraviolet, visible light, and entire infrared spectrum. Microwaves consist of such waves as radar, television, and radio. Generally, low frequency waves outside the band of thermal radiation are categorized as Hertzian waves and are of interest to electrical engineers.

Wavelength, λ in terms of the wave frequency is given as $\lambda = c/f$ where c is the speed of light and f is the wave frequency. In vacuum the speed of light is $c = 2.998\text{E}8\text{ m/s}$. Wavelength is usually expressed in μm .

Planck's constant, h is the proportionality factor to express wave energy in terms of the wave frequency. The plank constant is given as $h = 6.6256\text{E-}34\text{ J}\cdot\text{s}$. Hence, the wave energy is $E = hf$, where E is in joules. For example, to find the radiation energy having a frequency of 0.01 μm , we first calculate the wave frequency $f = c/\lambda = (2.998\text{E}8\text{ m/s})/(0.01\text{E-}6\text{ m}) = 2.998\text{E}16\text{ s}^{-1}$. We then find energy as $E = 6.6256\text{E-}34 \times 2.998\text{E}16 = 1.986\text{E-}17\text{ J}$.

1.2. Definitions Pertinent to Directions and Coordinates

Thermal radiation variables refer to the dependency of the emitted radiation on the wavelength (referred to as the spectral distribution) and on the direction (directional distribution).

Spectral distribution refers to the fact that the magnitude of radiation is a function of wavelength. This is shown in Figure IVd.1.2(a).

Monochromatic radiation emission refers to a radiation at a specific wavelength.

Directional distribution expresses the fact that surfaces may emit radiation in preferred directions as shown in Figure IVd.1.2(b). Figure IVd.1.2(c) shows an isotropic distribution of radiation.

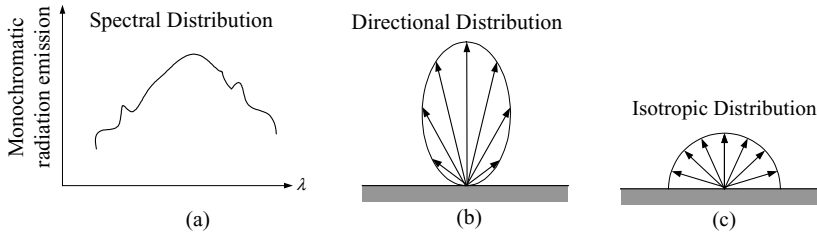


Figure IVd.1.2. Emission of radiation from surfaces (Incropera)

Radiation intensity is an energy density radiated from (emissive) or incident upon a surface. As we will see in this section, the radiation intensity in general depends on the wavelength and direction. Therefore, the radiation intensity is expressed in units of energy per unit time, unit area, unit wavelength, and unit angular direction.

Zenith and azimuthal angles in conjunction with the position vector specify the location of a point in the spherical coordinate system, Figure IVd.1.3(a). The zenith angle, measured from the x -axis, is shown by θ and is used in polar coordinates. The zenith angle ranges from 0 to 2π . The azimuthal angle, measured from the z -axis is shown by φ . The azimuthal angle ranges from 0 to $\pi/2$ for the top hemisphere ($+z$). The solid angle, as defined next, ranges from 0 to 2π for the top hemisphere.

Solid angle being a three dimensional angle is defined similar to a two dimensional or a plane angle*. To define these angles we consider the spherical coordinate system of Figure IVd.1.3(a). Angles θ and φ are the azimuthal and the zenith angles (also shown in Figure IVd.1.4). The differential plane angle, such as $d\varphi$ in Figure IVd.1.3(b) or IVd.1.3(c) is defined by the region between two rays of a circle and is measured as the ratio of the arc between the two rays (dl) divided by the radius of the circle (r) hence, $d\varphi = dl/r$. We define a differential solid angle in the same manner. Consider the elemental surface dA_1 as shown in Figure IVd.1.3(b). Surface dA_1 is defined in spherical coordinates by the azimuthal and the zenith angles θ and φ . The differential surface dA_n in space subtends a differential solid angle $d\Omega$ when viewed from a point on the differential surface dA_1 . Thus, the solid angle $d\Omega$ is defined by a region between two rays of a sphere and is measured as the ratio of the differential surface area dA_n between the two rays divided by the square of the sphere radius $d\Omega = dA_n/r^2$.

* Solid angle is defined as “the angle formed by the vortex of a cone or subtended at the point of intersection by three or more planes.” In other words, a solid angle is the angle intercepted by a cone on a surface of a unit sphere. The unit sphere has a solid angle of 4π steradian (sr).

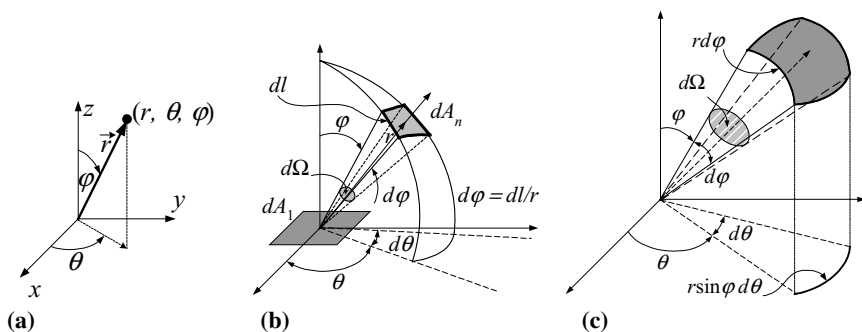


Figure IVd.1.3. (a) Spherical coordinates, (b) and (c) Elemental surface dA_n subtends solid angle $d\omega$

To eliminate the appearance of the arbitrarily taken differential space surface dA_n , we may substitute for dA_n in terms of the spherical coordinate system variables r , θ , and φ to obtain $dA_n = (r \sin \varphi d\theta)(rd\varphi)$. Thus, substituting in $d\Omega = dA_n/r^2$ we find $d\Omega = \sin \varphi d\theta d\varphi$. Plane angles have the unit of radians (rad) and solid angles are expressed in units of *steradian* (sr). Note that $0 \leq \Omega \leq 4\pi$.

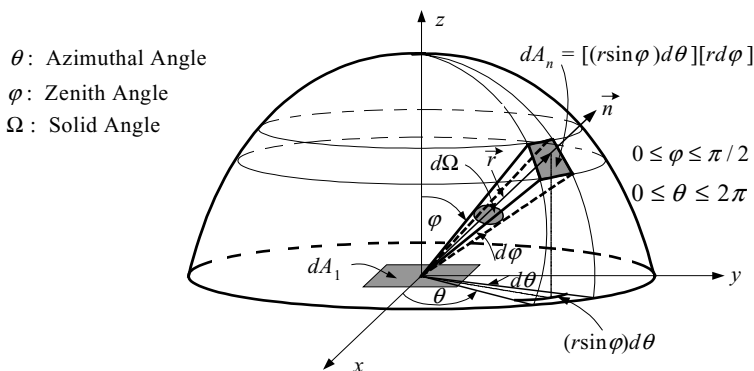


Figure IVd.1.4. Surface dA_n subtends solid angle $d\Omega$ at center of a hemisphere around dA_1

Projected area of surface dA_1 in the direction of n for example is $dA_1 \cos \varphi$, where φ is the zenith angle (Figure IVd.1.4).

1.3. Definitions Pertinent to Radiation Interaction with a Surface

Emission I_e , refers to the radiant energy emitted by a surface and is identified here by subscript e , as shown in Figures IVd.1.5(a) and IVd.1.5(c).

Irradiation I_i , is the radiant energy incident on a surface and is identified here by subscript i , as shown in Figure IVd.1.5(b) and IVd.1.5(c).

Radiosity J_r , refers to all of the radiant energy leaving a surface (including the radiation *reflected* by the surface) and is identified here by subscript r , as shown in Figure IVd.1.5(c).

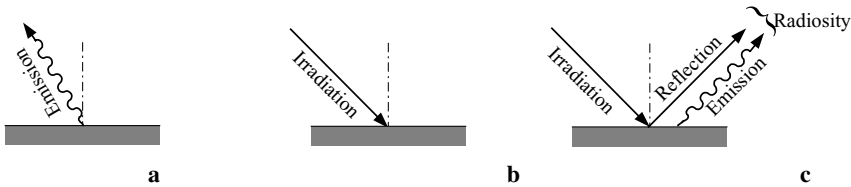


Figure IVd.1.5. Depiction of emission, irradiation, and radiosity

1.4. Definitions Pertinent to Emission

Emission spectral intensity, $I_{\lambda,e}(\lambda, \theta, \phi)$ is the rate of emitted radiant energy at the following characteristics:

- it has wavelength λ , per unit wavelength interval $d\lambda$ about λ
- it travels in the direction of θ and ϕ and per unit solid angle about this direction.
- it travels per unit area of the emitting surface normal to the direction θ and ϕ

Based on the above definition, if $d\dot{Q}$ is the total rate of energy emitted by the elemental surface dA_1 , the fraction in the (θ, ϕ) direction would be $d\dot{Q}/dA_1 \cos \phi$. Of this energy, the portion that is emitted in the interval $d\lambda$ about wavelength λ is $d\dot{Q}/dA_1 \cos \phi d\lambda$. Finally, the portion of this energy passing per unit time in the solid angle $d\Omega$ is $d\dot{Q}/dA_1 \cos \phi d\lambda d\Omega$. The spectral intensity has the units of $\text{W/m}^2 \cdot \mu\text{m} \cdot \text{sr}$ and is given by

$$I_{\lambda,e}(\lambda, \theta, \phi) = \frac{d\dot{Q}}{dA_1 \cos \phi d\lambda d\Omega} \quad \text{IVd.1.1}$$

Substituting for $d\Omega = \sin \phi d\theta d\phi$ we find:

$$I_{\lambda,e}(\lambda, \theta, \phi) = \frac{d\dot{Q}}{dA_1 \cos \phi \sin \phi d\theta d\phi d\lambda} \quad \text{IVd.1.1}$$

Spectral hemispheric emissive power, E_λ is defined as the rate of emission of radiation from a surface per unit surface area, at wavelength λ per unit wavelength $d\lambda$ about λ , in all directions. E_λ has units of $\text{W/m}^2 \cdot \mu\text{m}$. By defining the spectral hemispheric emissive power, we eliminated the directional dependency:

$$E_\lambda(\lambda) = \int_0^{2\pi} \int_0^{\pi/2} I_{\lambda,e}(\lambda, \theta, \phi) \cos \phi \sin \phi d\theta d\phi \quad \text{IVd.1.2}$$

Total emissive power, E is the rate of radiation emitted per unit surface area in all directions at all wavelengths. By this definition, we also eliminated the wavelength dependence:

$$E = \int_0^\infty E_\lambda(\lambda) d\lambda \quad \text{IVd.1.3}$$

Diffuse emitter refers to surfaces that emit radiation isotropically (i.e., independent of direction as shown in Figure IVd.1.2(c)). Therefore, in the case of an isotropic emitter, $I_{\lambda,e}(\lambda, \theta, \varphi)$ becomes only $I_{\lambda,e}$, which can be removed from the inside of the integral of Equation IVd.1.2:

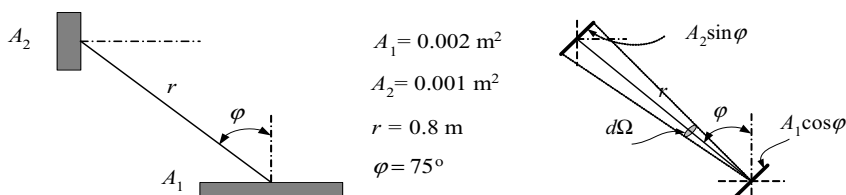
$$E_\lambda(\lambda) = I_{\lambda,e}(\lambda) \int_0^{2\pi} \left[\int_0^{\pi/2} \sin 2\varphi d\varphi / 2 \right] d\theta = I_{\lambda,e}(\lambda) \int_0^{2\pi} [-\cos 2\varphi / 4]_0^{\pi/2} d\theta = \pi I_{\lambda,e}(\lambda)$$

Total emissive power for a diffuse emitter is calculated from Equation IVd.1.3:

$$E = \int_0^\infty E_\lambda(\lambda) d\lambda = \int_0^\infty \pi I_{\lambda,e}(\lambda) d\lambda = \pi \int_0^\infty I_{\lambda,e}(\lambda) d\lambda = \pi I_e \quad \text{IVd.1.4}$$

where I_e is known as the total intensity, having units of $\text{W/m}^2\cdot\text{sr}$ and π is in sr.

Example IVd.1.1. Surface A_1 is a diffuse emitter with an emission intensity of $8,000 \text{ W/m}^2\cdot\text{sr}$ in the normal direction. Find the intensity of radiation received by surface A_2 for the data given below.



Solution: Since surface A_1 is a diffuse emitter, the intensity of emission is the same in all directions including the direction where A_2 is located. Since the given surfaces are small, we use them as elemental surfaces. To find the solid angle subtended by A_2 , we use the definition $d\Omega = dA_n/r^2$ where $dA_n = dA_2 \sin \varphi$. Substituting, we get $d\Omega = 0.001 \times \sin(75^\circ)/0.8^2 = 0.0015 \text{ sr}$. The intensity of radiation received by A_2 is given by:

$$d\dot{Q} = \int_0^\infty I_{\lambda,e}(\lambda, \theta, \varphi) (dA_1 \cos \varphi) d\lambda d\Omega = I_e dA_1 \cos \varphi d\Omega$$

$$d\dot{Q} = 8000 \times [0.0002 \times \cos(75^\circ)] \times 0.0015 = 6.2\text{E-4 W}.$$

1.5. Definitions Pertinent to Incident Radiant Energy on a Surface

Incident spectral intensity, $I_{\lambda,i}(\lambda, \theta, \varphi)$ is the rate of incident radiant energy at the following characteristics:

- it has wavelength λ , per unit wavelength interval $d\lambda$ about λ
- it travels in the direction of θ and φ and per unit solid angle about this direction.
- it is incident on a surface per unit area of the intercepting surface normal to the direction θ and φ .

Spectral irradiation G_λ , is the rate at which radiant energy of wavelength λ is incident on the unit area of a surface per unit wavelength interval $d\lambda$ about λ . Spectral irradiation is then related to the spectral intensity:

$$G_\lambda(\lambda) = \int_0^{2\pi} \left[\int_0^{\pi/2} I_{\lambda,i}(\lambda, \theta, \varphi) \cos \varphi \sin \varphi d\varphi \right] d\theta \quad \text{IVd.1.5}$$

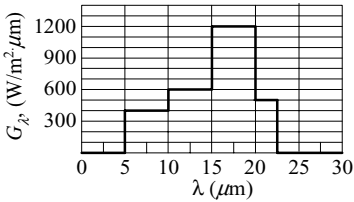
Since the incident spectral intensity has units of $\text{W/m}^2 \cdot \mu\text{m} \cdot \text{sr}$, the spectral irradiation has units of $\text{W/m}^2 \cdot \mu\text{m}$.

Total irradiation is that amount of radiant energy incident on the unit area of a surface in all directions and all wavelengths:

$$G = \int_0^\infty G_\lambda(\lambda) d\lambda \quad \text{IVd.1.6}$$

If the incident radiation is diffuse, then the integral of IVd.1.5 can be carried out to obtain $G_\lambda(\lambda) = \pi I_{\lambda,i}(\lambda)$.

Example IVd.1.1. Find total irradiation and total intensity for the given spectral irradiation distribution.



Solution: We find G from Equation IVd.1.6 by dividing the integral into several intervals:

$$G = \int_0^\infty G_\lambda(\lambda) d\lambda = \int_0^5 400 d\lambda + \int_5^{10} 600 d\lambda + \int_{10}^{15} 1200 d\lambda + \int_{15}^{20} 1200 d\lambda + \int_{20}^{22.5} 500 d\lambda + \int_{22.5}^\infty 0 d\lambda$$

$$G = 400 \times 5 + 600 \times 5 + 1200 \times 5 + 500 \times 2.5 = 12,250 \text{ W/m}^2.$$

Finally, we find total irradiation intensity from $I_i = 12,250/\pi = 3,899 \text{ W/m}^2$.

1.6. Definitions Pertinent to Surface Radiosity

Spectral radiosity, $J_\lambda(\lambda)$ is the rate at which radiant energy of wavelength λ per unit wavelength interval $d\lambda$ about λ leaves the unit area of a surface. Since spectral radiosity is the summation of the surface emission and reflection (r) of an incident radiation and appears in all directions, it has units of $\text{W/m}^2\cdot\mu\text{m}$:

$$J_\lambda(\lambda) = \int_0^{2\pi} \left[\int_0^{\pi/2} I_{\lambda,e+r}(\lambda, \theta, \phi) \cos \theta \sin \theta d\theta \right] d\phi \quad \text{IVd.1.7}$$

Total radiosity, J is defined similar to the definition of total emissive power and total irradiation. Thus, total radiosity is the total rate of radiant energy leaving the unit area of a surface:

$$J = \int_0^\infty J_\lambda(\lambda) d\lambda \quad \text{IVd.1.8}$$

If the surface is a diffuse emitter, then the integral can be carried out to obtain $J_\lambda(\lambda) = \pi I_{\lambda,e+r}(\lambda)$. Similarly, we find total radiosity given as $J = \pi I_{e+r}$.

2. Ideal Surfaces

In Section 1, we introduced such basic concepts for a surface as emissivity, irradiation, and radiosity. In this section, we further explore these concepts by first treating surfaces as ideal and then as real surfaces.

2.1. Blackbody Radiation

A blackbody is an ideal surface, which satisfies three conditions. First, it is a perfect emitter. Thus, for a specified temperature and wavelength, a blackbody emits more radiant energy than any other surface at the same temperature. Second, a blackbody is the best absorber of energy. Therefore, it absorbs all energies incident on it from all directions and at all wavelengths. Third, a blackbody is a diffuse emitter. In other words, the radiant energy emitted from a blackbody is only a function of temperature and wavelength but is independent of direction. Figure IVd.2.1(a) shows an isothermal cavity that approaches the definition of a blackbody.

Historically, Joseph Stefan in 1879 suggested that the total emissive power of a blackbody is proportional to the fourth power of the absolute temperature. It was Ludwig Boltzmann who in 1884 applied the principle of classical thermodynamics to analytically derive the same result. Hence, according to Stefan-Boltzmann:

$$E_b = \sigma T^4 \quad \text{IVd.2.1}$$

where σ is the Stefan-Boltzmann constant, $\sigma = 5.67\text{E}-8 \text{ W/m}^2\cdot\text{K}^4 = 0.1714\text{E}-8 \text{ Btu/ft}^2\cdot\text{h}\cdot\text{R}^4$. Note in Equation IVd.2.1, T is the absolute temperature and E_b is the total emissive power. To obtain the equation for spectral emissive power in terms

of temperature we turn to Max Planck, who in 1901 by treating radiation as “photon gas”, was able to express $I_{\lambda,b}$ in terms of wave length and temperature:

$$I_{\lambda,b}(\lambda, T) = \frac{(2\hbar c^2)\lambda^{-5}}{\exp(\hbar c / k\lambda T) - 1} \quad \text{IVd.2.2}$$

In Equation IVd.2.2, \hbar is the Planck’s constant, c is the speed of light in vacuum and k is the Boltzmann’s constant, $k = 1.3805\text{E-}23$ J/K. Since a blackbody is a diffuse surface, from Equation IVd.1.4 we find that:

$$E_{\lambda,b}(\lambda, T) = \pi I_{\lambda,b}(\lambda, T) = \frac{C_1 \lambda^{-5}}{\exp(C_2 / \lambda T) - 1} \quad \text{IVd.2.3}$$

where in Equation IVd.2.3, $C_1 = 2\pi\hbar c^2 = 3.742\text{E}8$ W· $\mu\text{m}^4/\text{m}^2$ and $C_2 = \hbar c/k = 1.439\text{E}4$ $\mu\text{m}\cdot\text{K}$. If we integrate Equation IVd.2.3 over all wavelengths we should obtain Equation IVd.2.1. This is easily verified:

$$E_b = \int_0^\infty E_{\lambda,b}(\lambda, T) d\lambda = \int_0^\infty \frac{C_1 \lambda^{-5}}{\exp(C_2 / \lambda T) - 1} d\lambda \equiv \sigma T^4$$

where the Stefan-Boltzmann constant $\sigma = f(C_1, C_2)$. Similarly, from Equation IVd.1.4 we conclude $I_b = E_b/\pi$. We may plot the Planck’s distribution (Equation IVd.2.3) by choosing a temperature and finding $E_{\lambda,b}$ for various values of λ . This is shown in Figure IVd.2.1(b). An interesting feature of these plots is that for a fixed temperature, the emitted radiation is a continuous function of wavelength. The magnitude of the spectral emissive power of a blackbody increases with the increasing wavelength until reaching a peak value after which, the magnitude decreases with increasing wavelength. Another interesting feature is the fact that as the surface temperature increases, the peak spectral emissive power shifts towards shorter wavelengths.

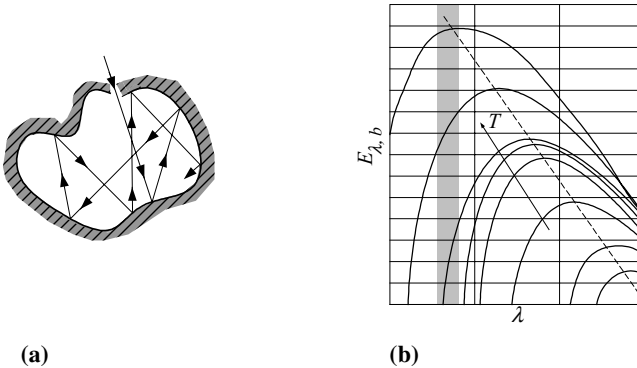


Figure IVd.2.1. (a) An isothermal blackbody cavity as an ideal absorber. (b) Planck’s distribution

The shaded area in Figure IVd.2.1(b) is the visible spectral region. To find the equation representing the locus of the peak emissive power, we should differentiate Equation IV.2.3 with respect to λ and set the result equal to zero. By doing so we find

$$\lambda_{\max} T = 2897.6 \mu\text{m}\cdot\text{K}$$

This is known as the Wien's displacement law who derived this equation in 1894.

Example IVd.2.1. The emissive power of a blackbody, at $1 \mu\text{m}$ wavelength is measured as $1000 \text{ W/m}^2\cdot\mu\text{m}$. Find the blackbody temperature.

Solution: We solve Equation IVd.2.3 for temperature to obtain

$T = C_2 / \lambda \ln[1 + C_1 \lambda^{-5} / E_{\lambda,b}]$. Substituting, we find

$$T = 1.439\text{E}4 \mu\text{m}\cdot\text{K} / \{1 \mu\text{m} \times \ln[1 + 3.742\text{E}8 \text{ W/m}^2\cdot\mu\text{m}^4 \times (1 \mu\text{m})^{-5} / 1000 \text{ W/m}^2\cdot\mu\text{m}]\} \\ = 1040 \text{ K}$$

Example IVd.2.2. The temperature of a blackbody surface is maintained at 3000 K . Find the wavelength associated with the emissive power.

Solution: We use the Wien's displacement law; $\lambda_{\max} = 2897.6/T = 2897.6/3000 = 0.966 \mu\text{m}$.

Example IVd.2.3. A metal rod having a length of 1 m and a diameter of 2 cm is maintained at 150 C (423 K). Fluid flows around the rod at an average temperature and heat transfer coefficient of 50 C (323 K) and $100 \text{ W/m}^2\cdot\text{K}$. If the rod surface can be approximated as a blackbody, find the percentage of heat transfer by radiation.

Solution: The amount of heat transfer by forced convection is calculated as:

$$\dot{Q}_C = (\pi L d) h (T_s - T_f) = (\pi \times 0.02 \times 1) \times 100 \times (423 - 323) = 628 \text{ W}$$

The net rate of heat transfer by radiation from a blackbody is given by:

$$\dot{Q}_R = \sigma A (T_s^4 - T_f^4) = (\pi \times 0.02 \times 1) \times (5.67\text{E}-8) \times (423^4 - 323^4) = 75 \text{ W}.$$

The contribution of radiation heat transfer to total rate of heat transfer is about $75/(75 + 628) = 10\%$.

Contribution of thermal radiation becomes more noticeable as the surface temperature rises.

Band emission. If we want to know the emissive power in a specific range of wavelength, say between λ_1 to λ_2 , we simply integrate the Planck distribution in this range:

$$(\Delta E_b)_{\lambda_1 \rightarrow \lambda_2} = \int_{\lambda_1}^{\lambda_2} \frac{C_1 \lambda^{-5}}{\exp(C_2 / \lambda T) - 1} d\lambda \quad \text{IVd.2.4}$$

Often, we are interested in the fraction of the emissive power. For example, if we want to find the fraction of emission in the range of λ_1 to λ_2 , as shown in Figure IVd.2.2, we integrate Equation IVd.2.3 in this range and divide over the entire emission, i.e. from zero to infinity.

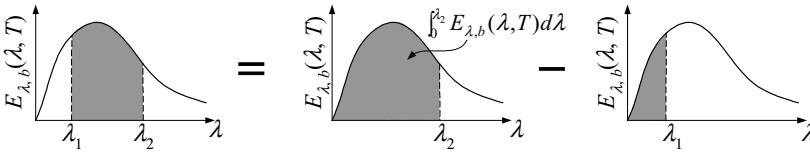


Figure IVd.2.2. Depiction of band emission calculation

If we show the fraction of emission between λ_1 to λ_2 with $F(\lambda_1 \rightarrow \lambda_2)$, then

$$F(\lambda_1 \rightarrow \lambda_2) = \frac{\int_{\lambda_1}^{\lambda_2} E_{\lambda,b} d\lambda}{\int_0^{\infty} E_{\lambda,b} d\lambda} = \frac{\int_0^{\lambda_2} E_{\lambda,b} d\lambda - \int_0^{\lambda_1} E_{\lambda,b} d\lambda}{\sigma T^4} = \frac{\int_0^{\lambda_2} E_{\lambda,b} d\lambda}{\sigma T^4} - \frac{\int_0^{\lambda_1} E_{\lambda,b} d\lambda}{\sigma T^4} = F(0 \rightarrow \lambda_2) - F(0 \rightarrow \lambda_1)$$

The integrals of Equation IVd.2.4 are developed between zero to various wavelengths and summarized in Table IVd.2.1. The integral representing $F(0 \rightarrow \lambda)$, does not have an analytical solution in closed form. However, it may be evaluated by the following series (Dunkle) in which $\zeta = C_2/\lambda T$:

$$F(0 \rightarrow \lambda) = (15/\pi^4) \sum_{i=1}^6 i^{-4} e^{-i\zeta} [(i\zeta)^3 + 3(i\zeta)^2 + 6(i\zeta) + 6]$$

Additional blackbody radiation functions are also summarized in Table IVd.2.1.

Example IVd.2.4. A blackbody is at 5489 C. Find a) the percentage of energy emitted in the shorter than visible range, b) the percentage of energy emitted in the longer than the visible range, c) the percentage of energy emitted in the visible range, and d) the rate of energy emitted in the visible range.

Solution: To find the fractions, we need the arguments, $\lambda_1 T$ and $\lambda_2 T$. These are calculated as:

$\lambda_1 T = 0.4 \times (5489 + 273) = 2304.8 \mu\text{m}\cdot\text{K}$, from the table we find the fraction for $F(0 \rightarrow \lambda_1) = 0.12057$

$\lambda_2 T = 0.7 \times (5489 + 273) = 4033.4 \mu\text{m}\cdot\text{K}$ from the table we find the fraction for $F(0 \rightarrow \lambda_2) = 0.48675$

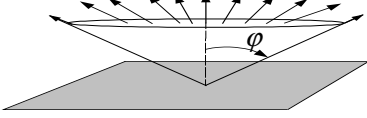
- Percentage of energy emitted in the shorter than the visible range is about 12%
- Percentage of energy emitted in the longer than the visible range is about $(1 - 0.48675) \equiv 51\%$
- Percentage of energy emitted in the visible range $= 0.48675 - 0.12057 \equiv 37\%$
- The rate of energy is: $(\Delta E_b)_{\lambda_1 \rightarrow \lambda_2} = (0.48675 - 0.12057) \times [5.67\text{E-}8 \times (5489 + 273)^4] = 22.88 \text{ MW/m}^2$

The blackbody represents our sun, which emits energy in the infrared, visible and ultraviolet as shown above.

Table IVd.2.1. Balckbody radiation functions (Incropera)

λT ($\mu\text{m}\cdot\text{K}$)	$F(0 \rightarrow \lambda)$	$I_{\lambda,b}(\lambda, T)/\sigma T^5$ ($\mu\text{m}\cdot\text{K}\cdot\text{Sr}$) ⁻¹	$\frac{I_{\lambda,b}(\lambda, T)}{I_{\lambda,b}(\lambda_{\text{max}}, T)}$	λT ($\mu\text{m}\cdot\text{K}$)	$F(0 \rightarrow \lambda)$	$I_{\lambda,b}(\lambda, T)/\sigma T^5$ ($\mu\text{m}\cdot\text{K}\cdot\text{Sr}$) ⁻¹	$\frac{I_{\lambda,b}(\lambda, T)}{I_{\lambda,b}(\lambda_{\text{max}}, T)}$
200	0	3.75E-28	0	6,200	0.75414	0.249E-04	0.345724
400	0	4.90E-14	0	6,400	0.769234	0.231E-04	0.319783
600	0	1.04E-09	0.000014	6,600	0.783199	0.214E-04	0.295973
800	0.000016	9.91E-08	0.001372	6,800	0.796129	0.198E-04	0.274128
1,000	0.000321	1.19E-06	0.016406	7,000	0.808109	0.183E-04	0.254090
1,200	0.002134	5.24E-06	0.072534	7,200	0.819217	0.170E-04	0.235708
1,400	0.007790	1.34E-05	0.186082	7,400	0.829527	0.158E-04	0.218842
1,600	0.019718	2.49E-05	0.344904	7,600	0.839102	0.147E-04	0.203360
1,800	0.039341	0.375E-04	0.519949	7,800	0.848005	0.136E-04	0.189143
2,000	0.066728	0.493E-04	0.683123	8,000	0.856288	0.127E-04	0.176079
2,200	0.100888	0.589E-04	0.816329	8,500	0.874608	0.107E-04	0.147819
2,400	0.140256	0.658E-04	0.912155	9,000	0.890029	0.901E-05	0.124801
2,600	0.183120	0.701E-04	0.970891	9,500	0.903085	0.765E-05	0.105956
2,800	0.227897	0.720E-04	0.997123	10,000	0.914199	0.653E-05	0.090442
2,898	0.250108	0.722E-04	1.000000	10,500	0.923710	0.560E-05	0.077600
3,000	0.273232	0.720E-04	0.997143	11,000	0.931890	0.483E-05	0.066913
3,200	0.318102	0.706E-04	0.977373	11,500	0.939959	0.418E-05	0.057970
3,400	0.361735	0.682E-04	0.943551	12,000	0.945098	0.364E-05	0.050448
3,600	0.403607	0.650E-04	0.900429	13,000	0.955139	0.279E-05	0.038689
3,800	0.443382	0.615E-04	0.851737	14,000	0.962898	0.217E-05	0.030131
4,000	0.480877	0.578E-04	0.800291	15,000	0.969981	0.172E-05	0.023794
4,200	0.516014	5.404E-04	0.748139	16,000	0.973814	0.137E-05	0.019026
4,400	0.548796	0.503E-04	0.696720	18,000	0.980860	0.908E-06	0.012574
4,600	0.579280	0.467E-04	0.647004	20,000	0.985602	0.623E-06	0.008629
4,800	0.607559	0.433E-04	0.599610	25,000	0.992215	0.276E-06	0.003828
5,000	0.633747	0.400E-04	0.554898	30,000	0.995340	0.140E-06	0.001945
5,200	0.658970	0.371E-04	0.513043	40,000	0.997967	0.474E-07	0.000656
5,400	0.680360	0.342E-04	0.474092	50,000	0.998953	0.201E-07	0.000279
5,600	0.701046	0.316E-04	0.438002	75,000	0.999713	0.419E-08	0.000058
5,800	0.720158	0.292E-04	0.404671	100,000	0.999905	0.136E-08	0.000019
6,000	0.737818	0.270E-04	0.373965				

Example IVd.2.5. A blackbody is at 2000 K. Find the rate of radiant energy emission in the cone shown in the figure for $\varphi = 45^\circ$ ($\varphi = \pi/4$ radian) at wavelength 1 to 5 μm .



Solution: The rate of radiant energy emission is given by Equation IVd.1.2. If integrated in the limits given:

$$E = \int_{\lambda_1}^{\lambda_2} E_{\lambda} d\lambda = \int_{\lambda_1}^{\lambda_2} \left[\int_0^{2\pi} \left(\int_0^{\pi/4} I_{\lambda,e} \cos \varphi \sin \varphi d\varphi \right) d\theta \right] d\lambda = \int_{\lambda_1}^{\lambda_2} I_{\lambda,e} \left[\int_0^{2\pi} \left(\int_0^{\pi/4} \cos \varphi \sin \varphi d\varphi \right) d\theta \right] d\lambda$$

where $I_{\lambda,e}$ is treated as a constant since a blackbody intensity is only a function of wavelength. Note that:

$$\int_{\alpha}^{\beta} \cos \varphi \sin \varphi d\varphi = (1/4) \int_{\alpha}^{\beta} \sin(2\varphi) d(2\varphi) = (1/4) [-\cos(2\varphi)]_{\alpha}^{\beta} = 0.25(\cos 2\alpha - \cos 2\beta)$$

$$E = 0.25 \int_{\lambda_1}^{\lambda_2} I_{\lambda,e} \left\{ \int_0^{2\pi} [\cos 0 - \cos(\pi/2)] d\theta \right\} d\lambda = 0.25 \int_{\lambda_1}^{\lambda_2} I_{\lambda,e} [2\pi] d\lambda = 0.5 \int_{\lambda_1}^{\lambda_2} \pi I_{\lambda,e} d\lambda$$

$$E = 0.5 \int_{\lambda_1}^{\lambda_2} \pi I_{\lambda,e} d\lambda = 0.5 \int_{\lambda_1}^{\lambda_2} E_{b,\lambda} d\lambda = 0.25 E_b \int_{\lambda_1}^{\lambda_2} E_{b,\lambda} / E_b d\lambda = 0.25 E_b [F(0 \rightarrow 5) - F(0 \rightarrow 1)]$$

To find the fractions, we need the arguments $\lambda_1 T$ and $\lambda_2 T$. These arguments are calculated as:

$\lambda_1 T = 1 \times 2000 = 2000 \mu\text{m}\cdot\text{K}$, from Table IVd.2.1 we find the fraction as $F(0 \rightarrow \lambda_1) = 0.0667$

$\lambda_2 T = 5 \times 2000 = 10000 \mu\text{m}\cdot\text{K}$ from Table IVd.2.1 we find the fraction as $F(0 \rightarrow \lambda_2) = 0.9142$. The fraction is $0.9142 - 0.0667 = 0.8475$

$$E = 0.25 \times 5.67\text{E-}8 \times 2000 = 0.227\text{E}6 \text{ W/m}^2.$$

3. Real Surfaces

Although the introduction of blackbody greatly simplified analysis, blackbody remains a mere concept. Real surfaces must be treated differently. For example, real surfaces in general are not diffuse emitters and their spectral emission does not fully conform to the Planck distribution. In this section, we discuss the emission of radiant energy from real surfaces in the context of a new surface property known as emissivity. We also discuss real surface response to irradiation. The irradiation will be discussed in the context of three additional surface properties known as reflectivity, absorptivity, and transmissivity.

3.1. Characteristics of Real Surfaces, Emissivity

For real surfaces we then define *spectral directional emissivity*, which implies that the emissivity from a real surface depends both on direction and on the wavelength. The spectral directional emissivity, $\varepsilon_{\lambda,\phi}(\lambda, \theta, \phi, T)$ is defined as the ratio of the radiation intensity emitted from a real surface having temperature T , at wavelength λ in the direction θ and ϕ , to the radiation intensity of a blackbody at temperature T and wavelength λ :

$$\varepsilon_{\lambda,\phi}(\lambda, \theta, \phi, T) = \frac{I_{\lambda,e}(\lambda, \theta, \phi, T)}{I_{\lambda,b}(\lambda, T)} \quad \text{IVd.3.1}$$

Expectedly, for real surfaces emissivity is always less than unity. Since a blackbody is a diffuse emitter, no directional dependency appears in the denominator of Equation IVd.3.1. To facilitate analysis, we eliminate directional dependence from the numerator by finding an average value for $\varepsilon_{\lambda,\phi}$ over all directions:

$$\varepsilon_{\lambda}(\lambda, T) = \frac{\int_0^{2\pi} \left[\int_0^{\pi/2} I_{\lambda,e}(\lambda, \theta, \phi, T) \sin \phi \cos \phi d\phi \right] d\theta}{\int_0^{2\pi} \left[\int_0^{\pi/2} I_{\lambda,b}(\lambda, T) \sin \phi \cos \phi d\phi \right] d\theta} = \frac{\int_0^{2\pi} \left[\int_0^{\pi/2} \varepsilon_{\lambda,e}(\lambda, \theta, \phi, T) \sin \phi \cos \phi d\phi \right] d\theta}{\int_0^{2\pi} \left[\int_0^{\pi/2} \sin \phi \cos \phi d\phi \right] d\theta}$$

where we replaced the intensity, $I_{\lambda,e}(\lambda, \theta, \phi, T)$ in the numerator from Equation IVd.3.1 by substituting for $I_{\lambda,e}(\lambda, \theta, \phi, T) = \varepsilon_{\lambda,\phi}(\lambda, \theta, \phi, T) I_{\lambda,b}(\lambda, T)$ and by canceling $I_{\lambda,b}(\lambda, T)$ from both numerator and denominator. For most surfaces, $\varepsilon_{\lambda,\phi}(\lambda, \theta, \phi, T)$ is not a strong function of θ . Hence, we can reasonably assume that $\varepsilon_{\lambda,\phi}(\lambda, \theta, \phi, T) \cong \varepsilon_{\lambda,\phi}(\lambda, \phi, T)$. Making this assumption and carrying out the integral we get:

$$\varepsilon_{\lambda}(\lambda, T) = 2 \int_0^{\pi/2} \varepsilon_{\lambda,e}(\lambda, \phi, T) \sin \phi \cos \phi d\phi \quad \text{IVd.3.2}$$

We may also define a spectral hemispheric emission as:

$$\varepsilon_{\lambda}(\lambda, T) = \frac{E_{\lambda}(\lambda, T)}{E_{\lambda,b}(\lambda, T)} \quad \text{IVd.3.3}$$

using this definition, we may find the total hemispherical emissive power, $\varepsilon(T)$ by using Equations IVd.1.3 :

$$\varepsilon(T) = \frac{E(T)}{E_b(T)} = \frac{\int_0^{\infty} \varepsilon_{\lambda}(\lambda, T) E_{\lambda,b}(\lambda, T) d\lambda}{E_b(T)} \quad \text{IVd.3.4}$$

Emissivity in general varies not only with temperature but also with such surface conditions as roughness, texture, color, degree of oxidation, and any coating. The above successive definitions allowed us to express emissivity only in terms of temperature. Emissivity for various materials and surface coatings are obtained

experimentally as shown in Tables A.IV.8 and A.IV.9 for metallic and nonmetallic surface, respectively.

Example IVd.3.1. The spectral emissivity of a substance is given as 0.1 for $0 \leq \lambda \leq 3 \mu\text{m}$ and 0.9 for $\lambda \geq 3 \mu\text{m}$. Find the total hemispherical emissivity at 2000 K.

Solution: Substituting numerical values for wavelengths and the corresponding emissivities, in Equation IVd.3.4, we find:

$$\varepsilon = \frac{0.1 \int_0^3 E_{\lambda,b}(\lambda, T) d\lambda + 0.9 \int_3^\infty E_{\lambda,b}(\lambda, T) d\lambda}{\sigma T^4}$$

By separating terms, we obtain the band emission:

$$\varepsilon = \frac{0.1 \int_0^3 E_{\lambda,b}(\lambda, T) d\lambda + 0.9 \int_3^\infty E_{\lambda,b}(\lambda, T) d\lambda}{\sigma T^4} = 0.1F(0 \rightarrow 3) + 0.9[1 - F(0 \rightarrow 3)] = 0.9 - 0.8F(0 \rightarrow 3)$$

For $\lambda T = 3 \times 2000 = 6000$ gives $F(0 \rightarrow 3) = 0.7378$

Therefore, $\varepsilon = 0.9 - 0.8 \times 0.7378 = 0.31$

3.2. Characteristics of Real Surfaces, Absorptivity, Reflectivity, Transmissivity

Earlier, we defined emissivity with respect to radiant energy emitted by a surface. Let's now consider radiant energy being intercepted by a surface. Such surface may constitute a medium. Semitransparent medium is a generic term for substances such as water and glass. In general, some of the incident radiation may be reflected (shown with subscript r), some may be absorbed (shown with subscript a) in the medium, and some transmitted (shown with subscript t) away from the medium. If the substance is opaque, then the incident energy is either reflected or absorbed (Figure IVd.3.1). The absorbed portion increases the internal energy of the medium. The reflected energy in the visible spectrum would constitute the color of a substance. The absorption and reflection of radiant energy occur in a very thin layer of the surface. From a radiation balance we find:

$$G_{\lambda,r} + G_{\lambda,a} + G_{\lambda,t} = G_\lambda$$

Dividing through by G_λ , we find:

$$\rho + \alpha + \tau = 1 \quad \text{IVd.3.6}$$

where ρ , α , and τ are the *reflectivity*, *absorptivity*, and *transmissivity*. In Equation IVd.3.6, average values are used for these parameters. In general however, ρ , α , and τ are functions of wavelength and direction.

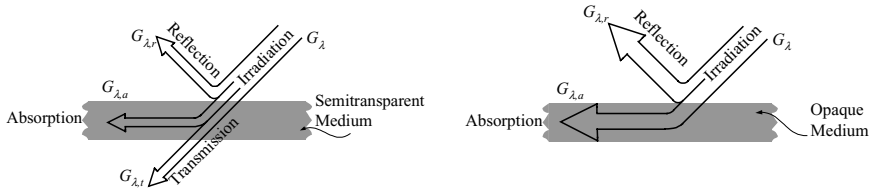


Figure IVd.3.1. Comparison of semitransparent and opaque surfaces

Absorptivity, $\alpha_{\lambda, \phi}(\lambda, \theta, \phi)$ determines the fraction of the incident energy absorbed by the surface:

$$\alpha_{\lambda, \phi}(\lambda, \theta, \phi) = \frac{I_{\lambda, i, a}(\lambda, \theta, \phi)}{I_{\lambda, i}(\lambda, \theta, \phi)} \quad \text{IVd.3.7}$$

To find the average surface absorptivity we substitute from Equation IVd.1.5 and integrate Equation IVd.3.7:

$$\alpha = \frac{G_a}{G} = \frac{\int_0^\infty \left\{ \int_0^{2\pi} \left[\int_0^{\pi/2} \alpha_{\lambda, \phi}(\lambda, \theta, \phi) I_{\lambda, i, a}(\lambda, \theta, \phi) \sin \phi \cos \phi d\phi \right] d\theta \right\} d\lambda}{\int_0^\infty \left\{ \int_0^{2\pi} \left[\int_0^{\pi/2} I_{\lambda, i}(\lambda, \theta, \phi) \sin \phi \cos \phi d\phi \right] d\theta \right\} d\lambda} \quad \text{IVd.3.8}$$

where α in Equation IVd.3.8 is known as the *total hemispherical absorptivity*.

Reflectivity, $\rho_{\lambda, \phi}(\lambda, \theta, \phi)$ determines the fraction of the incident energy reflected by the surface:

$$\rho_{\lambda, \phi}(\lambda, \theta, \phi) = \frac{I_{\lambda, i, r}(\lambda, \theta, \phi)}{I_{\lambda, i}(\lambda, \theta, \phi)} \quad \text{IVd.3.9}$$

To find the average surface reflectivity we substitute from Equation IVd.1.5 and integrate Equation IVd.3.9:

$$\rho = \frac{G_r}{G} = \frac{\int_0^\infty \left\{ \int_0^{2\pi} \left[\int_0^{\pi/2} \rho(\lambda, \theta, \phi) I_{\lambda, i, r}(\lambda, \theta, \phi) \sin \phi \cos \phi d\phi \right] d\theta \right\} d\lambda}{\int_0^\infty \left\{ \int_0^{2\pi} \left[\int_0^{\pi/2} I_{\lambda, i}(\lambda, \theta, \phi) \sin \phi \cos \phi d\phi \right] d\theta \right\} d\lambda}$$

where ρ in Equation IVd.3.10 is known as the *total hemispherical reflectivity*. Shown in Figure IVd.3.2. are two types of surface reflection. While polished surfaces are specular, most surfaces are diffuse reflectors.

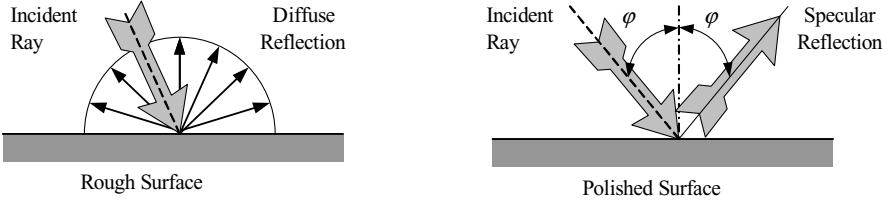
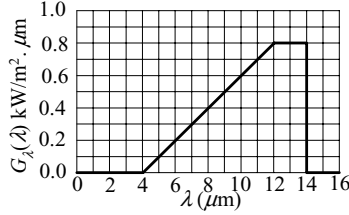
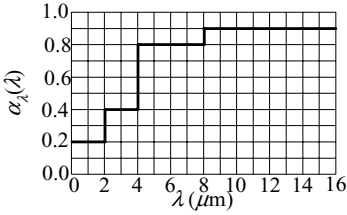


Figure IVd.3.2. Incident radiation on rough and polished surfaces

Transmissivity, $\tau_{\lambda, \phi}(\lambda, \theta, \phi)$ is the fraction of the incident energy transmitted. If averaged, $\tau = G_{\lambda, t}/G$.

Example IVd.3.2. An opaque surface is exposed to radiation. Use the spectral hemispherical absorptivity and irradiation profiles given below to find α .



Solution: To find total absorptivity, we carryout the integrals in Equation IVd.3.8. The numerator becomes:

$$\int_0^{\infty} \left\{ \int_0^{2\pi} \left[\int_0^{\pi/2} \alpha_{\lambda, \phi}(\lambda, \theta, \phi) I_{\lambda, i, a}(\lambda, \theta, \phi) \sin \phi \cos \phi d\phi \right] d\theta \right\} d\lambda =$$

$$\int_0^{\infty} \{ \alpha_{\lambda}(\lambda) I_{\lambda, i, a}(\lambda) [2\pi(1/2)] \} d\lambda$$

and denominator:

$$\int_0^{\infty} \left\{ \int_0^{2\pi} \left[\int_0^{\pi/2} I_{\lambda, i}(\lambda, \theta, \phi) \sin \phi \cos \phi d\phi \right] d\theta \right\} d\lambda = \int_0^{\infty} \{ I_{\lambda, i, a}(\lambda) [2\pi(1/2)] \} d\lambda$$

Using the definition of absorptivity, Equation IVd.3.8:

$$\alpha = \frac{\int_0^{\infty} \alpha_{\lambda}(\lambda) G_{\lambda}(\lambda) d\lambda}{\int_0^{\infty} G_{\lambda}(\lambda) d\lambda}$$

To carryout the numerator and denominator integrals we need to express α and G as functions of λ :

For $0 \mu\text{m} < \lambda < 2 \mu\text{m}$:

$$\alpha = 0.2$$

$$G_{\lambda} = 0 \text{ kW/m}^2 \cdot \mu\text{m}$$

For $2 \mu\text{m} < \lambda < 4 \mu\text{m}$:

$$\alpha = 0.4$$

$$G_{\lambda} = 0 \text{ kW/m}^2 \cdot \mu\text{m}$$

For $4\ \mu\text{m} < \lambda < 12\ \mu\text{m}$:

$$\alpha = 0.9$$

$$G_\lambda = (\lambda - 4)/10\ \text{kW/m}^2 \cdot \mu\text{m}$$

For $12\ \mu\text{m} < \lambda$:

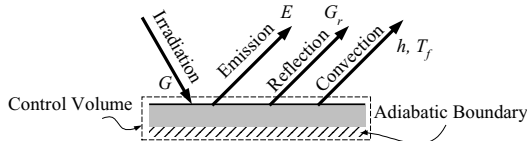
$$\alpha = 0.9$$

$$G_\lambda = 0.8\ \text{kW/m}^2 \cdot \mu\text{m}$$

We now substitute for G_λ to be able to integrate

$$\alpha = \left[\int_0^4 0.9(\lambda - 4)d\lambda + \int_4^{12} 0.9 \times 8d\lambda + \int_{12}^\infty 0.9 \times 8d\lambda \right] / \left[\int_0^4 (\lambda - 4)d\lambda + \int_4^{12} 8d\lambda + \int_{12}^\infty 8d\lambda \right] = 0.9$$

Example IVd.3.3. The surface temperature and total hemispherical emissivity in Example IVd.3.2 are 327 C and 0.85, respectively. Find the surface temperature after exposure.



Solution: We find the surface temperature from an energy balance for the control volume shown in the figure. In steady state, the net energy gain (loss) from the surface is equal to the rate of energy received by the surface from irradiation (G) minus the rate of energy removed from the surface by reflection, surface emission, heat convection, and heat condition in the surface. If the back surface is insulated and the whole surface can be assumed to have one temperature then there is no conduction heat transfer:

$$\dot{q}'' = G - (G_r + E + \dot{q}_C'')$$

If we ignore the heat loss due to convection and substitute for $G_r = \rho G = (1 - \alpha)G$ and for $E = \epsilon E_b$ we get the net heat gain (loss) as $\dot{q}'' = \alpha G - \epsilon E_b$.

Substituting for G , calculated in Example IVd.3.2 as $G = \int_0^\infty G_\lambda(\lambda)d\lambda = 7800\ \text{W/m}^2$, we find:

$$\dot{q}'' = \alpha G - \epsilon(\sigma T^4) = 0.728 \times 7800 - 0.85 \times [5.67\text{E-}8 \times (327 + 273)^4] = -568\ \text{W/m}^2.$$

4. Gray Surfaces

So far we defined four surface properties: emissivity, absorptivity, reflectivity, and transmissivity. If we obtain one more relation, we can then find any two properties if the other two properties are given. The additional relation is between emissivity and reflectivity. Kirchhoff in 1860 demonstrated that if a surface is encompassed by a blackbody at temperature T_s , Figure IVd.4.1(a), at thermal equilibrium (steady state), the energy received by the surface ($GA_1\alpha_1$ where α_1 is the surface absorptivity and A_1 is the surface area) must be equal to the energy emitted by the

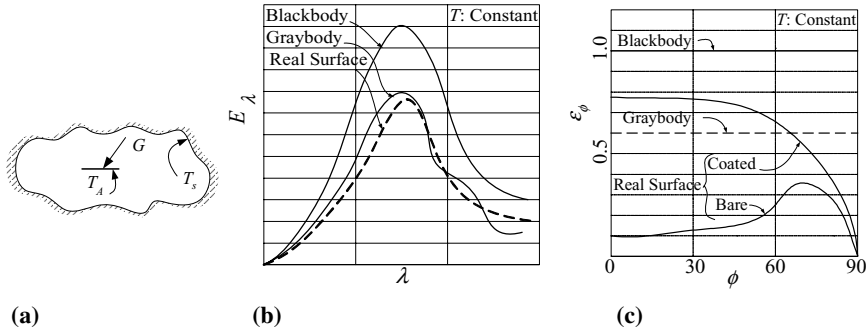


Figure IVd.4.1. (a) Emission, (b) total directional emissivity of ideal, gray, and real surfaces, and (c) emissivity for various surfaces

surface (E_1A_1), $GA_1\alpha_1 = E_1A_1$. Resulting in $E_1/\alpha_1 = G$. If we now replace surface 1 with surface 2 and let the steady state condition to prevail, we again can write $GA_2\alpha_2 = E_2A_2$ or $E_2/\alpha_2 = G$. We may repeat this experiment for many surfaces. If we finally place a blackbody in the enclosure and let it also comes to thermal equilibrium with the enclosure, we may write $E_b/1 = G$. As a result:

$$E_1/\alpha_1 = E_2/\alpha_2 = \dots = E_b$$

Using Equation IVd.3.3, we conclude that $\epsilon_{\lambda,\phi}(T_s) = \alpha_{\lambda,\phi}(T_s)$. In general, we want to know the circumstance under which we can have $\epsilon_\lambda = \alpha_\lambda$. It turns out that such condition exists if either surface or irradiation is diffuse. Condition $\epsilon = \alpha$ exists, if the irradiation corresponds to emission from a blackbody or if the surface is gray. That is to say that a gray surface is an idealized material, having constant emissivity independent of wavelength. A *diffuse gray surface* is a surface that has emissivity, $\epsilon_{\lambda,\phi}$ and absorptivity $\alpha_{\lambda,\phi}$ independent of direction (due to diffuse assumption) and wavelength (due to the gray surface assumption). A comparison is made between a blackbody, a gray surface and a real surface in Figure IVd.4.1(b). Figure IVd.4.1(c) shows the emissivity for the these surfaces.

5. Radiation Exchange Between Surfaces

So far we dealt with single surfaces emitting radiation and being irradiated. We also considered surfaces being contained in an enclosure. In general however, surfaces exchange radiation with other surfaces with arbitrary geometry and orientation. This complicates the calculation of the total heat transfer, as we should consider the surface geometry and orientation. To properly account for the amount of energy exchanged between surfaces, we introduce a parameter known as shape or view factor, $F < 1$. In this section we discuss means of calculating the view factor. We also introduce the concept of radiation exchange between surfaces by a network, which is series – parallel arrangement of the involved surfaces.

5.1. The View Factor

Consider two differential surfaces A_i and A_j oriented arbitrarily and exchanging radiation, as shown in Figure IVd.5.1. The view factor F_{ij} is defined as the ratio of the radiant energy leaving surface dA_i and reaching surface dA_j to the total radiant energy leaving surface dA_i . If the distance between these elemental surfaces is R and the angle between R and \vec{n}_j is ϕ_j , then the projected area of dA_i , normal to R is $dA_i \cos \phi_i$.

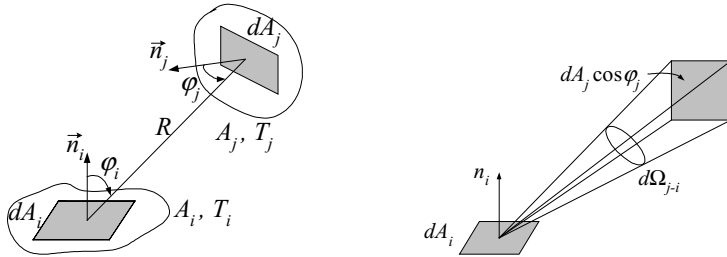


Figure IVd.5.1. Exchange of radiation for derivation of the view factor

The amount of radiant energy leaving differential area dA_i per unit time and unit area is the intensity of radiation, I_i of surface dA_i . Hence, the total radiant energy leaving the elemental area dA_i per unit time is $I_i dA_i$. The fraction of this energy radiated in the direction of dA_j is given by $(I_i dA_i) \cos \phi_i$. The amount of energy leaving dA_i in the direction of dA_j and received by dA_j is given by $(I_i dA_i) \cos \phi_i d\Omega_{j-i}$ where $d\Omega_{j-i}$ is the solid angle subtended by dA_j when viewed from dA_i . Since $d\Omega_{j-i} = (dA_j \cos \phi_j) / R^2$ then the fraction of energy leaving dA_i and reaching dA_j per unit time is obtained from $(I_i dA_i) \cos \phi_i (dA_j \cos \phi_j) / R^2$. This argument is summarized as follows:

Rate of energy leaving dA_i per s, per cm^2 , and per sr:	I_i
Rate of energy leaving the elemental area dA_i per s and per sr:	$I_i dA_i$
Rate of energy radiated in the direction of dA_j per s and per sr:	$(I_i dA_i) \cos \phi_i$
Rate of energy leaving dA_i and received by dA_j per s:	$(I_i dA_i) \cos \phi_i d\Omega_{j-i}$
Rate of energy leaving dA_i and received by dA_j per s:	$(I_i dA_i) \cos \phi_i (dA_j \cos \phi_j) / R^2$
Rate of energy leaving dA_i and received by dA_j per s:	$(J_i dA_i) \cos \phi_i (dA_j \cos \phi_j) / \pi R^2$

where in the last expression we have assumed that the surface emits and reflects diffusely and substituted for $I_{e+r} = J/\pi$, from the definition of total radiosity. This now represents hemispheric emission. Hence, the total rate of radiant energy leaving surface i and intercepted by surface j is:

$$\dot{Q}_{ij} = J_i \int_{A_i} \int_{A_j} [\cos \phi_i \cos \phi_j / \pi R^2] dA_i dA_j \quad \text{IVd.5.1}$$

Expressing $\dot{Q}_{ij} = F_{ij} A_i J_i$, by comparing to Equation IVd.5.1, we conclude that:

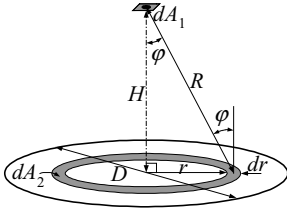
$$F_{ij}A_i = \int_{A_i} \int_{A_j} [\cos \varphi_i \cos \varphi_j / \pi R^2] dA_i dA_j \quad \text{IVd.5.2}$$

Similar arguments can be made for the radiant energy emitted from surface A_j and intercepted by surface A_i . Since the net energy exchange between these surfaces is the same we conclude that $F_{ij}A_i = F_{ji}A_j$. This is known as the *reciprocity relation*. Note that in this derivation we assumed that the surrounding is not participating in the radiation exchange. Having the view factors, the net rate of heat transfer by radiation is:

$$\dot{Q}_{ij} = \frac{J_i - J_j}{1/A_i F_{ij}} \quad \text{IVd.5.3}$$

where Equation IVd.5.3 is written similar to Equation IV3.6 for the reasons discussed in Section 5.4.

Example IVd.5.1. A differential area dA_1 is located parallel to and on the center-line of a finite disk of diameter D (radius of $c = D/2$). Find the view factor for this arrangement.



Solution: Since surface dA_1 is a differential surface, we choose the shaded area at an arbitrary $0 < r < c$ as the elemental area of surface A_2 . Clearly, if $dA_2 = 2\pi r dr$ is integrated in the above range, we would obtain $A_2 = \pi D^2/4$. In this problem, $\cos \varphi_1 = \cos \varphi_2 = r/R = H/(r^2 + H^2)^{1/2}$. Substituting values in Equation IVd.5.2:

$$F_{12}dA_1 = \int_{A_i} \int_{A_j} \left[\frac{\cos \varphi_i \cos \varphi_j}{\pi R^2} \right] dA_i dA_j = dA_1 \int_0^c \frac{H^2 / (H^2 + r^2)}{\pi (H^2 + r^2)} (2\pi r dr) = c^2 / (H^2 + c^2) dA_1$$

Hence, $F_{12} = c^2 / (H^2 + c^2)$.

Hamilton and Howell carried out the double integral of Equation IVd.5.2 for variety of surface orientations as shown in Figures IV5.5.2(a) through (d). In Equation IVd.5.2, F_{ij} is known as the *shape, configuration, or view factor*. Table IVd.5.1 includes the equations from which the above plots are obtained. These are also available on the accompanying CD-ROM. The user specifies dimensions and the program finds the F factor.

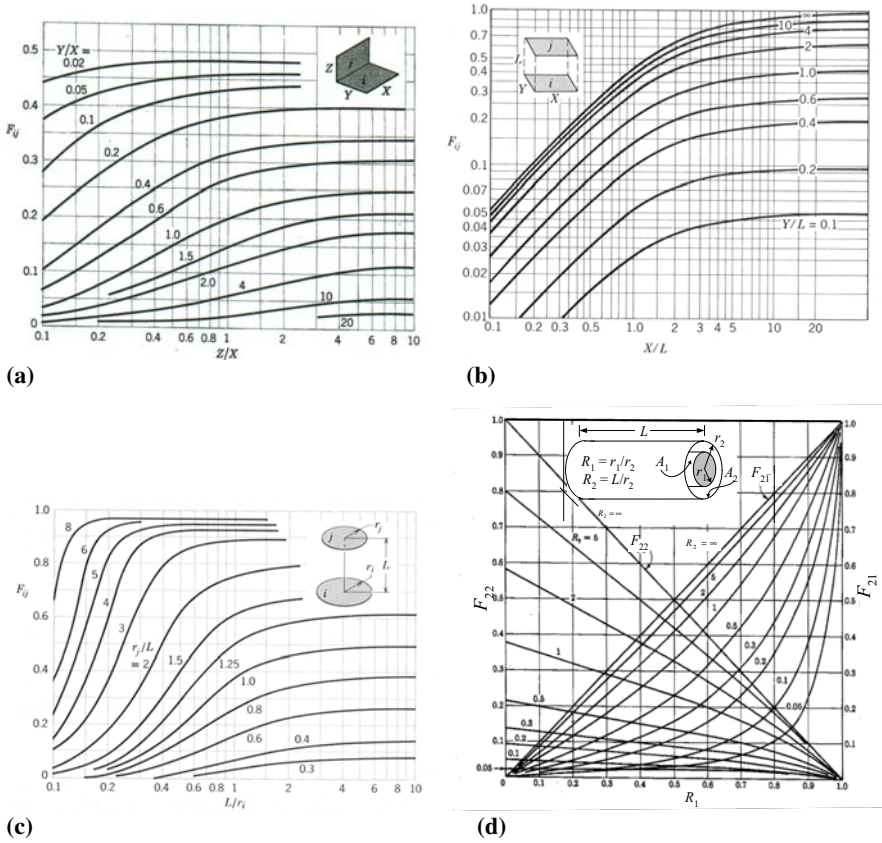
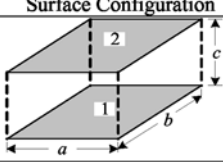
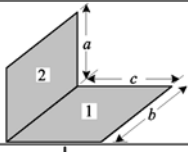
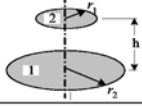
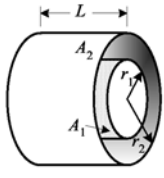


Figure IVd.5.2. Radiation view factor between (a) perpendicular rectangles with a common edge, (b) parallel rectangles, (c) parallel concentric disks, and (d) coaxial cylinders

Example IVd.5.2. Find the view factor for two parallel rectangles with $X = 20$ ft, $Y = 40.0$ ft, and $L = 10$ ft.

Solution: Since $Y/L = 4$ and $X/L = 2$ from Figure IVd.5.2(a) we find $F_{ij} \approx 0.52$.

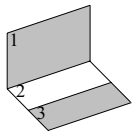
Table IVd.5.1. View factor for flat plates (Rohsenow 73)

Surface Configuration	View Factor
	$F_{12} = 2(Z_1 - Z_2 + Z_3 + Z_4)/(\pi XY)$ where $X = b/c$, $Y = a/c$, $L^2 = 1 + X^2$, $N^2 = 1 + Y^2$, $M^2 = 1 + X^2 + Y^2$, $Z_1 = \ln(LN/M)$, $Z_2 = X \tan^{-1} X + Y \tan^{-1} Y$, $Z_3 = NX \tan^{-1}(X/N)$, $Z_4 = LY \tan^{-1}(Y/L)$
	$F_{12} = (Z_1 + Z_5)/(\pi L)$ where $L = c/b$, $N = a/b$, and $M^2 = N^2 + L^2$, $W_1 = 1 + L^2$, $W_2 = 1 + N^2$, $W_3 = 1 + M^2$, $Z_1 = L \tan^{-1}(1/L) + N \tan^{-1}(1/N) - M \tan^{-1}(1/M)$, $Z_2 = W_1 W_2 / W_3$, $Z_3 = L^2 W_3 / (M^2 W_1)$, $Z_4 = N^2 W_3 / (M^2 W_2)$; $Z_5 = 0.25 \ln(Z_2 Z_3^2 Z_4^2)$
	$R_1 = r_1/h$ and $R_2 = r_2/h$, $F_{12} = 0.5(Z_1 - Z_3^{1/2})$ where $Z_1 = (1 + R_2^2)/R_1^2$, $Z_2 = 1 + Z_1$ and $Z_3 = Z_1^2 - 4(R_2/R_1)^2$
	$F_{12} = (1/X) - (Z_1 + Z_5)/(\pi X)$ where $X = r_2/r_1$, $Y = L/r_1$, $A = Y^2 + X^2 - 1$, $B = Y^2 - X^2 + 1$, $Z_1 = \cos^{-1}(B/A)$, $Z_2 = B \sin^{-1}(1/X) - \pi A/2$, $Z_3 = \cos^{-1}(B/XA)$, $Z_4 = [(A + 2)^2 - 4X^2]^{1/2} Z_3$, $Z_5 = (Z_2 + Z_4)/2Y$ Also $F_{22} = (1 - 1/X) + (2/\pi X) \tan^{-1}(Z_5) - (Y/2\pi X) Z_9$ where $Z_1 = X^2 - 1$, $Z_2 = X^2 - 2$, $Z_3 = 4X^2 + Y^2$, $Z_4 = (Z_3)^{1/2}$, $x = [4Z_1 + (Y^2 Z_2/X^2)]/[Y^2 + 4Z_1]$, $Z_5 = 2(Z_1)^{1/2}/Y$, $Z_6 = [(Z_3)^{1/2}/Y] \sin^{-1}(x)$, $Z_7 = \sin^{-1}(Z_2/X^2)$, $Z_8 = \pi[(Z_3)^{1/2}/Y - 1]/2$, and $Z_9 = Z_6 - Z_7 + Z_8$

5.2. View Factor Relations

Earlier we demonstrated that $F_{ij}A_i = F_{ji}A_j$. The reciprocity relation is useful in obtaining one view factor from the other known view factor. There are other useful relations for the view factor. For example if we use a well insulated cube as an enclosure, the view factor for a given side of this cube adds up to unity. This is because each side of the cube has only five other sides of the cube for the exchange of radiant energy. Hence, the summation of all the fractions of the radiant energy left the side of the cube adds up to unity. In general, for any enclosure we can write $\sum_j F_{ij} = 1$. We can also obtain view factor for non-standard orientations from view factor for standard geometry and orientations.

Example IVd.5.3. Find F_{13} and F_{31} for the arrangement below. All dimensions are known.

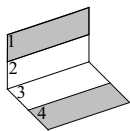


Solution: We reduce the view factor relations to obtain the intended view factor from standard orientations:

$A_1 F_{1,23} = A_1 (F_{12} + F_{13})$. Hence, $F_{13} = F_{1,23} - F_{12}$. To find F_{31} we use the reciprocity relation $A_1 F_{13} = A_3 F_{31}$.

$$F_{31} = A_1 F_{13} / A_3 = A_1 (F_{1,23} - F_{12}) / A_3.$$

Example IVd.5.4. Find F_{14} for the arrangement below. All dimensions are known.



Solution: We reduce the view factor relations to obtain the intended view factor from standard orientations: $A_{12} F_{12,34} = A_1 F_{1,34} + A_2 F_{2,34}$. This can be further expanded to:

$$A_{12} F_{12,34} = A_1 F_{1,34} + A_2 F_{2,34} = A_1 (F_{13} + F_{14}) + A_2 F_{2,34}.$$

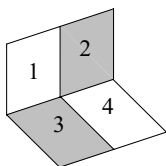
We still need to find F_{13} . From the reciprocity relation we know that

$$A_1 F_{13} = A_3 (F_{3,21} - F_{32}).$$

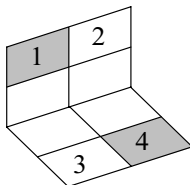
Substituting, we get

$$F_{14} = (A_{12} F_{12,34} + A_3 F_{32} - A_2 F_{2,34} - A_3 F_{3,21}) / A_1.$$

Example IVd.5.5. For the perpendicular rectangles in Figure (a), find F_{14} .



(a)



(b)

Solution: It can be shown that for the more general case of Figure (b):

$$A_1 F_{14} = A_4 F_{41} = A_2 F_{23} = A_3 F_{32}$$

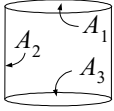
Returning to Figure (a), we note that:

$$A_{12} F_{12,34} = A_1 F_{13} + A_1 F_{14} + A_2 F_{23} + A_2 F_{24}$$

Substituting from the above rule (i.e., $A_1 F_{14} = A_2 F_{23}$), we find:

$$F_{14} = (A_{12} F_{12,34} - A_1 F_{13} - A_2 F_{24}) / 2A_1$$

Example IVd.5.6. Find F_{12} and F_{21} for a right circular cylinder of diameter D and height H .



Solution: Using the summation rule for an enclosure, $F_{11} + F_{12} + F_{13} = 1$.

Since $F_{11} = 0$ and F_{13} is known, we find $F_{12} = 1 - F_{13}$.

Finally, from the reciprocity relation, $F_{21} = A_1 F_{12} / A_2 = A_1 (1 - F_{13}) / A_3$

5.3. Radiation Exchange Between Black Surfaces

Exchange of radiation between blackbodies is straightforward since a blackbody is a perfect emitter and absorber. Consider for example black surface i exchanging radiation with black surface j . The total rate of energy from surface i intercepted by surface j is $A_i F_{ij} J_i$. Similarly, the total rate of energy from surface j intercepted by surface i is $A_j F_{ji} J_j$. Since for black surfaces $J \equiv E_b$, the net rate of radiant energy between blackbodies i and j is given by:

$$\dot{Q}_{ij} = A_i F_{ij} \sigma (T_i^4 - T_j^4) \quad \text{IVd.5.4}$$

Example IVd.5.7. The cylinder in Example IVd.5.6 represents a furnace. Surface A_1 is open to surroundings at 30 C while A_2 and A_3 are maintained at 500 C and 700 C, respectively. Find the power required to maintain furnace at these temperatures. There is no other heat loss from the furnace. $D = 2$ m, $h = 1$ m.

Solution: We treat surfaces A_2 and A_3 as black surfaces and find heat loss due to radiation by assuming A_1 is a fictitious surface. Hence, A_2 and A_3 lose heat to A_1 , which in turn loses heat to surroundings. Total heat loss is

$$\dot{Q} = \dot{Q}_{21} + \dot{Q}_{31} = A_2 F_{21} \sigma (T_2^4 - T_1^4) + A_3 F_{31} \sigma (T_3^4 - T_1^4)$$

$A_1 = A_3 = \pi D^2 / 4 = \pi$. We also find $A_2 = \pi D h = 2\pi$

From Figure IVd.5.2(c) or Table IVd.5.1: $F_{13} = F_{31} = 0.382$

From Example IVd.5.6: $F_{12} = 1 - F_{13} = 0.618$. Also $F_{21} = A_1 F_{12} / A_2 = 0.309$

$$\dot{Q} = (5.67 \times 10^{-8}) \times [2\pi \times 0.309 \times (773^4 - 303^4) + \pi \times 0.382 \times (973^4 - 303^4)] = 99 \text{ kW}$$

5.4. Radiation Exchange Between Gray Surfaces

In the previous section, we noticed that the only complication in the analysis of radiation exchange between black surfaces is the determination of the view factor. Since other surfaces are not perfect emitters and also reflect a fraction of the incident energy, the analysis of radiation exchange becomes more complicated. To simplify the analysis we make the following assumptions:

- all surfaces constitute an enclosure of *nonparticipating* medium
- all surfaces are *diffuse*, *gray*, and *opaque*
- temperature is uniform over the entire surface (i.e., *isothermal*)
- *reflective* and *emissive* properties are *constant* over the entire surface
- radiosity and irradiation are *uniform* over the entire surface
- heat conduction and heat convection mechanisms are absent

Consider the enclosure shown in the left side of Figure IVd.5.3. Details of surface i of this enclosure are shown in the right side of Figure IVd.5.3. The unit area of this surface receives irradiation G and emits radiosity J so that the net rate of energy loss from this surface is found as:

$$\dot{Q} = A(J - G) \quad \text{IVd.5.5}$$

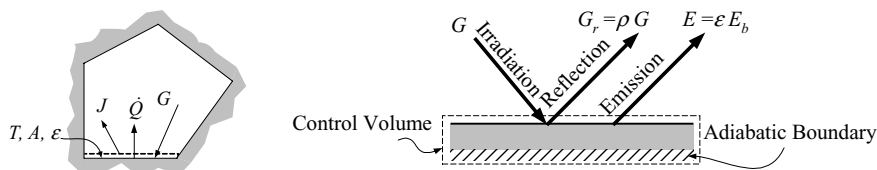


Figure IVd.5.3. Radiation emission in an enclosure

We may eliminate G by using the definition of radiosity, being the summation of emission and reflection:

$$J = \epsilon E_b + \rho G \quad \text{IVd.5.6}$$

To eliminate ρ , we use the assumption that the surfaces are opaque; $\rho = 1 - \alpha$. This can be further simplified by noting that for gray surfaces, $\alpha = \epsilon$. Substituting in Equation IVd.5.6., we get $J = \epsilon E_b + (1 - \epsilon)G$. We now solve this for $G = (J - \epsilon E_b)/(1 - \epsilon)$ and substitute for G in Equation IVd.5.5 and rearrange to get:

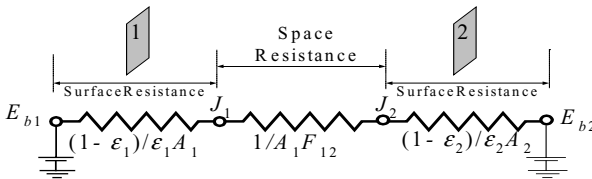
$$\dot{Q} = \frac{E_b - J}{(1 - \epsilon)/(\epsilon A)} \quad \text{IVd.5.7}$$

The advantage of arranging the result in the form of Equation IVd.5.7 is that it lends itself to an electrical engineering analogy, the electric potential represented by $E_b - J$ drives current \dot{Q} through the resistance $(1 - \epsilon)/(\epsilon A)$. This is a very useful approach, first suggested by Oppenheim, which allows problems involving complex radiation exchange to be solved by network representation. Note that Equation IVd.5.7 deals only with one surface. The rate of radiation exchange between two surfaces is given by Equation IVd.5.3. We can then summarize the thermal resistance for radiation heat transfer as the surface and the space resistances given as:

$$\begin{aligned} \text{Surface resistance due to surface conditions:} & R_s = (1 - \epsilon)/(\epsilon A) \\ \text{Space resistance due to geometry and orientation:} & R_g = 1/(A_i F_{ij}) \end{aligned}$$

Example IVd.5.8. Two gray plates at T_1 and T_2 exchange radiation in a nonparticipating medium. Find \dot{Q} .

Solution: Here we deal with three radiation resistances namely, the surface resistance of plate 1, the space resistance between plates 1 and 2, and the surface resistance of plate 2, as shown in the figure:



Hence, $\Sigma R = R_{s1} + R_g + R_{s2} = [(1 - \epsilon_1)/(\epsilon_1 A_1) + 1/(A_1 F_{12}) + (1 - \epsilon_2)/(\epsilon_2 A_2)]$ and $\dot{Q} = (E_{b1} - E_{b2})/\Sigma R$.

$$\dot{Q} = \frac{\sigma(T_1^4 - T_2^4)}{\frac{1 - \epsilon_1}{\epsilon_1 A_1} + \frac{1}{A_1 F_{12}} + \frac{1 - \epsilon_2}{\epsilon_2 A_2}} \quad \text{IVd.5.8}$$

We now apply Equation IVd.5.8 to four special cases including radiation exchange between parallel plates, long concentric cylinders, concentric spheres, and a small surface encompassed by a large volume.

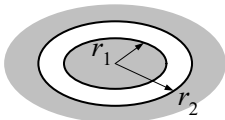
Example IVd.5.9. Find the net rate of heat transfer for two infinite parallel plates.



Solution: For these plates, $A_1 = A_2 = A$ and $F_{12} = 1$. Therefore, from Equation IVd.5.8, we find:

$$\dot{Q}_{12} = \frac{A\sigma(T_1^4 - T_2^4)}{1/\varepsilon_1 + 1/\varepsilon_2 - 1}$$

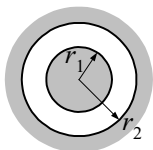
Example IVd.5.10. Find the net rate of heat transfer for two infinite concentric cylinders at radii r_1 and r_2 .



Solution: We use Figure IVd.5.2(d) for view factor between two concentric short cylinders. When cylinders are long, $F_{12} = 1.0$. Also substituting for $A_1 = 2\pi r_1 L$ and for $A_2 = 2\pi r_2 L$ into Equation IVd.5.8, we find:

$$\dot{Q}_{12} = \frac{A_1\sigma(T_1^4 - T_2^4)}{\frac{1}{\varepsilon_1} + \frac{1}{\varepsilon_2} \frac{r_1}{r_2} - \frac{r_1}{r_2}}$$

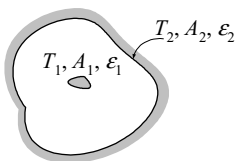
Example IVd.5.11. Find the net rate of heat transfer for two concentric spheres.



Solution: For these surfaces, $A_1/A_2 = (r_1/r_2)^2$ and $F_{12} = 1$ (note that $F_{22} \neq 0$). Substituting these into Equation IVd.5.8, we obtain:

$$\dot{Q}_{12} = A_1\sigma(T_1^4 - T_2^4)/[1/\varepsilon_1 + (r_1/r_2)^2/\varepsilon_2 - (r_1/r_2)^2]$$

Example IVd.5.12. Find the net rate of heat transfer for a small convex surface encompassed by a large cavity.



Solution: For these surfaces, $A_1/A_2 = 0$ and $F_{12} = 1$. Substituting these into Equation IVd.5.8, we obtain:

$$\dot{Q}_{12} = A_1 \sigma \epsilon_1 (T_1^4 - T_2^4)$$

The method shown in Example IVd.5.7 can be extended to three surfaces exchanging radiation, as shown in Figure IVd.5.4. However, as the number of participating surfaces increases, so is the number of equations. Since equations for unknown radiosities are linear, an easy way to handle such cases is to set up a matrix equation. Let's consider surfaces 1 and 2 in an enclosure whose walls are represented by surface 3. At steady state conditions, the rate of heat transferred into node J_1 is equal to the rate of heat transfer out of node J_1 (i.e., the net must be zero):

$$\frac{E_{b1} - J_1}{(1 - \epsilon_1)/(\epsilon_1 A_1)} + \frac{J_2 - J_1}{1/(A_1 F_{12})} + \frac{J_3 - J_1}{1/(A_1 F_{13})} = 0$$

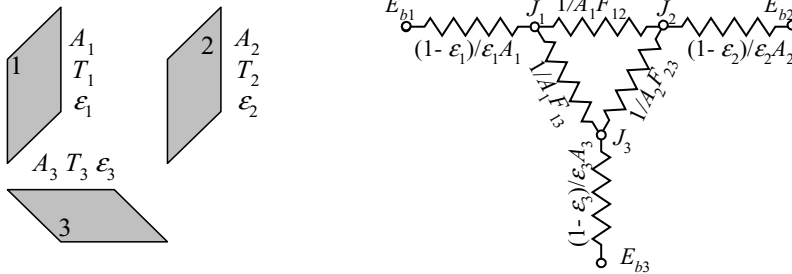


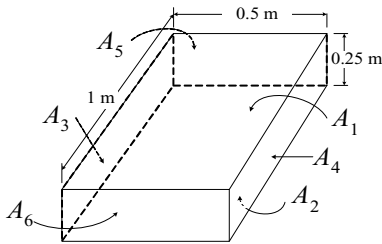
Figure IVd.5.4. Radiation exchange between three surfaces and the related radiation network

We can write similar equations for nodes 2 and 3. If we generalize and consider N gray and diffuse plates exchanging radiation, there will be N sets of linear algebraic equations for N unknown radiosities. Thus, for N surfaces, the set of equations may be arranged in a matrix equation of the form $\mathbf{AX} = \mathbf{B}$ with the coefficient matrix, the vector of unknowns and the vector of constants having the following elements:

$$\begin{bmatrix}
 \varepsilon_1 + (1 - \varepsilon_1) \sum F_{1i} & -(1 - \varepsilon_1)F_{12} & -(1 - \varepsilon_1)F_{13} & \cdots & -(1 - \varepsilon_1)F_{1N} \\
 -(1 - \varepsilon_2)F_{21} & \varepsilon_2 + (1 - \varepsilon_2) \sum F_{2i} & -(1 - \varepsilon_2)F_{23} & \cdots & -(1 - \varepsilon_2)F_{2N} \\
 -(1 - \varepsilon_3)F_{31} & -(1 - \varepsilon_3)F_{32} & \varepsilon_3 + (1 - \varepsilon_3) \sum F_{3i} & \cdots & -(1 - \varepsilon_3)F_{3N} \\
 \vdots & \vdots & \vdots & \vdots & \vdots \\
 -(1 - \varepsilon_N)F_{N1} & -(1 - \varepsilon_N)F_{N2} & -(1 - \varepsilon_N)F_{N3} & \cdots & \varepsilon_N + (1 - \varepsilon_N) \sum F_{Ni}
 \end{bmatrix}
 \begin{bmatrix}
 J_1 \\
 J_2 \\
 J_3 \\
 \vdots \\
 J_N
 \end{bmatrix}
 =
 \begin{bmatrix}
 \varepsilon_1 E_{b1} \\
 \varepsilon_2 E_{b2} \\
 \varepsilon_3 E_{b3} \\
 \vdots \\
 \varepsilon_N E_{bN}
 \end{bmatrix}
 \quad \text{IVd.5.9}$$

where index i in Equation IVd.5.9 ranges from 1 to N . Upon obtaining J_1 through J_N from Equation IVd.5.9, we then find the corresponding rates of heat transfer for each surface from Equation IVd.5.7. Since the surfaces do not “see” themselves (i.e., $F_{ii} = 0$) then the diagonal terms become unity.

Example IVd.5.13. The gray and diffuse surfaces of a rectangular parallelepiped are exchanging radiation with each other and nothing else. Use the following data to find the related radiosities and the rate of heat transfer to or from each surface.



Surface No.	T (K)	ε	A (m ²)	F :	1	2	3	4	5	6
1	500	0.3	0.500	F_{1j}	0.000	0.509	0.167	0.167	0.079	0.079
2	600	0.4	0.500	F_{2j}	0.509	0.000	0.167	0.167	0.079	0.079
3	550	0.8	0.250	F_{3j}	0.334	0.334	0.000	0.165	0.084	0.084
4	700	0.8	0.250	F_{4j}	0.334	0.334	0.165	0.000	0.084	0.084
5	650	0.6	0.125	F_{5j}	0.315	0.315	0.167	0.167	0.000	0.036
6	750	0.7	0.125	F_{6j}	0.315	0.315	0.167	0.167	0.036	0.000

Solution: The top and bottom surfaces are A_1 and A_2 , the left and right sides are A_3 and A_4 , and the back and front surfaces are A_5 and A_6 . The above view factors are found from Figures IVd.5.2(a) and IVd.5.2(b):

Parallel surfaces:

For $A_1 - A_2$, $X = 0.50$, $Y = 1.00$, $L = 0.25$, and $F_{12} = F_{21} = 0.509$

For $A_3 - A_4$, $X = 0.25$, $Y = 1.00$, $L = 0.50$, and $F_{34} = F_{43} = 0.165$

For $A_5 - A_6$, $X = 0.50$, $Y = 0.25$, $L = 1.00$, and $F_{56} = F_{65} = 0.036$

Perpendicular surfaces:

For surfaces $A_1 - A_3$, $A_1 - A_4$, $A_2 - A_3$, and $A_2 - A_4$:

$X = 1.00$, $Y = 0.50$, $Z = 0.25$ resulting in:

$F_{13} = F_{23} = F_{14} = F_{24} = 0.167$ and $F_{31} = F_{32} = F_{41} = F_{42} = (0.5/0.25) \times 0.167 = 0.334$

For surfaces $A_1 - A_5$, $A_1 - A_6$, $A_2 - A_5$, and $A_2 - A_6$:

$X = 0.50$, $Y = 1.00$, $Z = 0.25$ resulting in:

$F_{15} = F_{16} = F_{25} = F_{26} \approx 0.079$ and $F_{51} = F_{52} = F_{61} = F_{62} = (1.0/0.25) \times 0.079 = 0.315$

For surface $A_3 - A_5$, $A_3 - A_6$, $A_4 - A_5$, and $A_4 - A_6$:

$X = 0.25$, $Y = 1.00$, $Z = 0.50$ resulting in:

$F_{35} = F_{36} = F_{45} = F_{46} = 0.084$ and $F_{53} = F_{54} = F_{63} = F_{64} = (1.0/0.50) \times 0.084 = 0.167$

The emissive powers are found from Equation IVd.2.1. For example, $E_{b1} = 5.67\text{E}-8 \times 500^4 \text{ W/m}^2$. If we now substitute values in Equation IVd.5.9, we find:

$$\begin{bmatrix} 1.00 & -0.36 & -0.12 & -0.12 & -0.06 & -0.06 \\ -0.31 & 1.00 & -0.10 & -0.10 & -0.05 & -0.05 \\ -0.07 & -0.07 & 1.00 & -0.03 & -0.02 & -0.02 \\ -0.07 & -0.07 & -0.03 & 1.00 & -0.02 & -0.02 \\ -0.13 & -0.13 & -0.07 & -0.07 & 1.00 & -0.01 \\ -0.09 & -0.09 & -0.05 & -0.05 & -0.01 & 1.00 \end{bmatrix} \begin{bmatrix} J_1 \\ J_2 \\ J_3 \\ J_4 \\ J_5 \\ J_6 \end{bmatrix} = \begin{bmatrix} 1063.12 \\ 2939.33 \\ 4150.72 \\ 10890.94 \\ 6072.78 \\ 12558.16 \end{bmatrix}$$

Upon solving this set, we find; $J_1 = 7536.7 \text{ W/m}^2$, $J_2 = 8265.2 \text{ W/m}^2$, $J_3 = 6032.9 \text{ W/m}^2$, $J_4 = 12,556.5 \text{ W/m}^2$, $J_5 = 9522.8 \text{ W/m}^2$, and $J_6 = 15,085.6 \text{ W/m}^2$. The corresponding rates of heat transfer for the surfaces are:

$$\dot{Q}_1 = \frac{((5.67\text{E}-8) \times 500^4) - 7536.3}{(1-0.3)/(0.3 \times 0.5)} = -855.6 \text{ W. Similarly, we find } \dot{Q}_2 = -305.6$$

$$\text{W, } \dot{Q}_3 = -844.5 \text{ W, } \dot{Q}_4 = -1057.2 \text{ W, } \dot{Q}_5 = 112.2 \text{ W, and } \dot{Q}_6 = 832.6 \text{ W.}$$

Such problems involving radiation exchanges between isothermal surfaces can be easily solved with the software included on the accompanying CD-ROM.

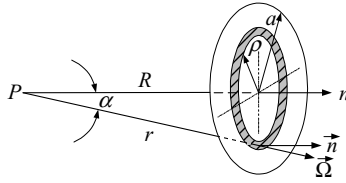
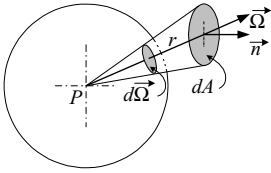
We use a similar method to solve problems in which instead of surface temperatures, the surface heat flux is specified. An adiabatic surface is a special case of the heat flux boundary conditions in which the heat flux is zero. Thus, if surface i is adiabatic, then $E_{bi} \equiv J_i$, which is equivalent with $\varepsilon_i \approx 0$.

QUESTIONS

- What was the role of ether in classical mechanics and electromagnetism?
- Who described the energy of particle-like waves?
- Does light travel as a wave or as a particle?
- Which broadcast wave is more energetic? AM or SW?
- If a radio station broadcasts on 100 m wavelength, what is the corresponding frequency?
- What is the difference between a plane angle and a solid angle?
- What is the value of a solid angle for a hemisphere? What is its value for a sphere?
- What is the difference between radiation intensity and radiosity?
- What are diffuse emitter and diffuse incident radiation?
- What are the Wien's distribution and Kirchhoff's radiation laws?
- What are the important features of the Planck distribution?
- What is meant by band emission? Calculate the band emission for $\lambda T = 3000 \mu\text{m}\cdot\text{K}$ and compare your result with the corresponding value given in the table of Section 2.1.
- Is it fair to say that a red rose absorbs all other colors but reflects the color red?
- For most engineering applications, are surfaces specular reflectors or diffuse reflectors?
- What is the unit of spectral irradiation?
- What are the advantages of a diffuse gray surface?
- What is the role of the view factor in thermal radiation?
- What is the reciprocity relation?
- What are the key assumptions in analyzing radiation exchanges in enclosures?
- What is the Oppenheim approach in solving problems involving radiation exchange?
- What is the physical interpretation of surface resistance? What other resistance to radiation heat transfer do you know?

PROBLEMS

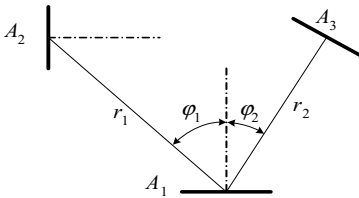
1. Shown in the left side figure, is the differential solid angle $d\Omega$ subtended by the differential area dA when viewed from point P . We define the solid angle at point P as the projection of the surface on a sphere of unit radius surrounding the point. Thus, the differential solid angle $d\Omega$ subtended by surface dA in the left side figure below is given by $d\Omega = |d\vec{\Omega}| = (d\vec{A} \cdot \vec{\Omega})/r^2$. a) Use this definition to compute the solid angle Ω subtended by a circular disk of radius a at a point P that is located a distance R from the disk, where P lies on the normal n passing through the center of the disk, as shown in the right figure. b) Find Ω as $a \rightarrow \infty$. [Ans.: b) Hemisphere].



2. The surface of a sphere of radius R emits S_0 photons isotropically towards the center of the sphere. Find total number of photons received at the center of the sphere per second and per unit area. [Ans. S_0].

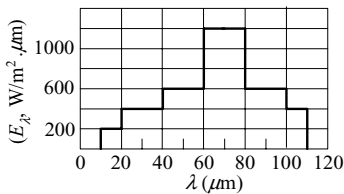
3. Surface A_1 is a diffuse emitter with an emission intensity of $10,000 \text{ W/m}^2\cdot\text{sr}$ in the normal direction. The orientation of surfaces A_2 and A_3 is such that $\varphi_1 = 60^\circ$ and $\varphi_2 = 30^\circ$. a) find the solid angles subtended by surfaces A_2 and A_3 , b) compare the intensity of the radiation emitted by surface A_1 in the direction of surface A_2 with the intensity of the radiation emitted by surface A_1 in the direction of surface A_3 . c) find the rate of energy received by surfaces A_2 and A_3 due to the radiation emission from surface A_1 .

Data: $A_1 = 0.0020$, $A_2 = 0.0015$, $A_3 = 0.0010 \text{ m}^2$, $r_1 = 35 \text{ cm}$, $r_2 = 65 \text{ cm}$.

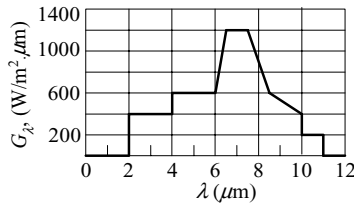


4. Find the energy associated with a radiation having a wavelength of $1\text{E-}3 \mu\text{m}$. (Ans.: $1.98\text{E-}16 \text{ J}$)

5. The spectral distribution of the radiation emitted by a diffuse surface is approximated in the figure. Find the total emissive power and the total intensity.



Problem 5



Problem 6

6. A spectral distribution for a surface irradiation is approximated as shown in the figure. Find the total irradiation.

7. The emissive power of a blackbody, at $0.8 \mu\text{m}$ wavelength is measured as $1\text{E}5 \text{ W/m}^2\cdot\mu\text{m}$. Find the blackbody temperature. [Ans. 1739 K]

8. Solve Example IVd.2.3 for a forced convection heat transfer coefficient of $7,500 \text{ W/m}^2\cdot\text{K}$. Solve the same example but for the surface temperature of 250°C .

9. A blackbody is at a temperature of 2000 K . Find a) the percentage of energy emitted in the shorter than visible range, b) the percentage of energy emitted in the longer than the visible range, c) the percentage of energy emitted in the visible range, and d) the rate of energy emitted in the visible range

10. A blackbody is radiating at a constant temperature of 2500 K . Find a) the emissive power of radiation from this blackbody, b) the wavelength below which 15% of the radiation of the blackbody is concentrated, c) the wavelength above which 10% of the emission is concentrated, d) the maximum spectral emissive power, e) the wavelength associated with the maximum spectral emissive power.

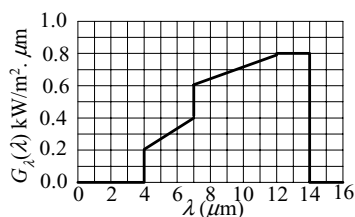
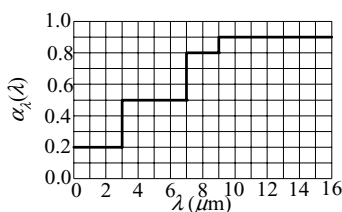
11. The blackbody in Problem 10 is a large isothermal enclosure. A small object is now placed inside this enclosure. Find the irradiation incident on this object.

12. The large isothermal enclosure of Problem 10 is a sphere, having a diameter of 10 m . The interior surface is smooth and completely covered with carbon. There is a small hole, 1 cm in diameter, on the surface of the sphere. The rate of radiant energy emitted through the small hole is 100 W . Find the temperature of the sphere.

10. A blackbody is at a temperature of 1500 K . Find the rate of radiant energy emission in the cone shown in the figure of Example IVd.2.5 for $\phi = 60^\circ$ at wavelength 2 to $4 \mu\text{m}$. [Ans. 0.1 MW/m^2].

11. Use the spectral hemispheric absorptivity of Example IVd.3.1 and find the surface spectral hemispherical reflectivity. [Hint: Recall that for an opaque surface $\alpha + \rho = 1$].

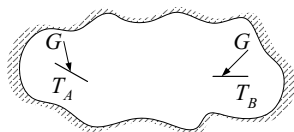
12. The spectral hemispherical absorptivity and irradiation profiles for an opaque surface are shown in the figure. Find the total hemispherical absorptivity.



13. The surface in Problem 12 has an absorptivity of 0.90 and is at a temperature of 550 K . Find the surface temperature after exposure to irradiation.

14. A large isothermal enclosure containing two small surfaces (surface A and surface B) is shown in the figure. The two surfaces are then irradiated by the enclosure at an equal rate of $10,000 \text{ W/m}^2$. Due to the differences in thermal properties of the surfaces, surface A absorbs the incident radiation at a rate of 8800 W/m^2 while surface B absorbs the incident radiation at a rate of irradiation at a rate of

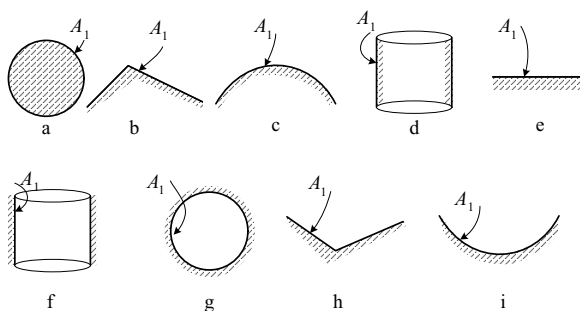
1000 W/m². Find the answer to the following questions under thermodynamic equilibrium condition a) the temperature of each surface, b) the absorptivity of each surface, and c) the emissivity of each surface



15. Radiant energy at a rate of 15.000 W/m² is received by a gray and diffuse surface. The surface is opaque and has an absorptivity of 0.65. Assume negligible heat transfer due to convection. The surface temperature is 400 C with a surface area of 1 m². Find a) the rate of energy absorbed by the surface, b) the rate of energy emitted by the surface, c) the total energy loss from the surface.

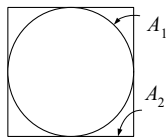
15. A flat metal plate ($\epsilon = 0.66$, and $\alpha = 0.35$) is exposed to solar radiation, at an irradiation rate of 1000 W/m². Find the plate temperature after a long time exposure (i.e., steady state condition). The convection heat transfer coefficient is estimated at about 20 W/m²·K.

16. For the purpose of calculating the view factor for radiation heat transfer, surfaces may be divided into three categories of convex, flat (plane), or concave. As shown in the figure, surfaces a, b, c, and d are examples of convex, and surfaces f, g, h, and i are examples of concave surface. If a surface can view itself then $F_{11} > 0$ otherwise, $F_{11} = 0$. Consider surfaces a through i, and specify the surfaces that have non-zero view factor.

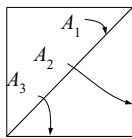


17. A disk, having a diameter of 1 m, is parallel to and on the centerline of another disk, having a diameter of 1.2 m. The two disks are 1 m apart. Find F_{12} and F_{21} . [Ans.: 0.232, 0.161].

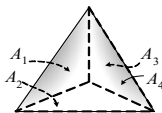
18. Find F_{12} and F_{21} for the following objects. a) Figure a shows a sphere placed inside a cube. The side of the cube is the same as the diameter of the sphere. b) Figure b shows a diagonally partitioned long square duct. c) Figure c shows a pyramid with equal sides. d) Figure d shows quarter of a cylinder exchanging radiation with the base surface of a half cylinder. [Ans.: a) $F_{12} = 1$, $F_{21} = \pi/6$, b) $F_{12} = 0.5$, $F_{21} = 0.71$].



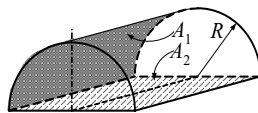
a



b



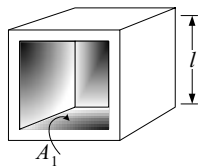
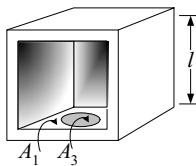
c



d

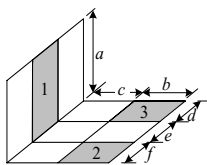
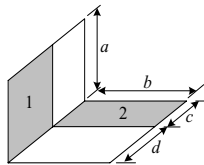
19. A right circular cylinder has a height of 1 m and diameter of 75 cm. Find the view factor for the cylindrical to the base.

20. An oven, as shown in the left figure, is in the shape of a cube of side l . The surface of the base is $A_1 = 0.1 \text{ m}^2$. All other surfaces have a combined surface area of $A_2 = 0.5 \text{ m}^2$. Find the view factor F_{21} and F_{22} .

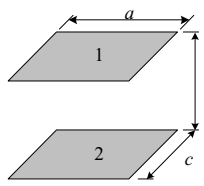
**Problem 20****Problem 21**

21. A circular disk of surface area $A_3 = 0.02 \text{ m}^2$ is placed on the base surface of the oven of Problem 20, as shown in the right figure. All other surfaces have a combined surface area of $A_2 = 0.5 \text{ m}^2$. Find F_{12} , F_{32} , and F_{23} .

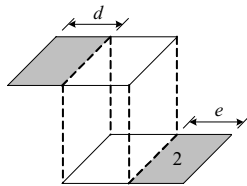
22. Two perpendicular rectangles are shown in the figure. Find F_{12} for both left and right figures. In the left figures, $a = b = 1 \text{ m}$, and $c = d = 0.5 \text{ m}$. In the right figure, $a = 1 \text{ m}$, $b = c = 0.5 \text{ m}$, $d = e = f = 0.3 \text{ m}$.



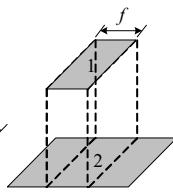
23. Find F_{12} for the two parallel plates shown in the figure, where 1 and 2 represent the shaded surfaces. The surfaces are $a = 1 \text{ m}$ by $c = 0.5 \text{ m}$ and are $b = 2 \text{ m}$ apart. For figure b use $d = 0.2 \text{ m}$ and $e = 0.3 \text{ m}$ and for figure c, use $f = 0.3 \text{ m}$. For Figure d, use $r_1 = 10 \text{ m}$, $r_2 = 5 \text{ m}$, and the vertical distance between surfaces A_1 and A_2 is 10 m. For figure d also find F_{31} and F_{33} .



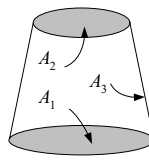
a



b

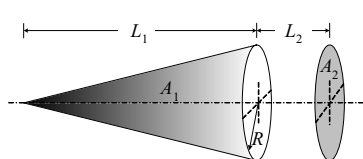


c

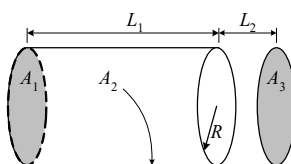


d

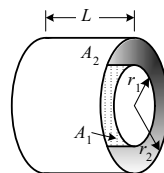
24. Find F_{12} for the cone shown in the figure. Use $R = 0.5$ m and $L_1 = 1.5$ m. Surface A_2 has the same diameter as the base of the cone and is located 0.5 m apart.



Problem 24



Problem 25



Problem 26

25. A right circular cylinder with $2R = 0.5$ and $L_1 = 1.5$ m, is open from the right end. Surface A_2 and A_3 have the same diameter as surface A_1 and is located $L_2 = 0.5$ m from the open end. Find a) F_{23} and b) F_{15} where surface 5 is the imaginary surface of a cylinder between the open end and surface A_3 .

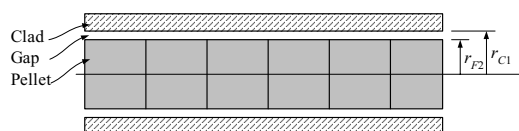
26. Find F_{21} for the two concentric cylinders given $r_1 = 35$ cm, $r_2 = 70$ cm, and $L = 0.7$ m.

27. The cross section of an enclosure is an isosceles triangle. The equal sides are 1 m in length and are at 600 C and 400 C. The base is adiabatic. a) Find the temperature of the base. b) Find the rate of heat transfer received by the side with temperature of 400 C.

28. Radiation is taking place between two parallel plates and nothing else. Each plates have a surface area of 1.5 m² with emissivities of 0.4 and 0.7. Find the rate of heat transfer for temperatures of 150 C and 250 C. [Ans.: 1243 W].

29. Shown is the figure is the theoretical configuration of the fuel pellet and cladding of a fuel rod. Assuming there is no contact between the pellet and the cladding, a gap region exists between the two materials. Find the rate of heat transfer from the fuel surface to the inside of the cladding by radiation.

Data: $T_{F2} = 400$ C, $T_{C1} = 350$ C, $r_{F2} = 4.8$ mm, $r_{C1} = 4.9$ mm, $L = 3.66$ m. In the temperature range of interest, use the following emissivities: for fuel $\epsilon_{UO2} \approx 0.8$ and for cladding $\epsilon_{Zircaloy} \approx 0.26$.



30. A filament, 1 cm in diameter is held in the center of a spherical bulb. The filament is at 250 C and the bulb, having a diameter of 5 cm, is at 80 C. Assuming radiation takes place only between the bulb and the filament, find the rate of heat transfer by radiation. $\epsilon_1 = \epsilon_2 = 0.75$.

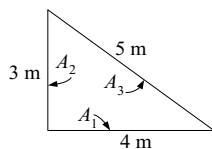
31. Two small rectangular flat plates, 5 ft by 10 ft are located 5 ft apart. These plates are located in a large room. The walls of the room are maintained at 65 F.

The plates exchange radiation with each other and with the room. However, consider only the plate surfaces facing each other. The temperature and diffusivity of the plates are $T_1 = 500$ F, $T_2 = 900$ F, $\varepsilon_1 = 0.7$, and $\varepsilon_2 = 0.9$, respectively. Find the rate of heat transfer from the plates to the room. [Ans.: $J_1 = 4240$ W/m², $J_2 = 16760$ W/m², $\dot{Q}_1 = -0.161$ E4 W, $\dot{Q}_2 = 0.7026$ E5 W].

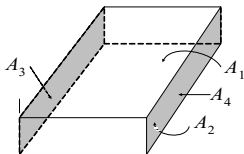
32. Two small rectangular flat plates, 0.5 m by 1 m are located 0.5 m apart. These plates are located in a large room. The walls of the room are maintained at 35 C. The plates exchange radiation with each other and with the room. However, consider only the plate surfaces facing each other. The temperature and diffusivity of the plates are $T_1 = 900$ C, $T_2 = 1200$ C, $\varepsilon_1 = 0.8$, and $\varepsilon_2 = 0.6$, respectively. Find the rate of heat transfer from the plates to the room. [Ans.: $J_1 = 95710$ W/m², $J_2 = 1.712$ E5 W/m², $\dot{Q}_1 = 23270$ W, $\dot{Q}_2 = 71790$ W].

33. The cross section of a duct is a right triangle as shown in the figure. The sides of this duct are isothermal and are exchanging radiation. Assuming a non-participating medium between the gray surfaces, find the rates of heat transfer. Data: $T_1 = 500$ K, $T_2 = 600$ K, $T_3 = 800$ K, $\varepsilon_1 = 0.625$, $\varepsilon_2 = 0.4$, and $\varepsilon_3 = 0.8$. [Ans.: -28150 W/m, -17070 W/m, 45200 W/m].

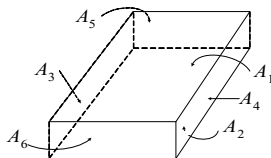
34. A duct, consisted of four rectangular flat plates, are radiating with each other and nothing else. Use the given data to find the radiosity and the rate of heat transfer for each surface. Data: Length = 1 m, depth, 2 m, height 0.5 m, $T_1 = 100$ C, $T_2 = 200$ C, $T_3 = 300$ C, $T_4 = 400$ C, $\varepsilon_1 = 0.5$, $\varepsilon_2 = 0.65$, $\varepsilon_3 = 0.75$, $\varepsilon_4 = 0.8$. The joins are well insulated so that there is no heat transfer between the plates by thermal conduction.



Problem 33



Problem 34



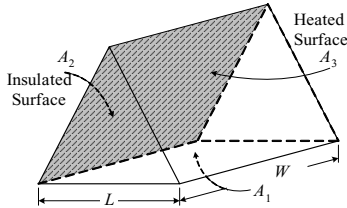
Problem 35

35. A rectangular parallelepiped consists of gray, diffuse, and flat surfaces, radiating with each other and nothing else. The surface temperatures are maintained at the specified values. There is a vacuum in the enclosure and thus, no other heat transfer mechanism except radiation exists. Use the given data to find the radiosity and the rate of heat transfer for each surface. Data: Length = 2 m, depth, 3 m, height 1 m, $T_1 = 100$ C, $T_2 = 200$ C, $T_3 = 250$ C, $T_4 = 400$ C, $T_5 = 500$ C, $T_6 = 550$ C, $\varepsilon_1 = 0.5$, $\varepsilon_2 = 0.65$, $\varepsilon_3 = 0.75$, $\varepsilon_4 = 0.8$, $\varepsilon_5 = 0.55$, $\varepsilon_6 = 0.65$, $\varepsilon_7 = 0.85$.

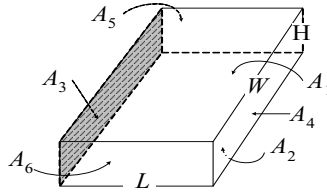
36. A triangular duct is shown in the figure. The base of the duct (surface 1) is maintained at a temperature of 600 K. The left panel (surface 2) is insulated and the right panel (surface 3) is heated and maintained at 1300 K. Find a) the radiosities of all surfaces, b) the required rate of heat transfer to surface 3 to maintain the

steady state temperatures as specified, and c) the temperature of the insulated surface. Data: $L = 1$ m, $W = 2$ m, $\varepsilon_1 = 0.7$, $\varepsilon_2 = 0.8$, and $\varepsilon_3 = 0.4$.

[Ans.: a) $J_1 = 129000$ W/m², $J_2 = 26,558$ W/m², $J_3 = 77,784$ W/m², b) 76.84 kW, and c) 1082 K].



Problem 36



Problem 37

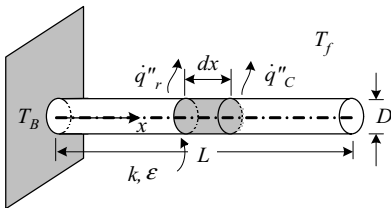
37. Consider the rectangular parallelepiped of Problem 34 with the back panel (surface A_3) is now insulated. All other surface temperatures remain unchanged. Find the rate of heat transfer to surface A_6 to maintain the temperatures at their specified values. Data: $T_1 = 500$ K, $T_2 = 600$ K, $T_3 = 550$ K, $T_4 = 650$ K, $T_5 = 700$ K, $T_6 = 1750$ K, $\varepsilon_1 = 0.3$, $\varepsilon_2 = 0.4$, $\varepsilon_3 = 0.18$, $\varepsilon_4 = 0.26$, $\varepsilon_5 = 0.25$, $L = 1$ m, $W = 0.5$ m, $H = 0.25$ m. [Ans.: 15.568 kW].

38. A cylindrical spine used as a fin to enhance the rate of heat transfer from a surface. Our goal is to find the one-dimensional temperature distribution in the spine. Write the conservation equation of energy for the control volume shown in the figure. Show that temperature at every location on this fin and at every time is found from the solution to:

$$\frac{\partial \theta(x, t)}{\partial t} = \frac{1}{\alpha} \frac{\partial^2 \theta(x, t)}{\partial x^2} - (m_c^2 + m_r^2) \theta(x, t) = 0$$

where $\theta = T(x, t) - T_f$, $a = \rho c / k$, $m_c = (Ph_c / \rho A c)^{0.5}$, and $m_r = (Ph_r / \rho A c)^{0.5}$. In these relations, h_c is the heat transfer coefficient for heat transfer by convection, and h_r is the heat transfer coefficient for heat transfer by radiation. Note that h_r is defined as:

$$h_r = \varepsilon \sigma (T + T_f) (T^2 + T_f^2)$$



Specify the required initial and boundary conditions.

39. Show that the steady state temperature distribution in a cylindrical spine is the solution to:

$$\frac{d^2\theta(x)}{dx^2} - (m_c^2 + m_r^2)\theta(x) = 0$$

where $m_c = (Ph_c/kA)^{0.5}$, and $m_r = (Ph_r/kA)^{0.5}$. Use the given data to find the temperature distribution at steady state in the above fin. Data: $L = 15$ cm, $D = 1$ cm, $T_B = 350$ C, $T_f = 27$ C, $k = 50$ W/m·C, $h_c = 15$ W/m²·C, $\varepsilon = 0.75$. The tip of the fin is losing energy by both radiation and convection.

[Hint: You may solve this problem analytically or numerically. The analytical solution follows the method described in Section 8 of Chapter IVa. Since we have linearized the differential equation by choosing the heat transfer coefficient, as shown in Problem 38, an iterative solution is required regardless of the solution method we choose (h_r , therefore, m_r are unknowns). The initial guess to estimate h_r for thermal radiation is obtained by ignoring thermal radiation (i.e., by setting $m_r = 0$). Upon obtaining the initial guess for temperature, we then include thermal radiation but evaluate h_r at the temperature calculated in the previous iteration. At the end of each trial, we find:

$$\varepsilon = \left| \frac{T^k - T^{k-1}}{T^k} \right|$$

where k is the iteration index. The iteration is terminated when $\varepsilon \leq \varepsilon_s$ where ε_s is the specified convergence criterion].

V. Two-Phase Flow and Heat Transfer

Va. Two-Phase Flow Fundamentals

At the first glance, two-phase or, in general, multi-phase flow seems an exotic topic used only in scientific experiments. In reality however, we may encounter two-phase flow in everyday activities. Flow of carbonated water pouring out of a bottle, ocean waves carrying oxygen, or even the action of the windshield wiper to remove rain involves two-phase flow. These are examples of isothermal flow. Of special interest is the flow of water and steam in heated channels such as in a BWR core or the tube-bundle of a PWR steam generator. Although continuous efforts are being made to formulate two-phase flow aspects by analytical means, most two-phase flow formulations are based on experimental data and hence are in the form of correlations. In this chapter, following the definition of pertinent terms, we discuss such important topics as calculation of two-phase flow pressure drop and critical flow.

1. Definition of Two-Phase Flow Terms

Two-phase flow generally refers to the flow of a liquid and a gas or vapor such as the flow of water and steam, water and air, etc.

Two-phase mixture refers to the mathematical analysis of two-phase flow where the two-phase mixture is treated as a pseudo single-phase.

Two-fluid model refers to the mathematical analysis of two-phase flow where phases are treated separately. Such treatment requires consideration of mass, momentum, and energy transfer between the phases. This model provides more information but also requires more experimentally based constitutive equations than a two-phase mixture model.

Multifluid flow refers to such cases as the flow of water droplets in bulk steam, surrounded by a film of flowing water.

Multi-phase flow refers to the flow of several phases such as steam, ice, and water.

Multicomponent flow refers to the flow of several phases having different chemical composition such as the flow of water, steam and air.

Thermodynamic equilibrium exists between phases when the liquid (l) and vapor (v) phases are at equal temperature, $T_l = T_v$.

Homogeneous is applied to two phases that flow at the same speed in the same direction.

Homogenous Equilibrium Model (HEM) is a means of mathematically describing two-phase flow, where $\bar{V}_l = \bar{V}_v$ (same flow direction at the same velocity) and also $T_l = T_v$ (thermodynamic equilibrium). If phase velocities are not equal ($|\bar{V}_l| \neq |\bar{V}_v|$) but temperature of the phases are, then the mathematical model for analysis of the two-phase flow is referred to as the *Separated Homogeneous Model* or SEM.

Quality is defined in various ways depending on the type of application. For example, considering steam and water, in Chapter II, we defined quality as $x = m_g/m$, referred to as the static quality, and may also be written as x_s . The thermodynamic quality is defined as $x = (h - h_f)/h_{fg}$, also written as x_e for equilibrium quality. The flow quality for a mixture of water and steam is defined as the ratio of mass flow rate of steam to mass flow rate of the mixture:

$$X = \frac{\dot{m}_g}{\dot{m}}$$

The flow quality, X , and thermodynamic quality, x , become equal only when thermal equilibrium conditions exist. Thus, $X = x$ only if $T_f = T_g$.

Void fraction in a control volume made up of liquid and gas mixture is the volume fraction of the gas phase. Hence, void fraction (α_g or simply α) is given by $\alpha = V_g/V$. Similarly, $1 - \alpha = V_f/V$. Note that void fraction is a space and time averaged quantity. The static quality, as defined above, can be expressed in terms of void fraction by noting that $x = m_g/(m_f + m_g) = \rho_g V_g/(\rho_f V_f + \rho_g V_g) = \rho_g \alpha V/[\rho_f(1 - \alpha) + \rho_g \alpha]V$. Hence,

$$x = \frac{\rho_g \alpha}{\rho_f(1 - \alpha) + \rho_g \alpha}$$

Mixture density is given by $\rho = (m_f + m_g)/V$. Substituting for $m_f = \rho_f V_f$ and $m_g = \rho_g V_g$, we find $\rho = \rho_f V_f/V + \rho_g V_g/V$. Since $V_f/V = 1 - \alpha$ and $V_g/V = \alpha$, the mixture density in terms of void fraction becomes:

$$\rho = (1 - \alpha)\rho_f + \alpha\rho_g$$

Phasic mass flux, is the mass flow of a given phase per mixture area. Thus, for a mixture of water and steam for example, $G_g = \dot{m}_g/A$. Using the definition of

flow quality, $G_g = X \dot{m} / A = XG$. Similarly, for water we have $G_f = \dot{m}_f / A$. Substituting, $G_f = (1 - X) \dot{m} / A = (1 - X)G$ where G is the mixture mass flux.

Mixing cup density is similar to the mixture density but is averaged with respect to the phasic mass flux; $v' = 1 / \rho' = [\rho_f (1 - \alpha) V_f^2 + \rho_g \alpha V_g^2] / G^2$. Similar to the mixing cup density, a mixing cup enthalpy is defined as; $h' = [\rho_f (1 - \alpha) V_f h_f + \rho_g \alpha V_g h_g] / G$

Phasic volumetric flow rate is defined similar to the single-phase flow hence, for the gas component of a mixture, $\dot{V}_g = \dot{m}_g / \rho_g = XGA / \rho_g$ and for the liquid component $\dot{V}_f = \dot{m}_f / \rho_f = (1 - X)GA / \rho_f$.

Superficial velocity is the velocity a phase would have if it were flowing alone in a channel. As such, the superficial velocity is obtained by dividing the related volumetric flow rate by the mixture area. For example, for the flow of water and steam in a channel, while water velocity is given by $V_f = \dot{V}_f / A_f$, where A_f is the water flow area, the superficial velocity for water is defined as $J_f = \dot{V}_f / A$ where A is total flow area of the channel. Similarly, the superficial velocity of steam is found as $J_g = \dot{V}_g / A$. To relate the superficial velocities to flow quality, we write:

$$J_g = \dot{V}_g / A = \dot{m}_g / (\rho_g A) = G_g / \rho_g = XG / \rho_g$$

Similarly, for J_f we find

$$J_f = (1 - X)G / \rho_f$$

We now define $J = J_f + J_g$. Substituting for J_f and J_g , we find J to be given by $J = [(1 - X) / \rho_f + X / \rho_g]G$. We also note that $J_g = \dot{V}_g / A = V_g A_g / A = \alpha V_g$. Similarly, for the liquid phase we have $J_f = (1 - \alpha)V_f$.

Slip ratio is defined as the ratio of the gas velocity to liquid velocity, $S = V_g / V_f$. Substituting, we find;

$$S = \frac{V_g}{V_f} = \frac{J_g / \alpha}{J_f / (1 - \alpha)} = \frac{1 - \alpha}{\alpha} \frac{XG / \rho_g}{(1 - X)G / \rho_f} = \left(\frac{1 - \alpha}{\alpha} \right) \left(\frac{X}{1 - X} \right) \left(\frac{\rho_f}{\rho_g} \right) \quad \text{Va.1.1}$$

Thus, the slip ratio relates X and α . If for simplicity, we represent the quality and the density ratios with y :

$$y = \frac{1-X}{X} \frac{\rho_g}{\rho_f}$$

Equation Va.1.1 simplifies to:

$$S = \frac{(1-\alpha)}{y\alpha} \quad \text{Va.1.2}$$

from which we can find void fraction as:

$$\alpha = (1 + yS)^{-1} \quad \text{Va.1.3}$$

Volumetric flow ratio as defined for the gas phase is given as $\beta = \dot{V}_g / \dot{V} = J_g / J$, which may be written as:

$$\beta = \frac{J_g}{J} = \frac{J - J_f}{J} = 1 - \frac{J_f}{J}$$

Substituting for the superficial velocities in terms of flow quality X and mass flux G , we find:

$$\beta = (1 + y)^{-1} \quad \text{Va.1.4}$$

Alternatively, by substituting for y from its definition above, we find:

$$\beta = \frac{X v_g}{v_f + X v_{fg}} \quad \text{Va.1.5}$$

Wallis number is the ratio of inertial force to hydrostatic force on a bubble or drop of diameter D . Hence, the Wallis number (Wa) can be defined for both gas and liquid. For example,

$$\text{Wa}_g = [\rho_g / g D (\rho_f - \rho_g)]^{0.5} J_g.$$

Kutateladze number is defined similarly to the Wa number except for the length scale D , which is replaced by the Laplace constant $[\sigma / g (\rho_f - \rho_g)]^{0.5}$. Hence for a gas the Ku number becomes;

$$\text{Ku}_g = [\rho_g / (g \sigma (\rho_f - \rho_g))]^{0.5} J_g$$

Flooding refers to the condition in which the upward flow of a gas stalls the downward flow of a liquid. This is accomplished through the momentum transfer at the liquid-gas interface. According to Wallis for flooding in vertical tubes,

$J_g^{0.5} + J_f^{0.5} = C$ where for round tubes $C = 0.9$ and for sharp-edged tubes $C = 0.75$.

Flow reversal refers to condition in which the upward flow of two phases is interrupted by a reduction in gas velocity. The lack of sufficient momentum transfer at the interface results in the gravity and frictional forces eventually stopping and finally reversing the flow of liquid. For flow reversal, $Ku_g = 3.2$.

Flow patterns of gas-liquid flow in an unheated pipe depend on such factors as pipe orientation, diameter, mass flux, flow quality, and phasic densities. Patterns of gas-liquid flow in a horizontal unheated tube and in upflow of a vertical unheated tube are shown in Figure Va.1.1.

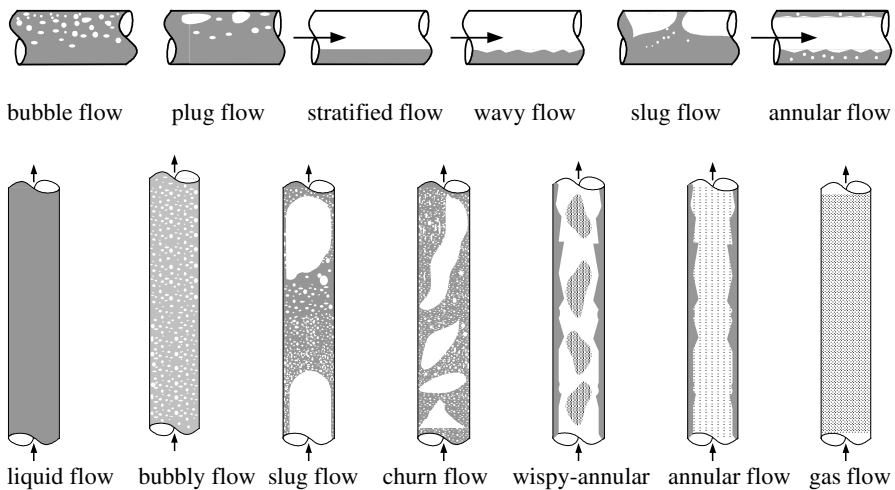


Figure Va.1.1. Flow patterns in horizontal and vertical tubes

Flow pattern map reduces various flow regimes to identifiable patterns. Such maps associate the key flow parameters to a specific pattern. For a given set of such parameters, the flow pattern map determines the corresponding flow regime. Conversely, by knowing the flow regime, we can find a specific range for the key parameters. An example of such maps is shown in Figure Va.1.2. Hewitt has suggested the left side map for upflow and the right side map is used in the RELAP-5 thermalhydraulic computer code.

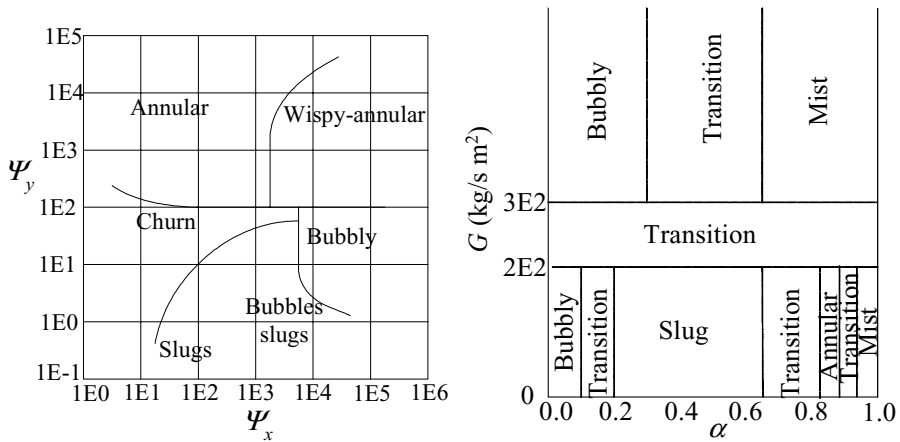


Figure Va.1.2. Flow pattern maps for vertical flow (low pressure air-water and high pressure steam-water)

The coordinates of the Hewitt map (left figure) are $\Psi_x = \rho_f J_f^2$ ($\text{kg/s}^2 \cdot \text{m}$) and $\Psi_y = \rho_g J_g^2$ ($\text{kg/s}^2 \cdot \text{m}$).

Example Va.1.1. Water and steam flow at 1000 psia (~ 7 MPa) and 2 lbm/s (~ 1 kg/s) in a 1 in (2.54 cm) diameter tube. Find the flow regime at a location where $X = 0.2$.

Solution: At 1000 psia, $\rho_f = 46.32$ lbm/ft³ and $\rho_g = 2.24$ lbm/ft³. Since $A = 3.14 \times (1/12)^2/4 = 5.45\text{E-}3$ ft², then $G = 2/5.45\text{E-}3 = 366.7$ lbm/ft² s (1790 kg/s m²). Using Hewitt's map, we find:

$$\rho_f J_f^2 = G^2 (1 - X)^2 / \rho_f = 366.7^2 (1 - 0.2)^2 / 46.32 = 1858 \text{ lbm/s}^2 \text{ ft} \\ (2765 \text{ kg/s}^2 \cdot \text{m})$$

$$\rho_g J_g^2 = G^2 X^2 / \rho_g = 366.7^2 (0.2)^2 / 2.24 = 2400 \text{ lbm/s}^2 \text{ ft} (3589 \text{ kg/s}^2 \text{ m})$$

Thus, the flow regime is Wispy – annular.

2. Two-Phase Flow Relation

For two-phase flow in a conduit, there are two methods for solving for such state parameters as pressure, temperature, and velocity. In the first method, we assign a control volume to each phase. We then write the three conservation equations of mass, momentum, and energy for each control volume and solve them simultaneously. These control volumes exchange mass, momentum, and energy with each

other and exchange momentum and energy with the surface of the conduit. This is called the two-fluid model. In the second method, being basically a pseudo single-phase flow model, we use such parameters as void fraction, slip ratio, and two-phase friction multiplier to solve for only the three conservation equations written for the mixture. In this section, we discuss the two-phase flow parameters used in the pseudo single-phase analysis such as void fraction, flow quality, and slip ratio as well as pressure differential terms for two-phase flow.

2.1. One Dimensional Relation for Void Fraction

Determination of void fraction is essential in several aspects of two-phase flow analysis such as calculation of pressure difference terms. Equation Va.1.3 shows that void fraction varies inversely with the slip ratio. Hence, for given P and X , as S increases, the void fraction decreases. For example, for the flow of water and steam at $P = 1000$ psia and $X = 12\%$, α drops from 75% to 40% when S increases from 1 to 4.

Example Va.2.1. Express the slip ratio only in terms of α and β .

Solution: We use the definition of β given by $\beta = \{1 + [(1 - X)/X] (\rho_g/\rho_f)\}^{-1}$ to find $1 - \beta$. We then divide these to get $(1 - \beta)/\beta = [(1 - X)/X] (\rho_f/\rho_g)$. Substituting in Equation Va.1.1, we obtain:

$$S = \frac{1 - \alpha}{\alpha} \frac{\beta}{1 - \beta}$$

The slip ratio in general is a function of pressure (P), quality (X), and mass flux (G).

Example Va.2.2. Compare X for the flow of water and steam at 1000 psia for $\alpha = 50\%$ and $S = 1, 2$, and 3.

Solution: We solve Equation Va.1.1 for X to get:

$$X = \frac{\alpha \rho_g S}{(1 - \alpha) \rho_f + \alpha \rho_g S}$$

At 1000 psia, $\rho_f = 46.32$ lbm/ft³ and $\rho_g = 2.24$ lbm/ft³. Substituting values, we find:

$X = 4.6\%, 9\%, 12.5\%$ for $S = 1, 2$, and 3, respectively.

Example Va.2.3. For the flow of steam - water, find α , β , ρ , and x . Use $T_{sat} = 270$ C, $X = 0.15$, and $S = 3$.

Solution: At 270 C, $\rho_f = 767.9$ kg/m³ and $\rho_g = 28.06$ kg/m³. Substitute values in y :

$$y = \frac{1-X}{X} \frac{\rho_g}{\rho_f} = \frac{1-0.15}{0.15} \frac{28.06}{767.9} = 0.207$$

Next, we find α , β , the mixture density, and quality:

$$\alpha = 1/(1 + yS) = 1/(1 + 0.207 \times 3) = 0.62$$

$$\beta = 1/(1 + y) = 0.83$$

$$\rho = (1 - \alpha)\rho_f + \alpha\rho_g = (1 - 0.62) \times 767.9 + 0.62 \times 28.06 = 309.2 \text{ kg/m}^3$$

$$x = \rho_g \alpha / [\rho_f(1 - \alpha) + \rho_g \alpha] = 28.06 \times 0.62 / [767.9(1 - 0.62) + 0.62 \times 28.06] = 0.056.$$

As specified in Example Va.2.1, slip ratio itself is a function of pressure, mass flux, density, and void fraction distribution at a given cross section. There are several correlations for the calculation of slip ratio. An analytical method is offered by Zivi. In this method, the flow kinetic energy is set to a minimum (i.e., $K.E. = \sum (\rho_i V_i^2 \dot{V}_i) = 0$ where subscript i refers to liquid and vapor). If we substitute for \dot{V}_f and \dot{V}_g from the definition of the phasic volumetric flow rate, we find:

$$K.E. = \left[\frac{X^3}{\alpha^2 \rho_g^2} + \frac{(1-X)^3}{(1-\alpha)^2 \rho_f^2} \right] \frac{AG^3}{2}$$

Taking the derivative with respect to α and setting it equal to zero, we obtain $d(1 - \alpha) = [X/(1 - X)](\rho_f/\rho_g)^{2/3}$. By comparing this result with Equation Va.1.1, we find that $S = (\rho_f/\rho_g)^{1/3}$. Since Zivi's method expresses the slip ratio only in terms of densities, Zivi's model does not compare well with experimental data. In Example Va.2.2, according to Zivi's method, S is always $S = (46.32/2.24)^{1/3} = 2.75$ for any mass flux. By definition, the homogenous model gives $S = 1$. Thom, recognizing the dependency of S on X , developed a relation for S based on best fit to data for various system pressures. Winterton collected these data in a single equation in terms of the saturated specific volumes:

$$S = 0.93(v_g/v_f)^{0.11} + 0.07(v_g/v_f)^{0.561} \quad \text{Va.2.1}$$

This correlation fits Thom's data well within 1% and can be used for pressures ranging from atmospheric up to the critical point. To estimate S from Equation Va.2.1, a thermal equilibrium condition must exist.

Example Va.2.4. Water enters a heated channel at rate of 20 kg/s with a degree of subcooling of 15 C. Use Equation Va.2.1 and a reference pressure of 7 MPa to find the rate of heat transfer to this channel to ensure the exit void fraction equals 75%.

Solution: To ensure the void fraction at the exit of the heated channel remains at the specified limit, we need to fix the value of the exit quality from Equation Va.1.1, with S given by Equation Va.2.1.

Next, having quality at the exit of the channel, we can find the flow enthalpy at the exit. The rate of heat transfer is subsequently found from a steady-state energy balance.

At 7 MPa, $v_f = 0.001351 \text{ m}^3/\text{kg}$, $v_g = 0.02737 \text{ m}^3/\text{kg}$, and $v_g/v_f = 20.26$

Substituting in Equation Va.2.1:

$$S = 0.93(20.26)^{0.11} + 0.07(20.26)^{0.561} = 1.67$$

Having S and α_e , we find $y \approx 0.2$ from Equation Va.1.2.

Having y , ρ_f , and ρ_g , we find x_e from $y = [(1 - x_e)/x_e](\rho_g/\rho_f)$
 $(1 - x_e)/x_e = y(v_g/v_f) = 0.2 \times 20.26 = 4$ resulting in $x_e = 0.198$

We now find the inlet and exit enthalpies. At 7 MPa, $T_{sat} = 285.88 \text{ C}$. To find h_i , we need to find the enthalpy of subcooled liquid at $P = 7 \text{ MPa}$ and $T = 285.88 - 15 = 273.85 \text{ C}$ resulting in $h_i \approx 1204 \text{ kJ/kg}$

The exit enthalpy is: $h_e = h_f + x_e h_{fg} = 1266.97 + 0.198 \times 1505.1 = 1565 \text{ kJ/kg}$

Therefore, $\dot{Q} = \dot{m}(h_e - h_i) = 20(1565 - 1204) = 7.22 \text{ MW}$.

2.2. Drift Flux Model for Void Fraction

This method, introduced by Zuber-Findlay, and also described by Wallis, is based on the relative motion of the phases and accounts for the void fraction dependency on mass flux and void distribution at a given cross section in the flow. The notable approach in this method is the introduction of a relative motion. In general, the liquid and gas in a mixture travel at different velocities for which we define the relative velocity between the phases as:

$$V_{gf} = V_g - V_f$$

Expressing the phasic velocities in terms of their corresponding superficial velocities, we find:

$$V_{gf} = J_g/\alpha - J_f/(1 - \alpha)$$

Multiplying both sides of this relation by $\alpha(1 - \alpha)$ we obtain;

$$\alpha(1 - \alpha)V_{gf} = (1 - \alpha)J_g - \alpha J_f.$$

The left side term has units of velocity known as the drift velocity or *drift flux*, J_{gf} . The right side term can be rearranged to get $J_g - \alpha(J_f + J_g) = J_g - \alpha J$. Thus; $J_{gf} = J_g - \alpha J$.

To get a physical interpretation of drift flux, we may say that drift flux is the gas volumetric rate passing through a unit area of a plane, normal to the channel axis and traveling at velocity αj .

While the above relation was derived for one-dimensional flow, the usefulness of the drift flux model is in the fact that it accounts for the void fraction distribution at a cross section. We now find the average value of variables over a flow cross section. For example:

$$\bar{\alpha} = \iint_A \alpha \frac{dA}{A} \quad \text{Va.2.2}$$

By so doing, the drift flux can be written as $\bar{J}_{gf} = \bar{J}_g - \bar{\alpha}\bar{J}$. Dividing this relation by $\bar{\alpha}$ and noting that $\bar{\alpha}\bar{J} \neq \bar{\alpha}\bar{J}$, we obtain:

$$\frac{\bar{J}_{gf}}{\bar{\alpha}} = \bar{V}_g - \frac{\bar{\alpha}\bar{J}}{\bar{\alpha}}$$

We simplify this relation by defining \bar{V}_{gJ} such that $\bar{J}_{gf} = \bar{\alpha} \bar{V}_{gJ}$ and a parameter C_o such that:

$$C_o = \frac{\bar{\alpha}\bar{J}}{\bar{\alpha}\bar{J}}$$

Substituting, we find $\bar{V}_{gJ} = \bar{V}_g - C_o\bar{J}$. Dividing both sides of this relation by \bar{J} and replacing $\bar{V}_g / \bar{J} = \bar{\beta} / \bar{\alpha}$ we obtain:

$$\bar{\alpha} = \frac{\bar{\beta}}{C_o + (\bar{V}_{gJ} / \bar{J})} \quad \text{Va.2.3}$$

Equation Va.2.3 is the Zuber-Findlay drift flux model for the calculation of void fraction. This equation is important for the fact that it also accounts for mass flux, G . The parameter C_o , as introduced by Zuber-Findlay, is the key in this model. This parameter helps to distinguish between the concentration profile at a cross section from the velocity profile. For example, for one-dimensional homogenous flow, we know that $\alpha = \beta$. From Equation Va.2.3, this is possible when $\bar{V}_{gJ} = 0$ and $C_o = 1$.

To write an alternative expression for Equation Va.2.3 we first substitute for $j_g = \beta j$ in Equation Va.2.3 to get $\bar{\alpha} = \bar{J}_g / (C_o\bar{J} + \bar{V}_{gJ})$. We then substitute for

$\bar{J}_g = XG / \rho_g$ and $\bar{J} = [(1 - X)/\rho_f + X/\rho_g]G$. Dividing both numerator and denominator by XG/ρ_g and using $y = (1 - X)\rho_g/X\rho_f$, as defined earlier, the drift flux model for void fraction becomes:

$$\alpha = \frac{1}{C_o(1 + y) + \frac{V_{gj}\rho_g}{XG}} \quad \text{Va.2.3}$$

where for simplicity, the volume-averaged symbol is now dropped. Substituting for void fraction from Equations Va.2.3 to Equation Va.1.3 and solving for the slip ratio, we find:

$$S = \left[C_o + \frac{C_o - 1}{y} \right] + \left[\frac{\rho_g V_{gj}}{yXG} \right] \quad \text{Va.2.4}$$

Equation Va.2.4 consists of two terms:

term 1: $C_o + [(C_o - 1)/y]$.

This term pertains to nonuniform void distribution in a given flow cross section

term 2: $V_{gj}\rho_g/(yXG)$.

This term pertains to velocity differential between the liquid and the gas phase.

If there is no void, then $C_o = 0$. Depending on the void fraction distribution, C_o ranges from 1.0 to 1.3. If the ratio of void fraction at the tube surface to the void fraction at the tube center is unity, then C_o is a minimum. The value of C_o increases to a maximum as the above ratio decreases to zero.

The Zuber-Findlay model for void fraction (Equation Va.2.3) is applicable for vertical upflow. If the flow regime is bubbly flow, Zuber and Findlay suggest $C_o = 1.13$ and V_{gj} is found from:

$$V_{gj} = 1.41 \left[\frac{g(\rho_f - \rho_g)\sigma}{\rho_f^2} \right]^{1/4} \cong 1.41 \left(\frac{g\sigma}{\rho_f} \right)^{1/4} \quad \text{Va.2.5}$$

These values correlate well to round tube data.

Example Va.2.5. A mixture of water and steam flows up a 20 mm diameter tube at a rate of 4000 kg/m²·s and temperature of 290 C. At a location where $X = 30\%$ find: a) void fraction, b) the mixture mixing cup density, c) mixture density using the HEM, d) mixture thermodynamic density.

Solution: For saturated mixture at $T = 290$ C, $\rho_f = 732$ kg/m³, $\rho_g = 39$ kg/m³, $\sigma = 0.0166$ N/m.

a) We find the parameter y from:

$$y = [(1 - X)/X](\rho_g/\rho_f) = (0.7/0.3)(39/732) = 0.124$$

$$\beta = 1/(1 + y) = 1/(1 + 0.124) = 0.89$$

Next, we calculate V_{gj} From Equation Va.2.5 and then find J , α , and S :

$$V_{gj} = 1.41[g(\rho_f - \rho_g)\sigma/\rho_f^2]^{0.25} = 1.41[9.81 \times (732 - 39) \times 0.0166/732^2]^{0.25} = 0.17 \text{ m/s}$$

$$J = (1 + y)XG/\rho_g = (1 + 0.124) \times 0.3 \times 4000/39 = 34.58 \text{ m/s}$$

$$\alpha = \beta/[C_o + V_{gj}/J] = 0.89/[1.13 + 0.17/34.58] = 0.78$$

(Compare with $\alpha_{\text{HEM}} = \beta = 0.89$)

$$S = \left[1.13 + \frac{1.13 - 1}{0.124} \right] + \left[\frac{39 \times 0.17}{0.124 \times 0.3 \times 4000} \right] = 2.2$$

b) For the mixing cup density we need phasic velocities. We find V_g and V_f from J_g and J_f :

$$V_g = J_g/\alpha = G_g/\alpha\rho_g = XG/\alpha\rho_g = 0.3 \times 4000/(0.78 \times 39) = 39 \text{ m/s}$$

$$V_f = (1 - X)G/(1 - \alpha)\rho_f = (1 - 0.3) \times 4000/[(1 - 0.78) \times 732] = 17.4 \text{ m/s}$$

(Note; $S = V_g/V_f = 2.2$)

$$1/\rho' = [39 \times 0.78 \times 39.25^2 + 732 \times (1 - 0.78) \times 17.38^2]/4000^2 = 5.97\text{E-}3 \text{ m}^3/\text{kg}$$

Thus, $\rho' = 167.5 \text{ kg/m}^3$. Find mixture density from:

$$\rho = (1 - \alpha)\rho_f + \alpha\rho_g = (1 - 0.78) \times 732 + 0.78 \times 39 = 191.46 \text{ kg/m}^3$$

c) The HEM density is obtained by substituting related values for specific volumes;

$$v = (1 - X)v_f + Xv_g. \text{ Thus, } \rho_{\text{HEM}} = (1 - X)/\rho_f + X/\rho_g = (1 - 0.3)/732 + 0.3/39 = 115.6 \text{ kg/m}^3.$$

d) Since we have used saturation properties, we have implicitly assumed thermal equilibrium exists between the phases hence, $x = X = 0.3$.

Whalley uses the definition of slip velocity to express drift flux in terms of void fraction as:

$$J_{gf} = V_b \alpha (1 - \alpha)^2 \quad \text{Va.2.6}$$

where V_b is the rising velocity of a single bubble as a function of pressure (Table Va.2.1).

Table Va.2.1. Values of V_b for water-steam flow (Whalley)

P (bar)	V_b (m/s)	P (psia)	V_b (ft/s)
1	0.22	14.5	0.722
3	0.21	43.5	0.689
10	0.20	145	0.656
30	0.19	435	0.623
100	0.16	1450	0.525
221.2*	0.0	3207.4*	0.00

*: At critical pressure $\rho_g \rightarrow \rho_f$, $\sigma \rightarrow 0$, and $V_b \rightarrow 0$

Example Va.2.6. A mixture of water and steam flows up a 10 mm diameter tube at a rate of $4000 \text{ kg/s}\cdot\text{m}^2$ and $2 \text{ kg/s}\cdot\text{m}^2$, respectively. Assume an adiabatic condition. Find void fraction in the tube.

Data: $P = 1 \text{ atm}$, $\rho_f = 1000 \text{ kg/m}^3$, $\rho_g = 0.598 \text{ kg/m}^3$.

Solution: One way to find α is to set Equation Va.2.5 equal to the definition of J_{gf} $= (1 - \alpha)J_g - \alpha J_f$:

$$V_b \alpha (1 - \alpha)^2 = J_{gf} = (1 - \alpha)J_g - \alpha J_f$$

We now need J_f and J_g , which are calculated as:

$$J_f = G_f / \rho_f = 4000 / 1000 = 4 \text{ m/s}$$

$$J_g = G_g / \rho_g = 2 / 0.598 = 3.34 \text{ m/s}$$

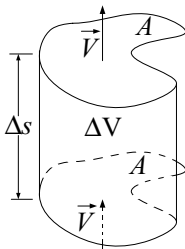
Finding V_b from Table Va.2.1 as 0.22 m/s, one obtains the following non-linear equation for α :

$$(J_f + J_g)\alpha + V_b \alpha (1 - \alpha)^2 - J_g = 0$$

By iteration, we find $\alpha \approx 0.455$.

2.3. Conservation Equations

Derivation of conservation equations for multi-phase and multi-dimensional flow in a control volume with a deformable boundary is beyond the scope of this book. Here, we consider a one-dimensional two-phase flow in a fixed boundary control volume with constant flow area, as shown in Figure Va.2.1 (Myer). To write the

**Figure Va.2.1.** One-dimensional control volume for conservation equations

conservation equation for the mixture, we use volume-averaged quantities similar to Equation Va.2.2, defined for void fraction. Since the flow area is assumed to be constant, the area averaged value for any quantity such as ψ is simplified to $\langle \psi \rangle = (\int \psi dA) / A$.

Beginning with the conservation equation of mass, we apply Equation IIIa.3.2 to the two-phase flow in the elemental control volume of Figure Va.2.1. We then divide each term by $A\Delta z$ and let Δz approach zero:

$$\frac{\partial}{\partial t} \langle \rho_g \alpha + \rho_f (1 - \alpha) \rangle + \frac{\partial}{\partial s} \langle \rho_f V_f (1 - \alpha) + \rho_g V_g \alpha \rangle = 0 \quad \text{Va.2.7}$$

If we now substitute for the mixture density, $\rho = (1 - \alpha)\rho_f + \alpha\rho_g$ and the mixture mass flux, defined as; $G = \langle \rho_f (1 - \alpha)V_f + \rho_g \alpha \rangle$, the one-dimensional continuity equation for the flow of a two-phase mixture becomes:

$$\frac{\partial \rho}{\partial t} + \frac{\partial G}{\partial s} = 0 \quad \text{Va.2.8}$$

If Equation Va.2.8 is integrated over a macroscopic control volume $V = sA$, we obtain Equation IIa.5.1.

Regarding the one-dimensional conservation equation of momentum for two-phase flow in a constant area channel, we use Equation IIIa.3.6. Assuming gravity to be the only body force and substituting for the shear stresses, such as surface force, we find the momentum equation for uniform flow at a cross section z :

$$\frac{\partial G}{\partial t} + \frac{\partial}{\partial s} \langle v' G^2 \rangle = -\frac{\partial P}{\partial s} - \frac{P_w \tau_s}{A} - \rho g \sin \gamma \quad \text{Va.2.9}$$

where τ_s is the shear stress at the wall of the channel, P_w is the channel wetted perimeter, and $\rho' = 1/v'$ is the mixing cup density. Also note that γ is the angle between the flow velocity vector and the horizontal plane (see Figure Va.2.2) and ranges from $-\pi/2 \leq \gamma \leq \pi/2$. For horizontal channels $\gamma = 0$. For vertical channels, if flow is upward, $\gamma = \pi/2$ and if flow is downward, $\gamma = -\pi/2$.

The term representing shear stresses in Equation Va.2.9 can be substituted from Equation IIIb.2.5 for single-phase flow so that $P_w \tau_s / A = f v |G| G / 2 D_h$ where f is the friction factor and using the absolute value of G ensures opposing force in the case of flow reversal in the channel. To obtain the momentum equation for a macroscopic control volume, we integrate Equation Va.2.9 over a finite length s :

$$\frac{s}{A} \frac{d\dot{m}}{dt} + \Delta \left(\frac{v' \dot{m}^2}{A^2} \right) = -\Delta P - \frac{f v |\dot{m}| \dot{m}}{2 A^2} \frac{s}{D_h} - \rho_m V g \sin \gamma \quad \text{Va.2.10}$$

The two-phase flow momentum equation is discussed in more detail in Section 2.4.

The conservation equation of energy for two-phase flow in a constant area channel can be derived from Equation IIIa.3.9 with work terms substituted from Equation IIIa.3.10. Ignoring the contribution by kinetic and potential energies and considering only pressure work, the energy equation simplifies to:

$$\frac{\partial}{\partial t}(\rho h) + \frac{\partial}{\partial s}(Gh') = \frac{\partial P}{\partial s} + \frac{\dot{q}'' P_h}{A} + \dot{q}''' \quad \text{Va.2.11}$$

where the mixture density h represents $h = \langle \rho_f h_f (1 - \alpha) + \rho_g h_g \alpha \rangle / \rho$ and h' is the mixing cup enthalpy. To obtain the energy equation for a macroscopic control volume, we integrate Equation Va.2.11 over control volume $V = sA$:

$$\frac{\partial}{\partial t}(\rho h V) + \Delta(\dot{m} h') = V \frac{\partial P}{\partial s} + \dot{q}'' P_h s + \dot{q}''' V \quad \text{Va.2.12}$$

2.4. Pressure Differential Terms

Equation Va.2.10 includes five pressure differential terms for two-phase flow which are similar to the pressure differential terms for single-phase flow defined in Equation IIIa.3.43 (with $\Delta P_{shaft} = 0$). At steady state, $\Delta P_{inertia} = 0$ and Equation IIIa.3.43 simplifies to:

$$\left(\frac{dP}{ds}\right)_{stat} + \left(\frac{dP}{ds}\right)_{acc} + \left(\frac{dP}{ds}\right)_{fric} + \left(\frac{dP}{ds}\right)_{grav} = 0 \quad \text{Va.2.13}$$

where the terms are differentiated with respect to s , the element of length as shown in Figure Va.2.2, not to be confused with the slip ratio, S . Let's now evaluate each term in Equation Va.2.13.

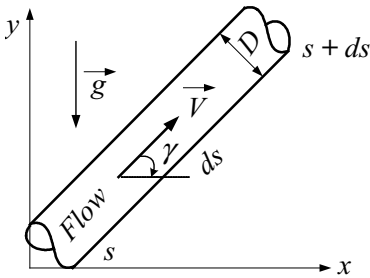


Figure Va.2.2. Steady-state flow of a two-phase mixture in a pipe

Static pressure gradient, $(dP/ds)_{stat}$ if integrated over a finite length in the flow path gives the total pressure drop from inlet (point i) to exit (point e):

$$\int_i^e \left(\frac{dP}{ds} \right)_{stat} ds = P_e - P_i. \quad \text{Va.2.14}$$

Pressure gradient due to acceleration is given by:

$$\left(\frac{dp}{ds} \right)_{acc} = \frac{1}{A} \frac{d(\dot{m}V)}{ds} = \frac{1}{A} \frac{d[(\rho VA)V]}{ds} = \frac{d}{ds} \left(\frac{G^2}{\rho'} \right) \quad \text{Va.2.15}$$

The derivative can be carried out based on the simplification made for the mixing cup density. For example, if velocities of both phases are uniform across the channel, we may substitute for V_g and V_f from $V_g = G_g/\alpha\rho_g = XG/\alpha\rho_g$ and $V_f = (1 - X)G/(1 - \alpha)\rho_f$ in the relation for mixing cup density to get;

$$\frac{1}{\rho'} = \frac{1 - X^2}{(1 - \alpha)\rho_f} + \frac{X^2}{\alpha\rho_g} \quad \text{Va.2.16}$$

Substituting for ρ' from Equation Va.2.16 into Va.2.15 and carrying out the derivative, we find:

$$\begin{aligned} \left(\frac{dP}{ds} \right)_{acc} = G^2 & \left[-\frac{2(1 - X)^2 v_f}{(1 - \alpha)} + \frac{2Xv_g}{\alpha} \right] \left(\frac{dX}{ds} \right) + G^2 \left[\frac{(1 - X)^2 v_f}{(1 - \alpha)^2} + \frac{X^2 v_g}{\alpha^2} \right] \left(\frac{d\alpha}{ds} \right) + \\ & G^2 \left[\frac{X^2}{\alpha} \frac{\partial v_g}{\partial P} \right] \left(\frac{dP}{ds} \right) \end{aligned} \quad \text{Va.2.17}$$

This derivation applies to separated flow. For HEM, the mixing cup density is calculated from $1/\rho' = v = (1 - X)v_f + Xv_g$. Substituting this relation in Equation Va.2.15 and using the equal phase velocity assumption, we get:

$$\left(\frac{dP}{ds} \right)_{acc} = G^2 \frac{d}{ds} [v_f + Xv_{fg}] = G^2 \frac{d}{ds} \left[X \frac{\partial v_{fg}}{\partial P} \frac{dP}{ds} + v_{fg} \frac{dX}{ds} \right] \quad \text{Va.2.18}$$

Neglecting the compressibility of liquid (i.e., setting $\partial v_f / \partial P = 0$), we find $(dP/ds)_{acc}$ for HEM as:

$$\left(\frac{dP}{ds} \right)_{acc} = G^2 \left[X \frac{\partial v_g}{\partial P} \frac{dP}{ds} + v_{fg} \frac{dX}{ds} \right] \quad \text{Va.2.19}$$

Pressure gradient due to friction for two-phase flow is similar to friction pressure drop for single-phase flow. For example, suppose a mixture of water and steam is flowing in a heated pipe of diameter D and length L at the mass flow rate of \dot{m} . The friction pressure drop for the two-phase mixture is obtained from:

$$\Delta P_{tp} = f_{tp} \frac{L}{D} \frac{\dot{m}^2}{2\rho_{tp} A^2} \quad \text{Va.2.20(a)}$$

where subscript tp stands for two-phase. To find f_{tp} , we now assume a case that *only water* is flowing in the same pipe at the same mass flow rate as the mixture of water and steam:

$$\Delta P_{sp} = f_{sp} \frac{L}{D} \frac{\dot{m}^2}{2\rho_{sp} A^2} \quad \text{Va.2.20(b)}$$

where sp stands for single-phase, hence, $\rho_{sp} = \rho_f$. Dividing Equation Va.2.20(a) by Va.2.20(b) we get:

$$\frac{\Delta P_{tp}}{\Delta P_{sp}} = \phi = \frac{f_{tp}}{f_{sp}} \frac{\rho_{sp}}{\rho_{tp}} \quad \text{Va.2.21}$$

This ratio is referred to as the *two-phase friction multiplier*. Substituting for $f_{tp}/\rho_{tp} = \phi(f_{sp}/\rho_{sp})$ from Equation Va.2.21 in Equation Va.2.20(a), we find the two-phase friction pressure drop as:

$$\Delta P_{tp} = \phi f_{sp} \frac{L}{D} \frac{\dot{m}^2}{2\rho_{sp} A^2} \quad \text{Va.2.22}$$

For homogeneous equilibrium conditions assuming $f_{tp} = f_{sp}$, the two-phase friction multiplier becomes:

$$\phi = \frac{\rho_{sp}}{\rho_{tp}} = \frac{v_{tp}}{v_{sp}} = [1 + X \frac{v_{fg}}{v_f}] \quad \text{Va.2.23}$$

This derivation was for a heated pipe. If the mixture is flowing in a pipe that is being cooled resulting in steam condensation, the comparison is made with *only steam* flowing in the pipe (i.e., $\rho_{sp} = \rho_g$).

Example Va.2.7. Derive alternative relations for the two-phase friction multiplier.

Solution: Rather than assuming equal single-phase and two-phase friction factors, let's substitute for friction factors in turbulent flow from Equation IIIb.3.6. In this case, Equation Va.2.23 becomes:

$$\phi = \frac{f_{tp}}{f_{sp}} \frac{\rho_{sp}}{\rho_{tp}} = \frac{0.184 / \text{Re}_{tp}^{0.2}}{0.184 / \text{Re}_{sp}^{0.2}} \frac{v_{tp}}{v_{sp}} = \left(\frac{\mu_{tp}}{\mu_{sp}} \right)^{0.2} \frac{v_{tp}}{v_{sp}}$$

The two-phase to single-phase viscosity ratio may be evaluated based on correlations by McAdams, Cichitti, or Dukler:

$$\left(\frac{\mu_{tp}}{\mu_{sp}} \right)_{\text{McAdams}} = [1 + X \left(\frac{\mu_f}{\mu_g} - 1 \right)]^{-1}; \quad \left(\frac{\mu_{tp}}{\mu_{sp}} \right)_{\text{Cichitti}} = [1 + X \left(\frac{\mu_g}{\mu_f} - 1 \right)];$$

$$\left(\frac{\mu_{tp}}{\mu_{sp}} \right)_{\text{Dukler}} = [1 + \beta \left(\frac{\mu_g}{\mu_f} - 1 \right)]$$

Reddy has recommended a relation similar to Equation Va.2.23:

$$\phi = 1 + X(v_{fg} / v_f)C \quad \text{Va.2.24}$$

where $C = C'X^{-0.175}G^{-0.45}$. If $P > 600$ psia then $C' = 1.02$ otherwise, $C' = 0.357[1 + (P/P_{critical})]$. In this relation, mass flux G , is in $\text{Mlbm/ft}^2\cdot\text{h}$. This correlation is valid for vertical upflow in tubes of 0.2 to 0.6 inches in diameter and 5 to 100 inches in length. The range for mass flux is 0.35 to 3.3 $\text{Mlbm/ft}^2\cdot\text{h}$. The advantage of Reddy's correlation is that it also accounts for the effect of mass flux.

A more recent correlation based on a vast bank of data is suggested by Friedel:

$$\phi = C_1 + \frac{3.24C_2C_3}{\text{Fr}^{0.045}\text{We}^{0.035}}$$

where Fr and We are the Froude and Weber numbers. The Froude number, the ratio of inertial to gravity force (Table A.I.6) is given as:

$$\text{Fr} = \frac{V^2}{gL} = \frac{\dot{m}}{\rho^2 gD}$$

and the Weber number, the ratio of inertial to surface tension force, is given as:

$$\text{We} = \frac{\rho VD^2}{\sigma} = \frac{(G_f + G_g)^2 D}{\rho\sigma}$$

where $\rho = 1/v = v_f + Xv_{fg}$. Constants C_1 , C_2 , and C_3 are related to steam quality and two-phase properties:

$$C_1 = (1 - X)^2 + X^2 \frac{\rho_f}{\rho_g} \frac{f_{sp,g}}{f_{sp,f}}, \quad C_2 = X^{0.78}(1 - X)^{0.24}, \quad \text{and}$$

$$C_3 = \left(\frac{\rho_f}{\rho_g}\right)^{0.91} \left(\frac{\mu_g}{\mu_f}\right)^{0.19} \left(1 - \frac{\mu_g}{\mu_f}\right)^{0.7}$$

Calculating the two-phase friction multiplier from any of the above relations, the frictional pressure gradient, $(dP/ds)_{fric}$, from Equation Va.2.22 can therefore be expressed as:

$$\left(\frac{dP}{ds}\right)_{fric} = \phi f_{sp} \frac{1}{D} \frac{G^2}{2\rho_{sp}} \quad \text{Va.2.25}$$

Pressure gradient due to gravity is given by:

$$\left(\frac{dP}{ds}\right)_{grav} = \rho g \sin \gamma = \frac{1}{v} \sin \gamma g = \frac{g \sin \gamma}{v_f [1 + X(v_{fg} / v_f)]} \quad \text{Va.2.26}$$

2.5. Static Pressure Gradient, HEM

We now can find $(dP/ds)_{stat,HEM}$ if we substitute for various pressure gradient terms into Equation Va.2.13. The result depends on whether we use Equation Va.2.17 or Va.2.19 to represent $(dP/ds)_{acc}$. If we use Equation Va.2.19, which is applicable to HEM, we find:

$$-\left(\frac{dP}{ds}\right)_{stat} = \frac{\phi f_{sp} \frac{1}{D_h} \frac{G^2}{2\rho_{sp}} + G^2 v_{fg} \frac{dX}{ds} + \rho g \cos \gamma}{1 + G^2 X \frac{\partial v_g}{\partial P}} \quad \text{Va.2.27}$$

where ϕ for HEM is given by Equation Va.2.23. We also used D_h so that Equation Va.2.15 is applicable to channels other than pipes and tubes. We may now integrate Equation Va.2.27 for the special case of a uniformly heated channel of length L and hydraulic diameter D_h . At the channel inlet (i) we have $s_i = 0$ and at the channel exit (e) we have $s_e = L$. In this integration, we assume saturated single-phase liquid enters the channel (i.e., $X_i = 0$). Since the channel is heated uniformly, we can make a change of variable from s to X according to:

$$\frac{dX}{ds} = \frac{X_e - X_i}{L}$$

so that $ds = (L/X_e)dX$. Note that the gas compressibility is generally very small, $|v_g/P| \ll 1$, which greatly simplifies the integration of Equation Va.2.27. Replacing ρ with $\rho = [v_f + Xv_{fg}]^{-1}$ and assuming that f_{sp} and v_{fg}/v_f remain constant, we integrate Equation Va.2.15 from the inlet to any point along the channel:

$$(P_i - P) = f_{sp} \frac{L}{D_e} \frac{G^2 v_f}{2} \left[1 + \left(\frac{v_{fg}}{v_f}\right) \frac{X}{2}\right] + G^2 v_{fg} X + \frac{gL \cos \gamma}{v_{fg} X} \ln \left[1 + X \left(\frac{v_{fg}}{v_f}\right)\right] \quad \text{Va.2.28}$$

where the quality and thermodynamic properties are evaluated at system pressure and $D_e = D_h$ is the equivalent hydraulic diameter.

Example Va.2.8. Water at 70 bar, 210 C, and a mass flow rate of 0.1 kg/s enters a uniformly heated vertical tube of diameter 2 cm and length 4 m. The applied heat flux is 600 kW/m². Find a) length of the tube over which water remains subcooled, b) pressure drop for the subcooled section, and c) total pressure drop.

Solution: At $P = 70$ bar; $T_{sat} = 285.9$ C, $h_f = 1267$ kJ/kg, $h_{fg} = 1505$ kJ/kg. $h_i(70$ bar & 210 C) $\cong 900$ kJ/kg.

a) Since $T_i < T_{sat}$, subcooled water enters the heated channel. The length of the single-phase or pre-heating section is found from a heat balance:

$$\dot{q}''(\pi d L_f) = \dot{m}(h_f - h_i)$$

Substituting values: $600[\pi \times (2/100) \times L_f] = 0.1[1267 - 900]$

Solving for L_f , we find: $L_f \cong 1$ m.

Water then boils over the remaining 3 m of the tube. To find the exit quality we write the energy balance over the boiling length:

$$600[\pi \times (2/100) \times (L - L_f)] = 0.1[h_e - 1267]$$

Substituting values we find: $h_e = 2398$ kJ/kg

$$X_e = (h_e - h_f)/h_{fg} = (2398 - 1267)/1505 = 0.75$$

b) Over the single-phase section, we find pressure drop due to friction, acceleration, and gravity:

$$\text{At } T_{sat} = 285.9 \text{ C; } v_f = 0.00135 \text{ m}^3/\text{kg}, v_{fg} = 0.026 \text{ m}^3/\text{kg}, \mu_f = 0.943\text{E-}4 \text{ N}\cdot\text{s}/\text{m}^2$$

$$\text{Tube flow area is: } A_f = \pi \times 0.02^2/4 = 3.14\text{E-}4 \text{ m}^2$$

$$\text{Thus, the mass flux is: } G = 0.1/3.14\text{E-}4 = 318.3 \text{ kg}/\text{m}^2\cdot\text{s}$$

$$(P_i - P_e)_{fric} = f_{sp} (L_f / D_e) v_f \dot{m}^2 / (2A_f^2)$$

To find f_{sp} , we must calculate the Reynolds number:

$$\text{Re}_{sp} = \dot{m} D_e / \mu A = 0.1 \times 0.02 / [0.943\text{E-}4 \times 3.14\text{E-}4] = 67,510 \text{ (Flow is turbulent)}$$

$$f_{sp} = 0.184/\text{Re}^{0.2} \cong 0.0199$$

The friction pressure drop over the single-phase section is found as:

$$(\Delta P)_{fric,sp} = \left(f_{sp} \frac{L_f}{D_e} \right) \frac{v_f \dot{m}^2}{2A_f^2} = \left(0.0199 \frac{1}{0.02} \right) \frac{0.00135 \times 0.1^2}{2 \times 9.87\text{E-}8} = 0.068 \text{ kPa}$$

$$(\Delta P)_{acc,sp} = G^2(v_f - v_i) = (318.3)^2 \times (0.00135 - 0.00117) = 0.018 \text{ kPa}$$

$$(\Delta P)_{grav,sp} = g L_f \cos \beta / [(v_i + v_f)/2] = 9.81 \times 1 / [(0.00117 + 0.00135)/2] = 7.8 \text{ kPa.}$$

c) We now find pressure drop due to friction, acceleration, and gravity over the two-phase section using the homogenous model:

$$(\Delta P)_{fric,tp} = f_{sp} \frac{L_b}{D_e} \frac{G^2 v_f}{2} \left[1 + \left(\frac{v_{fg}}{v_f} \right) \frac{X}{2} \right] =$$

$$0.0199 \frac{(4-1)}{0.02} \frac{(318.3)^2 \times 0.00135}{2} \left[1 + \left(\frac{0.026}{0.00135} \right) \frac{0.75}{2} \right] = 1.68 \text{ kPa}$$

$$(\Delta P)_{acc,tp} = G^2 v_{fg} X = (318.3)^2 \times 0.026 \times 0.75 = 1.97 \text{ kPa}$$

$$(\Delta P)_{grav,tp} = gL_b \cos \gamma \ln[1 + X(\frac{v_{fg}}{v_f})]/(v_{fg} X) =$$

$$9.81 \times 3 \times \ln[1 + 0.75(\frac{0.026}{0.00135})]/(0.026 \times 0.75) = 4.1 \text{ kPa}$$

$$\Delta P_{total} = (0.068 + 1.68) + (0.018 + 1.97) + (7.8 + 4.1) = 15.6 \text{ kPa}$$

Comment: Calculation of the properties at the inlet pressure is a reasonable assumption in this problem since the pressure drop is a small percentage of the inlet pressure ($\approx 0.2\%$). In general, an iterative solution may be required to find properties at an average pressure.

2.6. Static Pressure Gradient, Separated Flow Model (SFM)

To obtain $(dP/ds)_{stat}$ for the separated flow model, we substitute for various pressure gradient terms into Equation Va.2.13. For $(dP/ds)_{acc}$, we substitute from Equation Va.2.17. If we integrate the resulting equation between the channel inlet at $s_i = 0$ and any location along the channel, we find the gradient for static pressure as:

$$(P_i - P) = f_{sp} \frac{1}{D_h} \frac{G^2}{2\rho_{sp}} \int_{s_i}^s \phi ds + G^2 \left[\frac{(1-X)^2}{(1-\alpha)\rho_f} + \frac{X^2}{\alpha\rho_g} \right]_{X_i}^X + \int_{s_i}^s g \sin \gamma [(1-\alpha)\rho_f + \alpha\rho_g] ds$$

Va.2.29

The acceleration pressure drop, being a perfect differential, depends only on the end points and is independent of the flow path. Expressing mixture property variations as a function of s , we can integrate the first and the third terms of Equation Va.2.29. Similar to the case of HEM, for a special case of uniformly heated channel, a change of variable can be introduced by replacing the differential length, ds , with dX , the differential quality. Substituting the change of variable into Equation Va.2.29, for the special case of uniformly heated channels with $X_i = \alpha_i = 0$, we find:

$$(P_i - P_e) = f_{sp} \frac{1}{D_h} \frac{G^2 L}{2\rho_{sp}} \frac{\int_0^{X_e} \phi dX}{X_e} + \frac{G^2}{\rho_f} \left[\frac{(1-X_e)^2}{(1-\alpha_e)} + \frac{X_e^2 \rho_f}{\alpha_e \rho_g} - 1 \right] \\ + \frac{gL \cos \gamma}{X_e} \int_0^{X_e} [(1-\alpha)\rho_f + \alpha\rho_g] dX$$

This equation can alternatively be written as:

$$(P_i - P_e) = f_{sp} \frac{1}{D_h} \frac{G^2 L}{2\rho_{sp}} (C_1) + \frac{G^2}{\rho_f} (C_2) + gL \rho_f \sin \beta (C_3)$$

Va.2.30

Constants C_1 , C_2 , and C_3 may be obtained from the Martinelli-Nelson or the Thom correlation. Figure Va.2.3 gives the values of constants C_1 , C_2 , and C_3 according to Thom's correlation.

Example Va.2.9. Solve Example Va.2.8 based on the Separated Flow Model.

Solution: The same total pressure drop is applicable in the preheating section for both HEM and SFM. For the boiling section, we use Figure Va.2.3 for $(\Delta P)_{fric}$, $(\Delta P)_{acc}$ and $(\Delta P)_{grav}$ respectively. These result in: $C_1 \approx 8.5$, $C_2 \approx 14$, and $C_3 \approx 0.24$.

Substituting the constants in Equation Va.2.30, we find:

$$(\Delta P)_{fric,tp} = f_{sp} \frac{1}{D_h} \frac{G^2 L_b}{2\rho_{sp}} (C_1) =$$

$$0.0199 \frac{1}{0.02} \frac{(318.3)^2 \times 3 \times 0.00135}{2} \times 8.5 = 1.74 \text{ kPa}$$

$$(\Delta P)_{acc,tp} = [G^2 / \rho_f] (C_2) = (318.3)^2 \times 0.00135 \times 7.8 = 1.90 \text{ kPa}$$

$$(\Delta P)_{grav,tp} = g L_b \rho_f \cos \beta (C_3) = 9.81 \times (3/0.00135) \times 0.24 = 5.2 \text{ kPa}$$

Therefore, total pressure drop over the tube is found as:

$$\Delta P_{total} = (0.068 + 1.74) + (0.018 + 1.90) + (7.8 + 5.2) = 16.7 \text{ kPa}$$

This result is in reasonable agreement with the result obtained from the homogeneous model in Example Va.2.8.

3. Two Phase Critical Flow

Similar to the critical flow of compressible, single-phase fluid, as discussed in Chapter IIIc, flow of a two-phase mixture in a channel may also become critical. For cases where saturated water is contained under pressure, opening of a valve or sudden burst of a connecting pipe results in expulsion of the tank inventory. In such a case, the saturated water may partially flash to steam as it approaches the break area, which is at much lower pressure. We will seek an analytical solution for the two-phase critical flow of water and steam under the following conditions; flow is homogeneous ($V_f = V_g$), thermodynamic equilibrium exists between the phases ($T_f = T_g$), and the process is isentropic. These assumptions lead to the determination of critical flow for HEM. Maintaining the assumption of an isentropic process, analytical solutions are also extended to two equilibrium non-homogeneous cases. The first case uses a slip ratio calculated from either the Moody or the Fauske model. The second case uses models from Burnell and Henry-Fauske. These cases are summarized in Table Va.3.1 and then discussed in detail next.

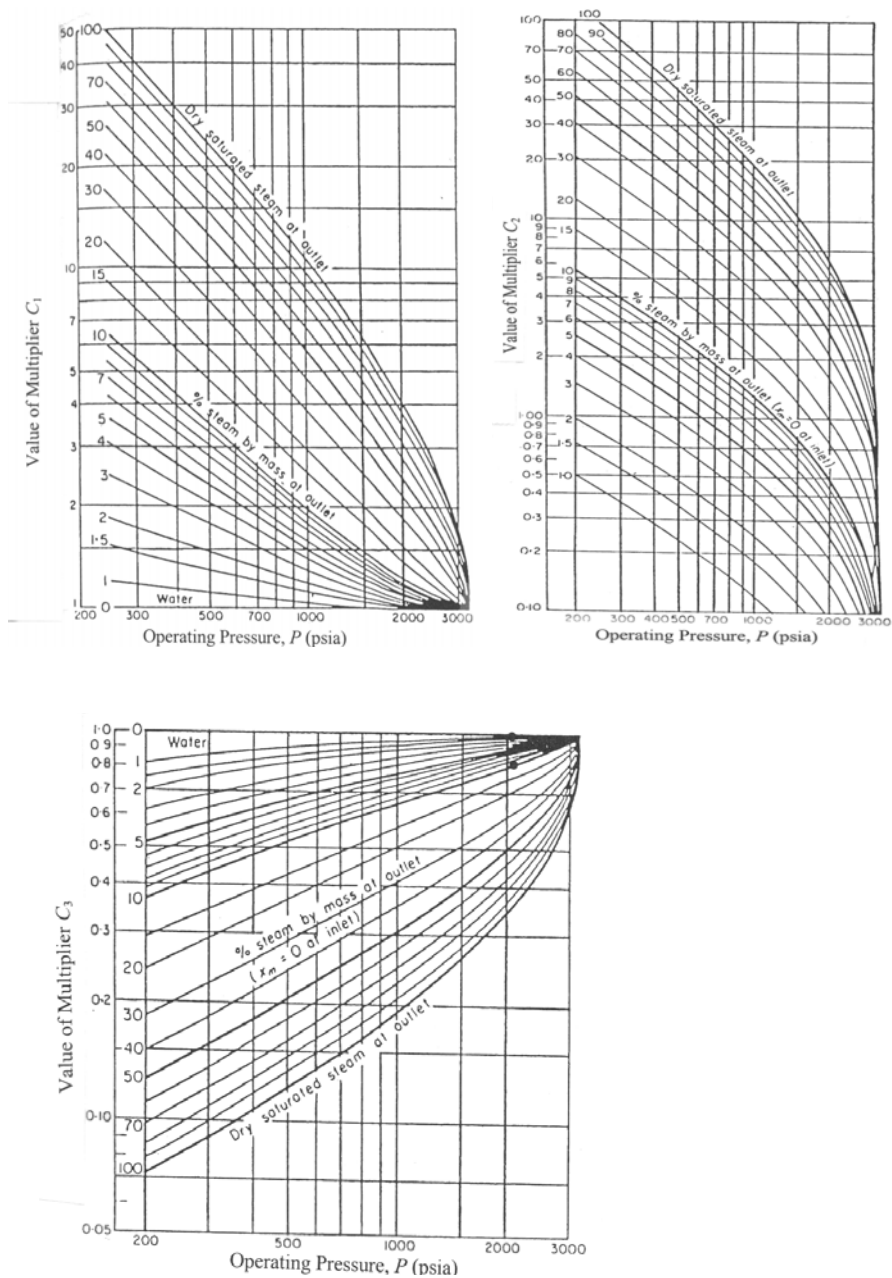


Figure Va.2.3. Coefficients for frictional, acceleration, and gravitational pressure drop (Thom 1964)

Table Va.3.1. Various critical flow models

	Homogenous Equilibrium	Equilibrium Non-homogenous		Homogenous Non-equilibrium
	(HEM)	(Moody Model)	(Fauske Model)	(Henry-Fauske Model)
$s_f = s_g$	Yes	Yes	Yes	Yes
$V_f = V_g$	Yes	No	No	Yes
$T_f = T_g$	Yes	Yes	Yes	No

3.1. Two-Phase Critical Flow (Homogeneous Equilibrium Flow)

This model is based on solving the conservation equations of mass and energy, in conjunction with the equations of state, under steady-state condition. The conservation equation of mass becomes:

$$\dot{m} = \rho VA = \text{constant} \quad \text{IIa.5.2}$$

where ρ is the mixture density. Note that no distinction is made between V_f and V_g . The energy equation for the mixture, using the upstream stagnation condition (shown with subscript o), becomes:

$$h_o = h + V^2/2 \quad \text{IIIc.2.1}$$

We may substitute for velocity from Equation IIIc.2.1 into IIa.5.2 and write the result in terms of mass flux:

$$G = \rho V = \frac{[2(h_o - (1-x)h_f - xh_g)]^{1/2}}{(1-x)v_f + xv_g} \quad \text{Va.3.1}$$

where we also made use of the equation of state for $h = (1-x)h_f + xh_g$. If we substitute for quality calculated from the mixture entropy

$$x = \frac{s_o - s_f}{s_g - s_f}$$

into Equation Va.3.1, we obtain a relation that is solely a function of pressure. By iteration with the steam tables, we can then find a pressure that maximizes mass flux. Alternatively, we may express all thermodynamic properties and their derivatives as functions of pressure (examples of such functions are given in Appendix II, Table A.II.3). To find the pressure that maximizes mass flux, we then substitute these functions into Equation Va.3.1, take the derivative of G and set it equal to zero.

3.2. Two-Phase Critical Flow (Equilibrium Non-homogeneous Flow)

This is similar to the homogenous flow, but we must account for $V_f \neq V_g$. The mass balance becomes:

$$G = \frac{W}{A} = \frac{W_g / x}{A_g / \alpha} = \left(\frac{\alpha}{x} \right) \frac{W_g}{A_g} = \left(\frac{\alpha}{x} \right) \frac{V_g}{v_g} = \left(\frac{1 - \alpha}{1 - x} \right) \frac{V_f}{v_f} \quad \text{Va.3.2}$$

The energy equation can be partitioned to account for the contribution of each phase as follows:

$$h_o = (1 - x) \left(h_f + \frac{V_f^2}{2} \right) + x \left(h_g + \frac{V_g^2}{2} \right) \quad \text{Va.3.3}$$

To find G , we first substitute for void fraction from Equation Va.1.3. We then find V_f and V_g in terms of G from Equation Va.3.1, substitute them into Equation Va.3.2, and solve for G to obtain:

$$G = \rho^* \sqrt{2 \left[h_o - h_f - (s_e - s_f) \frac{h_{fg}}{s_{fg}} \right]} \quad \text{Va.3.4}$$

where in Equation Va.3.4, ρ^* is given by:

$$\frac{1}{\rho^*} = \left[S(1 - x)v_f + xv_g \right]^2 \left[\frac{1 - x}{S^2} + x \right] \quad \text{Va.3.5}$$

Note that in Equation Va.3.5 the slip ratio S as given by Equation Va.1.1 should not be confused with s , the specific entropy. We now need to determine the slip ratio such that the mass flux is maximized. There are two models for this, as discussed next.

The Moody Model. In this model, the mass flux given by Equation Va.3.4 is maximized by setting the derivative of the kinetic energy with respect to slip ratio equal to zero, $\partial K.E. / \partial S = 0$:

$$\frac{\partial}{\partial S} \left[\frac{(1 - x)V_f^2}{2} + \frac{xV_g^2}{2} \right] = 0$$

Taking the derivative and setting it equal to zero, we obtain:

$$S_{\text{Moody}} = (v_g/v_f)^{1/3}$$

The Moody model compares well with data in the range of 14.7 – 400 psia.

The Fauske Model. In this model, the mass flux given by Equation Va.3.4 is maximized by setting the derivative of the flow momentum, with respect to slip ratio, equal to zero:

$$\frac{\partial}{\partial S} [(1-x)V_f + xV_g] = 0$$

This maximizes the axial pressure gradient for a given flow rate and steam quality. Substituting from Equation Va.3.1 for V_f and V_g , introducing Equation Va.1.3 for void fraction, and applying the chain rule for differentiation results in:

$$S_{Fauske} = (v_g/v_f)^{1/2}$$

Example Va.3.1. Derive the critical condition for annular flow using the conservation equation for mass and momentum.

Solution: We use the thermodynamic equilibrium and non-homogenous assumption, $V_f \neq V_g$. The combined continuity and momentum equations result in.

$$d(\dot{m}_f V_f + \dot{m}_g V_g) + AdP = 0$$

Substituting from Equation V.3.2 for V_f and V_g in terms of G , we find:

$$dP + d \left[\frac{(1-x)^2}{1-\alpha} v_f G^2 + \frac{x^2}{\alpha} v_g G^2 \right] = 0$$

Solving for G , we obtain:

$$G = \sqrt{-(dP/dv)_s} \quad \text{Va.3.6}$$

where specific volume in Equation Va.3.6 is given by:

$$v = \frac{(1-x)^2}{1-\alpha} v_f + \frac{x^2}{\alpha} v_g \quad \text{Va.3.7}$$

Having found the slip ratio by the Moody or the Fauske method, we express the thermodynamic properties and their derivatives in terms of pressure and substitute into Equation IIIa.3.6-2. For example, for the Fauske model, we use Equations IIIa.3.6-2, Va.1.3 (with $S = \sqrt{v_g/v_f}$), and Va.3.6 to obtain (Nahavandi):

$$\frac{-1}{G^2} = \left\{ [(1-x+xS)x] \frac{dv_g}{dP} + [(2xS-2S-2S^2x+S^2)v_f + (1+2xS-2x)v_g] \frac{dx}{dP} \right\}_s \quad \text{Va.3.8}$$

Nahavandi then plotted Equation Va.3.8 for mass flux as a function of the stagnation enthalpy and pressure, as shown in Figure Va.3.1.

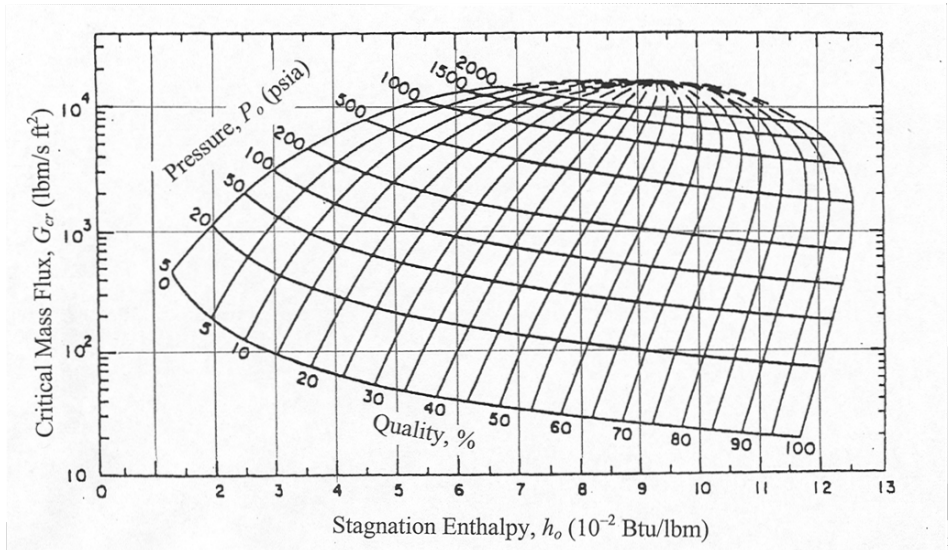


Figure Va.3.1. Critical mass flux versus stagnation enthalpy and pressure (Fauske)

Two observations can be made from Figure Va.3.1. First, the higher the source stagnation pressure, the higher the mass flux at the same steam quality. Second, for a given pressure, the critical mass flux increases with decreasing quality. Hence, as expected, the higher the liquid content, the higher the critical mass flux. For example, a stagnation pressure of 200 psia and $x = 75\%$ corresponds to the same mass flux of $1000 \text{ lbm/s}\cdot\text{ft}^2$ as a stagnation pressure of only 50 psia but steam quality of $x = 11\%$.

Example Va.3.2. Calculate the maximum mass flux for the flow of saturated water and steam at 2000 psia and enthalpy of 800 Btu/lbm, according to the Fauske model.

Solution: From Figure Va.3.1 for $P_o = 2000 \text{ psia}$ and $h_o = 800 \text{ Btu/lbm}$, we find $G_{max} \approx 11,000 \text{ lbm/s}\cdot\text{ft}^2$.

Example Va.3.3. A discharge line is connected to a pressurized tank, which contains saturated water at 1000 psia. The discharge line is equipped with a safety valve, having a flow area of 1.4 in^2 . We now open the valve. Find the maximum flow rate that leaves the tank. Assume $C_d = 1$.

Solution: Since the discharge valve opens to atmosphere, the flow is definitely choked. The maximum flow rate occurs at the moment that pressure is still at 1000 psia and just begins to drop. Thus from Figure Va.3.1 we find the mass flux as $G_{cr} = 10,100 \text{ lbm/s}\cdot\text{ft}^2$ and the mass flow rate as:

$$\dot{m} = 0.8(1.4/144) \times 10,100 = 78.5 \text{ lbm/s}$$

As for the Moody model, if we substitute $S = (v_g/v_f)^{1/3}$ into Equation Va.3.5 and then use the result in Equation Va.3.4, we find the following relation for the critical mass flux:

$$G^2 = \frac{2[h_o - xh_g - (1-x)h_f]}{v_g^2[x + (1-x)(v_f/v_g)^{2/3}]^3} \quad \text{Va.3.9}$$

Similar to the Fauske mode, mass flux from the Moody model is maximized and plotted for various values of the source stagnation pressure and enthalpy, as shown in Figure Va.3.2.

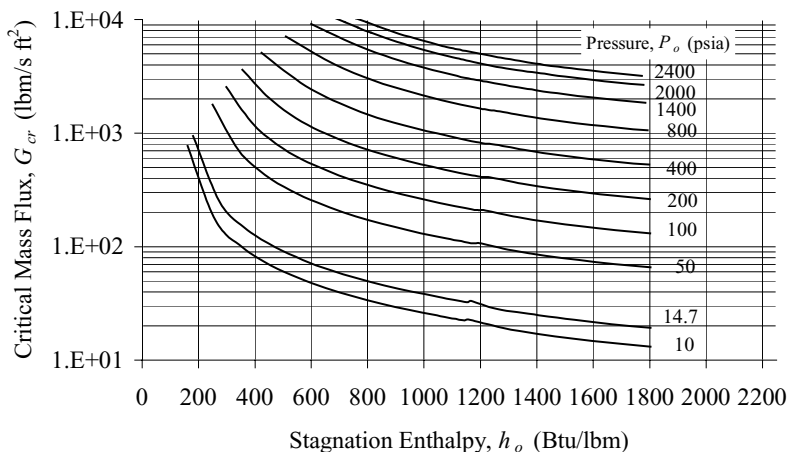


Figure Va.3.2. Critical mass flux versus stagnation enthalpy and pressure (Moody)

3.3. Two-Phase Critical Flow (Homogeneous Non-equilibrium Flow)

Earlier we showed that the existence of analytical solutions was primarily due to the isentropic process assumption. This assumption implies that the length and diameter of the flow path should be such that the frictional effects are minimized. Thermodynamic equilibrium in turn requires a reasonably long flow path to allow the phases to reach equilibrium. As such, the shorter the flow path, the higher the flow rate since less liquid would flash to steam. Fauske has identified three ranges for the L/D ; 0–3, 3–12, and 12–40 (Figure Va.3.3). For $0 < L/D < 3$, the flow path is too short for the phases to reach equilibrium while for $12 < L/D < 40$, the flow path allows the phases to reach equilibrium. Therefore, for the L/D range of 0–3, the critical flow can be estimated from such equations as IIIa.3.46, IIIb.3.14, IIIb.4.3, and IIIb.4.4:

$$G = 0.61\sqrt{2\rho_f(P_o - P_{cr})} \quad \text{Va.3.10}$$

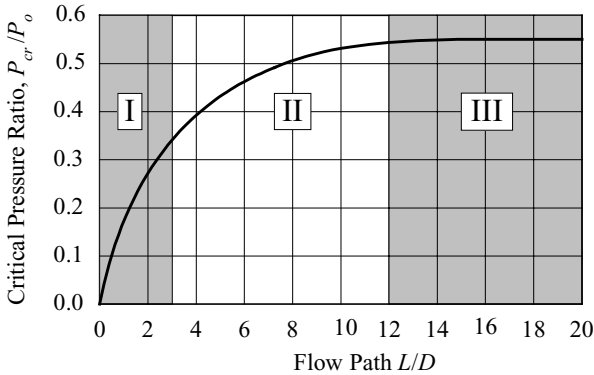
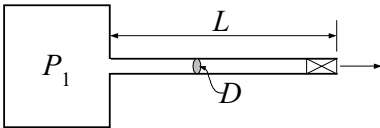


Figure Va.3.3. Critical pressure ratio versus flow path length over diameter (Fauske)

where in Equation Va.3.10, a discharge coefficient of 0.61 is accounted for. In this equation, P_{cr} stands for the critical pressure. According to Fauske, the value of P_{cr} depends on the value of the L/D ratio as shown in Figure Va.3.2. Note that, for an orifice, ($L/D = 0$), P_{cr} is the actual back pressure.

In conclusion, Region I in Figure Va.3.3 is applicable to non-equilibrium flow regimes and Region III of this figure is well suited for the HEM, since the sufficient flow path length allows the phases to reach thermal equilibrium. Note that Figure Va.3.1 would under-predict flow in Regions I and II of Figure Va.3.3.

Example Va.3.4. A pressurized tank containing saturated liquid at 2000 psia is connected to atmosphere by a 0.5 in diameter pipe. A frictionless valve on the pipe is suddenly opened. Find the maximum mass flux for three different pipe lengths of $L_1 = 0.1$ ft, $L_2 = 0.25$ ft, and $L_3 = 1$ ft at this pressure.



Solution:

$$\text{Find } G = 0.61 \sqrt{2 \times 32.2 \times 38.98 \times 144 (P_o - P_{cr})} = 366.78 \sqrt{(P_o - P_{cr})}$$

Next, we need to find $P_o - P_{cr}$, having L/D . Since $D = 0.5/12 = 0.042$ ft $L_1/D = 0.1/0.042 = 2.4$, $L_2/D = 6$, and $L_3/D = 24$.

We now use Figure Va.3.3:

For $L_1/D = 2.4$, we find $P_{cr}/P_o = 0.30$. Thus,

$$G = 366.78 \sqrt{(2000 - 600)} = 13,720 \text{ lbm/s} \cdot \text{ft}^2.$$

This is in good agreement with G from Figure Va.3.1 at

$P_o = 600$ psia and $h_o = h_f(2000) = 672$ Btu/lbm.

For $L_2/D = 6.0$, we find $P_{cr}/P_o = 0.48$. Thus,

$$G = 366.78\sqrt{(2000 - 960)} = 11,830 \text{ lbm/s}\cdot\text{ft}^2$$

For $L_3/D = 24$, we find $P_{cr}/P_o = 0.55$.

$$\text{Thus, } G = 366.78\sqrt{(2000 - 1100)} = 11,000 \text{ lbm/s}\cdot\text{ft}^2$$

As expected, G_{cr} is over-predicted compared to $G_{cr} \approx 8500 \text{ lbm/s}\cdot\text{ft}^2$ read from Figure Va.3.1 at $P_o = 1100 \text{ psia}$ and $h_o = h_f(2000 \text{ psia}) = 672 \text{ Btu/lbm}$.

Henry (1970) and later Henry-Fauske (1971) analytically derived the relation for two-phase critical mass flux for homogenous non-equilibrium flow, based on the isentropic assumption. This is a reasonable assumption for short flow paths for which the frictional pressure drop due to the wall shear forces is negligible compared to the momentum and pressure gradient terms. The RELAP4 (Moore) and GOTHIC (George) computer codes have tabulated the Henry correlation for various stagnation pressure and enthalpy. These are plotted in Figure Va.3.4.

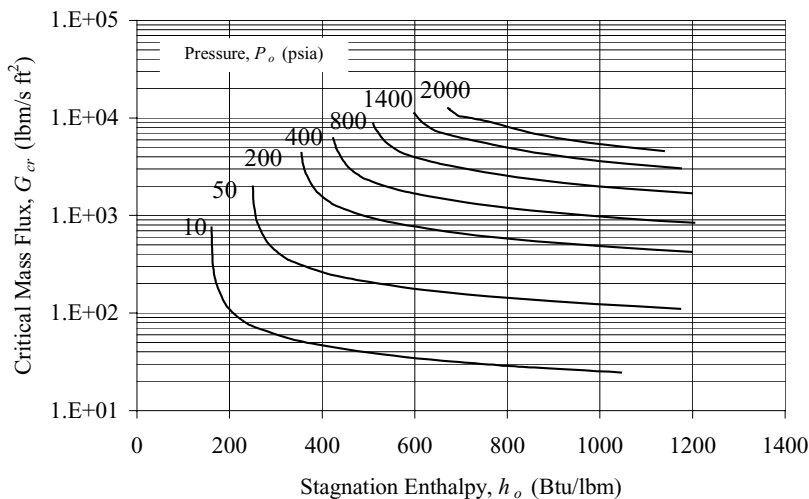


Figure Va.3.4. Critical mass flux versus stagnation enthalpy and pressure (Henry non-equilibrium model)

Example Va.3.5. In Example Va.3.5, find the maximum mass flux for $L_1 = 0.1 \text{ ft}$.

Solution: From Figure Va.3.4 for $P_o = 2000 \text{ psia}$ and saturated water, we find $G_{max} \approx 10,500 \text{ lbm/s}\cdot\text{ft}^2$.

3.4. Two-Phase Critical Flow (Homogeneous Non-equilibrium, Subcooled Fluid)

So far we dealt with saturated water and two-phase mixture. If the pressurized water is subcooled, then the percentage of flashing decreases, resulting in higher mass flow rate. Indeed test data indicates that the higher the degree of subcooling, the higher the critical mass flow rate. The Henry-Fauske correlation is extended to cover subcooled liquid. The extended Henry-Fauske correlation for maximum mass flux is plotted as a function of stagnation enthalpy and pressure in Figure Va.3.5.

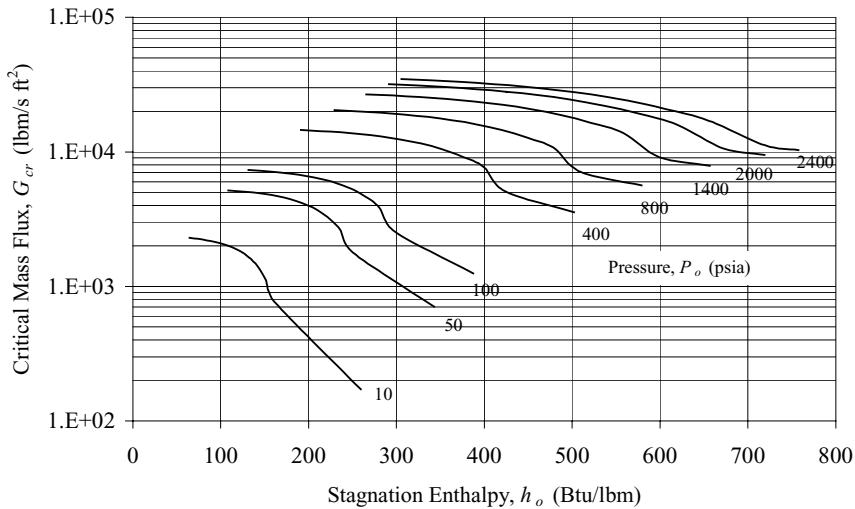


Figure Va.3.5. Critical mass flux versus stagnation enthalpy and pressure (Henry-Fauske model)

Example Va.3.6. A pressurized tank containing subcooled liquid at 2000 psia is connected to atmosphere by a frictionless valve. Find the maximum mass flux for two cases of $h_1 = 400$ Btu/lbm and $h_2 = 600$ Btu/lbm.

Solution: We expect to obtain higher mass flux at lower upstream enthalpy. According to Figure Va.3.5, at a upstream pressure of 2000 psia and enthalpy of 400, the critical mass flux is about 12,000 lbm/s. At the same pressure but enthalpy of 600 Btu/lbm, the critical mass flux is about 10,800 lbm/s.

QUESTIONS

- When does flow quality become equal to the thermodynamic quality?
- What is the slip ratio?
- What is superficial velocity?
- What does the slip ratio signify? What is its value for homogenous flow?
- Does the Zivi model predict data well? Why or why not?
- What is the physical significance of the drift flux model?
- Comparing drift flux and the relative velocity between phases, which one is always larger than the other?
- What is the advantage of the drift flux model compared to other void fraction models?
- Is the drift flux model suited for the annular flow regime?
- What is the purpose of defining a two-phase friction multiplier?
- What is the advantage of Reddy's two-phase friction multiplier?
- Regarding friction pressure drop, what is the distinction between two-phase flow in a heated pipe and in a pipe being cooled down?
- The acceleration pressure gradient, per Equation Va.2.5, is a perfect differential. Hence, it depends only on the end points. Why, then, do we carry out the derivative per Equations Va.2.5 and Va.2.6?
- Why does the critical mass flow rate increase with decreasing steam quality?
- For the exact same conditions, which model predicts higher mass flow rate, the Moody or the Fauske model?
- What is the major difference between the HEM, the Moody model, and the Fauske model?
- Are water and steam more likely to reach equilibrium in a shorter flow path or a longer flow path?
- How do we know if a two-phase flow is choked in a given flow path?

PROBLEMS

1. Consider the annular flow regime in a tube. If the thickness of the liquid film on the tube wall is much smaller than the tube diameter ($\delta \ll D$), show that the void fraction is given by $\alpha = 1 - (4d/D)$.
2. In this problem you are asked to investigate the effect of system pressure and steam quality on void fraction. For this purpose, use Equation Va.1.1, where $S = 1$, and produce a graph of $\alpha = f(x)$. You need to first choose a pressure and plot void fraction as a function of quality, ranging from 0% to 20%. Repeat this for another value for pressure. Choose $P = 14.7$ psia, 500 psia, 1000 psia, 2000 psia, and 3,206 psia. Outline your observations.
3. In this problem you are asked to investigate the effect of slip ratio and steam quality on void fraction. For this purpose, use Equation Va.1.1 where $P = 1000$

psia, and produce a graph of $\alpha = f(x)$. You need to first choose a value for void fraction. Try $S = 1, 2, 3$, and 4. Outline your observations.

4. Plot the density ratio ρ_f/ρ_g for the two-phase flow of water - air and water - steam versus pressure, ranging from 1 psia to 3200 psia. For water - air flow, use a temperature of 80 F (27 C). Outline your observation.

5. A tank is filled with a homogenous mixture of water and steam at thermal equilibrium. The tank pressure is 6.89 MPa. The liquid volume fraction in the tank is 40%. Find the mixture density and static quality. [Ans.: 318 kg/m³ and 0.07].

6. Use the definition of the mixture density and show that for homogenous flow ($S = 1$), $v = (1 - x)v_f + xv_g$.

7. Liquid enters a heated tube at velocity V_f . Derive a relation for the superficial velocity in terms of V_f , X , v_f , and v_g . [Hint: Use $j = [(1 - X)/\rho_f + X/\rho_g]G$ and substitute for ρ_f , ρ_g , and G]. [Ans.: $j = \{1 + (v_g/v_f - 1)X\}V_f$].

8. A BWR plant is operating at steady state, producing 1260 kg/s (1E7 lbm/h) dry, saturated steam for the turbine. Pressure in the vessel is 7 MPa (1000 psia). Feedwater enters the vessel at 150 C (~ 300 F). The average void fraction at the exit of the core is 40%. Assuming a uniform slip ratio of 2 throughout the core, find the recirculation ratio and total rate of heat transfer in the core. [Ans.: 15.476, 2703 MWth].

9. Two-phase mixture flows at a rate of 750 kg/m² s in a vertical tube of diameter 3 cm at 70 bar. Find the flow pattern at a cross section where $X = 10\%$.

10. Use Figure Va.1.1 and find the most likely flow pattern for the following six cases:

Case	G (kg/s m ²)	P (bar)	x	Case	G (kg/s m ²)	P (bar)	x
1	600	35	0.01	4	2600	35	0.01
2	600	75	0.10	5	2600	75	0.10
3	600	180	0.50	6	2600	180	0.50

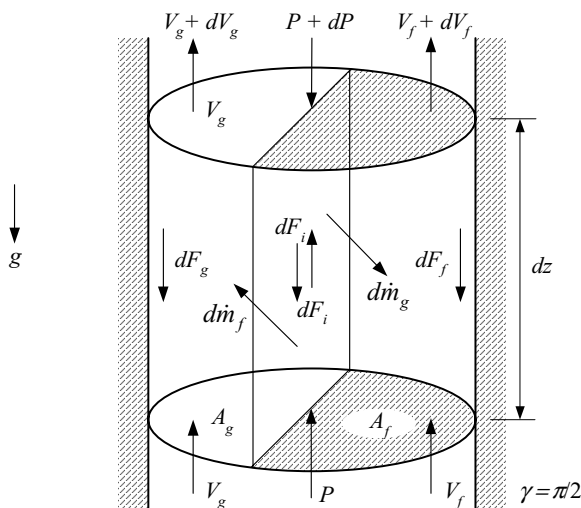
11. Estimate the slip ratio for a two-phase mixture flowing in a channel. The channel pressure is maintained at 1200 psia and at thermal equilibrium. [Ans.: 1.6].

12. A heated channel is operating at 7.5 MPa. Water enters the channel at a rate of 17 kg/s and an inlet subcooling of 18 C. Find the maximum rate of heat transfer that can be transferred to this channel while the void fraction at the channel exit is maintained at 0.8. Ignore pressure drop in the channel.

13. A mixture of water and steam is flowing up a 25 mm diameter channel at a rate of 4500 kg/s m² and temperature of 295 C. Assume thermal equilibrium and find the following items at an elevation where $x = 25\%$: a) void fraction, b) the mixture mixing cup density, c) mixture density using the HEM, d) mixture thermodynamic density.

14. Steam and water flow in a 25 mm tube at 300 C, 3500 kg/m² s, and $X = 0.4$. Use the drift flux model and find α and S . [Ans. 0.68 and 4.7]

15. An element of volume for the separated up-flow of water and steam in a channel is shown in the figure. Use the conservation equation of momentum at steady-state and directly derive Equation Va.2.4.



16. Use $(dP/ds)_{acc}$ according to the HEM and derive ΔP_{acc} for two-phase flow in a uniformly heated channel of length L . [Ans.: $(gL \cos) \ln(1 + X v_{fg}/v_f)/(X v_{fg})$].

17. Derive ΔP_{acc} by applying the momentum equation between inlet and outlet. [Hint: $F = \Delta(\text{momentum flux})$. Use $F = A \Delta P$ and substitute for momentum out = $\dot{m}_f V_f + \dot{m}_g V_g$ and for momentum in = $\dot{m}_i V_i$. Then replace each velocity by mass flow rate divided by ρA and introduce α and x to replace area and mass ratios].

18. In order to integrate the differential pressure drop, we ignored the compressibility of the gaseous phase, (v_g/P). Show the reasonableness of this assumption. Find the magnitude of this term at an operating pressure of 1000 psia (82.75 bar). [Ans.: $-7.57E-8 \text{ ft}^4 \cdot \text{s}^2/\text{lbm}^2$].

19. Consider two-phase flow in a tube of diameter 0.5 in and length 3 ft. For $P = 1000$ psia, $\dot{m} = 0.35$ lbm/s and $X = 50\%$ compare ϕ_{HEM} with ϕ_{Reddy} . [Ans.: $\phi_{HEM} = 10.83$. $\phi_{Reddy} = 12.73$].

20. Consider flow of water in two identical pipes of $D_e = 5$ cm and $L = 3$ m. One pipe is insulated while the other is heated so that $X_o = 0.2$. In both pipes, $P = 100$ bar and $G = 0.3$ kg/s. Compare $(\Delta P_1)_{fric}$ with $(\Delta P_2)_{fric}$.

21. Use the data of the above problem and compare $(\Delta P_1)_{\text{grav}}$ with $(\Delta P_2)_{\text{grav}}$ if $\beta_1 = 0$ and $\beta_2 = 30^\circ$.

22. For the flow of water and steam in a vertical insulated channel, calculate total pressure drop in the channel.

Data: channel diameter: 1 cm, channel length: 3 m, mass flow rate: 0.3 kg/s, pressure: 7.4 MPa, steam quality at inlet: 0.025. [Ans.: 77.7 kPa].

23. Find the total pressure drop for flow of water in a heated vertical tube. The diameter and the length of the tube are 12.7 mm and 1.55 m, respectively. The tube is heated uniformly at a rate of 39 kW. Water enters the tube at a rate of 0.0882 kg/s, temperature of 277 C and pressure of 70 bar. [Ans.: 10.6 kPa].

24. Water enters a uniformly heated vertical tube of diameter 2.5 cm and length 4.5 m. Total heat applied to the tube is 650 kW. Inlet pressure, temperature, and mass flow rate of water are given as 100 bar, 285 C, and 1.5 kg/s, respectively. Find the pre-heating length, exit quality, and various pressure differential terms. [Ans.: $L_f = 1.52$ m, $X_o = 0.22$, $(\Delta P)_{\text{fric},sp} = 5$ kPa, $(\Delta P)_{\text{fric},tp} = 21.73$ kPa, $(\Delta P)_{\text{acc},sp} = 1.05$ kPa, $(\Delta P)_{\text{acc},tp} = 34.17$ kPa, $(\Delta P)_{\text{grav},sp} = 10.7$ kPa, $(\Delta P)_{\text{grav},tp} = 10.05$ kPa, $(\Delta P)_{\text{total}} = 82.7$ kPa. All based on HEM]

25. Water enters a uniformly heated vertical tube of diameter 3 cm and length 5 m. Total heat applied to the tube is 1250 kW. Inlet pressure, temperature, and mass flow rate of water are given as 100 bar, 300 C, and 3 kg/s, respectively. Find the pre-heating length, exit quality, and various pressure differential terms. [Ans.: $L_f = 0.72$ m, $X_o = 0.29$, $(\Delta P)_{\text{fric},sp} = 3.38$ kPa, $(\Delta P)_{\text{fric},tp} = 54.61$ kPa, $(\Delta P)_{\text{acc},sp} = 0.905$ kPa, $(\Delta P)_{\text{acc},tp} = 89.72$ kPa, $(\Delta P)_{\text{grav},sp} = 4.93$ kPa, $(\Delta P)_{\text{grav},tp} = 12.57$ kPa, $(\Delta P)_{\text{total}} = 166.12$ kPa. All based on HEM]

26. In a certain adiabatic air – water flow experiment, it is desired to create the same pressure gradient in two vertical channels having hydraulic diameters D_1 and D_2 , respectively. Given the conditions for channel 1 (i.e. the total mass flow rate \dot{m}_1 and steam quality x_1), determine the corresponding values in channel 2 so that

a) the two channels have almost the same void fraction, $\alpha_1 = \alpha_2$

b) the two channels have also the same liquid mass flow rate, $\dot{m}_1 = \dot{m}_2$ (in this case $\alpha_1 \neq \alpha_2$)

c) same as b but for horizontal channels.

Pressure, temperature, and surface roughness are the same for the both channels. Assume single-phase friction factor is only a function of the Reynolds number, $f_{sp} = f(\text{Re})$.

27. Water enters a uniformly heated vertical tube of diameter 2 in and length 15 ft. Total heat applied to the tube is 100 kW. Inlet pressure, temperature, and mass flow rate of water are given as 1000 psia, 500 F, and 0.5 lbm/s, respectively. Find the pre-heating length, exit quality, and various pressure differential terms.

[Ans.: $L_f = 4.32$ ft, $X_o = 0.21$, $(\Delta P)_{fric,sp} = 0.001$ psia, $(\Delta P)_{fric,tp} = 0.005$ psia, $(\Delta P)_{acc,sp} \approx 0$ psia, $(\Delta P)_{acc,tp} = 0.01$ psia, $(\Delta P)_{grav,sp} = 1.43$ psia, $(\Delta P)_{grav,tp} = 1.36$ psia, $(\Delta P)_{total} = 2.81$ psia. All based on HEM]

28. A mixture of water and steam flowing out of a vent at 2000 psia and 798 Btu/lbm. Find quality and the void fraction at critical flow condition according to Moody and Fauske models. [Ans. $x = 0.27$, $\alpha_{Moody} = 0.42$, and $\alpha_{Fauske} = 0.50$].

29. A mixture of water and steam flowing out of a vent at 200 psia and quality of 0.27. Find the void fraction at critical flow condition according to Moody and Fauske models. [Ans. $\alpha_{Moody} = 0.65$ and $\alpha_{Fauske} = 0.81$].

30. In Example Va.3.1, show that mass flux can be expressed as:

$$\frac{-1}{G^2} = \left\{ \left[\frac{2(1-x)v_f}{1-\alpha} - \frac{2xv_g}{\alpha} \right] \frac{dx}{dP} + \left[\frac{(1-x)^2}{1-\alpha} \frac{dv_f}{dP} + \frac{x^2}{\alpha} \frac{dv_g}{dP} \right] + \left[\frac{(1-x)^2 v_f}{(1-\alpha)^2} - \frac{x^2 v_g}{\alpha^2} \right] \frac{d\alpha}{dP} \right\}_s$$

31. Water flows in a vertical channel. Use the given data to find the frictional pressure drop from the inlet to the exit of the channel. Compare the calculated values for $\Delta P_{friction}$ by using the homogenous, the Reddy, the Friedel, and the Thom model. Data: $H = 6$ ft, $D_h = 0.145$ ft, $P = 1000$ psia, $X_e = 8\%$, $V_i = 3$ ft/s, and $T_i = 522$ F.

32. Find the maximum flow rate for a mixture of water and steam flowing at 500 psia and $x = 50\%$. What is the stagnation enthalpy for this mixture?

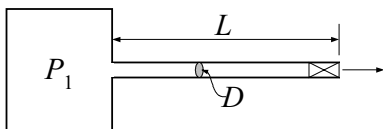
33. Derive an exact formulation for dP_{acc} for homogeneous, one-dimensional, steady, two-phase flow in a constant area channel assuming thermodynamic equilibrium. [Hint: Start with Equation Va.2.5 but written as $dP_{acc} = G^2 dv$, substitute for $v = v_f + x v_{fg}$, for x from $h = h_f + x h_{fg}$, and for h from the energy equation:

$$\dot{q}''(\pi D ds) = \dot{m}(dh + dV^2/2)$$

[Ans.: $(dP/ds)_{acc} = 4(G/D)\dot{q}''(v_{fg}/h_{fg})$].

34. A pressurized tank contains saturated water. A frictionless valve on the pipe is now opened to discharge the tank inventory to the atmosphere. Find if at the given pressure the flow rate is choked.

Data: $P_1 = 200$ psia, $L = 4$ ft, $D = 2$ in.



Vb. Boiling

Bubbles may be induced in a liquid in two ways. First, by sudden depressurization of the liquid referred to as flashing. For example, bubbles appear in a pressurized water tank if the sudden opening of a pressure relief valve results in the tank pressure dropping below the liquid saturation pressure. Similarly, if the flow of a liquid is accelerated or the flow encounters valve or fittings, vapor bubbles may appear as the result of the associated pressure drop. The second way is by addition of heat to a liquid at constant pressure. Boiling generally refers to the evaporation from the interface between a liquid and a heated surface. In boiling, liquid temperature remains practically constant and slightly higher than the saturation temperature at system pressure.

Knowledge about boiling heat transfer is essential in cases where we need a liquid to boil to enhance the rate of heat transfer and in such other cases in which preventing boiling is required by design. Boiling is the fundamental mode of heat transfer in the steam generator of a PWR, in the core of a BWR, and in the boiler of a fossil power plant. On the other hand PWRs must be operated to prevent boiling in the core. Boiling is also important to the cooling of rocket combustion chamber and electronic cooling. An interesting aspect of boiling heat transfer is the method that heat from a heated surface is transferred to the liquid (i.e., whether by carefully controlling the heated surface temperature or by controlling heat flux). The latter could be associated with a phenomenon referred to as boiling crises or critical heat flux. Boiling is the most desirable mode of heat transfer when a very high heat transfer coefficient (on the order of $1 \text{ MBtu/ft}^2\cdot\text{h}\cdot\text{F}$ or higher) is required. Boiling heat transfer consists of various modes as are discussed in this chapter.

1. Definition of Boiling Heat Transfer Terms

Nucleation refers to the inception of the embryonic bubble.

Homogeneous nucleation (also known as spontaneous vaporization) refers to the appearance of bubbles in the bulk of a liquid without any need for a heated surface. Such nucleation occurs only if the liquid is contained in a mirror-finished container and very high degree of superheat is provided. That is to say, the liquid temperature should be increased by hundreds of degrees beyond the saturation temperature for homogeneous boiling to take place. Sufficiently superheated liquids in containers with very smooth surfaces would vigorously produce bubbles if nucleation sites (rough surfaces) are introduced into the liquid.

Heterogeneous nucleation refers to the appearance of boiling bubbles, as a result of liquid vaporization at the interface with a heated surface. This is the most common form of boiling. In Section 2, we demonstrate that boiling in a superheated liquid subject to the introduction of a rough surface is distinctly different than boiling in a liquid with a heated rough surface.

Local or subcooled boiling refers to heterogeneous nucleation occurring at a specific region in a liquid with the bulk liquid being subcooled. In local boiling, if bubbles grow and detach from the surface, they would soon collapse upon reaching the colder liquid. The energy contained in the collapsed bubble is transferred to the liquid, raising the liquid average temperature.

Bulk or saturation boiling starts following subcooled boiling after a sufficient number of bubbles have burst in the liquid, transferring their energy to and raising the subcooled liquid temperature to saturation.

Nucleate boiling refers to a specific boiling mode where bubbles appear as a result of the nucleation process on the heated surface. Initiation of nucleate boiling strongly depends on surface roughness.

Film boiling refers to vaporization of liquid while the heated surface is covered by a film of vapor. Film boiling takes place at elevated surface temperatures. The heat for liquid vaporization is transferred to the liquid by conduction through the film of vapor. Hence, surface roughness has no effect on film boiling.

Pool boiling refers to boiling in a quiescent liquid. The only liquid flow in pool boiling is due to free convection and mixing as a result of bubble departure from the heated surface.

Flow boiling, as is the case in the core of BWRs and PWR steam generators takes place with bulk liquid in motion. Liquid flow is due to external forces as well as free convection and bubble-induced mixing.

Bubble equilibrium is a result of three types of equilibrium. Consider an isolated bubble in the bulk of a liquid, Figure Vb.1.1(a). For this bubble to remain intact (i.e., neither grow nor collapse) three conditions must be met. These are mechanical equilibrium, thermal equilibrium, and equal chemical potentials.

Mechanical equilibrium requires the algebraic summation of all the forces applied to the bubble to be zero, as shown in Figures Vb.1.1(a).

$$\Sigma F = \text{internal pressure force} + \text{external pressure force} + \text{surface tension force} = 0$$

Substituting for the three forces, we find:

$$(\pi r_e^2 P_v) + (\pi r_e^2 P_l) + (2\pi r_e \sigma) = 0$$

where r_e is the radius of the bubble at equilibrium. This equation simplifies to $P_v - P_l = 2\sigma/r_e$. Since $P_v > P_l$ but $T_v = T_l$, as shown in Figure Vb.1.1(b), liquid surrounding the bubble must be superheated. If there are gases dissolved in the liquid, then r_e is given by $r_e = 2\sigma/[(P_v + P_a) - P_l]$ where P_a is the gas pressure.

Thermal equilibrium requires the temperature of the vapor and liquid to be equal, $T_v = T_l$, Figure Vb.1.1(b). Otherwise, a combination of heat and mass transfer processes would occur to establish thermal equilibrium at a larger bubble size or cause the bubble to collapse, depending on the magnitude of T_v and T_l .

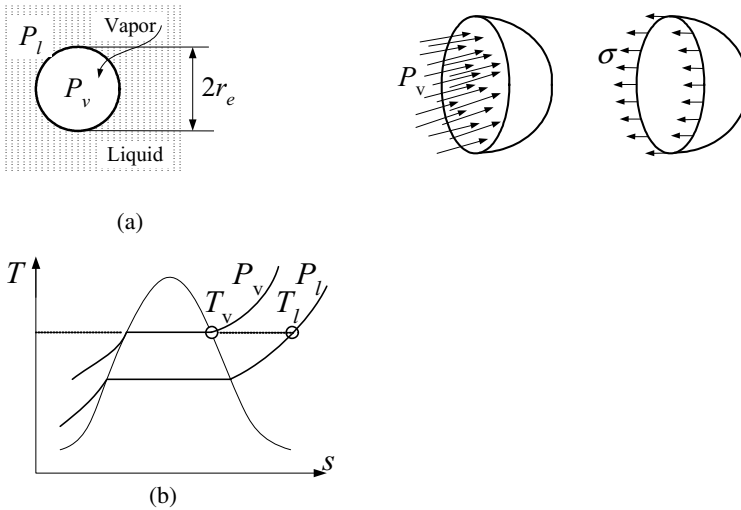


Figure Vb.1.1. Applied forces on a vapor bubble in equilibrium

Equal chemical potential ($g_v = g_l$) is the third condition for the bubble to be in equilibrium. Substituting for the Gibbs function we get $(h - Ts)_v = (h - Ts)_l$. For discussion on equal chemical potential see Section 2.2.

Surface roughness has a profound effect on nucleate boiling initiation. Unless a surface is mirror finished, surfaces consist of tiny pits and scratches also referred to as cavities. Most cavities on metal surfaces may be considered conical as shown in Figure Vb.1.2. Bubble nucleation generally begins at the cavities, referred to as the nucleation sites. When a wall is first wetted, nuclei of size 2.5–7.5 μm are generally present.

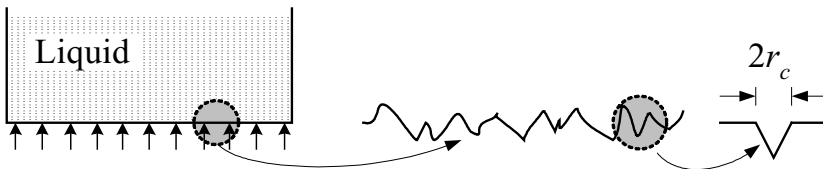


Figure Vb.1.2. Surface roughness acting as cavities or nucleation sites for bubble nucleation

Contact angle is a measure of the wet-ability of a liquid. Wetting itself is defined as the ability of liquids to form a boundary surface with solids. Figure Vb.1.3 shows a liquid in a capillary tube and in a surface cavity. Due to the action of surface tension, a wetting liquid in a capillary tube has a surface with a contact angle of $\phi < 90^\circ$ where ϕ is measured in the liquid. Non-wetting liquids

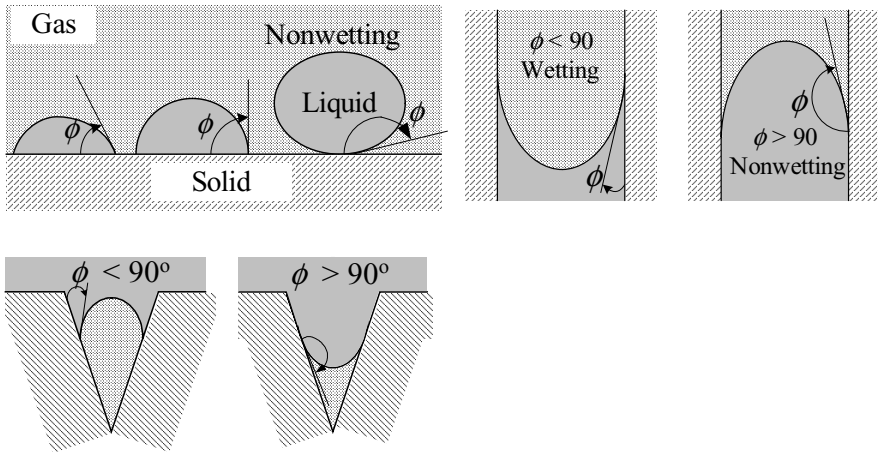


Figure Vb.1.3. Contact angle for liquid on horizontal surfaces, in capillary tubes, and in cavities

have convex surfaces and an angle of contact $\phi > 90^\circ$. Surface treatment affects liquid wet-ability. Wetting liquids fill surface cavities, preventing nucleation.

Bubble growth is the appearance and growth of a vapor bubble from cavities in a surface. Figure Vb.1.4(a) shows a surface cavity or nucleation site. Figure Vb.1.4(b) shows the inverse of the bubble radius ($1/r_b$) versus the bubble volume (V_b). The energy transferred from the heated surface to the trapped gas or vapor in this cavity (stage A) causes it to grow. As vapor volume increases, its radius (r_b) decreases. Stage B shows the moment that the bubble has reached at the mouth of the cavity. At this point, the bubble volume keeps increasing while the radius keeps decreasing. The minimum radius is reached when the bubble radius becomes equal to the radius of the cavity $r_b = r_c$ (stage C). Growth of the bubble beyond this point depends on the degree of superheat of the liquid. If sufficient superheat exists, bubbles eventually leave the nucleation sites towards the bulk. These stages are known as waiting period, growth period, agitation or displacement of liquid in the thermal sub-layer period, and departure (or collapse) period, as shown in Figure Vb.1.4(c) through Vb.1.4(f). As shown in Section 2, $1/r_b$ is proportional to the liquid superheat, $T_l - T_{sat}$.

Returning to Figure Vb.1.4(a), this discussion shows that the radius of the mouth of the cavity (r_c) determines the amount of superheat required for the vapor bubble to nucleate at that site (see Section 2.2).

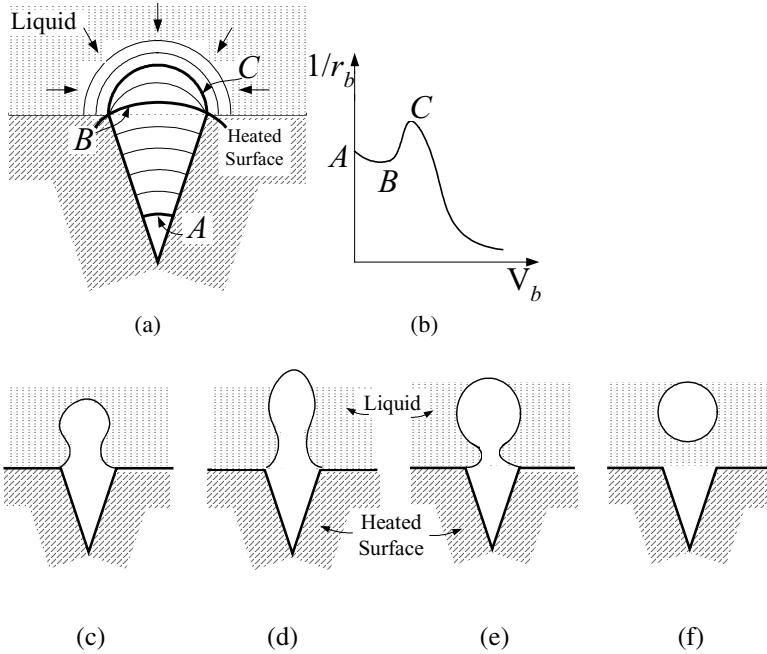


Figure Vb.1.4. Appearance and growth of a vapor bubble on a rough surface from conical cavities

Departure diameter, refers to the diameter of a bubble at the moment the bubble leaves the heated surface. We may estimate the bubble departure diameter from a force balance between buoyancy and surface tension:

$$\pi D \sigma = \frac{\pi D^3}{3} (\rho_f - \rho_g) g$$

Solving for the bubble departure diameter, we find:

$$D_d = \left[3 \frac{\sigma}{g(\rho_f - \rho_g)} \right]^{1/2} = 1.73 \left[\frac{\sigma}{g(\rho_f - \rho_g)} \right]^{1/2} \quad \text{Vb.1.1}$$

2. Convective Boiling, Analytical Solutions

Certain aspects of boiling heat transfer are amenable to analytical solutions. However, due to the inherent complications associated with the boiling mechanisms, there is no general analytical solution for derivation of such an important parameter as the heat transfer coefficient, for example. Here we discuss few aspects of the boiling mechanism.

2.1. Dimensionless Groups

Practical aspects of boiling heat transfer are based on experimental data. To correlate such data we need to find the dominant factors in heat transfer associated with phase change. Such factors include the involved forces, key fluid properties, and the operational conditions. Viscous and buoyancy forces play a major role in heat transfer with phase change. Pertinent fluid properties include latent and specific heat (h_{fg} , c_p), density and thermal conductivity (ρ , k), and viscosity and surface tension (μ , σ). Finally, operational conditions include pressure, fluid and surface temperature, and the surface geometry (L). Since the effect of pressure appears in fluid properties, we can reduce the number of variables to 10. These are ρ_l , ρ_v , h_{fg} , c_p , k , μ , σ , ΔT , L and h . Incropera finds five dimensionless groups for these parameters; $Nu = hL/k = f[\rho g(\rho_l - \rho_v)L^3/\mu^2, Ja, Pr, Bo]$ where the Bond number (Bo) is similar to the Gr number (Table A.I.6).

2.2. Determination of Degree of Superheat for Equilibrium Bubble

Homogeneous nucleation: Earlier we noticed that for a bubble to be in equilibrium in the bulk of a liquid, three conditions must be met. To maintain equilibrium, we can use these conditions to find the minimum degree of superheat for a liquid; i.e. $T_l - T_{sat}$. From the requirement for equal chemical potential, we obtain the Clausius-Clapeyron equation $dP/dT = h_{fg}/(T_{sat}v_{fg})$. We integrate this equation assuming $T_{sat}v_{fg}/h_{fg}$ remains constant. We then substitute for $P_v - P_l = 2\sigma/r_e$ from the second requirement to find:

$$\Delta T = T_l - T_{sat} = \frac{T_{sat}v_{fg}}{h_{fg}}\Delta P = \frac{T_{sat}v_{fg}}{h_{fg}}\left(\frac{2\sigma}{r_e}\right) \cong \frac{2\sigma T_{sat}}{h_{fg}\rho_g r_e} \quad \text{Vb.2.1}$$

where r_e is the radius of the equilibrium bubble. Equation Vb.2.1 shows that the degree of superheat is inversely proportional to the bubble radius. Thus, the smaller the bubble, the higher the required degree of superheat. That is why the homogenous nucleation requires very high degrees of superheat.

Heterogeneous nucleation: Regarding nucleation from a heated surface, we noticed that the minimum radius of a growing bubble is when $r_b = r_c$, where r_c is the radius of the cavity. Substituting into Equation Vb.2.1, we conclude that bubbles that have made it to the mouth of the cavity will grow if the degree of superheat in the liquid is at least equal to ΔT as given by Equation Vb.2.1. This is indeed the case if the bulk liquid is superheated. Superheating is achieved by heating the liquid in a pressurized vessel until liquid becomes saturated. When the heating process is terminated and the vessel is perfectly insulated, we reduce the liquid pressure. As the pressure drops, bubbles begin to form on the surface of the vessel when the liquid superheat becomes at least equal to that given by Equation Vb.2.1.

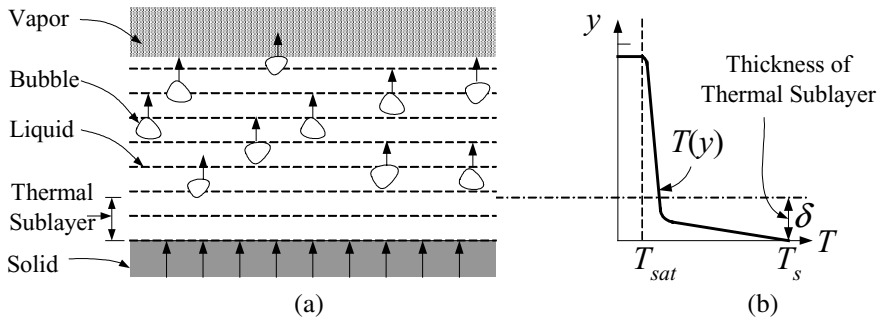


Figure Vb.2.1. Heterogeneous boiling and temperature gradient in liquid

It is fascinating to note that if boiling is induced solely by continuing to heat the vessel, the degree of superheat required for boiling is much higher than that predicted by Equation Vb.2.1. Indeed, some data have shown that the required degree of superheat for bubble growth is three times as much as that predicted by Equation Vb.2.1 (Hsu). The reason turns out to be the existence of a region (Figure Vb.2.1) referred to as the *thermal sub-layer*. Liquid temperature increases markedly in this region from T_{sat} to T_s , Figure Vb.2.1(b). It is in this thermal sub-layer near the heated surface that liquid becomes superheated to provide sufficient heat for the bubble to grow and depart.

We may estimate the thickness of the thermal sub-layer by using the definition of heat transfer coefficient (h). Thus, the thickness of the thermal sub-layer is related to the liquid thermal conductivity as $\delta = k/h$ where h can be estimated from a correlation such as that of Fishenden for turbulent natural convection from a horizontal flat surface:

$$Nu = 0.14(Gr Pr)^{1/3}$$

where the Gr and Pr numbers are calculated for the liquid phase. Next, we focus on the heat transfer mechanism taking place in the thermal sub-layer.

Let's investigate the relation between the bubble equilibrium temperature (Equation Vb.2.1) and water temperature in the thermal sub-layer. Shown in Figure Vb.2.2 is a cavity of radius r_c on the heated surface.

Originally, both liquid and surface have the same temperature as the bulk liquid T_f (line ZO). We add heat to the surface and bring its temperature to T_A . The temperature in the thermal sub-layer is shown by line ZA where we have assumed a linear temperature profile in the thermal sub-layer. Since we do not observe any bubble in the liquid we increase the surface temperature to T_B with the liquid temperature shown by line ZB. As we heat up the surface, the bubble in the cavity begins to grow. We keep increasing the surface temperature until eventually the line representing temperature in the thermal sub-layer (line ZC) becomes tangential to the curve representing Equation Vb.2.1 for an equilibrium bubble. At this point, the bubble in the cavity has reached the mouth of the cavity and has the smallest radius of curvature. Hsu's condition for the bubble to grow is that the

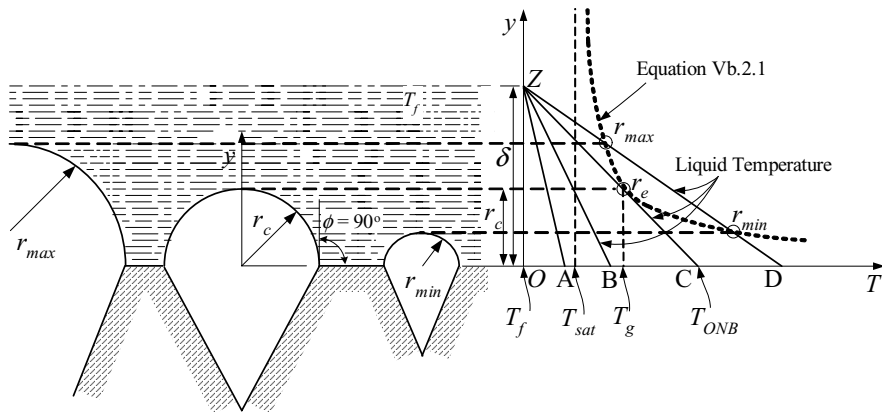


Figure Vb.2.2. Depiction of the onset of nucleate boiling (Hsu)

Next, we find the required surface superheat, $\Delta T_s = T_s - T_{sat}$ from Equation Vb.2.1:

$$\Delta T_s = 2\sigma T_{sat}/(h_{fg}\rho_g r_e) = 2 \times 0.059 \times (100 + 273)/(2.257E6 \times 0.593 \times r_b) = 3.3E-5/r_b \quad (2)$$

Substituting for $r_b = r_c = \delta/2$ into (2) yields: $\Delta T_s = 6.6E-5/\delta$. Substituting ΔT_s into (1) to find δ as:

$$\delta = 1.35E-3[6.6E-5/\delta]^{-1/3}. \text{ We, therefore, find } \delta = 6 \text{ mm. Thus, } \Delta T_s = 0.019 \text{ C.}$$

Comment: It is seen when cavities of all sizes are present, the required degree of superheat is very small.

Let's assume only cavities of $8 \mu\text{m}$ exist. In this case, $r_c = 8E-6 \text{ m}$ and $(\Delta T_s)_{\text{required}} = 3.3E-3/8E-6 = 4 \text{ C.}$

Heterogeneous nucleation formulation: We now want to quantify our qualitative argument regarding the vapor temperature and the thermal sub-layer temperature. For this purpose we find the equation for liquid temperature in the thermal sub-layer and set it equal to the vapor temperature in the bubble as given by Equation Vb.2.1. This method was originally suggested in 1962 by Hsu. Since the thermal sub-layer is thin, we use a linear temperature profile in this region which must satisfy the following boundary conditions:

$$\text{At } y = 0, T(y = 0) = T_s \text{ and at } y = \delta, T(y = \delta) = T_f$$

where T_s and T_f are the surface and the free stream temperatures of the bulk liquid, respectively. The profile is obtained as:

$$\frac{T_l - T_f}{T_s - T_f} = \frac{\delta - y}{\delta} \quad \text{Vb.2.2}$$

We make a change of variable from y with r_c (See Figure Vb.2.3) to obtain:

$$y = c_1 r_c = (1 + \cos\phi)r_b \quad \text{Vb.2.3}$$

We now set Equation Vb.2.1 equal to Equation Vb.2.2, while substituting for y from Equation Vb.2.3.

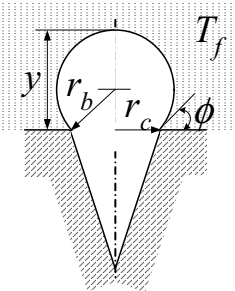


Figure Vb.2.3. Depiction of bubble height, radius, and cavity radius

Depending on the boiling condition, the curves representing the two temperature profiles may a) not meet, b) be tangent to each other, or c) intersect at two locations. These conditions are obtained from the solution to the following equation:

$$T_{sat} + \frac{2\sigma T_{sat}}{h_{fg} \rho_g c_2 r_c} = T_f + (T_s - T_f) \frac{\delta - c_1 r_c}{\delta}$$

This results in a second order algebraic equation for r_c . The solution is found as:

$$r_c = \frac{\delta(T_s - T_{sat})}{2c_1(T_s - T_f)} \left[1 \pm \sqrt{1 - \frac{8c_1}{c_2} \frac{(T_s - T_f)T_{sat}\sigma}{(T_s - T_{sat})^2 \delta \rho_g h_{fg}}} \right] \quad \text{Vb.2.4}$$

The results are plotted in Figure Vb.2.4.

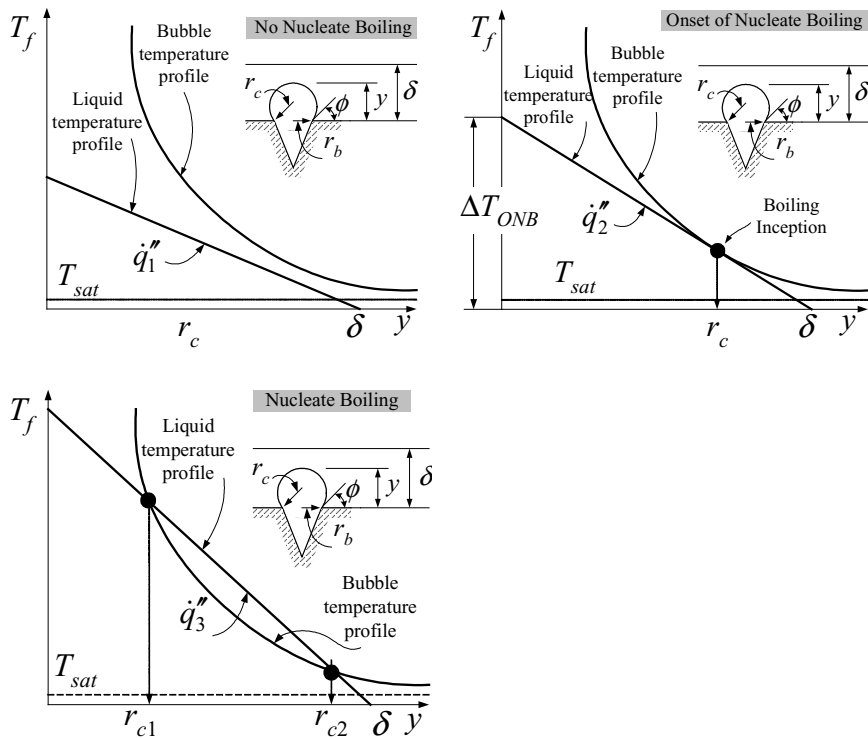


Figure Vb.2.4. Comparison of the vapor bubble and liquid temperature profiles

These concepts are further developed in Chapter VIe.

2.3. Prediction of Bubble Growth

We can predict the growth rate of a vapor bubble rather accurately by treating the surrounding superheated liquid as a semi-infinite body. In this case, the specified boundary condition is heat flux at the interface between the liquid and the vapor bubble, as shown in Figure Vb.2.5. Since liquid is being cooled at the interface we can write the following energy balance:

Rate of increase in bubble internal energy = Rate of liquid cooldown at the interface

$$\rho_g h_{fg} \frac{dV}{dt} = (4\pi R^2) \dot{q}''$$

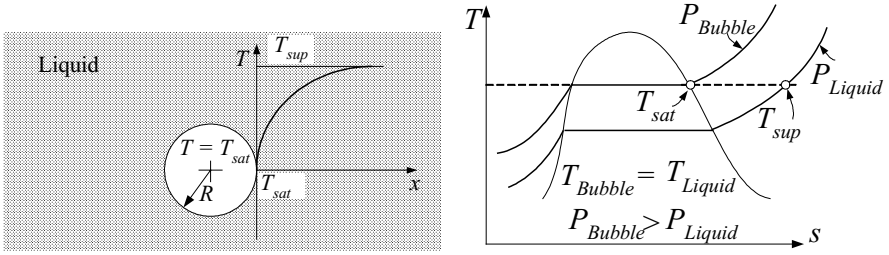


Figure Vb.2.5. Growth of a vapor bubble in the pool of superheated liquid

Substituting for heat flux at the interface from Equation IVa.9.10 and for volume in terms of radius yields:

$$\rho_g h_{fg} \frac{d}{dt} \left(\frac{4}{3} \pi R^3 \right) = (4\pi R^2) \frac{k(T_s - T_i)}{\sqrt{\pi \alpha t}}$$

Note in this case, the semi-infinite body is initially at $T_i = T_{sup}$ when the interface is suddenly cooled to $T_s = T_{sat}$. Subscripts *sup* and *sat* stand for superheated and saturated, respectively. Carrying out the derivative, canceling similar terms ($4\pi R^2$) from both sides of the equation, and rearranging, we obtain:

$$\rho_g h_{fg} dR = \frac{k(T_s - T_i)}{\sqrt{\pi \alpha}} \frac{dt}{\sqrt{t}}$$

Using the initial condition of $R = 0$ at $t = 0$, we find:

$$R(t) = \frac{2}{\sqrt{\pi}} \frac{k(T_{sup} - T_{sat})}{\rho_g h_{fg} \sqrt{\alpha}} t^{1/2} \quad \text{Vb.2.5}$$

As Lienhard describes, Jakob initially suggested the method that led to the derivation of Equation Vb.2.5. As shown in Figure Vb.2.4, this equation under-predicts the data obtained by Dergarabedian. Hence, Scriven used a more rigorous method and found that $R_{bubble} = \sqrt{3} R_{Jakob}$, which closely matches the data.

Figure Vb.2.6 shows that the trend predicted by Jakob is as expected but the absolute value under-predicts the data. The reason is that the bubble growth increases the temperature gradient, which has been treated as constant in Jakob's model. Scriven accounts for this and practically matches the data.

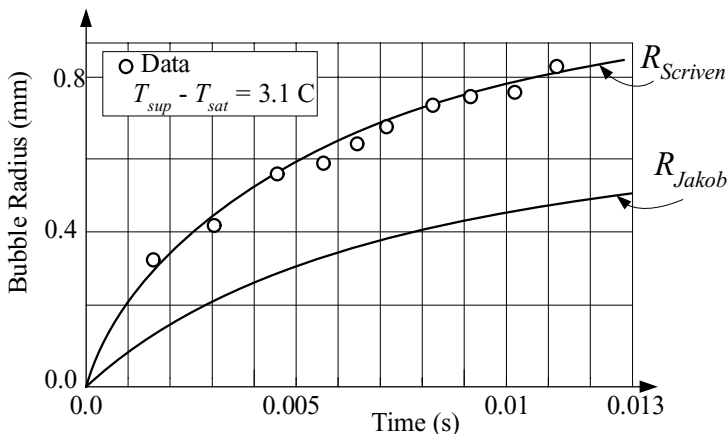


Figure Vb.2.6. Comparison of R_{Jakob} and $R_{Scriven}$ with data

Example Vb.2.2. Find the bubble diameter 0.01 s into the bubble growth for water boiling at 1 atm and $\Delta T = 3$ C. Data: $k_f = 0.68$ W/m·K, $\rho_g = 0.593$ kg/m³, $\alpha_f = 1.68$ E-7 m²/s, and $h_{fg} = 2.257$ E6 J/kg.

Solution: From Equation Vb.2.5, we find $R(0.01$ s) as:

$$R(t) = \frac{2}{\sqrt{\pi}} \frac{k(T_{sup} - T_{sat})}{\rho_g h_{fg} \sqrt{\alpha}} t^{1/2} =$$

$$\frac{2}{\sqrt{\pi}} \frac{0.68 \times 3.1}{0.593 \times 2.257 \text{E}6 \sqrt{1.68 \text{E} - 7}} \sqrt{0.01} \times 1\text{E}3 = 0.4336 \text{ mm}$$

3. Convective, Boiling, Experimental Observation

Before discussing the two distinct modes of pool and flow boiling, we consider the landmark experiment performed by Nukiyama in 1934, which led to the estab-

lishment of the boiling curve. The importance of this curve is in its clear depiction of various modes of heat transfer and demonstration of the effect of the method of heat addition to the liquid. This was the first experiment for the measurement of surface heat flux versus surface superheat ($\Delta T_{sl} = T_s - T_{sat}$). As shown in Figure Vb.3.1(a) the experiment consists of an electrically heated wire in a water container at atmospheric pressure. Nukiyama used a nichrome wire connected to an electric voltage. Data were obtained by varying the electric power measuring wire temperature after steady-state is achieved. This is referred to as power-controlled or heat flux controlled heating where \dot{q}_s'' is the independent variable and surface temperature (hence $\Delta T_{sl} = T_s - T_{sat}$) is the dependent variable. As power increased, there was a sudden jump in the wire temperature and eventual burnout. The heat up path is shown in Figure b with the arrows. The cool down path was obtained by reducing electric power to the wire as shown in Figure c by the arrows. As these figures indicate, on both heat up and cooldown paths, there is a jump from one side of the curve to the other. This is typical of power-controlled heat up and cooldown. Figure d shows how the entire boiling curve can be constructed if the process is temperature-controlled. In this case, there is a specific heat flux for a specific wall temperature. In practice, most processes such as production of heat in the core of nuclear reactors are power-controlled. As a results, in such applications, care must be exercised no to exceed the maximum heat flux as damage to the surface would follow.

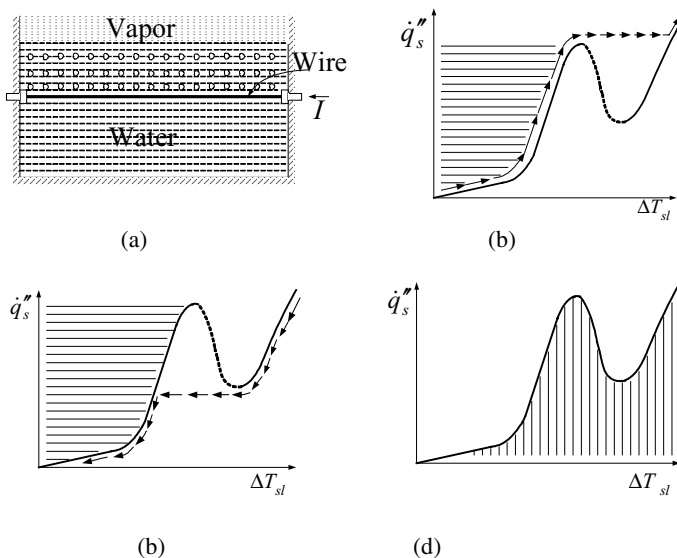


Figure Vb.3.1. Nukiyama experiment for developing the boiling curve

4. Pool Boiling Modes

The boiling curve for pool boiling heat transfer at atmospheric condition is shown in Figure Vb.4.1. Temperature is in degrees centigrade. Since the bulk liquid is quiescent, there is no heat flux when $\Delta T_{sl} = 0$. With an increasing degree of superheat, the surface heat flux increases solely due to free convection. At about $\Delta T_{sl} = 5$ C, the bubbles begin to grow and some may depart the surface. The buoyancy driven bubble causes agitation in the liquid. This mixing of liquid enhances heat flux. With increasing ΔT_{sl} , more bubbles are formed and the rate of carrying energy from the surface to the bulk liquid increases. Eventually, the rate of bubble production becomes so great that at ΔT_{sl} about 30 C, heat flux reaches its peak value. Beyond this point, the bubble population is so dense that it prevents liquid from reaching the surface. When this happens, heat transfer takes place only by conduction through the layer of vapor, which has blanketed the surface. With the surface being deprived of an efficient means of heat transfer by boiling bubbles, surface temperature jumps to elevated values. With heat flux maintained at its peak value, the jump in the surface temperature compensates for the sudden drop in the heat transfer coefficient. The heat transfer regime with vapor blanketing the surface is referred to as film boiling. The peak heat flux is referred to as the critical heat flux (CHF). A modest increase in heat flux beyond the CHF is due to both conduction through the vapor film and radiation due to the surface elevated temperature. On the cool down path, the reverse process occurs. When ΔT_{sl} reaches around 100 C, the vapor production is not vigorous enough to keep liquid away from the surface. With liquid in contact with the surface, the efficient heat transfer resumes. The point at which liquid contacts the surface again is known as the minimum stable film boiling (MSFB) or the Leidenfrost point. In 1756 Leidenfrost observed droplet boil off on hot surfaces. For surface temperature-controlled processes, the path between CHF and MSFB can be constructed. In this path, liquid and surface contact intermittently. This mode is known as *transition boiling*.

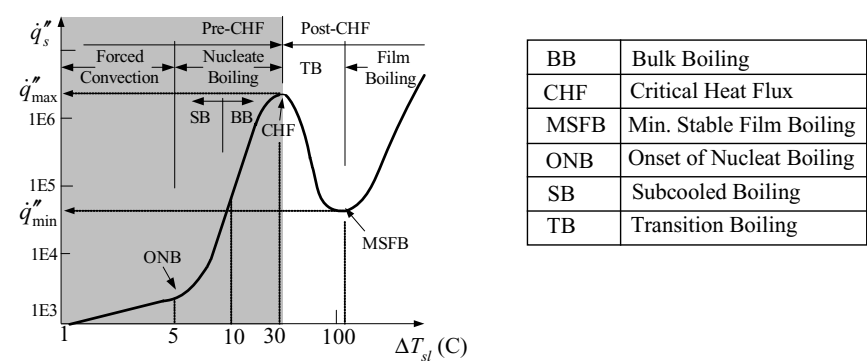


Figure Vb.4.1. The boiling curve for water at 1 atm and various heat transfer regimes

4.1. Nucleate Pool Boiling

Rohsenow, in 1952, obtained the nucleate pool boiling correlation in the form of $Ja = f(Re, Pr)$. The Reynolds number was defined for the bubbles as $Re = G_b D_b / \mu_b$ where G_b is bubble mass flux, D_b is bubble diameter, and μ_b is liquid viscosity. Therefore, $c_{p,f} \Delta T / h_{fg} = C_{s,f} (G_b D_b / \mu_b)^r Pr^n$. Rohsenow introduced $C_{s,f}$, r , and n so that nucleation on a variety of heated surfaces and liquids can be represented by the same relation. Expressing the bubble diameter in terms of contact angle, surface tension, and fluid density as $D_b = 1.48 \phi [2g_c \sigma / (g \Delta \rho)]^{0.5}$ and the bubble mass flux in terms of $G_b = \dot{q}'' / h_{fg}$, we find:

$$\frac{c_{p,f} (T_s - T_{sat})}{h_{fg} Pr_f^n} = C_{s-f} \left[\frac{\dot{Q} / A}{\mu_f h_{fg}} \sqrt{\frac{g_c \sigma}{g(\rho_f - \rho_g)}} \right]^{0.33} \quad \text{Vb.4.1a}$$

Solving for heat flux:

$$\dot{q}'' = \mu_f h_{fg} \left[\frac{g(\rho_f - \rho_g)}{\sigma} \right]^{0.5} \left(\frac{c_{p,f} (T_s - T_{sat})}{C_{s-f} h_{fg} Pr_f^n} \right)^3 \quad \text{Vb.4.1b}$$

The values for coefficient C_{s-f} and n for various surfaces and liquids are given in Table Vb.4.1.

Table Vb.4.1. Values for coefficients C_{s-f} and n for various liquid and surfaces

Fluid	Surface	C_{s-f}	n
Benzene	Chromium	0.1010	1.7
Carbon tetrachloride	Copper, polished	0.0070	1.7
Ethyl alcohol	Chromium	0.0027	1.7
Isopropyl alcohol	Copper	0.0025	1.7
n-Butyl alcohol	Copper	0.0030	1.7
n-Pentane	Copper, polished	0.0154	1.7
	Nickel, polished	0.0127	1.7
	Copper, emery-robbed	0.0074	1.7
	Chromium	0.0150	1.7
Water	Brass	0.0060	1.0
	Copper, polished	0.0128	1.0
	lapped	0.0147	1.0
	scored	0.0068	1.0
	Nickel	0.0060	1.0
	Stainless steel, ground & polished	0.0080	1.0
	, Teflon pitted	0.0058	1.0
	, chemically etched	0.0133	1.0
	, mechanically polished	0.0132	1.0
	Platinum	0.0130	1.0

Example Vb.4.1. Water is boiling in a container at atmospheric pressure. The heated surface area is 0.1 m^2 and is made of mechanically polished stainless steel. An electric heater is used to carefully maintain the heated surface superheat at 17 C . Find a) the required power, b) the heat transfer coefficient, and c) the rate of evaporation from the heated surface.

Solution: From Table AIV5(SI) for saturated water and steam at $T_{sat} = 100 \text{ C}$, we find $\rho_f = 958 \text{ kg/m}^3$, $\rho_g = 0.595 \text{ kg/m}^3$, $h_{fg} = 2257 \text{ kJ/kg}$, $c_{p,f} = 4.217 \text{ kJ/kg}\cdot\text{K}$, $\mu_f = 0.279\text{E-}3 \text{ N}\cdot\text{s/m}^2$, $Pr_f = 1.76$, $\sigma = 0.0589 \text{ N/m}$

a) Since the surface superheat, $T_s - T_{sat} = 17 \text{ C}$, thus $T_s = 100 + 17 = 117 \text{ C}$. From Table Vb.4.1 for mechanically polished stainless steel and water, we find $C_{sf} = 0.0132$ and $n = 1$. Equation Vb.4.1b yields:

$$\begin{aligned} \dot{q}'' &= 0.279\text{E-}3 \times 2257\text{E}3 \times \left[\frac{9.8 \times (958 - 0.595)}{0.0589} \right]^{0.5} \left(\frac{4.217 \times 17}{0.0132 \times 2257 \times 1.76} \right)^3 \\ &= 642 \text{ kW/m}^2 \end{aligned}$$

The required power for boiling at the specified condition is $\dot{Q} = \dot{q}'' \times A = 642 \times 0.1 = 64.2 \text{ kW}$.

b) Having the surface superheat and heat flux, the related heat transfer coefficient is found as:

$$h = \frac{\dot{q}''}{T_s - T_{sat}} = \frac{642,000}{17} = 37.8 \text{ kW/m}^2\cdot\text{C}$$

c) At steady state, the power delivered to saturated water is converted to the latent heat of vaporization, Equation IIa.7.2:

$$\dot{m} = \frac{\dot{Q}}{h_{fg}} = \frac{64.2}{2257} = 0.0284 \text{ kg/s} = 102.4 \text{ kg/h}$$

Comment: By using the software included on the accompanying CD-ROM, it can be easily verified that for a specified surface and surface superheat, the heat flux increases with increasing system pressure.

4.2. Critical Heat Flux in Pool Boiling

Kutateladze and later Zuber devised the following CHF correlation, which is only a function of pressure:

$$\dot{q}_{CHF}'' = 0.149 h_{fg} \rho_g \left[\frac{\sigma g (\rho_f - \rho_g)}{\rho_g^2} \right]^{0.25} \quad \text{Vb.4.2}$$

To avoid damage to heated surfaces, a safety factor is applied in the design of the heating elements to maintain heat flux well below the value predicted by Equation Vb.4.2.

Example Vb.4.2. A PWR rod is operating at a linear heat generation rate of 7 kW/ft. Find the safety factor according to the pool boiling CHF.

Solution: We first find the maximum heat flux from Equation Vb.4.2.

Using properties at $P = 2250$ psia we find:

$$\dot{q}_{CHF}'' = 0.149(416.4 \times 6.4)[0.000335 \times 32.2^2 (37.1 - 6.4)/6.4^2] = 283.6 \text{ Btu/ft}^2 \cdot \text{s}$$

A typical PWR rod diameter is about 0.44 inch, thus:

$$\dot{q}'' = \dot{q}' / \pi D = 7 / (3.14 \times 0.44 / 12) = 60.8 \text{ Btu/ft}^2 \cdot \text{s}$$

The safety factor is $283.6 / 60.8 = 4.70$.

4.3. Transition Pool Boiling

Transition boiling refers to the region between T_{CHF} and T_{MSFB} . This region is experienced in a temperature-controlled boiling process. In this region, both nucleate and film boiling mechanisms coexist as the surface temperature is not high enough for film boiling to dominate. Due to the complicated nature of the transition boiling mechanism, there is no correlation that can reliably predict the wall heat flux. Most correlations use a weighted average value between the heat flux corresponding to maximum heat flux (\dot{q}_{CHF}'') and the heat flux corresponding to the minimum stable film boiling (\dot{q}_{MSFB}'').

4.4. Minimum Stable Film Boiling

In temperature-controlled boiling, sufficiently high wall temperature in the transition boiling mode precludes nucleate boiling and covers the surface with a film of vapor. The temperature at which nucleation is completely ceased is the minimum stable film boiling (MSFB) temperature. To determine the heat flux at the point of minimum stable film boiling, we may use the definition of the Stanton number given as:

$$St = \frac{\dot{Q}}{\dot{m}\Delta h} = \frac{\dot{Q}}{(\rho VA)(c_p \Delta T)} = \frac{\dot{q}''}{\rho V c_p \Delta T}$$

when applied to conditions where a change of phase is involved, St becomes:

$$St = \frac{\dot{q}_{\min}''}{\rho_g V_{\min} h'_{fg}}$$

where V_{\min} in the denominator is given by:

$$V_{\min} = \left(\frac{g(\rho_l - \rho_v)L_c}{(\rho_l + \rho_v)} \right)^{1/2}$$

where L_c is a characteristic length given by Equation Vb.1.1. For large horizontal surfaces, Berenson suggested $St = 0.09$. Using Berenson's value and substituting for the characteristic length, the minimum heat flux is found as:

$$\dot{q}_{MSFB}'' = 0.09 \rho_v h_{fg} \left[\frac{\sigma g(\rho_l - \rho_v)}{(\rho_l - \rho_v)^2} \right]^{\frac{1}{4}} \quad \text{Vb.4.3}$$

Example Vb.4.3. Find the heat flux at the Leidenfrost point. Use $P = 1$ atm.

Solution: Using the saturated water properties at 100 C, Equation Vb.4.3 gives

$$\dot{q}_{MSFB}'' = 0.09 \times 0.59 \times (2257 \text{E}3) \left[\frac{0.059 \times 9.81(958 - 0.59)}{(958 + 0.59)^2} \right]^{\frac{1}{4}} = 19 \text{ kW/m}^2$$

4.5. Film Pool Boiling

The resemblance of the vapor film in the film boiling heat transfer to the condensate film in the laminar film condensation heat transfer prompted Bromley to suggest a correlation similar to Equation Va.2.6 for boiling on cylinders and spheres:

$$\bar{h} \frac{D}{k_v} = C \left[\frac{g(\rho_f - \rho_v)\rho_v h'_{fg} D^3}{\mu_v k_v (T_s - T_{sat})} \right]^{1/4} \quad \text{Vb.4.4}$$

In Equation Vb.4.4, $C = 0.62$ for horizontal cylinders and 0.67 for spheres. Also $h'_{fg} = h_{fg} + 0.4c_{p,v}(T_s - T_{sat})$. Vapor properties are evaluated at $T_{film} = (T_s + T_{sat})/2$. Since the contribution of radiation heat transfer becomes noticeable as the surface temperature approaches and exceeds 300 C, Bromley recommends the following h :

$$\bar{h} = \bar{h}_{convection} + 0.75 \bar{h}_{radiation} \quad \text{Vb.4.5}$$

where in Equation Vb.4.5, the heat transfer coefficient due to radiation is given as:

$$\bar{h}_{radiation} = \varepsilon \sigma (T_s^4 - T_{sat}^4) / (T_s - T_{sat})$$

In this relation ε and σ are surface emissivity and the Stefan-Boltzmann constant, respectively.

Example Vb.4.4. A horizontal cylinder, having a surface temperature of 300 C is submerged in saturated water at 100 C. Estimate the surface heat flux. Cylinder diameter is 4 cm and $\varepsilon = 0.85$.

Solution: Using saturation properties at 100 C we find $\rho_f = 958 \text{ kg/m}^3$, and $h_{fg} = 2257 \text{ kJ/kg}$. For superheated properties at 1 atm and a film temperature of 200 C: $\rho_v = 0.46 \text{ kg/cm}^3$, $c_{p,v} = 1.98 \text{ kJ/kg}\cdot\text{K}$, $\mu_v = 0.16\text{E-}4 \text{ Pa}\cdot\text{s}$, and $k_v = 0.033 \text{ W/m}\cdot\text{K}$.

$$h'_{fg} = h_{fg} + 0.4c_{p,v}\Delta T$$

$$= 2257 + 0.4 \times 1.98 \times 200 = 2415 \text{ kJ/kg.}$$

Using Equation Vb.4.4:

$$\bar{h}_{convection} = 0.62 \frac{0.033}{0.04} \left[\frac{9.81 \times (958 - 0.46) \times 0.46 \times 2415 \times 0.04^3}{(0.16\text{E-}4) \times 0.033 \times (300 - 100)} \right]^{1/4}$$

$$= 144 \text{ W/m}^2\cdot\text{K}$$

$$\bar{h}_{radiation} = 0.85 \times 5.67\text{E-}8 (573^4 - 373^4) / (573 - 373) = 21 \text{ W/m}^2\cdot\text{K}$$

$$h = \bar{h}_{convection} + 0.75 \bar{h}_{radiation} = 144 + 0.75 \times 21 = 160 \text{ W/m}^2\cdot\text{K}$$

$$\dot{q}'' = h\Delta T = 160 \times 200 = 32 \text{ kW/m}^2.$$

For film boiling on horizontal plates, Berenson's correlation is given as:

$$\text{Nu} = h\delta_v / k_v = 0.425 \quad \text{Vb.4.6}$$

where δ_v , an average vapor film thickness, used in the Nu number is given by:

$$\delta_v = \left[\frac{v_v^2 L_c}{g} \frac{\rho_v}{\rho_f - \rho_v} \frac{1}{\text{Pr}_v} \frac{\text{Ja}_v}{1 + 0.4\text{Ja}_v} \right]^{1/4} \quad \text{Vb.4.7}$$

In Equation Vb.4.7, L_c is the characteristic length as given in Equation Vb.1.1 and vapor properties are evaluated at T_{film} .

Example Vb.4.5. Find the convection heat flux for film boiling of water at 1 atm on top of a horizontal plate with $T_s = 900$ K.

Solution: Film temperature is $T_{film} = 0.5(373 + 900) = 636.5$ K. At atmospheric conditions, $\rho_f = 958$ kg/m³, $h_{fg} = 2.257$ E6 J/kg and $\sigma = 0.06$ N/m.

For superheated steam at 636.5 K:

$$c_{pv} = 2048 \text{ J/kg}\cdot\text{K}, \quad v_v = 66.4\text{E-}6 \text{ m}^3/\text{s}, \quad \rho_v = 0.345 \text{ kg/m}^3, \quad \text{and } k_v = 0.05 \text{ W/m}\cdot\text{K}$$

$$\text{Ja}_v = c_{p,v} \Delta T / h_{fg} = 2048 \times (900 - 373) / 2.257\text{E}6 = 0.48$$

$$L_c = (\sigma / g \Delta \rho)^{1/2} = [0.06 / (9.81 \times 958)]^{0.5} = 2.53\text{E-}3 \text{ m}$$

$$\delta_g = \left[\frac{(66.4\text{E-}6)^2 \times 2.53\text{E-}3}{9.81} - \frac{0.345}{958 - 0.349} \frac{1}{0.93} \frac{0.48}{1 + 0.4 \times 0.48} \right]^{0.25} = 0.115 \text{ mm}$$

$$h_{convection} = (k_v / \delta_v) \text{Nu} = (0.05 / 0.115\text{E-}3) \times 0.425 = 185 \text{ W/m}^2\cdot\text{K}$$

$$\dot{q}_{Convection}'' = h_{convection} \Delta T = 185 \times (900 - 373) = 98 \text{ kW/m}^2.$$

4.6. Minimum Stable Film Boiling Temperature

Temperature at the MSFB point may be found by using Newton's law of cooling and substituting for heat flux from Equation Vb.4.3 and for heat transfer coefficient from Equation Vb.4.4, for horizontal cylinders and spheres, or from Equation Vb.4.5 for horizontal plates. For horizontal cylinders and sphere we find:

$$T_{MSFB} - T_{sat} = 0.126 \frac{\rho_v h'_{fg}}{k_v} \left[\frac{g(\rho_l - \rho_v) \mu_v}{(\rho_l + \rho_v)^2} \right]^{1/3} \left[\frac{\sigma}{g(\rho_l - \rho_v)} \right]^{1/2} \quad \text{Vb.4.8}$$

where the vapor physical properties are developed at the film temperature.

Example Vb.4.6. For heat treatment, a long steel cylindrical rod is immersed horizontally in a pool of water at atmospheric pressure. The rod diameter is 4 cm. Find T_{MSFB} and the heat flux when surface is at 400 C. Use $\mathcal{E} = 0.66$.

Solution: For sufficiently hot surface, the entire boiling curve is traversed when the rod is immersed. If the initial heat transfer regime is film boiling, surface temperature begins to drop by both convection and radiation mechanisms until the MSFB point is reached. When T_{rod} drops below T_{MSFB} , partial nucleation takes place in the transition boiling region, increasing heat flux. This trend continues until the maximum heat flux is reached, further cooling the rod. As the rod gets colder, the required superheat for nucleation diminishes and heat begins to transfer by single-phase natural convection. We then start by calculating T_{MSFB} :

To find T_{MSFB} , we need T_{film} . We assume $T_s = 200$ C and use Equation Vb.4.8:

$$\Delta T_{MSFB} = 0.126 \frac{0.52 \times 2336E3}{0.029} \left[\frac{9.81(958 - 0.52) \times (0.14E - 4)}{(958 + 0.52)^2} \right]^{1/3} \left[\frac{0.06}{9.81(957 - 0.52)} \right]^{1/2}$$

We find $T_{MSFB} = 170$ C. Next, we assume $T_s = 180$ C and find $T_{MSFB} = 173$ C. We continue iteration until the answer converges to $T_{MSFB} \approx 185$ C. Thus initially heat transfer regime is film boiling. We find the initial heat flux from Equation Vb.4.4:

$$h = 0.62 \frac{0.038}{0.04} \left[\frac{9.81(958 - 0.42) \times 0.42 \times 2496E3 \times 0.04^3}{(0.18E - 4) \times 0.038 \times (400 - 100)} \right]^{0.25} = 140 \text{ W/m}^2 \cdot \text{K}$$

$$\begin{aligned} \dot{q}'' &= h\Delta T + 0.75\varepsilon\sigma(T_s^4 - T_f^4) \\ &= 140 \times 300 + 0.75 \times 0.66 \times 5.67E - 8 \times (673^4 - 373^4) = 47 \text{ kW/m}^2 \end{aligned}$$

4.7. Factors Affecting Pool Boiling

The pool boiling mode is influenced by several factors including gravity, pressure, surface roughness, aging, and the presence of noncondensable gases.

Effect of gravity. Among all the boiling modes, gravity primarily affects nucleation. In zero gravity, there is no nucleation as a large bubble would surround the heated surface. As gravity increases, heat transfer becomes more efficient due to enhanced free convection. If boiling is used as a cooling mechanism in the rotating machinery and in space vehicles, changes in gravity become a design consideration.

Effect of pressure. The rate of heat transfer in nucleate boiling is increased with pressure. This is apparent from the Clausius-Clapeyron equation. By treating vapor as an ideal gas, it can be shown that the degree of superheat is inversely proportional to pressure. Hence, at high pressures less ΔT_{sl} is needed for the same number of nucleation sites to become active. For example, if $\Delta T_{sl} = 12$ F, when pressure is increased by about 6.5 times (from 383 psia to 2465 psia) heat flux increases by 12.5 times (from 8E4 Btu/ft²·h to 1E6 Btu/ft²·h).

Effect of surface roughness was extensively studied by Berenson who demonstrated that the effect of surface roughness on heat transfer depends on the boiling mode. Berenson showed that pre-CHF is affected strongly, transition boiling moderately, and film boiling is not affected by surface conditions.

Effect of aging. Aging adversely affects boiling heat transfer due to surface oxidation. The layer of oxide increases thermal resistance, but it also increases the population of cavities.

Effect of noncondensable gases on boiling is to enhance surface heat flux. The dissolved gases in the liquid are released near the heated surface, agitating the liquid and increasing mixing.

5. Flow Boiling Modes

Flow boiling is associated with the flow of liquids into a heated conduit. As shown in Figure Vb.5.1, flow at the entrance of the conduit is single-phase liquid and heat transfer from the heated wall is found from forced convection correlation (A). As the liquid travels in the conduit, the layer adjacent to the heated surface enters the surface cavities. If sufficient superheat is available, the site becomes active. Bubbles generated in such sites would migrate toward the bulk liquid, which is still subcooled (B). This constitutes the subcooled flow boiling regime. Expectedly, heat transfer in this regime is due to both subcooled boiling as discussed in Section 4 for subcooled pool boiling and forced convection for single-phase liquid. Collapse of a bubble increases liquid energy, more bubbles are produced, resulting in the related flow regime being referred to as *bubbly flow* (C). Wall temperature remains constant the moment subcooled boiling is initiated. On the other hand, liquid temperature keeps increasing until the bulk liquid eventually reaches saturation. Hence, the related heat transfer regime is called *saturated nucleate boiling* (D).

As flow travels further in the conduit, the nucleation process becomes so effective that bubble population grows to a point that bubbles eventually begin to coalesce to form a slug. The related flow regime is known as *slug flow* (D). When slugs coalesce, a central vapor core is formed. The flow pattern where the vapor core is surrounded by a film of liquid is known as annular flow (E). The related heat transfer regime remains saturated nucleate boiling. However, the process of nucleation is soon replaced by evaporation (E and F). In this regime, surface heat is transferred to the liquid film by forced convection, which is then transferred to the liquid-vapor interface where evaporation takes place. The corresponding heat transfer regime is often called *forced convection vaporization*. With continuous evaporation, the liquid film eventually dries out. Following *dryout*, surface temperature jumps to elevated values due to the lack of effective liquid cooling. There is a slight drop in the surface temperature due to the lingering droplets, which would randomly touch the surface (G). These drops soon vaporize, resulting in a continuous rise in surface temperature due to heat transfer to single-phase vapor.

5.1. Subcooled Flow Boiling

There are several correlations for the calculation of the heat transfer coefficient in subcooled flow boiling (Delhaye, Ginoux, and Problem 9). However, the most widely used correlation, which is applied to both subcooled and saturation regions, is the Chen correlation as discussed next.

5.2. Saturated Flow Boiling

The Chen correlation accounts for both macro-convection due to flow and micro-convection due to boiling. As such, the Chen correlation is applicable over the en-

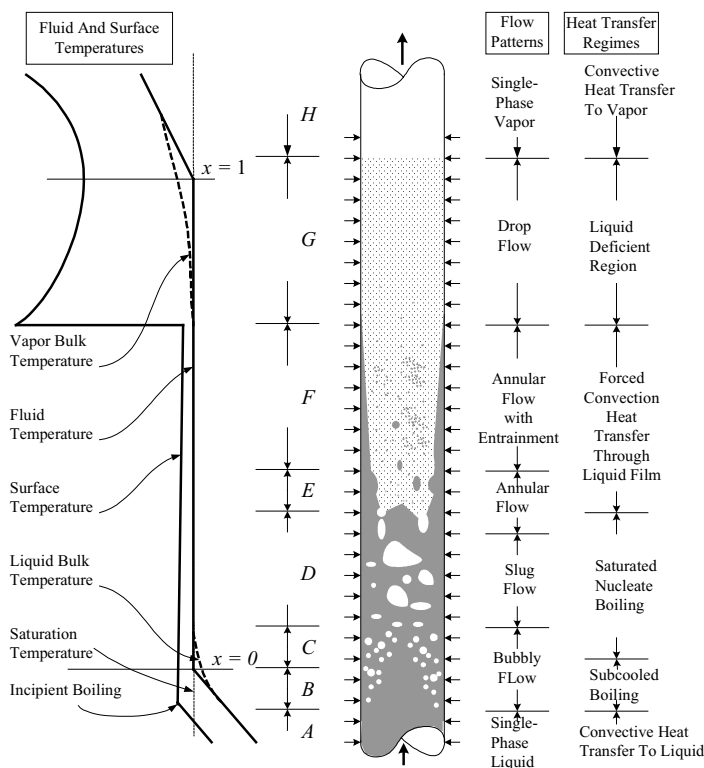


Figure Vb.5.1. Flow and heat transfer regimes in a sufficiently long heated conduit (Collier)

ture range of subcooled boiling, saturation boiling, and forced convection vaporization regions. The Chen correlation in SI units is given as:

$$h_{SI} = \frac{0.023k_f}{D_h} (\text{Re}_f)^{0.8} \text{Pr}_f^{0.4} F + 0.00122 \frac{k_f^{0.79} c_{p,f}^{0.45} \rho_f^{0.49}}{\mu_f^{0.29} \sigma^{0.5} h_{fg}^{0.24} \rho_g^{0.24}} \Delta T_{sat}^{0.24} \Delta P^{0.75} S \quad \text{Vb.5.1a}$$

substituting for ΔP from the Clapeyron equation, the Chen correlation in British units becomes:

$$h_{BU} = \frac{0.023k_f}{D_h} (\text{Re}_f)^{0.8} \text{Pr}_f^{0.4} F + 0.00122 \frac{k_f^{0.79} c_{p,f}^{0.45} \rho_f^{0.49} g_c^{0.25}}{\mu_f^{0.29} \sigma^{0.5} h_{fg}^{0.24} \rho_g^{0.24}} \left[\frac{778h_{fg}}{v_{fg}(T_{sat} + 460)} \right]^{0.75} \Delta T_{sat}^{0.99} S \quad \text{Vb.5.1b}$$

where $\text{Re}_f = G(1 - x)D_h/\mu_f$ and the conversion factor g_c is defined in Chapter IIa. The first term in Equation Vb.5.1 applies to subcooled boiling and follows the Dittus–Boelter correlation with a modification factor F , which accounts for the en-

hanced flow and turbulence due to the presence of vapor. The second term in Equation Vb.5.1 applies to nucleation and follows the Forster-Zuber analysis, modified with the suppression factor S . The modification factors F is given in terms of X_M :

$$X_M = \left(\frac{x}{1-x} \right)^{0.9} \left(\frac{\rho_f}{\rho_g} \right)^{0.5} \left(\frac{\mu_g}{\mu_f} \right)^{0.1}$$

so that for the F factor, $F = 2.35[0.213 + X_M]^{0.736}$, which applies if $X_M > 0.1$.

Otherwise, $F = 1$. Also, the S factor is given as $S = [1 + (2.53E - 6) \text{Re}^{1.17}]^{-1}$

where $\text{Re} = \text{Re}_f F^{1.25} = [G(1-x)D_h/\mu_f]F^{1.25}$.

Example Vb.5.1. Water flows in a vertical 1 in heated tube at a rate of 0.5 lbm/s. System pressure is 1000 psia. Find heat flux at a point where steam quality is 25% and surface superheat is $\Delta T_{sat} = T_s - T_{sat} = 8$ F.

Solution: First, we find properties at 1000 psia:

$\rho_f = 46.33 \text{ lbm/ft}^3$, $\mu_f = 0.229 \text{ lbm/ft}\cdot\text{h}$, $c_{p,f} = 1.286 \text{ Btu/lbm}$, $h_{fg} = 650.5 \text{ Btu/lbm}$, $\sigma = 0.0012 \text{ lbf/ft}$

$\rho_g = 2.23 \text{ lbm/ft}^3$, $\mu_g = 0.046 \text{ lbm/ft}\cdot\text{h}$, $k_f = 0.33 \text{ Btu/ft}\cdot\text{h}\cdot\text{F}$, $v_{fg} = 0.43 \text{ ft}^3/\text{lbm}$, $\text{Pr}_f = 0.899$, $T_{sat} = 544.33 \text{ F}$

$\rho_f = 46.33 \text{ lbm/ft}^3$, $\rho_g = 2.23 \text{ lbm/ft}^3$, $h_{fg} = 650.5 \text{ Btu/lbm}$, $c_{p,f} = 1.286 \text{ Btu/lbm}$, $\mu_f = 0.229 \text{ lbm/ft}\cdot\text{h}$, $\mu_g = 0.046 \text{ lbm/ft}\cdot\text{h}$, $k_f = 0.33 \text{ Btu/ft}\cdot\text{h}\cdot\text{F}$, $\text{Pr}_f = 0.899$, $\sigma = 0.0012 \text{ lbf/ft}$, $v_{fg} = 0.43 \text{ ft}^3/\text{lbm}$ and $T_{sat} = 544.33 \text{ F}$.

We now find X_M , F , S , and finally h . First X_M is found from:

$$X_M = \left(\frac{0.25}{0.75} \right)^{0.9} \left(\frac{46.33}{2.23} \right)^{0.5} \left(\frac{0.046}{0.23} \right)^{0.1} = 1.44$$

The F factor becomes

$$F = 2.35[0.213 + X_M]^{0.736} = 2.35(0.213 + 1.44)^{0.736} = 3.41$$

Diameter and flow area are: $d = 1/12 = 0.0833 \text{ ft}$ and $A = \pi d^2/4 = 3.14 \times 0.0833^2/4 = 5.45\text{E-}3 \text{ ft}^2$

$$G = \dot{m} / A = 0.5/5.45\text{E-}3 = 92 \text{ lbm/ft}^2\cdot\text{s}$$

To find S , we need to find:

$$\text{Re}_f = (0.5 \times 3600)(1 - 0.25) \times 0.0833 / (0.229 \times 5.45\text{E-}3) = 90,072$$

$$\text{Re} = \text{Re}_f \times F^{1.25} = 90,072 \times 3.41^{1.25} = 417,381$$

$$S = (1 + 2.53\text{E-}6 \times 417,381^{1.17})^{-1} = 0.095$$

The convection heat transfer coefficient (h_c) from Equation Vb.5.1b is:

$$h_c = 0.023(0.33/0.0833)(90,072)^{0.8} \times 0.899^{0.4} \times 3.55 = 2737 \text{ Btu/ft}^2\cdot\text{h}\cdot\text{F}$$

The nucleation heat transfer coefficient (h_b) from Equation Vb.5.1b is:

$$\text{Numerator: } 0.00122 \times 0.33^{-.79} \times 1.286^{.45} \times 46.33^{.49} \times (32.2 \times 3600^2)^{.25} = 0.533$$

$$\text{Denominator: } 0.229^{.29} \times 0.0012^{.5} \times 650.5^{.24} \times 2.23^{.24} = 0.13$$

$$\text{Bracket: } [778 \times 650.5 / (0.43 \times 1004.33)]^{.75} = 200.3$$

$$h_n = (0.533/0.13) \times 200.3 \times 8^{.99} \times 0.095 = 611 \text{ Btu/ft}^2 \cdot \text{h} \cdot \text{F}$$

$$h = h_c + h_n = 2737 + 611 = 3348 \text{ Btu/ft}^2 \cdot \text{h} \cdot \text{F}$$

$$\dot{q}'' = h\Delta T = 3348 \times 8 = 26,786 \text{ Btu/ft}^2 \cdot \text{h} = 84 \text{ kW/m}^2.$$

Example Vb.5.2. Water at a rate of 1200 kg/h flows in a tube having an inside diameter of 30 mm. Pressure is 10 MPa. Find the heat transfer coefficient and the surface heat flux at a location where surface superheat is 10 C and quality is 15%.

Solution: First, we find properties at 10 MPa:

$$\rho_f = 688.7 \text{ kg/m}^3, \mu_f = 0.86\text{E-}4 \text{ N}\cdot\text{s/m}^2, h_{fg} = 1320 \text{ kJ/kg}, c_{p,f} = 6.159 \text{ kJ/kg}\cdot\text{K}, \sigma = 0.012 \text{ N/m},$$

$$\rho_g = 55.14 \text{ kg/m}^3, \mu_g = 0.21\text{E-}4 \text{ N}\cdot\text{s/m}^2, v_{fg} = 0.016 \text{ m}^3/\text{kg}, k_f = 0.522 \text{ W/m}\cdot\text{K}, \text{Pr}_f = 1.02, T_{sat} = 310.88 \text{ C}.$$

Similar to Example Vb.5.1, we find X_M , F and S factors, and h_c and h_n :

$$\text{Find } X_M \text{ from: } X_M = (0.15/0.85)^{0.9} (688.7/55.14)^{0.5} (0.21\text{E-}4/0.86\text{E-}4)^{0.1} = 0.644$$

The F factor becomes:

$$F = 2.35 [0.213 + X_M]^{0.736} = 2.35 (0.213 + 0.644)^{0.736} = 2.1$$

$$d = 0.03 \text{ m}, A = \pi d^2/4 = 3.14 \times 0.03^2/4 = 7.068\text{E-}4 \text{ m}^2, \text{ and } G = 1200/7.068\text{E-}4 = 471.6 \text{ kg/m}^2 \cdot \text{s}$$

$$\text{To find } S, \text{Re}_f = G(1-x)D_h/\mu_f = 471.6 \times (1-0.15) \times 0.03/0.86\text{E-}4 = 139,835$$

$$\text{Re} = \text{Re}_f \times F^{1.25} = 139,835 \times 2.1^{1.25} = 353,500 \text{ and}$$

$$S = (1 + 2.53\text{E-}6 \times 353,500^{1.17})^{-1} = 0.11$$

The convection heat transfer coefficient (h_c) from Equation Vb.5.1a is:

$$h_c = 0.023(0.522/0.03)(139,835)^{0.8} \times 1.02^{0.4} \times 2.1 = 11,077 \text{ W/m}^2 \cdot \text{K}$$

The nucleation heat transfer coefficient (h_n) from Equation Vb.5.1a is:

$$\text{Numerator: } 0.00122 \times 0.522^{.79} \times (6.159\text{E}3)^{.45} \times 688.7^{.49} = 0.91$$

$$\text{Denominator: } (0.86\text{E-}4)^{.29} \times 0.012^{.5} \times (1320\text{E}3)^{.24} \times 55.14^{.24} = 0.559$$

$$\Delta T_{sat} = 10 \text{ C}, T_{surface} = T_{sat} + 10 = 320.88 \text{ C}$$

$$\Delta P = P_{sat}(320.88) - P_{sat}(310.88) = 11.42 - 10 = 1.42\text{E}6 \text{ Pa}$$

$$h_n = (0.91/0.559) \times (1.42\text{E}6)^{0.75} (10)^{0.24} \times 0.11 = 12800 \text{ W/m}\cdot\text{K}$$

$$h = h_c + h_n = 11,077 + 12,800 = 23,878 \text{ W/m}\cdot\text{K}$$

$$\dot{q}'' = h\Delta T = 23,878 \times 10 = 238.7 \text{ kW/m}^2.$$

In the above examples, surface temperature was specified. Otherwise, we should solve the problem by iteration. In an iterative solution, we assume a value for the surface temperature to find ΔT_{sat} and subsequently calculate h_{Chen} from the Chen correlation, Equation Vb.5.1b. Having h , we then recalculate ΔT_{sat} from a heat balance between the surface and the fluid; $\dot{q}'' = h\Delta T_{sat}$. We continue this until we reach the intended convergence criterion, for example $\varepsilon \leq 1\%$. Kandlikar has introduced a more recent correlation, which, according to Lienhard, leads to mean deviations of 16% for water and 19% for refrigerants.

5.3. Critical Heat Flux in Flow Boiling

Due to the importance of flow boiling especially in the operation of nuclear reactors, extensive research has been performed in flow boiling CHF. The CHF mechanism in flow boiling is a function of the flow regime and is either in the form of departure from nucleate boiling, DNB, or dryout. DNB is the mechanism of concern in the design and operation of PWRs. A PWR core contains pressurized subcooled water. In a high power channel, the rate of vaporization at the surface may become so vigorous that it may prevent liquid from reaching the surface, Figure Vb.5.2(a). Depriving the surface of liquid for nucleation results in elevated surface temperature, which may lead to fuel failure. On the other hand, the dryout mechanism is of concern in the design and operation of BWRs. This is because, in high power channels, the flow regime may become annular. With further increase in power, the liquid film may simply dryout as shown in Figure Vb.5.2(b). For this reason, the operational heat flux is maintained well below the CHF, through the application of a variety of safety factors. As shown in Figure Vb.5.2(c), the magnitude of CHF is either a direct or an inverse function of the mass flux, depending on quality. In the DNB region (low x), CHF is a direct function of mass flux whereas in the dryout region (high x) CHF depends inversely on mass flux.

There are many CHF correlations for water in the literature, including Babcock & Wilcox, Combustion Engineering, EPRI, General Electric, Westinghouse,

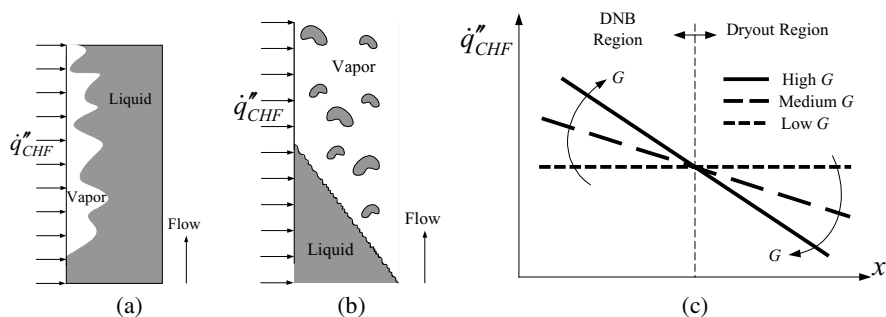


Figure Vb.5.2. Depiction of (a) DNB, (b) Dryout, and (c) Dependency of CHF on Mass Flux (Todreas)

Barnett, Biasi, Bernath, Bowring, Gaspari (CISE-4), and Katto. Next we discuss several of these correlations.

Barnett correlation. The critical heat flux in this correlation is expressed in terms of channel geometry (hydraulic diameter, heated diameter and heated length) as well as coolant mass flux and specific enthalpies. The Barnett correlation covers a narrow range for pressure (i.e., 4 – 10 MPa). The Barnett correlation in SI units is given as:

$$\dot{q}_{CHF}'' = 3.1546 \times 10^6 \frac{3.584 C_1 h_{fg} + 4.3 \times 10^{-4} C_2 (h_f - h_i)}{C_3 + 39.37z} \quad \text{Vb.5.2}$$

where constants C_1 , C_2 , and C_3 are expressed in terms of G and D as

$$C_1 = 230.7 D_h^{0.68} G^{0.192} [1 - 0.744 \exp(-0.3477 D_e G)],$$

$$C_2 = 0.1206 D_h^{1.415} G^{0.817}, \text{ and } C_3 = 8249 D_e^{1.415} G^{0.212}.$$

Bernath correlation is $\dot{q}_{CHF}'' = h_{CHF} (T_{s,CHF} - T_f)$ where h_{CHF} and $T_{s,CHF}$ are in turn obtained from the following relations:

$$h_{CHF} = 10,890 \frac{1}{1 + (P_h / \pi D_e)} + \frac{48V}{D_e^{0.6}}$$

$$T_{s,CHF} = 32 + 102.6 \ln P - \frac{97.2}{1 + (15/P)} - 0.45V$$

where P is system pressure in psia, V is coolant velocity in ft/s, T_f is bulk temperature of the coolant in F, D_e is the equivalent diameter in ft and P_h is the heated perimeter in ft. This correlation is valid for pressure ranging from 23 – 3000 psia, coolant velocity in the range of 4.0 – 54 ft/s, and equivalent diameter in the range of 0.143 – 0.66 in.

Biasi correlation expressed in terms of pressure, mass flux, quality, and diameter, has a much wider range of application for pressure compared to the Barnett correlation. Since the database covers both low and high steam quality, the Biasi correlation is applicable to both DNB and dryout. In SI units, the Biasi correlation for $G < 300 \text{ kg/s}\cdot\text{m}^2$ is given as:

$$\dot{q}_{CHF}'' = S_1 (1 - x) \quad \text{Vb.5.3}$$

where $S_1 = 15.048E7(100D)^{-n}G^{-1/6}C_1$ and heat flux is in W/m^2 . For mass fluxes higher than $300 \text{ kg/s}\cdot\text{m}^2$, the heat flux in W/m^2 is obtained from:

$$\dot{q}_{CHF}'' = S_2 (S_3 - x) \quad \text{Vb.5.4}$$

where $S_2 = 2.764 \times 10^7 (100D)^{-n} G^{-1/6}$ and $S_3 = 1.468 C_2 G^{-1/6}$. In Equations Vb.5.3 and Vb.5.4, constants C_1 and C_2 are only functions of pressure and are given as

$$C_1 = -1.159 + 1.49P \exp(-0.19P) + 9P(1 + 10P^2)^{-1} \quad \text{and} \\ C_2 = 0.7249 + 0.99P \exp(-0.32P)$$

Exponent n is 0.4 if the $D_{\text{channel}} \geq 0.01$ m. Otherwise, its value is 0.6. Also P is in MPa.

If the channel is heated uniformly, an energy balance for a control volume extended from the inlet to height z (where CHF occurs) gives:

$$\dot{q}''(\pi D z) = (\pi D^2 / 4) G (h_l - h_i) \quad \text{Vb.5.5}$$

Substituting for the local enthalpy from $h_l = h_f + x_l h_{fg}$ in Equation Vb.5.5, solving for x_l and substituting into Equations Vb.5.3 and Vb.5.4, the Biasi correlation for uniformly heated tubes becomes:

$$\dot{q}_{CHF}'' = S_1 (1 + \beta) / (1 + \alpha S_1) \quad \text{Vb.5.3}$$

$$\dot{q}_{CHF}'' = S_2 (S_3 + \beta) / (1 + \alpha S_2) \quad \text{Vb.5.4}$$

where $\alpha = 4z / (GD h_{fg})$ and $\beta = \Delta h_{sub,l} / h_{fg}$.

Bowring correlation has a wide range of applicability. It is based on the works of MacBeth and Barnett and in SI units is given as:

$$\dot{q}_{CHF}'' = (C_1 - C_2 x h_{fg}) / C_3 \quad \text{Vb.5.6}$$

where coefficients C_1 , C_2 and C_3 are functions of pressure, mass flux and channel diameter as follows:

$$C_1 = \frac{2.317 C_2 C_4 h_{fg}}{1 + 0.0143 C_5 D^{1/2} G}, \quad C_2 = \frac{DG}{4}, \quad C_3 = \frac{0.308 C_2 C_6}{1 + 0.347 C_7 (G/1356)^n}$$

where exponent n is a function of the reduced pressure (i.e., $n = 2 - 0.5P_R$). The reduced pressure in turn is defined as $P_R = 0.145P$ MPa. Coefficients C_4 through C_7 are functions of reduced pressure. For $P_R < 1$ MPa;

$$C_4 = 0.478 + 0.52 P_R^{18.942} \exp[20.89(1 - P_R)], \\ C_5 = C_4 \left\{ 0.236 + 0.764 P_R^{1.316} \exp[2.444(1 - P_R)] \right\}^{-1}, \\ C_6 = 0.4 + 0.6 P_R^{17.023} \exp[16.658(1 - P_R)], \text{ and } C_7 = C_6 P_R^{1.649}$$

and for $P_R > 1$ MPa, the above coefficients are given as:

$$C_4 = P_R^{-0.368} \exp[0.648(1 - P_R)], \quad C_5 = C_4 \{P_R^{-0.448} \exp[2.445(1 - P_R)]\}^{-1},$$

$$C_6 = P_R^{0.219}, \quad C_7 = C_6 P_R^{1.649}.$$

For uniformly heated channels, we use Equation Vb.5.5 and substitute $h_l = h_f + x h_{fg}$. The same procedure was used for the Biasi correlation to write the Bowring correlation as:

$$\dot{q}_{CHF}'' = \frac{C_1 + C_2 \Delta h_{sub}}{C_3 + z} \quad \text{Vb.5.7}$$

CISE-4 correlation is applicable to BWRs and has a narrow range of application for both pressure and mass flux. This correlation is expressed in terms of CHF quality (x_{CHF}) whose value approaches unity when mass flux approaches 0.0. This correlation in SI units is given as:

$$x_{CHF} = \frac{D_h}{D_e} \left(\frac{C_1 L_{CHF}}{C_2 + L_{CHF}} \right) \quad \text{Vb.5.8}$$

where C_1 and C_2 are functions of mass flux, pressure and critical pressure: The value of coefficient C_1 depends on mass flux as compared with a reference flux (G_R given by $G_R = 3375(1 - P/P_c)^3$). Hence;

$$C_1 = [1 + 1.481 \times 10^{-4} (1 - P/P_c)^{-3} G]^1; \quad G \leq G_R$$

$$C_1 = (1 - P/P_c)(G/1000)^{-1/3}; \quad G > G_R$$

and coefficient C_2 is given by $C_2 = 0.199(P_c/P - 1)^{0.4} GD^{1.4}$. Also L_{CHF} is the boiling length to the point where CHF occurs. To find \dot{q}_{CHF}'' by the CISE-4 correlation, we need to find relations for x_{CHF} and L_{CHF} . To find L_{CHF} , we use an energy balance, Equation Vb.5.5. If the entire tube is uniformly heated at \dot{q}_{CHF}'' , the portion of energy consumed to bring the subcooled water at the inlet of the tube to saturation, is found from:

$$\dot{q}_{CHF}'' [\pi D (L - L_{CHF})] = G (\pi D^2 / 4) (h_f - h_{in})$$

Similarly, we can find x_{CHF} from Equation Vb.5.6 applied to the boiling section:

$$\dot{q}_{CHF}'' \pi D L_{CHF} = G (\pi D^2 / 4) (h - h_f) = G (\pi D^2 / 4) x_{CHF} h_{fg}$$

Eliminating L_{CHF} between these equations and substituting, we obtain x_{CHF} as:

$$x_{CHF} = [4 L \dot{q}_{CHF}'' / (G D h_{fg})] - [(h_f - h_{in}) / h_{fg}] \quad \text{Vb.5.9}$$

Substituting into Equation Vb.5.8, we find the following implicit equation for \dot{q}_{CHF}'' :

$$y / h_{fg} = C_1 (D_h / D_e) [C_2 + L - (h_f - h_{in}) / y] \quad \text{Vb.5.10}$$

where in Equation Vb.5.10, $y = 4 \dot{q}_{CHF}'' / (GD)$.

EPRI-1 correlation as reported by Pei, is based on a vast bank of data:

$$\dot{q}_{CHF}'' = \frac{C_1 - x_{in}}{C_2 + (x_l - x_{in}) / \dot{q}_l''} \quad \text{Vb.5.11}$$

where \dot{q}_l'' is the local heat flux and both heat flux terms in Equation Vb.5.11 are in MBtu/h·ft². Mass flux G is in Mlbm/h·ft². Coefficients C_1 and C_2 are given as:

$$C_1 = P_1 P_r^{P_2} G^{(P_3 + P_7 P_r)}$$

$$C_2 = P_3 P_r^{P_4} G^{(P_6 + P_8 P_r)}$$

Note the reduced pressure is $P_r = P / P_{critical}$. Constants P_1 through P_8 are given as $P_1 = 0.5328$, $P_2 = 0.1212$, $P_3 = 1.6151$, $P_4 = 1.4066$, $P_5 = -0.3040$, $P_6 = 0.4843$, $P_7 = -0.3285$, and $P_8 = -2.0749$.

For uniformly heated channels, we may substitute for the local quality from $x_l = (h_l - h_f) / h_{fg}$ and for the local heat flux from Equation Vb.5.5 to write the EPRI-1 correlation as:

$$\dot{q}_{CHF}'' = \frac{C_1 - x_{in}}{C_2 + [4z / (GDh_{fg})]} \quad \text{Vb.5.12}$$

Katto correlation (Collier) is expressed in terms of quality, mass flux, and enthalpy as:

$$\dot{q}_{CHF}'' = XG[h_{fg} + K(h_f - h_i)] \quad \text{Vb.5.13}$$

where h_i is the inlet enthalpy calculated at P and T_i . Coefficients X and K in Equation Vb.5.13 are functions of dimensionless numbers Z , R , and W defined as:

$$Z = \frac{z}{D}, \quad R = \frac{\rho_f}{\rho_g}, \quad W = \frac{\sigma \rho_f}{zG^2}$$

We need to calculate five values for X and three values for K as follows:

$$X_1 = CW^{0.043} / Z, \quad X_2 = 0.1R^{0.133}W^{0.433}Z / y,$$

$$X_3 = 0.098R^{0.133}W^{0.433}Z^{0.27} / y,$$

$$X_4 = 0.0384R^{0.6}W^{0.173} / (1 + 0.28W^{0.233}Z),$$

$$X_5 = 0.234R^{0.513}W^{0.433}Z^{0.27} / y$$

$$K_1 = 0.261 / (CW^{0.043}), \quad K_2 = 0.833[0.0124 + Z^{-1}] / (R^{0.133}W^{0.333}),$$

$$K_3 = 1.12[1.52W^{0.233} + Z^{-1}] / (R^{0.6}W^{0.173})$$

where $y = 1 + 0.0031Z$ and the value of C in these relations is found as:

$$\begin{aligned} C &= 0.25 & \text{if } Z < 50, \\ C &= 0.25 + 0.0009(Z - 50) & \text{if } 50 < Z < 150, \\ C &= 0.34 & \text{if } Z > 150. \end{aligned}$$

The following logic should be used to find the applicable values of X and K :

$R < 0.15$

If $X_1 < X_2$, $X = X_1$

If $X_1 > X_2$ and $X_2 < X_3$, $X = X_2$

If $X_1 > X_2$ and $X_2 > X_3$, $X = X$

If $K_1 > K_2$, $K = K_1$

If $K_1 < K_2$, $K = K_2$

$R > 0.15$

If $X_1 < X_5$, $X = X_1$

If $X_1 > X_5$ and $X_4 < X_5$, $X = X_5$

If $X_1 > X_5$ and $X_4 > X_5$, $X = X_4$

If $K_1 > K_2$, $K = K_1$

If $K_1 < K_2$ and $K_2 < K_3$, $K = K_2$

If $K_1 < K_2$ and $K_2 > K_3$, $K = K_3$

General Electric correlation, devised for BWRs, expresses the lowest measured values of critical heat flux as a function of mass flux and quality:

$$\dot{q}_{CHF}'' = 0.705 + 0.237G \quad X < C_1$$

$$\dot{q}_{CHF}'' = 1.634 - 0.27G - 4.71X \quad C_1 < X < C_2$$

$$\dot{q}_{CHF}'' = 0.605 - 0.164G - 0.653X \quad C_2 < X$$

where constants C_1 and C_2 are given in terms of mass flux:

$$C_1 = 0.197 - 0.108G$$

$$C_2 = 0.254 - 0.026G$$

In these relations, X is the flow quality, mass flux G is in Mlbm/h-ft^2 , and heat flux \dot{q}_{CHF}'' is in MBtu/h-ft^2 . The above relations apply to a system at a pressure of 1000 psia. For other pressures, we find \dot{q}_{CHF}'' from:

$$\dot{q}_{CHF}''(P) = \dot{q}_{CHF}''(1000) + 440(1000 - P)$$

The GE correlation is valid for P in the range of 600 – 1450 spia, G in the range of 0.4 – 6 Mlbm/h-ft^2 , quality in the range of 0 – 0.45, channel length in the range of 29 – 108 in, and equivalent diameter in the range of 0.245 – 1.25 in. As reported

by Tong, the GE lower envelope correlation for low mass velocity CHF at pressures less than 1000 psia is obtained from:

$$\begin{aligned}\dot{q}_{CHF}'' &= 0.84 - x, & G < 0.5 \text{ Mlbm/h}\cdot\text{ft}^2 \\ \dot{q}_{CHF}'' &= 0.80 - x, & 0.5 < G < 0.75 \text{ Mlbm/h}\cdot\text{ft}^2\end{aligned}$$

where the critical heat flux is in MBtu/h·ft². The range of applicability of these correlations are shown in Table Vb.5.1.

Table Vb.5.1. Data base for various CHF correlations

Correlation	D (m)	L (m)	P (MPa)	G (kg/m ² s)
Biasi	0.0030 – 0.3750	0.20 – 6.00	0.27 – 14	100 – 6000
Bowring	0.0020 – 0.0450	0.15 – 3.70	0.20 – 19	136–18,600
Barnett	0.0095 – 0.0960	0.61 – 2.74	6.9	190 – 8409
CISE-4	0.0102 – 0.0198	0.76 – 3.66	4.96 – 7.0	1085 – 4069
EPRI-1	0.0420 – 0.0139	0.76 – 4.27	1.38 – 17	271 – 5553
Katto	0.0010 – 0.038	0.01 – 8.80	00.1 – 21*	**
General Electric	0.0060 – 0.0320	0.74 – 2.74	4.14 – 10	550 – 8000

* Specified in terms of $0.0003 < \rho_g/\rho_f < 0.41$. ** Specified in term of $3\text{E-}9 < W < 2\text{E-}2$.

Predictions of several CHF correlations are compared in the following example.

Example Vb.5.3. Water at 288 C (550 F) enters a uniformly heated vertical tube of diameter 13.4 mm (0.528 in) and length 3.66 m (12 ft) at 3508 kg/s·m² (2.59 Mlb/s·ft²). The system pressure is 15.51 MPa (2250 psia). Find CHF from the Biasi, the Bowring, the EPRI-1, and the Katto correlations.

Solution: We first find water properties at 15.51 MPa: $h_f = 1631$ kJ/kg (701 Btu/lbm), $h_g = 2600$ kJ/kg (1118 Btu/lbm), $h_{fg} = 969$ kJ/kg (417 Btu/lbm), $h_i(P = 15.51 \text{ \& } T = 288) = 1273.7$ kJ/kg (547 Btu/lbm).

Biasi correlation: Since $G > 300$ kg/s·m², we use Equation Vb.5.4:

$$C_1 = -1.159 + 1.49P \exp(-0.19P) + 9P(1 + 10P^2)^{-1} = 0.1123$$

$$C_2 = 0.7249 + 0.99P \exp(-0.32P) = 0.8322$$

$$S_2 = 2.764 \times 10^7 (100D)^{-n} G^{-1/6} = 0.5949\text{E}7,$$

$$S_3 = 1.468C_2 G^{-1/6} = 0.3134$$

$$\alpha = 4z/(GDh_{fg}) = 4 \times 3.66/(3508 \times 0.0134 \times 969\text{E}3) = 3.2\text{E-}7$$

$$\beta = (h_f - h_{in})/h_{fg} = (1631 - 1273)/2600 = 0.3686$$

$$\dot{q}_{CHF}'' = S_2 (S_3 + \beta) / (1 + \alpha S_2) = 0.5949\text{E}7 \times (0.3134 + 0.3686) / (1 + 3.2\text{E-}7 \times 0.5949\text{E}7) = 1.39 \text{ MW/m}^2$$

Bowring correlation: We first obtain $C_4 = 0.478$, $C_5 = 0.4912$, $C_6 = 0.4$, and $C_7 = 0.0345$. We then find:

$$C_1 = 2.317C_2C_4h_{fg} / (1 + 0.0143C_5D^{1/2}G) = 0.3274E7, C_2 = DG/4 = 11.75,$$

$$C_3 = 0.308C_2C_6 / [1 + 0.347C_7(G/1356)^n] = 1.3507$$

$$\dot{q}_{CHF}'' = (C_1 + C_2\Delta h_{sub}) / (C_3 + z) = (0.3274E7 + 11.75 \times (1631 - 1273.7)E3 / (1.3507 + 3.66) = 1.49 \text{ MW/m}^2$$

EPRI-1 correlation: We use Equation Vb.5.12 for which we find coefficients C_1 and C_2 from:

$$C_1 = P_1 P_r^{P_2} G^{(P_3 + P_7 P_r)} = 0.5328 \times (2250/3205.6)^{0.1212} \times 2.56^{[-0.3040 - 0.3285 \times (2250/3205.6)]} = 0.3069$$

$$C_2 = P_3 P_r^{P_4} G^{(P_6 + P_8 P_r)} = 1.6151 \times (2250/3205.6)^{1.4066} \times 2.56^{[0.4843 - 2.0749 \times (2250/3205.6)]} = 0.3892$$

$$\begin{aligned} \dot{q}_{CHF}'' &= \frac{C_1 + (\Delta h_{sub,i} / h_{fg})}{C_2 + [4z / (GDh_{fg})]} \\ &= \frac{0.3069 + [(701 - 547) / 417]}{0.3892 + (4 \times 3.66 / (2.59 \times 0.0134 \times 417))} 0.48 \text{ MBtu/h}\cdot\text{ft}^2 = 1.52 \text{ MW/m}^2 \end{aligned}$$

Katto correlation: We first find $Z = z/D = 272.95$, $R = \rho_g/\rho_f = 0.17$, and $W = 0.65E-7$. Now find X_i & K_i :

$$X_1 = 0.6114E-3, X_2 = 0.1732E-3, X_3 = 0.1475E-3, X_4 = 0.2881E-3, X_5 = 0.1803E-3, K_1 = 1.564, K_2 = 4.185, K_3 = 2.022.$$

Using the selection logic, we find $X = 0.2881E-3$ and $K = 2.022$

$$\dot{q}_{CHF}'' = XG[h_{fg} + K(h_f - h_i)] = 0.2881E-3 \times 3508[969E3 + 2.022(1631 - 1273.7)E3] = 1.71 \text{ MW/m}^2$$

Example Vb.5.4. Water at 400 F and 1000 psia enters a uniformly heated channel at a rate of $1E6 \text{ lbm/h}\cdot\text{ft}^2$. The channel heated and equivalent diameters are $D_h = D_e = 0.3 \text{ in}$. Channel length is 1.5 ft. Find the critical heat flux and wall temperature at CHF.

Solution: We first use a CHF correlation, such as EPRI-1 for example to find the critical heat flux:

$$\begin{aligned} \dot{q}_{CHF}'' &= \frac{C_1 + (\Delta h_{sub,i} / h_{fg})}{C_2 + (4z / GDh_{fg})} = \frac{0.4627 + (166.5 / 650.5)}{0.3140 + (4 \times 1.5 / 1 \times 0.025 \times 650.5)} \\ &= 1.05E6 \text{ Btu/h}\cdot\text{ft}^2 \end{aligned}$$

The solution to find T_{CHF} is basically iterative. However, we may use the Bernath correlation to find the onset of the boiling crisis. For this purpose, we need the local enthalpy:

$$h_l = h_i + (4z \dot{q}_{CHF}'' / GD) = 375.8 + [4 \times 1.5 \times 1.05 / (1 \times 0.025)] = 627.8 \text{ Btu/lbm}$$

Density at the onset of CHF is $\rho = \rho(1000 \text{ psia}, 627.8 \text{ Btu/lbm})$. Hence, $\rho_l = 46.3 \text{ lbm/ft}^3$:

$$V = G/\rho = (1E6/3600)/46.3 = 6 \text{ ft/s}$$

$$T_{s,CHF} = 32 + 102.6 \ln 1000 - [97.2 / (1 + 15 / 1000)] - 0.45 \times 6 = 642.3 \text{ F.}$$

5.4. Factors Affecting CHF

Critical heat flux correlations show the dependency of CHF on flow path diameter (d), flow path length (L), mass flux (G), inlet subcooling (Δh_{in}), and pressure (P). To determine the effect of each parameter, the rest of the parameters are kept constant. Let's first consider the case of upward flow of a liquid in a heated tube having diameter d and length L . Figure Vb.5.3 shows that CHF varies directly with Δh_{in} , G , and d and varies inversely with L . Pressure has a more interesting effect as CHF for water in both pool and flow boiling reaches a maximum at about 70 bar. To investigate the effect of heat flux on CHF, we try three cases of low, medium, and high heat fluxes, as shown by dashed lines 1, 2, and 3 in Figure Vb.5.4(A).

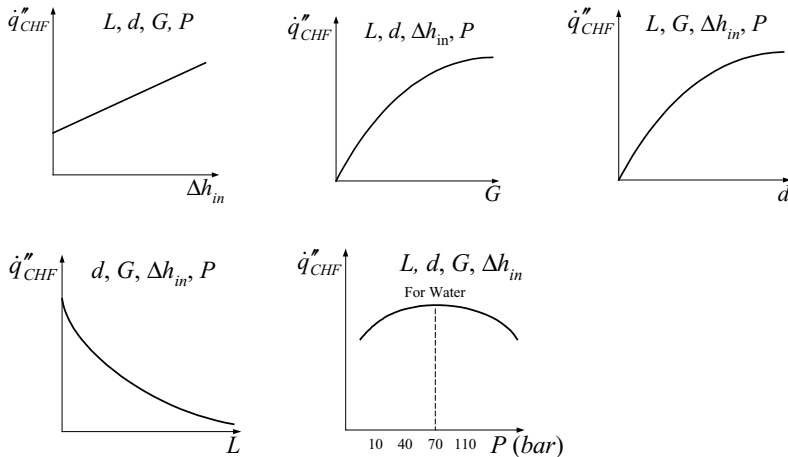


Figure Vb.5.3. Effect of various design parameters on CHF (Whalley)

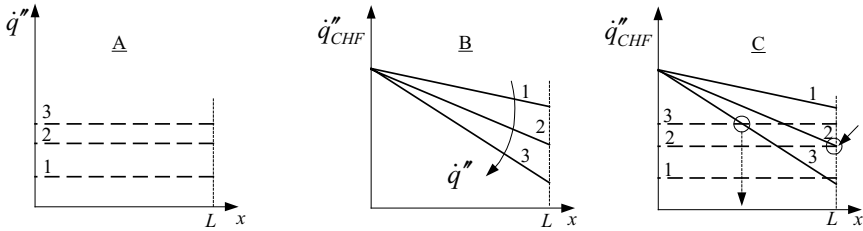


Figure Vb.5.4. Effect of uniform heat flux on critical heat flux

Expectedly, the critical heat flux correlations show that CHF inversely depends on heat flux. This is shown in figure B. Superimposing figures A and B, we obtain figure C. Let's examine this figure. We observe that at low heat flux (dashed and solid lines 1), CHF does not occur. When we increase heat flux, (dashed and solid lines 2), they intersect right at the tube exit. If we further increase heat flux, CHF occurs at a lower part of the tube (intersection of dashed and solid lines 3). The point at which CHF occurs moves towards the exit of the tube, as the heat flux is reduced. Hence, in uniformly heated channels, CHF always occurs first at the exit of the channel. Let's us now examine the case of non-uniform heat flux, which is the case in the core of nuclear plants. Since neutron flux has a sinusoidal distribution in the axial direction, heat flux has also a sinusoidal distribution, as shown in Figure Vb.5.5 (A). In this figure, two curves are shown for low heat flux (curve 1) and for high heat flux (curve 2). CHF versus tube length for the same two heat fluxes is shown in figure B. We obtain figure C by superimposing figures A and B. As seen in figure C, CHF occurs first in the upper part of the tube. As heat flux is increased, then CHF occurs at other locations along the tube.

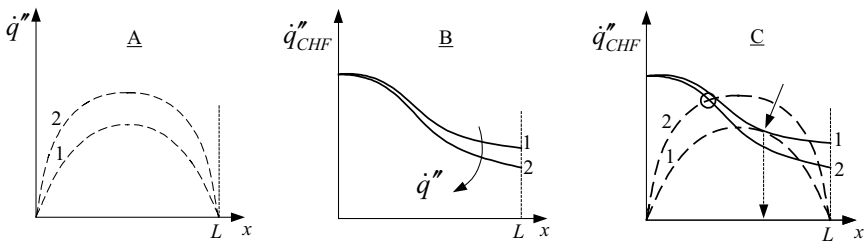


Figure Vb.5.5. Effect of non-uniform heat flux on critical heat flux

5.5. Transition Flow Boiling

In temperature controlled flow boiling, transition to film flow boiling occurs when the local heat flux exceeds the CHF. In this regime, heat transfer alternates between nucleate and film boiling regimes. The heat transfer coefficient for transition boiling may be calculated from the McDonough correlation:

$$\dot{q}'' = \dot{q}_{CHF}'' - C_1(T_s - T_{s,CHF}) \quad \text{Vb.5.10}$$

where T_s and $T_{s,CHF}$ are surface temperatures corresponding to \dot{q}'' and \dot{q}_{CHF}'' , respectively. Coefficient C_1 is given as a function of pressure. If $P > 1200$ psia, then $C_1 = 1180.8 - 0.252(P - 1200)$. Otherwise, $C_1 = 1180.8 - 0.801(P - 1200)$. The heat transfer coefficient for transition boiling is obtained by dividing \dot{q}'' calculated from Equation Vb.5.10 by $(T_s - T_{sat})$. The transition boiling correlation is valid until the heat flux calculated from Equation Vb.5.10 becomes smaller than the heat flux corresponding to stable film flow boiling. More recently, Cheng suggested a similar correlation:

$$\dot{q}'' = \dot{q}_{CHF}'' \left[(T_s - T_{sat}) / (T_{s,CHF} - T_{sat}) \right]^n \quad \text{Vb.5.11}$$

where for low-pressure $n = -1.25$. Bjornard tied the transition heat flux to CHF and MSFB:

$$\dot{q}'' = C_1 \dot{q}_{CHF}'' + (1 - C_1) \dot{q}_{MSFB}'' \quad \text{Vb.5.12}$$

where coefficient C_1 itself is tied to the T_{CHF} and T_{MSFB} as $C_1 = [(T_{MSFB} - T_s) / (T_{MSFB} - T_{CHF})]^2$.

5.6. Film Flow Boiling

The heat transfer coefficient in stable film flow boiling may be calculated from the correlation suggested by Dougal-Rohsenow. This correlation is a Reynolds number-modified Dittus-Boelter correlation given as:

$$h = (0.023k / D) [\text{Re}(v/v_g)]^{0.8} \text{Pr}^{0.4} \quad \text{Vb.5.14}$$

The appearance of v/v_g makes Equation Vb.5.14 also applicable to the flow of single-phase vapor.

QUESTIONS

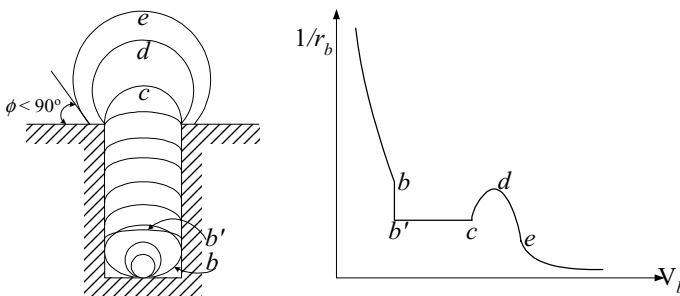
- What are the three conditions for bubble equilibrium? Why should the liquid be superheated?
- What is the difference between boiling by a heated surface and boiling by reducing the pressure of a saturated liquid? Why is Equation Vb.2.1 not sufficient to predict the degree of superheat required for nucleation?
- A heated plate is immersed in water. The temperature profiles of the thermal sub-layer and bubble as given by the Clausius-Clapeyron relation do not intersect. What should be done to start nucleation?
- Can we construct the entire boiling curve in a power-controlled process?
- In which medium (liquid or vapor) is the contact angle measured?
- Is it correct to say that the heat flux in nucleate pool boiling is a function of surface conditions, surface superheat, and pressure?

- Consider two electrically heated stainless steel surfaces. One surface is mechanically polished and the other is ground and polished. Both surfaces are maintained at the same temperature and boiling with the same liquid is taking place at the same pressure. Which surface requires higher power?
- Since ρ , h_{fg} , T_{sat} , and σ are functions of pressure, can we conclude that \dot{q}'' in pool nucleate boiling increases as pressure increases?
- Why does surface aging decrease the rate of surface heat flux?
- Explain the effect of non-condensable gases on boiling and on condensation heat transfer.
- Since g appears in boiling correlations, can we conclude that heat flux is a function of gravity?
- Why is boiling heat flux not affected by surface roughness in the film boiling mode?
- What is the difference between dryout CHF and DNB CHF? In what type reactor is DNB a concern?
- What effect does mass flux have on critical heat flux?
- Can transition boiling be experienced in heat flux controlled boiling?
- Is the Chen correlation for heat transfer coefficient applicable to post-CHF heat transfer?
- In a uniformly heated tube, at what location is CHF most likely to occur?

PROBLEMS

1. We noticed that the required degree of superheat depends both on the surface condition (the size of the nucleation sites) and the type of liquid (wetting versus non-wetting). Regarding the type of liquid, we want to examine two extreme cases. Find the required degree of superheat for nucleation for liquids that completely wet the surface ($\phi = 0^\circ$). Similarly, find the degree of superheat for completely non-wetting liquids ($\phi = 180^\circ$). [Ans.: For $\phi = 0$, there is no nucleation. For $\phi = 180$, no superheat is required].

2. Similar to the bubble growth in a conical cavity, the bubble growth in a cylindrical cavity is shown in the figure. Verify the accuracy of the plot of the inverse of bubble radius ($1/r$) versus bubble volume.



3. Find the degree of superheat ($T_s - T_{sat}$) for a horizontal flat plate in water at atmospheric pressure needed to cause nucleation if cavity sizes of $5\text{ }\mu\text{m}$ are present in the heated surface.
4. Use Equation Vb.2.4 to find the minimum degree of superheat for the onset of nucleate boiling.
5. Use Equation Vb.2.1 to compare the required degree of superheat for water and for sodium nucleation. [Hint: $\sigma_{\text{sodium}} > \sigma_{\text{water}}$].
6. A polished copper plate 0.05 m^2 in area is placed in water and electrically heated to 116 C . Find the rate of evaporation. [Ans.: $\dot{q}'' = 0.587\text{E}6\text{ W/m}^2$, $\dot{m} = 46.86\text{ kg/h}$, and $h = 36,688\text{ W/m}^2\cdot\text{C}$].
7. A pan made of stainless steel contains water at atmospheric pressure. The pan diameter is 25 cm and its surface is mechanically polished. The pan is now heated while its surface is maintained at 116 C . Find the surface heat flux, the boil off (evaporation) rate, and the peak heat flux. [Ans.: $\dot{q}'' = 5.6\text{E}5\text{ W/m}^2$, $\dot{m} = 44\text{ kg/h}$, and $\dot{q}_{CHF}'' = 1.27\text{ MW/m}^2$. Note that the operating heat flux is less than half of the peak heat flux hence, a safety factor of $1.27\text{E}6/0.56\text{E}6 = 2.26$].
8. A platinum wire having a diameter of 1.27 mm is used to boil water at atmospheric pressure. The surface superheat is 650 C . Find h and \dot{q}'' . [Ans.: $h_{conv} = 298\text{ W/m}^2\cdot\text{C}$, $h_{total} = 368\text{ W/m}^2\cdot\text{C}$, 240 kW/m^2]
9. Use the Rohsenow pool boiling correlation to find the heat flux at which incipient boiling occurs. The natural convection heat flux is given as $\dot{q}'' = 2.63\Delta T^{1.25}\text{ kW/m}^2$. Use water ($C_{sf} = 0.0132$) at $P = 3.5\text{ MPa}$. [Ans.: 4.2 kW/m^2].
10. A pool of liquid nitrogen at atmospheric pressure is used to cool an electronic device that generates a constant amount of heat. As the temperature of the device is unacceptably high, the following measures are proposed to lower the temperature:
 - a) substitute liquid hydrogen (a lower boiling point) for nitrogen
 - b) increase the heat transfer area by a factor of three
 - c) do both a and b.
 Use the given data and recommend the course of action that should be followed.
 Data: $(T_{Wall})_{Initial} = 1000\text{ R}$, $\dot{q}'' = 150,000\text{ Btu/h}\cdot\text{ft}^2$, properties in British Units are:

	T_{sat}	h_{fg}	ρ_v	ρ_l	σ	k_v	k_l	μ_v	μ_l
H_2	37	190	0.084	4.50	1.45E-4	0.0080	0.067	0.0027	0.032
N_2	140	86	0.280	50.0	5.90E-4	0.0034	0.088	0.0130	0.440

where T_{sat} (R), h_{fg} (Btu/lbm), ρ (lbm/ft³), σ (lbf/h), k (Btu/h·ft·F), μ (lbm/h·ft).

You may use the Rohsenow and Griffith correlation for critical heat flux:

$$\dot{q}_{CHF}'' = 143 \rho_v h_{fg} (\Delta \rho / \rho_v)^{0.6}.$$

11. A tank of water at atmospheric pressure is heated by an electric resistance heater. The voltage to the heater is held constant at 1000 V. Over the range of interest, the resistance of the heater in British units can be expressed as $R(T) = -21.07 + 0.11585T$ where T is in F and R is in ohms. The water is heated to saturation. At some location the heater temperature reaches 250 F, at which point CHF occurs, and the boiling regime changes to film boiling. Find the heat flux and the heater temperature at which the heater will be operating after this occurs. Data: $d_{\text{Heater}} = 0.25$ in, $A_{\text{Heater}} = 1$ ft². Neglect radiation effects.

12. Water at a rate of 1 lbm/s flows in a vertical heated tube ($d = 1.5$ in). System pressure is 1250 psia. Find heat flux at a point where steam quality is 15% and surface superheat is 12 F. [Ans.: $\dot{q}'' = 108$ kW/m²]

13. Water flows at a rate of 0.1 kg/s in a tube with a diameter of 250 mm. The tube is heated uniformly at a rate of 135 kW/m². Find the wall temperature at a location where $T_{\text{sat}} = 180$ C and $x = 25\%$. [Ans.: $T_s = 188$ C]

14. Consider the case of liquid flow in a uniformly heated channel. Initially, heat flux is so low that it only increases the liquid sensible heat. We then start to increase heat flux until water starts to boil. We keep increasing heat flux until eventually we attain a specific value for heat flux at which the tube first experiences CHF. Under this condition at what point does CHF first occur?

15. A test tube for boiling water has a diameter of 25 mm. Water at a rate of 1000 kg/h enters the uniformly heated tube. If pressure is 7.5 MPa, find the heat transfer coefficient and heat flux at a location where mixture quality is 0.25. $\Delta T_{\text{sat}} = 10$ C. [$h_c = 18,193$ W/m·K, $h_n = 6,669$ W/m·K, $\dot{q}'' = 249$ kW/m²]

16. Water at a rate of 0.25 lbm/s flows in a vertical heated tube having a diameter of 0.5 inches. Pressure in the tube is 900 psia. Find the heat flux at a point where the mixture enthalpy is 640 Btu/lbm and the surface superheat is 6 F. [Ans.: $\dot{q}'' = 97.6$ kW/m²].

17. Two simple correlations for nucleate flow boiling (subcooled and saturated) of water at $500 \text{ psia} \leq P \leq 1000 \text{ psia}$ are given by Jens-Lottes and by Thom-1966. These correlations in British units are:

$$\text{Jens-Lottes:} \quad \dot{q}'' / 1.E6 = \text{Exp}(4P / 900) \Delta T_{\text{sat}}^4 / 60^4$$

$$\text{Thom:} \quad \dot{q}'' / 1.E6 = \text{Exp}(2P / 1260) \Delta T_{\text{sat}}^2 / 72^4$$

where \dot{q}'' is in Btu/hr·ft², P is in psia, and T is in F. These correlations in SI units become:

$$\text{Jens-Lottes:} \quad \dot{q}'' / 1.E6 = \text{Exp}(4P / 6.2) \Delta T_{\text{sat}}^4 / 25^4$$

$$\text{Thom:} \quad \dot{q}'' / 1.E6 = \text{Exp}(2P / 8.7) \Delta T_{\text{sat}}^2 / 22.7^4$$

where \dot{q}'' is in W/m^2 , P is in MPa, and T is in C. Use these correlations to compare the results with the Chen correlation for $P = 800$ psia, $\Delta T_{sat} = 10$ F, and steam quality equal to 0.1.

18. In flow boiling, we often need to find the surface temperature and its location at which subcooled boiling begins. Although such local temperature for the incipience of subcooled boiling is not a single fixed temperature, we can estimate its value from the following relation:

$$T_{SB} = T_{sat} + (\Delta T_{sat})_{J-L} - (\dot{q}'' / h)$$

where $(\Delta T_{sat})_{J-L}$ is found from the Jens-Lottes correlation (see Problem 9). Find the location and value of the surface temperature for the following case:

Water enters a heated pipe of 0.7 in diameter at $T = 525$ F, $P = 1000$ psia, and $V = 8$ ft/s. Surface heat flux is uniform at a rate of $1000 \text{ Btu/h}\cdot\text{ft}^2\cdot\text{F}$. [Ans.: $(T_s)_{\text{incipient boiling}} = 547.8 \text{ F}$].

Vc. Condensation

Similar to boiling, condensation is another mode of heat transfer, which is associated with a phase change. Thus for constant system pressure, heat transfer takes place at constant fluid temperature. While boiling requires heat addition, in condensation, heat should be removed so that the process can take place. Such heat removal may be accomplished by employing a coolant or by transferring heat to a solid. Condensers are important components of steam power plants, refrigerators, and chemical plants. We begin this chapter with the definition of terms pertinent to condensation heat transfer.

1. Definition of Condensation Heat Transfer Terms

Sensible energy ($c_p\Delta T$) refers to the energy transfer due to the change in temperature.

Latent energy (h_{fg}) refers to the heat of vaporization, a process during which change of phase takes place at constant temperature. The latent energy is also known as latent heat.

Condensation is a process during which vapor changes phase and becomes liquid if vapor temperature is reduced to below the saturation temperature. If vapor also includes noncondensable gases, the saturation temperature corresponds to the condensable gas partial pressure. The condensable gas we consider in this chapter is steam. Modes of condensation are described below and shown in Figure Vc.1.1 (a) through (e).

Homogenous condensation is a mode of condensation, which occurs within the vapor field, where vapor forms tiny droplets of liquid suspended in the bulk of the vapor to form a fog (Figure a). At the formation, the drops are very small and fall so slowly that they can be considered suspended in the bulk vapor. As the concentration of these drops increases, they combine to form larger drops, falling as rain (*rainout*). If the vapor also contains gases, the fog is generated when the bulk vapor becomes supersaturated (relative humidity > 100%). That is to say that the vapor temperature drops below the saturation temperature at the steam partial pressure or the steam pressure is greater than the saturation pressure at the vapor temperature. A similar phenomenon, but for a liquid, is *flashing*, which occurs when the liquid temperature is above the saturation temperature at the total pressure.

Direct contact condensation is a mode of condensation where vapor is condensed directly on colder liquid. Examples for such mode of condensation include quench-tank of a PWR (Figure b) and the suppression pool of a BWR. Another example includes condensation of steam on the spray droplets.

Heterogeneous condensation occurs on a cooler surface (Figures c, d, and e). Heterogeneous condensation is the basis for the operation of condensers. During

the condensation process, the latent heat associated with the phase change is transferred to the cooler surface.

Dropwise condensation is a type of heterogeneous condensation (Figure c) where drops randomly appear on a cooler surface placed in the bulk vapor. This generally happens if the surface is not clean or the liquid does not wet the surface. Rate of heat transfer in dropwise condensation is very high due to the high exposure of surface area to the vapor. However, the tiny drops would eventually join, reducing exposed surface area for condensation. Liquid wet-ability is discussed in Chapter Vb.

Film condensation occurs when the liquid, which is formed from the condensation of vapor, wets a clean and uncontaminated cooler surface, blanketing it with a smooth film. In vertical plates, the thickness of the film increases as the condensate flows downward (Figures d and e). Appearance of the film on the surface reduces the effectiveness of condensation heat transfer, due to the temperature gradient across the film and the associated thermal resistance of the film. In this chapter, we consider only film condensation.

Jakob number, after Maxim Jakob, is the ratio of sensible heat to the latent heat, $Ja = c_p \Delta T / h_{fg}$.

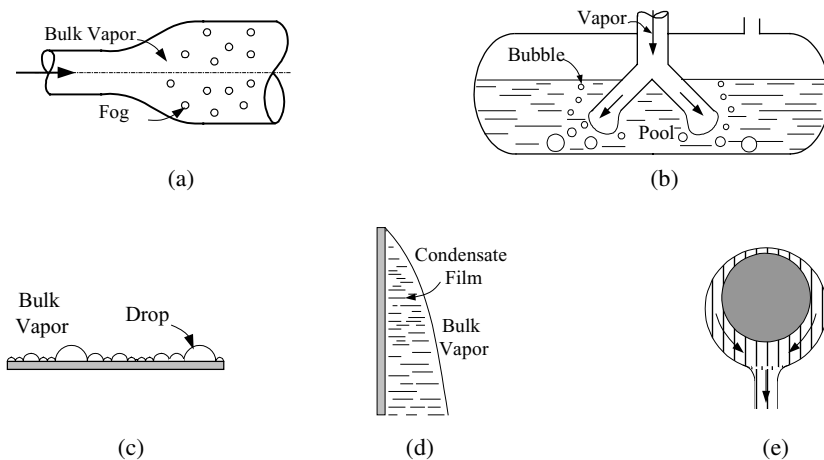


Figure Vc.1.1. Various modes of condensation

2. Analytical Solution

To find an analytical solution for the heat transfer coefficient in condensation, we consider the formation of a film of condensate on the cold surface of a vertical plate placed in a vapor. The vapor generally includes noncondensable gases. As shown in Figures Vc.2.1.(a and b), the film thickness increases as liquid flows

down since more vapor condenses on the film. Liquid velocity is zero at the wall, increasing to its maximum value at the edge of the boundary layer. Liquid temperature approaches surface temperature near the wall and increases to saturation temperature at the edge of the boundary layer. Nusselt's derivation for film condensation now follows.

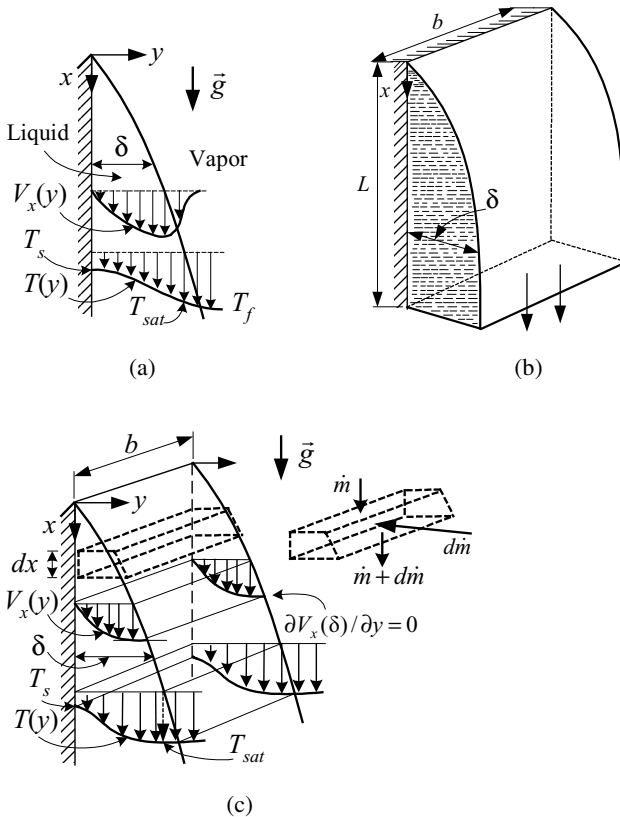


Figure Vc.2.1. (a) Film of condensate as boundary layer and (b) Nusselt model of the condensate film

2.1. Nusselt Derivation of Film Condensation

To be able to derive an analytical solution, several simplifying assumptions are made, per Nusselt. First we assume that vapor does not contain any noncondensable gas. Second, we assume that the flow of the film is laminar with thermal properties independent of temperature. Finally, we assume the shear stress at the edge of the boundary layer is negligible ($\partial u(\delta)/\partial y = 0$) and temperature profile in the film is linear. The governing equation for the hydrodynamic boundary layer is Equation IIIa.3.20-1, which reduces to:

$$0 = -\frac{1}{\rho} \frac{\partial P}{\partial x} + \nu \frac{\partial^2 V_x}{\partial y^2} + \frac{1}{\rho} X \quad \text{Vc.2.1}$$

where the body force in the film is now $X = \rho_f g$ and the pressure gradient is $dP/dx = \rho_g g$. Substituting in Equation Vc.2.1, yields:

$$\frac{\partial^2 V_x}{\partial y^2} = -g(\rho_f - \rho_g) / \mu_f \quad \text{Vc.2.2}$$

Integrating Equation Vc.2.2 and using the boundary conditions of $V_x(0) = 0$ and $\partial V_x(\delta)/\partial y = 0$ we find:

$$V_x(y) = \frac{g(\rho_f - \rho_g)\delta^2}{\mu_f} \left[\frac{y}{\delta} - \frac{1}{2} \left(\frac{y}{\delta} \right)^2 \right] \quad \text{Vc.2.3}$$

Note that V_x is also a function of x since $V_x = f[\delta(x)]$. Having the velocity profile, mass flow rate is:

$$\dot{m}(x) = \int_0^{\delta(x)} \rho V_x(y) b dy = b g \rho_f (\rho_f - \rho_g) \delta^3 / (3\mu_f) \quad \text{Vc.2.4}$$

Both V_x and \dot{m} are functions of δ , itself an unknown. To find δ , we use an energy balance for the control volume of Figure Vc.2.1. At steady state, the energy entering the control volume ($d\dot{m} h_{fg}$) is equal to the energy leaving the control volume and entering the colder surface, $d\dot{Q} = k_f(bdx)(T_{sat} - T_s)/\delta$. Setting these equal and using Equation Vc.2.4, we find that $[bg\rho_f(\rho_f - \rho_g)\delta^2 / \mu_f] h_{fg} d\delta/dx = k_f(bdx)(T_{sat} - T_s)/\delta$. So that δ becomes:

$$\delta(x) = \left(\frac{4k_f \mu_f (T_{sat} - T_s) x}{g\rho_f(\rho_f - \rho_g) h_{fg}} \right)^{0.25} \quad \text{Vc.2.5}$$

Having δ , we can find both V_x and \dot{m} as explicit functions of x . Since $h = k_f/\delta$ and $Nu = hL/k_f$, we then have both of these parameters also as functions of x . Integrating from x to L , we can find \bar{h} and \bar{Nu} :

$$\bar{h}_L = 0.943 \left(\frac{g\rho_f(\rho_f - \rho_g) k_f^3 h'_{fg}}{\mu_f (T_{sat} - T_s) L} \right)^{0.25} \quad \text{Vc.2.6}$$

Note that in Equation Vc.2.6, we replaced h_{fg} by $h'_{fg} = h_{fg}(1 + 0.68Ja)$, per Rohsenow's recommendation. This is to account for two effects: cooling of the film below the saturation temperature and the non-linear temperature profile in the

film. Total rate of heat transfer to the plate is $\dot{Q} = \bar{h}_L A (T_{sat} - T_s)$ and total rate of condensate produced is $\dot{m} = \dot{Q} / h'_{fg}$. To determine a condensation Reynolds number, we use Equation III.6.3, $Re = 4\dot{m} / (\pi\mu D)$, which is appropriate for condensation on a vertical cylinder. For a flat plate we have $\pi D \equiv b$ hence, $Re = 4\dot{m} / (\mu b)$. Substituting for \dot{m} in term of \dot{Q} , we obtain the Reynolds number as $Re_L = 4\bar{h}_L L (T_{sat} - T_s) / (h_{fg}\mu_f)$ where L is the plate length. Flow is laminar if $Re_L < 30$. For sufficiently large vertical plates the flow may become turbulent. For fully turbulent flow $Re > 1800$ and in the range of $30 < Re < 1800$, the condensate film becomes wavy and hence, referred to as the wavy laminar region.

Example Vc.2.1. A vertical flat plate 1.2 ft long and 2 ft wide is maintained at 424.8 F and exposed to saturated steam at 450 psia. Find the total rate of heat transfer to the plate and the condensate mass flow rate.

Solution: We first find $T_{sat}(450 \text{ psia}) = 456.4 \text{ F}$ then $T_{film} = (456.4 + 424.8)/2 = 440.6 \text{ F}$ to find the following:

For steam at $T_{sat} = 456.4 \text{ F}$: $h_{fg} = 768.2 \text{ Btu/lbm}$ and $\rho_v = 0.968 \text{ lbm/ft}^3$

For water at $T_{film} = 440.6 \text{ F}$: $k_f = 0.37 \text{ Btu/ft}\cdot\text{h}\cdot\text{F}$, $\mu_f = 0.285 \text{ lbm/ft}\cdot\text{h}$,

$\rho_f = 52 \text{ lbm/ft}^3$, $c_{pf} = 1.1 \text{ Btu/lbm}\cdot\text{F}$

Since $T_s \ll T_{sat}$ we need to find $h'_{fg} = h_{fg}(1 + 0.68Ja)$

$Ja = 1.1 \times (456.4 - 424.8)/768.2 = 0.045$. Thus, $h'_{fg} = 791.7 \text{ Btu/lbm}$

$$\begin{aligned}\bar{h}_L &= 0.943 \left[\frac{g\rho_f(\rho_f - \rho_g)k_f^3 h'_{fg}}{(\mu_f(T_{sat} - T_s)L)} \right]^{0.25} \\ &= 0.943 \left[\frac{(32.2 \times 3600^2) \times 52(52 - 0.968) \times 0.37^3 \times 791.7}{0.285 \times (456.4 - 424.8) \times 1.2} \right]^{0.25}\end{aligned}$$

$$\bar{h}_L = 1342.6 \text{ Btu/ft}^2\cdot\text{h}\cdot\text{F}$$

$$\dot{Q} = \bar{h}_L A (T_{sat} - T_s) = 1342.6 \times (1.2 \times 2) \times (456.4 - 424.8) = 101,823 \text{ Btu/h.}$$

$$\dot{m} = \dot{Q} / h'_{fg} = 101,823/791.7 = 0.036 \text{ lbm/s.}$$

Example Vc.2.2. A steel plate 1/8 in. thick with $L = 10 \text{ ft}$ is placed in saturated steam at 1 atm. At time zero, $T_{s0} = 200 \text{ F}$. Find the time when $T_s = T_{sat}$. For steel, $\rho = 488 \text{ lbm/ft}^3$, $c_p = 0.1 \text{ Btu/lbm}\cdot\text{F}$, and $k = 26.5 \text{ Btu/ft}\cdot\text{h}\cdot\text{F}$. For steam, $\rho_f = 59.8 \text{ lbm/ft}^3$, $\rho_g = 0.04 \text{ lbm/ft}^3$, and $h_{fg} = 970 \text{ Btu/lbm}$.

Solution: For this transient problem, we may estimate the plate temperature, from an energy balance using the lumped capacitance approach:

$$\frac{d(\rho c V T_s)}{dt} = hA(T_{film} - T_s)$$

In this relation, $T_{film} \approx (T_{sat} + T_s)/2$ and h in Equation Vc.2.6 may be written as:

$$h = \zeta(T_{sat} - T)^{-1/4} \text{ where } \zeta = 0.943(g\rho_f(\rho_f - \rho_g)k_f^3 h'_{fg}/(\mu_f L))^{0.25}$$

Assuming $\theta = T_{sat} - T_s$, the above energy balance simplifies to:

$$\int d\theta / \theta^{3/4} = -(\zeta A / 2\rho c V) \int dt$$

Integrating and setting $\theta = 0$, we find $t = \theta_0^{1/4} / (2\zeta A / \rho c V)$

$$\theta_0 = (T_{sat} - T_{s0}) = 212 - 200 = 12 \text{ F}, A/V = 12/0.125 \text{ ft}, \rho c = 48.8 \text{ Btu/ft}^3 \cdot \text{F}$$

For the condensate layer, we find film properties at $T_{film} = 209 \text{ F}$

$$\zeta = 0.943(32.2 \times 3600^2 \times 59.89(59.89 - 0.035)0.39^3 \times 970 / (0.69 \times 10))^{0.25} = 1772.5 \text{ Btu/ft}^2 \cdot \text{h} \cdot \text{F}^{3/4}$$

$$t = (12)^{1/4} / [2 \times 1772.5 \times 12 / (44.8 \times 0.125)] = 14 \text{ s}$$

3. Empirical Solution

Application of the empirical solutions depends on the value of the Reynolds number. If we substitute for mass flow rate, the Reynolds number can also be written as $Re_\delta = 4\dot{m}/(\mu b) = 4\rho \bar{V}_x \delta / \mu$ where the average film velocity is used and the plate width (b) cancels out from the numerator and the denominator.

3.1. Condensation on Vertical Plates and Cylinders

By defining a condensation Nusselt number, Nu_c also referred to as the *condensation number*, we may express the heat transfer coefficient in terms of the Reynolds number. These are shown in the table below. In the wavy laminar region, being the transition region between laminar and turbulent, the Kutateladze correlation and in the turbulent region the Labuntsov correlation are recommended.

Flow Regime	Range of Reynolds No.	Nusselt No.	Equation
Laminar	$Re_\delta \leq 30$	$Nu_c = 1.47 Re_\delta^{-1/3}$	Vc.3.1
Wavy laminar	$30 \leq Re_\delta \leq 1800$	$Nu_c = Re_\delta / [1.08 Re_\delta^{0.22} - 5.2]$	Vc.3.2
Turbulent	$1800 \leq Re_\delta$	$Nu_c = Re_\delta / [8750 + 58 Pr^{-0.5} (Re_\delta^{0.75} - 253)]$	Vc.3.3

$$Nu_c = \bar{h}_L (v_f^2 / g)^{1/3} / k_f \text{ where } v = \mu / \rho.$$

Example Vc.3.1. A vertical flat plate, 1.1 m long and 0.5 m wide maintained at 50 C is exposed to saturated steam at 0.5 bar. Find the total rate of heat transfer to the plate and the condensate mass flow rate.

Solution: We first find $T_{sat}(0.5 \text{ bar}) = 81.33 \text{ C}$ then $T_{film} = (81.33 + 50)/2 = 65.67 \text{ C}$:

For steam at $T_{sat} = 81.33 \text{ C}$: $h_{fg} = 2305.4 \text{ kJ/kg}$ and $\rho_v = 0.308 \text{ kg/m}^3$

For water at $T_{film} = 65.67 \text{ C}$: $k_f = 0.659 \text{ W/m}\cdot\text{K}$, $\mu_f = 429\text{E-}6 \text{ N}\cdot\text{s/m}^2$, $\rho_f = 980 \text{ kg/m}^3$, $c_{pf} = 4.2 \text{ kJ/kg}\cdot\text{K}$

Since $T_s \ll T_{sat}$, we calculate need to find h'_{fg} :

$$\text{Ja} = 4.2(81.33 - 50)/2305.4 = 0.057$$

$$h'_{fg} = 2305.4(1 + 0.68 \times 0.057) = 2395 \text{ kJ/kg}$$

$$\bar{h} = 0.943 \left(\frac{9.8 \times 980(980 - 0.308) \times 0.659^3 \times 2395\text{E}3}{429\text{E-}6 \times (81.33 - 50) \times 1.1} \right)^{0.25} = 4310 \text{ W/m}^2\cdot\text{K}$$

$$\dot{Q} = \bar{h}A(T_{sat} - T_s) = 4310 (1.1 \times 0.5) \times (81.33 - 50) = 74,268 \text{ W}$$

$$\dot{m} = \dot{Q} / h'_{fg} = 74,268/2.395\text{E}6 = 0.031 \text{ kg/s}$$

Finding $\text{Re}_\delta = 4 \dot{m} / \mu_f b = 4 \times 0.031/(429\text{E-}6 \times 0.5) = 578$ shows the flow regime is actually wavy laminar. We should then use the heat transfer coefficient based on the Kutateladze correlation as shown below:

$$\bar{h}_L = \frac{\dot{m} h'_{fg}}{A(T_{sat} - T_s)} = \frac{\text{Re}_\delta (\mu_f b) h'_{fg}}{4A(T_{sat} - T_s)} = \frac{\text{Re}_\delta}{1.08 \text{Re}_\delta^{1.22} - 5.2} \frac{k_f}{(v_f^2 / g)^{1/3}}$$

Solving for Re_δ , we find $\text{Re}_\delta = 716.5$. Using this in the Kutateladze correlation, we find:

$$\bar{h}_L = 716.5 \times 0.659 / \{ (1.08 \times 716.5^{1.22} - 5.2) [(429\text{E-}6/980)^2 / 9.8]^{1/3} \} = 5340 \text{ W/m}^2\cdot\text{K}$$

Revised values for \dot{Q} and \dot{m} are:

$$\dot{Q} = 5340 (1.1 \times 0.5) \times (81.33 - 50) = 92,016 \text{ W}$$

$$\dot{m} = 92,016/2.395\text{E}6 = 0.0384 \text{ kg/s.}$$

The same procedure used for vertical flat plates is applicable to vertical cylinders if $\delta_L \ll 0.5D$.

3.2. Condensation on Spheres, Horizontal Cylinders and on Banks of Tubes

Correlations similar to Equation Vc.2.6 are obtained for condensation on radial systems (Dhir & Lienhard):

$$\bar{h}_D = C \left(\frac{g \rho_f (\rho_f - \rho_g) k_f^3 h'_{fg}}{\mu_f (T_{sat} - T_s) D} \right)^{0.25} \quad \text{Vc.3.4}$$

where $C = 0.815$ for condensation on spheres and $C = 0.729$ for condensation on horizontal tubes. Equation Vc.3.4 is also applicable to condensers, which consist of banks of horizontal tubes with cold fluid flows inside the tubes and vapor condenses on the tubes. For film condensation inside horizontal tubes, $C = 0.555$.

Example Vc.3.2. Find the condensate flow rate for the following data of a power plant condenser: $P = 2$ in Hg, $D = 1\frac{1}{4}$ in, $L = 28.5$ ft, $N_{\text{tube}} = 16500$, $T_s = 75$ F.

Solution: We first find $T_{sat}(2 \text{ in Hg}) = 101$ F then $T_{film} = (101 + 75)/2 = 88$ F

For steam at $T_{sat} = 101$ F: $h_{fg} = 1036$ Btu/lbm and $\rho_g = 0.003$ lbm/ft³

For water at $T_{film} = 88$ F: $k_f = 0.36$ Btu/ft·h·F, $\mu_f = 1.9$ lbm/ft·h, $\rho_f = 62$ lbm/ft³, $c_{pf} = 1$ Btu/lbm·F

Since $T_s \ll T_{sat}$ we need to find $h'_{fg} = h_{fg}(1 + 0.68Ja)$

$Ja = 1 \times (101 - 75)/1036 = 0.025$ and $h'_{fg} = 1054$ Btu/lbm

e now use Equation Vc.3.4 to find the average heat transfer coefficient over a single tube:

$$\bar{h}_D = 0.729 \times \{(32.2 \times 3600^2) \times 62^2 \times 0.36^3 \times 1054 / [1.9 \times (101 - 75) \times (1/12)]\}^{0.25} = 1525 \text{ Btu/ft}^2 \cdot \text{h} \cdot \text{F}$$

$$\dot{Q} = \bar{h}_D A (T_{sat} - T_s) = 1525 \times (\pi \times 28.5 \times 1.25/12) \times (101 - 75) = 369,800 \text{ Btu/h}$$

$$\dot{m} = N_{\text{tube}} \dot{Q} / h'_{fg} = 16,500 \times 369,800 / 1054 = 5.8 \text{ Mlbm/h.}$$

4. Condensation Degradation

The presence of even a small amount of noncondensable gas significantly degrades the rate of condensation heat transfer. As shown in Figure Vc.4.1, these gases tend to migrate and accumulate near the colder surface, reducing the partial pressure of the vapor and subsequently the corresponding saturation temperature of the vapor. For containment response analysis, safety regulations require the use of the Tagami correlation for the case of a LOCA and the Uchida correlation during a MSLB analysis.

Tagami Correlation

Tagami, an empirical correlation, applies during the forced convection period following the blowdown phase of a LOCA. The key parameter in the Tagami corre-

lation is therefore time t_p , which marks the end of the blowdown-induced forced convection period. As such, the Tagami correlation is only applicable up to time t_p . The natural convection phase of a blowdown must be analyzed by using the Uchida or the turbulent natural convection correlation depending on the value of the Ra number. If h_{maximum} is the heat transfer coefficient corresponding to time t_p , then the heat transfer coefficients at other times ($t < t_p$) are obtained as $h = h_{\text{max}} (t / t_p)$. According to Tagami, h_{maximum} itself is calculated from: $h_{\text{max}} = C_T [U / (V t_p)]^{0.62}$, where U is the total blowdown energy released during t_p and V is containment free volume. In SI units, U is in J, t_p in s, V in m^3 , and C_T is 0.607. Time t_p is not known beforehand rather it should be obtained by iteration. A typical value for t_p given a large dry containment is about 13 seconds.

Uchida Correlation

The Uchida correlation is given as a table of heat transfer coefficient versus the ratio of air to steam mass. The maximum value is $1590 \text{ W/m}^2\cdot\text{K}$ and the minimum value is $11.4 \text{ W/m}^2\cdot\text{K}$.

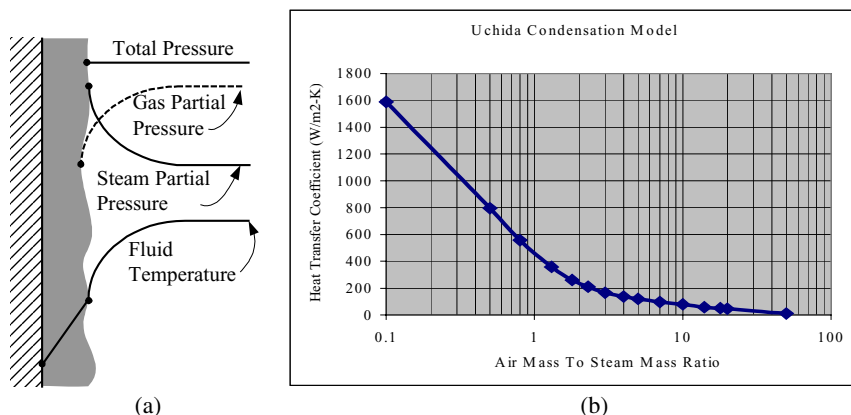


Figure Vc.4.1. (a) Effect of noncondensable gas on pressure and (b) on h (Uchida model)

QUESTIONS

- Find the condensation mode for the following examples, a power plant condenser, steam condensation on spray droplets, steam condensation in a suppression pool, rain.
- Which condensation mode is more efficient, dropwise or film?
- Does dropwise condensation occur if a liquid wets the surface
- Can the heat transfer coefficient in condensation reach $10,000 \text{ Btu/ft}^2\cdot\text{h}\cdot\text{F}$?
- Consider two condensers, one using horizontal tubes the other vertical tubes. Cold water flows inside the tubes. If all other parameters are identical which condenser is more efficient?

- Inside the condensate film, where can you find the minimum shear stress
- The flow of the condensate film beyond what Reynolds number becomes turbulent?

PROBLEMS

1. A vertical plate, 3 ft long and 5 ft wide is insulated from one side and the other side is exposed to steam at 15 psia. The plate temperature is maintained at 120 F. At what rate is condensate produced? [Ans.: $Ja = 0.033$, $Re = 287.5$, $Nu = 7004$, $h = 878 \text{ Btu/ft}^2\cdot\text{h}\cdot\text{F}$, $\dot{Q} = 126 \text{ kW}$, and $\dot{m} = 0.116 \text{ lbm/s}$].
2. steam at 4 psia is condensing on a vertical plate 1 m long and 2 m wide. The plate is at 50 C. Find \dot{m} . [Ans.: $Ja = 0.03$, $Re = 297$, $Nu = 7621$, $h = 4968 \text{ W/m}^2\cdot\text{K}$, $\dot{Q} = 278 \text{ kW}$, and $\dot{m} = 0.12 \text{ kgm/s}$].
3. A steam condenser consists of a square array of 529 horizontal tubes, 1 in diameter and 12 ft long. Tubes are maintained at 95 F to condense steam at 1 psia. Find the condensate production rate. [Ans.: 27 lbm/min.]
4. Find the condensation heat transfer coefficient for saturated Freon-12 at 50 C on a horizontal tube, having a diameter of 3 cm and maintained at 40 C. [Ans.: $1244 \text{ W/m}^2\cdot\text{C}$].
5. Consider condensation of benzene vapor at 1 bar on a vertical flat plate of height 0.3 m. If the plate is kept at 60 C, find the condensation heat transfer coefficient. At 1 bar, $T_{sat} = 80 \text{ C}$, $\rho_l = 823 \text{ kg/m}^3$, $\rho_g = 2.74 \text{ kg/m}^3$, $h_{fg} = 398 \text{ kJ/kg}$, $c_{p,l} = 1.88 \text{ kJ/kg}\cdot\text{K}$, $\mu_l = 321\text{E-}6 \text{ N}\cdot\text{s/m}^2$, $k_l = 0.131 \text{ W/m}\cdot\text{K}$. [Ans. $1270 \text{ W/m}^2\cdot\text{k}$].
6. Saturated steam at 1 atm is condensing on a horizontal tube at a rate of 300 kg/h. The tube is 2 m long and is maintained at 60 C. Find the tube diameter. [Ans.: 13 cm].
7. A steam power plant produces 2700 MWe at a thermal efficiency of 29%. Find the surface area and the number of tubes
8. A steel plate having $L = 3 \text{ m}$, $b = 1.5 \text{ m}$, and thickness of 0.5 cm is placed in steam at 1 atm. Initially, the plate is at 80 C. Plot the plate temperature versus time. Identify the simplifying assumptions made.
9. Water flows at a rate of 296 kg/h in a horizontal thin-walled tube ($d = 0.025 \text{ m}$) at 25 C. Benzene vapor condenses at 1 bar on the tube. Find the rate of condensation per meter. [Ans.: By iteration 24 kg/m·h].

VI. Applications

In this chapter we will study such important topics as heat exchangers, flow-meters, and turbomachines. We will also evaluate the thermal hydraulics response of systems to transients and heat generation from nuclear energy.

Vla. Heat Exchangers

Heat exchanger (HX) is a generic term applied to a wide range of mechanical systems, which are designed for the purpose of exchanging thermal energy between two streams of fluids separated by a solid surface. Some heat exchangers are used as heat sinks including automotive inter-coolers, containment air coolers, cooling towers, automotive radiators, and power plant condensers. Some other heat exchangers are used as a heat source including boilers, radiators for space heating, and steam generators. For example, a nuclear plant utilizes many heat exchangers. In a typical plant, feedwater heaters are employed in the balance of plant to improve plant thermal efficiency. Also, other heat exchangers, such as the component cooling water and shutdown cooling (also known as the residual heat removal) system, provide a heat sink for the reactor during the shutdown period. Finally, the service water heat exchanger provides a heat sink for the balance of plant equipment. Heat exchangers have a hot side and a cold side separated by tubes or plates. Heat transfer between the fluids in each side takes place through the surface dividing the hot side and the cold side. Heat transfer may take place between liquid and liquid, liquid and gas, and gas and gas. Heat exchangers may also carry two-phase flow resulting in boiling or in condensation. Heat exchangers may be operating at steady-state or transient conditions. Due to such design variations, heat exchangers require careful analysis in design optimization as well as in performance evaluation. In this chapter we will deal primarily with the thermal aspects of tubular heat exchangers.

1. Definition of Heat Exchanger Terms

Concentric parallel flow heat exchanger consists of a tube surrounded by a shell. In parallel flow heat exchangers, both hot and cold streams flow in the same direction as shown in Figure VIa.1.1.

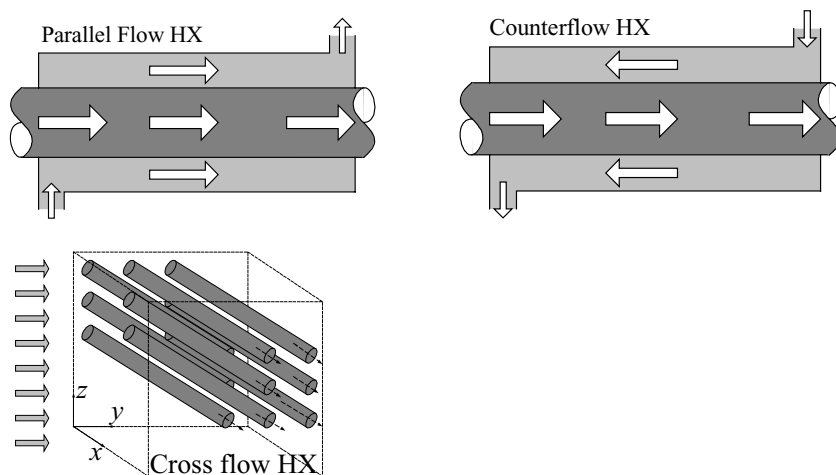


Figure VIa.1.1. Schematics of parallel, counterflow, and cross flow heat exchangers

Concentric counter flow heat exchanger consists of a tube surrounded by a shell. In counter flow heat exchangers, the hot and cold streams flow in opposite directions as shown in Figure VIa.1.1.

Cross flow heat exchangers are generally used in gas-liquid applications. They include tubes with a stream flowing parallel to the xy -plane and cross flow parallel to the yz -plane and perpendicular to the tube axis. The cross flow may be mixed, as shown in Figure VIa.1.1, or unmixed by passing cross flow through parallel plates.

Shell and tube heat exchanger is similar to the concentric heat exchanger. However, shell and tube heat exchangers consist of multi tubes held in place by baffle plates. These plates prevent tube vibration and enhance the rate of heat transfer by diverting the shell-side fluid in a cross flow manner, as shown in Figure VIa.1.2. Shell and tube heat exchangers may be arranged in series to obtain

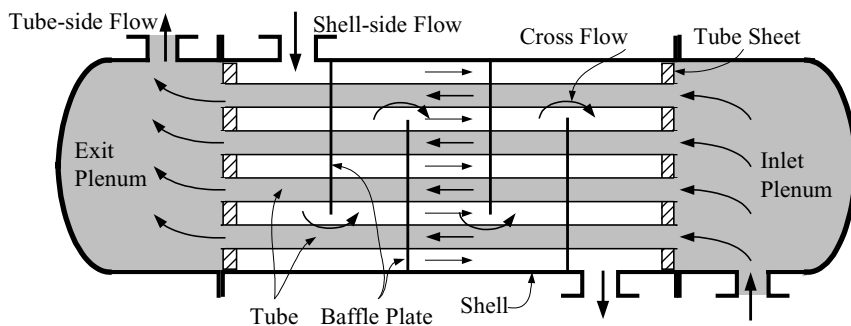


Figure VIa.1.2. Schematic of a shell and tube heat exchanger

several cascaded shells. Each heat exchanger has a minimum of four ports. As shown in Figure VIa.1.2, there is an inlet port and an outlet port in the hot side. Similarly, there is an inlet and an outlet port in the cold side. Tubes are either straight or bent in the form of a U. Heat exchangers including straight tubes have an inlet *plenum* and an outlet plenum. Tubes are installed inside tube sheets, which also act as barriers between the plenum fluids and the shell-side fluid.

Fouling factor f , is a measure of cleanliness of heat exchangers. Fluid streams generally carry impurities. Sedimentation of the impurities over time leads to a layer of deposit. This poses a resistance to heat transfer across the solid surface. The sedimentation may also consist of sludge that would pit and corrode solid surfaces. Maintaining a closely monitored chemistry of the fluid stream and periodic cleaning of heat exchangers is essential in ensuring proper operation of the device. In a shell and tube heat exchanger, for example, cleaning of the shell side is especially challenging due to the presence of the baffle plates. In such cases, the cleaner stream flows in the shell side, as cleaning the inside of the tubes is by far easier. In power plants using large bodies of water as the heat sink, steam always condenses on the tubes with river, lake, bay, or ocean water flowing in the tubes. Fouling may be categorized as particulate fouling, crystallization fouling, corrosion fouling, biofouling, and chemical reaction fouling (Kakac). One way to account for fouling in the design process of heat exchangers is to increase the surface area for heat transfer. Fouling factor has units of thermal resistance $\text{ft}^2\cdot\text{h}\cdot\text{F}/\text{Btu}$ or $\text{m}^2\cdot\text{K}/\text{W}$. Some typical values are as follows:

Fluid	$f(\text{m}^2\cdot\text{K}/\text{W})$	$f(\text{ft}^2\cdot\text{h}\cdot\text{F}/\text{Btu})$
Transformer oil	0.000176	0.0010
Engine lube oil	0.000176	0.0010
Crude oil	0.000352	0.0020
Heavy gas oil	0.000881	0.0050
Heavy fuel oil	0.001233	0.0070
Vegetable oil	0.000528	0.0030
Seawater	0.000176	0.0010
Brackish water	0.000528	0.0030
Muddy or silt water	0.000705	0.0040
River water (< 50 C)	0.001000	0.0060
Refrigerating liquid	0.000200	0.0011

From: Standards of Tubular Exchangers Manufacturers Association

Overall heat transfer coefficient is given in Equation IVa.6.8 for a clean concentric heat exchanger. To account for fouling resistance, Equation IVa.6.8 should be modified as follows:

$$UA = \left[\frac{1}{\pi d_i L h_i} + \frac{f_i}{\pi d_i L} + \frac{\ln(d_o / d_i)}{2\pi k L} + \frac{f_o}{\pi d_o L} + \frac{1}{\pi d_o L h_o} \right]^{-1} = U_i A_i = U_o A_o$$

VIa.1.1

where subscripts i and o stand for tube inside and tube outside, respectively. Tube outside is also known as the *tube bundle*, *shell side*, or *secondary-side*. In Equation VIa.1.1, f_i and f_o are the tube-side and shell-side fouling factors, respectively. Typical values of U for various streams are as follows.

Stream A / Stream B	U (W/m ² ·K)	U (Btu/ft ² ·h·F)
Condensing Steam / Water (Condenser & FWH)	1100 – 5500	200 – 1000
Freon 12 Condenser / Water	300 – 850	50 – 150
Water / Water	850 – 1700	150 – 300
Water / Oil	100 – 350	20 – 60
Gas / Gas	10 – 40	2 – 8

Cleanliness factor, C_F is another measure of heat exchanger cleanliness and is defined as the ratio of the overall heat transfer coefficient when a heat exchanger is fouled, to the overall heat transfer coefficient of the clean heat exchanger, $C_F = U_{fouled}/U_{clean}$. When defining C_F , we need not to consider any fouling (f_i and f_o) in Equation VIa.1.1, rather calculate U_{clean} and find U_{fouled} from $U_{fouled} = C_F U_{clean}$.

Heat Capacity, C is the product of mass flow rate and specific heat, $C = \dot{m}c_p$ having units of Btu/s·F or W/C.

2. Analytical Solution

In this section we discuss steady-state operation of heat exchangers. As shown in Figure VIa.2.1, we can assign control volumes to the entire hot-side, the cold-side and the solid surface separating the hot and cold sides. In steady state conditions, flow rates at the inlet and outlet ports for each control volume are equal hence:

$$\dot{m}_{h,in} = \dot{m}_{h,out} = \dot{m}_h \quad \text{VIa.2.1a}$$

$$\dot{m}_{c,in} = \dot{m}_{c,out} = \dot{m}_c \quad \text{VIa.2.1b}$$

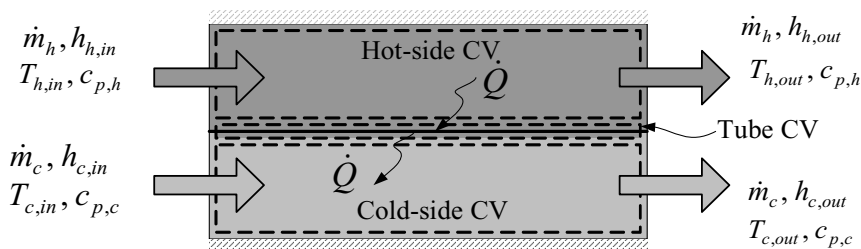


Figure VIa.2.1. Control volumes for the primary and secondary sides

The hot stream enters at an enthalpy of $h_{h,in}$ and leaves at an enthalpy of $h_{h,out} < h_{h,in}$. If the heat exchanger shell is fully insulated so that there is no heat loss to the environment, then under steady-state operation:

$$\dot{Q}_h = \dot{Q}_s = \dot{Q} \quad \text{VIa.2.2a}$$

On the other hand, the cold side fluid enters at an enthalpy of $h_{c,i}$ and leaves at an enthalpy of $h_{c,o} > h_{c,i}$. The gain in the cold stream energy is due to the transfer of heat from the solid surface. In steady-state:

$$\dot{Q}_c = \dot{Q}_s = \dot{Q} \quad \text{VIa.2.2b}$$

Substituting for the rate of heat transfer while assuming negligible potential and kinetic energies, we find:

$$\dot{Q} = \dot{m}_h (h_{h,in} - h_{h,out}) \quad \text{VIa.2.3a}$$

$$\dot{Q} = \dot{m}_c (h_{c,out} - h_{c,in}) \quad \text{VIa.2.3b}$$

For a special case where each stream exits at the same phase as it entered the heat exchanger, we may replace $\Delta h \approx c_p \Delta T$. Assuming variations in specific heat are small and using $c_p = f(T_{in} + T_{out})/2$, we can write the axial energy equations as:

$$\dot{Q} = C_h (T_{h,in} - T_{h,out}) \quad \text{VIa.2.4a}$$

$$\dot{Q} = C_c (T_{c,out} - T_{c,in}) \quad \text{VIa.2.4b}$$

So far we used the conservation equations of mass and energy in the axial direction. In the next section we use the conservation equation of energy in the transverse direction for elemental control volumes to tie the hot-side and cold-side temperatures by applying the overall heat transfer coefficient. The reason for using elemental control volume is that axial temperature profiles are generally not linear functions of the heat exchanger length. As a result, we cannot generally use average temperatures for the hot and cold side as:

$$\overline{\Delta T} = \left[\frac{T_{h,in} + T_{h,out}}{2} - \frac{T_{c,in} + T_{c,out}}{2} \right] \quad \text{VIa.2.5}$$

If it were possible, the rate of heat transfer would have been calculated from $\dot{Q} = UA\overline{\Delta T}$. The simple relation given in Equation VIa.2.5 provides only an estimation of ΔT . In the next section we will see that ΔT is a logarithmic function of the inlet and outlet temperatures referred to as the *logarithmic mean temperature difference* (LMTD).

2.1. LMTD Method of Analysis

The analysis performed below applies to parallel flow heat exchangers as shown in Figures VIa.2.2(a). Similar analysis can be performed for counterflow heat exchangers, shown in Figure VIa.2.2(b).

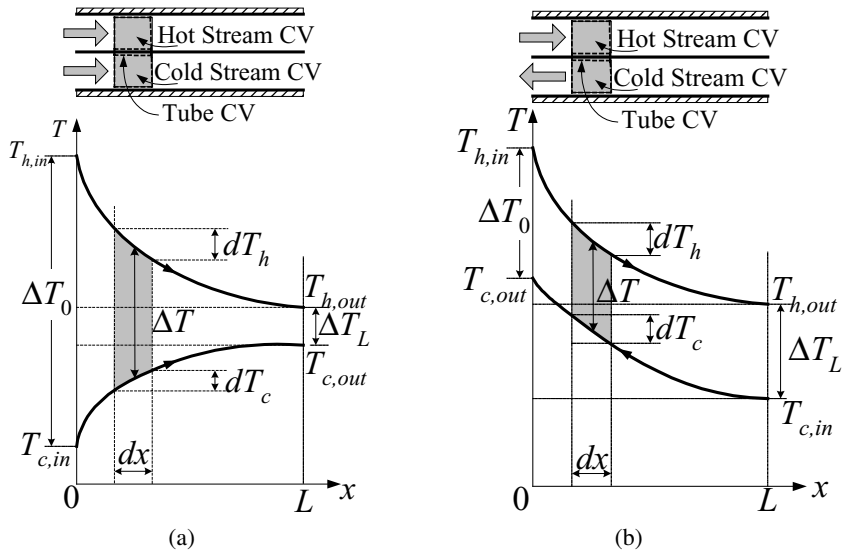


Figure VIa.2.2. Hot and cold temperature profiles for (a) parallel and (b) counterflow heat exchangers

Consider three elemental control volumes, one for the hot side, one for the tube surface, and one for the cold side of a heat exchanger, Figure VIa.2.2(a) and VIa.2.2(b). These figures show the temperature profiles as a function of the heat exchanger length. Similar to Equations VIa.2.4a and VIa.2.4b, we can write axial energy equations for the hot side and cold side of the elemental control volumes:

$$d\dot{Q} = -C_h dT_h \quad \text{VIa.2.6a}$$

$$d\dot{Q} = C_c dT_c \quad \text{VIa.2.6b}$$

We now write the transverse energy equation assuming negligible axial heat conduction in the tube. Such thermal resistances as flow, tube wall, and fouling are taken into account by the use of an overall heat transfer coefficient:

$$d\dot{Q} = [U(x)dA(x)]\Delta T \quad \text{VIa.2.7}$$

Note that the term ΔT in Equation VIa.2.7 represents the difference in the average temperatures of the hot and cold side elemental control volumes (i.e. $\Delta T = T_h - T_c$). To relate Equations VIa.2.6a and VIa.2.6b to Equation VIa.2.7, we differentiate ΔT and substitute for terms:

$$d(\Delta T) = dT_h - dT_c = -\frac{d\dot{Q}}{C_h} - \frac{d\dot{Q}}{C_c} = -d\dot{Q}\left(\frac{1}{C_h} + \frac{1}{C_c}\right) \quad \text{VIa.2.8}$$

If we integrate Equation VIa.2.8 from $x = 0$ to $x = L$, we get:

$$\Delta T_0 - \Delta T_L = \dot{Q} \left(\frac{1}{C_h} + \frac{1}{C_c} \right) \quad \text{VIa.2.9}$$

We may also substitute in Equation VIa.2.8 for $d\dot{Q}$ from Equation VIa.2.7 and divide by ΔT to obtain:

$$\frac{d(\Delta T)}{\Delta T} = -[U(x)dA(x)] \left(\frac{1}{C_h} + \frac{1}{C_c} \right)$$

Integrating the above equation from $x = 0$ to $x = L$, yields:

$$\int_0^L \frac{d(\Delta T)}{\Delta T} = - \left[\frac{1}{C_h} + \frac{1}{C_c} \right] \int_0^L U(x)dA(x) \quad \text{VIa.2.10}$$

We now define an overall heat transfer coefficient, which is averaged over the heat exchanger length:

$$U = \frac{\int_0^L U(x)dA(x)}{A}$$

where A is the heat exchanger surface area. By defining the average U , Equation VIa.2.10 becomes:

$$\ln \frac{\Delta T_0}{\Delta T_L} = UA \left(\frac{1}{C_h} + \frac{1}{C_c} \right) \quad \text{VIa.2.11}$$

Substituting for $1/C_h + 1/C_c$ from Equation VIa.2.9 we find:

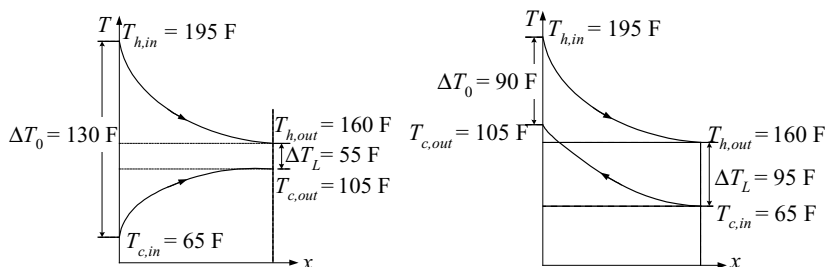
$$\dot{Q} = UA \frac{\Delta T_0 - \Delta T_L}{\ln(\Delta T_0 / \Delta T_L)} = UA \Delta T_{LMTD} \quad \text{VIa.2.12}$$

Note that in applying Equation VIa.2.12 to parallel and counterflow heat exchangers, we must recall that (see Figure VIa.2.2):

$$\begin{aligned} \text{Parallel Flow: } \Delta T_0 &= T_{h,in} - T_{c,in} \quad \text{and} \quad \Delta T_L = T_{h,out} - T_{c,out} \\ \text{Counterflow: } \Delta T_0 &= T_{h,in} - T_{c,out} \quad \text{and} \quad \Delta T_L = T_{h,out} - T_{c,in} \end{aligned}$$

For the same inlet and outlet temperatures, $(\Delta T_{LMTD})_{\text{Counterflow}} > (\Delta T_{LMTD})_{\text{Parallel}}$. This implies that for the same U and A , a counterflow heat exchanger has a higher rate of heat removal than a parallel flow heat exchanger. Comparing Equation VIa.2.5 with Equation VIa.2.12, we note that the temperature difference unfortunately contains a logarithmic term. This complicates analysis when unknown temperatures must be found from Equation VIa.2.12.

Example VIa.2.1. Use the given data to find a) ΔT_{LMTD} if the heat exchanger uses a parallel flow arrangement and b) ΔT_{LMTD} if the heat exchanger uses a counterflow arrangement. Data: $T_{h,i} = 195$ F, $T_{h,o} = 160$ F, $T_{c,i} = 65$ F, and $T_{c,o} = 105$ F.



Solution: a) For parallel flow, $\Delta T_0 = T_{h,i} - T_{c,i} = 195 - 65 = 130$ F, and $\Delta T_L = T_{h,o} - T_{c,o} = 160 - 105 = 55$ F

$$[\Delta T_{LMTD}]_{\text{Parallel}} = [130 - 55]/\ln(130/55) = 87.2 \text{ F}$$

b) For counterflow, $\Delta T_0 = T_{h,i} - T_{c,o} = 195 - 105 = 90$ F, and $\Delta T_L = T_{h,o} - T_{c,i} = 160 - 65 = 95$ F

$$[\Delta T_{LMTD}]_{\text{Counterflow}} = [90 - 95]/\ln(90/95) = 92.5 \text{ F}$$

Comment: Two observations can be made from this example. First, as discussed earlier and shown above $(\Delta T_{LMTD})_{\text{Counterflow}} > (\Delta T_{LMTD})_{\text{Parallel}}$. In this example, for the same U and A , the counterflow HX is more efficient than the parallel flow HX by about 6%. Second, an average temperature difference per Equation VIa.2.5 is $\Delta T = [(195 + 160) - (105 + 65)]/2 = 92.5$ F, which happens to agree with $(\Delta T_{LMTD})_{\text{Counterflow}}$.

Equations and Unknowns. For a concentric heat exchanger, we derived three equations, namely two axial energy equations (Equations VIa.2.4a and VIa.2.4b) and a transverse energy equation (Equation VIa.2.12). The number of unknowns, being nine, exceeds the number of equations by a wide margin. The unknowns are \dot{Q} , \dot{m}_h , \dot{m}_c , $T_{h,in}$, $T_{c,in}$, $T_{h,out}$, $T_{c,out}$, U , and A . Note that $c_{p,h}$ and $c_{p,c}$ are not unknowns as they are functions of the related temperatures. We have an additional equation for U given by Equation VIa.1.1, which introduces h_i , h_o , f_i , f_o , d_i , d_o , and L . However, the heat transfer coefficients are functions of Re , Pr , fluid temperature, d_i , and d_o . Also the heat exchanger surface area is related to tube diameter and tube length as $A = \pi dL$. An additional unknown is the shell diameter, which can be calculated from an appropriate equation. We increased the number of equations to eight. These are Equations VIa.2.4a, VIa.2.4b, VIa.2.12, VIa.1.1, V.3.4 (for h_i and a similar equation for h_o), the relation for $A = f(d, L)$, and the relation for D_{shell} . However, we increased the number of unknowns to seventeen! To have a consistent set, we must then specify nine of the unknowns. This argu-

ment indicates that, from the thermal analysis point of view, heat exchangers have a large degree of freedom. On the other hand, constraints for design optimization include:

- structural considerations (tube outside diameter to stand internal pressure)
- hydraulic considerations (tube inside diameter for pumping power and pressure drop in tube)
- performance (fouling characteristics of the working fluids)
- tube material (conductivity, erosion, and corrosion characteristics)
- size and weight limitations
- cost

Returning to the three equations and nine unknowns discussion, let's consider a case where two inlet temperatures ($T_{h,in}$ and $T_{c,in}$), two flow rates (\dot{m}_h , and \dot{m}_c), the heat transfer coefficient U , and the surface area A are specified. We solve for the two exit temperatures ($T_{h,out}$ and $T_{c,out}$) and the rate of heat transfer \dot{Q} . We substitute for the two exit temperatures from Equations VIa.2.4a and VIa.2.4b into Equation VIa.2.12 to solve for \dot{Q} :

$$\dot{Q} = \frac{(T_{h,in} - T_{c,in})(\beta - 1)}{(\beta / C_h) - (1 / C_c)} \quad \text{VIa.2.13}$$

where $\beta = e^{UA[1/\dot{m}_h c_{p,h} - 1/\dot{m}_c c_{p,c}]}$. This equation is applicable to counterflow heat exchangers. See Section 2.2 for generalization of this method.

Example VIa.2.2. Water flows in both sides of a counterflow heat exchanger. Find the rate of heat transfer \dot{Q} , and exit temperatures ($T_{h,out}$ and $T_{c,out}$) for the following data: $T_{h,i} = 130$ F, $T_{c,i} = 95$ F, $\dot{m}_h = 1.5\text{E}6$ lbm/h, $\dot{m}_c = 2.41\text{E}6$ lbm/h, $U = 259$ Btu/ft²·h·F, $A = 5,790$ ft², and $c_p = 1$ Btu/lbm·F.

Solution: To use Equation VIa.2.13, we find

$$\beta = \exp[259 \times 5,790(1/1.5\text{E}6 - 1/2.41\text{E}6)] = 1.4586$$

$$\dot{Q} = C_h(T_{h,in} - T_{h,out}) = (130 - 95) \times (1.4586 - 1)/[1.4586/1.5\text{E}6 - 1/2.41\text{E}6] = 28.8\text{E}6 \text{ Btu/h}$$

$$T_{h,out} = T_{h,in} - (\dot{Q} / C_h) = 130 - (28.8\text{E}6/1.5\text{E}6) = 111 \text{ F}$$

$$T_{c,out} = T_{c,in} + (\dot{Q} / C_c) = 95 + (28.8\text{E}6/2.41\text{E}6) = 107 \text{ F}.$$

Special Modes of Operation. Shown in Figure VIa.2.3 are three different modes of operations. Figure VIa.2.3(a) shows one stream is boiling while the other stream is cooling down. In this case (i.e., in the case of a steam generator) $\Delta T \rightarrow 0$ and $C_c \rightarrow \infty$. Figure VIa.2.3(b) shows one stream is condensing

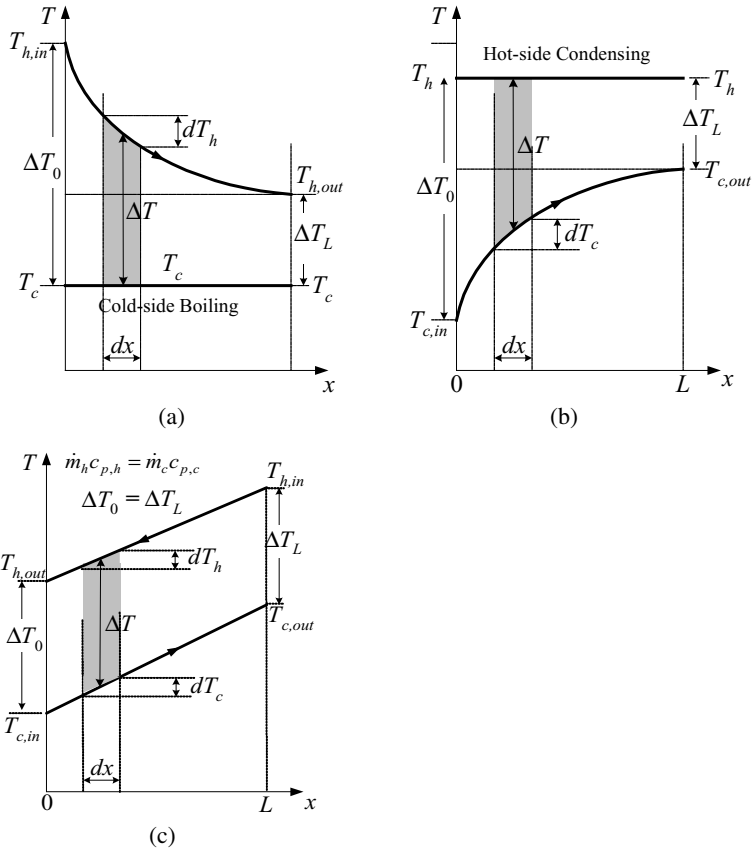


Figure VIa.2.3. (a) Steam generator, (b) Condenser, and (c) Special case of $\Delta T_h = \Delta T_c$

while the other stream is heating up. In this case (i.e. in the case of a condenser), we have $\Delta T \rightarrow 0$ and $C_h \rightarrow \infty$. Note that in these cases we should use Equations VIa.2.3a and VIa.2.3b. Finally, Figure VIa.2.3(c) shows a special case in which $C_h = C_c$. This requires that $\Delta T_h = \Delta T_c$.

Multi-pass Heat Exchangers. The LMTD method outlined above and the result culminated in Equation VIa.2.12 apply to concentric heat exchangers (Figure IVa.6.3). The same results can be applied to the shell and tube heat exchangers with multi-pass tubes and shell, by applying a correction factor $F_{multi-pass}$ so that:

$$\dot{Q} = F_{Multi-pass} UA \Delta T_{LMTD} \quad \text{VIa.2.12a}$$

The $F_{Multi-pass}$ factor is given in Figure VIa.2.4 for two cases. The left side figure is for any multiples of two tube pass (four, six, etc.) and one shell pass. The right

side figure is for any multiple of four tube and two shell passes. In these figures, the tube-side inlet and outlet temperatures are shown by t_i and t_o whereas the shell-side inlet and outlet temperatures are shown by T_i and T_o , respectively. The correction factor obtained from Figure VIa.2.3 should be used in conjunction with the ΔT_{LMTD} calculated for a counterflow configuration. The correction factor for one shell path, as shown in the left side plot of Figure VIa.2.4 is obtained from:

$$F_{Multi-pass} = \frac{\sqrt{R^2 + 1}}{R - 1} \times \frac{\ln[(1 - P)/(1 - PR)]}{\ln\{[2 - P(R + 1 - \sqrt{R^2 + 1})]/[2 - P(R + 1 + \sqrt{R^2 + 1})]\}} \quad \text{VIa.2.14}$$

Parameters P and R in Figure VIa.2.4 and in Equation VIa.2.11 are known as *capacity ratio* and *effectiveness*, respectively and are given as:

$$\text{Capacity Ratio: } P = \frac{C_c}{C_h} = \frac{t_o - t_i}{T_i - T_o}$$

$$\text{Effectiveness: } R = \frac{C_c(T_i - T_o)}{C_h(t_o - t_i)} = \frac{T_i - T_o}{t_o - t_i}$$

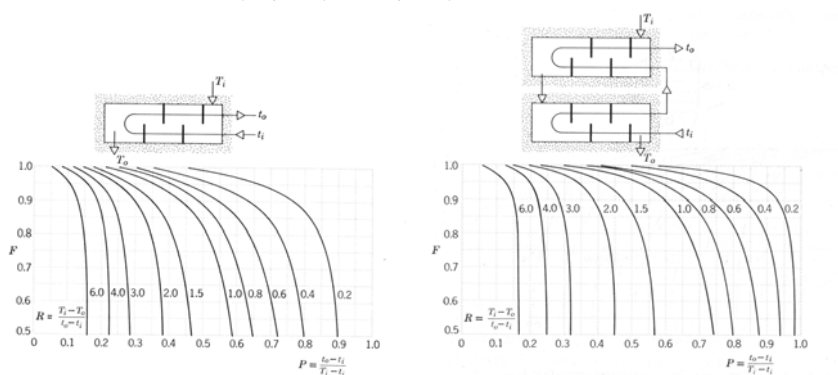


Figure VIa.2.4. Correction factor for multiple tube and shell passes

The LMTD correction factor (F) for multi-pass shell and tube heat exchangers can be calculated by using the software on the accompanying CD-ROM.

Example VIa.2.3. Seawater is used to cool the lubricating oil of a ship's diesel engine. The shell and tube heat exchanger has one shell and two tube passes. Tube surface area is 100 ft^2 and the overall heat transfer coefficient is given as $U = 250 \text{ Btu/ft}^2 \cdot \text{h} \cdot \text{F}$. Oil enters at 160 F and leaves at 125 F . Water enters the tube at 75 F and leaves at 100 F . Find the total rate of heat transfer.

Solution: We find the capacity ratio and the effectiveness as follows,
 $P = (100 - 75)/(160 - 75) = 0.294$. $R = (160 - 125)/(100 - 75) = 1.4$

Using the left plot of Figure VIa.2.3, we find $F_{Multi-pass} \approx 0.95$

$$\Delta T_{LMTD} = [(160 - 100) - (125 - 75)]/\ln[(160 - 100)/(125 - 75)] = 54.85 \text{ F}$$

$$\dot{Q} = F_{Multi-pass} UA \Delta T_{LMTD} = 0.95 \times 250 \times 100 \times 54.85 = 1.3\text{E6 Btu/h} \approx 0.4 \text{ MW.}$$

Cross Flow Heat Exchangers. Equation VIa.2.12 is also applicable to cross flow heat exchangers:

$$\dot{Q} = F_{CrossFlow} UA \Delta T_{LMTD} \quad \text{VIa.2.12b}$$

where $F_{CrossFlow}$ is given in Figure VIa.2.5 for two cases. The left figure is for a case where both streams are unmixed and the right figure is for one stream mixed and other stream unmixed.

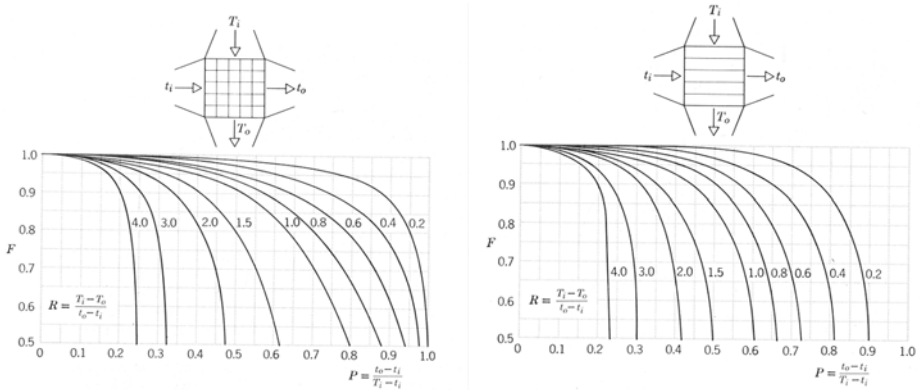


Figure VIa.2.5. Cross flow heat exchangers

2.2. NTU Method of Analysis

In cases where exit temperatures are unknown, we have to solve an equation involving the logarithmic term for ΔT_{LMTD} . An alternative method of analyzing heat exchangers is the ϵ – NTU method where $NTU = UA/C$ stands for *number of transfer units*, and effectiveness (now represented by ϵ) is given as:

$$\epsilon = \frac{\dot{Q}_{actual}}{\dot{Q}_{ideal}} = \frac{\dot{Q}_{actual}}{C_{\min} (T_{h,in} - T_{c,in})}$$

where C_{\min} is the minimum of C_h and C_c . The ideal or maximum rate of heat transfer is associated with maximum ΔT , which is $\Delta T_{\max} = T_{h,in} - T_{c,in}$. If we find ε , then we can calculate \dot{Q}_{actual} from:

$$\dot{Q}_{actual} = \varepsilon C_{\min} \Delta T_{\max}$$

Therefore, in the ε -NTU method, rather than calculating ΔT_{LMTD} we calculate ε , which depends on the type of heat exchanger and flow configuration. Since $\dot{Q}_{actual} = C_h (T_{h,in} - T_{h,out}) = C_c (T_{c,out} - T_{c,in})$, then

$$\varepsilon = \frac{C_h (T_{h,in} - T_{h,out})}{C_{\min} (T_{h,in} - T_{c,in})} \quad \text{Via.2.15a}$$

and

$$\varepsilon = \frac{C_c (T_{c,out} - T_{c,in})}{C_{\min} (T_{h,in} - T_{c,in})} \quad \text{Via.2.15b}$$

We use Equations Via.2.15a, Via.2.15b, and Via.2.11 to derive relations for ε for various types of heat exchangers. For example, for a parallel flow heat exchanger, we can write Equation Via.2.11 as:

$$\frac{\Delta T_L}{\Delta T_0} = \frac{T_{h,out} - T_{c,out}}{T_{h,in} - T_{c,in}} = \exp[-UA(1/C_h + 1/C_c)]$$

We now solve Equation Via.2.15a for $T_{h,out}$ and substitute in the above equation to get:

$$1 - \frac{T_{c,out} - T_{c,in}}{T_{h,in} - T_{c,in}} \left(1 + \frac{C_c}{C_h}\right) = \exp[-UA(1/C_h + 1/C_c)]$$

Substituting for the temperature ratio term in the above equation from Equation Via.2.15b yields:

$$\varepsilon = \frac{1 - \exp[-UA(1/C_h + 1/C_c)]}{C_{\min}/C_c + C_{\min}/C_h}$$

If it happens that $C_c < C_h$, then $C_{\min} = C_c$ and the denominator becomes $1 + C_c/C_h$. Conversely, for the case of $C_h < C_c$, the denominator becomes $1 + C_h/C_c$. We can write the result in compact form of $1 + C_r$ where $C_r = C_{\min}/C_{\max}$. Similarly, in the numerator, we factor out C_{\min} and substitute for $UA/C_{\min} = NTU$:

$$\varepsilon = \frac{1 - \exp[-NTU(1 + C_{\min}/C_{\max})]}{1 + C_{\min}/C_{\max}} \quad \text{VIa.2.16}$$

Equation VIa.2.16 gives the effectiveness as a function of NTU , $\varepsilon = f(NTU, C_r)$. We may also solve Equation VIa.2.16 for NTU as a function of ε , $NTU = f(\varepsilon, C_r)$. The same method used to derive Equation VIa.2.16 for the parallel flow heat exchangers can be applied to other types of heat exchangers and obtain similar relations for effectiveness (Kays). The results for ε as a function of NTU and $C_r = C_{\min}/C_{\max}$ are summarized in Table VIa.2.1. This is followed by the results obtained from Kays for $NTU = f(\varepsilon)$, as shown in Table VIa.2.2.

Example VIa.2.4. Water flows in both sides of a counterflow heat exchanger. Find the rate of heat transfer \dot{Q} , and exit temperatures, $T_{h,out}$, and $T_{c,out}$ for the following data: $T_{h,in} = 55^\circ\text{C}$, $T_{c,in} = 30^\circ\text{C}$, $\dot{m}_h = 200 \text{ kg/s}$, $\dot{m}_c = 300 \text{ kg/s}$, $U = 1.5 \text{ kW/m}^2\cdot\text{C}$, and $A = 540 \text{ m}^2$, $c_p = 4.18 \text{ kJ/kg}\cdot\text{K}$.

Solution: In this example, $C_{\min} = C_h = 200 \times 4.18 = 836 \text{ kW/C}$

$$NTU = \frac{UA}{C_{\min}} = \frac{1.5 \times 540}{836} = 0.97$$

$$C_r = \frac{200 \times 4.18}{300 \times 4.18} = 0.667$$

$$\varepsilon = \frac{1 - \exp[-NTU(1 - C_r)]}{1 - C_r \exp[-NTU(1 - C_r)]} = \frac{1 - \exp[-0.97 \times (1 - 0.667)]}{1 - 0.667 \times \exp[-0.97 \times (1 - 0.667)]} = 0.534$$

$$\dot{Q}_{\max} = C_{\min}(T_{h,in} - T_{c,in}) = 200 \times 4.18 \times (55 - 30) = 20,900 \text{ kW}$$

$$\dot{Q}_{\text{actual}} = \varepsilon \dot{Q}_{\max} = 0.534 \times 20,900 = 11,161 \text{ kW}$$

Having \dot{Q}_{actual} , we can find exit temperatures as:

$$T_{h,out} = 55 - \frac{11,161}{200 \times 4.18} = 42^\circ\text{C}$$

$$T_{c,out} = 30 + \frac{11,161}{300 \times 4.18} = 39^\circ\text{C}$$

Table VIa.2.1. Heat exchanger effectiveness for various flow arrangements

Flow Arrangement	Effectiveness
Parallel Flow:	$\varepsilon = \frac{1 - \exp[-NTU(1 + C_r)]}{1 + C_r}$
Counterflow:	$\varepsilon = \frac{1 - \exp[-NTU(1 - C_r)]}{1 - C_r \exp[-NTU(1 - C_r)]}$
Shell & tube (1 shell pass, 2, 4, ... n tubes passes):	$\varepsilon_1 = 2 \left\{ 1 + C_r + (1 + C_r^2)^{1/2} \frac{1 + \exp[-NTU(1 + C_r^2)^{1/2}]}{1 - \exp[-NTU(1 + C_r^2)^{1/2}]} \right\}^{-1}$
Shell & tube (n shell pass, $2n, 4n, \dots$ tube passes):	$\varepsilon = \left[\left(\frac{1 - \varepsilon_1 C_r}{1 - \varepsilon_1} \right)^n - 1 \right] \left[\left(\frac{1 - \varepsilon_1 C_r}{1 - \varepsilon_1} \right)^n - C_r \right]^{-1}$
Cross flow (single path, both streams unmixed):	$\varepsilon = 1 - \exp[(1/C_r)(NTU)^{0.22} \{ \exp[-C_r (NTU)^{0.78}] - 1 \}]$
Cross flow (C_{\max} mixed, C_{\min} unmixed):	$\varepsilon = (1/C_r)(1 - \exp\{-C_r[1 - \exp(-NTU)]\})$
Cross flow (C_{\max} unmixed, C_{\min} mixed):	$\varepsilon = 1 - \exp(-C_r^{-1} \{1 - \exp[-C_r (NTU)]\})$
Heat exchangers with $C_r = 0$:	$\varepsilon = 1 - \exp(-NTU)$

Table VIa.2.2. Heat exchanger NTU for various flow arrangements

Flow Arrangement	Number of Transfer Units
Parallel Flow:	$NTU = -\frac{\ln[1 - \varepsilon(1 + C_r)]}{1 + C_r}$
Counterflow:	$NTU = -\frac{1}{C_r - 1} \ln \left(\frac{\varepsilon - 1}{\varepsilon C_r - 1} \right)$
Shell & tube (1 shell pass, 2, 4, ... n tubes pass):	$NTU = -(1 + C_r^2)^{-1/2} \ln \left(\frac{E - 1}{E + 1} \right),$ $E = \frac{2/\varepsilon_1 - (1 + C_r)}{(1 + C_r^2)^{1/2}}$
Cross flow (C_{\max} mixed, C_{\min} unmixed):	$NTU = -\ln[1 + (1/C_r) \ln(1 - \varepsilon C_r)]$
Cross flow (C_{\max} unmixed, C_{\min} mixed):	$NTU = -(1/C_r) \ln[C_r \ln(1 - \varepsilon) + 1]$
Heat exchangers with $C_r = 0$:	$NTU = -\ln(1 - \varepsilon)$

3. Analysis of Shell and Tube Heat Exchanger

Shell and tube heat exchangers are the most widely used type of heat exchanger. They are used as steam generators, condensers, feedwater heaters, and in single-phase processes. In this section we consider shell and tube heat exchangers with subcooled water flowing in both tubes and the shell. In the next section, we consider shell and tube heat exchangers as condensers, followed by the section for shell and tube heat exchangers as steam generators. A schematic of a straight tube heat exchanger is shown in Section 1. Shown in Figure VIa.3.1 is the schematic of a U-tube heat exchanger of the shell and tube type. This figure shows a one-shell and two-tube pass. Shown on the right are examples of the tube arrangements. Tubes may be arranged in triangular, square, or other types of arrays. Earlier, it was mentioned that the chemically controlled stream should flow in the shell as tubes are easier to clean. Straight tube cleaning is generally performed with projectile guns to scrape tubes of deposits. There are other factors to consider in the allocation of the streams to the tube or the shell side. For example, high-pressure fluid should flow through tubes due to tube capability to withstand higher pressures. The stream with lower mass flow rate and heat transfer coefficient should generally flow in the shell. As discussed by Kakac, this facilitates installation of fins on the outside of the tubes. Also, mixing and redirecting flow by the baffle plates would enhance heat transfer. In the analysis that follows, subscripts i and o refer to the tube side and shell side, respectively.

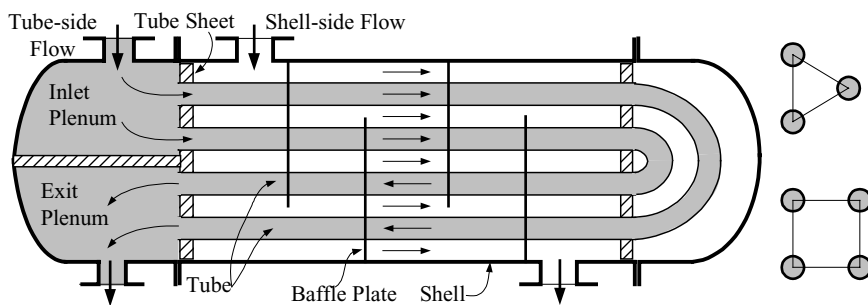


Figure VIa.3.1. Schematic of a one-shell, two-tube pass shell and tube heat exchanger and tube arrays

3.1. Performance Evaluation

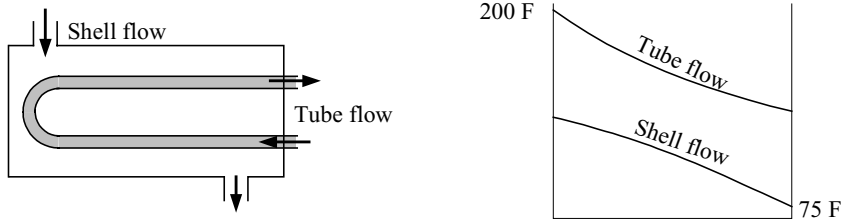
Heat exchangers are designed for a rated or nominal condition. Often we need to find the performance of a heat exchanger operating at conditions different than nominal. In such circumstance, we generally know the shell and tube mass flow rates and inlet temperatures. The goal is to determine the outlet temperatures as well as the rate of heat transfer and the overall heat transfer coefficient. Hence, performance evaluation of a shell and tube heat exchanger for which d_i , d_o , L , and N are known includes finding \dot{Q} , $T_{h,out}$, $T_{c,out}$, and U for given \dot{m}_h , \dot{m}_c , $T_{h,in}$, and

$T_{c,in}$. The solution requires iteration since properties must be evaluated at an average temperature while outlet temperatures are unknown. In the first trial, we assume either the outlet temperatures or determine fluid properties based on the known inlet temperatures. The solution steps are outlined as follows:

- 1- find A_o having d_o , L , and N
- 2- find h_h and h_c having \dot{m}_h , \dot{m}_c , and the thermophysical properties
- 3- find U_o having h_h , h_c , tube data, f_i , and f_o
- 4- find C_{min} , C_{max} , and C_r having \dot{m}_h , $c_{p,h}$ and \dot{m}_c , $c_{p,c}$
- 5- find NTU having UA and C_{min}
- 6- find ε having NTU and C_r
- 7- find \dot{Q} , $T_{h,o}$, $T_{c,o}$ having ε , $T_{h,in}$, and $T_{c,in}$
- 8- find F and the average temperatures having $T_{h,out}$, $T_{c,out}$, $T_{h,in}$, and $T_{c,in}$.

Repeat the above steps using updated properties until the required convergence criterion is met. These steps can be implemented in a spreadsheet or simple FORTRAN program, as shown in the next example.

Example VIa.3.1. Hot water flows inside tubes of a shell and tube heat exchanger. Find the total rate of heat transfer for the following data ($k_s = 10$ Btu/h·ft·F):



d_i	d_o	L	N	\dot{m}_h	\dot{m}_c	$T_{h,in}$	$T_{c,in}$	f_i	f_o
(in)	(in)	(ft)	(-)	(lbm/h)	(lbm/h)	(F)	(F)	(ft ² ·h·F/Btu)	(ft ² ·h·F/Btu)
0.652	0.75	40	1000	2E6	3E6	200	75	0.0005	0.0005

Solution: We follow the above solution steps. Since we do not have $T_{h,out}$ and $T_{c,out}$, we use an approximation and find properties at $T_{h,in}$ and $T_{c,in}$:

	T	ρ	c_p	μ	k	Pr
	(F)	(lbm/ft ³)	tu/lbm·F	(lbm/h·ft)	(Btu/h·ft·F)	(-)
Tube:	200	60.1	1.0	0.7293	0.392	1.87
Shell:	75	62.3	1.0	2.225	0.352	6.32

$$a_i = \pi d_i^2 / 4 = 3.14 \times 0.0543^2 / 4 = 2.32\text{E-}3 \text{ ft}^2$$

$$a_o = \pi d_o^2 / 4 = 3.14 \times 0.0625^2 / 4 = 3.07\text{E-}3 \text{ ft}^2$$

$$\text{Re}_i = \dot{m}_i d_i / (\mu_i a_i) = 2\text{E}3 \times 0.0543 / (0.7293 \times 2.32\text{E-}3) = 64,225$$

$$\text{Re}_o = \dot{m}_o d_o / (\mu_o a_o) = 3\text{E}3 \times 0.0625 / (2.225 \times 3.07\text{E}-3) = 27,144$$

$$h_i = (k_i/d_i)\text{Nu}_i = (k_i/d_i)(0.023 \text{Re}_i^{0.8} \text{Pr}_i^{0.3}) = (0.392/0.0543)(0.023 \times 64,225^{0.8} \times 1.87^{0.3}) = 1406 \text{ Btu/h}\cdot\text{ft}^2\cdot\text{F}$$

$$h_o = (k_o/d_o)\text{Nu}_o = (k_o/d_o)(0.023 \text{Re}_o^{0.8} \text{Pr}_o^{0.4}) = (0.352/0.0625)(0.023 \times 27,144^{0.8} \times 6.32^{0.4}) = 954 \text{ Btu/h}\cdot\text{ft}^2\cdot\text{F}$$

$$U_o = \left[\frac{d_o}{d_i h_i} + \frac{d_o f_i}{d_i} + \frac{d_o \ln(d_o/d_i)}{2k_s} + f_o + \frac{1}{h_o} \right]^{-1}$$

$$= [R_i + R_{fi} + R_s + R_{fo} + R_o]^{-1}$$

$$R_i = d_o/(d_i h_i) = 0.0625/(0.0543 \times 1406) = 8.1864\text{E}-4 \text{ h}\cdot\text{ft}^2\cdot\text{F/Btu}$$

$$R_{fi} = d_o f_i/d_i = 0.0625 \times 0.0005/0.0543 = 5.7551\text{E}-4 \text{ h}\cdot\text{ft}^2\cdot\text{F/Btu}$$

$$R_s = d_o \ln(d_o/d_i)/(2k_s) = 0.0625 \times \ln(0.0625/0.0543)/(2 \times 10) = 8.7901\text{E}-4 \text{ h}\cdot\text{ft}^2\cdot\text{F/Btu}$$

$$R_{fo} = f_o = 0.0005 \text{ h}\cdot\text{ft}^2\cdot\text{F/Btu}$$

$$R_o = 1/h_o = 1/954 = 1.0482\text{E}-4 \text{ h}\cdot\text{ft}^2\cdot\text{F/Btu}$$

$$\Sigma R = 8.1864\text{E}-4 + 5.7551\text{E}-4 + 8.7901\text{E}-4 + 5.00\text{E}-4 + 1.0482\text{E}-4 = 3.382\text{E}-3 \text{ h}\cdot\text{ft}^2\cdot\text{F/Btu}$$

$$U_o = 1/\Sigma R = 1/3.382\text{E}-3 = 295.7 \text{ Btu/h}\cdot\text{ft}^2\cdot\text{F}$$

$$C_{min} = 2\text{E}6 \text{ Btu/F and } C_{max} = 3\text{E}6 \text{ Btu/F. We find } C_r \text{ as: } C_r = C_{min}/C_{max} = 0.667$$

$$NTU = U_o A_o / C_{min} = 295.7 (\pi d_o NL)/2\text{E}6 = 295.7 \times 3.14 \times 0.0625 \times 1000 \times 40/2\text{E}6 = 1.161$$

Having $NTU = 1.161$ and $C_r = 0.667$, the effectiveness is found as: $\varepsilon = 0.55$

$$\dot{Q} = \varepsilon C_{min}(T_{h,in} - T_{c,in}) = 0.55 \times 2\text{E}6 \times (200 - 75) = 1.375\text{E}8 \text{ Btu/h.}$$

We should now use the calculated \dot{Q} to update tube and shell average temperature and repeat the steps that were performed above. These are implemented in the following FORTRAN program, which is also included on the accompanying CD-ROM.

```

c                                     Shell & Tube Heat Exchanger
c This program finds Th_o, Tc_o, Qdot, e, NTU, and DTlmtD Given:
c dmh, dmc, Th_i, Tc_i as well as di, do, aL, aN, fi, and fo for a Shell & Tube
c heat exchanger with water in both sides
c      implicit real*8 (a-h,o-z)
c
c Nomenclature:
c aa:   tube flow area (ft2)           ab:   shell flow area (ft2)
c aL:   total tube length (ft)         aN:   total number of tubes
c cpa:  tube-side specific heat (Btu/lbm-F)  cpb:  shell-side specific heat
c                                     (Btu/lbm-F)
c di:   tube inside diameter (in)       do:  tube outside diameter (in)
c ha:   tube-side HTC. (Btu/hr-ft2-F)   hb:  shell-side HTC (Btu/hr-ft2-F)
c Thi:  tube-side inlet temperature (F)  Tbi:  shell-side inlet temperature (F)

```

```

c      data pi/3.1415927/
      open(5,file='hx1.in')
      open(6,file='hx1.out')
      read(5,*) dmi,dmo
      read(5,*) Ti_in,To_in
      read(5,*) dip,dop,aL,aN
      read(5,*) aks
      read(5,*) fi,fo

c      di=dip/12.00
      do=dop/12.00
      fai=pi*di*di/4.
      fao=pi*do*do/4.
      Ao=pi*do*aL*aN
c      Only for the first trial, find properties based on the inlet temps.
      iter=0
      Ti_out=Ti_in
      To_out=To_in
100    continue
      iter=iter+1
      Ti_avg=0.5*(Ti_in+Ti_out)
      To_avg=0.5*(To_in+To_out)
      Ts=0.5*(Ti_avg+To_avg)
      call intrpl(Ti_avg,cpfi,cpgi,amufi,amug,akfi,akg,Prfi,Prg,
1      sigf,betaf,rofi,rog,anuf,anug,vf,vfg,vg)
      call intrpl(To_avg,cpfo,cpgo,amufo,amug,akfo,akg,Prfo,Prg,
1      sigf,betaf,rofo,rog,anuf,anug,vf,vfg,vg)
      call htc(Ti_avg,Ts,dmi,aN,di,fai,hi)
      call htc(To_avg,Ts,dmo,aN,do,fao,ho)

c      Call Uover(di,do,hi,ho,fi,fo,aks,Uo)
      Call NTU(dmi,cpfi,dmo,cpfo,Ao,Uo,Cmin,Cr,aNTU,eff)
      Qdot=eff*Cmin*abs(Ti_in-To_in)
      If(Ti_in.lt.To_in) go to 1
      Ti_out=Ti_in-(Qdot/(dmi*cpfi))
      To_out=To_in+(Qdot/(dmo*cpfo))
      go to 2
1      continue
      Ti_out=Ti_in+(Qdot/(dmi*cpfi))
      To_out=To_in-(Qdot/(dmo*cpfo))
2      continue
      DTlmtd=Qdot/(Uo*Ao)
      if(iter.eq.1) go to 100
      Tsn=0.5*(Ti_avg+To_avg)
      eps=abs(Tsn-Ts)/Tsn
      if(eps.le.1.e-6) go to 101
      if(iter.lt.30) go to 100
      print *, 'Steady-State Iteration Did Not Converge'
      stop
101    continue
      write(6,3) dip,dop,aL,aN,dmi,dmo,Ti_in,To_in,Ti_out,To_out,Ts,
1      DTlmtd,hi,ho,Qdot,Uo,aNTU,eff
3      format(
1' Tube inside diameter (in):.....',f8.3,5x,
1' Tube outside diameter (in):.....',f8.3,5x,/,
1' Tube total length (ft):.....',f8.1,5x,
1' Total number of tubes (-):.....',f8.1,5x,/,
1' Tube mass flow rate (lbm/h):...',e8.0,5x,
1' Shell mass flow rate (lbm/h):...',e8.0,5x,/,
1' Tube inlet temperature (F):....',f8.0,5x,
1' Shell inlet temperature (F):...',f8.0,5x,/,
1' Tube outlet temperature (F):...',f8.1,5x,
1' Shell outlet temperature (F):...',f8.1,5x,/,
1' Tube surface temperature (F):...',f8.1,5x,
1' Log mean temp. difference (F):...',f8.1,5x,/,
1' Tube-side HTC (Btu/ft2 h F):...',f8.1,5x,

```



```

1' Shell-side HTC (Btu/ft2 h F):...',f8.1,5x,/,
1' Rate of heat transfer (Btu/h):...',e8.1,5x,
1' Overall HTC (Btu/ft2 h F):...',f8.1,5x,/,
1' Number of transfer units (-):...',f8.1,5x,
1' Heat exchanger effectiveness:...',f8.3,5x,/)
stop
end

C.....
subroutine htc(Tflow,Ts,dm,aN,diam,fa,h)
implicit real*8 (a-h,o-z)
call intrpl(Tflow,cp,cpg,amu,amug,ak,akg,Pr,prg,sigf,betaf,
1 ro,rog,anuf,anug,vf,vfg,vg)
Re=dm*diam/(amu*aN*fa)
if(Re.gt.4000.) go to 1
h=(48/11)*ak/diam
return
1 continue
c n=0.4 for fluid being heated up and n=0.3 for fluid being cooled down
b=0.4
if(Ts.lt.Tflow) b=0.3
h=(ak/diam)*0.023*(Re**0.8)*(Pr**b)
return
end

C.....
Subroutine NTU(dmi,cpfi,dmo,cpfo,Ao,Uo,Cmin,Cr,aNTU,eff)
implicit real*8(a-h,o-z)
Cmin=dmi*cpfi
Cmax=dmo*cpfo
If(Cmax.gt.Cmin) go to 1
Cmin=dmo*cpfo
Cmax=dmi*cpfi
continue
Cr=Cmin/Cmax
aNTU=Uo*Ao/Cmin
arg=exp(-aNTU*sqrt(1.+Cr*Cr))
ratio=(1.+arg)/(1.-arg)
eff=2./(1.+Cr+sqrt(1.+Cr*Cr)*ratio)
return
end

C.....
Subroutine Uover(di,do,hi,ho,fi,fo,aks,Uo)
implicit real*8(a-h,o-z)
Resi=do/(di*hi)
Resfi=do*fi/di
Resso=do*alog(do/di)/(2.*aks)
Reso=1./ho
Uo=1./(Resi+Resfi+Resso+fo+Reso)
return
end

```

The results for the above data are obtained in 5 iterations as follows:

Tube inside diameter (in):	0.652	Tube outside diameter (in):	0.750
Tube total length (ft):	40.0	Total number of tubes (-):	1000
Tube mass flow rate (lbm/h):	2E+6	Shell mass flow rate (lbm/h):	3E+6
Tube inlet temperature (F):	200.	Shell inlet temperature (F):	75.
Tube outlet temperature (F):	131.6	Shell outlet temperature (F):	120.8
Tube surface temperature (F):	131.9	Log mean temp. difference (F):	58.6
Tube-side HTC (Btu/ft ² ·h·F):	1145.4	Shell-side HTC (Btu/ft ² ·h·F):	1186
Rate of heat transfer (Btu/h):	1.37E8	Overall HTC (Btu/ft ² ·h·F):	297.6
Number of transfer units (-):	1.2	Heat exchanger effectiveness:	0.547

3.2. Performance Monitoring

Performance of heat exchangers degrades over time primarily due to fouling. Two methods can be used to evaluate heat exchanger performance. The first method is to measure pressure drop and the second is to use measured flow rates and temperatures to calculate the fouling factor. The second method is accomplished by calculating the heat transfer coefficients in the tubes and in the shell (i.e., h_i and h_o). The fouling factor is then obtained from Equation VIa.1.1 and VIa.1.12:

$$\frac{f_i}{A_i} + \frac{f_o}{A_o} = \frac{F(\Delta T_{LMTD})_{Fouled}}{\dot{Q}_{Fouled}} - \left[\frac{1}{h_i A_i} + \frac{\ln(d_o/d_i)}{2\pi L k_s} + \frac{1}{h_o A_o} \right] \quad \text{VIa.3.1}$$

where in steady-state operation,

$$\dot{Q} = \dot{m}_c c_{p,c} (T_{c,out} - T_{c,in}) = \dot{m}_h c_{p,h} (T_{h,in} - T_{h,out}).$$

The software on the accompanying CD-ROM can be used to analyze the performance of the shell and tube heat exchangers including the calculation of the tube-side pressure drop.

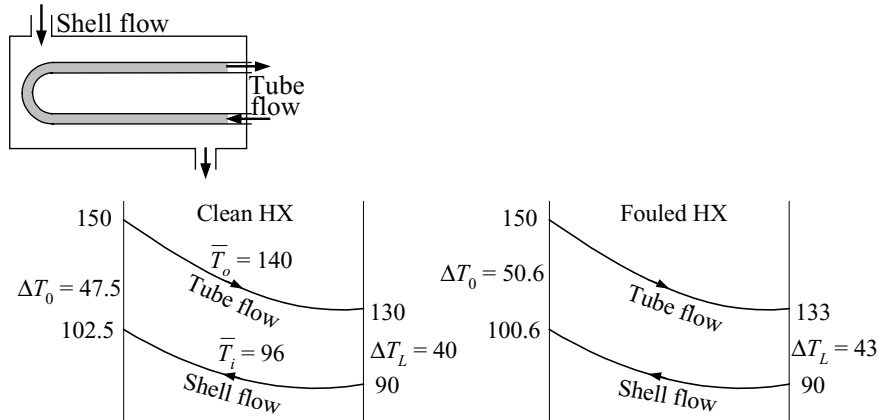
Example VIa.3.2. The rate of heat transfer in a shell and tube heat exchanger is 11.72 MW or about 4E7 Btu/h. Water flows in both tube and shell. The design values for the clean heat exchanger are as follows:

	T_{in} (F)	T_{out} (F)	\dot{m} (lbm/h)	d (in)	L (ft)	N
Tube:	150	130.0	2.0E6	0.652	13	773
Shell:	90	102.5	3.2E6	0.750	18	1

The data for the same heat exchange in a fouled condition are:

	T_{in} (F)	T_{out} (F)	\dot{m} (lbm/h)	d (in)	L (ft)	N
Tube:	150	133.0	2.0E6	0.652	13	773
Shell:	90	100.6	3.2E6	0.750	18	1

- Find the overall heat transfer coefficient for the clean heat exchanger. ($k_s = 8$ Btu/h-ft-F)
- Find the cleanliness factor for the fouled heat exchanger
- Find the fouling factor, assuming that the fouling occurs primarily in the tubes.



Solution: a) We find ΔT_{LMTD} for the clean heat exchanger and follow the steps outlined below:

$$[\Delta T_{LMTD}]_{Clean} = (47.5 - 40)/\ln(47.5/40) \approx 44 \text{ F}$$

$$P = (102.5 - 90)/(150 - 90) = 0.2 \text{ and } R = (90 - 102.5)/(130 - 150) = 0.21$$

Figure VIa.2.3 gives $F \approx 0.97$

$$A_o = \pi d_o L N = 3.14 \times (0.75/12) \times 13 \times 773 = 1973 \text{ ft}^2$$

$$\dot{Q}_{Clean} = F(U_o)_{Clean} A [\Delta T_{LMTD}]_{Clean}$$

$$(U_o)_{Clean} = 4E7/(0.97 \times 1973 \times 44) \approx 475 \text{ Btu/h}\cdot\text{F}$$

To confirm, $(U_o)_{Clean}$, we perform the following calculation:

	\bar{T} (F)	ρ (lbm/ft ³)	c_p (Btu/lbm·F)	μ (lbm/ft·h)	k (Btu/ft·h·F)	Pr
Tube	140	61.37	1.0	1.13	0.378	2.99
Shell	96	62.03	1.0	1.73	0.362	4.77

We use the Dittus-Boelter correlation to find heat transfer coefficient in both tube and shell:

$$d_i = 0.652/12 = 0.0543 \text{ ft} \rightarrow a_i = \pi d_i^2 / 4 = 3.14 \times 0.0543^2 / 4 = 2.32\text{E-}3 \text{ ft}^2.$$

$$d_o = 0.75/12 = 0.0625 \text{ ft} \rightarrow a_o = \pi d_o^2 / 4 = 3.14 \times 0.0625^2 / 4 = 3.06\text{E-}3 \text{ ft}^2.$$

$$\text{Re}_i = 4 \dot{m}_i / (\pi N \mu_i d_i) = 4 \times 2.0E6 / (3.14 \times 773 \times 1.13 \times 0.0543) = 53,688$$

$$\text{Re}_o = 4 \dot{m}_o / (\pi N \mu_o d_o) = 4 \times 3.2E6 / (3.14 \times 773 \times 1.73 \times 0.0625) = 48,748$$

$$h_i = (k_i/d_i)[0.023 \text{Re}_i^{0.8} \text{Pr}_i^{0.3}] = (0.378/0.0543) \times [0.023 \times 53,688^{0.8} \times 2.99^{0.3}] = 1352 \text{ Btu/h}\cdot\text{ft}^2\cdot\text{F}$$

$$h_o = (k_o/d_o)[0.023 \text{Re}_o^{0.8} \text{Pr}_o^{0.4}] = (0.362/0.0625) \times [0.023 \times 48,748^{0.8} \times 4.77^{0.4}] = 1401 \text{ Btu/h}\cdot\text{ft}^2\cdot\text{F}$$

$$1/(U_o)_{\text{Clean}} = [0.0625/(0.0543 \times 1352)] + [0.0625 \ln(0.0625/0.0543)/(2 \times 8)] + [1/1401] = 2.1126\text{E-}3$$

$$(U_o)_{\text{Clean}} = 1/2.1145\text{E-}3 = 473 \text{ Btu/h}\cdot\text{ft}^2\cdot\text{F}$$

b) For the fouled exchanger, the average temperatures and related properties are as follows:

	\bar{T} (F)	ρ (lbm/ft ³)	c_p (Btu/lbm·F)	μ (lbm/ft·h)	k (Btu/ft·h·F)	Pr
Tube	141.5	61.35	1.0	1.16	0.378	2.95
Shell	95.3	62.03	1.0	1.75	0.361	4.82

The related Re numbers, Nu numbers, and heat transfer coefficients become:

	\bar{T} (F)	Re	Nu	h (Btu/h·ft ² ·F)
Tube	141.5	53,023	191.5	1333
Shell	95.3	49,311	245.8	1420

$$[\Delta T_{LMTD}]_{\text{Fouled}} = (50.6 - 43)/\ln(50.6/43) \approx 46.7 \text{ F.}$$

$$P = (100.6 - 90)/(150 - 90) = 0.17 \text{ and } R = (90 - 100.6)/(133 - 150) = 0.62$$

Figure VIa.2.3 gives $F = 1.0$

$$\dot{Q}_{\text{Fouled}} = 2\text{E}6 \times 1 (150 - 133) = 3.4\text{E}7 \text{ Btu/h}$$

$$(U_o)_{\text{Fouled}} = \dot{Q}_{\text{Fouled}} / [FA_o(\Delta T_{LMTD})_{\text{Fouled}}] = 3.4\text{E}7 / (1973 \times 46.7) = 369 \text{ Btu/h}\cdot\text{F}$$

$$C_F = U_{\text{Fouled}}/U_{\text{Clean}} = 369/475 \approx 78\%$$

c) To find the fouling factor, we solve Equation VIa.1.1 for f_i as f_o is specified to be negligible:

$$\frac{d_o f_i}{d_i} = \frac{FA_o(\Delta T_{LMTD})_{\text{Fouled}}}{\dot{Q}_{\text{Fouled}}} - \left[\frac{d_o}{d_i h_i} + \frac{d_o \ln(d_o / d_i)}{2k_s} + \frac{1}{h_o} \right]$$

Substituting values

$$\frac{d_o f_i}{d_i} = \frac{1}{369} - \left[\frac{0.0625}{0.0543 \times 1333} + \frac{0.0625 \ln(0.0625/0.0543)}{2 \times 8} + \frac{1}{1420} \right]$$

$$= 2.71\text{E-}3 - 2.1\text{E-}3$$

This results in $f_i = 0.0005 \text{ h}\cdot\text{ft}^2\cdot\text{F/Btu}$. Note that the calculation of h_o was simplified in this problem.

As noted in the conclusion of Example VIa.3.1, calculation of the heat transfer coefficient for the tube bundle was based on a simplistic approach. Generally, the design of a heat exchanger shell depends on several factors including the number of tube passes, tube layout (type of array for tube bundle), baffle type, geometry, baffle spacing, operational pressure, weight, and size limitations. As a result, calculation of the shell-side h_o and ΔP_o is much more involved than h_i and ΔP_i for the tube side. For example, the baffle plates force fluid, which without the baffles flows parallel to the tube axis, to flow in a cross-flow manner over the tube bundle. Also, the diameter used in a correlation for h_o should be an appropriate hydraulic diameter. For a concentric or a double-pipe heat exchanger, the hydraulic diameter is found from:

$$D_c = 4 \frac{A_f}{C_w} = 4 \frac{\pi[D_{Sh}^2 - d_o^2]/4}{\pi(D_{Sh} + d_o)} = D_{Sh} - d_o$$

where A_f is the flow area, C_w the wetted perimeter, D_{Sh} the shell diameter, and d_o the tube outside diameter. The hydraulic diameter found above can then be used in a suitable correlation such as Dittus-Boelter to find the heat transfer coefficient. For shell and tube heat exchangers, the hydraulic diameter is calculated for the tube array. Perry suggests correlations for calculation of h_o and Kakac provides related examples.

4. Analysis of Condensers

Power plant condensers generally use coolant from large bodies of water such as a lake or bay to cooldown the condensing steam. The temperature difference between the condensing steam saturation temperature and circulating water inlet temperature is referred to as ITD , the initial temperature difference. The temperature difference at the tube exit is referred to as TTD , the terminal temperature difference (Figure VIa.4.1).

In condenser design, in addition to the steam pressure, hence steam saturation temperature (T_o), and the cooling water inlet temperature ($T_{c,in}$), we need to select an appropriate tube-side flow velocity to meet the heat transfer requirement while minimizing pumping power and tube erosion. Tube velocity may range from 3 to 12 ft/s. The tube side heat transfer coefficient can be found from the Dittus-Boelter correlation (Equation IVb.3.4) and the bundle-side heat transfer coefficient from condensation on horizontal tubes, given by Equation Vc.3.4. Temperature rise of the cooling water for large power plants is generally in the range of 12 to 15 F to minimize thermal pollution. Having the temperature rise, the flow rate of the cooling water is then found from $\dot{m}_c = \dot{Q}/\Delta T_i$. Knowing the heat sink water temperature, we can then find the temperature of the cooling water at the outlet. Selection of the tube diameter (tube flow area) combined with the cooling water density and velocity give the mass flow rate per condenser tube. The total number of tubes (N_{tube}) is obtained by dividing the cooling water mass flow rate by the mass flow rate of a tube. We then find the average tube length (L_{tube}) from \dot{Q} , ΔT_{LMTD} , and Equation VIa.2.12a.

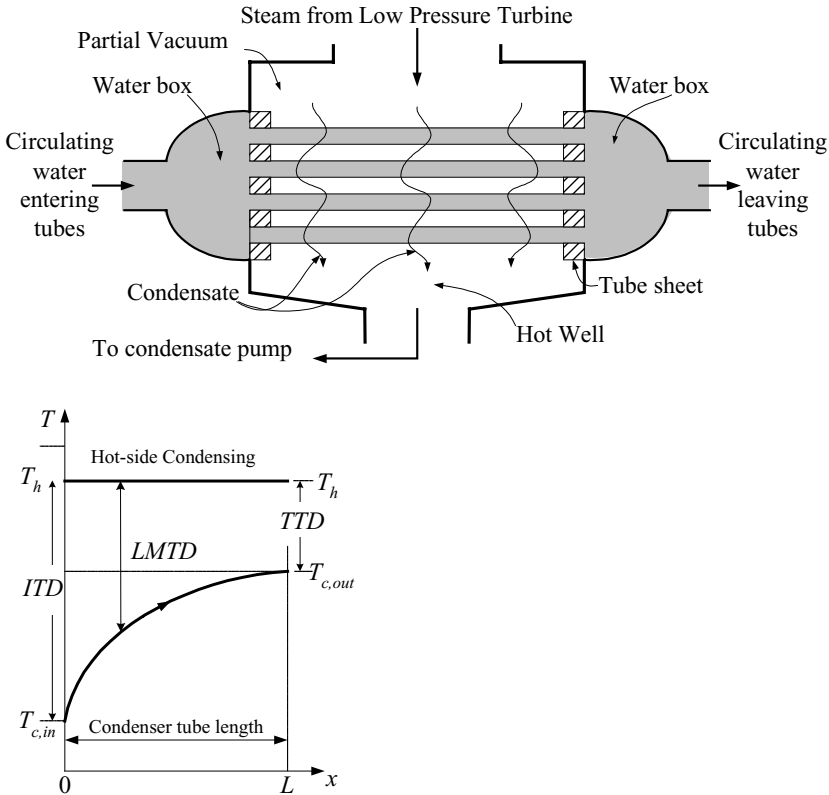
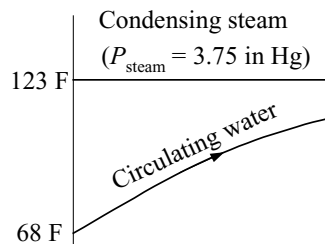
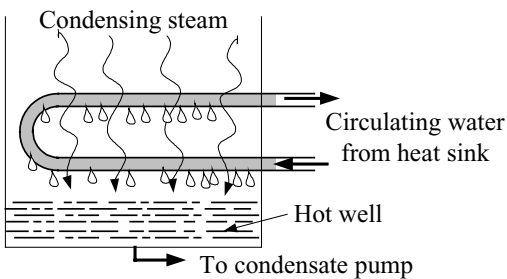


Figure VIa.4.1. Schematic of a condenser

Example VIa.4.1. A power plant produces 855 MWe at a thermal efficiency of $\eta_{\text{Thermal}} = 30\%$. Find: a) N_{tube} and L_{tube} , b) tube side pressure drop and c) Shell-side flow rate. Use the following data: $d_i = 0.93$ in, $d_o = 1$ in, $T_{c,in} = 68$ F, $\Delta T_c = 20$ F, $T_h = 123$ F, $V_i = 9$ ft/s, $k_s = 26$ Btu/ft \cdot h \cdot F, $c_{p,c} = 1$ Btu/lbm \cdot F.



Solution: a) First we calculate the rate of heat to be removed by the condenser. Total power produced is:

$\dot{Q}_H = \dot{W} / \eta_{Thermal} = 855/0.3 = 2850$ MWth. The rate of heat to be removed in the condenser is:

$$\dot{Q}_C = 2850 - 855 = 1995 \text{ MWth} = 6.8069\text{E}9 \text{ Btu/h}$$

- Tube-side mass flow rate: $\dot{m}_i = \dot{Q}_C / (c_{p,c} \Delta T_c) \cong 6.8069\text{E}9 / (1 \times 20) = 3.4\text{E}8$ lbm/h

- Since $T_{c,out} = 68 + 20 = 88$ F, the tube-side average temperature becomes $T_c = 0.5(68 + 88) = 78$ F.

- To find U we need h_i and h_o . To find h_o , we need tube temperature T_s , which varies along the tube length. We use T_s calculated at average temperatures to represent the entire tube temperature. Since we do not have tube surface area, for now we guess T_s from T_c and T_h : $T_s = 0.5(T_c + T_h) = 0.5(78 + 123) = 100.5$ F

- Properties for both tube-side and shell-side at the related film temperatures are:
 $(T_{film})_c = 0.5(T_c + T_s) = 89.25$ F. $(T_{film})_h = 0.5(100.5 + 123) = 111.75$ F

	\bar{T} (F)	ρ (lbm/ft ³)	c_p (Btu/lbm·F)	μ (lbm/ft·h)	k (Btu/ft·h·F)	Pr
Shell	111.75	61.82	0.998	1.466	0.368	-
Tube	89.25	62.12	0.998	1.868	0.358	5.207

For tube bundle (shell-side) we also find $h_{fg}(123 \text{ F}) = 1023.9$ Btu/lbm and $\rho_g(111.75 \text{ F}) = 0.004$ lbm/ft³

- Since $T_{sat} > T_s$, we find $Ja = c_{p,h}(T_h - T_s)/h_{fg} = 0.998 \times (123 - 100.5)/1023.9 = 0.0219$. Thus $h'_{fg} = 1023.9(1 + 0.68 \times 0.0219) = 1039.17$ Btu/lbm

$$h_o = 0.729 \left[\frac{g \rho_f (\rho_f - \rho_g) k_f^3 h'_{fg}}{\mu_f (T_h - T_s) d_o} \right]^{1/4} = 0.729 \left[\frac{4.173\text{E}8 \times 61.82^2 \times 0.368^3 \times 1039.17}{1.466 \times (123 - 100.5) \times (1./12)} \right]^{1/4}$$

$$= 1707 \text{ Btu/ft}^2 \cdot \text{h} \cdot \text{F}$$

- To calculate h_i we need to find $Re_i = \dot{m}_i d_i / (\mu_i Na_i)$. This in turn requires N and a_i , which are found as:

$$a_i = \pi d_i^2 / 4 = 3.14 \times (0.93/12)^2 / 4 = 0.004717 \text{ ft}^2$$

$$N = \dot{m}_i / (\rho_i V_i a_i) = 3.41\text{E}8 / [62.12 \times (9 \times 3600) \times 0.004717] = 35918$$

$$Re_i = 3.41\text{E}8 \times (0.93/12) / (1.868 \times 35918 \times 0.004717) = 83,500$$

$$h_i = (k_i/d_i) [0.023 Re_i^{0.8} Pr_i^{0.4}] = (0.358 \times 12/0.93) \times [0.023 \times 83500^{0.8} \times 5.207^{0.4}] = 1779.5 \text{ Btu/ft}^2 \cdot \text{h} \cdot \text{F}$$

- We now calculate U_o :

$$U_o = \left[\frac{d_o}{d_i h_i} + \frac{d_o \ln(d_o / d_i)}{2k_s} + \frac{1}{h_o} \right]^{-1} = \left[\frac{1}{0.93 \times 1779.5} + \frac{(1/12) \ln(1/0.93)}{2 \times 26} + \frac{1}{1707} \right]^{-1}$$

$$= 765.5 \text{ Btu/ft}^2 \cdot \text{h} \cdot \text{F}$$

- We also calculate $\Delta T_{LMTD} = \frac{(123 - 68) - (123 - 88)}{\ln[(123 - 68)/(123 - 88)]} = 44.25 \text{ F}$

- To find total tube length, we use the overall energy balance $\dot{Q}_C = U_o A_o \Delta T_{LMTD}$
 $= U_o (\pi d_o N L) \Delta T_{LMTD}$

$$- L = \frac{\dot{Q}_C}{U_o (\pi d_o N) \Delta T_{LMTD}} = \frac{6.8069 \text{E}9}{765.5 \times \pi \times (1/12) \times 35918 \times 44.25} = 21.2 \text{ ft.}$$

- For two-tube pass per shell, $L_{pass} = 21.2/2 = 10.68 \text{ ft.}$

b) The tube-side pressure drop is found from Equation III.6.7:

$$\Delta P_i = f \frac{L}{d_i} \frac{\dot{m}_i^2}{2 \rho_i g_c a_i^2} = \left(\frac{0.184}{\text{Re}_i^{0.2}} \right) \frac{21.2}{(0.93/12)} \frac{(3.41 \text{E}8/35918)^2}{2 \times 62.12 \times (32.2 \times 3600^2)(0.004717)^2}$$

$$= 408 \text{ lbf/ft}^2 = 2.83 \text{ psi.}$$

c) The rate of steam condensation is found from:

$$\dot{m}_o = \dot{Q}_C / h'_{fg} = 6.8069 \text{E}9 / 1039.17 = 6.55 \text{E}6 \text{ Btu/h}$$

The results are summarized below:

d_i (in)	d_o (in)	h_i (Btu/h·ft ² ·F)	h_o (Btu/h·ft ² ·F)	U_o (Btu/h·ft ² ·F)	L (ft)	ΔT_{LMTD} (F)	ΔP_i (psi)
0.93	1	1779.5	1707	765.5	21.2	44.25	2.83

Comment: we may use a transverse heat balance $h_i A_i (T_s - T_c) = h_o A_o (T_h - T_s)$ to update tube temperature, T_s . Note that due to high tube thermal conductivity, we assumed $T_{si} = T_{so}$. The updated average tube temperature becomes $T_s = [T_h + (h_i d_i / h_o d_o) T_c] / [1 + (h_i d_i / h_o d_o)] = 101.66 \text{ F}$. This is 1% larger than T_s used in the above analysis.

The above example shows the theoretical aspects of a condenser design. In practice, such problems as tube fouling and the ingress of non-condensable gases in the tube bundle need to be dealt with. The gas leakage in the tube bundle not only increases the hot well total pressure but also, as discussed by Harpster, tends to collect around some tubes, degrading condensation.

4.1. Condenser Design Optimization

For a given rate of heat transfer (\dot{Q}) and bundle-side pressure [$T_h = T_{sat}(P_{steam})$], we are interested in evaluating the effects of such parameters as tube velocity (V_i), tube diameter (d_i and d_o) and tube length (L) on the tube-side pressure drop and subsequently the required pumping power. To perform this parametric evaluation, we rearrange Equation VIa.3.1, noting that $F = 1$ for condensers:

$$\frac{1}{h_i(\pi d_i NL)} + \frac{\ln(d_o / d_i)}{2\pi k_s NL} + \frac{1}{h_o(\pi d_o NL)} = \frac{\Delta T_{LMTD}}{\dot{Q}} \quad \text{VIa.4.1}$$

where h_o may be calculated from Equation Vc.3.4. Hence, it is treated here as a constant. This is because the value of h_o depends only on the properties of the condensing fluid and the outside diameter of the tube. In Equation VIa.4.1, we need to substitute for h_i in terms of V_i and d_i . For this purpose, we use the definition of the Nusselt number:

$$\begin{aligned} h_i d_i &= k_i Nu_i = k_i \left[0.023 (\rho_i V_i d_i / \mu_i)^{0.8} \text{Pr}_i^{0.4} \right] \\ &= (0.023 k_i \text{Pr}_i^{0.4} \rho_i^{0.8} / \mu_i^{0.8}) (d_i V_i)^{0.8} \end{aligned}$$

Substituting for $h_i d_i$ in Equation VIa.4.1 and rearranging, we obtain:

$$\left(\frac{\pi \Delta T_{LMTD}}{\dot{Q}} \right) NL = \frac{1}{(0.023 k_i \text{Pr}_i^{0.4} \rho_i^{0.8} / \mu_i^{0.8}) (d_i V_i)^{0.8}} + \left[\frac{\ln(d_o / d_i)}{2k_s} - \frac{1}{d_o h_o} \right] \quad \text{VIa.4.2}$$

Equation VIa.4.2 provides a relation between N and L . We can find N in terms of d_i and V_i from an energy balance for the tube side:

$$N = \frac{4\dot{m}_i}{\rho_i V_i (\pi d_i^2)} = \left[\frac{4\dot{Q}}{(\pi d_i^2) c_{p,c} (T_{c,out} - T_{c,in})} \right] \frac{1}{\rho_i V_i} \quad \text{VIa.4.3}$$

Substituting N from Equation VIa.4.3 into Equation VIa.4.2, we find tube length L as:

$$L = \frac{\left[\frac{d_i^{1.2} V_i^{0.2}}{0.023 k_i \text{Pr}_i^{0.4} \rho_i^{0.8} / \mu_i^{0.8}} \right] - \left[\frac{\ln(d_o / d_i)}{2k_s} - \frac{1}{d_o h_o} \right] d_i^2 V_i}{\left[\left(\frac{4}{\rho_i c_{pi}} \right) \left(\frac{\Delta T_{LMTD}}{\Delta T_i} \right) \right]} \quad \text{VIa.4.4}$$

As shown in Tables A.III.1 and A.III.2, the selection of tube or pipe outside diameter and the specification of tube gage or pipe schedule results in the determination of the inside diameter. Equation VIa.4.3 shows that, for a specified tube size, the number of tubes is inversely proportional to the coolant velocity in the tubes. On the other hand, Equation VIa.4.4 shows that tube length is nearly a

tubes. On the other hand, Equation VIa.4.4 shows that tube length is nearly a linear function of tube-side velocity.

Using the above equations and the data of Example VIa.4.1, plots of tube length and number of tubes versus tube diameter are obtained as shown in Figure VIa.4.2. As expected, the plots show that for a specified flow velocity, the number of tubes increases, whereas tube length decreases with decreasing tube diameter. Also, for a given tube diameter, tube length increases and number of tubes decreases with increasing tube velocity. The same conclusion can be made for tube-side pressure drop and pumping power. The pumping power is given as:

$$\dot{W}_{\text{pump}} = \Delta P(\dot{m}_i / \rho) \quad \text{VIa.4.5}$$

For a given tube diameter, the required pumping power decreases as the number of tubes increases. This reduces operational cost. On the other hand, as shown by Nahavandi, the initial capital cost increases with an increasing number of tubes. Therefore, an optimized value for the number of tubes should be found to satisfy cost criterion.

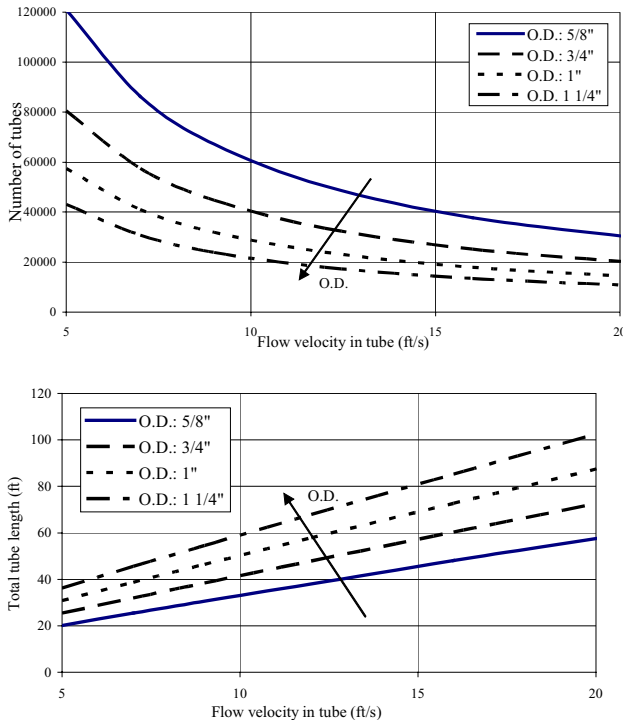


Figure VIa.4.2. Tube length and tube number versus flow velocity for various tube diameters

5. Analysis of Steam Generators

In the design of steam generators, the rate of heat transfer, inlet and outlet temperatures, and flow rates are generally known quantities (Figure VIa.5.1). The goal, therefore, is to calculate the heat transfer area of the tubes. In steam generators, the hot fluid generally flows in the tubes with water boiling in the tube bundle. In this analysis we consider the secondary side to be at saturation condition along the entire length of the tubes whether tubes are oriented horizontally or vertically. To be consistent, we show tube side values with subscript i and secondary-side values with subscript o , respectively. Also, $T_{h,in}$, $T_{h,out}$, and T_c are tube inlet, tube exit, and shell-side saturation temperatures, respectively. Known values are \dot{Q} , \dot{m}_i , $T_{h,in}$, $T_{h,out}$, T_c , f_i , f_o , d_i and d_o . We calculate the steam generator effectiveness from:

$$\varepsilon = \frac{T_{h,in} - T_{h,out}}{T_{h,in} - T_c} \quad \text{VIa.5.1}$$

Having ε from Equation VIa.5.1, we can calculate NTU from $NTU = UA / C_{\min} = -\ln(1 - \varepsilon)$. Therefore,

$$UA = -\dot{m}_i c_{p,i} \ln(1 - \varepsilon) \quad \text{VIa.5.2}$$

Combining Equations VIa.1.1 and VIa.5.2, writing the total tube length as $L = A_o / (\pi d_o)$, and the surface area of the inside of the tubes as $A_i = d_i A_o / d_o$ yields:

$$\left[\frac{d_o}{d_i} \frac{1}{h_i A_o} + \frac{d_o}{d_i} \frac{f_i}{A_o} + \frac{d_o}{2k_s} \frac{\ln(d_o / d_i)}{A_o} + \frac{f_o}{A_o} + \frac{1}{h_o A_o} \right]^{-1} = -\dot{m}_i c_{p,i} \ln(1 - \varepsilon) \quad \text{VIa.5.3}$$

Total tube surface area, A_o is obtained from Equation VIa.5.3 provided h_i and h_o are substituted in terms of known quantities. We use the Dittus-Boelter correlation (Equation IVb.3.4) for turbulent flow inside tubes to find h_i :

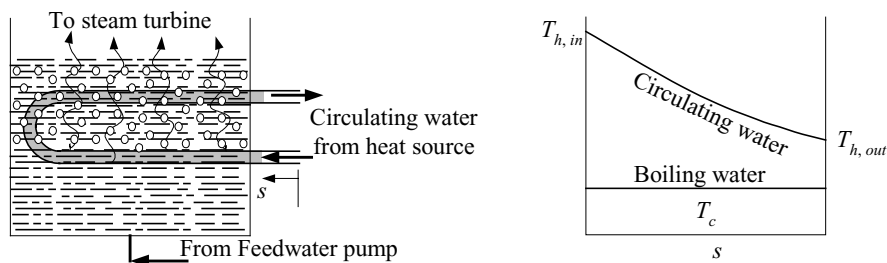


Figure VIa.5.1. Schematic of a steam generator

$$h_i = 0.023 \frac{k_i}{d_i} \left(\frac{4\dot{m}_i}{\pi \mu_i N d_i} \right)^{0.8} \text{Pr}_i^{0.3} \quad \text{VIa.5.4}$$

where the exponent of the Pr number is changed to 0.3 as the fluid is cooling down. Also physical properties in Equation VIa.5.4 are developed at the fluid bulk temperature. The secondary side heat transfer coefficient h_o may be found from Rohsenow's pool boiling correlation or the Chen correlation (Equations Vb.4.1a and Vb.5.1b, respectively). Selecting the Rohsenow correlation, we find:

$$T_s - T_c = \frac{C_{fs} h_{fg}}{c_{p,o}} \left[\frac{\dot{Q} / A_o}{\mu_o h_{fg}} \sqrt{\frac{g_c \sigma_o}{g(\rho_{f,o} - \rho_{g,o})}} \right]^{1/3} \text{Pr}_o^{1.7} \quad \text{VIa.5.5}$$

We now correlate the surface superheat to the secondary-side thermal resistance as

$$T_s - T_c = \left(\frac{f_o}{A_o} + \frac{1}{h_o A_o} \right) \dot{Q}$$

and substitute the result in Equation VIa.5.5:

$$\left(\frac{f_o}{A_o} + \frac{1}{h_o A_o} \right) = \left\{ \frac{C_{fs} h_{fg}}{c_{p,o}} \left[\frac{1}{\mu_o h_{fg}} \sqrt{\frac{g_c \sigma_o}{g(\rho_{f,o} - \rho_{g,o})}} \right]^{1/3} \text{Pr}_o^{1.7} \right\} \frac{1}{\dot{Q}^{2/3} A_o^{1/3}} \quad \text{VIa.5.6}$$

Substituting Equation VIa.5.6 into Equation VIa.5.3 results in:

$$C_1 A_o + C_2 A_o^{2/3} + C_3 = 0 \quad \text{VIa.5.7}$$

where $C_1 = [\dot{m}_i c_{p,i} \ln(1 - \varepsilon)]^{-1}$,

$$C_2 = \left\{ \frac{C_{fs} h_{fg}^{2/3}}{c_{p,o}} \left[\frac{1}{\mu_o} \sqrt{\frac{g_c \sigma_o}{g(\rho_{f,o} - \rho_{g,o})}} \right]^{1/3} \text{Pr}_o^{1.7} \right\} \frac{1}{\dot{Q}^{2/3}} \text{ and}$$

$$C_3 = \left[\frac{d_o}{d_i} \frac{1}{h_i} + \frac{d_o}{d_i} f_i + \frac{d_o}{2} \frac{\ln(d_o / d_i)}{k_s} \right],$$

where g_c is given in Chapter IIa. Equation VIa.5.7 is a non-linear algebraic equation that may be solved by Newton-Raphson iteration. The first guess for tube area is obtained from an approximate solution (i.e., by assuming that the second-

dary-side thermal resistance is negligible $(A_o)_{\text{Guess}} = C_3/C_1$). Upon solving Equation VIa.5.7, we can find the average tube length from $L = A_o/(\pi d_o N)$.

Example VIa.5.1. The following data are given for a steam generator. Find a) the average tube length L_{tube} , b) tube side pressure drop, and c) shell side flow rate. Data: $d_i = 0.654$ in, $d_o = 0.75$ in, $T_{h,\text{in}} = 604$ F, $T_{h,\text{out}} = 550$ F, $P_h = 2250$ psia, $P_c = 850$ psia, $k_s = 11.00$ Btu/ft·h·F, $N_{\text{tube}} = 8485$, $\dot{m}_i = 61\text{E}6$ lbm/h, $C_{fs} = 0.015$, $c_{p,o} = 1.24$ Btu/lbm·F, $f_i = 0.0002437$ ft²·h·F/Btu, $f_o = 0.0$ ft²·h·F/Btu.

Solution: The solution, in a FORTRAN program, is included on the accompanying CD-ROM.

The input data and results of calculation are summarized below.

Table VIa.5.1. Pertinent steam generator thermal hydraulic data

Total rate of heat transfer (Btu/h - MW):	4.386E9 - 1285.5
Tube inlet temperature (F - C):	604 - 318
Tube exit temperature (F - C):	550 - 288
Tube-side pressure (psia - MPa):	2250 - 15.51
Tube bundle-side pressure (psia - MPa):	850 - 5.86
Tube bundle-side temperature (F - C):	525.2 - 274
Total number of tubes:	8485
Tube outside diameter (in - mm):	0.75 - 19.05
Tube wall thickness (in - mm):	0.048 - 1.22
Tube inside diameter (in - mm):	0.654 - 16.61
Tube average heated length (ft - m):	54.16 - 16.5
Tube heat transfer area (ft ² - m ²):	90,232 - 8383
Overall heat transfer coefficient (Btu/h·ft ² ·F - W/m ² ·C):	1041 - 183.3
The log mean temperature difference, ΔT_{LMTD} (F - C):	46.7 - 25.9
Effectiveness:	0.684
Tube-side thermal resistance (h·ft ² ·F/Btu - m ² ·C/W):	0.0001744 - 0.00099
Tube-wall thermal resistance (h·ft ² ·F/Btu - m ² ·C/W):	0.0003950 - 0.00224
Tube bundle-side thermal resistance (h·ft ² ·F/Btu - m ² ·C/W):	0.0001475 - 0.00084
Tube-side fouling resistance (h·ft ² ·F/Btu - m ² ·C/W):	0.000 - 0.000
Tube bundle-side fouling resistance (h·ft ² ·F/Btu - m ² ·C/W):	0.0002437 - 0.00138

An alternative derivation for determination of the required surface area for the tubes takes into account the energy balance for an elemental control volume due to the change in temperature from tube inlet to tube exit (Nahavandi). Similar correlations can then be used for heat transfer coefficients and the resulting differential equation is integrated from tube inlet to tube outlet to obtain the required surface area. (see Problem VIa.18).

In steam generators, we often need to find the temperature of the hot fluid as it moves inside the tubes and transfers energy to the secondary side. This is shown in the next example.

Example VIa.5.2. Hot liquid is flowing steadily at a rate of \dot{m} inside the tubes of a steam generator having N tubes of outside diameter d_o . The secondary side is boiling, resulting in an overall heat transfer coefficient of U_o that remains uniform along the tube. Find the tube-side temperature profile as a function of flow path.

Solution: Applying Equation IIa.6.4-1 to the single-phase liquid inside the tubes over element ds , results in:

$$\frac{dT_h}{ds} = -\frac{N\pi d_o U_o}{\dot{m} c_p} (T_h - T_{sat})$$

where s is an element of length in the flow direction and T_{sat} is the secondary-side saturation temperature. Since \dot{m} , U_o , and T_{sat} remain constant, we can integrate from $T_{h,in}(s=0)$ to $T(s)$ to find:

$$T_h(s) = T_{h,in} - (T_{h,in} - T_{sat}) \left(1 - e^{-s/l^*}\right) \quad \text{VIa.5.8}$$

where s is an element of length along the tube and l^* is given by $l^* = \dot{m} c_p / (\pi N d_o U_o)$. This result is not applicable if liquid boils in the tube-side or liquid does not boil in the secondary side.

6. Transient Analysis of Concentric Heat Exchangers

A transient during heat exchanger operation is generally caused by throttling a valve located on the discharge line of the pump feeding the tube or the shell side. Heat exchanger transients also take place during starting or stopping the pump. Transients imposed by valves and pumps affect flow rate. Inlet temperatures to tube or shell may also change due to the loss of a feedwater heater if located upstream of the heat exchanger. In this analysis we consider concentric parallel and counterflow heat exchangers and divide the exchanger along its length to several nodes. Both streams are assumed to be incompressible and average fluid properties are used. By explicitly modeling the tube region, thermal inertia of the tube material would then appear in the formulation. Shown in Figure VIa.6.1 is the schematic of a concentric heat exchanger, divided into N nodes but only three nodes are shown. Node i , for example, receives mass and energy from node $i-1$, as carried by the mass flow rate of stream A and, in turn, delivers mass and enthalpy to node $i+1$. Due to the liquid incompressibility, mass flow rate into node i equals the mass flow rate into node $i+1$, as only energy would accumulate in

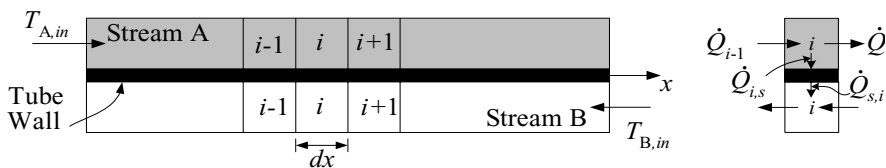


Figure VIa.6.1. Nodalization of a concentric heat exchanger

node i . There is also a transverse energy transfer out of node i of stream A, through the tube surface into node i of stream B. Hence, the energy balance in the axial direction for element i in stream A yields:

$$\dot{Q}_{i-1} - \dot{Q}_i - d\dot{Q}_{i-s} = \frac{\partial}{\partial t}(m_i c_v T_i) \quad \text{VIa.6.1}$$

where in Equation VIa.6.1, m_i is the mass of stream A fluid in control volume i . Note that in this derivation, we ignored heat conduction in the fluid compared with the rate of energy transfer by convection. Replacing $m_i = \rho_i A_i dx$, where A_i is the flow area of stream A, and expanding the second term in the left side, Equation VIa.6.1 becomes:

$$\dot{Q}_{i-1} - \left(\dot{Q}_{i-1} + \frac{\partial \dot{Q}_{i-1}}{\partial x} dx \right) - d\dot{Q}_{i-s} = \frac{\partial}{\partial t}[(\rho A dx)_i c_{v,i} T_i]$$

Since fluid is incompressible, we express enthalpy in terms of specific heat and temperature. Parameters ρ , $c_{p,i}$, and A_i are also constant. The formulation for stream A becomes:

$$-\frac{\partial}{\partial x}(\rho V A c_p T)_A dx - d\dot{Q}_{i-s} = \frac{\partial}{\partial t}(\rho A dx c_v T)_A$$

Substituting for the transverse energy term, yields:

$$-\frac{\partial}{\partial x}(\rho V A c_p T)_A dx - (Ph dx)_A (T_A - T_s) = \frac{\partial}{\partial t}(\rho A dx c_v T)_A$$

where P is the perimeter ($P = \pi d$) and h is the heat transfer coefficient. Note that we have represented the elemental tube since we are using average values for properties, ρ , c_p , c_v , and h remains constant. Since A_A and V_A are also assumed to be constant, we can write:

$$\frac{\partial T_A}{\partial t} + \left(V \frac{c_p}{c_v} \right)_A \frac{\partial T_A}{\partial x} + \left(\frac{Ph}{\rho A c_v} \right)_A (T_A - T_s) = 0 \quad \text{VIa.6.2}$$

Similarly, the differential equation describing axial energy of stream B becomes:

$$\frac{\partial T_B}{\partial t} + \lambda \left(V \frac{c_p}{c_v} \right)_B \frac{\partial T_B}{\partial x} - \left(\frac{Ph}{\rho A c_v} \right)_B (T_s - T_B) = 0 \quad \text{VIa.6.3}$$

where in this equation, $\lambda = 1$ for parallel flow and $\lambda = -1$ for counterflow heat exchangers. The rate of change of energy in the i th node of the tube material is due to the exchange of energy with streams A and B, hence the energy equation for the heat exchanger tube material becomes:

$$\frac{\partial T_s}{\partial t} - \frac{(Ph)_A}{(\rho c A)_s} (T_A - T_s) + \frac{(Ph)_B}{(\rho c A)_s} (T_s - T_B) = 0 \quad \text{VIa.6.4}$$

Equations VIa.6.2, VIa.6.3, and VIa.6.3 constitute an approximate formulation for transient analysis of parallel and counterflow heat exchangers. Various solution methods are proposed for this set of equations. For example, Li finds an exact solution for the parallel flow heat exchanger by using Laplace transforms. Lorenzini applies the finite element method while Romie uses several dimensionless ratios to describe the exit temperature response to a unit step change in the inlet temperatures. The following solution is based on the finite difference method. The energy equations for stream A, in finite difference form is:

$$\frac{T_{A,i}^{n+1} - T_{A,i}^n}{\Delta t} + \left(V \frac{c_p}{c_v} \right)_A \frac{T_{A,i}^{n+1} - T_{A,i-1}^{n+1}}{\Delta x} + \left(\frac{Ph}{\rho A c_v} \right)_A (T_{A,i}^{n+1} - T_{s,i}^{n+1}) = 0$$

The finite difference form of the tube wall energy equation becomes:

$$\frac{T_{s,i}^{n+1} - T_{s,i}^n}{\Delta t} - \frac{(Ph)_A}{(\rho c A)_s} (T_{A,i}^{n+1} - T_{s,i}^{n+1}) + \frac{(Ph)_B}{(\rho c A)_s} (T_{s,i}^{n+1} - T_{B,i}^{n+1}) = 0$$

and the finite difference form of stream B energy equation, considering a counter-flow heat exchanger is:

$$\frac{T_{B,i}^{n+1} - T_{B,i}^n}{\Delta t} - \left(V \frac{c_p}{c_v} \right)_B \frac{T_{B,i}^{n+1} - T_{B,i+1}^{n+1}}{\Delta x} - \left(\frac{Ph}{\rho A c_v} \right)_B (T_{s,i}^{n+1} - T_{B,i}^{n+1}) = 0$$

These equations can be simplified by introducing dimensionless constants for stream A:

$$\alpha_1 = \left(\frac{c_p}{c_v} \right)_A \frac{V_A}{(\Delta x / \Delta t)}; \quad \alpha_2 = 1 + \alpha_1 + \alpha_3; \quad \alpha_3 = \left(\frac{Ph}{\rho A c_v} \right)_A \Delta t$$

for the tube material:

$$\sigma_1 = \frac{(Ph)_A}{(\rho c A)_s} \Delta t; \quad \sigma_2 = 1 + \sigma_1 + \sigma_3; \quad \sigma_3 = \frac{(Ph)_B}{(\rho c A)_s} \Delta t$$

and for stream B:

$$\beta_1 = \left(\frac{Ph}{\rho A c_v} \right)_B \Delta t; \quad \beta_2 = 1 + \beta_1 + \beta_3; \quad \beta_3 = \lambda \left(\frac{c_p}{c_v} \right)_B \frac{V_B}{(\Delta x / \Delta t)}.$$

Definition of these dimensionless coefficients reduces the finite difference equations to:

$$\begin{aligned}
-\alpha_1 T_{A,i-1}^{n+1} + \alpha_2 T_{A,i}^{n+1} - \alpha_3 T_{s,i}^{n+1} &= T_{A,i}^n \\
-\sigma_1 T_{A,i}^{n+1} + \sigma_2 T_{s,i}^{n+1} - \sigma_3 T_{B,i}^{n+1} &= T_{s,i}^n \\
-\beta_1 T_{B,i-1}^{n+1} + \beta_2 T_{B,i}^{n+1} - \beta_3 T_{B,i+1}^{n+1} &= T_{B,i}^n
\end{aligned}$$

Writing similar equations for node $i = 1$ through $i = N$, the following set of equations is obtained:

$$\underline{A}^n \underline{Y}^{n+1} = \underline{C}^{n+1} \quad \text{VIa.6.5}$$

where vector \underline{Y} in Equation VIa.6.5 contains all unknown temperatures:

$$\underline{Y} = \left[\left(T_{A,1}^{n+1} \dots T_{A,i}^{n+1} \dots T_{A,N}^{n+1} \right), \left(T_{s,1}^{n+1} \dots T_{s,i}^{n+1} \dots T_{s,N}^{n+1} \right), \left(T_{B,1}^{n+1} \dots T_{B,i}^{n+1} \dots T_{B,N}^{n+1} \right) \right]^T$$

vector \underline{C} contains known temperatures and the boundary terms, added to the first and last terms:

$$\underline{C} = \left[\left(T_{A,1}^n + \alpha_1 T_{A,in} \dots T_{A,i}^n \dots T_{A,N}^n \right), \left(T_{s,1}^n \dots T_{s,i}^n \dots T_{s,N}^n \right), \left(T_{B,1}^n \dots T_{B,i}^n \dots T_{B,N}^n + \beta_3 T_{B,in} \right) \right]^T$$

and matrix A is a $3N \times 3N$ matrix having the structure shown in Figure VIa.6.2 (all other terms are zeroes). The left matrix is for parallel and the right matrix is for counterflow heat exchangers.

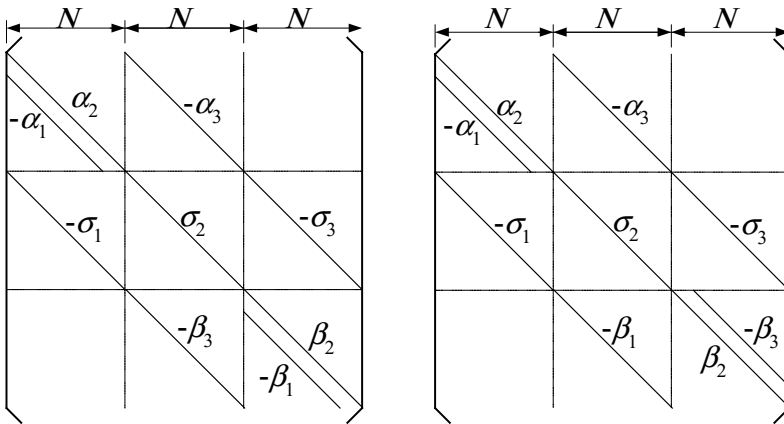


Figure VIa.6.2. Structure of the coefficient matrix for a parallel and a counterflow heat exchanger

Equation VIa.6.5 is written in a semi-implicit form where the terms of coefficient matrix A are developed at the previous time step. This prevents linearization of terms and formation of a Jacobian matrix. The initial conditions for the speci-

fied boundary conditions (inlet flows and temperatures) are obtained from the steady state solution to Equation Va.6.5:

$$(A - I)\underline{Y}^o = \underline{C}$$

where I is the identity matrix and \underline{Y}^o includes the steady-state temperature distribution in stream A, in tube material, and in stream B.

QUESTIONS

- What types of heat exchangers can be found in a house?
- What is the difference between a concentric heat exchanger and a shell and tube heat exchanger?
- Why a counterflow HX is more efficient than a parallel flow heat exchanger?
- What is the purpose of the baffle plates in a shell and tube heat exchanger? What are the advantages and disadvantages of baffle plates?
- Two streams are exchanging heat in a heat exchanger. One stream is cleaner than the other. Which stream should flow in the tubes and which stream should flow in the shell?
- What is the difference between fouling factor and the cleanliness factor (C_F)?
- If a heat exchanger has $C_F = 0.8$ and $U_{dirty} = 2000 \text{ W/m}^2\cdot\text{K}$ what is U_{clean} ?
- Why does tube temperature not appear in the steady-state formulation of heat exchangers?
- In a counterflow heat exchanger, can the outlet temperature of the cold stream be greater than the outlet temperature of the hot stream?
- What are the six major assumptions made in the derivation of the equations in Section 2 of this chapter?
- What heat exchanger design constraints are affected by the selection of tube diameter?
- What advantages and drawbacks can you identify for a horizontal versus a vertical steam generator?
- Why does the shell side of a power plant condenser operate at a partial vacuum?
- What effects does the ingress of non-condensable gases have on a condenser performance?

PROBLEMS

1. The following temperatures are obtained at the inlet and exit ports of a counterflow heat exchanger. Find ΔT_{LMTD} and compare it with $\overline{\Delta T}$ as given by Equation VIa.2.5. Data: $T_{h,i} = 130 \text{ F}$, $T_{h,o} = 111.9 \text{ F}$, $T_{c,i} = 95 \text{ F}$, and $T_{c,o} = 106.3 \text{ F}$ [Ans.: $\Delta T_{LMTD} = 20.1 \text{ F}$, $\overline{\Delta T} = 20.3 \text{ F}$. Temperature profiles are flat]
2. A concentric counterflow heat exchanger is used to cool oil by water. The oil flow rate is 0.1 kg/s and enters at 100 C . Water enters at 30 C and a flow rate of

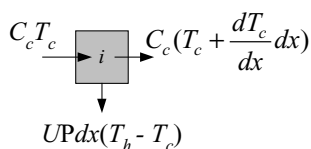
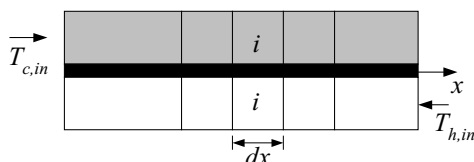
0.2 kg/s. The heat transfer area is 5.223 m^2 and the overall heat transfer coefficient is $37.8 \text{ W/m}^2\cdot\text{K}$. Find the rate of heat transfer and exit temperatures. Data: $c_{p,h} = 2131 \text{ J/kg}\cdot\text{K}$ and $c_{p,c} = 4178 \text{ J/kg}\cdot\text{K}$. [Ans.: $\dot{Q} = 8524 \text{ W}$, $T_{ho} = 60 \text{ C}$, and $T_{co} = 40 \text{ C}$].

3. A one-shell, two-tube pass shell and tube heat exchanger has 1580 tubes with $d_i = 13 \text{ mm}$ and $d_o = 16 \text{ mm}$. Tubes have an average length of 6 m per pass. Cold water enters the tubes at 30 C and a rate of 110 kg/s and hot water enters shell at 90 C and a rate of 125 kg/s . Find the rate of heat transfer, ΔT_{LMTD} , and the overall heat transfer coefficient. Use stainless steel tubes and $f_i = 0.001 \text{ m}^2\cdot\text{K/W}$. [Ans.: 13 MW , 10.7 C , and $493 \text{ W/m}^2\cdot\text{K}$].

4. A shell and tube heat exchanger uses 600 tubes of $\frac{3}{4}$ in B.W.G 20 ($d_o = 0.75 \text{ in}$ and $d_i = 0.68 \text{ in}$) and 17.5 ft per pass. Hot water enters the tubes at $1.5\text{E}6 \text{ lbm/h}$ and 180 F . The heat exchanger has one shell and two-tube pass per shell. Cold water enters the shell at $1.5\text{E}6 \text{ lbm/h}$ and 70 F . The fouling factors happen to be equal for both tube and shell sides, $f_i = f_o = 0.0003 \text{ h}\cdot\text{ft}^2\cdot\text{F/Btu}$. Find the tube and shell outlet temperatures and the heat exchanger effectiveness. [Ans.: 130 F , 120 F , and 0.456].

5. A shell and tube heat exchanger uses 650 tubes of $\frac{5}{8}$ in B.W.G 18 ($d_o = 0.625 \text{ in}$ and $d_i = 0.527 \text{ in}$) and 7.5 ft per pass. Tubes are stainless steel. The heat exchanger has one shell and two-tube passes per shell. Cold water enters the tubes at a velocity of 6.818 ft/s and a temperature of 75 F . Hot water enters the shell at 195 F and at a rate of $2.5\text{E}6 \text{ lbm/h}$. The fouling factors happen to be equal for both tube and shell sides, $f_i = f_o = 0.0005 \text{ h}\cdot\text{ft}^2\cdot\text{F/Btu}$. Find $T_{h,out}$, $T_{c,out}$, U_o , ε , total rate of heat transfer, and the tube-side pressure drop. [Ans.: 173.67 F , 110.75 F , $373.2 \text{ Btu/h}\cdot\text{ft}^2\cdot\text{F}$, 0.298 , and 2.38 psi].

6. Consider the steady-state operation of a counterflow heat exchanger. The energy balance for an elemental control volume in the cold stream is shown below. Write a similar energy balance for an elemental control volume in the hot stream. Then for each stream, derive the differential equation for temperature as function of the exchanger length. [Ans.: $dT_c/dx = (UP/C_c)(T_h - T_c)$ and $dT_h/dx = (UP/C_h)(T_h - T_c)$].



7. Solve the differential equations obtained in Problem VIa.6 using the following boundary conditions, $T_h(x=0) = T_{h,o}$ and $T_h(x=L) = T_{h,i}$ for the hot and $T_c(x=0) = T_{c,i}$ and $T_c(x=L) = T_{c,o}$ for the cold stream. [Ans.: if $C_c = C_{min}$, $T_h = \{T_{h,o} - C_r T_{c,i} - C_r(T_{h,o} - T_{c,i})\exp[-(1/C_c - 1/C_h)UPx] / (1 - C_r)$ similar relation for T_c].

8. Show that for condensers, $T_{c,out} = T_{c,in} + (T_h - T_{c,in})[1 - e^{-UA/C_c}]$.

9. In Example VIa.5.2, we derived the primary-side temperature profile for a steam generator. Derive a similar temperature profile but for a counter-current heat exchanger in terms of tube length, area, flow rates, and inlet temperatures.

[Ans.: $T_h(s) = T_{h,in} - (T_{h,in} - T^*)(1 - e^{(\beta-\alpha)s/L})$ where in this relation parameters α , β , and T^* are given as $\alpha = UA/\dot{m}_h c_{p,h}$, $\beta = UA/\dot{m}_c c_{p,c}$, and $T^* = (\beta T_{h,in} - \alpha T_{c,o})/(\beta - \alpha)$. Note, $T_{c,o}$ is obtained from Problem VIa.6 in terms of $T_{h,in}$, $T_{c,in}$, \dot{m}_h , \dot{m}_c , and UA].

10. In Example VIa.5.2, we derived the primary-side temperature profile for a steam generator. Now consider a case where fluid in the primary side is also boiling. Derive the profile for steam quality.

11. A shell and tube condenser uses saturated steam at 1 atm and 212 F (100 C) in the shell to heat water in the 18 tubes from 100 F (38 C) to 120 F (49 C). The tubes are thin wall with $d_o \approx d_i = 1$ in (2.54 cm) and are arranged in a triangular pitch. The velocity of water inside the tubes is 8 ft/s (2.44 m/s). Find a) the mass flow rate of water in the tubes, b) the heat transfer coefficient on the inside and outside of the tubes, c) the overall heat transfer coefficient for the tubes neglecting any fouling, d) the length of the tubes, and e) the rate of steam condensation in this condenser. Use carbon steel tubes.

12. In a tubular condenser, steam condenses on the tube bank at 50.5 C (123 F) while cooling water enters the tubes at a rate of 42.966 kg/s (3.41E8 lbm/h) and a temperature of 20 C (68 F). There are 35918 tubes having an outside diameter of 2.54 cm (1 inch) and a length of 6.5 m (21.3 ft). The overall heat transfer coefficient for the clean condenser is 4346 W/m²·C (765.5 Btu/h·F). Find the cooling water temperature at the outlet. Use copper tubes. [Ans.: 31 C (88 F)]

13. A condenser is used to reject 2000 MW to a large lake. Pressure of the condensing steam is 3 in Hg. Cooling water enters at 75 F. The maximum allowed temperature rise of the cooling water is 15 F. Tube velocity is 7 ft/s. Tubes are 1 1/4 in 18 BWG ($d_o = 1.250$ in and $d_i = 1.152$ in). Find the number of tubes, total tube length, and the tube-side pressure drop. Tubes are stainless steel. [Ans.: $N = 40276$, $L = 16.8$ ft, $\Delta P_i = 4.88$ psi].

14. A condenser is used to reject 2000 MW to a large lake. Pressure of the condensing steam is 3 in Hg. Cooling water enters at 75 F. The maximum allowed temperature rise of the cooling water is 15 F. Tube velocity is 7 ft/s. Tubes diameters are $d_o = 1.50$ in and $d_i = 1.402$ in. Find number of tubes, total tube length, and tube-side pressure drop. Tubes are stainless steel. [Ans.: $N = 23756$, $L = 19.6$ ft, $\Delta P_i = 0.93$ psi].

15. The core of a PWR produces 2,778.43 MWth. The PWR is equipped with two recirculating U-tube steam generators. Hot water leaves the core and enters the hot leg at 312.8 C (595.1 F). The system is fully insulated. Colder water

leaves the steam generator tubes and enters the cold legs at 286.7 C (548 F). Water is boiling in the shell-side at the saturation temperature of 277.6 C (531.64 F) corresponding to a pressure of 6.2 MPa ($P_o \cong 900$ psia). There are a total of 8471 tubes, each having an inside and outside diameter of 1.685 cm (0.6635 in) and 1.904 cm (0.7495 in), respectively. Use $f_o = 3.522\text{E-6 C}\cdot\text{m}^2/\text{W}$ (0.00002 F $\cdot\text{h}\cdot\text{ft}^2/\text{Btu}$) and $C_{sf} = 0.012$ to find A_o , ΔT_{LMTD} , h_i , h_o , U_o , L , ε , NTU , and ΔP_i . [Ans.: 8548 m² (92010 ft²), 19.3 C (34.75 F), 43420 W/m²·C (7647 Btu/ft²·h-F), 46877 W/m²·C (8256 Btu/ft²·h-F), 8417 W/m²·C (1482.4 Btu/ft²·h-F), 16.87 m (55.35 ft), 74.2%, 1.356, 0.2 MPa (29.67 psi)].

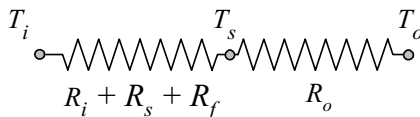
16. The design of a steam generator as described in Section 5 of this chapter uses the Rohsenow pool boiling correlation. Derive a relation for the calculation of the tube surface area using the Chen correlation.

17. The design of a steam generator as described in Section 5 ignores the preheating section of the tube bundle. a) Determine the expected tube length within which the feedwater reaches saturation, and b) revise the formulation to include the preheating calculation of the tube heat transfer area.

18. The steam generator design procedure outlined in Section 5 is based on the effectiveness. In this problem we want to design the steam generator by using a differential approach. [Hint: Writing a steady state energy balance in the axial and transverse directions for an element of length alongside the tubes gives:

$$\dot{q}'' = \frac{d\dot{Q}}{dA} = \dot{m}_i c_{p,i} \frac{dT_i}{dA} = U(T_i - T_o) = \frac{T_s - T_o}{R_s} \quad 1$$

where subscripts i , s , and o stand for tube side, tube, and tube-bundle-side. Use Equation IVa.6.8-2 to relate the various thermal resistances, as shown below, to the overall heat transfer coefficient.



From the last two terms of Equation 1 conclude that $T_i - T_o = \dot{q}''(R_c + R_o)$. Use Equation VIa.5.5, to find $T_s - T_o = f(P_o)\dot{q}''^{1/3}$ and from Equation 1 obtain $R_o = f(P_o)(\dot{q}'')^{-2/3}$. Substitute in Equation 1 and find:

$$T_i - T_o = \dot{q}'' R_c + \dot{q}'' R_o = \dot{q}'' R_c + (\dot{q}'')^{2/3} f(P_o) \quad 2$$

Integrate Equation 1 to find

$$A = \int_{inlet}^{exit} \dot{m}_i c_{p,i} \frac{dT_i}{\dot{q}''} = \dot{m}_i c_{p,i} \int_{inlet}^{exit} \frac{d(T_i - T_o)}{\dot{q}''}$$

Substitute for $T_i - T_o$ from Equation 2 and integrate from inlet (I) to exit (E) to obtain:

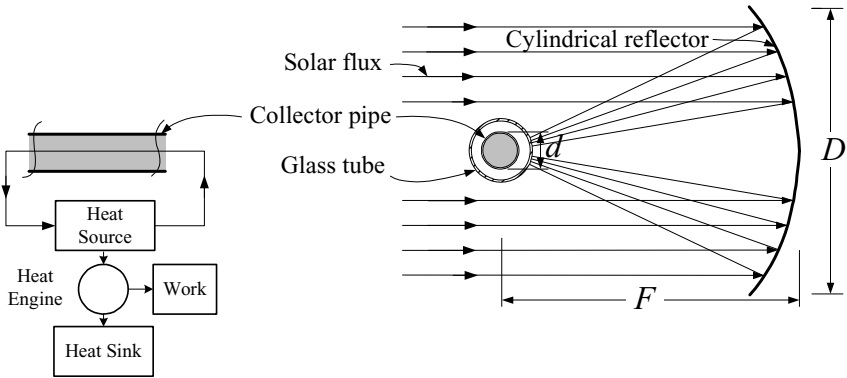
$$A = \dot{m}_i c_{p,i} \left\{ R_c \ln \frac{\dot{q}_E''}{\dot{q}_I''} + f(P_o) [(\dot{q}_E'')^{-2/3} - (\dot{q}_I'')^{-2/3}] \right\} \quad 3$$

To find the required tube surface area, you need to find the heat fluxes at the inlet and exit of the tubes. These are determined from Equation 2 by using the Newton-Raphson method].

19. A cylindrical reflecting lens focuses direct solar light on a collector pipe through which fluid circulates. The heated fluid is used as the heat source for a heat engine producing mechanical power. The collector tube is surrounded by a glass tube to reduce heat loss to the ambient atmosphere. The collector tube diameter is larger than the solar image formed by the reflecting lens. Use the given data and:

a) Find an analytical expression for the efficiency of the solar collector (i.e., the ratio of heat collected by the circulating fluid to the solar flux intercepted by the reflecting lens) as a function of the ratio $(T_c - T_a)/\dot{Q}_i$ and the fixed parameters listed below,

b) if the thermodynamic efficiency of the heat engine is a fixed fraction of the Carnot efficiency of a reversible heat engine operating between heat reservoirs having temperatures equal to the collecting fluid temperature and the ambient temperature, find an analytical expression for the collector temperature which will maximize the power output of the heat engine, and determine its nominal value.



Data:

Cord of cylindrical lens ($D = 1$ m), focal length of cylindrical lens ($F = 2$ m), collector tube outer diameter ($d = 0.03$ m), design direct solar flux ($\dot{q}_i'' = 950$ W/m²), ambient atmospheric temperature ($T_a = 20$ C), temperature of the collecting fluid (T_c), absorptivity-transmissivity product for the incident solar radiation focused on the collector tube ($\alpha\tau = 0.75$), reflectivity of lens surface for solar spectrum ($\rho = 0.9$).

VIb. Fundamentals of Flow Measurement

Flow measurement is an interesting application of the principals of fluid mechanics. Measurements in fluid mechanics are performed for a variety of properties including local (such as velocity, pressure, temperature, density, viscosity) and integrated (volume and mass flow rates) properties. In this section only measurement of local velocity and integrated properties are discussed. However, first some fundamental terms are defined.

1. Definition of Flow Measurement Terms

Invasive is a term applied mostly to classical flowmeters such as the Bernoulli obstruction meters, turbine meter, rotameter and even some modern instruments as vortex meter. Most modern flowmeters such as electromagnetic, ultrasonic, and laser Doppler anemometer are noninvasive instruments. The invasive meters must be integrated in the piping system. The invasive flowmeters generally disturb the flow.

Noninvasive flowmeters have several advantages compared with the invasive flowmeters including the lack of any moving parts, ease of installation, longevity as the instrument is not affected by the flow condition, cost savings, and capability to be bi-directional. Since the noninvasive flowmeters are not exposed to the fluid flow, they do not cause any pressure drop to the flow hence, there is no need for any *flow straightener*.

Error is the difference between the measured value and the true value. Error may be expressed as absolute error or relative error. If the true value of a ruler is 3 m, a measurement of 2.98 m has an absolute error of 0.02 m or relative error of $0.02/2.98 = 0.7\%$.

Fixed error is referred to as the amount of error appearing in repeated measurement by practically the same amount. In flow measurement, a leak upstream of the flowmeter introduces a fixed error regardless of the number of the times flow is measured. Similarly, in temperature measurements by thermometers, some heat is lost to the surroundings by the instrument itself. This additional heat transfer would cause the thermometer to read a lower temperature than the fluid temperature.

Random error is due to such factors as personal fluctuations, mechanical friction associated with certain processes, and electronic fluctuations.

Uncertainty refers to the *errors* associated with the measured data. Uncertainty is expressed in terms of percentage of the true value. An instrument reading with an uncertainty of $\pm 1\%$ implies that the reading falls within 1% of the true value in each direction.

Accuracy is the degree of proximity of the measurement to the actual value and refers to the fractional *error* in the instrument. Accuracy is a qualitative term to describe an instrument and is often confused with *uncertainty*.

Resolution of an instrument is the minimum change in output that the instrument can detect. As such, resolution can be defined as the smallest quantity that the instrument can measure.

Repeatability refers to the maximum difference between the same outputs for the same input, obtained in separate measurements but under similar test conditions. Any difference is generally due to *random error*.

Precision of an instrument is a measure of its repeatability with a specified degree of accuracy.

Calibration is a process to determine accuracy and resolution. Hence, the calibration of an instrument involves the measurement of known values. Such known values are primary standards or a previously calibrated instrument used as a reference. The calibration may also include the application of a primary measurement. Calibration of a flowmeter for example, may be based on a bucket and stop watch.

Drift is an undesirable change in the output of the instrument over a period of time. Drift is usually caused by the electronics of the device and not the process under measurement.

Hysteresis is a property of the instrument and is the difference in output when the measured value is approached with increasing and then with decreasing values. Hysteresis may be caused by friction, elastic deformation, thermal or magnetic effects.

Range refers to the domain within which the instrument works properly and beyond which the outputs are not reliable and the device may be damaged.

Response time is the time required for the output to rise to the value corresponding to the step change of the input.

Sensitivity is the ratio of change in the instrument output to the change in the value of the input.

Span is the difference between the limits of the range.

2. Repeatability, Accuracy, and Uncertainty

2.1. Repeatability and Accuracy

Due to the importance of repeatability and accuracy in measurement, we use an example dealing with throwing darts at a dartboard (Baker). In Figure VIb.2.1(a), 10 out of 10 darts are in the bulls-eye. Since the darts in this case have been accu-

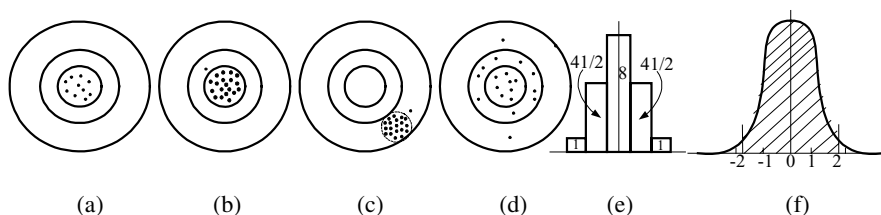


Figure VIb.2.1. Accuracy and repeatability in hitting a dart board

rate, the number of bulls-eyes is therefore, repeatable. In Figure VIb.2.1(b), 19 out of 20 ($19/20 = 95\%$) shots have hit the bulls-eye. Statistically this is a low value of uncertainty ($\pm 1\%$) with a 95% confidence level or within 2 standard deviations. In Figure VIb.2.1(c), the same repeatability is reached as in case (b) but with a certain bias causing all the shots to be off target. This indicates that good accuracy also means good repeatability whereas good repeatability does not necessarily imply good accuracy. In Figure VIb.2.1(d) 19 out of 20 have hit the target ($\pm 5\%$ uncertainty with 95% confidence level) but 8 out of 20 darts have hit the bulls-eye. Figure VIb.2.1(e) shows a depiction of case (d) on a linear plot. Figure VIb.2.1(f) shows the normal distribution, a good representation of flow measurement readings.

2.2. Uncertainty Analysis

Due to the importance of the uncertainty in measurement, more details are necessary for full understanding. During any measurement, there is always the possibility of errors entering the data acquisition process, and distorting data. This may be due to human error, fixed error, systematic error, or random error. It is therefore customary to express data along with some degree of uncertainty to clarify accuracy in the measurement. Uncertainties in the data are usually expressed as a percentage of the full-scale output of the instrument. Measurement of physical values consisting of several parameters, where each parameter is measured by separate instrument, is affected by the uncertainty associated with each instrument. One way to calculate the associated uncertainty in the result is to find the worst-case uncertainty. To explain, suppose that we are interested in calculating the uncertainty associated with pumping power from the flow rate and pressure rise over the pump:

$$\dot{W} = \Delta P \dot{V}$$

For a flow rate of $800 \text{ ft}^3/\text{h} \pm 12 \text{ ft}^3/\text{h}$ and a pressure rise of $45 \text{ psi} \pm 1 \text{ psi}$, the nominal pumping power is $\dot{W} = 36000 \text{ ft}\cdot\text{lbf}/\text{h}$. Applying the worst case uncertainty, pumping power can be calculated as $\dot{W}_{\max} = (800 + 12)(45 + 1) = 37352 \text{ ft}\cdot\text{lbf}/\text{h}$ and $\dot{W}_{\min} = (800 - 12)(45 - 1) = 34,672 \text{ ft}\cdot\text{lbf}/\text{h}$:

$$\dot{W} = 36000 \pm 3.7\%$$

However, it is very unlikely indeed that the highest measurement of pressure rise occurs at the highest measurement of flow rate as these are independent instruments. The same is true for the value of flow rate to coincide with the lowest measurement of pressure rise. The more accurate means of calculating the resulting uncertainty is the method referred to as the *mean squared error*. If output F is a function of n independent variables as:

$$F = f(x_1, x_2, \dots, x_i, \dots, x_n)$$

Then the uncertainty in F , also known as the *expected error*, is given by (Kline):

$$e_F = \pm \left[\left(\frac{\partial F}{\partial x_1} e_{x_1} \right)^2 + \left(\frac{\partial F}{\partial x_2} e_{x_2} \right)^2 + \dots + \left(\frac{\partial F}{\partial x_i} e_{x_i} \right)^2 + \dots + \left(\frac{\partial F}{\partial x_n} e_{x_n} \right)^2 \right]^{1/2} \quad \text{Vib.2.1}$$

where e_{x_i} is the uncertainty associated with each independent variable x_i .

Example Vib.2.1. The rated pressure rise and flow rate of a pump are given as $\Delta P_{\text{pump}} = 45 \pm 2\%$ psi and $\dot{V} = 800 \pm 1.5\%$ ft³/h, respectively. Find the uncertainty in pumping power using the mean squared error method.

Solution: The pumping power is found as $\dot{W} = \Delta P \dot{V}$. We first find the nominal pumping power as:

$\dot{W} = 800 \times 45 = 36000$ ft·lbf/h. To find the uncertainty in \dot{W} , we find:

$$\partial \dot{W} / \partial (\Delta P) = \dot{V} = 800 \text{ ft}^3/\text{h}.$$

The corresponding uncertainty is:

$$e_{\dot{V}} = 800 \times (1.5 / 100) = 12$$

$$\partial \dot{W} / \partial \dot{V} = \Delta P = 45 \text{ psi}.$$

The corresponding uncertainty is:

$$e_{\Delta P} = 45 \times (2 / 100) = 0.9 \text{ psi}.$$

Thus the uncertainty in \dot{W} is calculated as:

$$e_{\dot{W}} = \pm \left[\left(\frac{\partial \dot{W}}{\partial (\Delta P)} e_{\Delta P} \right)^2 + \left(\frac{\partial \dot{W}}{\partial \dot{V}} e_{\dot{V}} \right)^2 \right]^{1/2} = \pm \left[(800 \times 0.9)^2 + (45 \times 12)^2 \right]^{0.5} = \pm 900 \text{ ft} \cdot \text{lbf/h}$$

Therefore the pumping power is found as $\dot{W} = 36000 \pm (900/36000) = 36000 \pm 2.5\%$ ft·lbf/h. Earlier, the uncertainty was found as 3.7%.

To minimize the random error, several readings must be made. Such multiple observations allow the estimation of the *most probable error* from a normal probability distribution around an average value. For example, in the case of a ruler having an average length of \bar{L} , we take N measurements so that:

$$\bar{L} = \sum_{i=1}^N L_i / N$$

or σ being the standard deviation given by:

$$\sigma^2 = \sum_{i=1}^N (L_i - \bar{L})^2 / N$$

the error in measurement is estimated from $e_{\bar{L}} = \sigma / \sqrt{N-1}$ where the error is enhanced by subtracting unity from the number of observations to account for the fact that the true value of the length is not known.

Example VIb.2.2. The length of a ruler is measured 10 times and the following readings are obtained. Find the most probable error.

Reading:	1	2	3	4	5	6	7	8	9	10
Length (m):	3.97	3.82	4.10	4.01	4.16	3.87	4.15	4.05	3.89	3.92

Solution: Arithmetic average of the readings is $\bar{L} = 39.94/10 = 3.994$ m. Set up the following table:

Reading:	1	2	3	4	5	6	7	8	9	10
$L_i - \bar{L}$:	-0.024	-0.174	0.106	0.016	0.166	-0.124	0.156	0.056	-0.104	-0.074
$(L_i - \bar{L})^2 \times 100$:	0.058	3.030	1.12	0.026	2.75	1.54	2.43	0.314	1.08	0.55

Standard deviation is then found as $\sigma = (0.1047/10)^{1/2} = 0.102$ m. Hence, $e_{\bar{L}} = 0.135/\sqrt{9} = 0.034$ m.

3. Flowmeter Types

Recall that for fully developed flow, velocity varies as a function of pipe radius across the flow area and mass flow rate is given by (Equation IIb.2.3):

$$\dot{m} = \int_A \rho \vec{V} \cdot d\vec{A}$$

This equation was simplified for a stationary control surface, flow area normal to the control surface, and the uniform thermodynamic state uniform over the flow area at any instant to obtain Equation IIa.5.2, $\dot{m} = \rho \bar{V} A = \rho \dot{V}$. A flowmeter may then measure local flow velocity (\vec{V}), volumetric flow rate ($\dot{V} = \bar{V} A$) or mass flow rate (\dot{m}).

Flowmeters can be divided into several categories based on such factors as type of flow parameter to measure, cost, induced pressure drop, type of fluid, accuracy,

etc. A large class of flowmeters includes those meters that measure a change in the flow momentum. Examples of this class include the Bernoulli obstruction meters such as venturi, nozzle, and thin plate orifice as discussed in Section IIb.4.2.

Also included in this class are such devices as rotameter, pitot tube, and 90 degree elbows. Another large class of flowmeters includes instruments that measure the volumetric flow rate. Examples of this class include positive displacement of fluid and such devices as electromagnetic, vortex shedder and turbine meters. Devices that also measure volumetric flow rate and are noninvasive include the Laser Doppler anemometer, ultrasonic flowmeter, and pulsed neutron activation meters. To measure mass flow rate directly, such techniques as thermal mass flow measurement, Coriolis force meter, and angular momentum measurement are used. A summary of various types of flowmeters is shown in Table VIb.3.1, which provides information useful in the selection of flowmeters.

Depending on the application, as shown in Table VIb.3.1, the disadvantage of invasive flowmeters is the associated pressure loss. The invasive flowmeters are defined as those that cross the flow boundary. On the other hand, the noninvasive flowmeters, measure the flow by indirect means and are not associated with any head loss nor do they need to be integrated in the piping. For invasive flowmeters, it is important to install the device so that flow entering and leaving the instrument is not disturbed by the presence of fittings and valves. Manufacturers generally specify the minimum distance required upstream and downstream of the pipe. This distance is specified in terms of the diameter of the pipe on which the device would be installed. On occasions that such a possibility does not exist due to space limitations, a flow straightener is used to streamline the flow.

3.1. Momentum Sensing Flowmeters

Orifice, Nozzle, Venturi. The most famous momentum sensing instruments are Bernoulli obstruction meters as were discussed in Section IIb.4.2. Table VIb.3.1 shows that the orifice has the highest and the venturi has the lowest pressure loss. The cost of these devices is inversely proportional to the pressure drop they introduce to the flow. Hence, a venturi is the most expensive and a thin-plate orifice is the least expensive. The Bernoulli obstruction meters are found in various sizes. Thin plate orifices can be found as small as 1 inch in diameter. On the other hand the world's largest flowmeter is a venturi made for Southern Nevada Water authority. The diameter of this flowmeter is 180 inches (4.6 m), having a dry weight of 60,000 lbm and a volume of 6400 ft³ to measure a water flow rate in excess of 555,000 GPM (35 m³/s). The venturi flowmeter is 52 ft (15.85 m) long (Flow Control Magazine).

Rotameter: the trade name of a manufacturer has been applied to the variable area meter. Such meters consist of a tapered tube oriented vertically and a float as shown in Figure VIb.3.1(a). There are three forces acting on the float, the drag force (F_D), as a result of the external flow of fluid over the float, the buoyancy force (F_B) and the float weight (F_W). When $F_W = F_B + F_D$ then the float is at equilibrium and the flow rate is read from a calibrated scale.

Table VIb.3.1. Comparison of Various Flowmeters

Class	Type	Fluid	Accu- racy	Head Loss	Cost	UD/ DD	Advantages & Disadvantages
Momen- tum	Orifice	L/G	M	h	l	20/5	Corrosion & wear: su
	Nozzle	L/G/T	M	m	m	20/5	High temp. & velocity: su
	Venturi	L/G/S/T	M	l	h	15/5	High temp. & velocity: su
	Rotameter	L/G	L	m	l	n	Low flow: st, Pulsating flow: li
	Ave. Pitots	L/G	L	l	l	30/5	Probe flow eparation: su
	Laminar	G	L	h	m	15/5	Pulsating flow: st, Dirty fluid: li
	Elbow	L/G/S	L	l	l	25/10	Available performance data: li
Volume	Turbine	L/G	H	h	h	15/5	Bearing wear: su
	Paddle wheel	L/G	M	l	l	15/5	Bearing wear: su
	Vortex	L/G	H	h	h	20/5	Low flow: ns, Vibration: su
	Electro- magnetic	L/S/T	M	n	h	5/3	Non-conducting fluid: su
	Ultrasonic	L/G/T	H	n	h	15/5	Change in temperature: st
	Laser Doppler	L/G/S/T	M	n	h	15/5	Reynolds Number: li
	Positive displacement	L/G	H	h	l	n	Dirty fluid: su, Wear: su
Mass	Thermal	L/G	L	m	m	5/3	Dirty fluid: su, Low flow: st
	Angular	L	M	m	m	n	Aircraft fuel flow: st
	Coriolis	L/G/S	H	m	h	N	Pipe size: li, Fouling: su

Table abbreviations:

L: liquid, n: None
 G: gas, ns: Not suitable
 S: slurry, st: Suitable
 T: two-phase su: Susceptible
 h: high, li: Limitation
 m: medium UD: Straight piping, as multiples of pipe Diameter, required Upstream
 l: low DD: Straight piping, as multiples of pipe Diameter, required Downstream

Substituting for weight in terms of float volume and density, for buoyancy in terms of float volume and liquid density, and for drag in terms of specific kinetic energy:

$$\rho_F V_F g = \rho_f V_F g + C_D A_F (\rho_f \bar{V}^2) / 2$$

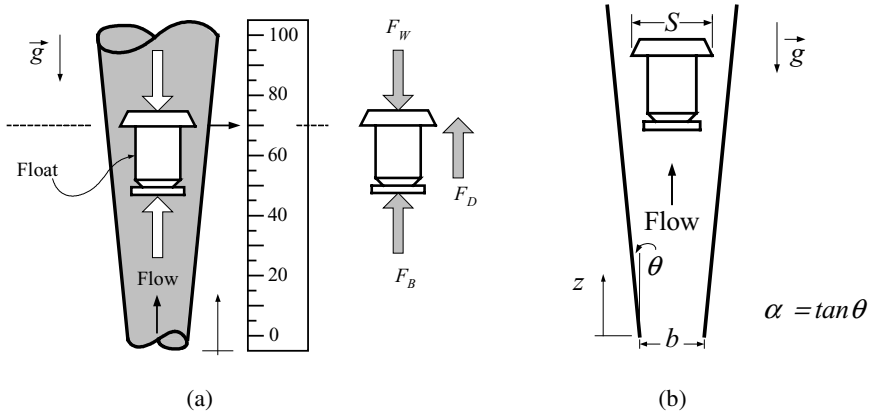


Figure VIb.3.1 A variable area flowmeter

where V is the float volume, \bar{V} is the mean flow velocity, and subscripts f and F stand for liquid and float, respectively. In this equation, C_D is the drag coefficient, which is pertinent to external flow over immersed bodies. For spherical floats, the drag coefficient is readily available as a function of the Reynolds number. For example, experimental data indicate that the drag coefficient for spheres remains practically constant at 0.5 if the Reynolds number is between 2000 to 200,000. At higher Reynolds number, the drag coefficient is even smaller. Solving the above equation for flow velocity:

$$\bar{V} = \left[\frac{1}{C_D} \frac{2gV_F}{A_F} \left(\frac{\rho_F}{\rho_f} - 1 \right) \right]^{1/2} \quad \text{VIb.3.1}$$

The volumetric flow rate can then be calculated from $\dot{V} = \bar{V}A(z)$ where $A(z) = \pi[(b + \alpha z)^2 - S^2]/4$. Although rotameters are generally made of glass or other special transparent materials, there are variable area flow meters made of metal where the reading is obtained by magnetic coupling so that the signal can be received and recorded remotely.

Elbow meter, as shown in Figure VIb.3.2(a), takes advantage of the centrifugal force applied on fluid elements when moving around a bend. The top and the bottom of the 90-degree elbow are drilled at 45 degrees for the insertion of the pressure taps. These pressure taps provide input to a differential-pressure measuring device (DP-cell), which, upon calibration, would show flow rate in the 90-degree elbow.

Laminar flowmeters, also known as viscous flowmeters, shown in Figure VIb.3.2(b), are used to measure gas flow rate based on Equation IIIb.2.3:

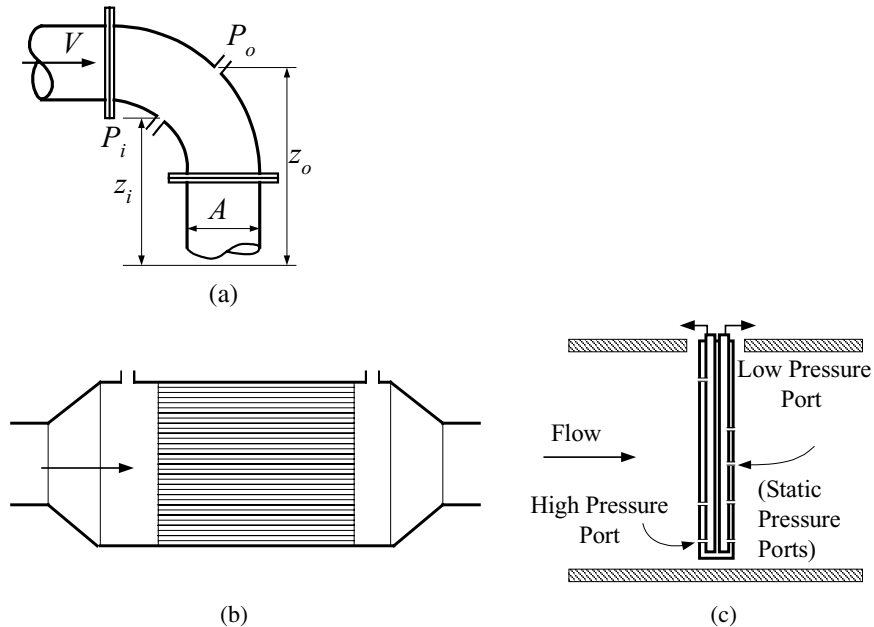


Figure VIb.3.2. (a) Elbow meter; (b) Laminar flowmeter; (c) Averaging pitot flowmeter

$$\dot{V} = \frac{\pi D^4}{128 \mu L} \Delta P \quad \text{VIb.3.2}$$

To change the flow regime from turbulent to laminar so that the viscous effects become dominant, a laminar flow element is used. The laminar flow element consists of capillary tubes with inside diameter as small as 0.01 inches (about 0.23 mm). The pressure taps for differential pressure measurement are located upstream and downstream of the laminar flow element.

Averaging Pitot device works on the basis of differential pressure. A bar that spans the pipe is inserted perpendicular to the flow. The bar may be a circular cylinder or have other profiles such as hexagonal, square, diamond, or elliptic cross section. Holes are drilled in the side facing the flow and in the downstream side of the bar, as shown in Figure VIb.3.2(c). The inputs to the pressure taps are carried to individual pressure sensors to be sent to a DP-cell. The advantage of an averaging pitot tube is its ease of installation and low impact on the flow. Underestimating the flow rate is its main disadvantage. This is because of a suction effect at the static pressure ports, due to the vortices created downstream of the probe. This is generally taken into account by a flow coefficient in calibration.

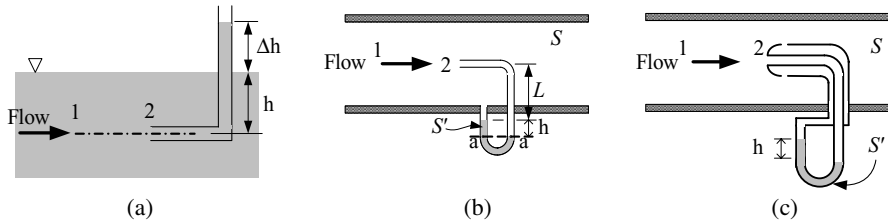


Figure VIb.3.3. (a) Simple pitot tube; (b) Differential pitot tube; (c) Pitot-static tube

It should be added that a pitot tube, invented by Henri Pitot in 1732, is itself a device for measuring flow velocity. Shown in Figure VIb.3.3(a), is a glass pitot tube in an open channel. Points 1 and 2 are on a streamline where point 2 is at the entrance to the tube, hence is at rest. Point 2 is called the *stagnation point*. Pressure at point 1 is $P_1 = \rho gh$. Pressure at point 2 is $P_2 = \rho g(h + \Delta h)$. From the Bernoulli equation between point 1 and point 2 we have; $P_1 + (\rho V_1^2/2) = P_2$. Substituting, we get $V_1 = \sqrt{2g\Delta h}$. We derived pressure at point 2 in terms of pressure at point 1 and pressure related to velocity head. Pressure at point 2 is *total* or *stagnation pressure* as it consists of static and dynamic heads of the flowing fluid. Shown in Figure VIb.3.3(b) is the differential pitot tube. If the flowing fluid has a specific gravity of S and the manometer liquid has a specific gravity of S' , a force balance at the level a-a gives:

$$P_1 + \rho_w g(LS + hS') = P_2 + \rho_w g(L + h)S \quad \text{VIb.3.3}$$

This simplifies to $P_2 - P_1 = \rho_w gS[(S'/S) - 1]h$. On the other hand, $P_1 + (\rho_w V_1^2/2) = P_2$. We find that $V_1 = V = \sqrt{2gh[(S'/S) - 1]}$. A more compact system is the pitot-static tube as shown in Figure VIb.3.3(c). For this case, similar expression can be derived.

3.2. Volume Measuring Flowmeters

Turbine flowmeter, Figure VIb.3.4(a), and its various forms have been in use for flow measurement for centuries. The turbine meter consists of a shaft equipped

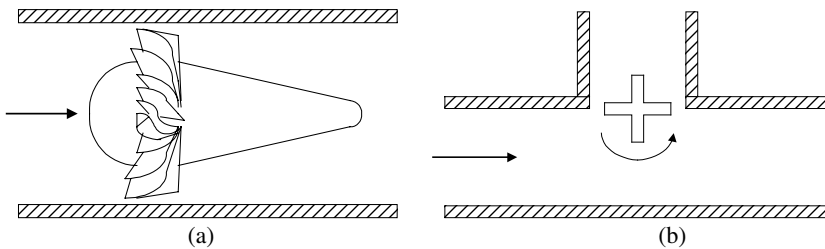


Figure VIb.3.4. (a) Turbine meter and (b) Paddle wheel

with blades and located centrally against the flow. The shaft and the blades are designed to minimize the adverse effect on the flow. The flow of fluid through the blades imparts momentum, causing rotation of the blade, which, in a magnetic field, produces current proportional to the flow volume passing over the shaft. In the absence of friction, this proportionality would have been a linear function. However, various frictional forces result in non-linearity. These forces include bearing friction, drag on the rotor and the blades, and friction due to the electromagnetic effects. Like the turbine meter, there are similar flowmeters, which work on the transfer of momentum from the flow to a turning wheel. These are paddle wheel or vane-type and the Pelton-wheel flowmeter, Figure VIb.3.4(b).

Vortex meter is a relatively new concept in flow measurement as the idea was introduced in the mid 1950s. The device became available in the mid 1970s. In a vortex meter, a bluff body is placed in the flow field to cause some flow separations downstream of the bluff body, Figure VIb.3.5(a). As flow increases, so does the rate of flow separation to a point that the separated flow is rolled back in the low-pressure area developed behind the bluff body. This backward curl is called a vortex. As the flow rate is increased, these vortices grow in size and begin to travel downstream to form a so-called *vortex street*. The notable feature of such vortex-shedding instruments is that the vortices are formed and depart in alternate manner from each side of the bluff body. This causes an alternating pressure gradient across the body. The frequency of vortex generation and pressure oscillations is proportional to flow rate.

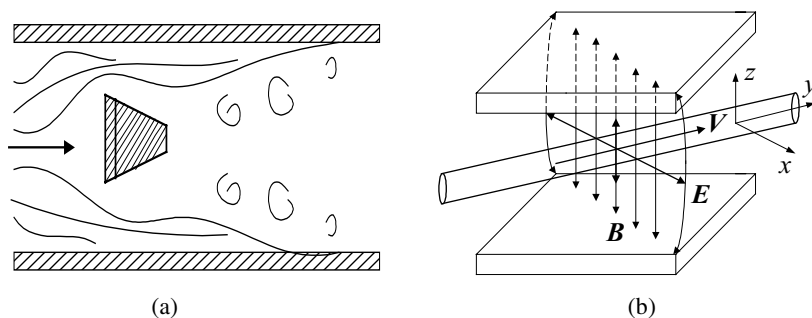


Figure VIb.3.5. (a) Schematics of Vortex flowmeter (b) Electromagnetic flowmeter

Electromagnetic flowmeter works on the basis of Michael Faraday's law of electromagnetic induction. As shown in Figure VIb.3.5(b), a magnetic field is created in the coil surrounding the pipe carrying a conducting liquid. The magnetic field may be created by an alternating current. The pipe carrying the conducting liquid is made of nonmagnetic material to allow penetration of a magnetic field. We now envision molecules of the conduction liquid on a line parallel to the vector E . Since these lines are moving with flow velocity V inside the coil, they cut through the magnetic lines, which, in turn, induce electrical current in these lines of fluid. Electrodes attached to both sides of the pipe pick these electric signals and transfer them to a signal processor. The flow of fluid is proportional with

the generated signals. Major advantages of this flowmeter are lack of moving parts and that it is noninvasive, resulting in no pressure loss. The major disadvantage is the limitation to electrically conducting liquids. It is not suited for such non-conducting fluids as hydrocarbons, hence is not widely used in petroleum industry.

Ultrasonic flowmeter, as shown in Figure VI3.6(a), is based on the travel time of acoustic waves in a flow field. Some clarification is needed regarding the term ultrasonic. Some flowmeters, such as a vortex-shedding meter, use ultrasonic sensing in their data acquisition systems. Ultrasonic flowmeters are of two types: ultrasonic doppler meter and ultrasonic transit-time meter. The ultrasonic transit time meter works on the basis that sound waves in the flow direction travel at a speed faster by $2V$ compared with the sound waves travelling against the flow. The time it takes for the wave to travel from the transmitter to the receiver is $t_1 = L/(c + V\cos\alpha)$. Similarly, the time it takes for the wave to travel from the receiver back to the transmitter is $t_2 = L/(c - V\cos\alpha)$. This results in:

$$\Delta t = \frac{2LV \cos \alpha}{c^2 - V^2 \cos^2 \alpha} \cong \frac{2LV \cos \alpha}{c} \quad \text{VIb.3.4}$$

indicating that the measured time is linearly proportional with the measured flow velocity. Note that V is the flow velocity and c the speed of sound in the fluid. The transit-time meter is by far more accurate than a Doppler meter, Figure VIb.3.6(b). The latter works on the basis of the Doppler frequency shift. This occurs when sound waves are reflected from an impurity in the fluid. If sound waves are reflected from stationary objects, there is no change in their wave characteristics wavelength and frequency. However, upon reflection from a moving target, there will be a shift in the wave characteristics hence the wave would have new amplitude, period, and frequency. The flow velocity by Doppler flowmeter is found from $V = c\Delta f/(2f\cos\alpha)$ where f is the transmission frequency and Δf is the doppler shift in frequency. Generally noninvasive flowmeters have the advantage of no moving parts, no induced pressure drop, no need for integration in the piping system, ease of use, capability to be bi-directional, and associated cost savings.

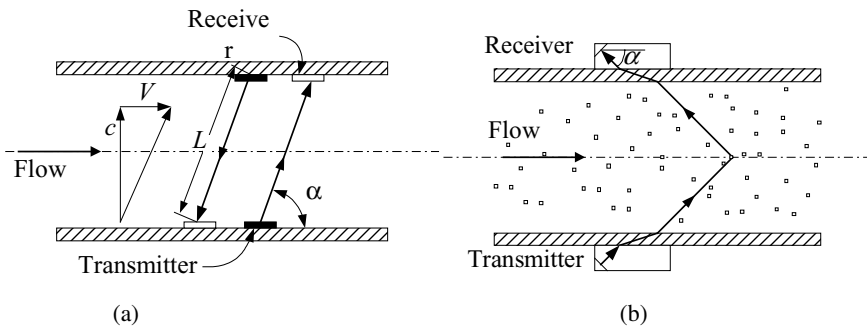


Figure VIb.3.6. (a) Ultrasonic Transit-Time flowmeter and (b) Ultrasonic Doppler flowmeter

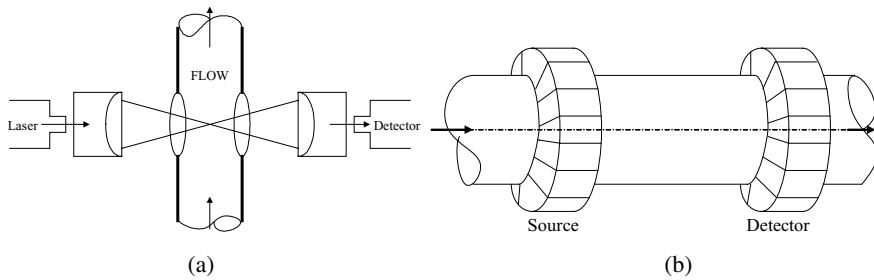


Figure VIb.3.7. Schematics of (a) Laser Doppler flowmeter; (b) Pulsed Neutron Activation Flowmeter

Laser Doppler anemometer or LDA is also used to measure flow rate using the concept of doppler shift. In this method a laser - a coherent monochromatic light beam - passes through the fluid flow and is highly focused in an LDA. Solid particles, in the order of 25 microns in the fluid will scatter the light beam. The scattered light would have a different frequency than the incident light. This is the Doppler shift. A photo multiplier device receives the scattered beam to electronically sense the change in frequency with respect to a reference (non-scattered) beam. Shown in Figure VIb.3.7(a) is a dual-beam LDA with α being the angle between the incident rays. If l is the frequency of the incident ray, the flow velocity is then given by $V = \lambda \Delta f / [2 \sin(\alpha/2)]$. The disadvantage of this method is the fact that it requires a glass window for light to pass through.

Pulsed neutron activation or PNA is another non-invasive means of measuring flow rate and is included in the class of radioisotope tracer technique. As shown in Figure VIb.3.7(b), an energetic neutron source is used to induce radioactivity into the flow field. The field velocity is determined by detecting the γ -ray emitted from the irradiated liquid, in a detector located downstream of the neutron source. There are disadvantages associated with this method. PNA uses high-energy neutrons. For example, for the $O^{16}(n, p)N^{16}$ reaction, which has a half-life of 7.14 seconds, the neutron activation threshold is 10.24 MeV. Such high levels of energy require extensive shielding. Additionally, the neutron source and the detector should be circumferentially distributed to minimize radiation bias. Indeed radiation bias occurring due to beam attenuation is another drawback of this method.

Elbow meter is another means of measuring volumetric flow rate, using the change of flow momentum and the associated centrifugal force. Lansford correlated the resulting differential pressure to volumetric flow rate to obtain a formula similar to Equation IIb.4.3:

$$\dot{V} = CA \sqrt{2g \left\{ [(P_o - P_i) / \rho g] + (z_o - z_i) \right\}} \quad \text{VIb.3.5}$$

where, in this relation, value of C ranges from 0.56 - 0.88 depending on the size and shape of the elbow.

Positive Displacement (PD) is the most widely used flowmeter for flow measurement of liquid and gas for industrial, commercial and residential applications. A recent survey indicates that the worldwide sale of the positive displacement flowmeters constituted half of all the flowmeters sold in 2001. Thus more PD flowmeters are sold than all other types, such as Ultrasonic, Electromagnetic, ΔP meter, Vortex meter and mass measuring flowmeters combined (Control magazine). The PD flowmeters are of various types. All function on the same principle of measuring a known volume of the fluid in a distinct compartment that is accurately measured by the manufacturer. The number of these measurements (i.e. the number of times these compartments are filled and emptied per unit time) would determine the flow rate. The PD flowmeters are suitable for viscous fluids (such as oil, paint, varnish, and cosmetics), for low flow rates (as low as about 2 liter/m), and for corrosive products.

3.3. Mass Measuring Flowmeters

There is no need to measure density in these flowmeters, as mass flow rate is directly measured. Several such instruments are discussed below.

Coriolis flowmeters are used in the flow measurement of liquids, suspensions, emulsions, and gases. The coriolis flowmeter is named after the French mathematician Gustave Coriolis who in 1835 showed that an inertial force must be taken into account when describing the motion of bodies in non-inertial frames. The

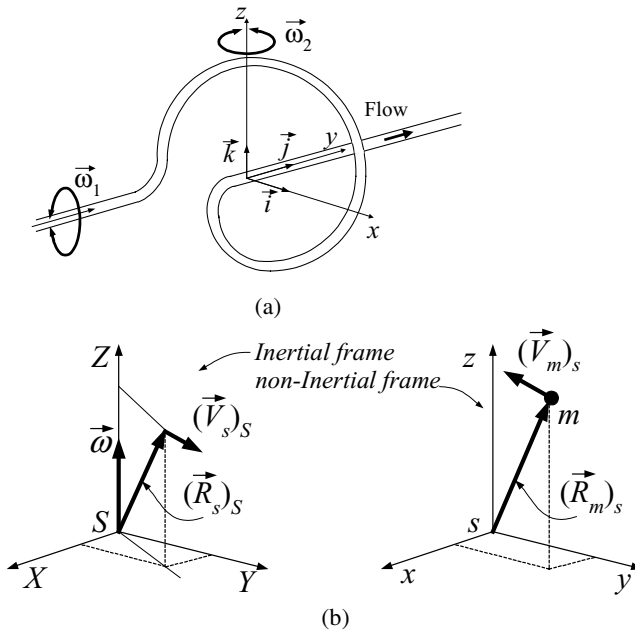


Figure Vlb.3.8. (a) A Coriolis flowmeter; (b) Depiction of an inertial and a non-inertial frame

coriolis flowmeter is an instrument consisting of a twisted tube resting on two flexible couplings. Figure VIb.3.8(a) shows the tube being alternatively rotated by a motor along the y -axis with an angular velocity of $\vec{\omega}_1 = \omega_1 \vec{j}$. Vibration of the tube coupled with the flow of fluid induces acceleration, causing the Coriolis force to deflect the tube ($\vec{\omega}_2 = \omega_2 \vec{k}$). Tube deflection is accurately measured. Since the applied rotation to the tube is known, the induced rotation can be used to find mass flow rate. To show the relation between the tube deflection and mass flow rate, let's consider mass m moving at a velocity V with respect to frame s ($(V_m)_s$). In general, frame s is a non-inertial frame, having its own linear velocity $(V_s)_S$ and angular velocity ($\vec{\omega}$) with respect to an inertial frame S . Vectors in frame s can be expressed in frame S using the following mathematical operator:

$$\left(\frac{d}{dt} \right)_s = \left(\frac{d}{dt} \right)_S + \vec{\omega} \times \quad \text{VIb.3.6}$$

Having the position vector $(\vec{R}_m)_s$ and velocity $(\vec{V}_m)_s$ of mass m in frame s , velocity of mass m in frame S (i.e., $(\vec{V}_m)_S$) is found by applying the operator given by Equation VIb.3.6 to the position vector of mass m :

$$(\vec{V}_m)_S = \frac{d(\vec{R}_m)_s}{dt} = \frac{d}{dt} [(\vec{R}_s)_S + (\vec{R}_m)_s] + \vec{\omega} \times (\vec{R}_m)_s$$

which simplifies to $(\vec{V}_m)_S = (\vec{V}_s)_S + (\vec{V}_m)_s + \vec{\omega} \times (\vec{R}_m)_s$. Similarly, the acceleration of mass m in frame S is:

$$(\vec{a}_m)_S = \left(\frac{d(\vec{V}_m)_S}{dt} \right)_S = \left[\left(\frac{d}{dt} \right)_S + \vec{\omega} \times \right] [(\vec{V}_s)_S + (\vec{V}_m)_s + \vec{\omega} \times (\vec{R}_m)_s] \quad \text{VIb.3.7}$$

carrying out an operation on each of the three terms of the right-hand side bracket in Equation VIb.3.7, we find:

$$(\vec{a}_m)_S = \frac{d}{dt} [(\vec{V}_s)_S + (\vec{V}_m)_s + \vec{\omega} \times (\vec{R}_m)_s] + \vec{\omega} \times [(\vec{V}_s)_S + (\vec{V}_m)_s + \vec{\omega} \times (\vec{R}_m)_s] \quad \text{VIb.3.8}$$

taking the derivative of the terms in the first bracket and performing multiplication in the second bracket yields:

$$(\vec{a}_m)_S = \left[\frac{d(\vec{V}_s)_S}{dt} + \frac{d(\vec{V}_m)_s}{dt} + \vec{\omega} \frac{d(\vec{R}_m)_s}{dt} + \frac{d\vec{\omega}}{dt} \times (\vec{R}_m)_s \right] + \left[\vec{\omega} \times (\vec{V}_s)_S + \vec{\omega} \times (\vec{V}_m)_s \right] + \vec{\omega} \times \left[\vec{\omega} \times (\vec{R}_m)_s \right]$$

Finally;

$$(\bar{a}_m)_s = (\bar{a}_s)_s + (\bar{a}_m)_s + 2\bar{\omega} \times (\bar{V}_m)_s + \frac{d\bar{\omega}}{dt} \times (\bar{R}_m)_s + \bar{\omega} \times \bar{\omega} \times (\bar{R}_m)_s$$

Newton's second law of motion applies to the absolute acceleration; $\Sigma \bar{F} = m(\bar{a}_m)_s$. Alternatively:

$$\Sigma \bar{F} = m \left[(\bar{a}_s)_s + (\bar{a}_m)_s + 2\bar{\omega} \times (\bar{V}_m)_s + \frac{d\bar{\omega}}{dt} \times (\bar{R}_m)_s + \bar{\omega} \times \bar{\omega} \times (\bar{R}_m)_s \right]$$

VIb.3.9

where;

$m(\bar{a}_s)_s :$	Force due to frame s acceleration
$m(\bar{a}_m)_s :$	Force due to local acceleration
$m[2\bar{\omega} \times (\bar{V}_m)_s] :$	Force due to Coriolis acceleration
$m \left[\frac{d\bar{\omega}}{dt} \times (\bar{R}_m)_s \right] :$	Force due to angular acceleration
$m[\bar{\omega} \times \bar{\omega} \times (\bar{R}_m)_s] :$	Force due to centripetal acceleration

Thermal mass flowmeters may be used for both liquids and gases to measure mass flow rate. For gases, a resistance heater is wrapped around a thin-wall pipe. Fluid temperatures upstream and downstream of the heater are measured. Having the rate of heat transferred to the fluid and the temperature difference, flow rate of the fluid is then calculated. For liquids, the instrument consists of a U-tube. A heat sink in addition to a heat source is used to bring the liquid temperature down to the inlet temperature at the exit. The obvious error is associated with axial heat transfer in the pipe wall.

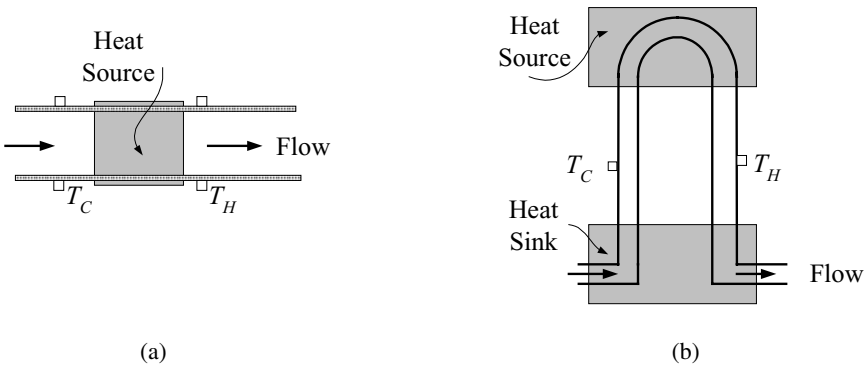


Figure VIb.3.9. Schematics of a thermal mass flow meter for (a) gas; (b) liquid

4. Flowmeter Installation

Since the majority of flow meters measure the average flow velocity and require fully developed flow, such meters should be installed in a way that ensures a symmetric and undisturbed velocity profile through the instrument (Figure VIb.4.1). Flow disturbance is primarily caused by valves and fittings in a piping system.

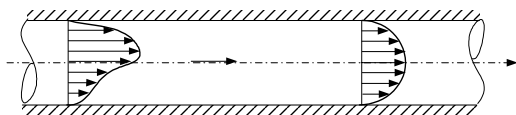


Figure VIb.4.1. Comparison of disturbed and unperturbed velocity profiles

Therefore, flow meter manufacturers require a minimum length of straight pipe to be considered upstream and downstream of the instrument. For example, the required lengths of straight pipe for a vortex meter for various fittings are shown in Figure VIb.4.2. When space is at a premium and the recommended straight pipe length cannot be accommodated, various flow straighteners, as shown in Figure VIb.4.3 are used to enforce a symmetric profile. This, however, is achieved at the cost of higher induced pressure drop.

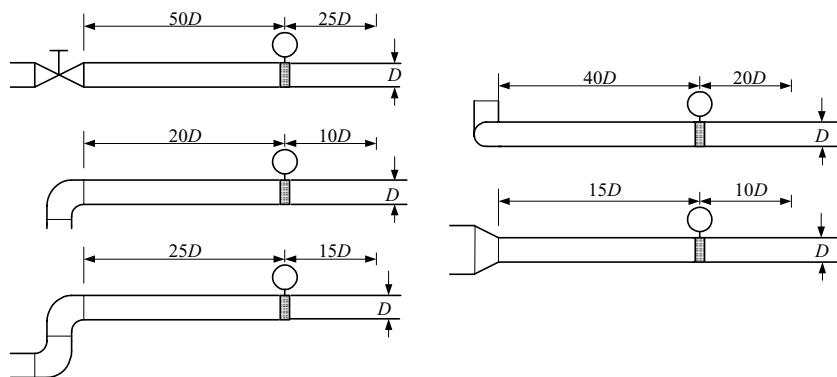


Figure VIb.4.2. Required straight pipe length upstream and downstream of a vortex meter

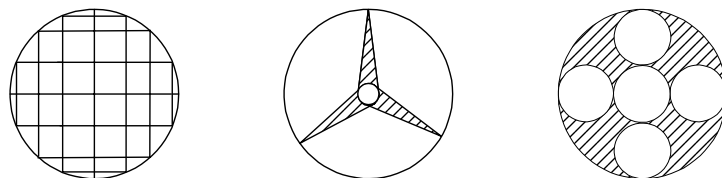


Figure VIb.4.3. Various flow straightener designs

QUESTIONS

- What is the difference between fixed errors and random errors?
- If an experiment has high degree of repeatability are the results necessarily highly accurate?
- List 5 types of noninvasive flowmeters.
- List 5 advantages associated with non-invasive flowmeters.
- Why are flow straighteners used? What is the major component of a laminar flowmeter?
- How does a positive displacement flowmeter measure flow?
- What type of flowmeter should be used when fluid flows at a low velocity?
- Why is a rotameter tube tapered?
- What are the advantages of the mass flowmeter?
- How do we measure the flow rate of slurry?
- What are the advantages of the electromagnetic flowmeter?
- What is the principle upon which a vortex flowmeter operates?
- What is the major drawback of the pulsed neutron activation flowmeter?

PROBLEMS

1. Two electric resistors are connected in series, thus $R = R_1 + R_2$. Find the uncertainty in power dissipated in these resistors noting that $E = RI$ where I is the electric current passing through each resistor.
Data: $R_1 = 0.005 \pm 0.25\%$, $R_2 = 0.008 \pm 0.20\%$, and $I = 150 \pm 1$ A.

2. The mass flow rate from a Bernoulli obstruction meter is given as:

$$\dot{m} = CA\sqrt{2P_1\Delta P/(RT_1)}$$

Find the percent uncertainty in the mass flow rate for the following data:

$C = 0.9 \pm 0.0075$, $P_1 = 30$ psia ± 0.8 psia, $T_1 = 85$ F ± 1 F, $\Delta P = 1.5$ psi ± 0.0035 psi, $A = 1.5$ in² ± 0.001 in²

3. In a shell & tube heat exchanger, total rate of heat transfer between the shell-side and the tube-side is given as $\dot{Q} = UA\Delta T$. Find the uncertainty percent in total rate of heat transfer using the following data:
 $U = 500$ Btu/ft²·h ± 5 Btu/ft²·h, $A = 1000$ ft² ± 2.5 ft², $\Delta T = 75$ F ± 2 F.

4. In the measurement of the water mass flow rate in a pipe, the following data are obtained: $A = 100$ cm² $\pm 0.5\%$, $\rho = 950 \pm 5$ kg/m³, and $V = 6$ m/s $\pm 7\%$. Using Equation VIb.2.1, show that the uncertainty in mass flow rate is dominated by the uncertainty in the velocity measurement. What conclusion can then be made from attempts in reducing the uncertainties in area and density measurement?

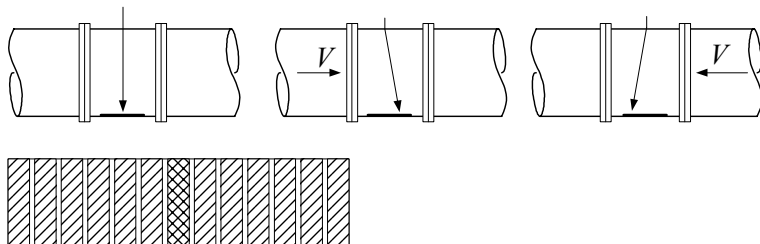
5. A variable area flowmeter (rotameter) is used to find the flow rate of water at room temperature. The rotameter is 18 inches long with the smallest and largest diameters of 1.75 and 4 inches, respectively. The floater is a stainless steel ball,

2 inches in diameter. Find the volumetric flow rate when the floater mid-plane is at 1 foot from the entrance to the meter. [Ans.: 27 GPM].

6. Apply the Bernoulli equation and the equation of state for an ideal gas to derive a relation similar to Equation IIIb.1.8 for velocity of compressible fluids flowing in the pipe.

$$(\text{Ans.: } V = \sqrt{2c_p T_1 \left[(P_2 / P_1)^{(k-1)/k} - 1 \right]}).$$

7. Suppose we want to use a small probe equipped with a camera at the end of the probe to measure the flow of a liquid. The probe is inserted in a pipe perpendicular to the flow. Attached to the wall opposite to the probe is a light sensitive patch consisted of solar cells, shown as cross-hatched regions in the figure. When inserted in the pipe, the probe behaves as a cantilever, bending in the direction of the flow. The device (i.e., the probe and the patch) is calibrated so that activation of each strip (i.e., solar cell) is associated with a certain flow rate. Comment on applicability, advantages, and disadvantages associated with the use of this flow-meter design.



8. Consider the pitot tube of Figure VIb.3.3-b. Gas is flowing over the tube at 40 C and 1 atm. The dynamic pressure is measured as 2 in-H₂O. Find the flow velocity. (Ans.: 29.7 m/s).

9. A hot-wire anemometer is a heated electric resistance placed in the pipe carrying the flow. King showed that the rate of heat transfer is proportional to the flow velocity as:

$$\dot{Q} = (a + bV^{0.5})(T_{\text{wire}} - T_f)$$

where constants a and b are determined from a calibration of the anemometer. The rate of heat transfer is also given by the electric power consumed to heat up the resistance:

$$\dot{Q} = R_{\text{wire}} I^2 = R_o [1 + \alpha(T_{\text{wire}} - T_o)] I^2$$

where I is the electric current, α is the temperature coefficient of resistance, and R_o is the wire resistance at temperature T_o . Obtain flow velocity as a function of the electric current.

Vlc. Fundamentals of Turbomachines

Turbomachines are mechanical devices that exchange momentum and energy with a fluid. Machines in which energy is transferred to the fluid are called pumps, compressors, blowers, and fans depending on the type of the fluid and pressurization. In turbines, transfer of energy is from the fluid to the rotating shaft. Such machines, depending on the type of working fluid, are called hydraulic turbine, steam turbine, or gas turbine. If a turbomachine contains a blade or vane, momentum is exchanged with a fluid by changing the direction and the velocity of the flow. The rate of change of fluid momentum results in a force that leads to transfer of work due to fluid displacement. Next, some fundamental terms are defined which help in the discussion of turbomachine operation.

1. Definition of Turbomachine Terms

Dimensional analysis is a third technique to analyze a flow field with the first and second techniques being the integral and differential methods that were discussed in Chapter IIIa. Dimensional analysis, being a means of reducing the number of variables that affect a physical phenomenon, is based on the identification of the pertinent *dimensionless groups*. In this chapter we make extensive use of dimensionless groups.

Scaling laws are a direct result of using the dimensional analysis technique. Scaling laws allow us to extrapolate the results of the study regarding the effects of fluid flow on a *model* to the *prototype*. When the scaling law is valid, it is said that a condition for *similarity* between model and prototype exists.

Velocity vector diagram refers to fluid velocity vector in the impeller of pumps or turbines. Figure Vlc.1.1. shows the velocity vector diagrams for a pump impeller rotating clockwise and for a centrifugal compressor rotating counter-clockwise. The fluid absolute velocity, whether at the blade inlet or outlet, has two components. One component is always perpendicular to the position vector

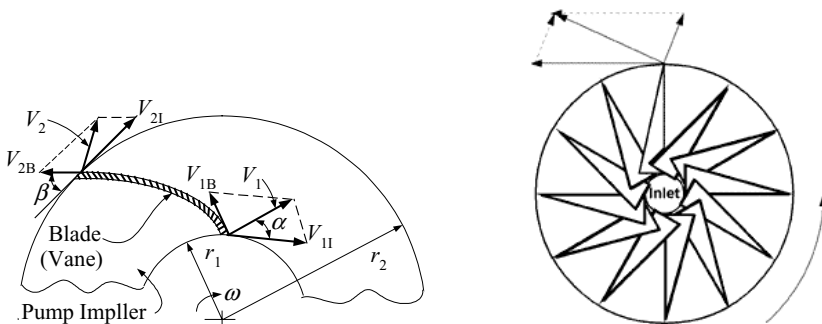


Figure Vlc.1.1. Velocity vector diagrams of impellers of a pump and a compressor

hence, tangent to the impeller (V_I) and another component tangent to the blade (V_B). The component tangent to the impeller is the peripheral speed of the impeller at that location ($r\omega$). The velocity component tangent to the blade is fluid velocity relative to the blade. The geometric similarity between the two systems requires that angle α , referred to here as the velocity angle, and angle β , known as the blade angle, are equal in both systems.

Homologous systems are any two systems that are geometrically similar and have a similar velocity vector diagram. For example, if a given pump (say pump A) is to be homologous with another pump (say pump B), the geometrical symmetry requires that $\alpha_A = \alpha_B$ and $\beta_A = \beta_B$. For angle α to be constant, it requires that $\dot{V} / \omega D^3 = \text{constant}$.

Dimensionless groups are generated by identifying pertinent parameters in the operation of turbomachines. For example, there are three groups containing pertinent pump parameters. Group one contains pump performance consisting of flow rate and pressure rise (\dot{V} , ΔP). Group two contains pump geometry data given by the impeller diameter, speed, and roughness (D , ω , ε). Group three contains fluid properties, the most pertinent being density and viscosity (ρ , μ). According to the *Buckingham Pi theorem*, the number of dimensionless groups between N independent variables is equal to $N - N'$ where N' is equal to the number of primary dimensions, such as Mass, Length, and Time (m , L , t).

Pump performance curve is a term applied to the head delivered by the pump versus the flow rate. A more comprehensive pump performance curve, discussed later in this chapter, includes head versus flow curves for a given rotor speed and various rotor sizes. The pump performance curve is constructed by the pump manufacturer from a wide range of data and generally includes plots of pump efficiency.

Classification of pumps. There are many types of pumps in various shapes and forms for different industrial, residential, and medical applications. Hence, pumps may be classified in various ways. Here we classify pumps based on the means of momentum transfer to the working fluid. This classification results in only two types of pumps, positive displacement and dynamic.

Positive displacement pumps are devices delivering fluid that, in each cycle, fills a known volume or closed compartment of the pump. This type of pump delivers periodic or pulsating flow. The means of delivering varies depending on a specific design. For example, fluid delivery may take place by the action of sliding vanes, rotating gears and screws, or moving plungers and pistons. Schematic of a piston-cylinder positive displacement pump is shown in Figure VIc.2.1.

Dynamic pumps basically deliver momentum to the fluid through the rotation of vanes or impellers. The momentum is converted to pressure head as the liquid passes through the pump diffuser. Dynamic pumps may in turn be divided into two major categories; rotary and special applications.

Dynamic pumps for special applications include such pumps as electromagnetic pumps for the delivery of liquid metals such as sodium and mercury, jet pumps for mixing two streams of fluids, and fluid actuated pumps. The electromagnetic pumps are of either direct-current (also known as the dc-Faraday pumps) or of the alternating-current type. The electromagnetic pumps operate on the same principle as electromagnetic flowmeters.

Dynamic rotary pumps are also referred to as *rotodynamic* pumps. They consist of radial, mixed, and axial flow designs. The design refers to the flow inside the pump. The rotor of the radial flow pump is generally referred to as an impeller and the rotor of the axial flow pump as a propeller. The impeller of the radial flow pumps, consists of vanes and the propeller of the axial flow pump consists of blades. In the radial flow pump, flow enters the inlet of the pump impeller and primarily flows in the radial direction until exiting the impeller. In the axial flow pumps, flow direction is along the axis of the pump propeller. The most widely used dynamic pump is the centrifugal pump.

2. Centrifugal Pumps

We begin the introduction of the centrifugal pump by comparing its characteristic curve with that of a positive displacement pump. As shown in Figure V1c.2.1, positive displacement pumps deliver nearly constant flow at a wide range of pressure while rotodynamic pumps deliver nearly constant pressure at a range of flow rate. Rotodynamic pumps provide high rate of flow rates (as high as 700 ft³/s) but with rather low head (in the range of 100 psi). On the other hand, positive displacement pumps supply high head (up to 3000 psia) but rather low flow rate (in the range of 2 ft³). For example, a typical PWR plant uses positive displacement pumps, each delivering about 45 GPM (3.5 lit/s) at 2250 psia (15.5 MPa).

To investigate the design and operation of rotodynamic pumps we consider centrifugal pumps as shown in Figure V1c.2.2. A centrifugal pump is a mechanical device, combining centrifugal force with mechanical impulse to produce an increase in pressure. In such pumps, kinetic energy is produced by the action of centrifugal force and then the energy is partially converted to pressure by efficiently reducing its velocity. Centrifugal pumps consist of rotating and stationary

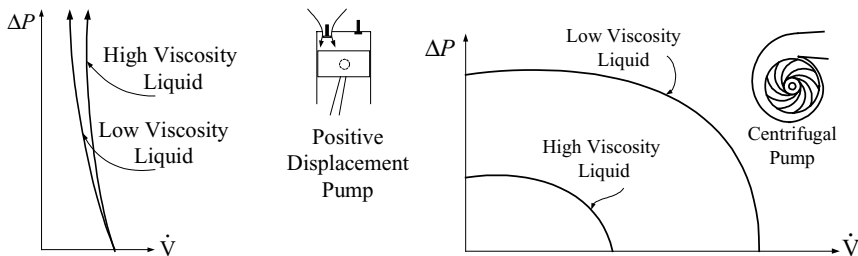


Figure V1c.2.1. Characteristic curve comparison of positive displacement and rotodynamic pumps (White)

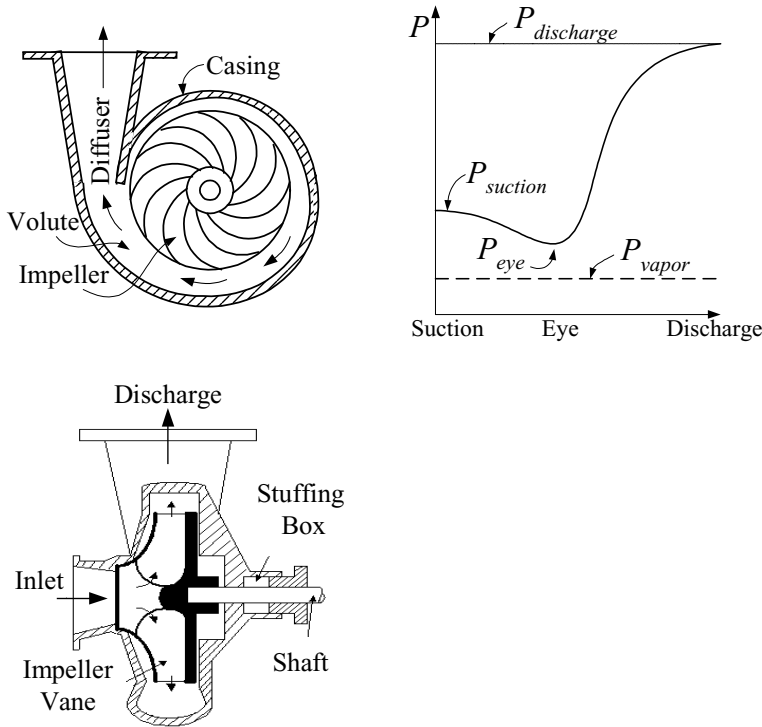


Figure VIc.2.2. Cross-section of a single-stage centrifugal pump

parts. Rotating parts include the impeller, mounted on a shaft, which, in turn, rests in the pump bearings. The impeller contains blades or vanes. Liquid enters the pump through the central hole or *eye* of the impeller, at the inlet to the blades. Stationary parts include the casing and the diffuser. Some casings are equipped with stationary blades acting as a diffuser. Note that we must have the liquid pressure at the eye of the pump greater than the liquid vapor pressure as described in Section 1.4 of Chapter IIa and Section 2.1 of this chapter.

Generally, casings have spiral shape, referred to as a volute, to change the liquid velocity to pressure head at the discharge. The casing may be solid with an opening in one side to access the impeller or may be split either axially or radially. In the latter case, bolts are used to fasten the two parts of the casing together.

Power to rotate the pump shaft is provided by the pump driver also referred to as the *prime mover*, which may be a reciprocal engine, a steam turbine, or an electrical motor. A pump coupling provides connection between the two units. Pressurized liquid in the pump has the tendency to leak at the shaft access through the casing. This is prevented by a pump seal, which also prevents air leakage into the pump in the case of a suction lift when pressure drops below atmospheric. The pump seal generally consists of a series of packing rings, the housing of which is

referred to as the *stuffing box*. Pumps may also use mechanical seals as are used in reactor coolant pumps. In such cases, the mechanical seals are cooled by the plant component cooling system. Seal cooling is required due to the high pumping power of such pumps (about 5 MW per pump for a typical 1000 MWe PWR).

2.1. Definition of Terms for Centrifugal Pumps

In the definitions below, reference is made to Figure IIb.4.1, but subscript i is used for suction- and e for discharge-side.

Useful work of a pump is defined as the product of two terms. The first term is the rate at which fluid passes through the pump. The second term is the height of a column of fluid equivalent, under adiabatic conditions, to the total pressure differential measured immediately before entering and right after leaving the pump. The first term is referred to as *capacity*, *discharge*, *volumetric flow rate*, *flow rate*, or simply *flow*. The second term is referred to as *pump pressure head*.

Velocity head is the vertical distance a body would have to fall to acquire the velocity V , $h_v = \frac{V^2}{2g}$.

Static suction head is the absolute pressure at the free level (Z_i) of the suction reservoir in feet of liquid plus the vertical distance from the pump centerline to this level. This definition applies only if $Z_i > Z_p$:

$$h_{ss} = \frac{P_i}{\rho g} + (Z_i - Z_p)$$

If $Z_i < Z_p$, the term is referred to as the static-suction lift.

Static discharge head is the absolute pressure at the pump discharge plus the elevation head with respect to the pump centerline:

$$h_{sd} = \frac{P_e}{\rho g} + (Z_e - Z_p)$$

Total static head is the difference between the static discharge and the static suction head.

$$h_{sd} = \frac{P_e - P_i}{\rho g} + (Z_e - Z_i)$$

Total dynamic suction head is the static suction plus the velocity head minus the suction friction head.

$$h_s = \left(\frac{P_i}{\rho g} + \frac{V_i^2}{2g} + Z_i - Z_p \right) - h_{sf}$$

Total dynamic discharge head is the static discharge head plus the velocity head plus the discharge friction head.

$$h_d = \left(\frac{P_e}{\rho g} + \frac{V_e^2}{2g} + Z_e - Z_p \right) + h_{df}$$

Total dynamic head is the difference between total dynamic discharge and total dynamic suction head:

$$H = \left(\frac{P_e}{\rho g} + \frac{V_e^2}{2g} + Z_e \right) - \left(\frac{P_i}{\rho g} + \frac{V_i^2}{2g} + Z_i \right) + h_f = h_s$$

where $h_f = h_{df} + h_{sf}$

Vapor pressure of a liquid is the absolute pressure at which liquid vaporizes and is in equilibrium with its vapor phase. If the liquid pressure drops below the vapor pressure, the liquid boils. If liquid pressure is greater than the vapor pressure, then the liquid vaporizes at the interface between the two phases. The vapor pressure of water at 80 F (27 C), for example, is $P_v = 0.50683$ psia (3.5 kPa). Similar definition is given in Section IIa.1.4. If pressure at the eye of the pump drops below the vapor pressure then the pump begins to cavitate.

Cavitation is the major cause of damage to pumps and valves where liquid experiences a large and sudden pressure drop. Cavitation is defined as formation, via vaporization, and subsequent collapse, via condensation, of vapor bubbles in a liquid. A pressure drop to or below the liquid vapor pressure coupled with existing nuclei (tiny voids containing vapor or gas) results in liquid vaporization. These voids appear as tiny bubbles that will grow if the surrounding pressure remains at or below the vapor pressure of the liquid or they will collapse at higher pressures. Pressure drop occurs at such locations as tip of a propeller, edges of a thin-plate orifice, or seats of a valve. These unrecoverable pressure losses in these places are associated with dissipation of energy, which constitutes the loss coefficient of valves and fittings. Collapse of bubbles in higher-pressure regions is associated with rapid pressure fluctuations that will eventually result in erosion and pitting of the hydraulic structure.

There are various means of preventing cavitation, primarily depending on the type of the hydraulic system. Prevention of cavitation in a pump is discussed in Section 3. In some hydraulics systems, it may be possible to introduce a gradual pressure drop to the flow. Cavitation control valves may use a tortuous flow path, cascaded orifices, or a combination of both to cause high velocity hence, large local frictional losses. Another means of preventing material erosion due to cavitation is to use erosion resistant materials at locations prone to cavitation, such as the use of stainless steel for a turbine blade, valve seat, or pump impeller. As shown in Figure VIc.2.2, during operation we must ensure that $P_{eye} > P_{vapor}$.

Best efficiency point (BEP) is an operation mode at which the pump efficiency is a maximum. While pumps should be operated at their BEP, it is especially im-

portant for pumps that operate with liquids with abrasive contents. At the BEP, the angle at which the impeller and the liquid meet is optimized, helping to reduce impingement and minimize erosion. In this chapter, the pump parameters at BEP are shown with subscript “o”.

Net positive suction head as required by the pump is usually given for the best efficiency point by the pump manufacturer. The available net positive suction head ($NPSH_A$) defined as $P_i + (V_i^2/2) - P_v$ is obtained from:

$$NPSH_A = \frac{P_i}{\rho g} - (Z_P - Z_i) - \frac{P_v}{\rho g} - h_{fs} \quad \text{VIc.2.1}$$

where point i is on the surface of the source reservoir and point P is at the pump inlet. However, for large pumps, point P should be taken at the top of the impeller. Pressure at the source reservoir is P_i . If the reservoir is open to atmosphere then $P_i = P_{atm}$. In Equation VIc.2.1, P_v shows the vapor pressure of the liquid at operating temperature. For example, water vapor pressure at $P = 14.7$ psia and $T = 80$ F is about $P_v = 0.5$ psia. Finally, h_{fs} represents frictional head loss in the suction piping and is found from Equation IIIb.3.12 with $L = s + \delta$ as depicted in Figure VIc.1.1 where h_{fi} is friction head loss between the suction-side reservoir and pump inlet and P_v is the working liquid saturation pressure at operating temperature.

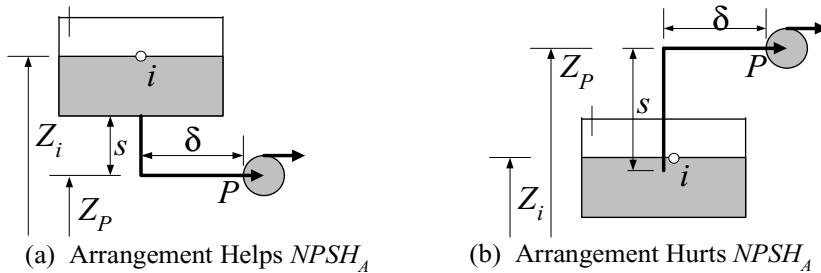


Figure VIc.1.1. Two arrangements for pump suction (P_i is maintained throughout the pumping process)

Shutoff head is the maximum head a pump develops corresponding to the minimum flow rate.

Runaway speed is the speed a centrifugal pump would reach when the pump impeller runs in the reverse direction. This occurs upon failure of the discharge valve to close when a running pump is stopped under a high static head.

Design pressure is the maximum pressure the pump casing can be exposed to before being structurally damaged.

Rated conditions are the values of pump head and pump flow rate corresponding to maximum pump efficiency. For all practical purposes, pumps should be operated at the BEP. However, we recognize that deviations will occur from

pump conditions during operations primarily variations in demand for flow rate. The more the operating conditions deviate from the BEP, the more a pump would be subject to degradation in performance and long-term deterioration of its components.

Hydraulic horsepower is the power transferred to the fluid to deliver a flow rate of \dot{V} at a total dynamic head of H . To calculate the pumping power, we use $\dot{W}_{HYD} = FV = (\Delta PA)(\dot{V}/A) = \rho g H \dot{V} = \dot{m} g H$.

Brake horsepower is the power delivered by the prime mover to drive the pump ($\dot{W}_{BHP} = \omega T$), where ω is the shaft angular velocity (radian/s) and T is the shaft torque delivered by the prime mover.

Pump efficiency is the ratio of hydraulic horsepower to brake horsepower,

$$\eta = \frac{\dot{W}_{HYD}}{\omega T} = \eta_v \eta_h \eta_m.$$

Substituting values, efficiency can be found from $\eta = \rho g h \dot{V} / (2\pi NT)$ where head is in ft, flow rate in GPM, torque in ft-lbf, and impeller speed in rpm.

Volumetric efficiency, as a component of pump efficiency, is defined as $\eta_v = \dot{V} / (\dot{V} + \dot{V}_L)$ where \dot{V}_L is the leakage flow rate to the casing from the impeller-casing clearance.

Hydraulic efficiency is defined by three types of losses occurring in the pump. The first type is the *shock* loss at the impeller inlet (eye) due to imperfect match between inlet flow and the impeller entrance. The second type is due to *frictional* losses in the impeller. The third type is the *circulation* loss caused by the imperfect match between the exit flow and the impeller outlet. Hence, we find $\eta_h = 1 - (h_f / h_s)$.

Mechanical efficiency is defined by the losses in pump bearings, packing-glands, or mechanical seals and other contact points. If \dot{W}_f is the power wasted in all the contact points, $\eta_m = 1 - (\dot{W}_f / \dot{W}_{BHP})$. Improvement of the pump seal and the bearing material may increase pump efficiency by as much as 2%.

Priming refers to the inability of rotodynamic pumps to operate if non-condensable gases have leaked into the pump. In positive displacement pumps, the moving element, whether piston, gear, screw, or sliding vane, readily evacuates gases from the pump. For this reason, positive displacement pumps are considered to be *self-priming*.

3. Dimensionless Centrifugal Pump Performance

Earlier in this section we identified three groups containing pertinent pump parameters, $(\dot{V}, \Delta P)$, (D, ω, ε) , and (ρ, μ) . To obtain a relation for $\Delta P_{\text{pump}} = \rho g H = f(\dot{V}, \rho, \mu, N, D, \varepsilon)$ with H being total dynamic head, we note that there are a total of seven variables. Choosing ρ , D , and ω to represent the three primary dimensions mass, length, and time, we can identify four dimensionless ratios. Two obvious ones are ε/D for roughness ratio and $\rho N D^2 / \mu$ for the Reynolds number. The non-dimensional flow rate and head rise become $\dot{V}/N D^3$ and $gH/N^2 D^2$, respectively. Hence, we can write:

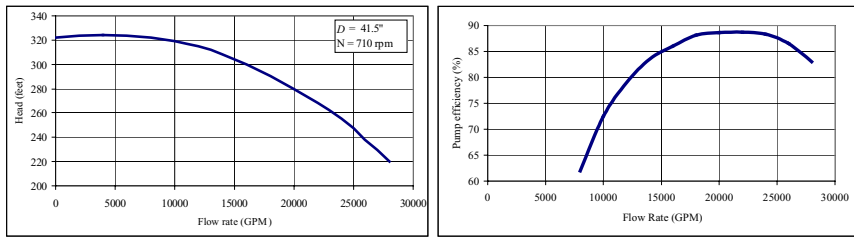
$$\frac{gH}{N^2 D^2} = f_1\left(\frac{\dot{V}}{N D^3}, \frac{\rho N D^2}{\mu}, \frac{\varepsilon}{D}\right)$$

Similar analysis can be performed for break horsepower and pump efficiency with dimensionless ratios of $\dot{W}_{BHP} / \rho N^3 D^5$ and η , respectively. The dimensionless ratios for flow, head, and break horsepower are referred to as *capacity coefficient* ($C_{\dot{V}} = \dot{V}/N D^3$), *head coefficient* ($C_H = gH/N^2 D^2$), and *power coefficient* ($C_{\dot{W}} = \dot{W}_{BHP} / \rho N^3 D^5$), respectively. Similar to the power coefficient, we may also define a *torque coefficient* ($C_T = T/\rho N^2 D^5$). If we assume that head and power coefficients are weak functions of Reynolds number and surface roughness, for all practical purposes we can then write:

$$C_H \cong C_H(C_{\dot{V}}) \quad C_{\dot{W}} \cong C_{\dot{W}}(C_{\dot{V}}) \quad \eta = \eta(C_{\dot{V}}) \quad \text{Vic.3.1}$$

Hence for two pumps to be homologous, we must have $C_{\dot{V}1} = C_{\dot{V}2}$, $C_{H1} = C_{H2}$, $C_{\dot{W}1} = C_{\dot{W}2}$, and $\eta_1 = \eta_2$. These conditions are known as the similarity rules. Using the similarity rules, not only can we predict the performance of other homologous units of pumps but we can also predict the performance of the same pump at various speeds.

Example Vic.3.1. A performance curve of a typical centrifugal pump having an impeller diameter of 41.5 inches at 710 rpm (pump A) is shown in the figure. Find the performance curve of the homologous pump (pump B) having a head and flow rate of 325 ft and 3000 GPM at the point of best efficiency.



Solution: We use the conditions for dynamic similarity given by three relations in Equation VIc.3.1. Since head and flow rate of pump B are specified at the point of best efficiency, to satisfy the third condition, we also use the head and flow rate of pump A in the first and the second relations at the point of best efficiency. Flow rate and head for pump A at the point of best efficiency (i.e. at $\eta \approx 88\%$) are about $\dot{V}_0 = 22000$ GPM and $H_0 = 270$ ft, respectively. Hence, from

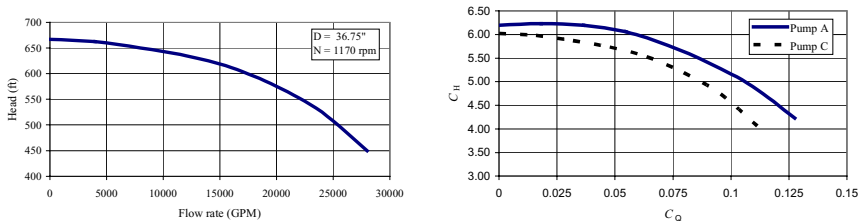
$$\frac{\dot{V}_B}{N_B D_B^3} = \frac{\dot{V}_A}{N_A D_A^3} \quad \text{and} \quad \frac{gH_B}{N_B^2 D_B^2} = \frac{gH_A}{N_A^2 D_A^2} \quad \text{we solve for } D_B \text{ and } N_B, \text{ to find}$$

$$D_B = (H_A / H_B)^{1/4} (\dot{V}_B / \dot{V}_A)^{1/2} D_A \quad \text{and} \quad N_B = \sqrt{\dot{V}_A / \dot{V}_B} (H_B / H_A)^{3/4} N_A.$$

Substituting for flow rates, heads, and D_A , we get $D_B = 14.63$ inches and $N_B = 2209$ rpm. Having, D_B and N_B , other points of the pump B characteristic curve at other efficiencies can be obtained by using similar points of pump A.

In the next example, we compare pump A of Example VIc.3.1 with another pump, which belongs to the same homologous series of pumps (say pump C). Our intention is to verify if the homologous pumps can be represented only with the non-dimensional groups.

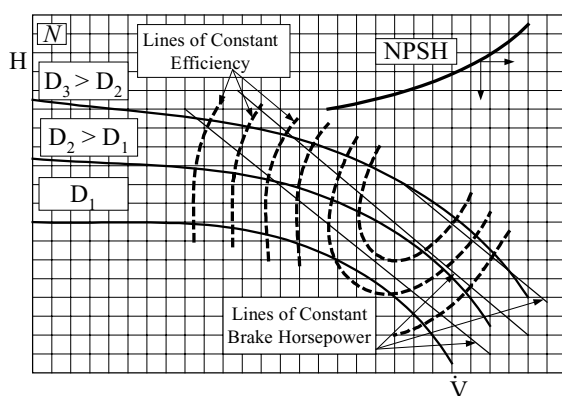
Example VIc.3.2. A performance curve of Pump C, which is homologous to pump A of Example VIc.3.1, is shown below in the left-hand side plot. Find the head versus the flow coefficient for these pumps.



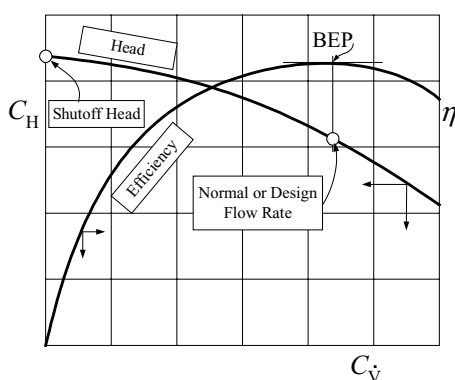
Solution: Having N and D for each pump, as well as the characteristic curves (H versus \dot{V}) for both pumps A and C, we find the head and flow coefficients as plotted in the right graph in the above figure. This figure shows that for geometrically similar pumps, the head coefficient is almost a unique function of the capacity coefficient. The reason for the slight difference is due to the assumptions we

made namely, ignoring the viscosity effects and the surface roughness. Similar comparison can be made for the brake horsepower coefficient and efficiency of pumps A and C.

Even with ignoring the effects of viscosity and surface roughness to find the two independent variables H and \dot{W}_{BHP} , we need to know the values of three independent variables: \dot{V} , N , and D . Shown in Figure VIc.3.1(a) are head and brake horsepower (also efficiency and NPSH) versus flow rate for a specified diameter and a specified impeller speed. These data, referred to as the pump characteristic curves, are produced empirically by the pump manufacturer. Due to the complexity of dealing with a multi-variable system, it is essential, especially for computer analysis, to use single graphs to represent the pump characteristic curves. Example VIc.3.1 showed that dimensionless homologous curves allow us to make such single graph representations, as shown in Figure VIc.3.1(b).



(a)



(b)

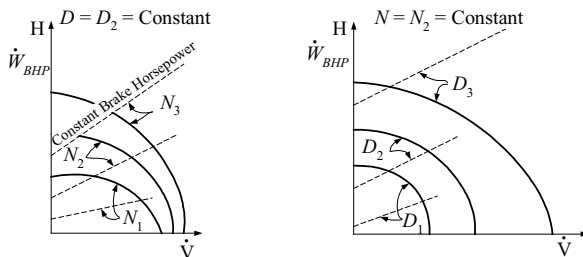
Figure VIc.3.1. Representation of (a) pump characteristic curves by (b) homologous curves

Example VIc.3.3. Use the similarity rules and compare the performance of a series of homologous pumps for various impeller diameters and impeller speeds.

Solution: The similarity rules require that;

$$\frac{\dot{V}_2}{\dot{V}_1} = \frac{N_2}{N_1} \left(\frac{D_2}{D_1} \right)^3, \quad \frac{H_2}{H_1} = \left(\frac{N_2}{N_1} \right)^2 \left(\frac{D_2}{D_1} \right)^2, \quad \text{and} \quad \frac{\dot{W}_2}{\dot{W}_1} = \frac{\rho_2}{\rho_1} \left(\frac{N_2}{N_1} \right)^3 \left(\frac{D_2}{D_1} \right)^5$$

These relations indicate that brake horsepower varies significantly with impeller size, as it depends on the diameter to the power of 5. The impeller size also affects flow rate since for the same total dynamic head, we get higher flow rate with higher diameter. Pump performance curves for various diameters and speed are plotted on the comparative diagrams where $D_1 < D_2 < D_3$ and $N_1 < N_2 < N_3$. Note that the similarity rules require that we also have $\eta_1 = \eta_2$. In reality however, larger pumps generally have higher efficiency than smaller pumps due to the smoother surfaces and tighter clearances.



3.1. Specific Speed

In Example VIc.3.1, we eliminated the impeller diameter and obtained $N_B = (\dot{V}_A / \dot{V}_B)^{1/2} (H_B / H_A)^{3/4} N_A$. If we now assume that for pump B, $\dot{V}_B = 1$ GPM and $H_B = 1$ ft, then N_B is known as specific speed of the pump (N_s) given by:

$$N_s = N \dot{V}_o^{1/2} / H_o^{3/4} \quad \text{VIc.3.2}$$

Therefore, for a homologous series of pumps, the specific speed is the pump speed that delivers a unit discharge at unit head at the BEP since N_s is generally calculated at the point of peak efficiency (shown by subscript o). Specific speed expressed in the *U.S. customary units* is calculated assuming speed in RPM, flow rate in GPM and head in feet. The advantage of specific speed is that it is associated with a particular range of values for each class of pumps. For example, high-head and low-flow pumps have a specific speed in the range of about 500 in U.S. customary units. As flow rate increases and dynamic head drops, the specific speed increases. Wislicenus showed (Figure VIc.3.2) that pump peak efficiency increases with increasing flow rate and specific speed.

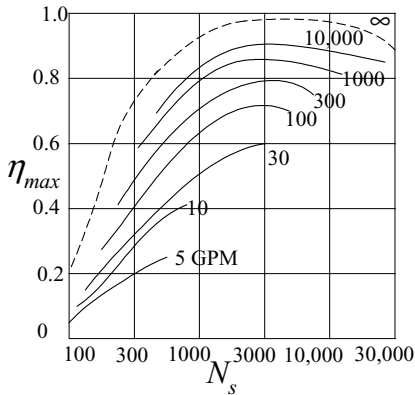


Figure VIc.3.2. Pump peak efficiency versus specific speed

Example VIc.3.4. Use the pump performance data of Example VIc.3.1 to find specific speed.

Solution: Specific speed is found at the point of peak efficiency. Therefore, given an impeller speed of 710 RPM, a flow rate of 22,000 GPM (8248 lit/s), and head of 270 ft (82.3 m), we find:

$$N_s = \frac{710 \times (22,000)^{0.5}}{(270)^{0.75}} = 1581$$

Example VIc.3.5. Find the specific speed of a pump with flow rate of 50,000 GPM and head of 23 ft. For this pump the capacity coefficient and the head coefficient at the BEP are 0.1 and 5.0, respectively.

Solution: Flow rate in ft^3/s is $50,000 \text{ GPM} \times (1 \text{ ft}^3/7.481 \text{ gallon}) \times (1 \text{ min}/60) = 111.4 \text{ ft}^3/\text{s}$.

$$C_V = \dot{V}/ND^3, \text{ therefore, } ND^3 = \dot{V}/C_V = 111.4/0.1 = 1114$$

$$C_H = gH/N^2D^2, \text{ therefore, } N^2D^2 = gH/C_H = 32.2 \times 23/5 = 148.12$$

Solving for N and D , we find $D = 9.6 \text{ ft}$ and $N = 1.3 \text{ revolution/s} = 76 \text{ RPM}$. Since high flow rate is pumped at a low head, the impeller diameter becomes too large and the impeller speed too slow. The specific speed is found as $N_s = 76(50,000)^{1/2}/(23)^{3/4} = 1619$.

The disadvantages associated with large diameter impeller and slow speed pumps include size accommodation and cost associated with parts (bearings, shaft, impeller, mechanical seals, and casing) in manufacturing and operation. As seen from the above example, the centrifugal pumps are well suited for low flow and

high head applications. Delivering high flow rates at lower head is better accomplished with pumps that reduce the radial component and increase the axial flow component. Figure VIc.3.3 shows that the large diameter radial flow impeller should be used for low specific speed. As specific speed increases, the shape of the impeller changes to reduce the centrifugal component in favor of the axial flow component. At very high specific speeds, pumps equipped with propeller should be used.

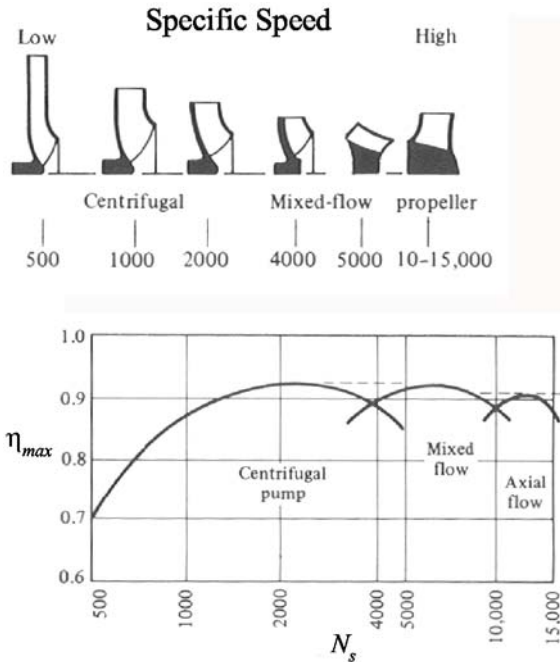


Figure VIc.3.3. Depiction of type and efficiency versus specific speed (White)

3.2. Prevention of Pump Cavitation

The required NPSH to avoid cavitation ($NPSH_R$) is specified by the pump manufacturer. As shown in Figure VIc.3.4, NPSH is a function of flow rate and impeller speed. Installation of the pump must ensure that the available NPSH remains always greater than the required NPSH. Therefore, to avoid cavitation, we must ensure that $NPSH_A > NPSH_R$ holds during pump operation. In fact, to enhance the margin to the onset of cavitation, it is recommended (Kreith) to increase the $NPSH_R$ by an additional 2 to 3 m (6.5 to 10 ft).

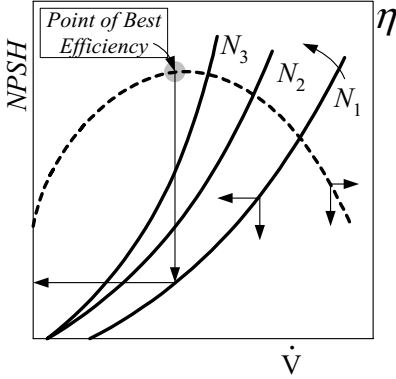


Figure VIc.3.4. Effect of flow rate and speed on the required NPSH

Example VIc.3.6. A centrifugal pump is used to deliver water at a rate of 250 GPM. The pump manufacturer has specified a minimum NPSH of 17 ft. The source reservoir is open to the atmosphere. The suction piping has a diameter of 3.5 in. with a total loss coefficient of $K = 8$. Find the maximum height that the pump can be placed above the reservoir to prevent cavitation. Water in the reservoir is at 14.7 psia and 75 F. The horizontal suction pipe run is 18 ft.

Solution: We use Equation VIc.2.1. Water is at $P_i = 14.7$ psia, and 75 F. The vapor pressure is about $P_v = 0.43$ psia. Total head loss in the suction piping is:

$$h_{fs} = \left(f \frac{s + \delta}{D} + K \right) \frac{V^2}{2g}$$

where s is the height we are looking for and $\delta = 18$ ft is the specified horizontal pipe run to pump intake. To find velocity, we use $\dot{V} = 250 / (7.481 \times 60) = 0.557$ ft³/s and $A = \pi D^2 / 4 = 3.14 \times (3.5/12)^2 / 4 = 0.0668$ ft². Hence, $V = 0.557 / 0.0668 = 8.34$ ft/s and $Re = \rho V D / \mu = 62.4 \times 8.34 \times (3.5/12) / 6.25E-4 = 0.243E6$. Assuming a smooth pipe, $f = 0.184 / Re^{0.2} = 0.0154$. Using Equation VIc.2.1:

$$\frac{14.7 \times 144}{62.4} - s - \left(0.0154 \frac{s + 18}{(3.5/12)} + 8 \right) \frac{8.34^2}{2 \times 32.2} - \frac{0.43 \times 144}{62.4} \geq NPSH_R = 17$$

From here $s = Z_p - Z_i = 6$ ft. Hence, $Z_p = Z_i + 6$ ft. This is the maximum elevation for the pump to avoid cavitation. Note that in this example head loss due to skin friction ($h_1 = 1.4$ ft) is by far smaller than losses due to valves, filters, and fittings ($h_2 = 8.64$ ft) on the suction line. In general, the suction line must be located as close to the source reservoir as possible with as few valves and fittings on the suction line as absolutely necessary. Head loss due to skin friction can become noticeable in cases where pumps cannot be located near the source reservoir with only few fittings on the suction line.

The likelihood for cavitation increases with increasing specific speed conservatively beyond about 8000.

Example VIc.3.7. The available NPSH for a pump delivering 50,000 GPM water is 40 ft. Find the maximum impeller speed to avoid cavitation.

Solution: We find N from Equation VIc.3.2 with NPSH substituted for H_o :

$$N = N_s(\text{NPSH})^{3/4} / \dot{V}^{1/2}.$$

$$N = 8000 \times (40)^{0.75} / (50,000)^{1/2} = 569 \text{ RPM.}$$

4. System and Pump Characteristic Curves

The challenge of selecting a pump is to meet the required capacity while providing the required head at the point of best efficiency. Equation IIb.4.8-1 (or IIb.4.8-2) gives serial-path system curves for laminar and turbulent flows. This is also plotted in Figure VIc.4.1(b). Pump head and flow rate is obtained from the intersection of the pump characteristic and system curves. If this point does not correspond with the point of peak efficiency, the pump speed should be adjusted otherwise alternate pumps should be sought. We may try an analytical solution for turbulent flow in pipes, for example where $H_{\text{System}} = c_1 + c_3 \dot{V}^2$. Representing pump head versus flow rate with a parabola, we find $H_{\text{Pump}} = a + b \dot{V}^2$. Setting the system head equal to the pump head, we find $(b - c_3) \dot{V}^2 + (a - c_1) = 0$. Flow rate is then found as

$$\dot{V} = \left(\frac{a - c_1}{c_3 - b} \right)^{1/2} = \left(\frac{H_{\text{Pump}}(\dot{V}=0) - (Z_e - Z_i)}{\sum fL'/(2gDA^2) + [H_{\text{Pump}}(\dot{V}=0)/\dot{V}^2 (H_{\text{Pump}}=0)]} \right)^{1/2} \quad \text{VIc.4.1}$$

where the two points to describe the $H_{\text{Pump}} = f(\dot{V})$ are taken at maximum H and maximum \dot{V} . The flow rate calculated above should be checked against \dot{V}_o , flow rate corresponding to best efficiency point. If significant difference exists, pump speed should be changed. If the change in speed still does not increase efficiency, an alternate pump should be sought. To find if a change in speed brings efficiency to its peak value, we use the homologous relations $C_{\dot{V}} = C_{\dot{V}_o}$ and $C_H = C_{H_o}$. If at N_o rpm, the flow rate and head corresponding to peak efficiency are \dot{V}_o and H_o , then at any other speed these are given by $\dot{V} = \dot{V}_o (N / N_o)$ and $H = H_o (N / N_o)^2$. We now substitute the new head and flow rate into the system curve to get $H_o (N / N_o)^2 = c_1 + c_3 [\dot{V}_o (N / N_o)]^2$. We solve this equation for N to get:

$$N = \left(\frac{C_1}{H_o - C_3 \dot{V}_o^2} \right) N_o = \left\{ \frac{Z_e - Z_i}{H_o - [\sum fL'/(2gDA^2)] \dot{V}_o^2} \right\}^{1/2} N_o \quad \text{Vic.4.2}$$

Equation Vic.4.2 yields an acceptable answer only if the argument is greater than zero. To increase accuracy, the pump curve should be represented by a higher order polynomial.

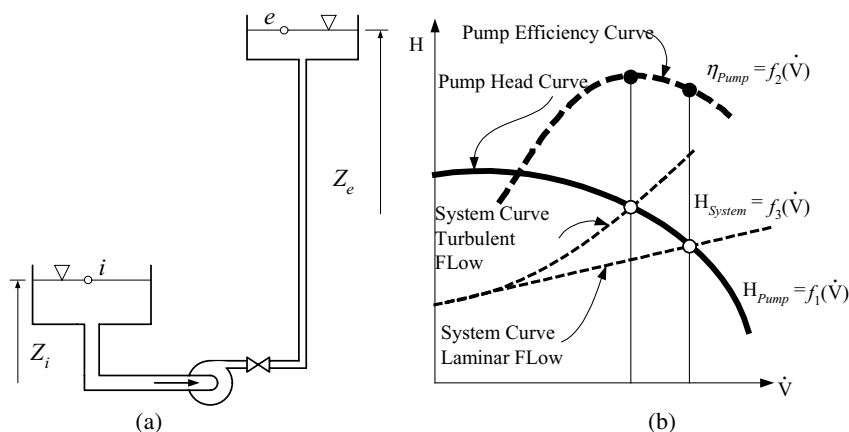


Figure Vic.4.1. (a) Pump in a single-path system (b) Pump and system curves

Example Vic.4.1. The pump in Example Vic.3.1 is used to deliver water to a height of 100 ft from the source reservoir. Total pipe length is 2000 ft and the pipe diameter is 14 in. The pipe run includes a swing check valve, a fully open gate valve, and a fully open globe valve as well as a total of 4 threaded 90° elbows. a) Find flow rate and efficiency. b) How do you maximize efficiency in part (a)?

Solution: a) We first find the system curve from $H_{\text{system}} = c_1 + c_3 \dot{V}^2$ where $c_1 = 100$ and c_3 is given by $c_3 = fL'/(2gDA^2)$.

However, $L' = L + L_e$. From Table III.6.3 (b), $L_e = 4 \times 30 + 50 + 8 + 340 = 518$ and from Table III.3.2, $f = 0.013$. Flow area becomes $A = \pi(14/12)^2/4 = 1.069 \text{ ft}^2$. Finally, $c_3 = 0.013 \times (2000 + 518)/[2 \times 32.2 \times (14/12) \times 1.069^2] = 0.38$. Therefore, $H_{\text{system}} = 100 + 0.38 \dot{V}^2$, where flow rate is in ft^3/s .

Approximating the pump head versus flow as a parabola ($H_{\text{pump}} = a + b \dot{V}^2$), we find coefficients a and b by using two points. The first point is at $\dot{V} = 0$, $H_{\text{pump}} = 322 \text{ ft}$. Picking the second point at the best efficiency gives $\dot{V} = 22000 \text{ GPM}/(7.481 \times 60) = 49 \text{ ft}^3/\text{s}$ and $H_{\text{pump}} = 270 \text{ ft}$. This results in, $a = 322$ and $b = -0.0216$ or $H_{\text{pump}} = 322 - 0.0216 \dot{V}_o^2$. From Equation Vic.4.1:

$\dot{V} = \sqrt{(c_1 - a)/(b - c_3)} = \sqrt{(100 - 322)/(-0.0216 - 0.38)} = 23.51 \text{ ft}^3/\text{s} = 10552 \text{ GPM}.$

This corresponds to a head of 310 ft and an efficiency of about 73%, far from the peak efficiency of 88%.

b) To increase the pump efficiency we may change the pump speed. To find the new pump speed, we use homologous relations to get $\dot{V}' = (N/710)\dot{V}_0$ and $H' = (N/710)^2 H_0$. We now substitute the new head and flow rate into the system curve to get: $(N/710)^2 \times 270 = 100 + 0.38 \{(N/710) [22000/(7.481 \times 60)]\}^2$. Thus, $-1.275\text{E-}3 N^2 = 100$. It is clear we cannot reach peak efficiency for the operational condition using this pump.

4.1. Compound Pumping System

Pumps may be used in serial or parallel arrangements depending on the flow or head requirement. Pumps combined in series, as shown in Figure VIc.4.2(a) provide a higher head for the same flow rate and pumps combined in parallel, provide the same head at higher flow rate. For optimum performance, not only the head and flow rate of the compound pumping system must meet the demand but they must also correspond to the point of best efficiency of each participating pump. Compound pumping systems are not always used to meet the head and flow rate demand. In many cases pumps are arranged in parallel to increase system availability.

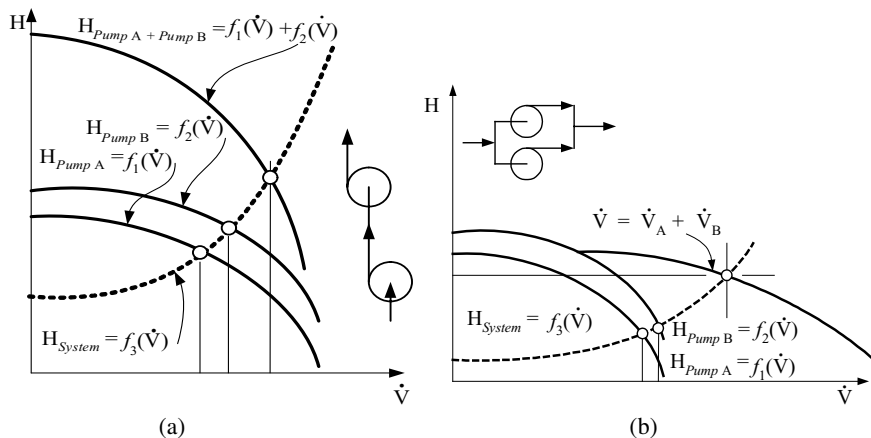


Figure VIc.4.2. Compound pumping system in (a) serial and (b) parallel arrangements

4.2. Extension of Pump Characteristic Curves

Earlier we discussed pump characteristic curves and the representation of the family of such curves with the pump homologous curves. While it is desired that pumps operate steadily at their rated condition, there are cases where pumps must be analyzed for such off normal conditions as flow reversal in the pump and reverse rotation of the impeller. Such off normal operations require the extension of the first-quadrant pump characteristic curves (positive flow rate and positive speed) to all four quadrants where any combination of positive and negative flow rate and speed exists. Unlike Figure VIc.3.1, where head and volumetric flow rate are chosen as coordinates, as shown in Figure VIc.4.3(a), the coordinates are chosen to be volumetric flow rate and the impeller speed. The resulting plots, as empirically produced by the pump manufacturer, are known as the *synoptic curves*, which constitute the *Karman-Knapp circle diagram*. In this figure, the solid lines represent constant head and the dotted lines show the constant pump hydraulic torque. Figure VIc.4.3(b) shows possible modes of operation of a pump during a transient. The first quadrant is normal pump (N). The solid lines between $H = 0$ and the speed coordinate are the familiar head versus flow rate curves. Expectedly, for a constant flow rate, head increases with increasing impeller speed. There are also lines representing negative pump head in this quadrant for positive flow and positive impeller speed.

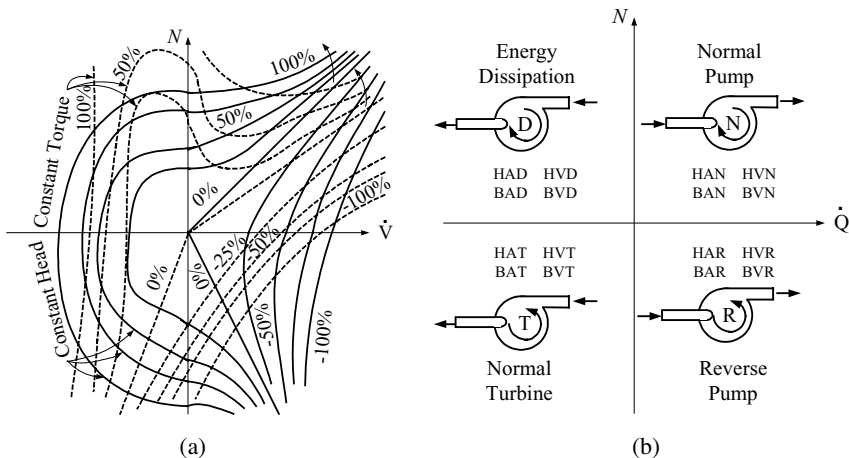


Figure VIc.4.3. (a) Pump characteristic curves in four quadrants and (b) Possible modes of operation

In the second quadrant (D), we find only positive pump head for positive impeller speed but negative flow rate. The third quadrant (T) is referred to as normal turbine where, for positive pump head, flow direction is into the pump with the impeller rotating in the reverse direction. Finally, in the fourth quadrant (R) there are both positive and negative pump heads for positive flow and reverse impeller rotation. It is obvious that representation of such massive pump characteristic data

in computer analysis is impractical. Therefore, we resort to the non-dimensional homologous curves to represent the pump characteristic curves. This, in turn, requires the definition of some additional non-dimensional groups.

For a given pump, we use the rated data, which correspond to the point of best efficiency, to normalize variables. Hence, we obtain *speed ratio* ($a = \omega/\omega_0 = N/N_0$), *flow ratio* ($v = \dot{V}/\dot{V}_0$), *head ratio* ($h = H/H_0$) and *torque ratio* ($b = T/T_0$). The flow, head, and torque coefficients now take the form of $C_V = b/v$, $C_H = h/a^2$, and $C_T = b/a^2$, respectively. We then can find C_H and C_T as functions of C_V . During analysis of pump response to a transient flow rate and impeller speed traverse positive and negative values. As such, both variables may encounter zero. In the case of the impeller speed, the values of the above coefficients would be undetermined. To avoid such conditions, we update our definition of the above coefficients and produce $C'_H = h/b^2$ and $C'_T = b/v^2$.

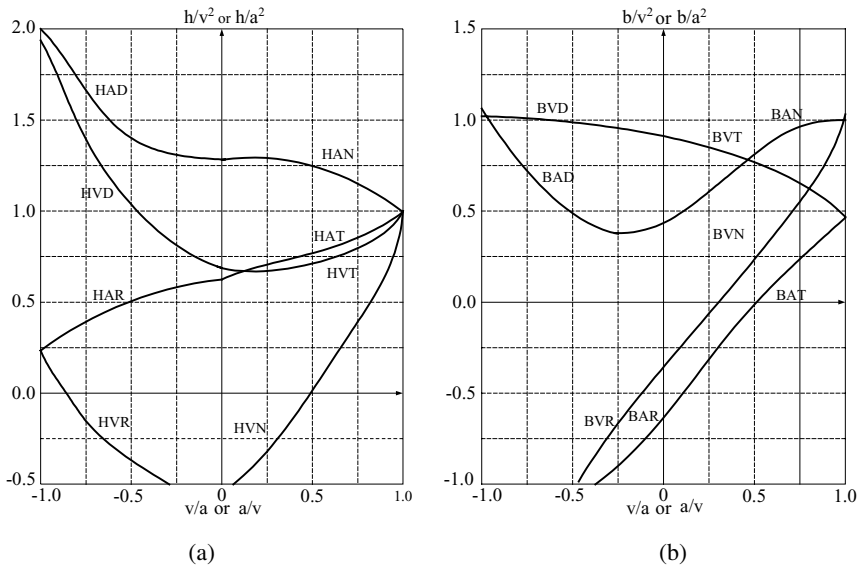
Generally, the head or torque coefficients (C_H and C_T or C'_H and C'_T) as independent variables are expressed in terms of flow and speed ratios (a and v). Since there are also four quadrants where these independent variables should be determined, it has become customary to use shorthand (a three-letter notation) to identify various variables in various quadrants. The first letter identifies the dependent variables (i.e., whether we are dealing with head or torque (h or b)). Hence, H designates head and T designates torque ratios. The second letter, as a representative of the independent variable, is such that A designates division by a for the independent variable, and division by a^2 for the dependent variable. Similarly, V designates division by v for the independent variable and division by v^2 for the dependent variable. Finally, the third letter indicates the mode in which the pump is operating, as shown in Figure VIc.4.3(b). These modes are N , R , T , and D for Normal pump, Reverse pump, normal Turbine, and energy Dissipation, respectively. These conventions are summarized in Table VIc.4.1, which defines 16 curves: 8 for head and 8 for torque. We now group similar curves of Table VIc.4.1 to obtain only four curves as summarized in Table VIc.4.2. These four homologous curves are shown for a typical centrifugal pump in Figure VIc.4.4(a) for homologous head and in Figure VIc.4.4(b) for homologous torque.

Table VIc.4.1. Summary of homologous curve notations

No.	a	v	v/a	Independent Variable	Dependent Variable		Dependent Variable	
					Type	Head	Type	Torque
1	> 0	≥ 0	≤ 1	v/a	HAN	h/a^2	BAN	b/a^2
2	> 0	> 0	> 1	a/v	HVN	h/v^2	BVN	b/v^2
3	> 0	< 0	≥ -1	v/a	HAD	h/a^2	BAD	b/a^2
4	> 0	< 0	< -1	a/v	HVD	h/v^2	BVD	b/v^2
5	< 0	≤ 0	≤ 1	v/a	HAT	h/a^2	BAT	b/a^2
6	≤ 0	< 0	> 1	a/v	HVT	h/v^2	BVT	b/v^2
7	< 0	> 0	≥ -1	v/a	HAR	h/a^2	BAR	b/a^2
8	≤ 0	> 0	< -1	a/v	HVR	h/v^2	BVR	b/v^2

Table VIc.4.2. Determination of pump homologous curves from pump characteristic curves

No.	Curves Paired		Independent Variable	v or a		Homologous Curve
	No.	No.				
I	3	1	$ v/a \leq 1$ $a > 0$	$v < 0$ HAD/BAD	$v \geq 0$ HAN/BAN	$h/a^2 = f(v/a)$ $b/a^2 = f(v/a)$
II	7	5	$ v/a \leq 1$ $a < 0$	$v > 0$ HAR/BAR	$v \leq 0$ HAT/BAT	$h/a^2 = f(v/a)$ $b/a^2 = f(v/a)$
III	8	2	$ a/v < 1$ $v > 0$	$a < 0$ HVR/BVR	$a \geq 0$ HVN/BVN	$h/v^2 = f(a/v)$ $b/v^2 = f(a/v)$
IV	4	6	$ a/v < 1$ $v < 0$	$a > 0$ HVD/BVD	$a \leq 0$ HVT/BVT	$h/v^2 = f(a/v)$ $b/v^2 = f(a/v)$


Figure VIc.4.4. Dimensionless homologous (a) pump head and (b) hydraulic torque

Example VIc.4.2. In a transient, the speed and flow rate of a centrifugal pump are given as $N = -600$ rpm and $\dot{V} = -200,000$ GPM. Find a) pump head and torque, b) pump efficiency, and c) the temperature rise of the liquid across the pump for rated conditions. The rated values of the pump are: $N_o = 900$ rpm, $\dot{V}_o = 370,000$ GPM, $H_o = 270$ ft, $T_o = 136,000$ ft-lbf, and $\rho = 50$ lbf/ft³.

Solution: a) Having \dot{V} and N , we obtain $v = \dot{V} / \dot{V}_o = -200,000 / 370,000 = -0.54$ and $a = N / N_o = -600 / 900 = -0.67$. Hence, $a/v = -0.54 / -0.67 = 0.81$.

From Figure VIc.4.4(a), using the HVT curve we find for $a/v = 0.81$, $h/v^2 = c_1 \cong 0.8$

From Figure VIc.4.4(b), using the BVT curve we find for $a/v = 0.81$, $b/v^2 = c_2 \cong 0.6$. Therefore,

$H = hH_o = 0.8 \times (0.54)^2 \times 270 = 63$ ft and $T = bT_o = 0.6 \times (0.54)^2 \times 136,000 = 24,588$ ft·lbf.

b) It can be easily shown that pump efficiency is related to the rated efficiency as $\eta/\eta_o = (c_1/c_2)(v/a)$

Having c_1 and c_2 from (a), and η_o , we can find η . However, pump efficiency is defined for the first quadrant. In the third quadrant for example, where the pump is in the turbine mode, efficiency should be redefined to fit the mode of operation.

c) Total power delivered to the liquid is $\dot{W}_{BHP} = \rho_o g \dot{V}_o H_o$. This is equal to the energy gained by the water as given by $\rho_o \dot{V}_o c_p \Delta T$. Hence, $\Delta T = H_o g / c_p$. If the liquid is water, $c_p = 1$ Btu/lbm F = 778 ft·lbf/lbm F. Hence, $\Delta T = 270/778 = 0.35$ F.

Since production of the pump homologous curves is tedious, there are several attempts to represent these by polynomial curve fits. For example, Streeter recommends parabolic functions for the representation of these curves in various quadrants. The dimensionless head becomes:

$$h = c_{11} + c_{12}(v/a) + c_{13}(v/a)^2 \quad 0 \leq |v/a| \leq 1 \quad \text{VIc.4.1-1}$$

$$h = c_{13} + c_{12}(a/v) + c_{11}(a/v)^2 \quad |v/a| > 1 \quad \text{VIc.4.1-2}$$

and the dimensionless hydraulic torque:

$$b = c_{21} + c_{22}(a/v) + c_{23}(a/v)^2 \quad 0 \leq |v/a| \leq 1 \quad \text{VIc.4.2-1}$$

$$b = c_{21} + c_{22}(a/v) + c_{23}(a/v)^2 \quad |v/a| > 1 \quad \text{VIc.4.2-2}$$

using the coefficients c_{ij} given in Table VIc.4.3.

Table VIc.4.3. Coefficient for parabolic fit to pump homologous curves

Quadrant	Curve	c_{11}	c_{12}	c_{13}	Sign	Curve	c_{21}	c_{22}	c_{23}
Normal Pump	HAN	1.30	-0.02	-0.28	-	BAN	-0.45	-0.85	-0.30
	HVN	0.70	0.85	-0.55	-	BVN	0.480	0.880	-0.36
Energy Dissipation	HAD	1.30	0.30	1.000	+	BAD	0.450	0.670	1.22
	HVD	1.20	-0.10	0.700	-	BVD	-0.20	0.340	0.86
Normal Turbine	HAT	0.65	0.25	0.100	+	BAT	-0.65	1.420	-0.32
	HVT	0.50	-0.15	0.650	+	BVT	-0.18	-0.23	0.86
Reverse Pump	HAR	0.65	0.15	-0.300	+	BAR	-0.65	1.250	0.28
	HVR	0.90	0.15	-0.550	+	BVR	-1.44	0.700	-0.36

Having the curve fit coefficients and the rated values, flow rate and hydraulic torque are found from:

$$\dot{V} = (\dot{V}_o / 2c_{13}) \left\{ -c_{12}a + \text{sign}[(c_{12}^2 - 4c_{11}c_{13})a + 4c_{13}h]^{1/2} \right\}$$

$$T_H = T_o (c_{21}a^2 + c_{22}av + c_{23}v^2)$$

Another example for curve fitting to the pump homologous curve is given by Kao as polynomials:

$$h/a^2 = \sum_{i=1}^4 c_{3i} (v/a)^{i-1} \quad \text{and} \quad b/a^2 = \sum_{i=1}^4 c_{4i} (v/a)^{i-1}$$

where coefficients c_{31} through c_{34} for positive impeller speed are 1.80, -0.30 , 0.35 and -0.85 and for negative impeller speed are 0.50 , 0.51 , -0.26 , 0.25 . For dimensionless torque, coefficients c_{41} through c_{44} for positive impeller speed are 1.37 , -1.28 , 1.61 , and -0.70 and for negative impeller speed are -0.65 , 1.9 , -1.28 , and 0.54 . In a transient, if the impeller speed goes to zero when changing direction from positive to negative speed, the pump head versus flow for these sets of polynomial curves may be found from:

$$h = (-4.181E - 3)|v|v$$

While theoretically a centrifugal pump may operate in all four quadrants, in practice, pump operation in the first quadrant can be ensured by pump and system modification. For example, installing a non-reversing ratchet prevents the impeller from rotating in the reverse direction and a check valve on the discharge line prevents reverse flow into the pump.

5. Analysis of Hydraulic Turbines

Turbines are mechanical devices to convert the energy of a fluid to mechanical energy. Turbines can be classified in various ways based on process, head conversion, or rotor type. Regarding the process, energy transfer in turbines may take place in either an adiabatic or in an isothermal process. Regarding head conversion, turbines may be divided into the reaction and the impulse type for momentum exchange between fluid and the turbine rotor. Finally, turbines may be classified depending on the velocity vector resulting in an axial, radial, or mixed-flow rotor.

5.1. Definition of Terms for Turbines

Adiabatic process turbines, as were studied in Chapter IIb, include gas and steam turbines where the means of energy transfer from fluid to the turbine rotor is primarily through the change in the fluid enthalpy. In this type of turbine, changes

in the fluid potential and kinetic energy are generally negligible, compared with the change in fluid enthalpy.

Isothermal process turbines include turbines used in greenpower production such as hydropower and wind turbines. In this type of turbine, the transfer of mechanical energy to the turbine rotor is due to the fluid kinetic energy, while changes in enthalpy are generally negligible compared with the change in the fluid kinetic energy.

Reaction type turbines or simply reaction turbines, have rotors equipped with blades. In the reaction type turbines, fluid fills the blade passages of the rotor to deliver momentum. Thus, the head conversion in the reaction type turbines occurs within the turbine rotor where fluid pressure changes from inlet to outlet. Examples of the reaction type turbines include adiabatic, wind, and most hydropower turbines.

Impulse type turbines convert the head in an injector. Thus, in an impulse turbine, the head conversion takes place outside the turbine rotor. The high velocity jet then strikes individual buckets attached to the Pelton wheel at a constant pressure. Imparting the momentum of the jet to a bucket produces a force, which results in a torque to turn the wheel and brings the adjacent bucket to face the jet.

5.2. Specific Speed for Turbines

The same dimensionless groups defined in Section 3 for pumps are also applicable to turbines. Recall that for pumps we expressed the head and the power coefficient in terms of the capacity coefficient. However, for turbines, we express the capacity and the head coefficient in terms of the power coefficient. In the U.S., it is customary to find specific speed for turbines from:

$$N_s = \frac{(N, \text{rpm})(\text{bhp})^{1/2}}{(\text{H}, \text{ft})^{5/4}} \quad \text{VIc.5.1}$$

5.3. Adiabatic Turbines, Steam Turbine

The adiabatic turbines, regardless of the type of working fluid, are generally of axial flow type. However, turbines used for turbo-charging are generally of radial flow type.

5.4. Isothermal Turbines, Pelton Turbine

As discussed in Chapter I, Pelton wheels are impulse turbines in which high head and low flow rate of water strikes the buckets attached to the wheel, as shown in Figure VIc.5.1. Our goal is to determine the Pelton wheel in terms of the jet velocity (V_j), the bucket velocity (V_t), and the bucket angle (β). This is shown in the example that follows.

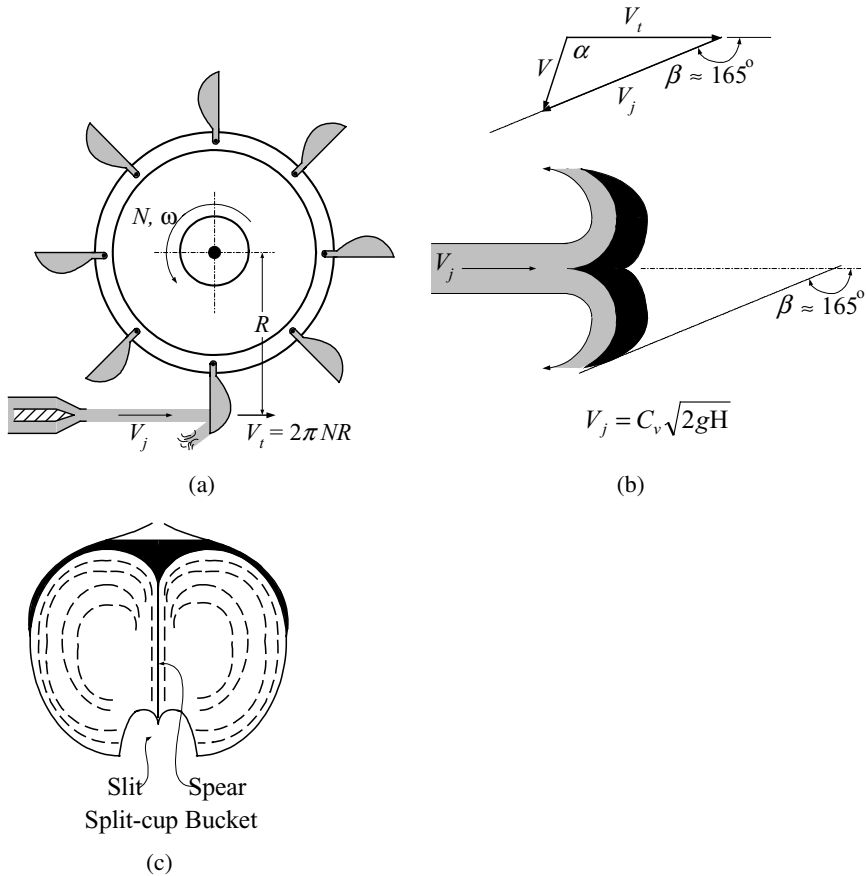


Figure V1c.5.1. Pelton wheel. (a) Side view of the wheel, (b) & (c) top and frontal views of the bucket.

Example V1c.5.1. Derive the efficiency of the Pelton wheel in terms of the constant velocities V_j , V_t , and the jet reflection angle of β .

Solution: Efficiency of the wheel is defined as the ratio of the power obtained from the wheel to the power delivered to the wheel $\eta = \dot{W}_{out} / \dot{W}_{in}$ (i.e., the break horsepower to the hydraulic horsepower).

$$\dot{W}_{in} = dE_j / dt = d(mV_j^2 / 2) / dt = (1/2) \left[(dm/dt)V_j^2 + m(dV_j^2/dt) \right] = \rho \dot{V} V_j^2 / 2$$

We find \dot{W}_{out} from the rate of change of momentum for which we must consider the relative velocities.

$F = d(mV)/dt = (dm/dt)V + (dV/dt)m = \rho V \dot{V}$. Note that $V = V_j - V_t$. The net force applied on the wheel is

$$\begin{aligned}
\Delta F &= F_j - F_t = \rho \dot{V}(V_j - V_t) - (\rho / g_c) \dot{V}(V_j - V_t) \cos \beta = \\
&\rho \dot{V}(V_j - V_t)(1 - \cos \beta) \\
\dot{W}_{out} &= \Delta F V = [\rho \dot{V}(V_j - V_t)(1 - \cos \beta)] V_t \\
\eta_{theoretical} &= \dot{W}_{out} / \dot{W}_{in} = [\rho \dot{V}(V_j - V_t)(1 - \cos \beta)] V_t / (\rho \dot{V} V_j^2 / 2) = \\
&2(1 - \cos \beta)(V_j - V_t) V_t / V_j^2.
\end{aligned}$$

To find $(\eta_{theoretical})_{max}$ we set $d\eta_{theoretical}/dV_t = 0$ resulting in $V_t = V_j/2$. Hence,
 $(\eta_{theoretical})_{max} = (1 - \cos \beta)/2$.

In the above example, we assumed an injector with maximum efficiency. In practice however, the bucket angle is about 165° and a velocity coefficient ($C_v \cong 0.94$) should also be considered for the nozzle. Hence, the efficiency becomes:

$$\eta = 2(1 - \cos \beta)(C_v - \phi) \phi \quad \text{VIc.5.2}$$

where $\phi = V_t / \sqrt{2gH}$. Maximum efficiency, considering the velocity coefficient, occurs when $\phi = C_v/2$. In practice, the Pelton wheel efficiency is even less than that given by Equation VIc.5.2 due to such losses as windage and mechanical friction. Additionally, the Pelton wheels suffer from two more losses, which are peculiar only to this type of turbine. The first has to do with the nature of a jet striking a turning wheel. As the bucket facing the jet moving away and the neighboring bucket approaches the jet, the back of the approaching bucket would first touch the jet before the front of the bucket faces the jet. Although a recess or a slit has been made in each bucket to minimize *back-splashing*, there are still some losses associated with this feature of the Pelton wheel. The second loss is due to the frontal structure of each bucket. Each bucket is made of two split cups, the common edge of which constitutes a spear, as shown in Figure VIc.5.1. The jet, upon entering the bucket, is divided up by the spear into two equal parts to pass the curvilinear surface of each cup and exit the bucket. Machining and surface finish of each split cup is essential for having a uniform flow in each cup of the bucket.

The Pelton wheel efficiency should, therefore, be calculated from experimentally obtained data such as the data shown in Figure VIc.5.2, which gives efficiency in terms of the turbine power specific speed. Figure VIc.5.2 indeed indicates that hydraulic turbines using the Pelton wheel have lower efficiency at their BEP than the Francis and the Kaplan turbines. Given this fact, it then appears that a Francis turbine is a better choice. Indeed Francis turbines, with radial-axial rotors, are used to harness the power of water at a height of up to 700 m (2,300 ft). However, the Pelton wheels are used for heads as high as 1500 m. Using a Francis turbine for such high heads, results in the rotor having to run at very high speeds. Furthermore, a thick casing is required to contain water at pressures that may exceed 2000 psia.

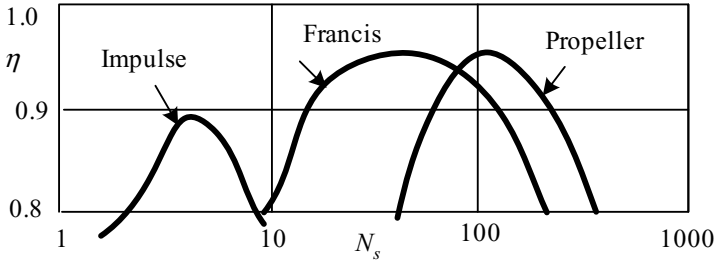


Figure VIc.5.2. Efficiency of hydraulic turbines as a function of specific speed (White)

Example VIc.5.2. The Pelton wheel of an impulse turbine has a wheel diameter of 4 m and an injector diameter of 10 cm. The turbine is operating at a net head of 600 m. Find the power output of this turbine for best efficiency.

Solution: We use a return angle of 165° , a velocity coefficient of 0.94, and perform the following steps:

$$V_j = C_v \sqrt{2gH} = 0.94(2 \times 9.8 \times 600) = 102 \text{ m/s and } (V_j)_{\max} = 108.4 \text{ m/s.}$$

Find flow rate from:

$$\dot{V} = (\pi d_j^2 / 4) V_j = \pi (10/100)^2 \times 102/4 = 0.8 \text{ m}^3/\text{s} = 12700 \text{ GPM.}$$

Find η from Figure VIc.5.2.

To use Figure VIc.5.2, we need N_s . Recall that at best efficiency, $\phi = C_v/2$, where $C_v \approx 0.94$, therefore

$$\phi = 0.94/2 \equiv 2\pi R N / (V_j)_{\max} = \pi \times 4 \times N / 108.4.$$

Solving for N , we obtain $N = 4 \text{ RPS} = 240 \text{ RPM}$.

We need to calculate the bhp:

$$\text{bhp} = [(\rho / g_c) \dot{V} (V_j - V_t) (1 - \cos \beta)] V_t = 999 \times 0.8 [102 - (102/2)] (1 - \cos 165^\circ) \times (102/2) = 5480 \text{ hp}$$

$$N_s = N(\text{bhp})^{0.5} / H^{5/4} = 240 \times (5480)^{0.5} / (600 \times 3.2808)^{5/4} = 1.355.$$

From Figure VIc.5.2, $\eta \approx 0.73\%$

$$\dot{W}_{\text{out}} = 5480 \times 0.73 = 3993 \text{ hp.}$$

5.5. Classification of Hydraulic Turbines

Classification of the hydraulic turbines in terms of specific speed and head is shown in Figure VIc.5.3. As shown in this figure, axial flow turbines are suitable for low head and high flow. As the available head of water increases, the runner is shaped so that the flow of water becomes mixed with respect to the axis of the turbine runner. Still at higher heads, the Francis wheel is used. At low flow rates and very high head, the Pelton wheel is the obvious choice.

As seen from Figure VIc.5.3, for reaction turbines, low specific speeds are associated with radial turbines and high specific speed with axial turbines. Similar association applies to pumps as shown in Figure VIc.3.2 for specific speed ranging from 500 – 15,000. Mott indicates that axial flow pumps may be used for pump specific speed in the range of 7,000 – 60,000.

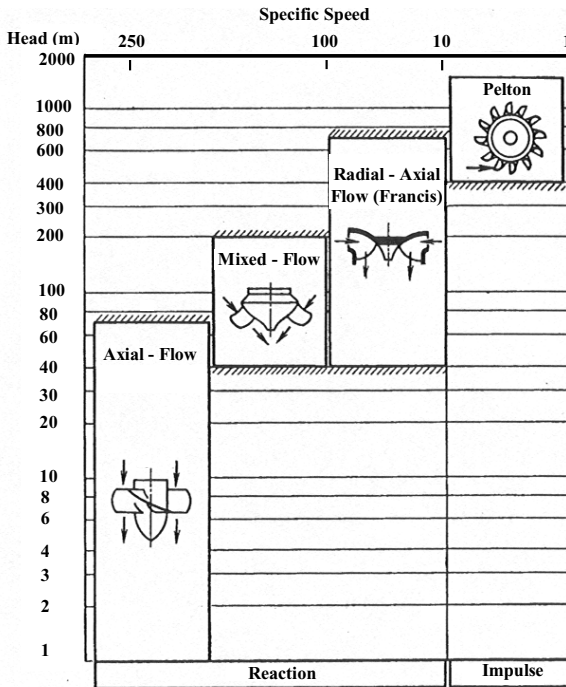


Figure VIc.5.3. Classification of hydraulic turbines (Krivchenko)

5.6. Isothermal Turbines, Wind Turbine

As was discussed in Chapter I, there are a variety of wind turbines in operation today. The most widely used is the wind turbine type of horizontal axis design equipped with propellers, as shown in Figure I.4.21. To derive the efficiency for the wind turbine, we use the method applied by White. For this purpose, we use the mass, momentum, and energy equations for the control volume consisting of a stream tube and a propeller, as shown in Figure VIc.5.4. We note that location 1 is the upstream of the propeller at velocity V_1 and pressure $P_1 = P_{atm}$. Locations 2 and 3 are right before and right after the propeller. Air velocity and pressure at these locations are V_2 , P_2 , V_3 , and P_3 , respectively. Finally, location 4 is downstream of the propeller at which air velocity is V_4 and air pressure reaches the atmospheric pressure, $P_4 = P_{atm}$. In the following derivation we assume uniform

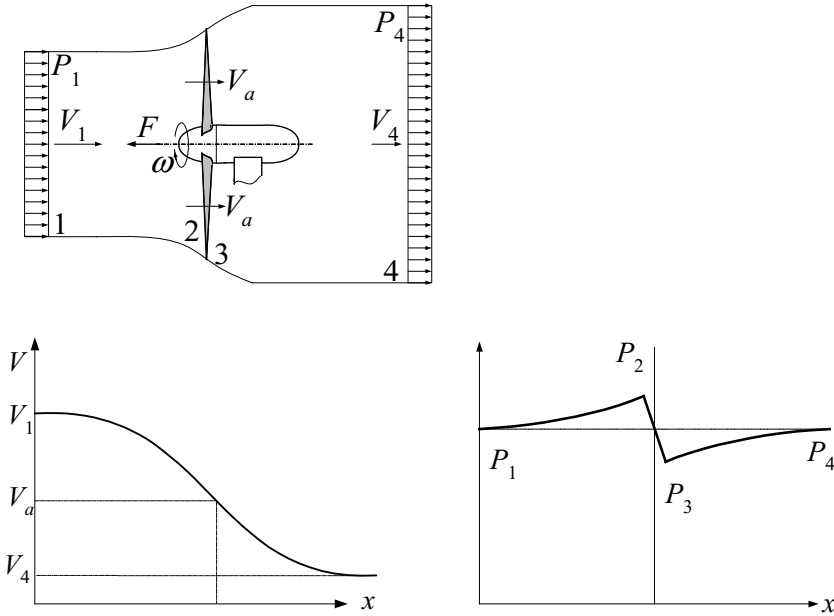


Figure VIc.5.4. The stream-tube for the flow of air through a wind turbine (White)

wake and ideal flow. There are reasonable assumptions for $V_1 < 20$ mph (32 km/h).

The continuity and the momentum equations. Regarding the continuity equation, we note that the mass flow rate of air through the propeller is found as $\dot{m} = \rho V_a A$ where A is the area swept by the propeller and V_a is the air velocity at the blade. As for the momentum equation, we apply the Bernoulli equation between locations 1 and 2 and between locations 3 and 4. Adding these equations and noting that $P_1 = P_4 = P_{atm}$ and $V_2 = V_3 = V_a$ we conclude:

$$P_2 - P_3 = \Delta P = \rho(V_1^2 - V_4^2)/2 \quad \text{VIc.5.3}$$

We now use the momentum equation over the turbine (i.e. between locations 2 and 3). A free-body diagram for the turbine shows that the net force applied in the wind direction to the turbine is equal to the rate of the change of air momentum passing through the propeller:

$$F = (P_2 - P_3)A = \rho V_a A(V_1 - V_4) \quad \text{VIc.5.4}$$

where we assume an ideal wind turbine for which no frictional losses exist. In reality, however, we must also include the friction force.

From Equation VIc.5.4, we find ΔP in terms of the turbine upstream and downstream velocities $\Delta P = \rho V_a(V_1 - V_4)$. Substituting ΔP in Equations VIc.5.3, we find:

$$V_a = (V_1 + V_4)/2 \quad \text{VIc.5.5}$$

If we define parameter $\alpha = V_4/V_1$, we note that for wind turbines, $0.5 < \alpha < 1$. For $\alpha < 1$, the wake flows towards the turbine. In an airplane equipped with a propeller, $\alpha > 1$.

The energy equation. To obtain the maximum power delivered to the wind turbine, we treat the incoming wind toward the blades as a jet having a flow area equal to the swept area of the propeller. Hence, the maximum power delivered to the impeller is:

$$\dot{W}_{available} = \frac{dE_{wind}}{dt} = \frac{d}{dt} \left(\frac{mV_1^2}{2} \right) = \left(\frac{1}{2} \right) \left[\frac{dm}{dt} V_1^2 + m \frac{dV_1^2}{dt} \right] = \frac{\dot{m}V_1^2}{2} \quad \text{VIc.5.6}$$

where the derivative of the wind velocity, for constant flow of wind, is zero. If we substitute for the wind mass flow rate, we find the wind power delivered to the propeller as:

$$\dot{W}_{available} = \frac{\rho A V_1^3}{2} \quad \text{VIc.5.7}$$

Having the rate of energy delivered to the propeller, we need to find the rate of energy extracted by the propeller to find the turbine efficiency. To find the latter, we use Equation VIc.5.4 in conjunction with the definition of power:

$$\dot{W}_{extracted} = FV = [\rho V_a A (V_1 - V_4)] V_a \quad \text{VIc.5.8}$$

where F is substituted from Equation VIc.5.4.

Turbine efficiency. We may find efficiency by dividing Equation VIc.5.8 by Equation VIc.5.7. However, we are more interested in finding the maximum efficiency, which requires the calculation of the maximum extracted work. The latter is found by taking the derivative of Equation VIc.5.8 and setting it equal to zero. To take the derivative of Equation VIc.5.8, we first substitute for V_a from Equation VIc.5.5:

$$\dot{W}_{extracted} = [\rho A (V_1 - V_4)] (V_1 + V_4)^2 / 4 \quad \text{VIc.5.9}$$

By taking the derivative of Equation VIc.5.9 with respect to V_4 and setting it equal to zero, we find that the maximum power is extracted if $V_4 = V_1/3$. The maximum extracted power is then obtained by substituting this result into Equation VIc.5.9:

$$(\dot{W}_{\text{extracted}})_{\max} = \frac{8}{27} \rho A V_1^3 \quad \text{VIc.5.10}$$

Having the maximum extracted power, we can now find the maximum efficiency from Equations VIc.5.7 and VIc.5.10:

$$(\eta_{\max})_{\text{windmill}} = \left(\frac{8}{27} \rho A V_1^3 \right) / \left(\frac{1}{2} \rho A V_1^3 \right) = \frac{16}{27} = 59.3\%$$

The result indicates that even at the ideal conditions (i.e., with no friction) this wind turbine can only extract about 60% of the wind energy.

Example VIc.5.3. A wind turbine is exposed to 50 mile/h wind. Wind speed downstream of the propeller is 40 mile/h. The propeller, consisting of two blades, has a diameter of 40 ft. Assume ideal gas and standard condition for air to find a) the thrust on the wind turbine, b) the power delivered to the wind turbine, c) the maximum power extracted by the wind turbine, and d) the wind turbine maximum efficiency.

Solution: First find the air speed in ft/s; $V_1 = 50 \times 5280/3600 = 73.3$ ft/s and $V_2 = 58.7$ ft/s. Next we find:

$$V_a = 0.5 (73.3 + 58.7) = 66 \text{ ft/s.}$$

The swept area is $A = \pi D^2/4 = \pi \times 40^2/4 = 1256.6 \text{ ft}^2$ and the air density is:

$$\rho = P/RT = 14.7 \times 144 / [(1535/28.97) \times (460 + 60)] = 0.077 \text{ lbm/ft}^3.$$

$$\text{a) } F = \rho V_a A (V_1 - V_4) = 0.077 \times 66 \times 1256.6 (73.3 - 58.7) / 32.2 = 2896 \text{ lbf}$$

$$\text{b) } \dot{W}_{\text{available}} = \rho A V_1^3 / 2 = 0.077 \times 1256.6 \times 73.3^3 / 64.4 = 0.592 \text{E6 ft}\cdot\text{lbf/s} = 0.8 \text{ MW}$$

$$\text{c) } \dot{W}_{\text{extracted}} = [\rho V_a A (V_1 - V_4)] V_a = [0.077 \times 66 \times 1256.6 (73.3 - 58.7)] \times 66 / 32.2 = 0.26 \text{ MW}$$

$$\text{d) } \eta = 0.26 / 0.8 = 32\%$$

6. Analysis of Turbojets for Propulsion

In Chapter I, various types of gas turbines for aircraft propulsion were described. In Chapter IIb, we discussed the air-standard cycle for reaction engines, and in Example IIb.1.7, we used the processes of an air-standard cycle to find the gas velocity at the exit of a turbojet for a specified sets of conditions. Our goal in this chapter is to find the thrust developed by various types of turbojets.

Derivation of Thrust for Aircraft Propulsion:

Shown in Figure VIc.6.1 are schematics of a turbojet, a turbofan, and a turboprop. The free stream properties are shown with subscript i . Let's first consider the control volume representing the turbojet. Air enters this control volume at velocity V_i ,

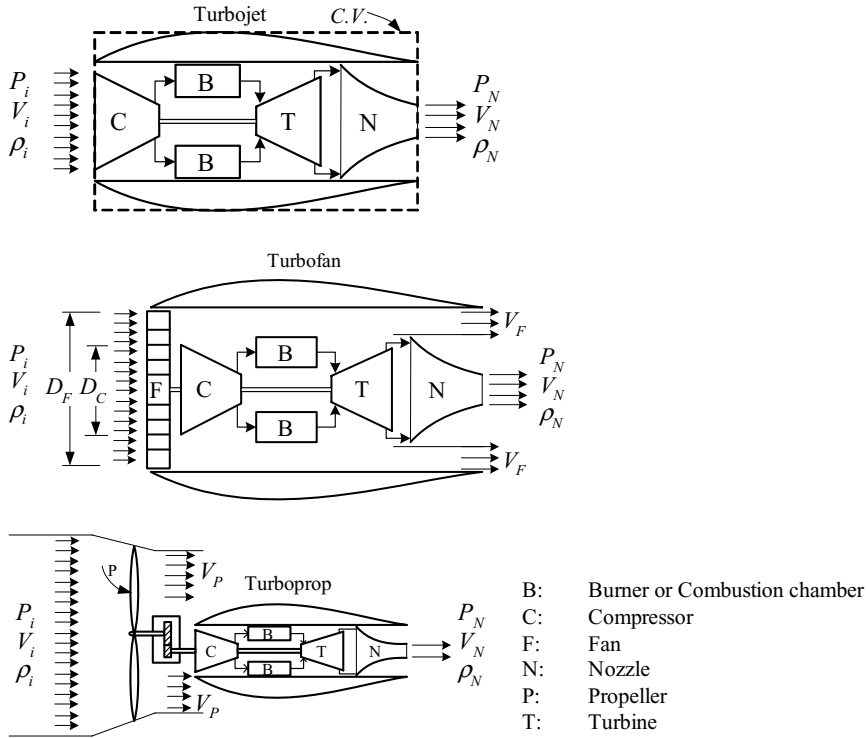


Figure VIc.6.1. Schematics of turbojet, turbofan, and turboprop

pressure P_i , and density ρ_i . These properties at the exit of the nozzle are V_N , P_N , and ρ_N , respectively. To obtain the thrust developed by this engine, we use the integral form of the conservation equations of mass (Equation IIa.5.1) and linear momentum (Equation IIIa.3.6). In this derivation, we are interested in calculating the engine thrust for steady state conditions. Therefore, the time dependent terms cancel out. Thus, the net forces acting on the control volume are balanced by the momentum flux. The net forces include such surface forces as the thrust on the engine and the pressure force at the inlet and exit of the control volume. We then write Equation IIIa.3.6 as:

$$F_x + (P_i - P_{atm})A_C - (P_N - P_{atm})A_N = \dot{m}_e V_e - \dot{m}_i V_i$$

Note that we assumed fuel enters the combustion chamber normal to the flow of air, hence it does not contribute to the momentum along the x -axis. The difference between the mass flow rates at the inlet and exit is due to the contribution of the fuel injected into the combustion chamber.

Example VIc.6.1. Air enters a turbojet at 500 km/h, 90 kPa, and a mass flow rate of 22 kg/s. Fuel enters the combustion chamber at a rate of 0.45 kg/s. The exhaust gases leave the nozzle at 2000 km/h and 130 kPa. Find the thrust on this engine. Other data: $P_{atm} = 100$ kPa, $A_C = 0.16$ m², $A_N = 0.08$ m². Ignore the momentum of the fuel entering the control volume.

Solution: For the control volume encompassing the engine:

$$F_{x,E} + (P_i - P_{atm})A_C - (P_N - P_{atm})A_N = (\dot{m}_i + \dot{m}_f)V_e - \dot{m}_i V_i$$

where subscripts E and f stand for engine and fuel, respectively. Substituting values, we find:

$$F_{x,E} = -(90 - 100) \times 0.16 + (130 - 100) \times 0.08 + (22 + 0.45) \times (2E6 / 3600) - 22 \times (0.5E6 / 3600) = 9417 \text{ N}$$

In turbfans and turboprops, the thrust developed by the engine is primarily due to the action of the fan and the propeller, respectively. Thus, in the case of turbfans and turboprops, we use the conservations of energy in addition to the conservation equations of mass and momentum. We write the conservation equation of energy for a control volume encompassing the fan or the propeller. The flow velocity exiting the fan or the propeller is then calculated from the energy equation for the specified rate of shaft work based on the power delivered to the fan or the propeller.

QUESTIONS

- To pump highly viscous liquids, do you use rotodynamic pumps or positive displacement pumps?
- Is a centrifugal pump a radial-type or an axial-type pump?
- What is a driver or a prime mover? Give three examples of a prime mover.
- What does total dynamic head of a pump represent?
- When are two centrifugal pumps homologous?
- Why do we try to find non-dimensional groups and what are the applications of the similarity rules?
- What is the significance of specific speed? A centrifugal pump has a specific speed of 500. What is the relation of head and flow to a similar pump but with specific speed of 1000?
- Why are the reactor coolant pumps in PWRs located on the cold legs and not the hot legs?
- Is it fair to say that operating the centrifugal pumps at the best efficiency point reduces impeller erosion?
- What are the four quadrants for pump operation? In which quadrant does a pump act like a turbine?

- What is the difference in head and flow rate between the impulse and the reaction type turbines?
- What type of turbine is a Pelton wheel?
- A hydropower plant has 100 m of head available to be used for power production. Is a Pelton wheel suitable for this purpose? What type of hydraulic turbine do you recommend?
- Consider two turbines producing identical power. One uses a Pelton wheel and the other a Kaplan type propeller. Which turbine has higher flow rate?
- What type of turbine do you use for a flow rate of $50 \text{ m}^3/\text{s}$ at a head of 10 m?
- Can a wind turbine of horizontal axis design achieve an efficiency of 65%?
- How is the engine thrust calculated in turbofans?
- How is the engine thrust calculated in turboprops?

PROBLEMS

1. A charging pump in a PWR plant operates at a volumetric flow rate of $\dot{V} = 44 \text{ GPM}$ (166.5 lit/min) at a head of $H = 7000 \text{ ft}$ (2134 m). What is the type of this pump?
2. A pump delivers water from a reservoir, which is open to atmosphere. Water level in the reservoir and the pump centerline are at elevations of 40 ft and 35 ft, respectively. Find the static suction head of the pump. [Ans.: 39 ft].
3. A pump is delivering water at atmospheric pressure to an elevation of 400 m. Elevation of the pump centerline is -10 m . Find the static discharge head. [Ans.: 444 ft].
4. The main feedwater pump of a PWR delivers water to the steam generator at a rate of 15,000 GPM (946.3 lit/s). The steam generator pressure is 900 psia (6.2 MPa). The difference between the discharge and the pump centerline elevation is 100 ft (30.48 m). Find the pump static discharge head. Water temperature is 450 F (232.2 C). [Ans.: 2600 ft (792.5 m)].
5. A pump delivering water at a temperature of 400 F (204.4 C) and a rate of 12,000 GPM (757 lit/s) to a pressurized vessel at 1000 psia. The discharge piping is 135 ft (41.15 m) long schedule 40 stainless steel, and nominal pipe size of 20 in (7.874 cm). Find the total dynamic discharge head.
6. A 3 horsepower compressor, circulating air at 20 C and a head of 20 m. Find the mass flow rate of the circulating air.
7. Use the data of Example VIc.3.1 and the definition of flow coefficient, head coefficient, and power coefficients to show that: $\eta_{\text{pump}} = C_{\dot{V}} C_H / C_{\dot{W}}$.
8. The rigorous way of calculating the pump specific speed is to use:

$$N'_s = C_{\dot{V}_o}^{1/2} / C_{H_o}^{3/4}$$

where $C_{\dot{V}_o}$ and C_{H_o} are the flow and head coefficients corresponding to the point of best efficiency. Use Equation VIc.3.2 to show that the specific speed, using the

customary definition (N_s) is related to N'_s as $N_s = 17182N'_s$. Also show that N_s or N'_s represents an entire family of pumps regardless of size or speed.

9. Using the performance curve of pump A given in Example VIc.3.2 (41.5" and 710 rpm) and find:

a) total dynamic head of a similar pump (pump B), at peak efficiency, having a diameter of 35 inches. Assume that both pumps A and B are operating at the same speed.

b) pump head if pump B is now operating at 1170 rpm. [Ans.: a) $H = 192$ ft and b) $H = 521.5$ ft].

10. A pump delivers 500 GPM water with a suction line 6 in. diameter. The reservoir is pressurized with to 17 psia. The required $NPSH_R$ is 15 ft. Due to the use of a filter and several bends on the suction line, the total loss coefficient adds up to $K = 35$. a) Find the maximum distance between pump centerline and water surface in the tank. Water is at 80 F for which, $\rho = 62.5$ lbm/ft³ and $\mu = 2.1$ lbm/ft-h. b) Find the $NPSH_A$ if the pump is located 5 ft below the source reservoir water level. [Ans.: a) 5 ft and b) 25 ft].

11. The rated conditions (at the point of best efficiency) of a centrifugal pump, having an impeller diameter of 40 in, are $\dot{V}_1 = 22000$ GPM, $N_1 = 700$ rpm, $N_s = 2000$, and $\eta_1 = 82\%$. To increase the flow rate, a 1000 rpm electric motor is suggested to replace the current prime mover. Find head brake horsepower and the size of the current and the replacement prime movers. $\rho_{\text{water}} = 62.4$ lbm/ft³.

[Ans.: $H_1 = 193.7$ ft (59 m), $\dot{W}_{BHP-1} = 1077$ hp, $\dot{W}_{PM-1} = 1313.4$ hp, $H_2 = 395.2$ ft (120.5 m), $\dot{W}_{BHP-2} = 3139$ hp, $\dot{W}_{PM-2} = 3832.6$ hp. Note, the available electric motors may not necessarily match the horsepower calculated. In such cases, the next largest standard size motor should be selected.]

12. A centrifugal pump is used for water delivery through a pipe having a diameter of 15.25 cm and total length of 61 m. Water level elevations of the source and the receiving reservoirs, both measured from the sea level, are 100 m and 103 m, respectively. There are losses due to pipe entrance, pipe exit and an elbow fitting with related loss coefficients of 0.5, 1.0, and 1.5, respectively. For the pump characteristic data given below, find flow rate and if this is a reasonably appropriate pump for this application.

Flow Rate (lit/s):	0	25	38	50	76	88	114	140
Pump Head (m):	27	26	25.8	24.7	22.8	21.3	18.3	14.3
Efficiency (%):	0	30	42	53	73	80	84	80

[Ans. 101 lit/s at 24 m].

13. The pump in Example VIc.3.1 is used to deliver water to a height of 110 ft above the source reservoir. Total pipe length is 600 ft and the pipe diameter is 14 in. The pipe run includes a fully open gate valve and 2 threaded 90 elbows.

a) Find the flow rate, b) How do you maximize efficiency? [Ans. a) $\dot{V} = 18,655$, and b) $N = 1432$ rpm].

14. Solve problem 3 for $\Delta Z = 50$ ft, $D = 16$ in, and $L = 500$ ft. All other data remain the same. [Ans. a) $\dot{V} = 28,880$, b) $N = 392$ rpm].

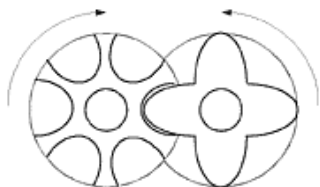
15. A pump delivering water at a rate of 100,000 GPM. The maximum available NPSH is 50 ft. Find the maximum speed to avoid cavitation.

16. In Example VIc.5.1, we derived the efficiency of a Pelton wheel in terms of V_w , V_t , and β . Use a deflection angle of 165° , $V_w = \sqrt{2gH}$, and $V_t = \omega R$, as shown in Figure VIc.5.1 and show that the Pelton wheel works most effectively when running at half the speed of the jet of water. Find the maximum efficiency. Comment on the actual Pelton wheel efficiency.

[Ans.: $\eta_{\max} = 97\%$. $\eta_{\text{actual}} < \eta_{\max}$ due to the involved frictions].

17. Find the maximum power produced by a Pelton wheel. The jet diameter is 10.45 in and the available head is 2,200 ft. [Ans.: Maximum power is the power delivered to the jet at a $C_v = 1$. Hence, $V_j = 376.4$, $A_j = 0.596$ ft², $\dot{W}_{in} = 56,000$ hp].

18. A screw-type reciprocating compressor having helically-grooved rotors is shown in the figure. Mention two advantages associated with this design. [Ans.: Pulse free and compact].



19. An impulse turbine is used to produce power from an available head of 500 m and flow rate of 100,000 GPM. Find the diameter of the jet and the maximum power that can conceivably be produced by the turbine.

[Ans.: $A_j = \dot{V} / \sqrt{2gH}$ and $(\dot{W}_j)_{\max} = \rho A_j V_j^3 / 2$].

20. An impulse turbine is operating at $h = 700$ m and $\dot{V} = 150,000$ gpm. The Pelton wheel has a diameter of 20 ft and rotating at 300 rpm. Find the power produced and the efficiency of the turbine. $C_v = 0.94$.

[Ans.: $V_j = 385.6$ ft/s, $V_t = V_j/2$].

21. An impulse turbine operating at a net head of 2000 ft uses a Pelton wheel of diameter 12 ft and a jet flow area of 5 in. Find the turbine power corresponding to the best efficiency. Use velocity coefficient of 0.94 and a bucket angle of 165° .

[Ans.: $V_j = 337$ ft/s, $V_t = 169$ ft/s, $\dot{V} = 45.95$ ft³/s].

- 22.** Use the Bernoulli equation and show that, for a wind turbine, the wind velocity is the arithmetic average of the velocity upstream and downstream of the propeller.
- 23.** Wind is approaching a wind turbine at 27 mph, as shown in Figure VIc.5.3. The wake wind has a velocity of 15 mph. Find a) the wind velocity at the blade and b) the corresponding power extracted by the turbine.
- 24.** A wind turbine has a diameter of 34 m and a power output of 350 kW at a wind velocity of 12.5 m/s. Find the efficiency of this turbine. Assume air at 27 C. [Ans. 33.6%].
- 25.** A wind turbine having an efficiency of 35% and rotor diameter of 33 m is exposed to air flowing at a speed of 6 m/s. Find the power developed by the turbine. Assume $\rho = 1.2 \text{ kg/m}^3$. [Ans.: 38.8 kW].
- 26.** A two-blade wind turbine is exposed to 60 mile/h wind. Downstream of the propeller the wind speed is 45 mile/h. The propeller has a diameter of 45 ft. Assume ideal gas and standard condition for air to find a) the thrust on the wind turbine, b) the power delivered to the wind turbine, c) the maximum power extracted by the wind turbine, d) the maximum efficiency obtained from this wind turbine.
- 27.** A two-blade wind turbine is installed on top of a hill experiencing winds of up to 80 mile/h. Downstream of the propeller the wind speed is 50 mile/h. Assume ideal gas and standard condition for air and find the tip to tip diameter of the propeller to obtain a theoretical efficiency of 50%.

VId. Simulation of Thermofluid Systems

In this chapter we study the response of such systems as reactor coolant pump (RCP), pressurizer, steam generator, containment, and the reactor coolant system (RCS) of a PWR to imposed transients. We begin by introducing some pertinent terms used in computer simulation and analysis of reactor thermal hydraulics.

1. Definition of Terms

Mathematical model refers to the application of the fundamental and constitutive equations to represent a physical phenomenon.

Computational cell is a control volume for which the physical phenomena are considered and mathematical models are developed. Since single-phase or two-phase fluid may flow through a computational cell, we need to identify the number of unknowns and set up a number of equations. For single-phase flow in a cell, there are five unknowns namely, P , T , V_x , V_y , and V_z . There are also five equations, conservation equation of mass, conservation equation of energy, and three conservation equations of momentum.

For two-phase flow through the cell, there are ten unknowns namely, P , T_l , T_v , $(V_x)_l$, $(V_y)_l$, $(V_z)_l$, $(V_x)_v$, $(V_y)_v$, $(V_z)_v$, and void fraction (α). Similarly, there are also ten equations consisting of two conservation equations of mass, two conservation equation of energy, and six conservation equations of momentum. Other unknowns are found from constitutive equations.

Node is the same as a computational cell. For the flow of water in a pipe, for example, we may divide the length L of the pipe into N sections. Therefore, the pipe now consists of N nodes, each having a length of $l = L/N$. For single-phase flow through the node, one pressure and one temperature would represent the entire node regardless of its size. Therefore, the higher the number of the nodes, the higher the amount of information obtained for the nodalized system. Pressure is generally calculated at the center of the node.

Node constituents in general may include several fluid fields such as continuous liquid, mixture of steam and gas, liquid droplets, and ice. The number of unknowns and equations increases with increasing number of the cell constituents. For example, if a cell contains liquid, steam, ice, drops, and 10 different non-condensable gases, there are as many as fourteen conservation equations of mass.

Nodalization. To determine the state parameters in a system, such as the primary side of a PWR, the system is broken down into several nodes. The process is generally referred to as nodalization. Figure VId.1.1 shows a section of a system, such as a hot leg, which is divided into N nodes with $1 \leq k \leq N$.

Control volume for mass and energy is shown in Figure VId.1.1(a). In this figure, nodes shown by $k-1$, k , and $k+1$ represent three sequential control volumes for calculation of mass and energy.

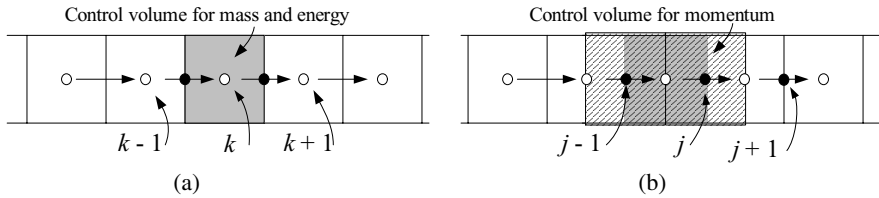


Figure VId.1.1. Nodalization of a horizontal pipe

Junctions or flow paths allow separate nodes to communicate. Hence, the mass and energy control volumes are connected together by junctions. Figure Id.1.1(b) shows junction j connecting the mass and energy control volume k to the mass and energy control volume $k + 1$.

Control volume for momentum. We may assign a control volume to node j extending from the center of node k to the center of node $k + 1$. This constitutes the control volume for the conservation of momentum for this one-dimensional flow. Momentum properties are calculated for this control volume. The most notable property calculated at node j is the flow velocity. Therefore, while pressure and temperature are calculated at the center of the mass and energy control volume, flow velocity is calculated at the junction.

Donor cell can be explained by considering two computational cells exchanging mass, momentum, and energy. The convective properties entering the receiving cell from the upstream cell are those of the upstream or so called donor cell. In Figure VId.1.1 for example, the enthalpy entering node k from node $k - 1$ is the enthalpy of node $k - 1$. Since there is no gradient inside a node, the enthalpy at the junction between nodes $k - 1$ and k is the same as enthalpy at the center of node $k - 1$.

Field, component, and phase. In Chapter IIIa and IIIb we dealt with homogeneous fields (all water, all air, etc.) In general, fields may also be heterogeneous (Chapter IIIc). Consider for example, a vapor consisted of steam and several non-condensable gases. Each of the constituents is referred to as a component of the field. Phase, on the other hand, is the various forms of the same substance such as ice, water, steam, mist, and drop.

Two-flow field model (two-fluid model) refers to the treatment of the flow fields in a computational cell. Assuming only water and steam exist in the cell, ten conservation equations are used in the two-fluid model to describe the conditions in the cell. Thus, in this mathematical model, water and steam can be at different temperatures flowing at different velocities.

HEM or the homogenous equilibrium model, refers to the treatment of the fluid in a computational cell. Assuming only water and steam exist in the cell, the two phases are assumed to be at thermodynamic equilibrium. Thus, both phases flow at the same velocity in the same direction having the same temperature.

SEM or the separated equilibrium model refers to a deviation from the HEM, by the introduction of the slip ratio. This in turn requires the inclusion of the in-

ter-phase friction force in the momentum equation. In both HEM and SEM the mixture properties such as ρ and u are obtained through the use of void fraction.

2. Mathematical Model for a PWR Loop

Determination of such parameters as pressure, temperature, and velocity in systems involving fluid flow and heat transfer is generally an involved task. A nuclear reactor is an example of a thermofluid system for which it is important to determine such parameters by mathematical modeling. For this reason many computer codes are developed to study various operational aspects of a nuclear power plant. For example, several codes are devised to evaluate the thermal hydraulic characteristics of only the reactor core. Among the computer codes developed to analyze the reactor coolant system are RELAP, RETRAN, and TRAC. In this section, we study the mathematical model based on the HEM for analysis of the reactor coolant system. A nodalization example of a two-loop PWR is show in Figure Vid.2.1.

Control volumes for mass and energy (shown with subscripts k and $k + 1$) and for momentum (shown with subscript j) are shown in Figure Vid.2.2 for constant and variable area channels. The conservation equations of mass, momentum, and

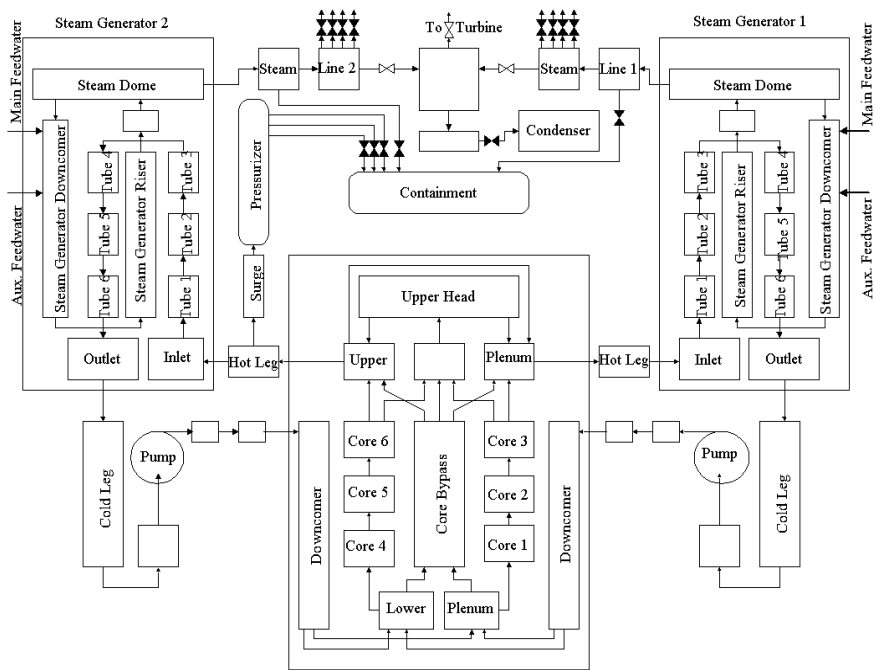


Figure Vid.2.1. Nodal diagram of a two-loop PWR primary side

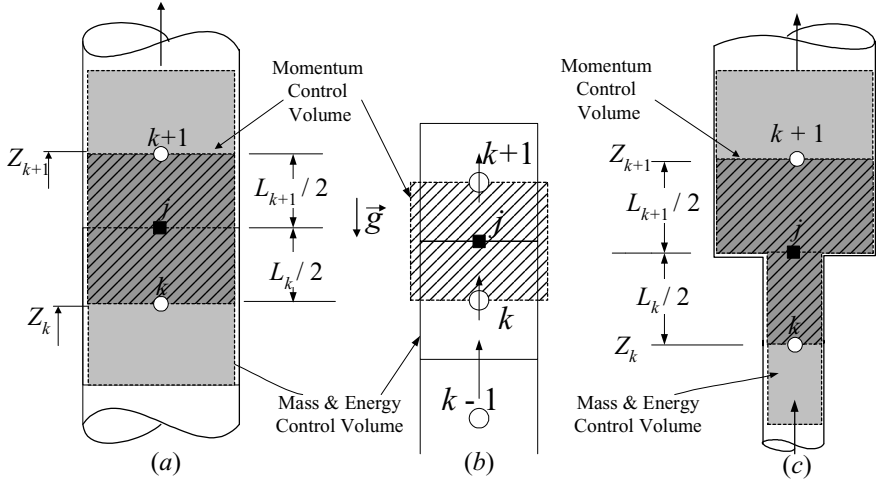


Figure VId.2.2. Mass, energy, and momentum control volume for channels with fixed or variable flow area

energy are described here. The area change plays no role for the conservation of mass and energy equations but the conservation equation of momentum, which is more involved, must consider the variable area channel. For node k , the conservation equation of mass, Equation IIa.5.1 can be written as:

$$\frac{d(\rho_m V)}{dt} = \sum_{inlet} (\rho V A) - \sum_{exit} (\rho V A) \quad \text{VId.2.1}$$

where $\rho_m = (1 - \alpha)\rho_f + \alpha\rho_g$ and α is given by Equation Va.1.3. We may also write Equation VId.2.1 as:

$$\frac{dM_k}{dt} = \dot{m}_{j-1} - \dot{m}_j \quad \text{VId.2.1-1}$$

The conservation equation of energy as given by Equation IIa.6.4 becomes:

$$\frac{dU_k}{dt} = \dot{m}_{j-1} \left[h_{j-1} + \frac{1}{2} \frac{\dot{m}_{j-1}^2}{\rho_{j-1}^2 A_{j-1}^2} + g(z_{j-1} - z_k) \right] - \dot{m}_j \left[h_j + \frac{1}{2} \frac{\dot{m}_j^2}{\rho_j^2 A_j^2} + g(z_k - z_j) \right] + \dot{Q}_k \quad \text{VId.2.2}$$

where in Equation VId.2.2, we ignored the rate of change in the kinetic energy as compared with the internal energy. Equation VId.2.2 includes enthalpy terms developed at the junctions. For fine nodalization, with good degree of approximation, we may use $h_{j-1} = h_{k-1}$ and $h_j = h_k$. This is consistent with the donor cell ap-

proach. However, there are certain nodes that require special treatment such as heated nodes within which density and enthalpy change substantially.

The one-dimensional momentum equation for the mixture can be readily obtained by applying Equation IIIa.3.44 to the variable channel area of Figure Vid.2.2. The momentum control volume is centered at j and it extends from $L_k/2$ and $L_{k+1}/2$. Substituting for various pressure drop terms, for the lower segment we get:

$$\frac{L_k}{2A_k} \frac{d\dot{m}_j}{dt} = -(P_j - P_k) + \left(\frac{\dot{m}_j^2}{\rho_k A_k^2} - \frac{\dot{m}_k^2}{\rho_k A_k^2} \right) + \frac{M_{k/2}}{A_k} g + f_k \phi \frac{L_k}{2D_k} \frac{\dot{m}_k |\dot{m}_k|}{2\rho_k A_k^2} + K_j \phi \frac{\dot{m}_j |\dot{m}_j|}{2\rho_j A_j^2}$$

where ϕ is the two-phase friction multiplier, as defined in Chapter VI. Now, we apply Equation IIIa.3.44 to the portion of the momentum control volume extending from j , right after the change in flow area to point $k+1$:

$$\frac{L_{k+1}}{2A_{k+1}} \frac{d\dot{m}_j}{dt} = -(P_{k+1} - P_j) + \left(\frac{\dot{m}_{k+1}^2}{\rho_{k+1} A_{k+1}^2} - \frac{\dot{m}_j^2}{\rho_{k+1} A_{k+1}^2} \right) + \frac{M_{(k+1)/2}}{A_{k+1}} + f_{k+1} \phi \frac{L_{k+1}}{2D_{k+1}} \frac{\dot{m}_{k+1} |\dot{m}_{k+1}|}{2\rho_{k+1} A_{k+1}^2} + K_j \frac{\dot{m}_j |\dot{m}_j|}{2\rho_j A_j^2}$$

Adding these equations, the result for the one dimensional momentum equation for variable area channel becomes:

$$\left[\frac{L_k}{2A_k} + \frac{L_{k+1}}{2A_{k+1}} \right] \frac{d\dot{m}_j}{dt} = \Delta P_{pump} - [(P_{k+1} - P_k) + \left(\frac{\dot{m}_{k+1}^2}{\rho_{k+1} A_{k+1}^2} - \frac{\dot{m}_k^2}{\rho_k A_k^2} \right) - \left(\frac{1}{A_{k+1}^2} - \frac{1}{A_k^2} \right) \frac{\dot{m}_j^2}{2\rho_j}] - \left(\frac{M_{(k+1)/2}}{A_{k+1}} - \frac{M_{k/2}}{A_k} \right) g + \phi \left(f_k \frac{L_k}{2D_k} \frac{\dot{m}_k |\dot{m}_k|}{2\rho_k A_k^2} + f_{k+1} \frac{L_{k+1}}{2D_{k+1}} \frac{\dot{m}_{k+1} |\dot{m}_{k+1}|}{2\rho_{k+1} A_{k+1}^2} + K_j \frac{\dot{m}_j |\dot{m}_j|}{2\rho_j A_j^2} \right)$$

Vid.2.3

Example Vid.2.1. Start with Newton's second law and derive Equation Vid.2.3.

Solution: The momentum equation expresses that the net momentum flux to or from a control volume plus the rate of change of momentum in the control volume is equal to the net external forces acting on the control volume. We now apply this principle to a differential control volume located between z and $z + dz$. This control volume has a flow area of A and a hydraulic diameter of D_e . External

forces are the body force and the surface forces. Hence, the net force acting on the control volume becomes:

$$\sum dF = A(P_z - P_{z+dz}) - s\rho(Adz)g - \phi\left(f\frac{dz}{D_e} + K\right)\frac{\dot{m}|\dot{m}|}{2\rho A}$$

where s is introduced to account for the flow direction. For upward flow $s = +1$, for horizontal flow, $s = 0$, and for downward flow $s = -1$. The absolute value for flow rate signifies the fact that the friction force acts always opposite to the flow direction. Hence using the convention of $\dot{m} > 0$ for up-flow, the friction force becomes negative i.e., $\vec{F} = -|F|\vec{k}$. Similarly for down-flow ($\dot{m} < 0$), the friction force would act in the direction of the z -axis, $\vec{F} = |F|\vec{k}$. Accounting for the rate of change in momentum flux, the rate of change of momentum of the control volume is therefore given by:

$$\frac{\partial \dot{m}}{\partial t} dz = A(P_z - P_{z+dz}) - s\rho(Adz)g - \phi\left(f\frac{dz}{D_e} + K\right)\frac{\dot{m}|\dot{m}|}{2\rho A} - \left[\left(\frac{\dot{m}^2}{\rho A}\right)_{z+dz} - \left(\frac{\dot{m}^2}{\rho A}\right)_z\right]$$

We now divide both sides of this equation by Adz and let dz approach zero:

$$\frac{1}{A} \frac{\partial \dot{m}}{\partial t} = -\frac{\partial P}{\partial z} - s\rho g - \phi f \frac{1}{D_e} \frac{\dot{m}|\dot{m}|}{2\rho A^2} - \frac{1}{A} \frac{\partial(\dot{m}^2 / \rho A)}{\partial z}$$

We may apply this equation to the control volume of Figure VI d.2.2(c), which is located between elevations Z_k and Z_{k+1} . To obtain the momentum equation for this control volume, we multiply both sides of this equation by dz and integrate the resulting equation first over the portion of the momentum control volume extending from k to j right before the flow area changes. Integration over the lower portion of the control volume yields:

$$\int_k^j \frac{1}{A} \frac{d\dot{m}}{dt} dz = -(P_i - P_k) - \int_k^j (s\rho g dz) - \int_k^j \frac{\phi}{2} \frac{f}{D_e} v_f \frac{\dot{m}^2}{A^2} dz - \int_k^j \frac{1}{A} d\left(\frac{\dot{m}^2 v}{A}\right)$$

Term by term integration is carried out as follows:

$$\int_k^j \frac{1}{A} \frac{d\dot{m}}{dt} dz \approx \frac{L_k}{2A_k} \frac{d\dot{m}_j}{dt}$$

$$\int_k^j s\rho g dz = \frac{sL_k g}{2\bar{v}} = \frac{sM_k g}{2A_k}$$

$$\int_k^j \frac{\phi}{2} \frac{f}{D_e} v_f \frac{\dot{m}^2}{A^2} dz = \frac{1}{2} \bar{\phi}(\bar{f}) \frac{L_k}{2D_{e,k}} + \sum_k K) \bar{v}_f \frac{\dot{m}_j |\dot{m}_j|}{A_k^2}$$

$$\int_k^j \frac{1}{A} d\left(\frac{\dot{m}v}{A}\right) = \frac{\dot{m}_j^2 v_j}{A_k^2} - \frac{\dot{m}_k^2 v_k}{A_k^2}$$

Adding up terms we get:

$$\frac{L_k}{2A_k} \frac{d\dot{m}_i}{dt} = -(P_j - P_k) - \frac{sL_k g}{2\bar{v}_k} - (f_k \frac{L_k}{2D_{e,k}} + \sum K_k) \bar{v}_k \frac{\dot{m}_k |\dot{m}_k|}{2A_k^2} - \left(\frac{\dot{m}_j^2 v_j}{A_k^2} - \frac{\dot{m}_k^2 v_k}{A_k^2} \right)$$

We now apply the resulting equation to the portion of the momentum control volume extending from j , right after the change in flow area, to point $k+1$, yielding:

$$\begin{aligned} \frac{L_{k+1}}{2A_{k+1}} \frac{d\dot{m}_i}{dt} = & -(P_{k+1} - P_j) - \frac{sL_{k+1} g}{2\bar{v}_{k+1}} - (f_{k+1} \frac{L_{k+1}}{2D_{e,k+1}} + \sum K_{k+1}) \bar{v}_{k+1} \frac{\dot{m}_{k+1} |\dot{m}_{k+1}|}{2A_{k+1}^2} \\ & - \left(\frac{\dot{m}_{k+1}^2 v_{k+1}}{A_{k+1}^2} - \frac{\dot{m}_j^2 v_j}{A_{k+1}^2} \right) \end{aligned}$$

Adding these equations, to get the one dimensional momentum equation for variable area channels:

$$\begin{aligned} \left[\frac{L_k}{2A_k} + \frac{L_{k+1}}{2A_{k+1}} \right] \frac{d\dot{m}_j}{dt} = & \Delta P_{pump,k} - [(P_{k+1} - P_k) + \frac{s_i(L_k + L_{k+1})g}{2\bar{v}_i} + \\ & \left(\frac{\dot{m}_{k+1}^2 v_{k+1}}{A_{k+1}^2} - \frac{\dot{m}_k^2 v_k}{A_k^2} \right) - \left(\frac{1}{A_{k+1}^2} - \frac{1}{A_k^2} \right) \frac{\dot{m}_j^2 \bar{v}_j}{2} \\ & + \phi \left(f_k \frac{L_k}{2D_{e,k}} \bar{v}_{f,i} \frac{\dot{m}_k |\dot{m}_k|}{2A_k^2} + f_{k+1} \frac{L_{k+1}}{2D_{e,k+1}} \bar{v}_{f,i} \frac{\dot{m}_{k+1} |\dot{m}_{k+1}|}{2A_{k+1}^2} + \sum K_i \bar{v}_i \frac{\dot{m}_j |\dot{m}_j|}{2A_j^2} \right)] \end{aligned}$$

This equation includes a pressure rise term in case there is a pump in the flow path. This equation while derived for single-phase flow is applied to two-phase mixture with the introduction of the multiplier ϕ and \bar{v} .

Equations VId.2.1, VId.2.2, and VId.2.3 constitute a set of differential equations in mass, internal energy, and mass flow rate. Writing similar sets for the rest of the nodes would result in a system of differential equations, which upon solution would result in obtaining the key parameters versus time. The initial conditions are found from the steady state operation prior to the imposition of a transient.

3. Simplified PWR Model

The level of information obtained from a mathematical model depends on the extent of complexities used in the model such as the multi-dimensional analysis of multi-component flow. We may introduce a variety of simplifying assumptions to reduce the computational burden and obtain results with reasonable accuracy. However, simplifying assumptions impose limitations on the applicability of the model. An example of a simplifying assumption is the application of an integral or loop-wide momentum equation. This assumption decouples the solution of the momentum equation from the mass and energy equations. To see the saving in the number of equations, consider a case where there are N nodes in each loop of Figure Vid.2.1. According to the model developed in Section 2, there are a total of $6N$ equations for the N nodes. By writing an integral momentum equation for each loop, the number of equations drops to $2N + N'$ where N' is the number of loops. An integral momentum equation ignores the compressibility of fluid due to the local pressure changes and assumes that the pressure and velocity disturbances are propagated at infinite velocity. This allows us to assign one pressure to the entire RCS and one loop flow rate to each loop.

Let's now obtain the set of equations for node k (Figure Vid.3.1) using the above simplifying assumption. For this purpose, we consider the various interactions with node k . Flow may enter this node from several inlet ports (shown with subscript i) and leaves from several exit ports (shown with subscript e). These are

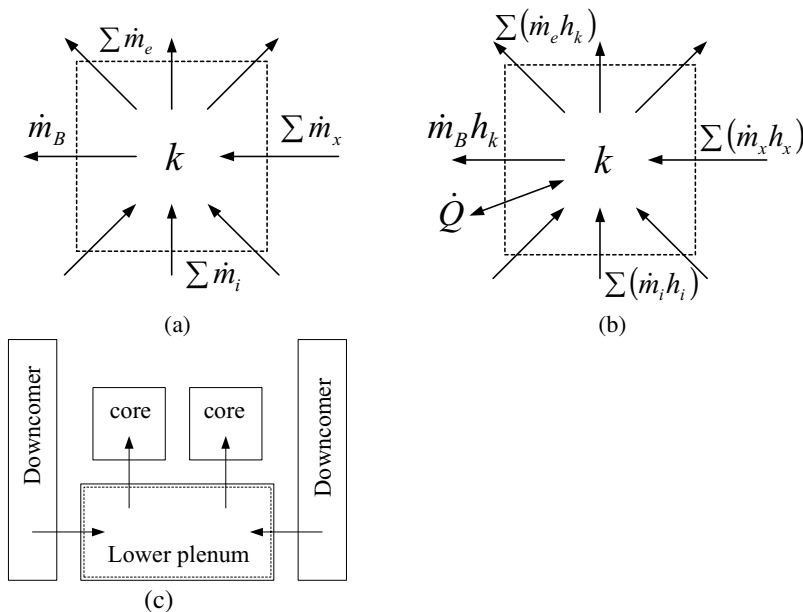


Figure Vid.3.1. (a) mass and (b) energy transfer for a typical node. (c) Example of a multi-port node

the inter-nodal flow rates. Node k may also receive flow from external sources (shown by subscript x), such as safety injection. This node may also discharge flow if a pipe break (shown with subscript B) happens to occur at this node. Not all these flow rates exist simultaneously or for all the nodes. However, we are considering them for the sake of generality. The conservation equation of mass, Equation IIa.5.1 for node k becomes:

$$\frac{dm_k}{dt} = \sum (\dot{m}_i)_k - \sum (\dot{m}_e)_k + \sum (\dot{m}_x)_k - (\dot{m}_B)_k \quad \text{VId.3.1}$$

Similarly, the conservation equation of energy, Equation IIa.6.4-1 for the node becomes:

$$\frac{d(m_k h_k)}{dt} = \sum (\dot{m}_i h_i)_k - \sum (\dot{m}_e h_k)_k + \sum (\dot{m}_x h_x)_k - \dot{m}_B h_k + \sum \dot{Q}_k + V_k \dot{P}_{RCS} \quad \text{VId.3.2}$$

Note that the work term includes only the pressure work as there is no shaft work and the shear work is ignored. Taking the derivative of the left side, substituting from the conservation equation of mass, and rearranging, yields:

$$m_k \dot{h}_k = [\sum (\dot{m}_i h_i)_k - h_k \sum (\dot{m}_i)_k] - [\sum (\dot{m}_x) h_k - \sum (\dot{m}_x)_k h_x] + \sum \dot{Q}_k + c V_k \dot{P}_{RCS} \quad \text{VId.3.3}$$

where c in Equation VId.3.3 is a conversion factor. We now use the volume constraint for node k , given the fact that V_k remains constant hence, $dV_k/dt = 0$:

$$\frac{dV_k}{dt} = \frac{d}{dt} (m_k v_k) = \dot{m}_k v_k + m_k \dot{v}_k = 0$$

The derivatives can be expanded in terms of the RCS pressure (P_{RCS}) and the node enthalpy (h_k):

$$\dot{m}_k v_k + m_k \left(\left. \frac{\partial v_k}{\partial h_k} \right|_{P_{RCS}} \dot{h}_k + \left. \frac{\partial v_k}{\partial P} \right|_{h_k} \dot{P}_{RCS} \right) = 0 \quad \text{VId.3.4}$$

Substitute from Equations VId.3.1 and VId.3.3, we obtain:

$$\begin{aligned} (v_k - h_k \frac{\partial v_k}{\partial h_k}) \sum (\dot{m}_i)_k + \frac{\partial v_k}{\partial h_k} \sum (\dot{m}_i h_i)_k - v_k \sum (\dot{m}_e)_k + (c V_k \frac{\partial v_k}{\partial h_k} + m_k \frac{\partial v_k}{\partial P}) \dot{P}_{RCS} = \\ (\dot{m}_B)_k v_k - \left[\frac{\partial v_k}{\partial h_k} \sum \dot{Q}_k + (v_k - h_k \frac{\partial v_k}{\partial h_k}) \sum (\dot{m}_x)_k + \frac{\partial v_k}{\partial h_k} \sum (\dot{m}_x h_x)_k \right] \end{aligned} \quad \text{VId.3.5}$$

This is the general form of the *mass-energy algorithm* for loops using an integral momentum equation. In this relation, the unknowns are inter-nodal flow rates and RCS pressure. These can be determined for specified break flow rate, rate of heat transfer to the node, and the external flow rates and enthalpies.

3.1. Determination of Nodal Flow Rates In a One Loop PWR

To demonstrate the application of the mass-energy algorithm, Equation Vid.3.5 is applied to a one-loop PWR as shown in Figure Vid.3.2. By using the donor cell concept, the algorithm simplifies to:

$$\left[v_k + \frac{\partial v_k}{\partial h_k} (h_{k-1} - h_k) \right] \dot{m}_{k-1} - v_k \dot{m}_k + \left(c V_k \frac{\partial v_k}{\partial h_k} + m_k \frac{\partial v_k}{\partial P} \right) \dot{P}_{RCS} =$$

$$(\dot{m}_B)_k v_k - \left[\frac{\partial v_k}{\partial h_k} \sum \dot{Q} + \left(v_k - \frac{\partial v_k}{\partial h_k} (h_x - h_k) \right) \sum (\dot{m}_x)_k \right]$$

Vid.3.6

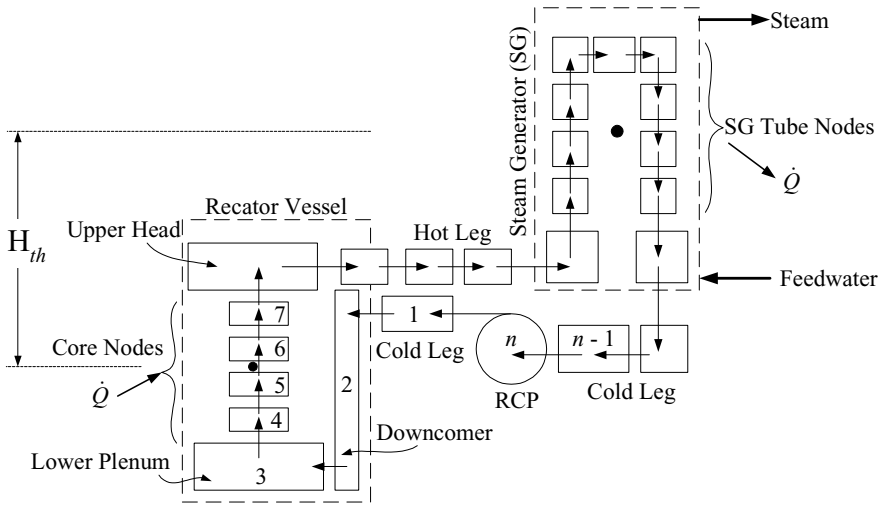


Figure Vid.3.2. A one-loop PWR, obtained by collapsing all the loops into one loop

Equation Vid.3.6 can be simply shown as:

$$\eta_k \dot{m}_{k-1} + \gamma_k \dot{m}_k + \delta_k \dot{P}_{RCS} = \varepsilon_k$$

where the coefficients η_k , γ_k , δ_k , and ε_k in this equation represent:

$$\begin{aligned}\eta_k &= v_k + \frac{\partial v_k}{\partial h_k}(h_{k-1} - h_k), \\ \gamma_k &= -v_k, \\ \delta_k &= c v_k \frac{\partial v_k}{\partial h_k} + m_k \frac{\partial v_k}{\partial P}, \text{ and} \\ \varepsilon_k &= (\dot{m}_B)_k v_k - \left\{ \frac{\partial v_k}{\partial h_k} \Sigma \dot{Q}_k + \left[v_k + \frac{\partial v_k}{\partial h_k}(h_x - h_k) \right] \Sigma (\dot{m}_x)_k \right\}\end{aligned}$$

We start from the discharge section of the cold leg as node 1. In this case, the flow entering this node is from the reactor coolant pump (RCP). Applying the mass-energy algorithm to all n nodes of the RCS, the following matrix equation is obtained:

$$\begin{bmatrix} \gamma_1 & 0 & 0 & 0 & \cdots & 0 & \delta_1 \\ \eta_2 & \gamma_2 & 0 & 0 & \cdots & 0 & \delta_2 \\ 0 & \eta_3 & \gamma_3 & 0 & \cdots & 0 & \delta_3 \\ 0 & 0 & \eta_4 & \gamma_4 & \cdots & 0 & \delta_4 \\ \vdots & \vdots & \vdots & \vdots & \ddots & \vdots & \vdots \\ \vdots & \vdots & \vdots & \vdots & \vdots & \gamma_{n-1} & \delta_{n-1} \\ 0 & 0 & 0 & 0 & \cdots & \gamma_n & \delta_n \end{bmatrix} \begin{bmatrix} \dot{m}_1 \\ \dot{m}_2 \\ \dot{m}_3 \\ \dot{m}_4 \\ \vdots \\ \dot{m}_{n-1} \\ \dot{P}_{RCS} \end{bmatrix} = \begin{bmatrix} \varepsilon_1 - \eta_1 \dot{m}_{RCP} \\ \varepsilon_2 \\ \varepsilon_3 \\ \varepsilon_4 \\ \vdots \\ \varepsilon_n - \gamma_n \dot{m}_{RCP} \end{bmatrix} \quad \text{VId.3.7}$$

At any time step, the thermodynamic properties and their derivatives are obtained from the equation of state by having the two independent variables of pressure and enthalpy of the previous time step. Hence, for a given pump flow rate, the RCS pressure and the inter-nodal flow rates are obtained from Equation VId.3.7 in an explicit manner. Subsequent to the calculation of the inter-nodal flow rates, nodal mass derivatives are found from back substitution of flow rates into the nodal conservation equations of mass. Upon integration over the time step this process yields the new nodal mass:

$$m_k^{N+1} = m_k^N + [\Sigma (\dot{m})_k + \Sigma (\dot{m}_x)_k - (\dot{m}_B)_k] \times \Delta t$$

Nodal enthalpy derivatives are determined from Equation VId.3.3 by using the calculated mass flow rates and the RCS pressure derivative as well as the updated nodal mass. The nodal enthalpies and the RCS pressure are then determined by explicit integration of the above quantities at the end of each time step. For example, the nodal enthalpy becomes $h_k^{N+1} = h_k^N + \dot{h}_k \times \Delta t$ and the RCS pressure $P_{RCS}^{N+1} = P_{RCS}^N + \dot{P}_{RCS} \times \Delta t$. This process is continued until the specified total

transient time is reached. In steady state operation, where no external flow or break flow rate exists, from Equation Vid.3.1 we find:

$$\dot{m}_{k-1} = \dot{m}_k = \dot{m}_{RCP}$$

Similarly, for each node from Equation Vid.3.2 we obtain the following energy balance:

$$\dot{Q}_k + \dot{m}_{RCP}(h_{k-1} - h_k) = 0$$

3.2. Integral Momentum Equation for a Multi-loop PWR

The primary side of a PWR may consist of two, three, four, or six loops. An integral momentum equation for loop L , for example, is obtained by integrating Equation IIIa.3.44 around the loop, which includes the reactor vessel:

$$\sum_L \left(\frac{L}{A} \right)_L \frac{d\dot{m}_L}{dt} + \sum_V \left(\frac{L}{A} \right)_V \frac{d\dot{m}_V}{dt} = (\Delta P_{pump,L}) - \left[\oint (\rho \bar{g} \cdot d\vec{s}) + \sum_{loop} (\Delta P_{fric,L}) + \Delta P_{fric,V} \right]$$

Vid.3.8

where subscripts L and V stand for Loop and vessel, respectively. We now evaluate various terms in the right side of Equation Vid.3.8, i.e. the friction pressure drop, the hydrostatic pressure head, and the pump head.

3.3. Friction Pressure Drop

The vessel and the rest of the loop friction pressure drops consists of skin friction and pressure losses at bends, the core support plate, the grid spacers, upper plenum, upper internals, entrance to hot leg, entrance to steam generator plenum, tubesheet, etc. As we did in Equation Vid.2.3, we also consider a two-phase friction multiplier for cases where subcooling is lost and a two-phase mixture is flowing in the primary side. Calculation of the loss coefficients is discussed in Chapter IIIb. The loss coefficients for components used exclusively in the nuclear industry, such as the fuel rod grid spacers used in a specific design, are provided by the nuclear reactor vendor. However, we may use the correlation suggested by Rust to estimate pressure drop due to the fuel rod grid spacers as:

$$\Delta P_{grid} = \frac{C_v \varepsilon \dot{m} |\dot{m}|}{2 \rho A^2}$$

where ε is the ratio of the projected grid spacer cross section to undisturbed flow cross section and C_v is the drag coefficient, in turn estimated from $C_v = 54.91 |\dot{m}|^{-0.0245}$.

3.4 Hydrostatic Pressure Head

The hydrostatic head in Equation Vid.3.8 represents the body force due to gravity. During normal operation when forced convection is the dominant flow regime, the hydrostatic force is negligible compared to such pressure forces as friction pressure drop and pressure rise over the pump. However, in thermal loops having natural circulation flow regime, the hydrostatic head is the driving force. The hydrostatic head then becomes:

$$\oint (\rho \vec{g} \cdot d\vec{s}) = \sum_{L+V} [(\rho_k g \Delta Z_k) \cos(\alpha_k)] \quad \text{Vid.3.9}$$

where in Equation Vid.3.9 the summation is over the vessel and other regions in the loop. These regions, as shown in Figure Vid.3.2, include downcomer, lower plenum, core, upper plenum, hot leg, steam generator, and cold leg. In this equation, α is the angle between the velocity vector and the vector representing the acceleration of gravity. Hence, $\cos(\alpha_k)$ is the same as index s introduced in Example Vid.2.1. For upward flow in the core, $\alpha_k = \pi$ and $\cos(\alpha_k) = -1$, for horizontal flow in the hot leg, $\alpha_k = \pi/2$ and $\cos(\alpha_k) = 0$, and for downward flow in the downcomer, $\alpha_k = 0$ and $\cos(\alpha_k) = 1$. In Equation Vid.3.9, ΔZ_k is the difference between the exit and the inlet elevations to a given region hence, $\Delta Z_k = Z_e - Z_i$.

Determination of the hydrostatic head where change in the liquid is linear is straightforward. For example in the core, Figure Vid.3.3(a), assuming a near linear density profile, the hydrostatic head becomes:

$$\int_{\text{Core inlet}}^{\text{Core exit}} (\rho \vec{g} \cdot d\vec{s}) = [(\rho_{\text{core}} g H_{\text{core}}) \cos(\alpha_{\text{core}})]_i^e = -\frac{(\rho_i + \rho_e)}{2} g H_{\text{core}}$$

Determination of the hydrostatic head in the steam generator is more involved. In the following example we evaluate the hydrostatic head for the single-phase flow inside the tubes of a U-tube steam generator. As shown in Figure Vid.3.3(b), the height of each leg of the average tube is l and the length of the horizontal section is δ , so the average tube length becomes $L = 2l + \delta$.

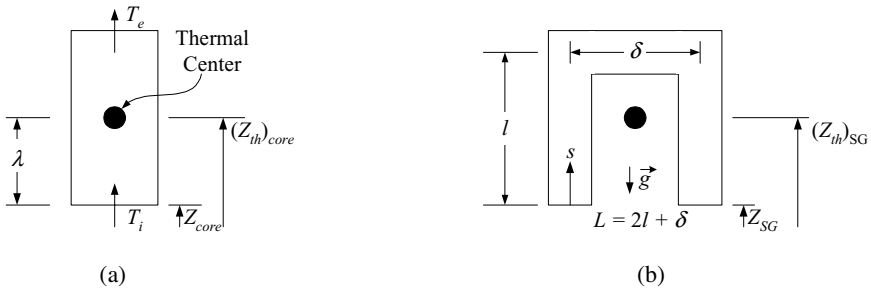


Figure Vid.3.3. Nodes representing (a) core and (b) tubes of a U-tube steam generator

Example VId.3.1. Develop the hydrostatic head for flow of water in the tubes of a U-tube steam generator. Flow enters tubes at pressure P and temperature T_H and leaves at temperature T_C . The tube average length is L .

Solution: To find the hydrostatic head in the steam generator, we find the following:

$\int_0^L [\rho(s) - \rho_H] \bar{g} \cdot d\bar{s} = \int_0^l [\rho(s) - \rho_H] \bar{g} \cdot d\bar{s} + \int_{l+\delta}^L [\rho(s) - \rho_H] \bar{g} \cdot d\bar{s}$ with respect to Figure VId.3.3(b). Since in the upward leg $\cos(\pi) = -1$ and in the downward leg $\cos(0) = 1$, we can write:

$$\int_0^L [\rho(s) - \rho_H] \bar{g} \cdot d\bar{s} = - \int_0^l [\rho(s) - \rho_H] g ds + \int_{l+\delta}^L [\rho(s) - \rho_H] g ds$$

We do not have the density profile to integrate. However, we have the temperature profile from Equation VIa.5.8 given as $T(s) = T_{sat} + (T_H - T_{sat}) e^{-s/l^*}$ where s is an element of length along the tube. To bridge the gap and relate the density difference to temperature difference, we use the definition of the thermal expansion coefficient of Chapter IIa, $\beta = -[(\partial\rho/\partial T)_P]/\rho$. It is assumed that β remains constant in the temperature range of T_C to T_H and β is approximated as $\beta \approx \Delta\rho/\Delta T$ or $\Delta\rho = \rho\beta\Delta T$. Thus, the integral becomes:

$$\int_0^L [\rho(s) - \rho_H] \bar{g} \cdot d\bar{s} = \beta g \rho_H (T_H - T_{sat}) \left\{ \int_0^l (1 - e^{-s/l^*}) ds + \int_{l+\delta}^L (1 - e^{-s/l^*}) ds \right\}$$

The integral of the argument is found as: $\int (1 - e^{-s/l^*}) ds = s + l^* e^{-s/l^*}$, subject to the limits 0 to l and $l + \delta$ to L :

$$\int_0^L [\rho(s) - \rho_H] \bar{g} \cdot d\bar{s} = \beta g \rho_H (T_H - T_{sat}) \left\{ - \left(l + l^* e^{-l/l^*} - l^* \right) + \left(L + l^* e^{-L/l^*} - (l + \delta) - l^* e^{-(l+\delta)/l^*} \right) \right\}$$

simplifies to:

$$\int_0^L [\rho(s) - \rho_H] \bar{g} \cdot d\bar{s} = \beta g \rho_H (T_H - T_{sat}) l^* \left(1 - e^{-l/l^*} - e^{-(l+\delta)/l^*} + e^{-L/l^*} \right).$$

Substituting from Equation (2), we get:

$$\int_0^L [\rho(s) - \rho_H] \bar{g} \cdot d\bar{s} = \beta g \rho_H (T_H - T_{sat}) l^* \left(1 - e^{-l/l^*} - e^{-(l+\delta)/l^*} + e^{-L/l^*} \right).$$

Replacing $T_H - T_{sat}$ with $T_H - T_C$, yields:

$$\int_0^L [\rho(s) - \rho_H] \bar{g} \cdot d\bar{s} = \beta g \rho_H (T_H - T_C) l^* \left(1 - e^{-l/l^*} - e^{-(l+\delta)/l^*} + e^{-L/l^*} \right) \left(1 - e^{-L/l^*} \right) \quad \text{VId.3.10}$$

Two-Phase Flow in Tubes. In Example Vid.3.1, we found the hydrostatic head for single-phase inside tubes. In the case of two-phase flow in the tubes, we must use the mixture density as defined in Chapter V, $\rho_m = (1 - \alpha)\rho_f + \alpha\rho_g$ where α is given by Equation Va.1.3 as $\alpha = X/(aX + b)$. Therefore, the hydrostatic head becomes:

$$\int_{SG} (\rho_m \bar{g} \cdot d\bar{s}) = \int_0^L \left(\rho_f + \frac{(\rho_g - \rho_f)X}{aX + b} \right) \bar{g} \cdot d\bar{s} \quad \text{Vid.3.11}$$

All we need to do now is to find the profile for flowing quality in the tubes. This is accomplished by using an energy balance in an elemental length of the tube, ds to obtain:

$$\dot{m} dh = -N \pi d_o U_o [T_{sat}(P_{primary}) - T_{sat}(P_{secondary})] ds$$

Substituting for $dh = h_{fg} dX$ in the above equation allows us to solve for $dX/ds = -N \pi d_o U_o [T_{sat}(P_{primary}) - T_{sat}(P_{secondary})] / \dot{m} h_{fg} = l_{2phase}^*$. We now integrate the result, which yields $X = l_{2phase}^* s + X_{in}$. Having the quality profile, we then substitute into Equation Vid.3.11 and integrate. The final answer depends on the length of the boiling section (L_B) i.e. whether $L_B < l$, of $l < L_B < l + \delta$, or $l + \delta < L_B < L$. For example if $L_B < l$ then the hydrostatic head becomes:

$$\int_0^{L_B} (\rho_m \bar{g} \cdot d\bar{s}) = -g \int_0^{L_B} \left(\rho_f + \frac{(\rho_g - \rho_f)(l_{2phase}^* s + X_{in})}{a(l_{2phase}^* s + X_{in}) + b} \right) ds = g l_{2phase}^* \left[a_1 x - a_2 \ln \frac{aX_{in} + b}{b} \right]$$

where $a_1 = \rho_f - (\rho_g - \rho_f)/a$ and $a_2 = (\rho_g - \rho_f)b/a^2$. Then from L_B to L we use the single-phase integral of Equation Vid.3.10. The solutions for all these cases are obtained by Kao.

Thermal Center. We now define a node property referred to as *thermal center*. In lumped nodes, the thermal center may be viewed as a point at which the heat transfer process takes place. For example, consider the node representing the core or the steam generator U-tubes in Figure Vid.3.3. Thermal center for these nodes may be defined as:

$$\lambda = \frac{\int_0^L [T(s) - T_H] ds}{T_C - T_H} \quad \text{Vid.3.12}$$

where λ is measured from the entrance to the node. For the core node, it is trivial to show that for linear temperature rise in the core, the thermal center is located at $\lambda_{core} = L_{core}/2$. Determination of the thermal center for the steam generator node, where temperature profile is not linear, is similar to the method used in Example Vid.3.1. For U-tube steam generators it can be shown (see Problem 2) that:

$$\lambda_{SG} = \frac{1 - e^{-l/l^*} - e^{-(l+\delta)/l^*} + e^{-L/l^*}}{1 - e^{-L/l^*}} l^* \quad \text{VId.3.13}$$

If we now substitute λ_{SG} into Equation VId.3.10, we obtain the steam generator hydrostatic head as:

$$\int_0^L [\rho(s) - \rho_H] \bar{g} \cdot d\bar{s} = \int_0^L \rho(s) \bar{g} \cdot d\bar{s} = \beta g \rho_H (T_H - T_C) \lambda_{SG}$$

Example VId.3.2. Find the distance to the thermal center of a steam generator from the tube sheet. Tube-side data: $\dot{m} = 61\text{E}6$ lbm/h, $c_p = 1.4$ Btu/lbm F, $N = 8485$, $d_o = 0.75$ in, $U_o = 1040$ Btu/h ft² F, $L = 56$ ft, $l = 26$ ft, average length of the U-tube horizontal section $\delta = 4$ ft, cold leg temperature $T_C = 550$ F, hot leg temperature $T_H = 600$ F.

Solution: According to Example VIa.6.2, $l^* = \dot{m} c_p / (\pi N d_o U_o)$. Therefore, l^* is found as:

$$l^* = 61\text{E}6 \times 1.4 / [\pi \times 8485 \times (0.75/12) \times 1040] = 49.3 \text{ ft.}$$

We now use Equation VId.3.13:

$$\lambda_{SG} = \frac{1 - e^{-l/l^*} - e^{-(l+\delta)/l^*} + e^{-L/l^*}}{1 - e^{-L/l^*}} l^* = \frac{1 - e^{-26/49.3} - e^{-(26+4)/49.3} + e^{-56/49.3}}{1 - e^{-56/49.3}} \times 49.3 = 13.57 \text{ ft}$$

This is almost equal to $l/2$. Indeed as $l^* \rightarrow \infty$, $\lambda_{SG} = 0.5(1 + \delta/L)l$.

Having the height of the core and the steam generator thermal centers, we can then find their corresponding elevations by adding the heights to the elevation of the bottom of the core and the tube sheet, respectively. Hence, $(Z_{th})_{core} = Z_{core} + \lambda_{core}$ and $(Z_{th})_{SG} = Z_{SG} + \lambda_{SG}$. These are shown in Figure VId.3.3.

The discussion on the hydrostatic head in a flow loop demonstrates that the hydrostatic head is primarily a function of the loop geometry and the working fluid density gradient. Therefore in flow loops, the hydrostatic force is given as:

$$\oint_{Loop} (\rho \bar{g} \cdot d\bar{s}) = (\rho_C - \rho_H) g H_{th} \quad \text{VId.3.14}$$

where H_{th} in Equation VId.3.14 is the difference between the steam generator and the core thermal centers given by $H_{th} = (Z_{th})_{SG} - (Z_{th})_{core}$. Note that elevations of the core and steam generator thermal centers are measured from a common reference.

Example Vid.3.3. Find the pressure difference due to the buoyancy force in a flow loop. Data: $P = 2250$, $T_{Hot} = 600$ F, $T_{Cold} = 550$ F, $Z_{Heat\ Sink} = 61$ ft, $Z_{Heat\ Source} = 31$ ft. Working fluid is water.

Solution: We use Equation Vid.3.14 to estimate $\Delta P_{gravity} = (47.2 - 43.1) \times (61 - 31) = 0.85$ psi.

3.5. Natural Circulation in Flow Loops

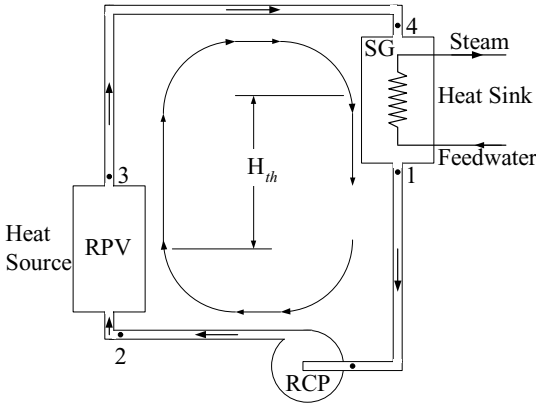
Natural circulation is the preferred mode of operation when the enhancement of the passive safety features, such as elimination of any pump failure, is a design requirement. Some high rise buildings use natural circulation for the heating of their units. This is accomplished by heating water in a boiler located in the basement resulting in warm water flowing upward inside the riser. As water passes various floors it deposits energy to heat the space. The colder and heavier water then flows downward and back to the boiler, pushing the warmer water upward. Hence, a necessary condition for establishment of natural circulation is that $H_{th} > 0$.

To estimate the natural circulation flow rate, we start with the single-loop of Figure Vid.3.4 and use Equation Vid.2.3. Since this equation is obtained for a single node, we integrate it over all the nodes comprising the loop. By doing so, the static pressure difference term cancels out. Integrating Equation Vid.2.3 is equivalent to summing up all the terms of Equation IIIa.3.44 around the loop. This results in:

$$\sum_{k=1}^n \left(\frac{L}{A} \right)_k \frac{d\dot{m}}{dt} = \Delta P_{pump} - \sum_{k=1}^n \bar{\rho}_k g (Z_{j+1} - Z_j)_k - \frac{\dot{m}^2}{2} \sum_{k=1}^n \frac{1}{\bar{\rho}_k} \left(\frac{1}{A_{j+1}^2} - \frac{1}{A_j^2} \right)_k - \frac{\dot{m}^2}{2} \sum_{k=1}^n \frac{1}{\bar{\rho}_k A_k^2} \left(f \frac{L}{D} + K \right)_k$$

Vid.3.15

where in the case of Figure Vid.3.4, $n = 5$. Equation Vid.3.15 can be simplified by noting that in a natural circulation loop, the pump head is zero. Note that the pump head being zero does not necessarily mean that there is no pump in the loop. Rather, the pump is simply not operating. A loop without a pump has by far less frictional losses than an identical loop but equipped with a pump that is turned off. This is because in the latter case, the working liquid must flow through the pump volute and among the blades of the impeller. The losses due to friction in pumps depend on the type of the pump and whether the impeller is locked or is free to spin. For example, for the canned-motor pump of the LOFT (Reeder) experiment, the loss coefficient for the free spinning impeller with flow in forward direction (from pump suction to pump discharge) was estimated to be $K = 3$, for flow in the reverse direction $K = 12$, and for flow through the pump with impeller locked $K = 20$.



Number	Name	A (ft ²)	L (ft)	D _h (ft)	K
1 - 2	Cold Leg	20	174	3.2	1
2 - 3	Heat Source	37	18	0.43	11
3 - 4	Hot Leg	20	75	3.0	1
4 - 1	Steam Generator	19.5	66	0.05	6

Figure VId.3.4. Schematics of a single-loop PWR primary side and related data

Returning to Equation VId.3.15, we may also ignore the pressure drop term due to the velocity change. Thus, in steady state operation, Equation VId.3.15 simplifies to:

$$\frac{\dot{m}^2}{2} \sum_{k=1}^n \frac{1}{\bar{\rho}_k A_k^2} \left(f \frac{L}{D} + K \right)_k = - \sum_{k=1}^n \bar{\rho}_k g (Z_{j+1} - Z_j)_k \approx (\rho_c - \rho_H) g H_{th} \quad \text{VId.3.16}$$

The left side of Equation VId.3.16 may be shown as $\dot{m}R/2\bar{\rho}$ where $R = \sum [(f_k L_k / D_k) + K_k] / A_k^2$, known as the loop *flow resistance*. In the right side of Equation VId.3.16, we made use of Equation VId.3.14 for the hydrostatic head. If we relate the density difference ($\Delta\rho$) to the corresponding temperature difference (ΔT) by $\Delta\rho \approx \beta\rho\Delta T$, assuming constant β in the temperature range of T_c to T_H , Equation VId.3.16 becomes:

$$\frac{1}{2} R \frac{\dot{m}^2}{\bar{\rho}} = \bar{\rho} \beta g H_{th} \Delta T \quad \text{VId.3.17}$$

The change in temperature in the loop is due to the rate of heat addition in the heat source (core) or the rate of heat rejection in the heat sink (steam generator). Therefore, from a steady state energy balance over the heat source, for example

we find that, $\dot{Q} = \dot{m} c_p (T_H - T_c)$. Substituting for ΔT we obtain the natural circulation flow rate in steady state operation as:

$$\dot{m}_{NC} = \left(\frac{2\beta g \bar{\rho}^2 H_{th} \dot{Q}_{Core}}{c_p R} \right)^{1/3} \quad \text{VId.3.18}$$

Equation VId.3.18 provides a reasonable estimate for the natural circulation flow rate provided that the system resistances are closely approximated and the flow regime is turbulent (see Problem 16).

Example VId.3.4. Find the natural circulation flow rate using the data of the simplified PWR loop shown in Figure VId.3.4. Core power during shutdown is 5 MW. Data: $f = 0.01$, $\bar{\rho} = 45 \text{ lbm/ft}^3$, $c_p = 1.3 \text{ Btu/lbm}\cdot\text{F}$, $\beta = 0.001 \text{ R}^{-1}$, $(Z_{th})_{SG} = 60 \text{ ft}$, $(Z_{th})_{RPV} = 30 \text{ ft}$.

Solution: We must first find the loop flow resistance using the specified friction factor of 0.01. Substituting values in $R_k = (f_k L_k / D_k + K_k) / A_k^2$ yields:

$$R_{1-2} = 3.86\text{E-}3 \text{ ft}^{-4}, R_{2-3} = 8.34\text{E-}3 \text{ ft}^{-4}, R_{3-4} = 3.12\text{E-}3 \text{ ft}^{-4}, \text{ and } R_{4-1} = 0.05 \text{ ft}^{-4}.$$

Thus, $\Sigma R = 0.065 \text{ ft}^{-4}$. We now substitute values into Equation VId.3.18:

$$\dot{m}_{NC} = \left(\frac{2 \times 0.001 \times 32.2 \times 45^2 \times (60 - 30) \times (5,000 \times 3412 / 3600)}{1.3 \times 0.065} \right)^{1/3} = 603 \text{ lbm/s}$$

Having determined the hydrostatic pressure head and the natural circulation flow rate we now proceed to deal with the pump head.

4. Mathematical Model for PWR Components, Pump

In Section 3, we used the pump flow rate as a known function. In this section, we want to find how such a function can be obtained. To find the pump speed, we apply the conservation equation of angular momentum to the impeller of a centrifugal pump. Assuming the prime mover is an electric motor, the electric torque (T_E) must provide for the hydraulic torque (T) and the frictional torque (T_F). The net torque according to Newton's second law is then equal to the moment of inertia times the rate of change of the impeller angular velocity:

$$T_E - T - T_F = I \frac{d\omega}{dt} \quad \text{VId.4.1}$$

where I in Equation VIId.4.1, represents the moment of inertia of the pump shaft, impeller, and flywheel. The electric torque delivered by the prime mover is a known quantity. If the pump is turned off, the electric torque drops exponentially as:

$$T_E = T_{E0} \frac{\omega}{\omega_0} e^{(-2t/\tau_e)}$$

where the rated electric torque, T_{E0} is provided by the electric motor manufacturer. Also τ_e is the electric motor decay constant, which accounts for the inertia of the electric motor. To obtain an instantaneous loss of the applied torque, the decay constant may be set equal to a small value such as $0.1 \mu s$. The hydraulic torque, T , due to the momentum transfer from the pump impeller to the liquid is obtained from the pump homologous curves as discussed in Chapter VIc. Finally, the frictional and windage torque, T_F accounts for all the losses in the contact points in such places as the bearings and the pump seals. The frictional and the windage torques may be correlated to the pump speed ratio by fitting a curve to pump coastdown data.

4.1. Implementation of Pump Model in Momentum Equation

Determination of flow rate as a function of time due to pump startup or shutdown in a multi-loop PWR requires simultaneous solution of the conservation equation of momentum, for the fluid, and conservation equation of angular momentum for the pump impeller. The momentum equation for the fluid is written as:

$$\sum_L \frac{L_k}{A_k} \frac{d\dot{m}_k}{dt} + \left(\frac{L}{A}\right)_V \frac{d\dot{m}_V}{dt} = F(\dot{m}_k, \omega_k, \dot{m}_V) \quad \text{VIId.4.2}$$

where \dot{m}_V represents flow rate through the vessel, being the common flow path, i.e. $\dot{m}_V = \sum_L \dot{m}_k$ where the summation is for the total number of loops. Function F , in Equation VIId.4.2, is given by the right side of Equation VIId.3.8 with pump head given by Equation VIc.4.1. Similarly, we may express Equation VIId.4.1 as:

$$\frac{d\omega_k}{dt} = G(\dot{m}_k, \omega_k)$$

If the transient is due to pump shutdown then, without the imposed electrical torque, the flow rate drops to the natural circulation flow rate at a rate determined by the pump inertia, pump frictional resistance, and the hydraulic torque. This set of equations can be generalized, using matrix notation for the multi-loop configuration, as:

$$A\dot{Y} = B(Y)$$

In this relation, matrix A is a square matrix. Elements of vector Y consist of all of the unknowns including the unknown loop flow rate, vessel flow area, and the pumps angular velocities:

$$Y = [\dot{m}_1, \omega_1, \dots, \dot{m}_n, \omega_n, \dot{m}_v]^T$$

and elements of vector B are:

$$B = [F_1, G_1, \dots, F_n, G_n]^T$$

To solve this set by a semi-implicit finite difference scheme, we first linearize the differential equations to set up the Jacobian matrix, which is given as $A^N \Delta Y^{N+1} = \Delta t [B(Y^N) + J^N \Delta Y^{N+1}]$ where superscript N represents the previous time step and J represents the Jacobian matrix. This equation can be rearranged to get:

$$[A - \Delta t J]^N \Delta Y^{N+1} = \Delta t B^N Y^N \quad \text{VId.4.3}$$

If we represent $[C] = [A - \Delta t J]$ then matrix $[C]$ would have the following structure:

$$[C] = \begin{bmatrix} c_{11}(1) & c_{12}(1) & 0 & 0 & 0 & 0 & 0 & 0 & c_{13}(1) \\ c_{21}(1) & c_{22}(1) & 0 & 0 & 0 & 0 & 0 & 0 & 0 \\ 0 & 0 & c_{11}(2) & c_{12}(2) & 0 & 0 & 0 & 0 & c_{13}(2) \\ 0 & 0 & c_{21}(2) & c_{22}(2) & 0 & 0 & 0 & 0 & 0 \\ 0 & 0 & 0 & 0 & c_{11}(3) & c_{12}(3) & 0 & 0 & c_{13}(3) \\ 0 & 0 & 0 & 0 & c_{21}(3) & c_{22}(3) & 0 & 0 & 0 \\ 0 & 0 & 0 & 0 & 0 & 0 & c_{11}(4) & c_{12}(4) & c_{13}(4) \\ 0 & 0 & 0 & 0 & 0 & 0 & c_{21}(4) & c_{22}(4) & 0 \\ -1 & 0 & -1 & 0 & -1 & 0 & -1 & 0 & 1 \end{bmatrix}$$

where elements of matrix C , as calculated by Kao, are given in Table VId.4.1.

Table VIc.4.1. Elements of matrix C

Element	Mathematical Expression
$c_{11}(k)$	$\sum_k (L/A)_k - \Delta t (\partial F / \partial \dot{m})_k^N$
$c_{12}(k)$	$-\Delta t (\partial F / \partial \omega)_k^N$
$c_{21}(k)$	$-\Delta t (\partial G / \partial \omega)_k^N$
$c_{22}(k)$	$1 - \Delta t (\partial G / \partial \omega)_k^N$
$c_{13}(k)$	$(L/A)_v - \Delta t (\partial F / \partial \dot{m}_v)_k^N$

In this section we found numerical solution for the loop flow rate as a function of time. Next we find analytical solutions for the loop flow rate versus time in two cases of pump imposed transients. In the first case, we assume that the pump head remains constant and is independent of flow rate and in the second case, we account for pump head being a function of the loop flow rate.

4.2. Analytical Solution for Flow Transients, Constant Pump Head

Our goal is to find an analytical solution to the loop flow rate in such transients as pump shutdown or pump start up. For now, we assume that the pump head is a weak function of flow rate so that it can be treated as a constant in the loop momentum equation. Later in this chapter, this assumption is relaxed and the pump head is treated as a function of flow rate. The pump head being a constant is a reasonable assumption in certain cases. For example, at low flow rates as shown in Figure VIc.3.1, pump head remains relatively flat and it changes rather slightly with flow rate. Another example includes cases where the pump inertia is small as compared with the loop fluid inertia, which makes an analytical albeit approximate solution possible.

To derive the analytical solution for flow transients we start with the single-loop of Figure VIId.3.4 and use Equation VIId.2.3. Since this equation is obtained for a single node, we integrate it over all the nodes comprising the loop. By doing so, the static pressure differential term cancels out. The integration of Equation VIId.2.3 is equivalent to summing up all the terms of Equation IIIa.3.44 around the loop. This results in:

$$\sum_{k=1}^n \left(\frac{L}{A} \right)_k \frac{d\dot{m}}{dt} = \Delta P_{pump} - \sum_{k=1}^n \bar{\rho}_k g (Z_{j+1} - Z_j)_k - \frac{\dot{m}^2}{2} \sum_{k=1}^n \frac{1}{\bar{\rho}_k} \left(\frac{1}{A_{j+1}^2} - \frac{1}{A_j^2} \right)_k - \frac{\dot{m}^2}{2} \sum_{k=1}^n \frac{1}{\bar{\rho}_k A_k^2} \left(f \frac{L}{D} + K \right)_k \quad \text{VIId.4.4}$$

where an average density is used for each node. For example, in the core $\bar{\rho}_{core} = (\rho_{CL} + \rho_{HL}) / 2$. Since in this example, flow area remains constant within each control volume, the summation term for the geometric inertia is simplified and is made over the five primary side nodes. Equation VIId.4.4 is a first order, linear differential equation of the following form:

$$\frac{d\dot{m}}{C_1^2 - C_2^2 \dot{m}^2} = dt \quad \text{VIId.4.5}$$

where coefficients C_1^2 and C_2^2 represent:

$$C_1^2 = \left[g_c \Delta P_{pump} + \sum_{k=1}^n \bar{\rho}_k g (Z_{j+1} - Z_j) \right] / \sum_{k=1}^n \left(\frac{L}{A} \right)_k$$

$$C_2^2 = \frac{1}{2} \left[\sum_{k=1}^n \frac{1}{\bar{\rho}_k} \left(\frac{1}{A_{j+1}^2} - \frac{1}{A_j^2} \right)_k + \sum_{k=1}^n \frac{1}{\bar{\rho}_k A_k^2} \left(f \frac{L}{D} + K \right)_k \right] / \sum_{k=1}^n \left(\frac{L}{A} \right)_k$$

To find an analytic solution for the above first order differential equation, we write it as

$$\frac{d\dot{m}}{C_1 - C_2\dot{m}} + \frac{d\dot{m}}{C_1 + C_2\dot{m}} = 2C_1 dt$$

this can be easily integrated to obtain:

$$\ln \frac{C_1 + C_2\dot{m}}{C_1 - C_2\dot{m}} = 2C_1 C_2 t + C_3 \quad \text{VId.4.6}$$

Where C_3 is the constant of integration and is determined from the initial condition. The above solution applies to both cases of pump start up in a stagnant loop and pump shutdown in a forced flow loop. The difference is in the application of the boundary condition to obtain the constant C_3 , as discussed next.

Case 1. Pump Start Up in a Stagnant Loop. Several conditions may lead to stagnation in flow loops. For example, there would be no flow if the thermal center of the heat sink is located below the thermal center of the heat source. Other examples include a flow loop with very high frictional losses resulting in insignificant rate of flow or an isothermal flow loop where $\rho_H = \rho_C$. In a stagnant loop, $\dot{m}(t=0) = 0$ hence, $C_3 = 0$. Equation VId.4.6 simplifies to:

$$\dot{m}(t) = \left(\frac{C_1}{C_2} \right) \frac{e^{2C_1 C_2 t} - 1}{e^{2C_1 C_2 t} + 1} \quad \text{VId.4.7}$$

At steady state, when $t \rightarrow \infty$, forced circulation flow rate is found as $\dot{m}_{FC} = C_1 / C_2$.

Case 2. Pump Start Up in a Natural Circulation Loop. If a flow loop with pump turned off operates in natural circulation mode then $\dot{m}(t=0) = \dot{m}_{NC}$ hence, $C_3 = \ln[(C_1 + C_2\dot{m}_{NC}) / (C_1 - C_2\dot{m}_{NC})]$. Substituting for C_3 , Equation VId.4.6 becomes:

$$\dot{m}(t) = \left(\frac{C_1}{C_2} \right) \frac{y_{NC} e^{2C_1 C_2 t} - 1}{y_{NC} e^{2C_1 C_2 t} + 1} \quad \text{VId.4.8}$$

where in Equation VId.4.8 $y_{NC} = (C_1 + C_2\dot{m}_{NC}) / (C_1 - C_2\dot{m}_{NC})$. At steady state, when $t \rightarrow \infty$, forced circulation flow rate is found as $\dot{m}_{FC} = C_1 / C_2$.

Example Vid.4.1. Consider the flow loop of Figure Vid.3.4 as described in Example Vid.3.4. We now start up the pump. Pressure rise over the pump is 50 psi. Find flow rate one second after start up and at steady state. $\rho_H = 44.5 \text{ lbm/ft}^3$ and $\rho_C = 45.5 \text{ lbm/ft}^3$.

Solution: To calculate coefficients C_1 and C_2 of Equation Vid.4.5 we find:

$$\Sigma(L/A)_k = (174/20) + (18/37) + (75/20) + (66/19.5) = 16.3 \text{ ft}^{-1}$$

$$\Sigma(\rho g \Delta Z)_k = (\rho_C - \rho_H)gH_{th} = (45.5 - 44.5) \times 32.2 \times (60 - 30) = 966 \text{ lbm-ft/s}^2$$

$$\Sigma(R/\rho)_k = (3.86\text{E-}3/45.5) + (8.34\text{E-}3/45) + (3.12\text{E-}3/44.5) + (0.05/45) = 1.45\text{E-}3 \text{ (ft-lbm)}^{-1}$$

$$C_1 = [(32.2 \times 50 \times 144 + 966)/16.3]^{1/2} = 119.5$$

$$C_2 \cong [(0.5 \times 1.45\text{E-}3)/16.3]^{1/2} = 6.7\text{E-}3$$

$$C_1 C_2 = 0.8 \text{ and } C_1/C_2 = 17,836 \text{ lbm/s}$$

$$y_{NC} = \frac{119.5 + 6.7\text{E-}3 \times 603}{119.5 - 6.7\text{E-}3 \times 603} = 1.07$$

$$\dot{m}(t) = 17,836 \frac{1.07 \exp(1.6t) - 1}{1.07 \exp(1.6t) + 1}$$

$$\dot{m}(t=1) = 17,836 \times (1.07e^{0.8} - 1)/(1.07e^{0.8} + 1) = 17,836 \times 0.41 = 7,313 \text{ lbm/s}$$

$$\dot{m}_{s-s} = 17,836 \text{ lbm/s.}$$

Case 3. Pump Shutdown in a Forced Circulation Loop. A similar solution can be found for the flow coast down due to the termination of pump operation. In this case, at time zero, the flow rate is equal to a specified steady state forced circulation flow. The intention is to obtain flow rate as a function of time after the pump is turned off. In this case, at time zero, $\dot{m} = \dot{m}_{FC}$, i.e., a known value. Therefore, for this case the constant C_3 can be determined as $C_3 = \ln[(C_1 + C_2 \dot{m}_{FC})/(C_1 - C_2 \dot{m}_{FC})]$. Substituting, the flow coastdown is found as:

$$\dot{m}(t) = \left(\frac{C_1}{C_2} \right) \frac{y_{FC} e^{2C_1 C_2 t} - 1}{y_{FC} e^{2C_1 C_2 t} + 1} \quad \text{Vid.4.9}$$

where in Equation Vid.4.9, $y_{FC} = (C_1 + C_2 \dot{m}_{FC})/(C_1 - C_2 \dot{m}_{FC})$.

In both cases of pump startup and shutdown, the integration of Equation Vid.4.6 was easily carried out due to our simplifying assumption that the pressure increase over the pump is independent of the flow rate. Next, we consider a more general case of pump pressure rise being a function of the loop flow rate.

4.3. Analytical Solution for Flow Transients, Pump Head a Function of Flow Rate

The rigorous approach that resulted in obtaining Equation Vid.4.3 requires numerical solution. Here we seek an approximate but analytical solution to the flow coastdown in a thermohydraulic loop. For this purpose we consider the reactor coolant pump in Figure Vid.3.2 being turned off. We are interested in the early part of the transient when flow is coasting down. In steady state operation, identified with subscript o, we have:

$$\frac{1}{2} \sum f_{k_o} \frac{L_k}{D_k A_k^2} \frac{\dot{m}_o^2}{\rho} = \rho g H_{p_o} + \oint \rho (\bar{g} \cdot d\bar{s}) \quad \text{Vid.4.10}$$

where H_{p_o} is the pump head in steady state. Approximating the hydrostatic force by using the thermal expansion coefficient, we get:

$$\oint \rho (\bar{g} \cdot d\bar{s}) = \rho_o g (\beta \Delta T_o Z_{th}) = \rho_o g H_{s_o} \quad \text{Vid.4.11}$$

where Z_{th} is the difference in the elevations of the heat source and heat sink thermal centers, as shown in Figure Vid.2.3, ρ_o is density at a reference temperature T_o , and H_{s_o} is the hydrostatic head at steady state. Assuming that the friction factors in the transient remain the same as in steady state and using an average flow rate for the entire loop, the momentum equation integrated over the loop yields:

$$\sum \left(\frac{L}{A} \right) \frac{d\dot{m}}{dt} = - \frac{\rho_o^2 g}{\rho} (H_{p_o} + H_{s_o}) (\dot{m} / \dot{m}_o)^2 + \rho g (H_p + H_s) \quad \text{Vid.4.12}$$

As recommended by Burgreen, we further assume that both the pump head ratio and the torque ratio in the transient will follow the same homologous curves as in steady state operation. For the pump head, using the pump affinity laws, we can then write $H_p/H_{p_o} = (\omega/\omega_o)^2$. Also noting that for the early part of the pump shut-down transient, $\rho \cong \rho_o$ and $H_s \cong H_{s_o}$, Equation Vid.4.12 simplifies to:

$$\sum \left(\frac{L}{A} \right) \frac{d\dot{V}}{dt} = -g (H_{p_o} + H_{s_o}) (\dot{V}/\dot{V}_o)^2 + g H_{p_o} (\omega/\omega_o)^2 + g H_{s_o} \quad \text{Vid.4.13}$$

For further simplification, we note that early in the flow coastdown event, the contribution to flow rate due to the natural circulation is exceedingly small. But as time goes on and the pump flywheel effect diminishes, the contribution of the hydrostatic force increases. Hence early in the event, we can assume that $H_{s_o} \cong 0$ so that:

$$I_L \frac{d\dot{V}}{dt} = -g H_{p_o} (\dot{V}/\dot{V}_o)^2 + g H_{p_o} (\omega/\omega_o)^2 \quad \text{Vid.4.14}$$

where in Equation Vid.4.14, I_L represents the loop inertia, $\Sigma(L/A)$. For pumps with negligible inertia, such as the canned motor and electromagnetic pumps, the third term in Equation Vid.4.14 can be ignored compared with the other two terms and Equation Vid.4.14 simplifies to $d\dot{V}/dt + (g H_{p_o} / I_L) (\dot{V}/\dot{V}_o)^2 = 0$. The so-

lution to this equation can be found as $t = (1/\dot{V} - 1/\dot{V}_o)\dot{V}_o^2 I_L / gH_{P_o}$. The time for flow to decay to half of its initial value, $\dot{V}_o^2 / 2$ is, therefore, found as: $(t_{1/2})_L = I_L \dot{V}_o / (gH_{P_o})$.

Returning to Equation VId.4.14, if we now define $\Phi = \dot{V} / \dot{V}_o$, $\theta = t/(t_{1/2})_L$, and $\Omega = \omega/\omega_o$ then Equation VId.4.14 simplifies to:

$$d\Phi / d\theta + \Phi^2 = \Omega^2 \quad \text{VId.4.15}$$

Having obtained the simplified form of the loop momentum equation following pump shutdown, we now turn to the impeller angular momentum given by Equation VId.4.1. Neglecting the frictional losses and noting that the electric torque goes to zero upon pump trip, we find for hydraulic torque that;

$$-T = I_p d\omega / dt \quad \text{VId.4.16}$$

Pump moment of inertia, I_p , typically consists of flywheel ($\cong 75\%$), electric motor ($\cong 23\%$), impeller ($\cong 1.5\%$) and shaft ($\cong 0.5\%$). Using the second approximation for pump break horsepower torque, $T/T_o = (\omega/\omega_o)^2$ where T_o is obtained from $T_o = \Delta P_o \dot{V}_o / (\eta_o \omega_o)$. Substituting, we find

$$d\omega/dt = -(1/I_p)T_o(\omega/\omega_o)^2 \quad \text{VId.4.17}$$

this upon integration from time zero to any time results in:

$$\frac{1}{\omega} - \frac{1}{\omega_o} = \frac{1}{I_p} \frac{T_o}{\omega_o^2} t$$

If at $(t_{1/2})_P$ we have $\omega = \omega_o/2$, then $(t_{1/2})_P = I_p(\omega_o/T_o)$. Equation VId.4.17 can then be written as $d\Omega/dt + \Omega^2/(t_{1/2})_P = 0$. Changing variable from t to θ , similar to Equation VId.4.15, Equation VId.4.17 becomes:

$$d\Omega/d\theta + \alpha\Omega^2 = 0 \quad \text{VId.4.18}$$

where parameter α in Equation VId.4.18 is given as $\alpha = (t_{1/2})_L/(t_{1/2})_P$. Equations VId.4.15 and VId.4.18 constitute a set of coupled first-order, nonlinear differential equations describing the effects of the pump on the loop flow rate. The solution to Equation VId.4.18 is obtained as:

$$\Omega = 1/(1 + \alpha\theta) \quad \text{VId.4.19}$$

Upon substituting Equation VId.4.19 into Equation VId.4.15, we obtain the governing equation during pump coastdown as:

$$d\Phi/d\theta + \Phi^2 = 1/(1 + \alpha\theta)^2 = 0 \quad \text{VId.4.20}$$

The solution to Equation VId.4.20, as offered by Burgreen, is shown graphically in Figure VId.4.1. To get a better interpretation of α , we note that the initial en-

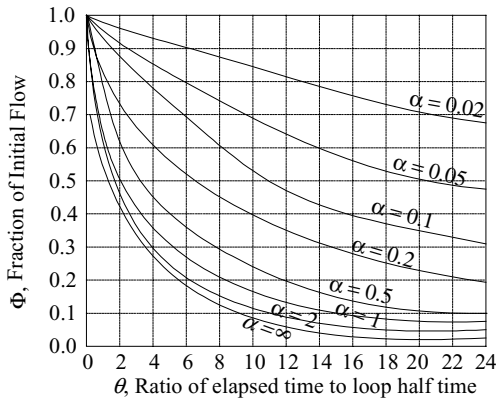


Figure Vid.4.1. Approximate fluid coastdown curves following pump shutdown

ergy stored in the pump is $E_{P0} = \frac{1}{2} I_P \omega_0^2$. Similarly, the initial stored energy in the loop circulating fluid is $E_{L0} = \frac{1}{2} \rho \Sigma (\dot{V}_0^2 / A) LA = \frac{1}{2} \rho \dot{V}_0^2 I_L$. We can now express pump and fluid half-lives in terms of their corresponding initial stored energies as

$$(t_{1/2})_P = 2E_{P0}/(T_0 \omega_0) \text{ and } (t_{1/2})_L = 2E_{L0}/[\rho g \dot{V}_0 H_{P0}]$$

Hence

$$\alpha = (t_{1/2})_P / (t_{1/2})_L = E_{L0} / (\eta_0 E_{P0})$$

where we also took advantage of the definition of pump efficiency. This relation indicates that the ratio of the fluid to pump half-lives is equal to the ratio of the fluid to pump effective initial stored energies. Expectedly, as shown in Figure Vid.5.1, if the pump flywheel contains high initial energy ($\alpha \ll 1$), reasonable amount of fluid circulates the loop following termination of the pump operation, due to the pump inertial effects. For small or no initial pump stored energy, as in the case of canned motor or electromagnetic pumps, termination of the pump operation results in rapid flow decay due to the action of the friction forces.

Example Vid.4.2. Find the coastdown flow fraction in a flow loop at 1, 5, 7 seconds into the event.

Loop Data: $I_L = \Sigma L/A = 108 \text{ ft}^{-1}$, $\Delta P_0 = 93 \text{ psi}$, $\rho_0 = 62.87 \text{ lbm/ft}^3$.

Pump Data: $T_0 = 636 \text{ ft lbf}$, $I_P = 19.5 \text{ lbm ft}^2$, $\omega_0 = 375 \text{ rad/s}$, $\eta_0 = 0.86$.

Solution: We first find volumetric flow rate at steady state:

$$\dot{V}_o = \frac{T_o \eta_o \omega_o}{\Delta P_o} = \frac{636 \times 0.86 \times 375}{93 \times 144} = 15.3 \text{ ft}^3/\text{s}$$

To find $t_{1/2}$, we note that $H_{P_o} = \Delta P_o / \rho_g = 93 \times 144 / 62.87 = 213 \text{ ft}$

$$(t_{1/2})_L = \frac{I_L}{g} \frac{\dot{V}_o}{H_{P_o}} = \frac{108}{32.2} \frac{15.3}{213} = 0.241 \text{ s}$$

To find α , we need to first find $(t_{1/2})_P$:

$(t_{1/2})_P = I_P(\omega_o/T_o) = (19.5/32.2)(375/636) = 0.357 \text{ s}$. Therefore, $\alpha = 0.241/0.357 = 0.68$

We now find $\theta_1 = 1/0.241 = 4.15$, $\theta_2 = 2/0.241 = 8.3$, and $\theta_3 = 3/0.241 = 12.4$. From Figure VId.5.1, we obtain $\Phi_1 \cong 0.4$, $\Phi_2 \cong 0.25$, and $\Phi_3 \cong 0.18$

Hence, $\dot{V}_1 \cong 0.4 \times 15.3 \cong 6 \text{ ft}^3/\text{s}$, $\dot{V}_2 \cong 0.25 \times 15.3 \cong 4 \text{ ft}^3/\text{s}$, and $\dot{V}_3 = 0.18 \times 15.3 \cong 2.7 \text{ ft}^3/\text{s}$.

5. Mathematical Model for PWR Components, Pressurizer

PWRs are filled with water, which remains subcooled during normal operation. Hence, a pressurizer is necessary to control water inventory and the system pressure. The volume of this tank is about 2% of the volume of the PWR primary system. A pressurizer is usually about half filled with water and half with steam. Since water and steam co-exist at equilibrium, both phases are saturated at the system pressure during normal operation. The pressurizer is attached to the hot leg through a pipe run referred to as the *surge line*. The vapor space allows for water to flow from the RCS into the pressurizer (in-surge) during transients that result in the expansion of the RCS water. The water region also allows water to flow from the pressurizer into the RCS (out-surge) during transients that result in contraction of the RCS inventory.

A pressurizer is equipped with spring loaded pressure safety valves (PSV), with pilot operated relief valves (PORV), with spray nozzles, and with two sets of heaters. The pressurizer design constraints include the existence of sufficient vapor space to prevent water from reaching the relief valves and sufficient water volume to prevent uncovering of the electric heaters. One set of heaters is designed to offset the heat loss through the insulation and maintain pressure. The other set of heaters is to produce steam following an out-surge, as shown in Figure VId.5.1.

Power increase. Events resulting in a power increase cause the RCS water temperature to rise. This is associated with an increase in water specific volume and subsequent expansion of water. The increase in water volume results in a rush of water from the surge line into the pressurizer and compression of steam in the bulk vapor region. The subsequent rise in the pressurizer pressure is controlled by

the spray control valve injecting colder water from the cold leg into the vapor space. Additional relief is provided by the chemical and volume control system (CVCS) by opening the letdown valve and allowing water to flow to the CVCS tank. Manual depressurization of the pressurizer is also possible by remote opening of the PORVs.

Power decrease. Events leading to a drop in the reactor power cause the water temperature, and hence, the water specific volume to decrease. The subsequent drop in the RCS water volume is compensated by the pressurizer water rushing to the RCS through the surge line. This results in the expansion of the bulk vapor space and a drop in the pressurizer pressure. Pressure is partially restored due to the flashing of water in the pressurizer. Additionally, the pressurizer heaters are activated by the pressure controller. If water drops below the low level set point, indicating the likelihood of heaters to be uncovered, the positive displacement charging pumps are automatically started to add coolant to the RCS from the CVCS tank.

Wall effect. The pressurizer wall also participates in the pressure control mechanism. During an in-surge, when steam may become superheated, the colder wall acts as a heat sink to condense some steam. In an out-surge, the warmer wall would heat up the expanding steam, which helps prevent excessive pressure drop. Also, during an out-surge, the warmer wall may result in boiling water adjacent to the wall. Hence, the heat transfer regime between wall and the fluid is either natural convection or results in the change of phase.

Mass and energy processes. Various mass and energy processes are discussed below. In this discussion, we use subscript l to represent the water region and v for the vapor region. To be consistent, we use subscripts f and g to represent the saturation properties. Hence, h_l stands for the enthalpy of water. If $h_l = h_f$ then the water is saturated. Otherwise, it is subcooled. Similarly, if $h_v = h_g$ then the steam is saturated. Otherwise, it is superheated. Figure VId.5.1 shows the various mass and associated energy transfer rates between regions. These include:

- surge flow rate to or from the water region, (\dot{m}_{su}, h_{su}) . In an in-surge, $h_{su} = h_{HL}$ and in an out-surge $h_{su} = h_l$
- spray flow rate, to lower pressure, added to the water region (\dot{m}_{sp}, h_{sp})
- spray condensation flow from the steam region to the water region (\dot{m}_{sc}, h_f)
- flashing from the water to the steam region due to depressurization (\dot{m}_{fl}, h_g)
- rainout from the steam to the water region due to depressurization (\dot{m}_{ro}, h_f)
- wall condensation from steam to the water region (\dot{m}_{wc}, h_f)
- wall boiling from water to the steam region (\dot{m}_{wb}, h_g)
- safety and relief valve flow rate from the steam region (\dot{m}_{rv}, h_v)

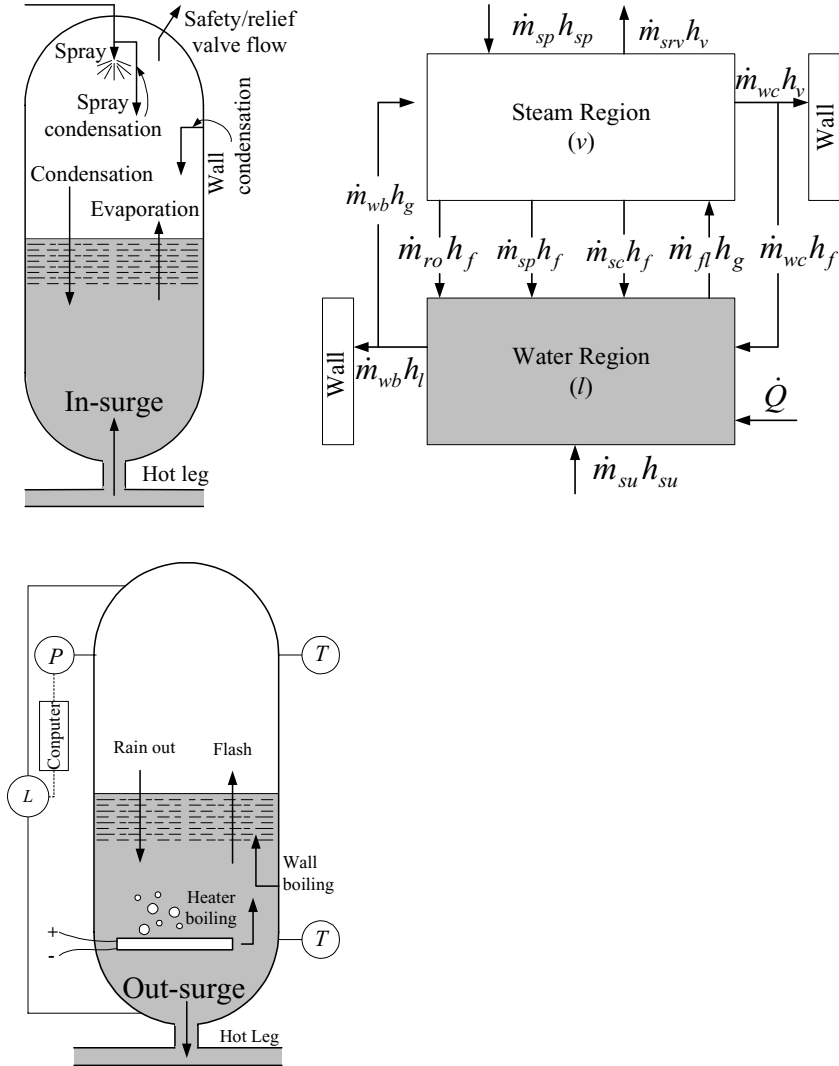


Figure Vid.5.1. Various mass and energy processes in a PWR pressurizer

- condensation on and evaporation from the bulk interface (\dot{m}_{ic}, h_f and \dot{m}_{ie}, h_g), not shown on Figure Vid.5.1
- non-condensable gases, released into the steam region (-).

- heater power in the water region and heat transfer to wall from water and steam, (\dot{Q}_h) , (\dot{Q}_{hw}) and (\dot{Q}_{vw}) .

Pressurizers use a surge sparger to dampen the momentum of the in-surge. The penetration depth of the in-surge water to the water region is generally limited to about 30 cm (1 ft).

Mathematical model. Generally, the extent of information obtained from a mathematical model depends on the degree of complexity of the model. While we may make reasonable assumptions to simplify a model, we should be careful about the effect of such assumptions on the accuracy of the results. For example, we may use one control volume to represent the entire pressurizer by assuming that water and steam are well mixed and remain at one pressure and temperature during a transient. While this approach simplifies the analysis it may actually lead to erroneous result in case of an in-surge into the pressurizer. During an in-surge, the bulk vapor region is compressed causing the pressurizer pressure to rise (condensation of steam on the colder wall somewhat reduces the rate of pressure increase). On the other hand, by using a one-node model in which the colder in-surge water mixes with the steam and water mixture, we would calculate a drop in the pressurizer pressure.

In a two-region model, we consider two deformable control volumes for the bulk water and bulk vapor region. We use the term “bulk” to distinguish the water droplets in the bulk vapor region from water in the bulk water region and steam bubbles in the bulk water region from steam in the bulk vapor region. A three-region model could allocate another deformable control volume to the colder in-surge in the lower portion of the pressurizer and a four region model could allocate a deformable control volume to each of the bulk water region, bulk vapor region, drops in the bulk vapor region, and bubbles in the bulk water region.

Example Vid.5.1. In a transient, water rushes into the pressurizer at 58.94 lbm/s for 17.5 seconds at an average pressure and temperature of 700 psia and 450 F. Estimate the pressurizer pressure. Ignore any interaction at the wall and at the bulk fluid interface. Assume that the pressurizer is a right circular cylinder, no spray or safety valve is actuated, and ignore condensation on the wall.

Data: $V_{\text{Pressurizer}} = 700 \text{ ft}^3$, $V_{\text{water}} = 100 \text{ ft}^3$, $T_{\text{initial}} = 500 \text{ F}$ ($P_{\text{initial}} = 680.86 \text{ psia}$).

Solution: a) No mixing assumption: If the transient is fast and there is not sufficient time for perfect mixing, we may find the peak pressure by assuming isentropic compression of the steam region.

Initially, at $P = 700 \text{ psia}$ and $T = 450 \text{ F}$, $v_{su} = 0.01939 \text{ ft}^3/\text{lbm}$ and $h_{su} = 430.38 \text{ Btu/lbm}$. To find the steam volume after compression, we need the in-surge mass and total volume:

$$m_{su} = \dot{m}_{su} \Delta t = 58.94 \times 17.5 = 1031.45 \text{ lbm}$$

Hence, $V_{su} = m_{su} v_{su} = (58.94 \times 17.5) \times 0.01939 = 20 \text{ ft}^3$. The steam volume following compression is:

$$(V_{\text{steam}})_2 = (V_{\text{steam}})_1 - V_{su} = 600 - 20 = 580 \text{ ft}^3$$

We find P_2 from Equation IIa.4.3:

$$P_2 = P_1 [(V_{\text{steam}})_1 / (V_{\text{steam}})_2]^{(0.445/0.335)} = 680.86 \times (600/580)^{1.328} = 712.2 \text{ psia.}$$

b) Perfect mixing assumption: At $T_1 = 500 \text{ psia}$, $v_{f1} = 0.0204 \text{ ft}^3/\text{lbm}$, $v_{g1} = 0.6749 \text{ ft}^3/\text{lbm}$

$$m_1 = m_{f1} + m_{g1} = 4901 + 889 = 5790 \text{ lbm and } x_1 = 0.153 \text{ so that } u_1 = 486.1 + 0.153 \times 631 = 572.98 \text{ Btu/lbm}$$

Using Equation IIa.6.4 gives: $\dot{m}_i h_i = d(mu)/dt$. The integration of this equation yields: $m_2 u_2 = m_1 u_1 + m_{su} h_{su}$

$$u_2 = [m_1 u_1 + m_{su} h_{su}] / (m_1 + m_{su}) \text{ and } v_2 = V / (m_1 + m_{su})$$

$$m_2 = m_1 + m_{su} = 5790 + 103.45 = 6821.7 \text{ lbm}$$

$$u_2 = [5790 \times 572.98 + 500 \times 613] / 6821.7 = 839 \text{ Btu/lbm}$$

$$v_2 = 1000 / 22,222 = 0.045 \text{ ft}^3/\text{lbm}$$

Pressure corresponding to $v_2 = 0.045 \text{ ft}^3/\text{lbm}$ and $u_2 = 839 \text{ Btu/lbm}$ is $P_2 = 672.85 \text{ psia}$. This model predicts a drop in pressure following the in-surge.

5.1. Two-Region Pressurizer Model

Development of the two-region mathematical model for the pressurizer is based on the Nahavandi method. We allocate one deformable control volume to the bulk water and another to the bulk vapor region. To find the various thermodynamic states of these two control volumes, we compare the enthalpy of each region (h_l and h_v) with $h_f(P)$ and $h_g(P)$. There are a total of 12 possible states as shown in Table VIc.5.2. However, we do not consider the meta-stable states where $h_l > h_f$ and $h_v < h_g$. These meta-stable states are shown in Figure VIc.5.2 for a depressurization process from an initial pressure of P_o to a final pressure of $P_o - \Delta P$. By not allowing such meta-stable states, we need to consider only four cases of a) saturated liquid, superheated vapor, b) saturated liquid, saturated vapor, c) subcooled liquid, saturated vapor, and d) subcooled liquid, superheated vapor. Selecting P and h as the state variables for each region, we begin with Equation IIa.5.1 and include all the transfer terms explicitly. For the water region we find:

Table VIc.5.2. Thermodynamic states in a 2-region model

$h_v < h_g$	$h_v = h_g$	$h_v > h_g$
$h_l < h_f$	$h_l < h_f$	$h_l < h_f$
$h_l = h_f$	$h_l = h_f$	$h_l = h_f$
$h_l > h_f$	$h_l > h_f$	$h_l > h_f$

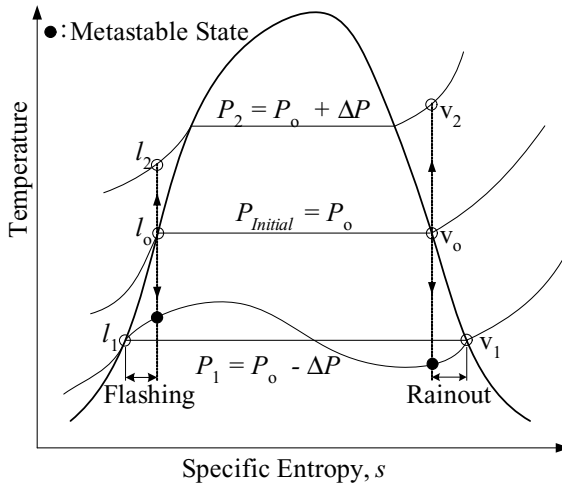


Figure VI.d.5.2. Isentropic rainout and flashing in a pressurizer during an out-surge transient (Todreas)

$$\frac{dm_l}{dt} = \dot{m}_{su} + \dot{m}_{sp} - \dot{m}_{fl} + \dot{m}_{ra} + \dot{m}_{wc} + \dot{m}_{sc} + \dot{m}_{ic} - \dot{m}_{ie} = \left(\sum_j \dot{m}_j \right)_l$$

and for the vapor region, the conservation equation of mass, Equation IIa.5.1 becomes:

$$\frac{dm_v}{dt} = \dot{m}_{fl} - \dot{m}_{ro} - \dot{m}_{wc} - \dot{m}_{sc} - \dot{m}_{rv} - \dot{m}_{ic} + \dot{m}_{ie} = \left(\sum_j \dot{m}_j \right)_v$$

We now use the conservation equation of energy for the water region, Equation IIa.6.4-1, to obtain:

$$\begin{aligned} \frac{d(m_l h_l)}{dt} = & \dot{m}_{su} h_{su} + \dot{m}_{sp} h_f - \dot{m}_{fl} h_g + \dot{m}_{ro} h_f + \dot{m}_{wc} h_f + \\ & \dot{m}_{wc} h_f + \dot{m}_{ic} h_f - \dot{m}_{ie} h_g + \dot{Q}_h - \dot{Q}_{lw} + cV_l \dot{P} \end{aligned}$$

and apply Equation IIa.6.4-1 to the vapor region to obtain:

$$\begin{aligned} \frac{d(m_v h_v)}{dt} = & \dot{m}_{sp} (h_{sp} - h_f) + \dot{m}_{fl} h_g - \dot{m}_{ro} h_f - \dot{m}_{wc} h_f - \\ & \dot{m}_{wc} h_f - \dot{m}_{rv} h_v - \dot{m}_{ic} h_f + \dot{m}_{ie} h_g - \dot{Q}_{vw} + cV_v \dot{P} \end{aligned}$$

Note that there is no shaft work and the shear work is ignored. Following the same method used in Chapter IIa to analyze the dynamics of gas-filled rigid vessels, we write the conservation equations as:

$$\frac{dm_k}{dt} = \left[\sum_j (\dot{m}_j) \right]_k$$

for mass in each control volume or region and as:

$$\frac{d(m_k h_k)}{dt} = \left[\sum_j (\dot{m}_j h_j + \dot{Q}_j + \dot{W}_{sj}) \right]_k + V_k \dot{P}$$

for energy. Subscript j represents the various processes associated with a region and subscript k is a region index. We now make use of the volume constraint as $V_l + V_v = V$ where V is the total volume of the pressurizer. Taking the derivative of the volume constraint relation and setting it to zero yields:

$$\frac{d(m_k v_k)}{dt} = \sum (\dot{m}_k v_k + m_k \dot{v}_k) = \sum \left[\dot{m}_k v_k + m_k \left(\frac{\partial v_k}{\partial h_k} \dot{h} + \frac{\partial v_k}{\partial P} \dot{P} \right) \right] = 0 \quad \text{VId.5.1}$$

where in Equation VId.5.1, the summation is over the two regions of liquid and vapor. Hence, $k = l$ and v . Also in Equation VId.5.1 noting that $v = f(P, h)$, the derivative of the specific volume of each region was expressed in terms of the partial derivatives with respect to pressure as well as the enthalpy of each region. We now carry out the derivatives of the energy equations. For the bulk liquid region we find:

$$\dot{h}_l = \left\{ \left[\sum_j (\dot{m}_j h_j + \dot{Q}_j + \dot{W}_{sj}) \right]_l + V_l \dot{P} - \left[\sum_j \dot{m}_j \right] h_l \right\} / m_l$$

Similarly, for the bulk vapor region, the enthalpy derivative becomes:

$$\dot{h}_v = \left\{ \left[\sum_j (\dot{m}_j h_j + \dot{Q}_j + \dot{W}_{sj}) \right]_v + V_v \dot{P} - \left[\sum_j \dot{m}_j \right] h_v \right\} / m_v$$

Substituting the enthalpy derivatives (\dot{h}_l and \dot{h}_v) into Equation VId.5.1 while also substituting from the conservation equations of mass we find the pressurizer pressure derivative as:

$$\dot{P} = - \frac{\sum_k \left\{ \left(\sum_j \dot{m}_j \right)_k v_k + \left[\sum_j (\dot{m}_j h_j + \dot{Q}_j + \dot{W}_{sj}) \right]_k - \left(\sum_j \dot{m}_j \right)_k h_k \right\} \frac{\partial v_k}{\partial h_k}}{\sum_k \left\{ m_k \frac{\partial v_k}{\partial P} + V_k \frac{\partial v_k}{\partial h_k} \right\}} \quad \text{VId.5.2}$$

Similar to the solution of Section 3, back substitution of pressure derivative results in finding the enthalpy derivatives. The mass and enthalpy of each region are then found by integration over each time step. As seen from Equation VIc.5.2, we also

need the derivatives of the properties. Such derivatives can be obtained by various means. For example, if properties are represented by least square fit to the data, we can then take the derivatives of the related functions.

This method of solution resulted in the explicit derivation for the control volume pressure. We used five equations (two conservation equations of mass, two conservation equations of energy, and one volume constraint) and we found five unknowns (P , h_l , h_v , m_l , and m_v). This in turn requires all other terms to be obtained from the related constitutive equations and the equations of state. Therefore, we need constitutive equations for such mass flow rates as flashing, rainout, spray condensation, wall condensation, surface evaporation, and condensation. If the pressurization of the vapor region results in the opening of a safety or relief valve, the corresponding flow rate is calculated from the momentum equation. If flow happens to be choked in a relief valve, the momentum equation appears in the form of the critical flow for the related valve.

5.2. Constitutive Models, Spray Condensation

To be able to find pressure from Equation Vid.5.2, in general we need to find constitutive equations for various mass flow rates. Constitutive equations are also needed for the rate of heat transfer to or from a region. An example for such an equation includes a model for the estimation of the rate of steam condensation on the spray droplets injected into the steam region. If we assume that the subcooled spray flow rate reaches saturation to condense steam, a steady state energy balance predicts the rate of steam condensation as:

$$\dot{m}_{sc} = \frac{h_f - h_{sp}}{h_s - h_f} \dot{m}_{sp}$$

where h_{sp} and h_s are the spray and the steam enthalpy, respectively. In this relation, we assumed that steam is saturated, then $h_s = h_g$.

Example Vid.5.2. A PWR pressurizer, operating at steady state condition at 15.51 MPa, is suddenly subject to a constant in-surge flow rate for 1 minute. Determine the pressurizer response to this event. For this purpose, use a two-region model for water and steam, ignore all transport processes at the fluid-fluid and solid fluid interfaces including water flashing to steam.

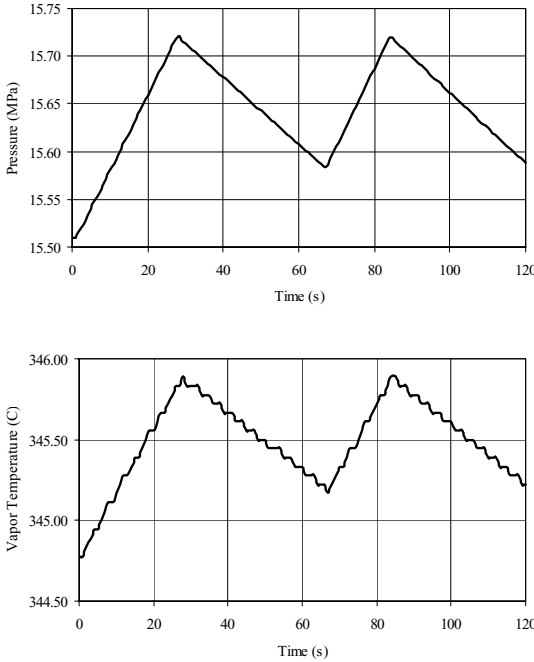
Data: $D = 2.5$ m, $H = 10$ m, $V_{water} = 25$ m³, surge flow rate = 7 kg/s for 60 s, surge enthalpy = 1442 kJ/kg, $A_{rv} = 1\text{E-}4$ m², $C_D = 0.61$, $(P_{Actuation})_{rv} = 17$ MPa, $(P_{Reset})_{rv} = 16$ MPa. Subscript rv stands for relief valve.

Solution: The rate of pressurization is given by Equation Vid.5.2, which for a two-region system becomes (subscripts i and e stand for into and exit from a region, respectively):

$$\dot{P} = - \frac{\left[(\Sigma \dot{m}_{i1} - \Sigma \dot{m}_{e1}) v_1 + (\Sigma \dot{m}_{i2} - \Sigma \dot{m}_{e2}) v_2 \right] + \left[\Sigma \dot{m}_{i1} (h_{i1} - h_{e1}) + \Sigma \dot{Q}_{i1} \right] \frac{\partial v_1}{\partial h_1} + \left[\Sigma \dot{m}_{i2} (h_{i2} - h_{e2}) + \Sigma \dot{Q}_{i2} \right] \frac{\partial v_2}{\partial h_2}}{\left(m_1 \frac{\partial v_1}{\partial P} + m_2 \frac{\partial v_2}{\partial P} \right) + \left(V_1 \frac{\partial v_1}{\partial h_1} + V_2 \frac{\partial v_2}{\partial h_2} \right)}$$

In this equation $\Sigma \dot{m}_{i1} = \dot{m}_{su}$, $\Sigma \dot{m}_{e1} = 0$, $\dot{m}_{i2} = 0$ and $\dot{m}_{e2} = \dot{m}_{rv}$.

Since no heater power is given and there is no interface heat transfer $\dot{Q}_1 = \dot{Q}_2 = 0$. The FORTRAN program is included on the accompanying CD-ROM. The results for pressure and steam temperature are shown below.



6. Mathematical Model for PWR Components, Containment

In addition to bulk water and bulk vapor regions, often control volumes may also include non-condensable gases in the bulk vapor region. Examples include the pressurizer with accumulated fission gases and the BWR and PWR plant containment. To solve for the pressures and temperatures, we use the method of Section 5. To simplify the formulation, we assign subscripts 1, 2, and 3 to water in the pool, steam in the bulk vapor region, and gas in the bulk vapor region. Figure VI.6.1(a) shows a system which consists of two control volumes, one for the bulk water region or the pool and one for the bulk vapor region. Various proc-

esses can take place for the system shown in Figure Vid.6.1(a) including water addition to or removal from the pool region, steam and gas addition or removal from the bulk vapor region, heat addition or removal from each region, and spray addition to the bulk vapor region. Figure Vid.6.1(b) shows steam injection into the bulk vapor region and the associated division of the injected two-phase into water and steam.

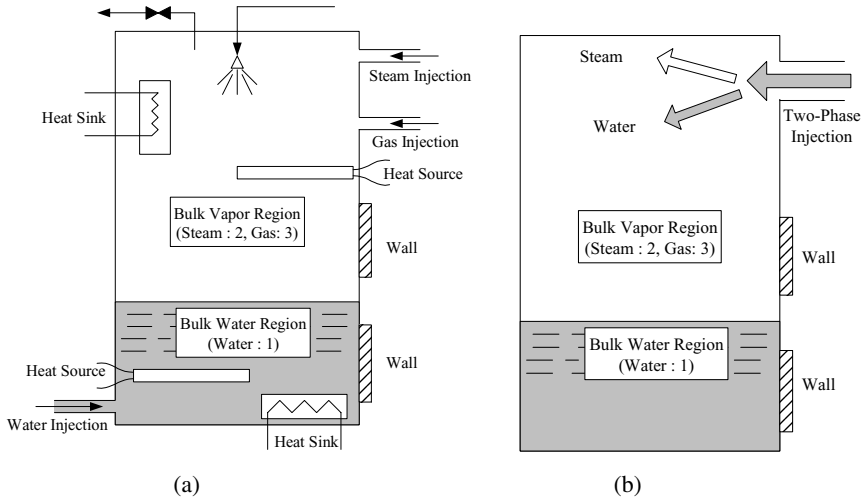


Figure Vid.6.1. (a) A control volume with water and a mixture of steam and gas and (b) Division at the break

Following the method of Section 5, we write the conservation equations of mass for water in the bulk water region, steam in the bulk vapor region, and gas in the bulk vapor region:

$$\frac{dm_k}{dt} = \alpha_k \quad \text{Vid.6.1}$$

where for water in the bulk water region

$$\alpha_1 = \sum \dot{m}_{j,1} = \dot{m}_{in,1} + \dot{m}_{sp} + \dot{m}_{sc} + \dot{m}_{wc} + \dot{m}_{ro} - \dot{m}_{fl} - \dot{m}_{ev} - \dot{m}_{wb} ,$$

for steam in the bulk vapor region,

$$\alpha_2 = \sum \dot{m}_{j,2} = \dot{m}_{in,2} + \dot{m}_{fl} + \dot{m}_{wb} + \dot{m}_{ev} - \dot{m}_{sc} - \dot{m}_{wc} - \dot{m}_{ro} - \dot{m}_{srv,2} ,$$

and for gas in the bulk vapor region, $\alpha_3 = \sum \dot{m}_{j,3} = \dot{m}_{in,3} - \dot{m}_{srv,3}$ where subscript *in* refers to the two-phase injection into the bulk vapor region. Other subscripts are the same as for pressurizer in Figure Vid.5.1.

Unlike the conservation equation of mass, we write two conservation equations of energy, one for the water in the bulk water region and one for steam and gas in the bulk vapor region. For the pool region, we have:

$$\frac{d(m_1 h_1)}{dt} = \beta_1 + c V_1 \dot{P}_1 \quad \text{VId.6.2}$$

where $\beta_1 = \sum (\dot{m}h)_{j,1} + \sum \dot{Q}_1$. Similarly, for the steam and gas in the vapor region we write:

$$\frac{d(m_2 h_2 + m_3 h_3)}{dt} = \beta_{2-3} + c V_2 (\dot{P}_2 + \dot{P}_3) \quad \text{VId.6.3}$$

where P_1 , P_2 , and P_3 in Equations VId.6.1 through VId.6.3 are the control volume total pressure and steam and gas partial pressures, respectively. Similar to β_1 , in Equation VId.6.3, $\beta_{2-3} = \sum (\dot{m}h)_{j,2-3} + \sum \dot{Q}_{2-3}$. Subscript 1 refers to the pool region and subscript 2-3 refers to the bulk vapor region.

In this formulation we have assumed only one non-condensable gas to exist in the bulk vapor region. If there are several gases in the bulk vapor region, we write as many conservation equations of mass as the number of gases in the bulk vapor region and include their effect in the related energy equation for the bulk vapor region (i.e., Equation VId.6.3).

There are a total of nine unknowns: m_1 , m_2 , m_3 , h_1 , h_2 , h_3 , P_1 , P_2 , and P_3 . So far we have obtained five equations. We find the sixth equation from the volume constraint as $V_1 + V_2 = V_{total}$. Substituting for $V = mv$ and taking the derivative of both sides we obtain:

$$\frac{d(m_1 v_1)}{dt} + \frac{d(m_2 v_2)}{dt} = 0 \quad \text{VId.6.4}$$

Three more equations are needed for which we use the principles of the Dalton model. From $P_1 = P_2 + P_3$:

$$\dot{P}_1 = \dot{P}_2 + \dot{P}_3 \quad \text{VId.6.5}$$

Also according to the Dalton model, $T_2 = T_3$ hence:

$$\dot{T}_2 - \dot{T}_3 = 0 \quad \text{VId.6.6}$$

The last remaining equation is obtained by noting that according to the Dalton model the same volume in the bulk vapor region is occupied by steam and gas so $V_2 = V_3$ and, thus $V_1 + V_3 = V_{total}$. Substituting and taking the derivative we get:

$$\frac{d(m_1 v_1)}{dt} + \frac{d(m_3 v_3)}{dt} = 0 \quad \text{VId.6.7}$$

The set of nine equations may be reduced to six by substitution from the continuity equations into the energy equations. The resulting set at every time step is found as:

$$\begin{bmatrix} m_1 & 0 & 0 & -cV_1 & 0 & 0 \\ 0 & m_2 & m_3 & -cV_2 & 0 & 0 \\ m_1 \frac{\partial v_1}{\partial h_1} & m_2 \frac{\partial v_2}{\partial h_2} & 0 & m_1 \frac{\partial v_1}{\partial P_1} & m_2 \frac{\partial v_2}{\partial P_2} & 0 \\ m_1 \frac{\partial v_1}{\partial h_1} & 0 & m_3 \frac{\partial v_3}{\partial h_3} & m_1 \frac{\partial v_1}{\partial P_1} & 0 & m_3 \frac{\partial v_3}{\partial P_3} \\ 0 & \frac{\partial T_2}{\partial h_2} & -\frac{\partial T_3}{\partial h_3} & 0 & \frac{\partial T_2}{\partial P_2} & -\frac{\partial T_3}{\partial P_3} \\ 0 & 0 & 0 & 1 & -1 & -1 \end{bmatrix} \begin{pmatrix} \dot{h}_1 \\ \dot{h}_2 \\ \dot{h}_3 \\ \dot{P}_1 \\ \dot{P}_2 \\ \dot{P}_3 \end{pmatrix} = \begin{pmatrix} \beta_1 - \alpha_1 h_1 \\ \beta_2 - \alpha_2 h_2 - \alpha_3 h_3 \\ -\alpha_1 v_1 - \alpha_2 v_2 \\ -\alpha_1 v_1 - \alpha_3 v_3 \\ 0 \\ 0 \end{pmatrix} \quad \text{VId.6.8}$$

Equation Vid.6.8 can be solved by Gaussian elimination. Having initial volumes, masses, enthalpies, physical properties and their derivatives, we can find enthalpy and pressure derivatives by solving the above set. The mass, enthalpy, pressure and volume derivatives are then integrated over a time step to find pressures, masses, volumes and enthalpies in a subsequent time step:

$$\begin{aligned} m_k^{N+1} &= m_k^N + \alpha_k \Delta t \\ h_k^{N+1} &= h_k^N + \dot{h}_k \Delta t \\ P_k^{N+1} &= P_k^N + \dot{P}_k \Delta t \\ V_k^{N+1} &= V_k^N + \dot{V}_k \Delta t \end{aligned}$$

This process is repeated until the end of the specified transient is reached.

In addition to the constitutive equations required to represent many of the processes as discussed in Section 5, we use three equations of states for water, steam, and gas to obtain

$$\begin{aligned} v_k &= f_{1,k}(P_k, h_k), \\ T_k &= f_{2,k}(P_k, h_k), \end{aligned}$$

$$\begin{aligned}\partial v_k / \partial h_k &= f_{3,k}(P_k, h_k), \\ \partial v_k / \partial P_k &= f_{3,k}(P_k, h_k), \\ \partial T_k / \partial h_k &= f_{5,i}(P_k, h_k), \text{ and} \\ \partial T_k / \partial P_k &= f_{65,k}(P_k, h_k),\end{aligned}$$

where index $k = 1, 2$, and 3 . Derivative of properties of the gas in the bulk vapor region, treated as an ideal gas, is readily obtained as:

$$\frac{\partial v_3}{\partial h_3} = \frac{R_3}{c_{p,3}P_3}, \quad \frac{\partial v_3}{\partial P_3} = -\frac{v_3}{P_3}, \quad \frac{\partial T_3}{\partial h_3} = \frac{1}{c_{p,3}}, \text{ and } \frac{\partial T_3}{\partial P_3} = 0.$$

Recall that properties of saturated water and saturated steam are functions of either pressure or temperature. However, properties of subcooled water and superheated steam are functions of two variables. Thermal hydraulic computer codes use curve fits to the steam tables. However, to simplify analysis in the following example, we are assuming that superheated steam can be treated as an ideal gas. This assumption is reasonable, especially for specific volume ($v = RT/P$) at low pressures and high temperatures. This assumption is less accurate for enthalpy of the superheated steam, $dh = c_p dT$, if c_p is treated as a constant.

Example VId.6.1. A heavy load drop inside a containment ruptures two pipes. One carrying superheated steam and the other compressed air. Estimate the containment response for the first 10 minutes to this event. Treat steam and air as ideal gases. Data: $V_{\text{containment}} = 2\text{E}6 \text{ ft}^3$ (56.6 m^3), $P_o = 14.7 \text{ psia}$ (101.3 kPa), $T_o = 120 \text{ F}$ (49 C), $\phi_o = 59\%$, $\dot{m}_{\text{steam}} = 100 \text{ lbm/s}$ (45.36 kg/s), $h_{\text{steam}} = 1200 \text{ Btu/lbm}$ (2791 kJ/kg), $\dot{m}_{\text{air}} = 50 \text{ lbm/s}$ (22.68 kg/s), $T_{\text{air}} = 350 \text{ F}$ (177 F). Ignore all safety systems and steam condensation.

Solution: We calculate the initial masses, pressures, volumes, and enthalpies. Since no pool region is specified, hence, $V_1 = 0$, and $V_2 = V_3 = 2\text{E}6 \text{ ft}^3$ (56.6 m^3)

$P_2 = 0.59 \times P_{\text{sat}}(120 \text{ F}) = 1 \text{ psia}$ (6.9 kPa), $P_3 = 14.7 - 1 = 13.7 \text{ psia}$ (0.094 kPa) and $P_1 = 14.7 \text{ psia}$ (101.3 kPa)

$h_2 = h_{100} + c_{p,2}(T - 100) = 1105.3 + 0.445(120 - 100) = 1114 \text{ Btu/lbm}$ (2591 kJ/kg)

$h_3 = 0.24(120 + 460) = 139.2 \text{ Btu/lbm}$ (323.7 kJ/kg)

$v_2 = R_2 T_2 / P_2 = 345.7 \text{ ft}^3/\text{lbm}$ ($21.58 \text{ m}^3/\text{kg}$). Thus, $m_2 = V/v_2 = 1.0\text{E}6/345.7 = 5785 \text{ lbm}$ (2624 kg)

$v_3 = R_3 T_3 / P_3 = 15.68 \text{ ft}^3/\text{lbm}$ ($0.978 \text{ m}^3/\text{kg}$). Thus, $m_3 = V/v_3 = 1.0\text{E}6/15.68 = 1.275\text{E}5 \text{ lbm}$ ($0.578\text{E}5 \text{ kg}$).

Since we have only the vapor region, Equation VId.6.8 simplifies to:

$$\begin{pmatrix} m_2 & 0 & -cV_2 & 0 \\ 0 & m_3 & 0 & -cV_3 \\ m_2 \frac{\partial v_2}{\partial h_2} & -m_3 \frac{\partial v_3}{\partial h_3} & m_2 \frac{\partial v_2}{\partial P_2} & -m_3 \frac{\partial v_3}{\partial P_3} \\ \frac{\partial T_2}{\partial h_2} & -\frac{\partial T_3}{\partial h_3} & \frac{\partial T_2}{\partial P_2} & -\frac{\partial T_3}{\partial P_2} \end{pmatrix} \begin{pmatrix} \dot{h}_2 \\ \dot{h}_3 \\ \dot{P}_2 \\ \dot{P}_3 \end{pmatrix} = \begin{pmatrix} \beta_2 - \alpha_2 h_2 \\ \beta_3 - \alpha_3 h_3 \\ -\alpha_2 v_2 + \alpha_3 v_3 \\ 0 \end{pmatrix}$$

Next, we find the forcing functions:

$\alpha_1 = 0$ lbm/s, $\alpha_2 = 100$ lbm/s, and $\alpha_3 = 50$ lbm/s

$\beta_2 = 100 \times 1200 = 1.2\text{E}5$ Btu/s, and $\beta_3 = 50 \times 0.24(350 + 460) = 0.972\text{E}4$ Btu/s

We now develop derivatives of specific volumes and temperatures:

$$\partial v_2 / \partial h_2 = R_2 / c_{p,2} P_2 = (1545/18) / (0.445 \times 144 P_2) = 1.339 / P_2$$

$$\partial v_3 / \partial h_3 = 1.543 / P_3$$

$$\partial v_2 / \partial P_2 = -v_2 / P_2 = -345.7 / P_2 = -2.4 \text{ ft}^3 / \text{lbm} \cdot \text{lbf}$$

$$\partial v_3 / \partial P_3 = -v_3 / P_3 = -15.68 / P_3 = 7.97\text{E}-3 \text{ ft}^3 / \text{lbm} \cdot \text{lbf}$$

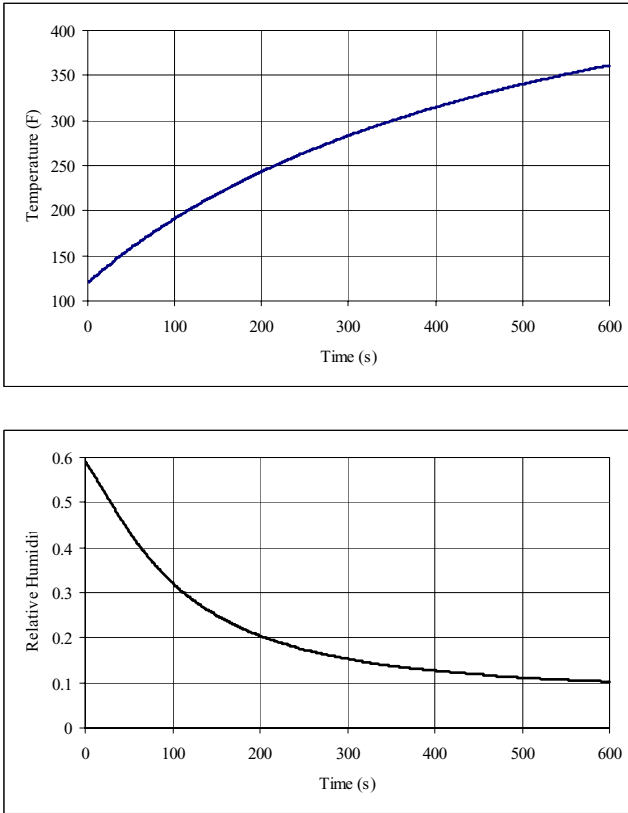
$$\partial T_2 / \partial h_2 = 1 / c_{p,2} = 2.247 \text{ lbm} \cdot \text{F} / \text{Btu}$$

$$\partial T_3 / \partial h_3 = 1 / c_{p,3} = 4.167 \text{ lbm} \cdot \text{F} / \text{Btu}$$

Upon substitution, the set of equations for the first time step becomes:

$$\begin{pmatrix} 5785 & 0 & -3.7\text{E}5 & 0 \\ 0 & 1.275\text{E}5 & 0 & -3.7\text{E}5 \\ 7746 & -14360 & -13888 & 1013.4 \\ 2.247 & -4.167 & 0 & 0 \end{pmatrix} \begin{pmatrix} \dot{h}_2 \\ \dot{h}_3 \\ \dot{P}_2 \\ \dot{P}_3 \end{pmatrix} = \begin{pmatrix} 8600 \\ 2760 \\ -33786 \\ 0 \end{pmatrix}$$

we find the four unknowns as $\dot{h}_2 = 1300$ Btu/lbm s, $\dot{h}_3 = 70$ Btu/lbm s, $\dot{P}_2 = 20.3$ psi/s and $\dot{P}_3 = 24.1$ psi/s. Having the derivatives, we find h_2 , h_3 , P_2 , and P_3 at the next time step. The FORTRAN program to solve this problem is included on the accompanying CD-ROM. The results for this problem for temperature and relative humidity are shown in the plots. Containment pressure in 10 minutes reaches 40 psia (2.76 bar).



6.1. Break Flow Split

Consider the containment of Figure VIId.6.1(b) initially being at P_o and T_o . We now inject saturated water or a two-phase mixture to the vapor region of this containment. The pressure and temperature of the injected flow are greater than those of the containment, $P_m > P_o$ and $T_m > T_o$, where subscript m stand for mixture. Our goal is to find the percentage of the injected flow that becomes steam and joins the vapor region and the portion that becomes water and flows to the pool region. Such injected flow split depends on the conditions at the plane of entrance to the containment. If the injected flow to the vapor region is saturated water for example, the flow partially flashes to steam upon entering the low pressure vapor region. The constitutive equations for determination of the injected flow split into two distinct phases in the containment are known as the *pressure flash* and the *temperature flash* models. Both models assume an isoenthalpic split of the injected flow so that:

$$\dot{m}_m h_m = \dot{m}_f h_f + \dot{m}_g h_g \quad \text{VId.6.8}$$

However, the difference between the two models lies in the evaluation of the saturated water and saturated steam enthalpies. To elaborate, let's define the fraction of the flow which flashes to steam, χ as:

$$\chi = \frac{h_m - h_f(y_1)}{h_g(y_2) - h_f(y_1)} \quad \text{VId.6.9}$$

In the pressure flash model, the saturation enthalpies are developed based on pressure. For example, $y_1 = y_2 = P_2$ (i.e. the partial pressure of steam). Another way to calculate the split fraction is to take $y_1 = P_1$ (i.e. total pressure in the containment) and $y_2 = P_2$ or to take $y_1 = y_2 = T_2$, as summarized in Table VId.6.1.

Table VId.6.1. Summary of various break flow split models

Break Flow Split		y_1	y_2
Pressure Flash	Model A	P_1	P_1
	Model B	P_1	P_2
	Model C	P_2	P_2
Temperature Flash		T	T

Note that in some references the temperature flash model is defined differently. In the temperature flash model described by Hargroves for example, the injected flow is instantaneously mixed and reaches equilibrium with the steam in the vapor region.

Example VId.6.2. A high energy pipe break occurs inside containment. Compare the split fraction of the break flow using various models of Table VId.6.1. Data: $P_o = 16.5$ psia, $T_o = 125$ F, $\phi_o = 51.5\%$, $h_m = 550$ Btu/lbm.

Solution: We find $P_2 = 0.515 \times P_{sat}(125 \text{ F}) = 1$ psia. Thus, $P_3 = P_1 - P_2 = 16.5 - 1 = 15.5$ psia.

(a) $y_1 = y_2 = 16.5$ psia;

$\chi_a = (550 - 186.11)/(1152.7 - 186.11) = 0.376$ steam and 62.4% water

(b) $y_1 = 16.5$ psia and $y_2 = 1$ psia;

$\chi_b = (550 - 186.11)/(1105.8 - 186.11) = 0.395$ steam and 60.5% water

(c) $y_1 = y_2 = 1$ psia;

$\chi_c = (550 - 69.730)/(1105.8 - 69.730) = 0.463$ steam and 53.7% water

(d) $y_1 = y_2 = 125$ F;

$\chi_d = (550 - 92.960)/(1115.7 - 92.960) = 0.447$ steam and 55.3% water

7. Mathematical Model for PWR Components, Steam Generator

The function of a PWR U-tube steam generator is described in Chapter I. Feed-water entering the downcomer, Figure I.6.6(b) and mixing with the saturated water returning from the separator assembly enters the tube bundle to reach saturation and begins to boil. Heat is transferred from the primary side through the tubes to the two-phase flow, which further increases steam quality. The two-phase flow eventually enters the risers or stand pipes of the moisture separator. The saturated water flows downward to mix with the feedwater while saturated steam enters the dryer and eventually the steam line.

The primary side response was discussed in Section 3. We now discuss mathematical modeling of the secondary side. Figure VI.7.1(a) shows a simple nodalization of the secondary side of the steam generator. We may use this simple nodalization to estimate the mass, enthalpy, pressure, and velocity distribution, which is helpful in refining the nodalization. Like before, we may also apply the simplifying assumption of an integral, loop-wide momentum equation as discussed in Section 3. However, the loop in the case of the secondary side of a steam generator consists of the following flow path; steam generator downcomer, tube bundle, riser, separator, dryer. The flow path then leads to the steam dome and the steam line for the dry saturated steam and back to the downcomer for the saturated recirculation water, as shown in Figure VI.7.1(b).

The one dimensional integral momentum equation for the flow loop in the secondary side of the SG is found by applying Equation VI.3.15 to the various regions shown in Figure VI.7.1(b).

Determination of the Boil Off Rate

To obtain a simple relation for estimation of the boil-off flow rate, we consider a pot-boiler (no circulation) where heat is added to the water region, steam exits the water region and enters the steam region, and feedwater is added to the water region to maintain inventory. The mass flow rate of steam is given by Equation IIa.5.3:

$$\dot{m}_g = \rho_g V_g A_g = \rho_g V_g (\alpha_e A_c) \quad \text{VI.7.1}$$

where α_e is the void fraction at the froth level (the interface between the water and the steam region) and A_c is the boiler cross sectional area at the froth level, perpendicular to the flow direction. Also in Equation VI.7.1, ρ_g and V_g are steam saturation density and steam velocity, respectively. Since ρ_g is a function of the operating pressure of the boiler (a known quantity) and A_c is the boiler flow area, also a known quantity, we need to find relations for α_e and V_g in terms of other known quantities. Void fraction is given by Equation III.2.2:

$$\alpha_e = \frac{X_e}{C_o [X_e + (\rho_g / \rho_f)(1 - X_e)] + (\rho_g V_{gj} A_c / \dot{m}_{boil})}$$

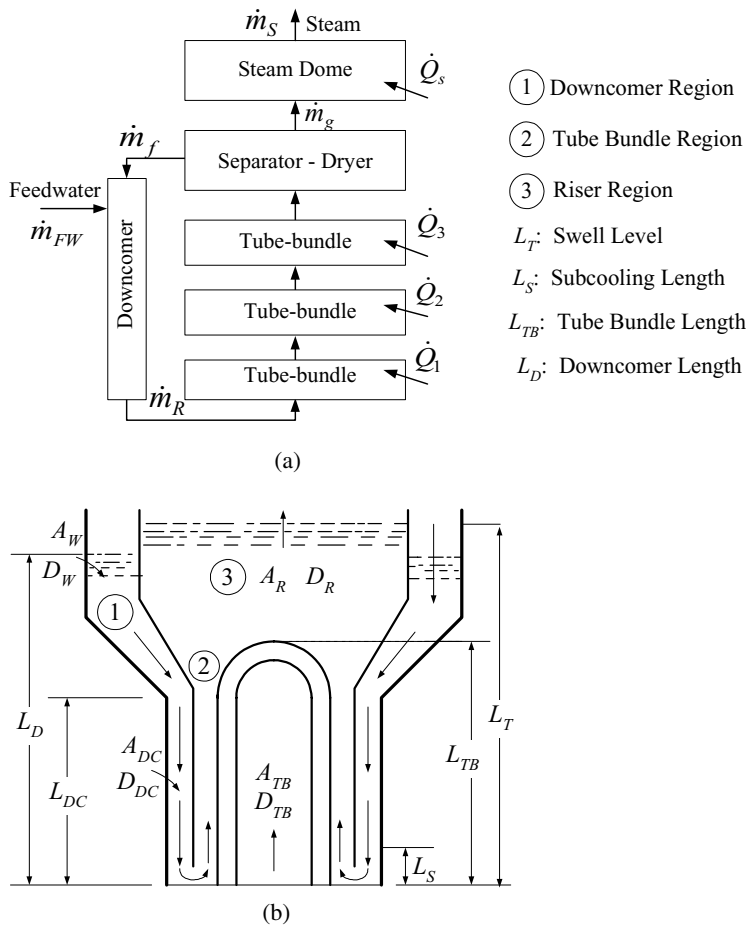


Figure VIId.7.1. Mass and energy control volumes and flow paths for conservation equation of momentum

where X_e may be calculated from $X_e = (h_e - h_f)/h_{fg}$ and V_{gj} from Equation IIIId.2.4. Finally, we find steam velocity, V_g from $V_g = J + V_{gj}$ where J may be estimated from $J = (\dot{m}_{FW} + \dot{m}_g)/(2\rho_e Ac)$. In this relation, subscript FW stands for feedwater and ρ_e is the mixture density. Substituting for a_e and V_g in Equation VIId.7.1, we find an implicit second-order algebraic equation for the boil off mass flow rate.

QUESTIONS

- An electromagnetic pump is used to circulate fluid around a flow loop. Describe the flow trend if the pump is tripped. Compare it with a pump equipped with a flywheel.
- What is the role of the buoyancy head in early flow coastdown of a forced circulation loop?
- Thermal center in Equation VId.3.12 is defined based on T_H . How do you define it based on T_C ?
- Can a natural circulation loop operate with the thermal center of the heat sink located slightly below that of the heat source?
- What are the important assumptions made that led to the derivation of Equation VId.3.16, used to estimate the natural circulation mass flow rate?
- What types of work should be considered in the derivation of the pressurizer pressure?
- In the derivation of the pressurizer pressure, only the conservation equations of mass and energy were used. What is the application of the momentum equation in the pressurizer?
- Consider the mass flow rate due to the condensation of steam on the wall of the pressurizer. Can we obtain this term from the conservation equations of mass and energy written for the water and the steam regions?
- Can Equation VIc.6.2 be applied to a three region pressurizer by taking $k = 3$?
- We used one pressure for the pressurizer, taken in the steam region. What assumption makes it possible to apply this same pressure to the water region?
- Plot the in-surge and the out-surge processes of a pressurizer on a T - s diagram.

PROBLEMS

1. Use the definition of thermal center and show that for the core, having near linear temperature profile, the thermal center is located at $H_{\text{core}}/2$ where H_{core} is the core height.
2. Derive Equation VId.3.13, the thermal center of a U-tube steam generator, where λ_{SG} is measured from the tube sheet. [Hint: Start with Equation VId.3.12. Then use the definition of the thermal expansion coefficient to relate density difference to temperature difference. Find λ_{SG} from:

$$\lambda_{SG} = \frac{\int_0^L [\rho(s) - \rho_H] \bar{g} \cdot d\bar{s}}{(\rho_C - \rho_H)g}$$

where the numerator is given in Example VId.3.1].

3. The following data are given for a U-tube steam generator. Tube mass flow rate $\dot{m} = 70\text{E}6$ lbm/h, total number of tubes $N = 8500$, tube outside diameter $d_o = 0.75$ in, overall heat transfer coefficient $U_o = 1000$ Btu/h ft² F, average tube length

$L = 60$ ft, average tube height $l = 28$ ft, cold leg temperature $T_C = 500$ F, hot leg temperature $T_H = 570$ F, pressure $P = 2265$ psia. For this steam generator find a) the hydrostatic head and b) the thermal center.

4. The U-tube steam generator of Problem 3 is located in a PWR loop. Use the following data to find the loop hydrostatic head (i.e., the difference in the elevations of the heat source and heat sink thermal centers). $Z_{SG} = 45$ ft and $(Z_{th})_{core} = 30$ ft.

5. A PWR is operating at a steady state condition. We now shutdown the plant and want to estimate the natural circulation flow rate. Although the reactor power decays after shutdown, we assume the core power remains steady for the duration of interest. Find the natural circulation flow rate 48 hours after shutdown. Data: Nominal reactor power: 3000 MWth, reactor pressure: 2265 psia, $T_C = 550$ F, $T_H = 610$ F, $\Sigma R = 0.28$ ft⁻⁴.

6. Show that for large values of l^* , given in Equation VIa.5.8, the thermal center of a U-tube steam generator approaches $Z_{SG} = (1 + \delta) l/2$.

7. Derive Equation VIId.3.14 by integrating the hydrostatic pressure term around a natural circulation flow loop. In this derivation assume a linear temperature profile over the heat source and apply Equation VIId.3.12 for the heat sink. [Hint: Find the density profile in the core and the related hydrostatic head. Take the height from the heat source exit to the heat sink inlet as h_H in which ρ_H remains constant. Take the height from the heat sink exit to the heat source inlet as h_C in which ρ_C remains constant. Then use $h_C - H_{core}/2 = h_H + H_{core}/2$]

8. An experimental flow loop is constructed to study events in a PWR plant. The core consists of electrically heated rods and the two steam generators are simulated by two shell and tube heat exchangers. The vessel is connected to the heat exchangers by two hot legs and four cold legs. Water flows from the hot leg in the tubes while the secondary side water is cooled by a cooling tower. The following flow resistances are measured for this facility $R_V = 227$ ft⁻⁴, $R_{HL} = 560$ ft⁻⁴, $R_{HX} = 369$ ft⁻⁴, $R_{CL} = 767$ ft⁻⁴. Find the natural circulation flow a) assuming no pump exists in the loop and b) considering four non-operating pumps on each cold leg, $R_{Pump} = 1793$ ft⁻⁴. Other design data are: core thermal power = 178 kW, core inlet temperature = 38 C, vertical distance between the core and the heat exchanger thermal centers = 0.75 m, average density = 985 kg/m³, average specific heat = 4.18 kJ/kg K, and $\beta = 0.37E-3$ 1/K.

9. Find the hydrostatic pressure in a flow loop operating at 3 MPa with $T_C = 150$ C and $T_H = 175$ C. In this loop, the distance between the heat source and heat sink thermal centers is 5 m. [Ans.: 1.6 kPa].

10. Derive the hydrostatic head for a once-through steam generator. Tubes are oriented vertically. Hot water enters the tubes from the top and leaves from the bottom. Water boils in the secondary side.

11. The flow resistance of a flow loop is given as 9.81 m^{-4} . The loop flow rate at steady state condition is $5 \text{ m}^3/\text{s}$. Find the total head loss in the loop. Also find the pressure drop in the loop. The average loop pressure and temperature are 2.5 MPa and 95 C , respectively. [Ans.: 12.5 m].

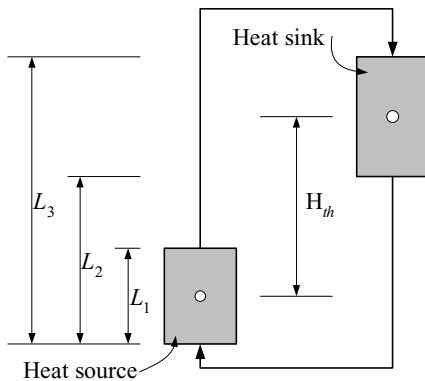
12. Show that the half life of a pump impeller is given by:

$$(t_{1/2})_P = I_P \frac{2\eta_o \omega_o^2}{\rho R \dot{V}_o^3}$$

where η is the pump efficiency, R is the loop flow resistance, and \dot{V} is the volumetric flow rate in the loop. Subscript o indicates nominal values.

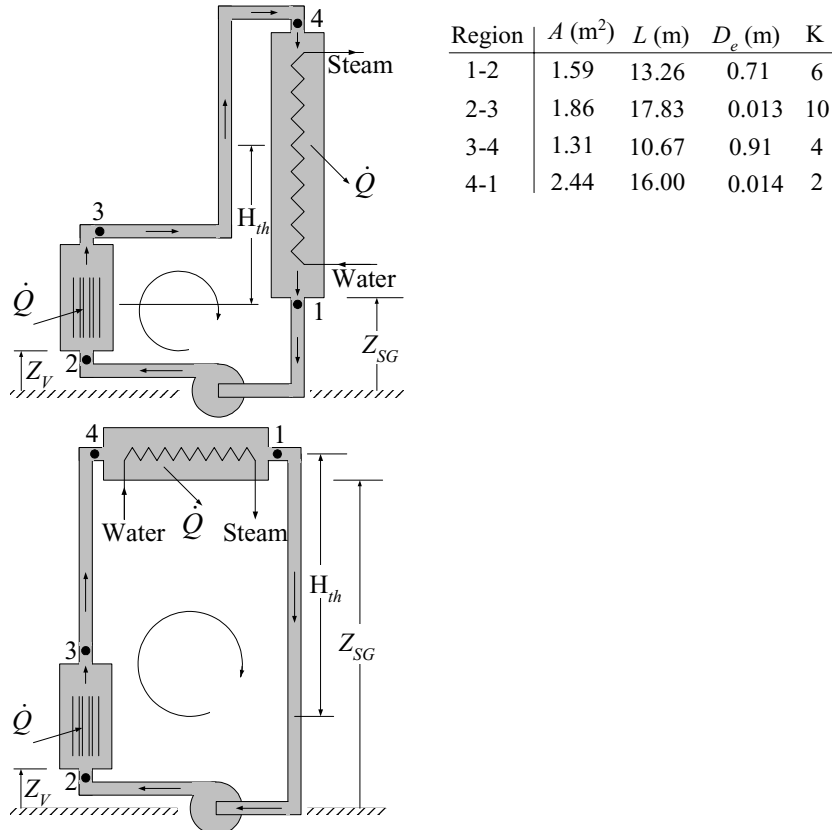
13. A pump is operating in a flow loop at nominal speed. We now turn off the pump. Find the time it takes the impeller to reach half of its nominal speed. Data: $\omega_o = 124 \text{ s}^{-1}$, $I_o = 2200 \text{ slug-ft}^2$, $\dot{V} = 85000 \text{ GPM}$, $\eta_o = 0.78$, $R = 0.076 \text{ ft}^{-4}$, $\rho_o = 38 \text{ lbm/ft}^3$. [Ans.: 2.7 s].

14. A natural circulation loop is shown in the figure. Verify the validity of Equation Vid.3.14. Assume that the thermal centers for the heat source and heat sink, in this case, are located at the geometrical center of each source. The vertical distance between the two sources is shown by H_{th} . Elevations L_1 , L_2 , and L_3 are given.



15. Define the system *thermal length* as the vertical distance between the thermal centers of the heat source and heat sink, $H_{th} = (Z_{th})_V - (Z_{th})_{SG}$ where subscript V stands for the heat source vessel and SG stands for the steam generator. In this problem we want to find the effect of the thermal length on the loop flow rate and the loop temperature gradient. Therefore, we keep changing the loop configuration with respect to the heat sink elevation. Due to height limitation of the building housing the loop, we would eventually have to place the steam generator horizontally. Assume all design parameters remain the same except for the increasing thermal length. a) Derive the loop flow rate as a function of the thermal length.

b) Prepare a table of loop flow rate and loop temperature gradient for various values of H_{th} . To do this, start from $H_{th} = 0.3$ m and conclude at $H_{th} = 15$ m using a 1 m height increment. c) Plot the values for \dot{m} and for T_H versus H_{th} . d) Compare the vertical and the horizontal orientation of the heat sink and comment on the advantages and drawbacks of each orientation. Other Data: $P = 4.48$ MPa, $\bar{T} = 243$ C, $\dot{Q} = 15$ MW



16. An approximate value for the mass flow rate in a natural circulation loop as given by Equation VI.d.3.18 was derived assuming a constant friction factor. a) By using Equations III.b.3.2 and III.b.3.6 show that in general, the mass flow rate is given by:

$$\dot{m}_{NC} = \left(\frac{2\beta g \bar{\rho}^2 H_{th} \dot{Q}_{Core}}{c_p R} \right)^{\frac{1}{3-n}}$$

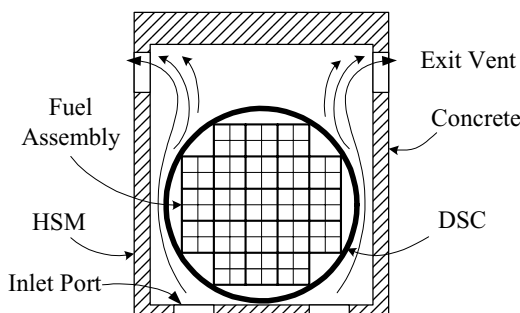
where $n = 0.2$ for turbulent flow in all the sections of the flow loop and $n = 1$ for laminar flow in all the sections of the flow loop. b) Show that the maximum power that can be removed from the heat source in a natural circulation loop is given by:

$$\dot{Q} = \left[\frac{2\beta g \bar{\rho}^2 H_{th}}{R} \right]^{\frac{1}{2-n}} (\Delta T)^{(3-n)/(2-n)} \bar{c}_p$$

where $\bar{\rho}$, \bar{c}_p , and \bar{T} are the loop average density, specific heat, and temperature. Also H_{th} is the system thermal length, as defined in Problem 15.

17. Some nuclear power plants, which are facing space limitation in their spent fuel pool, place older fuel assemblies in steel cylinders, referred to as dry shielded canisters (DSC). The DSC is then hermetically sealed and placed horizontally inside a concrete bunker, known as the horizontal storage module (HSM). Decay heat is removed by natural convection. Colder air entering the HSM through the inlet screen leaves through the vents located at the top of HSM. The loss coefficient and flow area of the inlet and exit ports are as follows:

	$K_{\text{Outer screen}}$	$K_{\text{Inner screen}}$	$K_{\text{Entrance/Exit}}$	Area (m^2)
Inlet port	0.4	0.5	1.4	0.5
Exit port	0.4	0.5	1.0	1.0



Total loss coefficient and flow area associated with the flow through the HSM are 2.5 and 0.5 m^2 , respectively. Total rate of decay heat for the DSC is 15 kW. The system thermal length, as defined in Problem 14 is 3.5 m. Air enters the HSM at a temperature of 22 C. Assume air at exit is well mixed. Use the given data to find a) temperature rise, b) flow rate of air through the HSM, and c) total pressure drop from inlet to exit.

18. A tank containing saturated liquid undergoes a rapid drop in pressure. This results in flashing to take place in the tank. In the absence of any other process, use the conservation equations of mass and energy to derive a relation for the flashing mass flow rate in terms of the depressurization rate.

[Ans.: $\dot{m}_{fl} = -(m_l / h_{fg})[(dh_f / dP) - v_v](dP / dt)$].

19. A tank containing saturated steam undergoes a rapid drop in pressure. This results in rainout from the steam. In the absence of any other process, use the conservation equations of mass and energy to derive a relation for the rainout mass flow rate in terms of the depressurization rate.

[Ans.: $\dot{m}_{fl} = (m_v / h_{fg})[(dh_g / dP) - v_v](dP / dt)$].

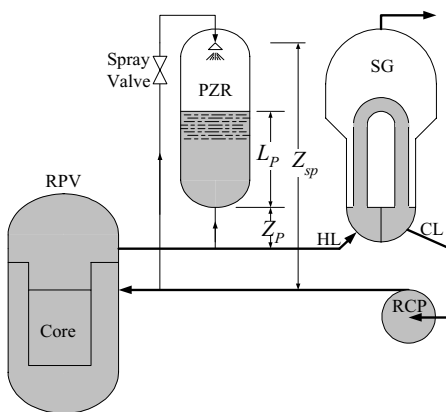
20. Consider a tank filled with steam at enthalpy h_v . A spray valve is opened allowing water at a rate of \dot{m}_{sr} and at enthalpy of h_{sp} to flow into the vapor space.

The rate of steam condensation on the spray droplets is \dot{m}_{sc} . Assuming both spray water and the condensate reach saturation, write a steady state energy balance and find the rate of spray condensation.

[Ans.: $\dot{m}_{sc} / \dot{m}_{sp} = (h_f - h_{sp}) / (h_v - h_f)$].

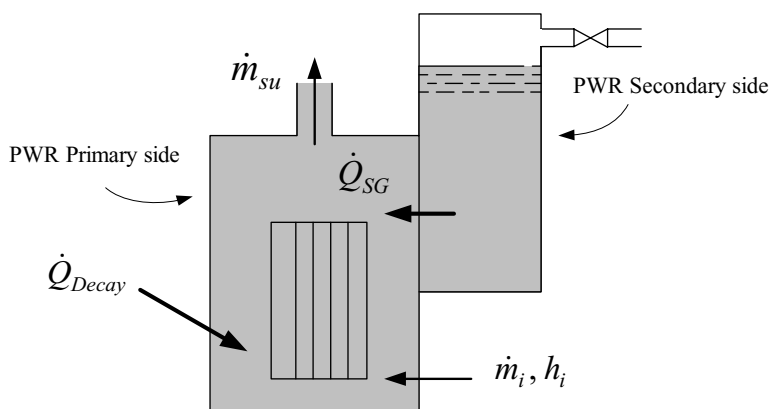
21. Find the spray flow rate into the pressurizer of a PWR by using a force balance around a closed loop. This loop starts from the inlet to the spray line and includes spray line, spray valve, pressurizer, surge line, hot leg, steam generator primary side, reactor coolant pump suction pipe, reactor coolant pump, and reactor coolant pump discharge line. The spray valve flow area and loss coefficient are A_{sp} and K_{sp} , respectively. For given height and elevations, find the spray flow rate and the condition at which there is no spray flow.

{ Ans.: $\dot{m}_{sp} = [(\Delta P_{HL} + \Delta P_{SG} + \Delta P_{CL}) + (\rho_{l,p} g / g_c)(L_p + Z_p) - (\rho_{CL} g / g_c)Z_{sp}]^{0.5} (A_{sp} / K_{sp}^{0.5})$ }.



22. Schematics of a PWR reactor coolant system and the secondary side of the steam generator are shown in the figure. The reactor is shutdown and the decay power is being steadily removed by the residual heat removal system (not shown in the figure). At this steady state operation, the average temperature in the primary side is equal to the temperature of water in the secondary side of the steam

generator, hence, there is no heat transfer taking place in the steam generator tubes. At time zero, we lose the cooling of the residual heat removal system, we inject water at a specified flow rate and enthalpy into the primary side, and we turn on the reactor coolant pumps (not shown in the figure). a) Set up the governing differential equations. Use one control volume for the primary side water and one for the secondary side water, b) solve the differential equations to find the primary side and secondary side temperatures as functions of time and other system parameters specified below, c) use the given data and plot the surge flow rate (out of the primary side) as a function of time for the first ten minutes from the start of the event. The primary and the secondary sides are identified with subscripts P and S, respectively.



Volume data: $V_P = 260 \text{ m}^3$ (9,181 ft^3), $V_S = 85 \text{ m}^3$ (3000 ft^3),

Pressure data: $P_P = 2 \text{ MPa}$ (290 psia), $P_S = 138 \text{ kPa}$ (20 psia),

Injection data: $\dot{V}_i = 8.33 \text{ lit/s}$ (132 GPM), $T_i = 43 \text{ C}$ (110 F),

Heat transfer data: $A_{SG-tubes} = 8,383 \text{ m}^2$ (90,232 ft^2), $U = 4531 \text{ W/m}^2\cdot\text{C}$ (798 $\text{Btu/h}\cdot\text{ft}^2\cdot\text{F}$)

Power addition data: $\dot{Q}_{decay} = 3 \text{ MW}$, $\dot{Q}_{pump} = 17 \text{ MW}$

Initial condition: $T_P = T_S = 105 \text{ C}$ (221 F).

Assumptions:

- The primary and secondary sides pressures remain constant throughout the event,
- water in both control volumes remains subcooled for the duration of interest such that $du \cong dh \cong c dT$,
- the overall heat transfer coefficient U remains constant,
- no water enters or leaves the secondary side.

23. The steam line in a BWR is equipped with a relief valve to discharge steam to the pressure suppression pool during an emergency. The valve opens upon the

closure of the isolation valve. To prevent overcooling of the reactor pressure vessel, the discharge of steam through the valve must not result in a cooldown rate in excess of 100 F/h. Use the data and the associated simplifying assumptions to find pressure in the reactor pressure vessel (RPV) and temperature in the suppression pool as functions of time for a discharge period of 10 minutes.

RPV initial condition:

Pressure: 1015 psia (7 MPa),
 water volume: 14,583 ft³ (413 m³),
 steam volume: 8370 ft³ (237 m³),

RPV injection data:

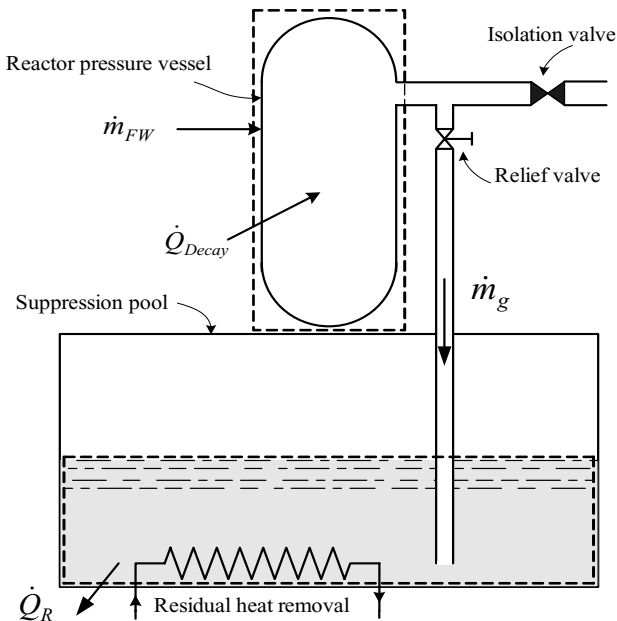
feedwater flow rate: 1,252,000 lbm/h (32 kg/s), feedwater enthalpy: 335 Btu/lbm (780 kJ/kg),

RPV power addition data:

rate of heat deposition to the mixture from the RPV internal structure: 950 Btu/s (≈ 1 MW), rate of heat deposition to the mixture from radioisotope decay: 1% of the reactor nominal power of 3434 MWth,

Suppression pool initial condition:

Water mass: 7.6E6 lbm (3,447 kg), water temperature: 90 F (32 C), pressure: 14.7 psia (1 atm).



RPV assumptions:

- water and steam are completely mixed and remain in thermodynamic equilibrium throughout the discharge period,
- only saturated steam leaves the RPV,
- the rate of heat deposition to the RPV from both sources remain constant throughout the discharge period.

Suppression pool assumptions:

- water in the suppression pool remains subcooled at atmospheric pressure throughout the event, and
- no residual heat removal system is activated for the suppression pool as long as the pool temperature remains below 110 F (43 C).

[Ans.: $P_{RPV} \approx 900$ psia and $T_{Pool} \approx 110$ F].

24. Find the cooldown rate and the suppression pool temperature in Problem 23 for a case that the relief valve has stuck open for five minutes. The valve flow area is 0.1 ft^2 ($\approx 0.01 \text{ m}^2$).

25. Our goal in this problem is to find the rate of depressurization in a PWR plant. In this case, the depressurization is due to the pressurizer spray valve failure in the open position. The stuck open spray valve allows colder water from the cold leg to be sprayed into the bulk vapor space. Find the time it takes for pressurizer pressure of 15.5 MPa to drop to 13 MPa. Also calculate the water volume. Assume no other processes take place in the pressurizer. Further assume that the spray flow rate and enthalpy remain constant and $\dot{m}_{sp} = \dot{m}_{out-surge}$.

Data: $\dot{m}_{sp} = 28 \text{ kg/s}$, $h_{sp} = 1250 \text{ kJ/kg}$, $(V_l)_{\text{initial}} = 18 \text{ m}^3$ and $(V_v)_{\text{initial}} = 28 \text{ m}^3$.

26. A hermetically sealed tank contains a mixture of water and steam at pressure P_1 . The tank wall is made of carbon steel. The wall on the inside is covered by a stainless steel cladding and on the outside by a layer of insulation. Use the specified data to find the time it takes for the tank pressure to drop to P_2 MPa.

Pressure data: Initial pressure: 2030.5 psia, final pressure: 1500.0 psia,

Geometry data: tank total volume: 1500 ft^3 , water volume fraction: 40%, tank height: 6 ft, cladding thickness: 0.5 in, carbon steel thickness: 5 in, insulation thickness: 3 in,

Heat transfer data: ambient temperature: 85 F, heat transfer coefficient from the mixture to the inside of the tank wall: $150 \text{ Btu/h}\cdot\text{ft}^2\cdot\text{F}$, heat transfer coefficient from the tank to the ambient: $25 \text{ Btu/h}\cdot\text{ft}^2\cdot\text{F}$,

Property data: stainless steel: $k = 8.6 \text{ Btu/h}\cdot\text{ft}\cdot\text{F}$, $c_p = 0.123 \text{ Btu/lbm}\cdot\text{F}$, $\rho = 488 \text{ lbm/ft}^3$,

carbon steel: $k_{\text{carbon steel}} = 29.6 \text{ Btu/h}\cdot\text{ft}\cdot\text{F}$, $c_p = 0.11 \text{ Btu/lbm}\cdot\text{F}$, $\rho = 487 \text{ lbm/ft}^3$,
insulation: $k = 0.3 \text{ Btu/h}\cdot\text{ft}\cdot\text{F}$, $c_p = 0.037 \text{ Btu/lbm}\cdot\text{F}$, and $\rho = 27 \text{ lbm/ft}^3$

Assumptions:

- heat loss takes place from all surfaces and
- heat transfer coefficients remain constant throughout the event.

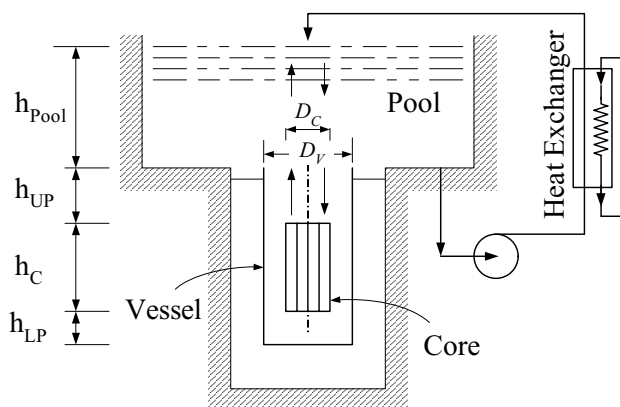
[Ans.: about 20 hours].

27. A tank contains saturated steam at 10.4 MPa. The height and the inside diameter of the tank are 9 m and 2.5 m, respectively. The bottom of the tank is connected to a supply piping with the admission valve fully closed. We open the admission valve and let water at a rate of 8 lit/s, a pressure of 17 MPa, and a temperature of 275 C enter the tank. We close the admission valve after 20 minutes.

- Use an isentropic compression assumption for the steam region to find the pressure in the steam dome immediately after the valve is closed.
- Revise your estimate by considering the effect of heat transfer to the wall and on the water surface.
- Find the tank pressure 15 minutes after the admission valve is closed. The tank has a wall thickness of 14 cm and is not insulated. The ambient temperature is 45 C and the heat transfer coefficient to ambient is 15 W/m²·C.

28. Shown in the figure is a PWR reactor vessel, with the vessel head removed. Initially there are no fuel assemblies in the core and the vessel and pool are full of water. We now place the assemblies in the core. The heat produced in the core, due to the decay of the radio-nuclides must be removed. For this purpose, water from the bottom of the pool is circulated through a heat exchanger and the colder water is returned to the top of the pool. In this way, the core is cooled solely by natural circulation. Use the specified data to estimate the flow rate through the core.

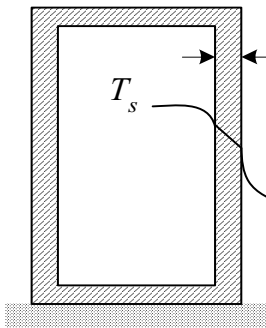
Data: $h_{LP} = 3$ m, $h_C = 3.5$ m, $h_{UP} = 3.8$ m, $h_{Pool} = 7$ m, $D_C = 2.5$ m, $D_V = 11.3$ m, $A_{Pool} = 162.5$ m², $T_{initial} = 50$ C, Core decay power = 10 MW, Flow rate through the pump = 200 lit/s.



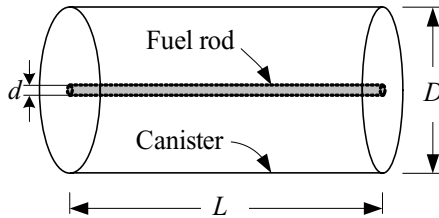
29. A right circular cylinder tank, having a volume of 44 m³, contains a saturated mixture of water and steam at 15 MPa. The tank has a height of 10 m and a wall thickness of 14 cm. The ambient is quiescent air at 35 C and 1 atm. The initial steam quality is 99%. The tank is fully insulated with negligible heat loss. We now, remove the insulation and let heat loss to ambient take place from the top

and the cylindrical surface. Estimate the value of the following variables after one hour a) steam pressure, b) steam temperature, c) wall temperature facing the steam, d) wall temperature facing the ambient air, e) water level in the tank.

[Ans. $P_2 = 14.17$ MPa, $T_2 = 337.5$ C, $T_{wi} = 337.5$ C, $T_{wo} = 333.6$ C, $L_{water} = 13$ cm].



Problem 29



Problem 30

30. A canister of diameter D , length L , and wall thickness δ has an initial temperature of T_c . We now evacuate the air from the canister by using a vacuum pump and place a spent fuel rod while maintaining the wall temperature at T_c . The spent fuel rod produces heat at rate of 5 W. The canister is exposed to air at 35 C and a heat transfer coefficient of 5 W/m²·C. Plot the spent fuel and the canister wall temperatures versus time for a duration of 18 hours. To simplify the analysis a) assume that the fuel rod is bare UO₂, b) ignore conduction heat transfer between the rod and the canister ends, c) use a lumped capacitance for the fuel as well as the canister wall. Heat transfer takes place at all surfaces. Use, $d = 2$ mm, $D = 10$ cm, $L = 3$ m, $\epsilon_{UO_2} = 0.8$. Canister is made of stainless steel with a wall thickness of 2 cm ($\epsilon = 0.4$).

31. The models developed in Chapter VIId to analyze the primary and the secondary sides of a PWR are based on the thermodynamic equilibrium assumption, except for the pressurizer and the secondary side of the steam generator, which were analyzed based on the thermodynamic non-equilibrium model. In the lumped parameter approach, the perfect mixing assumption is used and only one temperature is allocated to a node. Thus, a multi-node representation was required for regions such as the core and the steam generator primary side in which large temperature gradients exist (Figures VIId.2.1, VIId.3.2, and VIId.7.1).

Another approach, originally developed by Myers and employed by Kao, allocates only one node to a region even if there is a large temperature gradient in the region. For example, one node is used to represent the PWR core despite the large temperature rise over the core. Similarly, the tube bundle region of the steam generator with large density gradient is modeled by only one control volume. This is possible by the introduction of the *linear enthalpy profile* model. In this model a volume-averaged mixture density, ρ^* is defined as:

$$\rho^* = \frac{1}{V} \int_V \rho_m(P, h_m) dV$$

Similarly, a volume-averaged mixture enthalpy h^* is defined as:

$$h^* = \frac{1}{V} \int_V \rho_m(P, h_m) h_m dV$$

where subscript m stands for mixture. If the volume-averaged mixture density and enthalpy are known, then the mass and energy of a node can be found from $m = \rho^* V$ and $u = h^* V - PV$, respectively. To find the volume-averaged mixture density and enthalpy in closed form, the mixture density profile in terms of pressure and enthalpy is needed to develop the above integrals.

a) To find such profile, show that at a given pressure, density of saubcooled water decreases almost linearly with increasing enthalpy. Also show that the specific volume of a two-phase mixture and of superheated steam increases linearly with enthalpy.

b) Now consider control volume i , connected to the control volumes $i - 1$ and $I + 1$. Show that by a linear transformation, the volume-averaged density and enthalpy become functions of pressure and the inlet and exit mixture enthalpies, given by:

$$\rho_i^* = \frac{\int_{h_{m,i-1}}^{h_{m,i}} \rho_{m,i}(P, h_{m,i}) dh_{m,i}}{h_{m,i} - h_{m,i-1}} \quad \text{and} \quad h_i^* = \frac{\int_{h_{m,i-1}}^{h_{m,i}} \rho_{m,i}(P, h_{m,i}) h_{m,i} dh_{m,i}}{h_{m,i} - h_{m,i-1}}$$

c) Using the linear enthalpy profile assumption show that in the single-phase region:

$$\rho_{m,i} = \rho_{i-1} + \frac{\partial \rho_{m,i}}{\partial h_{m,i}} (h_{m,i} - h_{i-1})$$

where in this region, $\rho_{m,i} / h_{m,i}$ is a constant. Also show that in the two-phase region:

$$v_{m,i} = v_{i-1} + \frac{\partial v_{m,i}}{\partial h_{m,i}} (h_{m,i} - h_{i-1})$$

where in this region, $v_{m,i} / h_{m,i}$ is a constant.

d) Substitute these profiles in the above integrals to obtain expressions for ρ_i^* and h_i^* .

Vle. Nuclear Heat Generation

In Chapter IVa, we treated the volumetric heat generation rate, \dot{q}''' as a known quantity. The internal heat generation in a substance may be due to various processes such as electrical resistance, chemical, or nuclear reactions. If the internal heat generation is due to an electrical resistance, then the calculation of \dot{q}''' is rather trivial. Examples of chemical heat generation include the exothermic reaction of some alloys with water at high temperatures. Zircaloy, for example, reacts with water at elevated temperatures to produce heat and hydrogen gas. In the case of the nuclear reaction, however, calculation of the volumetric heat generation rate is more involved since it requires the study of neutron transport as a result of neutron-nucleus interactions. This is further complicated by the interdependency of neutron populations on the state of the medium, such as the composition, pressure, and temperature. In this chapter we first introduce several key terms that play major roles in nuclear engineering. This is followed by the derivation of the neutron transport equation, which is difficult to solve. Therefore, we introduce the application of Fick's law as our constitutive equation to turn the neutron transport equation into an equation known as the neutron diffusion equation. This is because the neutron diffusion equation provides nearly accurate results for many applications and has the additional advantage of being amenable to even analytical solutions for some familiar geometries. We then proceed to find the rate of nuclear heat generation from fission. Finally, we investigate the effect of the neutron flux on temperature distribution in conventional reactor cores.

1. Definition of Some Nuclear Engineering Terms

1.1. Definitions Pertinent to the Atom and the Nucleus

Atom is defined as the smallest unit of an element that can combine with other elements. Democritus in the fifth century B.C. believed that an atom is the simplest thing from which all other things are made. The Greek word *atomos* means *indivisible*. It was not until the early 20th century that subatomic particles were identified and the structure of the atom was described in terms of the nucleus and electrons. The nucleus consists of positively charged protons and neutral neutrons. The protons and neutrons are tightly clustered in the nucleus. The negatively charged electrons encircle the nucleus on far away orbits. Indeed the distance between the closest electron orbit to the nucleus is about 100,000 times the radius of the nucleus. Even further away is the neighboring nucleus, which is as far away as about 200,000 times the radius of the nucleus. The diameter of an atom is generally expressed in terms of angstrom (\AA), which is $1\text{E}-10$ m. For example, the diameter of a chlorine atom is 2\AA . The hydrogen atom has the simplest structure. Its nucleus consists of a proton with one electron in its orbit, which makes the atom neutral. Helium has two protons and two neutrons in the nucleus with two electrons orbiting the nucleus. There are a maximum number of

electrons that each orbit, or shell, can possess. In chemical reactions, electrons of the last shell, which is not filled to capacity, bond with the shells of other atoms to produce a molecule. In this reaction, the nucleus remains intact. In nuclear reactions, the nucleus itself is affected.

Nucleon is referred to a particle that exists in the nucleus. Thus protons and neutrons are *nucleons*.

Nuclide refers to a specific atom or nucleus. If a nuclide is not stable, it is referred to as a *radionuclide*.

Atomic number (Z) represents the number of protons in an atom. If N is the number of neutrons, then the *mass number* (A) is equal to the total number of neutrons and protons, $A = N + Z$. We generally show elements as ${}_Z^A\text{E}$. For example, natural uranium is shown as ${}_{92}^{238}\text{U}$. There are elements for which we can find various mass numbers. Atoms of these elements have the same number of protons but a different number of neutrons. These are known as *isotopes*. For example, naturally occurring uranium ore has 99.28% atoms of ${}_{92}^{238}\text{U}$, 0.714% atoms of ${}_{92}^{235}\text{U}$, and 0.006% atoms of ${}_{92}^{234}\text{U}$. Thus U-233, U-234, U-235 and U-238 are isotopes of uranium. The effect of isotopes on mass number is shown in Figure VIe.1.1(a). We may enhance the number of atoms in an isotope in the naturally occurring substance; this process is referred to as *enrichment*.

Atomic mass unit (amu) is equal to the one-twelfth of the mass of carbon 12. Since one mole of ${}^{12}_6\text{C}$ has 6.023E23 atoms and weighs 12 gram, then 1 amu = $(1/12) \times (12/6.023\text{E}23) = 1.66\text{E}-24$ gram. On this basis, $m_{\text{proton}} = 1.007277$ amu, $m_{\text{neutron}} = 1.008665$ amu, and $m_{\text{electron}} = 0.000548597$ amu as summarized in Table VIe.1.1. Based on Einstein's equation, the energy equivalent with 1 amu is $E = mc^2 = (1.66\text{E}-27 \text{ kg})(3\text{E}8 \text{ m/s})^2 = 1.49\text{E}-10 \text{ J}$. Since 1 MeV = 1.602E-13 J, then 1 amu = 931.5 MeV.

Table VIe.1.1. Approximate classical characteristics of atoms and particles

Object	Mass (amu)	Mass (g)	Charge (coul)	Radius (cm)
Electron	0.000548597	9.11E-28	-1.6E-19	2.822E-13
Proton	1.007277	1.67E-24	+1.6E-19	2.103E-14
Neutron	1.008665	1.67E-24	0.0	2.100E-14
Nucleus	$Zm_p + Nm_n$	$Zm_p + Nm_n$	$Z \times 1.6\text{E}-19$	$(1.2\text{E}-13)A^{1/3}$
Atom	$Z(m_p + m_e) + Nm_n$	$Z(m_p + m_e) + Nm_n$	$Z \times 1.6\text{E}-19$	1.0E-8

Atom density, N is the number of the atoms of an element per unit volume ($\#/\text{m}^3$). Atom density is given by $N = \rho N_A/M$. Atom density is generally a function of space and time, $N = N(\vec{r}, t)$.

Mass defect is defined as the difference in measured mass between the conglomerate mass of a coalesced nucleus and the sum of the masses of the individual

constituent particles of that nucleus. The mass defect for element ${}^A_Z\text{E}$, for example, is found as $\Delta m = Z(m_{\text{proton}}) + N(m_{\text{neutron}}) - (M_E - Zm_{\text{electron}})$.

Binding energy ($B.E.$) of a nucleus is the energy-equivalent of the mass defect of that nucleus ($B.E. = \Delta mc^2$). The binding energy may be thought of as the energy that would be required to break the nucleus into its individual constituents or as the amount of energy that would be released upon an instantaneous coalescence of all individual constituents to form the nucleus.

Example VIe.1.1. Find the mass defect and the binding energy per nucleon for Beryllium, ${}^9_4\text{Be}$. The mass of this element is given as 9.01219 amu.

Solution: The mass defect is found as:

$$\Delta m = 4 \times 1.007277 + 5 \times 1.008665 - (9.01219 - 4 \times 0.000549) = 0.062439 \text{ amu}$$

The equivalent energy is found as:

$$E = mc^2 = (0.062439 \times 1.66 \times 10^{-27} \text{ kg})(3 \times 10^8 \text{ m/s})^2 = 9.328 \times 10^{-12} \text{ J} = 58.2 \text{ MeV}.$$

The binding energy per nucleon is found as:

$$58.2/9 = 6.5 \text{ MeV/nucleon}.$$

Binding energy per nucleon, Figure VIe.1.1(b) is a minimum for hydrogen and reaches a maximum of about 9 MeV per nucleon for iron. As mass number increases beyond 60, binding energy per nucleon keeps dropping. The slope of the curve is an indication of relative stability and potential sources for energy release. For example, for such heavy elements as Uranium and Plutonium, the binding energy drops to about 7.5 MeV/nucleon. If the atom of such materials split, energy is released and more stable nuclei appear.

Neutron-nucleus interactions are of two types. Consider bombardment of a target material with a beam of neutrons. Depending on the energy and the direction of the neutrons as well as the atoms of the target, we may have an interaction. If an interaction occurs, it results in the neutrons being scattered from the nucleus or absorbed by the nucleus.

Scattering is one of two outcomes resulting from interaction between a target nucleus and the bombarding neutron. If the total kinetic energy of the neutron and the nucleus before and after the scattering event remains the same, the event is referred to as *elastic scattering*. Otherwise, the interaction is known as *inelastic scattering*. For low neutron energies in elastic scattering, the passing neutron is bounced due to the force exerted by the nucleus, hence the process is referred to as *potential scattering*. However, for higher neutron energies, the neutron and nucleus may combine to form a *compound nucleus* from which a neutron emerges. For inelastic scattering to occur, the energy of the neutron must exceed the minimum energy required for a compound nucleus to form.

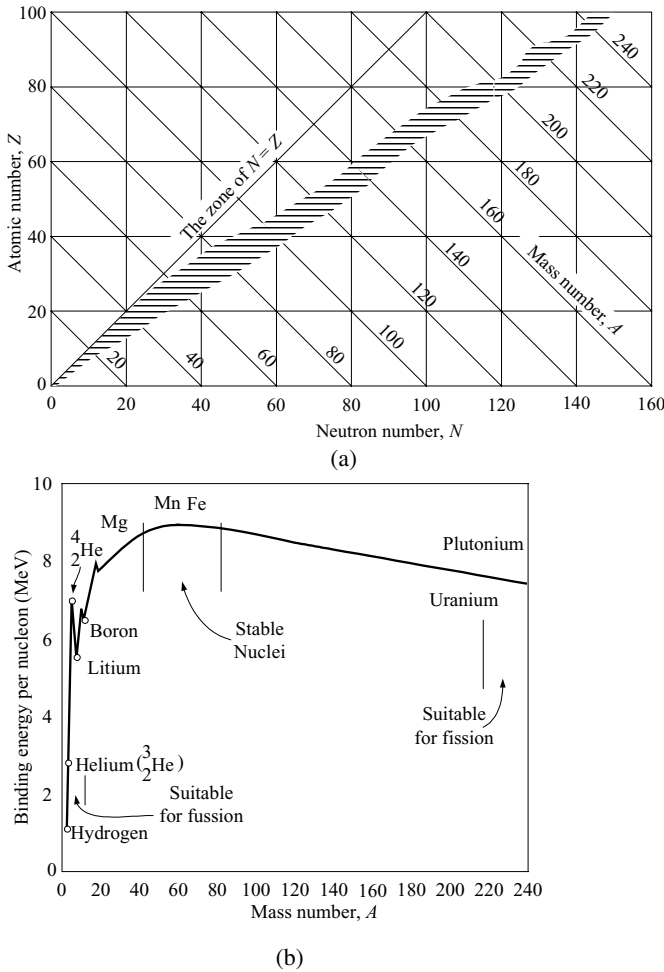


Figure VIe.1.1. (a) Effect of isotopes on mass number and (b) Binding energy per nucleon

Absorption is the second outcome in a neutron-nucleus interaction. Absorption in turn may lead to several types of interactions. The absorption of a neutron by the nucleus places the resulting compound nucleus in an excited state. The compound nucleus may then break up, leading to fission, or it may de-excite itself by emitting energetic radiation such as alpha (α), gamma (γ), neutron (n), or protons (p). Although the excited state of a nucleus can be as short as $1\text{E}-14$ seconds, it is considered a well-defined state compared with the approximately $1\text{E}-22$ seconds it takes for a neutron to travel across the nucleus.

Resonance. Application of the wave or quantum mechanics to the atomic nucleus shows that the internal energy of a nucleus is quantized (see the solution to Equation VIIb.1.32). If a neutron has a sufficient amount of $K.E.$ for the creation

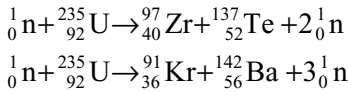
of a compound nucleus then the neutron and the nucleus are said to be in resonance.

Microscopic cross section σ_i , represents probability of occurrence of a given type of interaction between an incident neutron and the target nucleus of the medium through which the neutron travels. In this case, the subscripted variable, i , represents the type of interaction, whereby the relative probability of occurrence of a scattering reaction would be represented as σ_s (σ_a for absorption and σ_f for fission). This property, which represents probabilities of certain types of interaction, is specific to the target nucleus type (as it is a property) and is also dependent upon incident neutron energy and type of interaction. This probability is generally represented in units of area, cm^2 , or barns (b) where $1 \text{ barn} = 1.0\text{E}-24 \text{ cm}^2$.

Macroscopic cross section, Σ_i is the probability of interaction of type i per unit length (1/cm) of neutron travel. Thus, the chance of interaction with an atom per unit distance traveled is σ and for N atoms is $\Sigma_i = N\sigma_i$.

Resonance cross section refers to the range of neutron energy of 1 eV to $1\text{E}5$ eV where for many isotopes the absorption cross section of the target nucleus displays extreme variations in magnitude as shown in Figure VIe.1.2(a). The resonance cross section, indicating a high probability of interaction, occurs when the energy quantized or the excited state of the compound nucleus matches the summation of the neutron K.E. and the compound nucleus binding energy.

Fission event. Figure VIe.1.1 shows that, following the stable region, binding energy decreases with increasing number of neutrons. This implies that if we break up heavy nuclei such as uranium, we would end up with two nuclei having mass numbers of about one-half of the original nucleus hence being more stable. This is indeed the case, as the breaking up, referred to as fission, results in lighter and more stable nuclei with respect to fission. The appearance of a fission products is a probabilistic event. For example, the fission of uranium-235 may result in excess of 200 different isotopes of 35 different elements. Examples for fission of a Uranium-235 nucleus include the appearance of Zr, Te, Kr, and Ba:



It must be emphasized that the fission products are generally highly radioactive and thus hazardous.

The above reactions indicate that, in a sustained interaction leading to fission, between 2 to 3 neutrons emerge for each neutron that is absorbed to cause fission in U-235. The number of neutrons emerging in a fission is represented by ν . These newly emerged neutrons have a spectrum of energy as shown in Figure VIe.1.2(b) and mathematically described as:

$$\chi(E) = 0.453e^{-1.036E} \sinh \sqrt{2.29E}$$

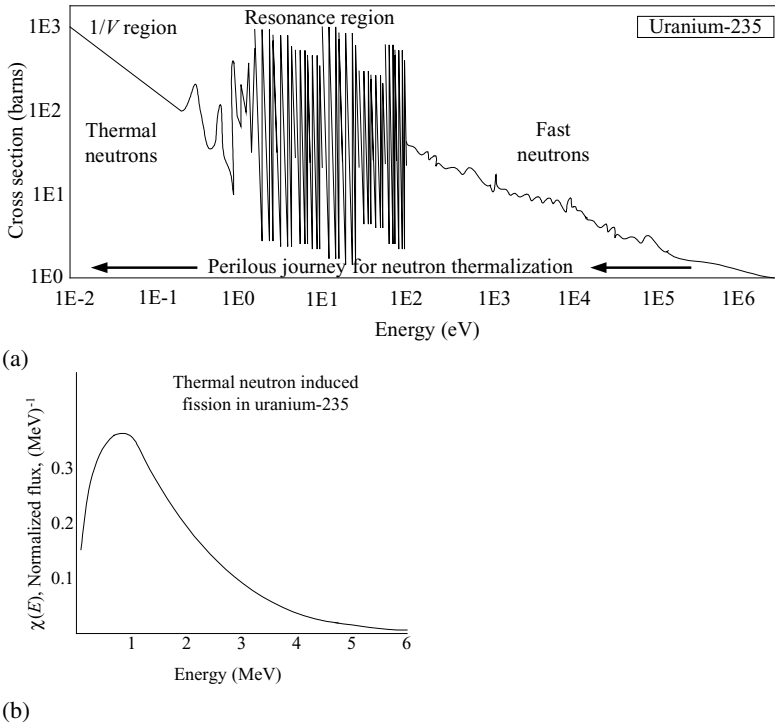


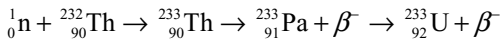
Figure VIe.1.2. U-235 (a) Fission cross-section and (b) prompt fission neutron spectrum

where E is in MeV. While some newly emerged neutrons have energies as low as a fraction of MeV and a few up to 17 MeV, the most probable energy is found as 0.73 MeV and the average energy as 1.98 MeV. The U-235 isotope has a large fission cross section for slow neutrons, (i.e., neutrons that have energy in the range of 0.025 eV). Hence, we must use some means of slowing down neutrons to such low energies. However, the journey for neutrons from about 2 MeV to about 0.025 eV is quite perilous. This is because the U-235 cross section for fission is highly energy dependent (Figure VIe.1.2(a)). Thus, there is a high probability that the neutron, before being slowed down is captured in the isotope, especially in the resonance region, hence not leading to fission. In the low energy range, referred to as the thermal region, the nucleus cross-section is proportional with the inverse square root of energy, known as the $1/V$ region.

Fissile, fissionable, and fertile isotopes. A fissile material is an isotope that would fission upon the absorption of a neutron of essentially no kinetic energy. In other words, simply the binding energy of that last neutron in the compound system is enough to overcome the critical energy required for fission to occur. This type of isotope proves to be the most useful for producing the neutron chain reaction necessary to produce power with a thermal pressurized water reactor. Fissile isotopes include ^{233}U , ^{235}U , ^{239}Pu , and ^{241}Pu . Plutonium-239 is found in abun-

dance in spent fuel rods and can be recovered in reprocessing facilities. During normal operation of a nuclear reactor, plutonium-239 is produced inside the fuel rod such that towards the end of a fuel cycle, it is one of the major contributors (up to 50%) of the power produced by the reactor. Fissionable materials are isotopes that, like fissile materials, fission, but only with fast or energetic neutrons (energies higher than 2 MeV for U-238). An important fissionable isotope is the naturally occurring U-238. The contribution of this isotope to the power level of a thermal reactor is about 5%. Other fissionable isotopes are ^{232}Th and Pu-240.

Fertile materials are isotopes that do not fission but produce fissile materials as a result of an interaction with neutrons. An example of a fertile isotope is $^{232}_{90}\text{Th}$:



where β^- refers to beta-decay. The most important fertile isotope is uranium-238 resulting in the fissile isotope plutonium-239.

Since there are isotopes that are suited for fission if exposed to fast neutrons and similarly isotopes suited for fission by slow (or thermal) neutrons, there are also two types of reactors, fast and thermal. However, there are many more nuclear reactors based on thermal fission than based on fast fission.

Moderator is used to slow down the newly born fast neutrons in thermal reactors. The moderator in thermal reactors generally has a dual role as it is also used as a coolant. Water (H_2O) is used in “light water reactors” and heavy water (D_2O), using deuterium instead of hydrogen, in “heavy water reactors”. The latter reactor is of Canadian design and is known as the Canada Deuterium Uranium or CANDU reactor, for short. Since a neutron loses most of its energy in scattering events with light nuclei, a moderator should be a substance made of light nuclei with low absorption and a high scattering cross section. Properties of widely used moderators are listed in Table VIe.1.2, where D is the diffusion coefficient and Σ_a is the macroscopic absorption cross sections.

Table VIe.1.2. Properties of some moderators (at 20 C) for thermal neutrons (Lamarsh)

Moderator	Density (g/cm^3)	D (cm)	Σ_a (1/cm)
Water (H_2O)	1.00	0.16	1.97E-2
Heavy Water (D_2O)	1.00	0.87	9.3E-5
Beryllium (Be)	1.85	0.50	1.04E-3
Graphite (C)	1.60	0.84	2.4E-4

1.2. Definitions Pertinent to Neutrons

Neutron density, $n(\vec{r}, E, \vec{\Omega}, t)$ as shown in Figure VIe.1.3(a) is the number of neutrons that at time t are at location x, y, z in volume dV , of energy E about dE and travelling in the direction of Ω_x, Ω_y , and Ω_z (or Ω_r, Ω_θ and Ω_ϕ) in $d\vec{\Omega}$ (the solid angle is shown in Figure IVd.5.1). If, for example, we want to find the num-

ber of neutrons having all ranges of energy and travelling in all directions, we integrate over energy and solid angle*:

$$n(\vec{r}, t) = \int_{\Omega} \left(\int_0^{\infty} n(\vec{r}, \vec{\Omega}, E, t) dE \right) d\vec{\Omega} \quad \text{VIe.1.1}$$

While $n(\vec{r}, \vec{\Omega}, E, t)$ has units of $\text{s}^{-1} \text{cm}^{-3} \text{eV}^{-1} \text{sr}^{-1}$, $n(\vec{r}, t)$ has units of neutrons/ cm^3 .

Neutron velocity, $V(E)$ is the length per unit time traveled by the neutrons, (cm/s). Neutron velocities may range from 8,000 to 80,000,000 km/h. The newly born neutrons due to fission are very energetic (average energy is about 2 MeV but some may emerge with energies up to 20 MeV). Such neutrons lose their energy due to collision with the moderator nuclei. The loss of energy would eventually result in neutrons coming to thermal equilibrium with their surrounding medium. This is why the slowed down neutrons are referred to as being *thermalized*. Energy of neutrons in a neutron population can be approximately obtained from the Maxwell-Boltzmann distribution (see Problem 4). Using the Maxwellian distribution, we can find the most probable velocity in terms of neutron temperature as $V = (2\kappa T/m)^{1/2}$ where κ is the Boltzmann constant, $\kappa = R_u/N_A = 8.314/6.023\text{E}23 = 1.38\text{E}-23 \text{ J/K}$. Thus, neutrons at room temperature of 20 C have a velocity of $V = (2 \times 1.38\text{E}-23 \times [20 + 273.16/(1.008665 \times 1.66\text{E}-27)])^{1/2} \approx 2200 \text{ m/s}$. The kinetic energy at this velocity is:

$$\begin{aligned} K.E. &= mV^2/2 = 0.5 \times [(1.008665 \times 1.66\text{E}-27)/(1.602\text{E}-13)] (2200)^2 \\ &= (5.226\text{E}-15) V^2 = 0.0253 \text{ eV} \end{aligned}$$

Neutron angular flux, $\phi(\vec{r}, E, \vec{\Omega}, t) dE d\vec{\Omega}$ is the number of neutrons at location r , energy (E) about dE and traveling at time t through a unit area perpendicular to $\vec{\Omega}$, in the differential solid angle $d\vec{\Omega}$ in the direction of $\vec{\Omega}$. As shown in Figure VIe.1.3(a), $\vec{\Omega}$ is the unit vector of the neutron velocity vector, hence, $\vec{V} = V\vec{\Omega}$. To find the integrated steady state neutron flux, we integrate the steady state angular flux over all solid angles to obtain:

$$\phi(\vec{r}, E) = \int_{\Omega} \phi(\vec{r}, E, \vec{\Omega}) d\vec{\Omega} \quad \text{VIe.1.2}$$

For the special case of isotropic emission of neutrons, where neutrons are distributed uniformly over the surface area of a sphere having a radius of unity, the angular flux is related to the integrated flux through:

$$\phi(\vec{r}, E, \vec{\Omega}) = \frac{\phi(\vec{r}, E)}{4\pi} \quad \text{VIe.1.3}$$

* Another way of representing $n(\vec{r}, E, \vec{\Omega}, t)$ is to write

$$d^6 n / dx dy dz dE d\vec{\Omega} dt = d^7 n / dx dy dz dE (\sin \varphi d\theta d\varphi) dt$$

The integrated flux is shown in Figure VIe.1.3(b). To relate neutron flux to the number density of the neutrons, we may treat neutrons as a fluid and use the similarity between neutron flux (ϕ), neutron density (n), and neutron velocity (V) with mass flux (G), density (ρ) and flow velocity (V) per Equation IIa.5.3, ($G = \rho V$). Thus, for neutron flux we find:

$$\phi(\vec{r}, E) = n(\vec{r}, E)V(E) \quad \text{VIe.1.4}$$

If the integrated flux over all directions is also integrated over all energies, we find neutron flux $\phi(\vec{r}, t)$ or the steady state flux $\phi(\vec{r})$. This is referred to as the *one-speed neutron flux*.

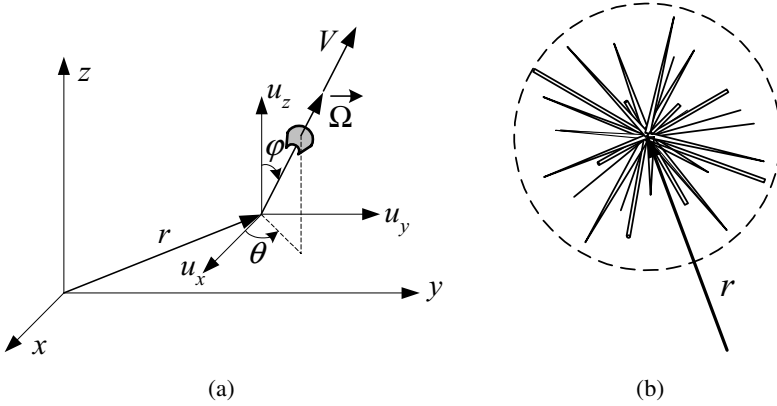


Figure VIe.1.3. (a) Depiction of position and direction of a neutron. (b) Integrated flux over all directions at position \vec{r} (Ott).

Angular current density is a vector defined by the following relation $\vec{J}(\vec{r}, E, \vec{\Omega}, t) = \phi(\vec{r}, E, \vec{\Omega}, t)\vec{\Omega}$, hence, it has an absolute value equal to the angular flux. Thus $\vec{J}(\vec{r}, E, \vec{\Omega}, t)dE dS d\vec{\Omega}$ represents the rate of neutrons at location \vec{r} , passing at time t through differential area dS , with an energy (E) in dE and in the direction of $\vec{\Omega}$ in $d\vec{\Omega}$.

Neutron current density or simply neutron current is obtained by the integration of the angular current density over all possible directions:

$$\vec{J}(\vec{r}, E, t) = \int_{\Omega} \vec{J}(\vec{r}, E, \vec{\Omega}, t) d\vec{\Omega} \quad \text{VIe.1.5}$$

If we integrate the neutron current density over all ranges of energy we obtain the neutron current as $\vec{J}(\vec{r}, t)$. The neutron current, being a vector, is instrumental in describing the leakage of neutron, into or out of a region.

Rate of neutron interaction, is obtained by multiplying the neutron flux by the macroscopic cross section of the nucleus for a specific outcome. Thus $R_i = \phi \Sigma_i$ (neutron/s·cm²) \times (atoms/cm) = interaction/s·cm³.

Rate of heat generation \dot{q}''' (W/cm³) is found from the rate of interaction. If we consider the interaction of type i as that leads to fission, then $i = f$ and $R_f = \phi \Sigma_{fr}$, where subscript fr stands for fission in the fuel rod. If the energy produced per fission is E_R , then the total power produced per unit volume is given by:

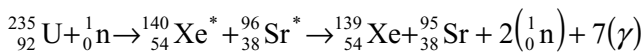
$$\dot{q}''' = E_R \phi \Sigma_{fr} \quad \text{VIe.1.6}$$

The energy produced per fission, E_R is about 200 MeV (1 eV = 1.6E–19 joules hence $E_R = 3.2\text{E}–11$ J). When the nucleus of a heavy element undergoes fission, most of the resulting energy is due to the kinetic energy of the fission fragments as shown in Table VIe.1.2. Note that the deposited energy is $E_d = 90\%$ $E_R = 180$ MeV.

Table VIe.1.2 Approximate distribution and deposition of fission energy (El-Wakil)

Type	Process	Percent of total energy	Energy deposition
Fission (prompt)	Kinetic energy of fission fragments	80.5	Fuel material
	Kinetic energy of the emergent fast neutrons	2.5	Moderator
	γ Energy associated with fission	2.5	Fuel & structure
Fission (delayed)	Kinetic energy of delayed neutrons	0.02	Moderator
	β^- -decay energy of fission products	3.0	Fuel material
	Neutrinos from β^-	5.0	Nonrecoverable
	γ -decay of fission products	3.0	Fuel & structure
Capture	β^- and γ -decay energy of (n, γ) product	3.5	Fuel & structure
Total	100		

Example VIe.1.2. Find the prompt energy of U-235 fission resulting in the appearance of Xe and Sr:



Solution: The prompt energy related to the mass defect is found from:

$$\begin{aligned} E_p &= [M({}_{92}^{235}\text{U}) + m_n - M({}_{54}^{139}\text{Xe}) - M({}_{38}^{95}\text{Sr}) - 2m_n]c^2 \\ &= [235.043923 + 1.008665 - 138.918787 - 94.919358 - 2(1.008665)] \end{aligned}$$

Thus $E_p = 0.197113$ amu = 0.197113×931.5 MeV/amu = 183.61 MeV. This includes 5.2 MeV kinetic energy of the two prompt neutrons and 6.7 MeV energy of the emerging gamma rays.

The six factor formula. Earlier we discussed that the emerging fast neutrons from the fission of U-235 have a perilous journey from the fast to the thermal region before being used for the next fission cycle. Aside from being absorbed in the nucleus (fuel) without causing fission, they may leak out of our control volume or may be absorbed by elements other than the fuel, such as the reactor structure (Table VIe.3.1). To formulate this verbal discussion in mathematical terms, we consider two cases of infinite and finite media. The infinite medium consists of fuel, structure, and neutrons. In such a medium, no neutron can be lost to leakage. However, for the finite medium case, we do lose neutrons to leakage. Such leakage is due to scattering out of the region of interest. To keep track of the neutron inventory in each cycle, we define k , the *multiplication factor*, as the ratio of the number of neutrons in the new cycle to the number of neutrons in the previous cycle. We represent this ratio by k_∞ for the infinite and by k_{eff} for the finite medium. If we divide the energy spectrum to fast and thermal, we may lose neutrons to leakage in both energy regions. The relation between the ratios is:

$$k_{\text{eff}} = k_\infty P_{\text{FNL}} P_{\text{TNL}}$$

where P_{FNL} is the probability that a fast neutron not leak out and P_{TNL} is the probability that a thermal neutron does not leak out. Having taken care of the leakage term for now, we begin to focus on k_∞ . By definition, in an infinite medium, the ratio of neutrons in the present cycle to that of the previous cycle is:

$$k_\infty = \frac{\int_{\text{medium}} dV \int_0^\infty v \Sigma_f(\vec{r}, E) \phi(\vec{r}, E)}{\int_{\text{medium}} dV \int_0^\infty \Sigma_a(\vec{r}, E) \phi(\vec{r}, E)} = \frac{\int_{\text{fuel}} dV \int_0^\infty v \Sigma_f(\vec{r}, E) \phi(\vec{r}, E)}{\int_{\text{medium}} dV \int_0^\infty \Sigma_a(\vec{r}, E) \phi(\vec{r}, E)}$$

where we changed the numerator to an integral over the fuel region, as there is no fission anywhere else in the medium. We further break down the above ratio by introducing terms in the numerator and denominator.

$$k_\infty = \frac{\int_{\text{fuel}} dV \int_0^\infty v \Sigma_f(\vec{r}, E) \phi(\vec{r}, E)}{\int_{\text{fuel}} dV \int_0^{E_T} v \Sigma_f(\vec{r}, E) \phi(\vec{r}, E)} \times \frac{\int_{\text{fuel}} dV \int_0^{E_T} v \Sigma_f(\vec{r}, E) \phi(\vec{r}, E)}{\int_{\text{fuel}} dV \int_0^{E_T} \Sigma_a(\vec{r}, E) \phi(\vec{r}, E)} \times \frac{\int_{\text{fuel}} dV \int_0^{E_T} \Sigma_a(\vec{r}, E) \phi(\vec{r}, E)}{\int_{\text{medium}} dV \int_0^{E_T} \Sigma_a(\vec{r}, E) \phi(\vec{r}, E)} \times \frac{\int_{\text{medium}} dV \int_0^{E_T} \Sigma_a(\vec{r}, E) \phi(\vec{r}, E)}{\int_{\text{medium}} dV \int_0^\infty \Sigma_a(\vec{r}, E) \phi(\vec{r}, E)}$$

VIe.1.7

where $E_T \cong 1$ eV is a cutoff energy separating the thermal region from the slowing down region. The first ratio represents the neutron production rate as a result of both fast and thermal fission to the neutron production rate due only to thermal fission. This ratio is shown by ε and referred to as the *fast fission factor*:

$$\varepsilon = \frac{\text{No. of neutrons produced in fast and thermal fission}}{\text{No. of neutrons produced in thermal fission}} = \frac{\int_{\text{fuel}} dV \int_0^\infty v \Sigma_f(\vec{r}, E) \phi(\vec{r}, E)}{\int_{\text{fuel}} dV \int_0^{E_T} v \Sigma_f(\vec{r}, E) \phi(\vec{r}, E)}$$

The second ratio in Equation VIe.1.7 represents the rate of neutron production due to thermal fission to the rate of absorption of thermal neutrons:

$$\eta = \frac{\text{No. of neutrons produced in thermal fission}}{\text{No. of thermal neutrons absorbed in fuel}} = \frac{\int_{\text{fuel}} dV \int_0^{E_T} v \Sigma_f(\bar{r}, E) \phi(\bar{r}, E)}{\int_{\text{fuel}} dV \int_0^{E_T} \Sigma_a(\bar{r}, E) \phi(\bar{r}, E)}$$

$$\cong \frac{v \Sigma_f}{\Sigma_{aF}}$$

where Σ_{aF} is the macroscopic cross section for absorption of the fuel material. This ratio is referred to as the *eta factor*. The third ratio in Equation VIe.1.7 is the rate of thermal neutrons absorbed in the fuel to the rate of thermal neutrons absorbed in the entire medium:

$$f = \frac{\text{No. of thermal neutrons absorbed in fuel}}{\text{No. of thermal neutrons absorbed in medium}} = \frac{\int_{\text{fuel}} dV \int_0^{E_T} \Sigma_a(\bar{r}, E) \phi(\bar{r}, E)}{\int_{\text{medium}} dV \int_0^{E_T} \Sigma_a(\bar{r}, E) \phi(\bar{r}, E)}$$

$$\cong \frac{\Sigma_{aF}}{\Sigma_a}$$

where Σ_a is the macroscopic cross section for absorption of the entire medium. This ratio is known as the *thermal utilization factor*. Finally, the last ratio in Equation VIe.1.7 represents the absorption rate of thermal neutrons to the absorption rate of all neutrons in the medium:

$$p = \frac{\text{No. of thermal neutrons absorbed in medium}}{\text{No. of all neutrons absorbed in medium}} = \frac{\int_{\text{medium}} dV \int_0^{E_T} \Sigma_a(\bar{r}, E) \phi(\bar{r}, E)}{\int_{\text{medium}} dV \int_0^{\infty} \Sigma_a(\bar{r}, E) \phi(\bar{r}, E)}$$

This ratio is known as the resonance escape probability. Therefore, we can write the multiplication factor of the infinite medium as $k_{\infty} = \epsilon \eta f p$. Upon substitution, the six-factor formula then becomes:

$$k_{\text{eff}} = \epsilon \eta f p P_{\text{FNL}} P_{\text{TNL}}$$

Some one-group key constants for fast reactors are shown in Table VIe.1.3.

Table VIe.1.3 Nominal one-group constants for a fast reactor (Lamarsh)

Element	σ_f	σ_a	σ_{tr}	ν	η
Na	0	0.0008	3.3	—	—
Al	0	0.0020	3.1	—	—
Fe	0	0.0060	2.7	—	—
U-235	1.4	1.6500	6.8	2.6	2.2
U-238	0.095	0.2550	6.9	2.6	0.97
Pu-239	1.85	2.1100	6.8	2.98	2.61

Cross sections are in barn (i.e., $1\text{E}-24\text{ cm}^2$)

2. Neutron Transport Equation

The neutron transport equation is the mathematical expression of the following fact:

$$\begin{aligned} & \text{rate of change of neutron population in a control volume} = \\ & \text{rate of neutron appearance in the control volume} - \\ & \text{rate of neutron disappearance in the control volume} \end{aligned}$$

We now evaluate each term in this neutron balance statement for a differential control volume dV and integrate over the volume of interest:

- Rate of change of neutron population in a control volume:

$$\int_V (dn(\bar{r}, E, \bar{\Omega}, t) / dt) dV$$

- Rate of neutron production by the source^{*}. If by fission then:

$$\int_V v \Sigma_f(\bar{r}, E) \phi(\bar{r}, E, \bar{\Omega}, t) dV$$

- Rate of neutron production due to scattering from all energy groups and all directions into the differential control volume:

$$\int_V \left\{ \int_0^\infty \int_{4\pi} [\phi(\bar{r}, E', \bar{\Omega}', t) \Sigma_s(E' \rightarrow E, \bar{\Omega}' \rightarrow \bar{\Omega})] dE' d\bar{\Omega}' \right\} dV$$

- Rate of net neutron leakage into or out of dV :

$$\oint_V \bar{J}(\bar{r}, E, \bar{\Omega}, t) \cdot d\bar{S} = \int_V \bar{\nabla} \cdot \bar{J}(\bar{r}, E, \bar{\Omega}, t) dV$$

- Rate of neutron scattering out of dV and absorption in dV :

$$\int_V [\phi(\bar{r}, E, \bar{\Omega}, t) \Sigma_t(\bar{r}, E) dV] dE d\bar{\Omega}$$

where the divergence theorem related the surface to volume integral, $\oint_A [\bar{J}(r, t) \cdot \bar{n}] dA = \iiint_V [\bar{\nabla} \cdot \bar{J}(r, t)] dV$. Substituting these in the above statement for neutron balance and dropping the integral over V , gives:

$$\begin{aligned} & \frac{1}{V} \frac{\partial \phi}{\partial t} + \bar{\nabla} \cdot \bar{J}(\bar{r}, E, \bar{\Omega}, t) + \phi(\bar{r}, E, \bar{\Omega}, t) \Sigma_t(\bar{r}, E) \\ & = v \phi(\bar{r}, E, \bar{\Omega}, t) \Sigma_f(\bar{r}, E) + \int_0^\infty \int_{4\pi} \phi(\bar{r}, E', \bar{\Omega}', t) \Sigma_s(E' \rightarrow E, \bar{\Omega}' \rightarrow \bar{\Omega}) dE' d\bar{\Omega}' \end{aligned}$$

VIe.2.1

where we also substituted for n in terms of ϕ from Equation VIe.1.4. Equation VIe.2.1, known as the neutron transport equation, is a linear partial differential equation. The angular flux in this equation is a function of seven variable; $\bar{r}(x, y, z)$, $\bar{\Omega}(\theta, \phi)$, E , and t . Since both space and time derivatives of the angular flux, as well as integrals over energy and solid angle, appear together in Equation VIe.2.1, the neutron transport equation is considered an integrodifferential equation. Appearance of both flux and current in Equation VIe.2.1 further complicates finding a solution. It is, therefore, important to find a more useful expression for

^{*} See Section 2.2 and Problem 42 for the discussion on the type of neutron source.

neutron current in terms of neutron flux than the one we already have, $\vec{J} = \phi \vec{\Omega}$. Introduction of any type of simplification to allow us deal with Equation VI.2.1 undoubtedly requires introduction of assumptions. One of the most important assumptions is the scattering-dominant reaction as discussed next.

2.1. Neutron Current In Weakly Absorbing Media

To express neutron current density, appearing in Equation VIe.2.1 in terms of neutron flux, we consider isotropic scattering of neutrons in a weakly absorbing medium. Figure VIe.2.1(a) shows neutrons being scattered isotropically out of the differential control volume dV . We want to find the neutron current density arriving at the differential surface dS at the origin located at a distance r from dV . If the macroscopic scattering of the nuclei located in volume dV is Σ_s and the flux of neutron in dV is ϕ , then the rate of neutrons scattered out of dV in all directions is $(\phi\Sigma_s)dV$. Thus, neutrons streaming out of dV are distributed over a sphere centered at dV at a rate of $(\phi\Sigma_s)dV/(4\pi r^2)$. The fraction of these neutrons that should reach dS at the origin should be $[(\phi\Sigma_s)dV/(4\pi r^2)]dS\cos\varphi$. However, neutron interaction with nuclei in the medium attenuates the rate of neutrons (see Problem 30) arriving at dS by a factor of $\exp(-\Sigma r)$. This factor is the probability of no collision between position r and the origin. In this relation, $\Sigma = \Sigma_a + \Sigma_s$. Since we considered weakly absorbing medium $\Sigma_a \approx 0$ we may then use $\Sigma \approx \Sigma_s$. As a result, the rate of neutrons arriving per unit area of the differential surface dS at the origin due to the neutrons streaming out of dV is:

$$[(\phi \Sigma_s) dV / (4\pi r^2)] dS \cos \varphi \exp(-\Sigma_s r)$$

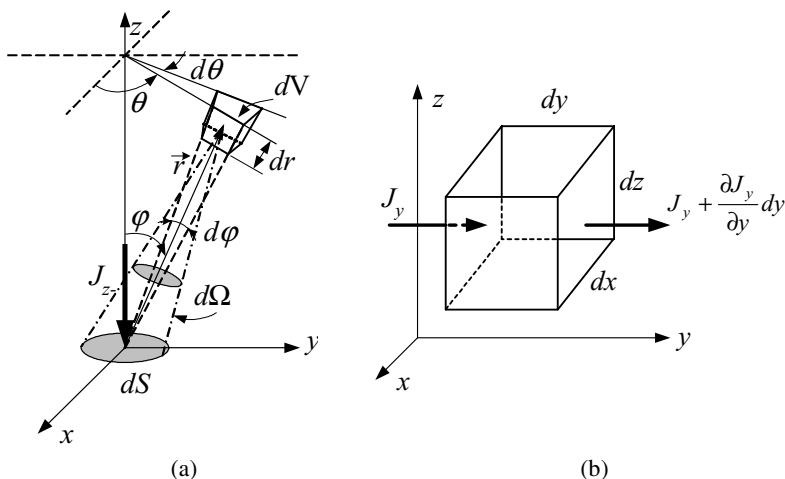


Figure VIe.2.1. (a) Neutron scattering in dV and (b) Neutron leakage from dV

The resulting neutron current in the direction shown in Figure VIe.2.1(a) is:

$$\overrightarrow{dJ}_{z-} \cdot \overrightarrow{dS} = dJ_{z-} dS = (\phi \Sigma_s) dV e^{-\Sigma_s r} \frac{\cos \phi dS}{4\pi r^2}$$

Substituting for differential volume $dV = (dr)(r \sin \phi d\theta)(rd\phi)$ and integrating, we get:

$$J_{z-} = \int_{\theta=0}^{2\pi} \int_{\phi=0}^{\pi} \int_0^{\infty} \frac{\Sigma_s}{4\pi} \left[\phi(x, y, z) e^{-\Sigma_s r} \cos \phi \sin \phi d\theta d\phi dr \right] \quad \text{VIe.2.2}$$

We now expand $\phi(x, y, z)$ using the Maclaurin series in terms of flux at the origin, $\phi_o = \phi_o(x_o, y_o, z_o)$:

$$\begin{aligned} \phi(x, y, z) = & \phi_o + x \left(\frac{\partial \phi}{\partial x} \right)_o + y \left(\frac{\partial \phi}{\partial y} \right)_o + z \left(\frac{\partial \phi}{\partial z} \right)_o + \\ & \frac{x^2}{2} \left(\frac{\partial^2 \phi}{\partial x^2} \right)_o + \frac{y^2}{2} \left(\frac{\partial^2 \phi}{\partial y^2} \right)_o + \frac{z^2}{2} \left(\frac{\partial^2 \phi}{\partial z^2} \right)_o + \dots \end{aligned}$$

Ignoring the higher order terms and substituting flux in Equation VIe.2.2, we obtain:

$$\begin{aligned} J_{z-} = & \phi_o \int_{\theta=0}^{2\pi} \int_{\phi=0}^{\pi/2} \int_0^{\infty} \frac{\Sigma_s}{4\pi} \left[e^{-\Sigma_s r} \cos \phi \sin \phi d\theta d\phi dr \right] + \\ & \frac{\partial \phi_o}{\partial z} \int_{\theta=0}^{2\pi} \int_{\phi=0}^{\pi/2} \int_0^{\infty} \frac{\Sigma_s}{4\pi} \left[(r \cos \phi) e^{-\Sigma_s r} \cos \phi \sin \phi d\theta d\phi dr \right] \end{aligned}$$

where we have also substituted for $z = r \cos \phi$ and noted that the integral over $x(\partial \phi / \partial x)_o$ and $y(\partial \phi / \partial y)_o$ vanishes (see Problem 31). Integrating this equation results in:

$$\begin{aligned} J_{z-} = & \frac{\Sigma_s \phi_o}{4\pi} \left[\frac{-e^{-\Sigma_s r}}{\Sigma_s} \right]_0^{\infty} \left[\frac{\sin^2 \phi}{2} \right]_0^{\pi/2} [\theta]_0^{2\pi} + \\ & \frac{\Sigma_s \phi_o}{4\pi} \left(\frac{\partial \phi}{\partial z} \right)_o \left[\frac{-e^{-\Sigma_s r}}{\Sigma_s} (-\Sigma_s r - 1) \right]_0^{\infty} \left[\frac{\sin^2 \phi}{3} \right]_0^{\pi/2} [\theta]_0^{2\pi} \end{aligned}$$

After the substitution of the integral limits we obtain:

$$J_{z-} = \frac{\phi}{4} + \frac{1}{6\Sigma_s} \left(\frac{\partial \phi}{\partial z} \right)_o \quad \text{VIe.2.3}$$

In order to find the net current in the z -direction at the origin due to the neutrons scattered from dV , we also need to find J_{z+} . This component is easily obtained by integrating Equation VIe.2.4 for $\pi/2 \leq \phi \leq \pi$.

$$J_{z+} = \frac{\phi}{4} - \frac{1}{6\Sigma_s} \left(\frac{\partial \phi}{\partial z} \right)_o \quad \text{VIe.2.4}$$

Thus the net neutron current at the origin in the z -direction becomes:

$$\vec{J}_z = \vec{J}_{z+} - \vec{J}_{z-} = -\frac{1}{3\Sigma_s} \left(\frac{\partial \phi}{\partial z} \right)_o \quad \text{VIe.2.5}$$

Similar analyses can be performed for the x and y directions. Thus the total neutron current becomes:

$$\vec{J} = -\frac{1}{3\Sigma_s} \left(\frac{\partial \phi}{\partial x} + \frac{\partial \phi}{\partial y} + \frac{\partial \phi}{\partial z} \right) \quad \text{VIe.2.6}$$

Note that in Equation VIe.2.6 we dropped subscript o (i.e., the reference to the origin). This is because we can carry out similar analyses for any other point, taken as the origin of the coordinate system, in space. We may further simplify Equation VIe.2.6 as:

$$\vec{J}(\vec{r}, E) = -D(\vec{r}) \vec{\nabla} \phi(\vec{r}, E) \quad \text{VIe.2.7}$$

where D in Equation VIe.2.7, is known as the diffusion coefficient (Table VIe.1.2) and is given by $D = 1/3\Sigma_s$. Recall that we derived Equation VIe.2.7 assuming isotropic scattering in a weakly absorbing medium. We may still apply Equation VIe.2.7 to cases where scattering is not isotropic by including the mass number of the moderating nuclei and using $D = A/(3A + 2)\Sigma_s$. In a homogeneous medium Σ_s and D are constant values independent of location. Thus Equation VIe.2.7 in the thermal region, for example, simply becomes $\vec{J}(\vec{r}) = -D \vec{\nabla} \phi(\vec{r})$. This is known as *Fick's law* expressing the fact that in weakly absorbing media, the current of neutrons is from the highly populated region to the sparsely populated region simply due to the net diffusion of the neutrons.

2.2. The One-Speed Neutron Diffusion Equation

The neutron diffusion equation may be obtained from the neutron transport equation or derived directly by applying the balance of neutrons for the control volume of Figure VIe.2.1(b). Choosing the latter method, we find the net rate of leakage into the differential volume in the y -direction as:

$$J_y(dx dz) - \left[J_y + \frac{\partial J_y}{\partial y} dy \right] (dx dz) = -\frac{\partial J_y}{\partial y} dx dy dz$$

Adding the leakage terms in the x - and z - directions, we find the total leakage for the control volume dV as $-\vec{\nabla} \cdot \vec{J}$. Thus the rate of change of neutrons in the control volume, $(1/V)(\partial\phi/\partial t)$ is equal to the rate of production from a neutron source such as s and the net in-leakage minus the net absorption or removal. Expressed mathematically;

$$\frac{1}{V} \frac{\partial\phi(\vec{r}, t)}{\partial t} = s(\vec{r}, t) - \vec{\nabla} \cdot \vec{J}(\vec{r}, t) - \Sigma_a(\vec{r})\phi(\vec{r}, t) \quad \text{VIe.2.8}$$

Substituting for the neutron current density from Fick's law given by Equation VIe.2.7, we find:

$$\frac{1}{V} \frac{\partial\phi(\vec{r}, t)}{\partial t} = s(\vec{r}, t) - [\Sigma_a(\vec{r})\phi(\vec{r}, t) + \vec{\nabla} \cdot [-D(\vec{r})\vec{\nabla}\phi(\vec{r}, t)]] \quad \text{VIe.2.9}$$

Expectedly, Equation VIe.2.9 is similar to Equation IVa.2.1 as it was derived for diffusion of heat in solids. For a homogeneous medium, D can be treated as a constant and the diffusion equation is obtained as:

$$\frac{1}{V} \frac{\partial\phi(\vec{r}, t)}{\partial t} = s(\vec{r}, t) - \Sigma_a(\vec{r})\phi(\vec{r}, t) + D\nabla^2\phi(\vec{r}, t) \quad \text{VIe.2.10}$$

Note that in the derivation of the neutron diffusion equation we assumed that the flux of neutrons is isotropic (i.e., with no directional preference), otherwise the diffusion model does not apply. For example, while the diffusion model is applicable in water, it breaks down at the water-air boundary. This is due to the fact that water is much denser than air hence more neutrons move from water to air than from air to water. If we are interested only in the steady state solution, the diffusion equation further simplifies to:

$$D\nabla^2\phi(\vec{r}) - \Sigma_a\phi(\vec{r}) = -s(\vec{r}) \quad \text{VIe.2.11}$$

In Equation VIe.2.11, the Laplacian operator for a rectangular parallelepiped, a cylinder, or a sphere is given by Equation VIIc.1.9, VIIc.1.10, or VIIc.1.11, respectively. For example, neutron flux in a slab is only a function of x , thus Equation VIe.2.11 simplifies to:

$$\frac{d^2\phi(x)}{dx^2} - \frac{\Sigma_a}{D}\phi(x) = -\frac{s(x)}{D} \quad \text{VIe.2.12}$$

Since Σ_a/D is referred to as the diffusion area $L^2 = \Sigma_a/D$ then L is known as the *diffusion length*. In cylindrical coordinates, assuming flux varies only in the r -direction, Equation VIe.2.11 simplifies to:

$$\frac{1}{r} \frac{d}{dr} \left[r \frac{d\phi(r)}{dr} \right] - \frac{\Sigma_a}{D}\phi(r) = -\frac{s(r)}{D} \quad \text{VIe.2.13}$$

and in spherical coordinates, assuming flux varies only in the r -direction, Equation VIe.2.11 becomes:

$$\frac{1}{r^2} \frac{d}{dr} \left[r^2 \frac{d\phi(r)}{dr} \right] - \frac{\Sigma_a}{D} \phi(r) = -\frac{s(r)}{D} \quad \text{VIe.2.14}$$

To find neutron flux we need two boundary conditions for the second order differential equation VIe.2.11. These boundary conditions depend not only on the geometry of the medium but also on the type of the neutron source. These are discussed next.

Medium geometry: The simplest geometry for Equations IVe.2.11 through IVe.2.14 is an infinite medium. Other geometries include infinite slab, finite slab, parallelepiped, infinite cylinder, finite cylinder, and sphere.

Type of source: Neutron sources may be of flux-dependent or flux-independent types. Flux dependent sources are due to fission. Flux-independent sources are sources that emit neutrons at a constant rate and are the driving force for the existence of neutron flux in a medium such as a moderator. The flux-independent sources may either be of a localized or distributed type. We can find analytical solutions for flux-independent sources of point, line, or planar types located in a sphere, cylinder, or slab (See Problems 32 through 41). If we are solving Equations VIe.2.11 through VIe.2.14 for flux-independent localized sources, s in these equations should be set to zero, as the neutron source would appear in the boundary condition.

Type of boundary condition: If we are dealing with an infinite medium, one boundary condition is obtained by the fact that as the variable approaches infinity, the flux must become zero. On the other hand, if we are dealing with finite medium, the flux must be zero at the extent of the medium.

The second boundary condition is obtained from the type of the neutron source. For example, the neutron current is generally known as the independent variable approaches the source. For a distributed neutron source, we can take advantage of symmetry if the source is distributed uniformly. If a medium is one that is covered by a blanket, also known as a reflector (see Problem 35), then at the interface between two regions A and B , we must satisfy:

$$\phi_A = \phi_B \quad \& \quad J_A \cdot \vec{n} = J_B \cdot \vec{n} \quad \text{VIe.2.15}$$

For the continuity of current in a reflected slab, for example;

$$-D_A(\partial\phi_A/\partial x)_{\text{boundary}} = -D_B(\partial\phi_B/\partial x)_{\text{boundary}}$$

For flux-dependent distributed sources, where the neutron flux and the neutron source are intertwined, we can write:

$$s = \eta \Sigma_{aF} \phi = \eta \frac{\Sigma_{aF}}{\Sigma_a} \Sigma_a \phi = \eta f \Sigma_a \phi$$

where f , the fuel utilization factor, is simply given as $f = \Sigma_{aF} / \Sigma_a$ and the multiplication factor k_∞ :

$$k_\infty = \frac{\eta \Sigma_a \phi}{\Sigma_a \phi}$$

Table VIe.1.3 gives useful data such as σ_f , σ_a , ν , and η for various materials, where η is the average number of fission neutrons emitted per neutron absorbed. Substituting k_∞ into the diffusion equation, we find:

$$D \nabla^2 \phi - \Sigma_a \phi = -k_\infty \Sigma_a \phi$$

Dividing through by the diffusion coefficient, we get:

$$\nabla^2 \phi + \frac{\Sigma_a}{D} (k_\infty - 1) \phi = 0$$

Defining $L^2 = D/\Sigma_a$ as the *diffusion area*, we find:

$$\nabla^2 \phi + B^2 \phi = 0 \quad \text{VIe.2.16}$$

where $B^2 = (k_\infty - 1)/L^2$ is known as *Material Buckling*. Equation VIe.2.16 is a one-group (i.e., one-energy group) diffusion equation. We can express the one group diffusion equation for a variety of sources such as infinite planar source, point source, and bare slab. However, we are more interested in reactor cores having such familiar geometries as parallelepiped, cylindrical, and spherical. All we need to do is to express the Laplacian operator for the specified core geometry as discussed next.

3. Determination of Neutron Flux in an Infinite Cylindrical Core

Since the cylindrical geometry is most applicable to actual reactor cores, we begin with an infinite circular cylinder and then reduce the solution to the finite right circular cylinder.

Flux in infinite cylindrical core. An infinite cylindrical core is a theoretical concept. We analyze it to eliminate the variation of neutron flux in the z -direction, which will be considered later. Assuming symmetry in the θ -direction, neutron flux becomes only a function of r . The diffusion equation then becomes:

$$\frac{1}{r} \frac{d}{dr} \left(r \frac{d\phi(r)}{dr} \right) + B^2 \phi(r) = 0$$

If we compare this equation with Equation VIIb.1.13, we note that we are dealing with a Bessel differential equation of order zero ($\nu = 0$) with m also being zero. The solution is given by Equation VIIb.1.14:

$$\phi = c_1 J_0(Br) + c_2 Y_0(Br)$$

where we must find constants c_1 and c_2 from the following boundary conditions:

$$\text{at } r = 0, \phi = \text{finite and at } r = R, \phi \cong 0$$

From the first boundary condition and Figure VIIb.3.1, we conclude that $c_2 = 0$ hence, $\phi = c_1 J_0(Br)$. The second boundary condition is even more interesting, as we get a host of answers. Figure VIIb.3.1 shows that function $J_0(x)$ goes to zero for three values of x when x ranges only from 0 to 8. This indicates that we are dealing with a Sturm-Liouville problem. The diffusion equation is a boundary-value problem having two homogenous boundary conditions. The Sturm-Liouville problem is discussed in Chapter VIIb. Hence, from the second boundary condition we find the n answers that satisfy the secondary boundary conditions as:

$$B_n R = x_n$$

where x_n stands for all n zeros of $J_0(x)$, the Bessel function of the first kind of order zero. As seen from Figure VIIb.3.1, the first zero occurs at 2.405. Hence, $B_1 R = 2.405$ and $B_1 = 2.405/R$. Thus the flux becomes:

$$\phi = c_1 J_0\left(\frac{2.405r}{R}\right)$$

Although we were not able to find c_1 , we managed to find the square root of the buckling term. To find coefficient c_1 , we use the power produced by the reactor. The power produced per unit volume is given by Equation VIe.1.5 as $\dot{q}''' = E_R \phi \Sigma_f$. Thus, power produced by a unit length of the infinite cylinder reactor is found as:

$$\begin{aligned} \dot{Q} &= \int_V E_R (\phi \Sigma_f) dV = \int_0^R E_R (\phi \Sigma_f) (2\pi r dr) \\ &= \int_0^R E_R \left[c_1 J_0\left(\frac{2.405r}{R}\right) \Sigma_f \right] (2\pi r dr) = \left(2\pi c_1 E_R \Sigma_f \right) \int_0^R J_0\left(\frac{2.405r}{R}\right) r dr \end{aligned}$$

In Chapter VIIb the above integral is carried out so that:

$$\begin{aligned} \int_0^R J_0\left(\frac{2.405r}{R}\right) r dr &= \frac{R}{2.405} \left[r J_1\left(\frac{2.405r}{R}\right) \right]_{r=0}^{r=R} \\ &= \frac{R}{2.405} [R J_1(2.405) - 0 \times J_1(0)] = \frac{0.51911R^2}{2.405} = 0.2158R^2 \end{aligned}$$

Substituting for the integral and solving for c_1 , neutron flux distribution in an infinite cylinder core becomes:

$$\phi = \frac{\dot{Q}}{1.356 E_R R^2 \Sigma_f} J_0\left(\frac{2.405r}{R}\right) \quad \text{VIe.3.1}$$

Flux in a finite cylinder core. Having solved the infinite cylinder core, we may apply the same method of solution to other geometries such as an infinite slab, rectangular parallelepiped or a spherical core. The results for all these cases are summarized in Table VIe.3.1. Note that the solution for a rectangular parallelepiped is obtained from the solution for an infinite slab. Similarly, the solution for a finite cylinder is obtained from the solutions for an infinite slab and an infinite cylinder. This is the same method we used for the determination of temperature distribution in these geometries, as shown in Table IVa.9.2. The reason for the similarity in mathematical solution is the fact that diffusion is the mechanism for both heat and flux transfer. As seen from Table VIe.3.1, for a finite cylinder, which resembles actual nuclear reactor cores, neutron flux varies as a cosine function in the axial and as the Bessel function of the first kind of order zero in the radial direction. Hence, maximum flux occurs in the center of the reactor. As will be discussed later in this chapter, neutron flux should be as uniform as possible in nuclear reactors. In practice this goal is approached by variety of means including the arrangement of higher power fuel assemblies in the core periphery. From Table VIe.3.1, neutron flux in a finite cylinder and homogenous core is then given as:

$$\phi(r, z) = \left(\frac{3.63\dot{Q}}{VE_R\Sigma_f} \right) J_0\left(\frac{2.405r}{R}\right) \cos\left(\frac{\pi z}{H}\right) \quad \text{VIe.3.2}$$

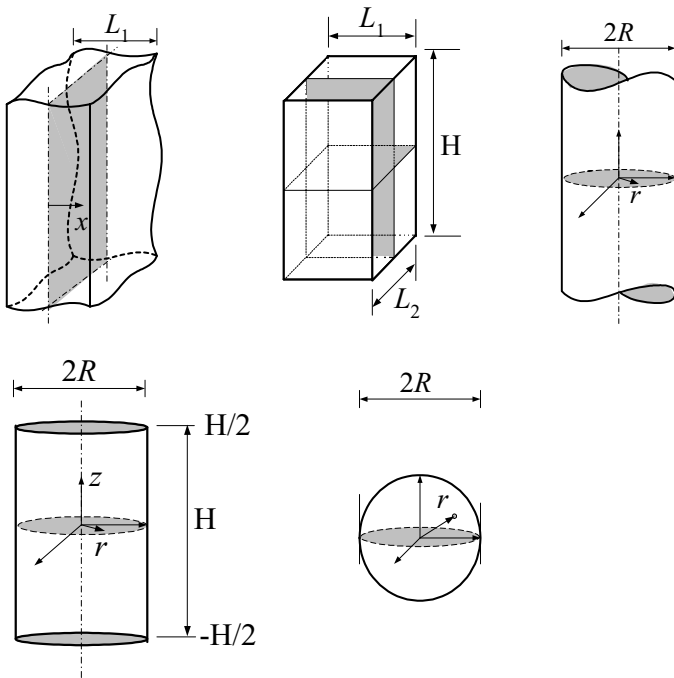


Figure VIe.3.1. Infinite slab, rectangular parallelepiped, infinite cylinder, finite cylinder and sphere

Table VIe.3.1. Flux and geometrical buckling for various critical core geometries

Type	Geometrical Buckling	ϕ	$\zeta = \phi_{\max}/\phi_{av}$
Infinite Slab	$\left(\frac{\pi}{L_1}\right)^2$	$\left(\frac{1.57\dot{Q}}{L_1 E_R \Sigma_f}\right) \cos\left(\frac{\pi x}{L_1}\right)$	$\pi/2 = 1.57$
Parallelepiped	$\left(\frac{\pi}{L_1}\right)^2 + \left(\frac{\pi}{L_2}\right)^2 + \left(\frac{\pi}{H}\right)^2$	$\left(\frac{3.87\dot{Q}}{V E_R \Sigma_f}\right) \cos\left(\frac{\pi x}{L_1}\right) \cos\left(\frac{\pi y}{L_2}\right) \cos\left(\frac{\pi z}{H}\right)$	$(\pi/2)^3 = 3.88$
Infinite Cylide	$\left(\frac{2.405}{R}\right)^2$	$\left(\frac{0.738\dot{Q}}{R^2 E_R \Sigma_f}\right) J_0\left(\frac{2.405r}{R}\right)$	2.32
Finite Cylinder	$\left(\frac{2.405}{R}\right)^2 + \left(\frac{\pi}{H}\right)^2$	$\left(\frac{3.63\dot{Q}}{V E_R \Sigma_f}\right) J_0\left(\frac{2.405r}{R}\right) \cos\left(\frac{\pi z}{H}\right)$	3.64
Sphere	$\left(\frac{\pi}{R}\right)^2$	$\left(\frac{\dot{Q}}{4R^2 E_R \Sigma_f}\right) \frac{1}{r} \sin\left(\frac{\pi r}{R}\right)$	3.29

where H is the total height of the core, as shown in Figure VIe.3.1. Reactor cores consist of thousands of fuel rods. To be able to apply Equation VIe.3.2 to reactors, we relate Σ_f for the entire core to that of the fuel rods by:

$$[(\pi a^2 H) N_{rod}] \Sigma_{fr} = \pi R^2 H \Sigma_f$$

where N_{rod} is the number of fuel rods in the core. Solving for Σ_f , we find:

$$\Sigma_f = [a^2 N_{rod}] \Sigma_{fr} / R^2.$$

where a is the fuel rod radius. Substituting Σ_{aF} in Equation VIe.3.1.2, we get:

$$\begin{aligned} \phi(r, z) &= \left(\frac{3.63 \dot{Q} R^2}{V E_R \Sigma_{fr} N_{rod} a^2} \right) J_0\left(\frac{2.405r}{R}\right) \cos\left(\frac{\pi}{H}\right) \\ &= \left(\frac{1.16 \dot{Q}}{E_R \Sigma_{fr} N_{rod} a^2 H} \right) J_0\left(\frac{2.405r}{R}\right) \cos\left(\frac{\pi z}{H}\right) \end{aligned}$$

Multiplying $\phi(r, z)$ by energy deposited per fission (E_d) and substitute from Equation VIe.1.5, we obtain:

$$\dot{q}'''(r, z) = \left(\frac{1.16 E_d \dot{Q}}{E_R N_{rod} a^2 H} \right) J_0\left(\frac{2.405r}{R}\right) \cos\left(\frac{\pi z}{H}\right) \quad \text{VIe.3.3}$$

Equation VIe.3.3 gives the distribution of the volumetric heat generation rate in reactor cores of finite cylinder. Since $[J_0(x)]_{\max} = 1$ and $[\cos(x)]_{\max} = 1$, the maximum volumetric heat generation rate occurs at the center of the cylinder where $r = z = 0$. Hence, Equation VIe.3.3 can be expressed as:

$$\dot{q}'''(r, z) = \dot{q}_{\max}''' J_0 \left(\frac{2.405r}{R} \right) \cos \left(\frac{\pi z}{H} \right) \quad \text{Vie.3.4}$$

Example Vie.3.1. A reactor core contains 41,000 fuel rods. The nuclear plant is operating at 1000 MWe and 29% thermal efficiency. Fuel pellet diameter is 0.44 in. Core dimensions are, $D = H = 4$ m. Find the volumetric heat generation rate at $z = H/3$ and $r = R/2$.

Solution: We find the maximum volumetric heat generation rate occurring at $z = r = 0$ from:

$$\begin{aligned} \dot{q}_{\max}''' &= \left(\frac{1.16 E_d \dot{Q}}{E_R N_{\text{rod}} a^2 H} \right) = \frac{1.16 \times 180 \times (1000 / 29\%)}{200 \times 41000 \times [(0.44 / 2) / 12]^2 \times 4} = 65.31 \text{ MW/ft}^3 \\ &= 2.23\text{E}8 \text{ Btu/h}\cdot\text{ft}^3 \end{aligned}$$

Therefore, $\dot{q}'''(r, z) = 2.23\text{E}8 [J_0(2.405 \times R/2R) \cos(\pi \times H/3H)] = 2.23\text{E}8 \times 0.67 \times 0.5 = 0.75\text{E}8 \text{ Btu/h}\cdot\text{ft}^3$.

Actual versus bare reactor cores. In actual reactor cores the maximum volumetric heat generation rate, is less than that calculated in the above example. To find \dot{q}_{\max}''' in actual cores, we write:

$$\begin{aligned} (\dot{q}_{\max}''')_{\text{actual}} &= \Sigma_{fr} E_d \phi_{\max} = \Sigma_{fr} E_d (\phi_{\text{av}} \zeta) = \Sigma_{fr} E_d \left(\frac{\dot{Q} \zeta}{\Sigma_f E_R V} \right) \\ &= \Sigma_{fr} E_d \left(\frac{\dot{Q} \zeta}{(\Sigma_{fr} N_{\text{rod}} a^2 / R_2) E_R V} \right) \end{aligned}$$

or alternatively;

$$(\dot{q}_{\max}''')_{\text{actual}} = \frac{\dot{Q} E_d \zeta}{\pi H a^2 N_{\text{rod}} E_R}$$

Heat flux distribution. We obtained the volumetric heat generation rate in a cylindrical core in Equation Vie.3.4. To obtain similar distribution, but for core heat flux, we write the relation between power, linear heat generation rate, heat flux and volumetric heat generation rate for a fuel rod as:

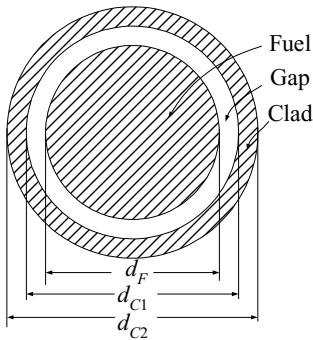
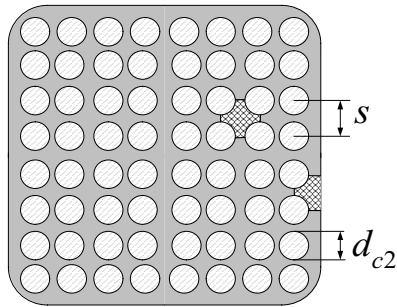
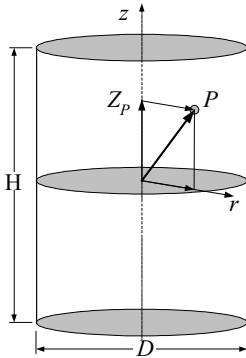
$$\dot{Q} = \dot{q}' H = \dot{q}'' P_F H = \dot{q}''' A_F H \quad \text{Vie.3.5}$$

where H is the rod length, P_F is the fuel pellet perimeter, and A_F is the fuel pellet cross sectional area. Thus, Equation Vie.3.4 can also be written as:

$$\dot{q}''(r, z) = \dot{q}_{\max}'' J_0 \left(\frac{2.405r}{R} \right) \cos \left(\frac{\pi z}{H} \right) \quad \text{VIe.3.6}$$

where \dot{q}'' is the local and \dot{q}_{\max}'' is the maximum fuel rod heat flux.

Example VIe.3.2. Data for a BWR core, bundle, and rod are given as follows:



D : Core diameter (ft):	16	H : Core height (ft):	12
n : Rods per bundle:	64	s : Pitch (in):	0.74
d_{c1} : Clad in-dia. (in):	0.50	d_{c2} : Clad out-dia. (in):	0.56
\dot{Q} : Core power (MWth):	3,300	ρ : UO_2 density (lbm/ft^3):	644
N : Number of fuel bundles:	585		
d_F : Pellet diameter (in):	0.48		
δ : Clad thickness (in):	0.03		
Ω : $\dot{q}_{\max}'' / \dot{q}_{av}''$:	2.5		

Find,

- total weight of UO_2 in kg,
- core average power density in kW/lit,
- specific power in kW/kg,
- average linear heat generation rate in kW/ft,
- average heat flux in kW/ft²,
- the maximum volumetric heat generation rate in kW/ft³, and g) the volumetric heat generation rate at $r = R/2$ and $z = H/3$.

Solution:

- a) We first find total volume and mass of UO_2 :

$$V_{\text{UO}_2} = \pi d_F^2 H / 4 = \pi \times (0.48 / 12)^2 \times (12 / 4) \times (8 \times 8 \times 585) = 564.58 \text{ ft}^3$$

$$M_{\text{UO}_2} = \rho V = 643.85 \times 564.58 = 363,505 \text{ lbm} = 164,667.7 \text{ kg} \cong 165 \text{ tons}$$

- b) We now calculate core volume:

$$V_{\text{Core}} = \pi D^2 H / 4 = \pi \times (16 / 3.2808)^2 \times (12 / 3.2808) / 4 = 68.32 \text{ E3 lit}$$

By definition: $\overline{P.D.} = \dot{Q}_{\text{Core}} / V_{\text{Core}} = 3,300 \times 1000 / 68.32 \text{ E3} = 48.3 \text{ kW/lit}$

c) By definition: $S.P. = \dot{Q}_{\text{Core}} / M_{\text{UO}_2} = 3,300 \times 1000 / 164,667.7 = 20 \text{ kW/kg}$

d) By definition: $\bar{q}' = \dot{Q}_{\text{Core}} / (N_{\text{Rod}} \times H) = 3,300 \times 1000 / [(585 \times 8 \times 8) \times 12] = 7.3 \text{ kW/ft}$

e) $\bar{q}'' = \dot{Q}_{\text{Core}} / (N_{\text{Rod}} \times \pi d_{c2} H) = 3,300 \times 1000 / [(585 \times 8 \times 8) \times \pi \times (0.56 / 12) \times 12] = 50 \text{ kW/ft}^2$

f) $(\dot{q}_{\text{max}}''')_{\text{Bare}} = \frac{1.16 P E_d}{H a^2 N_{\text{Rod}} E_R} = \frac{1.16 \times 3,300 \times 1000 \times 180}{12 \times (0.48 / 12)^2 \times (64 \times 585) \times 200} = 4792.67 \text{ kW/ft}^3$

$$\dot{q}_{\text{max}}''' = \frac{1.16 P E_d}{H a^2 N_{\text{Rod}} E_R} \left(\frac{\zeta}{1.16 \pi} \right) = 4792.67 \times \frac{2.5}{1.16 \pi} = 3287.83 \text{ kW/ft}^3$$

g) Since $\dot{q}'''(r, z) = \dot{q}_{\text{max}}''' J_0 \left(\frac{2.405 r}{R} \right) \cos \left(\frac{\pi z}{H} \right)$

then $\dot{q}'''(r, z) = 3287.83 \times J_0[(2.405 \times R/2)/R] \times \cos[(\pi \times H/3)/H] = 3287.83 \times 0.669 \times 0.5 = 1099.78 \text{ kW/ft}^3$

Average heat generation rate. We find the core average heat generation rate from:

$$\overline{\dot{q}'''} = \frac{\int_V \dot{q}'''(r, z) dV}{V} = \left(\frac{1}{\pi R^2 H} \right) \left(\frac{1.16 E_d \dot{Q}}{E_R N_{rod} a^2 H} \right) \left[\int_0^R J_0 \left(\frac{2.405 r}{R} \right) (2\pi r dr) \right] \left[\int_{-H/2}^{H/2} \cos \left(\frac{\pi z}{H} \right) dz \right]$$

If we carryout the integrals in the radial and the axial directions, we find $\overline{\dot{q}'''} = \dot{q}'''_{\max} / (2.316 \times 1.57)$. Writing in terms of heat flux by using Equation VIe.3.5 and representing $F_N = 2.316 \times 1.57$ we obtain:

$$\dot{q}''_{\max} = \overline{\dot{q}''} \times F_N \quad \text{VIe.3.7}$$

where in Equation VIe.3.7, F_N is known as the *nuclear peaking factor*. The first multiplier, $F_N^{\text{axial}} = 2.316$, is the axial peaking sub-factor and the second multiplier, $F_N^{\text{radial}} = 1.57$, is the radial peaking sub-factor.

3.1. Axial Temperature Distribution

We use the volumetric heat generation rate, as given by Equation VIe.3.3 to determine the axial temperature distribution in the reactor core. To limit the analysis to only one variable, we choose the central channel for which $r = 0$ hence $J_0 = 1$. We also limit the analysis to PWRs* where coolant entering and leaving the core remains subcooled. This assumption allows us to write $dh = c_p dT$. Using subscript f for the bulk coolant, F for the fuel, and applying Equation IIa.6.6 to an elemental control volume taken at axial location z (Figure VIe.3.2(c)), yields:

$$\dot{m}h + d\dot{Q} = \dot{m}(h + dh)$$

Simplifying, we find $\dot{m}c_p dT_f = d\dot{Q}$. For the fuel rod of Figure VIe.3.2, $\dot{Q} = \dot{q}'H = \dot{q}''P_{C2}H = \dot{q}'''A_FH$ where $P_{C2} = \pi d_{C2}$, and $A_F = \pi d_F^2/4$. Substituting for total rate of heat generation we get:

$$\dot{m}c_p dT_f = d\dot{q} = \dot{q}'''(z)A_F dz$$

We now substitute from Equation VIe.3.3 and integrate from the core inlet to any elevation:

* Note we are assuming that boiling does not occur even in the hot channel.

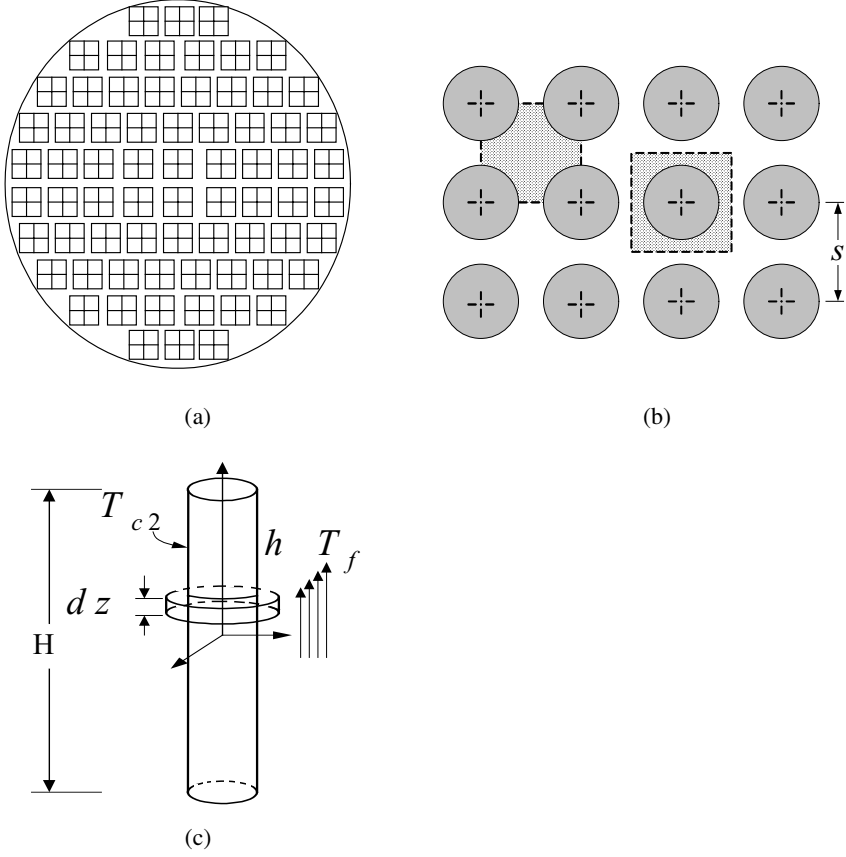


Figure VIe.3.2. (a) Core, (b) Fuel rods, and (c) Central rod and channel

$$\int_{-H/2}^z \dot{m} c_p dT_f = A_F \dot{q}_{\max}'' \int_{-H/2}^z \cos\left(\frac{\pi z}{H}\right) dz$$

Carrying out the integral and simplifying, we obtain the coolant temperature as:

$$T_f(z) = T_{f,in} + \frac{\dot{q}_{\max}'' A_F H}{\pi \dot{m} c_p} \left[1 + \sin\left(\frac{\pi z}{H}\right) \right] \quad \text{VIe.3.8}$$

Having the coolant temperature, we can find the clad outside temperature from a steady state heat balance:

$$d\dot{Q} = h(P_{C2} dz)(T_{C2} - T_f)$$

Substituting for the rate of heat transfer and for fluid temperature and solving for clad temperature, we get:

$$T_{C2}(z) = T_{f,in} + \frac{\dot{q}_{\max}''' V_F}{\pi \dot{m} c_p} \left[1 + \sin\left(\frac{\pi z}{H}\right) \right] + \frac{\dot{q}_{\max}''' A_F}{h P_{C2}} \cos\left(\frac{\pi z}{H}\right) \quad \text{VIe.3.9}$$

In this equation, we assumed that the heat transfer coefficient, h , remains constant from inlet to any elevation. Having the clad outside temperature, we can find clad inside temperature, T_{C1} , fuel surface temperature, T_{F2} , and fuel centerline temperature by using the corresponding thermal resistances. Following the procedure that led to derivation of Equation IVa.6.15, we can find each temperature in terms of $T_{f,in}$, \dot{m} , and \dot{q}_{\max}''' as:

$$T_{C1}(z) = T_{f,in} + \frac{\dot{q}_{\max}''' V_F}{\pi \dot{m} c_p} \left[1 + \sin\left(\frac{\pi z}{H}\right) \right] + V_F (R_f + R_C) \dot{q}_{\max}''' \cos\left(\frac{\pi z}{H}\right) \quad \text{VIe.3.10}$$

$$T_{F2}(z) = T_{f,in} + \frac{\dot{q}_{\max}''' V_F}{\pi \dot{m} c_p} \left[1 + \sin\left(\frac{\pi z}{H}\right) \right] + V_F (R_f + R_C + R_G) \dot{q}_{\max}''' \cos\left(\frac{\pi z}{H}\right) \quad \text{VIe.3.11}$$

$$T_{F1}(z) = T_{f,in} + \frac{\dot{q}_{\max}''' V_F}{\pi \dot{m} c_p} \left[1 + \sin\left(\frac{\pi z}{H}\right) \right] + V_F (R_f + R_C + R_G + R_F) \dot{q}_{\max}''' \cos\left(\frac{\pi z}{H}\right) \quad \text{VIe.3.12}$$

where the thermal resistance of fuel (R_F), gap (R_G), clad (R_C), and flow (R_f) are the terms in the denominator of Equation IVa.6.15. Temperature distributions of the coolant, clad, and fuel are shown in Figure VIe.3.3.

As we expect, the coolant temperature peaks at the channel exit due to the accumulation of heat. However, the fuel rod temperature is a function of both coolant temperature and the volumetric heat generation rate. While the coolant temperature keeps increasing along the channel, the volumetric heat generation rate is at its maximum at the center and then keeps decreasing, due to the $\cos(\pi z/H)$ multiplier. Therefore, the axial fuel rod temperature increases until a maximum temperature is reached, the location of which is expectedly above the core center-plane and below the channel exit.

Now that we evaluated the axial temperature distribution of the fuel rod at a given radius, let's evaluate the radial temperature distribution of the fuel rod at a given axial location. By expressing fuel rod temperature at various radial locations (Equations VIe.3.9 through VIe.3.12) with temperature at each location being a function of z , we have used a two-dimensional approach for the fuel rod temperature, albeit for selected nodes. Note that by using a single control volume for the coolant, its temperature in the radial direction is lumped. Since at any axial location, fuel rod temperature is a function of both T_f and \dot{q}_{\max}''' , it is then expected that temperature further inside the fuel rod is influenced more by \dot{q}_{\max}''' and less by

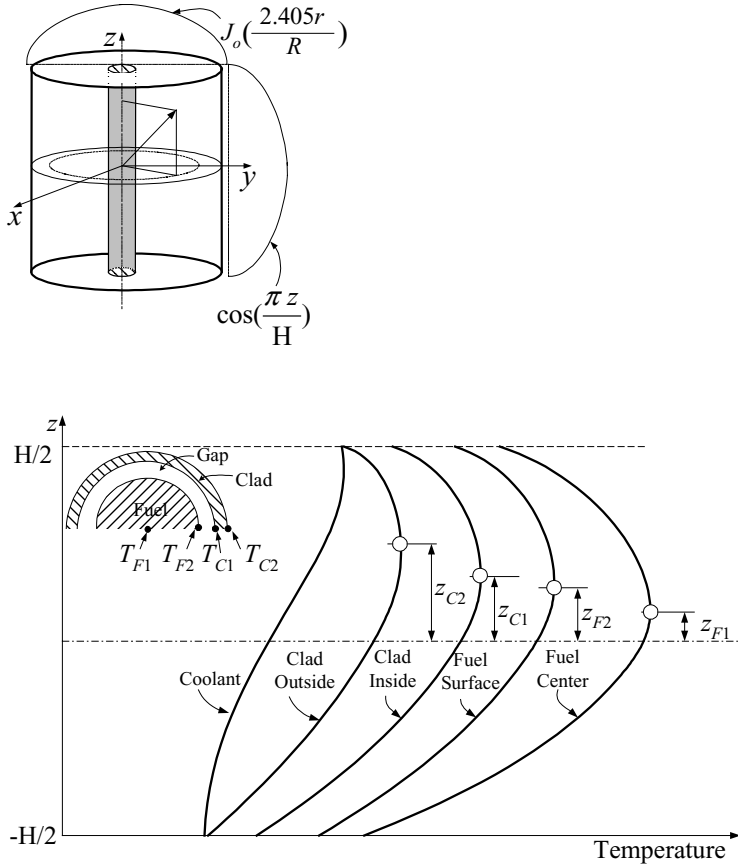


Figure VIe.3.3. Two dimensional temperature distribution of a fuel rod in the hot channel of a PWR

T_f . This is shown by the elevations from the point of maximum temperature to the core center-plane for various radial location as clad outside (z_{C2}), clad inside (z_{C1}), fuel surface (z_{F2}), and fuel centerline (z_{F1}).

To find the location of the maximum temperatures, we take the derivative of the related equation for temperature and set it equal to zero. By substituting the location at which temperature is maximum, we can obtain the value of T_{max} in terms of all the known variables for any radial location of the fuel rod. For example, for clad outside temperature, we take the derivative of Equation VIe.3.9 and set it equal to zero:

$$z_{c2,max} = (H/\pi) / \tan^{-1}(\pi i n c_p R_f)$$

Example VIe.3.3. A PWR core contains 217 fuel assemblies, each on the average containing 176 fuel rods, operating at 2700 MWth.. Use the data given below and find the location and the value of the peak clad outside temperature. Data: $H = 12$ ft, $\dot{m} = 138.5E6$ lbm/h, $d_{F2} = 0.377$ in, $d_{C2} = 0.44$ in, $h = 4000$ Btu/h·ft²·F, $c_p = 1.392$ Btu/lbm·F, $T_{f, in} = 550$ F, and $\Omega = 2.56$.

Solution: We first find the number and volume of the rods:

$$N_{rod} = 217 \times 176 = 38,192$$

$$V_F = \pi(d_{F2})^2/4 \times H = \pi(0.377/12)^2 \times 12/4 = 9.3E-3 \text{ ft}^3$$

We now find thermal resistance of the coolant film:

$$R_f = (\pi d_{C2} H) h = 1/[\pi \times (0.44/12) \times 12 \times 4000] =$$

$$1.81E-4 \text{ h} \cdot \text{ft}^2 \cdot \text{F/Btu} \quad (3.186E-5 \text{ m}^2 \cdot \text{K/W})$$

$$Z_{C2, max} = (12/\pi) / \tan^{-1}[\pi \times (138.5E6/38,192) \times 1.392 \times 1.81E-4] = (12/\pi) / 1.235 = 3.1 \text{ ft (1 m)}$$

The maximum volumetric heat generation rate is found from:

$$\dot{q}_{max}''' = \left(\frac{E_d \dot{Q} \zeta}{\pi E_R N_{rod} a^2 H} \right) = \frac{180 \times 2700 \times 2.56}{\pi \times 200 \times 38,192 \times [(0.377/2)/12]^2 \times 12} = 17.51 \text{ W/ft}^3$$

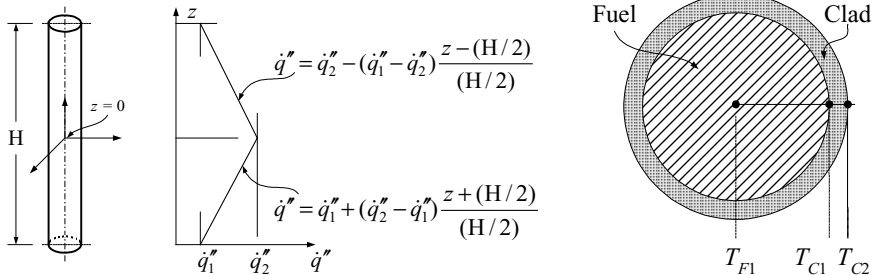
$$= 5.97E7 \text{ Btu/h} \cdot \text{ft}^3$$

The peak clad outside temperature is found from Equation VIe.3.9 by substituting for $z = z_{C2, max} = 3.1$:

$$T_{C2, max} = 550 + \frac{5.97E7 \times 9.3E-3}{\pi \times (138.5E6/38,192) \times 1.392} \left(1 + \sin \frac{\pi \times 3.1}{12} \right) +$$

$$\frac{5.97E7 \times 9.3E-3}{1/181E-4} \cos \frac{\pi \times 3.1}{12} = 680 \text{ F}$$

Example VIe.3.4. Shown in the figure is the surface heat flux of a rod in an experimental reactor. Use the given data and find a) coolant temperature, b) clad surface temperature, and c) fuel centerline temperature at $z = H/2$. Data: $H = 6$ ft, $d_{F2} = d_{C1} = 0.4$ in, $d_{C2} = 0.5$ in, $T_{f, in} = 155$ F, $\dot{m} = 375$ lb/hr per rod, $h = 2000$ Btu/h·ft²·F, $k_F = 1$ and $k_C = 3$ Btu/h·ft·F, $\dot{q}_1'' = 120,000$ Btu/hr ft², $\dot{q}_1''' = 250,000$ Btu/hr·ft².



Solution:

a) We write an energy balance for an elemental control volume and integrate:

$$\dot{m}c_p [T_f(z) - T_{f,in}] = \int_{-H/2}^0 \dot{q}''(z)(\pi d) dz + \int_0^z \dot{q}''(z)(\pi d) dz$$

We then substitute for heat flux and carrying out the integral:

$$\dot{m}c_p [T_f(z) - T_{f,in}] = \pi d \left[\left(\dot{q}_1'' z + (\dot{q}_2'' - \dot{q}_1'') \frac{(z^2/2) + (H/2)z}{H/2} \right)_{-H/2}^0 + \left(\dot{q}_1'' - (\dot{q}_2'' - \dot{q}_1'') \frac{(z^2/2) - (H/2)z}{H/2} \right)_0^z \right]$$

Solving for $T_f(z)$ and substituting values, we find:

$$T_f(z) = T_{f,in} + \frac{\pi d H}{2 \dot{m} c_p} (\dot{q}_1'' + \dot{q}_2'') = 155 + \frac{\pi \times (0.5/12) \times 6}{2 \times 375 \times 1} (1.2E5 + 2.5E5) = 542.5 \text{ F}$$

b) From a transverse heat balance we also find:

$$T_{C2}(z) = T_f(z) + [\dot{q}''(z) / h]$$

Substituting values to get:

$$T_{C2} = T_f(z) + \left[\dot{q}_1'' - (\dot{q}_2'' - \dot{q}_1'') \frac{z - (H/2)}{H/2} \right] / h = 542.5 + \frac{1.2E5}{2000} = 602.5 \text{ F}$$

c) We find, T_{F1} from another energy balance:

$$\dot{Q}(z) = \dot{q}''(z)(\pi d_{C2} z) = [T_{F1}(z) - T_{C2}(z)] / \Sigma R$$

$$T_{F1} = T_{C2} + d_{C2} \left[\frac{1}{4k_F} + \frac{\ln(d_{C2}/d_{C1})}{2k_C} \right] (\dot{q}_1'')$$

$$= T_{F1} = 474 + \frac{0.5}{12} \left[\frac{1}{4 \times 1} + \frac{\ln(0.5/0.4)}{2 \times 3} \right] \times 1.2E5 = 1910 \text{ F}$$

3.2. Determination of Incipient Boiling

In BWRs we often need to find the surface temperature and its location corresponding to the inception of subcooled boiling. As was discussed in Chapter Vb, such local temperature is not a single fixed temperature. Still, we can estimate a value for it from the following relation:

$$T_{SB} = T_{sat} + (T_{C2} - T_{sat})_{J-L} - (\dot{q}''/h) \quad \text{VIe.3.13}$$

where $(\Delta T_{sat})_{J-L}$ is given by the Jens-Lottes correlation, for example:

$$T_{C2} - T_{sat} = \frac{60(\dot{q}''/1E6)^{1/4}}{e^{P/900}}$$

In British units, P is in psia, temperatures are in F, \dot{q}'' is in Btu/h·ft² and h is in Btu/h·ft²·F. In general, the heat flux is given as a function of elevation, based on $\dot{q}''' = \dot{q}_{\max}''' \cos(\pi z/H)$, where the clad surface temperature is given by Equation VIe.3.9. Thus, $T_{SB} = T_{C2}$ and Z_{SB} are found by solving Equations VIe.3.9 and VIe.3.13 simultaneously. We may solve the resultant set by plotting each equation and finding the intersection. Or we set these equations equal and solve the resultant nonlinear equation by numerical means. Using the second method, the equation becomes:

$$T_{f,in} + \frac{\dot{q}_{\max}''' V_F}{\pi \dot{m} c_p} \left[1 + \sin\left(\frac{\pi z}{H}\right) \right] + \frac{\dot{q}_{\max}''' A_F}{h P_{C2}} \cos\left(\frac{\pi z}{H}\right) =$$

$$T_{sat} + \frac{60(\dot{q}''/1E6)^{1/4}}{e^{P/900}} - \frac{\dot{q}''}{h}$$

We now substitute for $\dot{q}'' = \dot{q}_{\max}''' (A_F/P_{C2}) \cos(\pi z/H)$ and rearrange the above relation to get:

$$\lambda_1 Y - \lambda_2 (1 - Y^2)^{1/2} - \lambda_3 Y^{1/4} + \lambda_4 = 0$$

where, in this relation, $Y = \cos(\pi z/H)$, and coefficients λ_1 through λ_4 are given as $\lambda_1 = 2(A_F/P_{C2}) \dot{q}_{\max}'''/h$, $\lambda_2 = \dot{q}_{\max}''' V_F/(\pi \dot{m} c_p)$, $\lambda_3 = 60[(A_F/P_{C2}) \dot{q}_{\max}'''/1E6]^{1/4}/e^{P/900}$, and $\lambda_4 = T_{f,in} + \lambda_2 - T_{sat}$.

Example VIe.3.5. Water enters the hot channel of a BWR at a velocity of $V = 8$ ft/s, temperature of 525 F, and pressure of 1020 psia. Fuel rods are arranged in square array on a pitch of 0.738 in. Heat flux can be closely represented as $\dot{q}'' = \dot{q}_{\max}''' \cos(\pi z/12)$ where z is in ft. Find the clad temperature and its location of the inception of subcooled boiling. Data: $\dot{q}_{\max}''' = 1.28E7$ Btu/h·ft³, $d_{C2} = 0.563$ in and $d_F = 0.487$ in.

Solution: At 1020 psia & 525 F, $\rho = 47.6$ lbm/ft³, $c_p = 1.24$ Btu/lbm·F, $\mu = 6.6E-5$ lbm·ft/s, $k = 0.3$ Btu/h·ft·F

$$A_F = \pi d_F^2/4 = \pi(0.487)^2/4 = 1.293E-3 \text{ ft}^2, P_{C2} = \pi d_{C2} = 0.147 \text{ ft}, V_F = A_F H = 1.293E-3 \times 12 = 0.0155 \text{ ft}^3$$

$$A_{Flow} = p^2 - \pi d_{C2}^2 / 4 = (0.738/12)^2 - \pi(0.563)^2 / 4 = 2.05E-3 \text{ ft}^2 (1.9 \text{ cm}^2)$$

$$D_e = 4A_{Flow}/P_{C2} = 4 \times 2.05E-3 / (\pi \times 0.563/12) = 5.58E-2 \text{ ft} (1.7 \text{ cm})$$

$$\dot{m} = \rho \times V \times A_{Flow} = 47.6 \times 8 \times 2.05E-3 = 0.78 \text{ lbm/s} = 2810 \text{ lbm/h} (0.354 \text{ kg/s})$$

Calculate h from Equation IVb.3.6 for forced single phase flow:

$$C = 0.042(0.7382/0.563) - 0.024 = 0.031$$

$$\text{Nu} = hD_e/k_{Water} = 0.031\text{Re}^{0.8}\text{Pr}^{1/3} = 0.031[47.6 \times 8 \times 5.58E-2/6.6E-5]^{0.8}(0.873)^{1/3} = 754$$

$$\text{Hence, } h = 754 \times 0.3377/5.58E-2 = 4563 \text{ Btu/h}\cdot\text{ft}^2\cdot\text{F} (25.91 \text{ kW/m}^2\cdot\text{K})$$

$$\lambda_1 = 2(A_F/P_{C2}) \dot{q}_{\max}''' / h = 2(1.293E-3/0.147) \times 1.28E7/4563 = 49.35 \text{ F} (9.6 \text{ C})$$

$$\lambda_2 = \dot{q}_{\max}'' V_F / (\pi \rho_p \dot{m}) = 1.28E7 \times 0.0155 / (\pi \times 1.24 \times 2810) = 18.12 \text{ F} (-7.7 \text{ C})$$

$$\lambda_3 = 60[(A_F/P_{C2}) \dot{q}_{\max}''' / 1E6]^{1/4} / e^{P/900} = 60(8.78E-3 \times 1.28E7/1E6)^{1/4} / e^{1020/900} = 11.18 \text{ F} (-11.56 \text{ C})$$

$$\lambda_4 = T_{f,in} + C_2 - T_{sat} = 525 + 18.12 - 546.99 = -3.87 \text{ F} (-15.63 \text{ C})$$

$$49.35Y - 18.12(1 - Y^2)^{1/2} - 11.18Y^{1/4} - 3.87 = 0$$

By iteration we find $Y = \cos(\pi z/H) = 0.5732$

Hence, $z_{SB} = -44$ in (i.e., 44 in below the core centerline or $(144/2) - 44 = 28$ in from the core inlet). Upon substitution in either Equation VIe.3.9 or VIe.3.12, we find $T_{SB} = 542.4 \text{ F} (283.5 \text{ C})$. Note, $T_{sat} (1020 \text{ psia}) = 547 \text{ F} (286 \text{ C})$.

In the above example we determined incipient boiling in a BWR. Let us now investigate a similar question for a PWR. Although there is no bulk boiling under normal operation, during certain transients or for the hot-channel even at steady state, local boiling may take place. While PWR channels are interconnected and heat flux profile is not uniform, we still consider fluid flow in a single vertical channel, subject to uniform heating to characterize flow in a PWR hot channel. For this channel, the temperature profiles of water and of channel surface as well as the void fraction profile versus the flow quality, X are shown in Figure VIe.3.4. Water enters this heated channel and flows upward. Heat transfer takes place from the channel wall to the single phase water in forced convection. Somewhere along the channel, at the point of the incipient boiling, the first bubble appears. As discussed in Chapter Vb, the surface temperature would remain nearly unchanged subsequent to the inception of subcooled boiling. The bubbles eventually manage to leave the surface, migrate into the bulk liquid, and collapse to heat up water, which is eventually brought to saturation.

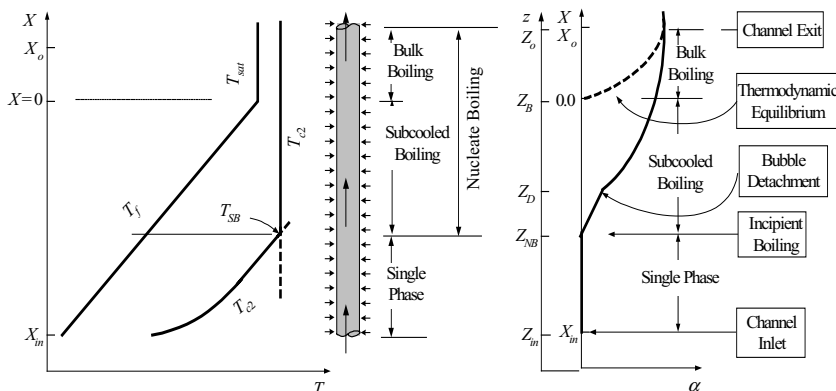


Figure VIe.3.4. Incipient boiling and void-quality profile for uniform heating of water

As the void-flow quality profile of Figure VIe.3.4 indicates, void fraction remains zero as long as water remains subcooled. At the incipient boiling, void fraction becomes nonzero and rises steadily. Upon more vigorous bubble production, which then results in bubble detachment, the increase in void fraction occurs at a larger slope, which continues up to the channel exit. The dotted curve shows void fraction starting from $X = 0$, which conforms to the assumption of thermodynamic equilibrium.

3.3. Margin for Thermal Design

Nuclear peaking factors. We derived the nuclear peaking factor, F_N in Equation VIe.3.7 for a right circular cylinder core using assemblies that produce equal power and are distributed uniformly in the core. These peaking factors are shown in Table VIe.3.1 for various core geometries. Equation VIe.3.3 shows that the maximum heat flux for a set of operational conditions is a fixed value and to increase the core average heat flux, we must reduce the nuclear peaking factors. Thus, for the same \dot{q}_{\max}''' , the flatter the neutron flux, the smaller the nuclear peaking factors and the larger the core average heat flux. In practice, there are various means of flattening the neutron flux in the core. For example, to flatten the radial distribution of neutron flux, fuel assemblies with higher enrichment are placed in the core periphery and less enriched assemblies in the center of the core. Instead of using higher enrichment, we may place older assemblies closer to the center and fresh assemblies in the core periphery during the plant scheduled shutdown for reload. The same goal may also be achieved by using burnable poisons or chemical shim (neutron absorbing material such as boron). However, placing higher enrichment or fresh assemblies at the core periphery would also increase neutron leakage. In the axial direction, fuel rods are loaded with less enriched fuel or even fuel mixed with burnable poison in the center of the rod. Figure VIe.3.5 shows two axial distributions. Figure VIe.3.5(a) shows the flux profile with cosine distribution at the beginning of cycle (BOC) and dipping in the central region to-

wards the end of cycle (EOC) due to higher flux. Figure VIe.3.5(b) shows the effect of burnable poison on flattening the neutron flux profile, hence, reducing the axial peaking factor.

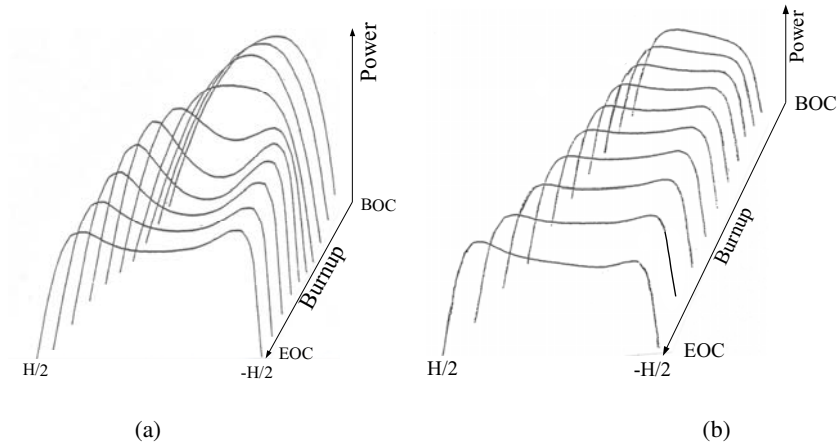


Figure VIe.3.5. Axial power distribution (a) Uniformly loaded rod and (b) rod loaded with poison

Engineering peaking factors, F_E , enhance the total peaking factor, $F = F_N \times F_E$ and further reduce the core average heat flux. The engineering peaking factors are those that affect the temperatures of clad and fuel centerline. These can be easily identified from Equations VIe.3.9 through VIe.3.12 as follows:

- *channel flow rate (\dot{m})*. Reduction in flow rate to the central channel increases bulk temperature.
- *heat transfer coefficient (h)*. Reduction in flow rate would adversely affect h through the Reynolds number.
- *clad thickness ($d_{C2} - d_{C1}$)*. Increase in clad thickness increases thermal resistance to the flow of heat
- *pellet diameter (d_{F2})*. Larger fuel diameter than nominal increases pellet/clad interaction.
- *gap heat transfer coefficient (h_G)*. Reduction in h_G increases thermal resistance to the flow of heat.
- *clad thermal conductivity (k_C)*. Reduction in k_C increases thermal resistance to the flow of heat.
- *fuel thermal conductivity (k_F)*. Reduction in k_F increases thermal resistance to the flow of heat.
- *fuel density*. Increase in fuel density increases neutron flux, hence, the linear heat generation rate.

Examples for such engineering sub-factors include: heat flux; 1.03, hot channel; 1.02, rod bowing; 1.065, axial fuel densification; 1.002, and azimuth power tilt;

1.03. The engineering peaking factors are primarily due to the manufacturing tolerances resulting in the finished product slightly deviating from the specified nominal value. The deviation from the nominal is a probabilistic event. Hence, the deviation can be higher or lower than the nominal value. However, to be conservative, we may consider only deviations that result in undesirable outcome. In this case, deviations that result in the fuel rod temperature to increase. For example, for the specified nominal value of 0.42 for clad outside diameter, the finished product may be $d_{C2} = 0.42 \pm 0.005$ inch. It is conservative to use $d_{C2} = 0.425$ in.

We may calculate the engineering peaking factor F_E from the various peaking sub-factors (itemized above) in two ways. The most conservative method is to assume that all sub-factors occur for the most limiting, or the hottest channel. Mathematically, this is equivalent to:

$$F_E = F_E^{\dot{m}} \times F_E^{d_{C2}} \times F_E^{d_{F2}} \times F_E^{k_C} \times F_E^{k_F} \times \dots$$

In this method, F_E is a maximum, $\overline{q''}$ is a minimum, and, economically, the operation of the reactor is least desirable. Obviously, such a doomsday scenario does not occur in practice. A reasonable way to account for all the engineering sub-factors is to use a method based on statistical combination of uncertainties.

Transient peaking factors. So far, we discussed nuclear and engineering peaking factors. These are applicable when plant is operating at steady state condition and producing nominal power. Two more sets of peaking factors are also considered. The first sub-factor (F_P), accounts for deviations from nominal power during normal operation and second peaking sub-factor (F_T) accounts for such conditions as the build up of thermal stresses in the clad due to plant transients. The result is to further increase the safety factor:

$$F = F_N \times F_E \times F_P \times F_T$$

Figure VIe.3.7 shows the effect of various peaking factors on core heat flux. In addition to the above mentioned factors, we need to consider another safety factor to provide margin to the critical heat flux as discussed next.

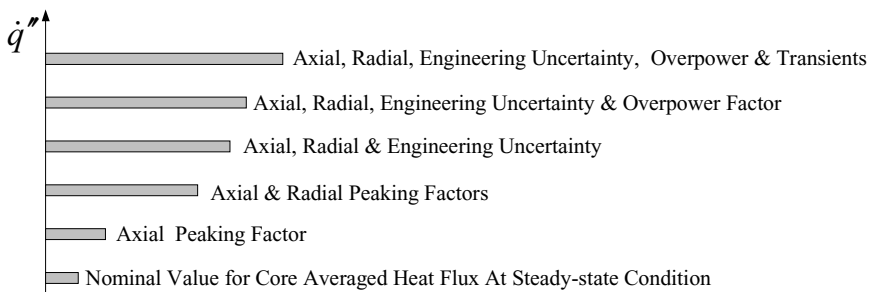


Figure VIe.3.7. Determination of peaking factors for reactor thermal design (Todreas)

4. Reactor Thermal Design

In the design of a power plant, many aspects must be evaluated and several constraints must be met. Some of the aspects that must be evaluated include federal, state, and local regulations, economical and environmental considerations, site suitability, structural, electrical, thermal, and hydraulic constraints. Focusing only on the thermalhydraulics of a water-cooled nuclear power plant, we start from the electric power demand that should be met by the utility. The balance of plant is designed based on the demand on the electric grid. This design consists of the steam cycle including turbine, steam extraction, feedwater heaters, and other heat exchangers. The site selected for the power plant determines the ultimate heat sink. If located on sites close to a bay, a lake, or other large bodies of water, selection of a condenser is warranted. Otherwise, cooling ponds or cooling towers should be used. If a condenser is used, the appropriate condensate pumps and condensate booster pumps to provide the design head and flow rate must be selected. This is also applied to such other pumps as the main feedwater and the feedwater heater pump.

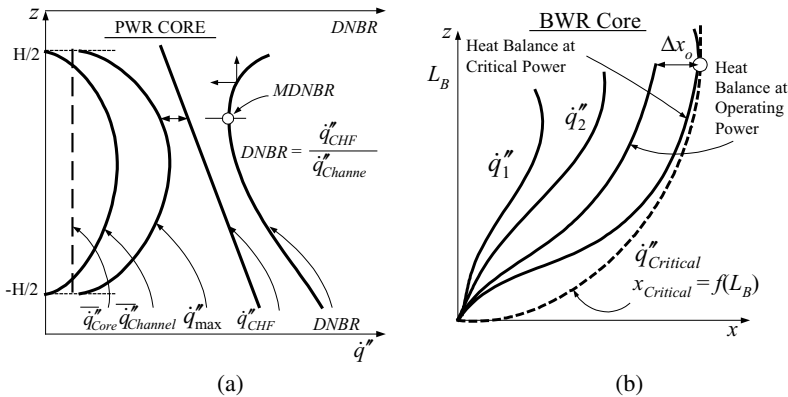


Figure VIe.4.1. Determination of CHF in (a) PWRs and (b) BWRs

The selection of the steam supply system is the most crucial decision. For nuclear plants the choice in the United States is primarily between a PWR or a BWR, although, gas cooled reactors may also be an alternative. To determine the required thermal power of the reactor core, we need to first calculate thermal efficiency of the steam cycle. Having thermal efficiency, we then design the core.

It is important to note that according to Carnot's efficiency, Equation IIa.9.2, the higher the heat source temperature, the higher the thermal efficiency. In BWRs, this is the core exit temperature and in PWRs this is the steam temperature in the steam dome. The highest temperature, being directly related to the integrity of the fuel rods, must remain well below the melting temperature of the cladding metal. The Code of Federal Regulations (10 CFR 50-46) requires the peak clad temperature not to exceed 2200 F (1500 K) during design basis events, as described later in this Chapter. If a nuclear reactor was a temperature-controlled sys-

tem, we could have defined a safety factor for the maximum temperature and operate the plant such that temperature does not exceed the calculated value. However, as Equation VIe.3.2 shows, reactors are flux-controlled systems. In such systems as Figure VIe.4.1 shows, the CHF point must not be approached since temperature jumps from the value corresponding to nucleate boiling to the elevated value corresponding to the film-boiling region. Thus, to ensure fuel rod temperature remains below limit, a regulatory approved correlation is first used to calculate critical heat flux. A safety factor, F_{CHF} , is then applied for conservatism. This safety factor is the critical heat flux ratio (CHFR).

The CHF in PWRs is due to the departure from nucleate boiling (DNB), which is a local phenomenon. Therefore, in PWRs this safety factor is referred to as the DNBR (departure from nucleate boiling ratio). To demonstrate this graphically, let's evaluate the plots of Figure VIe.4.1(a). The dashed line shows the core average heat flux. Note that the core average heat flux is related to the fuel rod surface area according to:

$$\overline{\dot{q}''_{av}} = \frac{\dot{Q}}{P_F H N_{rod}} = \frac{\dot{W}}{(P_F H N_{rod}) \eta} \quad \text{VIe.4.1}$$

where \dot{W} is the required power on the grid (MWe), $\dot{Q} = \dot{W} / \eta$ is core thermal power (MWth), and η is plant thermal efficiency. The first cosine curve in Figure VIe.4.1(a) shows the axial heat flux distribution in an average channel. The second cosine curve shows the axial heat flux distribution in the hot channel. Note that, similar to Equation VIe.3.7 and from our earlier discussion, the relationship between heat flux in an average channel to the heat flux in the hot channel is in the form of:

$$\overline{\dot{q}''_{av}} = \frac{\dot{q}''_{\max}}{F} \quad \text{VIe.4.2}$$

In Figure VIe.4.1(a), $\overline{\dot{q}''}$ is followed by the axial critical heat flux distribution, $\dot{q}''_{CHF}(z)$. The last curve on the right side shows the plot of:

$$DNBR(z) = \frac{\dot{q}''_{CHF}(z)}{\dot{q}''_{\max} \cos(\pi z / H)}$$

which is the departure from nucleate boiling ratios for various points along the hot channel. The minimum point on this plot is the minimum departure from nucleate boiling ratio, $MDNBR$:

$$MDNBR = \frac{\dot{q}''_{CHF}(z_{DNB})}{\dot{q}''_{\max} \cos(\pi z_{DNB} / H)} \quad \text{VIe.4.3}$$

If we substitute from Equation VIe.4.3 into Equation VIe.4.2 and subsequently in Equation VIe.4.1, we find:

$$N_{rod} = \left[\frac{\cos(\pi z_{DNB} / H)}{(P_F H \eta)} \right] F \times MDNBR \times \frac{\dot{W}}{\dot{q}_{CHF}''(z_{DNB})} \quad \text{VIe.4.4}$$

Equation VIe.4.4 shows the intricate relationship between power production, hot channel factor, and the minimum departure from nucleate boiling ratio. Economically, for the same core design parameters, higher power is obtained when the *MDNBR* and the hot channel factor are minimized.

Example VIe.4.1. The axial power distribution in a PWR core is represented as $\dot{q}''' = C \cos(\pi z / 12)$ where z is in ft. Use the given data and the Bernath correlation for CHF to find the *MDNBR*.

Data: $\dot{Q}_{core} = 2700$ MWth, $P = 2250$ psia (15.5 MPa), $T_{f,in} = 550$ F (560.7 K), $\dot{m}_{core} = 138.5\text{E}6$ lbm/h (62.82 kg/h), $N_{Rod} = 38,000$, $H_{core} = 12$ ft (3.66 m), $d_F = 0.38$ in (0.96 cm), $d_{C1} = 0.39$ in (0.99 cm), $d_{C2} = 0.45$ in (1.14 cm), $s = 0.588$ in (1.493 cm), $c_p = 1.3$ Btu/lbm·F (5.44 kJ/kg·K), $N_{Rod} = 38,000$.

Solution: Find $\dot{q}_{max}''' = \left(\frac{1.16 \dot{Q}_{core} E_d}{HN_{rod} a^2 E_R} \right) = \frac{1.16 \times 2700 \times 3412,000 \times 180}{12 \times (0.38 / 2 \times 12)^2 \times 38,000 \times 200} = 84.13\text{E}6$ Btu/h·ft³ (870.7 MW/m³)

$$(\dot{q}_{max}''')_{actual} = 2\dot{q}_{max}''' / 3 = 56\text{E}6 \text{ Btu/h·ft}^3 (579.6 \text{ MW/m}^3)$$

$A_F = \pi d_F^2 / 4 = 7.87\text{E}-4$ ft². We also find the channel flow area $A_{Flow} = s^2 - \pi d_{C2}^2 / 4 = 1.296\text{E}-3$ ft² (1.2 cm²)

$$D_e = 4A_{Flow} / P_{C2} = 4 \times 1.296\text{E}-3 / (\pi \times 0.45 / 12) = 0.044 \text{ ft (1.34 cm)}$$

$$\dot{m} = 135.5\text{E}6 / 38000 = 3565.8 \text{ lbm/h (0.45 kg/s)}$$

$$\dot{q}''(z) = (d_F^2 / 4d_{C2}) \dot{q}_{max}''' \cos(\pi z / H) = [(0.38/12)^2 / (4 \times 0.45/12)] \times 56\text{E}6 \cos(\pi z / H) = 0.374\text{E}6 \cos(\pi z / H)$$

$$T_f(z) = T_{f,in} + \frac{\dot{q}_{max}''' A_F H}{\dot{m} c_p} \left[1 + \sin\left(\frac{\pi z}{H}\right) \right] =$$

$$550 + \frac{56\text{E}6 \times 7.87\text{E}-4 \times 12}{\pi \times 3565.8 \times 1.3} \left[1 + \sin\left(\frac{\pi z}{H}\right) \right] = 550 + 36 \left[1 + \sin\left(\frac{\pi z}{H}\right) \right]$$

We now set up the following table for the hot channel in the core:

z	-5H/10	-4H/10	-3H/10	-2H/10	-H/10	0.0	H/10	2H/10	3H/10	4H/10	5H/10
$T_f(z)$	550.0	551.8	556.9	563.5	575.0	586.3	597.5	607.6	615.6	620.8	622.6
$\rho(z)$	47.17	46.95	46.73	46.08	45.25	44.44	43.48	42.55	41.67	41.15	40.98
$V(z)$	16.19	16.27	16.35	16.58	16.88	17.19	17.57	17.95	18.33	18.56	18.64
\dot{q}_{DNB}''	1.36	1.35	1.32	1.27	1.19	1.11	1.03	0.98	0.90	0.86	0.850
\dot{q}''	0.00	0.116	0.220	0.303	0.356	0.374	0.356	0.303	0.220	0.116	0.000
$MDNBR$	-	11.6	6.0	4.2	3.3	2.9	2.7	3.2	4.1	7.4	-

z : ft, $T_{f,in}$: F, ρ : lbm/ft³, V : ft/s, heat flux: MBtu/h·ft².
Note that we have assumed flux at $z = 0$ and $z = L$ is zero. In reality, flux goes to zero at *extrapolation lengths*

where \dot{q}_{DNB}'' is calculated from:

$$\dot{q}_{CHF}'' = h_{CHF} (T_{s,CHF} - T_f)$$

In this equation, h_{CHF} and $T_{s,CHF}$ are obtained from (the Bernoth correlation):

$$h_{CHF} = 10,890 \frac{1}{1 + (P_h / \pi D_e)} + \frac{48V}{D_e^{0.6}}$$

and $T_{s,CHF} = 32 + 102.6 \ln P - \frac{97.2}{1 + (15 / P)} - 0.45V$, respectively.

More accurate results are obtained if we use smaller increments from $z = 0.0$ to $z = 2H/10$. According to the Bernath correlation, the $MDNBR = 2.7$. Expectedly, the determination of the $MDNBR$ strongly depends on the correlation used to predict CHF in the hot channel. Note that we ignored small changes in pressure due to friction, elevation, and acceleration pressure drops. In this table, water temperature at each node is calculated from Equation VIe.3.9, which is used in turn to find water density and to obtain water velocity in the channel from Equation IIa.5.2.

As discussed in Chapter Vb, the critical heat flux in BWRs is due to the total heat deposited in the channel resulting in an annular flow regime and eventually leading to dryout. For this reason, in BWRs the CHFR is referred to as the critical power ratio, CPR. Shown in Figure VIe.4(b), the first curve on the left side is the flux distribution in a channel. The second shows the increased heat flux from \dot{q}_1'' to \dot{q}_2'' . We may keep increasing the heat flux and obtaining similar curves. The third plot, for example, shows the curve corresponding to the normal operational condition. The heat flux may be further increased so that the corresponding curve is tangent to the curve representing the critical condition. This is the limiting power that must not be approached. The curve representing CHF, in terms of critical quality versus boiling length, is known as GEXL and is obtained by General Electric (GE) from proprietary data.

Example VIe.4.2. The axial power distribution in a PWR core is represented as $\dot{q}''' = \dot{q}'''_{\max} \cos(\pi z / 12)$ where z is in ft. The core active length is 12 ft. The MDNBR of 2.0 occurs 20 inches from the core mid-plane where the critical heat flux is calculated as $1.2\text{E}6 \text{ Btu/h}\cdot\text{ft}^2$. Find a) \dot{q}'''_{\max} , b) \dot{q}''_{av} , and c) total fuel rod surface area. Data: Hot channel factor: 2.8, Required power on grid: 1000 MWe, $\eta = 29\%$.

Solution: We find the heat flux profile from \dot{q}''' profile since $\dot{q}'''(\pi d_F^2 / 4)H = \dot{q}''(\pi d_{C2})H$. Therefore, we find $\dot{q}'' = \dot{q}''' (A_F / P_{C2})$ where A_F and P are the fuel cross sectional area and perimeter, respectively. The heat flux profile becomes:

$$\dot{q}''(z) = (A_F / P_{C2}) \dot{q}'''_{\max} \cos\left(\frac{\pi z}{12}\right) = \dot{q}''_{\max} \cos\left(\frac{\pi z}{12}\right)$$

a) The maximum heat flux is found from the fact that at $z = 20$ in, $MDNBR = 2.0$

$$\dot{q}''(20) = \dot{q}''_{\max} \cos\left(\frac{20\pi}{144}\right) = \frac{\dot{q}''_{CHF}}{MDNBR} = \frac{1.2\text{E}6}{2.0} = 600,000 \text{ Btu/h}\cdot\text{ft}^2$$

Therefore, the maximum heat flux is found as,

$$\dot{q}''_{\max} = \frac{600,000}{\cos(20\pi / 144)} = \frac{600,000}{0.906} = 662,026.75 \text{ Btu/h}\cdot\text{ft}^2$$

b) The average heat flux is found as $\dot{q}''_{av} = \frac{\dot{q}''_{\max}}{F} = \frac{662,026.75}{2.8} = 236,438 \text{ Btu/h}\cdot\text{ft}^2$.

c) The required surface area is found from, $A = \dot{Q}_{Core} / \dot{q}''_{av}$ where $\dot{Q}_{Core} = (\dot{W} / \eta_{th})$. Hence, we find total fuel rod surface area from $A = (1000 \times 3412,000 / 0.29) / 236,438 = 50,000 \text{ ft}^2$.

Example VIe.4.3. Use the following data and plot the temperature profile of water in a PWR.

Data: $\dot{Q} = 2700 \text{ MWth}$, $\dot{m}_{Core} = 138\text{E}6 \text{ lbm/h}$, $T_{CL} = 550 \text{ F}$, $T_{FW} = 430 \text{ F}$, $P_{Core} = 2250 \text{ psia}$, $P_{SG} = 900 \text{ psia}$, $P_{Condenser} = 1 \text{ psia}$, $\dot{m}_{Heat Sink} = \text{lbm/h}$, $d_{C2} = 0.45 \text{ in}$, $H_{Core} = 12 \text{ ft}$, $F = 2.5$, $T_{sink,in} = 70 \text{ F}$, and $T_{sink,o} = 80 \text{ F}$.

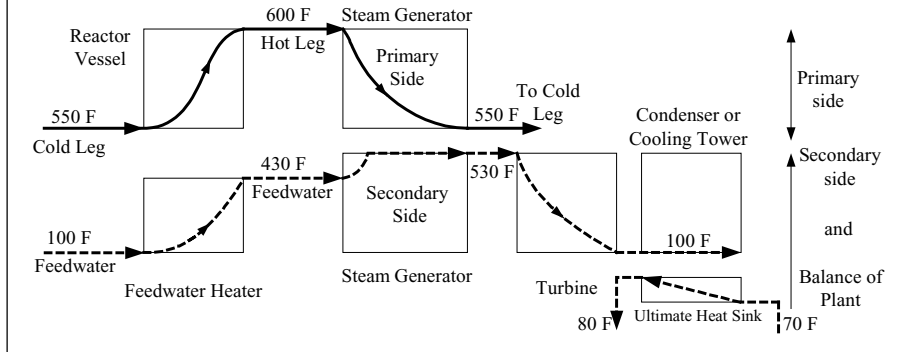
Solution: To find the plant temperature profile, we assume pipe runs are fully insulated. Then find

– core exit temperature by applying Equation IIa.6.6 to the core:

$$h_e = h_i + (\dot{Q} / \dot{m}) = 547.15 + (2700 \times 3412000 / 138\text{E}6) = 614 \text{ Btu/lbm}$$

Hence, $T_{HL} \cong 600$ F

- the profile of the water temperature in the average channel from Equation VIe.3.8
- steam generator inlet temperature from $T_{h,in} = T_{HL} = 600$ F
- the profile of water in the steam generator tubes from Equation VIa.6.8. Note, $T_{h,o} = T_{CL} = 550$ F
- steam generator secondary-side inlet temperature, $T_{c,i} = T_{FW} = 430$ F.
- turbine exit temperature from the condenser pressure, $T_{turbine,o} = 100$ F.



5. Shutdown Power Production

Unlike other power producing systems, nuclear reactors continue to produce power, albeit at a much smaller rate, even after being shutdown. Power generation in nuclear reactors following shutdown is due to two sources: the power produced by fission caused by the delayed neutrons and the power due to β and γ decays of radioisotopes. Power produced by delayed neutrons is short lived. It can be calculated by solving the neutron kinetic equation with the insertion of a large negative reactivity (-0.09). Such solution would show that the reactor power due to delayed neutrons would decrease exponentially over a period of about 80 seconds (the half-life of the longest lived delayed neutron precursor). Hence, the most dominant source of power following a reactor shutdown is the decay of radioisotopes.

The rate of decay heat, as shown in Figure VIe.5.1 is generally obtained from the models developed by the American Nuclear Society (ANS). In this figure, ANS 1971_1 refers to the nominal value for the decay of fission products. ANS 1971_2 refers to the nominal value plus the decay of the heavy elements (U-239 and NP-239). ANS 1971_3 is the same as ANS 1971_2 but it accounts for 20% uncertainty in the nominal and 10% uncertainty in the decay of the heavy elements. ANS 1971_4 applies 20% instead of 10% uncertainty to the decay of the heavy elements.

ANS 1979_1 refers to the nominal value for the decay of fission products plus the decay of the heavy elements. The ANS 1979_2 model also accounts for 2σ

uncertainty. The Branch Technical Position (BTP) in this figure is similar to ANS 1971_3. To highlight the differences between these model, the bottom figure focuses on the first 1000 seconds after shutdown.

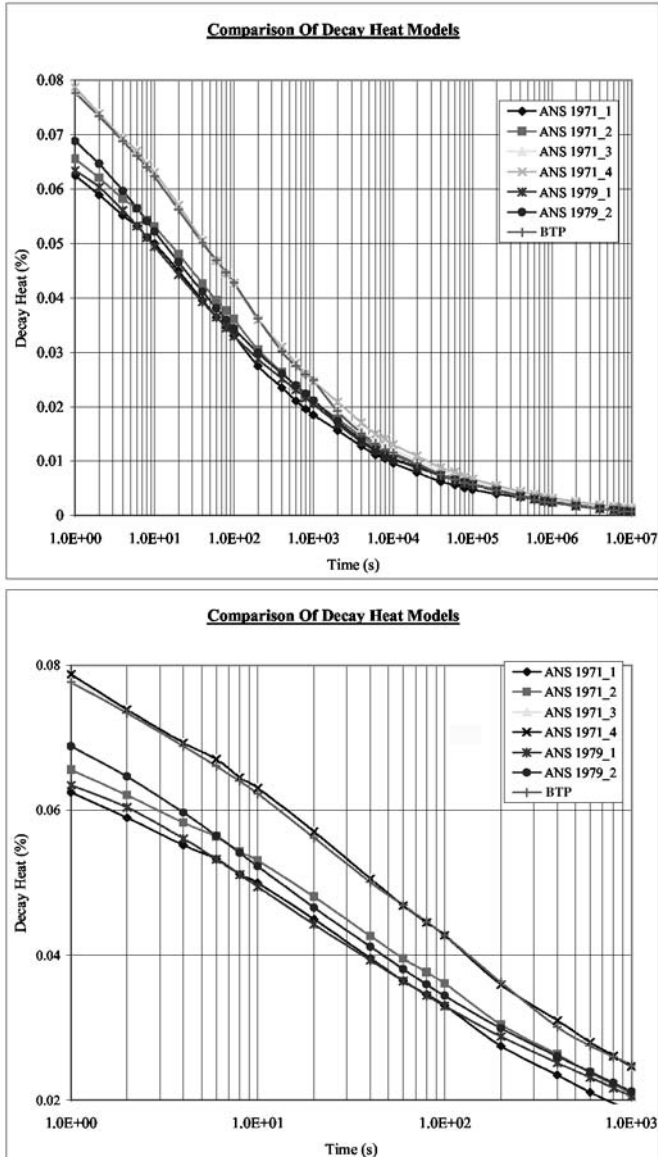


Figure VIe.5.1. Various models for the estimation of decay power

As shown in Figure VIe.5.1, reactor decay power following shutdown drops rapidly in the short term (about 1000 s) and in the long term approaches zero asymptotically. Obtaining a general formula for decay power is difficult due to such factors as dependency on the fuel cycle and duration of operation (resulting in differences in heavy nuclide concentration and their decay characteristics). See Problem 55 for a best estimate prediction of decay heat as recommended by El-Wakil. This correlation is applicable for time greater than 200 s after shutdown.

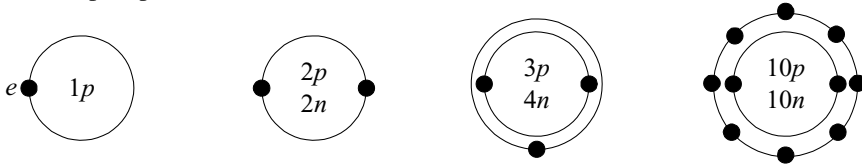
QUESTIONS

- What is the diameter of the chlorine atom?
- What are *subatomic* particles?
- What is an isotope? What are the isotopes of uranium?
- Define atomic mass unit. How much energy in MeV is associated with 1 amu?
- Explain the difference between a chemical and a nuclear reaction
- What is the abundance of the U-235 isotope in naturally occurring uranium?
- What is the process by which we increase the mass of certain isotopes in naturally occurring substance?
- What is mass defect? Why is the mass of a nucleus less than the total mass of its constituents?
- Why are heavy elements such as uranium and plutonium more amenable to fission?
- In how many ways may a neutron interact with a nucleus?
- What are the differences between elastic and inelastic scattering?
- Are microscopic and macroscopic cross sections properties of the neutron or of the nucleus?
- What does the macroscopic cross section physically represent?
- Why do we refer to slow neutrons as thermal neutrons?
- What major assumption constitutes the basis of the diffusion equation?
- Mathematically speaking, what do temperature distribution in a rectangular plate (Figure VIIb.2.1) and neutron flux distribution in a cylindrical core have in common?
- Why, in an elastic scattering between a fast neutron and a nucleus, is most energy lost in collision with light nuclei than with heavier nuclei?

PROBLEMS

1. The atomic nucleus contains protons and neutrons while the electrons are orbiting the nucleus on specific shells or orbits. Each shell is filled with a certain number of electrons. The shells are identified with quantum numbers 1, 2, 3, ..., etc. The shell with the quantum number 1 is the closest orbit to the nucleus. These are also referred to as orbits K , L , M , N , etc. Usually the shells closest to the nucleus are filled first. The number of electrons each shell is filled is given by $2n^2$. Thus, shell K is filled with 2, shell L with 8, shell M with 18, and shell N with 32 electrons. Electrons that orbit in the outermost shell of an atom are called

the valance electrons. Shown in the figure are the structure and the valance electrons for hydrogen, helium, lithium, and neon. Draw similar atomic structures for sodium, phosphorous, and xenon.



2. How much energy corresponds to 1 lbm?
3. If the energy released by the Hoover dam in 2.5 days is 2.7×10^{14} J, find the equivalent mass associated with this amount of energy. [Ans. 3 grams].
4. Treating neutrons as a gas, we may describe the total number of neutrons per unit volume by the Maxwellian distribution. If $n(E)$ is the number of neutrons per unit volume having energy E per unit energy, then $n(E)dE$ is the number of neutrons per unit volume having energies in the range of E and $E + dE$ so that:

$$n(E) = \frac{2\pi n}{(\pi \kappa T)^{3/2}} E^{1/2} e^{-E/\kappa T}$$

where N is the total number of neutrons and T is the absolute temperature of the medium. In this relation, κ is Boltzmann's constant $\kappa = 1.3806 \times 10^{-23}$ kJ/K = 8.617×10^{-5} eV/K. Use the above information and find:

- a) similar distribution for neutron velocity. [Hint: Substitute for E from the $K.E.$]
- b) the most probable energy, the most probable velocity, and the energy corresponding to the most probable velocity.
- c) the average energy

[Hint: use the averaging method given by $\bar{E} = \left(\int_0^E n(E) E dE \right) / n$].

[Ans.: a) $E_p = \kappa T/2$, b) $V_p = (2\kappa T/m)^{1/2}$, and c) $\bar{E} = 3\kappa T/2$].

5. Calculate the most probable neutron velocity and the neutron energy corresponding to the most probable velocity. Use room temperature of 20 C. [Ans.: $V_p = 2200$ m/s, and $E = 0.0253$ eV].

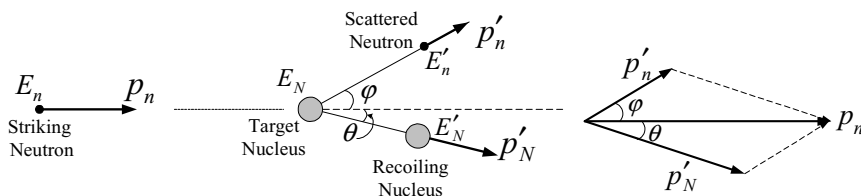
6. Steady state neutron flux in a bare spherical reactor of radius R is approximately expressed as:

$$\phi(\bar{r}, E, \bar{\Omega}) = \frac{\phi_o}{4\pi} E \exp\left(-\frac{E}{\kappa T}\right) \frac{\sin(\pi \bar{r} / R)}{r}$$

where ϕ_o is the maximum flux at the center of the reactor. Use Equation VIe.1.4 and the relation between energy and velocity to find the number of neutrons in the reactor. Gamma function properties are given in Chapter VIIb. [Ans. $\phi_o (2\pi m)^{1/2} (\kappa T)^{3/2} R^2$].

7. Show that the atom density of an element is given by $N = \rho N_A / M$ where N_A is Avogadro's number (6.023×10^{23}) and M is the molecular weight. Find the atom density of C-12. Use the data for scattering and absorption cross sections and find the total macroscopic cross section of C-12. Since the mean free path is $\lambda = 1/\Sigma$, show that C-12 is an excellent moderator.

8. Collision between neutrons and nucleus of the moderator results in slowing down the newly born fast neutrons. Such a collision is depicted in the figure. The striking fast neutron has an initial energy E_n and an initial momentum p_n . The target nucleus is initially at rest. Considering an elastic scattering, following the collision, the scattered neutron has an energy of E'_n and momentum of p'_n while the recoiling nucleus has an energy of E'_N and momentum of p'_N . Use the conservation of momentum and energy to drive a relation for energy of the scattered neutron in terms of the initial neutron energy and mass number of the target nucleus. [Hint: Find the momentum of the recoiling nucleus in terms of the momentum of the initial and the scattered neutron. Substitute for momentum terms ($p^2 = 2mE$) and for the recoiling energy from the energy balance].

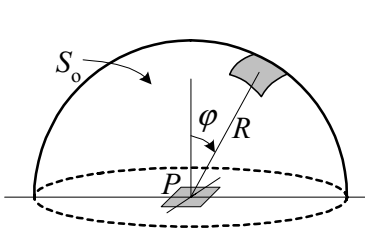


9. The energy of the scattered neutron following an elastic scattering between the neutron and the target atom is given as (note that the molecular mass of the nucleus, M divided by the mass of neutron, m is $M/m = A$):

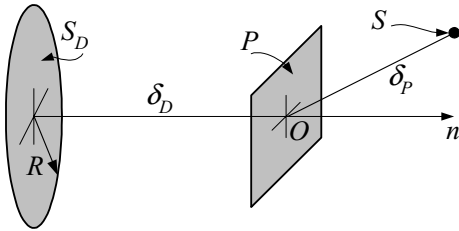
$$E'_n = \frac{E_n}{(A+1)^2} \left[\cos \phi + \sqrt{A^2 - \sin^2 \phi} \right]^2$$

Find the minimum energy of the scattered neutron following a collision with the atom of C-12. The striking neutron has an initial energy of 5 MeV.

10. An isotropic neutron source emitting S_0 neutrons/s·cm² is located on the surface of a sphere of radius R . Find a) neutron flux at the center of the sphere and b) neutron current at the center of the sphere through a mid plane. [Ans.: $S_0/2$ and $S_0/4$ downward].



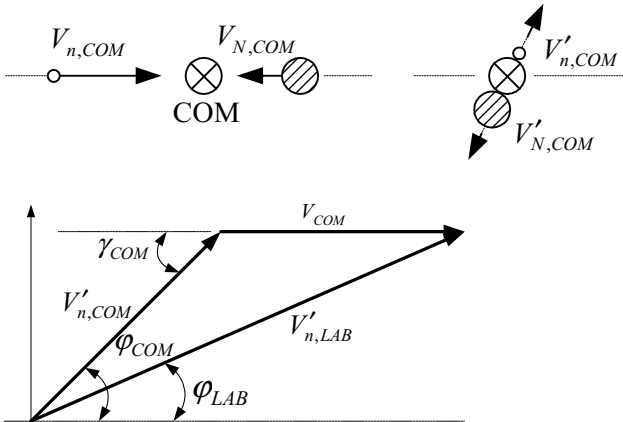
Problem 10



Problem 11

11. A plane (P) is located between a disk (D) and a point source. The disk emits S_D particles isotropically and is located at a distance δ_D from plane P . The point source emits S particles isotropically and is located at a distance δ_P from point O on plane P . Find neutron flux and current at point O .

12. The collision in Problems 8 and 9 is described from the point of view of a stationary observer, referred to as the laboratory (LAB) system. Now, consider a case where the observer is instead located at the center of momentum of the neutron and nucleus, referred to as the center of momentum (COM) system. In this case the total momentum before and after the collision is zero. Show that the velocity of the center of momentum (which for non-relativistic events is the same as the center of mass) for the stationary nucleus is given by $V_{COM} = V_{n,LAB}/(A + 1)$ where $V_{n,LAB}$ is the neutron velocity in the LAB system before collision. Also show that $V_{n,COM} = A V_{n,LAB}/(A + 1)$ and $V_{N,COM} = -V_{n,LAB}/(A + 1)$ where $V_{N,COM}$ is the velocity of the nucleus before the collision in the COM system.



Problems 12, 13, and 15

13. Use the diagram showing neutron velocity before and after a collision to conclude that:

$$\frac{E'_n}{E_n} = \frac{A^2 + 2A \cos(\varphi_{COM}) + 1}{(A+1)^2} = \frac{1+\alpha}{2} + \frac{1-\alpha}{2} \cos \varphi_{COM}$$

where $a = [(A-1)/(A+1)]^2$ is known as the *collision parameter*. Use this relation to:

- find the angle corresponding to the minimum energy of the emerging neutron (E'_{\min})
- find E'_{\min} , the minimum energy of the emerging neutron

14. Neutron lethargy is defined as $\lambda = \ln E - \ln E' = -\ln(E'/E)$. Use the result of Problem 13 and show that neutron lethargy in terms of the nucleus mass number may be expressed as $\lambda \approx 2/(A+2/3)$. [Hint: Find an energy-averaged lethargy. The probability distribution function for elastic scattering and isotropic in the center of mass is $1/(1-\alpha)E$].

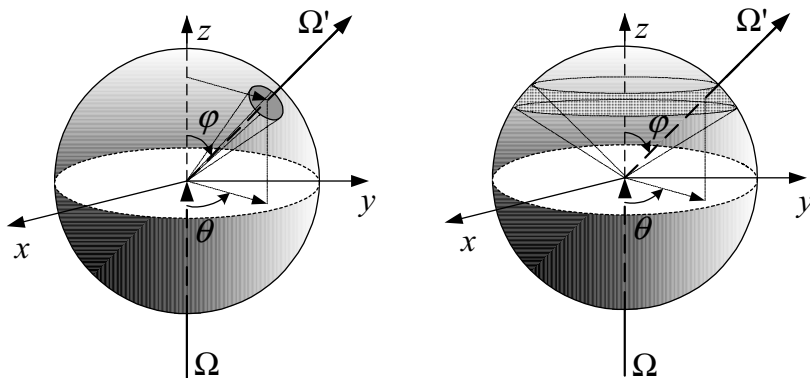
15. Use the diagram to conclude that the cosine of the scattering angle in the LAB system in terms of the cosine of the scattering angle in the COM system is given as:

$$\cos(\varphi_{LAB}) = \frac{A \cos(\varphi_{COM})}{\sqrt{A^2 + 2A \cos(\varphi_{COM}) + 1}}$$

16. Use the results of Problems 13 and 15 to plot E'/E as a function of both φ_{LAB} and φ_{COM} .

17. Consider the case of linearly anisotropic elastic scattering in the COM system $\sigma_s(\mu_{COM}) = \sigma_0 + \sigma_1 \mu_{COM}$ where σ_0 and σ_1 are known constants. Find and plot the distribution of the nuclear recoil energies

18. Find the probability of isotropic scattering into a differential solid angle is $d\Omega/4\pi^2$ where the differential solid angle $d\Omega$ is given as $2\pi \sin(\varphi_{COM})(rd\varphi_{COM})$. [Hint: Integrate over θ to get scattering in the segment]



19. Show that scattering in the COM system is isotropic. For this purpose, find $\cos(\varphi_{COM})$ and interpret the result. [Hint: Multiply the cosine of the scattering angle in the COM by the probability of scattering and integrate from 0 to π].

20. Use the result of Problem 15 and the method of Problem 18 to find the cosine of the scattering angle in the LAB system, $\cos(\varphi_{LAB})$. Does the result show that scattering in the LAB system is backward, isotropic, or forward scattering? [Ans.: $2/(3A)$].

21. In Problem 13 it is shown that there is a one-to-one relation between the change in neutron energy and the change in the scattering angle. Thus, it can be concluded that $p(E \rightarrow E')dE' = -p(\Omega \rightarrow \Omega')d\Omega'$ where p is probability and the minus sign reflects the fact that the larger the scattering angle, the lower the energy of the scattered neutron. We represent $p(\Omega \rightarrow \Omega') = 4\pi\sigma_s(\Omega \rightarrow \Omega')/\sigma_s$ where $\sigma_s(\Omega \rightarrow \Omega')$ is the differential scattering cross section and $\int_{\Omega} \sigma_s(\Omega \rightarrow \Omega')d\Omega' = \sigma_s$. Use this information and find $p(E \rightarrow E')$ for an elastic scattering and isotropic in the COM where $\sigma_s(\Omega \rightarrow \Omega') = \sigma_s/4\pi$. [Ans.: $p(E \rightarrow E') = 1/(1 - \alpha)E$].

22. Use the result of Problem 21 to find the *average fractional energy loss* in an elastic scattering collision. The average fractional energy loss is defined as $\overline{\Delta E}/E$. [Ans. $(1 - \alpha)/2$].

23. Regarding neutron-nucleus interaction, so far we dealt with elastic collision for *isotropic* and *anisotropic* scatterings. In this problem, we want to find E'/E for an inelastic scattering in which the target nucleus absorbs an amount of energy Q . Use the energy equation, which now accounts for Q and the velocity diagram of Problem 12 to show that:

$$\frac{E'}{E} = \frac{A^2\xi^2 + 2A\xi \cos \varphi_{COM} + 1}{(1 + A)^2}; \quad \xi = \left(1 - \frac{1 + A}{EA}Q\right)^{1/2}$$

24. Consider two groups of isotopes. Group A consisting of U-233, U-235, Pu-239, Pu-241 and group B of Th-232, U-238, Pu-240, and Pu-242. Identify the group that represents fissile and the group that represents fissionable nuclides.

25. Find velocity (m/s) and kinetic energy (eV) of a thermal neutron at a temperature of 500 F. [Ans.: 2964].

26. Find the temperature of a thermal neutron having energy of 0.11 eV. [Ans.: 1000 C].

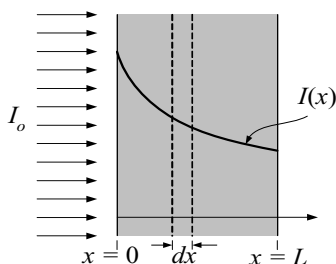
27. Start with the one-group neutron diffusion equation and derive the relation for neutron flux in a bare critical slab reactor. Find the maximum to average flux for this reactor.

28. An isotropic surface source of S_0 neutrons/s-cm² is located on the surface of a sphere of radius R . The sphere consists of a non-absorbing material. Find a) the

flux density at the center of the sphere and b) the net current of neutrons at the center of the sphere through a mid plane. [Ans.: a) S_0 and b) 0].

29. An isotropic surface source emits S_0 neutrons/s·cm² and is distributed on the surface of a hemisphere of radius R . The hemisphere consists of a non-absorbing material. a) Find the flux density at the center of the hemisphere. b) Find the net current of neutrons at the center of the hemisphere through a mid plane. [Ans.: $S_0/2$ and $S_0/4$].

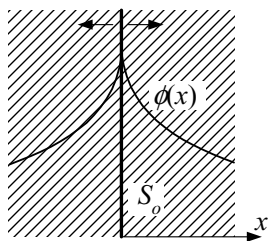
30. The left side of the slab shown in the figure is exposed to a monoenergetic neutron beam of an intensity I_0 neutrons/s cm². The slab material is homogeneously distributed and has an atom density of N atoms/cm³ and a cross section of σ for interactions with incident neutrons. Show that the neutron distribution inside the slab is given by $I(x) = I_0 \exp(-\Sigma_t x)$ where $\Sigma_t = N\sigma$. Find a) the probability that a neutron does not have an interaction when moves a distance dx , b) the fraction of neutrons without any interaction at $x = L$, and c) the average distance a neutron travels before interacting with a nucleus located in dx .



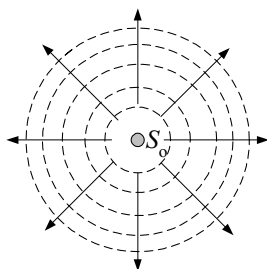
31. Show that the following integral is zero:

$$\frac{\partial \phi_0}{\partial x} \int_{\alpha=0}^{2\pi} \int_{\beta=0}^{\pi} \int_0^{\infty} \frac{\Sigma_s}{4\pi} \left[(r \sin \beta \cos \alpha) e^{-\Sigma_s r} \cos \beta d\alpha d\beta dr \right] = 0$$

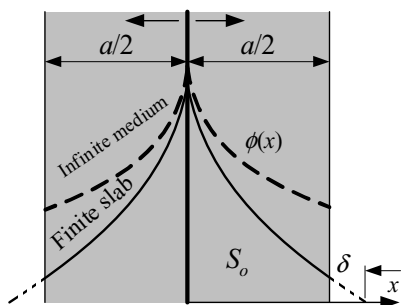
32. Consider a plane neutron source emitting S_0 neutrons/s·cm² in a non-multiplying, infinite, homogenous medium. The material of the medium has high scattering and low absorption cross section for neutrons. Find an expression for neutron flux in terms of D and L of the medium. [Hint: Solve Equation VIe.2.12 in the x -direction with $s = 0$ subject to the boundary conditions given by VIe.2.15]. [Ans.: $\phi(x) = (S_0 L / 2D) e^{-|x|/L}$].



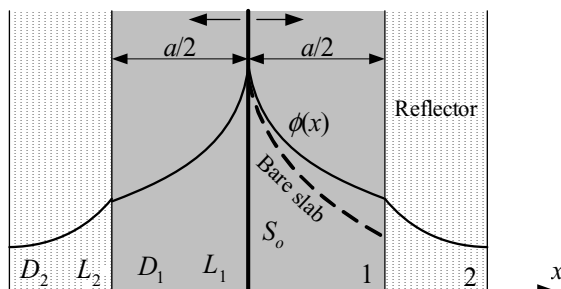
33. An isotropic point source emits S_o neutrons per second in an infinite non-multiplying weakly absorbing medium. Find neutron flux as a function of r , D , and L of the medium. [Ans.: $\phi(x) = (S_o/4\pi Dr)e^{-r/L}$].



34. A plane neutron source emitting S_o neutrons/s·cm² is located at the center of a non-multiplying homogenous bare slab. The material of the medium has high scattering and low absorption cross section for neutrons. Find an expression for the neutron flux in the slab. [Ans.: $\phi(x) = (S_o L/2D) \sinh(c_1)/\cosh(c_2)$ where $c_1 = (b - 2x)/2L$ and $c_2 = b/2L$ with $b = \delta + a/2$].

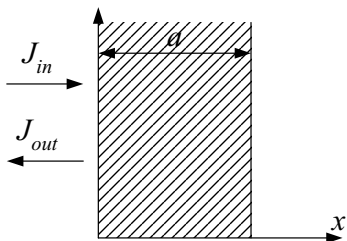


35. The slab of Problem 32 is now placed between two slabs of weakly absorbing materials. Slab 2, which is blanketing slab 1 is referred to as a blanket or reflector.



36. Consider the slab of Problem 34. However, in this case the localized planar source is replaced with a uniformly distributed neutron source emitting S_o neutrons/s cm^2 . Find the flux in the slab. [Ans.: $\{1 - (\cosh x/L)/\cosh a/L\}(S_o/\Sigma_a)$].

37. Albedo, or the reflection coefficient (α), is defined as the ratio of the reflected to the incident current, $\alpha = J_{\text{out}}/J_{\text{in}}$. Derive the albedo expression for a slab of thickness a . [Ans.: $\alpha = (1 - b)/(1 + b)$ where $b = (2D/L)\coth(a/L)$]. [Hint: Use Equations VIe.2.3 and VIe.2.4].

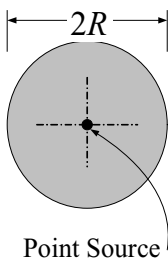


38. Consider an infinite medium through which monoenergetic sources of neutron emitting S_o neutrons/s cm^2 are uniformly distributed. Find neutron flux in this medium. [Ans.: $\phi = S_o/\Sigma_a$].

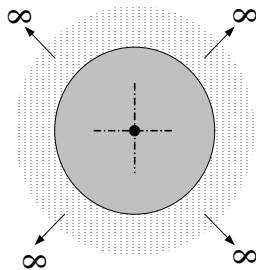
39. An isotropic point source emitting S_o neutrons/s is placed in the center of a bare sphere of radius R . The sphere is made up of carbon ($L^2 = D/\Sigma_a$). Show that the general solution for flux inside the sphere is given by:

$$\phi(r) = \frac{C_1}{r} e^{-r/L} + \frac{C_2}{r} e^{r/L}$$

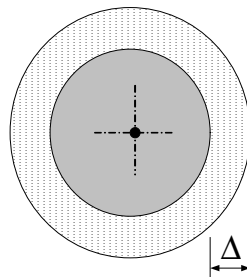
where C_1 and C_2 are constants of integration. Apply the boundary conditions and find the neutron flux anywhere at $r = R/2$. [Hint: Start with Equation VIe.2.14 and make a change of function; $\phi = \phi/r$].



Problem 39



Problem 40



Problem 41

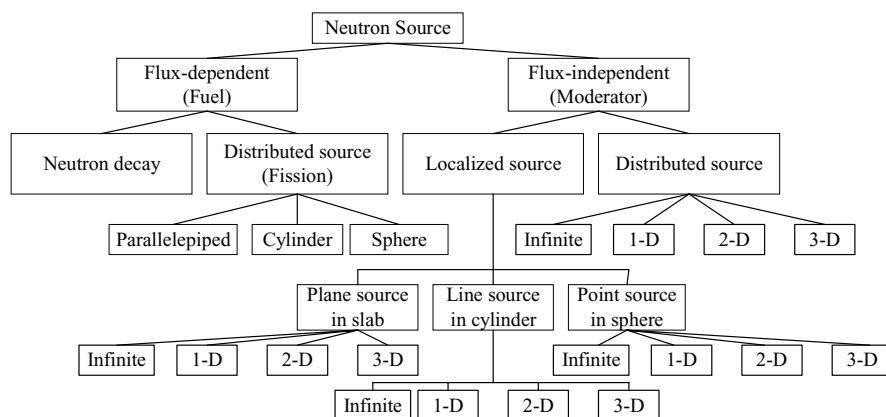
40. Solve problem 39 considering the sphere is located in an infinite medium made up of water.

41. Solve problem 40 considering the thickness of the water region is Δ and beyond $2R + \Delta$ is vacuum.

42. Start with the one-group neutron diffusion equation and derive the relation for neutron flux in a bare critical parallelepiped reactor. Find the maximum to average flux for this reactor.

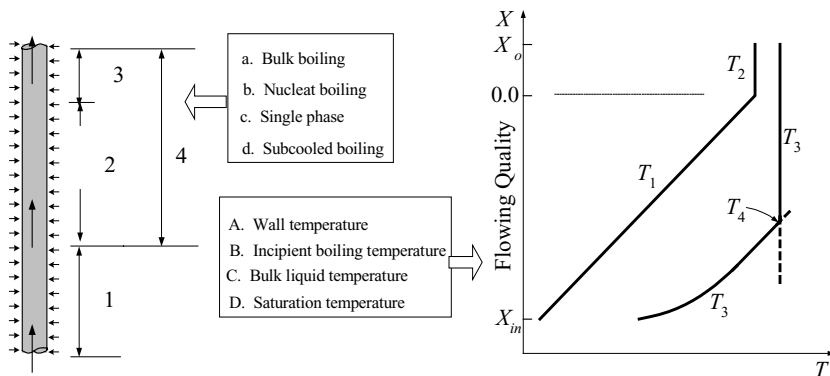
43. Start with the one-group neutron diffusion equation and derive the relation for neutron flux in a bare critical spherical reactor. Find the maximum to average flux for this reactor.

44. Categorize the type of neutron source used in problems 32 through 43. For this purpose, use the flow chart as shown below and find the box that best matches the source of neutron used in the above problems. In this figure, 1-D for example, stands for neutron diffusion equation in a one dimensional medium.



45. Determine the maximum linear heat generation rate to limit the average exit void fraction of a BWR to 0.60. Use the power profile of $\dot{q}'(z) = \dot{q}'_{\max} \sin(\pi z / L)$ where z is the distance from the assembly inlet and L is the assembly length. Use both homogeneous and drift flux models for void fraction. $H = 12$ ft, $P = 1000$ psia, $T_{f,in} = 530$ F, $(A_{Flow})_{\text{Assembly}} = 15$ in², $\dot{m} = 68\text{E}6$ lbm/h.

46. Water flows in a uniformly heated tube. At the entrance to the tube, water is subcooled at system pressure. Water leaves the tube as a saturated two-phase mixture. The figure below shows the heated tube and the plots of temperature versus quality. Match a) numbers with the lower case letters and b) temperatures with the upper case letters.



47. Water enters a BWR channel. Use the following data and find the location of the incipient boiling and the clad temperature corresponding to the incipient boiling.

Data: Pellet diameter: 0.45 in, Rod diameter: 0.55 in, Square array pitch: 0.8 in, core height = 12 ft, flow velocity: 8.5 ft/s, water inlet temperature: 530 F, system pressure: 1035 psia, $\dot{q}_{\max}'' = 1.25 \text{E}7 \text{ Btu/h}\cdot\text{ft}^2$.

[Ans.: $Nu = 1239$, $h = 5355 \text{ Btu/h}\cdot\text{ft}^2\cdot\text{F}$, $Y = 0.7$, $z_{SB} = -36.2 \text{ in}$, and $T_{SB} = 545.6 \text{ F}$].

48. Water enters a BWR channel. Use the following data and find the location of the incipient boiling and the clad temperature corresponding to the incipient boiling.

Data: Pellet diameter: 0.5 in, Rod diameter: 0.6 in, Square array pitch: 0.9 in, core height = 12 ft, flow velocity: 9 ft/s, water inlet temperature: 550 F, system pressure: 1050 psia, $\dot{q}_{\max}'' = 1.3 \text{E}7 \text{ Btu/h}\cdot\text{ft}^2$.

[Ans.: $z_{SB} = -63.72 \text{ in}$ and $T_{SB} = 553.77 \text{ F}$].

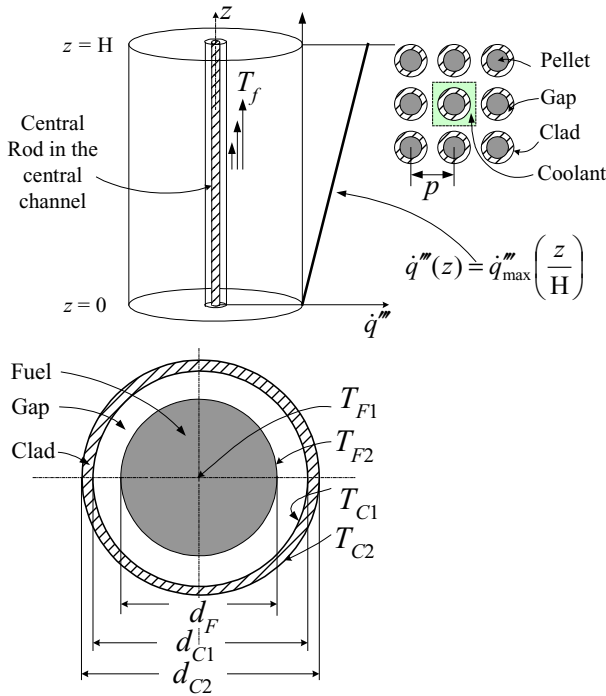
49. In this problem we want to find the bulk temperature corresponding to the incipient boiling temperature of the surface. Use the data of Example VIe.3.5 and find $T_i(z_{SB})$. [Ans.: $T_i(z_{SB}) = 528.3 \text{ F}$].

50. Find the bulk temperature corresponding to the incipient boiling temperature of problem 45.

51. Use the Bowring correlation for the calculation of CHF and solve Example VIe.4.1. Plot the results and find the $MDNBR$. [Ans.: CHF in $\text{MBtu/h}\cdot\text{ft}^2$ for various nodes: 1.85, 1.388, 0.11, 0.9251, 0.7929, 0.6937, 0.6166, 0.5549, 0.504, 0.4624, 0.4268. The $MDNBR = 1.5$].

52. Find the required number of rods for a PWR producing 1200 MWe having an efficiency of 30%. Other pertinent data at steady state operation are as follows: $MDNBR = 2.5$, $F = 2.3$, $z_{DNB} = 25''$ from the core mid-plane, $H = 12 \text{ ft}$, $d_{c2} = 0.45 \text{ in}$, $\dot{q}_{CHF}''(z_{DNB}) = 1.5 \text{E}6 \text{ Btu/h}\cdot\text{ft}^2$. [Ans.: $N_{Rod} = 31,638$].

53. We would like to load a core with fuel rods in which fuel pellet enrichment is such that the neutron flux increases linearly along the vertical axis as shown in the figure. Water is used as coolant. Use the given data

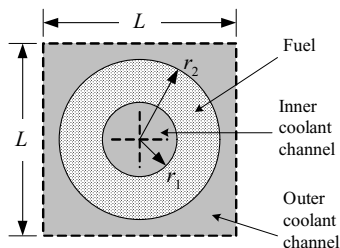
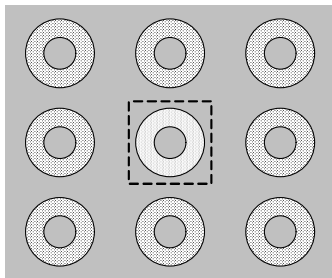


and find a) water temperature at the exit of the channel, b) peak temperatures of clad outside, clad inside, fuel surface, and fuel center, c) the incipient boiling temperature, and d) critical heat flux at the channel exit.

Data:

d_F (in):	0.38	P (psia):	1000
d_{C1} (in)	0.39	T_{in} (F):	500
d_{C2} (in):	0.44	\dot{m} (lbm/s):	1.00 (per rod)
p (in):	0.59	\dot{q}''' (Btu/h ft ³):	0.01E6

54. The fuel assembly shown in the left figure consists of periodic arrays of annular bare fuel rods, which are cooled by passing water through the center of the rods as well as over the outer surface. We want to analyze the thermal performance of the fuel rods by dividing the assembly into a number of unit cells (control volumes) and evaluating the performance of a cell, as shown in the right figure.



- a) Find the ratio of the average coolant velocities in the inner and outer channels at the axial level z . At this level, the pressure drop per unit length is the same in both channels and the bulk coolant temperature is 293 C. Assume that the flow is turbulent and fully developed in both channels.
- b) Find the maximum temperature in the rod, and the radius at which the maximum temperature occurs, for a particular axial location where the inner and outer surface temperatures of the rod are 371 C. At that level the volumetric heat generation rate may be assumed to be uniform and equal to 0.1 MW/m^3 . Assume constant fuel conductivity for the fuel.
- c) Find the mean temperature of the coolant at the core exit (i.e., the mixture of the coolant passing through the inner channel and that passing through the outer channel). The fuel rod is 4.3 m long and the axial power profile along the channel is give by:

$$\dot{q}'''(z) = \dot{q}_o''' \cos\left(\frac{\pi z}{4.3}\right)$$

where z is in m and $\dot{q}_o''' = 0.52 \text{ MW/m}^3$. Other pertinent data: Inlet water temperature = 293 C, water pressure at the outlet = 14 MPa, water flow rate per unit cell = 18.37 kg/s, unit cell side (L) = 6.35 cm, fuel inner radius (r_1) = 1.27 cm, and fuel outer radius (r_2) = 2.54 cm.

55. A reactor that has been operating at nominal power level of 2700 MWth for 2 years is shut down. The decay power from this reactor, for any time after shut-down, can be fairly well estimated from:

$$\frac{\dot{Q}(t)}{\dot{Q}_{\text{nominal}}} = 0.095t^{-0.26}$$

where t in this formula is the time after reactor shutdown in seconds. Find a) the power obtained from the reactor 1 day after shutdown, and b) the amount of energy produced by the decay power in a period of 24 hours. [Ans.: 13.35 MWth and 1.56E6 MJ].

56. A curve fit to the rate of the decay heat data of a typical PWR fuel cycle resulted in the following equation:

$$\frac{\dot{Q}(t)}{\dot{Q}_{\text{nominal}}} = A + \sum_{i=1}^6 \frac{B_i}{t^i}$$

where $\dot{Q}(t)$ is the decay power at time t , \dot{Q}_{nominal} is the nominal reactor power, and t is the time after reactor shutdown. Coefficients A and B_i are: $A = 0.3826033\text{E-}2$, $B_1 = 276.6013$, $B_2 = -5,124,569$, $B_3 = 0.6344872\text{E}11$, $B_4 = -0.4427653\text{E}15$, $B_5 = 0.1551979\text{E}19$, and $B_6 = -0.2086165\text{E}22$. Evaluate the accuracy of the formula given in Problem 55 by plotting both equations and comparing the results.

57. This problem deals with a CE-designed 2×4 PWR (i.e., 2 hot legs and 4 cold legs as shown in Figures I.6.2(b), I.6.4(CE), I.6.5, I.6.6(a), and I.6.6(b)). Use the given data to find the answers to the questions that follow the set of data.

Primary side data (BU - SI):

Core power (Btu/h - MWth):	9.2124E9 - 2700
Pressure in lower plenum (psia - MPa):	2595 - 18
Core pressure drop (psia - kPa):	14 - 100
Vessel pressure drop (psia - kPa)	37.1 - 256
Cold leg temperature (F - C):	550 - 288
Mass flow rate through core (lbm/h - kg/s):	138.5E6 - 17451
Number of fuel assemblies:	217
Number of rods per assembly:	14×14 (square array)
Fuel rod (Core) length (ft - m):	12 - 3.657
Fuel rod outside diameter (in - cm):	0.44 - 1.12
Fuel rod inside diameter (in - cm):	0.388 - 0.98
Fuel pellet diameter (in - cm):	0.377 - 0.96
Fuel pellet length (in - cm):	0.45 - 1.14
Fuel rod pitch (in - cm)	0.58 - 1.473
Gap heat transfer coefficient (Btu/h-ft ² ·F - W/m ² ·K):	1000 - 5678
Thermal conductivity of fuel pellet, UO ₂ (Btu/h-ft·F - W/m·K):	1.5 - 2.6
Thermal conductivity of Zircaloy (Btu/h-ft·F - W/m·K):	3.0 - 5.2
Hot leg inside diameter (ft - m):	3.5 - 1.067
Cold leg inside diameter (ft - m):	2.5 - 0.762
Volume of one hot leg (ft ³ - m ³):	138 - 3.9078
Volume of one cold leg (ft ³ - m ³):	224 - 6.343
Total peaking factor:	1.15

Steam generator (SG) data (BU - SI):

Number of steam generators:	2
Number of tubes per SG:	8485
Tube inside diameter (in - cm):	0.654 - 1.66

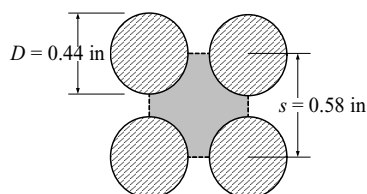
Tube outside diameter (in - cm):	0.750 - 1.905
Volume of the SG inlet plenum (ft^3 - m^3):	250 - 7.079
Volume of the SG outlet plenum (ft^3 - m^3):	250 - 7.079
Inlet plenum hydraulic diameter (ft - m):	7.6 - 2.316
Outlet plenum hydraulic diameter (ft - m):	7.6 - 2.316
Steam dome pressure (psia - MPa):	880 - 6.067
Feedwater pressure (psia - MPa):	1095 - 7.5
Feedwater temperature (F - C):	440 - 227
Tube material:	Stainless steel
Boiling heat transfer coefficient ($\text{Btu/h}\cdot\text{ft}^2\cdot\text{F}$ - $\text{W/m}^2\cdot\text{K}$):	6400 - 36340

Pressurizer data (BU - SI):

Geometry:	Circular cylinder
Steam dome Pressure (psia - MPa):	2250 - 15.51
Volume (ft^3 - m^3):	1500 - 42.477
Height (ft - m):	30 - 9.15
Water level (ft - m):	18 - 5.486
Wall thickness (in - cm):	4.5 - 11.43
Insulation thickness (in - cm):	0.00
Wall material:	Carbon Steel
Number of Relief Valves:	2
Relief valve flow area (ft^2 - cm^2):	0.01 - 0.01
Relief valve discharge coefficient	0.61
Ambient temperature (F - C):	90 - 32
Ambient pressure (psia - kPa):	14.7 - 101.35

Balance of plant data (BU - SI):

Total pumping power (condensate, booster, heater, and feedwater) (MW):	190
Condenser Pressure (in Hg - mm Hg):	26 - 660
Circulating water inlet temperature (F - C):	60
Circulating water flow rate (lbm/h - kg/s):	5.2E8 - 65,520



Find the answer to the following questions:

1. The centerline temperature in an average fuel rod
2. The centerline temperature in the fuel rod located in the hot assembly

3. Total power developed by the turbine (MW). Assume $\eta_{turbine} = 100\%$
4. The core total ΔP due to skin friction and the core total loss coefficient ($K = \sum K_i$)
5. The overall heat transfer coefficient in SG (a: assume feedwater is saturated, b: fouling = 0)
6. The average tube length of one SG (for questions 5 and 6 use Equations VIa.1.1 and VIa.2.12)
7. Pressure drop across the primary side of the SG (i.e., from the hot leg inlet to the outlet to cold leg)
8. The ΔP across the reactor coolant pump and the total power used by a reactor coolant pump
9. The temperature rise of the circulating water
10. We open one of the pressurizer relief valves. Find the maximum flow rate through the valve if one of the pressurizer relief valves is lifted.
11. Find the steam mass flow rate through the relief valve and the pressurizer pressure versus time if the relief valve is stuck open for one minute. Assume that the pressurizer is isolated from the rest of the reactor.

VII. Engineering Mathematics

The purpose of this chapter is to discuss the commonly used mathematical concepts and formulae in mathematical physics and engineering applications. This includes such topics as differential equations, mathematical functions, vector and matrix operations, and numerical analysis. Many of these topics are applied in various chapters of this book.

VIIa. Fundamentals

This chapter deals exclusively with the definitions of terminologies pertinent to engineering mathematics.

1. Definition of Terms

Independent variable is a quantity that may be equal to any one of a specified set of values.

Dependent variables are variables that denote values of a function. A function is a relationship between two variables such that each value of the independent variable corresponds exactly to one value of the dependent variable. For example, x in equation $dy/dx + e^x y = \sin x$ is the independent variable and y is the function or the dependent variable.

Domain includes the collection of all values assumed by the independent variable.

Range is the collection of all values assumed by the dependent variable. For example, the domain and range of the function $y = \sqrt{x-1}$ is determined as follows. Since the radical should be positive for y to be defined, then the domain of x is $1 \leq x < \infty$ and the range of y is $0 \leq y < \infty$.

Coordinate systems. As described in Section 1 of Chapter VIIc.

Explicit and implicit functions. A dependent variable is an explicit function of an independent variable if the function can be expressed in terms of the independent variable. For example, $y = 2x + \sin x + \ln x$ is an explicit function of x and the y in $\sqrt{y} + y \sin x + xy^5 - 1 = 0$ is an implicit function of x .

Continuous function. A function in the interval (a, b) is continuous if for any positive number ε there is a positive number δ so that when $x_0 - \delta < x < x_0 + \delta$ we have $|f(x) - f(x_0)| < \varepsilon$. For example, $f(x)$ in Figure VIIa.1.1 is not continuous at x_0 because for $h_2 - h_1 < \varepsilon$ there is no δ to satisfy the condition for continuity.

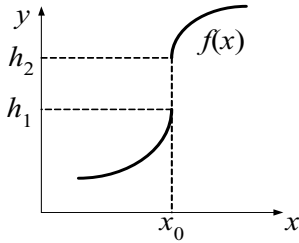


Figure VIIa.1.1. Example of a discontinuous function

Periodic functions. Function $f(x)$ is considered periodic if for any fixed number such as P , we could have the following relation $f(x + P) = f(x)$. If P is the smallest number for which the periodic condition exists, then x is called the *period* of the function.

Harmonic function. A harmonic function is a solution to the Laplace partial differential equation (defined in Section 2.2) which has continuous second-order partial derivatives.

Homogeneous function. A function $f(x, y)$ is considered to be homogeneous of degree n if for any number s and constant n , we have $f(sx, sy) = s^n f(x, y)$. For example, $x^3 + xy^2$ is homogeneous of degree 3 because $(sx)(sx)(sx) + (sx)(sy)(sy) = s^3(x^3 + xy^2)$ but $x^3 + y$ is not homogeneous.

Power series is defined as

$$\lim_{N \rightarrow \infty} \left[\sum_{i=0}^N C_i (x - x_0)^i \right]$$

for those values of x where the limit exists. For such values of x , the series is said to converge. An important aspect of a power series is that convergent power series can be treated as polynomials. We now consider function $f(x)$ which, along with all its derivatives, is continuous in an interval including $x = x_0$. This function can be expressed as a finite Taylor series plus a residual as follows:

$$f(x) = \left[\sum_{i=0}^{N-1} \frac{1}{i!} \frac{d^i f(x_0)}{dx^i} (x - x_0)^i \right] + \left[\frac{1}{N!} \frac{d^N f(\eta)}{dx^N} (x - x_0)^N \right]$$

where η is a point in the interval (x_0, x) . If $x_0 = 0$, the Taylor series becomes a Maclaurin series:

$$f(x) = \left[\sum_{i=0}^{N-1} \frac{1}{i!} \frac{d^i f(0)}{dx^i} x^i \right] + \left[\frac{1}{N!} \frac{d^N f(\eta)}{dx^N} x^N \right]$$

Differential equation is an equation that relates two or more dependent variables in terms of derivatives. Formulating the behavior of many physical phenomena by a mathematical model results in differential equations as discussed in Section 2.

Ordinary differential equation is a differential equation in which all derivatives are taken with respect to a single independent variable. For example, the differential equation $d^2y/dx^2 + f(x)dy/dx + g(x)y = h(x)$ is an ordinary differential equation.

Partial differential equation is a differential equation that contains at least one partial derivative with respect to some dependent variable. For example, the differential equation:

$$\frac{\partial^2 T}{\partial x^2} + \frac{\partial^2 T}{\partial y^2} + \frac{\partial^2 T}{\partial z^2} = \nabla^2 T = 0 \quad \text{VIIa.1.1}$$

(known as Laplace equation) is a partial differential equation. In Equation VIIa.1.1, ∇^2 is the Laplacian operator, as discussed in Chapter VIIc.

Exact differential is a first-order differential equation in the form of $M(x, y)dx + N(x, y)dy = 0$ (also called perfect differential) if and only if a function $f(x, y)$ exists so that $df(x, y) = M(x, y)dx + N(x, y)dy$. For exact differential equations $df(x, y) = 0$. Hence, $f(x, y) = C$. If such a function exists, $M(x, y)dx + N(x, y)dy$ is also called an exact differential. The necessary and sufficient condition for an expression to be an exact differential is that

$$\frac{\partial M(x, y)}{\partial y} = \frac{\partial N(x, y)}{\partial x}$$

Order of a differential equation is the highest order derivative in the differential equation. For example,

$$\frac{d^3 y}{dx^3} + y^4 \frac{d^2 y}{dx^2} + P(x) \frac{dy}{dx} + x^6 y^5 = Q(x)$$

is a differential equation of order three.

Degree of a differential equation is the power of the highest order derivative. For example, the following differential equation:

$$\left(\frac{d^4 y}{dx^4} \right)^3 + 4 \left(\frac{dy}{dx} \right)^4 = f(x)$$

is of order four and degree three.

Linear differential equations are those in which no dependent variable appears in the form of a product by itself or any of its derivatives. For example, Equation VII.a.1.1 is a linear differential equations while the following differential equation:

$$y \frac{d^2 y}{dx^2} + f(x) \frac{dy}{dx} + g(x)y = h(x)$$

is a nonlinear differential equation due to the first term in the left side, which includes the product of the dependent variable y and its derivative.

Homogeneous differential equation is a linear equation when all its terms include either the dependent function or one of its derivatives. Hence, the following is a homogeneous differential equation:

$$c_0 \frac{d^n y}{dx^n} + c_1 \frac{d^{n-1} y}{dx^{n-1}} + \dots + c_{n-1} \frac{dy}{dx} + c_n y = 0$$

Non-homogeneous differential equations are equations that include a term that is a function of only the independent variable. Therefore, the following is a non-homogeneous differential equation:

$$c_0 \frac{d^n y}{dx^n} + c_1 \frac{d^{n-1} y}{dx^{n-1}} + \dots + c_{n-1} \frac{dy}{dx} + c_n y = q(x) \quad \text{VIIa.1.2}$$

for $q(x) \neq 0$. However, if $q(x) = 0$ then Equation VIIa.1.2 becomes a *homogeneous differential equation*.

Homogeneous boundary condition is a boundary condition when the dependent variable or its derivatives, or any linear combination of the dependent variable and its derivatives, vanishes at the boundary. For example, if at $x = a$, $y(a) = 0$, then the boundary condition at $x = a$ is a *homogeneous boundary condition*. Similarly, boundary conditions $y'(a) = 0$ and $c_1 y(a) + c_2 y'(a) = 0$ are also homogeneous boundary conditions whereas, boundary conditions $y(a) = b$, or $c_1 y(a) + c_2 y'(a) = b$ are *nonhomogeneous boundary conditions*.

Trivial solution is any homogeneous differential equation subject to homogeneous boundary conditions that always has a solution in the form of $y(x) = 0$. This solution, referred to as the trivial solution, is usually of no interest.

General or homogeneous solution to a differential equation is a non-trivial function for the dependent variable that satisfies the homogeneous differential equation. For example, the general solution to $dy/dx = 2$ should satisfy $dy/dx = 0$. The general solution is, therefore, $y = C$. This is also shown as $y_H = C$. General solutions to various differential equations are discussed in Section 3.

Particular solution to a differential equation is a solution that satisfies the non-homogeneous equation. For example, a particular solution to $dy/dx = 2$ is $y_P = 2x$. Finding particular solutions relies on the type of the function $q(x)$, in Equa-

tion VIIa.1.2. For example, $q(x)$ may be of an algebraic, trigonometric, or exponential function:

$$q(x): 1, x, x^2, \dots x^n$$

$$q(x): \sin ax, \cos ax$$

$$q(x): e^{ax}$$

or a combination of all the above functions.

Complete solution to a differential equation is the summation of the homogeneous and the particular solutions. For example, the general solution to $dy/dx = 2$ is $y = y_H + y_P = 2x + C$. Since the solution must also satisfy the boundary or initial conditions, the value of the constants of integration should be obtained from the specified boundary or initial conditions (when x represents time).

Initial-value problems are differential equations that require particular solutions so that the function and its derivatives all satisfy a specified set of conditions corresponding to the same value of the independent variable. For example, the general solution to an n th-order linear differential equation has n arbitrary constants. These constants should be determined from n specified sets of conditions. In initial-value problems, these specified sets of conditions require that $y(x_0) = a$, $y'(x_0) = b$, $y''(x_0) = c$, etc. where a, b, c, \dots are specified constants. The differential equation of displacement of mass in a spring – dashpot system is an initial value problem where initial conditions at a specified time are used to determine constants of integration.

Boundary-value problems are differential equations that require particular solutions so that the function and its derivatives satisfy a specified set of conditions. In boundary-value problems, the several values of the function or its derivatives are not all known at the same independent variable, rather at different values of the independent variable. For example, the general solution to an n th-order linear differential equation has n arbitrary constants. These constants can be determined from n specified sets of conditions at point $x = a_1$ through point $x = a_n$. Certain classes of boundary-value problems fall in the category of the *characteristic-value* or *eigenvalue* problems as discussed later. Determination of the deflection of a simply supported beam, thermal conduction, and wave equation are examples of boundary-value problems.

Total differential of a function of several variables, such as $f(x, y, z)$, is defined as:

$$df = \frac{\partial f}{\partial x} dx + \frac{\partial f}{\partial y} dy + \frac{\partial f}{\partial z} dz$$

provided that the partial derivatives are continuous. In general, the variables x, y , and z can themselves be functions of the independent variables s and t . In this case, the variables x, y , and z are referred to as the intermediate variables and the partial derivative of f with respect to s becomes:

$$\left(\frac{\partial f}{\partial s}\right)_t = \frac{\partial f}{\partial x} \left(\frac{\partial x}{\partial s}\right)_t + \frac{\partial f}{\partial y} \left(\frac{\partial y}{\partial s}\right)_t + \frac{\partial f}{\partial z} \left(\frac{\partial z}{\partial s}\right)_t$$

where the subscript t implies that the derivatives are carried out with respect to s only. For example, for the function $f[x(t,s), y(t,s), z(t,s)] = xy + z^2x + y^2z$, we can carry the derivative of f with respect to s as:

$$\left(\frac{\partial f}{\partial s}\right)_t = \left(y \frac{\partial x}{\partial s} + x \frac{\partial y}{\partial s}\right) + (2xz \frac{\partial z}{\partial s} + z^2 \frac{\partial x}{\partial s}) + (2yz \frac{\partial y}{\partial s} + y^2 \frac{\partial z}{\partial s})$$

If the intermediate variables are given as $x = 2s$, $y = st$, and $z = t$, we can then find the partial derivative of f with respect to s as:

$$\left(\frac{\partial f}{\partial s}\right)_t = (2y + xt) + (2z^2) + (2yzt)$$

This equation can be further simplified if the intermediate variables are substituted in terms of independent variables.

Chain rule for derivatives follows the total differential defined above. Consider a composite function such as $F = f[s, U(s)]$. According to the chain rule for taking the derivative of composite functions, dF/ds is:

$$\frac{dF}{ds} = \frac{\partial F}{\partial s} + \frac{\partial F}{\partial U} \frac{\partial U}{\partial s}$$

Linear dependence of n functions is given by $c_1 f_1(x) + c_2 f_2(x) + \dots + c_n f_n(x)$. If at least one constant coefficient (c_i) is nonzero then the linear dependence is nontrivial. These functions are linearly independent in the domain ab (i.e., $a \leq x \leq b$) if, over the domain, no function is linearly dependent on the other functions. For example, x , $\sin x$ and xy are linearly independent over any domain while $\sin^2 x$, $\cos^2 x$, and -1 are linearly dependent over any domain.

Wronskian determinant of n functions, f_1 through f_n , is defined as:

$$W(f_1, f_2, \dots, f_n) = \begin{vmatrix} f_1 & f_2 & \dots & f_n \\ \frac{\partial f_1}{\partial x} & \frac{\partial f_2}{\partial x} & \dots & \frac{\partial f_n}{\partial x} \\ \vdots & \vdots & \ddots & \vdots \\ \frac{\partial^{n-1} f_1}{\partial x^{n-1}} & \frac{\partial^{n-1} f_2}{\partial x^{n-1}} & \dots & \frac{\partial^{n-1} f_n}{\partial x^{n-1}} \end{vmatrix}$$

For function f_1 through f_n to be linearly independent over a specific domain, it is necessary that the Wronskian determinant is not equal zero over that domain. However, if the Wronskian determinant vanishes in a specific domain, it does not necessarily mean that the related functions are linearly dependent.

Eigenvalue or characteristic-value problems are special cases of the boundary-value problems having particular solutions in periodic forms. Problems dealing with classical wave equation, quantum mechanics, elasticity, and vibration are characteristic-value problems. To elaborate the characteristic-value problems, consider the following differential equation:

$$\frac{d^2 y}{dx^2} + y = 0 \quad \text{VIIa.1.3}$$

which is subject to homogeneous boundary conditions $y(0) = 0$ and $y(L) = 0$. This equation has a solution in the form of:

$$y = c_1 \sin x + c_2 \cos x$$

From the first boundary condition, $c_2 = 0$. From the second boundary condition $c_1 = 0$. We, therefore, find $y = 0$ which is a trivial solution. Now consider the following differential equation:

$$\frac{d^2 y}{dx^2} + \lambda^2 y = 0 \quad \text{VIIa.1.4}$$

subject to the same boundary conditions. The solution to this equation is $y = c_1 \sin \lambda x + c_2 \cos \lambda x$. From the first boundary condition, $c_2 = 0$. From the second boundary condition $\lambda_n = n\pi/L$ where $n = 1, 2, 3, 4, \dots$ and the solution to the differential equation becomes $y_n = c_n \phi_n$ where $\phi_n = \sin(n\pi x/L)$. Hence:

$$y_n = c_n \phi_n = c_n \sin \frac{n\pi}{L} x \quad \text{VIIa.1.5}$$

Comparing these two differential equations and related solutions, we conclude that in the case of Equation VIIa.1.4, the second boundary condition was actually used to determine the parameter λ . The reason we were able to obtain a nontrivial solution for Equation VIIa.1.4 is that certain values of λ_n , as given by $n\pi/L$, cause the determinant of the coefficients to vanish. Equation VIIa.1.4 is a characteristic-value equation. Values obtained for λ_n are called characteristic or eigenvalues and the corresponding solutions (ϕ_n) are called the characteristic or eigenfunctions.

In problems dealing with mechanical vibration, the eigenvalues give the natural frequency of the system. The knowledge of natural frequencies of a load bearing system is essential. To avoid failure, external loads should not be applied at or near these frequencies as resonance will cause an amplification of displacement, leading to failure. An interesting aspect of the characteristic value equations is the fact that we now have to determine many more unknown coefficients (i.e., $c_1, c_2, c_3, c_4, \dots$), yet no more boundary conditions are left. In the next definition, we'll see how we can use the orthogonality aspect of the eigenfunctions to our advantage.

Orthogonality of characteristic functions is where the scalar product of two vectors is zero, as discussed in Section 5. Having this in mind, we now consider two functions, $y_m(x)$ and $y_n(x)$ and a weighting function, $r(x)$. These functions are orthogonal in the interval (a, b) , with respect to the weighting function $r(x)$, if the integral of their product over the given interval vanishes:

$$\int_a^b r(x)\varphi_m(x)\varphi_n(x)dx = 0$$

The characteristic functions are orthogonal. To verify, we may use the above example by assuming $r(x) = 1$:

$$\int_0^L \sin \frac{m\pi x}{L} \sin \frac{n\pi x}{L} dx = 0$$

An important aspect of the orthogonal functions is the ability to expand arbitrary functions in terms of orthogonal functions. If a set of functions such as φ_n are orthogonal in the interval (a, b) with respect to the weighting function $r(x)$, then an arbitrary function $f(x)$ can be expanded in terms of these functions as:

$$f(x) = c_0\varphi_0(x) + c_1\varphi_1(x) + c_2\varphi_2(x) + \cdots = \sum_{n=0}^{\infty} c_n\varphi_n(x)$$

If such expansion exists, then we may multiply both sides by the following functions and integrate over the above interval to get:

$$\int_a^b r(x)f(x)\varphi_k(x)dx = \sum_{n=0}^{\infty} c_n \int_a^b r(x)\varphi_k(x)\varphi_n(x)dx \quad \text{VIIa.1.6}$$

Using the orthogonality property of the eigenfunctions, the integral on the left side becomes zero except for $k = n$. Therefore, Equation VIIa.1.6 reduces to:

$$\int_a^b r(x)f(x)\varphi_n(x)dx = c_n \int_a^b r(x)[\varphi_n(x)]^2 dx$$

From here we can find the unknown coefficients $c_1, c_2, c_3, c_4, \dots$. For the characteristic equation of a matrix see Chapter VIId.

Fourier transform. It can be shown that any reasonably well-behaved function, $f(x)$ can be represented in the interval $-L, L$ by a series of trigonometric functions such as *sines* or *cosines*. Indeed it can be shown that any piecewise differentiable function in the interval $-L, L$ can be represented by both sine and cosine functions of a common period $2L$, i.e.:

$$f(x) = A_0 + \sum_{n=0}^{\infty} \left(A_n \cos \frac{n\pi x}{L} + B_n \sin \frac{n\pi x}{L} \right) \quad -L < x < L$$

where the coefficients are given as:

$$A_0 = \frac{1}{2L} \int_{-L}^L f(x) dx$$

$$A_n = \frac{1}{L} \int_{-L}^L f(x) \cos \frac{n\pi x}{L} dx$$

$$B_n = \frac{1}{L} \int_{-L}^L f(x) \sin \frac{n\pi x}{L} dx$$

Laplace transform is a mathematical conversion to simplify operations. To convert a function such as $f(t)$ by this means, we multiply the function by $\exp(-st)$ and take the integral from zero to infinity:

$$\ell\{f(t)\} = \int_0^\infty f(t) e^{-st} dt$$

The advantage of this type of conversion is that exponential and trigonometric functions are transformed into simple algebraic functions. This simplifies the integration task. For example, the reader may verify that

$$\ell\{\sin at\} = \int_0^\infty \sin(ate^{-st}) dt = \frac{a}{a^2 + s^2} \quad \text{and} \quad \ell\{\cos at\} = \int_0^\infty \cos(ate^{-st}) dt = \frac{s}{a^2 + s^2}$$

It is important to note that the conversion of a function by Laplace transform is a *linear* conversion. Therefore, we conclude that:

$$\ell\{af_1(t) + bf_2(t)\} = a\ell\{f_1(t)\} + b\ell\{f_2(t)\}$$

$$\ell\left\{\frac{d^n f(t)}{dt^n}\right\} = s^n \ell\{f(t)\} - \left[s^{n-1} f(0) + s^{n-2} \frac{df(0)}{dt} + \dots + \frac{d^{n-1} f(0)}{dt^{n-1}}\right] \quad \text{VIIa.1.7}$$

$$\ell\{f[u(t)]\} = \frac{1}{s} \ell\{f(t)\}$$

$$\ell\{e^{at} f(t)\} = \ell\{f(t-a)\}$$

$$\ell\{t^n f(t)\} = (-1)^n \frac{d^n [\ell\{f(t)\}]}{ds^n}$$

$$\ell\left\{\int_0^\infty f_1(t-u) f_2(u) du\right\} = \ell\{f_1(t)\} \ell\{f_2(t)\}$$

$$\ell\left\{\int_a^b f(t)dt\right\} = \frac{1}{s} \ell\{f(t)\} + \frac{1}{s} \int_a^0 f(t)dt$$

In this text, the Laplace transform of a function is shown as $\ell\{f(t)\} = \hat{f}$. The Laplace transforms of some exponential and trigonometric functions are presented in Table VIIa.1.1

Table VIIa.1.1. Laplace transforms of some familiar functions

Function, $f(t)$	Transform, \hat{f}
1	$1/s$
t	$1/s^2$
$t^{n-1}/(n-1)!$	$1/s^n$
e^{-at}	$1/(s+a)$
$t^{n-1}e^{-at}/(n-1)!$	$1/(s+a)^n$
$(e^{-bt} - e^{-at})/(a-b)$	$1/(s+a)(s+b)$
$(be^{-bt} - ae^{-at})/(b-a)$	$s/(s+a)(s+b)$
$\sin at$	$a/(s^2 + a^2)$
$\cos at$	$s/(s^2 + a^2)$
$\sinh at$	$a/(s^2 - a^2)$
$\cosh at$	$s/(s^2 - a^2)$
$t \sin at$	$2as/(s^2 + a^2)^2$
$t \cos at$	$(s^2 - a^2)/(s^2 + a^2)^2$
$\sin at - at \cos at$	$2a^3/(s^2 + a^2)^2$
$t \sinh at$	$2as/(s^2 - a^2)^2$
$t \cosh at$	$(s^2 + a^2)/(s^2 - a^2)^2$
$at \cosh at - \sinh at$	$2a^3/(s^2 - a^2)^2$
$e^{-bt} \sin at$	$a/[a^2 + (s+b)^2]$
$e^{-bt} \cos at$	$(s+b)/[a^2 + (s+b)^2]$
$\sin at \cosh at - \cos at \sinh at$	$4a^3/(s^4 + 4a^4)$
$\sin at \sinh at$	$2a^2s/(s^4 + 4a^4)$
$\sinh at - \sin at$	$2a^3/(s^4 - a^4)$
$\cosh at - \cos at$	$2a^2s/(s^4 - a^4)$
$\delta(t)$	1
$\delta(t - t_0)$	$\exp(-st_0)$
$\delta'(t)$	s
$\delta'(t - t_0)$	$s \exp(-st_0)$
t^n	$n!/s^{n+1}$
$t^{n-1}/(n-1)!$	$1/s^n$
$t^{n-1}e^{-at}/(n-1)!$	$1/(s+a)^n$
$[(n-1) - at] t^{n-2}e^{-at}/(n-1)!$	$s/(s+a)^n$

VIIb. Differential Equations

This chapter includes two types of differential equations used in most engineering applications and applied physics. These are the ordinary and the partial differential equations, ODE and PDE, respectively. We begin with the ordinary differential equations.

1. Famous Differential Equations

In this section several differential equations often used in engineering applications are discussed. Solutions to some ordinary differential equations are discussed in Section 2.

1.1. Ordinary Differential Equations

Bernoulli differential equation: The following equation is known as the Bernoulli differential equation:

$$\frac{dy}{dx} + P(x)y = Q(x)y^n \quad \text{VIIb.1.1}$$

where n may have any real value. Unless n is 0 or 1, the Bernoulli differential equation is non-linear. The Bernoulli differential equation appears in such fields as the study of population dynamics and hydrodynamic stability. The Bernoulli differential equation can be transformed into a linear differential equation by a change of dependent variable from y to $z = y^{1-n}$ to obtain:

$$\frac{dz}{dx} + (1-n)P(x)z = (1-n)Q(x)$$

resulting in a first-order linear differential equation, the solution of which is presented in Section 2 of this chapter.

Riccati differential equation: This is another first order non-linear differential equation named after Italian mathematician J. F. Riccati, and has the following form:

$$\frac{dy}{dx} + P(x)y^2 + Q(x)y = R(x) \quad \text{VIIb.1.2}$$

For $R(x) = 0$, Equation VIIb.1.2 becomes the Bernoulli differential equation ($n = 2$) with $z = 1/y$ transforming it to a first-order linear differential equation. If $u(x)$ is one solution to the Riccati differential equation, the substitution $y = u(x) + 1/z$ will transform the Riccati equation:

$$\frac{dz}{dx} - [uP(x) + Q(x)]z = 2P(x)$$

into a first-order linear differential equation. Since there is no general rule to solve non-linear differential equations analytically, a change of variable, as demonstrated for Bernoulli and Riccati differential equations, is an effective means of solving such classes of non-linear equations.

Euler-Cauchy differential equation: This is a linear, non-homogeneous differential equation with coefficients being functions of the independent variable. Euler-Cauchy equation has the form of:

$$c_0 x^n \frac{d^n y}{dx^n} + c_1 x^{n-1} \frac{d^{n-1} y}{dx^{n-1}} + \dots + c_{n-1} x \frac{dy}{dx} + c_n y = q(x) \quad \text{VIIb.1.3}$$

This equation can be transformed into an n th-order linear differential equation by a change of the independent variable from x to $z = \ln|x|$. The solution to Equation VIIb.1.3 is presented in Section 2.

Special Class of Differential Equations

Famous differential equations used in many engineering applications can be derived from ordinary second-order differential equations written in the general form of:

$$(1 + R_M x^M) \frac{d^2 y}{dx^2} + \frac{1}{x} (P_0 + P_M x^M) \frac{dy}{dx} + \frac{1}{x^2} (Q_0 + Q_M x^M) y = 0 \quad \text{VIIb.1.4}$$

Some examples are as follows.

Jacobi differential equation is given as:

$$x(1-x) \frac{d^2 y}{dx^2} + [a - (1+bx)] \frac{dy}{dx} + n(b+n)y = 0 \quad \text{VIIb.1.5}$$

The solution to the Jacobi differential equation is the Jacobi polynomial as discussed in Section 4. A special case of the Jacobi equation is:

$$(1-x^2) \frac{d^2 y}{dx^2} - cx \frac{dy}{dx} + n(n+c-1)y = 0$$

Chebyshev differential equation is obtained from the special form of the Jacobi equation if $c = 1$:

$$(1-x^2) \frac{d^2 y}{dx^2} - x \frac{dy}{dx} + n^2 y = 0 \quad \text{VIIb.1.6}$$

The solution to this equation is known as Chebyshev's polynomials.

Laguerre differential equation is a second-order linear differential equation given as:

$$x \frac{d^2 y}{dx^2} + (1-x) \frac{dy}{dx} + 2ny = 0 \quad \text{VIIb.1.7}$$

The solution to the Laguerre differential equation is known as the Laguerre polynomials.

Gauss differential equation is given as:

$$x(1-x) \frac{d^2 y}{dx^2} + [\gamma - (\alpha + \beta + 1)x] \frac{dy}{dx} - \alpha\beta y = 0 \quad \text{VIIb.1.8}$$

Hermite differential equation is a second-order linear differential equation given as:

$$x \frac{d^2 y}{dx^2} - 2x \frac{dy}{dx} + 2ny = 0 \quad \text{VIIb.1.9}$$

The solution to the Hermite Differential equation is known as the Hermite polynomials. One of the applications of the Hermite differential equation is in the investigation of the Schrodinger equation for a harmonic oscillator. Solution to the Hermit equation is discussed in Section 2.

Legendre differential equation is developed by applying the technique of the separation of variables in the spherical coordinate system to the Laplace differential equation, which results in Legendre differential equation:

$$(1-x^2) \frac{d^2 y}{dx^2} - 2x \frac{dy}{dx} + n(n+1)y = 0 \quad \text{VIIb.1.10-1}$$

The solution to this second-order linear differential equation is known as Legendre polynomials. An important application of the Legendre polynomials is that any polynomial of degree n can be expressed as a linear combination of the first $n+1$ Legendre polynomials.

Associated Legendre differential equation is similar to Equation VIIb.1.10-1 except for the coefficient of y , as follows:

$$(1-x^2) \frac{d^2 y}{dx^2} - 2x \frac{dy}{dx} + \left(n(n+1) - \frac{m^2}{1-x^2} \right) y = 0 \quad \text{VIIb.1.10-2}$$

Sturm-Liouville problem is any boundary value problem that is described by a differential equation in the form of:

$$\frac{d}{dx} \left(p(x) \frac{dy}{dx} \right) + [q(x) + \lambda r(x)] y = 0 \quad \text{VIIb.1.11}$$

and has two homogeneous boundary conditions, is known as a Sturm-Liouville problem. We can reduce the Legendre differential equation, Equation VIIb.1.10 from the Sturm-Liouville problem. To demonstrate, we first write the Legendre differential equation as:

$$\frac{d}{dx} \left[(1-x^2) \frac{dy}{dx} \right] + n(n+1)y = 0 \quad \text{VIIb.1.12}$$

Comparing Equation VIIb.1.11 with Equation VIIb.1.12, we conclude that $p(x) = 1-x^2$, $q(x) = 0$, $r(x) = 1$, $\lambda = n(n+1)$. Therefore, the Legendre differential equation is a special case of a Sturm-Liouville problem. The Sturm-Liouville problem possesses the orthogonality property associated with boundary-value differential equations. Hence, the nontrivial solutions y_1, y_2, y_3, \dots corresponding to distinct values $\lambda_1, \lambda_2, \lambda_3, \dots$ of parameter λ form an orthogonal system with respect to the weighting function, $p(x)$.

Bessel differential equation, widely used in various engineering disciplines, is a second-order linear differential equation and has the general form of:

$$x \frac{d}{dx} \left[x \frac{dy}{dx} \right] + (m^2 x^2 - \nu^2)y = 0 \quad \text{VIIb.1.13}$$

where m is a parameter and ν can be an integer, a fractional number, or zero. Bessel differential equations appear in such fields as neutron flux distribution in a cylindrical core, and heat transfer in fins with a triangular profile, as well as elasticity, electric field theory, and aerodynamics. The solution to the Bessel differential equation is given by:

$$y(x) = c_1 J_\nu(x) + c_2 Y_\nu(x) \quad \text{VIIb.1.14}$$

where $J_\nu(x)$ is the Bessel function of the first kind of order ν and $Y_\nu(x)$ is the Bessel function of the second kind of order ν . These functions are given as:

$$J_\nu(mx) = \sum_{k=0}^{\infty} (-1)^k \frac{(mx/2)^{2k+\nu}}{k! \Gamma(k+\nu+1)} \quad \text{VIIb.1.15}$$

$$Y_\nu(mx) = \frac{\cos(\nu\pi) J_\nu(mx) - J_{-\nu}(mx)}{\sin(\nu\pi)} \quad \text{VIIb.1.16}$$

where $J_{-\nu}(mx)$ is given by:

$$J_{-\nu}(mx) = \sum_{k=0}^{\infty} (-1)^k \frac{(mx/2)^{2k-\nu}}{k! \Gamma(k-\nu+1)} \quad \text{VIIb.1.17}$$

where $k!$ is the factorial of k and Γ is the gamma function as described in Section 3.

Modified Bessel equation: If in Equation VIIb.1.13, we replace x by ix where $i = \sqrt{-1}$, we get the modified Bessel equation as:

$$x \frac{d}{dx} \left[x \frac{dy}{dx} \right] - (m^2 x^2 + \nu^2) y = 0 \quad \text{VIIb.1.18}$$

The solution to the modified Bessel equation is given as:

$$y(x) = c_1 I_\nu(mx) + c_2 K_\nu(mx) \quad \text{VIIb.1.19}$$

where $I_\nu(x)$ is the modified Bessel function of the first kind of order ν and $K_\nu(x)$ is the modified Bessel function of second kind of order ν . where

$$I_\nu(mx) = \sum_{k=0}^{\infty} \frac{(mx/2)^{2k+\nu}}{k! \Gamma(k+\nu+1)} \quad \text{VIIb.1.20}$$

and

$$K_\nu(mx) = \frac{\pi}{2} \frac{I_{-\nu}(mx) - I_\nu(mx)}{\sin(\nu\pi)} \quad \text{VIIb.1.21}$$

where $I_{-\nu}(mx)$ is given by:

$$I_{-\nu}(mx) = \sum_{k=0}^{\infty} \frac{(mx/2)^{2k-\nu}}{k! \Gamma(k-\nu+1)} \quad \text{VIIb.1.22}$$

Bessel Type 1 differential equations: It can be shown that equations of the general form:

$$x^2 \frac{d^2 y}{dx^2} + ax \frac{dy}{dx} + b^2 x^2 y = 0 \quad \text{VIIb.1.23}$$

can be expressed in terms of Bessel functions by a change of function from y to $y = x^\nu z$ to get:

$$x \frac{d}{dx} \left(x \frac{dz}{dx} \right) + (b^2 x^2 - \nu^2) z = 0 \quad \text{VIIb.1.24}$$

Bessel Type 2 differential equations: Consider second order linear differential equations in the form of:

$$\frac{d}{dx} \left(x^\alpha \frac{dy}{dx} \right) + \eta^2 x^\beta y = 0 \quad \text{VIIb.1.25}$$

where α and β are positive and η may be real or imaginary. Similar to Bessel Type 1 equations, it can be shown that differential equations in the general form of Equation VIIb.1.25 can also be reduced to a Bessel differential equation by a change of variable from x to $x = t^\mu$ to get:

$$t^2 \frac{d^2 y}{dx^2} + t[\mu(\alpha - 1) + 1] \frac{dy}{dx} + \eta^2 \mu^2 t^2 y = 0$$

This equation has the form of Equation VIIb.1.23. Hence, the answer can be written as $y = x^{v/\mu} Z_v(\eta \mu x^{1/\mu})$ where $v = (1 - \alpha)/(\beta - \alpha + 2)$ and $\mu = 2v/(1 - \alpha)$.

The reader can verify that the Euler-Cauchy equation can also be reduced from Equation VIIb.1.25 if we have $\alpha - \beta = 2$ to obtain:

$$x^2 \frac{d^2 y}{dx^2} + \alpha x \frac{dy}{dx} + \eta^2 y = 0$$

We can solve this equation by introducing a change of variable from x to x^r .

1.2. Partial Differential Equations

Many linear partial differential equations representing physical phenomena can be reduced from:

$$\nabla^2 \psi = \lambda \frac{\partial^2 \psi}{\partial t^2} + \mu \frac{\partial \psi}{\partial t} + f(r) \quad \text{VIIb.1.26}$$

where the unknown function, ψ is, in general, a function of position and time (i.e., $\psi = f(r, t)$). Coefficients μ and λ are some physical parameters and function f is generally a function of position.

Laplace differential equation is the steady-state homogeneous form of Equation VIIb.1.26. This equation is used to describe several physical phenomena such as flow of fluids and flow of heat. The equation in the Cartesian coordinate system is written as:

$$\nabla^2 u = \frac{\partial^2 u}{\partial x^2} + \frac{\partial^2 u}{\partial y^2} + \frac{\partial^2 u}{\partial z^2} = 0 \quad \text{VIIb.1.27}$$

This is a 2nd-order linear partial differential equation with coefficients μ and λ as well as function f in Equation VIIb.1.26 being zero. The derivation of this equation for fluid flow is shown in Chapter IIIa.

Poisson equation is given as:

$$\nabla^2 \psi = f(r) \quad \text{VIIb.1.28}$$

It describes several physical phenomena. For example, it is the governing equation in potential flow, describing the velocity potential of an incompressible, irrotational, ideal fluid with a continuously distributed sink or source. The Poisson equation also describes the steady-state temperature distribution in a field with distributed heat sources. It also describes stress due to elastic torsion of bars.

Heat conduction equation, in general form, may be written as:

$$\nabla^2 \psi = \mu \frac{\partial \psi}{\partial t} + f(r) \quad \text{VIIb.1.29}$$

This equation describes the diffusion phenomenon. If used to determine temperature distribution due to heat diffusion, it is called the conduction equation, in which case $\mu = 1/\alpha$ where α is thermal diffusivity. If Equation VIIb.1.29 is used as the heat conduction equation, then the function $f(r)$ is described as $f(r) = -\dot{q}'''(x, y, z)/k$ where \dot{q}''' is the volumetric heat generation rate and k is the thermal conductivity of the diffusing medium. The derivation of the heat conduction equation is shown in Chapter IVa.2.1.

Telephone equation is a one-dimensional equation describing the rate of change of electric voltage ψ along a transmission cable and is written as:

$$\frac{\partial^2 \psi}{\partial x^2} = \lambda \frac{\partial^2 \psi}{\partial t^2} + \mu \frac{\partial \psi}{\partial t} + \zeta \psi \quad \text{VIIb.1.30}$$

where $\lambda = LC$, $\mu = (RC + GL)$, and $\zeta = RG$. Here, R and L represent resistance and inductance per unit length of the cable. Also, C and G stand for the capacitance and conductance to ground per unit length of the cable.

Wave equation is given as:

$$\nabla^2 \psi = \lambda \frac{\partial^2 \psi}{\partial t^2} \quad \text{VIIb.1.31}$$

where $\lambda = 1/c^2$ and c is the velocity of sound. This equation is used in the fields of acoustics, elastic vibration, and electromagnetics. The solution to the unknown function ψ determines the velocity potential in acoustics, displacement in elastic vibration, and an electric or a magnetic vector in electromagnetism. Equation VIIb.1.31, in three dimensions, represents the equation for sound waves in air. In two dimensions it represents the wave equation for a membrane, and in one dimension it represents the transverse wave equation in a string. The latter case can be easily derived from Newton's second law of motion. To perform such a derivation, consider a small element of a uniform string having a linear density of ρ and being under tension T as shown in Figure VIIb.1.1. Net force in the y -direction must be set equal to the acceleration of the string. The net force in the vertical direction is given by:

$$dF_y = (T \sin \theta)_{x+dx} - (T \sin \theta)_x$$

We now expand the first term in the right side in the Taylor series and use the first two terms:

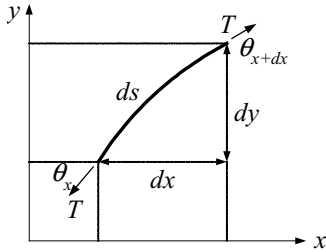


Figure VIIb.1.1. An elemental string in tension

$$dF_y = (T \sin \theta)_{x+dx} - (T \sin \theta)_x = \left[(T \sin \theta)_x + \frac{\partial(T \sin \theta)_x}{\partial x} dx \right] - (T \sin \theta)_x = \frac{\partial(T \sin \theta)_x}{\partial x} dx$$

From Newton's 2nd law ($dF = dm \frac{d^2 y}{dt^2}$):

$$\frac{\partial}{\partial x} \left(T \frac{\partial y}{\partial x} \right) = \rho \frac{\partial^2 y}{\partial t^2}$$

Since tension T is constant, it can be removed from the derivative. Also representing $T/\rho = b^2$ we obtain:

$$\frac{\partial^2 y}{\partial x^2} = \frac{1}{b^2} \frac{\partial^2 y}{\partial t^2} \quad \text{VIIb.1.31-1}$$

Note that b has the dimension of velocity. Having derived the one-dimensional wave equation, it is useful to briefly describe the fundamentals of mechanical waves. A wave is the motion of a disturbance in a medium. Wavelength (λ), frequency (ν), and the propagation velocity (b) are used to characterize waves.

Wavelength is the minimum distance between any two points on a wave that behave identically. Frequency is the rate at which the disturbance repeats itself. The wave amplitude is the maximum displacement of a particle disturbed by the wave. Waves are either transverse or longitudinal. In transverse waves, the motion of the particles of the medium is perpendicular to the wave velocity and in longitudinal waves, the motion of particles is parallel to the wave velocity. The propagation velocity (i.e., the velocity at which a wave travels) depends on the properties of the medium being disturbed. While waves generally require a medium to travel (referred to as mechanical waves), the electromagnetic waves such as photon travel in vacuum (i.e. require no medium).

Schroedinger wave equation in its general time-dependent form is given as:

$$-\frac{\hbar^2}{2m} \nabla^2 \psi(\vec{r}, t) + V(\vec{r}) \psi(\vec{r}, t) = i\hbar \frac{\partial \psi(\vec{r}, t)}{\partial t} \quad \text{VIIb.1.32}$$

where $i = \sqrt{-1}$, $\hbar = h/2\pi$, where Plank's constant $h = 6.626\text{E-}34$ J-s. In Equation VIIb.1.32, m is mass, V is potential energy, and r is the location vector. Potential energy in general is a function of location and time, $V = V(x, y, z, t)$ but most often only a function of location. Equation VIIb.1.32, as suggested by Erwin Schroedinger in 1926, has some similarities with Equation VIIb.1.31, the classic wave equation. However, unlike the wave equation derived above, the Schroedinger equation as a hypothesis, can only be verified and has no rigorous derivation. As such, Equation VIIb.1.32 is a statement similar to that of Newton's second law of motion, which has no proof. Furthermore, ψ in Equation VIIb.1.32 (referred to as the *wave function*) is not displacement. Rather; it is a measure of probability known as *probability amplitude* and the square of its absolute value is known as the *probability density* ($|\psi|^2$). By definition, $|\psi|^2 dx dy dz$ represents the probability that measurement of the particle's position at the time t finds the particle in the volume element dV about the point x, y , and z . Solution to the Schrödinger equation is given in Section 2.

2. Analytical Solutions to Differential Equations

Differential equations can be divided into two categories. The first category includes equations for which we can find analytical solutions. The second category includes equations for which, due to complications, we cannot find the analytical solutions and have to solve numerically. We start with the first category due to the importance of analytical solutions, then we deal with the second category.

2.1. Solution to First-Order Linear Ordinary Differential Equations

The general form of a first order linear differential equation is given as:

$$\frac{dy}{dx} + p(x)y = q(x) \quad \text{VIIb.2.1}$$

To seek an analytic solution in closed form, we note that if the equation was written as:

$$\frac{d}{dx}[F(x)y] = G(x) \quad \text{VIIb.2.2}$$

the solution could be readily found as:

$$y = \frac{1}{F(x)} \left[\int G(x) dx + C \right] \quad \text{VIIb.2.3}$$

where C is the constant of integration. To express the unknown functions $F(x)$ and $G(x)$ in terms of the specified functions $p(x)$ and $q(x)$, respectively, we carry out the differential on the left-hand side of Equation VIIb.2.2, and rearrange the results to get:

$$\frac{dy}{dx} + \left[\frac{1}{F(x)} \frac{dF(x)}{dx} \right] y = \frac{G(x)}{F(x)}$$

By comparing with the original equation, we find that:

$$\frac{1}{F(x)} \frac{dF(x)}{dx} = p(x)$$

Integrating this first order equation, the unknown function can be determined as $F(x) = e^{\int p(x) dx}$. Similarly, by comparing the right-hand sides, we find that:

$$\frac{G(x)}{F(x)} = q(x)$$

From here, the unknown function $G(x)$ can be determined as $G(x) = q(x)e^{\int p(x) dx}$. Substituting $F(x)$ and $G(x)$ in the solution (i.e. Equation VIIb.2.3) yields:

$$y = e^{-\int p(x) dx} \left\{ \int q(x) e^{\int p(x) dx} dx + C \right\} \quad \text{VIIb.2.4}$$

Example: Find the solution to the following equation, given $y = 1$ for $x = 1$:

$$x \frac{dy}{dx} + 2y = \sin x$$

We divide both sides by $x \neq 0$, to find $p(x) = 2/x$ and $q(x) = \sin x/x$. We first find:

$$\int p(x) dx = \int 2 \frac{dx}{x} = \ln x^2$$

We then find:

$$\int \frac{\sin x}{x} e^{\ln x^2} dx = \int x \sin x dx = \sin x - x \cos x$$

Substituting in Equation VIIb.2.4, we obtain:

$$y = e^{-\ln x^2} \{ \sin x - x \cos x + C \}$$

Applying the boundary condition, $C \cong 0.7$. Hence, $y = e^{-\ln x^2} \{ \sin x - x \cos x + 0.7 \}$

Special Case: In many engineering applications, both $p(x)$ and $q(x)$ are constant values, say P and Q . In this case, Equation VIIb.2.4 simplifies to:

$$y = Ce^{-Px} + \frac{Q}{P} \quad \text{VIIb.2.5}$$

The constant of integration can be found from a boundary condition. For example, if at $x = 0$, we have $y = y_0$, then $C = y_0 - Q/P$. The final solution for this special case becomes:

$$\frac{y - (Q/P)}{y_0 - (Q/P)} = e^{-Px} \quad \text{VIIb.2.6}$$

Example: Find the solution to the following first order equation where coefficients a and b are given constants. For the boundary condition, use $x = 0, y = a/b$.

$$\frac{dy}{dx} + ay = b$$

Solution: For this case, $P = a$, $Q = b$, and $y_0 = a/b$. Hence, from Equation VIIb.2.6, $y = (a/b - b/a)e^{-ax} + b/a$.

2.2. Solution to Higher Order Linear Ordinary Differential Equations

Solution to Linear Differential Equations with Constant Coefficients

Such equations have the general form of:

$$\frac{d^n y}{dx^n} + a_1 \frac{d^{n-1} y}{dx^{n-1}} + a_2 \frac{d^{n-2} y}{dx^{n-2}} + \cdots + a_{n-1} \frac{dy}{dx} + a_n y = q(x) \quad \text{VIIb.2.7}$$

where a_1 through a_n are constants. This linear non-homogeneous differential equation of order n is also written in the shorthand form of:

$$Dy = q(x) \quad \text{VIIb.2.8}$$

where D is a linear operator

$$D = \frac{d^n}{dx^n} + a_1 \frac{d^{n-1}}{dx^{n-1}} + a_2 \frac{d^{n-2}}{dx^{n-2}} + \cdots + a_{n-1} \frac{d}{dx} + a_n$$

We can verify that a solution in the form of $y = e^{rx}$ satisfies the homogeneous form of Equation VIIb.2.7 so that

$$Dy = (r^n + a_1 r^{n-1} + a_2 r^{n-2} + \cdots + a_{n-1} r + a_n) e^{rx} = 0 \quad \text{VIIb.2.9}$$

the solution to Equation VIIb.2.9 may yield real or complex values for r .

Real and distinct roots. The solution to the homogeneous Equation VIIb.2.9 becomes:

$$y_H = \sum_{i=1}^n c_i e^{r_i x}$$

For example, the solution to the differential equation

$$\frac{d^2y}{dx^2} - 3\frac{dy}{dx} + 2 = 0$$

has two distinct roots for $r^2 - 3r + 2 = 0$ namely, $r_1 = 1$ and $r_2 = 2$. Hence, the solution is $y = c_1e^x + c_2e^{2x}$.

Real but not distinct roots. Consider the case where the solution to Equation VIIb.2.9 yields real roots but roots (r_1) are repeated n -times where n is the degree of r in Equation VIIb.2.9. In such case, the solution is given by:

$$y = (c_1 + c_2x + c_3x^2 + \cdots + c_nx^{n-1})e^{r_1x}$$

For example, the linear differential operator for

$$\frac{d^3y}{dx^3} - 8\frac{d^2y}{dx^2} + 21\frac{dy}{dx} - 18 = 0$$

is $r^3 - 8r^2 + 21r - 18 = 0$ which yields $r_1 = 2$, $r_2 = 3$, and $r_3 = 3$. Hence, the solution to the differential equation becomes:

$$y = c_1e^{2x} + c_2e^{3x} + c_3xe^{3x}$$

As an another example, consider

$$\frac{d^4y}{dx^4} - 4\frac{d^3y}{dx^3} + 6\frac{d^2y}{dx^2} - 4\frac{dy}{dx} + 1 = 0$$

The linear operator is given by $r^4 - 4r^3 + 6r^2 - 4r + 1 = 0$. This equation yields 4-fold roots of $r_1 = 1$. Solution to the differential equation then becomes

$$y = (c_1 + c_2x + c_3x^2 + c_4x^3)e^x$$

Complex and distinct roots. If the solution to Equation VIIb.2.9 yields distinct complex roots such as $r_1 = a + ib$ and $r_2 = a - ib$, then the solution has the form of:

$$y = e^{ax}(c_1 \sin bx + c_2 \cos bx)$$

For example, the linear operator for

$$\frac{d^2y}{dx^2} - 4\frac{dy}{dx} + 5 = 0$$

is $r^2 - 4r + 5 = 0$, which has the roots of $r_1 = 2 + i$ and $r_2 = 2 - i$. Hence, the solution to the differential equation is found as:

$$y = e^{2x}(c_1 \sin x + c_2 \cos x)$$

Complex but not distinct roots. If the roots are complex and not distinct, then the solution becomes:

$$y = e^{ax} [(c_1 + c_2x + c_3x^2 + \cdots + c_nx^{n-1}) \sin bx + (c_{n+1} + c_{n+2}x + c_{n+3}x^2 + \cdots + c_{2n}x^{n-1}) \cos bx]$$

For example, the linear operator for

$$\frac{d^4y}{dx^4} + 2\frac{d^2y}{dx^2} + y = 0$$

is $r^4 + 2r^2 + 1 = 0$, which has two sets of identical roots $r_1 = r_2 = i$ and $r_3 = r_4 = -i$. The solution to the equation is:

$$y = (c_1 + c_2x) \sin x + (c_3 + c_4x) \cos x.$$

Solution to Equidimensional Linear Differential Equations

These are linear non-homogeneous differential equations with coefficients that are functions of the independent variable in the form of:

$$c_0x^n \frac{d^ny}{dx^n} + c_1x^{n-1} \frac{d^{n-1}y}{dx^{n-1}} + \cdots + c_{n-1}x \frac{dy}{dx} + c_ny = q(x) \quad \text{VIIb.2.10}$$

Such equations are known as Euler-Cauchy differential equations. This equation can be transformed into an n th-order linear differential equation, given by Equation VIIb.2.7, by change of independent variable from x to $z = \ln|x|$.

Solution to Differential Equations by Reduction of Order

This interesting method, as generally applied to second order linear differential equations, requires us to have one of the solutions to find the other solution. If we have one solution to the following general form of the second order differential equation as $y_1(x)$,

$$\frac{d^2y}{dx^2} + a_1(x) \frac{dy}{dx} + a_2(x)y = q(x) \quad \text{VIIb.2.11}$$

the second solution, as shown by Hildebrand, is then given by:

$$y_2(x) = \left[c_1 \int \frac{1}{zy_1^2(x)} dx + c_2 \right] y_1(x) \quad \text{VIIb.2.12}$$

where c_1 and c_2 are arbitrary constants and z is given by $z = e^{\int a_1(x) dx}$. One particular solution is obtained from:

$$y_P(x) = y_1(x) \int \frac{q(x)zy_1(x)dx}{zy_1^2(x)} dx \quad \text{VIIb.2.13}$$

No additional constants of integration are necessary for $y_2(x)$, since already arbitrary constant c_1 and c_2 are chosen. The complete solution is then given by:

$$y(x) = y_1(x) + y_2(x) + y_P(x) \quad \text{VIIb.2.14}$$

To ensure that the answers y_1 and y_2 are not linearly dependent, we should show that the Wronskian determinant is not zero. The Wronskian determinant is given by:

$$W(y_1, y_2) = c_1 e^{-\int a_1(x) dx}$$

As an example, let's try to solve the following differential equation by the method of reduction of order:

$$\frac{d^2 y}{dx^2} - 3 \frac{dy}{dx} + 2 = 0$$

Suppose the first answer is in the form of $y_1 = e^x$. We find the second answer by first calculating:

$$z = e^{\int a_1(x) dx} = e^{\int -3 dx} = e^{-3x}$$

then find y_2 from Equation VIIb.2.12:

$$y_2(x) = \left[c_1 \int \frac{1}{zy_1^2(x)} dx + c_2 \right] y_1(x) = e^x \left[c_1 \int e^x dx + c_2 \right] = c_1 e^{2x} + c_2 e^x$$

Note that $y_P(x) = 0$. Since c_1 and c_2 are arbitrary constants, the answer is therefore $y(x) = c_1 e^x + c_2 e^{2x}$.

Solution to Differential Equations by Laplace Transform

This approach is based on converting differential equations to algebraic equations by Laplace transform, finding the unknown in the converted equation, and finding the solution to the differential equation by an inverse transform. In this process, the properties of the Laplace transform as outlined in Section VIIa-1 and the functions with associated Laplace transforms of Table VIIa.1.1 are employed. For example to solve

$$\frac{d^2 y}{dx^2} + 9y = 0$$

with the boundary conditions of $y(0) = 0$ and $dy(0)/dx = 2$, we first find the Laplace transform of each term. The Laplace transform of the first term is ob-

tained from the general relation for the transform of the derivatives repeated here from Section 1 of this chapter:

$$\ell[f^{(n)}] = s^n \ell[f] - s^{n-1} f(0) - s^{n-2} f'(0) - \dots - f^{(n-1)}(0)$$

Hence, the equation becomes; $[s^2 \hat{y} - sy(0) - dy(0)/dx] + 9\hat{y} = 0$. Substituting for the values at $x = 0$ from the boundary conditions we get;

$$(s^2 + 9)\hat{y} = 2$$

From the inverse transform we find; $y = 2/3 \sin 3x$.

Solution to Differential Equations by Power Series

The solution to a large class of second order differential equations, where the coefficients are functions of the independent variable, can be found in terms of a power series. The general homogeneous form of such equations is given as:

$$P(x) \frac{d^2 y}{dx^2} + Q(x) \frac{dy}{dx} + R(x)y = 0 \quad \text{VIIb.2.15}$$

To demonstrate the solution by power series, let's solve an example where $P(x) = Q(x) = R(x) = 1$. We now assume a solution to exist in the form of:

$$y = A_0 + A_1 x + A_2 x^2 + A_3 x^3 + A_4 x^4 + A_5 x^5 + \dots \quad \text{VIIb.2.16}$$

Integrate Equation VIIb.2.16 twice for dy/dx and d^2y/dx^2 , substitute in Equation VIIb.2.15, and collecting similar terms we get:

$$[A_0 + A_1 + 2A_2] + [A_1 + 2A_2 + 6A_3]x + [A_2 + 3A_3 + 12A_4]x^2 + \dots = 0$$

For the summation of terms with the increasing power of x to become equal to zero, we must have the coefficient of each term to be equal to zero:

$$\begin{aligned} A_2 &= -[A_0 + A_1]/2 \\ A_3 &= -[A_1 + 2A_2]/6 \\ \vdots & \quad \quad \quad \vdots \end{aligned}$$

As seen above, we have solved for all the unknown coefficients in terms of two coefficients A_0 and A_1 , which in turn, can be found from the boundary conditions. We may generalize this to obtain an algorithm. To do this, we write Equation VIIb.2.16 in the more convenient way as:

$$y(x) = \sum_{i=0}^{\infty} A_i x^i \quad \text{VIIb.2.17}$$

The first and second differentials of Equation VIIb.2.17 become:

$$\begin{aligned}\frac{dy(x)}{dx} &= \sum_{i=0}^{\infty} iA_i x^{i-1} = \sum_{i=1}^{\infty} (i-1)A_{i-1} x^{i-2} = \sum_{i=2}^{\infty} (i-1)A_{i-1} x^{i-2} \\ \frac{d^2 y(x)}{dx^2} &= \sum_{i=0}^{\infty} i(i-1)A_i x^{i-2} = \sum_{i=2}^{\infty} i(i-1)A_i x^{i-2}\end{aligned}$$

where we have manipulated the indices to facilitate collection of the coefficients of like powers. We may now substitute these terms in Equation VIIb.2.15 to obtain:

$$\sum_{i=2}^{\infty} i(i-1)A_i x^{i-2} + \sum_{i=2}^{\infty} (i-1)A_{i-1} x^{i-2} + \sum_{i=2}^{\infty} A_{i-2} x^{i-2} = 0$$

This equation can be further simplified when the coefficients of like powers are grouped together:

$$\sum_{i=2}^{\infty} [i(i-1)A_i + (i-1)A_{i-1} + A_{i-2}] x^{i-2} = 0 \quad \text{VIIb.2.18}$$

From Equation VIIb.2.18, we can find the algorithm as:

$$A_i = -[(i-1)A_{i-1} + A_{i-2}] / i(i-1)$$

This algorithm is also referred to as the *recurrence formula*. To compare with our previous calculation of A_2 , we now choose $i = 2$ which results in $A_2 = -[A_1 + A_0]/2$, as was found earlier.

2.3. Solution to Solvable Non-linear Ordinary Differential Equations

Generally, the non-linear differential equations cannot be solved by analytical means to obtain answers in closed form. However, there are certain types of non-linear differential equations, which are amenable to analytical solution. These are discussed next.

Separable Equations

These are implicit equations that can be grouped in terms of the dependent and independent variables. For example, any equation in the form of:

$$f_1(x)f_2(y)dx + f_3(x)f_4(y)dy = 0$$

can be grouped as:

$$\frac{f_1(x)}{f_3(x)} dx + \frac{f_4(y)}{f_2(y)} dy = 0$$

Let's consider a specific example such as $xy^2dx + dy = 0$. This equation can be written as $xdx + dy/y^2 = 0$, integration of which gives $x^2/2 - 1/y = C$. A second example for non-linearity involving dy/dx is $(dy/dx)^2 + f(y) + C = 0$. Equations of this sort can be solved as $(dy/dx)^2 = -[f(y) + C]$. If the right-hand side is real then, $dy/dx = \pm \sqrt{-[f(y) + C]}$. This is a first order equation in the form of:

$$\frac{dy}{\sqrt{-[f(y) + C]}} = \pm dx \quad \text{VIIb.2.19}$$

This can be solved if the numerator is amenable to integration. As an exercise, the reader may solve the case of $f(x) = e^x$ and $C = -1$. It should be mentioned that Equation VIIb.2.19 was obtained by multiplying both sides by dx and dividing both sides by the radical. In doing so, we have excluded the special case of $f(y) = -C$. To see if this is indeed a solution, it must be verified separately. The reader may try another exercise where $f(y) = -y$ and $C = 1$ which shows that $f(y) = -C$ is indeed a solution.

Exact First-Order Equations

According to the definition of Section VIIa.1, the following differential equation

$$df(x, y) = M(x, y)dx + N(x, y)dy = 0$$

is an exact differential equation if:

$$\frac{\partial M(x, y)}{\partial y} = \frac{\partial N(x, y)}{\partial x}$$

Since the derivative of (x, y) is given as:

$$df(x, y) = \frac{\partial f(x, y)}{\partial x} dx + \frac{\partial f(x, y)}{\partial y} dy = 0$$

we then conclude that $\frac{\partial f(x, y)}{\partial x} = M$ and $\frac{\partial f(x, y)}{\partial y} = N$. Integrating the first relation gives:

$$f(x, y) = \int_{x_0}^x M(x, y)dx + g(y)$$

where $g(y)$ in this equation is the constant of integration. We can find its value by taking the derivative with respect to y and using the second relation:

$$\frac{\partial f(x, y)}{\partial y} = \int_{x_0}^x \frac{\partial M(x, y)}{\partial y} dx + g'(y) = N$$

Solving to get $g'(y) = N - \int^x \frac{\partial M(x, y)}{\partial y} dx$, from which $g(y)$ is found and the equation is solved. Let's try an example. The goal is to solve the following non-linear differential equation

$$\frac{dy}{dx} + \frac{x^2 + y^2}{2xy} = 0$$

this equation can also be written in the more familiar form of $(x^2 + y^2) dx + 2xy dy = 0$. Hence, $M = x^2 + y^2$ and $N = 2xy$. We first see if the expression $(x^2 + y^2) dx + 2xy dy$ is an exact differential. This can be easily verified that the derivative of M with respect to y (i.e. $2y$) is the same as the derivative of N with respect to x (i.e. $2y$). Similarly, we may verify this for N . To solve the differential equation, we integrate M to get $f(x, y) = x^3/3 + xy^2 + g(y)$. We now take the derivative of this with respect to y and set it equal to N to get: $2xy + g'(y) = 2xy$. From here, $g(y) = C$. Hence, the solution to the differential equation is given as:

$$f(x, y) = \frac{x^3}{3} + xy^2 + C$$

where C is found from the boundary condition. The following is left for exercise, $M = 2x + y$ and $N = x + 2y$.

Change of Variable

This technique is applicable to first-order nonlinear differential equations. For example, the Bernoulli differential equation:

$$\frac{dy}{dx} + P(x)y = Q(x)y^n$$

can be transformed into a linear differential equation by a change of dependent variable from y to $z = y^{1-n}$ to obtain:

$$\frac{dz}{dx} + (1-n)P(x)z = (1-n)Q(x)$$

resulting in a first-order linear differential equation. The second example includes the Riccati equation:

$$\frac{dy}{dx} + P(x)y^2 + Q(x)y = R(x)$$

If $u(x)$ is one solution to the Riccati differential equation, the substitution $y = u(x) + 1/z$ will transform the Riccati equation:

$$\frac{dz}{dx} - [uP(x) + Q(x)]z = 2P(x)$$

into a first-order linear differential equation. The third example includes equations in the form of:

$$\left(\frac{dy}{dx}\right)^2 + c_1 \frac{dy}{dx} + c_2 y = f(x) \quad \text{VIIb.2.20}$$

By assuming $dy/dx = z$, we may solve Equation VIIb.2.20 as an algebraic equation for z to obtain:

$$z = \frac{dy}{dx} = \frac{-c_1 \pm \sqrt{c_1^2 - 4[c_2 y - f(x)]}}{2} \quad \text{VIIb.2.21}$$

Depending on the function $f(x)$ and coefficients c_1 and c_2 , Equation VIIb.2.21 may be amenable to integration. This can be tried, as an exercise, for the case where $c_1 = -2$, $c_2 = 4$, and $f(x) = 4x - 1$.

Reduction of Order

This method is applied to the second-order differential equations lacking a variable (i.e. lacking either x , y or both). In such cases, we can reduce the order of the equation by using a substitute for a derivation. For example, consider the following second-order nonlinear equation:

$$\frac{d^2 y}{dx^2} + \left(\frac{dy}{dx}\right)^3 = 0$$

If we assume $dy/dx = M$, then $d^2 y/dx^2 = dM/dx$. Therefore, $dM/M^3 = -dx$. This can now be easily solved to find $1/M^2 = 2x + C$. Substituting for M , we get $dy = dx/(2x + C)^{1/2}$, which is a simple first order equation.

2.4. Solution to Partial Differential Equations

Generally, partial differential equations of mathematical physics and engineering applications are solved by the method of separation of variables. In this method, we seek particular product solutions. To illustrate this method, we present two examples. The first example deals with determination of temperature distribution in a plate and the second deals with determination of the probability amplitude of a subatomic particle.

Solution to the Heat Conduction Equation

The idea is to determine temperature distribution (i.e., $T = f(x, y)$) in a plate as shown in the figure under steady state conditions. The two-dimensional heat conduction equation in steady state, as derived in Chapter IVa, reduces to the two-dimensional Laplace differential equation:

$$\frac{\partial^2 T}{\partial x^2} + \frac{\partial^2 T}{\partial y^2} = 0 \quad \text{VIIb.2.22}$$

subject to the x -direction and y -direction boundary conditions as follows. In the x -direction, $T(0, y) = 0$ and $T(a, y) = 0$. In the y -direction, $T(x, 0) = 0$ and $T(x, b) = f(x)$ as shown in Figure VII.2.1.

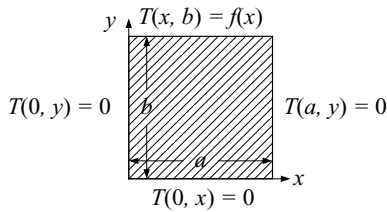


Figure VIIb.2.1. Boundary conditions for obtaining temperature distribution in a rectangle

Our goal is to find a product solution such as

$$T_P(x, y) = X(x)Y(y) \quad \text{VIIb.2.23}$$

Substituting Equation VIIb.2.23 to VII.2.22, we find:

$$Y \frac{d^2 X}{dx^2} + X \frac{d^2 Y}{dy^2} = 0$$

Separating variables, we obtain

$$-\frac{1}{X} \frac{d^2 X}{dx^2} = \frac{1}{Y} \frac{d^2 Y}{dy^2} = \pm k^2 \quad \text{VIIb.2.24}$$

where the right side of this equation is only a function of x and the left side is only a function of y . This is possible only if both sides are equal to a constant such as k^2 . By choosing the square of a real number, we made sure that k^2 is positive. The next task is to choose an appropriate sign for k^2 , which is discussed next. Meanwhile, note that by the method of separation of variables, we managed to replace a second order linear partial differential equation with two second-order linear ordinary differential equations, which can be readily solved.

To solve Equation VIIb.2.24, we must determine which sign we should use for k^2 . The selection of a sign for the constant k^2 depends on the boundary conditions. A direction involving homogeneous boundary conditions must be associated with a periodic function and the direction involving nonhomogeneous boundary condition must be associated with an exponential function. For example, in Figure VIIb.2.1, the homogeneous boundary conditions are specified in the x -direction whereas the y -direction includes one nonhomogeneous boundary condition. Therefore, we select the plus sign for k^2 to get:

$$\frac{d^2 X}{dx^2} + k^2 X = 0 \quad \text{VIIb.2.25}$$

Recall that Equation VIIb.2.25 is a Sturm-Liouville problem. Hence, constant k will result in appearance of the eigenvalues. The solution to Equation VIIb.2.25 subject to the above boundary conditions was obtained in Section VIIb.1.1 as:

$$X = A_n \sin \frac{n\pi x}{a}$$

where n is a positive integer, $n = 1, 2, 3, \dots$. Choosing plus sign for k^2 , the equation involving y becomes:

$$\frac{d^2 Y}{dy^2} - k^2 Y = 0 \quad \text{VIIb.2.26}$$

The solution to Equation VIIb.2.26 is given in Section VIIb.2.2 as:

$$Y = B_n \sinh \frac{n\pi y}{a}$$

Since $X(x)Y(y)$ is a particular solution to Equation VIIb.2.22, the following is also a solution:

$$T(x, y) = \sum_{n=1}^{\infty} C_n \sinh \frac{n\pi y}{a} \sin \frac{n\pi x}{a}$$

Where $C_n = A_n B_n$. To find the set of unknown coefficients C_n , we use the last boundary condition:

$$f(x) = \sum_{n=1}^{\infty} \left(C_n \sinh \frac{n\pi b}{a} \right) \sin \frac{n\pi x}{a} \quad 0 < x < a$$

We now use the Fourier series expansion for $f(x)$ to find the unknown coefficients C_n :

$$C_n \sinh \frac{n\pi b}{a} = \frac{2}{a} \int_0^a f(x) \sin \frac{n\pi x}{a} dx$$

Therefore,

$$T(x, y) = \sum_{n=1}^{\infty} C_n \sinh \frac{n\pi b}{a} \sin \frac{n\pi x}{a} \frac{\sinh(n\pi y/a)}{\sinh(n\pi b/a)} \quad \text{VIIb.2.27}$$

Thus, temperature at any point in the plate can be determined from Equation VIIb.2.27. Following the same logic of the two-dimensional temperature distribution in the Cartesian coordinate system, as an exercise, the reader may solve for the three-dimensional temperature distribution. To do this, consider a rectangular parallelepiped where all five faces are maintained at zero and the sixth face is maintained at a specified temperature $T(x, y, z = c) = f(x, y)$.

Solution to Schrödinger Wave Equation *

Erwin Schrödinger discovered the wave equation for matter waves. It was Max Born who interpreted the Shroedinger – de Broglie waves as waves of probability, which became the wave mechanics version of quantum mechanics. Consider the classical properties of electromagnetic waves in free space such as frequency (ν),

* **Historical perspective.** Physicists have traditionally tried to unify all physical phenomena under one set of mathematical rules. For example, Newton applied the terrestrial laws to describe the motion of celestial bodies. Boltzmann integrated thermodynamics into classical mechanics, Ampere and Faraday demonstrated that electricity and magnetism are two sides of the same coin, and James Clerk Maxwell explained optics in terms of electromagnetic waves (Figure VIIb.2.2). This pursuit of unification continued until around the turn of the 20th century, when classical physics then tried to explain every phenomenon in terms of two independent branches; classical mechanics and electromagnetism. However, with this approach classical physics could not describe phenomena on a microscopic scale. For example, blackbody radiation, the photoelectric effect, and the emission of sharp spectral lines by atoms in a gas discharge could not be explained within the framework of classical physics. The most challenging task facing classical physics was explaining the nature of light, which behaves as both wave and particle. In classical mechanics, every elementary object is either wave, obeying Maxwell's equations or a particle, obeying Newtonian laws. The discrepancy between the Newtonian concept of relative motion and Michelson's optical experiment in 1881 gave birth to Einstein's theory of relativity. Prior to Michelson's experiment, the nature of light was based solely on the electromagnetic theory of Maxwell dating back to 1862. Treating light only as an electromagnetic wave requires a medium for light to travel through an empty space. Still, classical physics was in dire need of modernization to be able to explain such new challenging phenomena as photoelectric effects and emission of sharp spectral light in a gas discharge. The shortcomings of classical physics led to the development of modern physics (based on wave or quantum mechanics), which quantitatively describes the behavior of nature on a microscopic scale. In quantum mechanics, where particles and waves are two distinct modes of behavior shared by all objects, there is no distinction between wave and particle as in classical theories. We may then consider the classical mechanics as a special case of the more general wave mechanics.

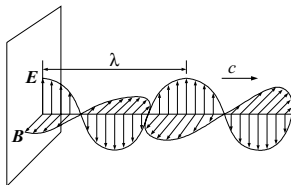


Figure VIIb.2.2. A plane monochromatic electromagnetic wave

The discovery of quantum physics proceeded in two tracks. Max Plank, Neils Bohr, and Werner Heisenberg's work led to the realization that the allowed values of energy exchange between subatomic particles are discrete. The second track based on the works of Albert Einstein, Louis de Broglie, Erwin Schrödinger, and Max Born focused on the duality of light as both wave and particle. Paul Dirac later showed that these two tracks are entirely equivalent.

wavelength (λ), and wave velocity (c). The introduction of Plank's constant ($h = 6.62559 \times 10^{-34}$ J·s) in 1901 allowed the introduction of particle properties such as energy ($E = h\nu$), momentum ($M = E/c = h\nu/c$), and relativistic mass ($m = W/c^2 = h\nu/c^2$) into the description of the electromagnetic waves. Hence, a photon would have a wavelength given by $\lambda = h/M$.

In 1924, De Broglie extended this definition of wavelength to other particles. Hence, such particles as electron, proton, neutron, or any other subatomic particle having momentum M , would have a "De Broglie wavelength" given by $\lambda = h/M$. Equation VIIb.1.32 gives the general time-dependent form of the Shroedinger wave equation. This equation predicts the behavior of the probability amplitude (ψ) of a particle having a mass of m and potential energy V as a function of position and time. We now solve Equation VIIb.1.32 for the spherical waves. Such waves represent, for example, a scattered particle by a nucleus or the emission of an α ray from the parent nucleus. The differential equation to solve is given by Equation VIIb.1.32, repeated here:

$$-\frac{\hbar^2}{2m}\nabla^2\psi(\vec{r},t) + V(\vec{r})\psi(\vec{r},t) = i\hbar\frac{\partial\psi(\vec{r},t)}{\partial t} \quad \text{VIIb.1.32}$$

where $\hbar = h/2\pi$. This equation, therefore, describes the wave behavior of a particle having mass m in a field that induces potential energy $V(r)$. Since we consider the potential energy to be only a function of location, we are able to separate variables and obtain a set of spatial and temporal functions by defining ψ as:

$$\psi(\vec{r},t) = \varphi(\vec{r})\xi(t) \quad \text{VIIb.2.28}$$

so that time is expressed as a separate factor, then the phase of ψ at any instant is the same throughout the entire wave. Such waves are called *standing waves*. Substituting for ψ in Equation VIIb.1.32, we get:

$$-\frac{\hbar^2}{2m}\xi(t)\nabla^2\varphi(\vec{r}) + V(\vec{r})\xi(t)\varphi(\vec{r}) = i\hbar\varphi(\vec{r})\frac{\partial\xi(t)}{\partial t}$$

If we divide both sides of this equation by that given by Equation VIIb.2.28, we get:

$$-\frac{\hbar^2}{2m}\frac{1}{\varphi(\vec{r})}\nabla^2\varphi(\vec{r}) + V(\vec{r}) = i\hbar\frac{1}{\xi(t)}\frac{\partial\xi(t)}{\partial t} = E$$

where E is the total energy of the state. The *time-independent Shroedinger equation* is then obtained as:

$$\nabla^2\varphi(\vec{r}) + \frac{2m}{\hbar^2}[E - V(\vec{r})]\varphi(\vec{r}) = 0 \quad \text{VIIb.2.29}$$

The simplest case to investigate is the atom of hydrogen where an electron is orbiting the nucleus at a distance r , having an electrostatic potential energy of $-e^2/r$. In the solution below, we leave the potential energy in its general form of

In the solution below, we leave the potential energy in its general form of $V(r)$. To further simplify the solution, rather than writing the equation for both electron and nucleus, we solve the time independent Shroedinger equation in the spherical co-ordinate system whose origin is at the center of mass. Since the nucleus is much more massive than the electron, the center of mass is very close to the nucleus. In this case, mass m in Equation VIIb.2.29 represents the mass of electron and nucleus and is given by:

$$m = \frac{m_e m_n}{m_e + m_n}$$

Substituting for the Laplacian operator (see Section VIIc.1.1), Equation VIIb.2.29 for a system representing both the electron and the hydrogen nucleus becomes:

$$\frac{1}{r^2} \frac{\partial}{\partial r} (r^2 \frac{\partial \phi}{\partial r}) + \frac{1}{r^2 \sin \theta} \frac{\partial}{\partial \theta} (\sin \theta \frac{\partial \phi}{\partial \theta}) + \frac{1}{r^2 \sin^2 \theta} \frac{\partial^2 \phi}{\partial \phi^2} + \frac{2m}{\hbar^2} [E - V(r)] \phi = 0$$

Again, we may use the method of separation of variables if potential energy is only a function of r . For $\phi(r, \theta, \phi) = R(r)S(\theta, \phi)$, the equation can be separated as:

$$\frac{1}{R} \frac{d}{dr} (r^2 \frac{dR}{dr}) + \frac{2m}{\hbar^2} [E - V(r)] r^2 = -\frac{1}{S} [\frac{1}{\sin \theta} \frac{\partial}{\partial \theta} (\sin \theta \frac{\partial S}{\partial \theta}) + \frac{1}{\sin^2 \theta} \frac{\partial^2 S}{\partial \phi^2}] \quad \text{VIIb.2.30}$$

For this relation to hold, both sides of this equation must be equal to some constant. We call this separation constant $l(l+1)$ because the differential equation of the wave function in the θ direction is a Legendre differential equation. Before proceeding to solve for R , let's use the same method of the separation of variables for the right side of Equation VIIb.2.30. In this case, we use $S(\theta, \phi) = \Theta(\theta)\Phi(\phi)$ to get:

$$\sin^2 \theta [\frac{1}{\Theta \sin \theta} \frac{d}{d\theta} (\sin \theta \frac{d\Theta}{d\theta}) + l(l+1)] = -\frac{1}{\Phi} \frac{d^2 \Phi}{d\phi^2}$$

Again, for this relation to hold, both sides must be equal to some constant such as n^2 . To summarize, we managed to break down the Shroedinger partial differential equation into three ordinary differential equations for radial, polar, and azimuthal directions:

$$\text{Radial: } \frac{1}{Rr^2} \frac{d}{dr} (r^2 \frac{dR}{dr}) + \frac{2m}{\hbar^2} [E - V(r)] - \frac{l(l+1)}{2mr^2} = 0 \quad \text{VIIb.2.31}$$

$$\text{Polar: } \frac{1}{\Theta \sin \theta} \frac{d}{d\theta} (\sin \theta \frac{d\Theta}{d\theta}) + l(l+1) - \frac{n^2}{\sin^2 \theta} = 0 \quad \text{VIIb.2.32}$$

$$\text{Azimuthal:} \quad \frac{d^2\Phi}{d\phi^2} - n^2\Phi = 0 \quad \text{VIIb.2.33}$$

These equations are valid if the potential energy $V(r)$ is spherically symmetric and if l and n , referred to as quantum numbers, are suitably chosen. The solution to the azimuthal differential equation is straightforward and is given as $\Phi = c_1 \exp(in\phi) + c_2 \exp(-in\phi)$. The integer n is known as the *magnetic quantum number* because the energy of the hydrogen atom depends on this quantum number only if the atom is placed in a magnetic field. If the atom is placed in a magnetic field, then distinct values for n determine the allowed energy levels.

We now try to find the solution to the polar differential equation. To see if this equation can be cast in the form of Equation VIIb.1.7, we make a change of variable as $x = \cos\theta$. We find the required derivative terms from:

$$\frac{d\theta}{dx} = -\sin\theta \frac{d\Theta}{dx}$$

and

$$\frac{d^2\Theta}{d\theta^2} = \sin^2\theta \frac{d^2\Theta}{dx^2} - \cos\theta \frac{d\Theta}{dx}.$$

Substituting into Equation VII.2.32, it simplifies to:

$$\frac{1}{\sin\theta} \frac{d}{d\theta} \left[\sin\theta \frac{d\Theta}{d\theta} \right] + \left[l(l+1) - \frac{n^2}{\sin^2\theta} \right] \Theta = 0 \quad \text{VIIb.2.34}$$

We can now carry out the derivative of the first term in Equation VIIb.2.34 to get:

$$\frac{d^2\Theta}{d\theta^2} + \frac{\cos\theta}{\sin\theta} \frac{d\Theta}{d\theta} + \left[l(l+1) - \frac{n^2}{\sin^2\theta} \right] \Theta = 0$$

We now substitute for the derivative terms in terms of $x = \cos\theta$, which yields:

$$\sin^2\theta \frac{d^2\Theta}{dx^2} - \cos\theta \frac{d\Theta}{dx} + \frac{\cos\theta}{\sin\theta} \left(-\sin\theta \frac{d\Theta}{dx} \right) + \left[l(l+1) - \frac{n^2}{\sin^2\theta} \right] \Theta = 0$$

where we have used $dy/d\theta = (dy/dx)(dx/d\theta)$. Collecting terms and substituting for $\sin\theta = \sqrt{1-x^2}$, we get:

$$(1-x^2) \frac{d^2\Theta}{dx^2} - 2x \frac{d\Theta}{dx} + \left[l(l+1) - \frac{n^2}{1-x^2} \right] \Theta = 0 \quad \text{VIIb.2.35}$$

If there is no magnetic field, then $n = 0$ (hence, $\Phi = \text{constant}$) and Equation VIIb.2.35 can be simplified to Equation VIIb.1.7. If l takes distinct integers such as 0, 1, 2, 3, etc., then $l(l+1) = 0, 2, 6, 12$, etc.

In Equation VIIb.2.35, constant l is known as the *angular-momentum quantum number*. To have a satisfactory answer for the wave function, n must have integral values between $-l$ and $+l$. For example, for $l = 3$, n can be $-3, -2, -1, 0, 1, 2$, and 3.

Finally, the solution to the radial differential equation can be obtained by making a change in function from $R(r)$ to $R(r) = Y/r$:

$$\frac{d^2 Y}{dr^2} + \frac{2m}{\hbar^2} [E - V(r) - \frac{l(l+1)\hbar^2}{2mr^2}] Y = 0$$

This is a linear second order differential equation similar to the one-dimensional wave equation. The final solution for the probability amplitude is then found as:

$$\psi(r, \theta, \phi) = Y_l(r) \Theta_n(\theta) \Phi_n(\phi) / r$$

3. Pertinent Functions and Polynomials

We now briefly discuss such important functions and polynomials as Dirac delta-function, the Gaussian error function, the Gamma function, and the Bessel functions.

Dirac δ -function. This function is defined as:

$$\delta(x - x_0) = \begin{cases} 0, & x \neq x_0 \\ \infty, & x = x_0 \end{cases}, \quad \int_{-\infty}^{\infty} \delta(x - x_0) dx = 1$$

The most useful property of the Dirac δ -function is when integrated along a well-behaved function $f(x)$:

$$\int \delta(x - x_0) f(x) dx = f(x_0)$$

Error function. The Gaussian error function is used in such engineering applications as conduction heat transfer and reliability engineering. The Gaussian Error function is defined as:

$$\text{erf}(x) = \frac{2}{\sqrt{\pi}} \int_0^x e^{-z^2} dz$$

Note that the complementary error function is $\text{erfc}(x) = 1 - \text{erf}(x)$ (i.e., the integral limits are from x to ∞).

Gamma function is defined by the integral:

$$\Gamma(x) = \int_0^{\infty} e^{-t} t^{x-1} dt$$

Note the following property of the gamma function $\Gamma(z + 1) = z\Gamma(z)$. It can be verified that $\Gamma(1/2) = (\pi)^{1/2}$, $\Gamma(0) = \infty$, $\Gamma(1) = 1, \dots$, $\Gamma(n) = (n - 1)!$

Exponential integrals are obtained by substituting values for the index n in the following integral:

$$E_n(x) = \int_1^\infty \frac{e^{-xt}}{t^n} dt$$

For example, $E_0(x) = e^{-x}/x$ and $E_n(x) = (e^{-x} - xE_{n-1}(x))/(n-1)$. Also $E'_n(x) = -E_{n-1}(x)$.

Bessel functions, having engineering applications in cylindrical coordinates for nuclear reactor core design, thermal conduction and electricity, are solutions of the Bessel differential equation:

$$x^2 \frac{d^2 y}{dx^2} + x \frac{dy}{dx} + (x^2 - \nu^2)y = 0 \quad \text{VIIb.3.1}$$

This second order differential equation is of order ν and has the following general solution:

$$y(x) = C_1 J_\nu(x) + C_2 Y_\nu(x)$$

where real functions J_ν and Y_ν are referred to as *Bessel functions of the first and the second kind of order ν* , respectively.

Modified Bessel functions: The complex form of the Bessel function is obtained if x is replaced by ix :

$$x^2 \frac{d^2 y}{dx^2} + x \frac{dy}{dx} - (x^2 + \nu^2)y = 0$$

The solution to this equation is given as:

$$y(x) = C_3 I_\nu(x) + C_4 K_\nu(x)$$

where real functions I_ν and K_ν are called the modified Bessel functions of the first and second kind. The Bessel functions of the first and the second kind are of the following form:

$$J_\nu(x) = x^\nu \sum_{m=0}^{\infty} \frac{(-1)^m x^{2m}}{2^{2m+\nu} m! \Gamma(\nu + m + 1)}$$

$$Y_\nu(x) = \frac{J_\nu(x) \cos(\nu\pi) - J_{-\nu}(x)}{\sin(\nu\pi)}$$

Bessel functions of order $\nu = 0$ and $\nu = 1$ are used more frequently. The polynomial for the Bessel function of the first kind of order 0 is given as (Abramowitz):

$$J_0(x) = 1 - 2.249997(x/3)^2 + 1.2656208(x/3)^4 - 0.316386(x/3)^6 + 0.444479(x/3)^8 - 0.0039444(x/3)^{10} \\ + 0.000210(x/3)^{12} + \varepsilon \\ -3 \leq x \leq 3, \quad |\varepsilon| < 5 \times 10^{-8}$$

The polynomial for the Bessel function of the first kind of order 1 is given as:

$$x^{-1}J_1(x) = 0.5 - 0.5624998(x/3)^2 + 0.21093573(x/3)^4 - 0.03954289(x/3)^6 + 0.00443319(x/3)^8 \\ - 0.003176(x/3)^{10} + 0.00001109(x/3)^{12} + \varepsilon \\ -3 \leq x \leq 3, \quad |\varepsilon| < 1.3 \times 10^{-8}$$

The polynomial for the Bessel function of the second kind of order 0 is given as:

$$Y_0(x) = (2/\pi)\ln(x/2)J_0(x) + 0.36746691 + 0.60559366(x/3)^2 - 0.74350384(x/3)^4 + 0.25300117(x/3)^6 \\ - 0.04261214(x/3)^8 + 0.00427916(x/3)^{10} + 0.00024846(x/3)^{12} + \varepsilon \\ 0 \leq x \leq 3, \quad |\varepsilon| < 1.4 \times 10^{-8}$$

The polynomial for the Bessel function of the second kind of order 1 is given as:

$$xY_1(x) = (2/\pi)x\ln(x/2)J_1(x) - 0.6366198 + 0.221209(x/3)^2 + 2.1682709(x/3)^4 - 1.3164827(x/3)^6 \\ + 0.312395(x/3)^8 - 0.040097(x/3)^{10} + 0.0027873(x/3)^{12} + \varepsilon \\ 0 \leq x \leq 3, \quad |\varepsilon| < 1.1 \times 10^{-7}$$

The polynomial for the modified Bessel function of the first kind of order 0 is given as:

$$I_0(x) = 1 + 3.5156229(x/3.75)^2 + 3.0899424(x/3.75)^4 + 1.2067492(x/3.75)^6 + 0.2659732(x/3.75)^8 \\ + 0.0360768(x/3.75)^{10} + 0.0045813(x/3.75)^{12} + \varepsilon \\ -3.75 \leq x \leq 3.75 \quad |\varepsilon| < 1.6 \times 10^{-7}$$

The polynomial for the modified Bessel function of the first kind of order 1 is given as:

$$x^{-1}I_1(x) = 0.5 + 0.878906(x/3.75)^2 + 0.51498869(x/3.75)^4 + 0.15084934(x/3.75)^6 + 0.2658733(x/3.75)^8 \\ + 0.0301532(x/3.75)^{10} + 0.00032411(x/3.75)^{12} + \varepsilon \\ -3.75 \leq x \leq 3.75 \quad |\varepsilon| < 8 \times 10^{-9}$$

The polynomial for the modified Bessel function of the second kind of order 0, is given as:

$$K_0(x) = -\ln(x/2)I_0(x) - 0.57721566 + 0.42278420(x/2)^2 + 0.23069756(x/2)^4 + 0.03488590(x/2)^6 + \\ 0.00262698(x/2)^8 + 0.00010750(x/2)^{10} + 0.00000740(x/2)^{12} + \varepsilon \\ 0 < x < 2, \quad |\varepsilon| < 1 \times 10^{-8}$$

The polynomial for the modified Bessel function of the second kind of order 1, is given as:

$$xK_1(x) = x\ln(x/2)I_1(x) + 1 + 0.15443144(x/2)^2 - 0.67278579(x/2)^4 - 0.18156897(x/2)^6 \\ - 0.01919402(x/2)^8 - 0.00110404(x/2)^{10} - 0.00004686(x/2)^{12} + \varepsilon \\ 0 < x < 2, \quad |\varepsilon| < 8 \times 10^{-9}$$

Abramowitz gives polynomials for x outside the ranges shown above. Some useful derivatives of Bessel functions are as follows:

Derivatives of $J_0(x)$, $Y_0(x)$, $I_0(x)$, and $K_0(x)$:

$$\begin{aligned}\frac{dJ_0(x)}{dx} &= -J_1(x) & \frac{dY_0(x)}{dx} &= -Y_1(x) \\ \frac{dI_0(x)}{dx} &= I_1(x) & \frac{dK_0(x)}{dx} &= -K_1(x)\end{aligned}$$

Derivatives of $J_v(x)$, $Y_v(x)$, $I_v(x)$, and $K_v(x)$:

$$\begin{aligned}\frac{dJ_v(x)}{dx} &= [J_{v-1}(x) - J_{v+1}(x)]/2 & \frac{dY_v(x)}{dx} &= [Y_{v-1}(x) - Y_{v+1}(x)]/2 \\ \frac{dI_v(x)}{dx} &= [I_{v-1}(x) - I_{v+1}(x)]/2 & \frac{dK_v(x)}{dx} &= [K_{v-1}(x) - K_{v+1}(x)]/2\end{aligned}$$

Derivatives of $x^v J_v(x)$, $x^v Y_v(x)$, $x^v I_v(x)$, and $x^v K_v(x)$:

$$\begin{aligned}\frac{dx^v J_v(x)}{dx} &= x^v J_{v-1}(x) & \frac{dx^v Y_v(x)}{dx} &= x^v Y_{v-1}(x) \\ \frac{dx^v I_v(x)}{dx} &= x^v I_{v-1}(x) & \frac{dx^v K_v(x)}{dx} &= -x^v K_{v-1}(x)\end{aligned}$$

Derivatives of $x^{-v} J_v(x)$, $x^{-v} Y_v(x)$, $x^{-v} I_v(x)$, and $x^{-v} K_v(x)$:

$$\begin{aligned}\frac{dx^{-v} J_v(x)}{dx} &= -x^{-v} J_{v+1}(x) & \frac{dx^{-v} Y_v(x)}{dx} &= -x^{-v} Y_{v+1}(x) \\ \frac{dx^{-v} I_v(x)}{dx} &= x^{-v} I_{v+1}(x) & \frac{dx^{-v} K_v(x)}{dx} &= -x^{-v} K_{v+1}(x)\end{aligned}$$

Some useful integrals of Bessel functions are as follows:

$$\begin{aligned}\int J_1(x)dx &= -J_0(x) + c & \int Y_1(x)dx &= -Y_0(x) + c & \int I_1(x)dx &= -I_0(x) + c, \\ \int K_1(x)dx &= -K_0(x) + c & \int x^v J_{v-1}(x)dx &= x^v J_v(x) + c, & \int x^{-v} J_{v+1}(x)dx &= -x^{-v} J_v(x) + c\end{aligned}$$

Table VIIb.3.1 includes some Bessel functions for the range of $0 \leq x \leq 4$ and Figure VIIb.3.1 shows Bessel functions of order zero for the range of $0 \leq x \leq 7$.

Hankel functions: are obtained from the Bessel functions and defined as:

$$\begin{aligned}H_{v,1} &= J_v(x) + iY_v(x) \\ H_{v,2} &= J_v(x) - iY_v(x)\end{aligned}$$

Jacobi polynomial is the solution to the special Jacobi differential equation. The Jacobi polynomial is:

Table VIIb.3.1. Bessel functions

x	$J_0(x)$	$J_1(x)$	$Y_0(x)$	$Y_1(x)$	$I_0(x)$	$I_1(x)$	$K_0(x)$	$K_1(x)$
0	1.0000	0.0000	$-\infty$	$-\infty$	1.000	0.0000	∞	∞
.05	0.9994	0.0250	-1.979	-12.79	1.001	0.0250	3.114	19.91
.10	0.9975	0.0499	-1.534	-6.459	1.003	0.0501	2.427	9.854
.15	0.9944	0.0748	-1.271	-4.364	1.006	0.0752	2.030	6.477
.20	0.9900	0.0995	-1.081	-3.324	1.010	0.1005	1.753	4.776
.25	0.9844	0.1240	-0.9316	-2.704	1.016	0.1260	1.542	3.747
.30	0.9776	0.1483	-0.8073	-2.293	1.023	0.1517	1.372	3.056
.35	0.9696	0.1723	-0.7003	-2.000	1.031	0.1777	1.233	2.559
.40	0.9604	0.1960	-0.6060	-1.781	1.040	0.2040	1.115	2.184
.45	0.9500	0.2194	-0.5214	-1.610	1.051	0.2307	1.013	1.892
.50	0.9385	0.2423	-0.4445	-1.471	1.063	0.2579	0.9244	1.656
.55	0.9258	0.2647	-0.3739	-1.357	1.077	0.2855	0.8466	1.464
.60	0.9120	0.2867	-0.3085	-1.260	1.092	0.3137	0.7775	1.303
.65	0.8971	0.3081	-0.2476	-1.177	1.108	0.3425	0.7159	1.167
.70	0.8812	0.3290	-0.1907	-1.103	1.126	0.3719	0.6605	1.050
.75	0.8642	0.3492	-0.1372	-1.038	1.146	0.4020	0.6106	0.9496
.80	0.8463	0.3688	-0.0868	-0.9781	1.167	0.4329	0.5653	0.8618
.85	0.8274	0.3878	-0.0393	-0.9236	1.189	0.4646	0.5242	0.7847
.90	0.8075	0.4059	-0.0056	-0.8731	1.213	0.4971	0.4867	0.7165
.95	0.7868	0.4234	0.0481	-0.8258	1.239	0.5306	0.4524	0.6560
1.0	0.7652	0.4401	0.0883	-0.7812	1.266	0.5652	0.4210	0.6019
1.1	0.6957	0.4850	0.1622	-0.6981	1.326	0.6375	0.3656	0.5098
1.2	0.6711	0.4983	0.2281	-0.6211	1.394	0.7147	0.3185	0.4346
1.3	0.5937	0.5325	0.2865	-0.5485	1.469	0.7973	0.2782	0.3725
1.4	0.5669	0.5419	0.3379	-0.4791	1.553	0.8861	0.2437	0.3208
1.5	0.4838	0.5644	0.3824	-0.4123	1.647	0.9817	0.2138	0.2774
1.6	0.4554	0.5699	0.4204	-0.3476	1.750	1.085	0.1880	0.2406
1.7	0.3690	0.5802	0.4520	-0.2847	1.864	1.196	0.1655	0.2094
1.8	0.3400	0.5815	0.4774	-0.2237	1.990	1.317	0.1459	0.1826
1.9	0.2528	0.5794	0.4968	-0.1644	2.128	1.448	0.1288	0.1597
2.0	0.2239	0.5767	0.5104	-0.1070	2.280	1.591	0.1139	0.1399
2.1	0.1383	0.5626	0.5183	-0.0517	2.446	1.745	0.1008	0.1227
2.2	0.1104	0.5560	0.5208	-0.0015	2.629	1.914	0.0893	0.1079
2.3	0.0288	0.5305	0.5181	0.0523	2.830	2.098	0.0791	0.0950
2.4	0.0025	0.5202	0.5104	0.1005	3.049	2.298	0.0702	0.0837
2.5	0.0729	0.4843	0.4981	0.1459	3.290	2.517	0.0623	0.0739
2.6	-0.0968	0.4708	0.4813	0.1884	3.553	2.755	0.0554	0.0653
2.7	-0.1641	0.4260	0.4605	0.2276	3.842	3.016	0.0493	0.0577
2.8	-0.1850	0.4097	0.4359	0.2635	4.157	3.301	0.0438	0.0511
2.9	-0.2426	0.3575	0.4079	0.2959	4.503	3.613	0.0390	0.0453
3.0	-0.2601	0.3391	0.3769	0.3247	4.881	3.593	0.0347	0.0402
3.2	-0.3202	0.2613	0.3071	0.3707	5.747	4.734	0.0276	0.0316
3.4	-0.3643	0.1792	0.2296	0.4010	6.785	5.670	0.0220	0.0250
3.6	-0.3918	0.0955	0.1477	0.4154	8.028	6.793	0.0175	0.0198
3.8	-0.4026	0.0128	0.0645	0.4141	9.517	8.140	0.0140	0.0157
4.0	-0.3971	-0.0660	-0.0169	0.3979	11.302	9.759	0.0112	0.0125

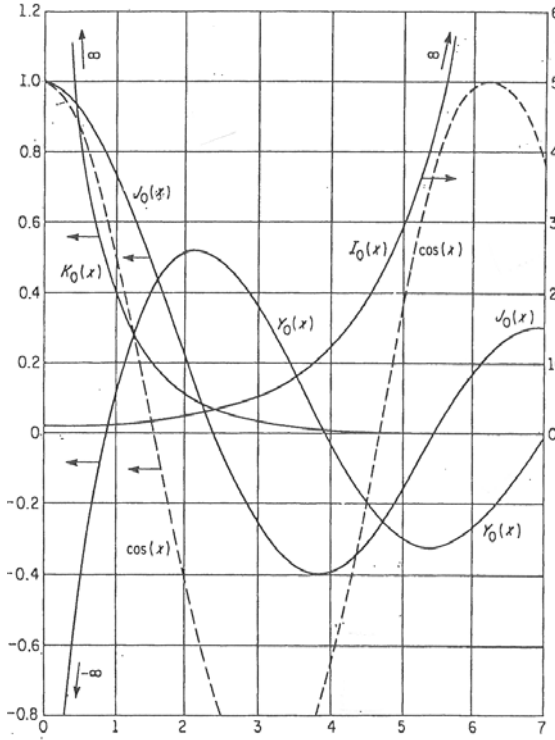


Figure VIIb.3.1. Bessel functions of order zero for the range of $0 \leq x \leq 7$

$$P_{Jacoby}(a, b, x) = 1 - \frac{n(n+b)}{a} \frac{x}{1!} + \frac{(n-1)n(n+b)(n+b+1)}{a(a+1)} \frac{x^2}{2!} + \dots$$

Chebyshev polynomial of the first kind is given as:

$$P_{Chebyshev}(x) = \cos(n \cos^{-1} x) = x^n - \binom{n}{2} x^{n-2} (1-x^2) + \binom{n}{4} x^{n-4} (1-x^2)^2 - \dots$$

Hermite polynomial is the solution to the Hermite differential equation and is given by *Rodrigue's* formula:

$$P_{Hermite}(x) = (-1)^n e^{x^2} \frac{d^n e^{-x^2}}{dx^n}$$

Hyperbolic functions are defined as $\sinh(x) = (e^x - e^{-x})/2$ and $\cosh(x) = (e^x + e^{-x})/2$.

Legendre polynomials are the solution to the Legendre differential equation and are given as:

$$P_{\text{Legendre}}(x) = \frac{1}{2^n n!} \frac{d^n (x^2 - 1)^n}{dx^n}$$

It can be verified that $P_0(x) = 1$, $P_1(x) = x$, $P_2(x) = (3x^2 - 1)/2$, $P_3(x) = (5x^3 - 3x)/2$, etc. Also

$$\int_{-1}^{+1} P_n(x) P_{n'}(x) dx = \frac{2}{2n+1} \delta_{nn'}$$

The recurrence relations for Legendre polynomials are as follows:

$$(n+1)P_{n+1}(x) - (2n+1)xP_n(x) + nP_{n-1}(x) = 0$$

$$P'_{n+1}(x) - xP'_n(x) = (n+1)P_n(x)$$

Associated Legendre polynomials are obtained from the following formula:

$$P_l^m(x) = (1-x^2)^{m/2} \frac{d^m}{dx^m} P_l(x)$$

and the spherical harmonics are given by:

$$Y_{lm}(\bar{\Omega}) = \left(\frac{(2l+1)(l-m)!}{4\pi(l+m)!} \right)^{1/2} P_l(\cos \varphi) e^{im\theta}$$

Laguerre polynomials are the solution to the Laguerre differential equation and are given as:

$$P_{\text{Laguerre}}(x) = e^x \frac{d^n (x^n e^{-x})}{dx^n}$$

VIIc. Vector Algebra

1. Definition of Terms

Types of physical quantities: There are three types of physical quantities, *scalar* (temperature), *vector* (velocity), and *tensor* (fluid stress and thermal conductivity). Scalars are zero order tensors. Vectors are first order tensors. A second order tensor is an array of nine components:

$$\tau = \begin{pmatrix} \tau_{xx} & \tau_{xy} & \tau_{xz} \\ \tau_{yx} & \tau_{yy} & \tau_{yz} \\ \tau_{zx} & \tau_{zy} & \tau_{zz} \end{pmatrix}$$

In this section, an arbitrary scalar is represented by f , an arbitrary vector is represented by \vec{A} and an arbitrary tensor is represented by τ .

Coordinate systems: There are three *Orthogonal* systems; Cartesian, cylindrical and spherical coordinates. The Cartesian refers to the rectangular coordinates for x , y , and z . The circular cylinder refers to r , θ , and z and the spherical refers to r , θ , and ϕ . The cylindrical and spherical are examples of *curvilinear* coordinates. The two-dimensional cylindrical coordinate in the x - y plane is referred to as the polar coordinate. The elemental area in the Cartesian coordinates is $dxdy$ and in a polar coordinate is $rdrd\theta$.

If earth is treated as a sphere and P is a point on the earth's surface in the northern hemisphere, for example, then the *latitude* of point P is angle $\alpha = 90^\circ - \phi^\circ$. The *longitude* of point P is $\beta = 360^\circ - \theta^\circ$. The semi-circle in the r - z plane is referred to as the *meridian*.

Differential volume: The elemental volume in Cartesian coordinates is $dV_{\text{Cartesian}} = dxdydz$, in a cylindrical coordinates is $dV_{\text{Cylindrical}} = rdrd\theta dz$, and in a spherical coordinates is $dV_{\text{Spherical}} = r^2 \sin\phi d\theta d\phi dr$.

Unit vector: A vector with the absolute value, magnitude, or length of unity is a unit vector. Thus the unit vector for vector \vec{A} is given by $\vec{u}_a = \vec{A}/|\vec{A}|$. Unit vectors in the Cartesian coordinate system are traditionally shown by \vec{i} , \vec{j} , and \vec{k} . Figure VIIc.1.2 shows the unit vectors in various coordinate systems.

Vector components: A vector, in general, is represented by three components:

$$\vec{A} = A_{u1}\vec{u}_1 + A_{u2}\vec{u}_2 + A_{u3}\vec{u}_3$$

where A_{ui} is the component along the i th axes having a unit vector \vec{u}_i . In the Cartesian coordinate system for example, the vector is represented as $\vec{A} = A_x\vec{i} + A_y\vec{j} + A_z\vec{k}$ where \vec{i} , \vec{j} , and \vec{k} are the unit vectors along x -, y -, and z -

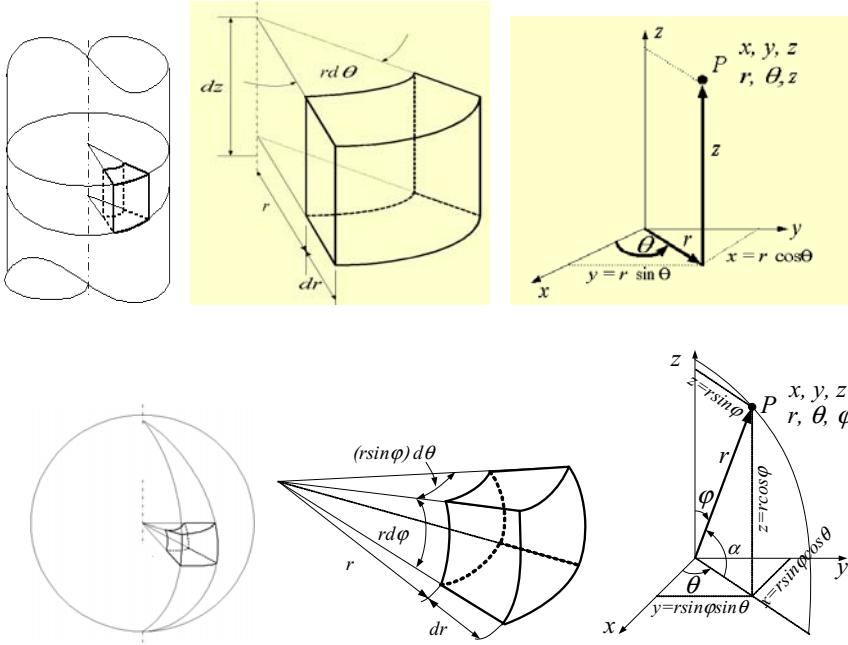


Figure VIIc.1.1. Cylindrical and spherical coordinates in the Cartesian coordinate system

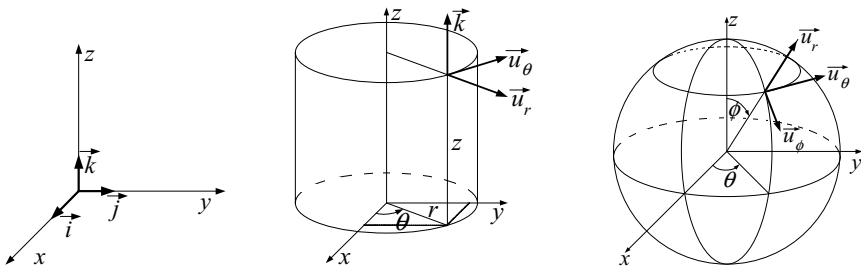


Figure VIIc.1.2. Unit vectors in Cartesian, cylindrical, and spherical coordinates

axes, respectively. In Figure VIIc.1.3, vector \vec{A} is represented by the line segment connecting point $P_1(x_1, y_1, z_1)$ to point $P_2(x_2, y_2, z_2)$ so that:

$$\vec{A} = \vec{r}_2 - \vec{r}_1$$

Substituting for the components comprising vectors r_1 and r_2 we get $A_x = x_2 - x_1$, $A_y = y_2 - y_1$, and $A_z = z_2 - z_1$.

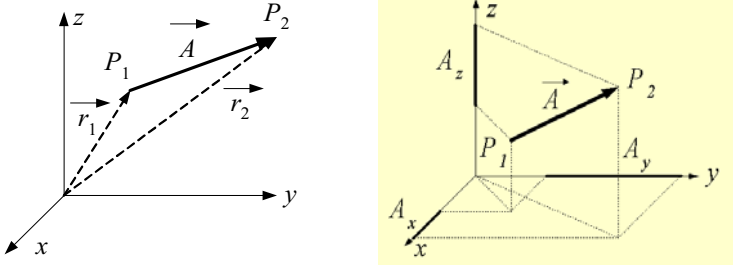


Figure VIIc.1.3. Depiction of vector \vec{A} in Cartesian coordinates

Absolute value of a vector written in the Cartesian coordinate system, for example, is defined as:

$$|\vec{A}| = \sqrt{A_x^2 + A_y^2 + A_z^2}$$

In case of Vector \vec{A} shown in Figure VIIc.1.2, the absolute value is given as:

$$|\vec{A}| = \sqrt{A_x^2 + A_y^2 + A_z^2} = \sqrt{(x_2 - x_1)^2 + (y_2 - y_1)^2 + (z_2 - z_1)^2}$$

Summation of vectors: For vectors \vec{A} and \vec{B} , the summation is defined as:

$$\vec{A} + \vec{B} = (A_x + B_x)\vec{i} + (A_y + B_y)\vec{j} + (A_z + B_z)\vec{k}$$

Scalar or dot product of two vectors results in a scalar. For vectors \vec{A} and \vec{B} , dot product is defined as:

$$\vec{A} \cdot \vec{B} = |\vec{A}||\vec{B}|\cos\varphi$$

Where φ is the angle between the two vectors. Thus, for two vectors in the Cartesian coordinate system, the dot product becomes:

$$\vec{A} \cdot \vec{B} = (A_x\vec{i} + A_y\vec{j} + A_z\vec{k}) \cdot (B_x\vec{i} + B_y\vec{j} + B_z\vec{k}) = (A_xB_x) + (A_yB_y) + (A_zB_z) \quad \text{VIIc.1.1}$$

According to this definition, $\vec{A} \cdot \vec{A} = A^2$.

Example: To find the angle between vector $\vec{A} = 3\vec{i} + 4\vec{j} - 6\vec{k}$ and $\vec{B} = -\vec{i} + 5\vec{j} + 11\vec{k}$, we first find: $\vec{A} \cdot \vec{B} = (3)(-1) + (4)(5) + (-6)(11) = -49$. Next find $|\vec{A}| = \sqrt{3^2 + 16 + 36} = 7.416$, $|\vec{B}| = \sqrt{1 + 25 + 121} = 12.124$, and $\cos(\varphi) = -49/(7.416 \times 12.124) = -0.545$. Therefore, $\varphi = 123^\circ$.

Vector or cross product of two vectors is another vector. The cross product of two vectors is defined as:

$$\vec{C} = \vec{A} \times \vec{B} = \begin{vmatrix} \vec{i} & \vec{j} & \vec{k} \\ A_x & A_y & A_z \\ B_x & B_y & B_z \end{vmatrix} \quad \text{VIIc.1.2}$$

The resultant vector has an absolute value of:

$$|\vec{C}| = |\vec{A} \times \vec{B}| = |\vec{A}| |\vec{B}| \sin \phi$$

According to this definition, $\vec{A} \times \vec{A} = 0$. The resultant vector \vec{C} is perpendicular to the plane of vectors \vec{A} and \vec{B} . The positive direction of vector \vec{C} follows the right-hand rule as shown in Figure VIIc.1.4. According to this definition, $\vec{A} \times \vec{B} = -\vec{B} \times \vec{A}$.

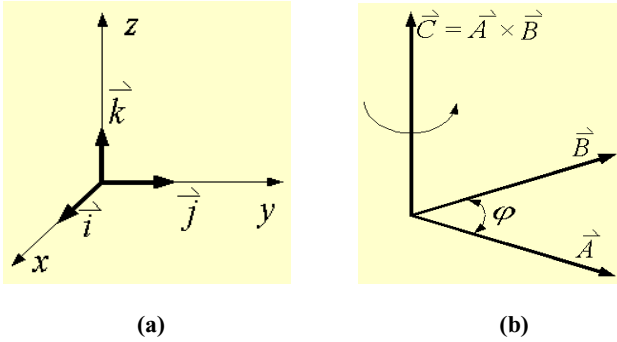


Figure VIIc.1.4. a) Unit vectors in a Cartesian coordinates. b) Depiction of a cross product vector

Differentiation of vectors. Since vector operations are not generally linear operations, care must be exercised in carrying out differentiation of vectors. For example, the dot product is a linear operation. Hence, the derivative of a dot product is also a linear operation:

$$\frac{d}{dt}(\vec{A} \cdot \vec{B}) = \frac{d\vec{A}}{dt} \cdot \vec{B} + \vec{A} \cdot \frac{d\vec{B}}{dt} = \vec{B} \cdot \frac{d\vec{A}}{dt} + \frac{d\vec{B}}{dt} \cdot \vec{A}$$

On the other hand, the cross product of two vectors is not a linear operation. Hence, the derivative of the cross product of two vectors is:

$$\frac{d}{dt}(\vec{A} \times \vec{B}) = \frac{d\vec{A}}{dt} \times \vec{B} + \vec{A} \times \frac{d\vec{B}}{dt} \neq \vec{B} \times \frac{d\vec{A}}{dt} + \frac{d\vec{B}}{dt} \times \vec{A}$$

Linear independence is defined for a set of vectors so that the relation

$$\sum_m c_i \bar{A}_i = 0$$

is satisfied only if the following condition exists for the coefficients

$$c_1 = c_2 = c_3 = \dots c_m = 0$$

Otherwise, the set of vectors would be *linearly dependent*.

Plane normal to a vector. Consider a vector given as $\bar{A} = A_x \bar{i} + A_y \bar{j} + A_z \bar{k}$. The equation of a plane normal to this vector at point $P_0(x_0, y_0, z_0)$ is given as:

$$A_x(x - x_0) + A_y(y - y_0) + A_z(z - z_0) = 0$$

Independence from coordinate system, Symbol *del* as a vector operator. It is very convenient and mathematically elegant to use a symbol for making formulae independent of the coordinate system. Such a symbol is called *del* ($\bar{\nabla}$) and used as a vector operator. For example, in the Cartesian coordinate system, *del* is defined as:

$$\bar{\nabla} = \frac{\partial}{\partial x} \bar{i} + \frac{\partial}{\partial y} \bar{j} + \frac{\partial}{\partial z} \bar{k}$$

Several uses of the *del* operator, such as *gradient*, *divergence*, and *Laplacian* are discussed below.

The Gradient operator ($\bar{\nabla}$). The gradient operator generally acts on a scalar and produces a vector. In the Cartesian coordinate system the *del* operator is written as:

$$\bar{\nabla}f = \frac{\partial f}{\partial x} \bar{i} + \frac{\partial f}{\partial y} \bar{j} + \frac{\partial f}{\partial z} \bar{k} \quad \text{VIIc.1.3}$$

In the cylindrical coordinate system as:

$$\bar{\nabla}f = \frac{\partial f}{\partial r} \bar{u}_r + \frac{1}{r} \frac{\partial f}{\partial \theta} \bar{u}_\theta + \frac{\partial f}{\partial z} \bar{u}_z \quad \text{VIIc.1.4}$$

and in the spherical coordinate system as:

$$\bar{\nabla}f = \frac{\partial f}{\partial r} \bar{u}_r + \frac{1}{r \sin \phi} \frac{\partial f}{\partial \theta} \bar{u}_\theta + \frac{1}{r} \frac{\partial f}{\partial \phi} \bar{u}_\phi \quad \text{VIIc.1.4}$$

The gradient operator may also operate on a vector to produce a tensor, referred to as a *dyad*. For example, in the Cartesian coordinate system:

$$\bar{\nabla}A = \begin{pmatrix} \frac{\partial A_x}{\partial x} & \frac{\partial A_y}{\partial y} & \frac{\partial A_z}{\partial z} \\ \frac{\partial A_y}{\partial x} & \frac{\partial A_x}{\partial y} & \frac{\partial A_z}{\partial y} \\ \frac{\partial A_z}{\partial x} & \frac{\partial A_z}{\partial y} & \frac{\partial A_z}{\partial z} \end{pmatrix}$$

In the discussion below we demonstrate that for $f(x, y, z)$, the gradient of f is in the direction of the normal to the surface S described by f (Figure VIIc.1.5)

$$\frac{\partial f}{\partial n} = \bar{n} \cdot \bar{\nabla}f \quad \text{VIIc.1.5}$$

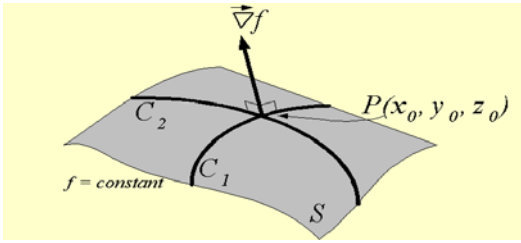


Figure VIIc.1.5. Gradient vector normal to an isothermal or equipotential surface

Consider a function such as $w = f(x, y, z)$. The points at which this function has the same value, such as w_0 has at a specific point $P_0(x_0, y_0, z_0)$, in general constitute a surface in space. The equation of this surface is given as $f(x, y, z) - w_0 = 0$ where w_0 is a constant. In electrical engineering, if w represents the electrical potential, then the surface is called an equipotential surface. In thermal sciences, if w represents temperature, then the surface is called an isothermal surface. It can be shown that the gradient vector is normal to these types of surfaces. For example, suppose we want to find the plane that is tangent to the surface $z = x^2 - y^2$ at point $P_0(2, 1, 3)$. To find the equation of such a plane we should find the gradient at point P_0 which, we know is normal to the above surface (i.e., surface $z = x^2 - y^2$). To do this, we first write the equation of the surface as $f(x, y, z) = x^2 - y^2 - z = 0$ and then find the gradient vector:

$$\bar{\nabla}f = \frac{\partial f}{\partial x} \bar{i} + \frac{\partial f}{\partial y} \bar{j} + \frac{\partial f}{\partial z} \bar{k} = 2x\bar{i} - 2y\bar{j} - \bar{k}$$

The gradient vector at the specified point is $\bar{\nabla}f = 2x\bar{i} - 2y\bar{j} - \bar{k} = 4\bar{i} - 2\bar{j} - \bar{k}$. This vector is normal to surface $z = x^2 - y^2$ at P_0 . The equation of the plane normal to this vector hence tangent to the surface at P_0 is $4(x - 2) - 2(y - 1) - 3(z - 3) = 0$ or $3z + 2y - 4x = 1$. Later in this section, the application of the gradient operator in developing surface integrals is discussed.

The divergence operator ($\bar{\nabla} \cdot$). Divergence acts on a vector and produces a scalar. In Cartesian coordinates system, the divergent operator is written as:

$$\bar{\nabla} \cdot \bar{A} = \frac{\partial A_x}{\partial x} + \frac{\partial A_y}{\partial y} + \frac{\partial A_z}{\partial z} \quad \text{VIIc.1.6}$$

in the cylindrical coordinate system as:

$$\bar{\nabla} \cdot \bar{A} = \frac{1}{r} \frac{\partial}{\partial r}(r A_r) + \frac{1}{r} \frac{\partial A_\theta}{\partial \theta} + \frac{\partial A_z}{\partial z} \quad \text{VIIc.1.7}$$

and in the spherical coordinate system as:

$$\bar{\nabla} \cdot \bar{A} = \frac{1}{r^2} \frac{\partial}{\partial r}(r^2 A_r) + \frac{1}{r \sin \phi} \frac{\partial A_\theta}{\partial \theta} + \frac{1}{r \sin \phi} \frac{\partial}{\partial \phi}(A_\phi \sin \phi) \quad \text{VIIc.1.8}$$

If vector \bar{A} happens to be the gradient of a scalar, then the divergence operation produces *Laplacian*:

$$\bar{\nabla} \cdot \bar{A} = \bar{\nabla} \cdot (\bar{\nabla} f) = \nabla^2 f$$

The Laplacian operator (∇^2). This operator primarily acts on scalars and produces scalars:

$$\nabla^2 f = \frac{\partial^2 f}{\partial x^2} + \frac{\partial^2 f}{\partial y^2} + \frac{\partial^2 f}{\partial z^2} \quad \text{VIIc.1.9}$$

The Laplacian operator in the cylindrical coordinate system is written as:

$$\nabla^2 f = \frac{1}{r} \frac{\partial}{\partial r}(r \frac{\partial f}{\partial r}) + \frac{1}{r^2} \frac{\partial^2 f}{\partial \theta^2} + \frac{\partial^2 f}{\partial z^2} \quad \text{VIIc.1.10}$$

and in the spherical coordinate system as:

$$\nabla^2 f = \frac{1}{r^2} \frac{\partial}{\partial r}(r^2 \frac{\partial f}{\partial r}) + \frac{1}{r^2 \sin^2 \phi} \frac{\partial^2 f}{\partial \theta^2} + \frac{1}{r^2 \sin \phi} \frac{\partial}{\partial \phi}(\sin \phi \frac{\partial f}{\partial \phi}) \quad \text{VIIc.1.11}$$

Laplacian may also operate on vectors but the vectors must be written in the Cartesian coordinate system. The Laplacian of vector \bar{A} in the Cartesian coordinate system is given as:

$$\nabla^2 \bar{A} = \left(\frac{\partial^2 A_x}{\partial x^2} + \frac{\partial^2 A_x}{\partial y^2} + \frac{\partial^2 A_x}{\partial z^2} \right) \bar{i} + \left(\frac{\partial^2 A_y}{\partial x^2} + \frac{\partial^2 A_y}{\partial y^2} + \frac{\partial^2 A_y}{\partial z^2} \right) \bar{j} + \left(\frac{\partial^2 A_z}{\partial x^2} + \frac{\partial^2 A_z}{\partial y^2} + \frac{\partial^2 A_z}{\partial z^2} \right) \bar{k}$$

For a vector written in other (i.e. cylindrical and spherical) orthogonal coordinate systems, the Laplacian can be found from:

$$\nabla^2 \vec{A} = \vec{\nabla}(\vec{\nabla} \cdot \vec{A}) - \vec{\nabla} \times (\vec{\nabla} \times \vec{A})$$

The Curl operator ($\vec{\nabla} \times$). This operator acts on vectors and produces vectors. The curl operator in the Cartesian coordinate system can be obtained from the definition of the cross products of two vectors:

$$\vec{\nabla} \times \vec{A} = \begin{vmatrix} \vec{i} & \vec{j} & \vec{k} \\ \frac{\partial}{\partial x} & \frac{\partial}{\partial y} & \frac{\partial}{\partial z} \\ A_x & A_y & A_z \end{vmatrix} \quad \text{VIIc.1.12}$$

The result is the following vector:

$$\vec{\nabla} \times \vec{A} = \left(\frac{\partial A_z}{\partial y} - \frac{\partial A_y}{\partial z} \right) \vec{i} - \left(\frac{\partial A_z}{\partial x} - \frac{\partial A_x}{\partial z} \right) \vec{j} + \left(\frac{\partial A_y}{\partial x} - \frac{\partial A_x}{\partial y} \right) \vec{k}$$

The curl operator in the cylindrical coordinate system is written as:

$$\vec{\nabla} \times \vec{A} = \frac{1}{r} \begin{vmatrix} \vec{u}_r & r\vec{u}_\theta & \vec{u}_z \\ \frac{\partial}{\partial r} & \frac{\partial}{\partial \theta} & \frac{\partial}{\partial z} \\ A_r & rA_\theta & A_z \end{vmatrix} \quad \text{VIIc.1.13}$$

Finally, the curl operator in the spherical coordinate system is given as:

$$\vec{\nabla} \times \vec{A} = \frac{1}{r^2 \sin \phi} \begin{vmatrix} \vec{u}_r & r \sin \phi \vec{u}_\theta & r\vec{u}_\phi \\ \frac{\partial}{\partial r} & \frac{\partial}{\partial \theta} & \frac{\partial}{\partial \phi} \\ A_r & r \sin \phi A_\theta & rA_\phi \end{vmatrix} \quad \text{VIIc.1.14}$$

If a vector is the gradient of a potential function, then the curl of such a vector is always equal to zero, $\vec{\nabla} \times (\vec{\nabla} f) = 0$. Later in this section, the application of the curl operator in Stokes' theorem is discussed.

Classical mechanics Hamiltonian operator in the Cartesian coordinate system is defined as:

$$H_{CM}(\vec{p}, \vec{r}, t) = \frac{1}{2m} (p_x^2 + p_y^2 + p_z^2) + V(x, y, z)$$

where m is mass, p is momentum, and V represents the potential energy of a particle.

Quantum mechanics Hamiltonian operator is defined as

$$H_{QM}(\vec{p}, \vec{r}, t) = \frac{-\hbar^2}{2m} \nabla^2 + V(\vec{r})$$

Some useful relations in vector algebra. The relations listed here are frequently used in vector algebra:

$$\begin{aligned}\bar{\nabla} \times (\bar{\nabla} f) &= 0 \\ \bar{\nabla} \cdot (\bar{\nabla} \times \vec{A}) &= 0 \\ \bar{\nabla} \cdot f\vec{A} &= f\bar{\nabla} \cdot \vec{A} + \vec{A} \cdot \bar{\nabla} f \\ \bar{\nabla} \times (f\vec{A}) &= f\bar{\nabla} \times \vec{A} + \bar{\nabla} f \times \vec{A} \\ (\vec{A} \cdot \bar{\nabla})\vec{A} &= \frac{1}{2}\bar{\nabla}(\vec{A} \cdot \vec{A}) - \vec{A} \times (\bar{\nabla} \times \vec{A}) \\ \bar{\nabla} \times (\vec{A} \times \vec{B}) &= \vec{B} \cdot (\bar{\nabla}\vec{A}) - \vec{A} \cdot (\bar{\nabla}\vec{B}) + \vec{A}(\bar{\nabla} \cdot \vec{B}) - \vec{B}(\bar{\nabla} \cdot \vec{A})\end{aligned}$$

Substantial derivative operator D/Dt . The substantial derivative is a mathematical operator that can operate on both scalars or vectors, provided the vector is written in the Cartesian coordinate system:

$$\frac{Df}{Dt} = (\vec{V} \cdot \bar{\nabla} f) + \frac{\partial f}{\partial t} \quad \text{VIIc.1.15}$$

where \vec{V} is the flow field velocity vector. We can find the substantial derivative of vectors written in other orthogonal coordinate systems by using Equation VIIc.1.15 in conjunction with the above vector relations.

Dyadic product of two vectors is a special form of a second-order tensor:

$$\vec{v}\vec{w} = \begin{pmatrix} v_1 w_1 & v_1 w_2 & v_1 w_3 \\ v_2 w_1 & v_2 w_2 & v_2 w_3 \\ v_3 w_1 & v_3 w_2 & v_3 w_3 \end{pmatrix}$$

Note that, according to this definition, $\vec{v}\vec{w} \neq \vec{w}\vec{v}$.

Line, surface, and volume integrals. Integration of vectors along lines and over surfaces and volumes are used to explain various physical phenomena. For example, the Stokes theorem as used in flow as well as electrical fields relates line integrals along a closed path to the surface integral enclosed by the path. The divergence or Gauss theorem relates a volume integral to the surface integral enclosing the volume.

Line integral of a vector along the segment path C , shown in Figure VIIc.1.6, is defined as:

$$\int_C \vec{A} \cdot d\vec{r} = \int_{P_1}^{P_2} (A_x dx + A_y dy + A_z dz) \quad \text{VIIc.1.19}$$

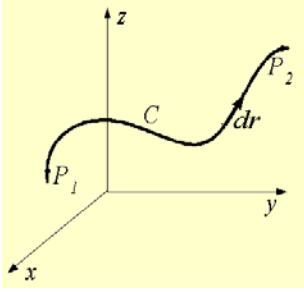


Figure VIIc.1.6. Line integral along a segment in Cartesian coordinate system

which indicates the path-dependence of line integrals. For example, consider the intersection of surface $z = xy^2$ and plane $z = 1$. We would like to integrate vector $\vec{A} = 3y\vec{i} + xz^3\vec{j} - zy^3\vec{k}$ along this segment from point P_1 located at 1, 1, 1 to point P_2 located at 0.25, 2, 1. We first find the dot product of the vector by the elemental segment as:

$$\vec{A} \cdot d\vec{r} = 3ydx + xz^3dy - zydz$$

Since $z = xy^2 = 1$ this results in $dz = 0$. Taking the derivative of the function representing the segment:

$$y^2dx + 2xydy = 0$$

from this equation, we find $dx = -x dy/y$. Substituting for x from $xy^2 = 1$, we obtain $dx = -dy/y^3$. Therefore, the integral of the dot product becomes:

$$\int_{P_1}^{P_2} \vec{A} \cdot d\vec{r} = \int_{P_1}^{P_2} 3ydx + xz^3dy - zydz = \int_{y=1}^{y=2} -3\frac{dy}{y^2} + \frac{dy}{y^2} = \left[\frac{2}{y} \right]_{y=1}^{y=2} = -1$$

To verify that the result depends on the path, we may assume a different path connecting the same points P_1 and P_2 , such as $z = xy^3$. In this case, the derivative of the function representing the path becomes $y^3dx + 3xy^2dy = 0$. Hence, we have $dx = -3x dy/y$. Substituting for x , the derivative becomes $dx = -3dy/y^4$. Finally

$$\int_{P_1}^{P_2} \vec{A} \cdot d\vec{r} = \int_{P_1}^{P_2} 3ydx + xz^3dy - zydz = \int_{y=1}^{y=2} -9\frac{dy}{y^3} + \frac{dy}{y^3} = \left[\frac{4}{y^2} \right]_{y=1}^{y=2} = -3$$

Special Case. Now, consider a case where vector \vec{A} is gradient of a potential function (i.e. $\vec{A} = \vec{\nabla}f$) (recall that $\vec{\nabla} \times \vec{A} = 0$). In this case, the line integral becomes independent of the path and depends only on the end points P_1 and P_2 . To demonstrate, we substitute the gradient in Equation VIIc.1.19. This results in the

argument of the integral to be an exact differential (see definition given in Section 1), which upon integration would depend only on the end points.

$$\int_C \vec{A} \cdot d\vec{r} = \int_C \vec{\nabla}f \cdot d\vec{r} = \int_{P_1}^{P_2} \left(\frac{\partial f}{\partial x} dx + \frac{\partial f}{\partial y} dy + \frac{\partial f}{\partial z} dz \right) = \int_{P_1}^{P_2} df = f(P_2) - f(P_1)$$

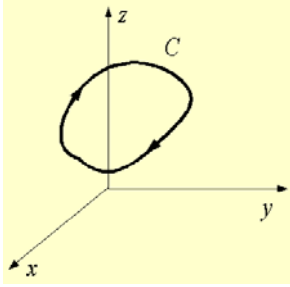


Figure VIIc.1.7. Line integral along a closed path or loop

If this differential is integrated along a loop, as shown in Figure VIIc.1.7, the line integral becomes zero:

$$\int_C \vec{A} \cdot d\vec{r} = \oint_C \vec{\nabla}f \cdot d\vec{r} = \oint df = 0$$

where the circle on the integral symbol emphasizes closed path integration. For example, if we want to find the integral of $\vec{A} = y^2 z^3 \vec{i} + 2xyz^3 \vec{j} + 3xy^2 z^2 \vec{k}$ along a segment from points $P_1(0, 0, 0)$ to $P_2(1, 1, 1)$, we need not to be concerned about the function that represents the segment, as the given vector is the gradient of the potential function $f = xy^2 z^3$. Therefore:

$$\int_C \vec{A} \cdot d\vec{r} = \int_{P_1}^{P_2} y^2 z^3 dx + 2xyz^3 dy + 3xy^2 z^2 dz = \int_{P_1}^{P_2} d(xy^2 z^3) = [xy^2 z^3]_{P_1}^{P_2} = 1$$

The integration of an exact differential depends only on the end points and is independent of the path. We may also try to find the result of the integration along a closed path:

$$\oint_C \vec{A} \cdot d\vec{r} = \oint_C y^2 z^3 dx + 2xyz^3 dy + 3xy^2 z^2 dz = \int_{P_1}^{P_1} d(xy^2 z^3) = [xy^2 z^3]_{P_1}^{P_1} = 0$$

Hence we conclude that if $\vec{\nabla} \times \vec{A} = 0$ then $\oint_C \vec{A} \cdot d\vec{r} = 0$.

Potential energy and conservative force. These terms are applied in the special case where the value of the line integral is independent of the path. In this case, if vector \vec{A} represents force, then the function f is known as the potential of \vec{A} . Additionally, $-f$ is called the *potential energy* associated with force \vec{A} and the force itself is said to be *conservative*.

Definition of surface and volume integrals. Integral of vector \vec{A} over surface S is defined as the summation of the dot products of \vec{A} and the normal vector \vec{n} representing an elemental area ds . If the elemental area is sufficiently small, then the summation becomes:

$$I = \iint_S \vec{A} \cdot d\vec{s} = \iint_S \vec{A} \cdot \vec{n} ds \quad \text{VIIc.1.20}$$

where \vec{n} is the unit vector normal to the elemental surface ds of surface S , as shown in Figure VIIc.1.8. Similar definition applies to a volume integral. If surface S is a closed surface (i.e., contains a volume), then the surface integral is written as:

$$I = \oiint_S \vec{A} \cdot d\vec{s} = \oiint_S \vec{A} \cdot \vec{n} ds \quad \text{VIIc.1.20-1}$$

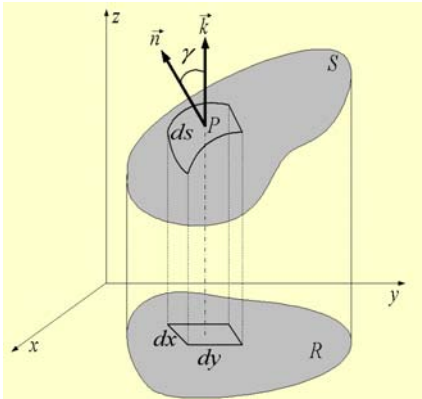


Figure VIIc.1.8. Depiction of surface and the normal vector

To find an alternative way to express Equation VIIc.1.20-1, we seek to express the unit vector normal to the surface in terms of the function representing the surface. To do this, you may recall that the gradient of function $w = f(x, y, z)$ is normal to the surface described by w . We may then express the gradient vector in terms of the unit vector of the surface:

$$\vec{\nabla} w = |\vec{\nabla} w| \vec{n}$$

Since $\vec{\nabla}w = (\partial w/\partial x)\vec{i} + (\partial w/\partial y)\vec{j} + (\partial w/\partial z)\vec{k}$ and

$|\vec{\nabla}| = \sqrt{(\partial w/\partial x)^2 + (\partial w/\partial y)^2 + (\partial w/\partial z)^2}$ then

$$\vec{n} = \frac{\partial w/\partial x\vec{i} + \partial w/\partial y\vec{j} + \partial w/\partial z\vec{k}}{\sqrt{(\partial w/\partial x)^2 + (\partial w/\partial y)^2 + (\partial w/\partial z)^2}} \quad \text{VIIc.1.21}$$

If the surface is closed (i.e. for surfaces that contain a volume), vector \vec{n} traditionally points outward. We now find projection of the elemental surface ds on the xy -plane. Since

$$ds = dx dy \cos \gamma$$

and the fact that the unit vector \vec{k} is perpendicular to the xy -plane, we alternatively write this as:

$$|\vec{n} \cdot \vec{k}| ds = dx dy$$

On the other hand, the dot product of two unit vectors is equal to the cosine of the angle between, hence:

$$\cos \gamma = \vec{n} \cdot \vec{k} = \pm \frac{\partial w/\partial z}{\sqrt{(\partial w/\partial x)^2 + (\partial w/\partial y)^2 + (\partial w/\partial z)^2}} \quad \text{VIIc.1.22}$$

Putting all these together, we can alternatively write the surface integral (Equation VIIc.1.20-1) as:

$$I = \iint_S \vec{A} \cdot d\vec{s} = \iint_S \vec{A} \cdot \vec{n} ds = \iint_S \vec{A} \cdot \vec{n} \frac{1}{\cos \gamma} dx dy \quad \text{VIIc.1.23}$$

For example, suppose we want to find the surface integral of vector $\vec{A} = 2x\vec{i} + 2y\vec{j}$ over the hemisphere shown in Figure VIIc.1.9. For this purpose, we first determine the unit vector normal to the surface. The surface function is $w = x^2 + y^2 + z^2 - 1$. The components of the unit vector then become $2x$, $2y$, and $2z$. The absolute value of the unit vector is 2. Therefore, the unit vector of the hemisphere is:

$$\vec{n} = x\vec{i} + y\vec{j} + z\vec{k}$$

Cosine of the angle between the unit vector normal to the surface and the unit vector normal to the xy -plane from Equation VIIc.1.22 becomes $\cos \gamma = z$. Therefore, from Equation VIIc.1.23, we have:

$$I = \iint_S \vec{A} \cdot \vec{n} \frac{1}{\cos \gamma} dx dy = \iint_S (2x\vec{i} + 2y\vec{j}) \cdot (x\vec{i} + y\vec{j} + z\vec{k}) \frac{dx dy}{z} = \iint_T 2(x^2 + y^2) \frac{dx dy}{z}$$

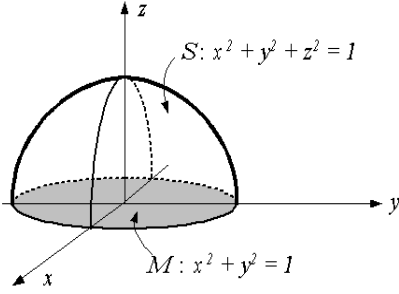


Figure VIIc.1.9. Hemisphere for calculation of a surface integral

Where the surface integral is now developed on the circle M which is the projection of the hemisphere. Replacing z from the function representing the hemisphere surface,

$$I = \iint_T 2(x^2 + y^2) \frac{dxdy}{z} = 4 \int_{x=0}^1 \int_{y=0}^{\sqrt{1-x^2}} \frac{2(x^2 + y^2)}{\sqrt{1-x^2-y^2}} dxdy$$

Note that the limits of the double integral span only one quarter of the circle in the xy -plane (i.e. in the $+x$ and $+y$ region). Due to symmetry we multiplied the integral by 4 to cover the entire surface of the circle. We practically solved the bulk of the problem. The rest deals with carrying out this integral. Generally, it is easier to carry out double integrals in a polar coordinate. Recall that in polar coordinates, $x = r \cos \theta$ and $y = r \sin \theta$. Therefore, $x^2 + y^2 = r^2$ and $dxdy = r dr d\theta$. Therefore, the integral becomes:

$$I = 8 \int_{x=0}^1 \int_{y=0}^{\sqrt{1-x^2}} \frac{(x^2 + y^2)}{\sqrt{1-x^2-y^2}} dxdy = 8 \int_{\theta=0}^{\pi/2} \int_{r=0}^1 \frac{r^2}{\sqrt{1-r^2}} r dr d\theta = 8\pi/3$$

Carrying out surface integrals is generally not a straightforward integration. This can be easily verified by trying to integrate $\vec{A} = x\vec{i} + y\vec{j} + z\vec{k}$ over the same hemisphere surface instead of the vector used in the above example. The difficulty of integration over surfaces is remedied by Gauss's divergence theorem.

Gauss divergence theorem relates an integral over a closed surface to an integral in the volume enclosed by the surface. For example, if volume V is enclosed by surface S , then:

$$\iiint_V (\nabla \cdot \vec{A}) dV = \oiint_S \vec{A} \cdot d\vec{s} = \oiint_S \vec{A} \cdot \vec{n} ds$$

An intuitive case is when volume V is a sphere and \vec{A} represents density of an incompressible fluid multiplied by the flow velocity (mass flux). In this case, the rate of change of mass inside the sphere is due to the flow of the incompressible liquid across the surface of the sphere.

We now try to solve the previous example of integration over the surface of a hemisphere. To obtain a closed surface, we use the circle obtained from the intersection of the xy -plane with the hemisphere to contain the volume. We note that the integral of the given vector over this surface is zero because the given vector has no component in the z -direction. Therefore, the integral over the surface of the hemisphere is equal to the divergence of the given vector in the volume of the hemisphere. The divergence of the given vector is $\vec{\nabla} \cdot \vec{A} = 4$. Therefore:

$$\oint_S \vec{A} \cdot \vec{n} ds = \iiint_V (\vec{\nabla} \cdot \vec{A}) dV = 4 \iiint_V dV = 4(2\pi/3) = 8\pi/3$$

As an exercise, the reader may develop the surface integral of $\vec{A} = x\vec{i} + y\vec{j} + z\vec{k}$ over the hemisphere of Figure VIIc.1.8.

Stokes curl theorem is the two dimensional form of the Gauss's theorem. It expresses that the circulation of a vector around a closed curve C is equal to the flux of the vector over S , the area enclosed by C :

$$\oint_C \vec{A} \cdot d\vec{r} = \iint_S (\vec{\nabla} \times \vec{A}) \cdot d\vec{S} = \iint_S (\vec{\nabla} \times \vec{A}) \cdot \vec{n} ds \quad \text{VIIc.1.24}$$

where $d\vec{r}$ is an elemental vector in the direction of integration along curve C and \vec{n} is the unit vector normal to the elemental area ds . Directions of these two vectors are as follows: if unit vector $d\vec{r}$ moves counterclockwise around the horizontal curve C (right-hand screw), the direction of unit vector \vec{n} is upward, if the elemental vector $d\vec{r}$ moves clockwise around the horizontal curve C (right-hand screw), the direction of unit vector \vec{n} is downward. For example, let us verify the Stokes curl theorem for the paraboloid of Figure VIIc.1.10. The function representing the surface is given by $z = 1 - x^2 - y^2$ and the function representing the intersection with the xy plane is given by $x^2 + y^2 = 1$. These are surfaces S and M in Figure VIIc.1.10, respectively.

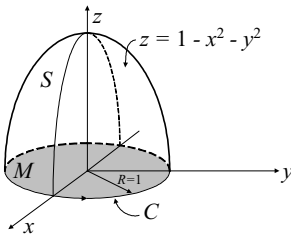


Figure VIIc.1.10. Depiction of a circular paraboloid

The goal is to first develop the line integral of the vector:

$$\vec{A} = (z - y)\vec{i} + (z + x)\vec{j} - (x + y)\vec{k}$$

along the closed path C , $I_1 = \oint_C \vec{A} \cdot d\vec{r}$. Then to carry out $I_2 = \iint_S \vec{\nabla} \times \vec{A} \cdot \vec{n} ds$ and

to show that $I_1 = I_2$. To develop the line integral:

$$I_1 = \oint_C [(z - y)\vec{i} + (z + x)\vec{j} - (x + y)\vec{k}] \cdot [dx\vec{i} + dy\vec{j} + dz\vec{k}] = \oint_C [(z - y)dx + (z + x)dy - (x + y)dz]$$

we first note that the integration is along path C , which is in the xy plane. As a result, I_1 simplifies to:

$$I_1 = \oint_C [(z - y)dx + (z + x)dy - (x + y)dz] = \oint_C [-ydx + xdy]$$

To simplify integration, we take advantage of the polar coordinates. This is true, as in this case, r remains constant ($r = R = 1$). Hence, we are replacing both x and y with a single variable θ . To do this, recall that $x = r \cos \theta$ and $y = r \sin \theta$. Setting $r = 1$ and substituting x and y into I_1 we get:

$$I_1 = \oint_C [-ydx + xdy] = \int_{\theta=0}^{2\pi} [-(\sin \theta)(-\sin \theta d\theta) + (\cos \theta)(\cos \theta d\theta)] = \int_{\theta=0}^{2\pi} d\theta = 2\pi$$

Let's now try the surface integral. For this purpose, we must first find the curl of the given vector:

$$\vec{\nabla} \times \vec{A} = \begin{vmatrix} \vec{i} & \vec{j} & \vec{k} \\ \frac{\partial}{\partial x} & \frac{\partial}{\partial y} & \frac{\partial}{\partial z} \\ z - y & z + x & -x - y \end{vmatrix} = 2(-\vec{i} + \vec{j} + \vec{k})$$

Next, we need to find the unit vector normal to surface S and the cosine of the angle between the unit vectors normal to the surfaces S and M . The unit vector normal to S is given by Equation VIIc.1.21 where w for a positive unit vector normal to the surface of the paraboloid is $w = z + x^2 + y^2 - 1$:

$$A = [a_{ij}]_{mn}$$

Therefore;

$$\vec{\nabla} \times \vec{A} \cdot \vec{n} = 2(-\vec{i} + \vec{j} + \vec{k}) \cdot \frac{2x\vec{i} + 2y\vec{j} + \vec{k}}{\sqrt{4(x^2 + y^2) + 1}} = \frac{-4x + 4y + 2}{\sqrt{4(x^2 + y^2) + 1}}$$

Finally the cosine of the angle between the unit vector normal to S and the unit vector normal to M is given by Equation VIIc.1.22 as:

$$6 \cos \gamma = \frac{\partial w / \partial z}{\sqrt{(\partial w / \partial x)^2 + (\partial w / \partial y)^2 + (\partial w / \partial z)^2}} = \frac{1}{\sqrt{4(x^2 + y^2) + 1}}$$

We now can find I_2 as:

$$I_2 = \iint_S \bar{\nabla} \times \bar{A} \cdot \bar{n} ds = \iint_S \bar{\nabla} \times \bar{A} \cdot \bar{n} \frac{dxdy}{\cos \gamma}$$

Substituting for the dot product of the cosine, I_2 becomes:

$$I_2 = \iint_M (-4x + 4y + 2) dxdy = -4 \iint_M x dxdy + 4 \iint_M y dxdy + \iint_M 2 dxdy$$

where the first two integrals on the right-hand side cancel out. Hence, I_2 finally becomes:

$$I_2 = 2 \int_{r=0}^1 r dr \int_{\theta=0}^{2\pi} d\theta = 2\pi$$

The Stokes curl theorem is useful in finding an alternative to complicated line integrals. This is because, in the Gauss divergence theorem and the Stokes curl theorem, the derivative of the vector is taken, which reduces the degree of the involved terms.

Green's theorem. Consider ϕ_1 and ϕ_2 as two scalar functions of position. Green's theorem states:

$$\iiint_V (\phi_1 \nabla^2 \phi_2 - \bar{\nabla} \phi_1 \cdot \bar{\nabla} \phi_2) dV = \oiint_S \phi_1 \bar{\nabla} \phi_2 \cdot \bar{n} ds$$

Green's theorem can alternatively be written as:

$$\iiint_V (\phi_1 \nabla^2 \phi_2 - \phi_2 \nabla^2 \phi_1) dV = \oiint_S (\phi_1 \nabla \phi_2 - \phi_2 \nabla \phi_1) \cdot \bar{n} ds$$

where surface S contains volume V . There are two special cases to this theorem. In the first case, the two scalar functions are equal. In this special case, Green's theorem becomes:

$$\iiint_V [\phi \nabla^2 \phi - (\nabla \phi)^2] dV = \oiint_S \phi \nabla \phi \cdot \bar{n} ds = \oiint_S \phi \frac{\partial \phi}{\partial n} ds$$

In the second special case, one function is zero:

$$\iiint_V \nabla^2 \phi dV = \oint_S \frac{\partial \phi}{\partial n} ds \quad \text{VIIc.1.25}$$

Leibnitz formula for differentiating integrals provides a useful means of differentiating integrals without the need to carry out integrals if there is no analytic means of integration. For example, if the derivative of $\phi(x)$ is needed where $\phi(x)$ is given as an integral function of $f(x)$,

$$\phi(x) = \int_{A(x)}^{B(x)} f(x, t) dt$$

then, $\phi'(x)$ is given as:

$$\frac{d}{dx} \int_{A(x)}^{B(x)} f(x, t) dt = \int_{A(x)}^{B(x)} \frac{\partial f(x, t)}{\partial x} dt + f(x, B) \frac{dB}{dx} - f(x, A) \frac{dA}{dx} \quad \text{VIIc.1.26}$$

where $f(x, t)$, $A(x)$, and $B(x)$ must be continuously differentiable with respect to x .

Example: Find the derivative of y with respect to x given $y(x) = \int_x^{x^2} tx^2 dt$

Solution: Since $f(x, t) = tx^2$, $A(x) = x$, and $B(x) = x^2$. Hence, $\partial f(x, t) / \partial x = 2xt$, $dB/dx = 2x$, and $dA/dx = 1$. Substituting in Equation VIIc.1.26 yields:

$$\frac{d}{dx} \int_x^{x^2} tx^2 dt = \int_x^{x^2} 2tx dt + (x^4)(2x) - (x^3)(1) = (xt^2)_x^{x^2} + 2x^5 - x^3 = 3x^5 - 2x^3$$

To verify the results we obtained, we may directly integrate the given function and substitute the limits:

$$y(x) = \int_x^{x^2} tx^2 dt = x^2 \left(t^2 / 2 \right)_x^{x^2} = (x^6 - x^4) / 2$$

Thus, $dy(x)/dx = (6x^5 - 4x^3)/2 = 3x^5 - 2x^3$, which verifies the results obtained above. In this example, we could easily carry out the integral with respect to t and then take the derivative with respect to x . However, the Leibnitz rule is helpful in cases where the integral can not be easily carried out. For example, see Equation IVa.9.10.

Leibnitz formula for differentiating a triple integral is a description of the Lagrangian versus Eulerian viewpoints in describing a flow field, as discussed in Chapter IIIa. The Leibnitz formula for differentiating a triple integral is an extension of the Leibnitz formula for differentiation of an integral. This formula states

that the rate of change of $c(x, y, z, t)$, either a scalar or a vector, in a closed region V is given by:

$$\frac{d}{dt} \iiint_V c(\vec{r}, t) dV = \iiint_V \frac{\partial c(\vec{r}, t)}{\partial t} dV + \oint_S c(\vec{r}, t) \vec{V}_S \cdot d\vec{S} \quad \text{VIIc.1.27}$$

In Equation VIIc.1.27, \vec{V}_S represents the velocity of surface S , encompassing volume V . If Volume V is a deformable volume then \vec{V}_S is a function of spatial coordinate. If volume V is accelerating or decelerating then \vec{V}_S is also a function of time. Thus in general, $\vec{V}_S = f(\vec{r}, t)$. Also $d\vec{S} = dS \vec{n}$, where \vec{n} is the unit vector of surface S .

Equation VIIc.1.27 is the expression of the *general transport theorem*. If volume V contains certain fluid mass encompassed by surface S , the surface velocity becomes the fluid velocity V (i.e., $\vec{V}_S = \vec{V}$), the total derivative (d/dt) is replaced by the substantial derivative, and Equation VIIc.1.27 is written as:

$$\frac{D}{Dt} \iiint_{V_m} c(\vec{r}, t) dV = \iiint_{V_m} \frac{\partial c(\vec{r}, t)}{\partial t} dV + \oint_{S_m} c \vec{V} \cdot d\vec{S} \quad \text{VIIc.1.28}$$

where V_m stands for the material volume enclosed by S_m . Equation VIIc.1.28 is now referred to as the *Reynolds transport theorem*. We may relate the total and the substantial derivatives by eliminating the volume integral of the partial derivative to obtain the relation between the control volume and the material volume at the instant they coincide:

$$\frac{D}{Dt} \iiint_V c(\vec{r}, t) dV = \frac{d}{dt} \iiint_V c(\vec{r}, t) dV + \oint_S c(\vec{r}, t) \vec{V}_r \cdot d\vec{S} \quad \text{VIIc.1.29}$$

where in Equation VIIc.1.29, $\vec{V}_r = \vec{V} - \vec{V}_s$ represents the relative velocity of the fluid in volume V with respect to the velocity of surface S encompassing volume V . The intensive and extensive properties of a system can be related if we introduce y such that $y = c(\vec{r}, t) / \rho$. The integral in the left side can then be replaced by Y so that $y = DY/Dm$. Substituting, Equation VIIc.1.29 simplifies to:

$$\frac{DY}{Dt} = \frac{d}{dt} \iiint_V y \rho dV + \oint_S y \rho \vec{V}_r \cdot d\vec{S} \quad \text{VIIc.1.30}$$

Equation VIIc.1.30 applies to a general case of deformable and moving control volumes. In a specific case that the control volume is fixed ($V_s = 0$, $V_r = V$), Equation VIIc.1.30 can be written as:

$$\frac{DY}{Dt} = \iiint_V \frac{\partial}{\partial t} (y \rho) dV + \oint_S y \rho \vec{V} \cdot d\vec{S} = \frac{\partial}{\partial t} \iiint_V y \rho dV + \oint_S y \rho \vec{V} \cdot d\vec{S} \quad \text{VIIc.1.31}$$

For example, a control volume representing a pump is a fixed control volume. In contrast, filling a balloon or draining a tank requires deformable control volumes to represent the air in the balloon or water in the tank.

Harmonic functions. A harmonic function is the solution to the Laplace differential equation VIIa.1.1 that has continuous second-order partial derivative.

Vllid. Linear Algebra

1. Definition of Terms

Row vector. A row vector is a group of real numbers written in a row. For example, the row vector A is defined as $A = [a_1, a_2, a_3, \dots, a_n]$. Each individual number in this vector is referred to as a component.

Column vector. A column vector is a group of real numbers written in a column. If the column vector has n numbers, then the column vector is an n -dimensional vector or a vector of order n .

Equal vectors. Two row vectors or two column vectors are equal if they are of the same order and have identical components.

Addition of vectors. Only vectors of the same type (row or column) and the same order can be added. For example, the addition of two row vectors of order n is given as:

$$A + B = [a_1, a_2, a_3, \dots, a_n] + [b_1, b_2, b_3, \dots, b_n] = [a_1 + b_1, a_2 + b_2, a_3 + b_3, \dots, a_n + b_n]$$

Commutative laws of addition. For any n -dimensional row (or column) vectors such as vectors A and B :

$$A + B = B + A$$

Associative laws of addition. If A , B , and C are any n -dimensional row (or column) vectors:

$$(A + B) + C = A + (B + C)$$

Multiplication of a vector by a number. If A is an n -dimensional row vector, then the product of A by a real number c is given as: $cA = [ca_1, ca_2, ca_3, \dots, ca_n]$.

Multiplication of vectors. If A is a row vector and B a column vector, then the product of $A \cdot B$ is a scalar given by:

$$A \cdot B = [a_{11}, a_{12}, a_{13}, \dots, a_{1n}] \begin{bmatrix} b_{11} \\ b_{21} \\ b_{31} \\ \vdots \\ b_{n1} \end{bmatrix} = (a_{11}b_{11} + a_{12}b_{21} + a_{13}b_{31} + \dots + a_{1n}b_{n1}) = \left[\sum_{k=1}^n a_{1k}b_{k1} \right]$$

Now consider multiplication of a column vector and a row vector:

$$A \cdot B = \begin{bmatrix} b_{11} \\ b_{21} \\ b_{31} \\ \vdots \\ b_{n1} \end{bmatrix} [a_{11}, a_{12}, a_{13}, \dots, a_{1n}] = \begin{bmatrix} a_{11}b_{11} & a_{12}b_{11} & a_{13}b_{11} & \cdots & a_{1n}b_{11} \\ a_{11}b_{21} & a_{12}b_{21} & a_{13}b_{21} & \cdots & a_{1n}b_{21} \\ a_{11}b_{31} & a_{12}b_{31} & a_{13}b_{31} & \cdots & a_{1n}b_{31} \\ \vdots & \vdots & \vdots & \vdots & \vdots \\ a_{11}b_{n1} & a_{12}b_{n1} & a_{13}b_{n1} & \cdots & a_{1n}b_{n1} \end{bmatrix}$$

The result is called a matrix as defined below.

The distributive law of vectors. If A is a row vector of dimension n and B and C are column vectors of dimension n , the distributive law specifies that:

$$A \cdot (B + C) = A \cdot B + A \cdot C$$

Matrix. A rectangular array of real numbers is called a matrix when arranged as shown in Figure VIId.1.1(a). Note that in general, the number of rows and columns are different.

$$A = \begin{pmatrix} a_{11} & a_{12} & \cdots & a_{1n} \\ a_{21} & a_{22} & \cdots & a_{2n} \\ \vdots & \vdots & \vdots & \vdots \\ a_{m1} & a_{m2} & \cdots & a_{mn} \end{pmatrix} \quad A = \begin{pmatrix} a_{11} & a_{12} & \cdots & a_{1n} \\ a_{21} & a_{22} & \cdots & a_{2n} \\ \vdots & \vdots & \vdots & \vdots \\ a_{n1} & a_{n2} & \cdots & a_{nn} \end{pmatrix}$$

(a) (b)

Figure VIId.1.1. Demonstrations of (a) a matrix and (b) a square matrix

Order of a matrix defines the number of rows and columns. For example, if a matrix has m rows and n columns then the matrix is of order m by n or alternatively $m \times n$. Hence, a row vector is a $1 \times m$ matrix and a column vector is an $m \times 1$ matrix. Two matrices of the same order are referred to as *comforbale*.

Square matrix. A $m \times n$ matrix would be referred to as a square matrix if $m = n$ as shown in Figure VIId.1.1(b).

Main diagonal. In a square matrix, the main diagonal consists of the a_{ii} elements.

Zero matrix. All the elements of a zero matrix are zeros.

Upper triangular matrix. A square matrix with elements $a_{ij} = 0$ for $i > j$ is called an upper triangular matrix (Figure VIId.1.2(a)).

Lower triangular matrix. A square matrix with elements $a_{ij} = 0$ for $i < j$ is called a lower triangular matrix (Figure VIId.1.2(b)).

$$\begin{aligned}
 \text{(a)} \quad A &= \begin{pmatrix} a_{11} & a_{12} & \cdots & a_{1n} \\ 0 & a_{22} & \cdots & a_{2n} \\ \vdots & \vdots & \ddots & \vdots \\ 0 & 0 & \cdots & a_{nn} \end{pmatrix} & \text{(b)} \quad A &= \begin{pmatrix} a_{11} & 0 & \cdots & 0 \\ a_{21} & a_{22} & \cdots & 0 \\ \vdots & \vdots & \ddots & \vdots \\ a_{n1} & a_{n2} & \cdots & a_{nn} \end{pmatrix} & \text{(c)} \quad A &= \begin{pmatrix} a_{11} & 0 & \cdots & 0 \\ 0 & a_{22} & \cdots & 0 \\ \vdots & \vdots & \ddots & \vdots \\ 0 & 0 & \cdots & a_{nn} \end{pmatrix}
 \end{aligned}$$

Figure VIIId.1.2. Demonstration of (a) upper triangular, (b) lower triangular, and (c) diagonal matrix

Diagonal matrix. All elements of a diagonal matrix are zeroes except for the elements of the main diagonal. In other words, a matrix which is both upper and lower triangular, is called a diagonal matrix:

Scalar matrix. A scalar matrix is a diagonal matrix with elements such that $a_{11} = a_{22} = \cdots = a_{nn} = k$.

Identity matrix. An identity matrix is a scalar matrix with $k = 1$.

Sums of matrices. If matrix $A = [a_{ij}]_{mn}$ is added to (or deducted from) matrix $B = [b_{ij}]_{mn}$, the result would be matrix C with elements given as $C = [a_{ij} \pm b_{ij}]_{mn}$. The commutative and associative laws of addition described for vectors also apply to matrices. Only matrices of the same order can be summed.

Multiplication of matrices. The product of matrix $A = [a_{ij}]_{mn}$ by matrix $B = [b_{ij}]_{np}$ is matrix $C = [c_{ij}]_{mp}$ with elements given as:

$$\begin{pmatrix} a_{11} & a_{12} & \cdots & a_{1n} \\ \vdots & \vdots & \ddots & \vdots \\ a_{i1} & a_{i2} & \cdots & a_{in} \\ \vdots & \vdots & \ddots & \vdots \\ a_{m1} & a_{m2} & \cdots & a_{mn} \end{pmatrix} \begin{pmatrix} b_{11} & \cdots & b_{1j} & \cdots & b_{1p} \\ b_{21} & \cdots & b_{2j} & \cdots & b_{2p} \\ \vdots & \cdots & \vdots & \cdots & \vdots \\ b_{n1} & \cdots & b_{nj} & \cdots & b_{np} \end{pmatrix} = \begin{pmatrix} c_{11} & \cdots & c_{1j} & \cdots & c_{1p} \\ \vdots & \vdots & \vdots & \vdots & \vdots \\ c_{i1} & \cdots & c_{ij} & \cdots & c_{ip} \\ \vdots & \vdots & \vdots & \vdots & \vdots \\ c_{m1} & \cdots & c_{mj} & \cdots & c_{mp} \end{pmatrix}$$

Where element c_{ij} of matrix C is given by:

$$c_{i,j} = a_{i1}b_{1j} + a_{i2}b_{2j} + \cdots + a_{in}b_{nj}$$

As shown above, in multiplication of two matrices A and B , these need not be square matrices. However, the number of columns of matrix A must be equal to the number of rows of matrix B . It is also important to note that matrix multiplication is not a linear operation hence, $AB \neq BA$. An example of multiplication of two square matrices is as follows

$$\begin{pmatrix} 1 & -1 & 2 \\ 3 & 9 & -4 \\ 5 & 1 & -3 \end{pmatrix} \begin{pmatrix} 7 & 11 & -6 \\ -1 & 3 & -5 \\ 6 & 1 & -8 \end{pmatrix} = \begin{pmatrix} 20 & 10 & -15 \\ -6 & 56 & 31 \\ 16 & 49 & 11 \end{pmatrix}$$

An example of the multiplication of two non-square matrices, $A(n_a, m)B(m, m_b) = C(n_a, m_b)$, is:

$$\begin{bmatrix} 1 & 5 & -8 & 11 & 10 \\ 0 & -7 & 3 & 5 & 7 \\ -6 & 2 & 1 & -9 & 4 \end{bmatrix} \begin{bmatrix} 1 & 5 \\ 0 & -4 \\ -2 & 7 \\ -3 & 6 \\ 9 & 12 \end{bmatrix} = \begin{bmatrix} 74 & 115 \\ 42 & 163 \\ 55 & -37 \end{bmatrix}$$

Transpose of a matrix. The transpose of matrix A is matrix A^T , obtained by interchanging the rows and columns of A :

$$A = \begin{pmatrix} a_{11} & a_{12} & \cdots & a_{1n} \\ a_{21} & a_{22} & \cdots & a_{2n} \\ \vdots & \vdots & \vdots & \vdots \\ a_{m1} & a_{m2} & \cdots & a_{mn} \end{pmatrix}, \quad A^T = \begin{pmatrix} a_{11} & a_{21} & \cdots & a_{m1} \\ a_{12} & a_{22} & \cdots & a_{m2} \\ \vdots & \vdots & \vdots & \vdots \\ a_{1n} & a_{2n} & \cdots & a_{mn} \end{pmatrix}$$

Note that $(A^T)^T = A$, $(A + B)^T = A^T + B^T$, $(AB)^T = B^T A^T$. Furthermore, matrix A is said to be symmetric if $A = A^T$ and is said to be skew symmetric if $A = -A^T$.

Determinant of a square matrix. A determinant of a square matrix is a functional value assigned to the numbers in the square array. While a matrix is represented by an array of numbers within brackets, the determinant of the matrix is represented by the same array of numbers within two parallel lines:

$$A = \begin{pmatrix} a_{11} & a_{12} & \cdots & a_{1n} \\ a_{21} & a_{22} & \cdots & a_{2n} \\ \vdots & \vdots & \vdots & \vdots \\ a_{n1} & a_{n2} & \cdots & a_{nn} \end{pmatrix} \quad |A| = \begin{vmatrix} a_{11} & a_{12} & \cdots & a_{1n} \\ a_{21} & a_{22} & \cdots & a_{2n} \\ \vdots & \vdots & \vdots & \vdots \\ a_{n1} & a_{n2} & \cdots & a_{nn} \end{vmatrix}$$

Minor determinant of a square matrix. If we eliminate the row and column associated with element a_{ij} of matrix A then the remaining array of numbers make up the elements of a minor determinant shown by M_{ij} . Therefore, there are as many minor determinants as the number of elements in the matrix. Note that if the order of matrix A is n , the order of each minor determinant is $n - 1$. . For example, for element a_{12} , of matrix A , the minor determinant is found as:

$$|A| = \begin{vmatrix} \boxed{a_{11}} & \boxed{a_{12}} & \cdots & a_{1n} \\ a_{21} & a_{22} & \cdots & a_{2n} \\ \vdots & \vdots & \vdots & \vdots \\ a_{n1} & a_{n2} & \cdots & a_{nn} \end{vmatrix}, \quad |M| = \begin{vmatrix} a_{21} & \cdots & a_{2n} \\ \vdots & \vdots & \vdots \\ a_{n1} & \cdots & a_{nn} \end{vmatrix}$$

Example: Let's find the minor determinant corresponding to elements a_{22} , a_{23} , and a_{32} of matrix A below:

$$A = \begin{pmatrix} -1 & 6 & 2 \\ 5 & 1 & -3 \\ 3 & -4 & 8 \end{pmatrix}, \quad M_{22} = \begin{vmatrix} -1 & 2 \\ 3 & 8 \end{vmatrix}, \quad M_{23} = \begin{vmatrix} -1 & 6 \\ 3 & -4 \end{vmatrix}, \quad M_{32} = \begin{vmatrix} -1 & 2 \\ 5 & -3 \end{vmatrix},$$

Cofactor of an element of a matrix. The minor determinant multiplied by $(-1)^{i+j}$ is called the cofactor of element a_{ij} of matrix A and is designated as A_{ij}^c . For example, the cofactors of a_{11} , a_{23} , and a_{33} of matrix A below are obtained as:

$$A = \begin{pmatrix} -2 & -1 & 3 \\ 0 & 5 & -4 \\ 9 & -7 & 2 \end{pmatrix}, \quad A_{11}^c = (-1)^2 \begin{vmatrix} 5 & -4 \\ -7 & 2 \end{vmatrix}, \quad A_{23}^c = (-1)^5 \begin{vmatrix} -2 & -1 \\ 9 & -7 \end{vmatrix}, \quad A_{33}^c = (-1)^6 \begin{vmatrix} -2 & -1 \\ 0 & 5 \end{vmatrix}$$

The cofactor matrix. A matrix whose elements are the cofactors of the elements of matrix A is known as the cofactor matrix of A . A matrix and its associated cofactor matrix are written as:

$$A = \begin{pmatrix} a_{11} & a_{12} & \cdots & a_{1n} \\ a_{21} & a_{22} & \cdots & a_{2n} \\ \vdots & \vdots & \vdots & \vdots \\ a_{n1} & a_{n2} & \cdots & a_{nn} \end{pmatrix}, \quad A^c = \begin{pmatrix} A_{11}^c & A_{12}^c & \cdots & A_{1n}^c \\ A_{21}^c & A_{22}^c & \cdots & A_{2n}^c \\ \vdots & \vdots & \vdots & \vdots \\ A_{n1}^c & A_{n2}^c & \cdots & A_{nn}^c \end{pmatrix}$$

Example: Consider matrix A and its associated cofactor matrix (A^c):

$$A = \begin{pmatrix} -5 & -2 & 3 \\ 1 & 5 & -8 \\ 9 & -7 & 6 \end{pmatrix} \quad A^c = \begin{pmatrix} -26 & -78 & -52 \\ -9 & 57 & -53 \\ 1 & -37 & -23 \end{pmatrix}$$

Determinant of a square matrix. For matrix A of order n , the value of the determinant is given as:

$$|A| = \sum (-1)^{i+j} a_{ij} M_{ij} = \sum a_{ij} A_{ij}^c \quad \text{VIIId.1.1}$$

where $A_{ij}^c = (-1)^{i+j} M_{ij}$ is the *cofactor* and M_{ij} is the *minor determinant* associated with element a_{ij} . This minor determinant is of order $n - 1$ and obtained by deleting the i th row and j th column, as discussed before. For a matrix of order n , there are $n!$ terms to evaluate. Consider first a matrix of order 2. There are $2! = 2$ terms to evaluate. Using Equation VIIId.1.1, the determination of a matrix of order 2 becomes:

$$|A| = \begin{vmatrix} a_{11} & a_{12} \\ a_{21} & a_{22} \end{vmatrix} = a_{11}a_{22} - a_{12}a_{21}$$

We now calculate the determinant of a matrix of order 3. In this case, there are $3! = 6$ terms to evaluate:

$$|A| = \begin{vmatrix} a_{11} & a_{12} & a_{13} \\ a_{21} & a_{22} & a_{23} \\ a_{31} & a_{32} & a_{33} \end{vmatrix} = a_{11} \begin{vmatrix} a_{22} & a_{23} \\ a_{32} & a_{33} \end{vmatrix} - a_{12} \begin{vmatrix} a_{21} & a_{23} \\ a_{31} & a_{33} \end{vmatrix} + a_{13} \begin{vmatrix} a_{21} & a_{22} \\ a_{31} & a_{32} \end{vmatrix} =$$

$$a_{11}(a_{22}a_{33} - a_{32}a_{23}) - a_{12}(a_{21}a_{33} - a_{31}a_{23}) + a_{13}(a_{21}a_{32} - a_{31}a_{22})$$

Example: The determinant of matrices A, B, and C are calculated as follows:

$$|A| = \begin{vmatrix} -2 & 4 & 9 \\ 1 & 6 & -5 \\ 10 & -3 & -1 \end{vmatrix} = -721, \quad |B| = \begin{vmatrix} 14 & -15 & 27 \\ -27 & 28 & -51 \\ 40 & -43 & 77 \end{vmatrix} = 4, \quad |C| = \begin{vmatrix} 10 & -20 & 25 \\ -15 & 30 & -40 \\ 45 & -50 & 30 \end{vmatrix} = 1000$$

Singular matrix. If the determinant of a matrix is zero, then the matrix is singular.

Adjoint matrix. The transpose of the cofactor matrix is called the adjoint matrix. Matrix A, the cofactor matrix A^c , and the adjoint matrix of A are shown in Figure VIId.1.3(a), (b), and (c), respectively.

$$A = \begin{pmatrix} a_{11} & a_{12} & \cdots & a_{1n} \\ a_{21} & a_{22} & \cdots & a_{2n} \\ \vdots & \vdots & \ddots & \vdots \\ a_{n1} & a_{n2} & \cdots & a_{nn} \end{pmatrix}, \quad C = \begin{pmatrix} A_{11} & A_{12} & \cdots & A_{1n} \\ A_{21} & A_{22} & \cdots & A_{2n} \\ \vdots & \vdots & \ddots & \vdots \\ A_{n1} & A_{n2} & \cdots & A_{nn} \end{pmatrix}, \quad \text{adj}A = \begin{pmatrix} A_{11} & A_{21} & \cdots & A_{n1} \\ A_{12} & A_{22} & \cdots & A_{n2} \\ \vdots & \vdots & \ddots & \vdots \\ A_{1n} & A_{2n} & \cdots & A_{nn} \end{pmatrix}$$

(a) (b) (c)

Figure VIId.1.3. Demonstration of (a) square matrix, (b) the cofactor matrix, and (c) the adjoint matrix.

Diagonally dominant matrix. In diagonally dominant matrices, the magnitude of the element located on the diagonal in each row is larger than the sum of the magnitude of all the other elements in that row:

$$|a_{ii}| > \sum_{\text{all } j \neq i} |a_{ij}|$$

2. The Inverse of a Matrix

The inversion of a matrix is very important in determining solutions to sets of algebraic equations. The process of matrix inversion is analogous to division for real numbers. If matrix B is the inverse of matrix A, then the product of matrices A and B is equal to the identity matrix, $AB = I$. The inverse of a matrix is denoted

$$\begin{array}{ccc}
 A = \begin{pmatrix} -5 & 10 & 1 \\ 2 & -9 & 7 \\ -11 & -1 & 4 \end{pmatrix}, & A^c = \begin{pmatrix} -29 & -85 & -101 \\ -41 & -9 & -115 \\ 79 & 37 & 25 \end{pmatrix}, & C = (A^c)^T = \text{adj}A = \begin{pmatrix} -29 & -41 & 79 \\ -85 & -9 & 37 \\ -101 & -115 & 25 \end{pmatrix} \\
 \text{(a)} & \text{(b)} & \text{(c)}
 \end{array}$$

Figure VIId.2.1. Demonstration of (a) a square matrix, (b) the cofactor matrix, and (c) the adjoint matrix

as $B = A^{-1}$. But not every matrix has an inverse. There are two conditions for a matrix to have an inverse. The first condition requires the matrix to be square so that a determinant can be calculated. The second condition requires the determinant of the matrix to be nonzero otherwise the matrix is singular. To inverse matrix A , we first replace all elements by their associated cofactors to obtain the cofactor matrix, A^c . We then transpose the cofactor matrix to obtain the adjoint matrix. The inverse of the matrix is the result of the division of the elements of the adjoint matrix by the determinant of matrix A :

$$A^{-1} = \frac{\text{adj}A}{|A|}$$

For example, if we want to find the inverse of matrix A , Figure VIId.2.1(a), we must first find the cofactor matrix by replacing each element of matrix A by its minor determinant, using the correct sign. This is shown in Figure VIId.2.1(b). The adjoint matrix of A is then obtained by transposing matrix A^c . Finally, the inverse matrix A^{-1} is obtained by dividing elements of matrix C by the determinant of matrix A .

Elements of the cofactor matrix are obtained as follows. For element $a_{11} = -5$, we substitute from the minor determinant obtained from eliminating elements in the first row and the first column of matrix A to get $[-9 \times 4 - (-1 \times 7)] = -29$. We retain the sign as the summation of first row and first column is an even number. Similarly, for element $a_{21} = 2$ we substitute from $[10 \times 4 - 1 \times (-1)] = 41$. However, the sign for this term would be minus since the summation of the row and column is an odd number.

We now calculate the determinant of matrix A . This is facilitated as we already have the minor matrices:

$$|A| = \begin{vmatrix} -5 & 10 & 1 \\ 2 & -9 & 7 \\ -11 & -1 & 4 \end{vmatrix} = -5(-29) - 2(41) - 11(79) = -806$$

Having the adjoint matrix, Figure VIId.2.1(c) and the determinant, the inverse matrix becomes:

$$A^{-1} = \begin{pmatrix} 0.036 & 0.0509 & -0.0980 \\ 0.105 & 0.0112 & -0.0459 \\ 0.125 & 0.1430 & -0.0310 \end{pmatrix}$$

To ensure that we have made no algebraic error, we should calculate the product of $AA^{-1} = I$:

$$\begin{pmatrix} -5 & 10 & 1 \\ 2 & -9 & 7 \\ -11 & -1 & 4 \end{pmatrix} \times \begin{pmatrix} 0.036 & 0.0509 & -0.0980 \\ 0.105 & 0.0112 & -0.0459 \\ 0.125 & 0.1430 & -0.0310 \end{pmatrix} = \begin{pmatrix} 1 & 0 & 0 \\ 0 & 1 & 0 \\ 0 & 0 & 1 \end{pmatrix}$$

Several matrices and their inverse matrices are provided below. The reader should try to follow the above procedure to inverse each matrix and compare the results with the inverse matrices presented.

Example 1:

$$A = \begin{pmatrix} 3 & 1 & 2 \\ -9 & 0 & -4 \\ 1 & -7 & 12 \end{pmatrix}, \quad A^{-1} = \begin{pmatrix} -0.192 & -0.178 & -0.0274 \\ 0.7120 & 0.2330 & -0.0411 \\ 0.4320 & 0.1510 & 0.06160 \end{pmatrix}, \quad |A| = 146$$

Example 2:

$$A = \begin{pmatrix} 0.15 & -1.00 & -0.079 \\ 0.30 & -0.56 & 0.4000 \\ -0.25 & 0.75 & -0.630 \end{pmatrix}, \quad A^{-1} = \begin{pmatrix} -0.601 & 7.85 & 5.060 \\ -1.01 & 1.30 & 0.953 \\ -0.968 & -1.57 & -2.46 \end{pmatrix}, \quad |A| = -0.0878$$

Example 3:

$$A = \begin{pmatrix} 10 & -14 & 15 & -8 \\ 13 & -3 & 21 & -13 \\ 18 & -12 & -7 & 11 \\ 2 & -19 & 14 & -10 \end{pmatrix}, \quad A^{-1} = \begin{pmatrix} -0.393 & 0.194 & 0.113 & 0.188 \\ 0.0441 & .0089 & -0.0229 & -0.072 \\ 1.12 & -0.431 & -0.243 & -0.602 \\ 1.40 & -0.581 & -0.274 & -0.769 \end{pmatrix}, \quad |A| = 6980$$

Example 4:

$$A = \begin{pmatrix} 4 & -5 & 6 & -7 \\ 2 & -3 & -9 & 11 \\ -8 & 0 & 1 & 10 \\ 3 & -2 & 0 & 9 \end{pmatrix}, \quad A^{-1} = \begin{pmatrix} -.0315 & -.0323 & -.1010 & .127 \\ -.1630 & -.1210 & -.0762 & .101 \\ .0162 & -.0977 & .0234 & .106 \\ -.0269 & -.0160 & .0168 & .091 \end{pmatrix}, \quad |A| = -5550$$

Such operations can be easily performed by using the accompanying CD-ROM.

3. Set of Linear Equations

Mathematical modeling of most physical phenomena reduces to a set of simultaneous differential equations the solution of which would determine the parameters of interest. The solution to such set of equations involves the approximation of the differential terms by finite difference, for example, and then linearization of the nonlinear terms. The linearization of a set of non-linear differential equations is discussed in Chapter VIIe. The net result is a set of linear simultaneous equations as given in Equation VIId.3.1, which must be solved in each time interval to obtain the trend of the parameters. There are several techniques for solving a set of n simultaneous linear equations in n unknowns:

$$\begin{cases} a_{11}x_1 + a_{12}x_2 + a_{13}x_3 + \cdots + a_{1n}x_n = c_1 \\ a_{21}x_1 + a_{22}x_2 + a_{23}x_3 + \cdots + a_{2n}x_n = c_2 \\ \vdots \\ a_{n1}x_1 + a_{n2}x_2 + a_{n3}x_3 + \cdots + a_{nn}x_n = c_n \end{cases} \quad \text{VIId.3.1}$$

such as matrix inversion and the Gauss – Seidel iteration method.

3.1. Solution to a Set of Linear Equations by Matrix Inversion

The above general set of linear equations can be written in the form of a matrix equation as:

$$Ax = c \quad \text{VIId.3.2}$$

where A is the *coefficient matrix*, x is the unknown vector, and c is the constant vector. If we now multiply both sides of Equation VIId.3.2 by A^{-1} we get $A^{-1}(Ax) = A^{-1}c$. Since $A^{-1}A = I$, the left hand-side becomes:

$$x = A^{-1}c$$

As a result, to solve a set of algebraic equations, we must find the inverse of the coefficient matrix and multiply it by the vector of the constants. If we place the vector of constants c as the last column inside the coefficient matrix A , the resultant is called the *augmented matrix*. Several examples are provided below. The reader should try to solve these sets and compare the results with those given below.

Example 1. Consider the set of linear equations as shown in Figure VIId.3.1(a). This set in matrix form is shown in Figure VIId.3.1(b). The augmented matrix of this set is shown in Figure VIId.3.1(c).

$$\begin{aligned}
 &\begin{cases} 2x_1 - 3x_2 + x_3 - 2x_4 = 5 \\ -x_1 + 4x_2 + 9x_3 + 3x_4 = 1 \\ x_1 + 6x_4 = -7 \\ 7x_1 - 3x_2 + 5x_3 - 6x_4 = -10 \end{cases} \quad \text{(a)} \\
 &\begin{pmatrix} 2 & -3 & 1 & -2 \\ -1 & 4 & 9 & 3 \\ 1 & 0 & 0 & 6 \\ 7 & -3 & 5 & -6 \end{pmatrix} \begin{pmatrix} x_1 \\ x_2 \\ x_3 \\ x_4 \end{pmatrix} = \begin{pmatrix} 5 \\ 1 \\ -7 \\ -10 \end{pmatrix} \quad \text{(b)} \\
 &\begin{pmatrix} 2 & -3 & 1 & -2 & 5 \\ -1 & 4 & 9 & 3 & 1 \\ 1 & 0 & 0 & 6 & -7 \\ 7 & -3 & 5 & -6 & -10 \end{pmatrix} \quad \text{(c)}
 \end{aligned}$$

Figure VIId.3.1. Demonstration of (a) set of linear equations, (b) matrix form, and (c) augmented matrix

Upon solving the above set, the solution vector becomes $x = [-4.52, -3.91, 1.48, -0.414]^T$.

Example 2:

$$\begin{cases} 12w - x - y + 2z = 15 \\ 4w + 4x - 3y - 13z = -10 \\ w - x + 6y + 6z = -5 \\ 7w + 13x - 4y - 3z = 10 \end{cases}, \quad \begin{pmatrix} 12 & -1 & -1 & 2 \\ 4 & 4 & -3 & -13 \\ 1 & -1 & 6 & 6 \\ 7 & 13 & -4 & -3 \end{pmatrix} \begin{pmatrix} w \\ x \\ y \\ z \end{pmatrix} = \begin{pmatrix} 15 \\ -10 \\ -5 \\ 10 \end{pmatrix}, \quad \begin{pmatrix} 12 & -1 & -1 & 2 & 15 \\ 4 & 4 & -3 & -13 & -10 \\ 1 & -1 & 6 & 6 & -5 \\ 7 & 13 & -4 & -3 & 10 \end{pmatrix}$$

The answers obtained for x_1 through x_4 is arranged in the transpose of the solution vector:

$$x^T = [0.0343, 0.405, -2.18, 1.41]^T.$$

3.2. Solution to a Set of Linear Equations by Gauss – Seidel Iteration

This is a simple and effective method to solve sets of linear algebraic equations. To explain the Gauss – Seidel iteration, let's consider a set of 3 equations in 3 unknowns:

$$\begin{cases} a_{11}x_1 + a_{12}x_2 + a_{13}x_3 = c_1 \\ a_{21}x_1 + a_{22}x_2 + a_{23}x_3 = c_2 \\ a_{31}x_1 + a_{32}x_2 + a_{33}x_3 = c_3 \end{cases} \quad \text{VIId.3.3}$$

This set can be arranged as:

$$\begin{pmatrix} a_{11} & a_{12} & a_{13} \\ a_{21} & a_{22} & a_{23} \\ a_{31} & a_{32} & a_{33} \end{pmatrix} \begin{pmatrix} x_1 \\ x_2 \\ x_3 \end{pmatrix} = \begin{pmatrix} c_1 \\ c_2 \\ c_3 \end{pmatrix}$$

We have arranged this set so that the diagonal elements in the coefficient matrix have the largest magnitude in each row. For example, for row 2 we have $a_{22} > a_{21}$ and $a_{22} > a_{23}$, etc. This arrangement expedites the iteration process. In fact, if the diagonal elements are larger than the summation of other elements of their corre-

sponding rows – in other words, the coefficient matrix is diagonally dominant – the convergence is guaranteed.

To demonstrate the Gauss – Seidel method, we try to solve the above set of linear equations. For this purpose, we obtain x_1 from the first, x_2 from the second, and x_3 from the third equation – assuming nonzero coefficients – as follows:

$$\begin{aligned}x_1 &= [c_1 - (a_{12}x_2 + a_{13}x_3)] / a_{11} \\x_2 &= [c_2 - (a_{21}x_1 + a_{23}x_3)] / a_{22} \\x_3 &= [c_3 - (a_{31}x_1 + a_{32}x_2)] / a_{33}\end{aligned}\tag{VIIId.3.4}$$

To calculate x_1 from Equation VIIId.3.4, for example, we need to have the values for x_2 and x_3 . Since we do not have these values before hand, we resort to guessing based on the knowledge we have about the system of equations. Using the initial guesses, we obtain updated values from Equation VIIId.3.4. We continue this process and at each trial we compare the updated values with the previous values. If the difference is less than a specified convergence criterion then we conclude that the iteration has converged. Using superscript k as an index of iteration, the values of each parameter at iteration number $k + 1$ become:

$$\begin{aligned}x_1^{(k+1)} &= [c_1 - (a_{12}x_2^{(k)} + a_{13}x_3^{(k)})] / a_{11} \\x_2^{(k+1)} &= [c_2 - (a_{21}x_1^{(k+1)} + a_{23}x_3^{(k)})] / a_{22} \\x_3^{(k+1)} &= [c_3 - (a_{31}x_1^{(k+1)} + a_{32}x_2^{(k+1)})] / a_{33}\end{aligned}$$

Note that as soon as a new value for a variable is calculated, it is used to obtain the new values for the rest of parameters. Let's try this iterative method for the following set of linear equations:

$$\begin{cases} 3x + y + z = 5 \\ 2x + 4y - z = -5 \\ x - y + 3z = 11 \end{cases}$$

For the first step we obtain:

$$\begin{cases} x = [5 - (y + z)] / 3 \\ y = [-5 - (2x - z)] / 4 \\ z = [11 - (x - y)] / 3 \end{cases}$$

To begin iteration, we may assume $x = y = z = 0$. From the first equation, new x becomes $x^{(1)} = 1.666$. From the second equation, new y becomes $y^{(1)} = [-5 - (3.333 + 0)] / 4 = -2.0833$. From the third equation, new value for z becomes $z^{(1)} = [11 - (1.666 + 2.0833)] / 3 = 2.4168$. We will use the updated values in the next step of the iteration process as is summarized below. Note that k is the iteration index:

$k = 1$	$k = 2$	$k = 3$	$k = 4$	$k = 5$	$k = 6$	$k = 7$	$k = 8$
0	1.666	1.555	1.2499	1.1195	1.0712	1.0370	1.0178
0	-2.083	-1.4235	-1.2065	-1.0978	-1.0656	-1.031	-1.0147
0	2.4168	2.6738	2.8478	2.880	2.9544	2.977	2.9892

As seen from this table, the values are approaching 1, -1, and 3 for x , y , and z , respectively. The criterion for terminating the iteration is that:

$$\left| \frac{x_i^{new} - x_i^{old}}{x_i^{old}} \right| < \mathcal{E}$$

where \mathcal{E} is a specified convergence criterion, such as 1×10^{-6} . As a result, to solve a set of linear equations given by $Ax = c$, we develop the following algorithm for the Gauss – Seidel iteration:

$$x_i^{(k+1)} = \frac{c_i}{a_{ii}} - \sum_{j=1}^{i-1} \frac{a_{ij}}{a_{ii}} x_j^{(k+1)} - \sum_{j=i+1}^N \frac{a_{ij}}{a_{ii}} x_j^{(k)} \quad k = 1, 2, \dots$$

Solution to a set of equations can be easily found by using the software included on the accompanying CD-ROM.

3.3. The Characteristic Equation of a Matrix

Mathematical modeling of engineering problems that are oscillatory in nature – such as mechanical vibration and alternating current – leads to linear algebraic systems of the type:

$$\begin{aligned} a_{11}x_1 + a_{12}x_2 + \dots + a_{1n}x_n &= \lambda x_1 \\ a_{21}x_1 + a_{22}x_2 + \dots + a_{2n}x_n &= \lambda x_2 \\ &\vdots \\ a_{n1}x_1 + a_{n2}x_2 + \dots + a_{nn}x_n &= \lambda x_n \end{aligned} \quad \text{VIIc.1.16}$$

or in the matrix form:

$$(A - \lambda I)\bar{x} = 0 \quad \text{VIIc.1.17}$$

where A is the square matrix of coefficients, x is the vector of unknowns, I is the identity matrix, and λ is a parameter. According to Cramer's rule, the only way of having a nontrivial solution for the above homogeneous system is for the determinant of the system of equations to be zero.

$$P(\lambda) = \det(A - \lambda I) = \begin{vmatrix} a_{11} - \lambda & a_{12} & \cdots & a_{1n} \\ a_{21} & a_{22} - \lambda & \cdots & a_{2n} \\ & & \ddots & \\ a_{n1} & a_{n2} & \cdots & a_{nn} - \lambda \end{vmatrix} = 0 \quad \text{VIIc.1.18}$$

The equation resulting from expansion of the above determinant is known as the *characteristic polynomial* of matrix A . The roots of the characteristic polynomial $(\lambda_1, \lambda_2, \dots, \lambda_n)$ are referred to as the *characteristic values* or *eigenvalues*. Vectors corresponding to the eigenvalues are referred to as *characteristic vectors* or *eigenvectors*.

VIIe. Numerical Analysis

In Chapter VIIIb, we studied analytical solutions of differential equations in closed form. Despite all the advantages associated with analytical solutions, we frequently have to resort to numerical solutions. This is due to the inability of analytical methods to deal with the involved complexities in dealing with many engineering problems. The primary advantage of analytical solutions is to provide exact answers in functional relationships. The latter makes analytical solutions independent of any specific problem to be analyzed. Numerical solutions, on the other hand, are problem dependent. For example, any change in a boundary condition requires the entire problem to be recalculated. Another key difference is that numerical solutions provide answers only in tabulated form. On the plus side, numerical solutions can handle complicated problems and therefore can, remove the limitations inherent in analytical methods when dealing with nonlinearities. Numerical methods can be divided into two groups: deterministic and statistic. The deterministic group consists of such techniques as finite difference and finite element. The statistical group deals primarily with such topics as the Monte Carlo method. Finite difference methods, for example, are used to solve ordinary and partial differential equations. Ordinary differential equations are solved based on either the Taylor's series technique or based on the predictor-corrector technique. The Taylor's series technique includes the Runge-Kotta and the Euler methods while the predictor-corrector technique includes Adams, Moulton, Milne, and Adams Bashford methods. Partial differential equations can be divided into three categories: Elliptic, Hyperbolic, and Parabolic. These equations are solved numerically by either the explicit, semi-implicit, or fully implicit method. In this chapter we consider only the finite difference methods.

1. Definiton of Terms

Accuracy. The reason this term is associated with numerical methods is that, unlike analytical solutions, numerical methods are always associated with certain degree of approximation. Accuracy is a measure of the closeness of the result obtained from a numerical solution to an exact answer obtained from an analytical solution. Although, in most cases, we do not have analytical answer to compare with, reduction of errors associated with numerical solutions leads to increased accuracy.

Backward difference. This definition is useful in the topic of interpolation. Consider a set of y values associated with a specified set of x values as $y_i = f(x_i)$. For simplicity, let's assume that all x values are equally spaced. We now define the first-order backward difference as $\nabla f_i = f(x_i) - f(x_{i-1})$.

Central difference. For the same set of values described above, the central difference is defined as:

$$\delta f(x) = f\left(x + \frac{\Delta x}{2}\right) - f\left(x - \frac{\Delta x}{2}\right)$$

Forward difference. For the same set of y values defined for backward difference, we may define the first-order difference as $\Delta f_i = f(x_{i+1}) - f(x_i)$. Similarly, a second-order difference is defined as:

$$\Delta^2 f_i = \Delta(\Delta f_i) = \Delta[f(x_{i+1}) - f(x_i)] = \Delta f(x_{i+1}) - \Delta f(x_i) = [f(x_{i+2}) - f(x_{i+1})] - [f(x_{i+1}) - f(x_i)]$$

Which simplifies to:

$$\Delta^2 f_i = f(x_{i+2}) - 2f(x_{i+1}) + f(x_i)$$

Using the same procedure, we can find the n th order difference as:

$$\Delta^n f(x_i) = f(x_{i+n}) - nf(x_{i+n-1}) + \frac{n(n-1)}{2!} f(x_{i+n-2}) - \frac{n(n-1)(n-2)}{3!} f(x_{i+n-3})$$

Round-off error. Most floating point operations involve some loss of significant digits due to the finite word length of the computer. This loss of digits is known as the round-off error. Arithmetic operations performed in single precession carry 7 or 8 significant digits for each variable. To reduce the round off error, we use double precession, which nearly doubles the number of significant digits assigned to the variable. The round-off error is also a function of the degree of the involved arithmetic as well as the step size. The cumulative round-off error increases as the step size is reduced.

Truncation error. In numerical analysis, we usually represent functions by a limited number of terms of their expansions in Taylor's series. As more terms in the expansions are used, the truncation error is reduced.

Mesh size. The step size or mesh size is the increment applied to dependent variables and is shown as Δx , Δy , Δz , Δt , etc. The mesh size affects the discretization error. The smaller the mesh sizes, the smaller the discretization error, the larger the number of arithmetic operations, and consequently the running time.

Discretization error. The discretization error stems from using a finite value for the step size, such as Δx to represent an infinitesimal value, such as dx . The discretization error is a direct function of the step size. The smaller the steps size, the smaller the discretization error. On the other hand, as was discussed earlier, the smaller the steps size, the larger the round off error. Therefore, there is basically an optimum value for the step size to have the minimum error, as shown in Figure VIIe.1.1.

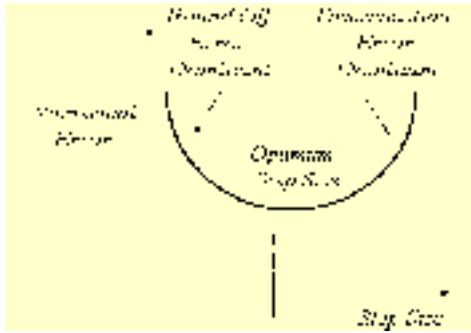


Figure VIIe.1.1. Depiction of dominance of numerical errors versus step or the increment size

Local error. An error that appears in the calculation of a variable at a specific step, of numerical integration for example, is known as the local error.

Propagated error. An error that appears in a step due to the accumulation of errors of the successive steps is a propagated error. The propagated error is in addition to the local error corresponding to that step.

Numerical stability. If the propagated error is further accumulated as the numerical process continues, a point may be reached where the error surpasses the true value of the variable. This results in invalid values known as a numerically unstable condition. A stable condition occurs where errors do not accumulate.

Nonlinear equation. An equation that contains multiples of a dependent variable by itself or its derivatives, is a nonlinear equation. Such equations can be linearized by the use of Taylor's series.

Explicit numerical scheme: Approximation of a first order differential equation $dy/dt = P(t)y + Q(t)$ in an explicit scheme is $[y(t^{n+1}) - y(t^n)]\Delta t = P(t^n)y(t^n) + Q(t^n)$ where n is the discretization index.

The partial differential equations of parabolic type can be solved by forward difference to explicitly calculate the dependent variable in terms of all the known quantities. The size of increments in this scheme must remain below limit to avoid numerical instability.

Implicit numerical scheme: Approximation of a first order differential equation $dy/dt = P(t)y + Q(t)$ in fully implicit numerical scheme is $[y(t^{n+1}) - y(t^n)]\Delta t = P(t^{n+1})y^{n+1} + Q(t^{n+1})$ where n is the discretization index. Approximation of the above equation in semi-implicit scheme is $[y(t^{n+1}) - y(t^n)]\Delta t = P(t^n)y^{n+1} + Q(t^n)$.

Also the partial differential equations of a parabolic type can be solved by forward difference to calculate the dependent variable in terms of all other dependent variables, which are also unknowns. This requires successive simultaneous solution of sets of equations. The implicit scheme is unconditionally stable.

2. Numerical Solutions of Ordinary Differential Equations

There are several methods for numerically solving the initial value problems of ordinary differential equations among which we mention such method as Taylor's series, Euler, Adams, Adams-Bashforth, Adams-Moulton, Milne, and Runge-Kutta. These methods can be basically divided into two groups. The first group includes methods based on Taylor's series. The second group are those based on the "predictor-corrector" method.

2.1. Methods Based on Taylor – Series

Three such methods are discussed below including Taylor's series, Euler, and Runge-Kutta.

Taylor's Series Method

To explain this method, we use a first order differential equation for which we can readily find an exact answer by analytical means. We then use the Taylor's Series method to find an approximate solution for comparison with the exact solution to determine the degree of approximation. Consider for example:

$$\frac{dy}{dx} - 2y = x^2$$

Subject to $y(0) = 1/2$. We may find the exact solution to this equation by using Equation VIIb.2.4:

$$y = e^{-\int -2dx} \{ [\int x^2 e^{\int -2dx} dx] + C \} = Ce^{2x} - \frac{1}{2}(x^2 + x + \frac{1}{2})$$

where the method of "integration by part" was used twice to carryout the integral. Applying the boundary condition, the exact solution becomes $y = 0.75e^{2x} - 0.5(x^2 + x + 0.5)$. Let's now try the Taylor's series method. In this method, the idea is to find a relation between y and x . Such relation exists when we expand y in terms of powers of x about the point x_0 by the Taylor's series (Section VIIa.1). In this example, since the boundary condition is given at $x = 0$, we may expand y about $x = 0$ and use Maclaurin's series to get:

$$y(x) = y(0) + \frac{(\Delta x)^1}{1!} y'(0) + \frac{(\Delta x)^2}{2!} y''(0) + \frac{(\Delta x)^3}{3!} y'''(0) + \dots$$

Starting from $x = x_0$, which in this case is $x = 0$, we can find y at any other interval provided that we have $y(0)$, $y'(0)$, $y''(0)$, $y'''(0)$, etc. We already have the first value (i.e. $y(0)$) from the boundary condition. The second value, $y'(0)$ is found from the differential equation itself as:

$$\frac{dy}{dx} = 2y + x^2 = f(x, y)$$

Hence $y'(0) = 2y(0) + 0 = 1$. The third and subsequent values are found from successive derivation of the differential equation:

$$y'' = \frac{d}{dx}\left(\frac{dy}{dx}\right) = 2y' + 2x$$

Since $y'(0) = 1$, then $y''(0) = 2$. For the third value:

$$y''' = \frac{d}{dx}(y'') = 2y'' + 2$$

Since $y''(0) = 2$, then $y'''(0) = 2 \times 2 + 2 = 6$. For the fourth derivative:

$$y^{iv} = \frac{d}{dx}(y''') = 2y'''$$

which gives $y^{iv}(0) = 12$. Similarly, for the fifth derivative;

$$y^v = \frac{d}{dx}(y^{iv}) = 2y^{iv}$$

Therefore, $y^v(0) = 24$. Let's stop here and substitute the values we obtained in the MacLaurin expansion of the function y to get:

$$y(x) = \frac{1}{2} + \Delta x + (\Delta x)^2 + (\Delta x)^3 + \frac{(\Delta x)^4}{2} + \frac{(\Delta x)^5}{5} + (\text{local truncation error})$$

We can now set up the following table to summarize the comparison between analytical and numerical answers corresponding to various values of x . Note that the increment of x values in Table VIIe.2.1 is 0.1.

These results indicate that we should have retained more terms in the Maclaurin series to increase accuracy. The disadvantage of this method is that, for any problem, the derivatives must be carried out individually.

Table VIIe.2.1. Taylor – series method versus the analytical solution

x	y_{Taylor}	$y_{\text{Analytical}}$
0.0	0.5	0.5
0.1	0.61052	0.611052
0.2	0.748864	0.748868
0.3	0.921536	0.921589
0.4	1.138848	1.139156
0.5	1.412500	1.413711
0.6	1.756352	1.760087

The Euler Method

The Euler method is a simplified form of the Taylor's series method where only the first derivative is retained. This method is simple to use as no higher order derivative needs to be carried out but, due to tendency to propagate local error, small increments must be used. In the Euler method values of the function are obtained at each increment or interval based on the value marching. To introduce the Euler method, we can either use the Taylor –series with only the first two terms retained or use Equation VIIb.2.1:

$$\frac{dy}{dx} = Q(x) - P(x)y \quad \text{VIIb.2.1}$$

and approximate the derivative term:

$$\frac{y_{i+1} - y_i}{\Delta x} = Q(x_i) - P(x_i)y_i = f(x_i, y_i)$$

This is the explicit numerical scheme. The recursive formula is then given by:

$$y_{i+1} = y_i + f(x_i, y_i)\Delta x$$

Let's apply this method to the earlier example for which we already have solutions from both the analytical and the Taylor's series methods. In that example, we have $f(x, y) = 2y + x^2$. The procedure is to start from the initial value we have, which in this case is $y(0) = 0.5$, and calculate the successive values for y by using an increment, of say, $\Delta x = 0.1$. This is summarized in Table VIIe.2.2.

Table VIIe.2.2. Euler method ($\Delta x = 0.1$)

x	y_n	$f(x_n, y_n)$	y_{n+1}
0.1	0.5000	0.101	0.6010
0.2	0.6010	0.121	0.7252
0.3	0.7252	0.15404	0.87924
0.4	0.87924	0.191848	1.071088
0.5	1.071088	0.2392176	1.3103056
0.6	1.3103056	0.2980611	1.6083667

By comparing the result of the Euler method corresponding to 0.6 with the Analytical solution we see that the error is nearly 9%. We then conclude that a smaller interval should be used. Let's try $\Delta x = 0.01$ and summarize results in Table VIIe.2.3. Note that the intermediate steps are not shown.

With the smaller increment, we improved the accuracy of the Euler method by reducing the error to 1%. Data of Table VIIe.2.3 are produced by FORTRAN Program VIIe.2.1, included on the accompanying CD-ROM.

Table VIIe.2.3. Euler method ($\Delta x = 0.01$)

x	y_n	$f(x_n, y_n)$	y_{n+1}
0.0	0.5	1.0001	0.510001
0.1	0.510001	1.2056847	0.60989922
0.2	0.60989922	1.50221459	0.746129443
0.3	0.746129443	1.88558226	0.916646955
0.4	0.916646955	2.37480475	1.131150425
0.5	1.131150425	2.9930636724	1.4014624778
0.6	1.4014624778	3.7686172858	1.7419948229

The Runge-Kutta Methods

Another means of solving ordinary differential equations, also derived from the methods based on the Taylor series expansion, is the Runge-Kutta methods. These methods consist of four algorithms, which are similar in approach but differ in the number of subintervals used in each interval. Like the Euler method, the function is assumed to remain constant over a subinterval. The advantage of the Runge-Kutta methods is the much higher order of truncation error obtained than in the Euler method. The general form of the Runge-Kutta methods is:

$$y_{i+1} = y_i + \Delta x g(x_i, y_i, \Delta x)$$

Where function $g(x_n, y_n, \Delta x)$ depends on the specific Runge – Kutta method chosen for the analysis. The simplest form for the function g is given by the *three-points* Runge-Kutta method:

$$y_{i+1} = y_i + \Delta x g(x_{i+1/2}, y_i + \frac{\Delta x}{2} y'_n)$$

The third and fourth-order Runge-Kutta methods are equivalent to the Taylor's series method carried as far as third and fourth derivatives, respectively. The four-point of the third-order Runge-Kutta method is in the form of:

$$y_{i+1} = y_i + \frac{\Delta x}{6}(k_1 + 4k_2 + k_3)$$

where k_1 , k_2 , and k_3 are given as

$$k_1 = f(x_i, y_i)$$

$$k_2 = f(x_i + \frac{\Delta x}{2}, y_i + \frac{\Delta x}{2} k_1)$$

$$k_3 = f(x_i + \Delta x, y_i + 2\Delta x k_2 - \Delta x k_1)$$

The five-point of fourth-order Runge-Kutta method is in the form of:

$$y_{i+1} = y_i + \frac{\Delta x}{6}(k_1 + 2k_2 + 2k_3 + k_4)$$

where k_1 , k_2 , and k_3 are given as

$$k_1 = f(x_i, y_i)$$

$$k_2 = f\left(x_i + \frac{\Delta x}{2}, y_i + \frac{\Delta x}{2} k_1\right)$$

$$k_3 = f\left(x_i + \frac{\Delta x}{2}, y_i + \frac{\Delta x}{2} k_2\right)$$

$$k_4 = f(x_i + \Delta x, y_i + \Delta x k_3)$$

The same example is solved with the fourth-order Runge – Kutta method and the results are summarized in Table VIIe.2.4.

Table VIIe.2.4. The fourth-order Runge-Kutta method ($\Delta x = 0.1$)

x	$y_{\text{Runge - Kutta}}$	$y_{\text{Analytical}}$
0.0	0.5000000	0.5
0.1	0.6110508	0.611052
0.2	0.7488653	0.748868
0.3	0.9215829	0.921589
0.4	1.1391452	1.139156
0.5	1.4136948	1.413711
0.6	1.7600627	1.760087

By this method, the error at $x = 0.6$ is now reduced to 0.001%. Data for Table VIIe.2.4 are produced by FORTRAN program VIIe.2.2, included on the accompanying CD-ROM.

2.2. Methods Based on Predictor-Corrector

There are several methods based on the predictor-corrector concept such as the modified Euler method, Adams method, and Milne method.

The Modified Euler Method

In the *marching* technique, as used in the Euler method, the value at each subsequent increment is calculated from the derivative at the previous increment (i.e., y_{n+1} is obtained from y_n rather than y'_{n+1}). In the modified Euler method, to better represent the function in the chosen interval, $y'(x)$ is obtained at the average of y_n and y_{n+1} . Since the value of y'_{n+1} is not known before hand, an iterative process must be used. The approach in the modified Euler method is as follows:

$$\text{Predictor:} \quad y(x_{i+1}) = y(x_i) + \Delta x \, y'(x_i) \quad \text{VIIe.2.1}$$

$$\text{Corrector:} \quad y(x_{i+1}) = y(x_i) + \frac{\Delta x}{2} [y'(x_i) + y'(x_{i+1})] \quad \text{VIIe.2.2}$$

The corrector (Equation VIIe.2.2) can alternatively be written as:

$$y(x_{i+1}) = y(x_i) + \frac{\Delta x}{2} [f(x_i, y_i) + f(x_{i+1}, y_{i+1}^{(k)})] \quad \text{VIIe.2.3}$$

where in Equation VIIe.2.3, k is the iteration index and is placed inside the parentheses to emphasize that it is not an exponent for y . To demonstrate the modified Euler method, let's apply the predictor-corrector concept to the same example used in Section 2.1. For this purpose, we substitute:

$$\frac{dy}{dx} = 2y + x^2 = f(x, y)$$

into Equation VIIe.1.3 to obtain:

$$y_{i+1}^{(k+1)} = y_i + \frac{\Delta x}{2} [(x_i^2 + 2y_i) + (x_{i+1}^2 + 2y_{i+1}^{(k)})]$$

To find the starting value (i.e. y_1^0) we use the *Predictor* (i.e. Equation VIIe.2.1). Using an interval size of $\Delta x = 0.05$, the iterations for y_1 progress as follows:

$$\begin{aligned} y_1^0 &= 0.5 + 0.05 (0 + 2 \times 0.5) = 0.55 \\ y_1^1 &= 0.5 + 0.025 [(0 + 2 \times 0.5) + (0.05^2 + 2 \times 0.55)] = 0.5525625 \\ y_1^2 &= 0.5 + 0.025 [(0 + 2 \times 0.5) + (0.05^2 + 2 \times 0.5525625)] = 0.5526906 \\ y_1^3 &= 0.5 + 0.025 [(0 + 2 \times 0.5) + (0.05^2 + 2 \times 0.5526906)] = 0.55269700 \\ y_1^4 &= 0.5 + 0.025 [(0 + 2 \times 0.5) + (0.05^2 + 2 \times 0.55269700)] = 0.55269730 \\ y_1^5 &= 0.5 + 0.025 [(0 + 2 \times 0.5) + (0.05^2 + 2 \times 0.55269730)] = 0.55269730 \end{aligned}$$

In this case, the iteration converged in five steps. Generally, however, we stop the process after the specified convergence criterion is met, then we proceed to calculate y_2, y_3, y_4, \dots until the specified interval is covered.

For higher accuracy, we may choose a smaller increment such as 0.01, 0.001, etc. The results obtained from the modified Euler method for $\Delta x = 0.05$, $\Delta x = 0.01$, and $\Delta x = 0.001$ are shown in Table VIIe.2.5. The data for Table VIIe.1.4 are produced by FORTRAN program Table VIIe.1.2, included on the accompanying CD-ROM.

Table VIIe.2.5. The modified Euler method

x	$\Delta x = 0.05$	$\Delta x = 0.01$	$\Delta x = 0.001$	$y_{\text{Analytical}}$
0.0	0.5000000	0.5000000	0.5000000	0.5000000
0.1	0.6112050	0.6110582	0.6110521	0.611052
0.2	0.7492421	0.7488834	0.7488687	0.748868
0.3	0.9222736	0.9216164	0.9215894	0.921589
0.4	1.1402705	1.1392002	1.1391562	1.139156
0.5	1.4154136	1.4137793	1.4137121	1.413711
0.6	1.7625828	1.7601872	1.7600888	1.760087

The Milne Method

In this method the predictor – corrector are as follows:

$$\text{Predictor: } y(x_{i+1}) = y(x_{i-3}) + \frac{4\Delta x}{3} [2y'(x_i) - y'(x_{i-1}) + 2y'(x_{i-2})] \quad \text{VIIe.2.4}$$

$$\text{Corrector: } y(x_{i+1}) = y(x_{i-1}) + \frac{\Delta x}{3} [y'(x_{i+1}) + 4y'(x_i) + y'(x_{i-1})] \quad \text{VIIe.2.5}$$

The Adams–Bashforth Method

In this method the predictor – corrector are as follows:

Predictor:

$$y(x_{i+1}) = y(x_{i-3}) + \frac{\Delta x}{24} [55y'(x_i) - 59y'(x_{i-1}) + 37y'(x_{i-2}) - 9y'(x_{i-3})] \quad \text{VIIe.2.6}$$

Corrector:

$$y(x_{i+1}) = y(x_i) + \frac{\Delta x}{24} [9y'(x_{i+1}) + 19y'(x_i) - 5y'(x_{i-1}) + y'(x_{i-2})] \quad \text{VIIe.2.7}$$

In the first glance, the Milne and the Adams-Bashford equations look complicated and convey laborious computation. However, these are simple relations for programming and once coded, they can be used for any function and with any step size increment.

3. Numerical Solution of Partial Differential Equations

Most second-order partial differential equations for engineering applications have a general form of:

$$A \frac{\partial^2 u}{\partial x^2} + B \frac{\partial^2 u}{\partial x \partial y} + C \frac{\partial^2 u}{\partial y^2} + D(x, y, u, \frac{\partial y}{\partial x}, \frac{\partial y}{\partial x}) = 0$$

Depending on the value of $B^2 - 4AC$, the equation may be of elliptic, parabolic, or hyperbolic type:

If $B^2 - 4AC < 0$ the differential equation is elliptic

If $B^2 - 4AC = 0$ the differential equation is parabolic

If $B^2 - 4AC > 0$ the differential equation is hyperbolic

We can alternatively describe differential equations of the elliptic type as having the general form of the diffusion equation:

$$-\nabla p(\vec{r}) \nabla \phi(\vec{r}) + q(\vec{r}) \phi(\vec{r}) = S(\vec{r}) \quad \text{VIIe.3.1}$$

If $q(\bar{r}) = 0$ and $p(\bar{r}) = \text{constant}$, Equation VIIe.3.1 becomes the Poisson equation as introduced in Chapter VIIb. If $q(\bar{r}) = S(\bar{r}) = 0$, Equation VIIe.3.1 becomes the Laplace equation.

Similarly, partial differential equations of the parabolic type are in the general form of:

$$\frac{\partial \phi(\bar{r}, t)}{\partial t} = \nabla p(\bar{r}, t) \nabla \phi(\bar{r}, t) - q(\bar{r}, t) \phi(\bar{r}, t) + S(\bar{r}) \quad \text{VIIe.3.2}$$

Finally, partial differential equations of the hyperbolic type are in the form of the wave equation:

$$\frac{\partial^2 u}{\partial t^2} = \alpha^2 \left(\frac{\partial^2 u}{\partial x^2} + \frac{\partial^2 u}{\partial y^2} + \frac{\partial^2 u}{\partial z^2} \right) \quad \text{VIIe.3.3}$$

To solve any of the elliptic, parabolic, or hyperbolic type partial differential equations numerically, we replace the derivatives by a difference quotient. To demonstrate the difference equivalent of a second order derivative, we make use of the Taylor series to expand $f(x_i - \Delta x)$ and $f(x_i + \Delta x)$ about point x and assume that the function has a continuous fourth derivative:

$$f(x_i - \Delta x) = f(x_i) - f'(x_i)\Delta x + \frac{f''(x_i)}{2}\Delta x^2 - \frac{f'''(x_i)}{6}\Delta x^3 + \frac{f^{iv}(x_i)}{24}\Delta x^4 + \dots$$

Similarly

$$f(x_i + \Delta x) = f(x_i) + f'(x_i)\Delta x + \frac{f''(x_i)}{2}\Delta x^2 + \frac{f'''(x_i)}{6}\Delta x^3 + \frac{f^{iv}(x_i)}{24}\Delta x^4 + \dots$$

We now sum these expansions to get:

$$f_i'' = \frac{f_{i+1} - 2f_i + f_{i-1}}{\Delta x^2}$$

The error in ignoring the remaining terms is of the order of Δx^2 . Similarly, we can use central difference approximation to represent the first derivative as:

$$f_i' = \frac{f_{i+1} - f_{i-1}}{2\Delta x}$$

with the same error of order Δx^2 as for the second derivative.

3.1. Elliptic Equations

An example of the elliptic partial differential equation is the steady-state heat conduction equation. In this section, we use two slightly different methods of solving this equation numerically. The first method uses the derived conduction equation in the form of a Laplace equation and applies the difference approximation where

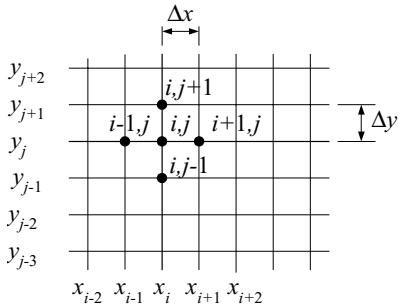


Figure VIIe.3.1. Subdivision of a region in the xy -plane

in the second method, we show how to derive the heat conduction equation in difference form.

Solving the Laplace Equation

First, to demonstrate the solution of partial differential equations by difference approximation, consider the two-dimensional Laplace equation:

$$\frac{\partial^2 u}{\partial x^2} + \frac{\partial^2 u}{\partial y^2} = 0$$

We now subdivide the region of interest into incremental values (Figure VIIe.3.1). The Laplace equation becomes:

$$\frac{u_{i-1,j} - 2u_{i,j} + u_{i+1,j}}{(\Delta x)^2} + \frac{u_{i,j-1} - 2u_{i,j} + u_{i,j+1}}{(\Delta y)^2} = 0 \quad \text{VIIe.3.4}$$

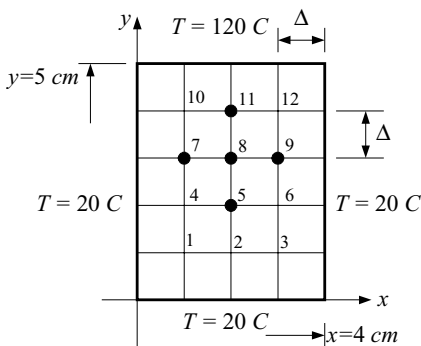


Figure VIIe.3.2. Temperature distribution in a homogeneous plate

If for simplicity we assume that the x increment and the y increments are equal, we get the algorithm as:

$$u_{i-1,j} + u_{i+1,j} - 4u_{i,j} + u_{i,j-1} + u_{i,j+1} = 0 \quad \text{VIIe.3.5}$$

or equivalently:

$$u_{i,j} = 0.25(u_{i-1,j} + u_{i+1,j} + u_{i,j-1} + u_{i,j+1})$$

implying that the dependent value at each node is the arithmetic average of the dependent value of all the neighboring nodes. As an example, we may use Equation VIIb.3.5 to find nodal temperatures in the interior of a plate made of a homogeneous material, having all the four boundary temperatures as shown in Figure VIIe.3.2. Using an equal increment of 1 cm for both x and y axes, we obtain the following sets of equations for nodes 1 through 12.

For node number 1:	$-4T_1 + T_2 + T_4 = -40$
For node number 2:	$T_1 + T_3 - 4T_2 + T_5 = -20$
For node number 3:	$T_2 - 4T_3 + T_6 = -40$
For node number 4:	$T_1 - 4T_4 + T_5 + T_7 = -20$
For node number 5:	$T_2 + T_4 - 4T_5 + T_6 + T_8 = 0$
For node number 6:	$T_3 + T_5 - 4T_6 + T_9 = -20$
For node number 7:	$T_4 - 4T_7 + T_8 + T_{10} = -20$
For node number 8:	$T_5 + T_7 - 4T_8 + T_9 + T_{11} = 0$
For node number 9:	$T_6 + T_8 - 4T_9 + T_{12} = -20$
For node number 10:	$T_7 - 4T_{10} + T_{11} = -140$
For node number 11:	$T_8 + T_{10} - 4T_{11} + T_{12} = -120$
For node number 12:	$T_9 + T_{11} - 4T_{12} = -140$

Since this is a set of linear algebraic equations, we can arrange it in a matrix as follows:

$$\begin{bmatrix} 1 & 2 & 3 & 4 & 5 & 6 & 7 & 8 & 9 & 10 & 11 & 12 \\ 1 & -4 & 1 & 0 & 0 & 0 & 0 & 0 & 0 & 0 & 0 & 0 \\ 2 & 1 & -4 & 1 & 0 & 1 & 0 & 0 & 0 & 0 & 0 & 0 \\ 3 & 0 & 1 & -4 & 0 & 0 & 1 & 0 & 0 & 0 & 0 & 0 \\ 4 & 1 & 0 & 1 & -4 & 0 & 0 & 1 & 0 & 0 & 0 & 0 \\ 5 & 0 & 1 & 0 & 1 & -4 & 0 & 0 & 1 & 0 & 0 & 0 \\ 6 & 0 & 0 & 1 & 0 & 1 & -4 & 0 & 0 & 1 & 0 & 0 \\ 7 & 0 & 0 & 0 & 1 & 0 & 1 & -4 & 0 & 0 & 1 & 0 \\ 8 & 0 & 0 & 0 & 0 & 1 & 0 & 1 & -4 & 0 & 0 & 1 \\ 9 & 0 & 0 & 0 & 0 & 0 & 1 & 0 & 1 & -4 & 0 & 0 \\ 10 & 0 & 0 & 0 & 0 & 0 & 0 & 1 & 0 & 1 & -4 & 0 \\ 11 & 0 & 0 & 0 & 0 & 0 & 0 & 0 & 1 & 0 & 1 & -4 \\ 12 & 0 & 0 & 0 & 0 & 0 & 0 & 0 & 0 & 1 & 0 & 1 \end{bmatrix} \begin{bmatrix} T_1 \\ T_2 \\ T_3 \\ T_4 \\ T_5 \\ T_6 \\ T_7 \\ T_8 \\ T_9 \\ T_{10} \\ T_{11} \\ T_{12} \end{bmatrix} = \begin{bmatrix} -40 \\ -20 \\ -40 \\ -20 \\ 0 \\ -20 \\ -20 \\ 0 \\ -20 \\ -140 \\ -120 \\ -140 \end{bmatrix}$$

As pointed out in Chapter VIId, there are several ways to solve this matrix equation including matrix inversion and Gauss-Seidel iteration. Solving this set of equations, we find the determinant of the coefficient matrix to be equal to 0.414E7 and the value of T_1 through T_{12} (in Centigrade) as:

T_1	T_2	T_3	T_4	T_5	T_6	T_7	T_8	T_9	T_{10}	T_{11}	T_{12}
23.3	24.7	23.3	28.7	32.0	28.7	39.5	46.0	39.5	63.1	73.1	63.1

Expectedly, the temperature of nodes 1, 4, 7, and 10 are the same as temperature of nodes 3, 6, 9, and 12. Hence, we could reduce the number of equations by taking advantage of symmetry.

Let's now solve a similar problem but this time as shown in Figure VII.3.3, the boundary conditions are specified such that there is no symmetry to reduce the number of equations. Following the same procedure outlined for the previous example, we find the following matrix equation:

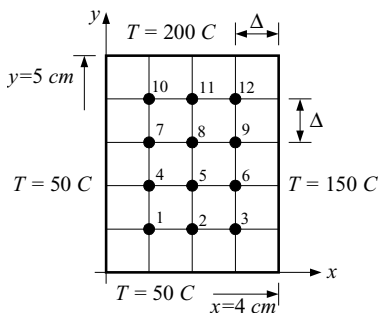


Figure VIIe.3.3. Temperature distribution in a heterogeneous plate

$$\begin{array}{cccccccccccc}
 & 1 & 2 & 3 & 4 & 5 & 6 & 7 & 8 & 9 & 10 & 11 & 12 \\
 \begin{array}{l} 1 \\ 2 \\ 3 \\ 4 \\ 5 \\ 6 \\ 7 \\ 8 \\ 9 \\ 10 \\ 11 \\ 12 \end{array} & \begin{bmatrix} -4 & 1 & 0 & 1 & 0 & 0 & 0 & 0 & 0 & 0 & 0 & 0 & 0 \\ 1 & -4 & 1 & 0 & 1 & 0 & 0 & 0 & 0 & 0 & 0 & 0 & 0 \\ 0 & 1 & -4 & 0 & 0 & 1 & 0 & 0 & 0 & 0 & 0 & 0 & 0 \\ 1 & 0 & 1 & -4 & 0 & 0 & 1 & 0 & 0 & 0 & 0 & 0 & 0 \\ 0 & 1 & 0 & 1 & -4 & 0 & 0 & 1 & 0 & 0 & 0 & 0 & 0 \\ 0 & 0 & 1 & 0 & 1 & -4 & 0 & 0 & 1 & 0 & 0 & 0 & 0 \\ 0 & 0 & 0 & 1 & 0 & 1 & -4 & 0 & 0 & 1 & 0 & 0 & 0 \\ 0 & 0 & 0 & 0 & 1 & 0 & 1 & -4 & 0 & 0 & 1 & 0 & 0 \\ 0 & 0 & 0 & 0 & 0 & 1 & 0 & 1 & -4 & 0 & 0 & 1 & 0 \\ 0 & 0 & 0 & 0 & 0 & 0 & 1 & 0 & 1 & -4 & 0 & 0 & 0 \\ 0 & 0 & 0 & 0 & 0 & 0 & 0 & 1 & 0 & 1 & -4 & 0 & 0 \\ 0 & 0 & 0 & 0 & 0 & 0 & 0 & 0 & 1 & 0 & 1 & -4 & 0 \end{bmatrix} & \begin{bmatrix} T_1 \\ T_2 \\ T_3 \\ T_4 \\ T_5 \\ T_6 \\ T_7 \\ T_8 \\ T_9 \\ T_{10} \\ T_{11} \\ T_{12} \end{bmatrix} & = & \begin{bmatrix} -100 \\ -50 \\ -200 \\ -50 \\ 0 \\ -150 \\ -50 \\ 0 \\ -150 \\ -50 \\ -200 \\ -350 \end{bmatrix}
 \end{array}$$

We expect to get the lowest temperature at node 1 and the highest temperature at node 12. Here are the results, in Centigrade, for this case:

T_1	T_2	T_3	T_4	T_5	T_6	T_7	T_8	T_9	T_{10}	T_{11}	T_{12}
63.6	78.1	100	76.3	99.0	122	92.4	120	138	123	151	160

We may use the same method to solve similar problems for other boundary temperatures or other mesh sizes such as 0.1 cm. Smaller mesh sizes give more detailed information about temperature distribution in the plate.

Direct Derivation of The Heat Conduction Equation

In the above examples, we used the Laplace equation to solve two cases that dealt only with temperature boundary condition. In the second method, we will derive the conduction equation in its difference form.

To do this, we use an arbitrary node such as node x_i, y_j for the medium shown in Figure VIIe.3.4. This node represents the shaded rectangle, one side at Δx and the other at Δy . In this method, we also consider an additional term for internal heat generation.

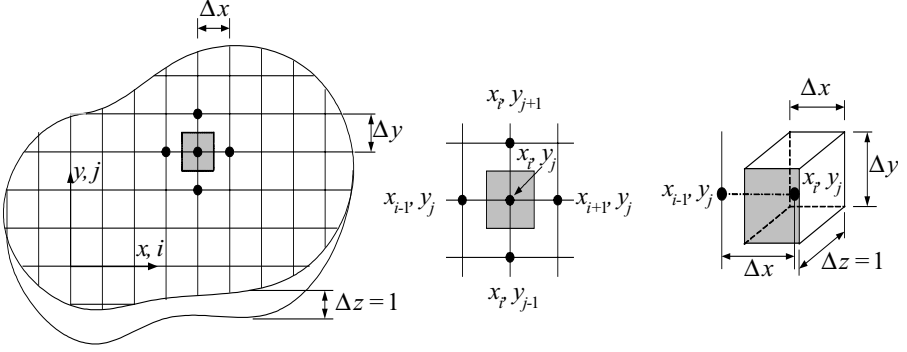


Figure VIIe.3.4. Determination of temperature distribution by direct derivation of heat conduction equation

In the Cartesian coordinate system, the adjacent nodes that exchange heat with node (x_i, y_j) are nodes (x_{i-1}, y_j) , (x_{i+1}, y_j) , (x_i, y_{j-1}) and (x_i, y_{j+1}) . For simplicity, we refer to these nodes by using only their indices hence, (x_i, y_j) is node (i, j) , etc. Each node in the center of a shaded area (parallelepiped of unit depth) represents the temperature of that area. This shows that in order to have more accurate temperature distribution, we should use a smaller mesh size or increment. Also note that we are using a unit depth which makes the temperature distribution two-dimensional. Generally, we must also consider temperature distribution in the z -direction, in other words, we should solve a three-dimensional problem. We now apply the first law of thermodynamics to the two-dimensional problem of Figure VIIe.3.5, using each shaded area as a control volume with unit depth perpendicular to the plane of Figure VIIe.3.5. The first law states that in steady state, summation of the rate of heat transfer from all of the adjacent nodes plus the rate of internal heat generation must be equal to zero:

$$\dot{Q}_{i-1,j \rightarrow i,j} + \dot{Q}_{i+1,j \rightarrow i,j} + \dot{Q}_{i,j-1 \rightarrow i,j} + \dot{Q}_{i,j+1 \rightarrow i,j} + \dot{q}''' V_{i,j} = 0$$

If there is no internal heat generation, by substituting from the Fourier's law of heat conduction we get:

$$k(\Delta y \times 1) \frac{T_{i-1,j} - T_{i,j}}{\Delta x} + k(\Delta y \times 1) \frac{T_{i+1,j} - T_{i,j}}{\Delta x} + k(\Delta x \times 1) \frac{T_{i,j-1} - T_{i,j}}{\Delta y} + k(\Delta x \times 1) \frac{T_{i,j+1} - T_{i,j}}{\Delta y} = 0$$

If we assume equal increments in the x and y directions, this equation reduces to Equation VIIe.3.5 as derived from the Laplace equation. Having derived the algorithm for interior nodes, we can proceed with the derivation of corner nodes and nodes exposed to convection boundary conditions shown in Figure VIIe.3.6.

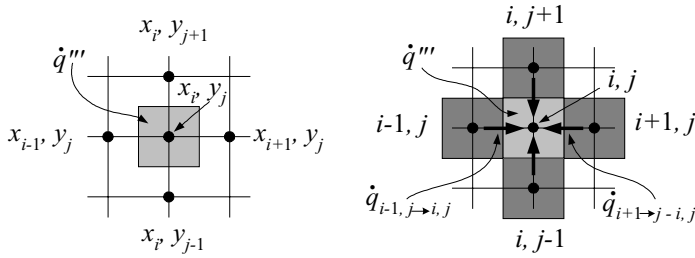


Figure VIIe.3.5. Nodal heat transfer in steady state two - dimensional conduction

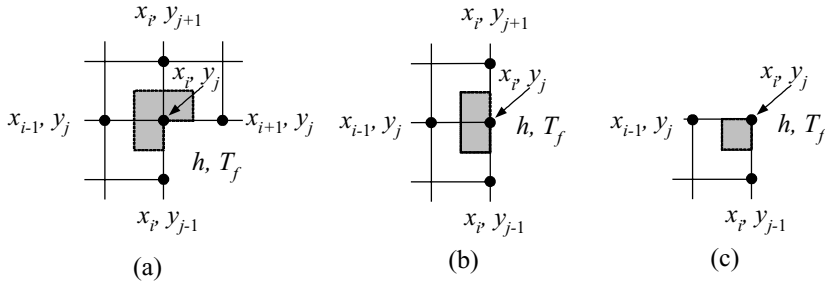


Figure VIIe.3.6. (a) Node at interior corner, (b) node at plane surface, and (c) node at external corner

For the internal corner node with convection of Figure VIIe.3.6(a), we must consider heat conduction from half of the area and heat convection from the rest of the area for nodes $i, j - 1$ and $i + 1, j$. The rate of heat transfer from nodes $i - 1, j$ and $i, j + 1$ is the same as given by Equation VIIe.3.4:

$$k(\Delta y \times 1) \frac{T_{i-1,j} - T_{i,j}}{\Delta x} + \left[k\left(\frac{\Delta y}{2} \times 1\right) \frac{T_{i+1,j} - T_{i,j}}{\Delta x} + h\left(\frac{\Delta y}{2} \times 1\right)(T_f - T_{i,j}) \right] +$$

$$\left[k\left(\frac{\Delta x}{2} \times 1\right) \frac{T_{i,j-1} - T_{i,j}}{\Delta y} + h\left(\frac{\Delta x}{2} \times 1\right)(T_f - T_{i,j}) \right] + k(\Delta x \times 1) \frac{T_{i,j+1} - T_{i,j}}{\Delta y} = 0$$

If the mesh sizes or increments are the same ($\Delta x = \Delta y$), we can simplify this equation to obtain:

$$2(T_{i-1,j} + T_{i,j+1}) + (T_{i+1,j} + T_{i,j-1}) - 2\left(3 + \frac{h\Delta x}{k}\right)T_{i,j} = -2\frac{h\Delta x}{k}T_f \quad \text{VIIe.3.6}$$

or the node at the plane surface with the convection boundary, Figure VIIe.3.5(b), we must consider heat conduction from half of the area and heat convection from the rest of the area for nodes $i, j - 1$ and $i, j + 1$. The rate of heat transfer from node $i - 1, j$ is the same as Figure VIIe.3.5(a):

$$k(\Delta y \times 1) \frac{T_{i-1,j} - T_{i,j}}{\Delta x} + \left[k\left(\frac{\Delta y}{2} \times 1\right) \frac{T_{i,j+1} - T_{i,j}}{\Delta x} + h\left(\frac{\Delta y}{2} \times 1\right)(T_f - T_{i,j}) \right] + \left[k\left(\frac{\Delta x}{2} \times 1\right) \frac{T_{i,j-1} - T_{i,j}}{\Delta y} + h\left(\frac{\Delta x}{2} \times 1\right)(T_f - T_{i,j}) \right] = 0 \quad \text{VIIe.3.7}$$

If the mesh sizes or increments are the same ($\Delta x = \Delta y$), we can simplify Equation VIIe.3.7 to get:

$$(2T_{i-1,j} + T_{i,j+1} + T_{i,j-1}) - 2\left(2 + \frac{h\Delta x}{k}\right)T_{i,j} = -2\frac{h\Delta x}{k}T_f \quad \text{VIIe.3.8}$$

For the corner node with convection boundary and different heat transfer coefficients, Figure VIIe.3.5(c), we must consider heat conduction from half of the area and heat convection from the rest of the area for nodes $i-1, j$ and $i, j-1$:

$$\left[k\left(\frac{\Delta y}{2} \times 1\right) \frac{T_{i-1,j} - T_{i,j}}{\Delta x} + h\left(\frac{\Delta y}{2} \times 1\right)(T_f - T_{i,j}) \right] + \left[k\left(\frac{\Delta x}{2} \times 1\right) \frac{T_{i,j-1} - T_{i,j}}{\Delta y} + h\left(\frac{\Delta x}{2} \times 1\right)(T_f - T_{i,j}) \right] = 0$$

Similarly, if the mesh sizes are the same ($\Delta x = \Delta y$), we can simplify this equation to get:

$$(T_{i-1,j} + T_{i,j-1}) - 2\left(1 + \frac{h\Delta x}{k}\right)T_{i,j} = -2\frac{h\Delta x}{k}T_f \quad \text{VIIe.3.9}$$

Two-Dimensional Temperature Distribution with Internal Heat Generation

We now derive similar algorithm for nodes considering internal heat generation in these nodes. This includes an interior node, an interior corner node, a node at a plane surface, and an external corner node.

Interior node (Figure VIIe.3.5):

$$T_{i-1,j} + T_{i+1,j} + T_{i,j-1} + T_{i,j+1} - 4T_{i,j} + \frac{(\Delta x)^2}{k} \dot{q}''' = 0$$

Internal corner node with convection boundary, Figure VIIe.3.6(a):

$$2(T_{i-1,j} + T_{i,j+1}) + (T_{i+1,j} + T_{i,j-1}) - [6 + (h_1 + h_2) \frac{\Delta x}{k}]T_{i,j} + \frac{3(\Delta x)^2}{2k} \dot{q}''' = -(h_1 + h_2) \frac{\Delta x}{k} T_f$$

Node at plane surface with convection boundary, Figure VIIe.3.6(b):

$$(2T_{i-1,j} + T_{i,j+1} + T_{i,j-1}) - 2\left(2 + \frac{h\Delta x}{k}\right)T_{i,j} + \frac{(\Delta x)^2}{k} \dot{q}''' = -2\frac{h\Delta x}{k}T_f$$

For the corner node with convection boundary and different heat transfer coefficients, Figure VIIe.3.6(c):

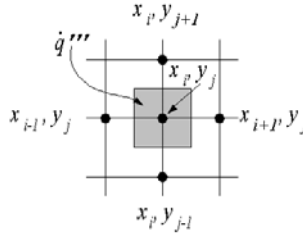
$$(T_{i-1,j} + T_{i,j-1}) - [2 + (h_1 + h_2) \frac{\Delta x}{k}] T_{i,j} + \frac{(\Delta x)^2}{2k} \dot{q}''' = -(h_1 + h_2) \frac{\Delta x}{k} T_f$$

These results are summarized in Table VIIe.3.1. A two-dimensional temperature distribution in a solid with internal heat generation is solved in Section 10 of Chapter IVa using the rectangular coordinates. We can use similar procedure to solve problems in other orthogonal but not rectangular coordinates, such as cylindrical and spherical coordinates.

3.2. Parabolic Equations

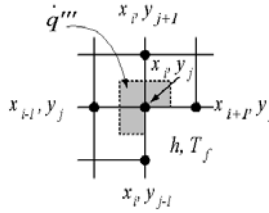
Partial differential equations of the parabolic type are the most important equations in the field of thermal science. The parabolic differential equations deal with physical problems, which are time-dependent (also known as unsteady-state or *transient*) in nature. As an example of a transient heat conduction problem, consider the same problem shown in Figure VIIe.3.7 when one or several of the inputs changes with time. This can either be due to a change in the ambient temperature (T_f) with time, change in the internal heat generation with time, or change in any of the boundary temperatures with time. In the differential equations of the parabolic type, we have to deal with space as well as time increments. In a three-dimensional problem, we have four increments such as Δx , Δy , Δz , and Δt . Since, in these types of problems, a whole set of distribution for the unknown parameter, temperature for example, changes from one time step to another, we then have to consider the concept of “values at the old time step” versus “values at the new time step”. This, in turn, brings up the concept of *explicit* versus *implicit* methods. In the explicit method, the unknown is defined only in terms of the known values, which are determined in the old or previous time step. In the implicit method on the other hand, all the values that are used to determine the unknown are themselves expressed in the new time step. There is also the *semi-implicit* method where, as the name implies, only some of the values that determine the unknown are expressed in terms of the new time step.

An example of a one-dimensional parabolic differential equation includes time dependent temperature distribution in a slender solid bar. In a slender bar, it is reasonable to assume that each cross section can be represented with one temperature. If the two ends are maintained at different but fixed temperatures, then temperature varies only along the length of the bar. Now, suppose that temperature at one or both ends begin to change with time. Temperature distribution along the length of the bar will respond to this change and produce a time dependent profile for each cross section along the length of the bar. Shown in Figure VIIe.3.8 is a schematic representation of the space and time nodalization for determination of temperature distribution in the solid bar. Functions $f_1(t)$ and $f_2(t)$ represent variation in temperatures at both ends of the solid bar while $f_3(x)$ shows the initial temperature distribution in the bar before the end temperatures begin to change with time.

Table VIIe.3.1. Finite difference equations for two-dimensional transient heat conduction


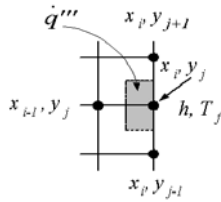
Interior Node:

$$T_{i-1,j} + T_{i+1,j} + T_{i,j-1} + T_{i,j+1} - 4T_{i,j} + \dot{q}'''[(\Delta x)^2 / k] = 0$$



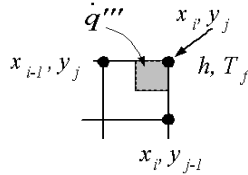
Interior Corner Node:

$$2(T_{i-1,j} + T_{i,j+1}) + (T_{i+1,j} + T_{i,j-1}) - 2(3 + h)(\Delta x / k)T_{i,j} + \left(\frac{3\dot{q}'''(\Delta x)^2}{2k}\right) = -2h(\Delta x / k)T_f$$



Plane Surface Node:

$$(2T_{i-1,j} + T_{i,j-1} + T_{i,j+1}) + 2[2 + (h\Delta x / k)]T_{i,j} + \dot{q}'''[(\Delta x)^2 / k] = -2(h\Delta x / k)T_f$$



Exterior Corner Node:

$$(T_{i-1,j} + T_{i,j-1}) - 2[1 + h(\Delta x / k)]T_{i,j} + \dot{q}'''[(\Delta x)^2 / 2k] = -2h(\Delta x / k)T_f$$

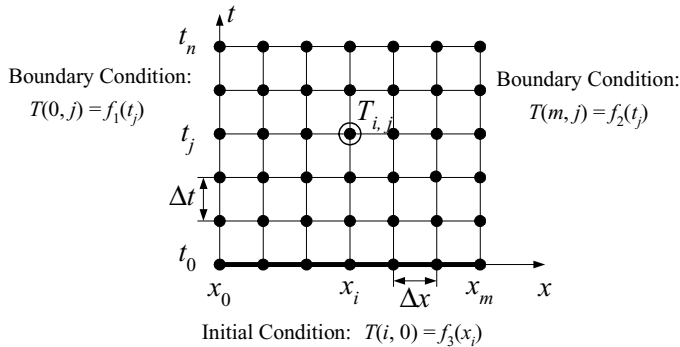


Figure VIIe.3.7. One-dimensional transient temperature distribution in a solid bar

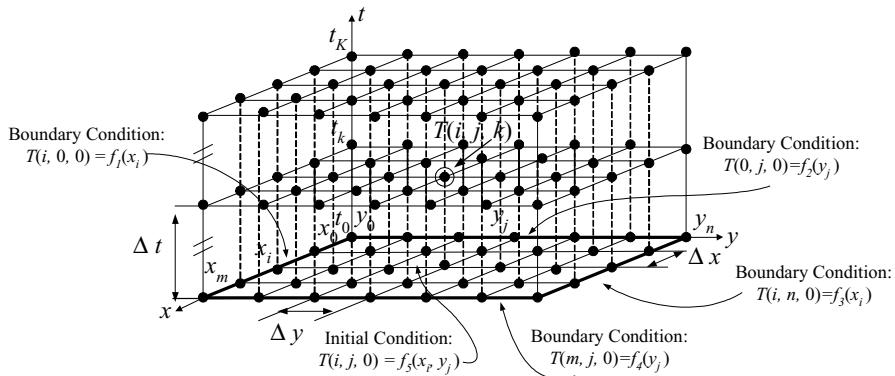


Figure VIIe.3.8. Two-dimensional transient temperature distribution in a plate

Similar discussion is applicable to a two-dimensional parabolic partial differential equation. For example, consider temperature distribution in the plate of Figure VIIe.3.8. Initially, temperature at the four boundaries is specified and the steady-state temperature distribution in the plate is given as $f_3(x, y)$. Then one or all of the four boundary temperatures are allowed to change with time. Nodal temperatures within the plate then become functions of x , y , and t .

Explicit and Implicit Numerical Schemes

The concepts of explicit and implicit numerical schemes appear when we try to discretize the differential terms. Let's consider the heat conduction equation describing time dependent temperature distribution in the plate of Figure VIIe.3.8:

$$\frac{\partial^2 T(x, y, t)}{\partial x^2} + \frac{\partial^2 T(x, y, t)}{\partial y^2} = \frac{1}{\alpha} \frac{\partial T(x, y, t)}{\partial t} \quad \text{VIIe.3.10}$$

We now begin to discretize the differential terms in finite difference. The more straightforward term to tackle is the time derivative term, which describes the rate of change of nodal temperature. In other words, this term describes the difference between nodal temperature in the new time step and the previous time step. Here, for the sake of consistency, we use the same notation as used in Figure VIIe.3.8. Subscripts i and j are used to represent nodal temperature in the x and y directions, respectively. The range of subscript i is from 0 to m and the range of subscript j is from 0 to n . Superscript k is used to represent nodal temperature at the previous time step and $k + 1$ for nodal temperature at the new time step:

$$\left. \frac{\partial T(x, y, t)}{\partial t} \right|_{i, j} = \frac{T_{i, j}^{k+1} - T_{i, j}^k}{\Delta t} \quad \text{VIIe.3.11}$$

Having discretized the temporal term, we now proceed to discretize the spatial terms. For this purpose, we may use the forward difference method where each nodal temperature is described in terms of its adjacent nodes as done in Equation VIIe.3.10:

$$\frac{\partial^2 T(x, y)}{\partial x^2} + \frac{\partial^2 T(x, y)}{\partial y^2} = \frac{T_{i-1, j} - 2T_{i, j} + T_{i+1, j}}{(\Delta x)^2} + \frac{T_{i, j-1} - 2T_{i, j} + T_{i, j+1}}{(\Delta y)^2}$$

What is missing in this expression is the lack of reference to time, as this expression is applicable to the steady-state condition. If we express all the above temperatures to correspond to the current time step:

$$\frac{\partial^2 T(x, y, t)}{\partial x^2} + \frac{\partial^2 T(x, y, t)}{\partial y^2} = \frac{T_{i-1, j}^k - 2T_{i, j}^k + T_{i+1, j}^k}{(\Delta x)^2} + \frac{T_{i, j-1}^k - 2T_{i, j}^k + T_{i, j+1}^k}{(\Delta y)^2} \quad \text{VIIe.3.12}$$

and substitute Equations VIIe.3.12 and VIIe.3.11 into Equation VIIe.3.10, we can find temperature of node i, j at the next time step ($T_{i, j}^{k+1}$) *explicitly* in terms of nodal temperatures at the current time step:

$$\frac{T_{i-1, j}^k - 2T_{i, j}^k + T_{i+1, j}^k}{(\Delta x)^2} + \frac{T_{i, j-1}^k - 2T_{i, j}^k + T_{i, j+1}^k}{(\Delta y)^2} = \frac{1}{\alpha} \frac{T_{i, j}^{k+1} - T_{i, j}^k}{\Delta t}$$

If we assume that $\Delta x = \Delta y$ and we also replace $\alpha \Delta t / (\Delta x)^2 = \text{Fo}$, the above expression simplifies to:

$$T_{i, j}^{k+1} = \text{Fo}(T_{i-1, j}^k + T_{i+1, j}^k + T_{i, j-1}^k + T_{i, j+1}^k) + (1 - 4\text{Fo})T_{i, j}^k \quad \text{VIIe.3.13}$$

Equation VIIe.3.13 provides the algorithm that allows us to calculate the nodal temperature of the new time step in terms of all the known temperatures of the previous time step. To compare this explicit approach with the *fully implicit* approach, we use the same equations and the same substitutions but develop the spa-

tial finite difference in Equation VIIe.3.12 with temperatures that correspond to the new time step to get:

$$\frac{T_{i-1,j}^{k+1} - 2T_{i,j}^{k+1} + T_{i+1,j}^{k+1}}{(\Delta x)^2} + \frac{T_{i,j-1}^{k+1} - 2T_{i,j}^{k+1} + T_{i,j+1}^{k+1}}{(\Delta y)^2} = \frac{1}{\alpha} \frac{T_{i,j}^{k+1} - T_{i,j}^k}{\Delta t}$$

If we assume that $\Delta x = \Delta y$ and we also replace $\alpha \Delta t / (\Delta x)^2 = \text{Fo}$, the above expression simplifies to:

$$(1 - 4\text{Fo})T_{i,j}^{k+1} - \text{Fo}(T_{i-1,j}^{k+1} + T_{i+1,j}^{k+1} + T_{i,j-1}^{k+1} + T_{i,j+1}^{k+1}) = T_{i,j}^k \quad \text{VIIe.3.14}$$

In Equation VIIe.3.14 the intended nodal temperature as well as all the neighboring temperatures are unknown. Equation VIIe.3.14 provides the algorithm to develop a set of algebraic equations, which should be solved simultaneously to find nodal temperatures corresponding to the new time step.

Stability of Explicit and Implicit Schemes

Comparing Equations VIIe.3.13 and VIIe.3.14, we see that the nodal temperature for the new time step in the explicit scheme is readily calculated in terms of known temperatures of the previous time step as opposed to the implicit scheme where sets of algebraic equations must be solved in each time step. On the other hand, the implicit scheme is unconditionally stable whereas in the explicit scheme we must ensure the spatial and temporal increments are small enough to obtain convergence and calculate meaningful physical quantities. As a result, to prevent instability due to the numerically induced oscillations, it can be both physically and mathematically shown that in Equation VIIe.3.13 we must have $1 - 4\text{Fo} \geq 0$. Hence, the condition for stability in the explicit numerical scheme requires that $\text{Fo} \leq 1/4$ or equivalently $\Delta t \leq \Delta x^2 / 4\alpha$. This implies that in solving two-dimensional problems by the explicit scheme, once the spatial increment is chosen, the temporal increment must remain smaller than the square of the spatial increment divided by 4α .

Derivation of Finite Difference Formulation for Nodal Temperature

Earlier we derived the finite difference formulation of the nodal temperatures from the heat conduction equation VIIe.3.10. We may derive the same formulation in both explicit and implicit schemes from the energy balance for each node. For example, for an interior node, as shown in Figure VIIe.3.4, we write:

Total rate of heat transfer into the node + Rate of internal heat generation in the node = Rate of change of nodal internal energy

We can substitute for each term, in either an explicit or implicit manner. For example, if we develop terms implicitly we get:

$$k(\Delta y \times 1) \frac{T_{i-1,j}^{k+1} - T_{i,j}^{k+1}}{\Delta x} + k(\Delta y \times 1) \frac{T_{i+1,j}^{k+1} - T_{i,j}^{k+1}}{\Delta x} + k(\Delta x \times 1) \frac{T_{i,j-1}^{k+1} - T_{i,j}^{k+1}}{\Delta y} + k(\Delta x \times 1) \frac{T_{i,j+1}^{k+1} - T_{i,j}^{k+1}}{\Delta y} + \dot{q}'''(\Delta x \times \Delta y \times 1) = \rho(\Delta x \times \Delta y \times 1) c_p \frac{T_{i,j}^{k+1} - T_{i,j}^k}{\Delta t}$$

Note that, in this derivation we have assumed a constant rate of heat generation and thermal properties that are independent of temperature. In general, thermal properties are temperature dependent and the rate of internal heat generation may change with time. In this case, we should also develop such terms in a discretize manner based on the constitutive equations explaining each term, which is rather straightforward in the explicit scheme. However, in the implicit scheme, development of the related constitutive equations would lead to the appearance of nonlinear terms, which should be linearized. Returning to the above equation, if we assume $\Delta x = \Delta y$ and make use of the definition of thermal diffusivity, we obtain Equation VIIe.3.14 with an additional term representing the internal heat generation. Using the derivation method described here, we can derive similar relations for interior corner, plane surface, and external corner nodes as shown in Figure VIIe.3.5. The derivation is left as an exercise to the reader. The results are summarized in Table VIIe.3.2.

Note that in Table VIIe.3.1, a constant internal heat generation is assumed. If there is no internal heat generation, then the volumetric heat generation rate (i.e. term \dot{q}''') should be set equal to zero. Also note that if a boundary is insulated rather than being exposed to a convection boundary, the heat transfer coefficient can be viewed as being zero. Hence, for insulated, adiabatic, or symmetric surfaces, the Bi in equations of Table VIIe.3.2 must be set equal to zero.

Slab Exposed to Convection Heat Transfer at the Boundary

As an example, let's consider the implicit formulation for temperature distribution in a slab of a specified initial temperature exposed to convection heat transfer at its boundaries. The formulation may take into account heterogeneous internal heat generation and material (i.e., both \dot{q}''' and k are functions of location). As shown in Figure VIIe.3.9, the slab is divided into N regions. The thickness of the interior regions is Δx and the thickness of the boundary regions is $\Delta x/2$. Thus, the interior nodes are located in the center of the interior regions. Due to the symmetry, we may write the energy equations for only half of the slab and apply an adiabatic boundary to the center of the slab. The energy equation for the i th interior node becomes:

$$k_{i-1} \frac{T_{i-1}^{k+1} - T_i^{k+1}}{\Delta x} + k_{i+1} \frac{T_{i+1}^{k+1} - T_i^{k+1}}{\Delta x} + (\dot{q}_i''')^{k+1} \times \Delta x = \rho \times \Delta x \times c_p \frac{T_i^{k+1} - T_i^k}{\Delta t}$$

Next, we consider the energy equation for the boundary nodes, nodes 1 and m .

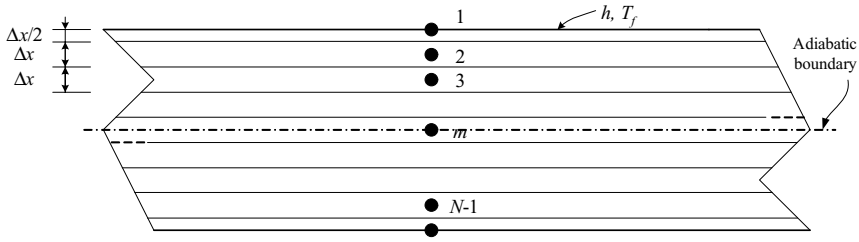


Figure VIIe.3.9. Schematic of a slab exposed to convection boundary

For node 1, exposed to heat transfer by convection, we write:

$$h(T_f^{k+1} - T_1^{k+1}) + k_2 \frac{T_2^{k+1} - T_1^{k+1}}{\Delta x} + (\dot{q}_1'')^{k+1} \times \Delta x / 2 = \rho \times \Delta x / 2 \times c_p \frac{T_1^{k+1} - T_1^k}{\Delta t}$$

and for node m , located on an adiabatic boundary, we write:

$$k_{m-1} \frac{T_m^{k+1} - T_{m-1}^{k+1}}{\Delta x} + (\dot{q}_m'')^{k+1} \times \Delta x / 2 = \rho \times \Delta x / 2 \times c_p \frac{T_m^{k+1} - T_m^k}{\Delta t}$$

where k is thermal conductivity and k , as the superscript, is an index to advance time. Writing the energy equation for all the interior nodes, we can summarize the results in the following matrix equation:

$$\begin{bmatrix} 1 + 2\text{Fo} + 2\text{FoBi} & -\text{Fo} & 0 & 0 & \dots & 0 \\ -\text{Fo} & 1 + 2\text{Fo} & -\text{Fo} & 0 & \dots & 0 \\ 0 & -\text{Fo} & 1 + 2\text{Fo} & -\text{Fo} & \dots & 0 \\ 0 & \dots & \dots & \dots & \dots & \dots \\ \dots & \dots & \dots & -\text{Fo} & 1 + 2\text{Fo} & -\text{Fo} \\ 0 & 0 & 0 & \dots & -2\text{Fo} & 1 + \text{Fo} \end{bmatrix} \begin{bmatrix} T_1^{k+1} \\ T_2^{k+1} \\ T_3^{k+1} \\ \dots \\ T_{m-1}^{k+1} \\ T_m^{k+1} \end{bmatrix} = \begin{bmatrix} 2\text{FoBi}T_f^{k+1} \\ T_2^k \\ T_3^k \\ \dots \\ T_{m-1}^k \\ T_m^k \end{bmatrix}$$

Starting at time zero (the superscript $k = 0$), all the nodal temperatures are known. Thus, we solve the above equation for nodal temperatures when time is advance one time step. We continue the solution to until the end of the specified transient time is reached. The accuracy of temperature distribution increases as the number of nodes increases. This however, means that the array sizes to hold the matrix elements increases as we must inverse larger coefficient matrices at each time step.

3.3. Hyperbolic Equations

Partial differential equations of the hyperbolic type appear basically in problems involving vibration and wave motion. As such, problems in waterhammer, neutron diffusion, radiation transfer, and supersonic flow are examples of hyperbolic

differential equations. The general form of the wave equation is given by Equation VIIb.1.31 and the one-dimensional equation in the Cartesian coordinate system is given in Equation VIIb.1.31-1 and repeated here:

$$\frac{\partial^2 y(x,t)}{\partial x^2} = \frac{1}{c^2} \frac{\partial^2 y(x,t)}{\partial t^2} \quad \text{VIIe.3.15}$$

where $c^2 = Tg_c / \rho$. If we now use an explicit numerical scheme, the finite differential form of Equation VIIe.3.15 for node i at time $k + 1$ becomes:

$$\frac{y_{i-1}^k - 2y_i^k + y_{i+1}^k}{(\Delta x)^2} = \frac{1}{c^2} \frac{y_i^{k-1} - 2y_i^k + y_i^{k+1}}{(\Delta t)^2}$$

Solving for the displacement at the new time step:

$$y_i^{k+1} = y_{i-1}^k - y_i^{k-1} + y_{i+1}^k \quad \text{VIIe.3.16}$$

where in this derivation we have taken the value of the coefficient as unity (i.e. $c^2(\Delta t)^2 / (\Delta x)^2 = 1$). From here, the time step size becomes:

$$\Delta t = \frac{\Delta x}{c}$$

It turns out that the time step calculated above is indeed the optimum time step size with respect to stability and convergence. An interesting feature of Equation VIIe.3.16, which involves a second derivative with respect to time, is the appearance of the lateral movement prior to time zero (i.e. term y^{-1}). Obviously, we find y^0 from the boundary condition. But we need to have another condition to find y^{-1} . One way is to use the initial velocity (i.e. $\partial y(x_i, t=0) / \partial t = 0$). Using the central-difference approximation, we find:

$$\frac{y_i^1 - y_i^{-1}}{2\Delta t} = 0$$

Substituting into Equation VIIe.3.16 to eliminate y^{-1} , we get displacement of the first time step as:

$$y_i^1 = \frac{1}{2}(y_{i-1}^0 + y_{i+1}^0)$$

Having displacement at the first time step in terms of displacements at time zero, we can proceed to find all other displacements at successive time steps from Equation VIIe.3.16.

Table VIIe.3.2. Finite difference equations for two-dimensional transient heat conduction

<p>Interior Node:</p> <p>Explicit: $T_{i,j}^{k+1} = \text{Fo}[T_{i-1,j}^k + T_{i+1,j}^k + T_{i,j-1}^k + T_{i,j+1}^k + \dot{q}'''(\Delta x)^2 / k] + (1 - 4\text{Fo})T_{i,j}^k$</p> <p>Implicit: $(1 + 4\text{Fo})T_{i,j}^{k+1} - \text{Fo}[T_{i-1,j}^{k+1} + T_{i+1,j}^{k+1} + T_{i,j-1}^{k+1} + T_{i,j+1}^{k+1} + \dot{q}'''(\Delta x)^2 / k] = T_{i,j}^k$</p>
<p>Interior Corner Node:</p> <p>Explicit: $T_{i,j}^{k+1} = \frac{2}{3}\text{Fo}[2T_{i-1,j}^k + T_{i+1,j}^k + T_{i,j-1}^k + 2T_{i,j+1}^k] + \frac{3\dot{q}'''(\Delta x)^2}{2k} + (1 - 4\text{Fo} - \frac{4}{3}\text{BiFo})T_{i,j}^k$</p> <p>Implicit: $(1 + 4\text{Fo} + \frac{4}{3}\text{BiFo})T_{i,j}^{k+1} - \frac{2}{3}\text{Fo}[T_{i-1,j}^{k+1} + T_{i+1,j}^{k+1} + T_{i,j-1}^{k+1} + T_{i,j+1}^{k+1} + \frac{2\dot{q}'''(\Delta x)^2}{3}] = T_{i,j}^k + \frac{4}{3}\text{BiFo}T_f$</p>
<p>Plane Surface Node:</p> <p>Explicit: $T_{i,j}^{k+1} = \text{Fo}[2T_{i-1,j}^k + T_{i+1,j}^k + T_{i,j-1}^k + 2\text{Bi}T_f + \dot{q}'''(\Delta x)^2 / k] + (1 - 4\text{Fo} - 2\text{BiFo})T_{i,j}^k$</p> <p>Implicit: $(1 + 4\text{Fo} + 2\text{BiFo})T_{i,j}^{k+1} - \text{Fo}[2T_{i-1,j}^{k+1} + T_{i+1,j}^{k+1} + T_{i,j-1}^{k+1} + \dot{q}'''(\Delta x)^2 / k] = T_{i,j}^k + 2\text{BiFo}T_f$</p>
<p>Exterior Corner Node:</p> <p>Explicit: $T_{i,j}^{k+1} = 2\text{Fo}[T_{i-1,j}^k + T_{i,j-1}^k + 2\text{Bi}T_f + \dot{q}'''(\Delta x)^2 / 2k] + (1 - 4\text{Fo} - 4\text{BiFo})T_{i,j}^k$</p> <p>Implicit: $(1 + 4\text{Fo} + 4\text{BiFo})T_{i,j}^{k+1} - 2\text{Fo}[T_{i-1,j}^{k+1} + T_{i,j-1}^{k+1} + \dot{q}'''(\Delta x)^2 / 2k] = T_{i,j}^k + 4\text{BiFo}T_f$</p>

Note: The superscript k, indicating a time step index should not be confused with k, thermal conductivity.

Solution of One-Dimensional Wave Equation by Method of D'Alembert

The D'Alembert method, like the Laplace transform and the method of separation of variables, provides an analytical solution to the one-dimensional wave equation. It can be easily shown that a function in the form of $y(x, t) = f_1(x + ct) + f_2(x - ct)$ is a solution to Equation VIIe.3.15. For this equation to be the final solution, it must satisfy the initial and the boundary conditions. For the initial conditions of $y(x, 0) = f(x)$ and $\partial y(x, 0)/\partial t = g(x)$, we find the solution as:

$$y(x, t) = \frac{1}{2}[f(x + ct) + f(x - ct)] + \frac{1}{2c} \int_{x-ct}^{x+ct} g(s) ds \quad \text{VIIe.3.17}$$

where s is a dummy variable. For example, consider a string, fixed at the end points, having a length of 4 feet. The wire density and the tension force are so that $c = 2$. Choosing a length increment of 1 ft, gives the optimum time step of 0.5 seconds. The string is now pulled to vibrate with an initial velocity of:

$$\frac{\partial y(x, 0)}{\partial t} = \sin \frac{\pi x}{L}$$

We want to find the displacement of a point located 1/5 of the length from the left end, 1 second after the string is disturbed. To solve the problem, we use Equation VIIe.3.17 as follows:

$$y = \frac{1}{2c} \int_{x-ct}^{x+ct} 4 \sin \frac{\pi s}{L} ds = \frac{L}{\pi} \left[\cos \left(\frac{\pi x}{L} - \frac{2\pi t}{L} \right) - \cos \left[\frac{\pi x}{L} + \frac{2\pi t}{L} \right] \right]$$

From here, we find y for $x = L/5$ ft and $t = 1$ second as:

$$y = \frac{4}{\pi} \left[\cos \left(\frac{\pi}{5} - \frac{\pi}{3} \right) - \cos \left(\frac{\pi}{5} + \frac{\pi}{3} \right) \right] = \frac{4}{\pi} \left(\cos \frac{2\pi}{15} - \cos \frac{8\pi}{15} \right) = \frac{4}{\pi} (0.913 + 0.104) = 1.296 \text{ ft}$$

The reader should use the finite-difference method and compare the results.

Solution of the Two-Dimensional Wave Equation

Displacement of a vibrating membrane can be predicted by the solution to the two-dimensional wave equation:

$$\frac{\partial^2 u(x, y, t)}{\partial x^2} + \frac{\partial^2 u(x, y, t)}{\partial y^2} = \frac{1}{c^2} \frac{\partial^2 u(x, y, t)}{\partial t^2}$$

This equation can be solved explicitly by substituting for the derivative terms from the central-difference approximation.

$$\frac{u_{i-1,j}^k - 2u_{i,j}^k + u_{i+1,j}^k}{(\Delta x)^2} + \frac{u_{i,j-1}^k - 2u_{i,j}^k + u_{i,j+1}^k}{(\Delta y)^2} = \frac{1}{c^2} \frac{u_{i,j}^{k-1} - 2u_{i,j}^k + u_{i,j}^{k+1}}{(\Delta t)^2}$$

If the increments along the x and the y -axis are equal, we get:

$$u_{i,j}^{k+1} = \frac{c^2 (\Delta t)^2}{(\Delta x)^2} (u_{i-1,j}^k + u_{i+1,j}^k + u_{i,j-1}^k + u_{i,j+1}^k) - u_{i,j}^{k-1} + [2 - 4 \frac{c^2 (\Delta t)^2}{(\Delta x)^2}] u_{i,j}^k$$

To further simplify this relation, we may choose the spatial and the temporal increments so that the last term vanishes and we simply get:

$$u_{i,j}^{k+1} = \frac{1}{2} (u_{i-1,j}^k + u_{i+1,j}^k + u_{i,j-1}^k + u_{i,j+1}^k) - u_{i,j}^{k-1}$$

This equation applies when $c^2 (\Delta t)^2 / (\Delta x)^2 = 1/2$. Similar to the one-dimensional wave problem, to find displacement corresponding to $k - 1$ when we begin the first time step, we take advantage of the specified initial velocity. If the initial velocity is zero, then displacement corresponding to the first time step is obtained from:

$$u_{i,j}^1 = \frac{1}{4} (u_{i-1,j}^0 + u_{i+1,j}^0 + u_{i,j-1}^0 + u_{i,j+1}^0)$$

4. The Newton–Raphson Method

As was discussed in Chapter VIId, the mathematical modeling of most physical phenomena reduces to a set of simultaneous differential equations the solution of which would determine the parameters of interest. The solution to such a set of equations involves the approximation of the differential terms by finite difference, for example, and then linearization of the nonlinear terms. The Newton-Raphson method is most often used for the transformation of a set of differential equations. Consider the following set of first order non-linear differential equations, consisted of N equations and N unknowns:

$$\frac{d}{dt} \begin{pmatrix} y_1 \\ y_2 \\ \vdots \\ y_N \end{pmatrix} = \begin{pmatrix} F_1(t, y_1, y_2, \dots, y_N) \\ F_2(t, y_1, y_2, \dots, y_N) \\ \vdots \\ F_N(t, y_1, y_2, \dots, y_N) \end{pmatrix} \quad \text{VIIe.4.1}$$

Functions in the right side of the above set can be linearized. To do this, each function is expanded in Taylor's series and then approximated by using only the first derivative term:

$$F_i(t, y_1, y_2, \dots, y_N) = F_i(t^n, y_1^n, y_2^n, \dots, y_N^n) + \sum_N \frac{\partial [F_i(t^n, y_1^n, y_2^n, \dots, y_N^n)]}{\partial y_i} (y_i^{n+1} - y_i^n)$$

We now substitute the approximated functions in the right side of Equation VIIe.4.1. We also expand the left side of the set of differential equations by using a discrete difference at consecutive time steps. Equation VIIe.4.1 can then be written as:

$$\begin{pmatrix} y_1^{n+1} - y_1^n \\ y_2^{n+1} - y_2^n \\ \vdots \\ y_N^{n+1} - y_N^n \end{pmatrix} = \Delta t \begin{pmatrix} F_1(t^n, y_1^n, y_2^n, \dots, y_N^n) \\ F_2(t^n, y_1^n, y_2^n, \dots, y_N^n) \\ \vdots \\ F_N(t^n, y_1^n, y_2^n, \dots, y_N^n) \end{pmatrix} + \Delta t \begin{pmatrix} \partial F_1^n / \partial y_1 & \partial F_1^n / \partial y_2 & \dots & \partial F_1^n / \partial y_N \\ \partial F_2^n / \partial y_1 & \partial F_2^n / \partial y_2 & \dots & \partial F_2^n / \partial y_N \\ \vdots & \vdots & \ddots & \vdots \\ \partial F_N^n / \partial y_1 & \partial F_N^n / \partial y_2 & \dots & \partial F_N^n / \partial y_N \end{pmatrix} \begin{pmatrix} y_1^{n+1} - y_1^n \\ y_2^{n+1} - y_2^n \\ \vdots \\ y_N^{n+1} - y_N^n \end{pmatrix} \quad \text{VIIe.4.2}$$

The matrix on the right hand side of Equation VIIe.4.2, which contains the partial derivative terms, is called the *Jacobian matrix*. The above set can now be solved for the increment in each variable. To do this, the Jacobian matrix multiplied by the time step should be deducted from the unity matrix. Final answer is obtained as:

$$\begin{pmatrix} y_1^{n+1} - y_1^n \\ y_2^{n+1} - y_2^n \\ \vdots \\ y_N^{n+1} - y_N^n \end{pmatrix} = \Delta t \begin{pmatrix} F_1(t^n, y_1^n, y_2^n, \dots, y_N^n) \\ F_2(t^n, y_1^n, y_2^n, \dots, y_N^n) \\ \vdots \\ F_N(t^n, y_1^n, y_2^n, \dots, y_N^n) \end{pmatrix} \left\{ \begin{pmatrix} 1 & 1 & \dots & 1 \\ 1 & 1 & \dots & 1 \\ \vdots & \vdots & \ddots & \vdots \\ 1 & 1 & \dots & 1 \end{pmatrix} - \Delta t \begin{pmatrix} \partial F_1^n / \partial y_1 & \partial F_1^n / \partial y_2 & \dots & \partial F_1^n / \partial y_N \\ \partial F_2^n / \partial y_1 & \partial F_2^n / \partial y_2 & \dots & \partial F_2^n / \partial y_N \\ \vdots & \vdots & \ddots & \vdots \\ \partial F_N^n / \partial y_1 & \partial F_N^n / \partial y_2 & \dots & \partial F_N^n / \partial y_N \end{pmatrix} \right\}^{-1}$$

Let's demonstrate the application of the Newton-Raphson linearization method by solving a simple example.

Example. Find the friction factor from:

$$f = \left[1.74 - 2 \log_{10} \left(\frac{2\varepsilon}{D_e} + \frac{18.7}{\text{Re} \sqrt{f}} \right) \right]^{-2}$$

Data: $D_e = 1$ in, $\varepsilon = 0.004$ in, $\text{Re} = 1.0\text{E}7$.

Solution: Since f appears in both sides of the correlation, we use the Newton-Raphson method where:

$$F = f - \left[1.74 - 2 \log_{10} \left(\frac{2\varepsilon}{D_e} + \frac{18.7}{\text{Re} \sqrt{f}} \right) \right]^{-2} = 0$$

we then expand F as:

$$F = F(x_o) + (x - x_o) \frac{dF}{dx} = 0$$

Solving for x , we find:

$$x = x_o - \frac{F(x_o)}{dF(x_o)/dx}$$

This procedure is summarized in the following FORTRAN program.

```

implicit real*8 (a-h,o-z)
data a1,a2,eps,De,Re,e/1.74,-2.00,4.00E-3,1.0,1.0E7,1.e-8/
f=0.1
1  continue
   i=i+1
   a3=2.00*eps/De
   a4=18.7/Re
   W=a3+(a4/sqrt(f))
   Wp=-a4*(f**(-1.5))/2.00
   V=a1+a2*log10(W)
   Vp=0.4343*a2*Wp/W
   U=1./(V*V)
   Up=-2.00*Vp/(V*V*V)
   Fof=f-U
   dFdf=1.00-Up
   error=Fof/dFdf
   f=f-error
   if(abs(error).le.e) go to 3
   if(i.gt.30) go to 2
   go to 1
2  continue
   Print *, 'Iteration did not converge'
   go to 4
3  continue
   Write(*,*) i,f
4  continue
9  format(i5,f15.9)
   stop
   end

```

Using the above data, the program finds the answer after 3 iterations as 0.0284.

5. Curve Fitting to Experimental Data

In many engineering applications, we prefer to use an equation to represent a set of experimental data. It is therefore our goal here to represent a set of experimental data by a curve that would best fit the data. The simplest case is fitting a line between points in a set of data. In general however, the experimental data are such that a nonlinear curve needs to be found to best fit the data. The most widely used technique for curve fitting is the method of least squares. A polynomial of degree n passes exactly through a set of N data points, if $n = N - 1$. Hence, in fitting polynomials to a set of experimental data, we require $n < N - 1$.

5.1. Regression Analysis, the Method of Least Squares

Since polynomials can be readily manipulated, to describe the method of least squares, we consider the case of fitting a polynomial to a specified set of data. In

this method, the goal is to find the coefficients of a function of a single variable in the form of:

$$f(x) = \sum_{i=1}^M c_i f_i(x) \quad \text{VIIe.5.1}$$

to fit the data pairs $(x_1, y_1), (x_2, y_2), \dots (x_N, y_N)$ so that the summation of the square of the errors as in the following summation:

$$E = \sum_{i=1}^N [f(x_i) - y_i]^2$$

is minimized. Since functions $f_i(x)$ comprising the function $f(x)$ are known, the unknown coefficients c_i should then be determined. This is accomplished by setting the derivative of E with respect to the unknown coefficients (i.e. c_i) to zero:

$$\frac{\partial E}{\partial c_1} = 2 \sum_{i=1}^N \{ [c_1 f_1(x_i) + c_2 f_2(x_i) + \dots + c_M f_M(x_i) - y_i] f_1(x_i) \} = 0$$

$$\frac{\partial E}{\partial c_2} = 2 \sum_{i=1}^N \{ [c_1 f_1(x_i) + c_2 f_2(x_i) + \dots + c_M f_M(x_i) - y_i] f_2(x_i) \} = 0$$

$$\frac{\partial E}{\partial c_M} = 2 \sum_{i=1}^N \{ [c_1 f_1(x_i) + c_2 f_2(x_i) + \dots + c_M f_M(x_i) - y_i] f_M(x_i) \} = 0$$

This results in the following set of M equations and M unknowns:

$$\begin{bmatrix} \sum_{i=1}^N f_1(x_i) f_1(x_i) & \sum_{i=1}^N f_1(x_i) f_2(x_i) & \dots & \sum_{i=1}^N f_1(x_i) f_M(x_i) \\ \sum_{i=1}^N f_2(x_i) f_1(x_i) & \sum_{i=1}^N f_2(x_i) f_2(x_i) & \dots & \sum_{i=1}^N f_2(x_i) f_M(x_i) \\ \vdots & \vdots & \ddots & \vdots \\ \sum_{i=1}^N f_M(x_i) f_1(x_i) & \sum_{i=1}^N f_M(x_i) f_2(x_i) & \dots & \sum_{i=1}^N f_M(x_i) f_M(x_i) \end{bmatrix} \begin{bmatrix} c_1 \\ c_2 \\ \vdots \\ c_M \end{bmatrix} = \begin{bmatrix} \sum_{i=1}^N f_1(x_i) y_i \\ \sum_{i=1}^N f_2(x_i) y_i \\ \vdots \\ \sum_{i=1}^N f_M(x_i) y_i \end{bmatrix}$$

VIIe.5.2

This set can be solved for the unknown coefficients c_i using the methods described in Chapter VIId. We may now apply the set given in Equation VIIf.4.2 to the following simple polynomials with linear terms:

$$y = a_0 + a_1x + a_2x^2 + \cdots + a_nx^n$$

Functions f_i then become $f_1 = a_0, f_2 = a_1x$, etc. Substituting into Equation VIIe.5.2, we obtain:

$$\begin{bmatrix} N & \sum_{i=1}^N x_i & \sum_{i=1}^N x_i^2 & \cdots & \sum_{i=1}^N x_i^n \\ \sum_{i=1}^N x_i & \sum_{i=1}^N x_i^2 & \sum_{i=1}^N x_i^3 & \cdots & \sum_{i=1}^N x_i^{n+1} \\ \vdots & \vdots & \vdots & \ddots & \vdots \\ \sum_{i=1}^N x_i^n & \sum_{i=1}^N x_i^{n+1} & \sum_{i=1}^N x_i^{n+2} & \cdots & \sum_{i=1}^N x_i^{2n} \end{bmatrix} \begin{bmatrix} a_0 \\ a_1 \\ \vdots \\ a_n \end{bmatrix} = \begin{bmatrix} \sum_{i=1}^N y_i \\ \sum_{i=1}^N x_i y_i \\ \vdots \\ \sum_{i=1}^N x_i^n y_i \end{bmatrix} \quad \text{VIIe.5.3}$$

Note that the degree of the polynomial N is not known before hand. Rather, N should be found by iteration. The criterion is to choose N to minimize the standard deviation.

Example VIIe.5.1. Find the coefficients of a polynomial to fit a portion of the steam tables, in the range of $100 \text{ psia} \leq P \leq 122 \text{ psia}$, for saturated steam pressure as a function of steam temperature (F):

$x_i (T_{sat})$	327.82	329.97	332.06	333.44	334.79	336.12	337.43	338.73	340.01	341.27	342.51
$y_i (P_{sat})$	100.00	103.00	106.0	108.0	110.00	112.00	114.00	116.00	118.00	120.00	122.00

Solution: We fit polynomials of degree 1, 2, 3, etc. The results of this polynomial fit in the form of:

$$P = a_0 + a_1T + a_2T^2 + \cdots$$

are tabulated below:

N	a_0	a_1	a_2	a_3	a_4	a_5	a_6	a_7	σ
1	-0.392E3	0.1499E1	-	-	-	-	-	-	0.1716E0
2	0.515E-2	-0.391E1	0.807E-2	-	-	-	-	-	0.5043E-2
3	-0.306E3	0.344E1	-0.1386E-1	0.218E-4	-	-	-	-	0.4987E-2
4	-0.972E4	0.1158E3	-0.5166E0	0.1022E-2	-0.7456E-6	-	-	-	0.5431E-2
5	0.3052E4	0.2611E1	-0.3029E0	0.1762E-2	-0.3904E-5	0.3110E-8	-	-	0.5808E-2
6	0.1504E5	-0.1229E3	0.2345E0	0.1539E-3	0.8715E-6	-0.6815E-8	0.844E-11	-	0.6307E-2

As the trend in this table indicates, the best fit occurs at $N = 3$. Hence, the answer is found as:

$$P = -305.7 + 3.438T - 0.01386T^2 + (0.2181E - 4)T^3$$

We may use this equation to find saturation pressure corresponding to $T_{sat} = 338.08$ F. According to the above fit

$$P_{sat} = -305.7 + 3.438 \times 338.08 - 0.01386 \times (338.08)^2 + (0.2181\text{E-}4) \times (338.08)^3 = 115.2 \text{ psia}$$

The corresponding pressure from the steam tables is $P = 115$ psia, resulting in an error of less than 0.2%.

The most important task in curve fitting by the method of least squares is the selection of the type of functions (i.e. $f_i(x)$) comprising function $f(x)$. The function may be in any of the following forms:

$$y = A + \sum_{i=1}^n B_i x^i, \quad \ln(y) = A + \sum_{i=1}^n B_i x^i, \quad \ln(y) = A + \sum_{i=1}^n B_i \ln(x^i),$$

$$y = x / \left(A + \sum_{i=1}^n B_i x^i \right), \quad y = A + \sum_{i=1}^n B_i / x^i, \quad \ln(y) = A + \sum_{i=1}^n B_i / x^i,$$

$$y = 1 / \left(A + \sum_{i=1}^n B_i x^i \right), \quad y = \sqrt{A + \sum_{i=1}^n B_i x^i}.$$

Polynomial fits to data (similar to the first equation shown above) can be made by using the regression analysis available on the accompanying CD-ROM.

VIII. Appendices

Table of Contents

Appendix I. Unit Systems, Constants, and Numbers	1013
Table A.I.1. Primary SI Units	1014
Table A.I.2. Derived SI Units	1014
Table A.I.3. Associated SI Units	1014
Table A.I.4. Common Physical Quantities in Two Systems of Dimensions.....	1015
Table A.I.5. Physical Constants	1016
Table A.I.6. Dimensionless Numbers	1017
Table A.I.7. Multiples of SI Units.....	1017
Table A.I.8. Unit Conversion Tables	1018
Appendix II. Thermodynamic Data	1023
Table A.II.1(SI). Saturated Water and Dry Saturated Steam Properties, $f(P)$	1024
Table A.II.2(SI). Saturated Water and Dry Saturated Steam Properties, $f(T)$	1028
Table A.II.3(SI). Superheated Steam Properties	1032
Table A.II.4(SI). Subcooled Water Properties	1036
Table A.II.5(SI). Properties of Various Ideal Gases.....	1037
Table A.II.1(BU). Saturated Water and Dry Saturated Steam Properties, $f(T)$	1038
Table A.II.2(BU). Saturated Water and Dry Saturated Steam Properties, $f(P)$	1040
Table A.II.3(BU). Superheated Steam Properties	1042
Table A.II.4(BU). Subcooled Water Properties	1046
Table A.II.5(BU). Properties of Various Ideal Gases.....	1047
Table A.II.6. Examples of Least-Square Fit to Saturated Water and Dry Saturated Steam.....	1047
Appendix III. Pipe and Tube Data	1049
Table A.III.1(SI). Commercial Steel Pipe (Schedule Wall Thickness)	1050
Table A.III.2(SI). Commercial Steel Pipe (Nominal Pipe Size, NPS)	1051
Table A.III.3(SI). Tube Data, Birmingham Gauges to millimeter and inches	1053
Table A.III.1(BU). Pipe Data, Carbon & Alloy Steel	1054
Table A.III.2(BU). Tube Data	1055

Table A.III.4. Navier-Stokes Equations in the Cylindrical Coordinate System	1056
Table A.III.5. Navier-Stokes Equations in the Spherical Coordinate System	1056
Table A.III.6. Substantial Derivative and Flow Acceleration Components (Cylindrical Coordinates).....	1057
Table A.III.7. Substantial Derivative and Flow Acceleration Components (Spherical Coordinates).....	1057
Appendix IV. Thermophysical Data	1059
Table A.IV.1(SI). Thermophysical Properties of Selected Metallic Solids.....	1060
Table A.IV.2(SI). Thermophysical Properties of Selected Nonmetallic Solids	1064
Table A.IV.3(SI). Thermophysical Properties of Common Materials at 300 K.....	1066
Table A.IV.4(SI). Thermophysical Properties of Gases at Atmospheric Pressure.....	1072
Table A.IV.5(SI). Thermophysical Properties of Saturated Water and Saturated Steam	1077
Table A.IV.6(SI). Thermophysical Properties of Liquid Metals.....	1079
Table A.IV.4(BU). Thermophysical Properties of Gases at Atmospheric Pressure.....	1080
Table A.IV.5(BU). Thermophysical Properties of Saturated Water	1082
Table A.IV.6(BU). Thermophysical Properties of Saturated Steam	1082
Table A.IV.7(BU). Thermophysical Properties of Superheated Steam.....	1083
Table A.IV.8(BU). Thermal Properties of Solid Dielectrics at Normal Temperature	1084
Table A.IV.9(BU). Normal, Total Emissivity of Metallic Surfaces.....	1086
Table A.IV.10(BU). Normal, Total Emissivity of Non-Metallic Surfaces	1088
Appendix V. Nuclear Properties of Elements	1091
Table A.V.1(SI). Absorption Coefficient of Gamma Rays	1092
Table A.V.2(SI). Cross Sections for Neutron Interaction	1093

Appendix I

Unit Systems, Constants, and Numbers

Table A.I.1. Primary SI Units	1014
Table A.I.2. Derived SI Units	1014
Table A.I.3. Associated SI Units	1014
Table A.I.4. Common Physical Quantities in Two Systems of Dimensions.....	1015
Table A.I.5. Physical constants	1016
Table A.I.6. Dimensionless Numbers	1017
Table A.I.7. Multiples of SI Units.....	1017
Table A.I.8. Unit Conversion Tables	1018

Table A.I.1. Primary SI Units

Quantity	Name	Symbol
Length	meter	m
Mass	kilogram	kg
Time	second	s
Electric current	ampere	A
Temperature	kelvin	K
Amount of substance	mole	mol
Luminous intensity	candela	cd
Plane Angle	radian	rd
Solid Angle	steradian	sr
Radioactive decay	becquerel	Bq

Table A.I.2. Derived SI Units

Quantity	Name	Symbol	Unit
Frequency	hertz	Hz	s^{-1}
Force	newton	N	$kg \cdot m/s^2$
Pressure & stress	pascal	Pa	N/m^2
Energy & work	joule	J	$N \cdot m$
Power	watt	W	J/s
Electric charge	coulomb	C	$A \cdot s$
Electric potential	volt	V	J/C
Electrical capacitance	farad	F	C/V
Electrical resistance	ohm	Ω	V/A
Electrical conductance	siemens	S	Ω^{-1}
Magnetic flux	weber	Wb	$V \cdot s$
Magnetic flux density	tesla	T	Wb/m^2
Inductance	henry	H	Wb/A
Luminous flux	lumen	lm	$cd \cdot sr$
Illuminance	lux	lx	lm/m^2

Table A.I.3. Associated SI Units

Quantity	Name	Symbol	Unit
Energy	electron volt	eV	$1.60219E-19$ J
Mass	metric ton	t	10^3 kg
Mass of atom	atomic mass unit	amu	$1.66057E-27$ kg
Plane angle	degree, minute, second	$^{\circ}, ', ''$	$(\pi/180)^{\circ}, (1/60)^{\circ}, (1/60)'$
Pressure of fluid	bar	bar	10^5 Pa
Temperature	degree Celsius	C	C
Time	minute, hour, day	min, h, d	60 s, 60 min, 24 h
Volume	liter	l	10^{-3} m ³

Table A.I.4. Common Physical Quantities in Two Systems of Dimensions

Quantity	MLT	FLT
Acceleration	LT^{-2}	LT^{-2}
Angle	$M^0L^0T^0$	$F^0L^0T^0$
Angular acceleration	T^{-2}	T^{-2}
Angular velocity	T^{-1}	T^{-1}
Area	L^2	L^2
Density	ML^{-3}	$FL^{-4}T^2$
Energy	ML^2T^{-2}	FL
Enthalpy	ML^2T^{-2}	FL
Entropy	$ML^2T^{-2}\theta^{-1}$	$FL\theta^{-1}$
Force	MLT^{-2}	F
Frequency	T^{-1}	T^{-1}
Heat	ML^2T^{-2}	FL
Heat flux	MT^{-2}	FL^{-1}
Heat transfer coefficient	$MT^{-2}\theta^{-1}$	$FL^{-1}\theta^{-1}$
Length	L	L
Mass	M	$FL^{-1}T^2$
Mass flow rate	MT^{-1}	$FL^{-1}T$
Modulus of elasticity	$ML^{-1}T^{-2}$	FL^{-2}
Moment of force	ML^2T^{-2}	FL
Moment of inertia (area)	L^4	L^4
Moment of inertia (mass)	ML^2	FLT^2
Momentum	MLT^{-1}	FT
Power	ML^2T^{-3}	FLT^{-1}
Pressure	$ML^{-1}T^{-2}$	FL^{-2}
Specific heat	$L^2T^{-2}\theta^{-1}$	$L^2T^{-2}\theta^{-1}$
Specific weight	$ML^{-2}T^{-2}$	FL^{-3}
Strain	$M^0L^0T^0$	$F^0L^0T^0$
Stress	$ML^{-1}T^{-2}$	FL^{-2}
Surface tension	MT^{-2}	FL^{-1}
Temperature	θ	θ
Thermal conductivity	$MT^{-3}\theta^{-1}$	$FL^{-1}T^{-1}\theta^{-1}$
Time	T	T
Torque	ML^2T^{-2}	FL
Velocity	LT^{-1}	LT^{-1}
Viscosity (dynamic)	$ML^{-1}T^{-1}$	$FL^{-2}T$
Viscosity (kinematic)	L^2T^{-1}	L^2T^{-1}
Void fraction	$M^0L^0T^0$	$F^0L^0T^0$
Volume	L^3	L^3
Work	ML^2T^{-2}	FL

Table A.I.5. Physical Constants

Parameter	Symbol	Value	Unit
Avogadro's number	A_v or N_v	0.602252E24	molecules/gm·mole
		0.273177E27	molecules/lbm·mole
Atomic mass unit	amu	1.66057E-27	Kg
		931.478	MeV
		4.1471E-17	kw·h
Barn	b	1.0E-24	Cm
Boltzmann's constant	κ	1.38066E-26	J/K
Curie	Ci	3.7E10	disintegration/s
Becquerel	Bq	1.0E00	disintegration/s
Electron charge	e	4.80298E-10	Esu
		1.60218E-19	coulomb
Faraday's constant	F	9.64800E14	coulomb/mole
Gravitational acceleration	g	9.80665	m/s ²
		32.1739	ft/s ²
Joule's constant	J_c	4.184	J/cal
		778.16	ft·lbf/Btu
Molecular volume	-	22,413.6	cm ³ /g·mole
Plank's constant	h	6.62608E-34	J·s
Rest mass of electron	-	5.48597E-4	Amu
Rest mass of proton	-	1.0072766	Amu
Rest mass of neutron	-	1.0086654	Amu
Stefan-Boltzmann constant	σ	5.67E-12	W/cm ² ·K ⁴
Speed of light in vacuum	c	2.997925E10	cm/s
		9.83619E8	ft/s
Universal gas constant	R_u	8.31434	kJ/kmol·K
		8.31451E3	kg m ² /s ² ·kgmol·K
		1.98545	cal/gm·mol·K
		0.08314	bar·m ³ /kmol·K
		1,545.08	ft·lbf/lbmole·R
		0.73000	atm·ft ³ /lbmol·R
		1.98545	Btu/lbmole·R
		4.9686E4	lbm·ft ² /s ² ·lbmol·R

Table A.I.6. Dimensionless Numbers

Number	Symbol	Formula	Significance
Biot	Bi	hx/L	Surface conductance/Internal conduction of solid
Bond	Bo	$g(\rho_l - \rho_v)L^2/\sigma$	Gravitational force/Surface tension force
Cauchy	Ca	$\rho V^2/F$	Inertial force/compressive force
Eckert	Ec	$V^2/c_p \Delta T$	Temperature rise due to energy conversion/temp. diff.
Euler	Eu	$\Delta P/\rho V^2$	Pressure force/Inertial force
Fourier	Fo	α/L^2	Rate of heat conduction/Rate of energy storage
Froude	Fr	V^2/gL	Inertial force/Gravity force
Graetz	Gz	$(D/L)(\rho V c_p D/k)$	Heat transfer convection/Heat transfer by conduction
Grashof	Gr	$g\beta\Delta T L^3/\nu^2$	Buoyancy force/Viscous force
Jakob	Ja	$c_p(T_s - T_{sat})/h_{fg}$	Ratio of sensible to latent heat
Knudsen	Kn	λ/L	Molecular mean free path/Object characteristic length
Lewis	Le	α/D_c	Thermal diffusivity/Molecular diffusivity
Mach	Ma	V/c	Velocity in a medium/Speed of sound in that medium
Nusselt	Nu	hL/k	Surface temp. gradient/Overall temp. gradient
Peclet	Pe	$\rho c_p V D/k$	Heat transfer by convection/Heat transfer by conduction
Prandtl	Pr	$\mu c_p/k$	Diffusion of momentum/Diffusion of heat
Reynolds	Re	$\rho V L/\mu$	Inertial force/Viscous force
Schmidt	Sc	$\mu/\rho D_c$	Diffusion of momentum/Diffusion of mass
Sherwood	Sh	$h_p L/D_c$	Molecular diffusivity/Diffusion of mass
Stanton	St	$h/\rho V c_p$	Heat transfer at surface/Energy transferred by stream
Stokes	Sk	$L\Delta P/\mu V$	Pressure force/Viscous force
Strouhal	Sl	L/tV	Frequency of vibration/Characteristic frequency
Weber	We	$\rho V^2 L/\sigma$	Inertial force/Surface tension force

Table A.I.7. Multiples of SI Units

Prefix	Symbol	Factor
yotta	Y	1.0E24
zeta	Z	1.0E21
exa	E	1.0E18
peta	P	1.0E15
tera	T	1.0E12
giga	G	1.0E09
mega	M	1.0E06
kilo	k	1.0E3
heco	h	1.0E02
deka	da	1.0E01
deci	d	1.0E-01
centi	c	1.0E-02
milli	m	1.0E-03
micro	μ	1.0E-06
nano	n	1.0E-09
pico	p	1.0E-12
femto	f	1.0E-15
atto	a	1.0E-18
zepto	z	1.0E-21
yocto	y	1.0E-24

The conversion tables are arranged in the form of a square matrix. Values on the diagonal are all unity. To convert units in each row of the first column to units in each column of the first row, multiply by the corresponding value in the matrix. Values below the diagonal are the inverse of the values above the diagonal. Unit conversion can be performed by using the software on the accompanying CD-ROM.

Table A.I.8.1. Conversion Factors (Length)

	cm	m	in	ft	mile	Micron (μ)	Angstrom (A)
cm	1	0.01	0.3937	0.03281	6.214E-6	1E4	1.E8
m	100	1	39.37	3.281	6.214E-4	1E6	1.E10
in	2.54	0.0254	1	0.08333	1.578E-5	2.54E4	2.54E8
ft	30.48	0.3048	12.00	1	1.894E-4	0.3048E6	30.48E8
Mile	1.6093E5	1609.344	6.336E4	5280	1	1.6093E9	1.6093E13
Micron	1E-4	1E-6	3.937E-5	3.281E-6	6.2139E-10	1	1.E4
Angstrom	1E-8	1E-10	3.937E-9	3.281E-10	6.2139E-14	1E-4	1

Example: 1 m = 100 cm = 39.37 in = 3.281 ft = 6.214E-4 miles

Note: 1 in = 1000 mil and 1 yard = 0.9144 m

Table A.I.8.2. Conversion Factors (Area)

	cm ²	m ²	in ²	ft ²	mile ²	acre	barn
cm ²	1	1E-4	0.155	1.0764E-3	3.861E-11	2.4711E-8	1E24
m ²	1E4	1	1550	10.764	3.861E-7	2.4711E-4	1E28
in ²	6.4516	6.4516E-4	1	6.944E-3	2.491E-10	1.5944E-7	6.4517E24
ft ²	929	0.0929	144	1	3.587E-8	2.2957E-5	9.29E26
mile ²	2.59E10	2.59E6	4.0144E11	2.7878E7	1	640	2.59E34
acre	4.0469E7	4.0469E3	6.2726E6	4.35E4	1.5625E-3	1	4.0469E31
barn	1E-24	1E-28	1.55E-25	1.0764E-27	3.861E-35	2.4711E-32	1

1 Hectare = 2.471054 acre, 1 km² = 100 hectare, 1 mile² = 258.9988 hectare

Table A.I.8.3. Conversion Factors (Volume)

	cm ³	liter	m ³	in ³	ft ³	U.S. gallon
cm ³	1	1E-3	1E-6	0.06102	3.532E-5	2.642E-4
liter	1E3	1	1E-3	61.02	0.03532	0.2642
m ³	1E6	1E3	1	6.102E4	35.31	264.2
in ³	16.39	0.01639	1.639E-5	1	5.787E-4	4.329E-3
ft ³	2.832E4	28.32	0.02832	1728	1	7.481
U.S. gallon	3785	3.785	3.785E-3	231.0	0.1337	1

Table A.I.8.4. Conversion Factors (Mass)

	g	kg	lbm	tons	amu
g	1	1E-3	2.2046E-3	1E-6	0.60225E24
kg	1E3	1	2.2046	1E-3	6.0225E26
lbm	453.6	0.4536	1	4.536E-4	2.7318E26
ton	1E6	1E3	2.2047E3	1	6.0225E29
amu	1.6604E-24	1.6604E-27	3.6606E-27	1.6604E-30	1

* refers to the metric tonnes.

Table A.I.8.5. Conversion Factors (Density)

	g/cm ³	kg/m ³	lbm/in ³	lbm/ft ³	lbm/US gallon
g/cm ³	1	1E3	0.03613	62.43	8.345
kg/m ³	1E-3	1	3.613E-5	0.06243	8.345E-3
lbm/in ³	27.68	2.768E4	1	1728	231
lbm/ft ³	0.01602	16.02	5.787E-4	1	0.1337
lbm/US gallon	0.1198	119.8	4.329E-3	7.481	1

Table A.I.8.6. Conversion Factors (Time)

	s	min	h	day	year
s	1	1.667E-2	2.778E-4	1.157E-5	3.169E-8
min	60	1	1.667E-2	6.944E-4	1.901E-6
h	3600	60	1	0.04167	1.141E-4
day	86400	1440	24	1	2.737E-3
years (yr)	3.1557E7	5.259E5	8766	365.24	1

Table A.I.8.7. Conversion Factors (Flow)

	cm ³ /s	ft ³ /min	U.S. gal/min (GPM)
cm ³ /s	1	0.002119	0.01585
ft ³ /min	472.0	1	7.481
U.S. gal/min (GPM)	63.09	0.1337	1

Table A.I.8.8. Conversion Factors (Force)

	Newton	dynes	poundal	lbf
Newton (N = kg m/s ²)	1	1E5	7.2330	0.224881
dynes (g·cm/s ²)	1E-5	1	7.2330E-5	2.24881E-6
poundal (lbm·ft/s ²)	0.13826	1.3826E4	1	3.10810E-2
pound force (lbf)	4.4482	4.4482E5	32.1740	1

Table A.I.8.9. Conversion Factors (Pressure and Momentum Flux)

	Pa	dyne/cm ²	lbf/ft ²	lbf/in ² (psia)	atm	mm Hg	in Hg	ft H ₂ O
Pa = N/m ²	1	10	2.0886E-2	1.4504E-4	9.8692E-6	7.5006E-3	2.9530E-4	3.3488E-4
dyne/cm ²	1E-1	1	2.0886E-3	1.4504E-3	9.8692E-7	7.5006E-4	2.9530E-5	3.3488E-5
lbf/ft ²	4.788E1	4.7880E2	1	6.9444E-3	4.7254E-4	3.5913E-1	1.4139E-2	0.0160350
lbf/in ² (psi)	6.8947E3	6.8947E4	144.00	1	6.8046E-2	5.1715E1	2.0360	2.3090422
atm	1.0133E5	1.0133E6	2.1162E3	14.696	1	760	29.921	33.933333
mm Hg	1.3332E2	1.3332E3	2.7845	1.9337E-2	1.3158E-3	1	3.9370E-2	0.0446033
in Hg	3.3864E3	3.3864E4	7.0727E1	4.9116E-1	3.3421E-2	25.400	1	1.1340954
ft H ₂ O	2.9861E3	2.9889E4	62.36352	0.43308	0.029469	22.419	0.88176	1

Hg at 0°C (32°F) and H₂O at 15.5°C (60°F).

1 bar = 1E5 Pa (1 atm = 1.01325E5 Pa, 1 bar ≈ 1 atm, 1 bar = 14.5 psia)

1 torr = 1 mm Hg (0°C) = 1.316E-3 atm = 133.322 Pa

Table A.I.8.10. Conversion Factors (Energy, Work, Enthalpy, and Torque)

	J	ergs	ft-lbf	calorie	Btu	hp-h	kWh	MeV
J = N·m	1	1E7	7.3756E-1	2.3901E-1	9.4783E-4	3.7251E-7	2.7778E-7	6.242E12
ergs*	1E-7	1	7.3756E-8	2.3901E-8	9.4783E-1	3.7251E-14	2.7778E-14	6.245E5
ft-lbf	1.3558	1.3558E7	1	3.2405E-1	1.2851E-3	5.0505E-7	3.7662E-7	8.462E12
calorie	4.1840	4.1840E7	3.0860	1	3.9657E-3	1.5586E-6	1.1622E-6	2.616E13
Btu	1.0550E3	1.0550E10	778.16	2.5216E2	1	3.9301E-4	2.9307E-4	6.584E15
hp-h	2.6845E6	2.6845E13	1.9800E6	6.4162E5	2.5445E3	1	7.4570E-1	1.677E19
kWh	3.6000E6	3.6000E13	2.6552E6	8.6042E5	3.4122E3	1.3410	1	2.25E19
MeV	1.6021E-13	1.6021E-6	1.178E-13	3.826E-14	1.519E-16	5.950E-20	4.44E-20	1

ergs = dynes·cm = g·cm²/s².

specific enthalpy: 1 Btu/lbm = 2.3258 kJ/kg

specific entropy: 1 Btu/lbm·R = 4.186 kJ/kg·K, 1 kJ/kg·K = 0.23886 Btu/lbm·R

Table A.I.8.11. Conversion Factors (Power)

	ergs/s	W	kW	Btu/h	hp	eV/s
ergs/s	1	1E-7	1E-10	3.412E-7	1.341E-10	6.241E11
W (J/s)	1E7	1	1E-3	3.412	0.001341	6.2421E18
kW	1E10	1E3	1	3412	1.341	6.2421E21
Btu/h	2.931E6	0.2931	2.931E-4	1	3.93E-4	1.8294E18
hp	7.457E9	745.7	0.7457	2545	1	4.6548E21
eV/s	1.6021E-12	1.0621E-19	1.6021E-22	5.4664E-19	2.1483E-22	1

Table A.I.8.12. Conversion Factors (Power Density)

	kW/liter	cal/s·cm ³	Btu/h·in ³	Btu/h·ft ³
kW/liter*	1	0.2388	55.91	9.662E4
cal/s·cm ³	4.187	1	234.1	4.045E5
Btu/h·in ³	0.01788	4.272E-3	1	1728
Btu/h·ft ³	1.035E-5	2.472E-6	5.787E-4	1

* kW/liter = W/cm³

Table A.I.8.13. Conversion Factors (Heat Flux)

	W/cm ²	cal/s·cm ²	Btu/h·ft ²	MeV/s·cm ²
W/cm ²	1	0.2388	3170.2	6.2420E12
cal/s·cm ²	4.187	1	1.3272E4	2.6134E13
Btu/h·ft ²	3.155E-4	7.535E-5	1	1.9691E9
MeV/s·cm ²	1.602E-13	3.826E-14	5.0785E-10	1

Table A.I.8.14. Conversion Factors (Thermal Conductivity)

	W/cm·C	W/m·K	cal/s·cm·C	Btu/h·ft·F	Btu-in/h·ft ² ·F
W/cm·C	1	100	0.2388	57.782	693.3
W/m·K	0.01	1	0.002388	0.57782	6.933
cal/s·cm·C	4.187	0.4187	1	241.9	2902.9
Btu/h·ft·F	0.01731	1.731	4.134E-3	1	12.00
Btu-in/h·ft ² ·F	1.441E-3	0.1441	3.445E-4	0.08333	1

Table A.I.8.15. Conversion Factors (Heat Transfer Coefficient)

	W/m ² ·K	Btu/h·ft ² ·F	cal/s·cm ² ·K	lb _f /s·ft·F
W/m ² ·K	1	0.17611	2.3901E-5	3.8068E-2
Btu/h·ft ² ·F	5.6782	1	1.3571E-4	2.1616E-1
cal/s·cm ² ·K	4.184E4	7.3686E3	1	1.5928E3
lb _f /s·ft·F	26.269	4.6263	6.2784E-4	1

Table A.I.8.16. Conversion Factors (Viscosity)

	Poise	kg/s·m	lbm/s·ft	lbm/h·ft	lb _f ·s/ft ²
Poise	1	0.1	0.06720	241.9	2.089E-3
kg/s·m	10	1	0.672	2.419E3	0.02089
lbm/s·ft	14.88	1.488	1	3.600E3	0.03108
lbm/h·ft	4.134E-3	4.134E-4	2.778E-4	1	8.634E-6
lb _f ·s/ft ²	478.8	47.88	32.17	1.158E5	1

1 Centipoise = 1E-2 Poise

1 Poise = 1 dyne·s/cm²

Appendix II

Thermodynamic Data

Table A.II.1(SI). Saturated Water and Dry Saturated Steam Properties, $f(P)$	1024
Table A.II.2(SI). Saturated Water and Dry Saturated Steam Properties, $f(T)$	1028
Table A.II.3(SI). Superheated Steam Properties	1032
Table A.II.4(SI). Subcooled Water Properties	1036
Table A.II.5(SI). Properties of Various Ideal Gases.....	1037
Table A.II.1(BU). Saturated Water and Dry Saturated Steam Properties, $f(T)$	1038
Table A.II.2(BU). Saturated Water and Dry Saturated Steam Properties, $f(P)$	1040
Table A.II.3(BU). Superheated Steam Properties	1042
Table A.II.4(BU). Subcooled Water Properties	1046
Table A.II.5(BU). Properties of Various Ideal Gases.....	1047
Table A.II.6. Examples of Least-Square Fit to Saturated Water and Dry Saturated Steam.....	1047

Table A.II.1(SI). Saturated Water and Dry Saturated Steam Properties, $f(P)$

(kPa) P	(C) T	(m ³ /kg)			(kJ/kg)		
		v_f	v_{fg}	v_g	u_f	u_{fg}	u_g
0.6113	0.01	0.001000	206.1310	206132	0	2375.30	2375.30
1.0	6.98	0.001000	129.2070	129.2080	29.29	2355.69	2384.98
1.5	13.03	0.001001	87.97913	87.9801	54.70	2338.63	2393.32
2.0	17.50	0.001001	67.00285	67.0039	73.47	2326.02	2399.48
2.5	21.08	0.001002	54.25285	54.2539	88.47	2315.93	2404.40
3.0	24.08	0.001003	45.66402	45.6650	101.03	2307.48	2408.51
4.0	28.96	0.001004	34.79915	34.8002	121.44	2293.73	2415.17
5.0	32.88	0.001005	28.19150	28.1925	137.79	2282.70	2420.49
7.5	40.29	0.001008	19.23674	19.2378	168.76	2261.74	2430.50
10	45.81	0.001010	14.67254	14.6736	191.79	2246.10	2437.89
15	53.97	0.001014	10.02117	10.0222	225.90	2222.83	2448.73
20	60.06	0.001017	7.64835	7.6494	251.35	2205.36	2456.71
25	64.97	0.001020	6.20322	6.2042	271.88	2191.21	2463.08
30	69.10	0.001022	5.22816	5.2292	289.18	2179.22	2468.40
40	75.87	0.001026	3.99243	3.9935	317.51	2159.49	2477.00
50	81.33	0.001030	3.23931	3.2403	340.42	2143.43	2483.85
75	91.77	0.001037	2.21607	2.2171	384.29	2112.39	2496.67
100	99.62	0.001043	1.69296	1.6940	417.33	2088.72	2506.06
125	105.99	0.001048	1.37385	1.3749	444.16	2069.32	2513.48
150	111.37	0.001053	1.15828	1.1593	466.92	2052.72	2519.64
175	116.06	0.001057	1.00257	1.0036	486.78	2038.12	2524.90
200	120.23	0.001061	0.88467	0.8857	504.47	2025.02	2529.49
225	124.00	0.001064	0.79219	0.7933	520.45	2013.10	2533.56
250	127.43	0.001067	0.71765	0.7187	535.08	2002.14	2537.23
275	130.60	0.001070	0.65624	0.6573	548.57	1991.95	2540.53
300	133.55	0.001073	0.60475	0.6058	561.13	1982.43	2543.55
325	136.30	0.001076	0.56093	0.5620	572.88	1973.46	2546.34
350	138.88	0.001079	0.52317	0.5243	583.93	1964.98	2548.92
375	141.32	0.001081	0.49029	0.4914	594.38	1956.93	2551.31
400	143.63	0.001084	0.46138	0.4625	604.29	1949.26	2553.55
450	147.93	0.001088	0.41289	0.4140	622.75	1934.87	2557.62
500	151.86	0.001093	0.37380	0.3749	639.66	1921.57	2561.23
550	155.48	0.001097	0.34159	0.3427	655.30	1909.17	2564.47
600	158.85	0.001101	0.31457	0.3357	669.88	1897.52	2567.40
650	162.01	0.001104	0.29158	0.2927	683.55	1886.51	2570.06
700	164.97	0.001108	0.27176	0.2729	696.43	1876.07	2572.49
750	167.77	0.001111	0.25449	0.2556	708.62	1866.12	2574.73
800	170.43	0.001115	0.23931	0.2404	720.20	1856.58	2576.79
850	172.96	0.001118	0.22586	0.22698	731.25	1847.45	2578.69
900	175.38	0.001121	0.21385	0.21497	741.81	1838.65	2580.46
950	177.69	0.001124	0.20306	0.20419	751.94	1830.17	2582.11
1000	179.91	0.001127	0.19332	0.19444	761.67	1821.97	2583.64
1100	184.09	0.001133	0.17639	0.17753	780.08	1806.32	2586.40
1200	187.99	0.001139	0.16220	0.16333	797.27	1791.55	2588.82
1300	191.64	0.001144	0.15011	0.15125	813.42	1777.53	2590.95
1400	195.07	0.001149	0.13969	0.14084	828.68	1764.15	2592.83

Table A.II.1(SI). Saturated Water and Dry Saturated Steam Properties, $f(P)$ (continued)

(kPa)	(C)	(kJ/kg)			(kJ/kg·K)		
P	T	h_f	h_{fg}	h_g	s_f	s_{fg}	s_g
0.611	0.01	0.00	2501.30	2501.30	0	9.1562	9.1562
1.0	6.98	29.29	2484.89	2514.18	0.1059	8.8697	8.9756
1.5	13.03	54.70	2470.59	2525.30	0.1956	8.6322	8.8278
2.0	17.50	73.47	2460.02	2533.49	0.2607	8.4629	8.7236
2.5	21.08	88.47	2451.56	2540.03	0.3120	8.3311	8.6431
3.0	24.08	101.03	2444.47	2545.50	0.3545	8.2231	8.5775
4.0	28.96	121.44	2432.93	2554.37	0.4226	8.0520	8.4746
5.0	32.88	137.79	2423.66	2561.45	0.4763	7.9187	8.3950
7.5	40.29	168.77	2406.02	2574.79	0.5763	7.6751	8.2514
10	45.81	191.81	2392.82	2584.63	0.6492	7.5010	8.3501
15	53.97	225.91	2373.14	2599.06	0.7548	7.2536	8.0084
20	60.06	251.38	2358.33	2609.70	0.8319	7.0766	7.9085
25	64.97	271.90	2346.29	2618.19	0.8930	6.9383	7.8313
30	69.10	289.21	2336.07	2625.28	0.9439	6.8247	7.7686
40	75.87	317.55	2319.19	2636.74	1.0258	6.6441	7.6700
50	81.33	340.47	2305.40	2645.87	1.0910	6.5029	7.5939
75	91.77	384.36	2278.59	2662.96	1.2129	6.2434	7.4563
100	99.62	417.44	2258.02	2675.46	1.3025	6.0568	7.3593
125	101.99	444.30	2241.05	2685.35	1.3739	5.9104	7.2843
150	111.37	467.08	2226.46	2693.54	1.4335	5.7897	7.2232
175	116.06	486.97	2213.57	2700.53	1.4848	5.6868	7.1717
200	120.23	504.68	2201.96	2706.63	1.5300	5.5970	7.1271
225	124.00	520.69	2191.35	2712.04	1.5705	5.5173	7.0878
250	127.43	535.34	2181.55	2716.89	1.6072	5.4455	7.0526
275	130.60	548.87	2172.42	2721.29	1.6407	5.3801	7.0208
300	133.55	561.45	2163.85	2725.30	1.6717	5.3201	6.9918
325	136.30	573.23	2155.76	2728.99	1.7005	5.2646	6.9651
350	138.88	584.31	2148.10	2732.40	1.7274	5.2130	6.9404
375	141.32	594.79	2140.79	2735.58	1.7527	5.1647	6.9174
400	143.63	604.73	2133.81	2738.53	1.7766	5.1193	6.8958
450	147.93	623.24	2120.67	2743.91	1.8206	5.0359	6.8565
500	151.86	640.21	2108.47	2748.67	1.8606	4.9606	6.8212
550	155.48	655.91	2097.04	2752.94	1.8972	4.8920	6.7892
600	158.85	670.54	2086.26	2756.80	1.9311	4.8289	6.7600
650	162.01	684.26	2076.04	2760.30	1.9627	4.7704	6.7330
700	164.97	697.20	2066.30	2763.50	1.9922	4.7158	6.7080
750	167.77	709.45	2056.98	2766.43	2.0199	4.6647	6.6846
800	170.43	721.10	2048.04	2769.13	2.0461	4.6166	6.6627
850	172.96	732.20	2039.43	2771.63	2.0709	4.5711	6.6421
900	175.38	742.82	2031.12	2773.94	2.0946	4.5280	6.6225
950	177.69	753.00	2023.08	2776.08	2.1171	4.4869	6.6040
1000	179.91	762.79	2015.29	2778.08	2.1386	4.4478	6.5864
1100	184.09	781.32	2000.36	2781.68	2.1791	4.3744	6.5535
1200	187.99	798.64	1986.19	2784.82	2.2165	4.3067	6.5233
1300	191.64	814.91	1972.67	2787.58	2.2514	4.2438	6.4953
1400	195.07	830.29	1959.72	2790.00	2.2842	4.1850	6.4692

Table A.II.1(SI). Saturated Water and Dry Saturated Steam Properties, $f(P)$ (continued)

(kPa) P	(C) T	(m ³ /kg)			(kJ/kg)		
		v_f	v_{fg}	v_g	u_f	u_{fg}	u_g
1500	198.32	0.001154	0.13062	0.13177	843.14	1751.30	2594.50
1750	205.76	0.001166	0.11232	0.11349	876.44	1721.39	2597.83
2000	212.42	0.001177	0.09845	0.09963	906.42	1693.84	2600.26
2250	218.45	0.001187	0.08756	0.08875	933.81	1668.18	2601.98
2500	223.99	0.001197	0.07878	0.07998	959.09	1644.04	2603.13
2750	229.12	0.001207	0.07154	0.07275	982.65	1621.16	2603.81
3000	233.90	0.001216	0.06546	0.06668	1004.76	1599.34	2604.10
3250	238.38	0.001226	0.06029	0.06152	1025.62	1578.43	2604.04
3500	242.60	0.001235	0.05583	0.05707	1045.41	1558.29	2603.70
4000	250.40	0.001252	0.04853	0.04978	1082.28	1519.99	2602.27
5000	263.99	0.001286	0.03815	0.03944	1147.78	1449.34	2597.12
6000	275.64	0.001319	0.03112	0.03244	1205.41	1384.27	2589.69
7000	285.88	0.001351	0.02602	0.02737	1257.51	1322.97	2580.48
8000	295.06	0.001384	0.02213	0.02352	1305.54	1264.25	2569.79
9000	303.40	0.001418	0.01907	0.02048	1350.47	1207.28	2557.75
10000	311.06	0.001452	0.01657	0.01802	1393.00	1151.40	2544.41
11000	318.15	0.001489	0.01450	0.01599	1433.68	1096.06	2529.74
12000	324.75	0.001527	0.01274	0.01426	1472.92	1040.76	2513.67
13000	330.93	0.001567	0.01121	0.01278	1511.09	984.99	2496.08
14000	336.75	0.001611	0.00987	0.01149	1548.53	928.23	2476.76
15000	342.24	0.001658	0.00868	0.01034	1585.58	869.85	2455.43
16000	347.43	0.001711	0.00760	0.00931	1622.63	809.07	2431.70
17000	352.37	0.001770	0.00659	0.00836	1660.16	744.80	2404.96
18000	357.06	0.001840	0.00565	0.00749	1698.86	675.42	2374.28
19000	361.54	0.001924	0.00473	0.00666	1739.87	598.18	2338.05
20000	365.81	0.002035	0.00380	0.00583	1785.47	507.58	2293.05
21000	369.89	0.002206	0.00275	0.00495	1841.97	388.74	2230.71
22000	373.80	0.002808	0.00072	0.00353	1973.16	108.24	2081.39
22089	374.14	0.003155	0	0.00315	2029.58	0	2029.58

Table A.II.1(SI). Saturated Water and Dry Saturated Steam Properties, $f(P)$ (continued)

(kPa)	(C)	(kJ/kg)			(kJ/kg·K)		
P	T	h_f	h_{fg}	h_g	s_f	s_{fg}	s_g
1500	198.32	844.87	1947.28	2792.15	2.3150	4.1298	6.4448
1750	205.76	878.48	1917.95	2796.43	2.3851	4.0044	6.3895
2000	212.42	908.77	1890.74	2799.51	2.4473	3.8935	6.3408
2250	218.45	936.48	1865.19	2801.67	2.5034	3.7938	6.2971
2500	223.99	962.09	1840.98	2803.07	2.5546	3.7028	6.2574
2750	229.12	985.97	1817.89	2803.86	2.6018	3.6190	6.2208
3000	233.90	1008.41	1795.73	2804.14	2.6456	3.5412	6.1869
3250	238.38	1029.60	1774.37	2803.97	2.6866	3.4685	6.1551
3500	242.60	1049.73	1753.70	2803.43	2.7252	3.4000	6.1252
4000	250.40	1087.29	1714.09	2801.38	2.7963	3.2737	6.0700
5000	263.99	1154.21	1640.12	2794.33	2.9201	3.0532	5.9733
6000	275.64	1213.32	1571.00	2784.33	3.0266	2.8625	5.8891
7000	285.88	1266.97	1505.10	2772.07	3.1210	2.6922	5.8132
8000	295.06	1316.61	1441.33	2757.94	3.2067	2.5365	5.7431
9000	303.40	1363.23	1378.88	2742.11	3.2857	2.3915	5.6771
10000	311.06	1407.53	1317.14	2724.67	3.3595	2.2545	5.6140
11000	318.15	1450.05	1255.55	2705.60	3.4294	2.1233	5.5527
12000	324.75	1491.24	1193.59	2684.83	3.4961	1.9962	5.4923
13000	330.93	1531.46	1130.76	2662.22	3.5604	1.8718	5.4323
14000	336.75	1571.00	1066.47	2637.55	3.6231	1.7485	5.3716
15000	342.24	1610.45	1000.04	2610.49	3.6847	1.6250	5.3097
16000	347.43	1650.00	930.59	2580.59	3.7460	1.4995	5.2454
17000	352.37	1690.25	856.90	2547.15	3.8078	1.3698	5.1776
18000	357.06	1731.97	777.13	2509.09	3.8713	1.2330	5.1044
19000	361.54	1776.43	688.11	2464.54	3.9387	1.0841	5.0227
20000	365.81	1826.18	583.56	2409.74	4.0137	0.9132	4.9269
21000	369.89	1888.30	446.42	2334.72	4.1073	0.6942	4.8015
22000	373.80	2034.92	124.04	2158.97	4.3307	0.1917	4.5224
22089	374.14	2099.26	0	2099.26	4.4297	0	4.4297

See the reference for the table. This material is used by permission of John Wiley & Sons, Inc.

Table A.II.2(SI). Saturated Water and Dry Saturated Steam Properties, $f(T)$

(C) T	(kPa) P	(m ³ /kg)			(kJ/kg)		
		v_f	v_{fg}	v_g	u_f	u_{fg}	u_g
0.01	0.611	0.001000	206.131	206.13	0	2375.33	2375.33
5	0.872	0.001000	147.117	147.12	20.97	2361.27	2382.24
10	1.228	0.001000	106.376	106.38	41.99	2347.16	2389.15
15	1.71	0.001001	77.9240	77.930	62.98	2333.06	2396.04
20	2.34	0.001002	57.7887	57.790	83.94	2318.98	2402.91
25	3.17	0.001003	43.3583	43.359	104.86	2304.90	2409.76
30	4.25	0.001004	32.8922	32.893	125.77	2290.81	2416.58
35	5.63	0.001006	25.2148	25.216	146.65	2276.71	2423.36
40	7.38	0.001008	19.5219	19.523	167.53	2262.57	2430.11
45	9.59	0.001010	15.2571	15.258	188.41	2248.40	2436.81
50	12.35	0.001012	12.0308	12.032	209.30	2234.17	2443.47
55	15.76	0.001015	9.56734	9.56835	230.19	2219.89	2450.08
60	19.94	0.001017	7.66969	7.67071	251.09	2205.54	2456.63
65	25.03	0.001020	6.19554	6.19656	272.00	2191.12	2463.12
70	31.19	0.001023	5.04114	5.04217	292.93	2176.62	2469.55
75	38.58	0.001026	4.13021	4.13123	313.87	2162.03	2475.91
80	47.39	0.001029	3.40612	3.40715	334.84	2147.36	2482.19
85	57.83	0.001032	2.82654	2.82757	355.82	2132.58	2488.40
90	70.14	0.001036	2.35953	2.36056	376.82	2117.70	2494.52
95	84.55	0.001040	1.98082	1.98186	397.86	2102.70	2500.56
100	101.30	0.001044	1.67185	1.67290	418.91	2087.58	2506.50
105	120.80	0.001047	1.41831	1.41936	440.00	2072.34	2512.34
110	143.30	0.001052	1.20909	1.21014	461.12	2056.96	2518.09
115	169.10	0.001056	1.03552	1.03658	482.28	2041.44	2523.72
120	198.50	0.001060	0.89080	0.89186	503.48	2025.76	2529.24
125	232.10	0.001065	0.76953	0.77059	524.72	2009.91	2534.63
130	270.10	0.001070	0.66744	0.66850	546.00	1993.90	2539.90
135	313.00	0.001075	0.58110	0.58217	567.34	1977.69	2545.03
140	361.30	0.001080	0.50777	0.50885	588.72	1961.30	2550.02
145	415.40	0.001085	0.44524	0.44632	610.16	1944.69	2554.86
150	475.90	0.001090	0.39169	0.39278	631.66	1927.87	2559.50
155	543.10	0.001096	0.34566	0.34676	653.23	1910.82	2564.04
160	617.80	0.001102	0.30596	0.30706	674.85	1893.52	2568.37
165	700.50	0.001108	0.27158	0.27269	696.55	1875.85	2572.51
170	791.70	0.001114	0.24171	0.24283	718.31	1858.14	2576.46
175	892.00	0.001121	0.21568	0.21680	740.16	1840.03	2580.19
180	1002.20	0.001127	0.19292	0.19405	762.08	1821.62	2583.00
185	1122.70	0.001134	0.17295	0.17409	784.08	1802.90	2586.98
190	1254.40	0.001141	0.15539	0.15654	806.17	1783.84	2590.01
195	1397.8	0.001149	0.1399	0.1411	828.36	1764.43	2592.79
200	1553.8	0.001156	0.1262	0.1274	850.64	1744.66	2595.29
205	1723.0	0.001164	0.1141	0.1152	873.02	1724.49	2597.52
210	1906.3	0.001173	0.1032	0.1044	895.51	1703.93	2599.44
215	2104.2	0.001181	0.0936	0.0948	918.12	1682.94	2601.06
220	2317.8	0.001190	0.0850	0.0862	940.85	1661.49	2602.35
225	2547.7	0.001199	0.0773	0.0785	963.72	1639.58	2603.30

Table A.II.2(SI). Saturated Water and Dry Saturated Steam Properties, $f(T)$ (continued)

(C) T	(kPa) P	(kJ/kg)			(kJ/kg·K)		
		h_f	h_{fg}	h_g	s_f	s_{fg}	s_g
0.01	0.611	0.00	2501.35	2501.35	0	9.156	9.156
5	0.872	20.98	2489.57	2510.54	0.076	8.950	9.026
10	1.228	41.99	2477.75	2519.74	0.151	8.750	8.901
15	1.705	62.98	2465.93	2528.91	0.225	8.557	8.781
20	2.339	83.94	2454.12	2538.06	0.297	8.371	8.667
25	3.169	104.87	2442.30	2547.17	0.367	8.191	8.558
30	4.246	125.77	2430.48	2556.25	0.437	8.016	8.453
35	5.628	146.66	2418.62	2565.28	0.505	7.848	8.353
40	7.384	167.54	2406.72	2574.26	0.572	7.685	8.257
45	9.593	188.42	2394.77	2583.19	0.639	7.526	8.165
50	12.35	209.31	2382.75	2592.06	0.704	7.373	8.076
55	15.76	230.20	2370.66	2600.86	0.768	7.223	7.991
60	19.94	251.11	2358.48	2609.59	0.831	7.078	7.910
65	25.03	272.03	2346.21	2618.24	0.893	6.938	7.831
70	31.19	292.96	2333.85	2626.80	0.955	6.800	7.755
75	38.58	313.91	2321.37	2635.28	1.015	6.667	7.682
80	47.39	334.88	2308.77	2643.66	1.075	6.537	7.612
85	57.83	355.88	2296.05	2651.93	1.134	6.410	7.544
90	70.14	376.90	2283.19	2660.09	1.192	6.287	7.479
95	84.55	397.94	2270.19	2668.13	1.250	6.166	7.416
100	101.30	419.02	2257.03	2676.05	1.307	6.048	7.355
105	120.80	440.13	2243.70	2683.83	1.363	5.933	7.296
110	143.30	461.27	2230.20	2691.47	1.418	5.820	7.239
115	169.10	482.46	2216.50	2698.96	1.473	5.710	7.183
120	198.50	503.69	2202.60	2706.30	1.528	5.602	7.130
125	232.10	524.96	2188.50	2713.46	1.581	5.496	7.077
130	270.10	546.29	2174.16	2720.46	1.634	5.393	7.027
135	313.00	567.67	2159.59	2727.26	1.687	5.291	6.978
140	361.30	589.11	2144.75	2733.87	1.739	5.191	6.930
145	415.40	610.61	2129.65	2740.26	1.791	5.093	6.883
150	475.90	632.18	2114.26	2746.44	1.842	4.996	6.838
155	543.10	653.82	2098.56	2752.39	1.892	4.901	6.793
160	617.80	675.53	2082.55	2758.09	1.943	4.808	6.750
165	700.50	697.32	2066.20	2763.53	1.992	4.715	6.708
170	791.70	719.20	2049.50	2768.70	2.042	4.624	6.666
175	892.0	741.16	2032.42	2773.58	2.091	4.535	6.626
180	1002.2	763.21	2014.96	2778.16	2.140	4.446	6.586
185	1122.7	785.36	1997.07	2782.43	2.188	4.359	6.546
190	1254.4	807.61	1978.76	2786.37	2.236	4.272	6.508
195	1397.8	829.96	1959.99	2789.96	2.2835	4.1863	6.4697
200	1553.8	852.43	1940.75	2793.18	2.3308	4.1014	6.4322
205	1723.0	875.03	1921.00	2796.03	2.3779	4.0172	6.3951
210	1906.3	897.75	1900.73	2798.48	2.4247	3.9337	6.3584
215	2104.2	920.61	1879.90	2800.51	2.4713	3.8507	6.3221
220	2317.8	943.61	1858.51	2802.12	2.5177	3.7683	6.2860
225	2547.7	966.77	1836.50	2803.27	2.5639	3.6863	6.2502

Table A.II.2(SI). Saturated Water and Dry Saturated Steam Properties, $f(T)$ (continued)

(C) T	(kPa) P	(m ³ /kg)			(kJ/kg)		
		v_f	v_{fg}	v_g	u_f	u_{fg}	u_g
230	2794.9	0.001209	0.0704	0.0716	986.72	1617.17	2603.89
235	3060.1	0.001219	0.0642	0.0654	1009.88	1594.24	2604.11
240	3344.2	0.001229	0.0585	0.0598	1033.19	1570.75	2603.95
245	3648.2	0.001240	0.0535	0.0547	1056.69	1546.68	2603.37
250	3973.0	0.001251	0.0489	0.0501	1080.37	1522.00	2602.37
255	4319.5	0.001263	0.0447	0.0460	1104.26	1496.66	2600.93
260	4688.6	0.001276	0.0409	0.0422	1128.37	1470.64	2599.01
265	5081.3	0.001289	0.0375	0.0388	1152.72	1443.87	2596.60
270	5498.7	0.001302	0.0343	0.0356	1177.33	1416.33	2593.66
275	5941.8	0.001317	0.0315	0.0328	1202.23	1387.94	2590.17
280	6411.7	0.001332	0.0288	0.0302	1227.43	1358.66	2586.09
285	6909.4	0.001348	0.0264	0.0278	1252.98	1328.41	2581.38
290	7436.0	0.001366	0.0242	0.0256	1278.89	1297.11	2575.99
295	7992.8	0.001384	0.0222	0.0235	1305.21	1264.67	2569.87
300	8581.0	0.001404	0.0203	0.0217	1331.97	1230.99	2562.96
305	9201.8	0.001425	0.0185	0.0200	1359.22	1195.94	2555.16
310	9856.6	0.001447	0.0169	0.0184	1387.03	1159.37	2546.40
315	10547	0.001472	0.0154	0.0169	1415.44	1121.11	2536.55
320	11274	0.001499	0.0140	0.0155	1444.55	1080.93	2525.48
325	12040	0.001528	0.0127	0.0142	1474.44	1038.57	2513.01
330	12845	0.001561	0.0114	0.0130	1505.24	993.66	2498.91
335	13694	0.001597	0.0103	0.0119	1537.11	945.77	2482.88
340	14586	0.001638	0.0092	0.0108	1570.26	894.26	2464.53
345	15525	0.001685	0.0081	0.0098	1605.01	838.29	2443.30
350	16514	0.001740	0.0071	0.0088	1641.81	776.58	2418.39
355	17554	0.001807	0.0061	0.0079	1681.41	707.11	2388.52
360	18651	0.001892	0.0051	0.0069	1725.19	626.29	2351.47
365	19807	0.002011	0.0040	0.0060	1776.13	526.54	2302.67
370	21028	0.002213	0.0027	0.0049	1843.84	384.69	2228.53
374.10	22089	0.003155	0	0.0032	2029.58	0	2029.58

Table A.II.2(SI). Saturated Water and Dry Saturated Steam Properties, $f(T)$ (continued)

(C) T	(kPa) P	(kJ/kg)			(kJ/kg·K)		
		h_f	h_{fg}	h_g	s_f	s_{fg}	s_g
230	2794.9	990.10	1813.85	2803.95	2.6099	3.6047	6.2146
235	3060.1	1013.61	1790.53	2804.13	2.6557	3.5233	6.1791
240	3344.2	1037.31	1766.50	2803.81	2.7015	3.4422	6.1436
245	3648.2	1061.21	1741.73	2802.95	2.7471	3.3612	6.1083
250	3973.0	1085.34	1716.18	2801.52	2.7927	3.2802	6.0729
255	4319.5	1109.72	1689.80	2799.51	2.8382	3.1992	6.0374
260	4688.6	1134.35	1662.54	2796.89	2.8837	3.1181	6.0018
265	5081.3	1159.27	1634.34	2793.61	2.9293	3.0368	5.9661
270	5498.7	1184.49	1605.16	2789.65	2.9750	2.9551	5.9301
275	5941.8	1210.05	1574.92	2784.97	3.0208	2.8730	5.8937
280	6411.7	1235.97	1543.55	2779.53	3.0667	2.7903	5.8570
285	6909.4	1262.29	1510.97	2773.27	3.1129	2.7069	5.8198
290	7436.0	1289.04	1477.08	2766.13	3.1593	2.6227	5.7821
295	7992.8	1316.27	1441.78	2758.05	3.2061	2.5375	5.7436
300	8581.0	1344.01	1404.93	2748.94	3.2533	2.4511	5.7044
305	9201.8	1372.33	1366.38	2738.72	3.3009	2.3633	5.6642
310	9856.6	1401.29	1325.97	2727.27	3.3492	2.2737	5.6229
315	10547	1430.97	1283.48	2714.44	3.3981	2.1821	5.5803
320	11274	1461.45	1238.64	2700.08	3.4479	2.0882	5.5361
325	12040	1492.84	1191.13	2683.97	3.4987	1.9913	5.4900
330	12845	1525.29	1140.56	2665.85	3.5506	1.8909	5.4416
335	13694	1558.98	1086.37	2645.35	3.6040	1.7863	5.3903
340	14586	1594.15	1027.86	2622.01	3.6593	1.6763	5.3356
345	15525	1631.17	964.02	2595.19	3.7169	1.5594	5.2763
350	16514	1670.54	893.38	2563.92	3.7776	1.4336	5.2111
355	17554	1713.13	813.59	2526.72	3.8427	1.2951	5.1378
360	18651	1760.48	720.52	2481.00	0.3000	1.1379	5.0525
365	19807	1815.96	605.44	2421.40	3.9983	0.9487	4.9470
370	21028	1890.37	441.75	2332.12	4.1104	0.6868	4.7972
374.10	22089	2099.26	0	2099.26	4.4297	0	4.4297

See the reference for this table. This material is used by permission of John Wiley & Sons, Inc.

Table A.II.3(SI). Superheated Steam Properties

C	v u h s				v u h s				v u h s			
	P = 0.01 MPa (45.81)				P = 0.05 MPa (81.33)				P = 0.10 MPa (99.63)			
Sat.	14.674	2437.9	2584.7	8.1502	3.240	2483.9	2645.9	7.594	1.694	2506.1	2675.5	7.3594
50	14.869	2443.9	2592.6	8.1749								
100	17.196	2515.5	2687.5	8.4479	3.418	2511.6	2682.5	7.695	1.696	2506.7	2676.2	7.3614
150	19.512	2587.9	2783.0	8.6882	3.889	2585.6	2780.1	7.940	1.936	2582.8	2776.4	7.6134
200	21.825	2661.3	2879.5	8.9038	4.356	2659.9	2877.7	8.158	2.172	2658.1	2875.3	7.8343
250	24.136	2736.0	2977.3	9.1002	4.820	2735.0	2976.0	8.356	2.406	2733.7	2974.3	8.0333
300	26.445	2812.1	3076.5	9.2813	5.284	2811.3	3075.5	8.537	2.639	2810.4	3074.3	8.2158
400	31.063	2968.9	3279.6	9.6077	6.209	2968.5	3278.9	8.864	3.103	2967.9	3278.2	8.5435
500	35.679	3132.3	3489.1	9.8978	7.134	3132.0	3488.7	9.155	3.565	3131.6	3488.1	8.8342
600	40.295	3302.5	3705.4	10.1608	8.057	3302.2	3705.1	9.418	4.028	3301.9	3704.7	9.0976
700	44.911	3479.6	3928.7	10.4028	8.981	3479.4	3928.5	9.660	4.490	3479.2	3928.2	9.3398
800	49.526	3663.8	4159.0	10.6281	9.904	3663.6	4158.9	9.885	4.952	3663.5	4158.6	9.5652
900	54.141	3855.0	4396.4	10.8396	10.828	3854.9	4396.3	10.097	5.414	3854.8	4396.1	9.7767
1000	58.757	4053.0	4640.6	11.0393	11.751	4052.9	4640.5	10.296	5.875	4052.8	4640.3	9.9764
1100	63.372	4257.5	4891.2	11.2287	12.674	4257.4	4891.1	10.486	6.337	4257.3	4891.0	10.1659
1200	67.987	4467.9	5147.8	11.4091	13.597	4467.8	5147.7	10.666	6.799	4467.7	5147.6	10.3463
1300	72.602	4683.7	5409.7	11.5811	14.521	4683.6	5409.6	10.838	7.260	4683.5	5409.5	10.5183

C	v u h s				v u h s				v u h s			
	P = 0.20 MPa (120.23)				P = 0.30 MPa (133.55)				P = 0.40 MPa (143.63)			
Sat.	0.8857	2529.5	2706.7	7.1272	0.605	2543.6	2725.3	6.9919	0.4625	2553.6	2738.6	6.8959
150	0.9596	2576.9	2768.8	7.2795	0.634	2570.8	2761.0	7.0778	0.4708	2564.5	2752.8	6.9299
200	1.0803	2654.4	2870.5	7.5066	0.716	2650.7	2865.6	7.3115	0.5342	2646.8	2860.5	7.1706
250	1.1988	2731.2	2971.0	7.7086	0.796	2728.7	2967.6	7.5166	0.5951	2726.1	2964.2	7.3789
300	1.3162	2808.6	3071.8	7.8926	0.875	2806.7	3069.3	7.7022	0.6548	2804.8	3066.8	7.5662
400	1.5493	2966.7	3276.6	8.2218	1.032	2965.6	3275.0	8.0330	0.7726	2964.4	3273.4	7.8985
500	1.7814	3130.8	3487.1	8.5133	1.187	3130.0	3486.0	8.3251	0.8893	3129.2	3484.9	8.1913
600	2.0130	3301.4	3704.0	8.7770	1.341	3300.8	3703.2	8.5892	1.0055	3300.2	3702.4	8.4558
700	2.2440	3478.8	3927.6	9.0194	1.496	3478.4	3927.1	8.8319	1.1215	3477.9	3926.5	8.6987
800	2.4750	3663.1	4158.2	9.2449	1.650	3662.9	4157.8	9.0576	1.2372	3662.4	4157.3	8.9244
900	2.7060	3854.5	4395.8	9.4566	1.804	3854.2	4395.4	9.2692	1.3529	3853.9	4395.1	9.1362
1000	2.9370	4052.5	4640.0	9.6563	1.958	4052.3	4639.7	9.4690	1.4685	4052.0	4639.4	9.3360
1100	3.1680	4257.0	4890.7	9.8458	2.112	4256.8	4890.4	9.6585	1.5840	4256.5	4890.2	9.5256
1200	3.3990	4467.5	5147.3	10.0262	2.266	4467.2	5147.1	9.8389	1.6996	4467.0	5146.8	9.7060
1300	3.6300	4683.2	5409.3	10.1982	2.420	4683.0	5409.0	10.0110	1.8151	4682.8	5408.8	9.8780

C	v u h s				v u h s				v u h s			
	P = 0.50 MPa (151.86)				P = 0.60 MPa (158.85)				P = 0.80 MPa (170.43)			
Sat.	0.3749	2561.2	2748.7	6.8213	0.316	2567.4	2756.8	6.7600	0.240	2576.8	2769.1	6.6628
200	0.4249	2642.9	2855.4	7.0592	0.352	2638.9	2850.1	6.9665	0.261	2630.6	2839.3	6.8158
250	0.4744	2723.5	2960.7	7.2709	0.394	2720.9	2957.2	7.1816	0.293	2715.5	2950.0	7.0384
300	0.5226	2802.9	3064.2	7.4599	0.434	2801.0	3061.6	7.3724	0.324	2797.2	3056.5	7.2328
350	0.5701	2882.6	3167.7	7.6329	0.474	2881.2	3165.7	7.5464	0.354	2878.2	3161.7	7.4089
400	0.6173	2963.2	3271.5	7.7938	0.514	2962.1	3270.3	7.7079	0.384	2959.7	3267.1	7.5716
500	0.7109	3128.4	3483.9	8.0873	0.592	3127.6	3482.8	8.0021	0.443	3126.0	3480.6	7.8673
600	0.8041	3299.6	3701.7	8.3522	0.670	3299.1	3700.9	8.2674	0.502	3297.9	3699.4	8.1333
700	0.8969	3477.5	3925.9	8.5952	0.747	3477.0	3925.3	8.5107	0.560	3476.2	3924.2	8.3770
800	0.9896	3662.1	4156.9	8.8211	0.825	3661.8	4156.5	8.7367	0.618	3661.1	4155.6	8.6033
900	1.0822	3853.6	4394.7	9.0329	0.90	3853.4	4394.4	8.9486	0.676	3852.8	4393.7	8.8153
1000	1.1247	4051.8	4639.1	9.2328	0.979	4051.5	4638.8	9.1485	0.734	4051.0	4638.2	9.0153
1100	1.2672	4256.3	4889.9	9.4224	1.056	4256.1	4889.6	9.3381	0.792	4255.6	4889.1	9.2050
1200	1.3596	4466.8	5146.6	9.6029	1.133	4466.5	5146.3	9.5185	0.850	4466.1	5145.9	9.3855
1300	1.4521	4682.5	5408.6	9.7749	1.210	4682.3	5408.3	9.6906	0.908	4681.8	5407.8	9.5575

Table A.II.3(SI). Superheated Steam Properties (continued)

C	v u h s				v u h s				v u h s			
	P = 1.00 MPa (179.91)				P = 1.20 MPa (187.99)				P = 1.40 MPa (195.07)			
Sat.	0.1944	2583.6	2778.1	6.5865	0.1633	2588.8	2784.8	6.5233	0.1408	2592.8	2790.0	6.4693
200	0.2060	2621.9	2827.9	6.6940	0.1690	2612.8	2815.9	6.5898	0.1430	2603.1	2803.3	6.4975
250	0.2327	2709.9	2942.6	6.9247	0.1923	2704.2	2935.0	6.8294	0.1635	2698.3	2927.2	6.7467
300	0.2579	2793.2	3051.2	7.1229	0.2138	2789.2	3045.8	7.0317	0.1823	2785.2	3040.4	6.9534
350	0.2825	2875.2	3157.7	7.3011	0.2345	2872.2	3153.6	7.2121	0.2003	2869.2	3149.5	7.1360
400	0.3066	2957.3	3263.9	7.4651	0.2548	2954.9	3260.7	7.3774	0.2178	2952.5	3257.5	7.3026
500	0.3541	3124.4	3478.5	7.7622	0.2946	3122.8	3476.3	7.6759	0.2521	3121.1	3474.1	7.6027
600	0.4011	3296.8	3697.9	8.0290	0.3339	3295.6	3696.3	7.9435	0.2860	3294.4	3694.8	7.8710
700	0.4478	3475.3	3923.1	8.2731	0.3729	3474.4	3922.0	8.1881	0.3195	3473.6	3920.8	8.1160
800	0.4943	3660.4	4154.7	8.4996	0.4118	3659.7	4153.8	8.4148	0.3528	3659.0	4153.0	8.3431
900	0.5407	3852.2	4392.9	8.7118	0.4505	3851.6	4392.2	8.6272	0.3861	3851.1	4391.5	8.5556
1000	0.5871	4050.5	4637.6	8.9119	0.4892	4050.0	4637.0	8.8274	0.4192	4049.5	4636.4	8.7559
1100	0.6335	4255.1	4888.6	9.1017	0.5278	4254.6	4888.0	9.0172	0.4524	4254.1	4887.5	8.9457
1200	0.6798	4465.6	5145.4	9.2822	0.5665	4465.1	5144.9	9.1977	0.4855	4464.7	5144.4	9.1262
1300	0.7261	4681.3	5407.4	9.4543	0.6051	4680.9	5407.0	9.3698	0.5186	4680.4	5406.5	9.2984

C	v u h s				v u h s				v u h s			
	P = 1.60 MPa (201.41)				P = 1.80 MPa (207.15)				P = 2.00 MPa (212.42)			
Sat.	0.12380	2596.0	2794.0	6.4218	0.11042	2598.4	2797.1	6.3794	0.09963	2600.3	2799.5	6.3409
225	0.13287	2644.7	2857.3	6.5518	0.11673	2636.6	2846.7	6.4808	0.10377	2628.3	2835.8	6.4147
250	0.14184	2692.3	2919.2	6.6732	0.12497	2686.0	2911.0	6.7664	0.11100	2679.6	2902.5	6.5453
300	0.15862	2781.1	3034.8	6.8844	0.14021	2776.9	3029.2	6.8226	0.12547	2772.6	3023.5	6.7664
350	0.17456	2866.0	3145.4	7.0694	0.15457	2863.0	3141.2	7.0100	0.13857	2859.8	3137.0	6.9563
400	0.19005	2950.1	3254.2	7.2374	0.16847	2947.7	3250.9	7.1794	0.15120	2945.2	3247.6	7.1271
500	0.2203	3119.5	3472.0	7.5390	0.19550	3469.8	3472.0	7.5390	0.17568	3116.2	3467.6	7.4317
600	0.2500	3293.3	3693.2	7.8080	0.22200	3292.1	3691.7	7.7523	0.19960	3290.9	3690.1	7.7024
700	0.2794	3472.7	3919.7	8.0535	0.24820	3471.8	3918.5	7.9983	0.22320	3470.9	3917.4	7.9487
800	0.3086	3658.3	4152.1	8.2808	0.2742	3657.6	4151.2	8.2258	0.2467	3657.0	4150.3	8.1765
900	0.3377	3850.5	4390.8	8.4935	0.3001	3849.9	4390.1	8.4386	0.2700	3849.3	4389.4	8.3895
1000	0.3668	4049.0	4635.8	8.6938	0.3260	4048.5	4635.2	8.6391	0.2933	4048.0	4634.6	8.5901
1100	0.3958	4253.7	4887.0	8.8837	0.3518	4253.2	4886.4	8.8290	0.3166	4252.7	4885.9	8.7800
1200	0.4248	4464.2	5143.9	9.0643	0.3776	4463.7	5143.4	9.0096	0.3398	4463.3	5142.9	8.9607
1300	0.4538	4679.9	5406.0	9.2364	0.4034	4679.5	5405.6	9.1818	0.3631	4679.0	5405.1	9.1329

C	v u h s				v u h s				v u h s			
	P = 2.50 MPa (223.99)				P = 3.00 MPa (233.90)				P = 3.50 MPa (242.60)			
Sat.	0.0800	2603.1	2803.1	6.2575	0.06668	2604.1	2804.2	6.1869	0.05707	2603.7	2803.4	6.1253
225	0.0803	2605.6	2806.3	6.2639								
250	0.0870	2662.6	2880.1	6.4085	0.07000	2644.0	2855.8	6.2872	0.05872	2623.7	2829.2	6.1749
300	0.0989	2761.6	3008.8	6.6438	0.08100	2750.1	2993.5	6.5390	0.06842	2738.0	2977.5	6.4461
350	0.1098	2851.9	3126.3	6.8403	0.09000	2843.7	3115.3	6.7428	0.07678	2835.3	3104.0	6.6579
400	0.1201	2939.1	3239.3	7.0148	0.09900	2932.8	3230.9	6.9212	0.08453	2926.4	3222.3	6.8405
450	0.13014	3025.5	3350.8	7.1746	0.10787	3020.4	3344.0	7.0834	0.09196	3015.3	3337.2	7.0052
500	0.1400	3112.1	3462.1	7.3234	0.11619	3108.0	3456.5	7.2338	0.09918	3103.0	3450.9	7.1572
600	0.1593	3288.0	3686.3	7.5960	0.13243	3285.0	3682.3	7.5085	0.11324	3282.1	3678.4	7.4339
700	0.1783	3468.7	3914.5	7.8435	0.14838	3466.5	3911.7	7.7571	0.12699	3464.3	3908.8	7.6837
800	0.19716	3655.3	4148.2	8.0720	0.16414	3653.5	4145.9	7.9862	0.14056	3651.8	4143.7	7.9134
900	0.2159	3847.9	4387.6	8.2853	0.17900	3846.5	4385.9	8.1999	0.15402	3845.0	4384.1	8.1276
1000	0.2346	4046.7	4633.1	8.4861	0.19541	4045.4	4631.6	8.4009	0.16743	4044.1	4630.1	8.3288
1100	0.2532	4251.5	4884.6	8.6762	0.21098	4250.3	4883.3	8.5912	0.18080	4249.2	4881.9	8.5192
1200	0.2718	4462.1	5141.7	8.8569	0.22600	4460.9	5140.5	8.7720	0.19415	4459.8	5139.3	8.7000
1300	0.2905	4677.8	5404.0	9.0291	0.24200	4676.6	5402.8	8.9442	0.20749	4675.5	5401.7	8.8723

Table A.II.3(SI). Superheated Steam Properties (continued)

C	v u h s				v u h s				v u h s			
	P = 4.0 MPa (250.40)				P = 4.5 MPa (257.49)				P = 5.0 MPa (263.99)			
Sat.	0.0498	2602.3	2801.4	6.0701	0.0440	2600.1	2798.3	6.0198	0.0394	2597.1	2794.3	5.9734
275	0.0546	2667.9	2886.2	6.2285	0.0473	2650.3	2863.2	6.1401	0.0414	2631.3	2838.3	6.0544
300	0.0588	2725.3	2960.7	6.3615	0.0514	2712.0	2943.1	6.2828	0.0453	2698.0	2924.5	6.2084
350	0.0665	2826.7	3092.5	6.5821	0.0584	2817.8	3080.6	6.5131	0.0519	2808.7	3068.4	6.4493
400	0.0734	2919.9	3213.6	6.7690	0.0648	2913.3	3204.7	6.7047	0.0578	2906.6	3195.7	6.6459
450	0.0800	3010.2	3330.3	6.9363	0.0707	3005.0	3323.3	6.8746	0.0633	2999.7	3316.2	6.8186
500	0.0864	3099.5	3445.3	7.0900	0.0765	3095.3	3439.6	7.0301	0.0686	3091.0	3433.8	6.9759
600	0.0989	3279.1	3674.4	7.3688	0.0877	3276.0	3670.5	7.3110	0.0787	3273.0	3666.5	7.2589
700	0.1110	3462.1	3905.9	7.6198	0.0985	3459.9	3903.0	7.5631	0.0885	3457.6	3900.1	7.5122
800	0.1229	3650.0	4141.5	7.8502	0.1091	3648.3	4139.3	7.7942	0.0981	3646.6	4137.1	7.7440
900	0.1347	3843.6	4382.3	8.0647	0.1197	3842.2	4380.6	8.0091	0.1076	3840.7	4378.8	7.9593
1000	0.1465	4042.9	4628.7	8.2662	0.1301	4041.6	4627.2	8.2108	0.1171	4040.4	4625.7	8.1612
1100	0.1582	4248.0	4880.6	8.4567	0.1406	4246.8	4879.3	8.4015	0.1265	4245.6	4878.0	8.3520
1200	0.1699	4458.6	5138.1	8.6376	0.1510	4457.5	5136.9	8.5825	0.1359	4456.3	5135.7	8.5331
1300	0.1816	4674.3	5400.5	8.8100	0.1614	4673.1	5399.4	8.7549	0.1453	4672.0	5398.2	8.7055

C	v u h s				v u h s				v u h s			
	P = 6.0 MPa (275.64)				P = 7.0 MPa (285.88)				P = 8.0 MPa (295.06)			
Sat.	0.0324	2589.7	2784.3	5.8892	0.0274	2580.5	2772.1	5.8133	0.0235	2569.8	2758.0	5.7432
300	0.0362	2667.2	2884.2	6.0674	0.0295	2632.2	2838.4	5.9305	0.0243	2590.9	2785.0	5.7906
350	0.0422	2789.6	3043.0	6.3335	0.0352	27694.0	3016.0	6.2283	0.0300	2747.7	2987.3	6.1301
400	0.0474	2892.9	3177.2	6.5408	0.0399	2878.6	3158.1	6.4478	0.0343	2863.8	3138.3	6.3634
450	0.0521	2988.9	3301.8	6.7193	0.0442	2978.0	3287.1	6.6327	0.0382	2966.7	3272.0	6.5551
500	0.0567	3082.2	3422.2	6.8803	0.0481	3073.4	3410.3	6.7975	0.0418	3064.3	3398.3	6.7240
550	0.0610	3174.6	3540.6	7.0288	0.0520	3167.2	3530.9	6.9486	0.0452	3159.8	3521.0	6.8778
600	0.0653	3266.9	3658.4	7.1677	0.0557	3260.7	3650.3	7.0894	0.0485	3254.4	3642.0	7.2589
700	0.0735	3453.1	3894.2	7.4234	0.0628	3448.5	3888.3	7.3476	0.0548	3443.9	3882.4	7.2812
800	0.0816	3643.1	4132.7	7.6566	0.0698	3639.5	4128.2	7.5822	0.0610	3636.0	4123.8	7.5173
900	0.0896	3837.8	4375.3	7.8727	0.0767	3835.0	4371.8	7.7991	0.0670	3832.1	4368.3	7.7351
1000	0.0975	4037.8	4622.7	8.0751	0.0835	4035.3	4619.8	8.0020	0.0730	4032.8	4616.9	7.9384
1100	0.1054	4243.3	4875.4	8.2661	0.0903	4240.9	4872.8	8.1933	0.0790	4238.6	4870.3	8.1300
1200	0.11321	4454.0	5133.3	8.4474	0.09703	4451.7	5130.9	8.3747	0.08489	4449.5	5128.5	8.3115
1300	0.12106	4669.6	5396.0	8.6199	0.10377	4667.3	5393.7	8.5473	0.0908	4665.0	5391.5	8.4842

C	v u h s				v u h s				v u h s			
	P = 9.0 MPa (303.40)				P = 10.0 MPa (311.06)				P = 12.5 MPa (327.89)			
Sat.	0.0205	2557.8	2742.1	5.6772	0.0180	2544.4	2724.7	5.6141	0.0135	2505.1	2673.0	5.4624
325	0.0233	2646.6	2856.0	5.8712	0.0186	2610.4	2809.1	5.7568				
350	0.0258	2724.4	2956.6	6.0361	0.0224	2699.2	2923.4	5.9443	0.0161	2624.6	2826.2	5.7118
400	0.0299	2848.4	3117.8	6.2854	0.0264	2832.4	3096.5	6.2120	0.0200	2789.3	3039.3	6.0417
450	0.0335	2955.2	3256.6	6.4844	0.0298	2943.4	3240.9	6.4190	0.0230	2912.5	3199.8	6.2719
500	0.0368	3055.2	3386.1	6.6576	0.0328	3045.8	3373.7	6.5966	0.0256	3021.7	3341.8	6.4618
550	0.0399	3152.2	3511.0	6.8142	0.0356	3144.6	3500.9	6.7561	0.0280	3125.0	3475.2	6.6290
600	0.0429	3248.1	3633.7	6.9589	0.0384	3241.7	3625.3	6.9029	0.0303	3225.4	36040.0	6.7810
650	0.0457	3343.6	3755.3	7.0943	0.0410	3338.2	3748.2	7.0398	0.0325	3324.4	3730.4	6.9218
700	0.0486	3439.3	3876.5	7.2221	0.0436	3434.7	3870.5	7.1687	0.0346	3422.9	3855.3	7.0536
800	0.0541	3632.5	4119.3	7.4596	0.0486	3628.9	4114.8	7.4077	0.0387	3620.0	4103.6	7.2965
900	0.0595	3829.2	4364.8	7.6783	0.0535	3826.3	4361.2	7.6272	0.0427	3819.1	4352.5	7.5182
1000	0.0649	4030.3	4614.0	7.8821	0.0583	4027.8	4611.0	7.8315	0.0466	4021.6	4603.8	7.7237
1100	0.0702	4236.3	4867.7	8.0740	0.0631	4234.0	4865.1	8.0237	0.0505	4228.2	4858.8	7.9165
1200	0.0754	4447.2	5126.2	8.2556	0.0679	4444.9	5123.8	8.2055	0.0543	4439.3	5118.0	8.0987
1300	0.0807	4662.7	5389.2	8.4284	0.0727	4460.5	5387.0	8.3783	0.0581	4654.8	5381.4	8.2717

Table A.II.3(SI). Superheated Steam Properties (continued)

C	v u h s				v u h s				v u h s			
	P = 15.0 MPa (342.24)				P = 17.5 MPa (354.75)				P = 20.0 MPa (365.81)			
Sat	0.010337	2455.5	2610.5	5.3098	0.00792	2390.2	2528.8	5.1419	0.005834	2293.0	2409.7	4.9269
350	0.01147	2520.4	2692.4	5.4421								
400	0.015649	2740.7	2975.5	5.8811	0.01245	2685.0	2902.9	5.7213	0.00994	2619.3	2818.1	5.5540
450	0.018445	2879.5	3156.2	6.1404	0.01517	2844.2	3109.7	6.0184	0.01270	2806.2	3060.1	5.9017
500	0.02800	2996.6	3308.6	6.3443	0.01736	2970.3	3274.1	6.2383	0.01477	2942.9	3238.2	6.1401
550	0.02293	3104.7	3448.6	6.5199	0.01929	3083.9	3421.4	6.4230	0.01656	3062.4	3393.5	6.3348
600	0.02491	3208.6	3582.3	6.6776	0.02106	3191.5	3560.1	6.5866	0.01818	3174.0	3537.6	6.5048
650	0.02680	3310.3	3712.3	6.8224	0.02274	3296.0	3693.9	6.7357	0.01969	3281.4	3675.3	6.6582
700	0.02861	3410.9	3840.1	6.9572	0.02434	3398.7	3824.6	6.8736	0.02113	3386.4	3809.0	6.7993
800	0.03210	3610.9	4092.4	7.2040	0.02738	3601.8	4081.1	7.1244	0.02385	3592.7	4069.7	7.0544
900	0.03546	3811.9	4343.8	7.4279	0.03031	3804.7	4335.1	7.3507	0.02645	3797.5	4326.4	7.2830
1000	0.03875	4015.4	4596.6	7.6348	0.03316	4009.3	4589.5	7.5589	0.02897	4003.1	4582.5	7.4925
1100	0.04200	4222.6	4852.6	7.8283	0.03597	4216.9	4846.4	7.7531	0.03145	4211.3	4840.2	7.6874
1200	0.04523	4433.8	5112.3	8.0108	0.03876	4428.3	5106.6	7.9360	0.03391	4422.8	5101.0	7.8707
1300	0.04845	4649.1	5376.0	8.1840	0.04154	4643.5	5370.5	8.1093	0.03636	4638.0	5365.1	8.0442

C	v u h s				v u h s				v u h s			
	P = 25.0 MPa				P = 30.0 MPa				P = 35.0 MPa			
375	0.00197	1798.7	1848.0	4.0320	0.00179	1737.8	1791.5	3.9305	0.00170	1702.9	1762.4	3.8722
400	0.00600	2430.1	2580.2	5.1418	0.00279	2067.4	2151.1	4.4728	0.00210	1914.1	1987.6	4.2126
425	0.00788	2609.2	2806.3	5.4723	0.00530	2455.1	2614.2	5.1504	0.00343	2253.4	2373.4	4.7747
450	0.00916	2720.7	2949.7	5.6744	0.00674	2619.3	2821.4	5.4424	0.00496	2498.7	2672.4	5.1962
500	0.01112	2884.3	3162.4	5.9592	0.00868	2820.7	3081.1	5.7905	0.00693	2751.9	2994.4	5.6282
550	0.01272	3017.5	3335.6	6.1765	0.01017	2970.3	3275.4	6.0342	0.00835	2921.0	3213.0	5.9026
600	0.01414	3137.9	3491.4	6.3602	0.01145	3100.5	3443.9	6.2331	0.00953	3062.0	3395.5	6.1179
650	0.01543	3251.6	3637.4	6.5229	0.01260	3221.0	3598.9	6.4058	0.01058	3189.8	3559.9	6.3010
700	0.01665	3361.3	3777.5	6.6707	0.01366	3335.8	3745.6	6.5606	0.01153	3309.8	3713.5	6.4631
800	0.01891	3574.3	4047.1	6.9345	0.01562	3555.5	4024.2	6.8332	0.01328	3536.7	4001.5	6.7450
900	0.02145	3783.0	4309.1	7.1680	0.01745	3768.5	4291.9	7.0718	0.01488	3754.0	4274.9	6.9886
1000	0.02310	3990.9	4568.5	7.3802	0.01920	3978.8	4554.7	7.2867	0.01641	3966.7	4541.1	7.2064
1100	0.02512	4200.2	4828.2	7.5765	0.02090	4189.2	4816.3	7.4845	0.01790	4178.3	4804.6	7.4057
1200	0.02711	4412.0	5089.9	7.7605	0.02259	4401.3	5079.0	7.6692	0.01936	4390.7	5068.3	7.5910
1300	0.0291	4626.9	5354.4	7.9342	0.02427	4616.0	5344.0	7.8432	0.02082	4605.1	5333.6	7.7653

C	v u h s				v u h s				v u h s			
	P = 40.0 MPa				P = 50.0 MPa				P = 60.0 MPa			
375	0.001641	1677.1	1742.8	3.8290	0.00156	1638.6	1716.6	3.7639	0.00150	1609.4	1699.5	3.7141
400	0.001908	1854.6	1930.9	4.1135	0.00173	1788.1	1874.6	4.0031	0.00163	1745.4	1843.4	3.9318
425	0.002532	2096.9	2198.1	4.5029	0.00201	1959.7	2060.0	4.2734	0.00182	1892.7	2001.7	4.1626
450	0.003693	2365.1	2512.8	4.9459	0.00249	2159.6	2284.0	4.5884	0.00209	2053.9	2179.0	4.4121
500	0.005622	2678.4	2903.3	5.4700	0.00389	2525.5	2720.1	5.1726	0.00296	2390.6	2567.9	4.9321
550	0.006984	2869.7	3149.1	5.7785	0.00512	2763.6	3019.5	5.5485	0.00396	2658.8	2896.2	5.3440
600	0.008000	3022.6	3346.4	6.0114	0.00611	2942.0	3247.6	5.8178	0.00483	2861.1	3151.2	5.6452
650	0.009063	3158.0	3520.6	6.2054	0.00697	3093.5	3441.8	6.0342	0.00560	3028.8	3364.5	5.8829
700	0.009941	3283.6	3681.2	6.3750	0.00773	3230.5	3616.8	6.2189	0.00627	3177.2	3553.5	6.0824
800	0.011523	3517.8	3978.7	6.6662	0.00908	3479.8	3933.6	6.5290	0.00746	3441.5	3889.1	6.4109
900	0.012962	3739.4	4257.9	6.9150	0.01028	3710.3	4224.4	6.7882	0.00851	3681.0	4191.5	6.6805
1000	0.014324	3954.6	4527.6	7.1356	0.01141	3930.5	4501.1	7.0146	0.00948	3906.4	4475.2	6.9127
1100	0.015642	4167.4	4793.1	7.3364	0.01250	4145.7	4770.5	7.2184	0.01041	4124.1	4748.6	7.1195
1200	0.016940	4380.1	5057.7	7.5224	0.01356	4359.1	5037.2	7.4058	0.01132	4338.2	5017.2	7.3083
1300	0.018229	4594.3	5323.5	7.6969	0.01462	4512.8	5303.6	7.5808	0.01222	4551.4	5284.3	7.4837

Table A.II.4(SI). Subcooled Water Properties

C	v u h s				v u h s				v u h s			
	P = 5.0 MPa (263.99 C)				P = 10 MPa (311.06 C)				P = 15 MPa (342.24 C)			
Sat	0.001286	1147.78	1154.20	2.920	0.0014524	1393.00	1407.60	3.360	0.001658	1585.60	1610.50	3.685
0	0.000998	0.03	5.02	0.000	0.0009952	0.09	10.04	0.000	0.000993	0.15	15.05	0.000
20	0.000999	83.64	88.64	0.296	0.0009972	83.36	93.33	0.295	0.000995	83.06	97.99	0.293
40	0.001005	166.93	171.95	0.571	0.0010034	166.35	176.38	0.569	0.001001	165.76	180.78	0.567
60	0.001014	250.21	255.28	0.829	0.0010127	249.36	259.49	0.826	0.001011	248.51	263.67	0.823
80	0.001026	333.69	338.83	1.072	0.0010245	332.59	342.83	1.069	0.001022	331.48	346.81	1.066
100	0.001041	417.50	422.71	1.303	0.0010385	416.12	426.50	1.299	0.001036	414.74	430.28	1.296
120	0.001057	501.79	507.07	1.523	0.0010549	500.08	510.64	1.519	0.001052	498.40	514.19	1.515
140	0.001076	586.74	592.13	1.734	0.0010737	584.68	595.42	1.729	0.001071	582.66	598.72	1.724
160	0.001099	672.61	678.10	1.938	0.0010953	670.13	681.08	1.932	0.001092	667.71	684.09	1.926
180	0.001124	759.62	765.24	2.134	0.0011199	756.65	767.84	2.128	0.001116	753.76	770.50	2.121
200	0.001153	848.08	853.85	2.326	0.0011480	844.50	856.00	2.318	0.001143	841.00	858.20	2.310
220	0.001187	938.43	944.36	2.513	0.0011805	934.10	945.90	2.504	0.001175	929.90	947.50	2.495
240	0.001226	1031.34	1037.47	2.698	0.0012187	1026.00	1038.10	2.687	0.001211	1020.80	1039.00	2.677
260	0.001275	1127.92	1134.30	2.883	0.0012645	1121.10	1133.70	2.870	0.001255	1114.60	1133.40	2.858
280					0.0013216	1220.90	1234.10	3.055	0.001308	1212.50	1232.10	3.039
300					0.0013972	1328.40	1342.30	3.247	0.001377	1316.60	1337.30	3.226
320									0.001472	1431.10	1453.20	3.425
340									0.001631	1567.50	1591.90	3.655

C	v u h s				v u h s				v u h s			
	P = 20.0 MPa (365.81 C)				P = 30 MPa				P = 50 MPa			
Sat	0.0020360	1785.60	1826.30	4.014								
0	0.0009904	0.19	20.01	0.000	0.000986	0.25	29.82	0.000	0.000977	0.20	49.03	-0.0014
20	0.0009928	82.77	102.62	0.292	0.000989	82.17	111.84	0.290	0.000980	81.00	130.02	0.2848
40	0.0009992	165.17	185.16	0.565	0.000995	164.04	193.89	0.561	0.000987	161.86	211.21	0.5527
60	0.0010084	247.68	267.85	0.821	0.001004	246.06	276.19	0.815	0.000996	242.98	292.79	0.8052
80	0.0010199	330.40	350.80	1.062	0.001016	328.30	358.77	1.056	0.001007	324.34	374.70	1.0440
100	0.0010337	413.39	434.06	1.292	0.001029	410.78	441.66	1.284	0.001020	405.88	456.89	1.2703
120	0.0010496	496.76	517.76	1.510	0.001045	493.59	524.93	1.502	0.001035	487.65	539.39	1.4857
140	0.0010678	580.69	602.04	1.719	0.001062	576.88	608.75	1.710	0.001052	569.77	622.35	1.6915
160	0.0010885	665.35	687.12	1.920	0.001082	660.82	693.28	1.910	0.001070	652.41	705.92	1.8891
180	0.0011120	750.95	773.20	2.115	0.001105	745.59	778.73	2.102	0.001091	735.69	790.25	2.0794
200	0.0011389	837.70	860.50	2.303	0.001130	831.40	865.30	2.289	0.001115	819.70	875.50	2.2634
220	0.0011693	925.90	949.30	2.487	0.001159	918.30	953.10	2.471	0.001141	904.70	961.70	2.4419
240	0.0012046	1016.00	1040.00	2.667	0.001192	1006.90	1042.60	2.649	0.001170	990.70	1049.20	2.6158
260	0.0012462	1108.60	1133.50	2.846	0.001230	1097.40	1134.30	2.824	0.001203	1078.10	1138.20	2.7860
280	0.0012965	1204.70	1230.60	3.025	0.001276	1190.70	1229.00	2.999	0.001242	1167.20	1229.30	2.9537
300	0.0013596	1306.10	1333.30	3.207	0.001330	1287.90	1327.80	3.174	0.001286	1258.70	1323.00	3.1200
320	0.0014437	1415.70	1444.60	3.398	0.001400	1390.70	1432.70	3.354	0.001339	1353.30	1420.20	3.2868
340	0.0015684	1539.70	1571	3.608	0.001492	1501.70	1546.50	3.543	0.001403	1452.00	1522.10	3.4557
360	0.0018226	1702.80	1739.30	3.877	0.001627	1626.60	16754	3.749	0.001484	1556.00	1630.20	3.6291
380					0.001869	1781.40	1837.5	4.001	0.001588	1667.20	1746.60	3.8101

Units: v: m³/kg, u: kJ/kg, h: kJ/kg, s: kJ/kg·C

See the reference for this table. This material is used by permission of John Wiley & Sons, Inc.

Table A.II.5(SI). Properties of Various Ideal Gases

Substance	Formula	M	R (kJ/kg·K)	c_p (kJ/kg·K)	c_v (kJ/kg·K)	γ (c_p/c_v)
Acetylene	C_2H_2	26.038	0.3196	1.6872	1.3677	1.234
Air		28.967	0.2871	1.0064	0.7192	1.399
Ammonia	NH_3	17.032	0.4885	2.0958	1.6076	1.304
Argon	A	39.944	0.2084	0.5208	0.3123	1.668
Benzene	C_6H_6	78.114	0.1064	1.0454	0.9390	1.113
n-Butane	C_4H_{10}	58.124	0.1432	1.6763	1.5331	1.093
Isobutane	C_4H_{10}	58.124	0.1431	1.6658	1.5226	1.094
1-Butene	C_4H_8	56.108	0.1483	1.5264	1.3740	1.111
Carbon dioxide	CO_2	44.011	0.1890	0.8436	0.6548	1.288
Carbon monoxide	CO	28.011	0.2970	1.0194	0.7435	1.399
Dodecane	$C_{12}H_{26}$	170.340	0.0488	1.6457	1.5967	1.031
Ethane	C_2H_6	30.070	0.2768	1.7512	1.4745	1.188
Ethyl ether	$C_4H_{10}O$	74.124				
Ethylene	C_2H_4	28.054	0.2967	1.5524	1.2559	1.236
Freon, F-12	CCl_2F_2	120.925	0.0688	0.5731	0.5041	1.136
Helium	He	4.003	2.0789	5.1954	3.1173	1.667
n-Heptane	C_7H_{16}	100.205	0.0830	1.6562	1.5733	1.053
n-Hexane	C_6H_{14}	86.178	0.0965	1.6604	1.5641	1.062
Hydrogen	H_2	2.016	4.1249	14.302	10.177	1.405
Hydrogen sulfide	H_2S	34.082				
Mercury	Hg	200.610				
Methane	CH_4	16.043	0.5188	2.2264	1.7077	1.304
Methyl fluoride	CH_3F	34.035				
Neon	Ne	20.183	0.4121	1.0299	0.6179	1.667
Nitric oxide	NO	30.008	0.2771	0.9951	0.7180	1.386
Nitrogen	N_2	28.016	0.2968	1.0395	0.7427	1.400
Octane	C_8H_{18}	114.232	0.0729	1.6532	1.5804	1.046
Oxygen	O_2	32.000	0.2599	0.9173	0.6573	1.396
n-Pentant	C_5H_{12}	72.151	0.1153	1.6662	1.5511	1.074
Isopentane	C_5H_{12}	72.151	0.1153	1.6629	1.5477	1.074
Propane	C_3H_8	44.097	0.1887	1.6671	1.4783	1.120
Propylene	C_3H_6	42.081	0.1976	1.5184	1.2790	1.187
Sulfur dioxide	SO_2	64.066	0.1298	0.6209	0.4911	1.264
Water vapor	H_2O	18.016	0.4617	1.8638	1.4021	1.329
Xenon	Xe	131.300	0.0602	0.1583	0.0950	1.667

M: Molecular weight

See the reference for this table.

Table A.II.1(BU). Saturated Water and Dry Saturated Steam Properties, $f(P)$

(psia)	(F)	(ft ³ /lbm)		(Btu/lbm)			(Btu/lbm·R)		
P	T	v_f	v_g	h_f	h_{fg}	h_g	s_f	s_{fg}	s_g
0.40	72.84	0.01606	792.000	40.94	1052.30	1093.30	0.0800	1.9799	2.0559
0.60	85.19	0.01609	540.000	53.27	1045.40	1098.60	0.1029	1.9184	2.0213
0.80	94.35	0.01611	411.700	62.41	1040.20	1102.60	0.1195	1.8773	1.9968
1.0	101.74	0.01614	333.600	69.70	1036.30	1106.00	0.1326	1.8456	1.9782
2.0	126.08	0.01623	173.730	93.99	1022.20	1116.20	0.1749	1.7451	1.9200
3.0	141.48	0.01630	118.710	109.37	1013.20	1122.60	0.2008	1.6855	1.8863
4.0	152.97	0.01636	90.630	120.86	1006.40	1127.30	0.2198	1.6427	1.8625
5.0	162.24	0.01640	73.520	130.13	1001.00	1131.10	0.2347	2.6094	1.8441
6.0	170.06	0.01645	61.980	137.96	996.20	1134.20	0.2472	1.5820	1.8292
7.0	176.85	0.01649	53.640	144.76	992.10	1136.90	0.2581	1.5586	1.8167
8.0	182.86	0.01653	47.340	150.79	988.50	1139.30	0.2674	1.5383	1.8057
9.0	188.28	0.01656	42.400	156.22	985.20	1141.40	0.2759	1.5203	1.7962
10.0	193.21	0.01659	38.420	161.17	982.10	1143.30	0.2835	1.5041	1.7876
14.696	212.00	0.01672	26.800	180.07	970.30	1150.40	0.3120	1.4446	1.7566
15	213.03	0.01672	26.290	181.11	969.70	1150.80	0.3135	1.4415	1.7549
20	227.96	0.01683	20.089	196.16	960.10	1156.30	0.3356	1.3962	1.7319
25	240.07	0.01692	16.303	208.42	952.10	1160.60	0.3533	1.3606	1.7139
30	250.33	0.01701	13.746	218.82	945.30	1164.10	0.3680	1.3313	1.6993
35	259.28	0.01708	11.898	227.91	939.20	1167.10	0.3807	1.3063	1.6870
40	267.25	0.01715	10.498	236.03	933.70	1169.70	0.3919	1.2844	1.6763
45	274.44	0.01721	9.401	243.36	928.60	1172.00	0.4019	1.2650	1.6669
50	281.01	0.01727	8.515	250.09	924.00	1174.10	0.4110	1.2474	1.6585
55	287.07	0.01732	7.787	256.30	919.60	1175.90	0.4193	1.2316	1.6509
60	292.71	0.01738	7.175	262.09	915.50	1177.60	0.4270	1.2168	1.6438
65	297.97	0.01743	6.655	267.50	911.60	1179.10	0.4342	1.2032	1.6374
70	302.92	0.01748	6.206	272.61	907.90	1180.60	0.4409	1.1906	1.6315
75	307.60	0.01753	5.816	277.43	904.50	1181.90	0.4472	1.1787	1.6259
80	312.03	0.01757	5.472	282.02	901.10	1183.10	0.4531	1.1676	1.6207
85	316.25	0.01761	5.168	286.39	897.80	1184.20	0.4587	1.1571	1.6158
90	320.27	0.01766	4.896	290.56	894.70	1185.30	0.4641	1.1471	1.6112
95	324.12	0.01770	4.652	294.56	891.70	1186.20	0.4692	1.1376	1.6068
100	327.81	0.01774	4.432	298.40	888.80	1187.20	0.4740	1.1286	1.6026
110	335	0.01782	4.049	305.66	883.20	1188.90	0.4832	1.1117	1.5948
120	341.25	0.01789	3.7280	312.44	877.90	1190.40	0.4916	1.0962	1.5878
130	347.32	0.01796	3.4550	318.81	872.90	1191.70	0.4995	1.0817	1.5812
140	353.02	0.01802	3.2200	324.82	868.20	1193.00	0.5069	1.0682	1.5751
150	358.42	0.01809	3.0150	330.51	863.60	1194.10	0.5138	1.0556	1.5694
160	363.53	0.01815	2.8340	335.93	859.20	1195.10	0.5204	1.0436	1.5640
170	368.41	0.01822	2.6750	341.09	854.90	1196.00	0.5266	1.0324	1.5590
180	373.06	0.01827	2.5320	346.03	859.80	1196.90	0.5325	1.0217	1.5542
190	377.51	0.01833	2.4040	350.79	846.80	1197.60	0.5381	1.0116	1.5497

Table A.II.1(BU). Saturated Water and Dry Saturated Steam Properties, $f(P)$ (continued)

(psia)	(F)	(ft ³ /lbm)		(Btu/lbm)			(Btu/lbm·R)		
P	T	v_f	v_g	h_f	h_{fg}	h_g	s_f	s_{fg}	s_g
200	381.79	0.01839	2.2880	355.36	843.00	1198.40	0.5435	1.0018	1.5453
250	400.95	0.01865	1.8438	376.00	825.10	1201.10	0.5675	0.9588	1.5263
300	417.33	0.01890	1.5433	393.84	809.00	1202.80	0.5879	0.9225	1.5104
350	431.72	0.01913	1.3260	409.69	794.20	1203.90	0.6056	0.8910	1.4966
400	444.59	0.01930	1.1613	424.00	780.50	1204.50	0.6214	0.8630	1.4844
450	456.28	0.01950	1.0320	437.20	767.40	1204.60	0.6356	0.8378	1.4734
500	467.01	0.01970	0.9278	449.40	755.00	1204.40	0.6487	0.8147	1.4634
550	476.94	0.01990	0.8424	460.80	743.10	1203.90	0.6608	0.7934	1.4542
600	486.21	0.02010	0.7698	471.60	731.60	1203.20	0.6720	0.7734	1.4454
650	494.90	0.02030	0.7083	481.80	720.50	1202.30	0.6826	0.7548	1.4374
700	503.10	0.02050	0.6554	491.50	709.70	1201.20	0.6925	0.7371	1.4296
750	510.86	0.02070	0.6092	500.80	699.20	1200.00	0.7019	0.7204	1.4223
800	518.23	0.02090	0.5687	509.70	688.90	1198.60	0.7108	0.7045	1.4153
850	525.26	0.02100	0.5327	518.30	678.80	1197.10	0.7194	0.6891	1.4085
900	531.98	0.02120	0.5006	526.60	668.80	1195.40	0.7275	0.6744	1.4020
950	538.43	0.02140	0.4717	534.60	659.10	1193.70	0.7355	0.6602	1.3957
1000	544.61	0.02160	0.4456	542.40	649.40	1191.80	0.7430	0.6467	1.3897
1100	556.31	0.02200	0.4001	557.40	630.40	1187.70	0.7575	0.6205	1.3780
1200	567.22	0.02230	0.3619	571.70	611.70	1183.40	0.7711	0.5956	1.3667
1300	577.46	0.02270	0.3293	585.40	593.20	1178.60	0.7840	0.5719	1.3559
1400	587.10	0.02310	0.3012	598.70	574.70	1173.40	0.7963	0.5491	1.3454
1500	596.23	0.02350	0.2765	611.60	556.30	1167.90	0.8082	0.5269	1.3351
2000	635.82	0.02570	0.1878	671.70	463.40	1135.10	0.8619	0.4230	1.2849
2500	668.13	0.02870	0.1307	730.60	360.50	1091.10	0.9126	0.3197	1.2322
3000	695.36	0.03460	0.0858	802.50	217.80	1020.30	0.9731	0.1885	1.1615
3206.20	705.40	0.05030	0.0503	902.70	0	902.70	1.0580	0.0000	1.0580

See the reference for this table. This material is used by permission of John Wiley & Sons, Inc.

Table A.II.2(BU). Saturated Water and Dry Saturated Steam Properties, $f(T)$

(F)	(psia)	(ft ³ /lbm)		(Btu/lbm)			(Btu/lbm·R)		
T	P	v_f	v_g	h_f	h_{fg}	h_g	s_f	s_{fg}	s_g
32	0.08854	0.01602	3306	0	1075.8	1075.8	0.0000	2.1877	2.1877
35	0.09995	0.01602	2947	3.02	1074.1	1077.1	0.0061	2.1709	2.1770
40	0.12000	0.01602	2444	8.05	1071.3	1079.3	0.0162	2.1435	2.1597
45	0.14752	0.01602	2036.40	13.06	1068.4	1081.5	0.0262	2.1167	2.1429
50	0.17811	0.01603	1703.20	18.07	1065.6	1083.7	0.0361	2.0903	2.1264
60	0.2563	0.01604	1206.70	28.06	1059.9	1088.0	0.0555	2.0393	2.0948
70	0.363 I	0.01606	867.90	38.04	1054.3	1092.3	0.0745	1.9902	2.0647
80	0.5069	0.01608	633.10	48.02	1048.6	1096.6	0.0932	1.9428	2.0360
90	0.6982	0.01610	468.00	57.99	1042.9	1100.9	0.1115	1.8972	2.0087
100	0.9492	0.01613	350.40	67.97	1037.2	1105.2	0.1295	1.8531	1.9826
110	1.2748	0.01617	265.40	77.94	1031.6	1109.5	0.1411	1.8160	1.9577
120	1.6924	0.01620	203.27	87.92	1025.8	1113.7	0.1645	1.7694	1.9339
130	2.2225	0.01625	157.34	97.90	1020.0	1117.9	0.1816	1.7296	1.9112
140	2.8886	0.01629	123.01	107.89	1014.1	1122.0	0.1984	1.6910	1.8894
150	3.7180	0.01634	97.07	117.89	1008.2	1126.1	0.2149	1.6537	1.8685
160	4.741	0.01639	72.29	127.89	1002.3	1130.2	0.2310	1.6170	1.8485
170	5.992	0.01645	62.06	137.90	996.3	1134.2	0.2472	1.5822	1.8293
180	7.510	0.01650	50.23	147.92	990.2	1138.1	0.2630	1.5480	1.8109
190	9.339	0.01657	40.96	157.95	984.1	1142.0	0.2785	1.5147	1.7932
200	11.526	0.01663	33.64	161.99	977.9	1145.9	0.2938	1.4824	1.7762
210	14.123	0.01670	27.82	178.05	971.6	1149.7	0.3090	1.4508	1.7598
212	14.696	0.01672	26.80	180.07	970.3	1150.4	0.3120	1.4446	1.7566
220	17.186	0.01677	23.15	188.13	965.2	1153.4	0.3239	1.4201	1.7440
230	20.780	0.01684	19.382	198.23	958.8	1157.0	0.3387	1.3901	1.7288
240	24.969	0.01692	16.323	208.34	952.2	1160.5	0.3530	1.3610	1.7140
250	29.825	0.01700	13.821	216.48	945.5	1164.0	0.3675	1.3323	1.6998
260	35.429	0.01709	11.763	228.64	938.7	1167.3	0.3811	1.3043	1.6860
270	41.858	0.01717	10.061	238.84	931.8	1170.6	0.3958	1.2769	1.6727
280	49.203	0.01726	8.645	249.06	924.7	1173.8	0.4096	1.2501	1.6597
290	57.556	0.01735	7.461	259.31	917.5	1176.8	0.4234	1.2238	1.6472
300	67.013	0.01745	6.466	269.59	910.1	1179.7	0.4369	1.1980	1.6350
310	77.68	0.01755	5.626	279.92	902.6	1182.5	0.4504	1.1727	1.6231
320	89.66	0.01765	4.900	290.28	894.9	1185.2	0.4637	1.1478	1.6115
330	103.06	0.01776	4.307	300.68	887.0	1187.7	0.4769	1.1233	1.6002
340	118.01	0.01787	3.788	311.13	879.0	1190.1	0.4900	1.0992	1.5891
360	153.04	0.01811	2.957	332.18	852.20	1194.40	0.5158	1.0519	1.5677
370	173.37	0.01823	2.625	342.79	853.50	1196.30	0.5286	1.0287	1.5573
380	195.77	0.01836	2.335	353.45	844.60	1198.10	0.5413	1.5471	1.5471
390	220.37	0.01835	2.0836	364.17	835.40	1199.60	0.5539	0.9832	1.5371

Table A.II.2(BU). Saturated Water and Dry Saturated Steam Properties, $f(T)$ (continued)

(F)	(psia)	(ft ³ /lbm)		(Btu/lbm)			(Btu/lbm·R)		
T	P	v_f	v_g	h_f	h_{fg}	h_g	s_f	s_{fg}	s_g
400	247.31	0.01864	1.8633	374.97	826.00	1201.00	0.5664	0.9608	1.5272
410	276.75	0.18780	1.6700	385.83	816.30	1202.10	0.5788	0.9386	1.5174
420	308.83	0.01894	1.5000	396.77	806.30	1203.10	0.5912	0.9166	1.5078
430	343.72	0.01910	1.3499	407.79	796.00	1203.80	0.6035	0.8947	1.4982
440	381.59	0.01926	1.2171	418.90	785.40	1204.30	0.6158	0.8730	1.4887
450	422.60	0.01940	1.0993	430.10	774.50	1204.60	0.6280	0.8513	1.4793
460	466.90	0.01960	0.9944	441.40	763.20	1204.60	0.6402	0.8298	1.4700
470	514.70	0.01980	0.9009	452.80	751.50	1204.30	0.6523	0.8083	1.4606
480	566.10	0.02000	0.8172	464.40	739.40	1203.70	0.6645	0.7868	1.4513
490	621.40	0.02020	0.7423	476.00	726.80	1202.80	0.6766	0.7653	1.4419
500	680.80	0.02040	0.6749	487.80	713.90	1201.70	0.6887	0.7438	1.4325
520	812.40	0.02090	0.5594	511.90	686.40	1198.20	0.7130	0.7006	1.4136
540	962.50	0.02150	0.4649	536.60	656.60	1193.20	0.7374	0.6568	1.3942
560	1133.10	0.02210	0.3868	562.20	624.20	1186.40	0.7621	0.6121	1.3742
580	1325.80	0.02280	0.3217	588.90	588.40	1177.30	0.7872	0.5659	1.3532
600	1542.90	0.02360	0.2668	610.00	548.50	1165.50	0.8131	0.5176	1.3307
620	1786.60	0.02470	0.2201	646.70	503.60	1150.30	0.8398	0.4664	1.3062
640	2059.70	0.02600	0.1798	678.60	452.00	1130.50	0.8679	0.4110	1.2789
660	2365.40	0.02780	0.1442	714.20	390.20	1104.40	0.8987	0.3485	1.2472
680	2708.10	0.03050	0.1115	757.30	309.90	1067.21	0.9351	0.2720	1.2071
700	3093.70	0.03690	0.0761	823.30	172.10	995.40	0.9905	0.1484	1.1389
705.40	3206.20	0.05030	0.0503	902.70	0.00	902.70	1.0580	0.0000	1.0580

See the reference for this table. This material used by permission of John Wiley & Sons, Inc.

Table A.II.3(BU). Superheated Steam Properties

F	v u h s				v u h s				v u h s			
	P = 1 (101.70)				P = 5 (162.20)				P = 10 (193.19)			
200	392.51	1077.49	1150.12	2.0507	78.147	1076.25	1148.55	1.8715	38.85	1074.67	1146.56	1.7927
240	416.42	1091.22	1168.28	2.0775	83.001	1090.25	1167.05	1.8980	41.32	1089.03	1165.50	1.8205
280	440.32	1105.02	1186.50	2.1028	87.831	1104.27	1185.53	1.9240	43.77	1103.31	1184.31	1.8467
320	464.19	1118.92	1204.82	2.1269	92.645	1118.32	1204.04	1.9487	46.20	1117.56	1203.05	1.8713
360	488.05	1132.92	1223.23	2.1499	97.447	1132.42	1222.59	1.9719	48.62	1131.81	1221.78	1.8948
400	511.91	1147.02	1241.75	2.1720	102.240	1146.61	1241.21	1.9941	51.03	1146.10	1240.53	1.9171
440	535.76	1161.23	1260.37	2.1932	107.030	1160.89	1259.92	2.0154	53.44	1160.46	1259.34	1.9385
500	571.53	1182.77	1288.53	2.2235	114.210	1182.50	1288.17	2.0458	57.04	1182.16	1287.71	1.9690
600	631.13	1219.30	1336.09	2.2706	126.150	1219.10	1335.82	2.0930	63.03	1218.85	1335.48	2.0164
700	690.72	1256.65	1384.47	2.3142	138.080	1256.50	1384.26	2.1367	69.01	1256.30	1384.00	2.0601
800	750.30	1294.86	1433.70	2.3549	150.010	1294.73	1433.53	2.1774	74.98	1294.58	1433.32	2.1009
900	809.88	1333.94	1483.81	2.3932	161.940	1333.84	1483.68	2.2157	80.95	1333.72	1483.51	2.1392
1000	869.45	1373.93	1534.82	2.4294	173.860	1373.85	1534.71	2.2520	86.91	1373.74	1534.57	2.1755
1100	929.03	1414.83	1586.75	2.4638	185.780	1414.77	1586.66	2.2864	92.88	1414.68	1586.54	2.2099
1200	988.60	1456.67	1639.61	2.4967	197.700	1456.61	1639.53	2.3192	98.84	1456.53	1639.43	2.2428
1300	1048.17	1499.43	1693.40	2.5281	209.620	1499.38	1693.33	2.3507	104.80	1499.32	1693.25	2.2743
1400	1107.74	1543.13	1748.12	2.5584	221.530	1543.09	1748.06	2.3809	110.76	1543.03	1747.99	2.3045

F	v u h s				v u h s				v u h s			
	P = 14.696 (211.99)				P = 20 (227.96)				P = 40 (267.26)			
240	27.999	1087.87	1164.02	1.7764	20.475	1086.54	1162.32	1.741	-	-	-	-
280	29.687	1102.40	1183.14	1.8030	21.734	1101.36	1181.80	1.768	10.71	1097.31	1176.59	1.686
320	31.359	1116.83	1202.11	1.8280	22.976	1116.01	1201.04	1.793	11.36	1112.81	1196.90	1.712
360	33.018	1131.22	1221.01	1.8516	24.206	1130.55	1220.14	1.817	12.00	1127.98	1216.77	1.737
400	34.668	1145.62	1239.90	1.8741	25.427	1145.06	1239.17	1.840	12.62	1142.95	1236.38	1.761
440	36.313	1160.05	1258.80	1.8956	26.642	1159.59	1258.19	1.861	13.24	1157.82	1255.84	1.783
500	38.772	1181.83	1287.27	1.9262	28.456	1181.46	1286.78	1.892	14.16	1180.06	1284.91	1.814
600	42.857	1218.61	1335.16	1.9737	31.466	1218.35	1334.80	1.940	15.69	1217.33	1333.43	1.862
700	46.932	1256.12	1383.75	2.0175	34.466	1255.91	1383.47	1.983	17.20	1255.14	1382.42	1.906
800	51.001	1294.43	1433.13	2.0584	37.460	1294.27	1432.91	2.024	18.70	1293.65	1432.08	1.947
900	55.066	1333.60	1483.35	2.0967	40.450	1333.47	1483.17	2.063	20.20	1332.96	1482.50	1.986
1000	59.128	1373.65	1534.44	2.1330	43.437	1373.54	1534.30	2.099	21.70	1373.12	1533.74	2.022
1100	63.188	1414.60	1586.44	2.1674	46.422	1414.51	1586.32	2.133	23.20	1414.16	1585.86	2.057
1200	67.247	1456.47	1639.34	2.2003	49.406	1456.39	1639.24	2.166	24.69	1456.09	1638.85	2.090
1300	71.304	1499.26	1693.17	2.2318	52.389	1499.19	1693.08	2.198	26.18	1498.94	1692.75	2.121
1400	75.361	1542.98	1747.92	2.2620	55.371	1542.92	1747.85	2.228	27.68	1542.70	1747.56	2.152
1500	79.417	1587.63	1803.60	2.2912	58.352	1587.58	1803.54	2.257	29.17	1587.38	1803.29	2.181
1600	83.473	1633.20	1860.20	2.3194	61.333	1633.15	1860.14	2.285	30.66	1632.97	1859.92	2.209

F	v u h s				v u h s				v u h s			
	P = 60 (292.73)				P = 80 (312.06)				P = 100 (327.85)			
320	7.49	1109.46	1192.56	1.663	5.54	1105.95	1188.02	1.627	-	-	-	-
360	7.92	1125.31	1213.29	1.689	5.89	1122.53	1209.67	1.654	4.661	1119.23	1205.5	1.6255
400	8.35	1140.77	1233.52	1.713	6.22	1138.53	1230.56	1.679	4.934	1136.07	1227.4	1.6516
440	8.78	1156.01	1253.44	1.736	6.54	1154.15	1250.98	1.702	5.200	1152.25	1248.5	1.6756
500	9.40	1178.64	1283.00	1.768	7.02	1177.19	1281.07	1.735	5.587	1175.72	1279.1	1.7085
600	10.43	1216.31	1332.06	1.817	7.79	1215.28	1330.66	1.784	6.216	1214.23	1329.3	1.7582
700	11.44	1254.35	1381.37	1.861	8.56	1253.57	1380.31	1.829	6.834	1252.78	1379.2	1.8033
800	12.45	1293.03	1431.24	1.902	9.32	1292.41	1430.40	1.870	7.446	1291.78	1429.6	1.8449
900	13.45	1332.46	1481.82	1.941	10.08	1331.95	1481.14	1.909	8.053	1331.45	1480.5	1.8838
1000	14.45	1372.71	1533.19	1.977	10.83	1372.29	1532.63	1.945	8.657	1371.87	1532.1	1.9204
1200	16.452	1455.80	1638.48	2.045	12.33	1455.51	1638.08	2.013	9.861	1455.21	1637.7	1.9882
1400	18.445	1542.48	1747.28	2.107	13.83	1542.26	1746.99	2.075	11.060	1542.04	1746.7	2.0502

Table A.II.3(BU). Superheated Steam Properties (continued)

<i>F</i>	<i>v u h s</i>				<i>v u h s</i>				<i>v u h s</i>			
	<i>P = 120 (341.30)</i>				<i>P = 140 (353.08)</i>				<i>P = 160 (363.60)</i>			
500	4.633	1174.20	1277.1	1.6868	3.952	1172.7	1275.1	1.6682	3.440	1171.2	1273.0	1.6518
550	4.900	1193.80	1302.6	1.7127	4.184	1192.6	1300.9	1.6944	3.646	1191.3	1299.2	1.6784
600	5.164	1213.20	1327.8	1.7371	4.412	1212.1	1326.4	1.7191	3.848	1211.1	1325.0	1.7034
700	5.682	1252.00	1378.2	1.7825	4.860	1251.2	1377.1	1.7648	4.243	1250.4	1376.0	1.7494
800	6.195	1291.20	1428.7	1.8243	5.301	1290.5	1427.9	1.8068	4.631	1289.9	1427.0	1.7916
1000	7.208	1371.50	1531.5	1.9000	6.173	1371.0	1531.0	1.8827	5.397	1370.6	1530.4	1.8677
1200	8.213	1454.90	1637.3	1.9679	7.036	1454.6	1636.9	1.9507	6.154	1454.3	1636.5	1.9358
1400	9.214	1541.80	1746.4	2.0300	7.895	1541.6	1746.1	2.0129	6.906	1541.4	1745.9	1.9980
1600	10.212	1632.30	1859.0	2.0875	8.752	1632.1	1858.8	2.0704	7.656	1631.9	1858.6	2.0556
1800	11.209	1726.20	1975.1	2.1413	9.607	1726.1	1975.0	2.1242	8.405	1725.9	1974.8	2.1094
2000	12.205	1823.60	2094.6	2.1919	10.461	1823.5	2094.5	2.1749	9.153	1823.3	2094.3	2.1601

<i>F</i>	<i>v u h s</i>				<i>v u h s</i>				<i>v u h s</i>			
	<i>P = 180 (373.13)</i>				<i>P = 200 (381.86)</i>				<i>P = 225 (391.87)</i>			
400	2.648	1126.20	1214.4	1.5749	2.361	1123.5	1210.8	1.5600	2.073	1119.9	1206.2	1.5427
450	2.850	1148.50	1243.4	1.6078	2.548	1146.4	1240.7	1.5938	2.245	1143.8	1237.3	1.5779
500	3.042	1169.60	1270.9	1.6372	2.724	1168.0	1268.8	1.6239	2.405	1165.9	1266.1	1.6087
550	3.228	1190.00	1297.5	1.6642	2.893	1188.7	1295.7	1.6512	2.558	1187.0	1293.5	1.6366
600	3.409	1210.00	1323.5	1.6893	3.058	1208.9	1322.1	1.6767	2.707	1207.5	1320.2	1.6624
700	3.763	1249.60	1374.9	1.7357	3.379	1248.8	1373.8	1.7234	2.995	1247.7	1372.4	1.7095
800	4.110	1289.30	1426.2	1.7781	3.693	1288.6	1425.3	1.7660	3.276	1287.8	1424.2	1.7523
900	4.453	1329.40	1477.7	1.8175	4.003	1328.9	1477.1	1.8055	3.553	1328.3	1476.2	1.7920
1000	4.793	1370.20	1529.8	1.8545	4.310	1369.8	1529.3	1.8425	3.827	1369.3	1528.6	1.8292
1200	5.467	1454.00	1636.1	1.9227	4.918	1453.7	1635.7	1.9109	4.369	1453.4	1635.3	1.8977
1400	6.137	1541.20	1745.6	1.9849	5.521	1540.9	1745.3	1.9732	4.906	1540.7	1744.9	1.9600
1600	6.804	1631.7	1858.4	2.0425	6.123	1631.6	1858.2	2.0308	5.441	1631.3	1857.9	2.0177
1800	7.470	1725.8	1974.6	2.0964	6.722	1725.6	1974.4	2.0847	5.975	1725.4	1974.2	2.0716
2000	8.135	1823.2	2094.2	2.1470	7.320	1823.0	2094.0	2.1354	6.507	1822.9	2093.8	2.1223

<i>F</i>	<i>v u h s</i>				<i>v u h s</i>				<i>v u h s</i>			
	<i>P = 250 (401.04)</i>				<i>P = 275 (409.52)</i>				<i>P = 300 (417.43)</i>			
sat	1.8448	1116.7	1202.1	1.5274	1.681	1117.5	1203.1	1.5192	1.544	1118.2	1203.9	1.5115
450	2.002	1141.1	1233.7	1.5632	1.803	1138.3	1230.0	1.5495	1.636	1135.4	1226.2	1.5365
500	2.150	1163.8	1263.3	1.5948	1.941	1161.7	1260.4	1.5820	1.766	1159.5	1257.5	1.5701
550	2.290	1185.3	1291.3	1.6233	2.071	1183.6	1289.0	1.6110	1.888	1181.9	1286.7	1.5997
600	2.426	1206.1	1318.3	1.6494	2.196	1204.7	1316.4	1.6376	2.004	1203.2	1314.5	1.6266
650	2.558	1226.5	1344.9	1.6739	2.317	1225.3	1343.2	1.6623	2.117	1224.1	1341.6	1.6516
700	2.688	1246.7	1371.1	1.6970	2.436	1245.7	1369.7	1.6856	2.227	1244.6	1368.3	1.6751
800	2.943	1287.0	1423.2	1.7401	2.670	1286.2	1422.1	1.7289	2.442	1285.4	1421.0	1.7187
900	3.193	1327.6	1475.3	1.7799	2.898	1327.0	1474.5	1.7689	2.653	1326.3	1473.6	1.7589
1000	3.440	1368.7	1527.9	1.8172	3.124	1368.2	1527.2	1.8064	2.860	1367.7	1526.5	1.7964
1200	3.929	1453.0	1634.8	1.8858	3.570	1452.6	1634.3	1.8751	3.270	1452.2	1633.8	1.8653
1400	4.414	1540.4	1744.6	1.9483	4.010	1540.1	1744.2	1.9376	3.675	1539.8	1743.8	1.9279
1600	4.896	1631.1	1857.6	2.0060	4.450	1630.9	1857.3	1.9954	4.078	1630.7	1857.0	1.9857
1800	5.376	1725.2	1974.0	2.0599	4.887	1725.0	1973.7	2.0493	4.479	1724.9	1973.5	2.0396
2000	5.856	1822.7	2093.6	2.1106	5.323	1822.5	2093.4	2.1000	4.879	1822.3	2093.2	2.0904

Table A.II.3(BU). Superheated Steam Properties (continued)

F	$P = 350 \text{ (431.82)}$				$P = 400 \text{ (444.70)}$				$P = 450 \text{ (456.39)}$			
	v	u	h	s	v	u	h	s	v	u	h	s
sat	1.3267	1119.0	1204.9	1.4978	1.1620	1119.5	1205.5	1.4856	1.0326	1119.6	1205.6	1.4746
450	1.3733	1129.2	1218.2	1.5125	1.1745	1122.6	1209.6	1.4901				
500	1.4913	1154.9	1251.5	1.5482	1.2843	1150.1	1245.2	1.5282	1.1226	1145.1	1238.5	1.5097
550	1.5998	1178.3	1281.9	1.5790	1.3833	1174.6	1277.0	1.5605	1.2146	1170.7	1271.9	1.5436
600	1.7025	1200.3	1310.6	1.6068	1.4760	1197.3	1306.6	1.5892	1.2996	1194.3	1302.5	1.5732
650	1.8013	1221.6	1338.3	1.6323	1.5645	1219.1	1334.9	1.6153	1.3803	1216.6	1331.5	1.6000
700	1.8975	1242.5	1365.4	1.6562	1.6503	1240.4	1362.5	1.6397	1.4580	1238.2	1359.6	1.6248
800	2.0850	1283.8	1418.8	1.7004	1.8163	1282.1	1416.6	1.6844	1.6077	1280.5	1414.4	1.6701
900	2.2670	1325.0	1471.8	1.7409	1.9776	1323.7	1470.1	1.7252	1.7524	1322.4	1468.3	1.7113
1000	2.446	1366.6	1525.0	1.7787	2.136	1365.5	1523.6	1.7632	1.8941	1364.4	1522.2	1.7495
1200	2.799	1451.5	1632.8	1.8478	2.446	1450.7	1631.8	1.8327	2.1720	1450.0	1630.8	1.8192
1400	3.148	1539.3	1743.1	1.9106	2.752	1538.7	1742.4	1.8956	2.4440	1538.1	1741.7	1.8823
1600	3.494	1630.2	1856.5	1.9685	3.055	1629.8	1855.9	1.9535	2.7150	1629.3	1855.4	1.9403
1800	3.838	1724.5	1973.1	2.0225	3.357	1724.1	1972.6	2.0076	2.9830	1723.7	1972.1	1.9944
2000	4.182	1822.0	2092.8	2.0733	3.658	1821.6	2092.4	2.0584	3.2510	1821.3	2092.0	2.0453

F	$P = 500 \text{ (467.13)}$				$P = 600 \text{ (486.33)}$				$P = 700 \text{ (503.23)}$			
	v	u	h	s	v	u	h	s	v	u	h	s
sat	0.928	1119.4	1205.3	1.4645	0.770	1118.5	1204.1	1.4464	0.656	1117.0	1202.0	1.4305
500	0.992	1139.7	1231.5	1.4923	0.795	1127.9	1216.2	1.4592				
550	1.079	1166.7	1266.6	1.5279	0.875	1158.2	1255.4	1.4990	0.728	1149.0	1243.2	1.4723
600	1.158	1191.1	1298.3	1.5585	0.946	1184.5	1289.5	1.5320	0.793	1177.5	1280.2	1.5080
650	1.233	1214.0	1328.0	1.5860	1.011	1208.6	1320.9	1.5609	0.852	1203.1	1313.4	1.5387
700	1.304	1236.0	1356.7	1.6112	1.073	1231.5	1350.6	1.5871	0.907	1226.9	1344.4	1.5661
800	1.441	1278.8	1412.1	1.6571	1.190	1275.4	1407.6	1.6343	1.011	1272.0	1402.9	1.6145
900	1.572	1321.0	1466.5	1.6987	1.302	1318.4	1462.9	1.6766	1.109	1315.6	1459.3	1.6576
1000	1.701	1363.3	1520.7	1.7371	1.411	1361.2	1517.8	1.7155	1.204	1358.9	1514.9	1.6970
1100	1.827	1406.0	1575.1	1.7731	1.517	1404.2	1572.7	1.7519	1.296	1402.4	1570.2	1.7337
1200	1.952	1449.2	1629.8	1.8072	1.622	1447.7	1627.8	1.7861	1.387	1446.2	1625.8	1.7682
1400	2.198	1537.0	1741.0	1.8704	1.823	1536.4	1739.5	1.8497	1.565	1535.3	1738.1	1.8321
1600	2.442	1628.9	1854.8	1.9285	2.033	1627.9	1853.7	1.9080	1.741	1627.1	1852.6	1.8906
1800	2.684	1723.3	1971.7	1.9821	2.236	1722.6	1970.8	1.9622	1.915	1721.8	1969.9	1.9449
2000	2.926	1820.9	2091.6	2.0335	2.438	1820.0	2091.0	2.0130	2.089	1819.5	2090.1	1.9958

F	$P = 800 \text{ (518.236)}$				$P = 1000 \text{ (544.75)}$				$P = 1250 \text{ (572.56)}$			
	v	u	h	s	v	u	h	s	v	u	h	s
sat	0.5690	1115.0	1199.3	1.4160	0.4459	1109.9	1292.4	1.390	0.3454	1101.7	1181.6	1.362
550	0.6154	1138.8	1229.9	1.4469	0.4534	1114.8	1198.7	1.397				
600	0.6776	1170.1	1270.4	1.4861	0.5140	1153.7	1248.8	1.445	0.3786	1129.0	1216.6	1.395
650	0.7324	1197.2	1305.6	1.5186	0.5637	1184.7	1289.1	1.482	0.4267	1167.2	1266.0	1.441
700	0.7829	1222.1	1338.0	1.5471	0.6080	1212.0	1324.6	1.514	0.4670	1198.4	1306.4	1.477
750	0.8306	1245.7	1368.6	1.5730	0.6490	1237.2	1357.3	1.541	0.5030	1226.1	1342.4	1.507
800	0.8764	1268.5	1398.2	1.5969	0.6878	1261.2	1388.5	1.566	0.5364	1251.8	1375.8	1.534
900	0.9640	1312.9	1455.6	1.6408	0.7610	1307.3	1448.1	1.612	0.5984	1300.0	1438.4	1.582
1000	1.0482	1356.7	1511.9	1.6807	0.8305	1352.2	1505.9	1.653	0.6563	1346.4	1498.2	1.624
1100	1.1300	1400.5	1567.8	1.7178	0.8976	1396.8	1562.9	1.691	0.7116	1392.0	1556.6	1.663
1200	1.2102	1444.6	1623.8	1.7526	0.9630	1441.5	1619.7	1.726	0.7652	1437.5	1614.5	1.699
1400	1.3674	1534.2	1736.6	1.8167	1.0905	1531.9	1733.7	1.791	0.8689	1529.0	1730.0	1.765
1600	1.5218	1626.2	1851.5	1.8754	1.2152	1624.4	1849.3	1.850	0.9699	1622.2	1846.5	1.824
1800	1.6749	1721.0	1969.0	1.9298	1.3384	1719.5	1967.2	1.905	1.0693	1717.6	1965.0	1.879
2000	1.8271	1818.8	2089.3	1.9808	1.4608	1817.4	2087.7	1.9557	1.1678	1815.7	2085.8	1.930

Table A.II.3(BU). Superheated Steam Properties (continued)

<i>F</i>	<i>P</i> = 1500 (596.39)				<i>P</i> = 1750 (617.31)				<i>P</i> = 2000 (636.00)			
	<i>v</i>	<i>u</i>	<i>h</i>	<i>s</i>	<i>v</i>	<i>u</i>	<i>h</i>	<i>s</i>	<i>v</i>	<i>u</i>	<i>h</i>	<i>s</i>
sat	0.2769	1091.8	1168.7	1.3359	0.2268	1080.2	1153.7	1.3109	0.1881	1066.6	1136.3	1.2861
600	0.2816	1096.6	1174.8	1.3416								
650	0.3329	1147.0	1239.4	1.4012	0.2627	1122.5	1207.6	1.3603	0.2057	1091.1	1167.2	1.3141
700	0.3716	1183.4	1286.6	1.4429	0.3022	1166.7	1264.6	1.4106	0.2487	1147.7	1239.8	1.3782
750	0.4049	1214.1	1326.5	1.4767	0.3341	1201.3	1309.5	1.4485	0.2803	1187.3	1291.1	1.4216
800	0.4350	1241.8	1362.5	1.5058	0.3622	1231.3	1348.6	1.4802	0.3071	1220.1	1333.8	1.4562
850	0.4631	1267.7	1396.2	1.5320	0.3878	1258.8	1384.4	1.5081	0.3312	1249.5	1372.0	1.4860
900	0.4897	1292.5	1428.5	1.5562	0.4119	1284.8	1418.2	1.5334	0.3534	1276.8	1407.6	1.5126
1000	0.5400	1340.4	1490.3	1.6001	0.4569	1334.3	1482.3	1.5789	0.3945	1328.1	1474.1	1.5598
1100	0.5876	1387.2	1550.3	1.6399	0.4990	1382.2	1543.8	1.6197	0.4325	1377.2	1537.2	1.6017
1200	0.6334	1433.5	1609.3	1.6765	0.5392	1429.4	1604.0	1.6571	0.4685	1425.2	1598.6	1.6398
1400	0.7213	1526.1	1726.3	1.7431	0.6158	1523.1	1722.6	1.7245	0.5368	1520.2	1718.8	1.7082
1600	0.8064	1619.9	1843.7	1.8031	0.6896	1617.6	1841.0	1.7850	0.6020	1615.4	1838.2	1.7692
1800	0.8899	1715.7	1962.7	1.8582	0.7617	1713.9	1960.5	1.8404	0.6656	1712.0	1958.3	1.8249
2000	0.9725	1814.0	2083.9	1.9096	0.8330	1812.3	2082.0	1.8919	0.7284	1810.6	2080.2	1.8765

<i>F</i>	<i>P</i> = 2500 (668.31)				<i>P</i> = 3000 (695.52)				<i>P</i> = 3500			
	<i>v</i>	<i>u</i>	<i>h</i>	<i>s</i>	<i>v</i>	<i>u</i>	<i>h</i>	<i>s</i>	<i>v</i>	<i>u</i>	<i>h</i>	<i>s</i>
sat	0.1306	1031.0	1091.4	1.1233	0.0108	968.8	1015.5	1.1575				
650									0.2491	663.5	679.7	0.8630
700	0.1684	1098.7	1176.6	1.3073	0.0977	1003.9	1058.1	1.1944	0.0306	759.5	779.3	0.9506
750	0.2030	1155.2	1249.1	1.3686	0.1483	1114.7	1197.1	1.3122	0.1040	1058.4	1126.1	1.2440
800	0.2291	1195.7	1301.7	1.4112	0.1757	1167.6	1265.2	1.3675	0.1363	1134.7	1223.0	1.3226
850	0.2513	1229.5	1345.8	1.4456	0.1973	1207.7	1317.2	1.4080	0.1582	1183.4	1285.9	1.3716
900	0.2712	1259.9	1385.4	1.4752	0.2160	1241.8	1361.7	1.4414	0.1763	1222.4	1336.5	1.4096
950	0.2896	1288.2	1422.2	1.5018	0.2328	1272.7	1402.0	1.4705	0.1921	1256.4	1380.8	1.4416
1000	0.3069	1315.2	1457.2	1.5262	0.2485	1301.7	1439.6	1.4967	0.2066	1287.6	1421.4	1.4699
1100	0.3393	1366.8	1523.8	1.5704	0.2772	1356.2	1510.1	1.5434	0.2328	1345.2	1496.0	1.5193
1200	0.3696	1416.7	1587.7	1.6101	0.3036	1408.0	1576.6	1.5848	0.2566	1399.2	1565.3	1.5624
1400	0.4261	1514.2	1711.3	1.6804	0.3524	1508.1	1703.7	1.6571	0.2997	1501.9	1696.1	1.6368
1600	0.4795	1610.2	1832.6	1.7424	0.3900	1606.3	1827.1	1.7201	0.3395	1601.7	1821.6	1.7010
1800	0.5312	1708.2	1954.0	1.7986	0.4416	1704.5	1949.6	1.7769	0.3776	1700.8	1945.4	1.7583
2000	0.5820	1807.2	2076.4	1.8506	0.4844	1803.9	2072.8	1.8291	0.4147	1800.6	2069.2	1.8108

<i>F</i>	<i>P</i> = 4000				<i>P</i> = 5000				<i>P</i> = 6000			
	<i>v</i>	<i>u</i>	<i>h</i>	<i>s</i>	<i>v</i>	<i>u</i>	<i>h</i>	<i>s</i>	<i>v</i>	<i>u</i>	<i>h</i>	<i>s</i>
650	0.02447	657.7	675.8	0.8574	0.0238	648.0	670.0	0.8482	0.02322	640.0	665.8	0.8405
700	0.02867	742.1	763.4	0.9345	0.0268	721.8	746.6	0.9156	0.02563	708.1	736.5	0.9028
750	0.06330	960.7	1007.5	1.1395	0.03364	821.4	852.6	1.0049	0.02978	788.6	821.7	0.9746
800	0.10522	1095.0	1172.9	1.2740	0.05932	987.2	1042.1	1.1583	0.03942	896.9	940.7	1.0708
850	0.12833	1156.5	1251.5	1.3352	0.08556	1092.7	1171.9	1.2596	0.05818	1018.8	1083.4	1.1820
900	0.14622	1201.5	1309.7	1.3789	0.10385	1155.1	1251.1	1.3190	0.07588	1102.9	1187.2	1.2599
950	0.16151	1239.2	1358.8	1.4144	0.11853	1202.2	1311.9	1.3629	0.09008	1162.0	1262.0	1.3140
1000	0.17520	1272.9	1402.6	1.4449	0.13120	1242.0	1363.4	1.3988	0.10207	1209.1	1322.4	1.3561
1100	0.19954	1333.9	1481.6	1.4973	0.15302	1310.6	1452.2	1.4577	0.12218	1286.4	1422.1	1.4222
1200	0.22130	1390.1	1553.9	1.5423	0.17199	1371.6	1530.8	1.5066	0.13927	1352.7	1507.3	1.4752
1300	0.24140	1443.7	1622.4	1.5823	0.18914	1428.6	1603.7	1.5493	0.15453	1413.3	1584.9	1.5206
1400	0.26030	1495.7	1688.4	1.6188	0.20517	1483.2	1673.0	1.5876	0.16854	1470.5	1657.6	1.5608
1600	0.29590	1597.1	1816.1	1.6841	0.23480	1587.9	1805.2	1.6551	0.19420	1578.3	1794.3	1.6307
1800	0.32960	1697.1	1941.1	1.7420	0.26260	1689.8	1932.7	1.7142	0.21801	1682.4	1924.5	1.6910
2000	0.36250	1797.3	2065.6	1.7948	0.2895	1790.8	2058.6	1.7676	0.24087	1784.3	2051.7	1.7450

See the reference for this table. This material used by permission of John Wiley & Sons, Inc.

Table A.II.4(BU). Subcooled Water Properties

<i>F</i>	<i>v u h s</i>				<i>v u h s</i>				<i>v u h s</i>			
	<i>P</i> = 50 (281.02)				<i>P</i> = 150 (358.43)				<i>P</i> = 300 (417.35)			
	<i>v</i>	<i>u</i>	<i>h</i>	<i>s</i>	<i>v</i>	<i>u</i>	<i>h</i>	<i>s</i>	<i>v</i>	<i>u</i>	<i>h</i>	<i>s</i>
Sat	0.01727	240.95	250.20	0.41120	0.01809	330.10	330.6	0.51410	0.01889	392.90	394.00	0.58820
32	0.01602	0.00	0.13	0.00000	0.01601	0.00	0.44	0.03600	0.01601	0.00	0.89	0.00000
50	0.01602	18.05	18.20	0.03610	0.01601	18.04	18.49	0.03600	0.01601	18.03	18.92	0.03600
100	0.01613	67.98	68.13	0.12950	0.01612	85.98	68.39	0.12940	0.01612	67.89	68.79	0.12940
150	0.01634	117.91	118.06	0.21500	0.01634	117.86	118.31	0.21490	0.01633	117.77	118.68	0.21470
200	0.01663	168.02	168.17	0.29400	0.01663	167.94	168.40	0.29380	0.01662	167.82	168.74	0.29370
250	0.01700	218.47	218.63	0.36770	0.01700	215.51	218.84	0.36750	0.01699	218.20	219.15	0.36730
300					0.01745	266.45	269.87	0.43700	0.01744	269.17	270.14	0.43670
350					0.01799	318.26	321.78	0.50320	0.01797	321.01	322.01	0.50290
400									0.01863	374.12	375.15	0.56650
450												
500												
550												

<i>F</i>	<i>v u h s</i>				<i>v u h s</i>				<i>v u h s</i>			
	<i>P</i> = 500 (465.13)				<i>P</i> = 1000 (544.75)				<i>P</i> = 1500 (596.39)			
	<i>v</i>	<i>u</i>	<i>h</i>	<i>s</i>	<i>v</i>	<i>u</i>	<i>h</i>	<i>s</i>	<i>v</i>	<i>u</i>	<i>h</i>	<i>s</i>
Sat	0.01975	447.70	449.53	0.64904	0.02159	538.39	54238	0.74320	0.02346	604.97	611.48	0.80824
32	0.01599	0.00	1.49	0.00000	0.01597	0.03	2.99	0.00005	0.01594	0.05	4.47	0.00007
50	0.01600	18.02	19.50	0.03599	0.01597	17.99	20.94	0.03592	0.01595	17.95	22.38	0.03584
100	0.01611	67.87	69.36	0.12932	0.01608	67.70	70.68	0.12901	0.01606	67.53	71.99	0.12870
150	0.01632	117.66	119.17	0.21457	0.01629	117.38	120.40	0.21410	0.01627	117.10	121.62	0.21364
200	0.01661	167.65	169.19	0.29341	0.01658	167.26	170.32	0.29281	0.01655	166.87	171.46	0.29221
250	0.01697	217.99	219.56	0.36702	0.01694	217.47	220.61	0.36628	0.01691	216.96	221.65	0.36554
300	0.01742	268.92	270.53	0.43641	0.01738	268.24	271.46	0.43552	0.01734	267.58	272.39	0.43463
350	0.01795	320.71	322.37	0.50249	0.01791	319.83	323.15	0.50140	0.01787	318.98	323.94	0.50034
400	0.01861	373.68	375.40	0.56604	0.01855	372.55	375.98	0.56472	0.01849	371.45	376.59	0.56343
450	0.01942	428.40	430.19	0.62798	0.01934	426.89	430.47	0.62632	0.01926	425.44	430.79	0.62470
500					0.02036	483.80	487.50	0.68740	0.02024	481.80	487.40	0.68530
550									0.02158	542.10	548.10	0.74690

<i>F</i>	<i>v u h s</i>				<i>v u h s</i>				<i>v u h s</i>			
	<i>P</i> = 2000 (636.00)				<i>P</i> = 3000 (695.52)				<i>P</i> = 5000			
	<i>v</i>	<i>u</i>	<i>h</i>	<i>s</i>	<i>v</i>	<i>u</i>	<i>h</i>	<i>s</i>	<i>v</i>	<i>u</i>	<i>h</i>	<i>s</i>
Sat	0.02565	662.40	671.89	0.86227	0.03431	783.45	802.50	0.97320				
32	0.01591	0.06	5.95	0.00008	0.01586	0.09	8.90	0.00900	0.01500	0.11	14.7	-0.00001
50	0.01592	17.91	23.81	0.03575	0.01587	11.84	26.65	0.03555	0.01577	1767	32.26	0.03508
100	0.01603	67.37	73.30	0.12839	0.01599	67.04	75.91	0.12777	0.01590	6640	81.11	0.12651
200	0.01653	166.49	172.60	0.29162	0.01648	165.74	174.89	0.29046	0.01600	16432	179.47	0.28818
300	0.01731	266.93	273.33	0.43376	0.01724	265.66	275.23	0.43205	0.01700	26325	27208	0.42875
400	0.01844	370.38	377.21	0.56216	0.01833	368.32	378.50	0.55970	0.01800	36447	381.25	0.55506
450	0.01919	424.04	431.14	0.62313	0.01905	421.36	431.93	0.62011	0.01800	416.44	433.84	0.61400
500	0.02014	479.80	487.30	0.68320	0.01994	476.20	487.30	0.67940	0.01900	469.80	487.90	0.67240
560	0.02172	551.80	559.80	0.75650	0.02138	546.20	558.00	0.75080	0.02000	536.70	556.00	0.74110
600	0.02330	605.40	614.00	0.80860	0.02274	597.00	609.60	0.80040	0.02191	584.00	604.20	0.78760
640					0.02475	654.30	668.00	0.85450	0.02334	634.60	656.20	0.83570
680					0.02879	728.4	744.3	0.9226	0.02535	690.60	714.10	0.88730
700									0.02676	721.8	746.6	0.9156

See the reference for this table. This material used by permission of John Wiley & Sons, Inc.

Table A.II.5(BU). Properties of Various Ideal Gases

Substance	Formula	M	R (ft·lbf/lbm·R)	c_p (Btu/lbm·R)	c_v (Btu/lbm·R)	γ (c_p/c_v)
Acetylene	C ₂ H ₂	26.038	59.39	0.4030	0.3267	1.234
Air		28.967	53.36	0.2404	0.1718	1.399
Ammonia	NH ₃	17.032	90.77	0.5006	0.3840	1.304
Argon	A	39.944	38.73	0.1244	0.0746	1.668
Benzene	C ₆ H ₆	78.114	19.78	0.2497	0.2243	1.113
n-Butane	C ₄ H ₁₀	58.124	26.61	0.4004	0.3662	1.093
Isobutane	C ₄ H ₁₀	58.124	26.59	0.3979	0.3637	1.094
1-Butene	C ₄ H ₈	56.108	27.55	0.3646	0.3282	1.111
Carbon dioxide	CO ₂	44.011	35.12	0.2015	0.1564	1.288
Carbon monoxide	CO	28.011	55.19	0.2435	0.1776	1.399
Dodecane	C ₁₂ H ₂₆	170.340	9.07	0.3931	0.3814	1.031
Ethane	C ₂ H ₆	30.070	51.43	0.4183	0.3522	1.188
Ethyl ether	C ₄ H ₁₀ O	74.124				
Ethylene	C ₂ H ₄	28.054	55.13	0.3708	0.3000	1.236
Freon, F-12	CCl ₂ F ₂	120.925	12.78	0.1369	0.1204	1.136
Helium	He	4.003	386.33	1.2410	0.7446	1.667
n-Heptane	C ₇ H ₁₆	100.205	15.42	0.3956	0.3758	1.053
n-Hexane	C ₆ H ₁₄	86.178	17.93	0.3966	0.3736	1.062
Hydrogen	H ₂	2.016	766.53	3.4162	2.4310	1.405
Hydrogen sulfide	H ₂ S	34.082				
Mercury	Hg	200.610				
Methane	CH ₄	16.043	96.40	0.5318	0.4079	1.304
Methyl fluoride	CH ₃ F	34.035				
Neon	Ne	20.183	76.58	0.246	0.1476	1.667
Nitric oxide	NO	30.008	51.49	0.2377	0.1715	1.386
Nitrogen	N ₂	28.016	55.15	0.2483	0.1774	1.400
Octane	C ₈ H ₁₈	114.232	13.54	0.3949	0.3775	1.046
Oxygen	O ₂	32.000	48.29	0.2191	0.1570	1.396
n-Pentant	C ₅ H ₁₂	72.151	21.42	0.3980	0.3705	1.074
Isopentane	C ₅ H ₁₂	72.151	21.42	0.3972	0.3697	1.074
Propane	C ₃ H ₈	44.097	35.07	0.3982	0.3531	1.120
Propylene	C ₃ H ₆	42.081	36.72	0.3627	0.3055	1.187
Sulfur dioxide	SO ₂	64.066	24.12	0.1483	0.1173	1.264
Water vapor	H ₂ O	18.016	85.80	0.4452	0.3349	1.329
Xenon	Xe	131.300	11.18	0.03781	0.0227	1.667

See the reference for this table.

Table A.II.6. Examples of least-square fit to saturated water and dry saturated steam properties

$P_{sat} = A + \sum_{i=1}^8 B_i (T_{sat})^i$ $A = 0.6962719,$ $B_4 = 0.4086826E-7,$ $B_8 = 0.1427914E-18$	$B_1 = -0.3579628E-1,$ $B_5 = -0.1124099E-9,$	$32 \text{ F} \leq T_{sat} \leq 656 \text{ F},$ $B_2 = 0.7568188E-3,$ $B_6 = 0.2708745E-12,$	$P_{sat} \text{ in psia}$ $B_3 = -0.6924369E-5$ $B_7 = -0.3145232E-15$
$T_{sat} = \exp \left[A + \sum_{i=1}^9 B_i \ln(P_{sat})^i \right]$ $A = 0.6962719,$ $B_4 = -0.1280366E-2,$ $B_8 = -0.5261809E-6,$	$B_1 = 0.3287797,$ $B_5 = 0.3129494E-3,$ $B_9 = 0.1480419E-7$	$0.1 \text{ psia} \leq P_{sat} \leq 2300 \text{ psia},$ $B_2 = -0.3147127E-1,$ $B_6 = -0.6129843E-4,$	$T_{sat} \text{ in F}$ $B_3 = 0.6053488E-2$ $B_7 = 0.7679802E-5$
$v_f = \left[A + \sum_{i=1}^8 \frac{B_i}{(T_{sat})^i} \right]^{-1},$ $A = 62.11036,$ $B_4 = -0.6087479E-8,$ $B_8 = -0.1077666E-19$	$B_1 = 0.1722592E-1,$ $B_5 = 0.16600974E-10,$	$32 \text{ F} \leq T_{sat} \leq 656 \text{ F},$ $B_2 = -0.2852652E-3,$ $B_6 = -0.2821841E-13,$	$v_f \text{ in ft}^3/\text{lbm}$ $B_3 = 0.1485193E-5$ $B_7 = 0.2669788E-16$
$v_{fg} = \exp \left[A + \sum_{i=1}^{10} B_i (T_{sat})^i \right],$ $A = 9.429309,$ $B_4 = -0.4738610E-10,$ $B_8 = 0.4408149E-19,$	$B_1 = -0.4471527E-1,$ $B_5 = 0.2567196E-11,$ $B_9 = 0.3543467E-22$	$32 \text{ F} \leq T_{sat} \leq 656 \text{ F},$ $B_2 = 0.1089104E-3,$ $B_6 = -0.1197328E-13,$ $B_{10} = -0.1208486E-25$	$v_{fg} \text{ in ft}^3/\text{lbm}$ $B_3 = -0.1994522E-6$ $B_7 = 0.3006035E-16$
$u_f = A + \sum_{i=1}^8 B_i (T_{sat})^i,$ $A = -31.33822,$ $B_4 = 0.3951334E-7,$ $B_8 = 0.9254311E-19$	$B_1 = 0.9664909,$ $B_5 = -0.1246218E-9,$	$32 \text{ F} \leq T_{sat} \leq 656 \text{ F},$ $B_2 = 0.6886926E-3,$ $B_6 = 0.2283063E-12,$	$u_f \text{ in Btu/lbm}$ $B_3 = -0.7099748E-5$ $B_7 = -0.2246668E-15$
$u_g = \sqrt{A + \sum_{i=1}^8 B_i T^i},$ $A = 1.016841E6,$ $B_4 = -0.2479441E-3,$ $B_8 = -0.5100722E-15$	$B_1 = 920.3534,$ $B_5 = 0.7584943E-6,$	$32 \text{ F} \leq T_{sat} \leq 656 \text{ F},$ $B_2 = -4.762259,$ $B_6 = -0.1346369E-8,$	$u_g \text{ in Btu/lbm}$ $B_3 = -0.4607905E-1$ $B_7 = 0.1283154E-11$
$h_{fg} = \sqrt{A + \sum_{i=1}^9 B_i T^i},$ $A = 1.208516E6,$ $B_4 = 0.12262E-2,$ $B_8 = 0.11569E-13,$	$B_1 = -2.0031710E3,$ $B_5 = -0.4690705E-5,$ $B_9 = -0.3706017E-17$	$32 \text{ F} \leq T_{sat} \leq 705 \text{ F}$ $B_2 = 17.61703,$ $B_6 = 0.1093905E-7,$	$h_{fg} \text{ in Btu/lbm}$ $B_3 = -0.19383,$ $B_7 = -0.1520656E-10$

Appendix III

Pipe and Tube Data

This appendix contains pipe and tube data in SI units followed by the same data in BU. This appendix also includes the Navier-Stokes equations in the cylindrical and spherical coordinates.

Table A.III.1(SI). Commercial Steel Pipe (Schedule Wall Thickness)	1050
Table A.III.2(SI). Commercial Steel Pipe (Nominal Pipe Size, NPS)	1051
Table A.III.3(SI). Tube Data, Birmingham Gauges to millimeter and inches	1053
Table A.III.1(BU). Pipe Data, Carbon & Alloy Steel	1054
Table A.III.2(BU). Tube Data	1055
Table A.III.4. Navier-Stokes Equations in the Cylindrical Coordinate System	1056
Table A.III.5. Navier-Stokes Equations in the Spherical Coordinate System	1056
Table A.III.6. Substantial Derivative and Flow Acceleration Components (Cylindrical Coordinates)	1057
Table A.III.7. Substantial Derivative and Flow Acceleration Components (Spherical Coordinates)	1057

Table A.III.1(SI). Commercial Steel Pipe (Schedule Wall Thickness)

	NPS (in)	O.D. (mm)	I.D. (mm)
Schedule 10	14	355.6	342.9
	16	406.4	393.7
	18	457.2	444.5
	20	508.0	495.3
	24	609.6	596.9
	30	762.0	746.2
Schedule 20	8	219.1	206.4
	10	273.0	260.3
	12	323.9	311.2
	14	355.6	339.8
	16	406.4	390.6
	18	457.2	441.4
	20	508.0	489.0
	24	609.6	590.6
Schedule 30	8	219.1	205.0
	10	273.0	257.4
	12	323.9	307.1
	14	355.6	336.6
	16	406.4	387.4
	18	457.2	434.9
	20	508.0	482.6
	24	609.6	581.1
Schedule 40	30	762.0	730.2
	1/8	10.3	6.8
	1/4	13.7	9.2
	3/8	17.1	12.5
	1/2	21.3	15.8
	3/4	26.7	21.0
	1	33.4	26.6
	1 1/4	42.2	35.1
	1 1/2	48.3	40.9
	2	60.3	52.5
	2 1/2	73.0	62.7
	3	88.9	77.9
	3 1/2	101.6	90.1
	4	114.3	102.3
	5	141.3	128.2
	6	168.3	154.1
	8	219.1	202.7
	10	273.0	254.5
	12	323.9	303.3
	14	355.6	333.3
	16	406.4	381.0
	18	457.2	428.7
	20	508.0	477.8
	24	609.6	574.6
Schedule 60	8	219.1	198.5
	10	273.0	247.6
	12	323.9	295.4
	14	355.6	325.4
	16	406.4	373.1
	18	457.2	419.1
	20	508.0	466.8
	24	609.6	560.4
Schedule 80	1/8	10.3	5.5
	1/4	13.7	7.7
	3/8	17.1	10.7
	1/2	21.3	13.8
	3/4	26.7	18.9
	1	33.4	24.3
	1 1/4	42.2	32.5
Schedule 80, Cont.	1 1/2	48.3	38.1
	2	60.3	49.2
	2 1/2	73.0	59.0
	3	88.9	73.7
	3 1/2	101.6	85.4
	4	114.3	97.2
	5	141.3	122.3
	6	168.3	146.4
	8	219.1	193.7
	10	273.0	242.8
	12	323.9	289.0
	14	355.6	317.5
	16	406.4	363.5
	18	457.2	409.6
	20	508.0	455.6
	24	609.6	547.7
Schedule 100	8	219.1	188.9
	10	273.0	236.5
	12	323.9	281.0
	14	355.6	308.0
	16	406.4	354.0
	18	457.2	398.5
	20	508.0	442.9
	24	609.6	531.8
Schedule 120	4	114.3	92.0
	5	141.3	115.9
	6	168.3	139.8
	8	219.1	182.6
	10	273.0	230.1
	12	323.9	273.1
	14	355.6	300.0
	16	406.4	344.5
	18	457.2	387.4
	20	508.0	431.8
Schedule 140	24	609.6	517.6
	8	219.1	177.9
	10	273.0	222.2
	12	323.9	266.7
	14	355.6	292.1
	16	406.4	333.4
	18	457.2	377.8
	20	508.0	419.1
Schedule 160	24	609.6	504.8
	1/2	21.3	11.7
	3/4	26.7	15.6
	1	33.4	20.7
	1 1/4	42.2	29.5
	1 1/2	48.3	34.0
	2	60.3	42.8
	2 1/2	73.0	54.0
	3	88.9	66.6
	4	114.3	87.3
	5	141.3	109.5
	6	168.3	131.8
	8	219.1	173.1
	10	273.0	215.8
	12	323.9	257.2
	14	355.6	284.2
	16	406.4	325.4
	18	457.2	366.7
	20	508.0	408.0
	24	609.6	490.5

Table A.III.2(SI). Commercial Steel Pipe (Nominal Pipe Size, NPS)

NPS (in)	O.D. (mm)	I.D. (mm)	NPS (in)	O.D. (mm)	I.D. (mm)	NPS (in)	O.D. (mm)	I.D. (mm)
1/8	10.2	7.0	1 1/4	42.4	30.6	3	88.9	60.5
		6.6			29.8			56.9
		6.2			28.2			90.4
		5.6			26.4			89.8
1/4	13.5	9.9	1 1/2	48.3	24.8	3 1/2	101.6	89.0
		9.5			41.9			87.4
		8.9			41.1			85.6
		8.3			40.3			84.0
3/8	17.2	7.7	1 1/2	48.3	30.3			81.6
		13.2			38.3			79.6
		12.6			37.5			76.6
		12.0			37.1			73.2
1/2	21.3	11.4			36.5			69.6
		10.8			35.7			66.6
		16.1			34.1	4	114.3	103.1
		15.5			32.3			102.5
		14.9			30.7			101.7
		14.1			28.3			100.1
		13.3	2	60.3	53.1			96.7
		12.3			52.3			94.3
3/4		11.3			51.0			92.3
		10.5			50.3			89.3
		21.7			49.5			85.9
		21.1			49.1			82.3
		20.5			48.5			79.3
		19.7			47.7			74.3
		18.9			46.1	5	139.7	127.9
		17.9			44.3			127.1
		16.9			42.7			125.5
1	33.7	16.1	2 1/2	76.1	40.3			123.7
		15.7			38.3			122.1
		15.1			66.1			119.7
		14.3			65.3			117.7
		12.7			64.9			114.7
		27.3			64.3			111.3
		26.5			63.5			107.7
		25.7			61.9			104.7
1 1/4	42.4	24.7			60.1	6	168.3	99.7
		23.7			58.5			155.7
		22.9			56.1			154.1
		22.5			54.1			152.3
		21.9	3	88.9	51.1			150.7
		21.1			47.7			148.3
		19.5			78.1			146.3
		17.7			77.7			143.3
		16.1			77.1			139.9
		36.0			76.3			136.3
		35.2			74.7			133.3
		34.4			72.9			128.3
		33.4			71.3			123.9
		32.4			68.9			
		31.6			66.9			
		31.2			63.9			

Table A.III.2(SI). Commercial Steel Pipe (Nominal Pipe Size, NPS), (continued)

NPS (in)	O.D. (mm)	I.D. (mm)	NPS (in)	O.D. (mm)	I.D. (mm)
8	219.1	206.5	16	406.4	393.8
		204.9			392.2
		203.1			390.4
		201.5			388.8
		199.1			386.4
		197.1			384.4
		194.1			381.4
		190.7			378.0
		187.1			374.4
		184.1			371.4
		179.1			366.4
		174.7			362.0
10	273.0	169.1			356.4
		260.4	18	457.0	444.4
		258.8			442.8
		257.0			441.0
		255.4			439.4
		253.0			437.0
		251.0			435.0
		248.0			432.0
		244.6			428.6
		241.0			425.0
		238.0			422.0
		233.0			417.0
12	323.9	228.6			412.0
		223.0			407.0
		311.3	20	508.0	495.4
		309.7			493.8
		307.9			492.0
		306.3			490.4
		303.9			488.0
		301.9			486.0
		298.9			483.0
		295.5			479.6
		291.9			476.0
		288.9			473.0
		283.9			468.0
14	355.6	279.5			463.6
		273.9			458.0
		343.0	22	610.0	597.4
		341.4			595.8
		339.6			594.0
		338.0			592.4
		335.6			590.0
		333.6			588.0
		330.6			585.0
		327.2			581.6
		323.6			578.0
		320.6			575.0
		315.6			570.0
		311.2			565.6
		305.6			560.0

Table A.III.3(SD). Tube data, Birmingham Gauges to millimeter and inches

B.G	Thickness (inch)	Thickness (mm)
15/0	1	25.4
14/0	0.9583	24.34
13/0	0.9167	23.38
12/0	0.875	22.22
11/0	0.8333	21.17
10/0	0.7917	20.11
9/0	0.75	19.05
8/0	0.7083	17.99
7/0	0.6666	16.93
6/0	0.625	15.88
5/0	0.5883	14.94
4/0	0.5416	13.75
3/0	0.5	12.7
2/0	0.4452	11.31
0	0.3964	10.07
1	0.3532	8.971
2	0.3147	7.993
3	0.2804	7.122
4	0.25	6.35
5	0.2225	5.652
6	0.1981	5.032
7	0.1764	4.481
8	0.157	3.988
9	0.1398	3.551
10	0.125	3.175
11	0.1113	2.827
12	0.0991	2.517
13	0.0882	2.24
14	0.0785	1.994
15	0.0699	1.775
16	0.0625	1.558
17	0.0556	1.412
18	0.0495	1.257
19	0.044	1.118
20	0.0392	0.9957

B.G	Thickness (inch)	Thickness (mm)
21	0.0349	0.8865
22	0.0313	0.7938
23	0.0278	0.7066
24	0.0248	0.6289
25	0.022	0.5598
26	0.0196	0.4981
27	0.0175	0.4432
28	0.0156	0.3969
29	0.0139	0.3531
30	0.0123	0.3124
31	0.011	0.2794
32	0.0098	0.2489
33	0.0087	0.221
34	0.0077	0.1956
35	0.0069	0.1753
36	0.0061	0.1549
37	0.0054	0.1372
38	0.0048	0.1219
39	0.0043	0.1092
40	0.00386	0.09804
41	0.00343	0.08712
42	0.00306	0.07772
43	0.00272	0.06909
44	0.00242	0.06147
45	0.00215	0.05461
46	0.00192	0.04877
47	0.0017	0.04318
48	0.00152	0.03861
49	0.00135	0.03429
50	0.0012	0.03048
51	0.00107	0.02718
52	0.00095	0.02413
-	-	-
-	-	-
-	-	-

Table A.III.1(BU). Pipe Data, Carbon & Alloy Steel

Nominal Size	Pipe Schedule	d_o (in)	d_i (in)	Nominal Size	Pipe Schedule	d_o (in)	d_i (in)	Nominal Size	Pipe Schedule	d_o (in)	d_i (in)		
1/8	40	0.405	0.269	8	20	8.625	8.125		40		16.876		
	80		0.215		30		8.071		60		16.500		
1/4	40	0.540	0.364		40		7.981		80		16.124		
	80		0.302		60		7.813		100		15.688		
3/8	40	0.675	0.493		80		7.625		120		15.250		
	80		0.423		100		7.437		140		14.876		
1/2	40	0.840	0.622		120		7.187		160		14.438		
	80		0.546		140		7.001		20	20.000	19.500		
	160		0.464		160		6.875		20		19.250		
3/4	40	1.050	0.824	10	20	10.750	10.250		30		19.000		
	80		0.742		30		10.136		40		18.812		
	160		0.612		40		10.020		60		18.376		
			0.434		60		9.750		80		17.938		
1	40	1.315	1.049		80		9.562		100		17.438		
	80		0.957		100		9.312		120		17.000		
	160		0.815		120		9.062		140		16.500		
			0.599		140		8.750		160		16.062		
1¼	40	1.660	1.610	12	20	12.750	12.250	22	10	22.000	21.500		
	80		1.500		30		12.090		20		21.250		
	160		1.338		40		12.000		30		21.000		
			1.100				11.938		60		20.250		
1½	40	1.900	1.610		60		11.750		80		19.750		
	80		1.500		80		11.626		100		19.250		
	160		1.338		100		11.374		120		18.750		
			1.100		120		11.062		140		18.250		
2	40	2.375	2.067		140		10.750		160		17.750		
	80		1.939	14	20	14.000	13.500	24	10	24.000	23.500		
	160		1.687		30		13.376		20		23.250		
			1.503		40		13.250		30		23.000		
2½	40	2.875	2.469		60		13.124		60		22.876		
	80		2.323		80		13.000		80		22.624		
	160		2.125		100		12.812		100		22.062		
			1.771		120		12.500		120		21.562		
3	40	3.500	3.068		140		12.124		140		20.938		
	80		2.900	16	20	16.000	15.500		160		19.876		
	160		2.624		30		15.376		26	26.000	25.376		
			2.300		40		15.250		20		25.250		
3½	40	4.000	3.548		60		15.000	28	10	28.000	25.000		
	80		3.364		80		14.688		20		27.376		
	160		3.026		100		14.312		30		27.250		
			2.624		120		13.938		20		27.000		
4	40	4.500	4.026		140		13.562	30	10	30.000	26.750		
	80		3.826		160		13.124		20		29.376		
	120		3.624	18	10	18.000	17.500		30		29.250		
	160		3.438		20		17.376		20		29.000		
5	40	5.563	5.047		30		17.250		30		28.750		
	80		4.813		40		16.876	32	10	32.000	31.376		
	160		4.563		60		16.500		20		31.250		
			4.313		80		16.124		30		31.000		
6	40	6.625	6.065		100		15.750		20		30.750		
	80		5.761		120		15.376		30		30.500		
	120		5.501		140		15.000		20		30.250		

Table A.III.2(BU). Tube Data

d_o (in)	BWG Gauge	d_i (in)	δ (in)	A_f (in ²)
1/4	22	0.194	0.028	0.0295
	24	0.206	0.022	0.0333
	26	0.214	0.018	0.0360
3/8	18	0.277	0.049	0.0603
	20	0.305	0.035	0.0731
	22	0.319	0.028	0.0799
	24	0.331	0.022	0.0860
1/2	16	0.370	0.065	0.1075
	18	0.402	0.049	0.1269
	20	0.430	0.035	0.1452
	22	0.444	0.028	0.1548
5/8	12	0.407	0.109	0.1301
	13	0.435	0.095	0.1486
	14	0.459	0.083	0.1655
	15	0.481	0.072	0.1817
	16	0.490	0.065	0.1924
	17	0.509	0.058	0.2035
	18	0.527	0.049	0.2181
	19	0.541	0.042	0.2298
	20	0.555	0.035	0.2419
3/4	10	0.482	0.134	0.1825
	11	0.510	0.120	0.2043
	12	0.532	0.109	0.2223
	13	0.560	0.095	0.2463
	14	0.584	0.083	0.2679
	15	0.606	0.072	0.2884
	16	0.620	0.065	0.3019
	17	0.634	0.058	0.3157
	18	0.652	0.049	0.3339
	20	0.680	0.035	0.3632
7/8	10	0.607	0.134	0.2892
	11	0.635	0.120	0.3166
	12	0.657	0.109	0.3390
	13	0.685	0.095	0.3685
	14	0.709	0.083	0.3948
	16	0.745	0.065	0.4359
	18	0.777	0.049	0.4742
	20	0.805	0.035	0.5090
1	8	0.670	0.165	0.3526
	10	0.732	0.134	0.4208
	11	0.760	0.120	0.4536
	12	0.782	0.109	0.4803
	13	0.810	0.095	0.5153
	14	0.834	0.083	0.5463
	15	0.856	0.072	0.5755
	16	0.870	0.065	0.5945
	18	0.902	0.049	0.6390
	20	0.930	0.035	0.6793

d_o (in)	BWG Gauge	d_i (in)	δ (in)	A_f (in ²)
1¼	7	0.890	0.180	0.6221
	8	0.920	0.165	0.6648
	10	0.982	0.134	0.7574
	11	1.010	0.120	0.8012
	12	1.032	0.109	0.8365
	13	1.060	0.095	0.8825
	14	1.084	0.083	0.9229
	16	1.120	0.065	0.9852
	18	1.152	0.049	1.042
	20	1.180	0.035	1.094
1½	10	1.232	0.134	1.192
	12	1.282	0.109	1.291
	14	1.334	0.083	1.398
	16	1.370	0.065	1.474
2	11	1.760	0.120	2.433
	13	1.810	0.095	2.573
2½		2.204	0.148	3.815

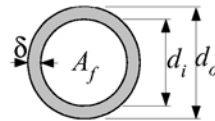


Table A.III.4. Navier-Stokes Equations in the Cylindrical Coordinate System

<p><u>r-direction:</u></p> $\rho \left(\frac{\partial V_r}{\partial t} + V_r \frac{\partial V_r}{\partial r} + \frac{V_\theta}{r} \frac{\partial V_r}{\partial \theta} - \frac{V_\theta^2}{r} + V_z \frac{\partial V_r}{\partial z} \right) = B_r - \frac{\partial P}{\partial r} + \mu \left(\frac{\partial^2 V_r}{\partial r^2} + \frac{1}{r} \frac{\partial V_r}{\partial r} - \frac{V_r}{r^2} + \frac{1}{r^2} \frac{\partial^2 V_r}{\partial \theta^2} - \frac{2}{r^2} \frac{\partial V_\theta}{\partial \theta} + \frac{\partial^2 V_r}{\partial z^2} \right)$ <p><u>θ-direction:</u></p> $\rho \left(\frac{\partial V_\theta}{\partial t} + V_r \frac{\partial V_\theta}{\partial r} + \frac{V_\theta}{r} \frac{\partial V_\theta}{\partial \theta} + \frac{V_r V_\theta}{r} + V_z \frac{\partial V_\theta}{\partial z} \right) = B_\theta - \frac{1}{r} \frac{\partial P}{\partial \theta} + \mu \left(\frac{\partial^2 V_\theta}{\partial r^2} + \frac{1}{r} \frac{\partial V_\theta}{\partial r} - \frac{V_\theta}{r^2} + \frac{1}{r^2} \frac{\partial^2 V_\theta}{\partial \theta^2} + \frac{2}{r^2} \frac{\partial V_r}{\partial \theta} + \frac{\partial^2 V_\theta}{\partial z^2} \right)$ <p><u>z-direction:</u></p> $\rho \left(\frac{\partial V_z}{\partial t} + V_r \frac{\partial V_z}{\partial r} + \frac{V_\theta}{r} \frac{\partial V_z}{\partial \theta} + V_z \frac{\partial V_z}{\partial z} \right) = B_z - \frac{\partial P}{\partial z} + \mu \left(\frac{\partial^2 V_z}{\partial r^2} + \frac{1}{r} \frac{\partial V_z}{\partial r} + \frac{1}{r^2} \frac{\partial^2 V_z}{\partial \theta^2} + \frac{\partial^2 V_z}{\partial z^2} \right)$

Table A.III.5. Navier-Stokes Equations in the Spherical Coordinate System

<p><u>r-direction:</u></p> $\rho \left(\frac{\partial V_r}{\partial t} + V_r \frac{\partial V_r}{\partial r} + \frac{V_\theta}{r} \frac{\partial V_r}{\partial \theta} + \frac{V_\theta}{r \sin \theta} \frac{\partial V_r}{\partial \varphi} - \frac{V_\theta^2}{r} - \frac{V_\varphi^2}{r} \right) = B_r - \frac{\partial P}{\partial r} + \mu \left(\frac{\partial^2 V_r}{\partial r^2} + \frac{2}{r} \frac{\partial V_r}{\partial r} - \frac{2V_r}{r^2} + \frac{1}{r^2} \frac{\partial^2 V_r}{\partial \theta^2} + \frac{\cot \theta}{r^2} \frac{\partial V_r}{\partial \theta} + \frac{1}{r^2 \sin^2 \theta} \frac{\partial^2 V_r}{\partial \varphi^2} - \frac{2}{r^2} \frac{\partial V_\theta}{\partial \theta} - \frac{2V_\theta \cot \theta}{r^2} - \frac{2}{r^2 \sin^2 \theta} \frac{\partial V_\varphi}{\partial \varphi} \right)$ <p><u>θ-direction:</u></p> $\rho \left(\frac{\partial V_\theta}{\partial t} + V_r \frac{\partial V_\theta}{\partial r} + \frac{V_\theta}{r} \frac{\partial V_\theta}{\partial \theta} + \frac{V_\theta}{r \sin \theta} \frac{\partial V_\theta}{\partial \varphi} - \frac{V_r V_\theta}{r} - \frac{V_\varphi^2 \cot \theta}{r} \right) = B_\theta - \frac{1}{r} \frac{\partial P}{\partial \theta} + \mu \left(\frac{\partial^2 V_\theta}{\partial r^2} + \frac{2}{r} \frac{\partial V_\theta}{\partial r} + \frac{V_\theta}{r^2 \sin^2 \theta} + \frac{1}{r^2} \frac{\partial^2 V_\theta}{\partial \theta^2} + \frac{\cot \theta}{r^2} \frac{\partial V_\theta}{\partial \theta} + \frac{1}{r^2 \sin^2 \theta} \frac{\partial^2 V_\theta}{\partial \varphi^2} + \frac{2}{r^2} \frac{\partial V_r}{\partial \theta} - \frac{2 \cot \theta}{r^2 \sin \theta} \frac{\partial V_\varphi}{\partial \varphi} \right)$ <p><u>φ-direction:</u></p> $\rho \left(\frac{\partial V_\varphi}{\partial t} + V_r \frac{\partial V_\varphi}{\partial r} + \frac{V_\theta}{r} \frac{\partial V_\varphi}{\partial \theta} + \frac{V_\varphi}{r \sin \theta} \frac{\partial V_\varphi}{\partial \varphi} - \frac{V_r V_\varphi}{r} - \frac{V_\theta V_\varphi \cot \theta}{r} \right) = B_\varphi - \frac{1}{r \sin \theta} \frac{\partial P}{\partial \varphi} + \mu \left(\frac{\partial^2 V_\varphi}{\partial r^2} + \frac{2}{r} \frac{\partial V_\varphi}{\partial r} - \frac{V_\varphi}{r^2 \sin^2 \theta} + \frac{2}{r^2 \sin^2 \theta} \frac{\partial V_r}{\partial \varphi} + \frac{1}{r^2 \sin^2 \theta} \frac{\partial^2 V_\varphi}{\partial \varphi^2} + \frac{2 \cot \theta}{r^2 \sin \theta} \frac{\partial V_\varphi}{\partial \varphi} \right)$
--

Table A.III.6. Substantial derivative and flow acceleration components (Cylindrical coordinates)**Substantial Derivative:**

$$\frac{D}{Dt} = \frac{\partial}{\partial t} + V_r \frac{\partial}{\partial r} + \frac{V_\theta}{r} \frac{\partial}{\partial \theta} + V_z \frac{\partial}{\partial z}$$

Flow acceleration:

$$a_r = \frac{\partial V_r}{\partial t} + V_r \frac{\partial V_r}{\partial r} + \frac{V_\theta}{r} \frac{\partial V_r}{\partial \theta} + V_z \frac{\partial V_r}{\partial z} - \frac{V_\theta^2}{r}$$

$$a_\theta = \frac{\partial V_\theta}{\partial t} + V_r \frac{\partial V_\theta}{\partial r} + \frac{V_\theta}{r} \frac{\partial V_\theta}{\partial \theta} + V_z \frac{\partial V_\theta}{\partial z} - \frac{V_r V_\theta}{r}$$

$$a_z = \frac{\partial V_z}{\partial t} + V_r \frac{\partial V_z}{\partial r} + \frac{V_\theta}{r} \frac{\partial V_z}{\partial \theta} + V_z \frac{\partial V_z}{\partial z}$$

Table A.III.7. Substantial derivative and flow acceleration components (Spherical coordinates)**Substantial Derivative:**

$$\frac{D}{Dt} = \frac{\partial}{\partial t} + V_r \frac{\partial}{\partial r} + \frac{V_\theta}{r} \frac{\partial}{\partial \theta} + \frac{V_\varphi}{r \sin \theta} \frac{\partial}{\partial \varphi}$$

Flow acceleration:

$$a_r = \frac{\partial V_r}{\partial t} + V_r \frac{\partial V_r}{\partial r} + \frac{V_\theta}{r} \frac{\partial V_r}{\partial \theta} + \frac{V_\varphi}{r \sin \theta} \frac{\partial V_r}{\partial \varphi} - \frac{V_\theta^2 + V_\varphi^2}{r}$$

$$a_\theta = \frac{\partial V_\theta}{\partial t} + V_r \frac{\partial V_\theta}{\partial r} + \frac{V_\theta}{r} \frac{\partial V_\theta}{\partial \theta} + \frac{V_\varphi}{r \sin \theta} \frac{\partial V_\theta}{\partial \varphi} + \frac{V_r V_\theta - V_\varphi^2 \cot \theta}{r}$$

$$a_\varphi = \frac{\partial V_\varphi}{\partial t} + V_r \frac{\partial V_\varphi}{\partial r} + \frac{V_\theta}{r} \frac{\partial V_\varphi}{\partial \theta} + \frac{V_\varphi}{r \sin \theta} \frac{\partial V_\varphi}{\partial \varphi} + \frac{V_r V_\varphi + V_\theta V_\varphi}{r}$$

Appendix IV

Thermophysical Data

Table A.IV.1(SI). Thermophysical Properties of Selected Metallic Solids.....	1060
Table A.IV.2(SI). Thermophysical Properties of Selected Nonmetallic Solids	1064
Table A.IV.3(SI). Thermophysical Properties of Common Materials at 300 K.....	1066
Table A.IV.4(SI). Thermophysical Properties of Gases at Atmospheric Pressure	1072
Table A.IV.5(SI). Thermophysical Properties of Saturated Water and Saturated Steam	1077
Table A.IV.6(SI). Thermophysical Properties of Liquid Metals.....	1079
Table A.IV.4(BU). Thermophysical Properties of Gases at Atmospheric Pressure.....	1080
Table A.IV.5(BU). Thermophysical Properties of Saturated Water	1082
Table A.IV.6(BU). Thermophysical Properties of Saturated Steam	1082
Table A.IV.7(BU). Thermophysical Properties of Superheated Steam.....	1083
Table A.IV.8(BU). Thermal Properties of Solid Dielectrics at Normal Temperature	1084
Table A.IV.9(BU). Normal, Total Emissivity of Metallic Surfaces.....	1086
Table A.IV.10(BU). Normal, Total Emissivity of Non-Metallic Surfaces.....	1088

Table A.IV.1(SI). Thermophysical Properties of Selected Metallic Solids

Composition	Melting Point (K)	Properties at 300 K				Properties at Various Temperatures (K)									
		ρ (kg/m ³)	c_p (J/kg·K)	k (W/m·K)	$\alpha \cdot 10^6$ (m ² /s)	$k(W/m\cdot K)/c_p(J/kg\cdot K)$									
						100	200	400	600	800	1000	1200	1500	2000	2500
Aluminum Pure	933	2702	903	237	97.1	302	237	240	231	218					
						482	798	949	1033	1146					
Alloy 2024-T6 (footnote 1)	775	2770	875	177	73.0	65	163	186	186						
						473	787	925	1042						
Alloy 195, Cast 4.5% Cu		2790	883	168	68.2			174	185						
Beryllium	1550	1850	1825	200	59.2	990	301	161	126	106	90.8	78.7			
						203	1114	2191	2604	2823	3018	3227	3519		
Bismuth	545	9780	122	7.86	6.59	16.5	9.69	7.04							
						112	120	127							
Boron	2573	2500	1107	27.0	9.76	190	55.5	16.8	10.6	9.60	9.85				
						128	600	1463	1892	2160	2338				
Cadmium	594	8650	231	96.8	48.4	203	99.3	94.7							
						198	222	242							
Chromium	2118	7160	449	93.7	29.1	159	111	90.9	80.7	71.3	65.4	61.9	57.2	49.4	
						192	384	484	542	581	616	682	779	937	
Cobalt	1769	8862	421	99.2	26.6	167	122	85.4	67.4	58.2	52.1	49.3	42.5		
						236	379	450	503	550	628	733	674		
Copper Pure	1358	8933	385	401	117	482	413	393	379	366	352	339			
						252	356	397	417	433	451	480			
Commercial Bronze, 90% Cu, 10% Al	1293	8800	420	52	14										
						785	460	545							
Phosphor Gear Bronze 89% Cu, 11% Sn	1104	8780	355	54	17										
						41	65	74							
Cartridge Brass 70% Cu, 30% Zn	1188	8530	380	110	33.9	75	95	137	149						
						360	395	425							
Constantan	1493	8920	384	23	6.71	17	19								
						237	362								

Table A.IV.1(SI). Thermophysical Properties of Selected Metallic Solids (continued)

Composition	Melting Point (K)	Properties at 300 K				Properties at Various Temperatures (K)									
		ρ (kg/m ³)	c_p (J/kg·K)	k (W/m·K)	$\alpha \cdot 10^6$ (m ² /s)	k (W/m·K)/ c_p (J/kg·K)									
						100	200	400	600	800	1000	1200	1500	2000	2500
Germanium	1211	5360	322	59.9	34.7	232	96.8	43.2	27.3	19.8	17.4	17.4			
Gold	1336	19300	129	317	127	327	323	311	298	284	270	255			
Iridium	2720	22500	130	147	50.3	172	153	144	138	132	126	120	111		
Iron Pure	1810	7870	447	80.2	23.1	134	94.0	69.5	54.7	43.3	32.8	28.3	32.1		
Armco 99.75% Pure		7870	447	72.7	20.7	95.6	80.6	65.7	53.1	42.2	32.3	28.7	31.4		
Carbon Steels (footnote 2)		7854	434	60.5	17.7	215	384	490	574	680	975	609	654		
AISI 1010		7832	434	63.9	18.8			58.7	48.8	39.2	31.3				
Carbon-Silicon (footnote 3)		7817	446	51.9	14.9			49.8	44.0	37.4	29.3				
Carbon-Manganese-Silicon , (footnote 4)		8131	434	41.0	11.6			42.2	39.7	35.0	27.6				
Chromium (low) Steels, (footnote 5)		7822	444	37.7	10.9			38.2	36.7	33.3	26.9				
(footnote 6)		7858	442	42.3	12.2			42.0	39.1	34.5	27.4				
(footnote 7)		7836	443	48.9	14.1			46.8	42.1	36.3	28.2				
Stainless Steels AISI 302		8055	480	15.1	3.91			17.3	20.0	22.8	25.4				
AISI 304	1670	7900	477	14.9	3.95	9.2	12.6	16.6	19.8	22.6	25.4	28.0	31.7		
AISI 316		8238	468	13.4	3.48	272	402	515	557	582	611	640	682		

Table A.IV.1(SI). Thermophysical Properties of Selected Metallic Solids (continued)

Composition	Melting Point (K)	Properties at 300 K				Properties at Various Temperatures (K)									
		ρ (kg/m ³)	c_p (J/kg·K)	k (W/m·K)	$\alpha \cdot 10^6$ (m ² /s)	k (W/m·K)/ c_p (J/kg·K)									
						100	200	400	600	800	1000	1200	1500	2000	2500
AISI 347		7978	480	14.2	3.71			15.8	18.9	21.9	24.7				
Lead	601	11340	129	35.3	24.1	39.7	36.7	34.0	31.4						
Magnesium	923	1740	1024	156	87.6	169	159	153	149	146					
Molybdenum	2894	10240	251	138	53.7	179	143	134	126	118	112	105	98	90	86
Nickel	1728	8900	444	90.7	23.0	141	224	261	275	285	295	308	330	380	459
Nichrome 80% Ni, 20% Cr	1672	8400	420	12	3.4	232	383	485	592	530	562	594	616		
Inconel X-750 (footnote 8)	1665	8510	439	11.7	3.1	8.7	10.3	13.5	17.0	20.5	24.0	27.6	33.0		
Niobium	2741	8570	265	53.7	23.6	55.2	52.6	55.2	58.2	61.3	64.4	67.5	72.1	79.1	
Palladium	1827	12020	244	71.8	24.5	188	249	274	283	292	301	310	324	347	
Platinum	2045	21450	133	71.6	25.1	76.5	71.6	73.6	79.7	86.9	94.2	102	110		
Pure						168	227	251	261	271	281	291	307		
						77.5	72.6	71.8	73.2	75.6	78.7	82.6	89.5	99.4	
(footnote 9)	1800	16630	162	47	17.4	100	125	136	141	146	152	157	165	179	
Rhenium	3453	21100	136	47.9	16.7	58.9	51.0	46.1	44.2	44.1	44.6	45.7	47.8	51.9	
Rhodium	2236	12450	243	150	49.6	186	154	146	136	127	121	116	110	112	
Silicon	1685	2330	712	148	89.2	147	220	253	274	293	311	327	349	376	
						884	264	98.9	61.9	42.2	31.2	25.7	22.7		
						259	556	790	867	913	946	967	992		

Table A.IV.1(SI). Thermophysical Properties of Selected Metallic Solids (continued)

Composition	Melting Point (K)	Properties at 300 K					Properties at Various Temperatures (K)									
		ρ (kg/m ³)	c_p (J/kg·K)	k (W/m·K)	$\alpha \cdot 10^6$ (m ² /s)	k (W/m·K)/ c_p (J/kg·K)	100	200	400	600	800	1000	1200	1500	2000	2500
Silver	1235	10500	235	429	174		444	430	425	412	396	379	361			
Tantalum	3269	16600	140	57.5	24.7		187	225	239	250	262	277	292			
Thorium	2023	11700	118	54.0	39.1		59.2	57.5	57.8	58.6	59.4	60.2	61.0	62.2	64.1	65.6
							110	133	144	146	149	152	155	160	172	189
Tin	505	7310	227	66.6	40.1		59.8	54.6	54.5	55.8	56.9	56.9	58.7			
							99	112	124	134	145	156	167			
							85.2	73.3	62.2							
							188	215	243							
Titanium	1953	4500	522	21.9	9.32		30.5	24.5	20.4	19.4	19.7	20.7	22.0	24.5		
							300	465	551	591	633	675	620	686		
Tungsten	3660	19300	132	174	68.3		208	186	159	137	125	118	113	107	100	95
							87	122	137	142	145	148	152	157	167	176
Uranium	1406	19070	116	27.6	12.5		21.7	25.1	29.6	34.0	38.8	43.9	49.0			
							94	108	125	146	176	180	161			
Vanadium	2192	6100	489	30.7	10.3		35.8	31.3	31.3	33.3	35.7	38.2	40.8	44.6	50.9	
							258	430	515	540	563	597	645	714	867	
Zinc	693	7140	389	116	41.8		117	118	111	103						
							297	367	402	436						
Zirconium	2125	6570	278	22.7	12.4		33.2	25.2	21.6	20.7	21.6	23.7	26.0	28.8	33.0	
							205	264	300	322	342	362	344	344	344	

- 1: 4.5% Cu, 1.5% Mg, .6% Mn
2: Plain Carbon, Mn ≤1%, Si ≤0.1%
3: Mn ≤1%, 0.1%<Si≤0.6%
4: 1%<Mn, ≤1.65% 0.1%<Si≤0.6%
5: 1/2 Cr, 1/4 Mo-Si (0.18% C, 0.65% Cr, 0.23% Mo, 0.6% Si)
6: 1 Cr-1/2 Mo (0.16% C, 1% Cr, 0.54% Mo, 0.39% Si)
7: 1 Cr-V (0.2% C, 1.02% Cr, 0.15% V)
8: X-750 (73% Ni, 15% Cr, 6.7% Fe
9: Alloy, 60Pt-40Rh, 60%Pt, 40%Rh

See the reference für this table.

Table A.IV.2(SI). Thermophysical Properties of Selected Nonmetallic Solids

Composition	Melting Point (K)	Properties at 300 K				Properties at Various Temperatures (K)									
		ρ (kg/m ³)	c_p (J/kg·K)	k (W/m·K)	$\alpha 10^6$ (m ² /s)	k (W/m·K)/ c_p (J/kg·K)									
						100	200	400	600	800	1000	1200	1500	2000	2500
Aluminum	2323	3970	765	46	15.1	450	82	32.4	18.9	13.0	10.5				
Oxide, Sapphire						---	---	940	1110	1180	1225				
Aluminum	2323	3970	765	36.0	11.9	133	55	26.4	15.8	10.4	7.85	6.55	5.66	6.00	
Oxide, Polycrystalline						---	---	940	1110	1180	1225	---	---	---	
Beryllium	2725	3000	1030	272	88.0			196	111	70	47	33	21.5	15	
Oxide								1350	1690	1865	1975	2055	2145	2750	
Boron	2573	2500	1105	27.6	9.99	190	52.5	18.7	11.3	8.1	6.3	5.2			
						---	---	1490	1880	2135	2350	2555			
Boron Fiber	590	2080													
Epoxy 30% Vol. Composite															
k_{\parallel} to Fibers				2.29		2.10	2.23	2.28							
k_{\perp} to Fibers				0.59		0.37	0.49	0.60							
c_p			1122			364	757	1431							
Carbon	1500	1950	---	1.60	---	0.67	1.18	1.89	2.19	2.37	2.53	2.84	3.48		
Amorphous						---	---	---	---	---	---	---	---		
Diamond, Type IIa Insulator	---	3500	509	2300		10000	4000	1540							
						21	194	853							
Graphite	2273	2210													
Pyrolytic															
k_{\parallel} to Layers				1950		4970	3230	1390	892	667	534	448	357	262	
k_{\perp} to Layers				5.70		16.8	9.23	4.09	2.68	2.01	1.60	1.34	1.08	0.81	
c_p			709			136	411	992	1406	1650	1793	1890	1974	2043	

Note: Symbols \parallel and \perp stand for parallel with and perpendicular to, respectively.

Table A.IV.2(SI). Thermophysical Properties of Selected Nonmetallic Solids (continued)

Composition	Melting Point (K)	Properties at 300 K				Properties at Various Temperatures (K)									
		ρ (kg/m ³)	c_p (J/kg·K)	k (W/m·K)	$\alpha \cdot 10^6$ (m ² /s)	k (W/m·K)/ c_p (J/kg·K)									
						100	200	400	600	800	1000	1200	1500	2000	2500
Graphite Fiber Epoxy 25% Vol. Composite	450	1400													
k , Heat Flow to Fibers				11.1		5.7	8.7	13.0							
k , Heat Flow \perp to Fibers				0.87		0.46	0.68	1.1							
c_p			935			337	642	1216							
Pyroceram, Corning 9606	1623	2600	808	3.98	1.89	5.25	4.78	3.64	3.28	3.08	2.96	2.87	2.79		
Silicon Carbide	3100	3160	675	490	230	---	---	---	---	---	87	58	30		
						880	1050	1135	1195	1243	1310				
Silicon Dioxide Crystalline	1883	2650													
k , to C Axis				10.4		39	16.4	7.6	5.0	4.2					
k , \perp to C Axis				6.21		20.8	9.5	4.70	3.4	3.1					
c_p			745			---	---	885	1075	1250					
Silicon Dioxide Polycrystalline (Fused Silica)	1883	2220	745	1.38	0.834	0.69	1.14	1.51	1.75	2.17	2.87	4.00			
						---	---	905	1040	1105	1155	1195			
Silicon Nitride	2173	2400	691	16.0	9.65	---	---	13.9	11.3	9.88	8.76	8.00	7.16	6.20	
	392	2070	708	0.206	0.141	0.165	0.185	578	778	937	1063	1155	1226	1306	1377
Sulfur						403	606								
Thorium Dioxide	3573	9110	235	13	6.1			10.2	6.6	4.7	3.68	3.12	2.73	2.5	
								255	274	285	295	303	315	330	
Titanium Dioxide Polycrystalline	2133	4157	710	8.4	2.8			7.01	5.02	3.94	3.46	3.28			
								805	880	910	930	945			

1: Also see Table A.IV.8.

See the reference for this table.

Table A.IV.3(SI). Thermophysical Properties of Common Materials at 300 K

<i>Structural building materials</i> DESCRIPTION/COMPOSITION	Density, ρ (kg/m ³)	Thermal Conductivity, k (W/m·K)	Specific Heat, c_p (J/kg·K)
Building Boards			
Asbestos-cement board	1,920	0.58	---
Gypsum or plaster board	800	0.17	---
Plywood	545	0.12	1,215
Sheathing, regular density	290	0.055	1,300
Acoustic tile	290	0.058	1,340
Hardboard, siding	640	0.094	1,170
Hardboard, high density	1,010	0.15	1,380
Particle board, low density	590	0.078	1,300
Particle board, high density	1,000	0.170	1,300
Woods			
Hardwoods (oak, maple)	720	0.16	1,255
Softwoods (fir, pine)	510	0.12	1,380
Masonry Materials			
Cement Mortar	1,860	0.72	780
Brick, common	1,920	0.72	835
Brick, face	2,083	1.3	---
Clay tile, hollow			
1 cell deep, 10 cm thick	---	0.52	---
3 cells deep, 30 cm thick	---	0.69	---
Concrete block, 3 oval cores			
Sand/gravel, 20 cm thick	---	1.0	---
Cinder aggregate, 20 cm thick	---	0.67	---
Concrete block, rectangular core			
2 cores, 20 cm thick, 16 kg	---	1.1	---
Same with filled cores	---	0.60	---
Plastering Materials			
Cement plaster, sand aggregate	1,860	0.72	---
Gypsum plaster, sand aggregate	1,680	0.22	1,085
Gypsum plaster, vermiculite aggregate	720	0.25	---
<i>Industrial materials and systems</i>			
Blanket and Batt			
Glass fiber, paper faced	16	0.046	---
	28	0.038	---
	40	0.035	---
Glass fiber, coated; duct liner	32	0.038	835
Board and Slab			
Cellular glass	145	0.058	1,000
Glass fiber, organic bonded	105	0.036	795
Polystyrene, expanded			
Extruded (R-12)	55	0.027	1,210
Molded beads	16	0.040	1,210
Mineral fiberboard; roofing material	265	0.049	---
Wood, shredded/cemented	350	0.087	1,590
Cork	120	0.039	1,800

Table A.IV.3(SI). Thermophysical Properties of Common Materials at 300 K (continued)

<i>Structural building materials</i> DESCRIPTION COMPOSITION	Density, ρ (kg/m ³)	Thermal Conductivity, k (W/m·K)	Specific Heat, c_p (J/kg·K)
Loose Fill			
Cork, granulated	160	0.045	---
Diatomaceous silica, coarse powder	350 400	0.069 0.091	---
Diatomaceous silica, fine powder	200 275	0.052 0.061	---
Glass fiber, poured or blown	16	0.043	835
Vermiculite, flakes	80 160	0.068 0.063	835 1,000
Formed/Foamed-in-Place			
Mineral wool granules with asbestos/ inorganic binders, sprayed	190	0.046	---
Polyvinyl acetate cork mastic; sprayed or troweled	---	0.100	---
Urethane, two-part mixture; rigid foam	70	0.026	1,045
Reflective			
Aluminum foil separating fluffy glass mats; 10-12 layers; evacuated; for cryogenic application (150 K)	40	0.00016	---
Aluminum foil and glass paper laminate; 75-150 layers; evacuated; for cryogenic application (150 K)	120	0.000017	---
Typical silica powder, evacuated	160	0.0017	---

Table A.IV.3(SI). Thermophysical Properties of Common Materials (continued)

Industrial Insulation DESCRIPTION/COMPOSITION	Max Service Temp. (K)	Typical Density (kg/m ³)	TYPICAL THERMAL CONDUCTIVITY, <i>k</i> (W/m·K), AT VARIOUS TEMPERATURES (K)													
			200	215	230	240	255	270	285	300	310	365	420	530	645	750
Blankets																
Blanket, mineral fiber, metal reinforced	920	96-192											0.038	0.046	0.056	0.078
	815	40-96											0.035	0.045	0.058	0.088
Blanket, mineral fiber, glass; fine fiber, organic bonded	450	10				0.036	0.038	0.040	0.043	0.048	0.052	0.076				
		12				0.035	0.036	0.039	0.042	0.046	0.049	0.069				
		16				0.033	0.035	0.036	0.039	0.042	0.046	0.062				
		24				0.030	0.032	0.033	0.036	0.039	0.040	0.053				
		32				0.029	0.030	0.032	0.033	0.036	0.038	0.048				
		48				0.027	0.029	0.030	0.032	0.033	0.035	0.045				
Blanket, alumina-silica fiber	1,530	48											0.071	0.105	0.150	
		64											0.059	0.087	0.125	
		96											0.052	0.076	0.100	
		128											0.049	0.068	0.091	
Felt, semirigid; organic bonded	480	50-125						0.035	0.036	0.038	0.039	0.051	0.063			
	730	50	0.023	0.025	0.026	0.027	0.029	0.030	0.032	0.033	0.035	0.051	0.079			
Felt, laminated; no binder	920	120											0.051	0.065	0.087	
Blocks, Boards, and Pipe Insulations																
Asbestos paper, laminated and corrugated																
	420	190								0.078	0.082	0.098				
	420	255								0.071	0.074	0.085				
	420	300								0.068	0.071	0.082				
Magnesia, 85% Calcium silicate	590	185									0.051	0.055	0.061			
	920	190									0.055	0.059	0.063	0.075	0.089	0.104
Cellular glass	700	145				0.046	0.048	0.051	0.052	0.055	0.058	0.062	0.069	0.079		
	1,145	345													0.092	0.098
Diatomaceous silica	1,310	385													0.101	0.100
															0.115	0.115
Polystyrene, rigid																
Extruded (R-12)	350	56	0.023	0.023	0.022	0.023	0.023	0.025	0.026	0.027	0.029					
	350	35	0.023	0.023	0.023	0.025	0.025	0.026	0.027	0.029						

Table A.IV.3(SI). Thermophysical Properties of Common Materials (continued)

Molded beads	350	16	0.026	0.029	0.030	0.033	0.035	0.036	0.038	0.040	
Rubber, rigid foamed	340	70					0.029	0.030	0.032	0.033	
Insulating Cement											
Mineral fiber (rock, slag, or glass)											
With clay binder	1,255	430									
With hydraulic setting binder	922	560						0.071	0.079	0.088	0.105 0.123
								0.108	0.115	0.123	0.137
Loose Fill											
Cellulose, wood or paper pulp	---	45						0.038	0.039	0.042	
Perlite, expanded	---	105	0.036	0.039	0.042	0.043	0.046	0.049	0.051	0.053	0.056
Vermiculite, expanded	---	122		0.056	0.058	0.061	0.063	0.065	0.068	0.071	
		80		0.049	0.051	0.055	0.058	0.061	0.063	0.066	

Table A.IV.3(SI). Thermophysical Properties of Common Materials (continued)

<i>Other Materials</i> DESCRIPTION/COMPOSITION	Temperature (K)	Density, ρ (kg/m ³)	Thermal Conductivity, k (W/m·K)	Specific Heat, c_p (J/kg·K)
Asphalt	300	2,115	0.062	920
Bakelite	300	1,300	1.4	1,465
Brick, refractory				
Carborundum	872	---	18.5	---
	1,672	---	11.0	---
Chrome brick	473	3,010	2.3	835
	823		2.5	
	1,173		2.0	
Diatomaceous silica, fired	478	---	0.25	---
	1,145	---	0.30	
Fire clay, burnt 1600 K	773	2,050	1.0	960
	1,073	---	1.1	
	1,373	---	1.1	
Fire clay, burnt 1725 K	773	2,325	1.3	960
	1,073		1.4	
	1,373		1.4	
Fire clay brick	478	2,645	1.0	960
	922		1.5	
	1,478		1.8	
Magnesite	478	---	3.8	1,130
	922	---	2.8	
	1,478		1.9	
Clay	300	1,460	1.3	880
Coal, Anthracite	300	1,350	0.26	1,260
Concrete (stone mix)	300	2,300	1.4	880
Cotton	300	80	0.06	1,300
Foodstuffs				
Banana (75.7% water content)	300	980	0.481	3,350
Apple, red (75% water content)	300	840	0.513	3,600
Cake, batter	300	720	0.223	---
Cake, fully baked	300	280	0.121	---
Chicken meat, white (74.4% water content)	198	---	1.60	---
	233	---	1.49	
	253		1.35	
	263		1.20	
	273		0.476	
	283		0.480	
	293		0.489	
Glass				
Plate (soda lime)	300	2,500	1.4	750
Pyrex	300	2,225	1.4	835
Ice	273	920	1.88	2,040
	253	---	2.03	1,945
Leather (sole)	300	998	0.159	---
Paper	300	930	0.180	1,340
Paraffin	300	900	0.240	2,890

Table A.IV.3(SI). Thermophysical Properties of Common Materials (continued)

<i>Other Materials</i> DESCRIPTION/COMPOSITION	Temperature (K)	Density, ρ (kg/m ³)	Thermal Conductivity, k (W/m·K)	Specific Heat, c_p (J/kg·K)
Rock				
Granite, Barre	300	2,630	2.79	775
Limestone, Salem	300	2,320	2.15	810
Marble, Halston	300	2,680	2.80	830
Quartzite, Sioux	300	2,640	5.38	1,105
Sandstone, Berea	300	2,150	2.90	745
Rubber, vulcanized				
Soft	300	1,100	0.13	2,010
Hard	300	1,190	0.16	---
Sand	300	1,515	0.27	800
Soil	300	2,050	0.52	1,840
Snow	273	110	0.049	---
		500	0.190	---
Teflon	300	2,200	0.35	---
	400		0.45	---
Tissue, human				
Skin	300	---	0.37	---
Fat layer (adipose)	300	---	0.2	---
Muscle	300	---	0.41	---
Wood, cross grain				
Balsa	300	140	0.055	---
Cypress	300	465	0.097	---
Fir	300	415	0.11	2,720
Oak	300	545	0.17	2,385
Yellow pine	300	640	0.15	2,805
White pine	300	435	0.11	---
Wood, radial				
Oak	300	545	0.19	2,385
Fir	300	420	0.14	2,720

See the reference for this table.

Table A.IV.4(SI). Thermophysical Properties of Gases at Atmospheric Pressure

T (K)	ρ (kg/m ³)	c_p (kJ/kg·K)	$\mu \cdot 10^7$ (N·s/m ²)	$\nu \cdot 10^6$ (m ² /s)	$k \cdot 10^3$ (W/m·K)	$\alpha \cdot 10^6$ (m ² /s)	Pr
Air							
100	3.5562	1.032	71.1	2.00	9.34	2.54	0.786
150	2.3364	1.012	103.4	4.426	13.8	5.84	0.758
200	1.7458	1.007	132.5	7.590	18.1	10.3	0.737
250	1.3947	1.006	159.6	11.44	22.3	15.9	0.720
300	1.1614	1.007	184.6	15.89	26.3	22.5	0.707
350	0.9950	1.009	208.2	20.92	30.0	29.9	0.700
400	0.8711	1.014	230.1	26.41	33.8	38.3	0.690
450	0.7740	1.021	250.7	32.39	37.3	47.2	0.686
500	0.6964	1.030	270.1	38.79	40.7	56.7	0.684
550	0.6329	1.040	288.4	45.57	43.9	66.7	0.683
600	0.5804	1.051	305.8	52.69	46.9	76.9	0.685
650	0.5356	1.063	322.5	60.21	49.7	87.3	0.690
700	0.4975	1.075	338.8	68.10	52.4	98.0	0.695
750	0.4643	1.087	354.6	76.37	54.9	109	0.702
800	0.4354	1.099	369.8	84.93	57.3	120	0.709
850	0.4097	1.110	384.3	93.80	59.6	131	0.716
900	0.3868	1.121	398.1	102.9	62.0	143	0.720
950	0.3666	1.131	411.3	112.2	64.3	155	0.723
1000	0.3482	1.141	424.4	121.9	66.7	168	0.726
1100	0.3166	1.159	449.0	141.8	71.5	195	0.728
1200	0.2902	1.175	473.0	162.9	76.3	224	0.728
1300	0.2679	1.189	496.0	185.1	82	238	0.719
1400	0.2488	1.207	530	213	91	303	0.703
1500	0.2322	1.230	557	240	100	350	0.685
1600	0.2177	1.248	584	268	106	390	0.688
1700	0.2049	1.267	611	298	113	435	0.685
1800	0.1935	1.286	637	329	120	482	0.683
1900	0.1833	1.307	663	362	128	534	0.677
2000	0.1741	1.337	689	396	137	589	0.672
2100	0.1658	1.372	715	431	147	646	0.667
2200	0.1582	1.417	740	468	160	714	0.655
2300	0.1513	1.478	766	506	175	783	0.647
2400	0.1448	1.558	792	547	196	869	0.630
2500	0.1389	1.665	818	589	222	960	0.613
3000	0.1135	2.726	955	841	486	1570	0.536
Ammonia (NH₃)							
300	0.6894	2.158	101.5	14.7	24.7	16.6	0.887
320	0.6448	2.170	109	16.9	27.2	19.4	0.870
340	0.6059	2.192	116.5	19.2	29.3	22.1	0.872
360	0.5716	2.221	124	21.7	31.6	24.9	0.872
380	0.5410	2.254	131	24.2	34.0	27.9	0.869

Table A.IV.4(SI). Thermophysical Properties of Gases at Atmospheric Pressure (continued)

T (K)	ρ (kg/m ³)	c_p (kJ/kg·K)	$\mu \cdot 10^7$ (N·s/m ²)	$\nu \cdot 10^6$ (m ² /s)	$k \cdot 10^3$ (W/m·K)	$\alpha \cdot 10^6$ (m ² /s)	Pr
Ammonia (NH₃) Continued							
400	0.5136	2.287	138	26.9	37.0	31.5	0.853
420	0.4888	2.322	145	29.7	40.4	35.6	0.833
440	0.4664	2.357	152.5	32.7	43.5	39.6	0.826
460	0.4460	2.393	159	35.7	46.3	43.4	0.822
480	0.4273	2.430	166.5	39.0	49.2	47.4	0.822
500	0.4101	2.467	173	42.2	52.5	51.9	0.813
520	0.3942	2.504	180	45.7	54.5	55.2	0.827
540	0.3795	2.540	186.5	49.1	57.5	59.7	0.824
560	0.3708	2.577	193	52.0	60.6	63.4	0.827
580	0.3533	2.613	199.5	56.5	63.8	69.1	0.817
Carbon Dioxide (CO₂)							
280	1.9022	0.830	140	7.36	15.20	9.63	0.765
300	1.7730	0.851	149	8.40	16.55	11.0	0.766
320	1.6609	0.872	156	9.39	18.05	12.5	0.754
340	1.5618	0.891	165	10.6	19.70	14.2	0.746
360	1.4743	0.908	173	11.7	21.2	15.8	0.741
380	1.3961	0.926	181	13.0	22.75	17.6	0.737
400	1.3257	0.942	190	14.3	24.3	19.5	0.737
450	1.1782	0.981	210	17.8	28.3	24.5	0.728
500	1.0594	1.02	231	21.8	32.5	30.1	0.725
550	0.9625	1.05	251	26.1	36.6	36.2	0.721
600	0.8826	1.08	270	30.6	40.7	42.7	0.717
650	0.8143	1.10	288	35.4	44.5	49.7	0.712
700	0.7564	1.13	305	40.3	48.1	56.3	0.717
750	0.7057	1.15	321	45.5	51.7	63.7	0.714
800	0.6614	1.17	337	51.0	55.1	71.2	0.716
Carbon Monoxide (CO)							
200	1.6888	1.045	127	7.52	17.0	9.63	0.781
220	1.5341	1.044	137	8.93	19.0	11.9	0.753
240	1.4055	1.043	147	10.5	20.6	14.1	0.744
260	1.2967	1.043	157	12.1	22.1	16.3	0.741
280	1.2038	1.042	166	13.8	23.6	18.8	0.733
300	1.1233	1.043	175	15.6	25.0	21.3	0.730
320	1.0529	1.043	184	17.5	26.3	23.9	0.730
340	0.9909	1.044	193	19.5	27.8	26.9	0.725
360	0.9357	1.045	202	21.6	29.1	29.8	0.725
380	0.8864	1.047	210	23.7	30.5	32.9	0.729
400	0.8421	1.049	218	25.9	31.8	36.0	0.719
450	0.7483	1.055	237	31.7	35.0	44.3	0.714
500	0.67352	1.065	254	37.7	38.1	53.1	0.710
550	0.61226	1.076	271	44.3	41.1	62.4	0.710
600	0.56126	1.088	286	51.0	44.0	72.1	0.707

Table A.IV.4(SI). Thermophysical Properties of Gases at Atmospheric Pressure (continued)

T (K)	ρ (kg/m ³)	c_p (kJ/kg·K)	$\mu \cdot 10^7$ (N·s/m ²)	$\nu \cdot 10^6$ (m ² /s)	$k \cdot 10^3$ (W/m·K)	$\alpha \cdot 10^6$ (m ² /s)	Pr
Carbon Monoxide (CO) Continued							
650	0.51806	1.101	301	58.1	47.0	82.4	0.705
700	0.48102	1.114	315	65.5	50.0	93.3	0.702
750	0.44899	1.127	329	73.3	52.8	104	0.702
800	0.42095	1.140	343	81.5	55.5	116	0.705
Helium (He)							
100	0.4871	5.193	96.3	19.8	73.0	28.9	0.686
120	0.4060	5.193	107	26.4	81.9	38.8	0.679
140	0.3481	5.193	118	33.9	90.7	50.2	0.676
160	---	5.193	129	---	99.2	---	---
180	0.2708	5.193	139	51.3	107.2	76.2	0.673
200	---	5.193	150	---	115.1	---	---
220	0.2216	5.193	160	72.2	123.1	107	0.675
240	---	5.193	170	---	130	---	---
260	0.1875	5.193	180	96.0	137	141	0.682
280	---	5.193	190	---	145	---	---
300	0.1625	5.193	199	122	152	180	0.680
350	---	5.193	221	---	170	---	---
400	0.1219	5.193	243	199	187	295	0.675
450	---	5.193	263	---	204	---	---
500	0.09754	5.193	283	290	220	434	0.668
550	---	5.193	---	---	---	---	---
600	---	5.193	320	---	252	---	---
650	---	5.193	332	---	264	---	---
700	0.06969	5.193	350	502	278	768	0.654
750	---	5.193	364	---	291	---	---
800	---	5.193	382	---	304	---	---
900	---	5.193	414	---	330	---	---
1000	0.04879	5.193	446	914	354	1400	0.654
Hydrogen (H₂)							
100	0.24255	11.23	42.1	17.4	67.0	24.6	0.707
150	0.16156	12.60	56.0	34.7	101	49.6	0.699
200	0.12115	13.54	68.1	56.2	131	79.9	0.704
250	0.09693	14.06	78.9	81.4	157	115	0.707
300	0.08078	14.31	89.6	111	183	158	0.701
350	0.06924	14.43	98.8	143	204	204	0.700
400	0.06059	14.48	108.2	179	226	258	0.695
450	0.05386	14.50	117.2	218	247	316	0.689
500	0.04848	14.52	126.4	261	266	378	0.691
550	0.04407	14.53	134.3	305	285	445	0.685
600	0.04040	14.55	142.4	352	305	519	0.678
700	0.03463	14.61	157.8	456	342	676	0.675

Table A.IV.4(SI). Thermophysical Properties of Gases at Atmospheric Pressure (continued)

T (K)	ρ (kg/m ³)	c_p (kJ/kg·K)	$\mu \cdot 10^7$ (N·s/m ²)	$\nu \cdot 10^6$ (m ² /s)	$k \cdot 10^3$ (W/m·K)	$\alpha \cdot 10^6$ (m ² /s)	Pr
Hydrogen (H₂) Continued							
800	0.03030	14.70	172.4	569	378	849	0.670
900	0.02694	14.83	186.5	692	412	1030	0.671
1000	0.02424	14.99	201.3	830	448	1230	0.673
1100	0.02204	15.17	213.0	966	488	1460	0.662
1200	0.02020	15.37	226.2	1120	528	1700	0.659
1300	0.01865	15.59	238.5	1279	568	1955	0.655
1400	0.01732	15.81	250.7	1447	610	2230	0.650
1500	0.01616	16.02	262.7	1626	655	2530	0.643
1600	0.0152	16.28	273.7	1801	697	2815	0.639
1700	0.0143	16.58	284.9	1992	742	3130	0.637
1800	0.0135	16.96	296.1	2193	786	3435	0.639
1900	0.0128	17.49	307.2	2400	835	3730	0.643
2000	0.0121	18.25	318.2	2630	878	3975	0.661
Nitrogen (N₂)							
100	3.4388	1.070	68.8	2.00	9.58	2.60	0.768
150	2.2594	1.050	100.6	4.45	13.9	5.86	0.759
200	1.6883	1.043	129.2	7.65	18.3	10.4	0.736
250	1.3488	1.042	154.9	11.48	22.2	15.8	0.727
300	1.1233	1.041	178.2	15.86	25.9	22.1	0.716
350	0.9625	1.042	200.0	20.78	29.3	29.2	0.711
400	0.8425	1.045	220.4	26.16	32.7	37.1	0.704
450	0.7485	1.050	239.6	32.01	35.8	45.6	0.703
500	0.6739	1.056	257.7	38.24	38.9	54.7	0.700
550	0.6124	1.065	274.7	44.86	41.7	63.9	0.702
600	0.5615	1.075	290.8	51.79	44.6	73.9	0.701
700	0.4812	1.098	321.0	66.71	49.9	94.4	0.706
800	0.4211	1.22	349.1	82.90	54.8	116	0.715
900	0.3743	1.146	375.3	100.3	59.7	139	0.721
1000	0.3368	1.167	399.9	118.7	64.7	165	0.721
1100	0.3062	1.187	423.2	138.2	70.0	193	0.718
1200	0.2807	1.204	445.3	158.6	75.8	224	0.707
1300	0.2591	1.219	466.2	179.9	81.0	256	0.701
Oxygen (O₂)							
100	3.945	0.962	76.4	1.94	9.25	2.44	0.796
150	2.585	0.921	114.8	4.44	13.8	5.80	0.766
200	1.930	0.915	147.5	7.64	18.3	10.4	0.737
250	1.542	0.915	178.6	11.58	22.6	16.0	0.723
300	1.284	0.920	207.2	16.14	26.8	22.7	0.711
350	1.100	0.929	233.5	21.23	29.6	29.0	0.733
400	0.9620	0.942	258.2	26.84	33.0	36.4	0.737
450	0.8554	0.956	281.4	32.90	36.3	44.4	0.741

Table A.IV.4(SI). Thermophysical Properties of Gases at Atmospheric Pressure (continued)

T (K)	ρ (kg/m ³)	c_p (kJ/kg·K)	$\mu \cdot 10^{-7}$ (N·s/m ²)	$\nu \cdot 10^6$ (m ² /s)	$k \cdot 10^3$ (W/m·K)	$\alpha \cdot 10^6$ (m ² /s)	Pr
Oxygen (O₂) Continued							
500	0.7698	0.972	303.3	39.40	41.2	55.1	0.716
550	0.6998	0.988	324.0	46.30	44.1	63.8	0.726
600	0.6414	1.003	343.7	53.59	47.3	73.5	0.729
700	0.5498	1.031	380.8	69.26	52.8	93.1	0.744
800	0.4810	1.054	415.2	86.32	58.9	116	0.743
900	0.4275	1.074	447.2	104.6	64.9	141	0.740
1000	0.3848	1.090	477.0	124.0	71.0	169	0.733
1100	0.3498	1.103	505.5	144.5	75.8	196	0.736
1200	0.3206	1.115	532.5	166.1	81.9	229	0.725
1300	0.2960	1.125	588.4	188.6	87.1	262	0.721
Water Vapor (steam)							
380	0.5863	2.060	127.1	21.68	24.6	20.4	1.06
400	0.5542	2.014	134.4	24.25	26.1	23.4	1.04
450	0.4902	1.980	152.5	31.11	29.9	30.8	1.01
500	0.4405	1.985	170.4	38.68	33.9	38.8	0.998
550	0.4005	1.997	188.4	47.04	37.9	47.4	0.993
600	0.3652	2.026	206.7	56.60	42.2	57.0	0.993
650	0.3380	2.056	224.7	66.48	46.4	66.8	0.996
700	0.3140	2.085	242.6	77.26	50.5	77.1	1.00
750	0.2931	2.119	260.4	88.84	54.9	88.4	1.00
800	0.2739	2.152	278.6	101.7	59.2	100	1.01
850	0.2579	2.186	296.9	115.1	63.7	113	1.02

See reference for this table.

Table A.IV.5(SI). Physical Properties of Saturated Water and Saturated Steam

T (K)	P (bars)	$c_{p,f}$ (kJ/kg·K)	$c_{p,g}$ (kJ/kg·K)	μ_f E6 (N·s/m ²)	μ_g E6 (N·s/m ²)	k_f E3 (W/m·K)	k_g E3 (W/m·K)	Pr_f (-)	Pr_g (-)	σ_f E3 (N/m)	β_f E6 (K ⁻¹)	T (K)
273.15	0.00611	4.217	1.854	1750	8.02	569	18.20	12.99	0.815	75.50	-68.05	273.15
275	0.00697	4.211	1.855	1652	8.09	574	18.30	12.22	0.817	75.30	-32.74	275
280	0.00990	4.198	1.858	1422	8.29	582	18.60	10.26	0.825	74.80	46.04	280
285	0.01387	4.189	1.861	1225	8.49	590	18.90	8.81	0.833	74.30	114.10	285
290	0.01917	4.184	1.864	1080	8.69	598	19.30	7.56	0.841	73.70	174.00	290
295	0.02617	4.181	1.868	959	8.89	606	19.50	6.62	0.849	72.70	227.50	295
300	0.03531	4.179	1.872	855	9.09	613	19.60	5.83	0.857	71.70	276.10	300
305	0.04712	4.178	1.877	769	9.29	620	20.10	5.20	0.865	70.90	320.60	305
310	0.06221	4.178	1.882	695	9.49	628	20.40	4.62	0.873	70.00	361.90	310
315	0.08132	4.179	1.888	631	9.69	634	20.70	4.16	0.883	69.20	400.40	315
320	0.1053	4.180	1.895	577	9.89	640	21.00	3.77	0.894	68.30	436.70	320
325	0.1351	4.182	1.903	528	10.09	645	21.30	3.42	0.901	67.50	471.20	325
330	0.1719	4.184	1.911	489	10.29	650	21.70	3.15	0.908	66.60	504.00	330
335	0.2167	4.186	1.920	453	10.49	656	22.00	2.88	0.916	65.80	535.50	335
340	0.2713	4.188	1.930	420	10.69	660	22.30	2.66	0.925	64.90	566.00	340
345	0.3372	4.191	1.941	389	10.89	668	22.60	2.45	0.933	641	595.40	345
350	0.4163	4.195	1.954	365	11.09	668	23.00	2.29	0.942	63.20	624.20	350
355	0.5100	4.199	1.968	343	11.29	671	23.30	2.14	0.951	62.30	652.30	355
360	0.6209	4.203	1.983	324	11.49	674	23.70	2.02	0.960	61.40	697.90	360
365	0.7514	4.209	1.999	306	11.69	677	24.10	1.91	0.969	60.5	707.10	365
370	0.9040	4.214	2.017	289	11.89	679	24.50	1.80	0.978	59.50	728.70	370
375	1.0815	4.217	2.029	279	12.02	680	24.80	1.76	0.984	58.90	750.10	375
380	1.2869	4.220	2.036	274	12.09	681	24.90	1.70	0.987	58.60	761.00	380
385	1.5233	4.226	2.057	260	12.29	683	25.40	1.61	0.999	57.60	788.00	385
390	1.794	4.232	2.080	248	12.49	685	25.80	1.53	1.004	56.60	814.00	390
400	2.455	4.239	2.104	237	12.69	686	26.30	1.47	1.013	55.60	841.00	400
410	3.302	4.256	2.158	217	13.05	688	27.20	1.34	1.033	53.60	896.00	410
420	4.370	4.278	2.221	200	13.42	688	28.20	1.24	1.054	51.50	952.00	420
430	5.699	4.302	2.291	185	13.79	688	29.80	1.16	1.075	49.40	1010.0	430
440	7.333	4.331	2.369	173	14.14	685	30.40	1.09	1.100	47.20		440
450	9.319	4.360	2.46	162	14.50	682	31.70	1.04	1.12	45.1		450
		4.400	2.56	152	14.85	678	33.10	0.99	1.14	42.90		450

Example, at 290 C, $\mu_f = 1080\text{E-6 N·s/m}^2$ and $k_f = 598\text{E-3 W/m·K}$.

Table A.IV.5(SI). Physical Properties of Saturated Water and Saturated Steam (continued)

T	P	$c_{p,f}$	$c_{p,g}$	μ_f	μ_g	k_f	k_g	Pr_f	Pr_g	σ_f	β_f	T
(K)	(bars)	(kJ/kg·K)		E6 (N·s/m ²)		E3 (W/m·K)		(-)		E3 (N/m)	E6 (K ⁻¹)	(K)
460	11.71	4.440	2.68	143	15.19	673	34.60	0.95	1.17	40.70		460
470	14.55	4.480	2.79	136	15.54	667	36.3	0.92	1.20	38.50		470
480	17.90	4.530	2.94	129	15.88	660	38.10	0.89	1.23	36.20		480
490	21.83	4.590	3.10	124	16.23	651	40.10	0.87	1.25	33.90		490
500	26.40	4.660	3.27	118	16.59	642	42.30	0.86	1.28	31.60		500
510	31.65	4.740	3.47	113	16.95	631	44.70	0.85	1.31	29.30		510
520	37.70	4.840	3.70	108	17.33	621	47.50	0.84	1.35	26.90		520
530	44.58	4.950	3.96	104	17.72	608	50.60	0.85	1.39	24.50		530
540	52.38	5.080	4.27	101	18.10	594	54.00	0.86	1.43	22.10		540
550	61.19	5.240	4.64	97	18.60	580	58.30	0.87	1.47	19.70		550
560	71.08	5.430	5.09	94	19.10	563	63.70	0.90	1.52	17.30		560
570	82.16	5.680	5.67	91	19.70	548	16.70	0.94	1.59	15.00		570
580	94.51	6.000	6.40	88	20.40	528	76.70	0.99	1.68	12.80		580
590	108.3	6.410	7.35	84	21.50	513	84.10	1.05	1.84	10.50		590
600	123.5	7.000	8.75	81	22.70	497	92.90	1.14	2.15	8.40		600
610	137.3	7.850	11.10	77	24.10	467	103.0	1.30	2.60	6.30		610
620	159.1	9.350	15.40	72	25.90	444	114.0	1.52	3.46	4.50		620
625	169.1	10.60	18.30	70	27.00	430	121.0	1.65	4.20	3.50		625
630	179.7	12.60	22.10	67	28.00	412	130.0	2.00	4.80	2.60		630
635	190.9	16.40	27.60	64	30.00	392	141.0	2.70	6.00	1.50		635
640	202.7	26.00	42.00	59	32.00	367	155.0	4.20	9.60	0.80		640
645	215.2	90.00	-	54	37.00	331	178.0	12.0	26.0	0.10		645
647.3	221.2	∞	∞	45	45.00	238	238.0	∞	∞	0.00		647.3

Example, at 600 C, $\mu_f = 81\text{E-6 N·s/m}^2$ and $k_g = 497\text{E-3 W/m·K}$.

See reference for this table.

Table A.IV.6(SI). Thermophysical Properties of Liquid Metals

Description/ Composition	Melting Point (K)	T (K)	ρ (kg/m ³)	c_p (kJ/kg·K)	$\nu \times 10^7$ (m ² /s)	k (W/m·K)	$\alpha \times 10^5$ (m ² /s)	Pr	Boiling Point (K)
Bismuth	544	589	10,011	0.1444	1.617	16.4	0.138	0.0142	
		811	9,739.	0.1545	1.133	15.6	1.035	0.0110	
		1033	9,467.	0.1645	0.8343	15.6	1.001	0.0083	
Lead	600	644	10,540	0.159	2.276	16.1	0.960	0.024	2020
		755	10,410	0.155	1.849	15.6	0.967	0.017	
		800	10,350	0.155	1.660	19.0	1.184	0.014	
		900	10,230	0.155	1.460	20.4	1.286	0.011	
		977	10,140	0.155	1.347	14.9	0.948	---	
Lithium	453	500	505.0	4.190	10.75	46.1	2.178	0.049	1613
		600	499.0	4.190	9.050	46.6	2.228	0.041	
		700	488.0	4.190	7.900	47.1	2.303	0.034	
		800	471.0	4.190	7.200	47.6	2.412	0.030	
		900	442.0	4.190	6.750	48.1	2.597	0.026	
Mercury	234	300	13,530	0.140	1.100	8.40	0.443	0.025	630
		400	13,280	0.140	0.850	9.80	0.527	0.016	
		500	13,040	0.140	0.750	11.0	0.603	0.012	
		600	12,780	0.140	0.650	12.1	0.676	0.010	
Potassium	337	400	814.0	0.800	6.000	45.5	6.98	0.0086	1049
		422	807.3	0.800	4.608	45.0	6.97	0.0066	
		500	790.0	0.790	3.500	43.6	6.89	0.0050	
		600	765.0	0.780	2.800	41.6	6.97	0.0040	
		700	741.0	0.770	2.500	39.5	6.92	0.0036	
		800	741.7	0.750	2.397	39.5	7.10	0.0034	
		900	692.0	0.740	2.100	34.4	6.72	0.0031	
		977	674.4	0.740	1.905	33.1	6.55	0.0029	
Sodium	371	366	929.1	1.380	7.516	86.2	6.71	0.0110	1156
		500	900.0	1.335	4.700	79.2	6.59	0.0071	
		600	868.0	1.310	3.600	74.7	6.57	0.0055	
		644	860.2	1.300	3.270	72.3	6.47	0.0051	
		700	840.0	1.280	3.000	70.1	6.52	0.0046	
		800	813.0	1.260	2.700	65.7	6.41	0.0042	
		900	792.0	1.255	2.500	62.1	6.25	0.0040	
		977	778.5	1.255	2.285	59.7	6.12	0.0037	
		1000	772.0	1.255	2.300	59.3	6.12	0.0038	
		1100	753.0	1.255	2.100	56.7	5.99	0.0035	
NaK, (45%/55%)	292	366	887.4	1.130	6.522	25.6	2.55	0.026	
		644	821.7	1.055	2.871	27.5	3.17	0.0091	
		977	740.1	1.043	2.174	28.9	3.74	0.0058	
NaK, (22%/78%)	262	366	849.0	0.946	5.797	24.4	3.05	0.019	
		672	775.3	0.879	2.666	26.7	3.92	0.0068	
		1033	690.4	0.883	2.118	---	---	---	
PbBi, (44.5%/55.5%)	398	422	10,524	0.147	---	9.05	0.586	---	
		644	10,236	0.147	1.496	11.86	0.790	0.189	
		922	9,835	---	1.171	---	---	---	

See reference for this table.

Table A.IV.4(BU). Thermophysical Properties of Gases at Atmospheric Pressure

	T (F)	ρ (lbm/ft ³)	c_p (Btu/lbm-F)	$\mu \times E5$ (lbm/ft-s)	$\nu \times E3$ (ft ² /s)	k (Btu/h-ft-F)	Pr	α (ft ² /h)	$\beta \times E3$ (1/F)	$g\beta\rho^2\mu^2$ (1/ft ³ -F)
Air	0	0.086	0.239	1.110	0.130	0.0133	0.73	0.646	2.18	4.2E6
	32	0.081	0.240	1.165	0.145	0.0140	0.72	0.720	2.03	3.16
	100	0.071	0.240	1.285	0.180	0.0154	0.72	0.905	1.79	1.76
	200	0.060	0.241	1.440	0.239	0.0174	0.72	1.20	1.52	0.850
	300	0.052	0.243	1.610	0.306	0.0193	0.71	1.53	1.32	0.444
	400	0.046	0.245	1.750	0.378	0.0212	0.689	1.88	1.16	0.258
	500	0.0412	0.247	1.890	0.455	0.0231	0.683	2.27	1.04	0.159
	600	0.0373	0.250	2.000	0.540	0.0250	0.685	2.68	0.943	0.106
	700	0.0341	0.253	2.14	0.625	0.0268	0.690	3.10	0.862	70.4E6
	800	0.0314	0.256	2.25	0.717	0.0286	0.697	3.56	0.794	49.8
	900	0.0291	0.259	2.36	0.815	0.0303	0.705	4.02	0.735	36.0
	1000	0.0271	0.262	2.47	0.917	0.0319	0.713	4.50	0.685	26.5
	1500	0.0202	0.276	3.00	1.47	0.0400	0.739	7.19	0.510	7.45
Steam	212	0.0372	0.451	0.870	0.234	0.0145	0.96	0.864	1.49	0.88E6
	300	0.0328	0.456	1.000	0.303	0.0171	0.95	1.14	1.32	0.459
	400	0.0288	0.462	1.130	0.395	0.0200	0.94	1.50	1.16	(.243)
	500	0.0258	0.470	1.265	0.490	0.0228	0.94	1.88	1.04	0.139
	600	0.0233	0.477	1.420	0.610	0.0257	0.94	2.31	0.943	82E3
	700	0.0213	0.485	1.555	0.725	0.0288	0.93	2.79	0.862	52.1
	800	0.0196	0.494	1.700	0.855	0.0321	0.92	3.32	0.794	34.0
	900	0.0181	0.50	1.810	0.987	0.0355	0.91	3.93	0.735	23.6
	1000	0.0169	0.51	1.920	1.13	0.0388	0.91	4.50	0.685	17.1
	1200	0.0149	0.53	2.14	1.44	0.0457	0.88	5.80	0.603	9.4
	1400	0.0133	0.55	2.36	1.78	0.053	0.87	7.25	0.537	5.49
	1600	0.0120	0.56	2.58	2.14	0.061	0.87	9.07	0.485	3.38
	1800	0.0109	0.58	2.81	2.58	0.068	0.87	10.8	0.442	2.14
Oxygen	2000	0.0100	0.60	3.03	3.03	0.076	0.86	12.7	0.406	1.43
	2500	0.0083	0.64	3.58	4.30	0.096	0.86	18.1	0.338	0.603
	3000	0.0071	0.67	4.00	5.75	0.114	0.86	24.0	0.289	0.293
	0	0.0955	0.2185	1.215	0.127	0.0131	0.73	0.627	2.18	4.33E6
	100	0.0785	0.2200	1.420	0.181	0.0159	0.71	0.880	1.79	1.76
	200	0.0666	0.2228	1.610	0.242	0.0179	0.722	1.20	1.52	0.84
	400	0.0511	0.2305	1.955	0.382	0.0228	0.710	1.94	1.16	0.256
	600	0.0415	0.2390	2.26	0.545	0.0277	0.704	2.79	0.943	0.103
	800	0.0349	0.2465	2.53	0.725	0.0324	0.695	3.76	0.794	48.5E3
	1000	0.0301	0.2528	2.78	0.924	0.0366	0.690	4.80	0.685	25.8
	1500	0.0224	0.2635	3.32	1.480	0.0465	0.677	7.88	0.510	7.50

Table A.IV.4(BU). Thermophysical Properties of Gases at Atmospheric Pressure (continued)

	T F	ρ lbm/ft ³	c_p Btu/lbm·F	$\mu \times E5$ lbm/ft·s	$\nu \times E3$ ft ² /s	k Btu/h·ft·F	Pr	α ft ² /h	$\beta \times E$ 1/F	$g\beta\rho^2/\mu^2$ 1/ft ³ ·F
Nitrogen	0	0.0840	0.2478	1.055	0.125	0.0132	0.713	0.635	0.635	4.55E6
	100	0.0690	0.2484	1.222	0.177	0.0154	0.71	0.898	1.79	1.84
	200	0.0585	0.2490	1.380	0.236	0.0174	0.71	1.20	1.52	0.876
	400	0.0449	0.2515	1.660	0.370	0.0212	0.71	1.88	1.16	0.272
	600	0.0304	0.2564	1.915	0.526	0.0252	0.70	2.70	0.943	0.110
	800	0.0306	0.2623	2.145	0.702	0.0291	0.70	3.62	0.794	52.0E3
	1000	0.0264	0.2689	2.355	0.891	0.0330	0.69	4.65	0.685	27.70
	1500	0.0197	0.2835	2.800	1.420	0.0423	0.676	7.58	0.510	8.120
Carbon Monoxide	0	0.835	0.2482	1.065	0.128	0.0129	0.75	0.621	2.18	4.32E6
	200	0.0572	0.2496	1.390	0.239	0.0169	0.74	1.16	1.52	0.860
	400	0.0446	0.2532	1.670	0.374	0.0208	0.73	1.84	1.16	0.268
	600	0.0362	0.2592	1.910	0.527	0.0246	0.725	2.62	0.943	0.109
	800	0.0305	0.2662	2.134	0.700	0.0285	0.72	3.50	0.794	52.1E3
	1000	0.0263	0.2730	2.336	0.887	0.0322	0.71	4.50	0.685	28.0
	1500	0.0196	0.2878	2.783	1.420	0.0414	0.70	7.33	0.510	8.13
Helium	0	0.012	1.24	1.140	0.950	0.078	0.67	5.25	2.18	77800
	200	0.00835	1.24	1.480	1.77	0.097	0.686	9.36	1.52	15600
	400	0.0064	1.24	1.780	2.78	0.115	0.70	14.5	1.16	4840
	600	0.0052	1.24	2.02	3.89	0.129	0.715	20.0	0.943	2010
	800	0.00436	1.24	2.285	5.24	0.138	0.73	25.5	0.794	932
	1000	0.00377	1.24	2.520	6.69				0.685	494
	1500	0.0028	1.24	3.160	11.30				0.510	129
H ₂	0	0.0060	3.39	0.540	0.89	0.094	0.70	4.62	2.18	86600
	100	0.0049	3.42	0.620	1.26	0.110	0.695	6.56	1.79	36600
	200	0.0042	3.44	0.692	1.65	0.122	0.69	8.45	1.52	18000
	500	0.0028	3.47	0.884	3.12	0.160	0.69	16.5	1.04	3360
	1000	0.0019	3.51	1.160	6.2	0.208	0.705	31.2	0.685	591
	1500	0.0014	3.62	1.415	10.2	0.260	0.71	51.4	0.510	161
	2000	0.0011	3.76	1.64	14.4	0.307	0.72	74.2	0.406	59
	3000	0.0008	4.02	1.72	24.2	0.380	0.66	118.0	0.289	20
Carbon Dioxide	0	0.132	0.184	0.88	0.067	0.0076	0.77	0.313	2.18	15.8E6
	100	0.108	0.203	1.05	0.098	0.0100	0.77	0.455	1.79	6.10
	200	0.092	0.216	1.22	0.133	0.0125	0.76	0.63	1.52	2.78
	500	0.063	0.247	1.67	0.266	0.0198	0.75	1.27	1.04	0.476
	1000	0.0414	0.280	2.30	0.558	0.0318	0.73	2.75	0.685	71.4E3
	1500	0.0308	0.298	2.86	0.925	0.0420	0.73	4.58	0.510	19.0
	2000	0.0247	0.309	3.30	1.34	0.050	0.735	6.55	0.406	7.34
	3000	0.0175	0.322	3.92	2.25	0.061	0.745	10.8	0.289	1.85

See the reference for this table.

Table A.IV.5(BU). Thermophysical Properties of Saturated Water

T (F)	k (Btu/h·ft·F)	ρ (lbm/ft ³)	c_p (Btu/lbm·F)	$\mu \times 10^7$ (lbf·s/ft ²)	$\nu \times 10^5$ (ft ² /s)	Pr
32	0.319	62.400	1.009	374.000	1.930	13.350
40	0.325	62.400	1.005	324.000	1.670	11.350
50	0.332	62.400	1.002	274.000	1.410	9.400
60	0.340	62.300	1.000	234.000	1.210	7.880
70	0.347	62.300	0.998	205.000	1.057	6.780
80	0.353	62.200	0.998	180.000	0.930	5.850
90	0.359	62.100	0.997	160.000	0.828	5.120
100	0.364	62.000	0.997	143.000	0.741	4.530
120	0.372	61.700	0.997	118.000	0.615	3.640
140	0.378	61.400	0.998	98.000	0.513	3.010
160	0.384	61.000	1.000	84.000	0.442	2.530
180	0.389	60.600	1.002	73.000	0.388	2.160
200	0.392	60.100	1.004	64.000	0.342	1.900
250	0.396	58.800	1.012	48.000	0.262	1.430
300	0.395	57.300	1.026	39.000	0.219	1.170
400	0.381	53.700	1.067	29.000	0.174	1.000
600	0.292	49.000	1.362	18.000	0.118	1.000

See the reference for this table.

Table A.IV.6(BU). Thermophysical Properties of Saturated Steam

T (F)	k (Btu/h·ft·F)	ρ (lbm/ft ³)	c_p (Btu/lbm·F)	$\mu \times 10^7$ (lbf·s/ft ²)	$\nu \times 10^5$ (ft ² /s)	Pr
32.00	0.0105	0.00030	0.449	1.68	1784.00	0.81
40.00	0.0107	0.00041	0.443	1.71	1348.00	0.82
50.00	0.0109	0.00059	0.444	1.76	965.00	0.83
60.00	0.0110	0.00083	0.441	1.80	702.00	0.84
70.00	0.0112	0.00115	0.442	1.85	517.00	0.85
80.00	0.0114	0.00158	0.443	1.90	387.00	0.86
90.00	0.0116	0.00214	0.445	1.94	293.00	0.87
100.00	0.0118	0.00285	0.449	1.99	225.00	0.88
120.00	0.0122	0.00492	0.451	2.08	136.5	0.89
140.00	0.0127	0.00813	0.459	2.18	86.2	0.91
160.00	0.0131	0.01290	0.464	2.27	56.6	0.93
180.00	0.0135	0.01990	0.467	2.36	38.3	0.95
200.00	0.0140	0.02980	0.479	2.45	26.5	0.97
212.00	0.0143	0.03730	0.482	2.51	21.7	0.98

See the reference for this table.

Table A.IV.7(BU). Thermophysical Properties of Superheated Steam at Atmospheric Pressure

T (F)	k (Btu/h·ft·F)	ρ (lbm/ft ³)	c_p (Btu/lbm·F)	$\mu \times 10^7$ (lb·s/ft ²)	$\nu \times 10^5$ (ft ² /s)	Pr
212.00	0.0145	0.0372	0.451	2.700	23.40	0.96
300.00	0.0171	0.0328	0.456	3.110	30.30	0.95
400.00	0.0200	0.0288	0.462	3.510	39.50	0.94
500.00	0.0228	0.0258	0.470	3.930	49.00	0.94
600.00	0.0257	0.0233	0.477	4.410	61.00	0.94
700.00	0.0288	0.0213	0.485	4.830	72.50	0.93
800.00	0.0321	0.0196	0.494	5.280	85.50	0.92
900.00	0.0355	0.0181	0.500	5.620	98.70	0.91
1000.00	0.0388	0.0169	0.510	5.960	113.00	0.91
1200.00	0.0457	0.0149	0.530	6.650	144.00	0.88
1400.00	0.0530	0.0133	0.550	7.340	178.00	0.87
1600.00	0.0610	0.0120	0.560	8.020	214.00	0.87
1800.00	0.0680	0.0109	0.580	8.730	258.00	0.87
2000.00	0.0760	0.0100	0.600	9.410	303.00	0.86
2500.00	0.0960	0.0083	0.640	11.12	430.00	0.86
3000.00	0.1140	0.0071	0.670	12.42	575.00	0.86

See the reference for this table.

Table A.IV.8. Thermal Properties of Solid Dielectrics at Normal Temperature

Selected Materials	k		ρ		c_p	
	W/m·K	Btu/hr·ft·F	kg/m ³	lb/ft ³	J/kg·K	Btu/lbm·F
Aluminum oxide (sapphire)	36	21	3700	231	800	0.19
Beryllium oxide, pressed	216	125	2960	185	1050	0.25
Brick, common	0.69	0.40	1600	100	840	0.20
Carbon (ATJ-S graphite) (300 K/540 R)	98	57	1810	113	1300	0.31
(1000 K/1800 R)	55	32	1810	113	1926	0.46
(2000 K/3600 R)	38	22	1810	113	2135	0.51
(3000K/5400 R)	33	19	1810	113	2180	0.52
Chrome brick (2000C/2930F)	1.42	0.82	3940	246	840	0.20
(1000 C/1832 F)	1.66	0.96				
Concrete	1.13	0.65	2240	140	880	0.21
Earth, dry	0.52	0.30	2050	128	1840	0.44
wet	2.60	1.50	2400	150	2180	0.52
Glass, borosilicate (pyrex):	1.09	0.63	2640	165	800	0.19
flint, 0.45 PbO, 0.10 misc.	0.76	0.44	2710	169	840	0.20
Silica (fused quartz)	1.35	0.78	2640	165	800	0.19
Soda-lime, 0.125 Na2O, 0.10 CaO	0.88	0.51	2400	150	840	0.20
Ice (0 C/32 F)	2.22	1.28	910	57	1930	0.46
Insulations:						
Asbestos	0.160	0.090	580	36	1050	0.25
Cork	0.043	0.025	160	10	1680	0.40
Diatomaceous earth (380C/100 F)	0.052	0.030	224	14	880	0.21
(316 C/600 F)	0.080	0.046				
Fiberglass (38 C/1000 F)	0.054	0.031	24	1.50	800	0.19
(93 C/200 F)	0.074	0.043				
Polystyrene foam	0.035	0.020	40	2.50	1130	0.27
Magnesium oxide, crystal	61	35	3570	223	920	0.22
Paper	0.130	0.075	930	58	2500	0.60
Plastics:						
Acrylic	0.210	0.120	1185	74	1470	0.35
Cellulose acetate	0.240	0.140	1300	81	1510	0.36
Neoprene rubber	0.190	0.110	1250	78	1930	0.46
Phenolic, filled	0.500	0.290	1760	110	1260	0.30
Polyamide (nylon)	0.240	0.140	1140	71	1670	0.40
Polyethylene (high density)	0.330	0.190	960	60	2090	0.50
Polypropylene	0.170	0.100	910	57	1930	0.46
Polystyrene	0.130	0.074	1170	73	1340	0.32
Polytetrafluoroethylene	0.240	0.140	2190	137	1050	0.25
Polyvinylchloride	0.092	0.053	1714	107	1050	0.25
Silicon dioxide (crystalline quartz)	6.200	3.600	2640	165	750	0.18

Table A.IV.8. Thermal Properties of Solid Dielectrics at Normal Temperature (continued)

Selected Materials	k		ρ		c_p	
	W/m·K	Btu/hr·ft·F	kg/m ³	lb/ft ³	J/kg·K	Btu/lb·F
Uranium oxide (20 C/68 F)	8.000	4.600	10,890	680	234	0.056
(80 C/1472 F)	3.600	2.100			310	0.074
(1600 C/2912 F)	2.300	1.300			350	0.083
(2400 C/4352 F)	2.900	1.700			450	0.108
Wood						
Oak, perpendicular to grain	0.210	0.120	820	51	2400	0.570
parallel to grain	0.350	0.200				
White pine, perpendicular to grain	0.100	0.060	500	31	2800	0.67
parallel to grain	0.240	0.140				
Zirconia brick (200 C/392 F)	1.450	0.840	4870	304	540	0.13
(1000 C/1832 F)	1.960	1.130				

1: See Table A.IV.2(SI).

See the reference for this table.

Table A.IV.9. Normal, Total Emissivity of Metallic Surfaces

Material	Temp. (K)	Temp. (F)	Emissivity
Aluminum			
Polished	300 - 900	80 - 1160	0.04 - 0.06
Rough plate	310	99	0.07
Commercial sheet	400	260	0.09
Heavily oxidized	400 - 800	260 - 980	0.20 - 0.33
Anodized	300 - 400	80 - 260	0.82 - 0.76
Antimony, polished	310 - 530	99 - 495	0.28 - 0.31
Brass			
Highly polished	500 - 650	440 - 710	0.03 - 0.04
Polished	350	170	0.09
Dull plate	300 - 600	80 - 620	0.22
Oxidized	450 - 800	350 - 980	0.66
Chromium, polished	300 - 1400	80 - 2060	0.08—0.27
Cobalt, unoxidized	530 - 810	495 - 998	0.13—0.23
Copper			
Highly polished	300	80	0.02
Polished	300 - 500	80 - 440	0.04 - 0.05
Commercial sheet	300	80	0.15
Oxidized	600 - 1000	620 - 1340	0.5 - 0.8
Gold, highly polished	300 - 1000	80 - 1340	0.03 - 0.06
Inconel			
X, stably oxidized	500 - 1145	440 - 1600	0.55 - 0.78
B, stably oxidized	500 - 1225	440 - 1745	0.32 - 0.55
X and B, polished	420-590	296 - 600	0.20
Iron			
Pure polished	366	200	0.06
Bright etched	423	300	0.13
Bright abraded	293	68	0.24
Red rusted	293	68	0.61
Hot rolled	293	68	0.77
Hot rolled	400	260	0.60
Heavily crusted	293	68	0.85
Heat-resistant oxidized	353	176	0.61
Heat-resistant oxidized	473	392	0.64
Cast iron, bright	366	200	0.21
Cast iron, oxidized	366	200	0.61
Black iron oxide	366	200	0.56
Wrought iron (polished)	400	260	0.28
Lead			
Polished	310 - 530	99 - 495	0.05 - 0.08
Gray, oxidized	310	99	0.28
Oxidized at 865 K	310	99	0.63
Magnesium (polished)	310 - 530	99 - 495	0.07 - 0.13
Mercury, pure and clean	310 - 365	99 - 198	0.10 - 0.12

Table A.IV.9. Normal, Total Emissivity of Metallic Surfaces (continued)

Material	Temp. (K)	Temp. (F)	Emissivity
Molybdenum			
Polished	310 - 530	99 - 495	0.06 - 0.08
Polished	810 - 1365	966 - 1998	0.11 - 0.18
Filament	810 - 3030	966 - 4995	0.08 - 0.29
Monel			
Repeated heating & cooling	505 - 1170	450 - 1647	0.45 - 0.70
Oxidized at 866 K	475 - 865	395 - 1098	0.41 - 0.46
Polished	310	99	0.17
Nickel			
Polished	500 - 1200	440 - 1700	0.07 - 0.17
Oxidized	450—1000	350 - 1340	0.37 - 0.57
Wire	530—1365	495 - 1998	0.10 - 0.19
Platinum			
Electrolytic	530 - 810	495 - 998	0.06 - 0.10
Filament	310 - 1365	99 - 1998	0.04 - 0.19
Oxidized at 865 K	530 - 810	495 - 998	0.07 - 0.11
Polished	500 - 1500	440 - 2240	0.06 - 0.18
Strip	810 - 1360	1000 - 1988	0.12 - 0.14
Wire	475 - 1645	395 - 2500	0.07 - 0.18
Silver			
Polished or deposited	310 - 810	99 - 1000	0.01 - 0.03
Oxidized	310 - 810	99 - 1000	0.02 - 0.04
Stainless Steel			
Polished	300 - 1000	80 - 1340	0.17 - 0.30
Lightly oxidized	600 - 1000	620 - 1340	0.30 - 0.40
Highly oxidized	600 - 1000	620 - 1340	0.70 - 0.80
Steel			
Commercial sheet	500-1200	440 - 1700	0.20 - 0.32
Heavily oxidized	300	80	0.81
Mild, polished	420 - 755	300 - 900	0.14 - 0.32
Polished	310 - 530	99 - 495	0.07 - 0.10
Sheet, ground	1200	1700	0.55
Sheet, rolled	310	99	0.66
Tin, bright	310 - 360	99 - 188	0.04-0.06
Tungsten			
Polished	300 - 2500	80 - 4040	0.03 - 0.29
Filament	810 - 1365	966 - 1998	0.11 - 0.16
Filament	3500	5840	0.39
Zinc			
Pure, polished	310 - 530	99 - 495	0.02 - 0.03
Oxidized at 1200 K	1200	1700	0.11
Galvanized, gray	310	99	0.28
Galvanized, fairly bright	310	99	0.23
Dull	310 - 530	99 - 495	0.21

See the reference for this table.

Table A.IV.10. Normal, Total Emissivity of Non-Metallic Surfaces

Material	Temp. (K)	Temp. (F)	Emissivity
Aluminum oxide	600 - 1500	620 - 2240	0.69 - 0.41
Asbestos	300	80	0.96
Brick			
Common	300	80	0.95
Fireclay	1200	1700	0.75
Ordinary, refractory	1350	1970	0.59
White, refractory	1350	1970	0.29
Carbon			
Filament	2000	3140	0.53
Lampsoot	310	99	0.95
Clay, fired	365	198	0.91
Cloth	300	80	0.80
Concrete, rough	300	80	0.94
Glass, window	300	80	0.93
Glass, pyrex	300 - 1200	80 - 1700	0.82 - 0.62
Glass, pyroceram	300 - 1500	80 - 2240	0.85 - 0.57
Gypsum	310	99	0.80 - 0.90
Ice	273	32	0.97
Limestone	500 - 700	440	0.95 - 0.83
Magnesium oxide	400 - 800	260 - 1000	0.69 - 0.55
Marble	300	80	0.94
Masonry	300	80	0.80
Mica	310	99	0.75
Mortar, lime			0.92
Paints			
Aluminum	300	80	0.45
Black, lacquer, shiny	300	80	0.88
Enamel	293	68	0.85 - 0.95
Lacquer white	273	32	0.93
Lampblack	325	125	0.94
Lacquer black matte	353	500	0.97
Oils, all colors	300	80	0.94
White, acrylic	300	80	0.90
Red primer	300	80	0.93
Varnish, dark glossy	311	100	0.89
Paper, white	300	80	0.95 - 0.98
Paper, other colors	300	80	0.92 - 0.94
Paper, roofing	300	80	0.91
Plaster, white	300	80	0.93
Porcelain, glazed	300	80	0.93
Quartz, rough, fused	300	80	0.93

Table A.IV.10. Normal, Total Emissivity of Non-Metallic Surfaces (continued)

Material	Temp. (K)	Temp. (F)	Emissivity
Rubber, soft	300	80	0.86
Rubber, hard	300	80	0.93
Sand	300	80	0.90
Silicon carbide	600 - 1500	620 - 2240	0.86
Skin, human	300	80	0.95
Snow	273	32	0.85
Soil, earth	300	80	0.95
Soot	300 - 500	80 - 440	0.95
Teflon	300 - 500	80 - 440	0.85 - 0.92
Water (thickness > 0.1 mm)	273 - 373	32 - 212	0.95
Wood, beech	300	80	0.94
Wood, oak	300	80	0.90

See the reference for this table.

Appendix V

Nuclear Properties of Elements

Table A.V.1(SI). Absorption Coefficient of Gamma Rays	1092
Table A.V.2(SI). Cross Sections for Neutron Interaction	1093

Table A.V.1(SI). Absorption Coefficients of Gamma Rays for Shielding Materials

Material	ρ (g/cm ³)	μ (1/cm)		
		1 MeV	3 MeV	6 MeV
Air	0.0012940	0.0000766	0.0000430	0.0000304
Aluminum.....	2.700	0.166	0.0953	0.0718
Ammonia(liquid).....	0.771	0.061	0.0322	0.0221
Beryllium.....	1.850	0.104	0.0579	0.0392
Beryllium carbide.....	1.900	0.112	0.0627	0.0429
Beryllium oxide (hot-pressed blocks).....	2.300	0.140	0.0789	0.0552
Bismuth.....	9.800	0.700	0.4090	0.4400
Boral.....	2.530	0.153	0.0865	0.0678
Boron (amorphous).....	2.450	0.144	0.7910	0.0679
Boron carbide (hot-pressed).....	2.500	0.150	0.0825	0.0675
Bricks:				
Fire clay.....	2.050	0.129	0.0738	0.0543
Kaolin.....	2.100	0.132	0.0750	0.0552
Silica.....	1.780	0.113	0.0646	0.0473
Carbon.....	2.250	0.143	0.0801	0.0554
Clay.....	2.200	0.130	0.0801	0.0590
Cements:				
Colemanite borated.....	1.950	0.128	0.0725	0.0528
Plain*.....	2.070	0.133	0.0760	0.0559
Concretes:				
Barytes.....	3.50	0.2130	0.1270	0.1100
Barytes-boron frits.....	3.25	0.1990	0.1190	0.1010
Barytes-limonite.....	3.25	0.2000	0.1190	0.0991
Barytes-lumite-colemanite.....	3.10	0.1890	0.1120	0.0939
Iron-portland.....	6.00	0.3640	0.2150	0.1810
MO (ORNL mixture).....	5.80	0.3740	0.2220	0.1840
Portland (1 cement:	2.20	0.1410	0.0805	0.0592
2 sand: 4 gravel mixture).....	2.40	0.1540	0.0878	0.0646
Flesh.....	1	0.0699	0.0393	0.0274
Fuel oil (medium weight).....	0.89	0.0716	0.0350	0.0239
Gasoline.....	0.738	0.0537	0.0299	0.0203
Glass:				
Borosilicate.....	2.23	0.1410	0.0805	0.0591
Lead (Hi-D).....	6.40	0.4390	0.2570	0.2570
Plate (av.).....	2.40	0.1520	0.0862	0.0629
Iron.....	7.86	0.4700	0.2820	0.2400
Lead.....	1.34	0.7970	0.4680	0.5050
Lithium hydride (pressed powder).....	0.70	0.0444	0.0239	0.0172
Lucite (polymethyl methacrylate).....	1.19	0.0816	0.0457	0.0317
Paraffin.....	80	0.0646	0.0360	0.0246
Rocks:				
Granite.....	2.45	0.5500	0.0887	0.0654
Limestone.....	2.91	0.1870	0.1090	0.0824
Sandstone.....	2.40	0.1520	0.0871	0.0641
Rubber:				
Butenediene copolymer.....	0.915	0.0662	0.0370	0.0254
Natural.....	0.92	0.0652	0.0364	0.0248
Neoprene.....	1.23	0.0813	0.0462	0.0333
Sand.....	2.20	0.1400	0.0825	0.0587
Stainless steel, Type 347.....	7.80	0.4620	0.2790	0.2360
Steel (1% carbon).....	7.83	0.4600	0.2760	0.2340

Table A.V.1(SI). Absorption Coefficients of Gamma Rays for Shielding Materials (continued)

Uranium.....	18.70	1.4600	0.8130	0.8810
Uranium hydride.....	115	0.9030	0.5040	0.5420
Water.....	1.00	0.0706	0.0396	0.0277
Wood:				
Ash.....	0.51	0.0345	0.0193	0.0134
Oak.....	0.77	0.0521	0.0293	0.0203
White pine.....	0.67	0.0452	0.0253	0.0175

* 1 Portland cement: 3 sand mixture

Table A.V.2(SI). Cross Sections for Neutron Interaction

Substance	Symbol	Z	M	ρ (g/cm ³)	N (1/cm ³)	σ_a (b)	σ_s (b)	Σ_a (cm ⁻¹)	Σ_s (cm ⁻¹)
Actinium	Ac	89	227			800			
Aluminum	Al	13	26.9815	2.699	0.06024	0.235	1.40	0.0142	0.0843
Antimony	Sb	51	121.750	6.62	0.03275	5.50	4.30	0.1801	0.1408
Argon	Ar	18	39.948	Gas		0.63	1.50		
Arsenic	As	33	74.922	5.73	0.04606	4.50	6	0.2073	0.2764
Barium	Ba	56	137.340	3.50	0.01535	1.20	8	0.0184	0.1228
Beryllium	Be	4	9.012	1.85	0.1236	0.00950	7.00	0.0012	0.8652
Beryllium oxide	BeO		25.012	2.96	0.07127	0.00950	6.80	0.0007	0.4846
Bismuth	Bi	83	208.980	9.80	0.0282	0.034	9	0.0010	0.2542
Boron	B	5	10.811	2.30	0.1281	759	4	97.23	0.5124
Bromine	Br	35	79.909	3.12	0.02351	6.70	6	0.1575	0.1411
Cadmium	Cd	48	112.400	8.65	0.04635	2450	7	113.60	0.3245
Calcium	Ca	20	40.080	1.55	0.02329	0.43	3.00	0.0100	0.0699
Carbon (graphite)	C	6	12.0112	1.60	0.08023	0.0034	4.80	0.0003	0.3851
Cerium	Ce	58	140.120	6.78	0.02914	0.70	9	0.0204	0.2623
Cesium	Cs	55	132.905	1.90	0.00861	30	20	0.2583	0.1722
Chlorine	Cl	17	35.453	Gas		33	16		
Chromium	Cr	24	51.996	7.19	0.08328	3.10	3	0.2582	0.2498
Cobalt	Co	27	58.933	8.80	0.08993	37	7	3.3270	0.6295
Copper	Cu	29	63.540	8.96	0.08493	3.80	7.20	0.3227	0.6115
Deuterium	D	1	2.0141	Gas		0.0005			
Dysprosium	Dy	66	162.5	8.56	0.03172	940	100	29.82	3.1720
Erbium	Er	68	167.260	9.16	0.03203	160	15	5.1250	0.4805
Europium	Eu	63	151.960	5.22	0.02069	4300	8	88.97	0.1655
Fluorine	F	9	18.998	Gas		0.0098	3.90		
Gadolinium	Gd	64	157.250	7.95	0.03045	46000	4	1401	0.1218
Gallium	Ga	31	69.720	5.91	0.05105	3.00		0.1532	
Germanium	Ge	32	72.590	5.36	0.04447	2.40	3	0.1067	0.1334
Gold	Au	79	196.967	19.32	0.05907	98.80	9.30	5.8360	0.5494
Hafnium	Hf	72	178.490	13.36	0.04508	105	8	4.7330	0.3606
Heavy water	D ₂ O		29.028	1.105	0.0332	13.60	13.6	3.323E-5	0.4519
Helium	He	2	4.003	Gas		0.0500	0.80		
Holmium	Ho	67	164.930	8.76	0.03199	65		2.0790	
Hydrogen	H	1	1.00797	Gas		0.332	38		
Indium	In	49	114.82	7.31	0.0383	194	2.20	7.438	0.0844
Iodine	I	53	126.904	4.93	0.0234	6.40	3.60	0.1498	0.0824
Iridium	Jr	77	192.22	22.50	0.0705	460		32.43	
Iron	Fe	26	55.847	7.87	0.0849	2.53	11	0.2147	0.9336
Krypton	Kr	36	83.80	Gas		24	7.20		
Lanthanum	La	57	138.91	6.19	0.0268	8.9	15	0.2389	0.4026
Lead	Pb	82	203.973	11.34	0.0335	0.17	11	0.00569	0.3683
Lithium	Li	3	6.939	0.53	0.0460	71	1.40	3.266	0.0644
Lutetium	Lu	71	174.91	9.74	0.0335	80		2.683	
Magnesium	Mg	12	24.312	1.74	0.0431	0.063	4	0.00272	0.1724
Manganese	Mn	25	54.938	7.43	0.0815	13.3	2.30	1.08	0.1873
Mercury	Hg	80	200.59	13.55	0.0407	360	20	14.64	0.8136
Molybdenum	Mo	42	95.94	10.20	0.0640	2.6	7	0.167	0.4482
Neodymium	Nd	60	144.24	6.98	0.0291	50	16	1.457	0.4662
Neon	Ne	10	20.183	Gas		0.032	2.40		

Table A.V.2(SI). Cross Sections for Neutron Interaction (continued)

Substance	Symbol	<i>Z</i>	<i>M</i>	ρ (g/cm ³)	<i>N</i> (1/cm ³)	σ_a (b)	σ_s (b)	Σ_a (cm ⁻¹)	Σ_s (cm ⁻¹)
Nickel	Ni	28	58.71	8.90	0.0913	4.6	17.50	0.420	1.597
Niobium	Nb	41	92.906	8.57	0.0556	1.1	5	0.0611	0.2778
Nitrogen	N	7	14.007	Gas		1.85	10		
Osmium	Os	76	190.20	22.50	0.0712	15	11	1.07	0.7836
Oxygen	O	8	15.999	.	Gas		<0.0002	4.20	
Palladium	Pd	46	106.40	12.00	0.0679	8	3.60	0.543	0.2445
Phosphorus	P	15	30.974	1.82	0.0354	0.19	5	0.00672	0.177
Platinum	Pt	78	195.09	21.45	0.0662	10	10	0.662	0.662
Plutonium	Pu	94	239	19.60	0.0494	1015	1015	9.60	49.88
	Pu					($\sigma_f = 741$)		($\Sigma_f = 36.55$)	
Polonium	Po	84	210	9.51	0.0273				
Potassium	K	19	39.10	0.86	0.0133	2.10	1.50	0.0278	0.0199
Piaseodymium	Pr	59	140.91	6.78	0.0290	12	4	0.197	0.116
Promethium	Pm	61							
Protactinium	Pa	91	231			210			
Radium	Ra	88	226	5.00	0.0133	20		0.266	
Rhenium	Re	75	186.20	20	0.0660	85	14	5.61	0.923
Rhodium	Rh	45	102.91	12.41	0.0726	155	5	11.26	0.363
Rubidium	Rb	37	85.47	1.53	0.0108	0.73	12	0.01	0.129
Ruthenium	Ru	44	101.07	12.20	0.0727	2.50	6	0.182	0.436
Samarium	Sm	62	150.35	6.93	0.0278	5800	5	161.00	0.139
Scandium	Sc	21	44.956	2.50	0.0335	23	24	0.770	0.804
Selenium	Se	34	78.96	4.81	0.0367	12	11	0.440	0.404
Silicon	Si	14	28.09	2.33	0.0500	0.16	1.70	0.116	0.0849
Silver	Ag	47	107.87	10.49	0.0586	63	6	3.69	0.351
Sodium	Na	11	22.990	0.97	0.0254	0.53	4	0.0135	0.102
Strontium	Sr	38	87.62	2.60	0.0179	1.30	10	0.0232	0.179
Sulfur (yellow)	S	16	32.06	2.07	0.0389	0.52	1.10	0.202	0.0428
Tantalum	Ta	73	180.95	16.60	0.0553	21	5	1.16	0.276
Technetium	Tc	43	99			22		0.138	0.147
Tellurium	Te	52	127.60	6.24	0.0295	4.70	5	1.45	
Terbium	Tb	65	158.92	8.33	0.0316	46		0.115	0.489
Thallium	Tl	81	204.37	11.85	0.0349	3.30	14	0.225	0.383
Thorium	Th	90	232.04	11.71	0.0304	7.40	12.60	4.14	0.232
Thulium	Tm	69	168.93	9.35	0.0331	125	7	0.0233	0.148
Tin	Sn	50	118.69	7.30	0.0370	0.63	4	0.346	0.227
Titanium	Ti	22	47.90	4.51	0.0567	6.10	4	1.20	0.315
Tungsten	W	74	183.85	19.20	0.0629	19	5		
Uranium	U	92	238.03	19.1	0.04833	7.6	8.3	0.3673	0.4011
	U					($\sigma_f = 4.2$)		($\Sigma_f = 0.0203$)	
Vanadium	V	23	50.942	6.10	0.0721	4.90	5	0.35340	0.3606
Water	H ₂ O		18.017	1.00	0.0334	0.664	103	0.02220	3.4430
Xenon	Xc	54	131.30	Gas		24	4.3		
Ytterbium	Yb	70	173.04	7.01	0.0244	37	12	0.92080	0.2928
Yttrium	Y	39	88.905	5.51	0.0373	1.30	3	0.04853	0.1120
Zinc	Zn	30	65.37	7.133	0.0657	110	3.60	0.07229	0.2366
Zirconium	Zr	40	91.22	6.50	0.0429	0.18	8	0.00772	0.3433

Z: Atomic number*M*: Atomic or molecular weight

References

Chapter I

- Del Frari, Bernard, "The Global Nuclear Fuel Market, World Nuclear Association Symposium, 2001.
- Dubrovsky, V., "Construction of Nuclear Power Plants," Mir Publishers, Moscow, 1981.
- Gavrilas, Mirela, et. al., "Safety Features of Operating Light Water Reactors of Western Design," CANES, Massachusetts Institute of Technology, 2000.
- Graham, James J., "The Uranium Market with fewer, Better & Faster Sources?," 27th Annual Meeting and International Conference on Nuclear Energy, Goteborg, Sweden, 2000.
- Marion Jerry B. and Marvin L. Roush, "Energy in Perspective," 2nd Edition, Academic Press, 1982.
- Marquand C. and D. Croft, "Thermofluids," John Wiley, 1994.
- Mayo, Robert M., "Introduction to Nuclear Concepts for Engineers," ANS Publications, 1998.
- Ramsey, Charles B. and Mohammad Modarres, "Commercial Nuclear Power," John Wiley, 1998.
- Suryanarayana, N. V. V., "Design and Simulation of Thermal Systems,"
- "US Bureau of the Census," www.census.gov/cgi-bin/ipc/popclockw
 - "Alternative sources of energy," www.altenergy.org
 - "Aviation Turbine Engines," chevron.com/prodserv/fuels/bulletin/aviationfuel
 - "British Petroleum Statistical Review of World Energy 2002," February 2003
 - CNN.com, October 12, 1999
 - "Code of Federal Regulations, 10 CFR 50-46," nrc.gov/NRC/CFR/Part050
 - "Energy Efficiency and Renewable Energy," www.eere.energy.gov
 - "Energy Information Administration," www.eia.doe.gov
 - "Geothermal Power Plant," Toshiba Power Systems and Services
 - "Hydro-electric Power," <http://acre.murdoch.edu.au/refiles>
 - "Iter Introduction to Fusion", itercanada.com.
 - "World Energy Beyond 2050," Journal of Petroleum Technology, JPT Online Feb. 2002
 - "Why Nuclear Power, Comparison of Various Energy Sources." Nucleartourist.com.
 - "World Nuclear Association, WNA" <http://www.world-nuclear.org/info/inf75.htm>

Chapter II

- Abbott, M. M., and H. C. Van Ness, "Thermodynamics," McGraw-Hill, 1972.

- Anderson, Edward E., "Thermodynamics," PWS Publishing Company, 1994.
- Bond, John W. Jr., Kenneth Watson, and Jasper A. Welsh, Jr., "Atomic Theory of Gas Dynamics," Addison-Wesley, 1965.
- Eastop, T. D. and A. McConkey, "Applied Thermodynamics for Engineering Technologies," 5th Edition, Longman Scientific & Technical, John Wiley 1993.
- El-Wakil, M. M., "Powerplant Technology," McGraw-Hill, 1984.
- Felder, Richard M. and Ronald W. Rousseau, "Elementary Principles of Chemical Engineering Processes," 3rd Edition, John Wiley and Sons, 1999.
- Hatsopoulos, G. N. and J. H. Keenan, "Principles of General Thermodynamics" John Wiley & Sons, Inc., 1965.
- Holman, J. P., "Thermodynamics," 3rd Edition, McGraw-Hill, 1980.
- Howell, John R. and Richard O. Buckius, "Fundamentals of Engineering Thermodynamics," 2nd Edition, McGraw-Hill, 1992.
- Huang, Francis F., "Engineering Thermodynamics, Fundamentals and Applications," Macmillan, 1976.
- Masi, J. F., "Trans. ASME," 76: 1067, October 1954.
- McQuiston, F. C. and J. D. Parker, "Heating, Ventilating, and Air Conditioning Analysis and Design," John Wiley, 1977.
- Meyer, C. A., et. al., "ASME Steam Tables," Thermodynamics and Transport Properties of Steam, Sixth Edition, 1993.
- Moran, Michael J. and Howard N. Shapiro, "Fundamentals of Engineering Thermodynamics," Second Edition, John Wiley & Sons, Inc. 1992.
- Nashchokin, V., "Engineering Thermodynamics and Heat Transfer," Mir Publishers, Moscow, 1979.
- Roth, Alexander, "Vacuum Technology," 3rd Edition, Elsevier, 1990.
- Reynolds, William C and Henry C. Perkins, "Engineering Thermodynamics," McGraw-Hill 1977.
- Smith, J. S. and H.C. Van Ness, "Introduction To Chemical Engineering Thermodynamics," Third Edition, McGraw-Hill, 1975.
- Sontag, Richard E., Claus Boorgnakke, and Gordon J. an Wylen," Fundamentals of Thermodynamics," fifth edition, John Wiley & Sons, Inc. 1998.
- Todreas, Neil E., and Mujid S. Kazimi, "Nuclear Systems I. Thermal Hydraulic Fundamentals," Hemisphere Publishing Company, 1990
- Van Wylen, Gordon J. and Richard E. Sonntag, "Fundamentals of Classical Thermodynamics," 3rd Edition, English/SI Version, John Wiley & Sons, Inc. 1986.
- Wark, Jr., Kenneth, "Thermodynamics," 5th Edition, McGraw-Hill, Inc., 1988.
- Zemansky, Mark W. and Richard H. Ditton, "Heat and Thermodynamics, an Intermediate Textbook," Sixth edition, McGraw Hill, Inc. 1981.
- Zemansky, Mark W., "Temperatures Very Low and Very High," Dover Publications Inc., 1964.

Chapter III

- Aris, Rutherford, "Vectors, Tensors, and Basic Equations of Fluid Mechanics," Dover Publications Inc., 1990.
- Baumeister T. and E. A. Avallone, "Mark's Standard Handbook for Mechanical Engineers, 8th ed. New York, McGrawHill, 1979.
- Bean, H. S., "Fluid Meters: Their Theory and Application," 6th ed., American Society of Mechanical Engineers, New York, 1971.

- Binder, Raymond C., "Fluid Mechanics," Fifth Edition, Prentice Hall, 1973
- Boussinesq, see Brodkey, R. S.
- Brodkey, R. S., "The Phenomena of Fluid Motion," 3rd printing, Addison-Wesley, 1967.
- Burgreen, D., "Flow Coastdown in a Loop After Pumping Power Cutoff," Nuclear Science and Engineering: 6, 306–312, 1959.
- Carnahan B., H. A. Luther and J. O. Wilkes, "Applied Numerical Methods," Wiley, 1969
- Chaudhry, M. H., "Applied Hydraulic Transients," 2nd Edition, Van Nostrand Reinhold, 1987.
- Churchill, S. W., Empirical Expressions for the Shear Stress in Tirbulent Flow in Commercial Pipe," A. IChE. J., Vol. 19, No. 2, pp. 375–376, 1973.
- Colebrook, see Fox, R. W. and A. T. McDonald. Also White, F. M.
- Cross, H., "Analysis of Flow in Networks of Conduits or Conductors," University of Illinois Bulletin 286, November 1936.
- Daily, J. W. and D. R. F. Harleman's, "Fluid Dynamics," Addison Wesley, 1966.
- Denn, Morton M., "Process Fluid Mechanics," Prentice Hall, 1980.
- Di Marco, P. et. al., "Experimental Study on Rising Velocity of Nitrogen Bubbles in FC-72," Int. Journal of Thermal Sciences, 42 (2003).
- Fox, R. W. and A. T. McDonald, "Introduction to Fluid Mechanics," 3rd Edition, Wiley, 1985
- Goldstein, S., "Modern Development in Fluid Dynamics," Vol. 1. Oxford Press 1952.
- Granger, Robert A., "Fluid Mechanics," Dover, 1995.
- Haaland, S. E., "Simple and Explicit Formulas for the Friction Factor in Turbulent Pipe Flow," Journal of Fluid Engineering, 1983.
- Henry, R. E. and H. K. Fauske, "The Two-Phase Critical Flow Of One Component Mixtures in Nozzles, Orifices, and Short Tubes," Journal of Heat Transfer, May 1971.
- Hildebrand, F. B., "Advanced Calculus for Applications, 2nd Edition, 1976.
- Hines, J. O., "Turbulence," McGraw-Hill 1959.
- Howell, John R. and Richard O. Buckius, "Fundamentals of Engineering Thermodynamics," Second Edition, McGraw-Hill, 1992.
- Hughes W. F. and J. A. Brighton, "Fluid Dynamics," McGraw-Hill, 1967.
- Idelchik, I. E., "Handbook of Hydraulic Resistance," 2nd Edition, Hemisphere Pub. Co., 1986.
- Kao, S. P., "A PWR mathematical model," Ph. D. Thesis, Dept. of Nuclear Eng., MIT 1984.
- Lansford, W. M., "The Use of an Elbow in a Pipe Line for Determining the Flow in the Pipe," Eng. Exp. Sta. University of Illinois, Bull. 289, 1936.
- Liepmann, H. W. and A. Roshko, "Elements of Gas Dynamics," 2001.
- Lyons, J. L., "Lyons' Valve Designers Handbook," Van Nostrand Reinhold, 1982.
- Meyer, Richard E., "Introduction to Mathematical Fluid Mechanics," Dover, 1971.
- Miller, R.W., "Flow Measurement Engineering Handbook," New York, McGraw-Hill, 1983.
- Moody, L. F., "Friction Factor for Pipe Flow," Transactions, ASME, Vol. 66, 1944, p. 671.
- Moody, F. J., "Maximum Discharge Rate of Liquid Vapor Mixtures From Vessels," In ASME Symposium: Nonequilibrium Two-Phase Flows. 1975, pp. 27–36.
- Moody, F. J., "Introduction to Unsteady Thermofluid Mechanics," Wiley, 1990.
- Nahavandi, Amir N. and Michael P. Rashevsky, "A Digital Computer Program for Critical Flow Discharge of Two-Phase Flow, Steam-Water Mixture (Critco Code). CVNA-128, February, 1962.
- Nahavandi, Amir N. and G. V. Catanzaro, "Matrix Method for Analysis of Hydraulic Networks," Journal of the Hydraulic Division, Proceedings of the American Society of Civil Engineers, January, 1973.

- Nayyar, M. L., "Piping Handbook," 6th Ed. McGraw-Hill. 1992.
- Nikuradze, see Fox, R. W. and A. T. McDonald. Also White, F. M.
- Pai, S. I., "Viscous Flow Theory," Vol. II – Turbulent Flow, D. Van Nostrand, Princeton, 1957.
- Parmakian, J., "Waterhammer Analysis," Prentice-Hall, 1955.
- Perry, R. H. and C. H. Chilton, "Chemical Engineer's Handbook," 5th Ed, McGraw-Hill, 1975.
- Peterson, C. E., et. al., "RETRAN-02, Volume 1: Theory & Numerics," Revision 4, EPRI NP-1850-CCM-A. 1988.
- Potter, Merle C. and David C. Wiggert, "Mechanics of Fluids," Prentice-Hall, 1991.
- Rust, James H., "Nuclear Power Plant Engineering," Haralson, 1979.
- Schlichting, H., "Boundary Layer Theory," 7th Edition, McGraw-Hill, 1979.
- Swamee, P. K. and A. K. Jain, "Explicit Expressions for Pipe Flow Problems," Journal of Hydraulic Division Proceedings, ASCE, pp. 657-664, May 1976.
- Todreas, N. E. and M. S. Kazimi, "Nuclear Systems, I," Taylor & Francis, 3rd. Printing, 2000.
- Thompson, L and O. E. Buxton, "Maximum Isentropic Flow of Dry Saturated Steam Through Pressure Relief Valves," 3rd. International Conference on Pressure Vessels and Piping, San Francisco, June 1979.
- Tomiyaama, Akio et. al., "Shapes of Rising Velocities of Single Bubbles Rising through an Inner Subchannel," Nuc. Science & Tech. Vol. 40, No. 3, March 2003
- Tullis, J. Paul, "Hydraulics of Pipelines, Pumps, Valves, Cavitation, Transients," John Wiley & Sons, 1989.
- Watters, Gary Z., "Analysis and Control of Unsteady Flow in Pipelines," Second Edition, Butterworth, Ann Arbor Science Book, 1984.
- Vennard, John K. and Robert L. Street, "Elementary Fluid Mechanics," 5th Edition, John Wiley & Sons, 1975.
- von Karman, T., "Über Laminaire und Turbulente Reibung," Angew. Math. Mech., vol. 1, pp. 233–252, 1921; also NACA Tech. Mem. 1092, 1946.
- Welty, J. R., C. E. Wicks, and R. E. Wilson, "Fundamentals of Momentum, Heat, and Mass Transfer," 2nd Edition, Wiley, 1976.
- White, F. M., "Fluid Mechanics," 2nd. Ed. McGraw Hill. 1986.
- White, F. M., "Viscous Fluid Flow," McGraw-Hill, 1974.
- Wiely, Benjamin E. and Victor L. Streeter, "Fluid Transients in Systems," Prentice Hall, 1997.
- Zucrow, Maurice J. and Joe D. Hoffman, "Gas Dynamics," Volume 1, John Wiley & Sons, 1976.
- , ASME Boiler and Pressure Vessel Code, Section III, Division 1- Subsection NB, Class 1 Components. ANSI/ASME BPV-III-1-NB, 1980 edition.
- , CRANE Tech. Paper 410, "Flow Of Fluids in Valves, Fittings, & Pipes," 1980.
- , EPRI Report, "Critical Flow Predictions through Safety & Relief Valves," EPRI-NP-2878 LD, February 1983.
- , EPRI Report, "Safety and Relief Valves in Light Water Recators," edited by Avtar Singh NP-4306-SR, December 1985.
- , FSAR, Yankee Atomic Electric Company.
- , Measurement of Fluid Flow by Means of Orifice Plates, Nozzles, and Venturi Tubes Inserted in Circular Cross Section Conduits Running Full," ISO Rep. DISTRIBUTION-5167, Geneva, 1976.

Chapter IV

- Arpaci, V. S., "Conduction Heat Transfer," Addison Wesley, 1966.
- Blasius, H. Z., Math. Phys., 56, 1, 1908.
- Carlsaw, H. S. and J. C. Jeager, "Conduction of Heat in Solids," 2nd ed., Oxford University Press, 1959.
- Chapman, Alan J., "Heat Transfer," 4th Ed., Macmillan, 1984.
- Churchill, S.W., "Free Convection Around Immersed Bodies," in Heat Exchanger Design Handbook, Hemisphere Publishing Co., 1983.
- Churchill, S. W., and H. H. S. Chu, "Correlating Equations for Laminar and Turbulent Free Convection from a Vertical Plate," Int. Journal of Heat Mass Transfer, vol. 18, p. 1323, 1975.
- Churchill, S. W., and H. H. S. Chu, "Correlating Equations for Laminar and Turbulent Free Convection from a Horizontal Cylinder," Int. Journal of Heat Mass Transfer, vol. 18, p. 1049, 1975.
- Churchill, S. W., and H. Ozoe, "Correlations for Laminar Forced Convection in Flow Over an Isothermal Flat Plate and in Developing and Fully Developed Flow in an Isothermal Tube," Journal of Heat Transfer, vol. 95, p. 46, 1973.
- Dittus, F. W. and L. M. K. Boelter, University of California, Berkley, Pub. Eng., vol. 2, 1930, p. 443.
- Dwyer, O. E., "Liquid Metals Handbook, Sodium and NaK Supplement," Washington D. C., U.S. Atomic Energy Commission, 1970, Chapter 5.
- Eckert, E. R. G. and Robert M. Drake, Jr., "Analysis of Heat and Mass Transfer," McGraw-Hill, 1972.
- El-Wakil, M. M., "Nuclear Heat Transport," ANS. 1978.
- Fishenden, M. and Saunders, O., "An Introduction to Heat Transfer," Oxford University Press, 1950.
- , "General Electric BWR Thermal Analysis Basis Data; Correlation and Design Applications. NADO-10958, 1973.
- Holman, J. P., "Heat Transfer," 7th Ed. McGraw Hill. 1990
- Howarth, L., "On the Solution of the Laminar Boundary Layer Equations," Proc. Royal Society. London, Series A, 164, 1938, p. 547.
- Lyon, R. N., "Liquid Metal Handbook," Department of the Navy, June 1952.
- Incropera, Frank P. and D. P. De Witt, "Fundamentals of Heat and Mass Transfer," 3rd Ed., Wiley, 1990.
- Jakob, M., Heat Transfer," vol. 1, John Wiley & Sons, Inc., 1949.
- Kakac, S. and R. K. Shah, W. Aung, "Handbook of Single-Phase Convective Heat Transfer," John Wiley. 1987.
- Kreith, F., "Principles Of Heat Transfer," 3rd. Ed. Harper & Row. 1973 & 1986.
- Kutateladze, S. S., "Fundamentals of Heat Transfer," Academic Press, New York, 1963.
- Lahey, R. T., and F. J. Moody, "The Thermal-Hydraulics of a Boiling Water Nuclear Reactor," American Nuclear Society, 1977.
- Lienhard, John H., "A Heat transfer Textbook," Prentice-Hall, Inc., 1981.
- Lamarsh, John R and Anthony J. Baratta, "Introduction to Nuclear Engineering," 3rd ed., Prentice Hall, 2001.
- McAdams, W.H., "Heat Transmission," 3rd. ed. McGraw Hill 1954.
- Ostrach, S., "An Analysis of Laminar Free Convection Flow and Heat Transfer About a Flat Plate Parallel to the Direction of the Generating Body Force," NACA Tech. Note 2635, 1952.
- Ozisik, M. N., "Basic Heat Transfer," McGraw Hill. 1977.

- Rohnesnow, W. M. and H. Choi, "Heat, Mass & Mom. Transfer," Prentice Hall. 1961.
- Rohsenow, W. M., "Handbook of Heat Transfer," McGrawHill, 1973.
- Schneider, P. J., "Conduction Heat Transfer," Addison Wesley, 1955.
- Seban, R. A., and T. Shimazaki, "Heat Transfer to Fluid Flowing Turbulently in a Smooth Pipe and with Walls at Constant Temperature," ASME Paper 50-A-128, 1950.
- Seider, E. N., and E. G. Tate, "Heat Transfer and Pressure Drop of Liquids in Tubes," Ind. Eng. Chem., Vol. 28, 1936, p. 1429.
- Suryanarayana, N. V., "Engineering Heat Transfer," West Publishing Company, 1995.
- Todreas, Neil E. and Mujid S. Kazimi, "Nuclear Systems I," 3rd Printing, Taylor & Francis, 2000.
- Whitaker, S., "Forced Convection Heat Transfer Correlations for Flow in Pipes, Past Flat Plates, Single Cylinders, Single Spheres, and Flow in Packed Beds and Tube Bundles," AIChE Journal, vol. 18, 1972.
- White, F. M., "Heat Transfer," Addison Wesley. 1984.
- Zhukauskas, A., "Heat Transfer from Tubes in Cross Flow," Adv. in Heat Transfer, vol. 8 Academic Press, 1972.

Chapter V

- Berenson, P. J., "Experiments of Pool Boiling Heat Transfer," Int. Journal of Heat Mass Transfer, 5, 1962.
- Bernath, L., Transactions of A.I.Ch.E., 1955.
- Biasi, L., et. al., "Studies on burnout, Part 3. Enrgy Nucl. 14:530, 1967.
- Bjornard, T. A. and P. Griffith, "PWR Blowdown Heat Transfer," Symposium on Thermal and Hydraulic Aspects of Nuclear Reactor Safety (Vol. 1). New York, ASME 1977.
- Bowring, R. W., "Simple but Accurate Round Tube, Uniform Heat Flux Dryout Correlation over the Pressure Range 0.7 to 17 MPa," AEEW-R-789, U.K. Atomic Energy Authority, 1972.
- Bromley, L. A., "Heat Transfer in Stable Film Boiling," Chem. Eng. Prog., 46, 221, 1950.
- Chen, John C., "A Correlation for Boiling Heat Transfer to Saturated Fluids in Convection Fow," ASME paper 63-HT-34, 1963.
- Cheng, S. C, W. Ng, and K. T. Heng, "Measurements of Boiling Curves of Subcooled Water Under Forced Convection Conditions," Int. Journal of Heat Mass Transfer 21:1385, 1978.
- Cichitti, A., et. al., "Two-Phase Cooling Experiments – Pressure Drop, Heat Transfer, and Burnout Measurements," Energia Nucl. 7:407, 1960.
- Collier, John G. and Thome, John R., "Convective Boiling and Condensation," Third Edition, Oxford University Press, 1996.
- Delhaye, J. M., M. Giot, and M. L. Riethmuller, "Thermohydraulics of Two-Phase Systems for Industrial Design and Nuclear Engineering," McGraw Hill/Hemisphere, 1981.
- Dergarabedian, P., "The Rate of Growth of Bubbles in Superheated Liquid," Journal of Appl. Mech. Trans. ASME, vol. 75, 1953.
- Dhir, V. K. and J. H. Lienhard, "Laminar Film Condensation on Planes and Axisymmetric Bodies in Non-uniform Gravity," Journal of Heat Transfer, 93, 97–100, 1971
- Duckler, A. E., et. al., "Pressure Drop and Hold-up in Two-Phase Flow: Part A – A Comparison of Existing Correlations. Part B – An Approach Through Similarity Analysis," AIChE Journal, 10:38, 1964.
- Fauske, H. F., "The Discharge of Saturated Water Through Tubes," Chem. Eng. Sym. Series 61:210, 1965.

- Friedel, L., "Improved Friction Pressure Drop Correlations for Horizontal and Vertical Two-Phase Pipe Flow, European Two-Phase Flow Group Meeting, Ispra, Italy, 1979.
- Forster, H. K. and N. Zuber, "Dynamics of Vapor Bubbles and Boiling Heat Transfer," *AIChE Journal*, 1 (4), 531–535, 1955.
- Gaspari, G. P., et. al., "A Rod-Centered Subchannel Analysis with Turbulent Mixing for Critical Heat Flux Prediction in Rod Clusters Cooled by Boiling Water," *Proceedings of 5th Int. Heat Transfer Conference*, Tokyo, Japan, 3–7, September 1974, CONF-740925, 1975.
- George, Thomas L., et. al., "GOTHIC Containment Analysis Package, Technical Manual," Numerical Applications, Inc., Richland, Washington, NAI 8907-06, Rev. 12, July 2001.
- Ginoux, J. N., "Two-Phase Flow and Heat Transfer," McGraw Hill/Hemisphere, 1978.
- Groeneveld, D. C., "Post Dryout Heat Transfer at Reactor Operating Conditions, AECL-4513, 1973.
- Henry, R. E., "The Two-Phase Critical Discharge of Initially Saturated or Subcooled Liquid," *Nuclear Science and Engineering*, 41, 1970, pp 336.
- Henry, R.E., and H. F. Fauske, "The Two-Phase Critical Flow of One-Component Mixtures in Nozzles, Orifices, and Short Tubes," *Transactions of ASME, Journal of Heat Transfer* 93, 179–187, May 1971.
- Hewitt, G. F. and D. N. Roberts, "Studies of Two-Phase Flow Patterns by Simultaneous X-Ray and Flash Photography," *AERE-M2159*, 1969.
- Hsu, Yih-Yun, "On the Size Range of Active Nucleation Cavities in Nucleate Boiling," *Journal of Heat Transfer*, 84C(3), 207–216, 1962.
- Hsu, Yih-Yun and Robert W. Graham, "Transport Processes in Boiling and Two-Phase Systems, McGraw Hill Publishing Company, 1976.
- Janssen, E. and Levy, S., "General Electric Company Report APED-3892, 1962.
- Jens, W. H. and P. A. Lottes, "Analysis of Heat Transfer, Burnout, Pressure Drop, and Density Data for High Pressure Water," *ANL-4627*, 1951.
- Kandlikar, S. G., "A General Correlation for Saturated Two-Phase Flow Boiling Heat Transfer Inside Horizontal and Vertical Tubes," *J. Heat Transfer*, 112(1):219–228, 1990.
- Katto, Y. and Haramura, Y., "Critical Heat Flux on a uniformly heated horizontal cylinder in an upward cross flow of saturated liquid," *Int. Journal Heat Mass Transfer*, 26, pp 1199–1205, 1983.
- Mandhane, J. M. et. al., "A Flow Pattern Map for Gas-Liquid Flow in Horizontal Pipes," *International Journal of Multiphase flow*, 1:537, 1974.
- , *RELAP-5, MOD1 Code Technical Manual*
- Labuntsov, D. A., "Heat Transfer in Film Condensation of Pure Steam on Vertical Surfaces and Horizontal Tubes," *Teploenergetika*, 4, 72, 1957.
- McAdams, W. H., et. al., "Vaporization Inside Horizontal Tubes. II. Benzene-Oil Mixture, *Trans. ASME* 64:193, 1942.
- MacBeth, R. V., "Burn-out Analysis, Part 4. Application of a local condition hypothesis to world data for uniformly heated round tubes and rectangular channels," *AEEW-R* 267, 1963.
- McDonough, J.B., W. Milich, W., and E.C. King, "An Experimental Study of Partial Film Boiling Region with Water at Elevated Pressures in a Round Vertical Tube. *Chem. Eng. Prog. Sym. Series* 57:197, 1961.
- Martinelli, R. C. and D. B. Nelson, "Prediction of Pressure Drop During Forced Circulation Boiling of Water," *Trans. ASME* 70:695, 1948.
- Moody, F. J., "Maximum Flow Rate of a Single-Component, Two-Phase Mixture," *Journal of Heat Transfer*, Vol. 87, 134–142, February 1965.

- Moore, K. V. and W. H. Rettig, "RELAP4 – A Computer Program for Transient Thermal-Hydraulic Analysis," ANCR-1127, Idaho National Laboratory, Idaho Falls, Idaho, 1975.
- Myer, John E., "Conservation Laws in One-Dimensional Hydrodynamics," WAPD-BT-20, Sept. 1960.
- Nahavandi, Amir N and Michael P. Rashevsky, "A Digital Computer Program for Critical Flow Discharge of Two-Phase Steam-Water Mixtures," CVNA-128, February 1962.
- Nukiyama, S., "The Maximum and Minimum Values of Heat Transmitted from Metal to Boiling Water Under Atmospheric Pressure," *Int. J. Heat Mass Transfer*, 9, 1966.
- Pei, B. S. et. al., "Evaluations and Modifications of the EPRI-1 Correlation of PWR Critical Heat Flux Predictions Under Normal & Abnormal Fuel Conditions," *Nuclear Tech.*, Vol. 75, N0. 2, November 1986.
- Reddy, D. G., R. S. Sreepada, and Amir. N. Nahavandi, "Two-Phase Friction Multiplier Correlation for High – Pressure Steam Water Flow," EPRI, NP-2522, July 1982.
- Scriven, L. E., "On the Dynamics of Bubbles in Superheated Water," *Chem. Eng. Sci.*, vol. 10, 1959.
- Stephen, Karl, "Heat Transfer in Condensation and Boiling," Springer-Verlag, 1992.
- Tong, L. S., "Boiling Crisis and Critical Heat Flux, TID-25887 NTIS, 1972.
- Thom, J. R. S., et. al., "Boiling in Subcooled Water During Flow in Tubes and Annuli," *Proc. Int. Mech. Eng.* 180:226, 1966.
- Thom, J. R. S., "Prediction of Pressure Drop During Forced Circulation Boiling of Water," *Int. Journal of Heat Mass Transfer* 7:709, 1964.
- Wallis, G. B., "One Dimensional Two-Phase Flow," McGraw Hill, New York. 1969.
- Whalley, P. B., "Boiling, Condensation, and Gas-Liquid Flow," Oxford University Press, 1990.
- Winterton, R. H. S., "Thermal Design of Nuclear Reactors," Pergamon Press, 1981.
- Zivi, S. M., "Estimation of Steady-State Steam Void Fraction By Means of The Principle of Minimum Entropy Production," *Trans. ASME (J. Heat Transfer)*, 86, 247–52.
- Zuber, N, and J. A. Findlay, "Average Volumetric Concentration in Two-Phase Flow Systems," *J. Heat Transfer*, 87:453, 1965.
- Zuber, N., "On the Stability of Boiling Heat Transfer," *Trans. ASME*, 80, 1958.
- Zuber, N. and M. Tribus, "Further Remarks on the Stability of Boiling Heat Transfer," UCLA, Report No. 58-5, January 1958.

Chapter VIa

- , "Standards of the Tubular Exchanger Manufacturers Association," 7th Edition, Tubular Exchanger Manufacturers association, New York, 1988.
- Fraas, A. P and M. N. Ozisik, "Heat Exchanger Design," Wiley, 1965
- Harpster, Joseph W., "An Impact on Plant Performance from Advanced Instrumentation," 44th Annual ISA Industry Symposium, July 2001, Fl. USA
- Harpster, Joseph W., "On Understanding the Behavior of Non-Condensables in the Shell Side of Steam Surface Condensers," ASME Conference, June 2001, Louisiana. USA
- Incropera, Frank P. and David P. De Witt, "Fundamentals of Heat And Mass Transfer," 3rd Edition, John Wiley & Sons, 1990
- Kakac, Sadik and Hongtan Liu, "Heat Exchangers Selection, Rating, and Thermal Design," CRC Press LLC, 1998.

- Kreith, F. and R. F. Boehm, "Direct – Contact Heat Exchangers," Hemisphere Pub. Corp., 1988
- Li, Chung Hsiung, "Exact Transient Solutions of Parallel-Current Transfer Processes," *Journal of Heat Transfer*, Vol. 108, 365–369, May 1986.
- Lorenzini, E., et. al., "Numerical Transient Analysis of Parallel and Counter Flow Heat Exchangers," *Journal of Heat and Technology*, Vol. 7, No. 2, 1989.
- Nahavandi A. N., M. A. Vorkas, and V. J. D'emidio, "Cost Optimization of Vertical Natural Circulation Steam Generators," *Nuclear Engineering and Design* 36, 1976.
- Romie, F. E., "Transient Response of the Counterflow Heat Exchanger," *Transactions of ASME*, Vol. 106, 620–626, August 1984
- Singh, K. P. and A. I. Soler, "Mechanical Design of Heat Exchangers," Arcturus Publishers, 1984
- Taborek, et. al., "Heat Exchangers, Theory and Practice" Hemisphere Publishing Corp. 1983

Chapter VIb

- , ASME Fluid Meters Research Committee, "The ISO-ASME Orifice Coefficient Equation", *Mech. Eng.* July 1981.
- , ASME, "Flowmeter Computation Handbook," New York, 1961.
- Baker, Roger C., "Flow Measurement Handbook, Industrial Designs, Operating Principles, Performance, and Applications," Cambridge University Press, 2000.
- , Flow Control Magazine, April/May, 2000.
- Bean, H. S., "Flow Meters: Their Theory and Application," 6th ed., ASME, New York, 1971 Control magazine, October 2002
- Cussler, E. L., "Diffusion. Mass Transfer in Fluid Systems," 2nd. Edition. Cambridge University Press, 1997.
- Holman, J. P., "Experimental Methods for Engineers," 7th edition, McGraw Hill 2001.
- King, L. V., "On the Convection of Heat from Small Cylinders in a Stream of Fluid, with Applications to Hot-Wire Anemometry," *Phil. Trans. Roy. Soc. London*, vol. 214, no. 14, p. 373, 1924.
- Kline, S. J. and F. A. McClitock, "Describing Uncertainties in Single-Sample Experiments," *Mechanical Engineering*, 75, 1, pp. 3–9. January 1953

Chapter VIc

- Karassik, I. J., "Pump Handbook," 2nd Ed. McGraw-Hill. 1986.
- Kreith, Frank and D. Yogi Goswami, "The CRC Handbook of Mechanical Engineering," 2nd edition, CRC Press, 2005.
- Krivchenko, G. I., "Hydraulic Machines, Turbines and Pumps," Mir Publishers, Moscow, 1986.
- Mott, Robert L., "Applied Fluid Mechanics," 4th ed., Macmillan Publishing Company, 1994.
- White, F. M., "Fluid Mechanics," 2nd. Ed. McGraw Hill. 1986.
- Wiely, Benjamin E. and Victor L. Streeter, "Fluid Transients in Systems," Prentice Hall, 1997.
- Wislicenus, G. F., "Fluid Mechanics of Turbomachinery," 2nd edition, McGraw Hill, 1965.

Chapter VI d

- Burgreen, David, "Flow Coastdown in a Loop after Pumping Power Cutoff," Nuclear Science and Engineering, 6, 306–312, 1959.
- Edwards D. K., et al, "Transfer Processes. An Introduction To Diffusion, Convection and Radiation," 2nd Edition, McGraw Hill.
- George, Thomas L., et. al., "GOTHIC Containment Analysis Package, Technical Manual," Version 6.1, July 1999. NAI 8907-06, Rev. 9
- Hargroves, D.W. and L. J. Metcalfe et. al., "CONTEMPT-LT/028A Computer Program for Predicting Containment Pressure – Temperature Response to a Loss-Of-Coolant-Accident," NUREG/CR-0255, 1979.
- Kao, Shih Ping, "A Multiple-Loop Primary System Model for Pressurized Water Reactor Plant Sensor Validation," Ph.D. Thesis, Department of Nuclear Engineering, MIT, 1984.
- Lin, C. C. et. al., "CONTEMPT4/MOD4, A Multi-compartment Containment System Analysis Program," NUREG/CR-3716, BNL-NUREG-51754, March 1984.
- McFadden, J. H. et. al., "RETRAN-02 – A Program for Transient Thermal-Hydraulic Analysis of Complex Fluid Flow Systems," EPRI NP-1850-CCM-A, Volume 1, Revision 4, 1988.
- Myer, John E., "Some Physical and Numerical Considerations for the SSC-S Code," Brookhaven National Lab., BNL-NUREG 50913, 1978.
- Reeder, Douglas L., "LOFT System and Test Description," NUREG/CR-0247, July 1978.
- Rust, J. H., "Nuclear Power Plant Engineering," Haralson Publishing Co., Buchanon, GA, 1979.
- , "LOFT Integral Test System Design Basis Report," DBR-1, Aerojet Nuclear Inc., Jan. 1974.
- Weisman, J., "Heat Transfer to Water Flowing Parallel to Tube Bundles," Nuc. Sci. & Eng. 6:78, 1979.

Chapter VI e

- , "American Nuclear Standard for Decay Heat Power in Light Water Reactors," American Nuclear Society (ANS), ANSI/ANS-5.1-1979. August 1979.
- Almenas, Kazys and Richard Lee, "Nuclear Engineering, An Introduction," Springer-Verlag, 1992.
- Bernath, L., Transactions A.I.Ch.E., 1955.
- Brown, Theodore L. and H. Eugene LeMay, Jr., "Chemistry, The Central Science," 2nd Edition, Prentice-Hall, Inc. 1981
- Collier, John G. and Geoffrey F. Hewitt, "Introduction to Nuclear Power," Hemisphere Publishing Company, 1987.
- Connolly, Thomas J., "Foundations of Nuclear Engineering," John Wiley & Sons, 1978.
- Duderstadt, James J. and Louis J. Hamilton, "Nuclear Reactor Analysis," John Wiley & Sons, 1976.
- Evans, Robley D., "The Atomic Nucleus," McGraw-Hill, Fourteenth Printing, 1972.
- Ferziger, Joel H. and P. F. Zweifel, "The Theory of Neutron Slowing Down in Nuclear Reactors, The MIT Press, 1966.
- Foster, Arthur R. and Robert L. Wright, Jr., "Basic Nuclear Engineering," 4th Ed. Allyn & Bacon, 1983.

- Glasstone, Samuel and Alexander Sesonske, "Nuclear Reactor Engineering," Van Nostrand Reinhold Company, 1967.
- Henry, Alan F., "Nuclear Reactor Analysis," The MIT Press, 1975.
- Klimov, A., "Nuclear Physics And Nuclear Reactors," MIR Publishers, Moscow, 1975.
- Knief, Ronald Allen, "Nuclear Criticality Safety, Theory and Practice", Sixth Printing, American Nuclear Society, 1998.
- Knoll, Glenn F., Radiation Detection And Measurement," John Wiley & Sons, 1979.
- Mayo, Robert M., "Introduction to Nuclear Concepts for Engineers," American Nuclear Society, 1998.
- Ott, Karl O. and Winfred A. Bezella, "Introductory Nuclear Reactor Statics," Revised edition, ANS 1989.
- Price, William J., "Nuclear Radiation Detection," second Edition, McGraw-Hill, 1964
- Rahman, Inam-Ur and Paulinus S. Shieh, "Introduction to Nuclear Engineering," Robert E. Krieger Publishing Company, 1981.
- Schaeffer, N. M., "Reactor Shielding for Nuclear Engineers," National Technical Information Center, TID-25951, 1973.
- Shultis, J. Kenneth and Richard E. Faw, "Radiation Shielding," American Nuclear Society, 2000.
- Shultis, J. Kenneth and Richard E. Faw, "Fundamentals of Nuclear Science and Engineering," Marcel Dekker, Inc. 2002.
- Walker, F. William, et. al., "Nuclides and Isotopes, Chart of Nuclides," Fourteenth Edition, GE Nuclear Energy, General Electric Company, 1989.
- Weisman, Joel, "Elements of Nuclear Reactor Design," Second Edition, Robert E. Krieger Publishing Company, 1983.
- , "Residual Decay Energy for Light Water Reactors for Long Term Cooling," NRC Standard Review Plan (NUREG-0800), Rev. 2, Section 9.2.5-8, Branch Technical Position ASB 9-2, July 1981.

Chapter VII

- Abramowitz, M. and I. A. Stegun, "Handbook of Mathematical Functions," Dover, 9th Printing, 1972.
- Acton, F. S., "Numerical Methods that Work," Harper & Row, 1970
- Agresti, A. and B. Finlay, "Statistical Methods for the Social Sciences," 2nd. Ed., Dellen Pub. Co., 1986.
- Bendat, Julis S. and Allan G. Piersol, "Random Data: Analysis and Measurement Procedures," Wiley-Interscience, 1971.
- Bird, R. B., W. E. Stewart, and E. N. Lightfoot, "Transport Phenomena," 2nd ed. Wiley, 2002.
- Byrkit, Donald R., "Elements of Statistics," D. Van Nostrand, 1972.
- Boyce, W. E. and R. C. DiPrima, "Elementary Differential Equations and Boundary Value Problems," 3rd Edition, Wiley, 1977.
- Carnahan B., H. A. Luther and J. O. Wilkes, "Applied Numerical Methods," Wiley, 1969.
- Curtis, F. G., "Applied Numerical Methods," 2nd Edition, Addison Wesley, 1980.
- Dankoo, P. E., et. al., "Higher Mathematics in Problems and Exercises," Mir Publishers, Moscow, 1983.
- Demidovich, B. P. and I. A. Maron, "Computational Mathematics," Mir Publishers, Moscow, 1987.
- Elsayed, E. A., "Reliability Engineering," Addison Wesley Longman, Inc., 1996.

- Evans, Robley D., "The Atomic Nucleus," McGraw Hill, 1972.
- Griffith D. V. and I. M. Smith, "Numerical Methods for Engineers," CRC Press, 1991.
- Hildebrand, F. B., "Introduction to Numerical Analysis," 2nd Edition, Dover 1974.
- Hildebrand, F. B., "Advanced Calculus for Applications," 2nd Edition, Prentice Hall, 1976.
- Hunt, R. A., "Calculus with Analytic Geometry," Harper & Row, 1988.
- Kellison, Stephen G., "Fundamentals of Numerical Analysis," Richard D. Irwin, Inc. 1975.
- Korn & Korn, "Mathematical Handbook," 2nd Edition, McGraw-Hill, 1968.
- Krasnov, M., et. al., "Mathematical Analysis for Engineers," Volume 2, Mir Publishers, Moscow, 1990.
- Kreyszig, E., "Advanced Engineering Mathematics," 7th Ed. Wiley, 1993.
- Kroemer, Herbert, "Quantum Mechanics for Engineering, Materials Science, and Applied Physics," Prentice Hall, 1994.
- Modarres, Mohammad, "Reliability and Risk Analysis," Marcel Dekker, Inc., 1993.
- Meyer, Richard E., "Introduction to Mathematical Fluid Mechanics," Dover Publication, Inc., 1971.
- Larson, Ronald E. and R. P. Hostetler, "Calculus with Analytic Geometry," D. C. Heat & Co., 1979.
- Liboff, Richard L., "Introductory Quantum Mechanics," Holden-Day Inc. 1980
- Nakamura, Shoichiro, "Computational Methods in Engineering & Science," Wiley, 1977.
- Ozisik, Necati, "Finite Difference Methods in Heat Transfer," CRC Press, 1994
- Park, David, "Introduction to Quantum Theory," McGraw Hill, 1964.
- Pauli, Wolfgang, "Wave Mechanics," Dover Publications, Inc., 1973.
- Rossing, Thomas D and N. H. Fletcher, "Principles of Vibration and Sound," Springer Verlag, 1995.
- Schiesser, W. E., "Computational Methods in Engineering & Applied Science," CRC, 1994.
- Spiegel, Murray R., "Applied Differential Equations," 3rd Ed., Prentice Hall, 1981.
- Thomas, Jr. George B., "Calculus and Analytic Geometry," Part 2, 4th Edition, Addison-Wesley, 1972
- Wylie, C. R. and L. C. Barnett, "Advanced Engineering Mathematics," 5th Edition, McGraw-Hill, 1982.

Appendix

Table A.II.1(SI), Table A.II.2(SI), Table A.II.3(SI), Table A.II.4(SI):

Sonntag, Richard E., Claus Borgnakke, and Gordon J. Van Wylen, "Fundamentals of Thermodynamics," Fifth Edition, John Wiley & Sons, Inc., 1998.

Table A.II.1(BU), Table A.II.2(BU):

El-Wakil, M. M., "Nuclear Heat Transport," International Textbook Company, 1971.

Table A.II.5(SI), Table A.II.5(BU):

Masi, J. F., Trans. ASME, 76:1067, October 1954.

—, National Bureau of Standards Circ. 500, February 1952.

—, API Research Project 44, national Bureau of Standards, Washington, December 1952.

Table A.III.1(SI), Table A.III.2(SI), Table A.III.1(BU):

CRANE, "Flow of Fluids through Valves, Fittings, and Pipe," Publication 410M (Metric Edition), 1988.

Table A.III.2(SI):

CRANE, "Flow of Fluids Through Valves, Fittings, and Pipe," Technical Paper No. 410, 1988.

Table A.IV.1(SI), Table A.IV.2(SI), Table A.IV.3(SI), Table A.IV.4(SI), Table A.IV.5(SI), Table A.IV.10:

Incropera, Frank P. and David P. De Witt, "Fundamentals of Heat and Mass Transfer," Third Edition, John Wiley and Sons, 1990.

Table A.IV.6(SI):

- Lyon, R. N., "Liquid Metal Handbook," Atomic Energy Commission and Department of the Navy, Washington D. C., 1952
- Weatherford, Jr., et al., "Energy Conversion and Heat-Transfer Fluids for Space Applications," WADD Technical Report 61-96, November 1961
- —, "Metallic Elements and Their Alloys," T. P. R. C. Data Book, Vol. 1, Purdue Research Foundation, 1966.

Table A.IV.9, Table A.IV.10:

Suryanarayana, N. V., "Engineering Heat Transfer," West Publishing Company, 1995.

Table A.IV.4(BU):

Kreith, Frank, "Principles of Heat Transfer," 3rd ed., Harper & Row, 1973.

Table A.IV.5(BU), Table A.IV.6(BU), Table A.IV.7(BU), Table A.IV.8:

Edwards, D. K., V. E. Denny, and A. F. Mills, "Transfer Processes, An Introduction to Diffusion, Convection, and Radiation," Second Edition, McGraw-Hill, 1979.

Table A.V.1:

Tipton, C. R., Jr., "Reactor Handbook," Vol. 1, Materials 2nd Edition, Interscience, 1960.

Table A.V.2:

Almenas, Kazys, and Richard Lee, "Nuclear Engineering, an Introduction," Springer-Verlag, 1992.

Index

- Absolute pressure, 36
- Absorption cross section, 845, 847
- Absorptivity, 573-727
- Acceleration
 - convective, 237-379
 - local, 235
 - pressure drop, 319, 621, 880
- Accuracy, 730
- Acoustic velocity, 372
- Adiabatic, 57
- Affinity laws, 808
- Air conditioning, 196
- Amagat model, 188
- Anemometer, 748-766
- Angle
 - contact, 659
 - solid, 563
 - valve, 309
- Angular velocity, 39
- Annular fuel rod, 466
- Annulus, 13
- Anisotropic, 432
- Aspect ratio, 366
- Atomic mass unit, 41
- Atomic number, 842
- Augmented matrix, 971
- Availability, 105
- Avogadro, 42
- Axial flow, 19, 749, 760, 770
- Azimuthal angle, 563

- Balance of plant, 162
- Ball valve, 306-309
- Barnett correlation, 663
- Barometric pressure, 36
- Bernath correlation, 663
- Bernoulli equation, 244
- Bernoulli-obstruction meters, 321
- Bessel
 - functions, 915
 - differential equation, 914
- Best efficiency point (BEP), 752
- Biasi correlation, 663
- Biomass, 24
- Biot number, 443
- Blackbody, 568
- Blasius, 524
- Body force, 226
- Boiling
 - departure from nucleate, 662
 - film, 638
 - flow, 638
 - inception, 646
 - pool, 638
 - saturated, 638
 - subcooled, 638
 - transition, 650, 653
 - water reactor, 13
- Bond number, 642
- Borda-Carnot equation, 304
- Boundary
 - layer, 231
 - value problem, 905
- Bowring correlation, 664
- Break flow split, 625
- Brayton, 154
- Breeder reactor, 5, 12
- Buckingham pi, 748
- Buckling, 859
- Bulk:
 - modulus, 230
 - temperature, 519
- Buoyancy, 366, 549
- Butterfly valve, 309

- Calibration, 729
- Carnot
 - efficiency 101
 - principle, 100
- Cavitation, 752
- CD-ROM, 53, 85, 89, 92, 320, 329, 426, 499, 581, 591, 652, 697, 707, 718, 824, 970, 974, 981, 983, 984, 1009
- Chain rule for derivatives, 906
- Chen correlation, 658
- Choked flow, 414
- Churchill and Ozoe correlation, 528
- Cladding, 17
- Clapeyron equation, 54
- Clausius statement, 97
- Clausius-Clapeyron equation, 54
- Cleanliness factor, 690
- Coal, 4, 6, 22
- Coefficient of:
 - contraction, 322
 - performance, 103
 - volume expansivity, 47
- Colburn analogy, 521
- Compressible flow, 399
- Compressibility:
 - isentropic, 47
 - isothermal, 47
- Compressed liquid, 46, 50
- Compressor, 10, 11, 71, 74
- Concentric heat exchanger, 688, 694
- Condensation, 435, 677, 678
- Condenser, 6, 710
- Conduction equation, 437-438
- Conservation equation, 26, 64, 67, 69
- Contact resistance, 436
- Containment, 12, 187, 207-221, 819
- Continuum, 225
- Continuity equation, 64
- Control valve, 306-309
- Convection, 256, 259, 260, 435
- Conversion factors, 1018
- Cooling tower, 6, 97, 209
- Control surface, 35
- Control volume, 57
- Coordinate systems, 225, 943, 944, 947
- Coriolis acceleration, 743
- Cramer's rule, 974
- Creeping flow, 252
- Critical flow, 414
 - Critco correlation, 424
 - Henry-Fauske correlation, 622-631
 - Moody model, 628
 - Rateau correlation, 425
- Critical heat flux (CHF), 650, 876
 - Barnett correlation, 663
 - Biasi correlation, 663
 - Bowring correlation, 664
 - CISE-4 correlation, 665
 - Katto correlation, 666
- Critical:
 - pressure, 41
 - temperature, 41
- Cryogenic, 464
- Curl operator, 950
- Curvilinear coordinate, 943
- Cycle:
 - Air standard, 147
 - Brayton, 147
 - Carnot, 104
 - Diesel, 152
 - Ericsson, 158
 - Joule, 154
 - Otto, 150
 - power, 144
 - refrigeration, 99, 103
 - regenerative, 157, 169, 171
 - reheat, 167
 - Stirling, 158
 - thermodynamic, 6
- Cylindrical coordinates, 943
- D'Alembert paradox, 233
- Dalton model, 189
- Darcy formula, 299
- Darcy-Weisbach, 301
- Darrieus wind machine, 21
- Dead state, 116
- Decay heat, 882

-
- Deformation of a fluid element, 264
 - Degree
 - Centigrade, 37
 - Fahrenheit, 37
 - of subcooling, 53
 - of superheat, 167
 - Del operator, 947
 - Density, 33
 - Departure from nucleate boiling (DNB), 662
 - Design parameters, 26
 - Determinant, 966
 - Deuterium, 5, 847
 - Dew point, 196
 - Diameter
 - equivalent, 309
 - heated, 663
 - hydraulic, 309
 - Differential analysis, 239
 - Differential equations
 - Bernoulli, 911
 - Bessel,
 - Chebyshev
 - Euler-Cauchy, 912
 - Gauss
 - Hermite
 - Jacobi, 912
 - Laguerre, 912
 - Legendre, 913
 - linear, 904, 911
 - nonlinear, 904
 - ordinary, 911
 - partial, 916
 - Poisson, 916
 - Riccati, 911
 - Diffuser, 71
 - Diffusion, 432
 - Diffusivity, 435
 - Dilatant fluid, 228
 - Discharge coefficient, 321
 - Dittus-Boelter correlation, 538
 - Divergence operator, 949
 - Division at the break, 820
 - Domain, 901
 - Downcomer, 12-16, 134, 791, 827
 - Drag, 232, 233, 365-366, 521, 733
 - Drift flux, 609
 - Dry-bulb temperature, 202
 - Dryout, 658, 662, 663
 - Dynamic viscosity, 227
 - Dynamics of
 - gas filled vessels, 90
 - mixing tanks, 83
 - Eckert number, 520
 - Eddy diffusivity, 289, 535
 - Effectiveness, 120
 - Efficiency
 - Carnot, 101
 - thermodynamic, 11, 100, 101
 - Eigenvalue, 905, 907
 - Einstein, 4, 842, 932
 - Elastic
 - analysis, 344
 - scattering, 843
 - Electromagnetic flowmeter, 738
 - Elbow meter, 735
 - Electron, 841
 - Electron volt, 842
 - Elevation head, 263
 - Emissivity, 436, 568-579, 1086
 - Empirical relations, 534
 - Energy
 - balance, 57
 - binding, 843
 - grade line, 263
 - internal, 39
 - kinetic, 38
 - mechanical, 1-3, 9, 261
 - potential, 39
 - Engine
 - internal combustion, 2-8
 - jet, 2, 9-10, 71, 97, 103, 160
 - reciprocal, 9-11, 750
 - rotary, 6, 8-9
 - English engineering system of units (BU), 33
 - Enthalpy, 39
 - Entrance length, 231
 - Entropy, 39
 - EPRI-1 correlation, 666
 - Equation

- Euler, 252, 265
 - of state, 26, 41-46
- Equilibrium
 - bubble, 642-644
 - thermal, 35
- Error, 728
 - fixed, 728
 - function, 488, 489, 491
 - random, 728
- Eta factor, 852
- Eulerian approach, 230
- Evaporation, 37, 49-50
- Exergy, 105
- Expansion coefficient, 413
 - thermal, 47
 - volumetric, 549
- Explicit method, 994
- Extended surfaces, 477
- Feedwater, 12-16
- Fertile, 5, 846, 847
- Fick's law, 26, 841
- Field, 225
- Film
 - boiling, 638
 - condensation, 678
 - temperature, 520
- Fin
 - annular, 480-484
 - cylindrical spine, 483
 - longitudinal, 483
- First law of thermodynamics, 67
- Fissile, 846
- Fission, 845
- Fissionable, 846
- Fittings, 175, 224, 286, 295, 302
- Flash, 79, 89, 173, 622, 637, 812
- Flooding, 604
- Flow
 - critical, 399, 622
 - coefficient, 307, 322
 - compressible, 399
 - dimensions, 232
 - external, 99, 223, 230-233
 - incompressible, 231
 - internal, 232
 - laminar, 230
 - loop, 20, 325, 549, 799
 - measurement, 321, 412, 728
 - over flat plate, 230, 521-535
 - pattern, 555, 605, 606
 - reversal, 605, 614, 765
 - turbulent, 230
 - two-phase, 602
- Flowmeter, 302, 321, 728
 - Bernoulli, 321
 - Coriolis, 733
 - elbow, 735
 - electromagnetic, 738
 - installation, 744
 - laser Doppler, 728, 740
 - mass, 741
 - nozzle, 321
 - positive displacement, 741
 - pulsed neutron, 740
 - rotameter, 733
 - straightener, 744
 - turbine, 737
 - ultrasonic, 739
 - venturi, 321
 - vortex, 738
- Fluid
 - ideal, 223-224
 - Newtonian, 228
 - non-Newtonian, 228
- Forced convection, 518
- Form loss, 175, 306, 419
- Forster-Zuber, 660
- Fouling
 - factor, 669, 690, 707
 - resistance, 690, 718
- Fourier equation, 439
- Fourier number, 437
- Fourier transform, 908
- Friction
 - factor, 292-299, 305, 1005
 - pressure drop, 242, 312, 617
 - velocity, 293
- Fuel
 - fossil, 4
 - nuclear, 4, 23
 - pellet, 17, 466, 468

-
- rod, 14, 16, 17
 - spent, 23, 459, 559, 833
 - utilization factor, 859
 - Fusion, 3, 5, 25
 - Gage pressure, 36
 - Gamma radiation, 436, 456-458
 - Gap, 17
 - Gas turbine, 6-11, 66, 97, 154
 - Gate valve, 305
 - Gauss divergence theorem, 956
 - Gauss-Seidel iteration, 971 - 974
 - General electric correlation, 667
 - Geothermal energy, 22
 - Gibbs function, 47, 639
 - Globe valve, 305
 - Gradient operator, 947
 - Grashof number, 549
 - Gray surface, 578
 - Greenhouse effect, 11
 - Greenpower, 17
 - Hagen-Poiseuille, 291
 - Hardy Cross method, 338
 - Hazen-Williams formula, 301
 - Head, 18, 224
 - Heat
 - engine, 99
 - flux, 129, 256, 432
 - pump, 25, 31, 97, 103
 - sink, 6, 21, 96, 97
 - source, 6, 20, 22, 70, 96, 97
 - Heat exchanger, 71, 76, 147-167, 687
 - Heat transfer coefficient, 435
 - Heisler, 493, 497
 - Helmholtz function, 46
 - HEM, 602, 616, 619, 621, 623, 785
 - Hemispherical, 574, 576
 - Homogeneous, 432
 - Heterogeneous, 432
 - Hewitt map, 606
 - Humidity ratio, 195
 - Hydraulic grade line, 263
 - Hydraulic jump, 270, 408
 - Hydrostatic head, 796-799
 - Hysteresis, 729
 - Ideal gas, 41
 - Implicit method, 976, 994
 - Integral analysis, 240, 248
 - Invasive, 728
 - Inviscid, 223, 228, 231, 252, 259
 - Irreversibility, 98, 99, 105, 109
 - Isotope, 5, 11, 740, 842, 844, 845
 - Isotropic, 229, 432, 562-566, 848
 - Jakob number, 678
 - Jacobian matrix, 1005
 - Jet pump, 13, 749
 - Katto correlation, 666
 - Kelvin, 33, 98
 - Kinematic viscosity, 228
 - Kinetic energy, 38
 - Kirchhoff, 338, 369, 442, 578
 - Kutateladze, 605, 652, 682
 - Lagrangian, 234, 237, 238-259
 - Laminar
 - boundary layer, 535
 - flow, 230
 - Laplace transform, 909
 - Laplacian operator, 949
 - Latent heat, 51, 53
 - Le System International d'Unites, 33
 - Leading edge, 232, 519
 - Least-square, 1006
 - Leidenfrost point, 650, 654
 - Leibnitz rule, 960
 - Line integral, 951
 - Linear heat generation rate, 432
 - Liquid compressibility, 373
 - Logarithmic mean temperature difference (LMTD), 691
 - correction factor, 696
 - Lumped, 57, 207, 255, 431, 443
 - Lyon-Martinelli correlation, 540
 - Mach number, 230
 - Maclaurin series, 855, 902

- Manning formula, 301
- Manometer, 36, 37, 272, 322
- Martinelli-Nelson, 622
- Mass defect, 842
- Mass flow rate, 58
- Mass flux, 65
- Mass number, 842
- Matrix inversion, 968
- McAdams correlation, 299
- Metastable state, 816
- Maxwell relations, 47
- MDNBR, 877
- Minimum stable film boiling (MSFB), 653
- Minimum stable film boiling temperature, 656
- Minor loss, 301, 302
- Moderator, 5, 11, 847
- Modulus of elasticity, 375
- Moist air, 187-189
- Moisture separator, 162
- Molecular diffusion, 431, 535
- Molecular weight, 41
- Momentum
 - conservation equation, 241, 248
 - flux, 242, 262, 372, 399, 526, 778
- Napier's correlation, 425
- Natural convection, 549
- Natural circulation, 549, 796, 800
- Navier-Stokes equations, 249, 251
- Net expansion factor, 412
- Net positive suction head (NPSH), 753, 757, 760-762
- Neutron
 - current, 849
 - fast, 5, 846, 847, 851
 - flux, 457, 466, 671, 841, 848
 - thermal, 11, 846, 847, 851, 852
 - transport equation, 841, 853
- Newton's law of cooling, 435
- Newton-Raphson method, 1004
- Nozzle, 10, 70-72, 321, 323, 324
- Nuclear
 - power plant, 4, 11, 144, 786
 - resonance, 844
- Nucleate boiling, 638
- Nucleation
 - homogeneous, 637
 - heterogeneous, 637
 - onset, 644, 646, 650
- Number of transfer unit (NTU)
 - method, 698
- Nusselt number, 520
- Nuclei, 5, 844, 845
- Opaque, 575, 576, 577
- Ordinary differential equations, 911
 - Adam's method, 985
 - Euler method, 981
 - Runge-Kutta methods, 982
- Orifice meter, 321
- Orthogonality, 908
- Partial differential equations, 903
- Partial pressure, 189
- Peaking factor, 866, 874-875
- Peclet number, 541
- Perfect gas, 42
- Pitot tube, 733, 736, 737
- Planck:
 - constant, 562
 - distribution, 569
 - statement, 97
- Poisson equation, 439
- Power
 - cycle, 144
 - density, 23, 865, 1020
 - hydro, 17
 - tidal, 22
- Prandtl number, 520
- Precision, 729
- Pressure drop in
 - bends, 302
 - internal flow, 295
 - Bernoulli obstruction meters, 323
- Pressure gradient due to:
 - acceleration, 616
 - friction, 616
 - gravity, 618
- Pressurized water reactor, 5
- Pressurizer, 12, 14, 811

-
- Primary dimensions, 33, 748
 - Primary side 784-785
 - Process
 - adiabatic, 57
 - isentropic, 59
 - isobaric, 59
 - isothermal, 59
 - polytropic, 59
 - reversible, 57
 - Property:
 - critical, 41
 - extensive, 40
 - intensive, 40
 - reduced, 41
 - Pump
 - Booster, 173, 877
 - canned-motor, 800
 - centrifugal, 749
 - characteristic curve, 749, 757
 - head, 263, 313, 762
 - homologous, 748, 755-769
 - jet, 13, 749
 - positive displacement, 749
 - Pumping power, 75, 76, 169, 314
 - Pure substance, 34
 - Quality
 - steam, 50
 - void and slip relation, 602
 - Quantum number, 884, 935
 - Quasi-steady, 348
 - Quench tank, 204
 - Quiescent fluid, 550, 650
 - Radial flow, 10, 20, 749
 - Radiation heat transfer, 26, 436, 561
 - Radiosity, 565
 - Range, 729
 - Rankine cycle, 161-162
 - Rateau correlation, 125
 - Rayleigh number, 550
 - Reactor shutdown, 882
 - Reciprocity, 581
 - Recirculation, 13, 16, 134, 827
 - Reduced pressure, 41
 - Reflectivity, 573, 575
 - Refrigerant, 662
 - Regression, 1007
 - Relative humidity, 194
 - Relative roughness, 312
 - Repeatability, 729
 - Resolution, 729
 - Resonance, 845
 - Reynolds-Colburn analogy, 521
 - Reynolds number, 230
 - Reynolds transport theorem, 240, 961
 - Rigid column theory, 344, 371
 - Rohsenow correlation, 651
 - Safety valve, 307
 - Saturation
 - pressure, 54, 637
 - temperature, 46
 - Scaling laws, 747
 - Scattering:
 - elastic, 843
 - inelastic, 843
 - Seban-Shimazaki correlation, 540
 - Second law of thermodynamics, 96
 - Secondary side, 12-16, 30, 97, 134
 - Seider-Tate correlation, 538
 - Semi-infinite solid, 485
 - Sensitivity, 729
 - Separated flow model, 616, 621
 - Shaft work, 60, 69-77
 - Shape factor, 581
 - Shear work, 60, 262, 792, 816
 - Shearing strain, 226
 - Shell and tube, 688
 - Shell side, 314-315, 465, 688
 - Shock wave, 98, 151, 408
 - Shroedinger wave equation, 932
 - Similarity, 747
 - Siphon, 284, 285
 - Six factor formula, 851
 - Skin friction, 302
 - Slab, 443
 - Slip ratio, 603
 - Solar, 3, 6, 17-22, 129, 133, 727
 - Solid angle, 563
 - Specific

- enthalpy, 40
- entropy, 40
- gravity
- heat, 40
- humidity, 195
- power, 9, 145, 156, 865
- speed, 758
- volume, 38
- Spherical coordinate system, 251
- Spray, 211-214, 329, 818
- Stagnation enthalpy, 417
- Standard temperature and pressure (STP), 37
- Standard temperature, 37
- Stanton number, 520
- State
 - equilibrium, 35
 - steady, 32, 66
 - unsteady, 66
 - thermodynamic, 38, 55, 815
- Steam extraction, 12, 167-172
- Steam generator, 2, 3, 12-16, 77, 702
- Stefan-Boltzmann law, 26, 436, 568
- Steradian, 564
- Stokes hypothesis, 249
- Streamline, 230
- Stress
 - normal, 224
 - shear, 224
 - tensor, 226
- Sturm-Liouville, 860, 913
- Subcooled, 46
- Sublimation, 48
- Subsonic, 230
- Substantial derivative, 235
- Sudden:
 - contraction, 303
 - expansion, 303
- Superheated vapor, 46
- Supersonic, 230, 407
- Surface force, 226
- Surface roughness, 98, 224-299
- Surface tension, 229, 618, 639, 651
- Surge tank, 357
- Surroundings
- System
 - closed, 56
 - isolated, 56
 - open, 57
- Taylor series, 902
- Terminal temperature difference (TTD), 710
- Terminal velocity, 366
- Thermal
 - capacitance, 434
 - center, 796
 - conductivity, 433
 - diffusion, 432
 - expansion, 40, 47
 - neutron, 846
 - pollution, 101
 - radiation, 436, 561
 - resistance, 435
- Thermodynamic
 - availability, 105
 - cycle, 6
 - efficiency, 100
 - irreversibility, 99
 - process, 36
 - property, 40
 - state, 38
 - system, 35
- Thermofluids, 1
- Time constant, 446
- Total directional emissivity, 579
- Total hemispherical absorptivity, 576
- Total hemispherical emissivity, 575
- Trailing edge, 519
- Transient, 32, 66, 81-95
- Translation, 39, 265
- Transmissivity, 575
- Tube bundle, 15, 77, 537, 690
- Tubesheet, 15, 16, 688, 795
- Turbine
 - efficiency, 175, 776
 - Francis, 20, 772
 - gas, 6-11, 66, 97, 154
 - impulse, 19, 770
 - Kaplan, 17, 19, 772

-
- Pelton, 18, 19, 738, 770-774
 - rotor, 9, 10, 17, 19, 769-770
 - steam, 4, 9, 15, 17, 25, 73
 - wind, 21, 770, 774-777
 - Turbofan, 9, 777-779
 - Turbomachine, 6, 747
 - Turboprop, 9, 777-779
 - Turbulence, 287, 535, 660
 - Turbulent flow, 230
 - Two-phase:
 - flow fundamentals, 601
 - friction multiplier, 617
 - U-tube
 - heat exchanger, 702
 - steam generator, 15, 16, 796
 - Uncertainty analysis, 730
 - Unit vector, 943
 - Universal gas constant, 42
 - Uranium
 - enrichment, 842
 - natural, 842
 - Valves, 72, 306
 - Van der Waals, 43
 - Vane, 15, 19, 748
 - Vapor pressure, 37
 - Velocity
 - angular, 39
 - distribution, 289
 - coefficient, 322, 772
 - head, 263
 - of sound, 917
 - Vena contracta, 303, 321, 322
 - Venturi meter, 71, 321
 - View factor, 436, 579, 580
 - Viscoelastic, 228, 229
 - Viscosity, 227-228
 - Viscous:
 - dissipation, 257
 - flow, 224, 230-232, 268
 - sublayer, 232, 294
 - Void fraction, 602
 - Volumetric flow rate, 58
 - Volumetric flow ratio, 604
 - Volumetric heat generation rate, 244
 - Von Karman, 293, 526
 - Vorticity, 226, 265
 - Wake, 233, 775, 776
 - Wallis number, 604
 - Water properties, 1077, 1082
 - Waterhammer, 371
 - Wave
 - equation, 917
 - mechanics, 932
 - Wavelength, 561
 - Weber number, 618
 - Wet bulb temperature, 202
 - Wetted perimeter, 309
 - Wien's displacement law, 570
 - Whitaker's correlation, 536
 - Work
 - definition, 57
 - optimum useful, 111
 - Zenith angle, 563-564
 - Zeroth law of thermodynamic, 56
 - Zhukauskas, 537
 - Zuber and Findlay, 609-611
 - Zuber correlation, 652